A study of the mixing of natural flows using ICP-MS and the elemental composition of waters

Thesis by

Susan C. Paulsen

In Partial Fulfillment of the Requirements

for the Degree of

Doctor of Philosophy

California Institute of Technology

Pasadena, California

1997

(Submitted May 22, 1997)

Acknowledgments

It is astonishing to me how little of the work presented in this thesis could have been done without the support, help, and encouragement of so many people. Thanks first of all to my friend and mentor John List, who provided the idea that grew into this thesis as well as good humor, always constructive criticism, and a sense of adventure in doing field work. Professors Jim Morgan and Norman Brooks, co-advisors on this work, were available and helpful and made me look at problems in ways I didn't necessarily want to (which, in hindsight, was a very good thing). Thanks also to Geoff Blake, whose participation on my candidacy and thesis committees and whose knowledge of geochemistry were greatly appreciated. Finally, many thanks are owed to Stanford's Jeff Koseff, whose enthusiasm and love of water and teaching got me started in this area, and Steve Monismith, who also provided encouragement throughout this work.

Many people helped me in conducting the field work necessary for this thesis. Hank Gebhard, Dick Gage, Doug Thompson, and Randy Brown of the State of California Department of Water Resources helped with locating, installing, and maintaining sampling equipment; Frank Schmiedel of the Boathouse Marina at Locke and Ralph and Ardith Wallace of Donavon's Marina at Bethel Island were kind enough to provide space, power, and easy access for sampling equipment. Rosemary Clark of the Sacramento Regional Wastewater Treatment Plant collected samples during the early part of the work in the Delta. Finally, Bob Rocheleau, Ted Durland, and the others at Sea Engineering, Inc., in Hawai'i were wonderful in collecting samples and plotting and analyzing results, and they were great hosts for the work conducted in Oahu.

Credit is also due to my friends and colleagues at Caltech, who helped with preparing for sampling trips, discussing ideas, learning new instrumentation and laboratory procedures, figuring out paperwork and problem sets, and keeping me (more or less) sane. In particular, Peter Green helped immeasurably with learning ICP-MS techniques and maintaining equipment; Fran Matzen, Linda Scott, and Rayma Harrison helped with a million not-so-little things; and master's students Tyler Erickson and Dina Del Conte helped in organizing references and mountains of data. Dr. Gerry Wasserburg and others in his laboratory helped with discussion and sample analysis. Thanks also to Fabrizio, Edye, Maryjean, Tom, Aaron, Hinrich, Bruce, Phil, Selena, Nicole, Mike, Roberto, Patrick, Ralf, Jeff, John, and many others. I feel blessed.

The writer wishes to thank all the organizations that supported this thesis research financially. The Andrew W. Mellon Foundation provided financial support for the initial development of the method and for thesis writing. Much of the work in the Delta was funded by the Research Enhancement Program for the San Francisco Bay/Delta, sponsored by the Interagency Ecological Studies Program. Funding for the work conducted in Hawai'i was provided by CEROS, the National Defense Center of Excellence for Research in Ocean Sciences. The analytical work for this research was performed both in the Environmental Analysis Center, sponsored by the Bank of America, and using an ICP-MS provided by Hewlett-Packard in a cooperative arrangement.

Finally, many thanks to my parents, Fred and Marjorie Paulsen - I don't think you knew what you were in for when I started this Ph.D. During this research, you provided a warm bed, great meals and company, even a surrogate cat when I was doing field work.

You put up with heavy, smoky vacuum pumps running late into the night, and you went with me to sampling sites when I was scared to be out alone during the worst flood in memory. None of this should surprise me, for you have always been there. I dedicate this thesis to you.

Abstract

Determining flow patterns and the distribution of chemical constituents in the environment is critical to understanding and solving problems in freshwater, estuarine, and coastal environments. Computer models describing flows in the environment usually use empirical estimates of key parameters and are difficult to validate. The objective of this research was to develop a method to trace flows in surface waters by directly measuring existing conditions. Inductively coupled plasma-mass spectrometry (ICP-MS) was used to establish elemental "fingerprints" for water sources, and fractions of "fingerprinted" waters in a sample containing these source waters were estimated. Two different, complex systems were studied: the Sacramento-San Joaquin Delta and the near-coastal environment of Oahu, Hawai'i. If the method could be successfully used in these highly complicated environments, it should be applicable in almost any other natural environment. Successful application in three smaller, simpler systems supports this conclusion.

Within the Delta, source "fingerprints" were established, and their variation both temporally and spatially was determined. Elemental behavior was determined by laboratory work and field studies, and a simple mathematical model was used to calculate the fraction of source water in samples collected throughout the system. Mixing was consistently determined for most flow conditions using the tracer elements sodium, magnesium, calcium, and strontium. The method was used to establish the sources of water pumped from the Delta into major aqueducts and the effects of various operational changes.

Because of Hawai'i's uniform geology and difficulties measuring trace elements in saline waters, the method was significantly less successful in Hawai'i. Concentrations of major ions were used to estimate dilution for stream and wastewater flows to 25:1 in receiving waters; rare earth elements (lanthanum, praseodymium, and neodymium) were added to a wastewater flow to qualitatively determine mixing at dilution levels of about 300:1.

The procedures for ICP-MS analysis developed for this study are presented, as are the criteria for selecting and using elemental tracers in freshwater, estuarine, and certain saltwater environments. The method can be used to directly determine mixing levels and the distribution of chemical constituents, to validate computer models, and to address a variety of specific environmental issues.

Table of Contents

List of Figures

Note: A table of figures is provided with each appendix as appropriate.

List of Tables

1 Introduction

1.1 Motivation

Determining the distribution of chemical constituents and flow patterns in the environment is vital to understanding and solving environmental problems in freshwater, estuarine, and coastal environments. Although computer models exist to describe flows and the transport of chemical constituents in the environment, these models are difficult to validate and usually rely upon empirical estimates of flow parameters obtained from tracer studies. The objective of this study was to develop an alternative method to analyze flows in surface waters, a method that would measure existing conditions directly using natural elements rather than depending upon added tracers. Whereas long-term flow predictions generally require computer modeling, the method proposed here would also allow the direct determination of flow conditions over periods ranging from hours to years.

The analytical technique that made this study possible was inductively coupled plasma-mass spectrometry (ICP-MS), a technique capable of measuring the aqueous concentrations of seventy-five elements rapidly and to very low detection limits. The concept is to use this technique to "fingerprint" specific water sources by obtaining their chemical elemental compositions. The fraction of a "fingerprinted" water could then be determined in a water sample that contains a mixture of source waters.

The greater part of this study focused on the application of ICP-MS to the analysis of various natural waters (see Chapter 2) and the development of a tracer method to

characterize the distribution of chemical constituents within two different and complex systems: the Sacramento-San Joaquin Delta in northern California (see Chapter 3) and the near coastal environment of southern Oahu (see Chapter 4). These locations were selected because they provide two distinct, complex environments: if the feasibility of this concept could be shown in these environments, it should be applicable in almost any other environment, as these localities are representative of the extremes of complexity that can be found in natural systems. Additionally, it was hoped that the method could be used to answer fundamental questions about the flow environments in each of these locations.

1.2 Literature review

Similar natural tracer investigations have been performed in the context of groundwater and air pollution studies. Chemical mass balances (CMBs) were first used in the early 1970s to estimate the contributions to air pollution from regional sources. Elemental concentrations were measured in source emissions and in samples collected from various locations within the region ("receptor" locations) (Friedlander, 1973). These models were developed based upon the observation that air pollution sources, whether natural or man-made, can be characterized based on the elements they emit and the proportions in which these elements are emitted (Gordon, 1988). The models then estimate contributions from each source in a sample by solving a set of simultaneous linear algebraic equations (Friedlander, 1973); they are objective methods, as data are manipulated only in the calculation of statistical measures (Olmez *et al.*, 1994). Since

their early development, many refinements have been made to the models, and they have been successfully used in a wide variety of air pollution studies. These studies include a CMB study of fine and coarse particulate matter in Philadelphia (Dzubay *et al.*, 1988) and a factor analysis study in Boston that utilized the concentrations of eighteen elements (Hopke *et al.*, 1976). Studies have been conducted that model source contributions based upon the ratios of the concentrations of six trace elements (Heaton *et al.*, 1992) and the concentrations of organic species (Rogge, 1993).

Receptor modeling has been used in groundwater studies to trace specific sources of contamination. Recent studies include the differentiation between sources of groundwater contamination in a site contaminated by multiple sources in central Pennsylvania (Olmez *et al.*, 1994) and a study to identify trace element patterns in leaks from hazardous waste impoundments (Olmez and Hayes, 1990). Additional studies have used simpler mass balance techniques or have investigated the spreading of released tracers that are distinct from surrounding groundwaters. Among these are studies of: accidentally released tritium in groundwaters and in surface waters in the Glatt Valley of Switzerland (Santschi *et al.*, 1987); transport of microspheres and indigenous bacteria in a sandy aquifer (Harvey *et al.*, 1989); inflow to seepage lakes using solute tracers released by weathering (Stauffer, 1985); and the distribution and mobility of selenium and other trace elements in groundwater in the San Joaquin Valley using factor analysis (Deverel and Millard, 1988). Additionally, at least two recent studies have been conducted specifically to confirm the potential of ICP-MS analysis to fingerprint waters: for spring

and well waters in southern Nevada (Stetzenbach *et al.*, 1994) and for lakes in the eastern U.S. (Henshaw *et al.*, 1989).

Several other techniques for tracing flows are reported in the literature; many of these techniques can be used to measure high dilution levels, and these techniques involve the addition of a tracer substance to the flow to be traced. Dye tracing, in which a dye such as fluorescein, rhodamine WT, rhodamine B, or acid yellow 7 is added to a source flow, involves the measurement of fluorescence in samples collected from a study area. Fluorescence can vary significantly with temperature and pH and can be affected by chemical reactions between the dye and the source water; sorption (both adsorption and absorption) can result in non-conservative behavior, particularly when concentrations of organic matter in the study area are high (Wilson *et al.*, 1986). Photolysis can result in the decomposition of dyes (Suijlen and Buyse, 1994). Elements that are added as tracers may cause toxicity in high concentrations, even for elements generally regarded as safe at naturally occurring levels (such as Li; see Stewart and Kszos, 1996). Two tracers that have been used more recently and that show fewer of these effects are sulfur hexafluoride (SF_6) and perfluorodecalin (PFD); however, their solubilities are low and their dissolution requires extremely large quantities of water or elaborate dissolution systems (Watson *et al.*, 1991; Wilson and Mackay, 1996).

Numerous studies have been performed in surface waters, including rivers, estuarine environments, and ocean waters, to study the concentrations and chemical behavior of elemental and chemical constituents as they are transported. A considerable

body of literature relevant to this study has been reviewed; results of this literature review are presented as Appendix A.

1.3 Criteria for tracer studies

To model flows accurately in the environment using receptor models or chemical mass balances, three conditions must be met:

(1) sources must have distinct chemical or elemental "fingerprints;"

(2) source fingerprints must not vary significantly on timescales shorter than the mixing timescales of the system; and

(3) fingerprints of sources must not be altered to any great extent either by chemical and/or biological reactions or by physical changes that occur during mixing (*i.e.*, mixing should be conservative, or very nearly conservative).

The first condition ensures that a source can be uniquely characterized by establishing a source fingerprint, defined as a vector containing the concentrations of certain elements in a given water sample. The second ensures that this characterization is preserved between the time elemental concentrations are measured in a parcel of water collected from a source and the time a sample is collected at a receptor site. Finally, if mixing is conservative, there is no gain or loss of the element, the concentration of the elements in a sample collected from a receptor site can be computed as:

$$C_i = \sum_j f_j x_{ij},$$

where C_i is the concentration of element i in the receptor sample and f_j is the source strength term, representing the fraction of an element contributed by source j. The term x_{ij} is the concentration of the ith element in water that originated in the jth source.

1.4 Study areas

1.4.1 Sacramento-San Joaquin Delta

A key problem in the future development of California is the allocation of freshwater resources in the Sacramento-San Joaquin Delta ("the Delta"). The Delta is a system in northern California in which two large rivers (the Sacramento and San Joaquin Rivers) and various smaller freshwater sources flow into a brackish bay. In this estuary, mixing between fresh and brackish waters of varying chemical compositions occurs over long distances. Currently, the primary factor controlling the use of the freshwater that passes into and through the Delta is the ecological health of the system; this has been directly related by some investigators to the distribution of salinity and to overall water quality within the system. Several hydrodynamic models exist to describe the hydraulic transport of salt and other chemical constituents in the Delta, including the Fisher Delta Model (FDM), the State of California Department of Water Resources Delta Simulation Model (DWRDSM), and the Resource Management Associates (RMA) model. Each of these models uses empirical estimates of the net consumptive water use within the Delta and semi-empirical flow estimates at some of the major channel connections in the Delta. In addition, these models have been calibrated to reproduce the salinity observed within

the Delta but not to estimate or reproduce the distribution of water from each of the freshwater sources. These factors have led to intense discussion about the specific route by which salt and other chemical constituents arrive at a given location and consequently about appropriate management and control strategies.

The development of a method using ICP-MS and receptor modeling would help resolve the flow distribution debate by establishing a technique with which flow patterns and mixing levels within the Delta could be objectively determined. Specifically, water arriving at pumps that export water from the Delta could be traced back to its source, thus determining the origin of lower quality water. During the study period, the distribution of water within the Delta would be established for various configurations of artificial flow control structures. This information could then be used (by others) to calibrate existing flow models for the distribution of freshwater within the system, and models could be used with far greater confidence to predict the outcome of various operations scenarios. ICP-MS analysis techniques and sampling protocols for the Delta study are presented in Chapter 2; the tracer method developed for use in this system and results from the application of this method are presented in Chapter 3.

1.4.2 Oahu, Hawai'i

Pollution in coastal waters is an important environmental, regulatory, and economic problem in many areas, including Hawai'i. An extension of the ICP-MS tracer technique into coastal and saline waters could help overcome existing monitoring limitations and could help provide definitive answers to the problems of coastal

degradation. Successful implementation of the technique in saline waters would require overcoming several technical problems, including the use of ICP-MS to analyze trace elements in saline waters and the identification of tracer elements that can be measured accurately in fully saline ocean waters.

The study area as defined for this research included ten freshwater streams that flowed either into Pearl Harbor or into the Pacific Ocean directly. In addition, Waianae outfall, one of several wastewater outfalls that discharges into the ocean, was studied. For all of these flows, mixing between fresh and fully saline waters occurs over short distances. The suitability of ICP-MS analysis for measuring elemental concentrations in highly saline waters is discussed in Chapter 2; after difficulties were identified, the study was modified to add a rare earth tracer to the wastewater flow. Details and results of the study are presented in Chapter 4.

1.4.3 Other studies

During the course of this research, there were several opportunities to collect samples from systems far simpler than those of the Delta and the near-shore environment of Oahu. Chapter 5 presents the results of three of these studies. In one, the mixing of two influent waters to a drinking water treatment plant was successfully predicted by measuring elemental concentrations in the treated effluent. The concentrations of several elements measured in the Napa River estuary were used to demonstrate the tidal flushing capacity of this estuary. Both of these studies used the natural elemental compositions of the water studied. Finally, the opportunity arose to evaluate the use of an added tracer in

the Delta environment. In this study, rubidium chloride was used to establish the mixing behavior of a wastewater discharged through an outfall located in the south Delta.

1.5 Overview

The use of the ICP-MS analysis technique and sample collection procedures are presented in Chapter 2. Chapter 3 presents analysis results, method development, and conclusions for the Delta study area. Results from the Oahu, Hawai'i, study area are presented as Chapter 4, and Chapter 5 includes the results from three smaller studies, also used for method development. Finally, Chapter 6 summarizes the results of the previous chapters and discusses additional applications and extensions of the method; areas for additional study are also presented. Throughout this document, terms are defined when they are first used; the exception is that elements are referred to throughout by their chemical symbols. A complete list of element names and symbols is provided in Appendix A.

2 Sample Collection and Analysis

2.1 Overview

This research was undertaken subsequent to the purchase by Caltech of an instrument to perform inductively coupled plasma-mass spectrometry (ICP-MS). Because of its ability to measure many elements in the periodic table quickly and accurately, a preliminary study was conducted to determine whether or not ICP-MS could be used to establish unique elemental compositions, or "fingerprints," for distinct water sources. When it appeared that water sources did indeed have different "fingerprints," a larger study was designed to develop a method for tracing flows using these "fingerprints." By its nature, such a study involves the collection and analysis of a large number of samples. Because the ICP-MS technique was new at Caltech, analysis procedures were refined through much trial-and-error. Sample handling and preservation techniques were also modified through the course of this study with the goal of providing reproducible, reliable data, and significant effort was made to extend the applicability of ICP-MS to brackish and highly saline oceanwater samples. This chapter presents both the analysis and sampling techniques developed during the course of this research.

2.2 ICP-MS

Inductively coupled plasma-mass spectrometry (ICP-MS) was first introduced commercially in 1983 as a method for rapid, highly accurate multi-elemental analysis. ICP-MS consists of two separate operations, the creation of a plasma and the analysis of

that plasma, connected by an interface. The plasma is produced from a water sample when the sample is nebulized, desolvated, dissociated, and excited; the plasma consists of ionized atoms from the original water sample in an argon submatrix. The plasma results from the desolvation of the sample (much of the original water substrate is driven away) and the destruction of chemical bonds and ionization of the resulting atoms at very high energies (temperatures to 6,000K).

After its creation, the plasma passes through an interface between the plasma torch and a quadrupole mass spectrometer. The mass spectrometer operates as a filter, and along its axis, a path exists for ions of only one mass-to-charge (m/z) ratio. Other ions are deflected away from the axis; ions that reach the detector are counted. The ICP-MS interfaces with a computer that records the sample intensity (ion counts per second) and calculates the standard deviation in the intensity. Additionally, the use of standards enables the computer to calculate elemental concentrations for a given sample. By tuning the mass spectrometer to varying m/z ratios, ion counts and concentrations for the various isotopes of the elements are determined and recorded by the computer.

ICP-MS allows the rapid and accurate determination of the concentrations of many elements in a small volume of sample. Operational costs are relatively low, and detection limits for most elements are much lower than with other analytical methods; detection limits are shown in Figure 2.1. The fundamental basis of the research conducted for this study is the ability of ICP-MS to measure elemental concentrations in water samples with exceptional accuracy. ICP-MS can rapidly determine the concentrations of seventy-five elements to very low detection limits, often in the part-per-

trillion (1 in 10^{12}) range. This capability allow the analysis of many more samples for more elements and to lower detection limits than possible with many other analysis techniques.

ICP-MS does not yield any chemical information about a sample other than its raw elemental composition, so the determination of concentrations of compounds or molecules such as sulfates, nitrates, or more complex chemicals cannot be made. The main disadvantages of ICP-MS result from interferences between ions which can cause inaccurate analysis if corrections are not made. ICP-MS can experience interferences from overlapping isotopes (isobaric interferences) and from molecular species such as oxides and doubly-charged ions that form in the plasma. Polyatomic ions such as argides may also form from the main components of the plasma itself. In general, most of these interferences are correctable by manipulating operating conditions to minimize oxides, doubly-charged ions, and polyatomic ions and by employing interference corrections, which are derived from the isotopic abundances of interfering species.

Two ICP-MS instruments are currently available at Caltech and have been used for this work. Initial sample analysis was performed with a Perkin-Elmer Elan 5000 ICP-MS; this is the older of the two instruments. More recently, a Hewlett-Packard 4500 ICP-MS was loaned to Caltech for use as a demonstration instrument and was later purchased by Caltech. The HP 4500 instrument has several advantages over the Perkin-Elmer instrument, including lower detection limits for many elements and software which is easier to use and more reliable. Additionally, the HP 4500 can be more easily tuned to optimize operating conditions; this instrument was used for most of the samples collected

later during this research, and most of the results upon which the conclusions of this research are based were obtained using the HP 4500.

Section 2.2.1 below presents the fundamentals of ICP-MS analysis, including the various components within the instrument, their functions, and optimization of performance by "tuning" the various components. Interference corrections and analysis procedures utilized during this research are presented in Sections 2.2.2 and 2.2.3, respectively.

2.2.1. Fundamentals of ICP-MS analysis

ICP-MS was developed in response to the requirement for a new generation of multi-elemental analytical instruments. At the time of its development, a variety of analytical techniques were available. These included atomic fluorescence spectrometry (AFS), instrumental neutron activation analysis (INAA), atomic absorption spectrometry (AAS), and x-ray fluorescence (XRF). None of these techniques provided coverage of most of the elements of the periodic table, the required mass resolution, or the enhanced sensitivity desired. Inductively coupled plasma-atomic emission spectrometry (ICP-AES), while providing analysis capability for a wide range of elements, suffered from problems due to matrix effects and high detection limits for high mass elements (for greater detail, see Date and Gray, 1989, p. 1). Coupling the creation of a plasma with mass spectrometry seemed the best solution to these problems. Creation of hotter, more efficient plasmas was achieved relatively easily in the 1970s; transferring the ions created in the plasma to the low pressure environment required for mass spectrometry proved the

most difficult obstacle. This obstacle was overcome in the early 1980s, and further improvements resulted in the instruments now commercially available. There is a rich literature on the development of ICP-MS and solutions to the technical problems encountered during its evolution; see Date and Gray, 1989, and Jarvis, *et al.*, 1992, for greater detail and further references.

The fundamental components of an ICP-MS system are shown in Figure 2.2. The sample introduction system usually consists of a peristaltic pump system, nebulizer, and spray chamber; these pump liquid solution into the system, create fine aerosol droplets from the solution, and select droplets so that only the finest droplets are incorporated into the plasma. The plasma is then created within a torch, where droplets are desolvated, salt particles are volatilized, molecular vapor is dissociated, and atoms are excited and ionized. The resulting plasma passes through a free space between the torch and the mass spectrometer. The central-most portion of the plasma flows through small orifices in two "cones." The pressure drops from ambient before the cones to very low pressure behind the cones, and the plasma passes finally into the mass spectrometer. In the mass spectrometer, ions of a selected m/z ratio are channeled to a detector, where they are counted. Greater detail on these components is provided below.

2.2.1.1 Sample introduction

ICP-MS analysis requires that a sample be introduced to the plasma as a gas, vapor, or aerosol of fine droplets or solid particles. The ICP-MS systems in use at Caltech pump sample solution into the instrument using a peristaltic pump; the solution passes into a nebulizer that disperses the sample using a stream of argon gas. Both

concentric and Babington type nebulizers are used in these instruments. The concentric nebulizer consists of a main channel through which the liquid sample is introduced and a smaller side channel through which the argon gas is introduced. The Babington nebulizer produces an aerosol of fine droplets by allowing a thin film of sample to flow over the surface of a sphere; gas is forced through a small aperture beneath this film to produce an aerosol. The Babington nebulizer has a greater tolerance for solutions with high dissolved solids and colloidal-sized particles and was used for most of the samples in this work.

The nebulizer produces a fine mist, which then passes through a double-pass spray chamber. Larger droplets are removed by collision with the spray chamber walls and only droplets finer than about 8 μm pass through to the plasma. The temperature within the spray chamber is maintained by a Peltier cooler, yielding a more stable ion signal and removing some of the water from the sample. This reduces the level of interfering oxide species formed.

2.2.1.2 Torch and plasma

An inductively coupled plasma is formed when energy from a radio frequency generator is coupled to an annulus in a gas stream. The gas used for most ICP-MS work, and for all of the work in this research, is argon. The plasma is generated inside the open end of a quartz torch, which is an assembly of three concentric tubes. The innermost tube is called the injector tube; sample from the sample introduction system and argon gas (carrier or nebulizer gas) flow through this tube into the plasma. The carrier gas flowrate is generally about 1 to 1.2 l min^{-1}. Side tubes inject gas into two annular regions formed

between the innermost and the middle tubes and between the middle and outer tubes. These side tubes are mounted to the torch tangentially and create vorticular flow within the annular regions. The outermost gas flow (the plasma gas flow) cools the tube walls and is the main plasma support gas; its flow rate is generally 10 - 15 l min^{-1}. The second gas flow in the innermost annular space is called the auxiliary gas. It serves to cool the central torch tube to prevent it from being melted by the plasma and to direct flow from the injector tube. The auxiliary gas flow rate is generally between 0 and 1.5 l min^{-1} and may be varied according to operating conditions. The gas flow from the central injector tube travels with a higher velocity than the flow in the annular regions, and this flow "punches through" the center of the plasma.

The end of the torch is located inside a coupling or load coil. A radio frequency (RF) current is passed through four windings of this copper coil. The RF current oscillates at 27.12 MHz and generates a magnetic field. In a cold torch, the discharge is initiated by a Tesla coil, which provides free electrons to "seed" the plasma. Electrons in the plasma collide with and transfer their energy to argon atoms, which heat the plasma. Most energy is coupled into the outer reaches of the plasma; the gas/sample mixture from the injector is heated mainly by radiation and conduction. In the outer portions of the flow, temperatures range from 8,000 to 10,000 K. The injector flow, which punches a hole through the outer plasma, is generally cooler. Because the injector flow punches through the center of the hotter plasma, the chemical composition of the sample can vary significantly without affecting the energy transfer processes from the coil to the plasma.

The plasma is very efficient at creating singly-charged ions. Most elements of interest are over 90% ionized under normal operating conditions (Houk and Thompson, 1988), and the plasma is efficient at ionizing elements with first ionization energies below 10 eV. For elements with first ionization energies above about 10 eV, fewer than 50% of atoms present in the plasma are ionized. Most elements have first ionization energies below 10 eV, as shown in Table 2.1 (adapted from Houk and Thompson, 1988). No elements have second ionization energies below 10 eV, which helps to minimize interferences caused by doubly-charged ions, discussed in greater detail in Section 2.2.2.

Table 2.1
Ionization energies for singly- and doubly-charged ions

Ionization energy (eV)	Elements forming singly-charged ions	Elements forming doubly-charged ions
< 7	Li, Na, Al, K, Ca, Sc, Ti, V, Cr, Ga, Rb, Sr, Y, Zr, Nb, In, Cs, Ba, La, Ce, Pr, Nd, Pm, Sm, Eu, Gd, Tb, Dy, Ho, Er, Tm, Yb, Lu, Hf, Tl, Ra, Ac, Th, U	
7 - 8	Mg, Mn, Fe, Co, Ni, Cu, Ge, Mo, Tc, Ru, Rh, Ag, Sn, Sb, Ta, W, Re, Pb, Bi	
8 - 9	B, Si, Pd, Cd, Os, Ir, Pt, Po	
9 - 10	Be, Zn, As, Se, Te, Au	
10 - 11	P, S, I, Hg, Rn	Ba, Ce, Pr, Nd, Ra
11 - 12	C, Br	Ca, Sr, La, Sm, Eu, Tb, Dy, Ho, Er
12 - 13	Xe	Sc, Y, Gd, Tm, Yb, Th, U, Ac
13 - 14	H, O, Cl, Kr	Ti, Zr, Lu
14 - 15	N	V, Nb, Hf
15 - 16	Ar	Mg, Mn, Ge, Pb
>16	He, F, Ne	All other elements

2.2.1.3 Interface and vacuum system

The ions created in the plasma at ambient pressure must be introduced into the mass spectrometer at very low pressures; this is achieved as the plasma passes through the interface zone or system. Ions flow into the first vacuum stage by passing through a sampling orifice, which is a hole in the front plate of the vacuum chamber about 1 mm in diameter, known as the sampling cone or "sampler." The interface zone behind this orifice is an expansion region evacuated by a rotary pump. Pressures in this interface zone are typically about 200 - 500 Pa. The ions then pass through a second orifice called the skimmer orifice or "skimmer," which is about 0.40 mm in diameter, and into the ion lens chamber. The ion lens chamber is evacuated by a turbomolecular pump backed by a rotary pump. Pressures in this chamber are typically 10 - 20 Pa. The extracted gas reaches supersonic velocities passing through the sampler cone, and travel times to the skimmer cone are on the order of microseconds (Jarvis *et al.*, 1992). Thus, the composition of the plasma should not change significantly as it passes into the analysis region of the instrument. Between the sampler and the skimmer cones, the flow forms a free jet bounded by a shock wave. A second shock wave called the Mach disc forms across the axis, generally about 10 mm behind the sampler orifice (Date and Gray, 1989). The skimmer is placed upstream of the Mach disc, beyond which flow becomes subsonic again. The skimmer cone is designed with a sharper angle than the sampling cone in order to minimize the formation of an additional shock at its tip. The temperature in the center of the jet passing through the skimmer cone is generally about 200 K, but the

skimmer must be cooled externally because the surrounding gas impacting the skimmer remains very hot.

Both the sampler and skimmer cones are replaceable and are made of a highly conductive metal, usually nickel, copper, platinum, or a combination of these metals. The cones are cooled by water from a chiller, which flows through the metal bases to which the cones attach. Periodic cleaning of the cones is necessary to minimize sample "carryover" and the formation of interfering polyatomic ions. Because the cones are exposed to such extreme conditions, the metals forming the cones may become pitted and annealed, particularly near the orifice; regular cleaning removes materials deposited on the cones, and occasional refinishing creates a smooth surface to which ions are less likely to "stick."

After passing through the cones, the sample passes through two extraction lenses and through a variety of other lenses as discussed below. A gate valve is located between these sets of lenses so that the vacuum within the high vacuum chamber can be maintained during normal maintenance of the cones and extraction lenses and while the instrument is not in use.

2.2.1.4 Ion lenses and quadrupole mass spectrometer

Ion lenses are used to focus the ion beam after it has passed through the skimmer and before it enters the quadrupole mass analyzer. The ion lens assembly also prevents photons and neutral species created in the plasma from reaching the detector. The ion lenses are electrically charged metal cylinders placed so that the ion stream flows along the axis of the lens assembly. An ion of a given charge is created in the plasma in a

region with a given electrical potential; this charge and potential define the potential energy of the ion. The ion will travel through a given region as long as the potential in that region is below the initial potential; otherwise, it will turn around and travel back toward the source or be deflected away from the axis of the flow. The ion lenses are used to create regions of varying potential as the ions travel through the lens assembly. Between adjacent lenses, equipotential surfaces serve to focus ions, bringing ions of a selected potential toward the axis of the flow. Ions with a potential other than that selected will be deflected away from the central axis. The transmission and focal properties of the lens assembly can be changed rapidly by varying the voltages applied to the individual lenses.

Both neutral species and photons travel with the ion beam through the sampler and skimmer, and both can activate the detector. Two methods are commonly used to minimize their transmission into the analyzer region. The first method involves the placement of "photon stops," small uncharged plates, on the axis of the lens assembly. Photon stops cast a shadow on the aperture to the analyzer, preventing direct photons from reaching the detector. The second method electronically deflects the charged, focused ion beam away from the axis of the flow and into the off-axis entrance to the analyzer. Uncharged species and photons, which are not deflected, do not enter this region.

The lens assembly typically includes two extraction lenses, which extract ions from the plasma and accelerate them into the Einzel lens; the extraction lenses are located just behind the skimmer and before the gate valve. The Einzel lenses focus the ion beam

from the extraction lenses and direct the beam to the analyzer region. Photon stops may be located just after the Einzel lenses; alternatively, a third lens assembly, known as the Omega lens assembly, may be used in place of photon stops to deflect the ion beam to an off-axis entrance to the analyzer region. The Hewlett Packard 4500 ICP-MS at Caltech utilizes the Omega lens assembly while the Perkin Elmer Elan 5000 at Caltech employs a conventional photon stop.

The focused ion beam passes into the quadrupole mass analyzer, which functions as a mass filter, allowing ions of a specific m/z to pass through the center of the quadrupole. The quadrupole is constructed of four long metal rods of hyperbolic cross-section; these are arranged parallel to each other along the axis of the analyzer region. Pressures in the analyzer region are maintained by a turbomolecular pump between 1 and 9×10^{-4} Pa. Both RF and DC potentials are supplied to the quadrupole rods from the RF generator; the transmitted mass is determined by the amplitude of these potentials and the resolution is determined by their ratio (Jarvis *et al.*, 1992). The RF and DC voltages can be changed easily and rapidly, and the entire mass range (spanning m/z from 2 to 260) can be analyzed in roughly 100 milliseconds.

Quadrupole mass analyzers provide limited mass resolution, sufficient to separate peaks at adjacent masses but not sufficient to separate elemental peaks from peaks created by interfering species. To some degree, resolution can be enhanced to minimize this problem, but generally interference corrections must be made as discussed in Section 2.2.2.

2.2.1.5 Ion detection

After passing through the quadrupole, ion signals are measured by an electron multiplier detector, located behind the quadrupole in the analyzer stage. Two modes of ion counting are normally used, depending upon the concentration of the analytes being measured. Pulse-counting mode is used for concentrations ranging from the detection limit to about 1 ppm. In pulse count mode, the detector releases a cascade of electrons when struck by a positively charged ion; this cascade is successively multiplied until it is detected as a single pulse. For concentrations higher than about 1 ppm, ions are counted in analog mode. Analog mode involves releasing the ion intensity as a current and converting that current to a pulse counting signal using a voltage-to-frequency converter.

Caltech's Perkin Elmer Elan 5000 ICP-MS operates only in pulse-counting mode but uses an ion lens "detuning" feature to focus high concentrations of ions less sharply and to allow even high concentrations to be measured in pulse-counting mode. The degree of "detuning" is specified by a user-supplied "omni-range" feature and is not automatic. The Hewlett Packard 4500 ICP-MS at Caltech allows one to specify analog-counting mode for elements known to be present in high concentration, or the instrument can automatically scan the mass range and select either pulse-counting or analog-counting mode depending upon the concentrations of ions detected in the scan. Initially, the analog-counting mode of the HP 4500 ICP-MS did not function properly, but after extensive testing and hardware and software redesign based largely upon work performed at Caltech, this mode of operation functions properly. The detectors used in these instruments are similar, but the lifetime of the detector in the HP 4500 is considerably

shorter than that of the detector in the Elan 5000. Presumably this is an artifact of the overall analyzer system design.

2.2.1.6 Scanning and data acquisition

As described in Section 2.2.1.5, the quadrupole mass analyzer transmits ions with a given m/z depending upon the RF and DC voltages applied to the quadrupole rods. The voltages applied to the rods are generally controlled by a DC voltage ramp from a computer controlled digital-to-analog converter (Jarvis *et al.*, 1992); these voltages can be changed rapidly between discrete values or the entire m/z range of interest can be scanned repetitively. The peak-hopping mode is generally used for quantitative analysis, as this mode spends more time on each discrete peak, and repetitive peak sampling can average out some of the fluctuations present in the ion signal.

The dwell time, defined as the amount of time spent analyzing a peak, is specified by the user through the computer interface. The intensity of the signal is transmitted from the detector to the computer as counts per second, and the computer reports this information directly or converts it to concentration values using calibration curves established by analyzing standards. A variety of calibration techniques can be used, including external calibration, standard addition calibration, and isotope dilution analysis. Except where noted, external calibration was used to obtain the results presented in this work; analysis and calibration procedures are described in greater detail in Section 2.2.3. Internal standards are used to correct for general fluctuations in plasma and operating conditions; these corrections are also performed by the computer. The equations used for

external calibrations with internal standards are included in Section 2.2.3.2. Interference corrections, described in Section 2.2.2, are automatically applied to the collected data.

In addition to these functions, the computer provides additional control and safety functions for the whole system. Start-up, shut-down, and tuning (controlling the operating parameters) of the instrument may be either manual (as with the Perkin Elmer Elan 5000 ICP-MS) or computer-controlled (as with the Hewlett Packard 4500 ICP-MS). The computer is also used to run automated sampling equipment. Protection against misoperation is also provided by the computer; this includes automatic shutdown, including closure of the gate valve behind the skimmer, which occurs if the plasma is extinguished, if there is a cone failure, or if normal, safe operating ranges for temperatures or pressures within the system are exceeded. When used with an autosampler, the ICP-MS instrument can be run unattended and can be programmed to shut down automatically at the end of a sampling program.

2.2.2 Interference corrections

Interferences in ICP-MS analysis result when ions other than the desired analyte ions reach the detector and are counted, adding to the peak caused by the desired analyte. These interferences fall into two categories, spectroscopic interferences and matrix effects. Spectroscopic interferences include isobaric interferences, polyatomic ions, oxide ions, and doubly-charged ions. Matrix effects are more general and include both suppression and enhancement effects as well as physical effects caused by samples containing high dissolved solids. The extent of the interference depends largely on the

nature of the sample matrix itself. To a certain extent, interferences can be minimized by changing the operating parameters of the instrument and by employing interference corrections. The major interferences and some solutions to the problems caused by interfering species are discussed below; a table of interferences is provided in Appendix B, with the isotopes chosen for analysis and interferences for which corrections were applied shown in bold type.

2.2.2.1 Isobaric overlaps

Isobaric overlaps occur when two elements have isotopes of nearly the same mass. Although the isotopes do generally have masses which differ slightly from one another, the differences are small and cannot be resolved by the quadrupole mass analyzer. Most elements in the periodic table have at least one isotope free from overlaps with an isotope of another element. The exception to this is indium (In), which overlaps at m/z 113 with ^{113}Cd and at m/z 115 with ^{115}Sn. There are no isobaric overlaps below m/z 36. Some elements experience a significant isobaric overlap for their most abundant isotope; for example, based upon natural isotopic abundances, 48.89% of zinc occurs at m/z 64 as $^{64}_{30}$Zn, where it overlaps with an isotope of nickel (1.08% of nickel occurs as $^{64}_{28}$Ni). In general, a different isotope may be chosen to measure concentrations of these elements; in this case, zinc can be measured at m/z 66, which experiences no isobaric overlaps. Additionally, corrections can be employed to quantify and subtract the overlapping species. Strontium, for example, can be accurately measured at m/z 87 if rubidium is measured at m/z 85 and the appropriate fraction of counts is subtracted from the total

counts measured at m/z 87. In this case, since 7.02% of Sr and 27.85% of Rb are found at m/z 87 and 72.15% of Rb is found at mass 85:

$$^{87}Sr = {}^{87}M - 0.2785\ Rb = {}^{87}M - (0.2785/0.7215)\ {}^{85}M = {}^{87}M - 0.3860\ {}^{85}M$$

$$\text{and } Sr_{total} = (0.0702)^{-1}\ {}^{87}Sr.$$

In using isobaric overlap corrections, care must be taken that the signal subtracted from the total intensity at a given m/z is smaller than the total signal, *i.e.*, that the noise on the signal subtracted is much smaller than the remaining signal.

Isobaric overlaps with the components of the plasma gas can also occur. The most obvious case is that of calcium; 96.97% of calcium occurs at m/z 40, overlapping with 99.6% of argon, the most abundant element in the plasma, and with potassium, with only 0.00118% occurring at m/z 40. In addition to overlaps with argon caused by the plasma gas, both krypton and xenon can occur as impurities in argon and may contribute to isobaric overlaps. These may be significant for a variety of elements, as krypton has six isotopes and xenon has nine.

2.2.2.2 Polyatomic ions

The plasma contains large populations of neutral species and ions of plasma gas and of matrix species. These highly abundant species may react with each other or with other species to form polyatomic ions that interfere with the ions of interest. These species typically include argon, hydrogen, and oxygen; these atoms are often present at concentrations as high as 10^8 times those of a trace analyte at about the 1 ppb level (Date and Gray, 1989). Examples of such interfering species include ArO (coinciding with ^{56}Fe), ArH (coinciding with ^{41}K), NaAr (overlapping with ^{63}Cu), and ClO (overlapping

with ^{51}V). Reaction rates between these species are typically very low under ambient conditions; both the abundance of the atoms comprising polyatomic species and the intense temperatures of the plasma contribute to their formation.

Major elements present in the sample or in reagents used in sample preparation and preservation may also react to form abundant polyatomic species. Examples of reagent-based polyatomic interferences include nitrogen species from nitric acid (*e.g.*, NO at ^{30}Si), chloride species from hydrochloric acid (*e.g.*, LiCl at ^{42}Ca), and sulfur species from sulfuric acid (*e.g.*, SS at ^{65}Cu). Nitric acid (HNO_3) is generally chosen for the acidification of natural water samples because it produces fewer polyatomic interferences than other acids (see for example Date and Gray, 1989, or Jarvis *et al.*, 1992; see also Section 2.3.1).

For some of these overlaps, corrections can be made. For example, it is possible to measure intensities at masses 51, 52, and 53 to correct for ClO interferences with V:

$$^{51}M = {}^{51}V + {}^{51}ClO$$

$$^{52}M = 0.8376\ Cr + 0.00029\ ClO$$

$$^{53}M = 0.0955\ Cr + 0.2432\ ClO$$

$$\text{so that } {}^{51}V = {}^{51}M - 3.1086\ {}^{53}M + 0.3544\ {}^{52}M.$$

By measuring a reagent blank and subtracting the intensity for the blank from the intensity measured for a given element at the same m/z, a correction may also be made. Generating calibration curves from standards that are made up in the same matrix as the samples to be analyzed can also help to overcome this problem. This is only reasonable if the intensity of the interfering polyatomic species is small compared to the intensity of the

analyte; otherwise, significant error may occur due to the noise on the signal of the peak which is subtracted. Additionally, work by Jarvis *et al.* (1992) has suggested that polyatomic gas peaks are less stable than analyte ions peaks, introducing additional sources of error in making corrections. To a certain extent, the formation of these species, particularly oxide species, can be minimized by adjusting the operating parameters of the instrument. The temperature of the spray chamber can be maintained near freezing, for example, to promote the condensation of water vapor arising from the dissociation of the sample, thereby minimizing the formation of oxide and hydride species.

2.2.2.3 Refractory oxide species

Refractory oxide species result either from the incomplete dissociation of the sample matrix or from recombination of elements as the plasma cools (Jarvis *et al.*, 1992). These species cause interferences 16, 32, and 48 mass units above the ion with which an oxide is formed; a peak from an ion M^+ will form the interfering species MO^+, MO^{2+}, and MO^{3+}. The levels of oxides expected from the analysis of a given matrix can be predicted from the monoxide bond strength and concentration of the element concerned (Jarvis *et al.*, 1992). Cerium seems to form oxides most readily, although oxide levels observed for Ce using the Hewlett Packard 4500 ICP-MS are generally below 1%. Other light rare earth elements (LREEs) may form oxides that interfere with the measurement of the heavy rare earth elements (HREEs), but this is generally only a problem in solutions with very high concentrations of rare earth elements. As with the other interferences, operating conditions, particularly nebulizer flow rate and carrier gas

flow rate, can be adjusted to minimize the formation of oxide ions in the plasma. With the exception of MoO (causing an interference with ^{111}Cd), these refractory oxides are generally not problematic in natural water samples. A correction can be made for the interference of MoO with ^{111}Cd as follows:

$$^{111}M = {}^{111}Cd + 0.15886\ MoO$$

$$^{108}M = 0.0088\ Cd + 0.14805\ MoO$$

$$^{106}M = 0.0122\ Cd$$

so that $^{111}Cd = {}^{111}M + 0.77398\ {}^{106}M - 1.0730\ {}^{108}M$.

2.2.2.4 Doubly-charged ions

Most of the ions produced in the plasma are singly-charged; some multiply-charged species may also occur, particularly for elements that have low second ionization potentials or are particularly abundant in the plasma. (See Table 2.1 for the first and second ionization energies of the elements.) Only elements with a second ionization energy smaller than the first ionization energy of argon will experience significant double ionization. The elements most likely to form interfering doubly-charged ions are the alkaline earths, some transition metals, and the rare earth elements (Jarvis *et al.*, 1992). Although some loss of signal occurs for the doubly-charged species, a more serious problem is the overlap caused at half the mass of the parent element. An example of this is the doubly-charged species formed by ^{138}Ba; barium is generally abundant enough in natural samples that the formation of $^{138}Ba^{2+}$ does not affect the quantitation of barium, but the overlap with ^{69}Ga, a less abundant element, can be significant. Corrections for this interference are difficult, as Ba^{2+} species also experience overlaps with several

isotopes of the transition metals, which may also be abundant in natural waters. In general, manipulation of operating conditions, particularly the nebulizer gas flow rate and plasma temperature, can minimize the formation of doubly-charged species.

2.2.2.5 Suppression and enhancement effects

Both signal suppression and enhancement have been observed for analytes in samples containing high levels of certain elements. Often, results for different instruments or different operating conditions have varied significantly. One of the earliest studies demonstrated signal suppression for cobalt in a NaCl matrix; suppression was observed for NaCl concentrations above about 10^{-3} mol l^{-1} (Olivares and Houk, 1986). Beauchemin *et al.* (1987) observed signal enhancement from some elements (including sodium, magnesium, potassium, calcium, and cesium) and suppression for others (including boron, aluminum, and uranium). Thompson and Houk (1987) concluded that analyte signals were generally suppressed by concomitant or matrix elements under all conditions tested; these conditions included variations in gas flow rates, RF power, nebulizers, and ion lens voltages. In general, the noise on the signal is higher when high concentrations of matrix ions are present. A number of explanations for the observed phenomena have been proposed and the issue is not fully resolved.

In practice, it is important to recognize that suppression or enhancement effects are likely to occur when samples containing high concentrations (about 1 ppm or higher) of non-analyte elements are analyzed. In general, lower mass analytes and those with lower degrees of ionization in the plasma are likely to experience this effect to a greater degree (Jarvis *et al.*, 1992). A number of strategies can be employed to overcome

difficulties caused by this effect, including: sample dilution to a degree sufficient to bring the concentration of matrix ions to lower levels; use of internal standards, with careful matching of mass and ionization energy; instrumental optimization; matrix matching of standards and samples; and ion exchange, precipitation, or other separation techniques to remove the high concentrations of matrix ions and to concentrate the analyte element(s). These techniques are discussed in greater detail in Section 2.2.4.

2.2.2.6 High dissolved solids concentrations

ICP-MS analysis of samples containing high concentrations of dissolved solids is subject to a number of difficulties. In addition to the matrix suppression and enhancement effects noted in Section 2.2.2.5, a number of physical effects may occur. These include blockages of the cones, significant downward drift of the signal, and viscosity effects. Blockage of the cones occurs when the dissolved solids in the sample precipitate onto the cones, progressively blocking the small orifices in the cones. Signal drift results both from cone blockage and from "seasoning" of the instrument, probably a stabilizing of the ion extraction process as temperatures and pressures within the instrument stabilize. Viscous effects may occur because samples containing high concentrations of dissolved solids are generally more viscous than standards or rinse solutions; variable sample introduction rates and carryover (or memory) effects, where high concentrations of solids or analyte can "tail" from one sample into the next, can result. Cone blockage can be minimized by diluting samples, and drift effects caused by cone blockage can be minimized by seasoning the cones by aspirating solutions containing high concentrations of dissolved solids prior to sample analysis. Seasoning

the cones in this way also stabilizes the ion extraction process, further minimizing drift. Tuning the instrument to predetermined values, established by tests using solutions containing high concentrations of dissolved solids, also minimizes drift. Such tuning includes setting the sample depth (the distance from the end of the torch to the sampler) to maximize the temperature of the sampler and setting the extraction lens voltages to values which stabilize the ion extraction process and minimize drift. Finally, use of internal standards and an external drift correction procedure can also improve the results obtained for samples containing high concentrations of dissolved solids. Even with these strategies, analysis of samples containing high concentrations of dissolved solids is difficult; additional details on the methods chosen for analyzing such samples for this work are included in Section 2.2.4.

2.2.3 Analysis procedures

Samples analyzed on the ICP-MS included freshwater, brackish water, and fully saline ocean water samples. Because thousands of samples are required for a study such as reported here, sample handling was minimized. Almost no sample pretreatment was conducted. Analysis was conducted quantitatively for forty-one elements. Most of these elements could be measured accurately and reproducibly; a few of them, however, were problematic and are discussed in greater detail below in Section 2.2.3.4. Analysis procedures involved calibration with external standards, use of internal standards, and use of samples of known concentration analyzed every five samples. Additionally, every tenth sample was reanalyzed during a separate "run" and concentration values were

compared to those obtained from the previous run. Most of the sample data presented in this thesis were obtained using the Hewlett Packard 4500 ICP-MS. The analysis procedures described below are those used with this instrument. Variations in analysis procedures for the Perkin Elmer instrument are noted where significant.

2.2.3.1 Instrument optimization

Prior to an analysis run, various components of the ICP-MS instrument were cleaned to minimize sample carryover from the previous run. The sampler and skimmer cones were removed and cleaned with 1% nitric acid; the chamber in between the cones and the interface between the skimmer and the analysis region were also cleaned with nitric acid and ultrapure (18 MΩ-cm) water. The quartz spray chamber, connector pieces, and torch were rinsed with deionized water and dried. Tubings were changed periodically (generally every second or third run) to minimize sample carryover from the sample introduction system. The instrument was then reassembled and started. After one hour of warm-up time, temperatures and operating pressures had stabilized, and the instrument parameters were fine-tuned to optimize performance.

The instrument was tuned using a tuning solution containing 10 ppb each of Li, Y, Ce, and Tl. Sensitivity (signal intensity and stability) was optimized by changing the sample depth (the distance from the end of the torch to the tip of the sampler cone) and by changing the voltages applied to the electron multiplier, the extraction lenses, and the Einzel lenses. Background signal caused by electrical noise within the instrument was minimized by adjusting the discriminator voltage. The occurrence of doubly-charged ions was minimized by changing the sample depth, carrier gas flow rate, and the RF

power; Ce^{2+} was used as the indicator ion by measuring the ratio of Ce^{2+}/Ce^{+}, or m/z 70 to m/z 140. Similarly, oxide species were minimized by varying the same parameters and by monitoring the ratio of CeO^{+}/Ce^{+}, or m/z 156 to m/z 140. Ce was chosen for both of these optimization steps because it has a very low second ionization potential (see Table 2.1) and readily forms both Ce^{2+} and CeO (see also Date and Gray, 1989, p. 26). The resolution and mass axis were adjusted by varying the AMU gain and AMU offset (both of which adjust the peak width), the axis gain and axis offset (to adjust the mass calibration), and the plate and pole bias (which refocus the ion beam and control the speed of the ions entering the analyzer region). Finally, the transition from pulse-to-analog counting was optimized by using an automated routine which adjusted the last dynode voltage and the pulse-to-analog adjustment factors.

Typically, the sensitivity after optimization was better than 8,000 counts per second [cps]/ppb Li and better than 12,000 cps/ppb Y, Ce, and Tl. The relative standard deviation on the signal (a measure of the noise of the signal) was generally less than 3%. The ratio of Ce^{2+}/Ce^{+} was typically about 2%, and the ratio of CeO/Ce was less than 1%. Background counts due to electronic noise were usually less than 5 counts per second at all masses.

Many of the operational parameters on the Perkin Elmer Elan 5000 ICP-MS must be adjusted manually rather than through a computer interface; these parameters were seldom adjusted when using the Perkin Elmer instrument. Accordingly, the sensitivity of this instrument was not as high, and the levels of interferences were not as low as with the Hewlett Packard instrument.

2.2.3.2 Calibration

After tuning, external calibration standards were analyzed and calibration curves were generated using weighted linear curve fits. Internal standards were used during the analysis of all standards and samples. For each point in a calibration curve, 5 replicates of 300 milliseconds each (for low concentration elements) or 100 milliseconds each (for high concentration elements) were used to compute the average intensity and the standard deviation of the intensity. Because the standard deviation, or count error, is generally greater for higher concentrations than for lower concentrations, a weighted regression was used to weight more heavily concentrations that had smaller standard deviations. Weighted curves will pass more closely to points having lower errors than points having higher errors. Calibration equations were taken from Miller and Miller (1988). The weight of each point was calculated as:

$$w_i = \frac{S_i^{-2}}{(\sum_i S_i^{-2} / n)}$$

where S_i = standard deviation of each point

and n = number of points.

Internal standards were used to divide the counts for each data point in the calibration curve by the ratio of the counts to the concentration of the internal standard, as follows:

$$y = y_o / y_i / x_i \qquad (y = y_o / y_i \text{ if } x_i = 0)$$

where x_i = concentration of internal standard

y_i = counts of internal standard

y_o = count of sample or standard.

A weighted linear calibration curve of the form $y = ax + b$ was generated using the following formulae for the coefficients a and b:

$$a = \frac{n(\sum_i x_i y_i w_i) - (\sum_i x_i w_i)(\sum_i y_i w_i)}{n(\sum_i x_i^2 w_i) - (\sum_i x_i w_i)^2}$$

$$b = \frac{\sum_i y_i w_i}{n} - a\frac{\sum_i x_i w_i}{n}.$$

The concentration in a sample is computed using the coefficients generated from the calibration as:

$$x = \frac{y - b}{a}.$$

The standard deviation on this concentration is computed as

$$SD = \frac{S_{(y/x)w}}{a}\left[\frac{1}{w_o} + \frac{1}{n} + \frac{(y_o - \bar{y}_w)^2}{a^2(\sum_i w_i x_i^2 - n\bar{x}_w^2)}\right]^{1/2}$$

where n = number of data points in the calibration curve

y_o = measured y (intensity) of the sample

$\bar{y}_w$ = average of y_w in the calibration curve $(\sum_i w_i y_i / n)$

$\bar{x}_w$ = average of x_w in the calibration curve $(\sum_i w_i x_i / n)$

w_o = weight for y_o $(w_o = S_o^{-2} / \sum_i S_i^{-2} / n)$

where S_o = standard deviation of y_o

$$S_{(y/x)w} = \left[\frac{(\sum_i w_i y_i^2 - n\bar{y}_w^2) - a^2(\sum_i w_i x_i^2 - n\bar{x}_w^2)}{n-2} \right]^{1/2}$$

Three sets of calibration standards were used as described in Table 2.2. The computer interfaced to the ICP-MS instrument generated the calibration curves after all standards were analyzed, and the curves were viewed individually and edited (points selectively deleted) as necessary. Data points at the high end of the calibration curve were deleted when concentrations in samples were expected to be significantly lower than the highest calibration values, *e.g.*, calibration points of 100 ppb were deleted for the rare earth elements when the highest concentration in the sample was known to be below 10 ppb. Data points at the low end of the curve were deleted when concentrations in samples were significantly higher than the lower values, *e.g.*, calibration points of 10 ppb or lower were deleted for Na, Mg, and Ca, as sample concentrations were generally 1,000 ppb or higher.

Table 2.2
Calibration solutions used for ICP-MS analysis

Solution	Matrix	Concentration range	Elements
Nitric acid-soluble elements	2% HNO_3	0.1 ppb - 10,000 ppb	Li, Na, Mg, K, Ca, Rb, Sr, Cs, Ba
		0.01 ppb - 1000 ppb	V, Cr, Mn, Fe, Co, Ni, Cu, Zn, Cd
		0.001 ppb - 100 ppb	Sc, Ga, Y, La, Ce, Pr, Nd, Sm, Eu, Gd, Tb, Dy, Ho, Er, Yb, Lu, Th, U
Hydrochloric acid-soluble elements	2% HCl	0.001 ppb - 100 ppb	B, Si, Mo
Water-soluble elements	Ultrapure water	0.001 ppb - 10 ppb	Br, I

An internal standard solution containing Be, In, and Tl was pumped into the ICP-MS using a peristaltic pump with small-diameter Tygon tubing. Larger diameter tubing was used for sample introduction with the same peristaltic pump. The ratio of sample flow rate to internal standard flow rate was about 50:1, and final concentrations of internal standard elements after mixing with sample were roughly 10 ppb. Ideally, internal standards are chosen to have mass and first ionization potential similar to the elements measured in a sample; they also must be present in negligible concentrations in the samples themselves. In and Tl both have masses suitable for measuring mid-mass and high-mass elements, and both have ionization potentials (5.785 eV and 6.106 eV, respectively) similar to those of the mid- and high-mass elements measured. Be, with a high first ionization potential of 9.320 eV, is a less obvious choice for use as an internal standard. It was chosen because Sc, the other choice for a low-mass internal standard, experiences significant interferences (false signals) from ions present in saline samples. Extensive testing demonstrated that the signals of all three internal standard elements chosen (Be, In, and Tl) were strong and stable.

Check standards were used to adjust for any residual variation in plasma parameters that could not be corrected by the use of internal standards; this correction procedure is described in greater detail below. Check standards contained known concentrations of all elements in the standards containing nitric acid. A typical check standard composition would be 100 ppb each of the alkali metals and alkaline earth elements, 10 ppb of the transition metals, and 1 ppb of the rare earth elements and uranium.

2.2.3.3 Sample analysis and data handling

After instrument calibration, samples and check standards were analyzed. As with standard solutions, both samples and check standards were analyzed using 5 replicates of 300 milliseconds or 100 milliseconds each. Internal standards were used with both samples and check standards, as described above. Check standards were analyzed every five samples. Particulate matter in samples was allowed to settle to the bottom of the sample container, and the autosampler probe was adjusted so that it was above this level. Field blanks, collected as described in Section 2.3.3, were diluted to a strength of 2% nitric acid in the laboratory using ultrapure water and analyzed in the same manner as samples. After each sample or check standard, the autosampler probe traveled to a flow-through rinse port supplied with ultrapure water, to a redistilled nitric acid (5%) rinse solution, back to the rinse port, and finally to the next sample. The probe was inserted fully into the flow-through rinse port, rinsing both the outside of the probe and the sample uptake tubing; the probe tip remained in the nitric acid rinse solution for 90 seconds, allowing a thorough rinsing of the uptake tubing with a solution slightly more acidic than the sample. This procedure served to minimize sample carryover in the tubing and to maintain a clean rinse solution.

The intensity and standard deviation measured for each element were recorded by the computer, which then converted this information to a concentration and a standard deviation using the equations given above. This information was written to the data file for each sample and to an analysis database, which also contained information about the sample, including the sample name, the data file name, the sample location, the sample

collection date, and the analysis date. The analysis database was copied as an Excel spreadsheet file, and these data were further manipulated to correct for instrumental drift and sample dilution and to subtract blank concentrations.

The check standards were used to compute a correction factor directly for most elements. The correction factor was computed by dividing the measured concentration for an element by the known concentration of that element in the check standard solution. Between check standards, correction factors were computed by linear interpolation. For each sample, a corrected concentration and standard deviation were obtained by dividing the measured concentration and standard deviation by the correction factor computed for that sample. For elements not measured directly in the check standard solutions (including boron, silicon, and molybdenum), composite correction factors were obtained by averaging the correction factors known for other elements. Correction factors were generally very near one (for most elements, ranging from 0.95 to 1.05). Elements that were more difficult to measure (including some of the transition elements and lithium, as discussed in greater detail below) were not included in the composite drift factor calculation. Finally, every tenth sample was reanalyzed during a separate run and after a separate tuning and calibration procedure was conducted. These results were then corrected for instrumental drift and compared to the results for those samples from the previous run. If agreement was good (generally less than a 10% difference for most elements), the results from the previous day's run were used; if agreement was poor, the entire sample analysis procedure was repeated.

After drift correction and comparison with reanalyzed samples, blank concentrations were subtracted from sample concentrations. Elevated blank concentrations, when they occurred, may have been caused by contamination in the field or in the laboratory or by interferences within the plasma; in any case, it was assumed that such contamination or interferences were the same for both blanks and samples. Standard deviations were computed as the square root of the sum of the squares of the standard deviations of the sample and the blank ($\sigma^2_{final} = \sigma^2_{measured} + \sigma^2_{blank}$). Finally, both the concentration and standard deviation of samples that had been diluted were multiplied by the dilution factor to obtain final results. Both the concentration and the standard deviation from each sample were then recorded in a database containing all sample information (called the project database) along with sample identification information, including the sample identifier, sample location, sample date, analysis date, analysis method, spreadsheet used for drift correction, dilution factor, and any special observations or comments. Results from field blanks were also recorded.

2.2.3.4 Problematic elements

During certain times of the year, concentrations of major ions at several locations within the brackish waters of the Delta were too high to be measured directly. These samples were diluted 10:1, 100:1, or 200:1, as appropriate, and reanalyzed for these major ions, including Na, Mg, K, and Ca. After dilution, concentrations of all elements except Na were within the range of standards. In the most saline samples, concentrations of Na were slightly higher than the concentration in the highest standard, but tests confirmed that the calibration curves were linear even at higher concentrations. Also, further

dilution would introduce additional error from the dilution procedure, so 200:1 was chosen as the maximum dilution. Both internal standards and check standards were used as described above, and results were multiplied by the applicable dilution factor; results were then entered into the project database.

Measurement of Li was also difficult with the Hewlett Packard 4500 ICP-MS. Because of the low mass of Li and the sharp angle on the sampler and skimmer cones, Li tended to scatter more in the plasma and build up on the analyzer (back) side of the cones. After measurement of samples or standards containing high concentrations of Li, the residual Li "bled" off the cones and caused falsely elevated concentrations of Li in subsequent samples. As cones aged, the cone surfaces became more pitted and rough, and the problem became more pronounced. The solution adopted for all samples collected after August 1, 1996, was to substitute clean, new cones for the cones used for general analysis. Analysis was then performed for Li alone by calibrating the instrument only to a Li concentration just higher than the highest concentration expected in samples. Samples were then analyzed for Li, again employing both an internal standard (Be) and check standards, and drift corrections were made. The corrected concentrations were then recorded in the project database. This solution seemed to minimize Li carryover, and concentrations obtained in this manner were highly reproducible and exhibited very little noise.

Measurements of Ca were less reproducible than measurements of other elements. When results from the original run were compared to results from a subsequent run, concentrations often varied by as much as 20% (compare to the maximum 10% variation

for other elements), even when concentrations for other elements were highly reproducible. These variations are likely due to the fact that Ca must be measured at a very minor isotope, ^{43}Ca, which accounts for only 0.14% of the natural abundance of calcium. The major isotopes of Ca are ^{40}Ca and ^{44}Ca (96.9% and 2.1% of the natural abundance, respectively), which suffer from significant interferences from ^{40}Ar (the main component of the plasma) and $^{12}C^{16}O_2$, respectively. The result of quantifying Ca using such a minor isotope is that small errors in the count rate at m/z 43 can cause larger errors in the extrapolated concentration of Ca.

Concentrations of the transition elements were also difficult to obtain using the Hewlett Packard 4500 ICP-MS for a variety of reasons. Because this instrument is located neither in a clean room facility nor in a clean laboratory, dust and lint built up within the instrument very quickly after installation. Argon gas cylinders, located immediately adjacent to the instrument, released metal dust each time the gas supply was changed from one cylinder to the next. The sampler cone was constructed of copper and nickel, and the skimmer cone was composed of nickel; these construction materials may also contribute to the problem of quantifying low concentrations of these transition elements. Finally, very clean sampling conditions are required to accurately measure many of these elements, and these conditions did not exist during the Delta sampling; concentrations of several of these elements in field blanks collected from autosamplers were near sample concentrations in the Delta. Despite these conditions, concentrations of a few of the transition metals could be quantified accurately at levels present in freshwater samples from the Delta; these elements included V, Mn, Co, and Zn. In

brackish waters, interferences caused by major ions are more severe, and measurement of any of the transition elements is more difficult (see Section 2.2.2, Section 2.2.3.5, and Appendix C for additional detail).

2.2.3.5 Confirmation of measurements

Standard addition testing was conducted to confirm the ability of ICP-MS to measure accurately the concentrations of many elements in samples collected from the Delta. Samples collected from coastal waters near Oahu, Hawai'i, were treated separately, and measurement of fully saline samples is discussed in Section 2.3 below.

Samples of several hundred milliliters were collected from each of the three end member water sources in the Delta; each was acidified to 2% nitric acid and divided into multiple subsamples. Each subsample was then spiked with a small volume of standard solution, and each spiked sample was then analyzed. For elements present in very high concentrations, *e.g.*, Na, Mg, K, and Ca, samples were diluted either 10:1 (for Sacramento River and San Joaquin River waters) or 100:1 or 200:1 (for Bay water) and then spiked. This was necessary because undiluted sample concentrations were too near the concentrations of the spiking solutions.

The expected concentration of each subsample was computed from the measured concentration of an unspiked subsample and the known volume and concentration of the standard solution added. This expected concentration was then plotted against the measured concentration to judge the accuracy of measurement of the ICP-MS technique. A straight regression line was fit through the plotted points and forced through an intercept of zero. The R^2 correlation coefficient and the slope of each line were

computed; results for each element measured quantitatively are included as plots in Appendix C. In addition, the correlation coefficient, slope, and relative standard deviation (RSD) for each sample are tabulated in Tables 2.2, 2.3, and 2.4 below. In general, elements that can be measured accurately show high R^2 correlation coefficients, slopes of near 1.00, and low RSDs. Values falling outside specified ranges are in boldface for emphasis. These values are: $R^2 < 0.9900$, slope < 0.95 or slope > 1.05, and RSD $> 10\%$. Where values fall outside these ranges, possible reasons are given in the tables and further discussed below.

Results of standard addition testing for Sacramento River water collected at Locke are summarized in Table 2.3. Because it has lower concentrations of major elements than the other two Delta water endmembers (see Chapter 3), analysis of Sacramento River water should suffer from fewer matrix interferences. Indeed, correlation coefficients and best-fit line slopes are very near 1.000 for most elements measured. Elements that are difficult to quantify include Mn, Fe, Cu, and Zn; difficulties could result from interferences and matrix effects but are most likely due to contamination problems. These problems are discussed in greater detail in Section 2.2.3.4. Because concentrations of several of the heavier rare earth elements are present near detection limits, these elements suffer from high RSDs. Further, thorium has a very high particle affinity and spiked concentrations are lower than expected values; this also indicates that thorium concentrations may change in stored samples. In general, the concentrations of most elements can be measured accurately and highly reproducibly.

Table 2.3
Standard addition testing for Sacramento River water
Sample collected at Locke on August 1, 1996

Element	R^2 correlation coefficient	Slope of best-fit regression line	RSD on unspiked sample [%]	Likely cause
Li	0.9991	0.9912	1.92	
B	0.9995	1.0090	4.16	
Na	0.9948	**1.0583**	1.44	matrix effects
Mg	0.9997	0.9796	0.84	
Si	**0.9327**	0.9813	0.46	NN, low ionization potential
K	0.9992	**1.0892**	2.74	ArH, NaO
Ca	0.9997	1.0024	1.11	
V	0.9990	0.982	2.71	
Cr	0.9996	0.9866	5.80	
Mn	**0.8788**	**1.0618**	0.81	KO, NAr
Fe	0.9980	0.9598	0.59	ArO, NAr
Co	0.9999	0.9952	3.20	NaAr, MgCl
Ni	0.9995	1.0275	1.94	
Cu63	**0.9841**	**1.2076**	3.03	NaAr, MgCl, contamination
Cu65	**0.9802**	**1.2367**	7.63	MgAr, contamination
Zn	0.9958	**1.2068**	4.10	MgAr, contamination
Ga	0.9995	0.9973	2.44	
Rb	1.0000	0.9925	3.29	
Sr	0.9998	1.0012	0.59	
Y	0.9995	1.0138	2.20	
Mo	0.9969	1.0074	4.15	
Cd	0.9997	0.9937	**11.09**	near detection limit
Cs	1.0000	0.9984	**11.05**	near detection limit
Ba	0.9997	1.0031	0.40	
La	0.9998	1.0251	4.70	
Ce	0.9988	1.0211	2.69	
Pr	0.9997	0.9937	4.58	
Nd	0.9954	1.0022	3.74	
Sm	0.9991	1.0123	7.47	
Eu	0.9999	1.0224	**14.24**	near detection limit
Gd	0.9992	0.9757	**15.90**	near detection limit
Tb	0.9989	0.9980	**18.09**	near detection limit
Dy	0.9987	1.0270	9.08	
Ho	0.9998	1.0214	**18.74**	near detection limit

Table 2.3
Standard addition testing for Sacramento River water
Sample collected at Locke on August 1, 1996

Element	R^2 correlation coefficient	Slope of best-fit regression line	RSD on unspiked sample [%]	Likely cause
Er	0.9996	1.0173	**57.05**	near detection limit
Yb	0.9997	1.0201	**15.99**	near detection limit
Lu	0.9990	1.0093	**32.22**	near detection limit
Th	0.9960	**0.7195**	**14.93**	near detection limit, low solubility
U	0.9999	0.9925	2.52	

Table 2.4 contains a summary of results from standard addition testing of San Joaquin River water. In general, these results are poorer than results from Sacramento River water. Still, by the criteria presented above, most elements can be measured accurately. As with Sacramento River water, quantitation of transition elements is poor, likely due to contamination and saline interferences. Also, concentrations of several of the HREEs are near detection limits, so RSDs are above acceptable values. Interestingly, potassium apparently cannot be measured accurately in this river water; this is likely due to the high concentrations of Na present in this river water. Sodium may form NaO in the plasma, creating an even larger background signal than is present from the interferent ArH alone. Finally, although the R^2 correlation coefficients of B, Mo, and U are below 0.9900, the slope of the best-fit regression lines are very near 1.000; because concentrations of these elements are significantly higher in this water than in Sacramento River water and Bay water, these results are used. See Chapter 3 for more details.

Table 2.4
Standard addition testing for San Joaquin River water
Sample collected at Mossdale Landing on August 1, 1996

Element	R^2 correlation coefficient	Slope of best-fit regression line	RSD on unspiked sample [%]	Likely interferences
Li	0.9932	1.0064	1.29	
B	**0.9786**	1.0059	2.38	C
Na	**0.9689**	1.0085	1.60	matrix effects
Mg	0.9987	0.9980	1.34	
Si	**0.9259**	0.9854	1.82	matrix effects, low ionization potential
K	0.9976	**1.2519**	1.99	NaO, ArH
Ca	0.9971	1.0060	1.67	
V	0.9958	0.9844	2.69	
Cr	0.9995	1.0184	**11.72**	ArO, Mg_2,ClO, contamination
Mn	0.9977	**1.0556**	2.04	KO, NAr
Fe	**0.9864**	0.9871	2.33	ArO, NAr
Co	0.9984	0.9922	1.96	
Ni	0.9983	0.9911	2.53	
Cu63	**0.9854**	1.0304	2.43	NaAr, MgCl, contamination
Cu65	**0.9881**	0.9878	2.05	MgAr, contamination
Zn	0.9957	1.0002	2.00	
Ga	0.9984	1.0138	1.74	
Rb	0.9998	0.9930	1.79	
Sr	0.9930	0.9893	2.07	
Y	0.9998	1.0473	2.50	
Mo	**0.9867**	0.9676	2.72	
Cd	0.9988	1.0166	**23.06**	near detection limit, contamination
Cs	0.9999	0.9795	3.35	near detection limit
Ba	0.9983	1.0033	2.10	
La	0.9997	1.0092	1.12	
Ce	0.9997	0.9991	1.71	
Pr	0.9998	1.0127	1.96	
Nd	0.9998	1.0105	1.26	
Sm	0.9994	1.0068	1.52	
Eu	0.9998	1.0275	3.44	

Table 2.4
Standard addition testing for San Joaquin River water
Sample collected at Mossdale Landing on August 1, 1996

Element	R^2 correlation coefficient	Slope of best-fit regression line	RSD on unspiked sample [%]	Likely interferences
Gd	0.9997	1.0176	3.45	
Tb	0.9991	1.0384	3.69	
Dy	0.9994	1.0213	2.36	
Ho	0.9996	1.0370	1.29	
Er	0.9996	1.0175	3.52	
Yb	0.9998	1.0299	3.19	
Lu	1.0000	1.0094	6.13	
Th	**0.9784**	**0.7125**	2.07	near detection limit, low solubility
U	**0.9617**	1.0143	1.95	matrix effects

Table 2.5 shows the results of standard addition testing for water collected from Martinez on December 18, 1996. In this sample, concentrations of many elements can be measured quite accurately. Those that cannot be measured accurately include K, the transition metals, Ce, and Th. This sample represents a mid-salinity sample from this site; results from a more saline sample are shown in Table 2.5. For this grab sample, concentrations of several high concentration components of seawater were: Li (37 ppb), B (356 ppb), Na (1,000 ppm), Mg (112 ppm), and Sr (674 ppb). By comparison, the concentrations of these elements a composite sample collected from this site on October 27, are: Li (111 ppb), B (1,680 ppb), Na (4,600 ppm), Mg (600 ppm), and Sr (3,710 ppb); this sample is among the most saline collected from this location. Although samples collected at this site are generally a mixture of waters from the Pacific Ocean, the Sacramento River, and the San Joaquin River, it is useful to compare these concentrations to those found in "average" world seawater. Concentrations of these elements in

seawater are: Li (178 ppb), B (4,600 ppb), Na (11,000 ppm), Mg (1,330 ppm), and Sr (8,000 ppb) (see for example Bruland, 1983). Thus, the sample represented in Table 2.5 is roughly 10% as saline as seawater, while the saltiest samples collected at this location are about 40% as saline as seawater. Standard addition testing was not performed for samples less saline than the sample of moderate salinity shown in Table 2.5, as these samples are composed largely of San Joaquin and Sacramento River waters, and results should be similar to those shown in Tables 2.3 and 2.4.

As shown in Table 2.5, quantitation of the transition elements is poor. Although contamination is probable, interferences caused by chloride species and species containing major ions become more prominent in these brackish waters. These interferences are the most likely causes of poor quantitation. As with San Joaquin River water, high concentrations of Na, which may form NaO in the plasma, are probably the cause of poor quantitation for K. Results for B are significantly better than in San Joaquin River water, while results for Mo and U are comparable.

Table 2.5
Standard addition testing for water from Carquinez Strait
Sample collected at Martinez on December 18, 1996 (moderate salinity)

Element	R^2 correlation coefficient	Slope of best-fit regression line	RSD on unspiked sample [%]	Likely interferences
Li	0.9975	1.0167	3.00	
B	0.9927	1.0005	2.38	
Na				
Mg	**0.9897**	0.9800	1.71	
Si	0.9931	0.9701	0.94	
K	0.9731	**1.0956**	1.97	matrix effects, ArH, NaO
Ca	0.9934	1.0389	1.82	
V	**0.9832**	**1.1069**	1.94	NCl, ClO, Mg_2
Cr	**0.8180**	**1.0527**	2.55	ArO, Mg_2,ClO,

Table 2.5
Standard addition testing for water from Carquinez Strait
Sample collected at Martinez on December 18, 1996 (moderate salinity)

Element	R^2 correlation coefficient	Slope of best-fit regression line	RSD on unspiked sample [%]	Likely interferences
				contamination
Mn	0.9998	1.0429	1.62	
Fe	**0.9673**	0.9553	1.83	KO, CaO
Co	0.9958	**1.1324**	1.55	MgCl, NaAr
Ni	**0.9876**	0.9568	2.61	NaCl, MgCl
Cu63	**0.9104**	1.0279	1.53	NaAr, MgCl, contamination
Cu65	0.9956	**1.1983**	2.13	MgAr, contamination
Zn	**0.8371**	0.9687	2.06	MgAr, contamination
Ga	0.9949	0.9750	2.37	
Rb	0.9996	0.9985	0.24	
Sr	0.9900	0.9886	0.59	
Y	0.9902	0.9868	1.33	
Mo	**0.9824**	1.0224	3.66	BrO, CuCl, matrix effects
Cd	0.9983	**0.8634**	**19.64**	near detection limit, matrix effects
Cs	0.9999	1.0047	2.71	
Ba	0.9990	0.9984	1.30	
La	0.9967	1.0103	1.85	
Ce	**0.9860**	1.0122	1.08	MoAr, matrix effects
Pr	0.9991	1.0103	5.22	
Nd	0.9949	1.0237	1.46	
Sm	0.9971	1.0068	4.54	
Eu	0.9995	1.0196	4.22	
Gd	0.9998	1.0186	6.24	
Tb	0.9992	1.0276	**11.72**	NdO, near detection limit
Dy	0.9963	1.0058	5.92	
Ho	0.9985	1.0294	5.62	
Er	0.9937	1.0282	**13.34**	near detection limit
Yb	0.9965	1.0119	6.71	
Lu	0.9984	**1.0519**	**11.21**	near detection limit
Th	**0.9838**	**0.5046**	7.09	near detection limit, low solubility
U	0.9979	**1.0515**	1.70	matrix effects

Standard addition tests were performed for a sample collected on March 4, 1997 from San Pablo Bay at at Pinole, which is west of Martinez and Carquinez Strait. Unfortunately, all samples collected at Martinez for standard addition tests were collected during the ebb tide, and this sample is the most saline of all Bay samples collected for these tests. The concentrations of major ions in this sample were: Li (46.4 ppb), B (842 ppb), Na (1,900 ppm), Mg (222 ppm), and Sr (1,550 ppb); thus, the salinity of this sample was roughly half the salinity of the most saline samples collected at Martinez and twice that of the sample used to obtain the results in Table 2.5. Comparison of the results in Table 2.6 with those in Table 2.5 indicates that quantitation of transition elements deteriorates as sample salinity increases, while quantitation of major ions, B, Mo, and U remains good. This is largely as expected, particularly for those elements that are measured after sample dilution. Na, for example, is diluted 200:1 in the most saline samples; the diluted sample thus is brought within the range of calibration standards and has a major ion composition resembling that of freshwater samples.

Table 2.6
Standard addition testing for water from near Carquinez Strait
Sample collected at Pinole on March 4, 1997 (high salinity)

Element	R^2 correlation coefficient	Slope of best-fit regression line	RSD on unspiked sample [%]	Likely interferences
Li	0.9945	1.0383	1.841	
B	0.9957	0.9964	1.079	
Na	**0.9876**	1.0144	0.936	matrix effects
Mg	0.9989	0.9940	1.329	
Si	[a]	[a]	2.849	
K	0.9994	1.0054	1.397	matrix effects, ArH, NaO
Ca	0.9988	1.0324	1.105	
V	**0.9870**	**1.0981**	3.579	NCl, ClO, Mg_2
Cr	**0.9866**	**1.1188**	0.525	ArO, Mg_2,ClO,

Table 2.6
Standard addition testing for water from near Carquinez Strait
Sample collected at Pinole on March 4, 1997 (high salinity)

Element	R^2 correlation coefficient	Slope of best-fit regression line	RSD on unspiked sample [%]	Likely interferences
				contamination
Mn	**0.9482**	**1.0604**	2.723	OCl, NeCl, KO
Fe	[a]	[a]	3.561	
Co	0.9955	**1.0967**	3.079	MgCl, NeCl, NaAr
Ni	**0.9733**	**0.8701**	1.696	SiCl, MgAr
Cu63	**-0.1359**	**1.178**	3.837	NaAr, MgCl, contamination
Cu65	0.9912	**1.0608**	4.572	MgAr, contamination
Zn	**-0.0233**	**0.9422**	2.866	MgAr, contamination
Ga	**0.8517**	0.9504	2.670	SCl
Rb	0.9998	1.0233	0.797	
Sr	0.9998	0.9744	1.043	
Y	0.9984	**1.0520**	1.205	SrH, CrCl, FeCl
Mo	0.9963	0.9968	1.733	
Cd	**0.9677**	**0.7137**	**70.814**	near detection limit, matrix effects
Cs	0.9977	0.9787	7.731	
Ba	0.9998	0.9958	0.394	
La	0.9989	0.9913	2.440	
Ce	**0.9971**	0.9722	**11.369**	MoAr, matrix effects
Pr	0.9937	**0.9384**	3.946	CdCl, matrix effects
Nd	0.9974	0.9913	5.114	
Sm	0.9937	1.0174	7.484	
Eu	0.9995	0.9920	**10.126**	matrix effects
Gd	0.9991	0.9847	**14.361**	matrix effects
Tb	0.9967	0.9852	3.726	
Dy	0.9991	**1.0560**	5.994	XeCl, matrix effects
Ho	0.9992	0.9662	5.931	
Er	0.9826	**0.9205**	**14.659**	near detection limit
Yb	0.9972	0.9842	**10.420**	near detection limit
Lu	0.9987	0.9962	**20.037**	near detection limit
Th	**0.9795**	**0.7402**	**11.109**	near detection limit, low solubility
U	0.9989	0.9984	1.230	

[a] Standard addition testing was not performed for these elements.

2.2.4 Saltwater analysis

Many of the samples collected off the coast of Oahu were fully saline seawater samples (see Chapter 4). Because the analysis of saltwater samples using ICP-MS is much more difficult than the analysis of freshwater samples, research was conducted to determine the best method for analyzing these samples. Many of the major interferences presented in Section 2.2.2 are enhanced in highly saline samples, making accurate quantitation of many elements nearly impossible. For example, "physical" effects are enhanced, including the "salting up" of cones and lenses within the instrument, where salt from the sample precipitates as a solid. Detector saturation, which results when the detector is hit by too many ions and loses sensitivity, and viscosity differences between fresh and saltwater samples can both introduce errors. Chemical effects are enhanced because the saltwater matrix contains very high concentrations (part-per-thousand levels) of major ions. Additionally, concentrations of many elements in seawater are several orders of magnitude higher than in freshwater, and interferences from molecular ions formed from these major ions are much more abundant than in freshwater samples. Examples of these include chlorides (such as CaCl at ^{75}As, MgCl and NaCl at ^{60}Ni, and SrCl at ^{121}Sb), oxides (such as BO at ^{27}Al and NaO at ^{39}K), argides (such as BAr at ^{51}V, NaAr at ^{63}Cu, MgAr at ^{66}Zn, and SrAr at ^{127}I), and hydrides (such as CaH at ^{39}K and ^{45}Sc and SrH at ^{89}Y).

Several approaches can be taken to overcome the difficulties of analyzing seawater samples. Common to all approaches is the manipulation of the ICP-MS tuning parameters (specifically, the sample depth and the voltages applied to the extraction and

Einzel lenses) to minimize the interferences, instrumental drift, and "salting-up" effects of samples with high dissolved solids content. The approaches evaluated are detailed below.

2.2.4.1 Dilution to freshwater strength

Dilution of saltwater samples to the ionic strength of freshwater would reduce interferences to the manageable levels found in freshwater samples. This approach would require very significant dilution (to at least 1000:1), and trace signals would be lost. Also, such signficant dilution introduces the possibility of measurement error during dilution. This approach was eliminated for these reasons.

2.2.4.2 Use of standard addition

Standard addition is a process in which each collected sample is split into three separate aliquots for analysis. Two of these aliquots are spiked with known concentrations of the elements to be measured, and the third is analyzed without spiking. A calibration curve (a straight line) is plotted through the points generated by the spiked samples, and the concentration of the unspiked sample is determined from this calibration. This method of analysis is very accurate, as it corrects for the effects of high interferences by generating calibration curves that include matrix effects separately for each sample. This method is very time-consuming, requiring each sample to be analyzed multiple times for each element of interest. Although equipment to perform standard addition automatically at the input to the ICP-MS is available commercially, it is expensive and was not available at Caltech during this research. Time constraints prohibited the use of this method for all seawater samples collected near Oahu. The

potential of this method was tested by spiking "clean" background Hawai'i seawater collected in October 1995. Results are discussed in Section 2.2.4.4.

2.2.4.3 Use of sample pretreatment

Saltwater samples can be pretreated through ion exchange, which effectively removes the ions of interest and allows major ions present in high concentrations in seawater to flow through the column. The ions of interest are then removed ("eluted") from the column in a concentrated solution, which is then analyzed. To perform ion exchange, samples are treated with reagents to attain a prescribed pH and then pumped through a column containing an ion exchange resin (such as Chelex 100). Columns are then eluted by passing various reagents through the column, and the eluted liquid is captured and analyzed. This procedure has been used successfully to measure concentrations of several rare earth elements in seawater (see for example Möller *et al.*, 1992, or Beauchemin and Berman, 1989). Although this technique, like standard addition, yields highly accurate results, great care is required in the implementation of the ion exchange process. Columns and exchange resins must be meticulously cleaned prior to use, and all reagents must be of the highest quality to avoid impurities. Processing time and sample handling is extensive, introducing the possibility of human error. This technique is suited for the highly accurate quantitation of a small number of samples. It was eliminated as an option because of the cost, in terms of time and materials, and the large number of samples to be analyzed.

2.2.4.4 Partial dilution and matrix matching

The final option considered, and the option chosen for this research, involved some dilution coupled with the use of standards made up in a salty solution. For this option, samples were diluted just to the level that would decrease the level of "salting up" of cones and lenses in the ICP-MS to acceptable levels. Standards were created in a salty matrix in order to mimic the effect of the major ions in solution. Because samples could be diluted upon collection (minimizing sample handling) and because calibration curves would be generated from a series of external standards analyzed before samples (as in freshwater analysis), this was the most practical option for this research.

Development of the analysis method entailed first establishing standards and calibration curves using a variety of elements, then selecting those elements that exhibited minimal interference effects with salt water during ICP-MS measurement. Because Na^+ and Cl^- are the most abundant ions in seawater (see Table 2.7) and because some of the other major ions present in seawater were possibilities for use as tracers, solutions were created using only Na^+ and Cl^- as the major ions. The ionic strength was set to 0.06 M, approximately the same as in the 9.5:1 seawater samples to be analyzed. Finding sodium solutions or salts that did not contain impurities that would impair the analyses of other elements was the most difficult part of standard creation; the solution chosen was an ICP-MS standard solution (10,000 ppm) created from the purest NaOH available (purchased from Inorganic Ventures, Inc.). Ultrapure hydrochloric acid (Baker Ultrex II) was added to the standards to provide the chloride component.

Table 2.7
Major ions in seawater

Cation	Abundance (‰ w/w)	Anion	Abundance (‰ w/w)
Na^+	10.556	Cl^-	18.980
Mg^{2+}	1.272	SO_4^{2-}	2.649
Ca^{2+}	0.400	HCO_3^-	0.140
K^+	0.380	Br^-	0.065
Sr^{2+}	0.013	$H_2BO_3^-$	0.026
		F^-	0.001

Standard solutions were made up in the NaCl solution, but were otherwise as described in Section 2.2.3.2. Calibration curves were generated to determine the effect of impurities in the NaCl solution on the measurement of elements in this solution. Calibration curves were linear for almost all elements of interest; exceptions were silver and arsenic, which experience strong chloride interferences in the plasma.

Finally, standard addition testing was performed to address two issues: (1) to determine detection limits in salt water for this chosen method of analysis; and (2) to test the potential of standard addition as an alternative analysis method. "Clean" background Hawai'i seawater was diluted to 10:1, acidified to 2% HNO_3, and spiked with known concentrations of various elements. Results for each element were plotted on a log-log plot to show the results for several samples spiked with a single element on a single graph (see Appendix C). The "actual concentration" shown is the generally accepted seawater concentration (from the literature for clean seawater, see for example Bruland, 1983) plus the spike; the "measured concentration" is the concentration value determined by ICP-MS analysis using the method described above. The straight line on each plot is the line on

which points would fall if no major interferences or matrix effects occurred. Error bars on each point represent the standard deviation on the measurement (computed from five replicates).

Most elements analyzed in this manner show a distinctive behavior: the measured concentration is higher than actual concentrations for low spiked concentrations. This indicates that, for elements that exhibit this behavior, matrix effects are strong near seawater concentrations. Without pretreatment, accurate measurement of these elements at low concentrations would be difficult if not impossible. Concentrations could be determined using these elements if concentrations in samples were significantly above the points on the graphs where the measured and actual concentrations begin to merge. These tests demonstrate, however, that standard addition analysis would not be an accurate analysis technique in salt water for measuring the very low concentrations of most elements in clean seawater. (Note that concentrations of many of these trace elements are much lower in background seawater than in the waters collected from the Delta study area; for this reason, many of these "trace" elements can be determined quantitatively in Delta waters but not in seawater.) Elements that can be measured accurately in seawater samples diluted 9.5:1 include Rb, Sr, and U; these elements can also be measured accurately using external calibration. This analysis technique was used to analyze seawater samples for these elements and for high concentrations of the REEs (specifically, La, Pr, and Nd) in seawater samples containing a REE tracer. Results are presented in Chapter 4.

2.3 Sample collection and handling

2.3.1 Sample preservation and container preparation

All samples were acidified to 2% nitric acid (HNO_3) upon collection. Acidification lowers the pH of the sample to inhibit adsorption of metal ions and cationic species onto container surfaces. Acidification also helps to minimize the formation of many insoluble precipitates that form by the interaction of trace metals with other major constituents (Ward, 1989). Creed *et al.* (1995) found that acidification of drinking waters to a pH < 2 effectively stabilized metal concentrations for 180 days. Nitric acid was generally used for acidification because it produces fewer interferences during ICP-MS analysis than other acids; also, its use is compatible with the materials found within the ICP-MS itself, including sample introduction tubing and the sampler and skimmer cones. Finally, HNO_3 is less reactive with many of the elements in solution than other acids. For these reasons, its use is commonly accepted for the preservation of natural water samples analyzed using ICP-MS (see, for example, Benoit, 1994; Creed *et al.*, 1995; Taylor and Garbarino, 1988; Henshaw *et al.*, 1989; Stetzenbach *et al.*, 1994; Long and Martin, 1991).

For this research, two types of nitric acid were used. For single grab samples of 15 ml or less in volume, ultrapure nitric acid (double-distilled Baker Ultrex II) was used. For larger samples, such as those collected using autosamplers, redistilled instrument-grade nitric acid (Tracepur Plus by EM Science) was used. This acid contains significantly fewer impurities than reagent grade acid but is much less expensive than double-distilled acid. Samples were collected and spiked with acid as described below.

Samples were collected in 16-mm diameter Teflon or polypropylene sample containers. Most samples were collected in 10-ml Teflon (FEP) centrifuge tubes with Teflon caps, manufactured by the Nalge company. These sample containers were reused after thorough cleaning between uses. For approximately one month of samples collected in the Delta (see Chapter 3), 15-ml polypropylene centrifuge tubes manufactured by Corning were used; these containers were not reused. The Corning tubes were also used for analysis of calibration standards. All containers were cleaned in a solution of 10% HNO_3 (redistilled) at 60°C for a minimum of 24 hours. After soaking in the HNO_3 bath, containers were triple-rinsed with Caltech tap deionized water and single-rinsed with Milli-Q 18.2 MΩ-cm water. Containers were dried, capped, and stored in low density polyethylene (LDPE) ziplock bags until use. This cleaning procedure yielded clean blanks for samples collected in both types of tubes; data for blanks collected with samples are provided with sample data in Chapter 3.

2.3.2 Collection of fresh and brackish water grab samples

Freshwater grab samples were collected on various occasions throughout the Delta and along the Sacramento River, as well as from the streams and wastewater flow in the study area in Hawai'i. Brackish water grab samples were collected in the Delta. Samples were collected in pre-cleaned 10-ml Teflon sample containers that contained 287 µl of ultrapure 70% HNO_3 (Baker Ultrex II); the final concentration of HNO_3 upon addition of the sample was thus 2% v/v. At most locations, a large sample was collected in a Teflon beaker or LDPE plastic container that had been double-rinsed in the water to

be collected. Occasionally, sample containers were lowered into the water and allowed to fill. Because the mouth of the sample containers was small, the containers filled slowly and could be removed quickly without loss of the nitric acid initially inside. After collection, sample containers were capped and agitated to mix the sample thoroughly with the nitric acid.

Almost all freshwater and brackish water grab samples were collected by hand from just below the surface to minimize contamination by surface films or rainwater. Samples collected from a boat (almost all samples collected along the Sacramento River) were collected from the bow of the boat while the boat was traveling upriver. Samples collected from shore or from docks were collected at locations that were as far into the river as possible and after any disturbance of near-shore sediments had settled or been swept downstream. A few surface samples were collected with spring-loaded drop bottles lowered into the water, generally from a bridge. All samples collected from near the channel bottom were collected with a drop bottle that was lowered until a suspended weight struck bottom; a messenger weight was then released to "trip" the bottle shut. Sample containers were then filled after the container had been raised by opening a valve located near the bottom of the drop bottle. The drop bottle method of collection was used only where access to the river or stream was restricted.

2.3.3 Collection of fresh- and brackish water composite samples

At five locations within the Delta study area (see Chapter 3), daily composite samples were collected using autosamplers (ISCO, Inc., Model 6700). These

autosamplers contained 24 500-ml HDPE plastic sample containers that were filled by a peristaltic pump. The peristaltic pump was programmed to deliver a specified volume (generally 45 ml) every 3 hours. Eight 45-ml volumes (360 ml total) were pumped into each sample container, which was filled prior to sample collection with 90 ml of 10% redistilled HNO_3 (Tracepur Plus by EM Science). Thus, the total volume in each container after sample collection was 450 ml, and the sample was diluted to 80% its original strength (dilution of 1.25) and spiked to 2% HNO_3 v/v. In addition, each sampler was fitted with a pH probe and thermometer that recorded data at 30-minute intervals. A computer controller was used to program each autosampler, to store data from the pH probe and thermometer, and to maintain a running log of autosampler operation.

The tubing through the peristaltic pump was silicone and was connected to more durable tygon tubing that traveled from the autosampler unit into the water body or to a flow connection. The samplers located at Locke and Bethel Island were bolted to docks, and water entered sample tubing through a strainer located approximately 4 feet below the water surface. Samplers at Mossdale Landing, Martinez, and Clifton Court Forebay were located in sampling stations managed by the State of California Department of Water Resources. Submerged pumps located near these stations delivered water from a fixed depth above the bottom (at Mossdale Landing and Clifton Court Forebay), or from a fixed depth below the water surface (at Martinez), through pipes and into each station. Tubing from each autosampler was spliced into this continuous-flow water supply.

Samples were collected from autosamplers on a roughly two-week service schedule. During each collection period, each sample container was capped and shaken

to evenly distribute particulate matter that had settled to the bottom. Ten milliliters of sample were then immediately decanted into pre-cleaned 10-ml Teflon sample containers. One field blank of 10% nitric acid was collected from each station during each sample collection period from the container immediately following the last collected sample. The remainder of the sample (or acid blank) in the autosampler container was discarded, and each container was filled with a solution of 10% redistilled HNO_3, capped, and shaken thoroughly. This rinse solution was also discarded, and containers were filled with 90 ml of redistilled 10% HNO_3. Data from the computer were downloaded into a portable datalogger device. The pH probe was then cleaned with a brush and deionized water and calibrated using buffer solutions of pH 4, 7, and 10. Finally, the autosampler was reassembled and the computer reprogrammed for the following sampling period.

2.3.4 Collection of saline samples

Saline samples were collected as described in this section for the research conducted in Hawai'i. Freshwater streams within this study area flow into highly saline receiving water bodies; the wastewater effluent studied is discharged through a diffuser structure at the bottom of the ocean off Waianae. Sampling procedures for these two types of samples differed slightly and are described in greater detail below. Additional details about the sampling sites are provided in Chapter 4.

Because the freshwater streams studied in Oahu discharge into relatively shallow water (usually about 8 feet deep and always less than 40 feet deep), only surface samples were collected in receiving water bodies. Samples were collected in a grid with roughly

200 meter point spacing from the point of discharge to beyond the visible limits of the surface plume. Presampling preparation included acid-washing of sample containers as described in Section 2.3.1. Additionally, 8.5 ml of ultrapure water (Milli-Q 18.2 MΩ-cm) and ultrapure nitric acid (Baker Ultrex II) were added to each sample container after cleaning.

At each station, a Teflon beaker was used to collect the sample. For each sample, the beaker was rinsed once with a 2% HNO_3 solution and twice with the receiving water to be sampled. Samples were collected from slightly below the water surface to avoid contamination by surface films of petroleum products or rainwater. To minimize surface contamination by the sampling vessel, samples were collected from the bow of the boat as the boat was moving slowly forward over the station. One milliliter of sample was pipetted from the beaker using an Eppendorf pipetter and pre-cleaned, polypropylene disposable pipette tips. This volume of sample was added to the sample container, which was then capped and shaken to mix the sample. The typical field sampling collection rate was approximately 20 samples per hour. Average time was 1.5 minutes on station and 1.5 minutes travel time between stations.

Water column sampling was conducted for samples collected near the Waianae Ocean Outfall discharge. For the first two sampling events, a peristaltic pump was used to pump the samples to the surface at the rate of 1.5 l/min through 3/16-inch inner diameter Teflon tubing. Samples were collected from the surface and from 20, 40, 65, and 90 foot depths at each station. Prior to sampling, the Teflon tube and all beakers used for sample handling were soaked in a 10% HNO_3 solution for 24 hours, then rinsed with

high purity distilled water. Sample container preparation was as described for receiving water samples.

Two sampling patterns were used during the collection of samples from Waianae Outfall. The first involved determining the current direction using a window-shade drogue and then measuring a transect of the plume in the direction of the current. Each transect consisted of five stations with three to five depths measured at each station. Transect directions were modified as the current direction changed during the day. This method was used on sampling days 2 (4/12/95), 3 (8/18/95), and part of day 4 (10/17/95). The second technique involved occupying stations in a grid surrounding the diffuser and sampling one to four depths per station. This method was used for part of day 4 (10/17/95) and all of day 5 (3/26/96).

With the vessel on station, the surface sample was collected with the Teflon beaker as described above. Plastic-coated dive weights, sealed in LDPE ziplock bags to prevent sample contamination, were attached to the end of the tube using plastic wire ties. This provided the weight to sink the tube to the sampling depth. The tube was then lowered to the desired depth. Prior to sample collection, three tubing volumes were pumped through the system. A sample was then pumped into the Teflon beaker, and 1 ml of sample was pipetted into a pre-diluted 10-ml Teflon sample container. The tube was then raised to the next depth, and the process was repeated. This sampling procedure was very time-consuming, mainly because of the time required to pump several volumes of water through the tubing. Obtaining a sample from a single depth took approximately five minutes. With any wind or current, it was impossible to hold the vessel on station

for the required amount of time (approximately 30 minutes). Anchoring at each station increased the time on that station to 45 to 60 minutes. This method of sample collection was abandoned due to low sampling rates.

The revised method utilized 1.2-liter Teflon-coated Niskin bottles (manufactured by General Oceanics, Inc.). Both the spring closure and messenger weights were also Teflon-coated. At each station, the surface sample was collected with the Teflon beaker. The Niskin bottles were lowered to the desired depth, and a messenger weight was released from the surface to close the bottles. The bottles were then recovered, and 1-ml volumes from each sample were pipetted into pre-diluted Teflon sample containers. This method was used for the last three sampling days at Waianae Outfall. Because only two of the Niskin bottles were purchased, two drops per station were necessary to recover four subsurface samples. Under these conditions, sampling rates increased to approximately 30 samples per hour.

2.3.5 Sample filtration

Brackish and fresh water grab samples samples collected throughout the Delta were filtered to determine which elements were associated largely with particles. Prior to use, 10-ml polypropylene disposable syringe filters (Benton & Dickinson) were removed from their packaging. The plunger portion was removed from the barrel, and the barrel was acid-washed in a 10% redistilled nitric acid bath (using Tracepur Plus HNO_3 by EM Science and Milli-Q water), followed by triple-rinsing with ultrapure water (also Milli-Q). The rubber stopper of the plunger was double-wrapped with Teflon tape (PTFE

thread sealant tape by Scienceware). A Teflon syringe filter with 0.45 μm pores (Acrodisc CR PTFE by Gelman Sciences) was attached to the barrel of the syringe. The syringe barrels (with filters attached) and plungers were then packaged into LDPE ziplock bags for storage.

In the field, the barrel of the syringe was filled with a 10% redistilled HNO_3 rinse solution. The plunger was reinserted into the barrel and the rinse solution was forced through the syringe filter. The plunger was then removed again from the barrel and both the inside of the barrel and the plunger were rinsed several times with the sample to be filtered. The syringe was then filled with sample and the plunger reinserted. The first several ml of sample were forced through the filter and discarded; the remaining volume in the syringe was then filtered into a 10-ml Teflon sample container containing 287 μl of ultrapure HNO_3 (Baker Ultrex II). The final filtered solution was thus acidified to 2% HNO_3 v/v. Unfiltered grab samples were also collected and acidified at the same time for analysis and comparison with filtered samples. Collection of these samples was as described in Section 2.3.2.

Figure 2.1: ICP-MS schematic

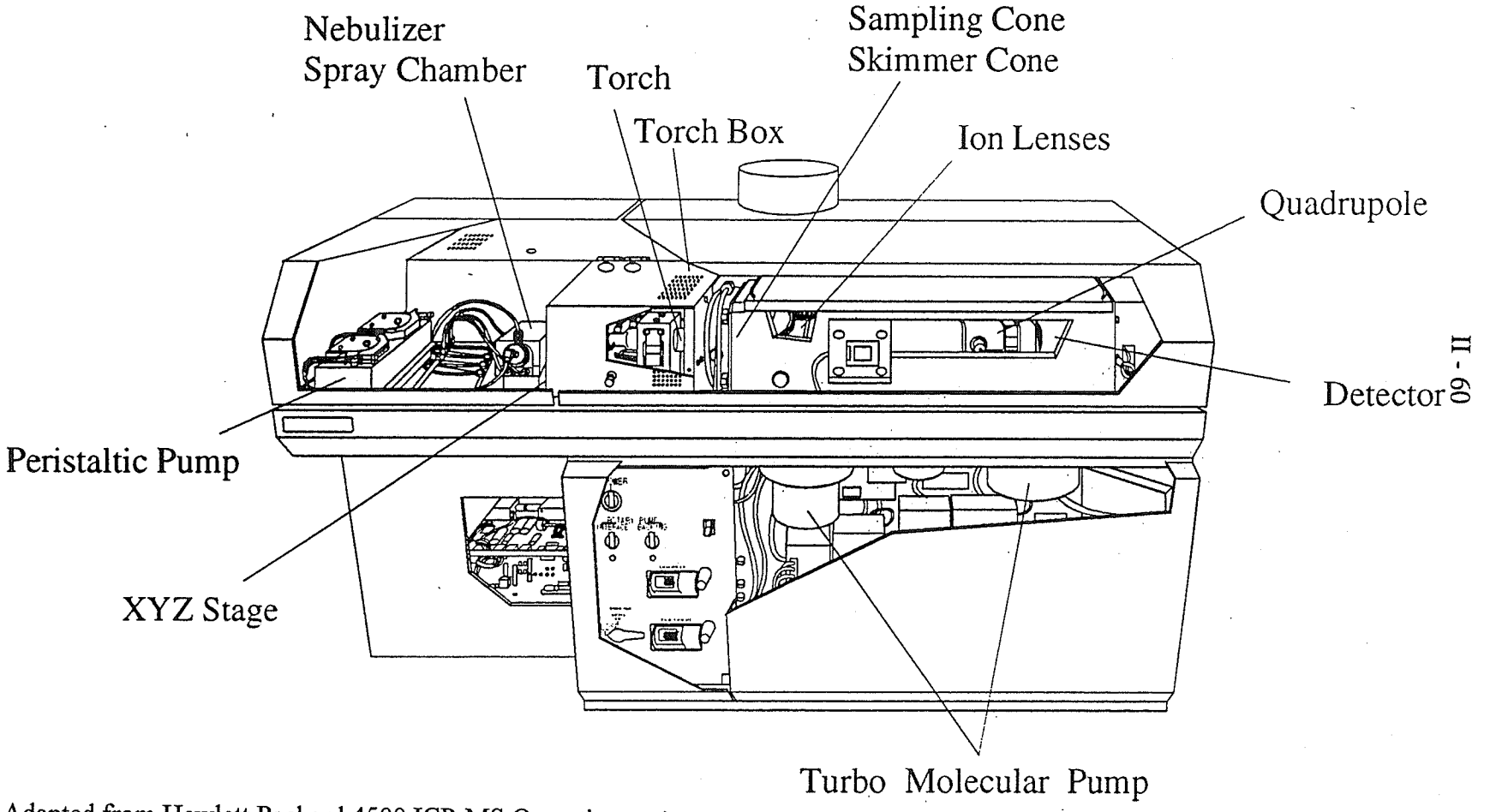

Adapted from Hewlett Packard 4500 ICP-MS Operation and Maintenance Manual.

Figure 2.2: ICP-MS detection limits

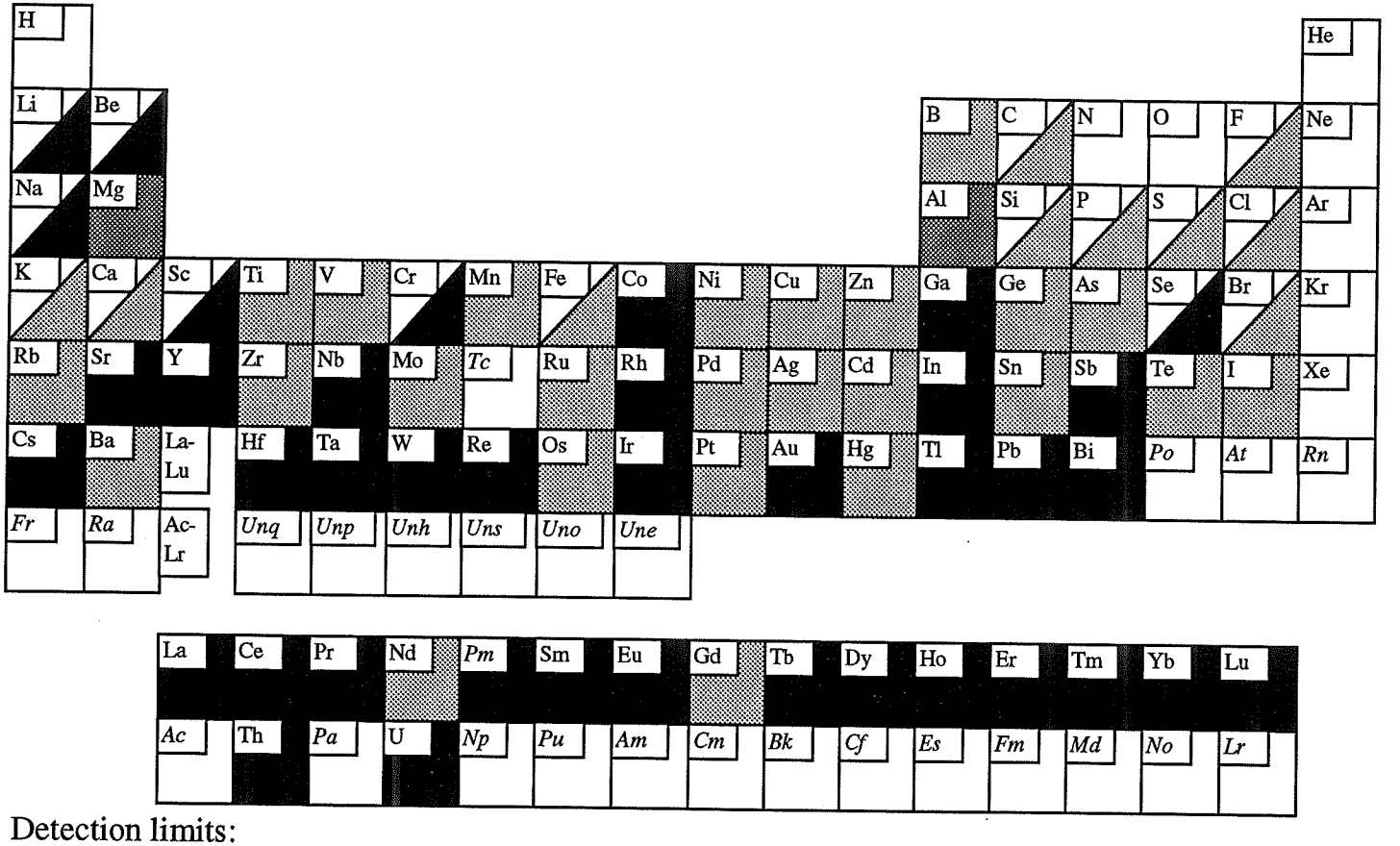

Detection limits:

- ≤ 0.001 µg/l (≤ 1 ppt)
- 0.001 - 0.01 µg/l (1 - 10 ppt)
- 0.01 - 0.1 µg/l (10 - 100 ppt)
- ≥ 0.1 µg/l (≥ 100 ppt)

3 Development of a tracer technique for the Sacramento-San Joaquin Delta

3.1 Introduction

The Sacramento-San Joaquin Delta (known as "the Delta"), which has been called a "reversed delta" by some, has an enclosed Bay at the mouth and a network of channels upstream that otherwise resembles a more traditional Delta. About 40% of the surface area of California is included within the watershed that drains through the Delta, and it is an important ecological resource, providing habitat for many species that are either permanent or seasonal residents. The Delta is also the heart of the state's extensive water resources system. Water that is exported from the Delta is delivered to the southern two-thirds of California, providing at least some drinking water for two-thirds of the state's residents. Roughly eighty-five percent of the water exported from the Delta (a total of 1.3×10^{10} m^3 yr^{-1}) is used to support the state's multibillion dollar agricultural economy.

The current primary factor controlling the use of the Delta's freshwater resource is the ecological health of the system, which has been tied to the distribution of salinity and overall water quality within the Delta. Although hydrodynamic models have been developed to describe the distribution of salt and other contaminants and chemical constituents within the system, these models rely upon empirical estimates of consumptive use within the Delta and semi-empirical flow estimates at some of the major channel connections and barrier locations within the Delta. The use of empirical factors has led to intense discussion about the specific route by which salt or other chemical constituents arrive at a given location. Even though hydrodynamic models can to some

extent be calibrated based upon the distribution of salinity within the Delta, the distribution within the Delta of freshwater from the two major rivers remains largely unknown. Some of the most intense debate has arisen over appropriate management strategies to control the distribution of both the salt and the flow.

This study was designed to provide an objective determination of actual flow patterns and levels of mixing within the Delta by determining the behavior of elements within the water. By direct measurement of conservative flow tracers naturally present in Delta river and Bay waters by ICP-MS, fractions of water arriving from the rivers and the Bay would be estimated in water samples that contain a mixture of these waters. As discussed in Chapter 1, this requires establishing three criteria for elements selected for use as tracers:

(1) sources must have distinct chemical or elemental "fingerprints;"

(2) source concentrations must not vary significantly on timescales shorter than the mixing timescales of the system; and

(3) fingerprints of sources must not be altered to any great extent during mixing, *i.e.*, chemical behavior during mixing should be very nearly "conservative."

In this study, the language developed for use in air pollution tracer studies was adopted: a "source" is defined as the point of origin for water entering the study area, and a "receptor" is defined as a sampling location within the study area, where water is a mixture of the source waters.

3.2 Study area

The Sacramento-San Joaquin Bay-Delta system ("the Delta") is located in northern California and consists of two large freshwater sources that flow into a brackish bay. The Sacramento River flows into the Delta from the north and contains water from its two major tributaries, the American and Feather Rivers; it provides roughly 85% of the freshwater that flows into the system. The San Joaquin River, flowing from the south, provides roughly 10% of the average freshwater inflow. The remainder of the freshwater inflow to the estuary arrives from eastside streams, including the Cosumnes and Mokelumne Rivers and other small local streams. The total drainage area is about 38 million acres (1.5×10^{11} m^2), or about 40% of the surface area of the state of California plus a small portion that extends into southern Oregon (California State Lands Commission, 1994). Over the past 150 years, the Delta has undergone significant changes; Figure 3.1 shows the Delta as it exists today. Major features of the system are noted, as are the sample collection locations used for this study.

Before development, the Delta looked much different than it does today (California State Lands Commission, 1991). It consisted largely of marshland and regularly experienced significant floods. Freshwater was delivered to the system primarily in two pulses: one from winter rainstorm events, and one during the spring snowmelt in the Sierra-Nevada Mountains. High tides also caused periodic flooding, particularly when coupled with high freshwater inflows. Infrequent high flood flows overtopped natural levees and filled floodplain basins.

As a result of the periodic flooding and growth of marsh plants, the soils within the Delta are fine silts and very fertile peat soils. Between 1860 and 1930, most of the Delta's freshwater marsh areas (a total of about 350,000 acres) were diked and put into agricultural production (California State Lands Commission, 1991). Currently there are about 1,100 miles of levees diking about 500,000 acres of farmland in the Delta, most of which is contained on 57 islands (*ibid.*). Other changes in stream channels resulted from hydraulic mining in the foothills of the Sierra-Nevada Mountains, which washed roughly 1 billion cubic yards (800×10^9 m^3) of sediment into the rivers between 1853 and 1884 (*ibid.*).

Freshwater flow patterns within the Delta have also been altered significantly by an extensive system of dams and water diversions upstream of the Delta and by exports of water, primarily from the south Delta. Because two-thirds of the state's water supply is in the rivers and streams of northern California while two-thirds of the state's water use is south of Sacramento, water is transferred from north to south through the Delta. The two main projects accomplishing this water transfer are the State Water Project (SWP) and the Central Valley Project (CVP).

The CVP is operated by the U.S. Department of the Interior's Bureau of Reclamation; it consists of 20 reservoirs and 500 miles of canals and other water conveyance facilities in the Sacramento, Trinity, American, and San Joaquin River basins (California State Lands Commission, 1991). The largest water storage facility in this project is Shasta Dam, completed in 1944, which stores up to 4.5 million acre-feet (5.5×10^9 m^3); Folsom Lake, completed in 1956 and located on the American River, stores up

to 1 million acre-feet (1.2×10^9 m^3). Within the Delta, the Delta Cross-Channel Gates (located just downstream of the sampling station at Locke, shown on Figure 3.1) provide a controlled connection between the Sacramento and Mokelumne Rivers, diverting flow from the Sacramento River channel into the eastern portion of the Delta. This diversion allows higher quality Sacramento River water to flow to the export pumps in the south Delta (located near the Clifton Court station as shown on Figure 3.1); its operations schedule for the period March 1996 - March 1997 is shown in Table 3.1 below. About 7 to 8 million acre-feet (8.6 to 9.9×10^9 m^3) of water is pumped annually at the Tracy Pumping Plant into the Delta-Mendota Canal, which then delivers this water to the lower San Joaquin Valley. Here it is used primarily for irrigation. Other stated functions of the CVP include urban water supply, water quality maintenance, flood control, power generation, recreation, and fish and wildlife enhancement (*ibid.*).

The SWP consists of reservoirs, aqueducts, power plants, and pumping plants extending 600 miles from Plumas County in northern California to Riverside County in southern California. It is operated by the State of California's Department of Water Resources (DWR). The main storage facility in this system is Lake Oroville, which impounds up to 3.5 million acre-feet (4.3×10^9 m^3) of water from the Feather River and was completed in 1968. This water is conveyed in the Sacramento River channel through the Delta to Clifton Court Forebay, where water is impounded briefly before being pumped into the California Aqueduct for delivery to southern California. The SWP is designed to deliver up to 4.2 million acre-feet (5.2×10^9 m^3) of water each year to 30 different water agencies in the southern part of the state; currently, it delivers an annual

average of about 2.4 million acre-feet (2.9×10^9 m^3). In addition, the North Bay Aqueduct diverts a small portion of this flow to Solano and Napa Counties.

In addition to freshwater diversions for CVP and SWP demands, agricultural diversions within the Delta account for close to 1 million acre-feet (1.2×10^9 m^3) of water annually. The Contra Costa Water District diverts about 0.1 million acre-feet (0.12×10^9 m^3) annually from Rock Slough in the Delta. Several other constructed facilities within the Delta also alter flow patterns within the system. During the study period, four barriers were constructed in the south Delta to alter flow patterns and water levels. The locations of these barriers are shown on Figure 3.1; Table 3.1 summarizes the locations, functions, and installation dates of these barriers during the period March 1996 - March 1997. Also included in Table 3.1 is the operations schedule for the Delta Cross-Channel Gates. The impact of these barriers and of Cross-Channel Gate operations on water quality and distribution within the Delta will be discussed in Section 3.7 below.

One result of water transfers and changes in channel configurations is a change in seasonal flows. Except during wet years, freshwater flows in the Delta are almost completely controlled by reservoir releases and export pumping. The pulse of freshwater flow resulting from snowmelt in the spring has largely been eliminated. When the amount of water exported from the Delta is high, flows in some channels in the south Delta "reverse;" this effect is particularly pronounced when freshwater flows into the system are low. This change in flow patterns also impacts water quality. For example, in the spring, agricultural drainage levels are high. Without a large spring flow pulse to dilute agricultural return flows, these flows constitute a significant fraction of the water

carried through the Delta. Agricultural return flows often carry toxic levels of pesticides and high levels of other pollutants, including metals, chlorinated hydrocarbons, and petrochemicals.

Table 3.1
Locations and operations of gates and barriers within the Delta: March 1996 - March 1997

Map label	Facility	Date operational	Date non-operational	Function
DXC	Delta Cross Channel	6/12/96 open 11/15/96 open	11/12/96 closed 11/20/96 closed	To convey Sacramento River water to south Delta
A	Barrier at head of Old River	5/12/96 10/3/96	5/16/96 11/19/96	To restrict fish conveyance to export pumps
B	Barrier at Grantline Canal	7/9/96	10/2/96	To impound water behind barrier for ag. diversions
C	Barrier at Middle River	6/5/96	9/29/96 (begun) 10/15/96 (complete)	To impound water behind barrier for ag. diversions
D	Barrier at Old River at Tracy	6/10/96	9/29/96 (begun) 10/15/96 (complete)	To impound water behind barrier for ag. diversions

Water quality within the Delta is an important issue in the management of water that flows through the Delta. In general, the quality of Sacramento River water is higher than the quality of San Joaquin River water. The Sacramento River at Freeport (just upstream of the sampling station at Locke) usually has a pH of about 7.4 to 7.9; the pH falls to about 7.0 during periods of high flow. Monthly measurements of alkalinity during the period February 1996 - February 1997 ranged from 19.78 mg/l as $CaCO_3$ to 61.5 mg/l as $CaCO_3$; excluding the low value, measured during the flood of January 1997, the

average measured alkalinity in the Sacramento River was 49.2 mg/l as $CaCO_3$ (Domagalski, personal communication, 1997). For the San Joaquin River, the most complete set of alkalinity measurements available were made by the USGS for the water year October 1992 - September 1993 at Vernalis (upstream of the Mossdale Landing sampling location). During this period, the alkalinity in the San Joaquin River ranged from 46 to 173 mg/l as $CaCO_3$, with an average of 104 mg/l as $CaCO_3$ (Mullen *et al.*, 1993). Measured pH values at Mossdale Landing during the period March 1996 - March 1997 generally ranged from about 7.5 to 8.2, with values up to 9.0 measured during algal blooms and below 7.0 during flood periods. Turbidity and total dissolved solids (salt) concentrations are generally significantly higher in the San Joaquin River than in the Sacramento River.

3.3 Sampling strategy and source fingerprints

The sampling strategy employed to obtain the results presented in this chapter was developed after two years of preliminary sample collection throughout the Delta. Information gathered during the preliminary phase included elemental concentrations in grab samples, information on sample collection methods, and laboratory results on mixing and analysis techniques. Based upon this information, five locations were selected for the collection of daily composite samples. Three locations were selected for the collection of source samples: Locke, on the Sacramento River just upstream of the Delta Cross-Channel; Mossdale Landing, on the San Joaquin River at the point where it flows into the Delta; and Martinez, located in Carquinez Strait between Suisun and San

Pablo Bays. Note that the samples collected at Martinez are a mix of freshwater from the rivers and of more saline Bay waters. It is difficult to define the "pure" Bay water source due to mixing from various freshwater sources throughout the estuary and beyond the Delta. Because all water leaving the area of interest must pass through this strait (or be exported from the south Delta), this collection point is used to define the Bay source for the study area. It is recognized that the composition of this source will vary with time and freshwater outflow. Two sample collection locations in the interior of the Delta were also selected: Bethel Island, located on the western edge of Frank's Tract in the central Delta; and the inlet to Clifton Court, the export point to the SWP in the south Delta. This export point is also near the Tracy Pumping Plant, the export point to the CVP. Additional detail on the configuration of these sampling stations and on sample collection and analysis methods is provided in Chapter 2.

The word "fingerprint" has come to mean "any unique or distinctive pattern that presents unambiguous evidence of a specific person, substance, etc." (Random House, 1995). In the context of this study, a "fingerprint" is a vector containing the concentrations of certain elements in a given water sample. For the purposes of a mathematical model, the fingerprints of various sources must be distinct, *i.e.*, the source vectors must be linearly independent, in order for such a model to resolve the relative proportions of source waters in a sample containing a mixture of those source waters. These source vectors are linearly independent if no vector can be expressed as a combination of any others (see, for example, Greenberg, 1995).

For this study, there are three clearly defined sources: the Sacramento River, the San Joaquin River, and the Bay at Martinez. Each can be assigned a vector consisting of the measured concentrations of various elements in that source: $\{c_1, c_2, c_3, ..., c_k\}$. Elements selected for use in a source fingerprint must form a vector that is unique for a given source and must also meet the other two criteria described in Section 3.1 above. In this section, several general observations are made concerning the compositions of source waters, and calculations are conducted for elements that are likely to meet all three criteria to confirm that the sources of water to this system do indeed have distinct fingerprints.

3.3.1 General observations

Daily composite samples were collected for a period of about one year at five stations within the Delta, as shown in Figure 3.1 and discussed above. Plots of elemental concentrations in these daily composite samples are included as Appendix D. Concentrations of all elements measured in daily composite samples were averaged for each source location; these average values are presented in Table 3.2. In general, concentration differences between sources were preserved except during the flood event of January 1997. Relative concentrations between sources (*i.e.*, the concentration of an element in one source divided by the concentration of the same element in a second source) changed in magnitude only. For example, the ratio of the concentration of Li in samples collected from the Bay to the concentration of Li in samples collected in the Sacramento River ($C_{Li,Martinez}/C_{Li,Locke}$) ranged from 2.29 to 100, with an average value of

36.5. (Note that this ratio differs from the ratio calculated using the values in Table 3.2 because the sampling period at Martinez was shorter than the sampling period at Locke.) Although the magnitude of this ratio changed, the concentration of Li at Martinez was always higher than the concentration of Li at Locke. Exceptions to this general trend occurred during the January 1997 flood, when river flows were large enough to flush saltwater from the Bay out of the study area. This situation is discussed in greater detail in Section 3.6.

Table 3.2
Average concentration in daily composite samples collected from Delta source locations

Element	Sacramento River at Locke 3/14/96 - 3/3/97	San Joaquin River at Mossdale Landing 3/15/96 - 3/1/97	San Pablo Bay at Martinez 4/13/96 - 3/3/97
Li [ppb]	1.75	17.91	56.85
B [ppb]	33.1	240	954
Na [ppm]	6.42	44.6	2,530
Mg [ppm]	5.02	16.1	312
Si [ppm] [a]	10.4	23.6	24.6
K [ppm] [a]	0.94	4.20	90.7
Ca [ppm]	4.52	15.2	66.9
V [ppb] [a]	5.33	32.4	25.5
Cr [ppb] [a]	4.42	14.3	47.2
Mn [ppb] [a]	40.0	627	264
Fe [ppm] [a]	0.944	13.7	10.0
Co [ppb] [a]	0.88	8.68	5.93
Ni [ppb] [a]	7.38	28.0	51.0
Cu [ppb] [a]	2.44	41.5	25.4
Zn [ppb] [a]	8.56	117	44.6
Ga [ppb]	0.27	1.80	0.74
Br [ppb] [a]	76	958	51,400
Rb [ppb]	1.46	25.9	35.1
Sr [ppb]	63.9	295	1,950
Y [ppb]	0.556	5.74	3.27
Mo [ppb]	0.27	0.94	2.09

Table 3.2
Average concentration in daily composite samples collected from Delta source locations

Element	Sacramento River at Locke 3/14/96 - 3/3/97	San Joaquin River at Mossdale Landing 3/15/96 - 3/1/97	San Pablo Bay at Martinez 4/13/96 - 3/3/97
Cd [ppb] [a]	0.70	0.42	2.48
I [ppb] [a]	16.6	50.0	20.3
Cs [ppb] [a]	0.08	1.52	0.62
Ba [ppb]	26.8	171	67.1
La [ppb]	0.452	10.1	2.74
Ce [ppb]	1.037	18.9	6.21
Pr [ppb]	0.132	2.38	0.81
Nd [ppb]	0.579	9.17	3.44
Sm [ppb]	0.129	1.67	0.789
Eu [ppb]	0.033	0.337	0.186
Gd [ppb]	0.125	1.50	0.748
Tb [ppb]	0.019	0.211	0.114
Dy [ppb] [a]	0.109	1.16	0.646
Ho [ppb] [a]	0.021	0.222	0.131
Er [ppb] [a]	0.058	0.604	0.336
Yb [ppb] [a]	0.049	0.249	0.114
Lu [ppb] [a]	0.007	0.074	0.039
Th [ppb] [a]	0.040	3.10	0.593
U [ppb]	0.18	7.25	1.35

[a] Reported concentrations of these elements are qualitative, not quantitative.

Ratios describing the concentration of an element in one source divided by the concentration of the same element in a second source were computed for all elements that were measured. Results are summarized in Figures 3.2 through 3.4, which sort these ratios into several bins. Figure 3.2, for example, shows the ratios computed for the Sacramento River and San Joaquin River sources. Concentrations of all elements measured (except Cd) were higher in samples collected from the San Joaquin River than in samples collected from the Sacramento River. Concentrations of Mg were between 1.5 and 4 times higher in the San Joaquin River than in the Sacramento River; concentrations

of B were between 4 and 10 times higher; and concentrations of most of the REEs were more than 10 times higher. In general, the San Joaquin River is significantly more saline than the Sacramento River, as seen by the higher concentrations of alkali metals and alkaline earth elements. However, the relative ratios of concentrations of these elements vary, suggesting that concentrations of these elements in the San Joaquin River are not simply a fixed multiple of the concentrations measured in Sacramento River water. This will be confirmed on a day-by-day basis in Section 3.3.2 below.

As shown in Figure 3.3, concentrations of all elements measured are higher in samples collected from the Bay at Martinez than in samples collected from the Sacramento River; this is expected, as samples collected from Martinez are a mixture of Bay water and water from both the Sacramento and San Joaquin Rivers. Since San Joaquin River water contains higher concentrations of most of these elements than Sacramento River water, concentrations at Martinez should be higher than concentrations in the Sacramento River. An additional factor may be resuspension at the Martinez site. The station at Martinez is located on the edge of a broad expanse of water, and high winds and large waves are common. As a result, the water at this station is often very turbid. Samples were collected from a fixed depth below the water surface, which was within a few feet of the bottom during low tide. Particles that had settled and that were resuspended later by wave action were collected along with the water flowing past the collection site; the result is an increase in the measured concentrations of elements that are associated with particulate matter. This effect is discussed in greater detail below, as it affects both the observed variations in the fingerprint of water collected from Martinez

and the conservative behavior of these elements within the estuary. Elements that are likely to be affected by resuspension include Si, the transition metals, and the REEs.

Concentrations of elements present in high concentrations in seawater (particularly major cations) are higher in water from Martinez than in water from the San Joaquin River; see Figure 3.4. However, concentrations of many other elements are higher in San Joaquin River water than in Bay water. Most notably, concentrations of several transition metals and of the rare earth elements (REEs) are a factor of about 2 to 3 higher in San Joaquin River water. Although the transition metals are difficult to measure quantitatively in samples of moderate to high salinity (see Chapter 2), these observed trends are likely real; if interferences caused by high salinity result in measurement error, measured concentrations will be higher than actual concentrations. Since concentrations in the more saline samples are lower than concentrations in San Joaquin River water, it can be safely concluded that these qualitative variations are real. It is also worth noting that concentrations of U are higher in the San Joaquin River than in Bay waters. This is significant because U tends to behave conservatively in seawater (see, for example, Bruland, 1983), suggesting that the world average concentration in river water is lower than in seawater. This is confirmed by studies of world average river water, for which dissolved concentrations of about 40 ppt (parts-per-trillion) have been estimated (Martin and Meybeck, 1979). The elevated concentrations in the San Joaquin River are likely due to high concentrations of U in soils derived from marine sediments in the western San Joaquin Valley (Bradford *et al.*, 1990). Concentrations of the REEs are also significantly elevated above world-average concentrations (again, see Martin and

Meybeck, 1979), and these may also originate from the same deposits. Here, note that the ratio of REE concentrations is relatively constant, suggesting that concentrations of the REEs in water collected from Martinez may be a multiple of REE concentrations in San Joaquin River water.

3.3.2 Element-specific observations

As noted in Section 3.3, a necessary condition for mixing ratios to be predicted accurately is that source vectors must be linearly independent. Linear independence was confirmed for source vectors containing concentrations of the elements Na, Mg, Ca, and Sr; this choice of elements will be justified in Sections 3.4 and 3.5 below. Because there are three major sources of water to this system (the Sacramento River, sampled at Locke; the San Joaquin River, sampled at Mossdale Landing; and San Pablo Bay, sampled at Martinez), a unique source vector, or fingerprint, must contain at least three elements. If source vectors containing only three elements are linearly independent, then any source vector containing these elements will be linearly independent of similar fingerprints for the other two sources.

To verify that this condition was satisfied for samples collected in the Delta, a matrix was formed of the source vectors for each of the three sources. Linear independence was tested by dividing each source vector by the concentration of Na in that source vector (multiplication by a constant for mathematical convenience) and by calculating the determinant of the matrix:

$$\begin{bmatrix} (c_{Mg} / c_{Na})_{Locke} & (c_{Ca} / c_{Na})_{Locke} & (c_{Sr} / c_{Na})_{Locke} \\ (c_{Mg} / c_{Na})_{Mossdale} & (c_{Ca} / c_{Na})_{Mossdale} & (c_{Sr} / c_{Na})_{Mossdale} \\ (c_{Mg} / c_{Na})_{Martinez} & (c_{Ca} / c_{Na})_{Martinez} & (c_{Sr} / c_{Na})_{Martinez} \end{bmatrix}.$$

If the determinant of this matrix is not zero, then the vectors in the matrix are linearly independent (see Greenberg, 1988), and source fingerprints containing concentrations of these elements are linearly independent. This calculation was made for all dates for which samples were collected at all three source locations.

Figure 3.5 shows the absolute value of the determinant of this matrix as a function of sample collection date. The sensitivity of the value of the determinant was tested by assuming values of the source vectors that were very nearly linearly dependent. For example, the value of the ratio of (c_{Mg}/c_{Na}) for the San Joaquin River (measured at Mossdale) was assumed to be 10% higher or lower than the value of that ratio as measured at Locke; the values of both (c_{Ca}/c_{Na}) and (c_{Sr}/c_{Na}) were assumed to be identical to those measured at Locke. Because measured concentrations of these elements were rejected unless they were within 10% of measured concentrations for repeat measurements (see Chapter 2), this value is roughly the error possible for the measured concentrations of these elements. These calculations were repeated for many combinations of a possible 10% error. Based upon this testing, values of the determinant below about 1×10^{-5} were determined to be within the error on a given measurement and therefore not truly linearly independent. As shown on Figure 3.5, the values for the determinant computed from the measured source concentrations of Na, Mg, Ca, and Sr were generally an order of magnitude higher than this value, confirming that source fingerprints are linearly independent.

It is noteworthy that values of this determinant remained above the 10^{-5} level even during the January 1997 flood period. During this flood event, concentrations of the major cations fell to freshwater levels at Martinez in San Pablo Bay. If Sacramento and San Joaquin River waters were the only source of water flowing past Martinez during this period, the value of the determinant should be below 10^{-5}. That it is not suggests that other sources were important during this period. As discussed in greater detail below, concentrations of major ions at the interior Delta stations of Bethel Island and Clifton Court were higher during this event than in samples collected from the Sacramento River, the San Joaquin River, or Martinez; this suggests a significant local source of salt in the south Delta (likely agricultural return water). During this period, a model using the Sacramento River, the San Joaquin River, and the Bay as the only sources is not likely to yield meaningful results.

3.4 Variations in source fingerprints

In order to predict mixing at a given location within a system, one must be able to predict accurately the concentration of a tracer arriving from a given source to that location. Operationally, this means that the source fingerprint must not vary significantly on timescales shorter than the timescale required for a parcel of water to travel from the source location to the receptor location. Additionally, source fingerprints should not vary significantly spatially, *i.e.*, elements should be chosen for inclusion in the fingerprint based upon predictable source vector behavior. As an example, an element that is strongly enriched in an irregular, seasonal manner (such as the REEs in particle-rich

agricultural drainage) would not be a wise choice for use as a tracer. To address these questions, elemental concentrations were determined for all the stations studied within the Delta, with data collection continuing for roughly one year; variations in concentration were compared to estimated travel times from source to receptor. Also, samples were collected along the length of the Sacramento River from Keswick Reservoir (near Redding) to Suisun Bay in the Delta; these samples were collected during a period at the end of June 1996 when river flow was relatively steady and when agricultural inputs were likely to be high.

3.4.1 Temporal variations in source fingerprints

Daily composite samples were collected from three source locations (Locke, Mossdale Landing, and Martinez) and from two receptor locations (Bethel Island and Clifton Court) during the period of March 1996 through March 1997. For each location, elemental concentrations were plotted as a function of the sample collection date; these plots are included, ordered primarily by location and secondarily by elemental mass, in Appendix D. Appendix D also contains river flowrates measured at Freeport (near Locke) and Vernalis (near Mossdale Landing); the combined export flow rate from the Tracy and Banks Pumping Plant is also included. Flow data were obtained from the California Data Exchange Center (California Data Exchange Center, 1997), while elemental concentrations were measured at Caltech as described in Chapter 2.

Travel times from the river source locations to receptor locations were approximated by measuring the travel distance along several flow paths from a source to

a receptor. Flow velocities for the Sacramento River at Freeport (upstream of Locke) were measured by the California Department of Water Resources (DWR). Flow velocities for the San Joaquin River were estimated from field observations and from data collected during September and November 1996; additional detail is provided in Section 5.4 of Chapter 5. These approximations, though crude, provide an order-of-magnitude estimate of the travel time from source to receptor. Details of these estimates are included as Table 3.3.

The travel time from the Bay at Martinez to the receptor locations is much more difficult to estimate. Water carried from the Bay to Bethel Island or to Clifton Court is carried by the tides and by dispersion as river water and Bay water mix together. In addition, processes such as tidal pumping affect the distribution of salinity within the Delta. As shown in Section 3.6 below, the fraction of Bay water at all receptor sites is small; the highest value observed at Bethel Island is about 0.025, or 2.5%, while the highest value observed at Clifton Court is less than 0.01, or 1%. Errors in the estimated concentrations of many elements in the Bay source water do not significantly affect the predicted fractions of river waters in a sample collected from a receptor site. This is because Bay waters contain significantly higher concentrations (factors of up to 100) of saline elements than river waters. Even a large error (say, 30%) in estimating the concentration of Bay water arriving at a receptor site using these high concentration elements will result in only a small error in the relative fractions of source waters at that site as determined by a model; this is illustrated in Section 3.6 below.

Table 3.3
Estimated travel times from source locations to receptor locations

Source	Receptor	Estimated travel distance [miles]	Estimated flow velocity [feet/second]	Estimated travel time [days]
Locke	Bethel Island	24[a]	1.2 (low flow)[a] 2.7 (high flow)[a]	1.5 0.5
Locke	Clifton Court	44[b]	1.2 (low flow)[b] 2.7 (high flow)[b]	2.7 1.0
Mossdale Landing	Bethel Island	27[c] 39[c]	0.8[c] 0.3[c]	2.1 7.9
Mossdale Landing	Clifton Court	19[d]	0.3[d]	3.9

[a] Low flow condition is 15,000 cfs; high flow condition is 70,000 cfs. Velocities used are 75% of those measured at Freeport. Travel path is roughly equal for (Sacramento River - Threemile Slough - San Joaquin River - Fisherman's Cut) and (DXC - North Fork Mokelumne River - Old River - Franks Tract).

[b] Flow conditions and velocities are the same as in [a]. Travel path is roughly equal for (Sacramento River - Threemile Slough - Bethel Island - Old River - Clifton Court) and (DXC - South Fork Mokelumne River - Old River - Clifton Court).

[c] Higher flow velocity is assumed from field observations of the San Joaquin River at Mossdale Landing during low to moderate flow conditions; low flow velocity was measured during the City of Tracy wastewater study during low San Joaquin River flow conditions. The shorter flow path (San Joaquin River - Old River - Franks Tract) is the most likely; the longer flow path (Old River - Grantline Canal - Old River - Franks Tract) is probably responsible for a much smaller fraction of transport, particularly when barriers are in place.

[d] Flow velocity is as measured during the City of Tracy wastewater study during low San Joaquin River flow conditions (see Chapter 5 for detail). Flow path is (Old River - Grantline Canal - Clifton Court).

3.4.1.1 Sacramento River

Based upon travel times estimated in Table 3.3, the source fingerprint of the Sacramento River as determined at Locke should be relatively constant on a timescale of about three days to accurately predict mixing at either of the receptor sites. The sample record at Locke is almost complete, with samples missing only for the period of May 16 - May 25, 1996; unfortunately, this was a period of high flow.

Measured flow rates at Freeport, just upstream of Locke, were relatively constant during the dry season, from about June 20, 1996 through about November 20, 1996. During this time period, changes in concentrations in daily composite samples collected at Locke were gradual. The concentrations of Na increased steadily through early September at a rate of about 120 ppb, or 2%, each day; the concentration declined at roughly the same rate through mid-October, then climbed at a slightly lower rate through mid-November. Concentrations of other alkali metals, the alkaline earth elements, B, Mo, and U exhibited the same patterns but generally at lower rates. Concentrations of the transition metals were nearly constant through this period, as were concentrations of the REEs. Almost all elements during the dry season have concentrations that are nearly constant on timescales of about three days.

In the wet period preceding this dry period (end of winter 1996), variations in elemental concentrations at Locke were more extreme. The concentrations of B, Na, Mg, K, Ca, and Sr varied in a regular manner, decreasing linearly from high concentrations in mid-March (at the start of collection) to moderate concentrations in mid-April. From mid-April to the start of the dry season, several small storms and one major storm caused increases in flow rates in the river; increased flow rates caused a general decline in the concentrations of these elements, with changes of about 20% on timescales of 2 to 3 days for the smaller storms. Concentration changes were most likely about 40% due to the major storm. Concentrations of Rb and Ba followed the same general trends but with much more scatter. Concentrations of Mo were nearly constant and concentrations of U decreased linearly and predictably during this period. Concentrations of other elements

responded to changes in flow more erratically. Rather than varying in a linear manner, concentrations of the transition metals and REEs varied by factors of 2 to 3 on timescales of a few days during this period. Except for the few days surrounding a high flow event, concentrations of B, Na, Mg, K, Ca, Sr, Mo, and U fluctuate only slightly on timescales of a few days.

Both flow rates and concentrations of most elements changed rapidly during the wet period that began in early December 1996. The Sacramento River experienced a four-fold increase in flow rate during the first major storm of the wet season, and concentrations of Na dropped linearly by a factor of about two in a period of five days. Concentrations of B, Mg, K, Ca, Sr, Mo, and U did not drop so precipitously but did vary by factors of about 20 - 40% from early through late December. Concentrations of Ga, Rb, and Ba increased significantly as the flow rate increased. Concentrations of the transition metals and REEs exhibited a first peak at the end of November at about double their dry season concentrations, then rose by a factor of 10 or more during a mid-December rain event.

The "New Year's Flood" of January 1997 caused significant flooding along the length of the Sacramento River and its major tributaries. Flow rates increased significantly (peak flows measured at Freeport were near 120,000 cfs, about seven times the dry season average flow), and turbidity along the river increased significantly also. Concentrations of B, Mg, K, Ca, and Sr fell to one-quarter to one-half their pre-flood values over a one-week period; concentrations of Mo and U also fell but only to about two-thirds their pre-flood values. Concentrations of all these elements rose steadily as

flow rates decreased, then fell again during a second storm toward the end of January; concentrations then rose linearly after this storm through the end of the study period. Concentrations of the transition metals, the REEs, Ga, Rb, and Ba behaved much more erratically through the flood period, with very high peaks during high flow events followed by short periods during which the concentrations of these elements varied by factors of 2 to 3.

Based upon this analysis, elements that should be most useful as tracers are those for which variations in concentration occur predictably and over relatively long periods of time. These elements include B, Na, Mg, Ca, Sr, Mo, and U. Elements that show significant variation over short timescales and are therefore not likely to be useful as tracers include the transition metals and the REEs. (These elements are shown in Section 3.4 to be strongly associated with particulate matter.) Elements that are intermediate in character include Rb, Ga, and Ba. During the end of June 1996 and during the periods between mid-December 1996 and mid-February 1997 when river flow rates changed very rapidly, concentrations of almost all elements vary significantly on short timescales periods.

3.4.1.2 San Joaquin River

Estimated travel times from the source location on the San Joaquin River at Mossdale Landing to the receptor sites within the study area are on the order of 4 - 5 days. The sample record at Mossdale Landing is almost complete between March 14, 1996 and March 3, 1997, with only a scattered handful of samples missing due to pump failures at the sampling station. The extended dry season in the San Joaquin River began in early

June 1996 and lasted through the end of November 1996; this dry season was slightly longer than that observed in the Sacramento River because of differences in storm and rainfall patterns immediately preceding the dry period.

During the extended dry period, elemental behavior was similar to that observed during the dry period for the Sacramento River. Concentrations of Na were very low at the end of the last rain event of the spring, and they rose quickly as flow rates in the river fell and then stabilized. Between May 26 and June 22, the concentration of Na rose from 8930 ppb to 81,500 ppb, an average increase of 2700 ppb, or 25% of the initial concentration, per day. Concentrations of B increased at roughly the same rate. Concentrations of Mg, Ca, Sr, Mo, and, to a lesser extent, U, also rose during this period but at lower rates. Concentrations of these elements then declined at rates of about 1% per day from early July through mid-October and then increased rapidly again from mid-October through mid-November at rates similar to those observed between May and June. In contrast to observations in the Sacramento River, concentrations of Li, K, Ga, Rb, and Ba remained relatively steady through this period; fluctuations in concentration on timescales of days were moderate and exhibited no clear trend. Concentrations of the transition metals and REEs fluctuated significantly on timescales of a few days. A small peak in the concentrations of these elements was observed toward the end of July; this peak corresponded to the peak observed for B, Na, Mg, Ca, Sr, and Mo and was perhaps due to agricultural drainage. From mid-July through mid-October, concentrations of these elements were steady on timescales longer than estimated travel times.

The storms that arrived during March, April, and May 1996 were wetter in the Sacramento River watershed than in the San Joaquin River watershed; therefore, flow rates in the San Joaquin river (measured at Vernalis, upstream of Mossdale Landing) did not vary as much as flow rates in the Sacramento River. Concentrations of B, Na, Ca, Sr, and Mo varied little on timescales of a few days, and concentrations remained relatively level through the beginning of May, then dropped linearly through the end of May during the largest of the storm events. Concentrations of Mg and U were much more variable on shorter timescales during this period. Concentrations of Li, K, Ga, Rb, and Ba were also highly variable during this period; no clear trends in the data are evident, although concentrations did fall with flow rate at the end of May. Concentrations of the transition metals and REEs were highest when flow rates were highest, and concentrations exhibited variations of factors of 2 to 3 on timescales of a few days between high flow events.

Flow rates in the San Joaquin River increased significantly in early December. As flow rates increased, concentrations of B, Na, Mg, Ca, Sr, and Mo decreased. The rate of decrease was fastest for B, Na, and Mg (roughly 8% per day) and slower for Ca, Sr, and Mo (roughly 1% - 3% per day); these variations were linear. Concentrations of Li, K, Ga, Rb, Ba, and U varied more erratically, with strong peaks in mid-December at values 3 to 7 times average dry season values. Concentrations of the transition metals and REEs behaved similarly but peaks were more pronounced.

The flood event of January 1997 was more severe on the San Joaquin River and its tributaries than along the Sacramento River. Maximum flow rates recorded at

Vernalis were about 50,000 cfs; the San Joaquin River channel and its levee system are designed to convey a maximum of 8,000 cfs. The peak flow was about 17 times the average dry season flow rate (contrast this to peak flows of 7 times the average dry season flow rate on the Sacramento River). Additionally, because of reservoir conditions upstream, high flows were released for a long period following the major rainfall events, and river flow rates and conditions did not return to "normal" levels until mid-March 1997. Because of this, the concentrations of elements in the river beyond mid-January may not be representative of "typical" years, in which high river flows are observed for only a few days to a week after a storm event. The initial flood pulse brought a sharp decrease in the concentrations of the alkali metals and alkaline earths, even for those elements that had responded with increased concentrations to the high flow rates of mid-December. Beyond mid-January, concentrations of B, Na, Ca, Sr, and Mo were steady on timescales of a few days. Concentrations of Li, Mg, K, Ga, Ba, and U were steady through early February then peaked as river flow rates again increased. The behavior of the transition metals and the REEs was similar, but again peaks were more pronounced.

Based upon these observations of temporal variation in the source fingerprint of the San Joaquin River, the elements for which concentrations at a receptor site can best be predicted include B, Na, Mg, Ca, Sr, Mo, and U. Elements for which concentrations vary by large amounts on timescales of a few days include the transition metals and the REEs. Elements exhibiting intermediate behavior include Li, K, Ga, Ba, and U. These observations are similar to those made for the Sacramento River; as on the Sacramento River, elements with the least varying fingerprints are those that are not strongly

associated with particulate matter. Concentrations of almost all elements vary significantly between the end of May 1996 and mid-June 1996 and between the end of November 1996 and early January 1997.

3.4.1.3 San Pablo Bay at Martinez

Fortunately, although it is difficult to estimate travel times from Martinez to either Bethel Island or Clifton Court, these travel times are less significant than for the sources located on either the Sacramento River or on the San Joaquin River. For detail, see Section 3.4.1 above and Section 3.6 below. Errors as high as 30% do not significantly affect the calculated fractions of source waters at a receptor location. Therefore, the criterion for evaluating the variation in the fingerprint of water collected at Martinez is different from the criterion for fingerprints at the river source locations. For elements present in much higher concentrations in Bay water than in river water, variations of 30% are acceptable. Elements that fall into this category include Li, B, Na, Mg, K, Ca, and Sr. Bay water concentrations of these elements are much higher (factors of 10 or greater) than river water concentrations through the entire study period with the exception of week-long periods in mid-April and mid-May 1996 and the end of the period beginning December 6, 1996. During and after the flood of January 1997, concentrations of these elements fell to freshwater levels throughout the estuary. Otherwise, variations were generally 30% or less on timescales of a week or more.

Elements that in the Sacramento and San Joaquin Rivers are strongly associated with particulate matter include the transition metals and the REEs. As is shown in Section 3.5.2, the concentrations of these elements at Martinez were higher than would be

expected based upon the likely proportions of river and ocean waters and the concentrations of these elements in those waters. The extra source at Martinez is believed to be resuspension of bottom sediments. Concentrations of these elements in samples collected at Martinez varied by factors of 3 to 10 on timescales of days.

Concentrations of Ba were relatively constant throughout the entire study period, with anomalously high concentrations observed during the flood of January 1997. Concentrations of U showed a pattern similar to that of Li, B, Na, Mg, K, Ca, and Sr, but concentrations of U increased steadily after this flood event; because the concentration of U is higher in the San Joaquin River than in Bay waters, variations in the concentration of U in Bay waters are significant. Often, the concentration of U varied by a factor of about 2 on timescales of a week. In conclusion, the elements Li, B, Na, Mg, K, Ca, and Sr exhibit concentrations that vary within acceptable limits during the entire dry season, from mid-June through the beginning of December 1996.

3.4.2 Spatial variation in source fingerprints

Between June 24, 1996 and June 28, 1996, samples were collected along the Sacramento River between Keswick Reservoir, near Redding, to Pittsburg, in Suisun Bay. Figure 3.6 shows this stretch of the Sacramento River, with major landmarks noted. Because the upper portion of the river was often only a few feet deep, two surface samples were collected at each sampling location along this reach of river. Beyond the Highway 32 Bridge (see Figure 3.6), a single bottom sample was also collected where the channel was more than about 8 feet deep. See Chapter 2 for detail regarding sample

collection procedures. Results are presented as plots of elemental concentrations along the length of the river; these plots are included as Appendix E and show the landmarks noted in Figure 3.6. Where three samples (two surface and one bottom) were collected at a given location, all three points are plotted; bottom samples, almost without exception, have higher elemental concentrations than surface samples. Concentrations of major bodies of water flowing into the Sacramento River are also shown on these plots. Their locations are noted; for example, elemental concentrations in samples collected from the Feather River are shown at mile 151, and concentrations in samples collected from the American River are plotted at mile 169. Concentrations in water collected from Georgiana Slough are plotted at mile 206; this sample was likely a mixture of Sacramento and Mokelumne River waters.

To facilitate discussion, elements are divided into three separate groups: the first group includes B, Na, Mg, K, Ca, and Sr; the second group includes Li, Si, Ga, Rb, Mo, Ba, and U; and the third group includes the transition metals and the REEs. The first group of elements includes B and those alkali metals and alkaline earths that were present in concentrations of 50 ppb or higher. Concentrations of all these elements except B and Sr were present at concentrations levels of about 1000 ppb (1 ppm) or higher in all samples collected within the Sacramento River channel. These elements showed remarkably consistent and predictable behavior. Concentrations were lowest near the head of the river, in the Feather and American Rivers, and in Georgiana Slough; concentrations increased moving downriver and were highest in samples collected at Pittsburg, in the more brackish water of Suisun Bay. Concentrations did not vary

significantly between samples collected from the surface and from the bottom of the channel. Despite these similarities, variations between the concentrations of the elements in this group were significant, indicating that the relative proportions of these elements varied in waters tributary to the river. For example, between mile 0 and mile 110, the concentrations of B and Sr increased by about 35%, the concentrations of Mg and Ca increased by 18% and 9%, respectively, and the concentrations of Na and K did not change significantly. These variations were likely due to differences between the sources of tributaries, *e.g.*, agricultural drainage, pristine mountain streams, or groundwater.

Concentrations of the second group of elements (including Li, Si, Ga, Rb, Mo, Ba, and U) were similar to those of the first group, but they exhibited more variation. As with the first group of elements, the relative proportions of these elements varied significantly in waters tributary to the main channel. As a result, general trends in concentration were similar, but the magnitude of variations differed by element. Concentrations in samples collected from the bottom of the channel were higher than concentrations in surface water samples; this effect became more pronounced closer to the Delta, where channels are deeper, and where velocities within the channel varied more than near the head of the river. This effect is likely due to higher concentrations of particulate matter in samples collected from the bottom of the channel, as particulate matter is often carried along in higher concentrations near the bed. If sampling using a drop bottle (see Chapter 2 for detail) disturbed the channel bed, samples collected near the bottom may have included bed sediments as well. As shown in Section 3.5, the

elements in this second group are often associated with particulate matter; acidification of whole water samples then releases at least part of the adsorbed mass of these elements.

The effect of adsorption to particulate matter is especially pronounced for the third group of elements, which includes the transition metals and the REEs. Near the head of the river, only surface samples were collected, as noted above. Where bottom samples were collected, concentrations near the bed were significantly higher (factors of two to three or more). As shown in Section 3.5, these elements are even more strongly adsorbed to particulate matter than the elements in the second group. Concentrations of most of these elements varied significantly over distances of a few miles; although concentrations increased along the entire length of the river, the scatter in the data makes it difficult to discern trends in concentration on shorter length scales. Exceptions to this general behavior were observed for V, which shows less scatter and a more easily observed, generally increasing concentration downriver, and Cd, for which concentrations are uniformly low and near detection limits (as reflected by the large error bars). Scatter in the data is more pronounced for the REEs than for the transition metals, again reflecting their stronger adsorption to particulate matter.

Based upon this analysis, the elements B, Na, Mg, K, Ca, and Sr are likely to be better tracers than the other two groups of elements. The uniformity of the concentrations of these elements along the length of the river indicates that their concentrations in tributary waters do not vary by as much as concentrations of the other two groups of elements. More importantly, the uniformity in concentration between surface and bottom water samples indicates that these elements are present primarily in the dissolved phase.

This does not necessarily indicate that there is no adsorption to particulate matter for these elements; rather, total concentrations are high enough that the fraction adsorbed to particulate matter is insignificant. This in turn means that localized increases in particulate matter concentration, the settling of particulate matter within the study area, and differences in sampling procedures (that may include or eliminate particulate matter before sample acidification) are less important to the use of these elements as tracers.

Initially, it was hoped that longitudinal sampling of elemental concentrations along the Sacramento River might establish clear correlations between easily measured parameters (or conservative elements) and removal or addition for a non-conservative element. For example, if a scatter plot of the concentrations of Li and Na revealed uniform loss of Li at high salinity (or Na concentration), then a correction could be determined. Such a correction might involve multiplying the concentration of Li by a factor determined by the salinity (or Na concentration) of a sample. Unfortunately, no such relationships were evident for the data collected on this sampling trip. This is perhaps because variations in the relative compositions of tributary waters overwhelm such correlations; because the Delta is not a closed system, correlations between elements are very difficult to establish. If it is possible to make corrections such as this within an estuary, it should first be established for a simpler, two-source system (such as a single river flowing into a bay).

3.5 Mixing behavior

To predict mixing accurately within a system, source fingerprints must not be altered to an great extent by chemical and/or biological reactions or by physical changes that occur during mixing (*i.e.*, mixing should be conservative, or very nearly conservative). Among the many possible causes of non-conservative mixing behavior are: formation of insoluble precipitates; uptake by organisms that later die and settle; volatilization and loss to the atmosphere; adsorption to particulate matter that settles; release by ion exchange from particulate matter that later settles; and adsorption to or desorption from particles caused by changes in redox state. To evaluate the "conservativeness" of the behavior of elements within the Delta, an extensive literature search was conducted. Detailed information on the expected speciation and behavior of elements is included in Appendix A; also included are observations from other estuaries. In addition to this literature search, laboratory mixing studies were conducted at Caltech to predict elemental mixing behavior under controlled conditions, and field work was conducted to predict mixing at the confluences of freshwater rivers within the study area (see Section 3.5.2.1). Grab samples were collected at the five autosampler locations at regular intervals to compare filtered and unfiltered samples and to determine an operationally defined maximum cation exchange capacity (see Section 3.5.2.2). Finally, data for daily composite field samples were analyzed to judge the behavior of elements at select locations within the Delta (Section 3.5.2.3).

3.5.1 General observations

Based upon literature review and work conducted to determine the uniqueness and variability of source fingerprints, many elements were eliminated from consideration as tracers early on. In addition, elements for which concentrations could not be readily determined by ICP-MS analysis were dismissed. These included elements that were present in concentrations at or below detection limits in samples collected from the study area (Be, Zr, Nb, Ru, Rh, Pd, Sb, Te, Hf, Ta, Re, Os, Ir, Pt, Au, and Bi), elements that cannot be determined using ICP-MS (H, He, N, O, Ne, Ar, Kr, and Xe), and elements with very high ionization potentials, for which results were not consistent (C, F, S, and Cl).

In addition, elements known to have highly non-conservative behavior in estuarine environments were disregarded. Elements that might volatilize were eliminated from consideration; these include F and I (perhaps lost by volatilization within the estuary but almost certainly lost during the process of sample acidification) and Se, which likely is transformed biologically to the volatile species dimethyl selenide (DMSe) in the San Joaquin River (Cooke and Bruland, 1987). Likewise, elements that may have a strong biological interaction were eliminated; these elements include Se, as noted above, As, and Ge. As is present in methylated forms in Suisun Bay (Anderson and Bruland, 1991), and, although these forms are not likely to be volatile, the distribution of As within the estuary may be affected by biological activity. Ge is involved in biological reactions in the ocean, where it is taken up by siliceous organisms along with Si (Bruland, 1983); although the total concentration of Si is not likely to be affected by biological uptake in

estuaries, Ge is present at much lower concentrations and biological activity may have a more significant effect. Finally, biological cycling can produce thermodynamically unstable oxidation states in estuarine environments (see, for example, Aston, 1978), and it can be difficult to predict the speciation and behavior of elements thus affected. Additional information on expected speciation and behavior of these elements can be found in Appendix A.

Precipitation reactions can also cause loss or gain of elements during estuarine mixing. Some common causes of precipitation probably do not occur within the Delta. These include oxidation-type precipitation, where Fe- and Mn-oxides or sulfur are precipitated by oxidation of reducing solutions (most, if not all, tributary waters to the Delta are well oxygenated). Reducing-type precipitation can occur for U, V, Cu, Se, and Ag, which can be precipitated as metals or lower-valency oxides by the reduction of oxidizing water; reducing sulfide-type precipitation can occur as Fe, Cu, Ag, Zn, Pb, Hg, Ni, Co, As, and Mo are precipitated as sulfides by the reduction of oxidizing sulfate waters. Neither of these is considered likely, as the waters of the Delta remain oxic, with the possible exception of the sediment-water interface in stagnant portions of the Delta. Ba, Sr, and Ca can be precipitated by increased sulfate or carbonate as a result of the mixing of waters or the oxidation of sulfide, conditions that are not believed to exist within the Delta. Finally, alkaline-type precipitation has been observed for Ca, Mg, Sr, Mn, Fe, Cu, Zn, Pb, and Cd, among others, when pH increases, usually from the mixing of acid waters with carbonates or silicate rocks or mixing with highly alkaline waters. This mechanism was not investigated further, as elements affected by this mechanism

were not considered as tracers. (See Salomons and Foerstner, 1984, for additional detail on these mechanisms.)

Precipitation within the Delta estuary is likely to occur for elements that adsorb on accumulations of Fe-Mn-oxides, clays, and organic matter. Such adsorption is particularly likely to occur for the transition metals and other high-valency cations, such as the REEs. An additional effect may be release of cations from particles as low salinity river waters mix with higher salinity Bay waters and Na, Mg, and Ca participate in ion exchange reactions with other cations adsorbed to particle surfaces. As fresh and saline waters mix, precipitation of particles is likely to be enhanced above natural particle settling rates due to a variety of mechanisms, including: neutralization of negative charge on colloidal-sized clay particles by specific adsorption of positively-charged species; a compression of the electrochemical double layer as ionic strength increases; formation of bridging bonds between particles, largely by organic substances; and the enmeshing of clay and hydroxide particles (Aston, 1978). Any one of these is likely to occur in the Delta, where particle-rich river waters mix with higher-salinity Bay waters. These particle-related effects are believed to be the most important causes of non-conservative behavior within the Delta, and additional study was designed to address the extent to which they render elemental behavior non-conservative.

3.5.2 Water-particle interactions

3.5.2.1 Studies of freshwater mixing

Mixing studies were conducted in the laboratory to determine the mixing characteristics of various elements. In these studies, waters collected from the San Joaquin River and the Sacramento River were mixed in known proportions. Samples were agitated for several hours after mixing, and particulate matter was then allowed to settle to the bottom of the mixing containers. Because acidifying these samples after mixing would change the mixing behavior, samples were not acidified prior to analysis; the analysis results are therefore qualitative rather than quantitative. Concentration data were plotted against the known fraction of river waters, and conservative behavior was determined by a straight line fit through the data points.

Figures 3.7 and 3.8 show examples of conservative and non-conservative behavior for different elements in these mixing series. Because of error in the generation of calibration curves, these data are plotted as intensities in counts per second (cps); calibration curves are linear, so there is a 1:1 correspondence between concentration and intensity. All mixtures in these plots were composed of Sacramento River water and San Joaquin River water, so that a point falling at 80% Sacramento River water contained 20% San Joaquin River water. Elements that demonstrated conservative behavior (as determined by a correlation coefficient for a straight line regression fit through the data points of $r^2 \geq 0.900$) in this mixing series included: Li, B, Mg, Si, K, Ca, Ga, Br, Rb, Sr, Mo, I, Ba, and U.

Additional studies were conducted at the confluences of the Sacramento River with the American River and with the Feather River. These confluences were beyond the reach of tides when test samples were collected. The samples obtained were used to predict the fractions of water downstream of the confluence contributed by each of the upstream rivers; this calculation was based upon linear (conservative) mixing of elemental concentrations. These fractions were computed for each element using the following equations:

$$(c_{Sacramento}Q_{Sacramento})_{upstream} + c_{Feather}Q_{Feather} = (c_{Sacramento}Q_{Sacramento})_{downstream};$$

$$(Q_{Sacramento})_{upstream} + Q_{Feather} = (Q_{Sacramento})_{downstream};$$

$$\text{so that } Percent_{Feather} = \frac{(c_{Sacramento})_{upstream} - (c_{Sacramento})_{downstream}}{(c_{Sacramento})_{upstream} - c_{Feather}} \times 100.$$

Predicted fractions were then compared to the fractions of flow known from reservoir release data and from measured flowrates. An example of these results is presented in Table 3.4 for mixing at the confluence of the Sacramento and Feather Rivers; samples were collected September 23, 1993, when flowrates were approximately 11,970 cfs and 1,280 cfs in the Sacramento River upstream of the confluence and in the Feather River, respectively. Results were calculated using elemental concentrations measured in samples that were acidified upon collection, either before or after filtration, as noted in the table. Sample analysis was performed using the qualitative analysis mode of the Perkin-Elmer Elan 5000 ICP-MS; although elemental concentrations were not accurate due to the use of a surrogate calibration procedure by the qualitative analysis mode, relative concentration differences between samples were accurate.

Table 3.4
Predicted mixing at the confluence of the Sacramento and Feather Rivers, September 21, 1993

Element	Results for filtered samples		Results for unfiltered samples	
	Percent from Sacramento River (Actual = 90%)	Percent from Feather River (Actual = 10%)	Percent from Sacramento River (Actual = 90%)	Percent from Feather River (Actual = 10%)
Li	52.8	47.2	39.6	60.4
B	41.6	58.4	69.1	30.9
C	69.0	31.0	74.3	25.7
Na	66.7	33.3	67.6	32.4
Mg	75.9	24.1	76.2	23.8
Al	64.9	35.1	70.6	29.4
Si	88.3	11.7	82.1	17.9
K	67.2	32.8	82.9	17.1
Ca	[a]	[a]	82.2	17.8
Sc	[a]	[a]	83.0	17.0
V	95.6	4.4	88.4	11.6
Mn	33.7	66.3	95.4	4.6
Fe	[a]	[a]	69.1	30.9
Ga	[a]	[a]	80.4	19.6
Rb	[a]	[a]	73.1	26.9
Sr	60.6	39.4	59.2	40.8
Y	72.2	27.8	89.5	10.5
Ba	81.5	18.5	65.0	35.0
La	13.3	86.7	59.8	40.2
Ce	[b]	[b]	87.9	12.1
Nd	[b]	[b]	80.5	19.5
U	[b]	[b]	91.5	8.5

[a] Computed fractions for these elements were less than zero and had no physical meaning.
[b] Filtration reduced concentrations of these elements to below detection limits.

As seen in Table 3.4, concentrations of most elements in unfiltered samples (whole water samples) that were acidified upon collection predicted mixing fractions better than samples that were filtered and then acidified. Concentrations of several elements in filtered samples, including Ca, Sc, Ga, several of the REEs, and U, were

either below detection limits or yielded computed source fractions that were meaningless, *e.g.*, negative; concentrations of these elements measured in unfiltered, acidified samples predicted mixing well. These data demonstrate that some elements predicted mixing to within 10% of the measured flow rates (Si, K, Ca, Sc, V, Mn, Ga, Y, Ce, Nd, and U in unfiltered samples) while others failed to predict mixing to within these limits (Li, B, C, Na, Mg, Al, Fe, Rb, Sr, Ba, and La in unfiltered samples). The discrepancy between predicted and measured flow fractions is likely due to errors in estimating the flow rates of the Sacramento and Feather Rivers upstream of the confluence. During this period, reservoir release rates were changing rapidly (California Data Exchange Center, 1997); travel times from the reservoirs to the locations at which samples were collected were on the order of a couple days, making the estimation of flow rates at the confluence difficult. In addition, the samples downstream of the confluence were collected from the edge of the river, and the two flows may not have been thoroughly mixed at this point. Nonetheless, it is clear from this and similar data collected at other confluences that unfiltered samples predicted mixing better than filtered samples; most samples collected subsequently were not filtered prior to acidification or analysis.

Both laboratory and field tests demonstrated that the same elements consistently predict conservative mixing when two freshwaters are mixed together. Some of these elements, however, may exhibit non-conservative behavior due to ion exchange and deposition of particulate matter when freshwaters mix with more saline waters. This effect is likely to be most pronounced at low to intermediate salinities, where sufficient river-borne particulate matter and high concentrations of Na^+ ions are available to

participate in exchange reactions and enhance coagulation processes. Further testing was designed to address this question.

3.5.2.2 Determination of maximum cation exchange capacities

Because exchange reactions are a likely cause of non-conservative behavior during estuarine mixing, both filtered and unfiltered grab samples were collected to determine the maximum possible cation exchange capacities. During most sampling trips, two sets of samples were collected: (1) whole water samples that were acidified upon collection; and (2) samples filtered as described in Chapter 2, with the filtrate immediately acidified.

Whole water samples, acidified to 2% nitric acid upon collection, were analyzed to determine maximum cation exchange capacities, defined operationally as the amount of an element released to solution from particles upon acidification. Such strong acidification (to a pH between 0 and 1) should result in the release of cations adsorbed to particle surfaces and possibly also in some dissolution of the particles themselves. Anionic species adsorbed to particle surfaces should also be partially released due to complexation of hydrogen ions with competing ligands, which are less likely to complex with the surfaces of particles that are positively charged due to acidification. In filtered samples, all particles larger than 0.45 μm were removed prior to acidification; the difference in elemental concentration between unfiltered and filtered samples therefore is indicative of the maximum possible release from particles for elements that would be present as cations in solution. Anionic release is likely also approximated by this measure.

Samples were collected and processed in this manner on twelve occasions between mid-August 1996 and the end of the study period in early March 1997. Appendix E contains the results of these investigations, plotted by element; each plot contains the results for each of the five sampling locations on each of the collection dates, expressed as a percent removal, with error bars representing the standard deviation on this estimate. The percent removal and standard deviation were computed as follows:

$$\% \text{ removed} = \frac{(c \pm SD)_{whole} - (c \pm SD)_{filtered}}{(c \pm SD)_{whole}} \times 100$$

$$= \left[\frac{c_{whole} - c_{filtered}}{c_{whole}} \pm \frac{SD_{whole} + SD_{filtered} + \left(\frac{c_{whole} - c_{filtered}}{c_{whole}}\right) \times SD_{whole}}{c_{whole}} \right] \times 100.$$

Also included in this Appendix are the measured flowrates on the San Joaquin and Sacramento Rivers for these dates. Plots are included in the order in which they are referred to below. A brief discussion of elemental speciation is provided below in an attempt to understand and explain observed behavior; additional detail, including considerable information from other studies and for other locations, is included in Appendix A

As seen in Appendix E, plots for B and Na show little or no removal by filtration in all samples collected, even in those collected during high flow events. The elements Ca and Sr show little or no removal except for samples collected during the extreme flood event of January 1997. During this peak of this flood event, as much as 30% of these elements is removed by filtration; the percentage removed declined as flow rates decreased after early January. Mg and K show similar behavior, but the percentages

removed by filtration during the January 1997 flood are as high as 65% and 35%, respectively; in samples collected as flow rates declined in late January, the percentage of these elements removed also declined. In samples collected prior to January 1997, the percentage removed remains below about 10% for both Mg and K. Based upon this analysis, these elements should behave conservatively, or nearly conservatively, within the estuary during non-flood periods.

Several elements were removed at levels of between 10% and 30% in samples collected at most stations before January 1997. These elements included Li, Si, Ga, Rb, Ba, and U. Exceptions occurred for Si and Ga, which were removed in higher amounts by filtration of water collected at Martinez, and Rb, which was removed in amounts exceeding 50% for all samples collected at Mossdale Landing on the San Joaquin River. The fraction of these elements removed by filtration during the January 1997 flood was high, ranging from about 60% to more than 90%.

Filtration resulted in significant removal for many other elements, including elements that are present in very high concentrations in particulate matter (*e.g.*, Fe and Mn) and elements that are known to have a strong affinity for particulate matter, including the REEs and Th. Additionally, the transition metals showed significant removal in freshwater samples, particularly during the January 1997 flood; although concentrations of transition metals could not be measured quantitatively in more saline samples, removal was still observed. Plots are included in Appendix E for V (which did not experience contamination during filtration and which is more easily measured in saline waters than other transition metals) and for La and Pr (chosen as representative of

the REEs). These elements are not likely to behave conservatively during estuarine mixing.

Boron is present in freshwaters and seawater primarily as H_3BO_3, the neutral species of boric acid. With a pK of about 9.3 (Stumm and Morgan, 1981), very little boric acid in the dissolved phase is ionized (1% or less). The fractionation between dissolved B and B adsorbed to particles is therefore not likely to be affected strongly by the acidification process used to treat these samples. (Note, however, that field observations have indicated that B is often removed during estuarine mixing; this effect is likely caused by adsorption to clay particles and is discussed in greater detail in Section 3.6.2 below and in Appendix A). In both river and saline waters, Na is present almost entirely as Na^+. Even if Na participated in ion exchange reactions on particles (adsorbing to particles and exchanging with other cations) and is subsequently removed, changes in dissolved phase concentrations would be negligible because of the very high concentrations of dissolved Na in natural waters.

The speciation of K is similar to that of Na, with only a very slight tendency to complexation with anions in river waters (0.08% occurring as $K\text{-}SO_4$ complexes, Aston, 1978) and a slightly larger tendency to complexation with anions in ocean waters (about 1%, Bruland, 1983). Mg, Ca, and Sr are all alkaline earth elements, and their behavior in solution is therefore expected to be similar. Mg and Ca are both present primarily as hydrated cations in river water (> 96%), with a slight tendency to complexation with sulfate, bicarbonate, and carbonate (Aston, 1978); Sr likely has similar speciation. All these elements are present in much higher concentrations in ocean (or Bay) waters than in

river waters, and ion exchange reactions with particles are likely to involve only a very small fraction of the total dissolved mass. During flood periods, there was very little Bay influence within the estuary, and samples had salinity levels typical of river waters at all stations; the particulate load carried by the rivers was, however, much larger than that carried during non-flood periods. The large percentage of these elements associated with particles during flood events was likely the result of partial dissolution of the particles themselves and ion exchange from particles caused by sample acidification. Removal by particle settling within the study area was possible, but ion exchange effects in the waters of the estuary were most likely a very minor effect during this period.

The elemental behavior of both Li and Rb should be similar to that of Na and K, the alkali metals discussed above. Li has an exceptionally large hydrated ion size (3.40 Å, compared to 2.76 Å for Na, 2.32 Å for K, and 2.28 Å for Rb, see Cotton and Wilkinson, 1988); because of this, it should be one of the least reactive of this group of elements in aqueous solution. Studies of Li speciation in seawater indicate that it is present primarily as a hydrated cation with only a slight tendency to complexation with SO_4^{2-} (Byrne *et al.*, 1988); it is probably present in freshwaters almost completely as a hydrated cation. Rb, on the other hand, is probably more reactive in aqueous solution, although its complexation in seawater is similar to that of Li (*ibid.*). The main factor accounting for differences in observed removal for these elements as compared with other members of this group is their lower concentration in freshwaters. During the study period, concentrations of Li and Rb were about 1000 times lower than concentrations of Na and K at all the sampling locations. Therefore, the amount adsorbed to particles is

likely to be a more significant fraction of the total mass of these elements present. This does not, however, explain why Rb is so strongly associated with particles in the San Joaquin River. Possibly a source of particulate matter in the river is enriched in Rb, and elevated concentrations in acidified whole water samples resulted from partial dissolution of these particles.

Like Li and Rb as compared to Na and K, Ba is present in much lower concentrations than the other alkaline earth elements. Concentrations of Sr range from 2 to about 50 times those of Ba, while concentrations of Mg and Ca are about 1000 times greater. This may account for its enhanced association with particles, as its speciation should be similar to that of the other alkaline earths (see, for example, Bruland, 1983, and Byrne *et al.*, 1988). Hanor and Chan (1977) found that concentrations of Ba were strongly enhanced in the Mississippi River estuary during mixing and proposed ion exchange onto and off of clay particles as the main mechanism.

Si and Ga exist in seawater in the dissolved phase primarily as hydrolyzed anions or neutral species (Bruland, 1983; Aston, 1978). Little data are reported for the speciation of Ga in fresh waters, but it is likely present primarily as $Ga(OH)_3$ and $Ga(OH)_4^-$, as in ocean water. Scavenging by particles in the ocean is reported to be a significant sink for Ga (Orians and Bruland, 1988a, 1988b). Significantly more information is available for Si than for Ga. Dissolved Si should be present almost entirely as silicic acid, $Si(OH)_4$, in both freshwaters and ocean waters (Aston, 1978; Bruland, 1983); the pK_1 of silicic acid is approximately 9.46 (Stumm and Morgan, 1988). Si has been shown to behave conservatively in some estuaries and to exhibit removal in

others; see Appendix A for detail. Non-conservative behavior is likely due to sedimentary fluxes of biogenic silica and biologically-mediated uptake; such processes have been observed in San Francisco Bay (Flegal *et al.*, 1991) and within the Delta estuary (Peterson *et al.*, 1985). These processes often involve conversion of dissolved silica to particulate silica and vice versa. Concentrations of Si are higher than concentrations of Ga in the estuary, and Si is therefore more likely to behave conservatively than Ga.

U is reported to behave conservatively in some estuaries and highly non-conservatively in others; where non-conservative behavior is observed, removal is likely due to reducing conditions, formation of insoluble phosphate compounds, and sorption onto sediment particles, particularly ferric oxyhydroxides (see, for example, Sarin and Church, 1994; Somayajulu, 1994; Plater *et al.*, 1992; Swarzenski *et al.*, 1995). In both fresh and saline waters, U probably occurs in the dissolved phase primarily as $UO_2(CO_3)_2^{2-}$ and $UO_2(CO_3)_3^{4-}$ (van den Berg, 1991 and 1993). Complexation of these uranyl ions with decaying organic matter can cause reduction of U(VI) to the insoluble U(IV) (Gascoyne, 1992). The behavior of U is highly dependent upon environmental conditions, which may vary between estuaries and with location in a given estuary; the behavior of U in the Delta was evaluated further by statistical comparison with other elements (see Section 3.6).

The transition metals (Ti through Zn, otherwise known as elements of the first transition series) show a strong affinity for particulate matter, with removals of 50% or greater for most of these elements for samples collected in the Delta. Compared to the

elements described above, the transition metals have a very complex chemistry. All except Zn can exist in multiple oxidation states, and most complex readily with organic matter. For many, including Fe and Cu, a large fraction of the total mass present may exist as colloidal particles; these are particularly prone to coagulation when freshwater mixes with saline waters. Because they are not likely to behave conservatively and because they cannot be measured accurately By ICP-MS in saline samples, their chemistry was not investigated further.

The REEs are known to adsorb strongly to particulate matter carried by rivers. Most adsorption is likely to Fe-organic colloids; removal during estuarine mixing is due to particle coagulation and is observed first for the lighter REEs and later for the heavier REEs (Sholkovitz, 1995); these observations are confirmed by laboratory tests (Koeppenkastrop and DeCarlo, 1992). The phosphorus geochemistry of an estuarine system may affect the coagulation behavior to a large degree, as the REEs readily form low solubility phosphate complexes (Byrne and Kim, 1993; Wood, 1990; Sholkovitz, 1995). In the dissolved phase, REEs are probably complexed with carbonate (Erel and Stolper, 1993; Goldstein and Jacobsen, 1988). Additional information is included in Appendix A; it is concluded from this literature review and from the field filtration studies that the REEs are not likely to behave conservatively within the Delta estuary.

In summary, those elements that are most likely to predict conservative mixing include the alkali metals and the alkaline earth elements that are present in relatively high concentrations, generally 50 ppb or larger in river waters (Na, Mg, K, Ca, and Sr) and B. These elements are present in much higher concentrations in seawater than in river water,

due largely to their conservative behavior. All except B are present primarily as hydrated cations in solution; B is present almost entirely as $B(OH)_3$. While they may participate in ion exchange reactions, the relative fraction of these elements that may exchange is small compared to the total mass present in the dissolved phase. Elements also present primarily as cations in the dissolved phase but that are present in lower concentrations (Li, Rb, and Ba) participate to a larger relative extent in ion exchange reactions, with subsequent removal on particles. The acidification of whole water samples may have resulted in the release of cations adsorbed to particles that may not have been released during estuarine mixing; for this reason, these elements may behave more conservatively during estuarine mixing than their maximum cation exchange capacities suggest. Other elements exhibiting some removal by filtration include Si, Ga, and U; Si and Ga have similar chemistry and may be removed by biologically mediated reactions, while U exhibits complex chemistry in estuarine environments and removal must be determined based upon ambient conditions. The remaining elements are strongly associated with particulate matter and are removed by particle coagulation and particle settling in estuarine environments.

3.5.2.3 Field observations

An additional consideration in the collection of field samples is that they be truly representative of conditions within the estuary. Local conditions that change the composition of samples may affect model results and predictions of mixing within the estuary. For example, resuspension of sediments at Martinez, mentioned in Section 3.3.1, probably causes elevated concentrations of elements that are associated with particulate

matter in samples collected at this location. If these elements were then used to predict mixing at receptor stations, the fraction of water arriving from Martinez would be strongly over- or underestimated. Similar processes at receptor sites would result in errors in the estimation of the distribution of source waters at that receptor site.

Evidence for resuspension at Martinez is two-fold: first, concentrations of many elements at Martinez are too high to be a combination of river and ocean waters, indicating an additional source; and second, element removal by filtration in samples collected at this location is anomalous when compared to observed removal at other locations. Based upon annually averaged river flow rates, samples collected at Martinez should be composed of about 85% Sacramento River water, 10% San Joaquin River water, and perhaps 5% water that originated from the Pacific Ocean. (Water originating from additional tributaries, such as the Mokelumne River, is typically lower in concentration than water from these other sources and is neglected in this simple analysis.) Concentrations of the transition metals, the REEs, Si, and Ga are in significantly lower in ocean water than in Delta river waters (see Bruland, 1983, for typical concentrations of these elements in ocean water). If mixing were conservative, concentrations of these elements would be much lower than concentrations measured in samples collected at Martinez. Filtration studies demonstrating that these elements adsorb strongly to particulate matter lead to the conclusion that resuspension is the most likely source of elevated concentrations at Martinez.

Additional evidence comes from looking at the plots of removal observed for Si and Ga, discussed in Section 3.5.2.2 and presented in Appendix E. Measured removal by

filtration for these elements is elevated for samples collected at Martinez, particularly for samples collected in August 1996 and on November 14, 1996; removals of 40% to 70% for Si and 30% to almost 60% for Ga were observed at Martinez, while removal of these elements at the other stations was generally 30% or below for both elements. Review of wind data collected for these periods confirms that winds were particularly strong over the Bay on these collection dates (U.S. Geological Survey, 1997). Although filtration experiments showed strong particle affinities for other elements, including Li and Rb, these elements are present in such high concentrations at Martinez (due to their high concentrations in ocean water) that any particle resuspension effects are masked. Elements for which concentrations at Martinez are enhanced due to resuspension were not used as tracers.

In addition to resuspension effects at Martinez, particle concentrations were enhanced at Bethel Island by extensive dredging conducted over a three-week period starting at the end of August 1996. In samples collected for filtration on September 18, 1996, observed removal by filtration for Li and U was strongly enhanced, indicating that particles suspended by dredging contained significant concentrations of these elements. Enhancement was less pronounced for other elements. The plots of element concentration in daily composite samples (included in Appendix D) also show these effects; concentrations of Li, Si, Ga, Rb, Ba, the transition metals, and the REEs are higher and exhibit more scatter between August 24 and September 24, 1996. These elements would not make good tracers, as their measured concentrations are highly dependent upon changes in the sampling environment. None of the elements that

exhibited low rates of removal by filtration exhibited enhanced removal rates or enhanced concentrations during dredging at Bethel Island.

3.6 Statistical analyses

3.6.1 General observations

To further understand the behavior of elements in source waters to the Delta, correlations between elements were determined by linear regression. In the Sacramento River, correlations were very high (r^2 correlation coefficients of 0.800 or higher) for elements that experienced strong increases in concentration when the river flow rate increased. Elements in this category included Rb, Ga, Ba, La and Nd (taken as representative of the REEs) and Co (representative of the transition metals). Elements that were not strongly correlated with one another included those for which concentrations decreased as flow rates increased; the r^2 correlation coefficients for these elements were generally less than 0.500. Exceptions include strong correlations between the following pairs of elements: Ca and Mg ($r^2 = 0.808$); Mg and Sr ($r^2 = 0.908$); and Ca and Sr ($r^2 = 0.733$).

More interesting were correlations computed for elemental concentrations and measured flow rate in the Sacramento River. Results of this computation are summarized in Table 3.5; the elements V and Co were included as representative of the transition metals, and La and Nd were included as representative of the REEs. As shown in Sections 3.5 and 3.6, elements for which concentration falls as flow rate rises are the

elements most likely to predict conservative mixing. Elements that exhibited a strong increase in concentration when the flow rate increased included Co, Ga, Rb, Ga, La, and Nd; these elements, as shown in Section 3.5, were strongly associated with high concentrations of particulate matter. The elements that exhibited relatively weak but positive correlations with flow, including Li, K, V, Mo, and U, were adsorbed to particulate matter to an intermediate extent.

Table 3.5
Correlations between measured flow rate and measured elemental concentrations in the Sacramento River

Parameter	$r^2 > 0.500$	$0.300 < r^2 < 0.500$	$r^2 < 0.300$
Positive correlation between flow rate and concentration	Ga, Co, Rb, Ba, La, Nd	K, V	Li, Mo, U
Inverse correlation between flow rate and concentration		B, Na	Mg, Ca, Sr

For data collected from the San Joaquin River, correlations between concentrations of pairs of elements were determined by linear regression, as were correlations between the concentration of an element and the river flow rate. Element-element correlations were strong ($r^2 > 0.800$) for all possible combinations of the following elements: Rb, Ba, Ga, La, V, Co, and Nd. In addition, strong correlations were observed for the following pairs of elements: B and Na ($r^2 = 0.898$); B and Sr ($r^2 = 0.868$); Na and Sr ($r^2 = 0.910$); and Li and Ba ($r^2 = 0.805$). In contrast to the correlations observed for the Sacramento River, the highest correlations between concentration and flow rate for the San Joaquin River were observed for B, Na, Mg, Ca, and Sr. For these elements, r^2 ranged from 0.330 to 0.542; for all other elements, the r^2 correlation

coefficient was below 0.179. As in the Sacramento River, concentrations of these elements decreased as river flow rate increased. Concentrations of K, Ga, Rb, Ba, V, Co, La, and Nd increased as flow rates decreased. This information is summarized in Table 3.6.

Table 3.6
Correlations between measured flow rate and measured elemental concentrations in the San Joaquin River

Parameter	$r^2 \geq 0.330$	$r^2 < 0.180$
Positive correlation between flow rate and concentration		K, Ga, V, Co, Rb, Ba, La, Nd
Inverse correlation between flow rate and concentration	B, Na, Mg, Ca, Sr	Li, Mo, U

Because reservoir releases remained abnormally high after early January 1997, flow rates in the San Joaquin River did not decline in a typical fashion after the flood of January 1997; excluding data collected beyond mid-January yields a dataset that is likely more typical of the "normal" range of flow conditions. The calculations made above were repeated for this truncated dataset. Between pairs of elements, computed correlation coefficients remain almost unchanged. Correlations between elemental concentrations and river flow rate do change significantly, however. Correlations remain highest for B, Na, Mg, Ca, and Sr (r^2 ranging from 0.236 to 0.454), but correlations between flow rate and concentration for Ga, Ba, V, Co, La, and Nd are higher (r^2 ranging from 0.260 to 0.325). Correlation coefficients for all other elements are below 0.130. Results are summarized in Table 3.7.

Table 3.7
Correlations between measured flow rate and measured elemental concentrations in the San Joaquin River for samples collected before January 18, 1997

Parameter	$r^2 > 0.236$	$r^2 \leq 0.236$
Positive correlation between flow rate and concentration	V, Co, La, Nd	Li, K, Ga, Rb, Ba
Inverse correlation between flow rate and concentration	B, Na, Ca, Sr	Mg, Mo, U

Differences in values between correlations computed for data obtained before mid-January and for the entire dataset show the importance of the origin of the water passing the sampling location (rather than simply the flow rate). Generally, very high flows are associated with storm events, and the water passing a sampling location includes a significant fraction of local runoff, which carries high concentrations of particulate matter. Low flows are associated with reservoir releases and, other than agricultural return flows, do not include a significant fraction of local runoff or very high particulate loads. After the flood of January 1997, river flow rates remained high due to high reservoir releases, but the fraction of flow from local runoff decreased steadily after mid-January. Consequently, concentrations of elements generally associated with high flow conditions fell even though flow rates remained high.

Elements that exhibited an inverse correlation between flow rate and concentration were less likely to be associated with particulate matter carried by rivers and exhibited steadier source concentrations both temporally and spatially. Although individual behavior from one estuary to another will vary, it is likely that elements that behave conservatively will exhibit the same inverse correlation; this simple analysis, therefore, might be used to screen elements for use as tracers in other estuaries.

3.6.2 Statistical analysis for selection of tracers

To further select elements for use as tracers and to predict the fractions of source waters ("source fractions") arriving at receptor sites within the Delta, a simple model was created based upon linear algebraic principles. This model assumed that all water arriving at a receptor site was from one of the three sources in the study area; further, it assumed conservative mixing, so that no correction was made to account for elemental adsorption to particles with subsequent removal or addition. This model was used to compare the behavior of elements that prior study had shown were likely to behave conservatively (see Section 3.5) to each other and to elements that were not likely to behave conservatively. The elements that were likely to behave conservatively, including B, Na, Mg, K, Ca, and Sr, exhibited source concentrations that varied little over timescales shorter than mixing timescales, and removal or addition processes leading to non-conservative behavior were believed to be minimal for these elements (this will be revisited below). Once conservative mixing was established for these elements (excluding B and K), the predicted mixing behavior of the elements only moderately associated with particulate matter (including Li, Ga, Rb, Ba, and U) was compared to that of the conservative elements. The model was used to confirm that the lack of certainty about travel times between Martinez and receptor sites was insignificant in determining the distribution of river waters in the Delta. Finally, the model was used to predict the relative fractions of source waters in samples collected at Bethel Island and Clifton Court; model results are presented in detail in Section 3.7 below.

In mathematical terms, mixing within the Delta was assumed to be conservative, so that:

$$c_{LK} f_{LK} + c_{ML} f_{ML} + c_{MZ} f_{MZ} = c_{receptor},$$

where the symbol f_{LK} represents the fraction of water arriving at the receptor location from the Sacramento River at Locke; f_{ML} represents the fraction from the San Joaquin River at Mossdale Landing, and f_{MZ} represents the fraction from the Bay at Martinez. Because all water at a receptor was assumed to arrive from these sources, these source fractions were forced to add to 1. The concentrations of the source waters and of water collected from a receptor location are known; a simple mathematical formulation was developed to solve for the unknown source fractions:

$$\begin{bmatrix} c_{a,LK} & c_{a,ML} & c_{a,MZ} \\ c_{b,LK} & c_{b,ML} & c_{b,MZ} \\ 1 & 1 & 1 \end{bmatrix} \times \begin{bmatrix} f_{LK} \\ f_{ML} \\ f_{MZ} \end{bmatrix} = \begin{bmatrix} c_{a,receptor} \\ c_{b,receptor} \\ 1 \end{bmatrix}.$$

This system solves for the source fractions at a receptor location using the concentrations of two elements, c_a and c_b. This model is similar to the model used to predict mixing downstream of a freshwater confluence in Section 3.5. At a freshwater confluence where there are two sources, source fractions are forced to add to 1, and a solution is obtained using the concentration of a single element; here, three unknown source fractions are forced to add to 1, and source fractions are predicted using a pair of elements. The solution for the source fractions in this system of equations was obtained using Mathematica. Note that this model does not determine error for the source fraction computed using a pair of elements. Also, the model does not exclude negative computed

source fractions, although these were not observed except during conditions of extremely high flow, *e.g.*, during the January 1997 flood. A more sophisticated model would allow inclusion of error on the measured concentrations and would yield a solution that is accompanied by an estimate of the error present in the computed result.

To evaluate elemental behavior within the estuary, source fractions were computed for all possible pairs of elements for weekly averages of the elemental concentrations for the entire study period. Concentration data were averaged on week-long timescales because source fingerprints were relatively constant over the period of a week; also, an averaging process such as this compensates for day-to-day variations in concentration and for differing travel times from source to receptor. Because source fingerprints changed least during the dry season, elements were selected as tracers based upon model evaluations during this period; results using the selected tracers were then evaluated during the wet periods preceding and following this dry period. A discussion of the validity of the model is provided in Sections 3.6.2.1 and 3.6.2.2, below; computed results are presented as Figures 3.9 through 3.21 and are discussed in detail in Section 3.7.

3.6.2.1 Model validity during the dry season

The first measure of the success of a pair of elements in predicting mixing at a receptor site was the "realism" of the predicted source fractions. Source fractions ranging between -0.05 and 1.05 were considered physically reasonable. Results consistently fell in this range during the dry season for the elements Na, Mg, Ca, and Sr; source fractions generated by these elements agree with expectations based upon river flow rates and

barrier and gate configurations (see Sections 3.7.2.1 through 3.7.2.4). Results for B and K were less consistent, usually falling within this range but occasionally predicting values dramatically outside this range. As shown in Tables 2.3 through 2.6 of Chapter 2, concentrations of K were difficult to measure accurately in the waters of the study area, particularly in San Joaquin River water. Measurement errors and inconsistencies are the likely cause of the failure of K to reasonably predict source fractions. This was not the case for B, which could be measured accurately in Delta waters. It is more likely that B did experience non-conservative behavior within the estuary, likely due to adsorption onto particulate matter that was then removed by coagulation and settling. This behavior may not have been reproduced by filtration studies because B is present predominantly as the neutral $B(OH)_3$ in solution, and therefore adsorption-desorption behavior would not be strongly affected by acidification. Extensive adsorption to particles has been observed both for soil-water solutions and for particles in other estuaries (see, for example, Sposito, 1989; Bergerson, 1984; Narvekar, 1983; details are included in Appendix A). Based upon this analysis, Na, Mg, Ca, and Sr were selected as tracer elements and are referred to below as "primary tracers;" their behavior during wet periods is discussed in greater detail below.

Because travel times from Martinez to the receptor sites could not be readily estimated, values of the primary tracers in waters from Martinez were varied to gauge the effect of such error on the model results. Typical of the results were the computed source fractions for the pair of elements (Na, Sr); measured values of the concentrations of these elements averaged over the week ending October 5, 1996 are given in Table 3.8. Shown

in Table 3.9 below are model results computed for this element pair. Concentrations of these elements were varied by 30% for data collected during the week ending October 5, 1996; as shown in the table, these variations produced only very minor changes (<1%) in the predicted source fractions for the Sacramento River and San Joaquin Rivers. The predicted source fraction for Martinez changed by a larger factor (up to 40%) but remained consistently low. Other pairs of the primary elements predicted similar results during the dry season.

Table 3.8
Measured concentrations of tracer elements averaged over the seven-day period ending October 5, 1996

Location	Na concentration [ppm]	Mg concentration [ppm]	Ca concentration [ppm]	Sr concentration [ppb]
Sacramento River at Locke	7.43	5.25	4.93	69.1
San Joaquin River at Mossdale Landing	61.4	18.2	17.2	362
Bay at Martinez	4,190	505	88.9	3,750
Bethel Island	29.3	9.45	5.38	114
Clifton Court	34.6	9.04	7.36	142

Table 3.9
Variation in model predictions caused by simulated error in measured concentrations at Martinez: Computed for the element pair (Na, Sr) using concentration values averaged over the seven-day period ending October 5, 1996

Condition	Source fraction from the Sacramento River $f_{Sacramento\ River}$	Source fraction from the San Joaquin River $f_{Mossdale\ Landing}$	Source fraction from the Bay at Martinez $f_{Martinezr}$
Bethel Island:			
original values	0.908	0.087	0.0054
original values - 30%	0.906	0.087	0.0077
original values + 30%	0.909	0.086	0.0041
Clifton Court:			
original values	0.780	0.218	0.0024
original values - 30%	0.779	0.218	0.0035
original values + 30%	0.781	0.217	0.0019

The second set of elements evaluated using this model included Li, Ga, Rb, Ba, and U. Concentrations of these elements varied more over time and adsorption to and possible removal with particles was enhanced when compared to the primary tracers. Still, if particles (and the elemental mass they carried) traveled through the estuary rather than settling out, mixing may still have been conservative for these elements. Source fractions generated by pairs of these elements with each other and with the primary tracers were evaluated; calculated source fractions varied considerably when compared to those predicted by the primary tracers. Still, values generally fell within the range of -0.05 to 1.05. Often, pairs of these elements (particularly pairs including Ga or Ba as one of the two elements) greatly overpredicted the source fraction from Martinez; resuspension effects are the likely cause. Pairs including U as one element predicted source fractions that were nearer those predicted by the primary elements, particularly for

samples collected from Bethel Island. These predictions were not consistent, however; at Bethel Island, predictions were particularly poor during the period of dredging, from the end of August 1996 through the end of September 1996. Because these results were not consistent, final model results were obtained using only the primary tracers.

Surprisingly, source fractions predicted by pairs including either a transition metal or a REE often fell within the range of reasonable values; these predictions exhibited a greater range than predictions made with the elements discussed above. This confirms that, as expected, not all particulate matter carried by the rivers is removed before it leaves the estuary. This analysis is complicated by the fact that resuspension effects at Martinez probably affected concentrations of these elements in water collected from this source; indeed, the source fraction for water from Martinez is generally overpredicted by these elements, particularly during periods of high winds (and therefore high resuspension). Because of these uncertainties, source fractions generated by these elements, even when falling within the range of reasonable values, are not reliable.

3.6.2.2 Model validity during high flow periods

During high flow periods, concentrations of all elements in source waters can vary significantly on timescales that are shorter than the mixing timescales estimated for the study area (see Section 3.4.1). Concentrations of particulate matter and the associated mass of elements are higher during these periods. Particle settling and element removal is likely enhanced, particularly in the channels of the central Delta, where channels are wider and more meandering and where flows are less turbulent. During extremely high flow periods, the portion of even the primary tracers associated with particulate matter is

high, ranging from about 25% for Ca and Sr to 40% - 60% for Mg. Only Na and B exhibit concentrations that are almost unchanged between samples that were filtered before acidification and whole water samples that were acidified upon collection, suggesting that they are present almost exclusively in the dissolved phase.

Because sampling at Martinez did not begin until April 13, 1996, source fractions are predicted at receptor stations only after this date. During the first high flow period, extending through mid-June, source fractions predicted by the primary tracers exhibit much more scatter and do not always fall within reasonable limits. The standard deviation computed for these source fractions is large, particularly for the weeks ending May 4, 1996, and May 11, 1996. During these weeks, flow rates on the San Joaquin River were relatively steady, but flow rates on the Sacramento River varied by a factor of about two. Presumably, the fraction of the total element flux carried by particles changed on the Sacramento River during this period also; this variation may account for the scatter in the predicted source fractions. During these period, several of the criteria for tracing flows are stretched, and predicted source fractions through this period should be regarded as qualitative at best.

The period following the dry season began in early December, when winter storms and high reservoir releases caused increased flow rates and particulate loads on both rivers. Variations in concentration were linear on the San Joaquin River. Variations were more dramatic on the Sacramento River, where concentrations dropped by as much as a factor of two in one five-day period. Still, concentrations varied in a linear fashion, and week-long averages of the data probably compensated for much of the day-to-day

variation. Model predictions through the period ending on December 21, 1996, were fairly consistent. Only when a major storm hit immediately after this period, signaling the start of the flood period of January 1997, did model predictions yield results that fell outside reasonable levels.

During the January 1997 flood, salinity throughout the study area fell to freshwater levels, and concentrations varied by factors of three to four on timescales of a few days. Variations in concentration, although dramatic, were fairly regular, but model predictions were unreasonable and erratic (see Appendix G). The most likely factor, as noted in Section 3.3.2, is an additional source of water in the south Delta. Because concentrations of Na and other major ions were higher at both Clifton Court and Bethel Island than at any of the source locations during this period, agricultural drainage (which often has elevated salinity levels) from the islands in the south Delta is the likely extra source. Flow rates of agricultural drainage were high enough to elevate salinities locally but not high enough to cause an increase in salinity at Martinez. During this period, the assumption that all water comes from the San Joaquin River, the Sacramento River, and the Bay as measured at Martinez is invalid, and the model cannot accurately predict source fractions. Model predictions for the entire study period, including this flood period, are included in Appendix G and show clearly the unrealistic source fractions computed when model assumptions are invalid.

3.7 Results and conclusions

3.7.1 Predicted mixing in the Delta

The statistical model described in Section 3.6.2 was used to predict source fractions at Bethel Island and Clifton Court for two different averaging timescales: for the entire study period, seven-day averages of the data were used to compute source fractions; and for the fall period, when barrier configurations and Delta Cross-Channel gate operations were changing, the model was used to compute source fractions for three-day averages of the data. The elements Na, Mg, Ca, and Sr were used in the model, as discussed above; for each seven-day (or three-day) period, the source fraction was computed using all six possible pairs of elements. Results are presented graphically; each plotted source fraction is the average of source fractions computed for the six possible pairs of these elements. The "error bars" represent the standard deviations on the source fractions computed for these element pairs. The discussion in Sections 3.7.1.1 through 3.7.1.4 and Figures 3.9 through 3.21 are based upon this method of source fraction computation. These data could also be evaluated using alternate methods for evaluating error or selecting a "best-fit" source fraction; some of these possibilities are discussed in Section 3.7.2 below.

3.7.1.1 Seven-day averages for Clifton Court

As discussed in Section 3.6.2, results of the statistical model were consistent during the dry period; results were qualitative and exhibited more scatter between April 20, 1996 and June 8, 1996. From December 21, 1996 through the end of the study period

in March 1997, model assumptions were invalid. Results computed over the entire sampling period including this flood period are included in Appendix G; they demonstrate the large "error," computed as the standard deviation of calculated source fractions, in source fractions computed from concentration data collected during the flood. During this period, the model fails because not all sources of water to the system are adequately described. Figures 3.9, 3.10, and 3.11 show the results of model computations through December 21, 1996, for samples collected at the Clifton Court receptor location. Note that data were missing due to pump failures for the weeks ending June 15 and 22, 1996, August 10 and 17, 1996, and from February 15, 1996, through the end of the study period; computations were not made for the weeks ending May 18 and 25, 1996, because of pump failures at the Locke sampling station.

The fraction of Sacramento River water computed by the model is shown in Figure 3.9. Initially, Sacramento River water comprises between 10% and 30% of the water collected at Clifton Court; error estimates for these fractions are large. This fraction grows beyond June 1, 1996, reaching 52.8 ± 15.3% (where 15.3% represents the standard deviation of the source fractions computed using six pairs of elements as described in Section 3.7.1) for the week ending June 8, 1996, and 71.7 ± 3.5% for the week ending June 29, 1996. The Delta Cross-Channel gates were opened on June 12, 1996. Flow rates in both the Sacramento and San Joaquin Rivers were changing significantly prior to this period, and steady-state conditions for low (dry season) river flow had not established prior to the opening of the gates. However, it is likely that the opening of the gates did allow Sacramento River water that otherwise would have flowed

directly to the Bay to reach the south Delta and Clifton Court. Through the remainder of the summer, the Cross-Channel gates remained open, and the fraction of water arriving from the Sacramento River to Clifton Court remained high, usually above 80%. A sharp decrease in this source fraction was computed for the weeks ending October 19 and 26, 1996; this is likely due to the removal of flow barriers in the south Delta (see Section 3.7.1.3 below for more detail). After this sharp decrease, the source fraction from the Sacramento River returned to values near 80% until the week ending November 16, 1996, when the source fraction declined to around 70%. This can be directly related to Delta Cross-Channel gate operations, as the gates were closed on November 12, 1996, and then reopened briefly from November 15 through 20, 1996. Clearly, the closure of these gates allowed less Sacramento River water to reach the south Delta.

The computed fraction of San Joaquin River water in samples collected at Clifton Court is shown in Figure 3.10. This fraction and the fraction from the Sacramento River very nearly add to one. The fraction of San Joaquin River water in Clifton Court samples is high at the start of the sampling period (about 83 ± 22%). An intermediate value of 49.4 ± 20.2% was computed for the week ending June 8, 1996, with values stabilizing for the remainder of the summer at 30% or below. The lowest value computed for this fraction was 7.9 ± 2.0% for the week ending August 31, 1996. In addition to the opening of the Delta Cross-Channel gates on June 12, 1996, two flow barriers were installed in the south Delta in this period. These barriers, located at Middle River and on the Old River at Tracy (features C and D on Figure 3.1), became operational on June 5 and 10, 1996, respectively. These barriers raised water levels in Middle and Old Rivers and changed

the hydraulic gradient between the San Joaquin River and Clifton Court so that flow through these channels was restricted. A slight increase in the San Joaquin River source fraction is observed between September 28 and October 12, 1996, when barriers were removed from the south Delta, followed by a decrease, then a rise again after the closure of the Cross-Channel gates. Additional detail on this fall period is provided in Section 3.7.1.3 below.

Perhaps the most important result of this modeling is the computed fraction of water arriving at Clifton Court from the Bay. The water quality at Clifton Court is monitored closely because this is an export location; when water quality is poor, usually due to high total dissolved solids (salinity), exports are curtailed. There has been considerable controversy as to the route by which poor quality (high salinity) water reaches the export pumps; many have speculated that it is carried in from the Bay by tidal action. For all dates through the end of December 1996, average values computed for this source fraction are less than 1% (although the standard deviations of the predicted source fractions are occasionally slightly larger than this value). The fraction of salinity arriving from each source location to Clifton Court is computed and discussed in detail in Section 3.7.1.3 below.

3.7.1.2 Seven-day averages for Bethel Island

The autosampler at Bethel Island functioned well during the entire sampling period; therefore, the only dates missing in the computations for source fractions at Bethel Island are for the weeks ending May 18 and 25, 1996, when samples were not collected at Locke. Figures 3.12, 3.13, and 3.14 show the computed fractions of water

from the Sacramento River, the San Joaquin River, and the Bay, respectively, for the period beginning April 20, 1996 and ending December 21, 1996. Computations for the entire study period are included in Appendix G and include results for the period when model assumptions were violated; as with the results computed at Clifton Court, model calculations during this period confirm that incomplete identification of all sources of water to the system causes nonsensical results.

Errors in the computed fraction of Sacramento River water arriving at Bethel Island are large through June 8, 1996. During this period, flow rates in both rivers were changing rapidly and mixing patterns throughout the estuary were probably unsettled. The estimated source fraction from the Sacramento River ranges from 30% to 80% during this period. After this period, conditions at Bethel Island were nearly constant through the end of September, 1996. The Cross-Channel gates were open and the barriers at Middle River and at Old River at Tracy in the south Delta had been installed. The source fraction is generally greater than 85% throughout this period and reaches a maximum for the week ending September 7, 1996, with a value of 98.1 ± 1.7%. This fraction falls to a value of 61.3 ± 36.8% for the week ending October 19, 1996, after the removal of barriers in the south Delta; the fraction then rises steadily again to about 95% for the week ending November 23, 1996, then falls to below 80% after the closure of the Delta Cross-Channel gates. When the fraction of water from the Sacramento River is high, the standard deviations of the computed source fractions are small; when this fraction falls, the standard deviation increases dramatically. This is likely due both to the rapidly changing

flow rates (and mixing patterns) and to possible losses of elements associated with particulate matter, which are present in higher concentrations in San Joaquin River water.

As at Clifton Court, the computed fractions of Sacramento and San Joaquin River waters in samples collected from Bethel Island add to nearly one; their sum decreases to about 0.975 near the end of December 1996. Therefore, many of the same observations apply. The fraction of San Joaquin River water is relatively high through June 8, 1996, when it falls to below 20%. It decreases from about 15% to about 2.5% through the summer to the beginning of September 1996 and shows a sharp increase to almost 40% for the week ending October 19, 1996. It then falls, almost linearly, to a value of 3.4 ± 10.0% for the week ending November 23, 1996. After the closure of the Delta Cross-Channel gates, the fraction of water collected from Bethel Island that originated in the San Joaquin River rises again to a value of 23.5 ± 10.5% on December 21, 1996. As with computed source fractions for the Sacramento River, standard deviations computed for these source fractions are largest when the fractions of flow from the San Joaquin River are highest.

The fraction of water arriving at Bethel Island from the Bay, as measured at Martinez, is also uniformly low. This fraction is near zero at the beginning of the dry season and rises to a value of 2.45 ± 0.20% for the week ending November 30, 1996. This provides additional confirmation of the low fraction of water from Martinez at Clifton Court; because Bethel Island is west of Clifton Court, the fraction of Bay water at Bethel Island must be higher than the fraction at Clifton Court. This source fraction

therefore provides an upper bound on the source fraction at Clifton Court, useful for the periods during which data is missing at Clifton Court due to station pump failures.

3.7.1.3 Three-day averages for Clifton Court during fall 1996

During the period beginning in mid-September 1996, barrier configurations and Delta Cross-Channel conditions were changed several times. To understand the effects of these changes on mixing patterns in the Delta, the model was used to compute source fractions for three-day averages of concentration data. To accommodate the travel time from source to receptor (now on the order of the three-day averaging time), a two-day lag time was selected between source concentrations and receptor concentrations. The barriers that had been installed in Middle River and in Old River at Tracy in June were breached on September 29, 1996; removal was completed at both locations on October 15, 1996. The Grantline Canal barrier was removed on October 2, 1996. The barrier at the head of Old River (near Mossdale Landing) was installed on October 3, 1996, and removed on November 19, 1996. Finally, the Delta Cross-Channel was open between the mid-June and November 12, 1996, and again between November 15 and November 20, 1996.

Measurements of the stage in Old River at Tracy illustrate dramatically the changes water surface elevation during this period (California Data Exchange Center, 1997). These are included as Figure 3.15. Before the removal of the barriers at Middle River, Old River at Tracy, and Grantline Canal, the water surface elevation near Tracy (behind, or to the east of, the barriers) is artificially elevated. After these barriers are removed and the barrier at the head of Old River is installed, the lowest water level in Old

River falls by about 2.5 feet and tidal fluctuations become much more pronounced. The removal of the barrier at the head of Old River and the closure of the Delta Cross-Channel gates in mid-November have little effect on the stage at this location.

The fraction of water at Clifton Court that originates in the Sacramento River is shown in Figure 3.16. This source fraction is 89.6 ± 6.6% for the three-day period ending September 18, 1996; it declines steadily to a value of 76.3 ± 2.4% for the period ending October 12, 1996. From this point it declines more steeply to a low value of 46.9 ± 20.1% for the period ending October 24, 1996. This steep decline is probably due to the removal of barriers at Middle River and in the Old River at Tracy. There was also a slight increase in the flow rate of the San Joaquin River beginning on October 12, 1996, which may have influenced this pattern. After this low, the computed fraction returned to values of about 80% before declining again toward the end of November 1996, presumably due to the closure of the Delta Cross-Channel and the removal of the barrier at the head of Old River.

The source fraction from the San Joaquin River is shown in Figure 3.17; again, source fractions from the San Joaquin and Sacramento Rivers add to nearly one. After the removal of the barriers at Middle River, Old River at Tracy, and Grantline Canal, and after the installation of the barrier at the head of Old River, the value of this source fraction increases from about 20% to just over 50%. The fraction then falls again to about 10%, rising only after the closure of the Cross-Channel gates and the installation of the barrier at the head of Old River.

The value of the source fraction for water arriving at Clifton Court from the Bay at Martinez remains below 1% for the entire fall period; see Figure 3.18. These results agree well with those for the seven-day averages of concentration data (shown in Figure 3.11). The standard deviation on the estimate of this source fraction increases in early November; the cause of this increase is unknown.

To assess the relative proportion of salinity at Clifton Court that is contributed by each source, the Na concentration was used as a surrogate for total salinity; computed source fractions were multiplied by observed Na concentrations for each water source. Results are plotted as percentages of total Na in Figure 3.19. "Error bars" were computed by multiplying the standard deviation obtained from the source fraction computation by the Na concentration averaged over each three-day period. Near the beginning of the fall period, approximately 35% of the Na at Clifton Court originated from the Sacramento River; through the end of September, the source fraction from the Sacramento River, representing the fraction of total flow, remained above 80%. The percent of Na contributed by the Sacramento River fell to about 10% later in the fall as the source fraction decreased to about 50%. Approximately 30% of Na at Clifton Court arrived from Martinez through the end of September, and between 25% (in mid-September) and 45% (at the end of September) arrived from the San Joaquin River. Through early November, these proportions fluctuated, but the proportion of Na from the Sacramento River remained small (less than 20%) and the fractions of Na from the San Joaquin River and from Martinez remained similar, with the San Joaquin River contributing slightly more Na on average to the water at Clifton Court. Both computed source fractions

(representing the fraction of total water flow) from Martinez to Clifton Court and Na concentrations measured at Martinez were highest during the fall period; therefore, the largest contribution to total Na in water arriving at Clifton Court from Martinez was made during this fall period. That the contribution from the San Joaquin River remained equal to or slightly more than the contribution from Martinez demonstrates the importance of San Joaquin River water in determining water quality at the export pumps at Clifton Court.

3.7.1.4 Three-day averages for Bethel Island during fall 1996

The model was used to compute source fractions for three-day averages of water collected at Bethel Island. Again, a two-day lag time was used to compensate for the travel time of water between source and receptor. The fraction of Sacramento River water in samples collected at Bethel Island is shown in Figure 3.20. This fraction remains near or above 90% for the entire fall period except between October 12, 1996, and November 2, 1996. During this period, source fractions fall to a low value of 60.5 ± 38.4%. The standard deviations of these estimates are large.

Source fractions from the San Joaquin River are shown in Figure 3.21. Fractions are relatively uniform at about 10 - 15% excluding the period between October 12, 1996, and November 2, 1996, when concentrations rise to a peak value of 38.7 ± 39.2%. Again, standard deviations for these fractions are large, but comparison with the peak in this source fraction at Clifton Court lends credence to these data. In Figure 3.17, we see that the peak of this source fraction at Clifton Court is 52.8 ± 20.3%; the width of this peak is about 15 days. The peak for data collected at Bethel Island is lower and lasts about 22

days. Although mixing with additional Sacramento River water has occurred, it appears that there is a "slug" of San Joaquin River water traveling toward the bay after the breaching of barriers in the study area. The decreased magnitude and the elongation of this slug reflect the effects of longitudinal dispersion.

Finally, source fractions for the Martinez source were computed and are shown in Figure 3.22. Again, results agree well with those computed for seven-day averages of the data, peaking at 2.42 ± 0.15% for the three-day period ending November 29, 1996. Other than this slug of water passing Bethel Island, the barrier and Cross-Channel gate configurations have little effect on the source fractions observed at Bethel Island.

3.7.2 Alternative approaches to computation of source fractions and error analysis

Section 3.6.2 presented the method used to obtain the results shown in Figures 3.9 through 3.14, Figures 3.16 through 3.19, and Figures 3.20 through 3.22. For this method, source fractions were computed for six possible pairs of the elements Na, Mg, Ca, and Sr; an average value was obtained by averaging the six computed source fractions, and a standard deviation was computed for these six pairs of elements to give a measure of the "scatter" of the source fractions computed by each of the possible pairs. Computing source fractions in this manner allowed the evaluation of source fractions computed using other elements; for example, B and K were eliminated as tracers based upon these calculations (see Section 3.6.2.1). This method also confirmed that model assumptions were invalid during certain time periods (*e.g.*, during the January 1997 flood event). There are several other possible methods to compute source fractions and provide

estimates of the error on source fractions. Two of these are discussed below. In Section 3.7.2.1, a method is presented for choosing the source fraction computed by elemental pairs that minimizes errors in predicted elemental concentrations (Brooks, 1997); in Section 3.7.2.2, an effective variance least-squares fitting technique for determining source fractions is discussed.

3.7.2.1 Selection of the "best" source fraction computed from elemental pairs

The method described in Section 3.6.2 computes the three major source fractions in the Delta using a pair of elements. When the selected tracer elements Na, Mg, Ca, and Sr are used, six separate sets of source fractions are computed, one for each possible element pair. The results described in Section 3.7.1 were obtained by averaging the source fractions calculated for each of these six pairs of elements and by computing the standard deviation for the six element pairs. Additional information can be obtained by computing the error in concentrations of all four elements predicted by source fractions computed by a single pair of elements. By comparing error computations for each of the six element pairs, the element pair that produces the least error can be identified. An example of this calculation is provided in Table 3.10.

In Table 3.10, concentrations of the four tracer elements measured in samples collected from the three sources and from Bethel Island were averaged over the seven-day period ending September 14, 1996. Source fractions were computed for each of the six element pairs (see Section 3.6.2) using these measured concentrations. Elemental

concentrations predicted by the source fractions were computed for a given element pair as:

$$C_{element,predicted} = f_{Sacramento}C_{element,Sacramento} + f_{San\ Joaquin}C_{element,San\ Joaquin} + f_{Martinez}C_{element,Martinez}.$$

Predicted concentrations corresponding to each element pair are shown in the table. Finally, the relative error was computed as:

$$Percent\ error_{element} = \frac{C_{measured,\ Bethel\ Island} - C_{predicted\ by\ source\ fraction}}{C_{measured,\ Bethel\ Island}} \times 100.$$

Because there is an exact solution for the two elements in the element pair used to compute source fractions, the relative error for these two elements is zero. The relative error for the predicted concentrations for the other two elements is used to evaluate the fit of the chosen element pair.

As shown in by the data in Table 3.10, source fractions predicted by the element pair containing Na and Sr (Na, Sr) yielded the smallest error in predicted concentrations; predicted concentrations for Mg and Ca differed by less than 5% from measured values. For this seven-day average of concentration data at Bethel Island, this source pair yielded the "best" prediction. Relative error predicted by the element pair (Na, Ca) was nearly as low as that for (Na, Sr); relative errors for the pairs (Na, Mg), (Mg, Ca), and (Mg, Sr) were below 20%. Relative error for the pair (Ca, Sr) was very large at 184%.

Table 3.10
Determining the "best fit" source fraction predicted by element pairs for Bethel Island, week ending September 14, 1996

Measured elemental concentrations:

	Na [ppm]	Mg [ppm]	Ca [ppm]	Sr [ppb]
Sacramento River at Locke	9.78	6.07	4.63	79.4
San Joaquin River at Mossdale Landing	62.9	19.5	16.4	391
San Pablo Bay at Martinez	3,980	481	75.3	2,621
Bethel Island	27.1	8.71	5.53	98.8

Source fractions predicted by pairs of elements:

Element pair:	**(Ca,Sr)**	**(Na,Mg)**	**(Na,Ca)**	**(Mg,Ca)**	**(Na,Sr)**	**(Mg,Sr)**
$f_{Sacramento}$	0.8917	0.9148	0.9418	0.9443	0.9659	0.9731
$f_{San\ Joaquin}$	0.1147	0.0819	0.0546	0.0516	0.0301	0.0220
$f_{Martinez}$	-0.0064	0.0033	0.0036	0.0041	0.0039	0.0049

Concentrations predicted by element pair source fractions (see text for details):

Element pair:	**(Ca,Sr)**	**(Na,Mg)**	**(Na,Ca)**	**(Mg,Ca)**	**(Na,Sr)**	**(Mg,Sr)**
Na [ppm]	-9.68	27.1	27.1	28.9	27.1	30.6
Mg [ppm]	4.55	8.71	8.52	8.71	8.35	8.71
Ca [ppm]	5.53	5.83	5.53	5.53	5.27	5.24
Sr [ppb]	98.8	113	106	106	98.8	98.8

Relative error in concentrations predicted by element pair source fractions (see text for details):

Element pair:	**(Ca,Sr)**	**(Na,Mg)**	**(Na,Ca)**	**(Mg,Ca)**	**(Na,Sr)**	**(Mg,Sr)**
Na (% error)	136	0	0	-6.60	0	-13.06
Mg (% error)	47.8	0	2.22	0	4.19	0
Ca (% error)	0	-5.38	0	0	4.80	5.26
Sr (% error)	0	-14.6	-6.87	-7.21	0	0
Sum of absolute values (%)	184	20.0	9.09	13.8	**9.00**	18.3

This calculation was repeated for average concentrations of Na, Mg, Ca, and Sr for the seven-day period ending September 14, 1996 at Clifton Court. These data are summarized in Table 3.11. Again, source fractions computed using the element pair (Na, Sr) yielded the least relative error in concentrations predicted for the other two elements.

Relative error for the (Na, Ca) element pair was below 20%; for the element pairs (Na, Mg), (Mg, Ca), and (Mg, Sr), relative errors were below 40%. As in Table 3.10, the element pair (Ca, Sr) yielded by far the largest relative error at 346%.

Table 3.11
Determining the "best fit" source fraction predicted by element pairs for Clifton Court, week ending September 14, 1996

Measured elemental concentrations:

	Na [ppm]	Mg [ppm]	Ca [ppm]	Sr [ppb]
Sacramento River at Locke	9.78	6.07	4.63	79.4
San Joaquin River at Mossdale Landing	62.9	19.5	16.4	391
San Pablo Bay at Martinez	3,980	481	75.3	2,621
Clifton Court	22.9	7.89	6.48	118

Source fractions predicted by pairs of elements:

Element pair:	**(Ca,Sr)**	**(Na,Mg)**	**(Na,Ca)**	**(Mg,Ca)**	**(Na,Sr)**	**(Mg,Sr)**
$f_{Sacramento}$	0.7651	0.9615	0.8498	0.8397	0.8906	0.8807
$f_{San\ Joaquin}$	0.2506	0.0357	0.1489	0.1610	0.1075	0.1188
$f_{Martinez}$	-0.0157	0.0028	0.0013	-0.0007	0.0019	0.0005

Concentrations predicted by element pair source fractions (see text for details):

Element pair:	**(Ca,Sr)**	**(Na,Mg)**	**(Na,Ca)**	**(Mg,Ca)**	**(Na,Sr)**	**(Mg,Sr)**
Na [ppm]	-39.2	22.9	22.9	15.5	22.9	18.0
Mg [ppm]	1.97	7.89	8.69	7.89	8.39	7.89
Ca [ppm]	6.48	5.25	6.48	6.48	6.03	6.07
Sr [ppb]	118	97.7	129	128	118	118

Relative error in concentrations predicted by element pair source fractions (see text for details):

Element pair:	**(Ca,Sr)**	**(Na,Mg)**	**(Na,Ca)**	**(Mg,Ca)**	**(Na,Sr)**	**(Mg,Sr)**
Na (% error)	271	0	0	32.2	0	21.4
Mg (% error)	75.0	0	-10.1	0	-6.42	0
Ca (% error)	0	19.0	0	0	6.93	6.39
Sr (% error)	0	17.0	-9.76	-8.60	0	0
Sum of absolute values (%)	346	36.0	19.9	40.9	**13.4**	27.8

For these weekly averages of concentration data, source fractions computed using the (Na, Sr) element pair minimized relative error at both Bethel Island and Clifton Court; for these data, the "best" source fractions were within the range predicted by the method described in Section 3.6.2. Source fractions computed using (Ca, Sr) yielded relative errors roughly an order of magnitude greater than the relative errors predicted by all other pairs. Repeating this procedure for calculating the relative error for computed source fractions would yield the "best fit" element pair source predictions and could yield additional information on the behavior of elements within the estuary. Additionally, errors for source fractions computed using a single pair of elements could be predicted using the standard deviation on the concentration measurements.

3.7.2.2 Use of a least squares estimation method

A least squares estimation method finds a "best solution" for source fractions in a chemical mass balance equation. Such a solution technique solves for source fractions using the entire source vector, or fingerprint, rather than solving for source fractions using a subset of all the available tracer element information. For the Delta study area, this would mean solving for source fractions using the concentrations of all tracer elements simultaneously rather than in element pairs. One example of a model that uses this type of solution technique is the Chemical Mass Balance (CMB) Model Version 7.0 (CMB 7.0) (Watson *et al.*, 1990).

CMB 7.0 finds a least squares solution to a set of linear equations of the following format:

$$C_i = F_{i1}S_1 + F_{i2}S_2 + \ldots + F_{iJ}S_J \text{ for } i = 1, 2, \ldots, I \text{ and } j = 1, 2, \ldots, J, \text{ where}$$

C_i is the concentration of species i measured at a receptor site

F_{ij} is the fraction of species i in emissions from source j

S_j is the estimated source fraction for source j

I is the number of elements in the fingerprint

J is the number of source types.

Input to this model consists of source and receptor concentrations, both with appropriate uncertainty estimates (*ibid.*). The model calculates contributions from each source (source fractions) and the uncertainties of those values. Uncertainty values for the input data are used both to weight the importance of input data values and to calculate the uncertainties of the source contributions. For a unique solution to exist, the number of elements (I) must be greater than or equal to the number of sources (J).

An effective variance least squares solution (either with or without an intercept) is used by this model to compute results. This solution was developed and tested by Watson *et al.* (1984) and minimizes the weighted sums of the squares of the differences between measured and calculated values of C_i and F_{ij}; the solution algorithm is an iterative procedure that calculates a new set of S_j based upon the S_j estimated from the previous iteration (see Watson *et al.* (1984) or Watson *et al.* (1990) for greater detail).

The model makes the following assumptions (taken from Watson *et al.*, 1990):

(1) Compositions of source emissions are constant over the period of source and receptor sampling;

(2) Chemical species do not react with each other, i.e., they add linearly;

(3) All sources with a potential for significantly contributing to the receptor have been identified and characterized;

(4) source compositions are linearly independent of one another;

(5) the number of sources is less than or equal to the number of chemical species; and

(6) measurement uncertainties are random, uncorrelated, and normally distributed.

These restrictions can never be fully met in practice. The CMB model can tolerate deviations from these assumptions; deviations are generally reflected in increases in the uncertainties of the computed source fractions. Many studies have been performed to address the effects of deviations from these assumptions in the context of air pollution studies (see Watson *et al.* (1990) for a summary). In the context of water source apportionment, deviations are likely to be less severe than in air pollution source apportionment, as sources and chemical or physical transformations that may lead to non-conservative elemental behavior are more easily identified.

Use of this model would provide "error bars" for estimated source fractions that are calculated based upon the uncertainty in the measured source and receptor element concentrations. This method, while more robust for the overall calculation, does not allow the behavior of individual elements to be viewed as directly as the method used in this thesis; nonetheless, it could also be used to evaluate the effect of including elements that do not behave completely conservatively by computing increased error in source apportionment calculations. Because of its ability to compute results for both a large

number of sources and a large number of element tracers, its use would be necessary if additional sources of water to the Delta (*e.g.*, agricultural drainage water) were used.

3.7.3 Areas for further study

The use of a procedure such as that described in Section 3.7.2.1 to select the "best fit" element pair could improve the confidence of model predictions. Alternatively, the use of a more sophisticated model to predict the relative fractions of water at a receptor location would improve the accuracy of the results presented above by computing the standard error on the estimated source fractions in a more robust manner (see Section 3.7.2.2). Such models have been developed for use in air pollution studies; the Chemical Mass Balance (CMB) Model Version 7.0 (CMB 7.0) is one model that would be relatively easy to adapt for use with these data. This model uses an effective variance least squares estimation algorithm to calculate source contributions and their standard errors. It also evaluates the model fit and validates the model results. The mathematical model developed above was used with only four elements and three sources, and computed source fractions for possible pairs of tracer elements agreed closely with one another (see Sections 3.7.1.1 through 3.7.1.4). A more sophisticated model would be useful, however, to further evaluate the behavior of elements that behaved less conservatively than those selected as tracers. Also, a more sophisticated model would be necessary if more sources were included in the model (*e.g.*, if agricultural drainage water was characterized and used as a source).

One of the greatest potential uses of this information is to calibrate the hydrodynamic models that describe transport through and mixing within the Delta. Calibration of the models to accurately reproduce the distribution of freshwater within the system would give greater confidence when flow models are used to evaluate different management options. For example, if a model could be calibrated to reproduce the slug of San Joaquin River water that travels to the Bay when the barriers in the south Delta are removed, this model could then be used to evaluate different barrier configurations and the timing of their installation and removal. A calibrated model could be used to more assuredly predict the effects of different management options on the quality of the water arriving at the export pumps. A calibrated model could also be used to better understand mixing patterns within the Delta and to establish the manner in which these mixing patterns develop. This information could also be used to construct a water chemistry module that would run concurrently with a flow model; a water chemistry module could be used to predict the distribution of conservative constituents within the estuary and to estimate the concentrations of non-conservative constituents. This would promote the understanding of general chemical behavior within the estuary and could be used to predict concentrations of various pollutants, such as pesticides, that would be observed within the estuary.

Inherently, the elements that behave conservatively and therefore make good tracers are elements that are present in significantly higher concentrations in seawater (and Bay water) than in the river waters. It was initially hoped that the results of this work could be used to estimate the net Delta outflow based upon the mass fluxes of

elements past Martinez; however, to estimate net outflow, there must be an element that is present in river water in much higher concentrations than in Bay water. None of the elements for which this is true behave conservatively within the estuary. Collection of filtered samples might help this situation, but only if the dissolved phase of an element passes through the estuary without undergoing ion exchange reactions or adsorbing to particulate matter. This is almost certainly not the case for Li, Rb, or Ba, which are present as cations in solution and participate in ion exchange reactions, but could possibly be the case for Ga, which is present primarily as neutral or anionic species.

Figure 3.1: Sacramento-San Joaquin Delta study area

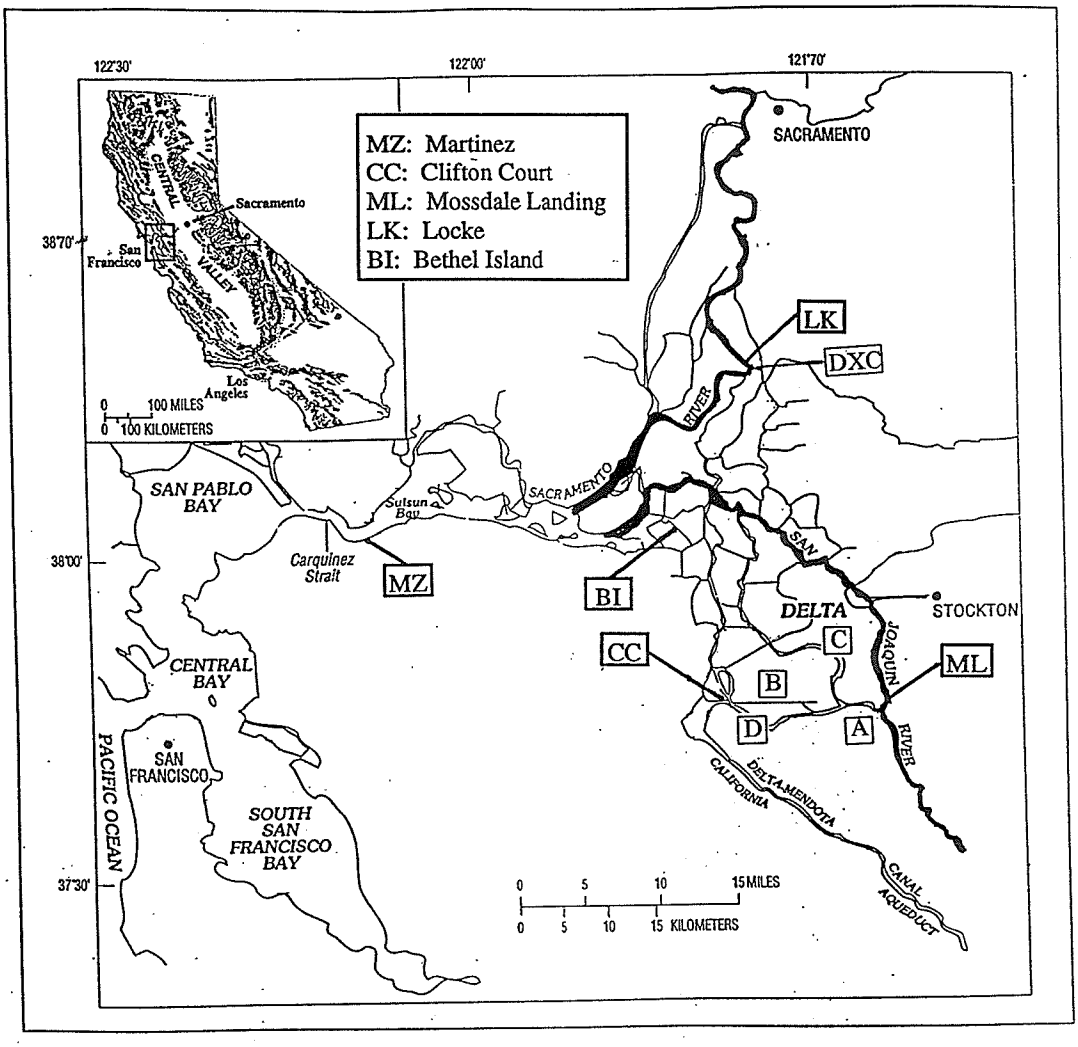

Barrier and gate locations:

DXC: Delta Cross-Channel
A: Barrier at the head of Old River
B: Barrier in Grantline Canal
C: Barrier in Middle River
D: Barrier in Old River at Tracy

Map adapted from Smith et al. (1995).

Figure 3.2: Variation in Elemental Concentration between the Sacramento River and the San Joaquin River

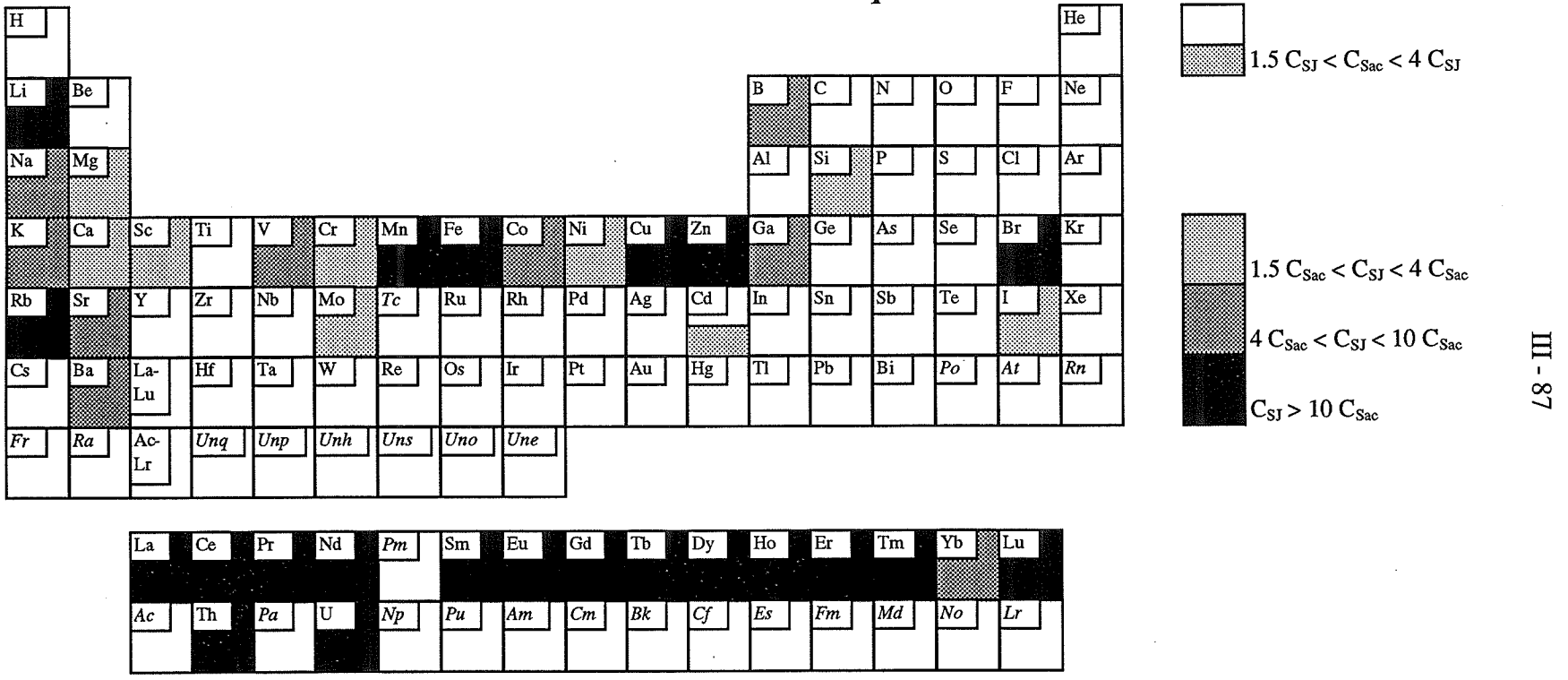

Figure 3.3: Variation in Elemental Concentration between the Sacramento River and the Bay at Martinez

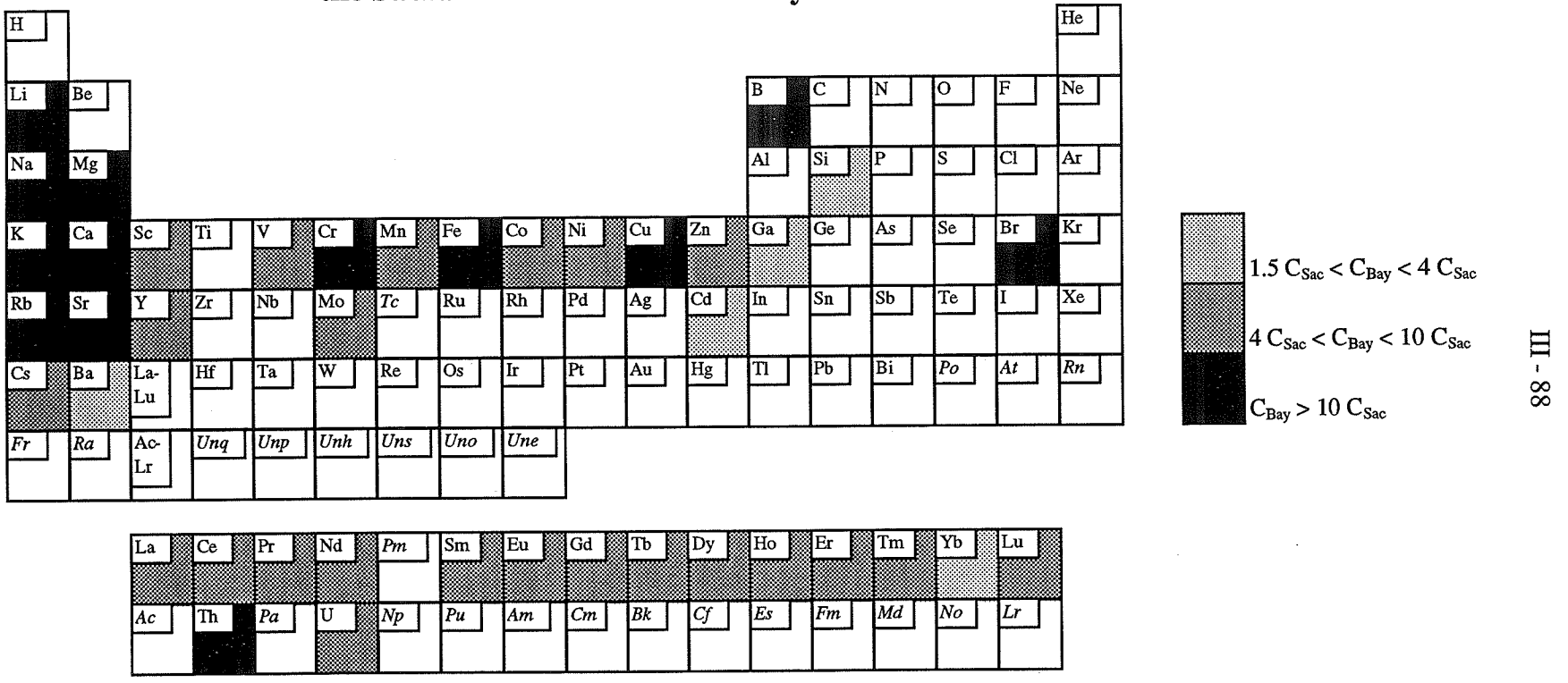

Figure 3.4: Variation in Elemental Concentration between the San Joaquin River and the Bay at Martinez

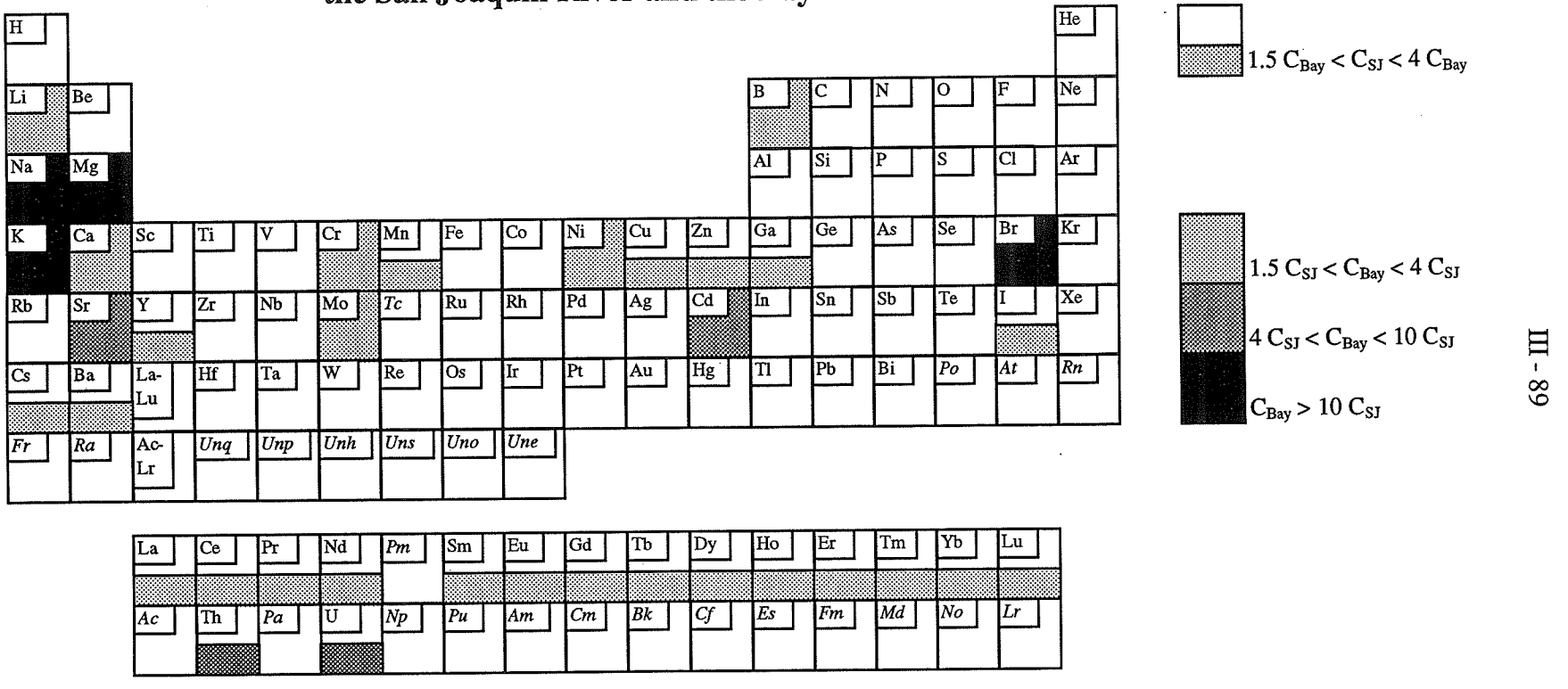

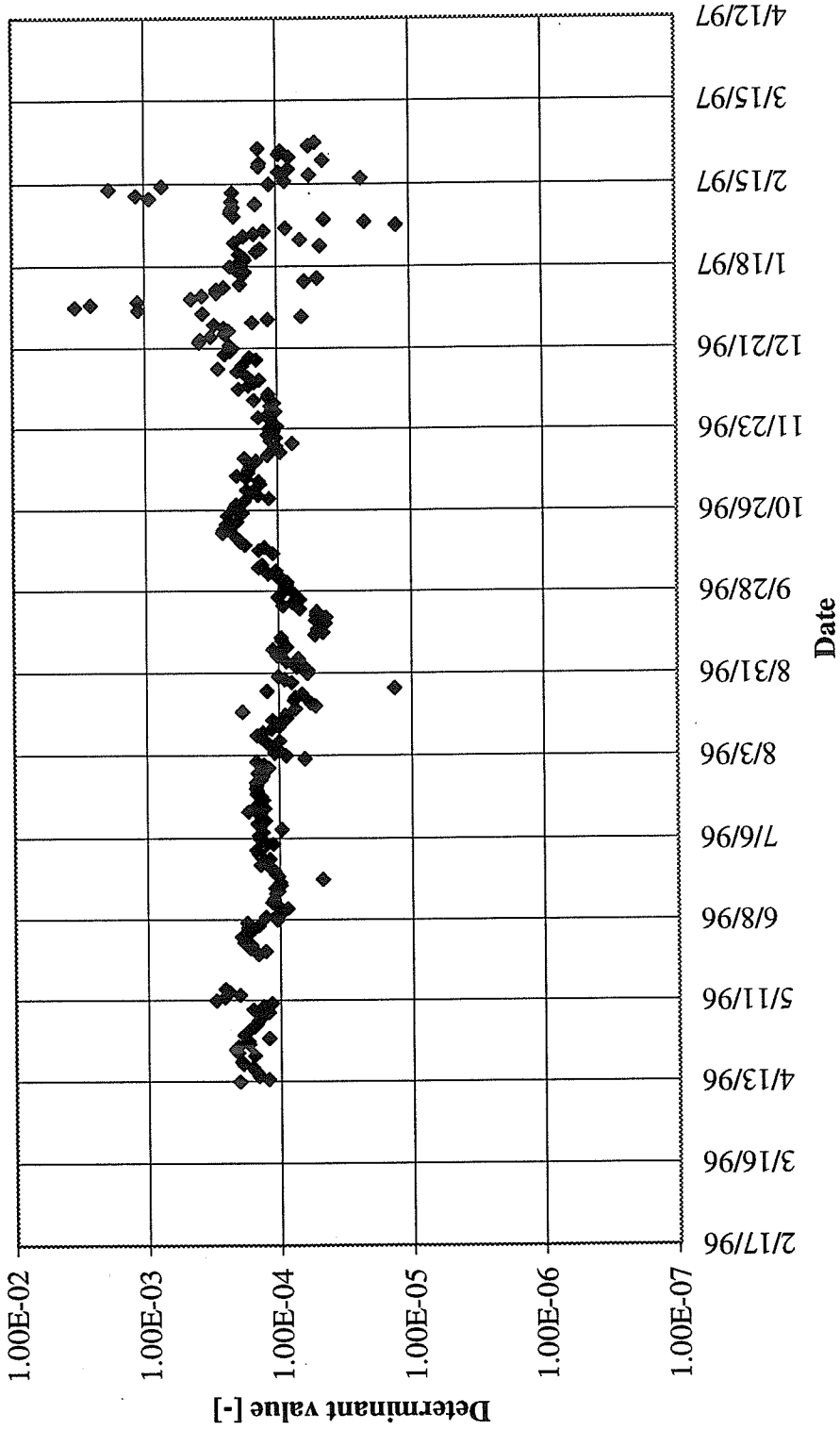

Figure 3.5: Absolute value of determinant computed from source vectors containing Mg, Ca, and Sr

Figure 3.6: Locations of samples collected along the Sacramento River June 1996

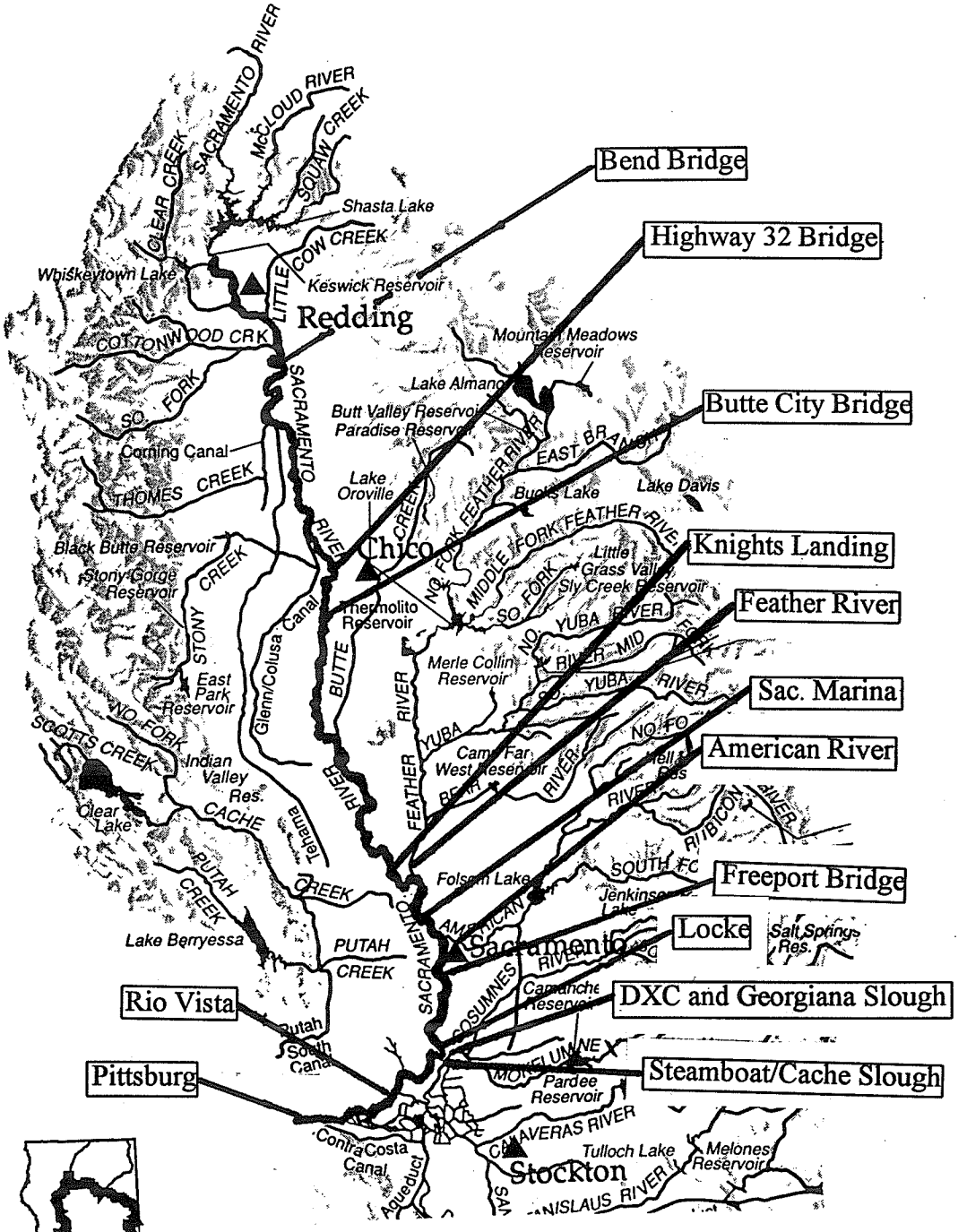

Map adapted from California State Lands Commission (1994).

Figure 3.7: Conservative mixing for laboratory mixtures of Sacramento and San Joaquin River waters: October 22 - 23, 1994

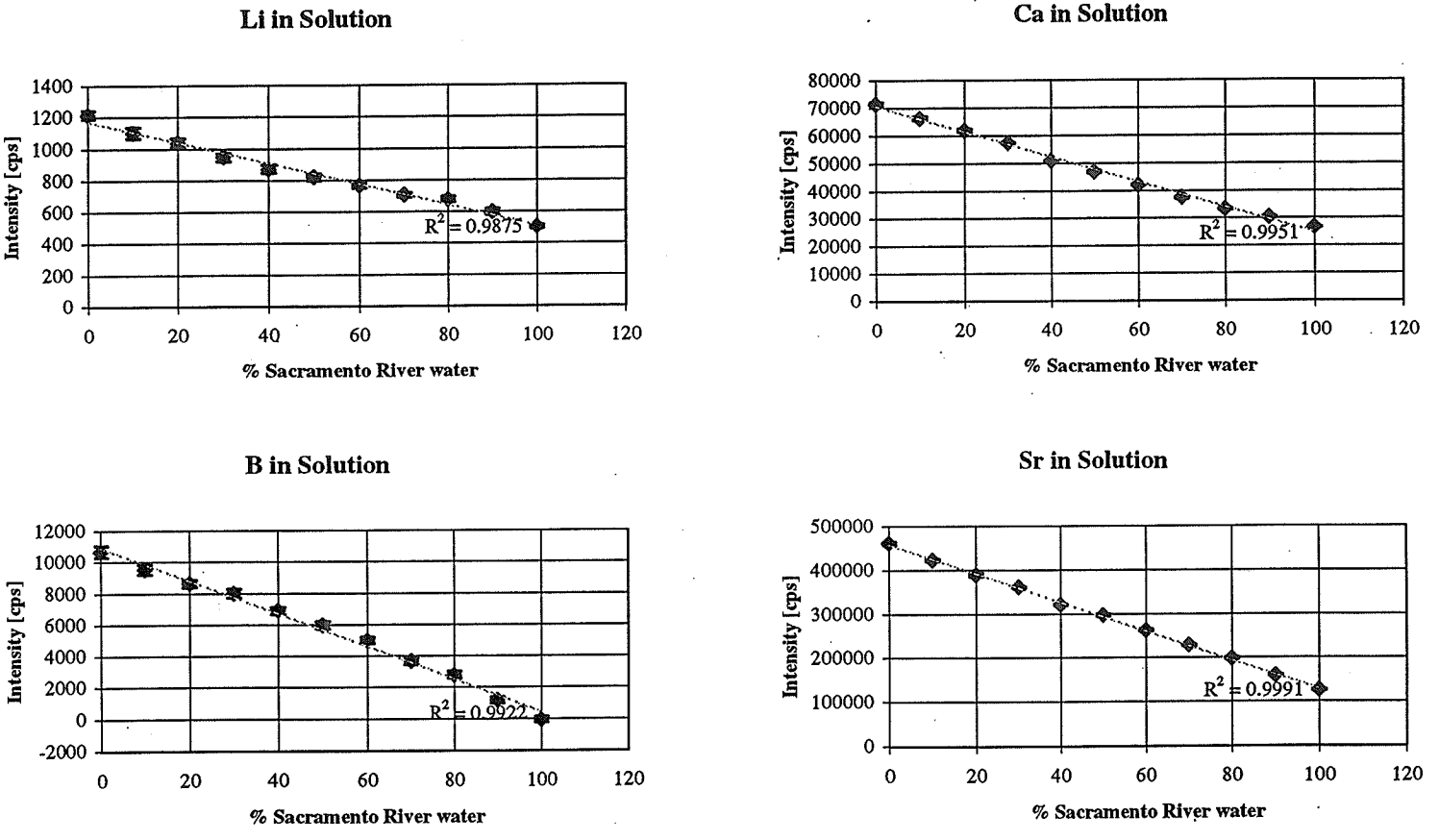

Figure 3.8: Non-conservative mixing for laboratory mixtures of Sacramento and San Joaquin River waters: October 22 - 23, 1994

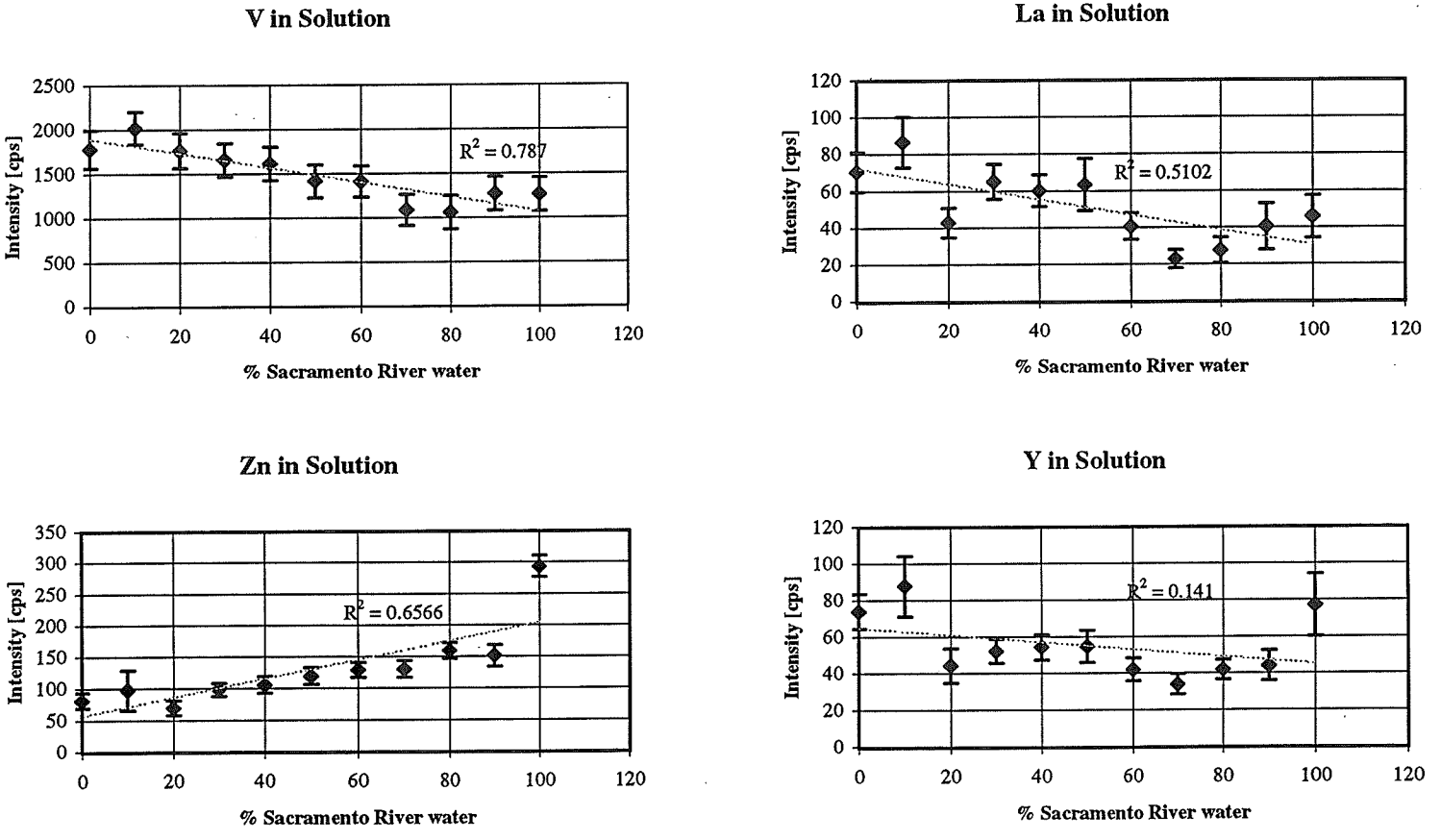

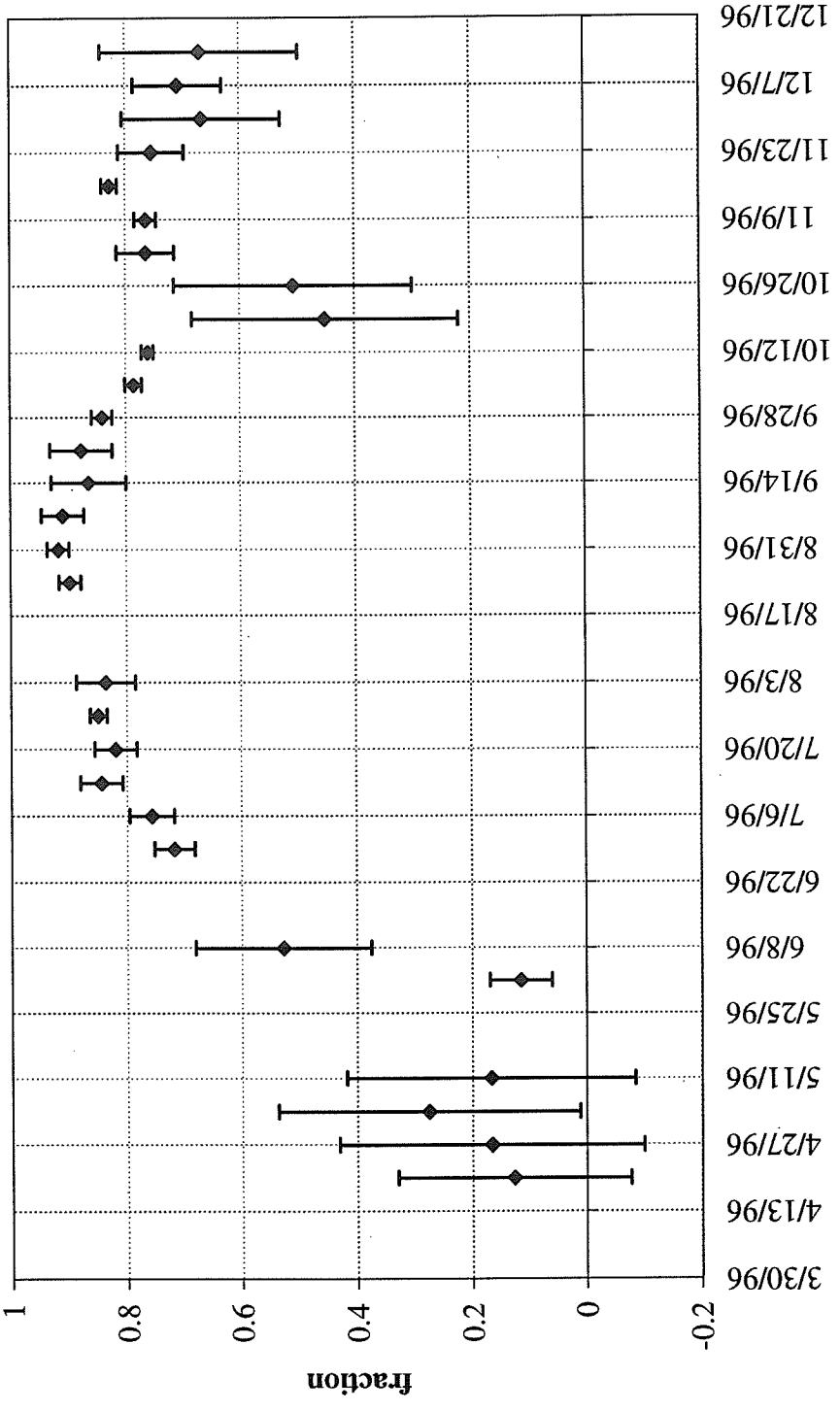

Figure 3.9: Computed fraction of Sacramento River water in samples collected at Clifton Court: Seven-day averages plotted by end date

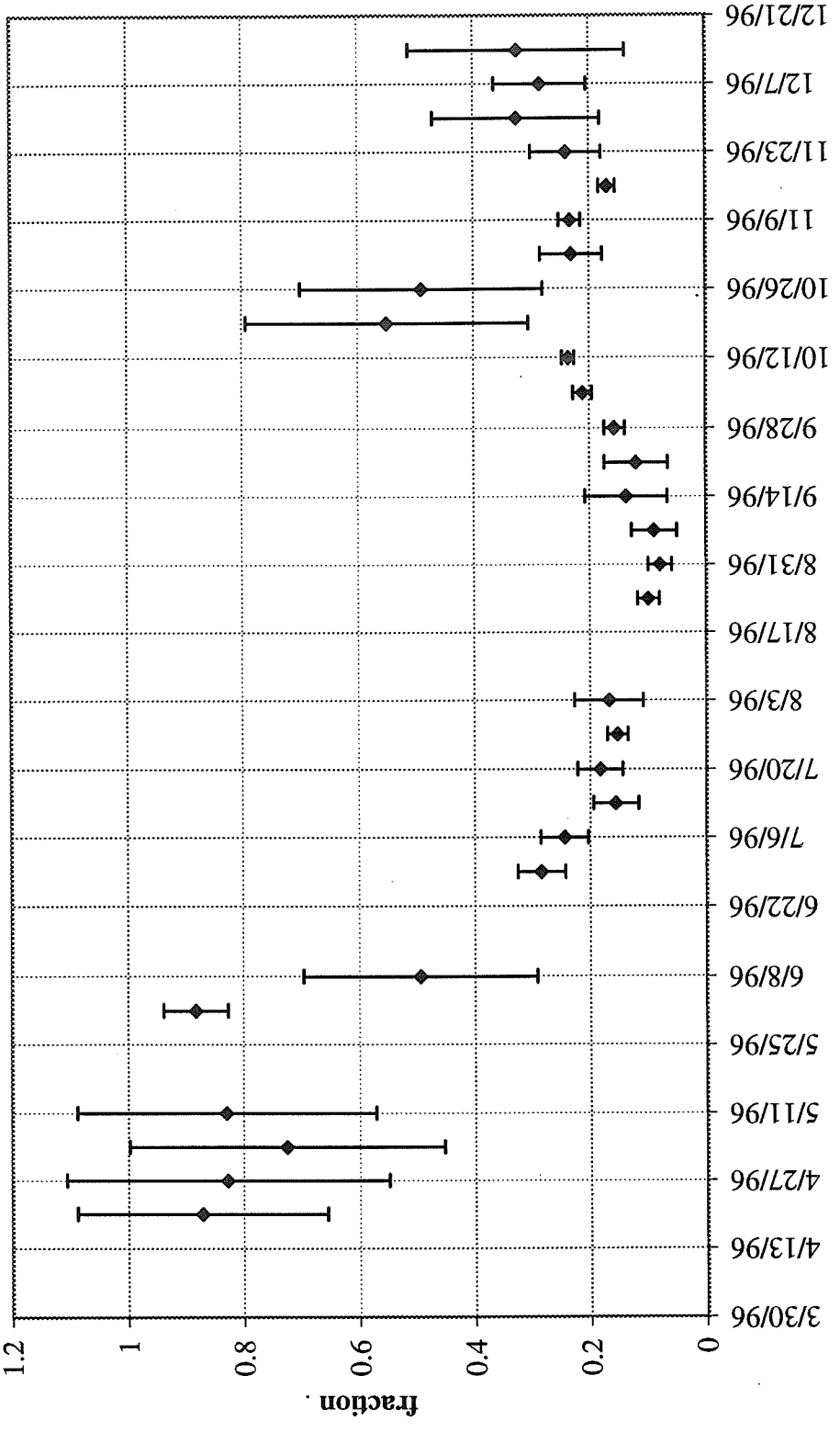

Figure 3.10: Computed fraction of San Joaquin River water in samples collected at Clifton Court: Seven-day averages plotted by end date

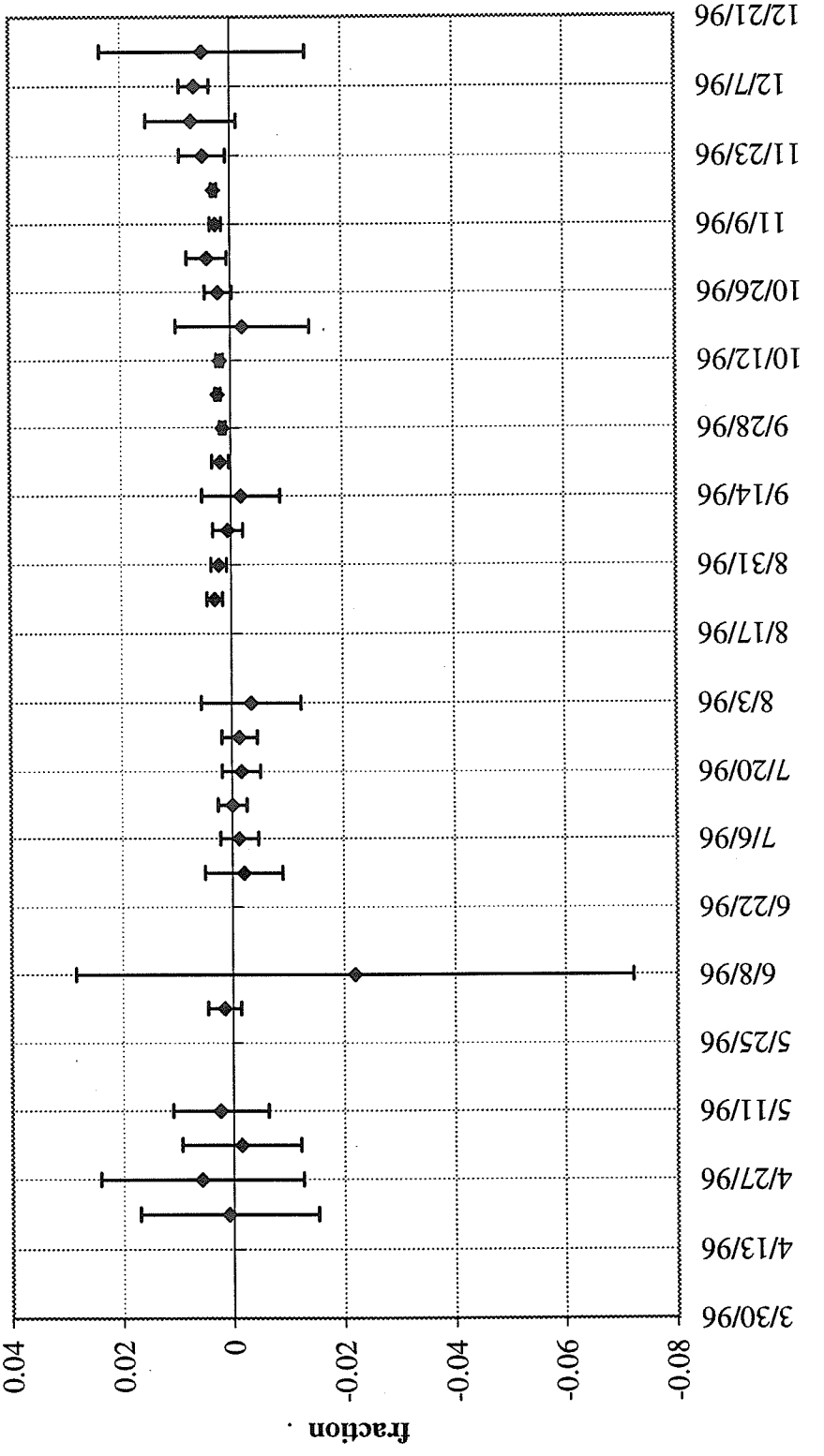

Figure 3.11: Computed fraction of Martinez River water in samples collected at Clifton Court: Seven-day averages plotted by end date

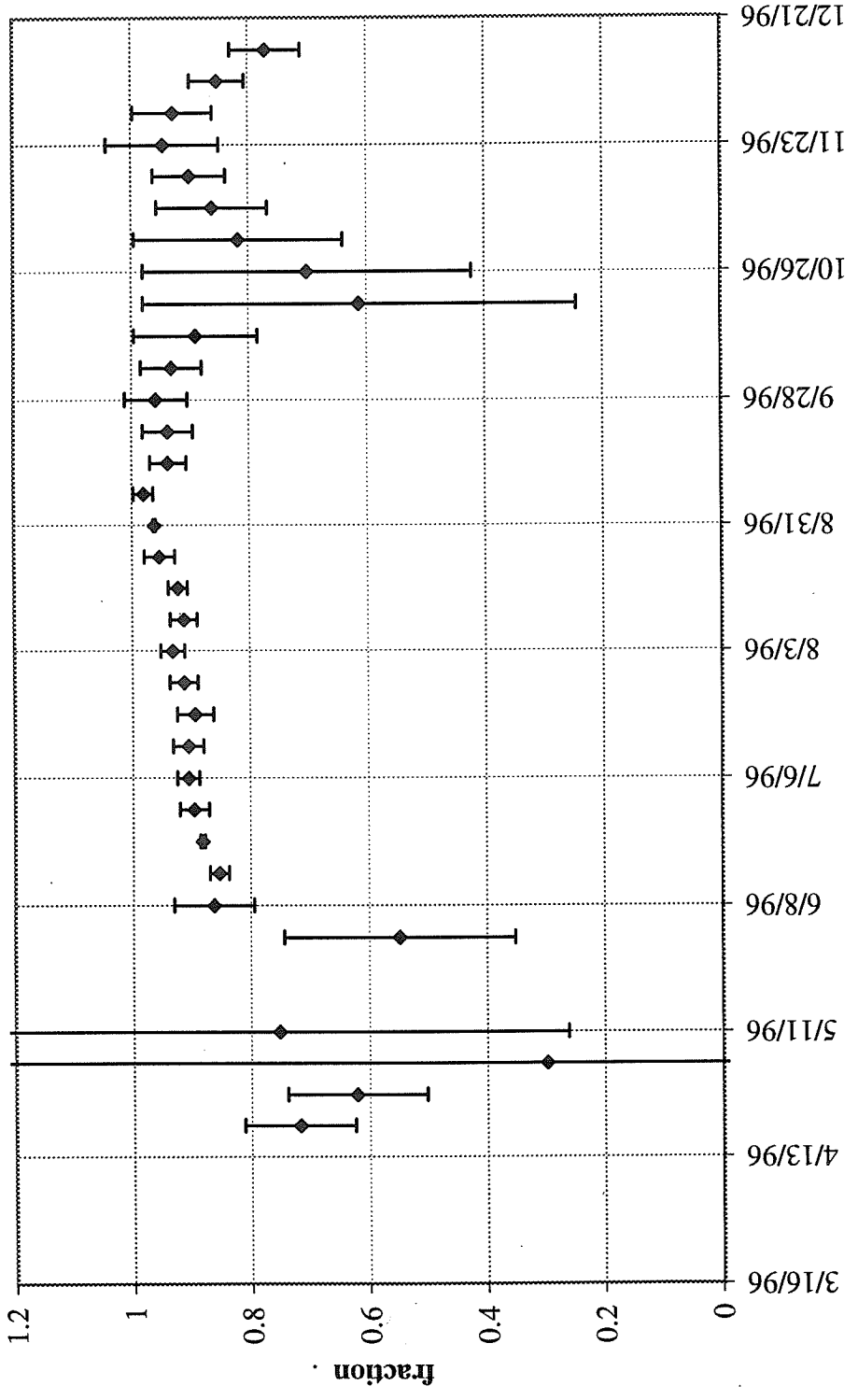

Figure 3.12: Computed fraction of Sacramento River water in samples collected at Bethel Island: Seven-day averages plotted by end date

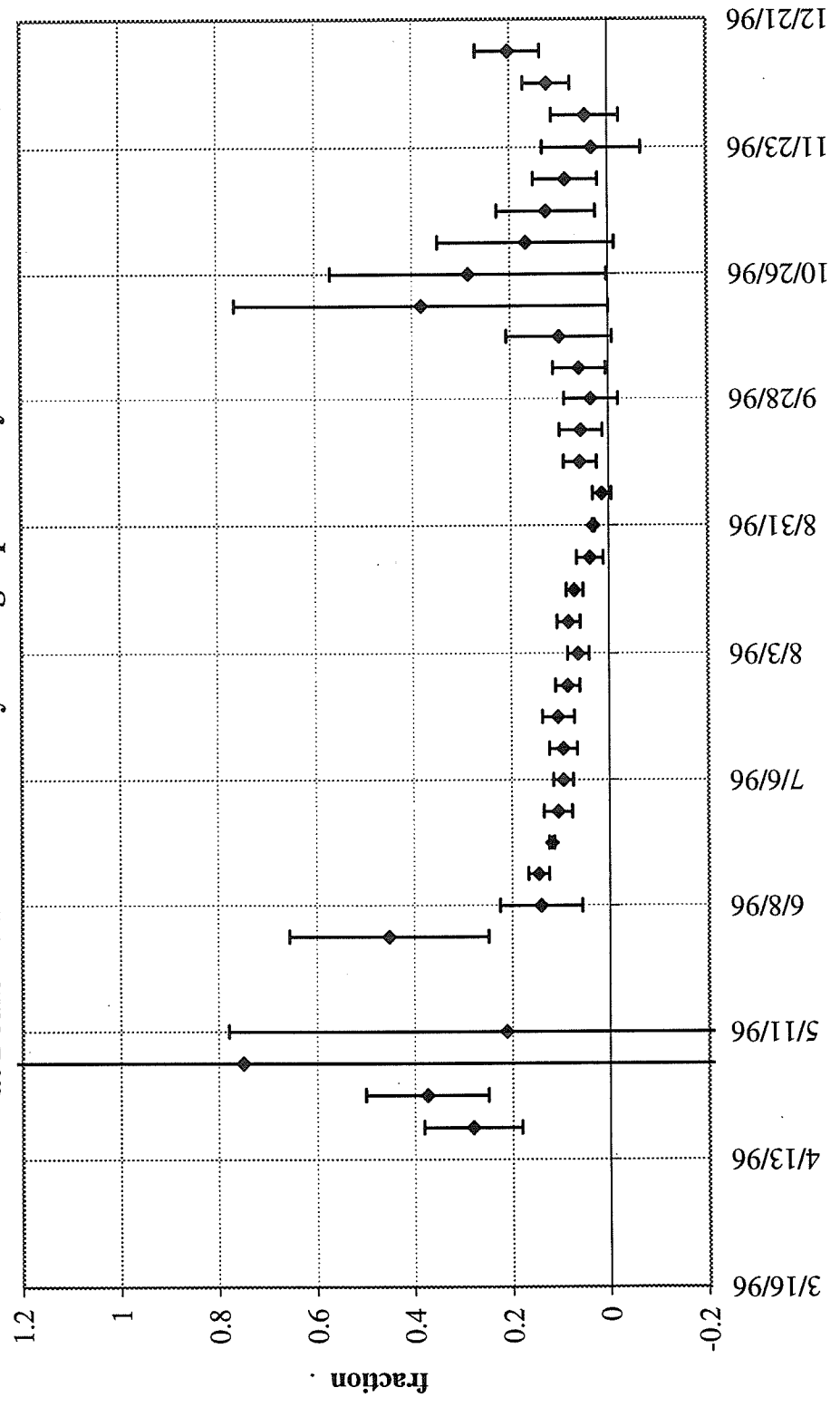

Figure 3.13: Computed fraction of San Joaquin River water in samples collected at Bethel Island: Seven-day averages plotted by end date

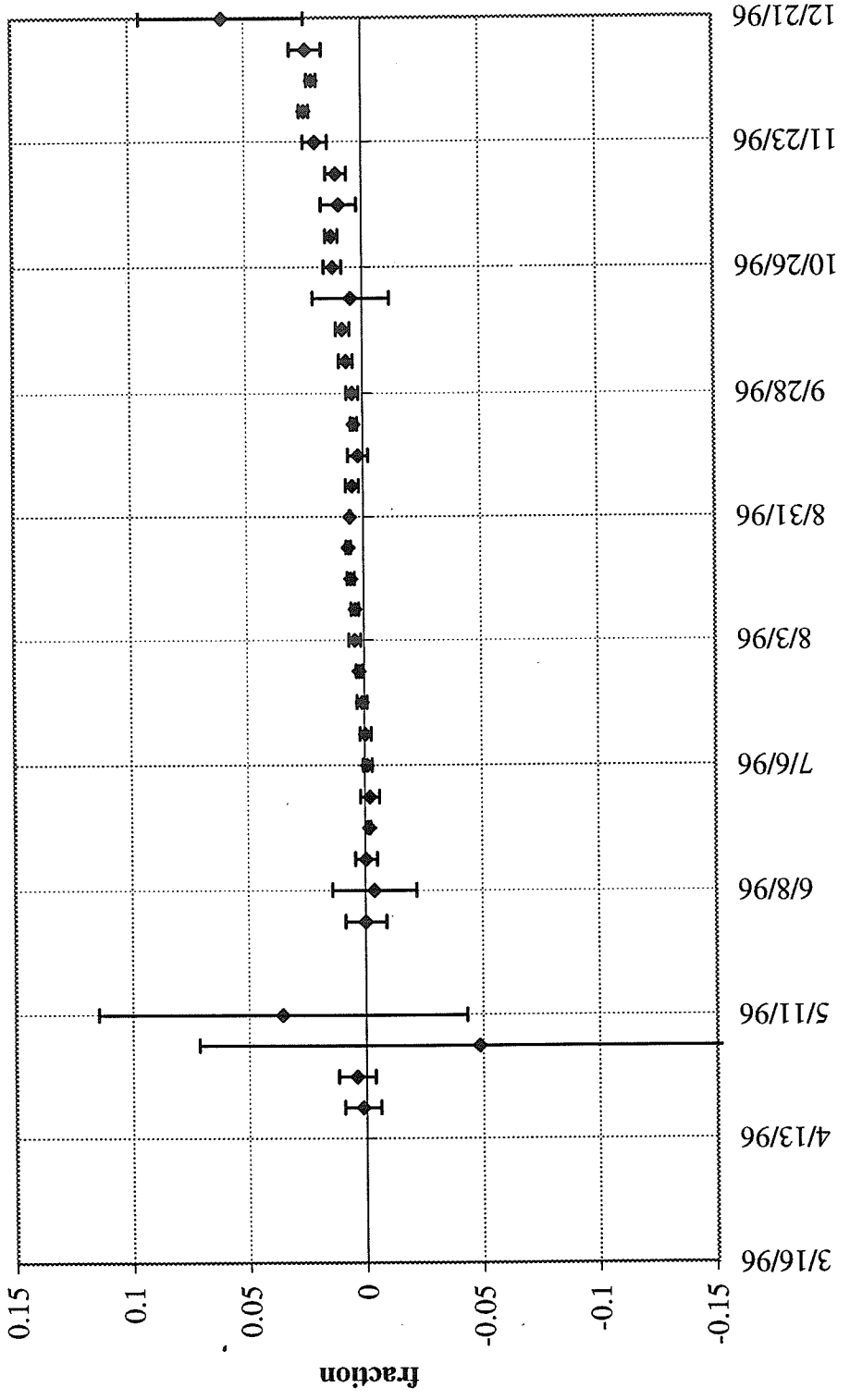

Figure 3.14: Computed fraction of Martinez water in samples collected at Bethel Island: Seven-day averages plotted by end date

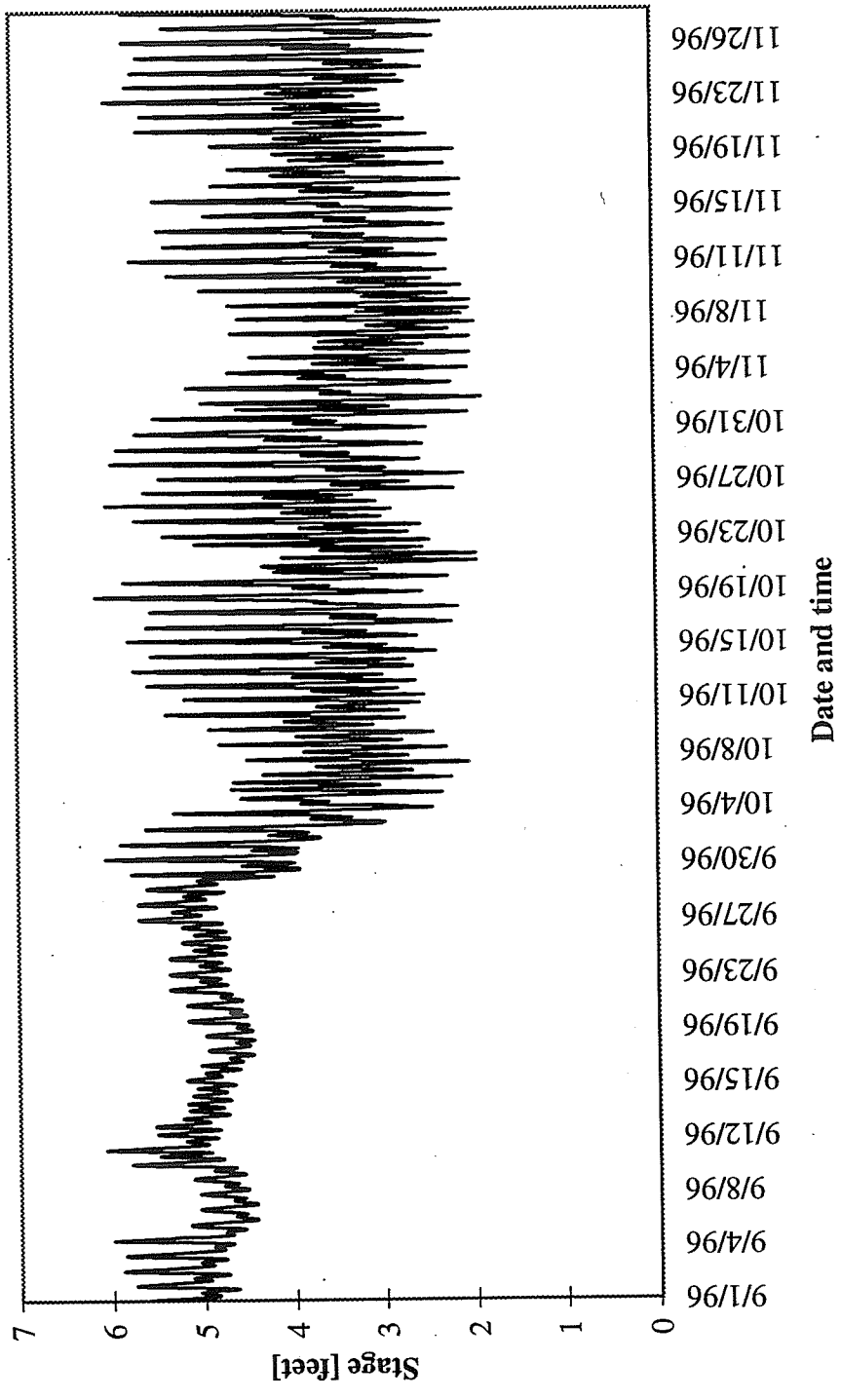

Figure 3.15: River Stage at Old River near Tracy

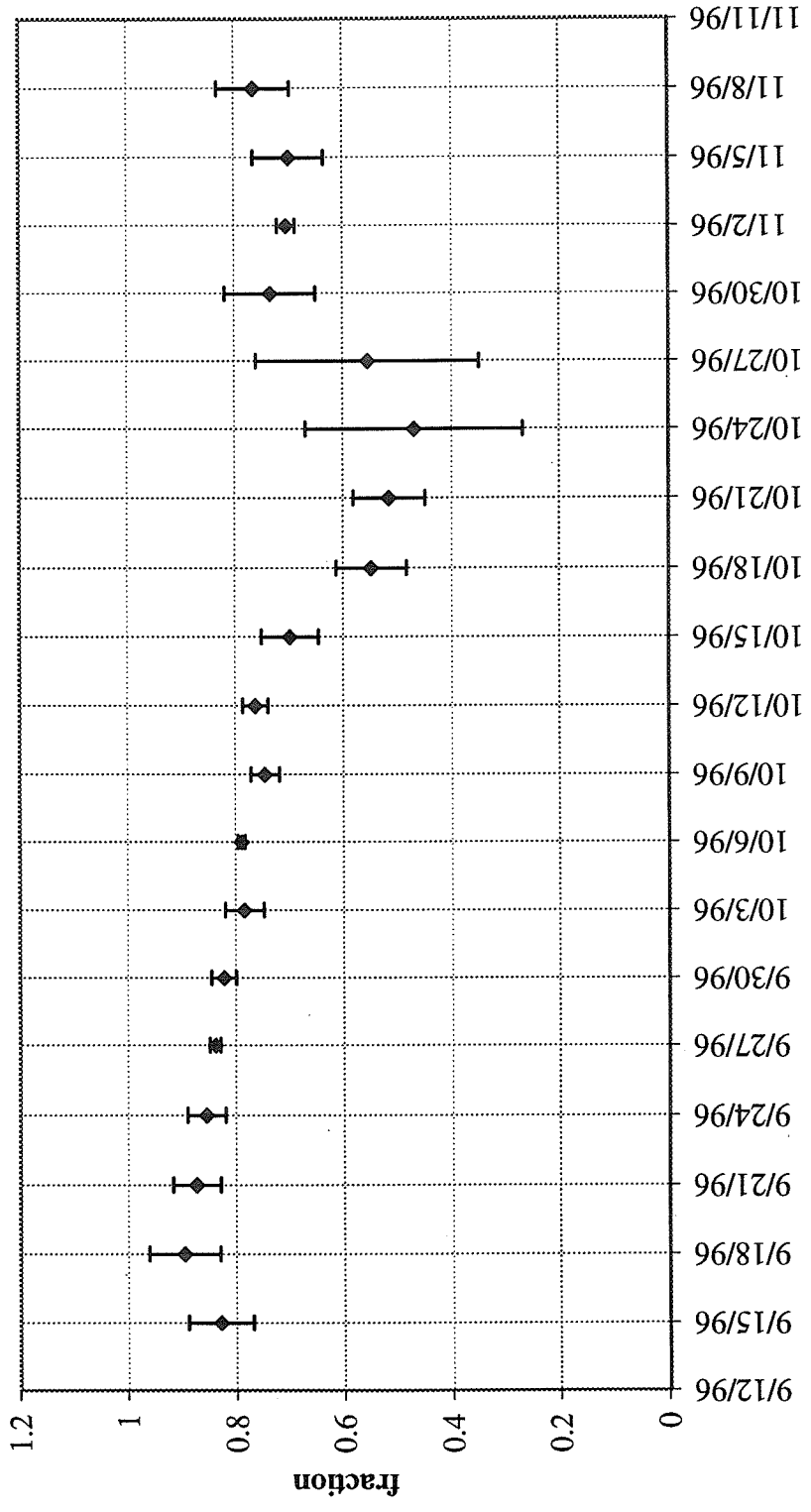

Figure 3.16: Computed fraction of Sacramento River water in samples collected at Clifton Court: Three-day averages plotted by end date

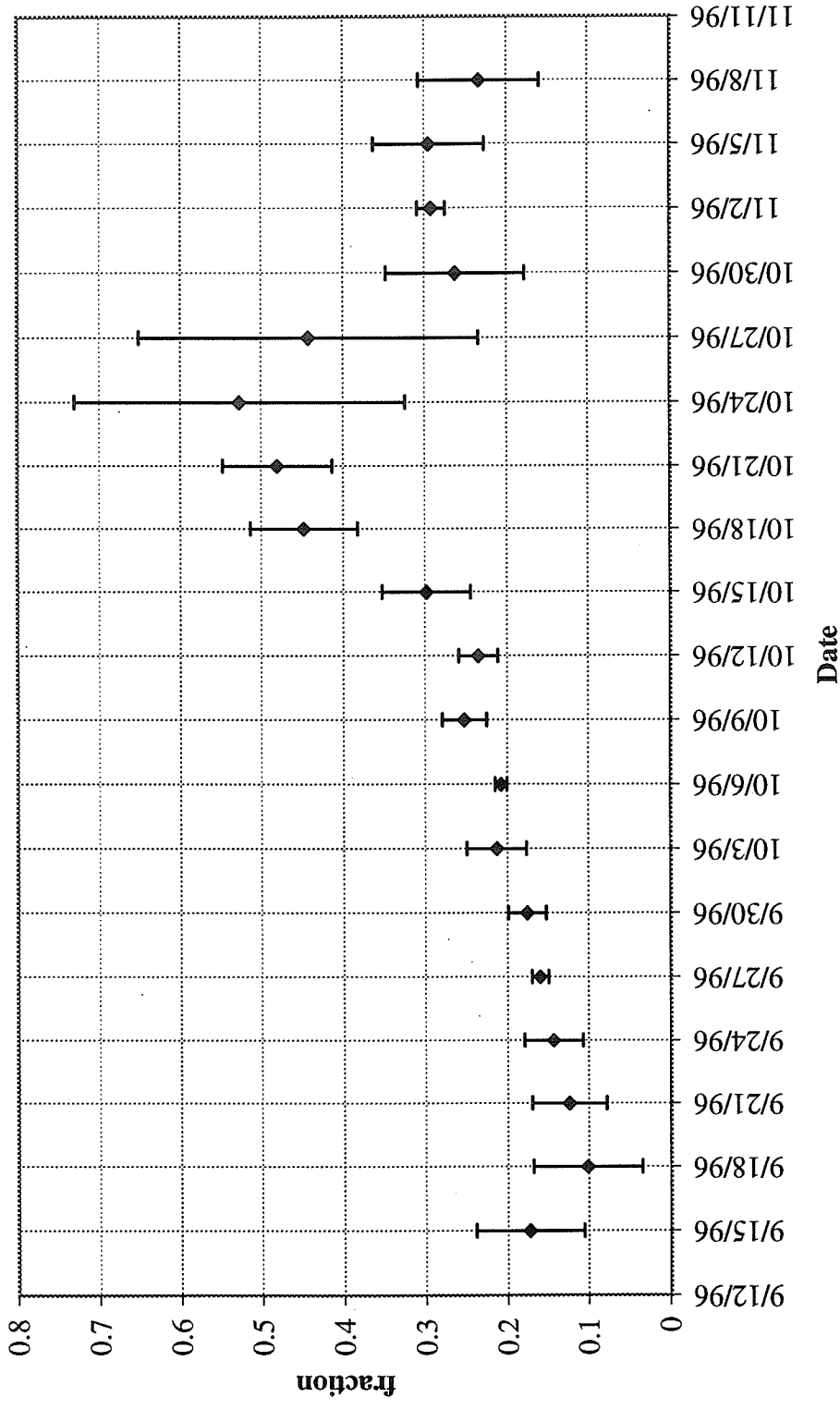

Figure 3.17: Computed fraction of San Joaquin River water in samples collected at Clifton Court: Three-day averages plotted by end date

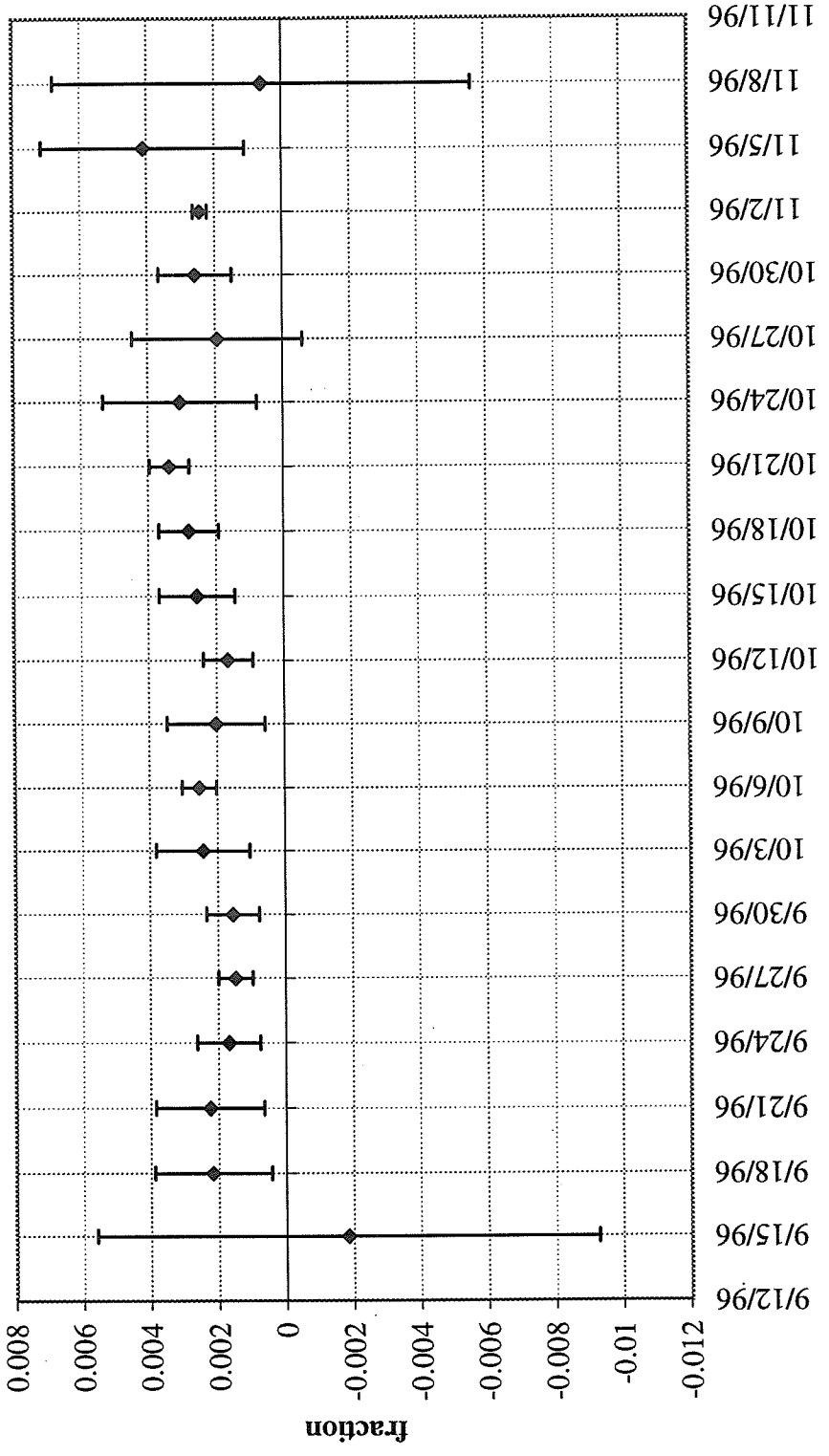

Figure 3.18: Computed fraction of Martinez water in samples collected at Clifton Court: Three-day averages plotted by end date

Figure 3.19: Source of Na in samples collected at Clifton Court: Three-day averages plotted by end date

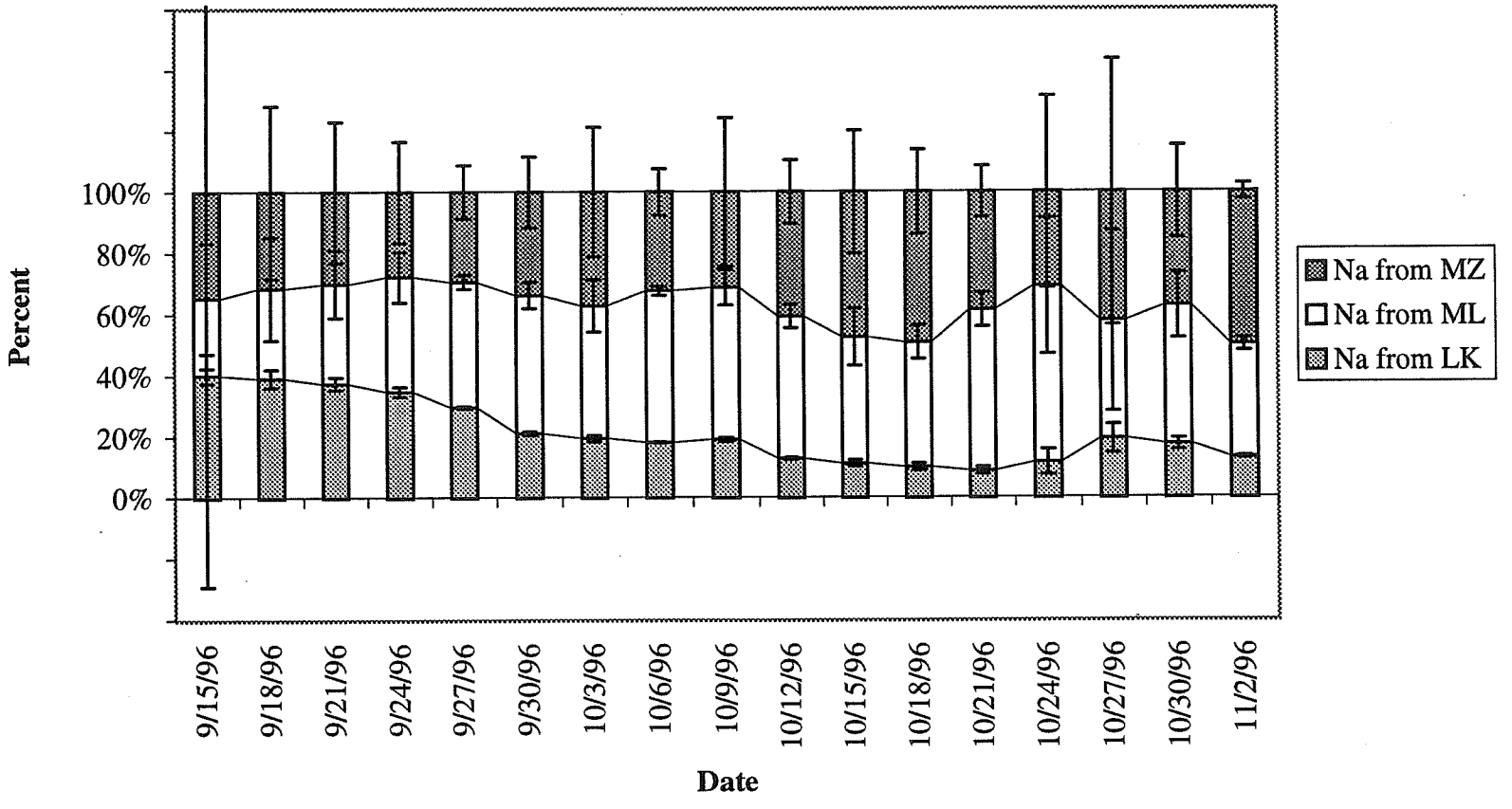

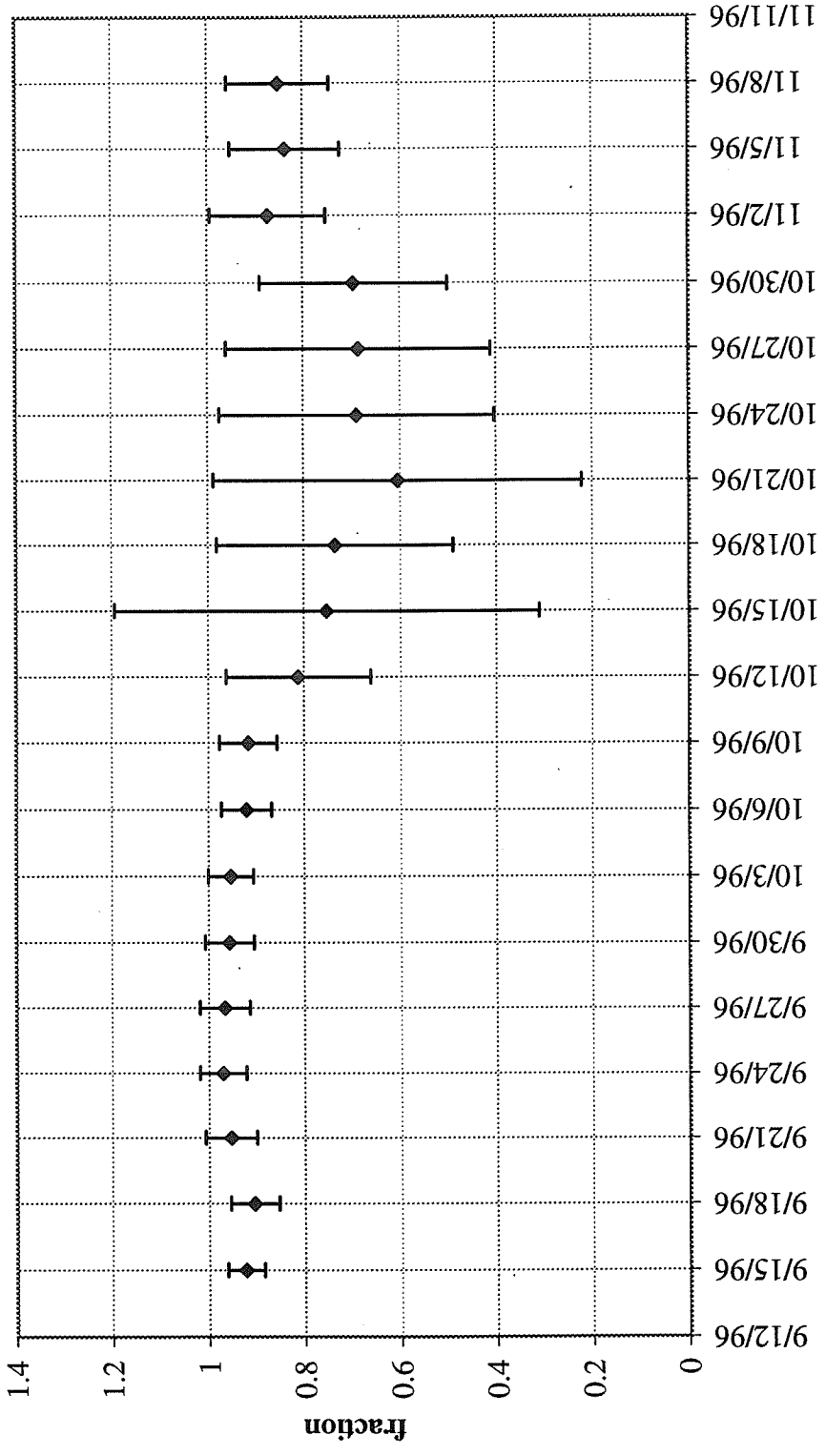

Figure 3.20: Computed fraction of Sacramento River water in samples collected at Bethel Island: Three-day averages plotted by end date

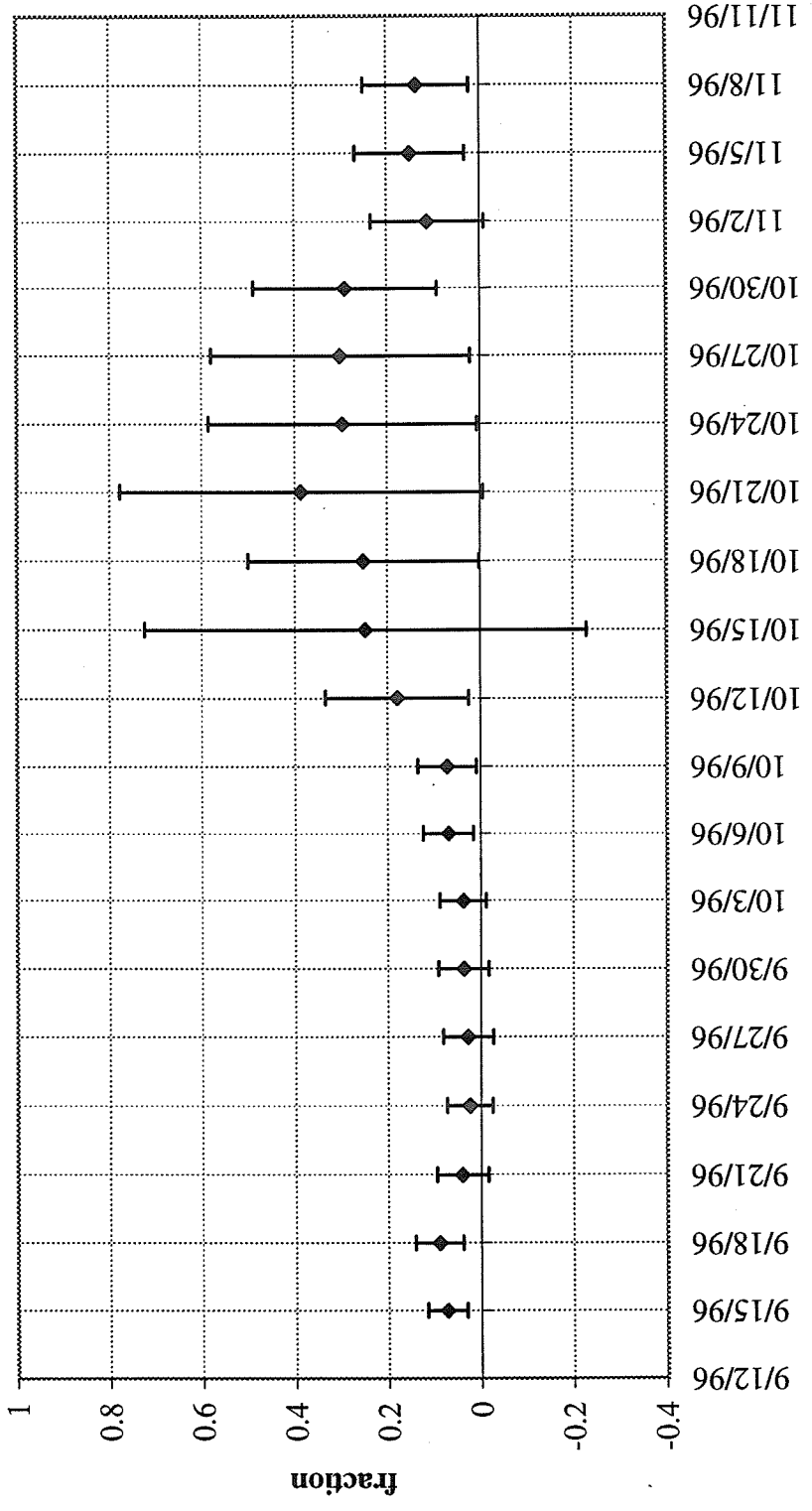

Figure 3.21: Computed fraction of San Joaquin River water in samples collected at Bethel Island: Three-day averages plotted by end date

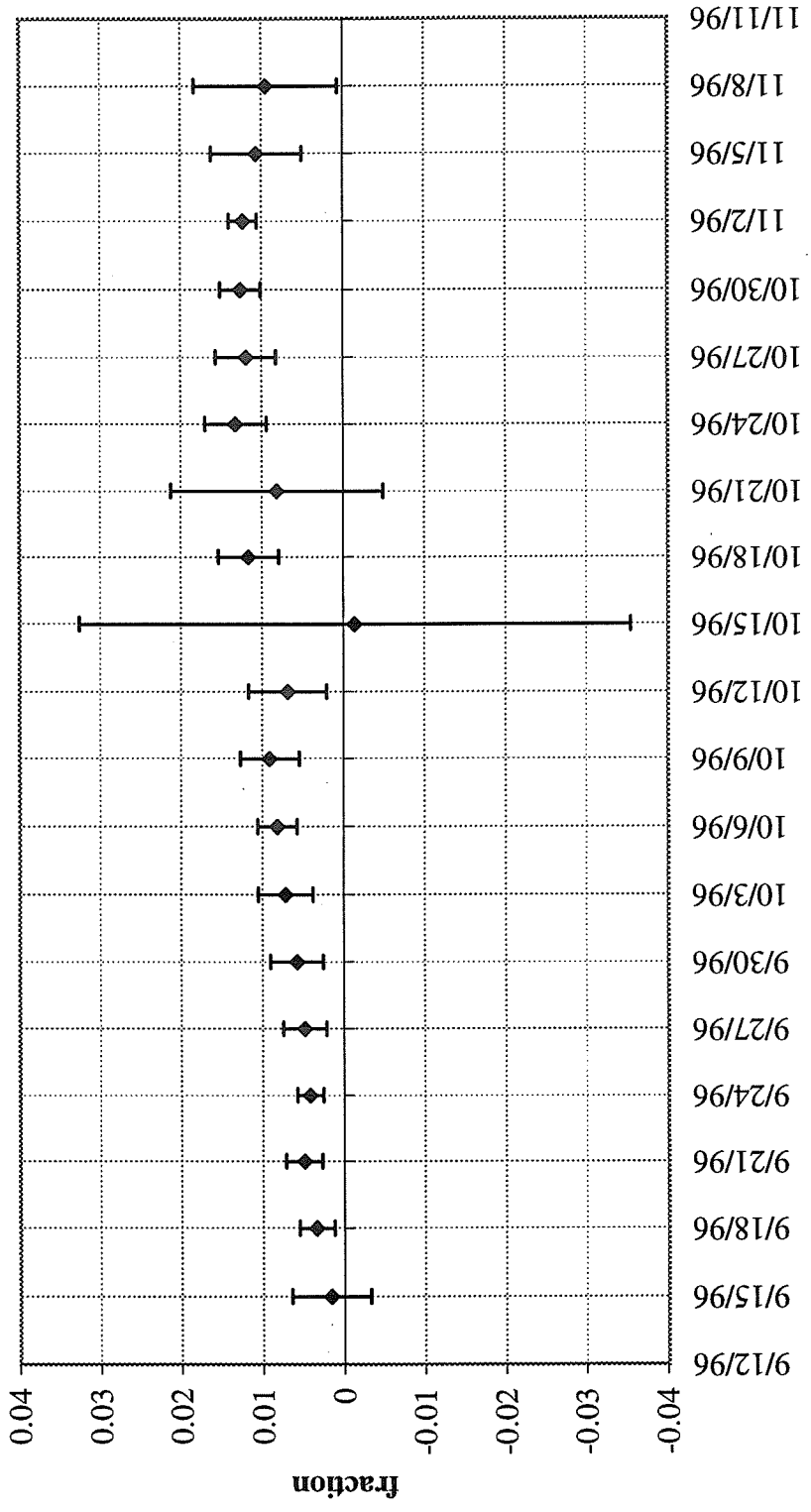

Figure 3.22: Computed fraction of Martinez water in samples collected at Bethel Island: Three-day averages plotted by end date

4 Development of a technique to identify pollutant sources and impacts in coastal and oceanic waters

4.1 Introduction

The objective of this study was to develop the technical means to determine mixing using ICP-MS analysis in coastal and ocean waters. The successful extension of the technique developed for the Delta into fully saline coastal waters could help overcome existing monitoring limitations, such as large natural fluctuations in water quality parameters and high laboratory costs, and could help determine the source of coastal pollution. Accurate determination of initial and far field dilution at sewage and industrial outfalls would assist in the calibration and verification of numerical mixing and advection models. Determination of individual and cumulative impacts of multiple point and non-point pollution sources and the tracking and monitoring of non-point discharges would help in the resolution of water quality controversies.

Prior to this study, no attempts had been made to apply this technique to coastal and oceanic waters. It was anticipated that the successful application of the ICP-MS technique to coastal waters would be dependent upon overcoming the technical problems listed below, and the study performed attempted to address these problems:

(1) Does high salinity interfere with laboratory analyses? If so, how would this be overcome?

(2) Do elemental tracers exist for the types of discharges that occur in coastal environments, *e.g.*, domestic sewage, stream and storm water discharges,

and industrial discharges? If so, can these tracers can be used as unique "fingerprints" for each discharge, distinct from that of the associated receiving water body?

(3) How important is the temporal variability of the discharge source fingerprints?

4.2 Study area and sampling schedule

4.2.1 Study area

Three types of discharges into fully saline coastal waters were selected for study: domestic sewage, perennial stream flow, and storm water runoff. Permission was obtained from the City and County of Honolulu to sample the discharge from the Waianae Ocean Outfall, one of Oahu's four municipal outfalls. This outfall is located on the leeward coast of Oahu and discharges an average of 3.0 million gallons per day of primary-treated domestic sewage; effluent is pumped to a diffuser structure approximately 5,250 feet offshore in 105 feet of water. The diffuser consists of 42 diffuser nozzles, each 6-inches in diameter; half the ports are presently flanged off and will remain so until the flow increases. The 21 nozzles currently in use are evenly spaced at 15-foot intervals.

The Pearl Harbor drainage basin was selected as the site for the study of perennial stream discharge. The drainage area for Pearl Harbor is approximately 145 square miles, approximately 24% of the total island. Eight streams enter the harbor, as shown on

Figure 4.1. Halawa, Kalauao, Waiawa, Waikele and Waimalu are perennial; Aiea, Honouliuli and Waiau are intermittent. Waikele stream has the largest flow of all the streams studied. Although Pearl Harbor receives only 20 to 30 inches of rain per year, the rainfall at the stream head ranges up to 250 inches per year. Runoff to Pearl Harbor drains forest, agricultural, commercial, industrial, military and residential lands. The water within Pearl Harbor is a mixture of ocean water and stream waters, and salinity within the harbor varies with runoff but is generally less than 85% of ocean water salinity.

The Ala Wai Canal, shown in Figure 4.2, is a two mile long man-made waterway constructed between 1921 and 1928; this canal drains three watersheds, the Manoa-Palolo, the Makiki, and the Kapahulu. Approximately 60-percent of the watershed is urban, with a dense road network and high automobile traffic. Under normal conditions, the canal has relatively low fresh water input, and tidal flushing is the primary circulation mechanism. During infrequent heavy rainfall events, the freshwater discharge increases greatly. The Mamala Bay Study (1996) defined a significant event as that producing more than 2,000,000 cubic feet of runoff from the watershed over the event duration (durations ranged from 12 to 72 hours). "Significant" events occurred 53 times during the 16-month period of January 1994 to April 1995. During four events, the runoff exceeded 50,000,000 cubic feet. The Mamala Bay Study (1996) concluded that during heavy rainfall events, the Ala Wai Canal contributed large concentrations of fecal coliforms to the bay and was a major source of contamination to Waikiki Beaches. Because of the intense interest in the Ala Wai Canal, it was selected to evaluate the possible application of the ICP-MS tracer method to this area.

4.2.2 Sampling schedule

Samples from the streams entering Pearl Harbor and the Waianae Treatment Plant were collected biweekly, for a total of 23 times, to determine if there was a unique "fingerprint" for each discharge and to address the question of temporal variability. Temporal variability is potentially most important at the stream discharges because of the possible differences between storm and non-storm events. Most of the initial samples were representative of dry weather, low flow conditions. As the study progressed, the sampling interval was modified in order to sample the streams during at least some significant rain events. During one of the sampling events, Waikele Stream was sampled hourly for 12 hours to investigate short term variations during a rain event.

The initial plan was to sample the receiving waters off the Waianae Outfall and at the discharge of one of the Pearl Harbor streams at quarterly intervals during the study year. The area off Waikele Stream was selected based upon volume and elemental characteristics of the stream flow. Several modifications were made in the course of the study, and the actual receiving water body sampling schedule is shown in Table 4.1.

Table 4.1
Receiving water body sampling schedule

Location	Sampling day	Date	Number of samples	Notes
Waianae	1	2/28/95	3	
	2	4/12/95	25	
	3	8/18/95	100	
	4	10/17/95	72	
	5	3/26/96	101	3-hour sampling at end of 12-hour LaCl injection into outfall

Table 4.1
Receiving water body sampling schedule

Location	Sampling day	Date	Number of samples	Notes
Waikele	1	4/5/95	104	
	2	8/2/95	113	
	3	1/10/96	84	
Ala Wai	1	1/25/96	76	Following high rainfall event
Canal	2	2/28/96	34	Following high rainfall event

Two types of samples were collected: discharge source samples and receiving water body samples. Discharge source samples were collected as freshwater grab samples; collection procedures for freshwater grab samples are described in Section 2.3.2. Receiving water samples were collected as saline samples; collection procedures are described in Section 2.3.4. Samples were analyzed as described in Sections 2.2.3 and 2.2.4.

4.3 Results

4.3.1 Stream variability

In order to trace discharges into receiving waters by using their naturally occurring elemental composition, the discharges must have distinct elemental fingerprints. Further, these fingerprints must remain distinct over time so that the characteristics of source waters are maintained over timescales longer than the timescales of mixing. Variation between sources could be either short-term, *i.e.*, occurring during a single rainfall event, or long-term, with variations changing over longer timescales, *i.e.*, seasonally. The sampling plan developed for this study investigated long-term variability by collecting

samples at regular intervals over fifteen months. Short-term fluctuations were investigated for Waikele Stream, which had the largest flow of any of the streams in the study area, by collecting hourly samples during a twelve-hour period encompassing part of a rainfall event.

4.3.1.1 Long-term variability

Twenty-three sets of stream samples were collected from streams within the study area; these streams are described in Section 4.2.1. The total number of samples collected from each stream varied, as samples were only collected when stream flow rates were high enough to allow collection of a sample. These samples were analyzed as described in Section 2.2.3.

Elements with concentrations that are higher in the streams than in the receiving waters include the transition metals and the REEs. However, difficulties in measuring their concentrations reliably at naturally occurring concentration levels in saline samples precluded the use of these elements as tracers. However, data on the concentrations of many of these elements were collected and could be used in the future if measurement techniques for these elements in seawater are improved. Included in Appendix H are graphs of the concentrations of Zn in Waikele Stream and V in Waiawa Stream. These data are representative of the patterns of concentrations of the transition metals observed in all the streams studied; concentrations of transition elements showed significant variation for the samples collected.

La concentrations (representative of the concentrations of the other rare earth elements except Ce) are also shown in Appendix H. Although higher than REE

concentrations measured in ocean water, stream water and wastewater effluent concentrations were consistently low (La concentrations below 1.5 ppb); the single exception to this trend was one outlying point for a sample collected from Waikele Stream on March 4, 1996. This high concentration was likely the result of sample collection during a rainfall event, consistent with samples collected during the rainfall event of January 25, 1996, and discussed in greater detail below.

As described in Section 2.2.4, standard addition analysis determined that Rb and U could be accurately and reproducibly measured in seawater; Sr could also be measured, but the accuracy was not as great as for either Rb or U. However, all three of these elements have concentrations that are higher in seawater than in freshwater; thus, in a sense they act as "inverse" tracers and indicate the amount of dilution in a given sample. Rb is present at roughly 120 ppb in seawater and about 1 ppb in freshwater; U was almost absent in the freshwater samples analyzed for this study and is present at approximately 3.2 ppb in seawater. Sr is present in seawater at 7.5 ppm; in streamwater its concentration was below 100 ppb, in wastewater below 1 ppm. These were the main elements were used to determine mixing within the Hawai'i study area.

Graphs of measured concentrations of Rb and U are included in Appendix H for the streams that flow into areas where receiving water samples were collected. Plots of Sr concentrations are very similar to the plots of Rb concentrations and are therefore not included. In general, although the concentrations of Rb, La, and U did vary in the freshwater analyzed, the variation between freshwaters was very small compared to the variation between fresh and saltwater. These elements therefore could not be used as

tracers of individual sources. However, where no other significant freshwater sources were present, such as the Waikele Stream discharge, dilution was determined using the inverse tracer technique (see Section 4.3.2 for detail).

4.3.1.2 Short-term variability

Samples were collected hourly over a ten-hour period in Waikele Stream during a rain event. Samples were analyzed as described in Section 2.2.3. The flow caused by the rain event peaked at 6:30 am on January 25, 1996, with a maximum flow of 1,890 cfs; the flow decreased to 117 cfs by the end of the sample collection period and returned to its average level of about 45 cfs during the following day. A plot of flow rates, measured at a gauging station on Waikele Stream at Waipahu, is included in Appendix H, as are plots of the concentrations of Rb, La, and U.

As with the long-term stream samples, concentrations of Sr during this rain event were quite similar to those of Rb; concentrations of Rb were remarkably constant, even with changes in flow rate. This unique feature indicates that no correction would need to be made for dilution measurements made with Rb or Sr during a rainfall event. Concentrations of both La and U were highest when flow rates were highest and decreased as the flow rate decreased. Concentrations of U for all samples analyzed remained well below the concentration of U in seawater, so that no correction would have to be made for the use of U as a "inverse tracer" during a rainfall event.

The trend of decreasing concentration with decreasing flow rate was very uniform in the data for La, and the highest concentration observed for La was significantly higher than the average concentration observed in samples collected during

dry weather. The maximum La concentration observed during this sampling event was 2.75 ppb (observed at 8 am, the start of sample collection during this January 25, 1996, rainfall event), while the maximum concentration observed during the dry season was less than 1 ppb. This excludes the single anomalous point observed on March 4, 1996, and discussed in Section 4.3.1.1 above. The daily average flow in Waikele Stream on March 4, 1996, was 252 cfs, while the average daily flow on January 25, 1996, was 370 cfs, supporting the generalization that La concentrations increase dramatically in proportion to flow during rainfall events. This characteristic could allow the measurement of dilution in receiving waters using La during rainfall events if analysis methods could be improved to allow lower detection limits in saline samples.

4.3.2 Receiving water

Concentrations of Rb, Sr, and U were used to track the discharges of the Ala Wai Canal into the ocean and of Waikele Stream into Pearl Harbor. Concentrations of these elements in the effluent from the Waianae Sewage Treatment Plant (STP) were higher than concentrations found in the streams but were still far below the concentrations found in all seawater samples analyzed, so these elements were also used as "inverse tracers" for the Waianae STP receiving water sampling events.

For each of these elements, the ratio of the measured concentration to the typical seawater concentration was calculated, and values agreed to within about 5%. The average of the three ratios was used for plotting. All plots of receiving water concentrations and dilutions (included as Figures 4.3 through 4.10) were generated by Sea

Engineering, Inc., of Waimanalo, Hawai'i. When using inverse tracers, the extent of dilution that can be measured depends in part upon the accuracy of measurement of the tracer element in the receiving water. This limit could be improved by making more extensive measurements of the naturally existing background levels of the receiving waters on the sampling days. In addition, computed dilution values are limited by the standard error on the ICP-MS measurements (a measure of the signal-to-noise ratio). For Rb, Sr, and U, the standard error on the measurement leads to a maximum computed error of 4% of the computed dilution (see the report by Sea Engineering, Inc. and California Institute of Technology (1996) for concentration data and computed dilution for each sample).

4.3.2.1 Waikele Stream

Figures 4.3 to 4.5 show the contoured data for the three Waikele sampling days. As shown in Table 4.1, between 84 and 113 samples were collected during these sampling events (see Sea Engineering and California Institute of Technology (1996) for detail). On all three days, mixing between stream and harbor waters occurred quickly, with dilution to near background levels occurring within approximately 1000 feet of the mouth of the stream. Note that background (harbor) concentrations reflect a salinity that is between 60% (for the first two sampling dates) and 80% (for the last sampling date) that of ocean water. Concentrations changed more gradually as the plume reached the middle of the bay. By contrast, a sharp edge of the muddy surface plume was visible near the middle of the bay on each of the field days. It may be that the leading edge of the plume consisted of a very thin surface layer and the technique of sampling just below the

surface to avoid surficial contaminants caused the discrepancy between the visual observations and the measurements.

Figure 4.3 also shows low concentration levels at the eastern shore of the harbor; these could be indicative of groundwater runoff. This highlights the fact that this method can serve well as a freshwater detector but not necessarily as a tracer for a specific body of water.

4.3.2.2 Ala Wai Canal

Figures 4.6 and 4.7 show the contoured data for the two Ala Wai sampling events. As at Waikele stream, dilution occurred quickly close to the channel. Figure 4.6 shows a distinct plume edge oriented along a north-south azimuth near channel markers "G1" and "R2." These measurements corresponded to visual observations. The plume actually extended inshore on the reef flat on the east side of the channel; because samples were not collected from the shallow reef flat, this is not shown on the plot. Also of interest on Figure 4.6 is the indication of freshwater discharges northwest and southeast of the Ala Wai Canal. Potential sources are the Kewalo Basin to the west and the Kapahulu Groin drainage culvert to the east. The results of the second sampling event are shown in Figure 4.7; during this event, rainfall was not as intense as on the first day, and the plume edge was not as well defined.

4.3.2.3 Waianae

Figure 4.8 shows the transect measured at the Waianae Outfall on April 12, 1995, and Figures 4.9A through 4.9D show four transects measured on August 18, 1995. Each transect shows a contour plot generated from dilutions computed from Rb, Sr, and

U concentrations, as described in Section 4.3.2. Each transect consists of five stations located approximately 0, 120, 240, 480, and 960 feet down-current from the diffuser. On April 12, 1995, five depths were sampled at each station. On August 18, 1995, the objective was to determine an optimum combination for sampling time versus plume resolution, and the depths sampled at each station varied from transect to transect. Five depths were sampled on Transect 1 (Figure 4.9A), four on transect 2 (Figure 4.9B), and three on each of Transects 3 and 5 (Figures 4.9C and 4.9D). The structure seen in Figures 4.8 and 4.9A indicates the value of sampling the greater number of depths. Figures 4.9B and 4.9D do not show freshwater concentrations as high as those in Figure 4.9A. This may be because the current was reversing during the measurement of Transects 2 through 5, resulting in greater mixing of the plume. In Figures 4.8 and 4.9A, evidence of the plume is well-defined up to 800 feet away from the diffuser.

Figures 4.10A, 4.10B, and 4.10C show horizontal sections of the plume at the 0, 30, and 60 foot depths on October 17, 1995. Thirteen stations were occupied in a grid extending approximately 300 feet to either side of the diffuser; three samples were taken at each station. The spacing provided sufficient resolution to identify areas of both high and low effluent concentration, and values at the edge of the grid were well within the measurement limits of this study, indicating that the grid could be expanded over a much larger area. Note that these sections show the plume to be somewhat "blobby," with "lumps" of fluid of higher concentration in the flow field. Many plume models currently in use compute averages over longer periods of time and may predict more uniform

plume mixing than exhibited by this instantaneous (1-hour average) "snapshot;" see Section 4.4.5 for greater detail.

4.3.3 Added rare earth tracer

To further explore the potential applicability of ICP-MS to salt water, the use of an added tracer was investigated during this study. Standard addition testing (see Chapter 2 and Appendix C) established that many of the rare earth elements could be measured to relatively low concentrations in seawater. Further, previous study results indicated that these elements were present in low concentrations in both fresh and salt water samples, so their use as tracers would not require the addition of a large amount of material. The Waianae Outfall receiving waters were selected because of the relatively constant, low flow rate and because of the potential applicability of tracer methods to the study of outfall plume dynamics; such a tracer could also be added to a streamwater discharge.

A rare earth salt called lanthanum lanthanide chloride (containing high concentrations of La, Ce, Pr, and Nd) was purchased from Molycorp. Background concentrations of these elements in seawater are 10 ppt or less (see, for example, Bruland, 1983). This salt was selected after a literature search was conducted to confirm that this salt would likely be non-toxic to aquatic life. Assuming an initial dilution upon discharge from the outfall of approximately 100:1 and an effluent concentration of 1,500 ppb, the near field concentration of tracer would immediately be reduced to 15 ppb, with additional dilution occurring as the plume mixed further with surrounding ocean water. Past fish toxicity studies using rainbow trout have shown that exposure to 20 ppb of La

for 28 days would kill 50% of exposed trout (The Royal Society of Chemistry, 1994). European Community standards for lanthanum chloride in drinking water set an upper limit at 25 ppm based upon chloride concentrations (*ibid.*). An earlier study conducted in a drinking water reservoir in San Diego resulted in added lanthanum chloride concentrations in excess of 10 ppb with no adverse effects observed (List, 1997). Based upon this information, 125 pounds were purchased for $1.25 per pound. The salt was dissolved in a water/hydrochloric acid matrix, and the tracer was added to the outfall discharge over a 12-hour period. The final concentrations of La, Pr, and Nd in the effluent exiting the diffuser were 1,525, 174, and 525 ppb, respectively. During the injection period, the measured effluent flow rate averaged 3.35 million gallons per day (150 liters per second) and varied by only 30% from this average value.

Anticipated detection limits of the method in seawater were about 1 ppb for La, 1 ppb for Pr, and 0.7 ppb for Nd, theoretically corresponding to estimated dilutions of roughly 1500:1 for La, 175:1 for Pr, and 750:1 for Nd. Standard addition testing was conducted using a single clean, background seawater sample, collected far offshore of Oahu, to assess detection limits of these elements in seawater. The plots shown in Appendix C are generated from these standard addition laboratory tests and show good agreement between measured and expected concentrations of each of these elements down to about 0.1 ppb for this "clean" control seawater sample; this detection limit would correspond to estimated dilutions of 15,000:1, 1,750:1, and 7,500:1 for La, Pr, and Nd, respectively. However, field samples exhibited more variability, and the ICP-MS signal

was "noisier;" actual detection limits in field samples (and corresponding estimated dilution levels) were likely between these values.

Dilution levels of 300 to 1 were estimated consistently from concentrations measured for La, Pr, and Nd; these dilution levels correspond to residual concentrations in the receiving water of 5 ppb, 0.58 ppb, and 1.75 ppb for La, Pr, and Nd, respectively. Below these concentrations, significantly different dilutions were obtained for each of the three elements in the samples. The relative concentrations of the elements should have been constant for all the samples, regardless of the absolute concentrations. Dilutions predicted by Pr and Nd agreed fairly well with each other (see Appendix I); dilutions predicted by La at concentrations below 5 ppb varied by a factor of 2 to 3 from these values. There are several possible explanations for these differences, including analysis error, preferential losses during mixing, or matrix effects within the plasma.

To ensure that the discrepancy was not due to analysis error, half the samples were reanalyzed; results did not differ by more than about 5% from the initial analysis. Because replicates agreed, it was concluded that the discrepancy was due neither to changing instrument parameters nor to instrumental drift.

Discrepancies may have been due to the loss of one element preferentially over another as the effluent mixed with ocean water. This would require either preferential adsorption of one of the elements onto particles in the effluent with subsequent particle removal or diffusion rates within the mixing fluid that differed significantly from one element to the next. This process would have had to occur quickly, as the travel time of the wastewater effluent from the point of tracer addition to release into the ocean was

short, probably one-half hour or less, and dilution was observed to occur quickly as the plume exited the diffuser structure (see Figures 4.8 through 4.10). No particle removal was observed visually during the sampling event, and particles were not observed to have settled in containers after sample collection. Indeed, if particle removal were the mechanism of error, Pr and Nd should have been preferentially removed, as their binding constants with particulate matter tend to be higher than those for La (de Baar *et al.*, 1985; Byrne and Kim, 1990; de Baar *et al.*, 1991; Erel and Stolper, 1993), although some evidence is contradictory (Sholkovitz *et al.*, 1994; see Appendix A for greater detail). If there was preferential removal of an element in these samples, it was preferential removal of La, as dilutions predicted by La were much higher than those predicted by either Pr or Nd. In addition, rare earth species adsorbed to particles in whole water samples would desorb from particles upon sample acidification; they would therefore be present in the bulk solution for analysis rather than settling out on particles to the bottom of the collection container. Turbulence, which carries particles as well as dissolved substances in the bulk fluid, is the main mixing mechanism at the study site. Since turbulent diffusion is dominant over molecular diffusion, no element removal or enhancement should have been observed as a result of different molecular diffusion coefficients for different elements. Even diffusional processes coupled with preferential desorption from particles cannot explain the differences observed in the data since there is no reason that particles and bulk fluid (and therefore the elements) should separate spatially.

To test the hypothesis that the discrepancy was due to matrix effects within the plasma, six of the seawater samples collected during the tracer addition experiment and

previously analyzed by ICP-MS were selected and sent to the geochemistry laboratory of Dr. Gerald Wasserburg at Caltech for independent analysis of Nd concentrations. Samples selected included two with the highest REE concentrations measured by ICP-MS analysis, two with intermediate concentrations, and two with relatively low concentrations. The independent analysis was performed using a highly accurate Nd-isotope spiking technique. Analysis results are presented in Table 4.2.

Table 4.2
Nd concentrations measured by ICP-MS and by Nd-isotopic dilution analysis

Sample ID	HP 4500 ICP-MS Nd analysis		Isotopic Nd analysis	
	Concentration [ppb]	Standard deviation [ppb]	Concentration [ppb]	Standard deviation [ppb]
LaCl002	15.97	0.83	16.69	0.09
LaCl007	1.92	0.22	5.32	0.02
LaCl015	0.734	0.148	2.97	0.02
LaCl055	2.43	0.27	2.53	0.01
LaCl078	0.625	0.177	1.77	0.01
LaCl097	1.53	0.20	3.71	0.03

Concentrations measured by this independent analysis agreed relatively well with concentrations measured by ICP-MS for samples 2 and 55. These samples contained the high concentrations which produced the two concentration peaks in the flow field shown in Figure 4.11, which was produced using the concentrations measured by ICP-MS analysis. The concentrations measured by Nd-isotope analysis for the other samples were much higher than the concentrations measured by ICP-MS. This was surprising because the standard addition analysis of detection limits (see Chapter 2 and Appendix C) indicated that measured concentrations, if in error because of matrix effects, would be higher than actual concentrations. The cause of this error has not been determined;

sample contamination, which may have occurred during or after the initial ICP-MS analyses and before samples were analyzed using Nd-isotope analysis, seems the most likely cause.

To illustrate the inconsistencies, dilutions predicted by each element were calculated for the six samples analyzed by the ICP-MS and Nd-isotopic analysis methods. The results are presented in Table 4.3. Dilutions predicted by all measurements agreed for sample 2; the highest dilution values were predicted by ICP-MS measurements for either sample 15 or sample 78. Dilutions predicted by each of the two methods for the other samples differ significantly and are disappointing. Nonetheless, the general trends observed in the plots are confirmed, but the exact magnitude of the predicted dilution varied by a factor of roughly three for many of the samples. Although the cause of the inconsistencies between the La, Pr, and Nd measurements was not resolved, the plots of plume dilution are in qualitative agreement, *i.e.*, the magnitude of observed peaks varies, but the location, shape, and footprint of peaks as determined by La, Pr, and Nd measurements agree.

Table 4.3
Dilutions measured by ICP-MS and by Nd-isotopic dilution analysis

Sample ID	HP 4500 ICP-MS analysis			Isotopic Nd analysis
	La dilution	Pr dilution	Nd dilution	Nd dilution
LaCl002	31.6 ± 1.1	30.7 ± 2.8	33.0 ± 2.3	31.6 ± 1.6
LaCl007	310 ± 10	260 ± 30	270 ± 30	100 ± 5
LaCl015	1600 ± 100	850 ± 120	720 ± 100	180 ± 10
LaCl055	660 ± 30	280 ± 30	220 ± 20	210 ± 10
LaCl078	2400 ± 100	500 ± 60	800 ± 100	300 ± 15
LaCl097	970 ± 30	340 ± 30	350 ± 40	140 ± 10

Appendix I includes both point value plots and contour plots generated from these concentrations, plotted as normalized concentrations × 1000, where the normalized concentration was defined as the measured concentration in a given sample divided by the effluent concentration. These plots were generated using samples collected at a given depth or from samples collected at the surface, as indicated on the plots. Plots generated using concentration data for each of the three elements show remarkably similar features. As an example, Figure 4.11 shows the plots for La and Pr at the surface and the 35 foot depth (note that plots for Nd are similar to those for Pr and are included in Appendix I, along with plots for all three elements at the 70 foot depth). Most notable are the various concentration peaks on the different levels. Apart from the unusually high value measured at the northwest corner of the sampling grid at the 35 foot depth, the ratio of the peak concentrations to background lay in the 3:1 to 6:1 range. Given the above mentioned uncertainties in some of the data, the plots could possibly misrepresent the intensity of the peaks, but the features themselves are probably real and confirm the "lumpy" or "blobby" nature of the plume observed in Figures 4.8 through 4.10.

4.4 Conclusions

The goal of this project was to identify the potential for ICP-MS to fingerprint and track possible sources of coastal pollution. The research has led to several important findings and conclusions regarding the applicability of ICP-MS analysis to saline waters and regarding the elemental characteristics of Hawai'i's streams, outfalls, and coastal waters.

4.4.1 Determination of fingerprints

Over 250 samples from the streams draining into Pearl Harbor, the Ala Wai Canal, and Inoaole Stream in Waimanalo were collected and analyzed during this study. The ICP-MS analysis of these samples revealed that the elemental fingerprints of these streams were not distinct from each other. This is in contrast to the findings from the Delta study area, where rivers showed very distinct elemental fingerprints. In Hawai'i, there may be special situations that result from unique industrial discharges, but in general the relative uniformity of surface water sources precludes the use of natural water composition for fingerprinting water sources. The homogeneity of the streams is likely due to the relatively uniform geologic composition of the island.

4.4.2 Determination of tracer elements

As discussed in Chapter 2, the technique chosen for analysis of saline samples (dilution to 10:1 and calibration using external standards created in a NaCl matrix) was not capable of measuring elements that were present in low concentrations in highly saline samples. This was due to matrix effects within the plasma caused by very high concentrations of major ions, resulting in an enhancement of signal (false "positives") at very low concentrations. This effect would also be present if the technique of standard addition were adopted; this effect precludes using as tracers elements that are present in higher concentrations in stream waters than in ocean waters.

Rb, Sr, and U were isolated as three easily identifiable elements that did occur in significantly different concentrations in freshwater discharges and in ocean water; the freshwater discharges showed a significant deficit in these elements relative to ocean water. This feature allowed the successful tracking of the discharges by measuring the reduction in ambient ocean concentrations caused by the discharges. This "inverse tracer" method demonstrated the ability to measure dilutions to 25:1 with good accuracy. Dilutions of this order can provide excellent visualization of plumes of effluent discharging to the ocean; indeed, the plume observed in this study appeared "lumpy" and "blobby." However, this technique did not permit the unique tracing of a specific discharge; all freshwater sources showed the same effect and were not separable. Comparable results could be obtained more economically by measuring conductivity, a surrogate for salinity.

4.4.3 Use of added tracers

Given the deficit of suitable tracer elements in the discharge sources studied, various elements were investigated for possible use as added tracers. A rare earth salt called lanthanum lanthanide-chloride, containing high concentrations of La, Nd, and Pr, was selected. A solution made from this salt was injected into the Waianae Outfall discharge prior to one of the receiving water sampling events. Dilution levels of 300:1 were subsequently estimated using elemental concentrations determined by ICP-MS analysis; these dilution levels corresponded to residual La concentrations of 5 ppb in the receiving water (see Appendix I). Below that concentration, different dilutions were

obtained from each of the three elements in the solution, with the implied La dilutions at least three times the dilution measured for the other two elements; separate analyses designed to resolve this issue were inconclusive and possibly flawed by contamination. Despite difficulties in quantifying dilution at levels higher than 300:1 (or greater than about 35:1, if Nd-isotope analysis techniques are used), dilution plots created from the data obtained for each of the three elements agreed qualitatively and showed a "lumpy" plume. These results indicate that above these dilution levels, the magnitude of dilution cannot be determined using current analysis techniques, but flow features can be determined. Increased dilution could be measured quantitatively by increasing the amount of tracer injected into the flow or by improving analytical techniques to lower detection limits. With the analytical techniques developed in this study, La tracer should be injected in sufficient volume that the residual concentrations would remain above 10 ppb. This tracer addition technique also could be used to distinguish stream water sources from one another.

4.4.4 Areas for further study

In principle, the "inverse tracer" method should be capable of measuring dilutions to at least 1000:1, but it would require the use of an exchange resin technique (described in Section 2.2.4) to remove major ions, which cause noise on the ICP-MS signal due to matrix effects. Use of ion exchange techniques would significantly increase sample processing and handling time; additionally, increasing ICP-MS dwell times (the amount of time spent analyzing a single isotope, see Chapter 2) to reduce the noise on the

signal would also increase sample analysis time. This technique is also the most promising for measuring very low concentrations of various elements in saline samples and would improve detection limits for added tracers significantly. Because of the extensive sample handling required, this technique is commonly used for small numbers of samples and has been successfully used for the measurement of rare earth elements in seawater in the part-per-trillion range (see, for example, de Baar *et al.*, 1985). This technique would require automation in order to be a rapid and economical means of measuring large numbers of samples in receiving waters. This advance would result in the greatest improvement in the methods developed for this study.

4.4.5 Application of plume models

Computer models are often used in engineering analyses to predict the behavior of buoyant plumes. Such computer models are useful in describing the time-averaged concentrations of an effluent in the receiving water, but these models are limited in their ability to describe instantaneous conditions.

As described by Fischer *et al.* (1979), plume behavior is highly dependent upon many factors, including: the characteristics of the plume itself, as described by the initial momentum and buoyancy fluxes and the flux of any tracer material; environmental parameters, including turbulence levels, currents, and density stratification; and the geometry of the problem, including the geometry of the outfall. The relationships between these parameters have been determined under laboratory conditions and are fairly well understood for the simplest of cases. Numerical models are based upon results

obtained from studying these simple cases; they are then used in environments and under conditions that are much more complex and where many of the assumptions used in the development of simple models may no longer apply. Most models assume that neither ocean currents nor the rate of effluent discharge vary with time, and necessary coefficients (accounting for such factors as ambient crossflow, buoyancy, flow curvature, etc.) are often estimated from asymptotic solutions obtained in the absence of other parameters.

Additionally, these models generally yield results that are "ensemble averages," which smooth out large concentrations gradients that may result from both small and large scale fluctuations in the turbulent flow field. Results from these models generally provide a statistical estimate of the size of a plume and of concentrations within the plume as an average over time; plumes represented in this way have smooth Gaussian concentration distributions that do not vary significantly at a given location on short timescales. Such a solution technique cannot reproduce the large peaks in concentration that may be observed on short timescales.

In contrast, field and short-timescale laboratory observations show that buoyant mixing is more likely to be "lumpy" or "blobby," with "puffs" of higher concentration present in the plume. Thus, the concentration at a given point in the flow field may fluctuate between zero and a concentration several times that predicted by plume models. Such a "strongly intermittent concentration field" has been observed in the laboratory by Papantoniou and List (1989), who also give more theoretical detail than is presented here.

Observations of the mixing of the outfall plume near Waianae indicate that "blobby" buoyant plume behavior also occurs over large length scales.

Figure 4.1: Pearl Harbor/Oahu study area

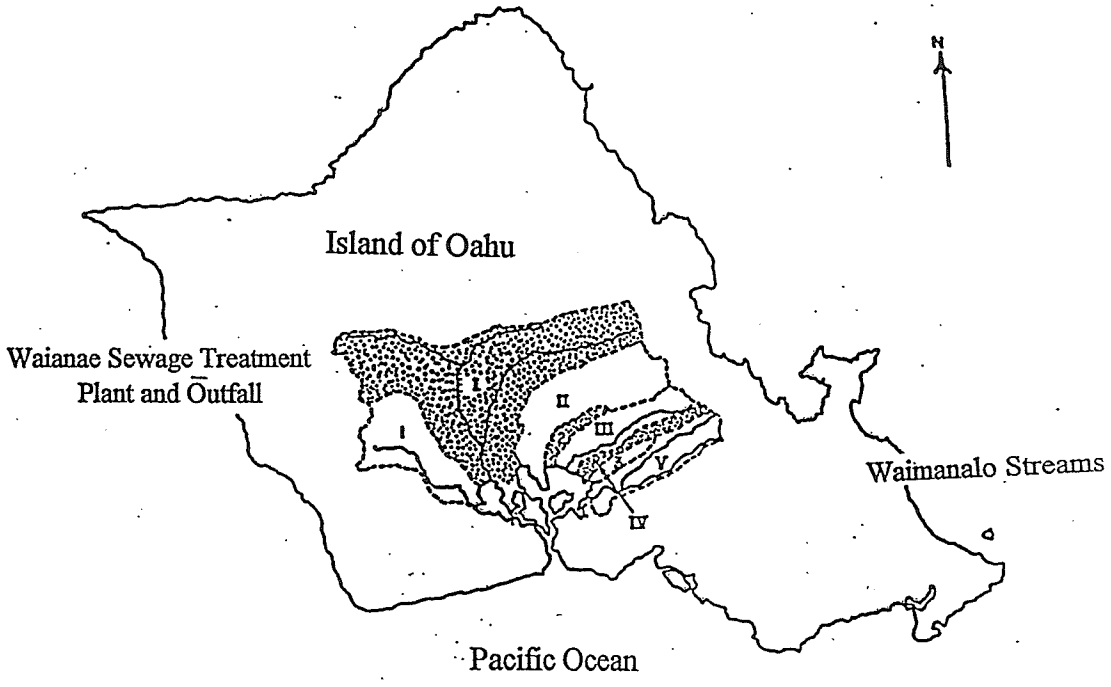

Drainage Areas as Shown
- I Waikele
- II Waiawa
- III Waimalu
- IV Kalauao
- V Halawa
- 1 Honouliuli
- 2 Waimanu
- 3 Aiea

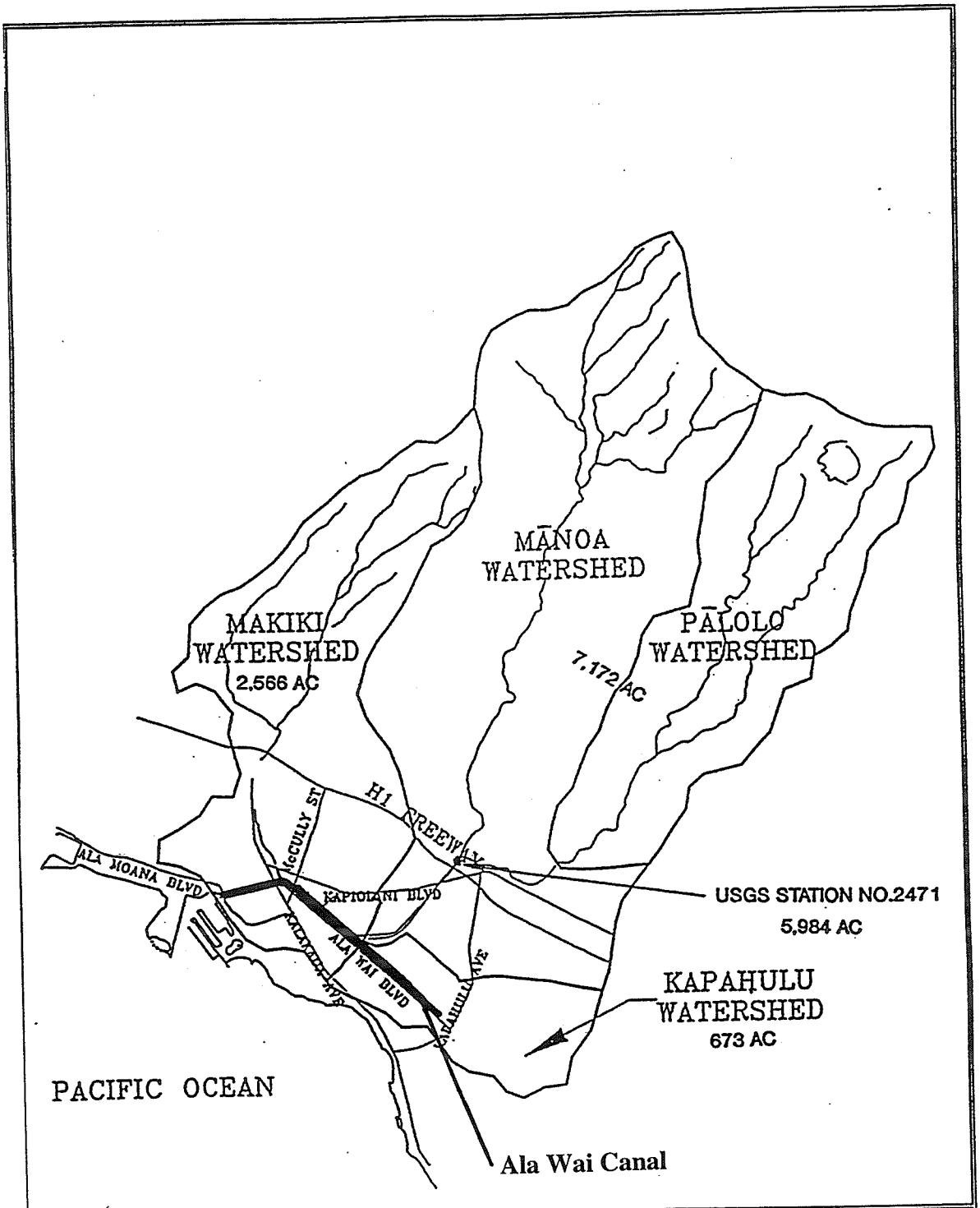

Figure 4.2: ALA WAI CANAL AND WATERSHEDS

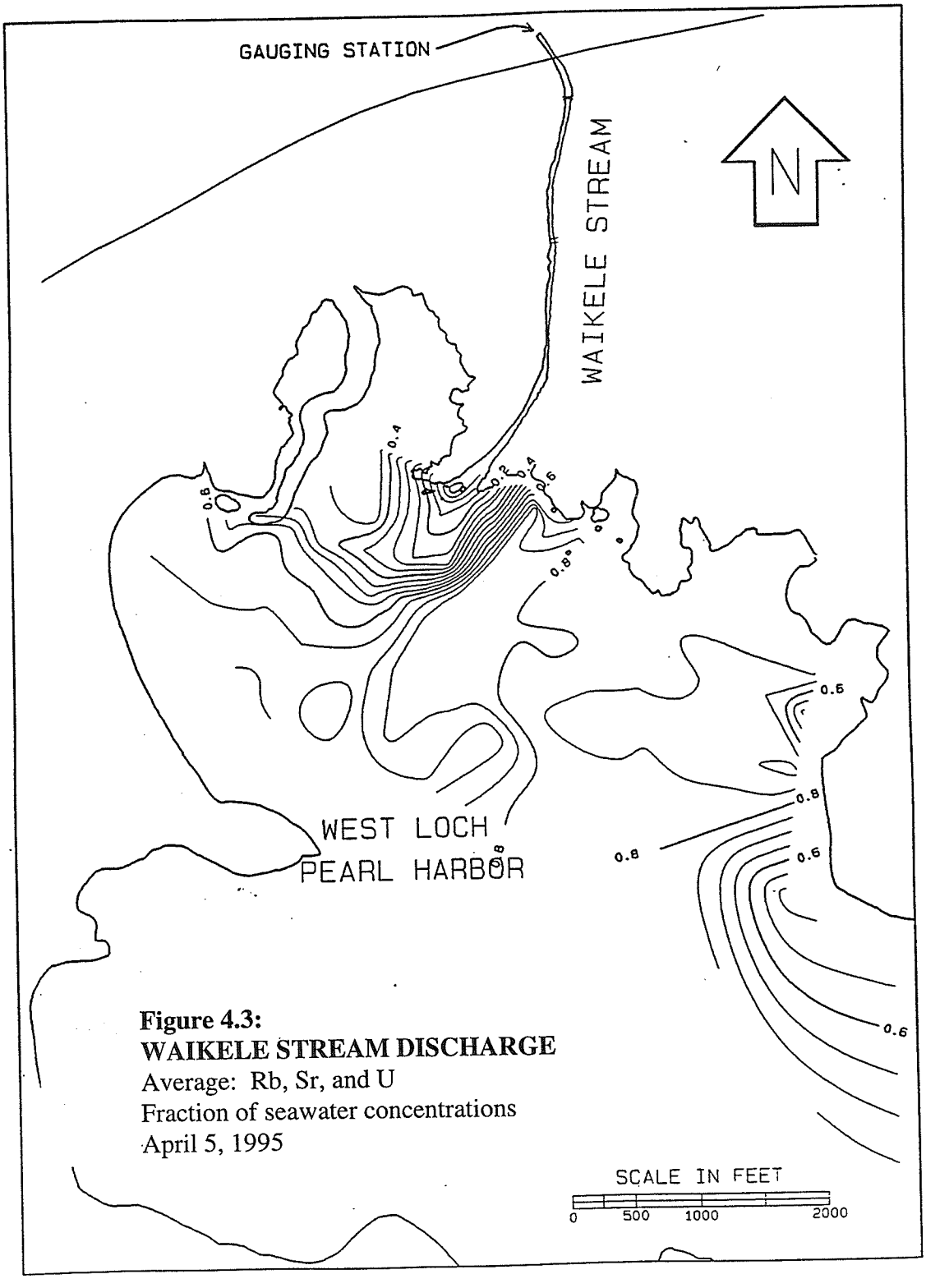

Figure 4.3:
WAIKELE STREAM DISCHARGE
Average: Rb, Sr, and U
Fraction of seawater concentrations
April 5, 1995

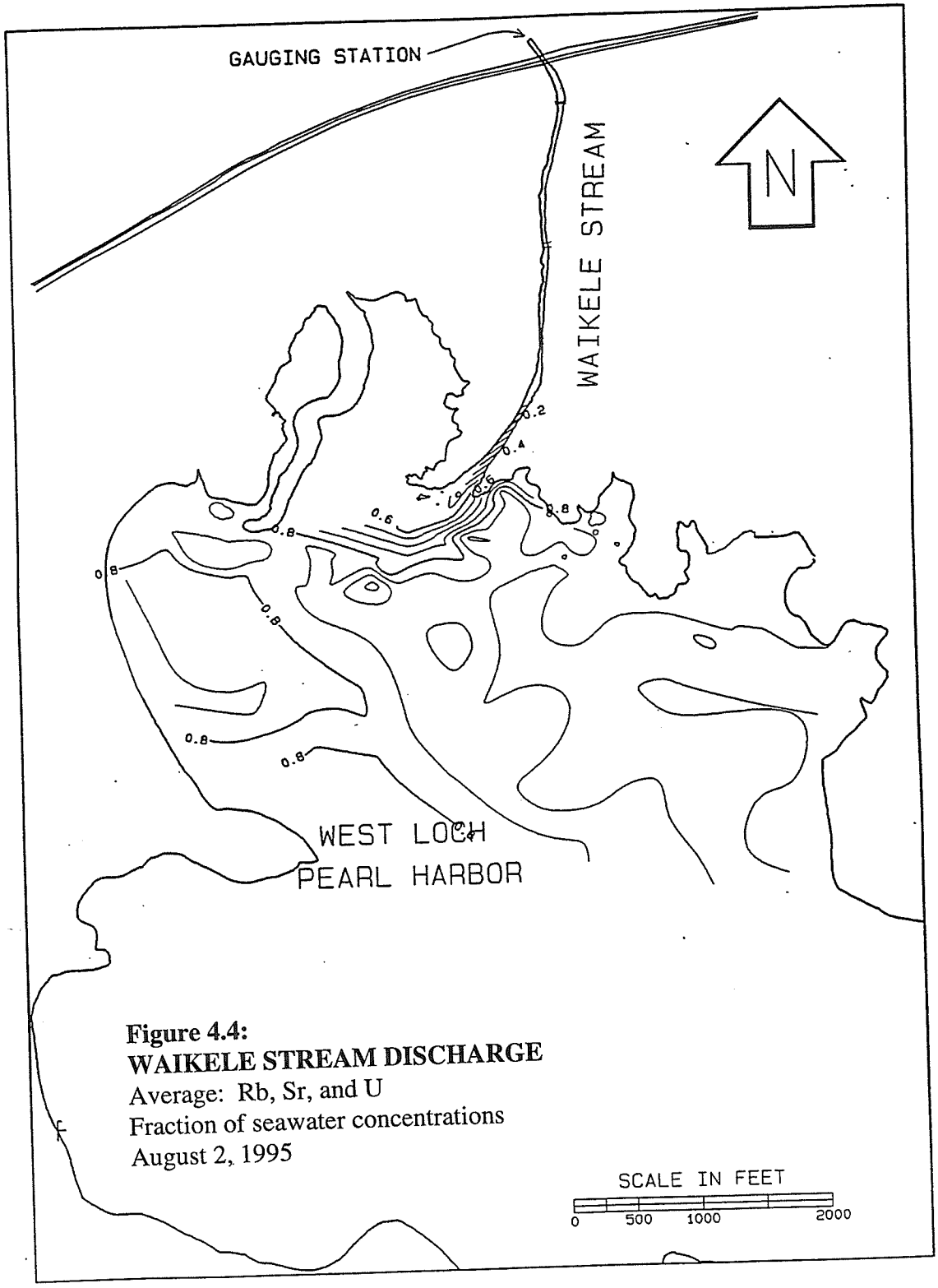

Figure 4.4:
WAIKELE STREAM DISCHARGE
Average: Rb, Sr, and U
Fraction of seawater concentrations
August 2, 1995

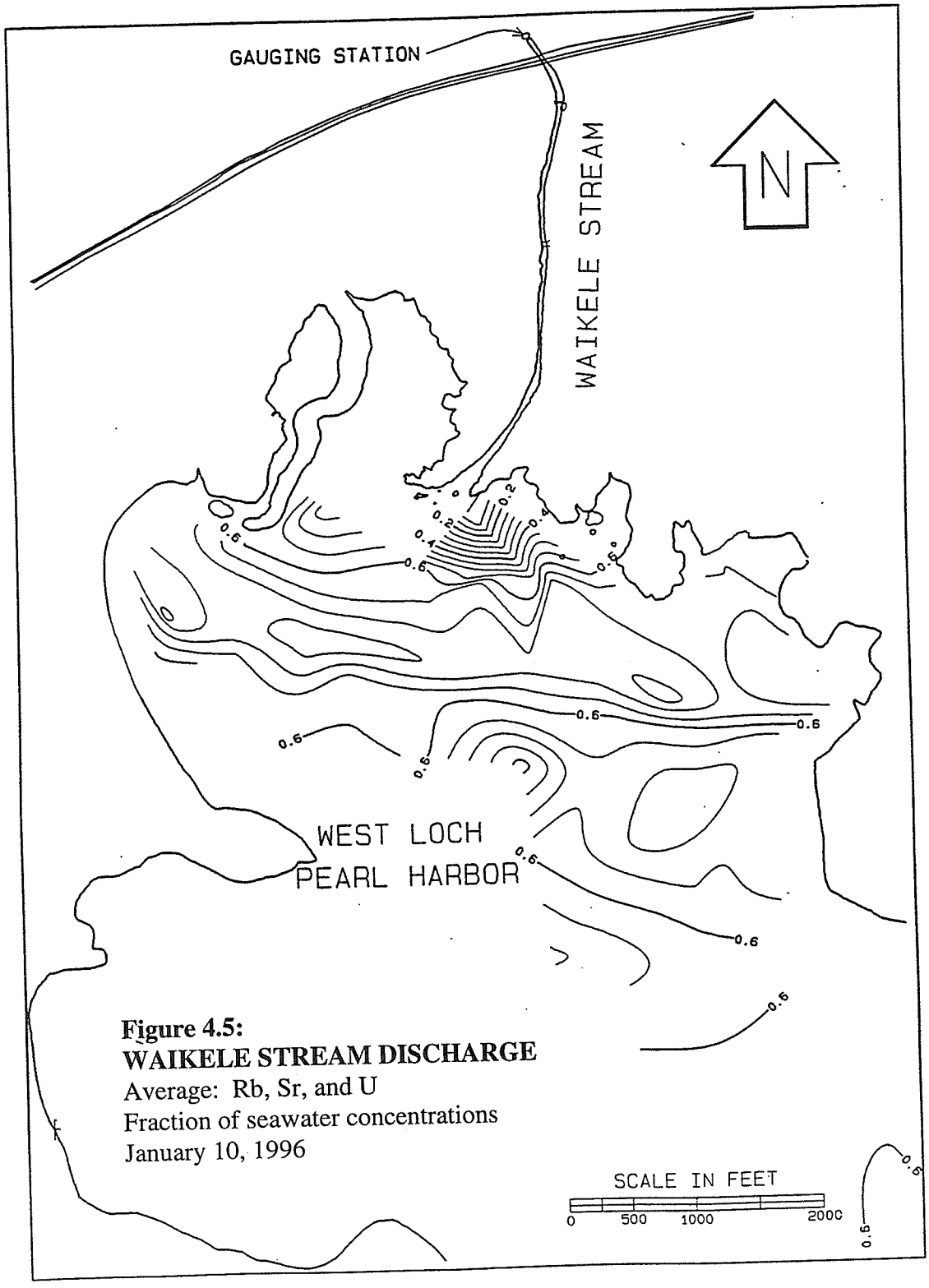

Figure 4.5:
WAIKELE STREAM DISCHARGE
Average: Rb, Sr, and U
Fraction of seawater concentrations
January 10, 1996

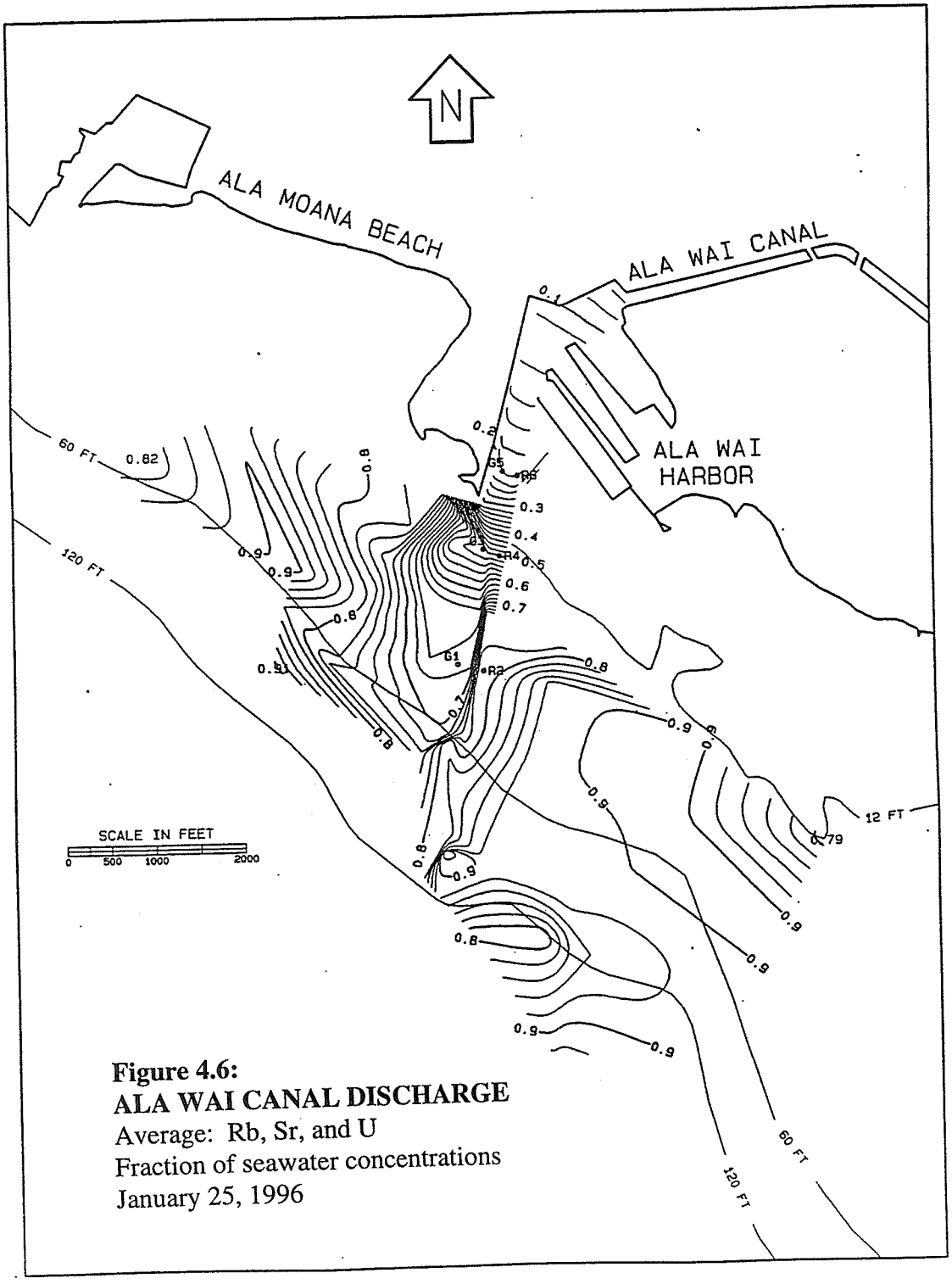

Figure 4.6:
ALA WAI CANAL DISCHARGE
Average: Rb, Sr, and U
Fraction of seawater concentrations
January 25, 1996

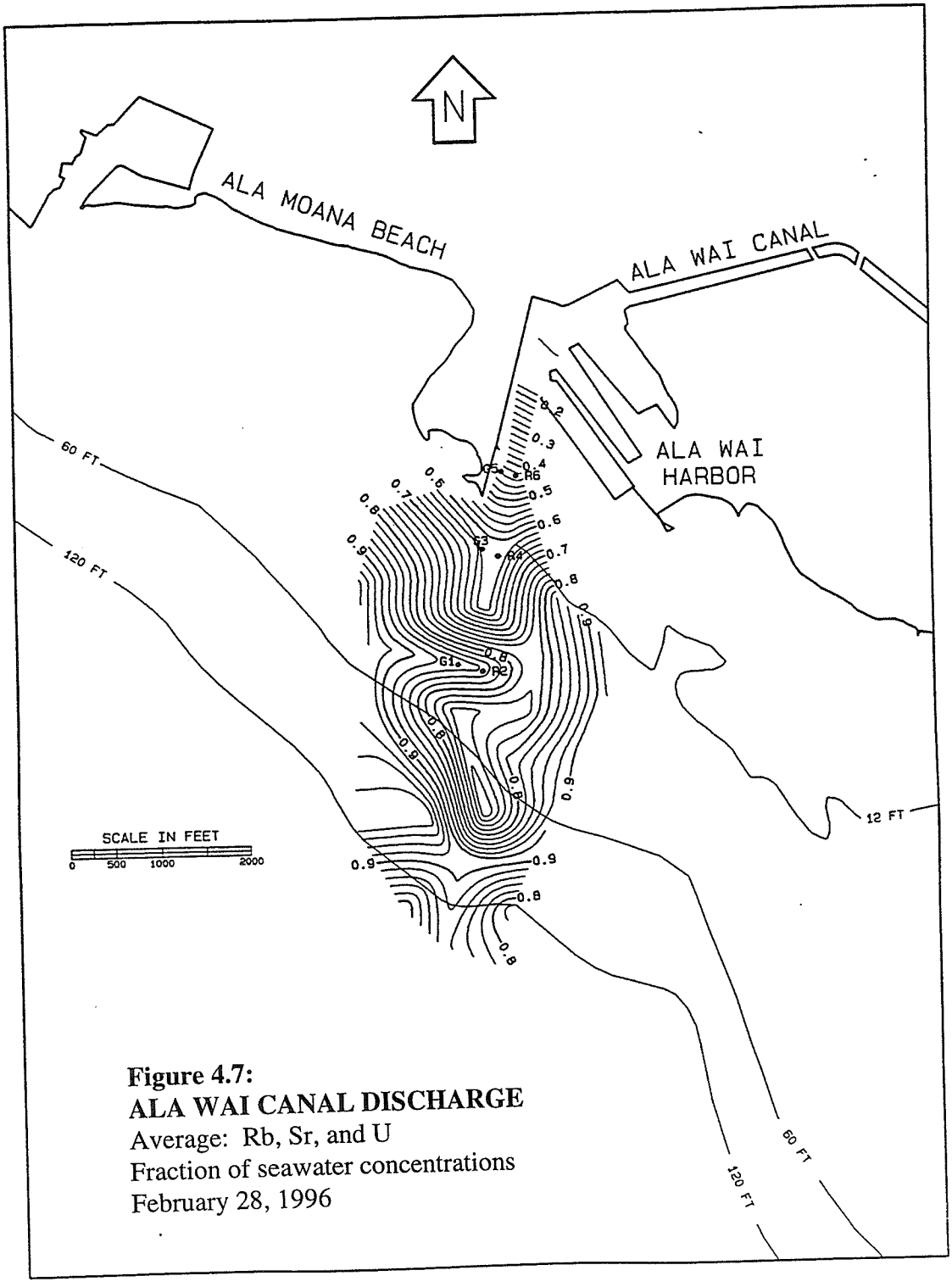

Figure 4.7:
ALA WAI CANAL DISCHARGE
Average: Rb, Sr, and U
Fraction of seawater concentrations
February 28, 1996

Figure 4.8:

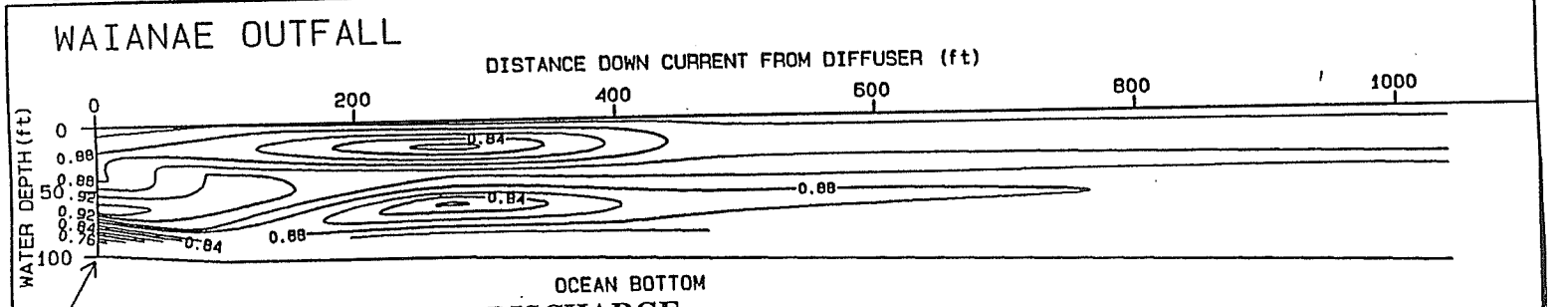

WAIANAE OUTFALL DISCHARGE
Average: Rb, Sr, and U
Fraction of seawater concentrations
April 12, 1995
Transect bearing 166 T

Figure 4.9A:

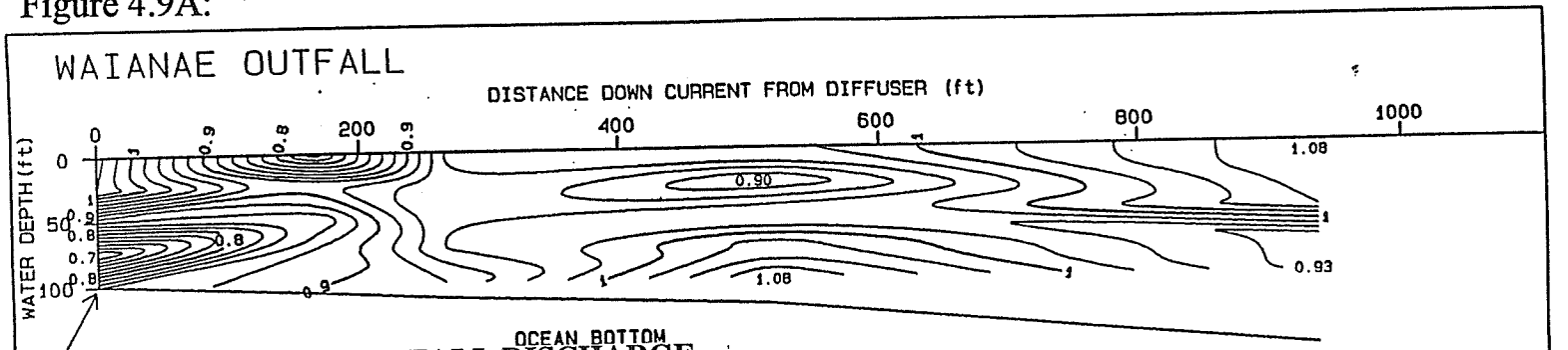

WAIANAE OUTFALL DISCHARGE
Average: Rb, Sr, and U
Fraction of seawater concentrations
August 18, 1995
Transect 1, bearing 184 T

Figure 4.9B:

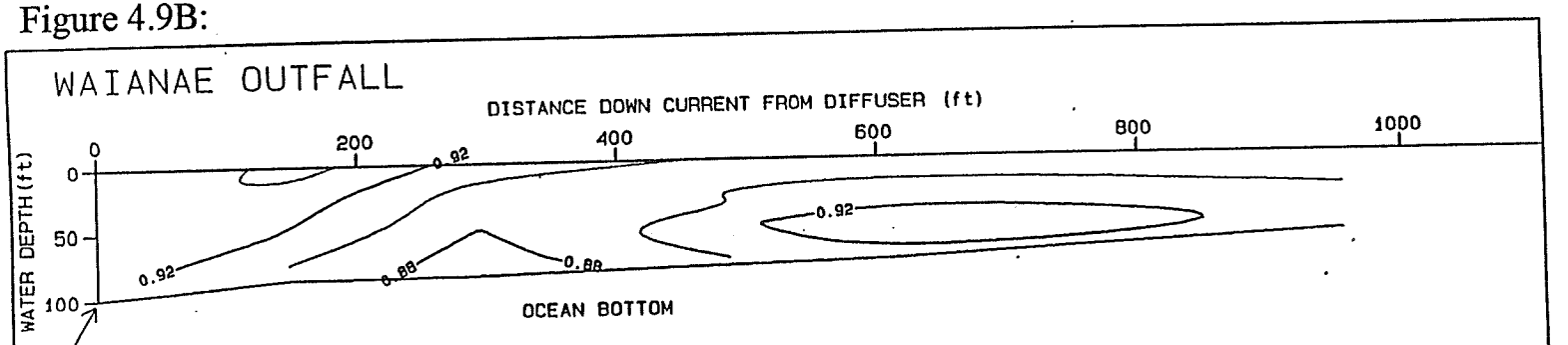

WAIANAE OUTFALL DISCHARGE
Average: Rb, Sr, and U
Fraction of seawater concentrations
August 18, 1995
Transect 2

Figure 4.9C:

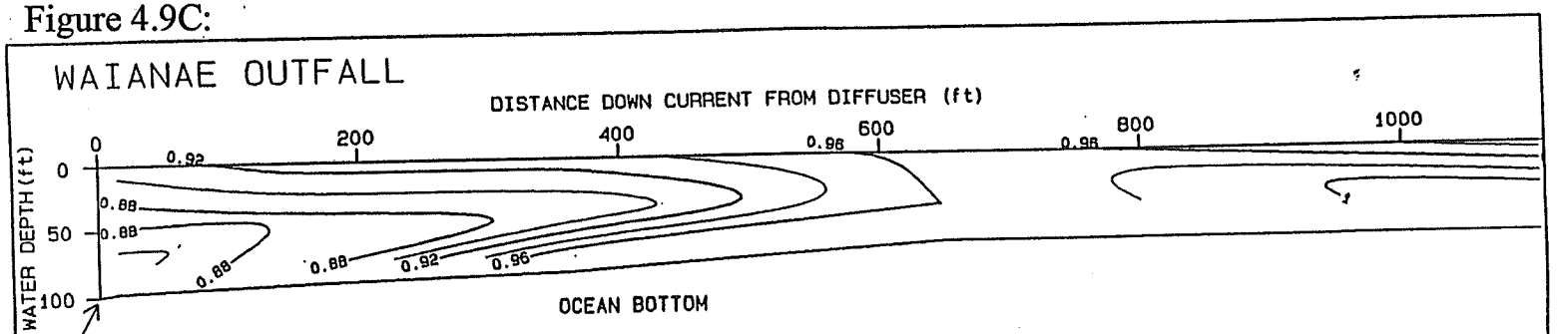

WAIANAE OUTFALL DISCHARGE
Average: Rb, Sr, and U
Fraction of seawater concentrations
August 18, 1995
Transect 3, bearing 324 T

Figure 4.9D:

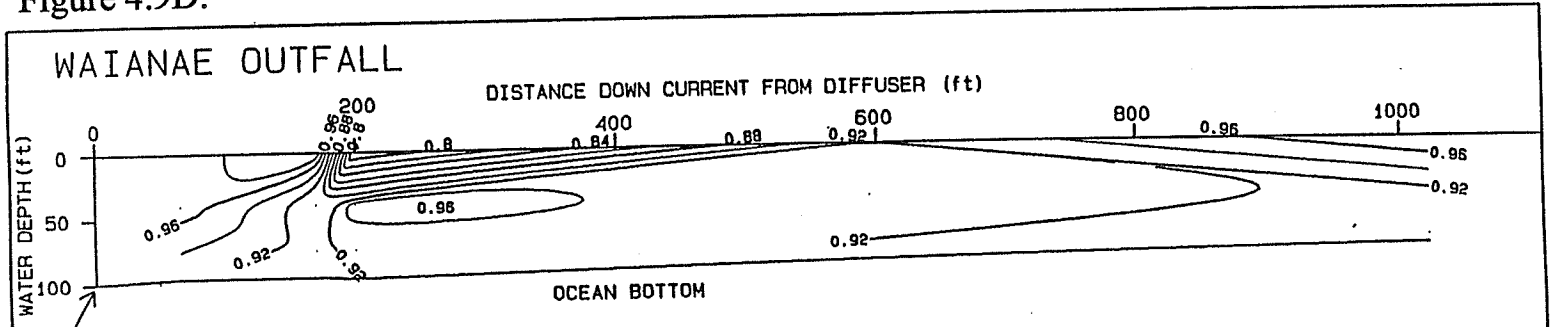

WAIANAE OUTFALL DISCHARGE
Average: Rb, Sr, and U
Fraction of seawater concentrations
August 18, 1995
Transect 5, bearing 117 T

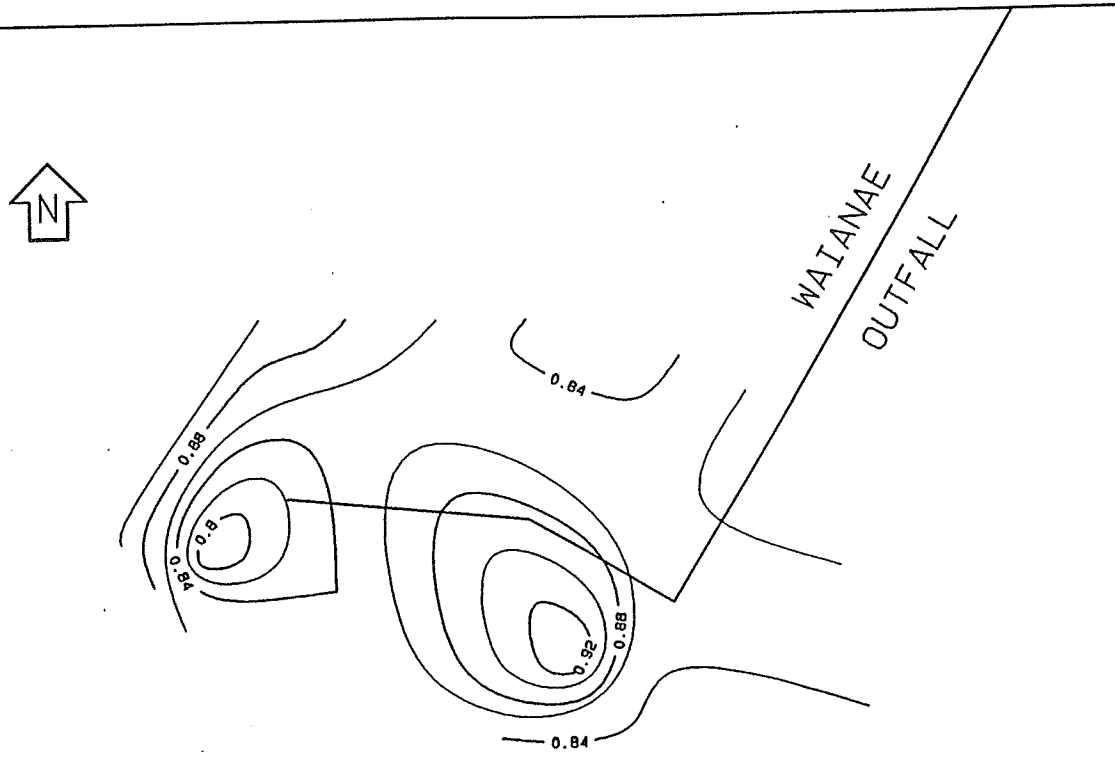

Figure 4.10A:
WAIANAE OUTFALL DISCHARGE
Average: Rb, Sr, and U
Fraction of seawater concentrations
October 17, 1995
Depth: 0 feet

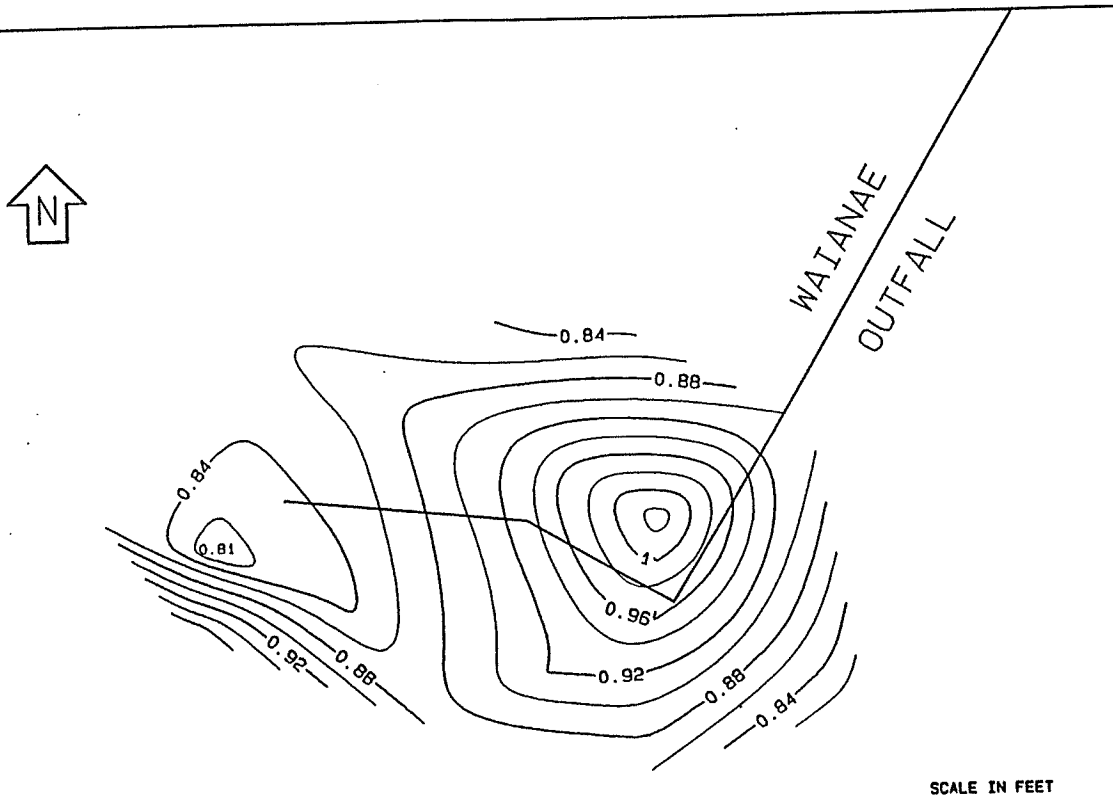

Figure 4.10B:
WAIANAE OUTFALL DISCHARGE
Average: Rb, Sr, and U
Fraction of seawater concentrations
October 17, 1995
Depth: 30 feet

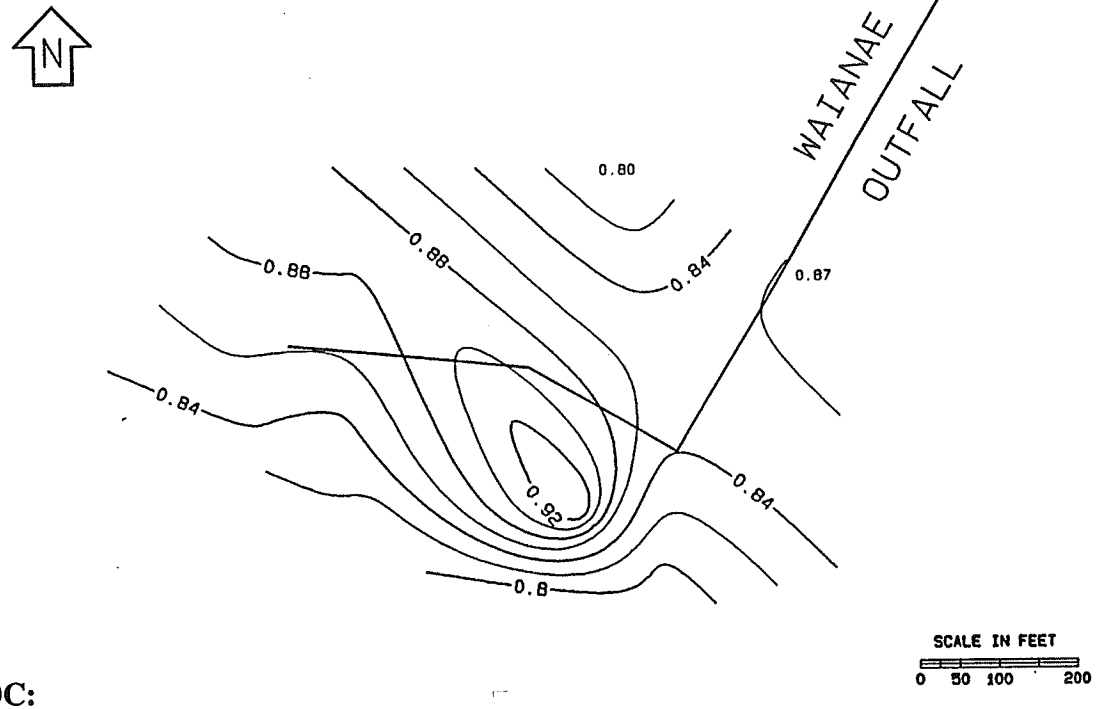

Figure 4.10C:
WAIANAE OUTFALL DISCHARGE
Average: Rb, Sr, and U
Fraction of seawater concentrations
October 17, 1995
Depth: 60 feet

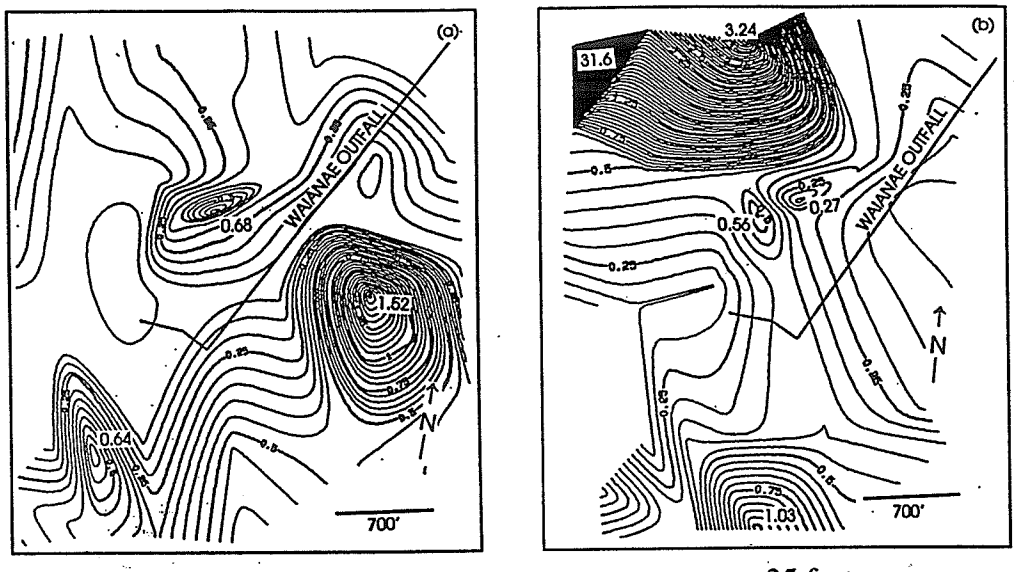

Surface -35 feet

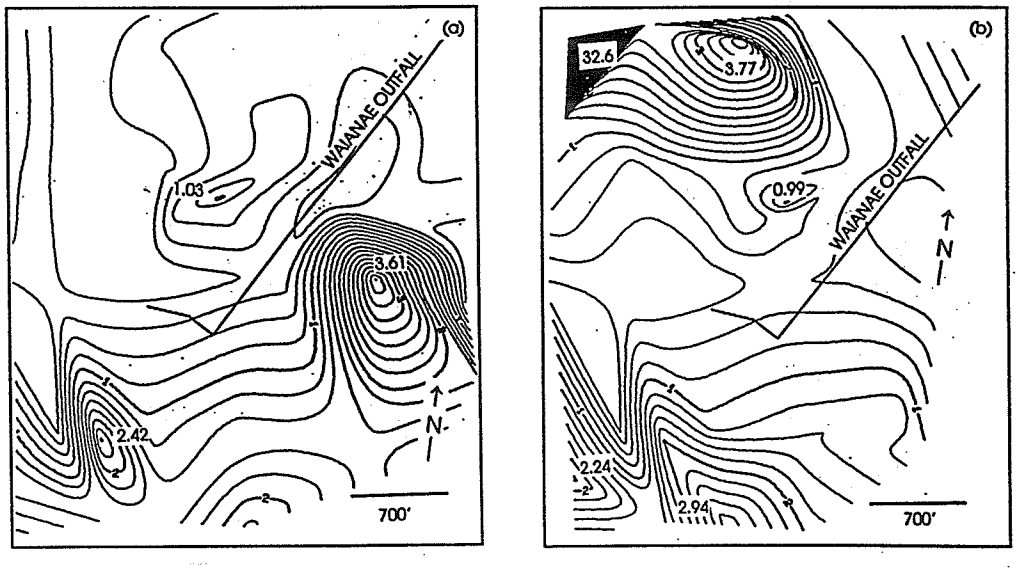

Surface -35 feet

Figure 4.11:
Normalized concentrations (×1000) of La (top) and Pr (bottom) at the surface and 35 feet below the surface during the Waianae Outfall tracer injection event. Peak values are indicated on plots.

5 Additional applications of tracer techniques

5.1 Introduction

The method developed above for tracing flows in the Delta and in the near-coastal environment of Oahu was also used to trace flows and predict mixing in simpler flow systems. Many of the elements used to predict mixing for the study areas presented in Chapters 3 and 4 were also found to predict mixing well in three quite diverse systems. In one simple study, ratios of inflows from two different sources were used to successfully predict mixing in treated water from a drinking water treatment plant. In another study in the Napa River estuary, concentrations of several elements were observed to predict the vertical and longitudinal distribution of saline water from San Pablo Bay and fresh water from the Napa River. A tracer was added to a treated wastewater discharging into the south Sacramento/San Joaquin Delta to predict mixing behavior and residence times in this system. This chapter presents the results of these studies, focusing on the application of the techniques presented in this thesis rather than on the specific details of each project.

5.2 Mixing in the Weymouth Filtration Plant

An initial test of the methodology presented in this study was conducted with water collected from the Weymouth Filtration Plant, which is operated by the Metropolitan Water District (MWD) and in Laverne, California. This plant blends water from two sources, treats it using several treatment processes, and then distributes it for

use. The two sources of water to the plant are the Colorado River Aqueduct and the California Aqueduct, which delivers water from the Sacramento/San Joaquin Delta in northern California. The water from the Delta is a mixture of waters from the Sacramento River, the San Joaquin River, and other smaller rivers and contains, depending upon location, a small component of water from San Francisco Bay (see Chapter 4 for greater detail); it is well-mixed by the time it reaches the treatment plant. Treatment processes in the plant include flocculation (with the addition of ferric chloride, $FeCl_3$), sedimentation, filtration through activated carbon beds, and chlorination. Several samples were collected from the plant on May 26, 1994, and analyzed using the Perkin-Elmer ICP-MS.

The mixing ratio of the two influent water sources was estimated based upon the measured concentrations in the two influent streams (before blending or treatment) and the measured concentration in the treated water leaving the plant after treatment. If the concentration of a tracer and the flowrates of the two influent streams are c_1 and Q_1 (for water from the Colorado Aqueduct) and c_2 and Q_2 (for water from the California Aqueduct), and the treated water has concentration c_3 and total flow Q_3, then for a conservative tracer:

$$c_1Q_1 + c_2Q_2 = c_3Q_3 \text{ and}$$

$$Q_3 = Q_1 + Q_2.$$

Dividing each equation by Q_3 and by substitution:

$$\frac{Q_1}{Q_3} = \frac{c_3 - c_1}{c_2 - c_1},$$

where Q_1/Q_3 is the fraction of water from the Colorado aqueduct in the treated water leaving the plant.

This computed fraction was compared to the measured fraction of the two influent water sources, known from flow monitoring devices in the plant. Results are shown in Table 5.1. In spite of the extensive treatment these waters receive (designed primarily to disinfect and remove particulate matter), mixing ratios are predicted accurately by many elements. Many of these same elements also predict mixing accurately in other systems (see Chapters 3 and 4 and detail later in this chapter). Although ion exchange effects are not important, particle removal effects may be, particularly since one of the treatment processes involves the precipitation of particles designed to remove impurities. However, these data indicate that particle settling may not be important in determining behavior for these conservative elements when two freshwaters are mixed together.

Table 5.1
Measured concentrations and predicted mixing ratios at Weymouth Filtration Plant

Element	Concentration in Colorado Aqueduct [ppb]	Concentration in California Aqueduct [ppb]	Concentration in treated outflow [ppb]	Computed fraction of Colorado water in outflow ($Q_1/Q_{3,measured}$=0.90)
Li	15.35	1.84	13.92	0.89
B	18.46	35.85	21.36	0.83
Si	706	1194	753	0.90
K	1511	1063	1475	0.92
Ca	27,490	1250	25,000	0.91
Sc	0.42	0.77	0.45	0.90
Rb	1.35	0.87	1.27	0.84
Sr	555	154	523	0.92
Mo	3.59	1.43	3.31	0.87
Sb	0.17	0.06	0.15	0.83
I	2.09	4.66	2.32	0.91
Ba	146	40	135	0.90
U	11.22	4.12	10.63	0.92

5.3 Napa River estuary

The Napa Marsh, located adjacent to the Napa River at the northern end of San Pablo Bay, is 48,000 acres in size and is very significant ecologically. It is a staging and wintering area for birds migrating along the Pacific Flyway, and over 100 species of water birds use the sloughs and marshes in this area. It is also home to several endangered species, including the California clapper rail and the Salt-marsh harvest mouse. Until 1990, the commodities company Cargill operated approximately 10,000 acres of evaporation ponds used for the solar production of salt. These ponds were located in the marsh immediately adjacent to the Napa River (see Figure 5.1). Cargill's property contained 52 miles (84 km) of rivers and dikes in addition to tidal sloughs and reclaimed wetlands and salt marshes once used for agriculture. After salt production ceased, a plan was developed to remove the salt from the evaporation ponds by pumping lower salinity Napa River water through them, thus flushing salts out of the ponds and restoring them to natural, brackish wetlands. As part of the analysis conducted to support this plan, samples were collected and analyzed at Caltech using ICP-MS to determine the tidal flushing capacity of the Napa River estuary. The data presented here illustrate that the determination of the concentrations of a few elements is sufficient to establish the distribution between saline water (delivered into the estuary from San Pablo Bay by tidal action) and fresh water (delivered by the Napa River) within this estuary.

Samples were collected at four locations along the main channel of the Napa River during a flood tide. These locations are marked on Figure 5.1. At each location, three sets of samples were collected: four samples were collected from just above the

bottom of the channel, four samples were collected from the mid-depth point of the channel, and four surface water samples were collected. Concentrations of many elements were measured in each of the samples using Caltech's Perkin-Elmer ICP-MS. Samples were analyzed qualitatively only, meaning that the absolute concentrations in the samples may not have been determined precisely, but ratios of concentrations between samples are probably accurate. Salinities were computed from conductivity measurements made in the field. Concentrations and mixing ratios are presented in Table 5.2. Mixing ratios were calculated using the minimum and maximum concentrations measured in the samples as endpoints for the river and Bay waters; the mixing ratio represents the fraction of water in a given sample from San Pablo Bay, with the remainder from the Napa River. The mixing ratio is computed as:

$$\frac{C_{sample} - C_{river}}{C_{Bay} - C_{river}}.$$

As can be seen from the data in Table 5.2, the data agree well for several of the elements measured. With the exception of the salinity measured in the surface sample collected at station 4, the elemental mixing estimates also agree well with mixing ratios predicted by salinity. All of the samples collected were highly saline (compare to seawater, with an average salinity of about 34.6‰ (Murray, 1992)), samples were not diluted, and measurement was qualitative. Considering these limitations, these results clearly show that these elemental tracers can be used to predict mixing ratios for mixing between brackish and more saline waters. Additionally, several other elements predicted mixing nearly as well when the saline endpoint concentration was chosen to improve the data fit. This is because of saturation effects, particularly pronounced in the Perkin-Elmer

ICP-MS, where very high concentrations of elements are underestimated. These elements include Mg, K, and Mo. Such manipulation also improves the agreement of the predicted data for Br.

Table 5.2
Measured concentrations and predicted mixing ratios[a] in the Napa River estuary

Constituent	Location 1	Location 2	Location 3	Location 4
Salinity [‰]				
surface	13.0 (0.00)	14.7 (0.23)	15.4 (0.33)	14.5 (0.20)
mid-depth	13.3 (0.02)	14.7 (0.22)	15.4 (0.32)	16.7 (0.50)
bottom	13.9 (0.11)	14.9 (0.24)	15.3 (0.31)	20.2 (1.00)
Li [ppb]				
surface	69.6 (0.08)	76.9 (0.18)	91.7 (0.37)	107.3 (0.56)
mid-depth	68.5 (0.07)	77.5 (0.19)	90.3 (0.35)	100.0 (0.47)
bottom	62.9 (0.00)	78.0 (0.19)	84.0 (0.27)	141.8 (1.00)
B [ppb]				
surface	537 (0.06)	591 (0.15)	741 (0.38)	881 (0.59)
mid-depth	535 (0.06)	614 (0.18)	749 (0.39)	874 (0.58)
bottom	496 (0.00)	615 (0.18)	663 (0.26)	1,145 (1.00)
Sr [ppb]				
surface	1,870 (0.04)	2,020 (0.13)	2,300 (0.30)	2,530 (0.43)
mid-depth	1,880 (0.04)	2,020 (0.13)	2,260 (0.27)	2,390 (0.35)
bottom	1,810 (0.00)	2,070 (0.15)	2,200 (0.24)	3,470 (1.00)
Br [ppb]				
surface	13,800 (0.07)	14,400 (0.12)	16,200 (0.27)	17,500 (0.38)
mid-depth	13,700 (0.06)	14,500 (0.12)	15,900 (0.24)	16,800 (0.32)
bottom	13,000 (0.00)	15,100 (0.18)	15,900 (0.24)	24,900 (1.00)

[a] Data in table include concentrations and mixing ratios for each location and depth; mixing ratios are in parentheses. Mixing ratios represent the fraction of water in a given sample from San Pablo Bay, with the remainder from the Napa River.

5.4 City of Tracy wastewater study

The City of Tracy, California, discharges treated wastewater to Old River in the southern part of the Delta system via an outfall diffuser. To fulfill the requirements of a Tentative NPDES permit, the City was required to determine the variability of the available dilution for the effluent discharge. Because of artificial barriers recently placed

in the channels near the study area, flow rates may be reduced from historic levels. To address this issue, a tracer was added to the effluent stream; concentrations of this tracer were then measured using ICP-MS, and dilution levels were estimated directly from the field data. In addition, the field data were used to calibrate an existing computer flow model for the Delta. Field studies were conducted under two different barrier configurations: once in September 1996 and again in November 1996.

The field measurements were scheduled to meet the requirements of the NPDES permit by determining the effects of the tides, Delta exports, and differing channel barrier configurations. In general, Old River flows past the outfall from east to west and is subject to strong tidal influence. Additionally, flow patterns are highly dependent on the configuration of flow barriers placed in the south Delta. Barriers have been proposed for and constructed in four locations: in the Old River near Tracy, toward the western end of the Grant Line Canal, in Middle River near Victoria Canal, and in Old River near the San Joaquin River (see Figure 3.1 of Chapter 3 for detail). Several barrier configurations are possible, but two configurations produce flow conditions past the outfall that are critical. From June through October, the barrier at the head of Old River is not in place but the other barriers are; during this period, flow is restricted to only that which spills over the notched barriers. From October through December, the barrier at the head of Old River is the only barrier in place. During this period, the flow of water from the San Joaquin River to the west through Old River is restricted, and tidal influences are strong. The tidal stage in the Old River at Tracy between September and December 1996 is shown in Figure 3.15 of Chapter 3.

Rubidium chloride (RbCl) was selected as a tracer for use in this study. River background concentrations of Rb were quite low (ranging from 1.75 to about 4 ppb during both study periods), and a literature search confirmed that Rb is not known to have significant health effects at the concentrations observed during the study. Dye was not selected as a tracer because it can decay with photolysis (Suijlen and Buyse, 1994) and is affected by changes in temperature and pH (Wilson *et al.*, 1986). In addition, when concentrations of organic matter are high (as they often are in the San Joaquin River, see California Data Exchange Center, 1997), both adsorption to and absorption by organic matter can result in non-conservative behavior (Wilson et al., 1986). Rb is not likely to experience any of these difficulties.

The Tracy Wastewater Treatment Plant outfall diffuser, through which the effluent is injected into Old River near Tracy, is 72 feet (22 m) long, with ten 8-inch (0.20 m) nozzles spaced 8 feet (2.4 m) apart. The outfall is perpendicular to the river flow. The diffuser is located an elevation of -11 feet (-3.4 m), approximately 9 feet (2.7 m) below the mean low water elevation. At this point, Old River is about 180 feet (55 m) wide and about 16 feet (4.9 m) deep. The flow rate per nozzle typically averages 1 cfs (0.028 m^3/s), producing an average velocity from each port of 2.87 feet per second (0.87 m/s).

5.4.1 September study

For the September study, five kilograms of RbCl were mixed with 42 gallons (about 160 liters) of treated wastewater in a recirculating tank, thus producing a well-

mixed solution with a Rb concentration of 22.2 grams per liter (22,200 ppm). This solution was discharged at a constant rate over a twelve-hour period in order to allow enough time to collect an adequate number of samples from the study area. The tracer injection raised the effluent Rb concentration values to between approximately 265 ppb and 380 ppb, depending upon plant flowrate; a concentration of 265 ppb corresponds to over 75 times the average river background concentration. The flowrate through the plant was expected to vary between 4.5 MGD (0.20 m^3s^{-1}) and 7 MGD (0.31 m^3s^{-1}) during the nighttime and daytime flow periods, respectively.

Samples were collected within the treatment plant both upstream and downstream of the tracer injection point. In the Delta, samples were collected from thirteen locations as shown on Figure 5.2; the station labeled "OF" is located directly over the outfall, and the other stations are labeled "A" through "L." Water samples were collected at each station from both the surface and the bottom of the channel. The dissolved oxygen (DO), surface water temperature, and the channel depth were recorded for each sample collected. Drifters were used to observed flow directions and to estimate the surface velocity of the river. After collection, samples were analyzed at Caltech by ICP-MS as described in Chapter 2. Results from the September study are presented in Table 5.3.

Table 5.3
Results from the Tracy wastewater dilution study: September 1996

Sample information			Rb [ppb]			DO [mg/l]			River data	
ID	Sta-tion	Day & Time	Btm.	Surf.	Avg.	Btm.	Surf.	Avg.	Depth [m]	Speed [m/s]
004	A	1 09:23	6.595	2.715	4.655	7.2	7.0	7.10	3.65	
014	A	1 11:30	3.650	2.355	3.003	7.4	7.7	7.55		0.17
032	A	1 14:23	3.944	2.435	3.189	7.7	8.3	8.00	4.88	
054	A	1 17:15	3.992	4.181	4.086	7.8	7.9	7.85	4.88	0.22
074	A	2 08:00	3.407	2.844	3.125	7.4	7.1	7.25		0.22
006	B	1 09:46	7.445	7.025	7.235	7.2	7.3	7.25	2.44	
018	B	1 11:54	10.55	8.756	9.651	7.2	7.2	7.20		
036	B	1 14:45	5.480	4.070	4.775	7.7	7.6	7.65	3.35	
058	B	1 17:30	3.807	3.515	3.661	7.5	7.4	7.45		
078	B	2 08:21	3.500	2.959	3.230	7.2	7.0	7.10		0.10
096	B	2 10:26	3.322	2.619	2.971	7.2	7.4	7.30		0.18
008	C	1 09:55	4.823	4.263	4.543	7.2	7.2	7.20	3.96	
020	C	1 12:00	6.059	4.472	5.266	7.0	7.4	7.20		
038	C	1 14:59	9.294	8.195	8.745	7.5	7.8	7.65	3.05	
060	C	1 17:37	4.432	4.089	4.260	7.6	7.4	7.50	3.35	0.09
080	C	2 08:20	3.160	2.828	2.994	7.2	6.8	7.00	3.81	
010	D	1 10:08	6.453	3.654	5.054	6.9	6.4	6.65	3.05	0.12
022	D	1 12:08	5.423	3.880	4.652	7.0	7.0	7.00		0.15
040	D	1 15:06	7.085	7.112	7.098	7.2	7.8	7.50		
062	D	1 17:42	5.936	5.946	5.941	7.6	7.6	7.60	2.74	0.05
082	D	2 08:40	3.146	2.912	3.029	7.2	7.4	7.30	2.90	0.48
098	D	2 10:38	3.303	2.813	3.058	7.1	7.0	7.05		
012	E	1 10:20	4.234	3.513	3.874				2.44	
028	E	1 12:57	3.814	3.370	3.592	7.3	7.3	7.30	2.44	
046	E	1 15:43	3.682	4.211	3.947	6.5	7.8	7.15	2.13	0.23
066	E	1 17:59	5.748	5.064	5.406	7.6	7.4	7.50	2.44	0.31
088	E	2 09:08	4.180	3.760	3.970	5.9	6.6	6.25	2.44	0.03
102	E	2 11:00	4.633	3.016	3.824	5.4	6.9	6.15	2.29	0.17
024	F	1 12:18	4.332	3.518	3.925	7.0	7.5	7.25		0.13
042	F	1 15:19	4.522	3.991	4.257	7.1	7.9	7.50	5.18	
064	F	1 17:58	7.411	6.866	7.139	7.4	7.9	7.65	6.10	
084	F	2 08:48	3.168	2.694	2.931	7.1	6.9	7.00	6.25	0.12
026	G	1 12:40	3.877	3.227	3.552	7.2	7.9	7.55	5.18	
044	G	1 15:30	4.039	3.185	3.612	7.1	8.2	7.65	4.88	
086	G	2 08:57	3.890	2.895	3.393	6.9	7.1	7.00	5.18	
100	G	2 10:50	3.213	2.792	3.002	7.1	7.3	7.20	5.18	
034	H	1 14:30	3.210	3.804	3.507	7.6	7.7	7.65	5.49	

Table 5.3
Results from the Tracy wastewater dilution study: September 1996

Sample information			Rb [ppb]			DO [mg/l]			River data	
ID	Sta-tion	Day & Time	Btm.	Surf.	Avg.	Btm.	Surf.	Avg.	Depth [m]	Speed [m/s]
048	I	1 15:55	3.715	3.334	3.525	6.5	6.9	6.70	2.44	0.16
070	I	1 18:30	5.500	5.748	5.624	7.2	7.0	7.10	2.44	0.21
090	I	2 09:20	3.850	2.770	3.310	6.8	7.2	7.00	2.59	0.35
104	I	2 11:09	3.898	3.210	3.554	6.9	7.0	6.95	2.59	0.09
050	J	1 16:08	3.639	3.278	3.459	6.4	6.7	6.55	2.13	0.30
072	J	1 18:39	4.934	4.865	4.900	7.3	7.1	7.20		0.13
092	J	2 09:29	3.035	3.141	3.088	7.0	7.0	7.00		0.18
052	K	1 16:24	3.166	2.788	2.977	6.2	6.7	6.45	2.29	
094	K	2 09:42	4.121	3.633	3.877	5.9	5.9	5.90		0.23
068	L	1 18:17	4.866	2.797	3.832	7.6	11.6	9.60	2.44	0.81
002	OF	1 08:50	14.11	11.71	12.91	6.8	6.7	6.75	3.66	0.23
016	OF	1 11:40	3.519	2.481	3.000	7.6	7.4	7.50		
030	OF	1 14:10	3.426	9.122	6.274	7.1	8.3	7.70		
056	OF	1 17:22	3.634	2.844	3.239	7.5	7.1	7.30	5.49	
076	OF	2 08:12	3.604	2.585	3.094	7.3	7.1	7.20		0.29
Samples collected from the treatment plant: "Upstream" is prior to tracer injection and "downstream" is after tracer injection:										
			Up	Down	stream					
01	STP	1 08:54	53.89	267.5						
02	STP	1 10:01	51.71	332.3						
03	STP	1 11:01	52.02	219.4						
04	STP	1 12:01	51.71	245.1						
05	STP	1 13:02	56.34	58.94						
06	STP	1 14:09	50.58	73.80						
07	STP	1 15:00	48.58	50.96						
08	STP	1 16:00	46.95	49.32						
09	STP	1 17:10	44.43	51.42						
10	STP	1 18:00	41.92	49.55						
11	STP	2 08:25	41.54	46.00						

A steady river flow rate past the outfall diffuser would produce a steady-state condition, where concentrations downstream of the outfall are independent of time. The data in Table 5.3 show that this is not the case. To determine the flowrate of the river, parcels of water were tracked from Station A past the outfall to Station B; the relative

concentrations of Rb in water samples collected at these locations at appropriate times will yield an estimate of the river's flowrate, as given by:

$$\frac{Q_A}{Q_{OF}} = \frac{C_{OF} - C_B}{C_B - C_A}.$$

This equation was derived using the same assumptions presented in Section 5.2 above. The concentration at Station A, C_A, was assumed to be the background concentration of Rb observed in the Delta near Tracy, approximately 3.0 ppb. The effluent flow rate from the treatment plant, Q_{OF}, was estimated from logs of daily outflow for the plant for the days immediately prior to the tracer study. Unfortunately, actual effluent flow rates during both study periods were unavailable due to plant flow meter failures. Because of the long travel times from the plant to the diffuser (between 2.9 and 4.5 hours, depending upon flow rate), the concentration of Rb in the effluent, C_{OF}, was estimated from nighttime flow rates and the rate at which tracer was added to the effluent. A velocity of 0.3 feet per second (0.09 m/s) was used to estimate the travel time for a water parcel between the stations; this speed was based upon data taken from drifter observations during the study period and is about half the measured surface velocity. Table 5.4 shows the values used in this calculation and the results for both Q_A and dilution.

Table 5.4
Estimation of flow and dilution in Old River near Tracy: September 1996

C_B [ppb]	Q_{OF} [m^3/s]	C_{OF} [ppb]	C_A [ppb]	Q_A [m^3/s]	Dilution
7.23 (09:46)	0.197 (07:00)	380 (03:00)[a]	3 (04:00)	17.4 (07:00)	89
9.65 (11:54)	0.351 (09:00)	381 (06:30)[a]	3 (06:00)	19.6 (09:00)	57
			Average	18.5	73

[a] C_{OF} is computed using the estimated nighttime effluent flow rates and the measured tracer addition flow rate.

5.4.2 November study

The tracer study conducted during September was repeated in November, after the barrier configuration had changed. During the November study, three kilograms of RbCl were mixed with about 25 gallons of treated wastewater in the same recirculating tank. Measured concentrations of Rb in the effluent ranged from 325 to about 400 ppb; effluent flow rates were expected to be the same as for the September study.

The data obtained from the second tracer release, summarized in Table 5.5, were more difficult to interpret than the data obtained from the first tracer release. During the second release, the flow rate in Old River changed much more rapidly; during part of the tidal cycle, flow past the outfall actually reversed, confirming that tidal influences were much more pronounced due to the winter barrier configuration. In addition, the pump that added the tracer to the effluent malfunctioned for approximately 1 - 2 hours during the middle of the injection period. These conditions made it much more difficult to predict the flow rates past the outfall and dilutions in Old River. Samples were collected from the same locations used for the September study with two exceptions: Stations K and L were inaccessible due to shallow water, and stations M, N, and O were added in Old River to the east of Station H.

Table 5.5
Results from the Tracy wastewater dilution study: November 1996

Sample information			Rb [ppb]			DO [mg/l]	River data		
ID	Sta-tion	Day & Time	Btm.	Surf.	Avg.	Surf.	Depth [m]	N Speed [m/s]	E Speed [m/s]
010	A	1 08:44	2.07	2.20	2.14	8.0	4.11	0.12	0.34
033	A	1 11:21	2.21	1.97	2.09	8.2	4.88	0.05	0.15
056	A	1 14:22	1.82	1.64	1.73	8.2	5.18	0.17	-0.07
079	A	2 07:30	2.63	1.99	2.31	8.2	4.11	0.08	-0.22
014	B	1 08:58	2.48	2.47	2.48	8.5	2.74	0.14	0.19
037	B	1 11:35	5.41	5.66	5.53	8.3	2.44	0.01	0.02
060	B	1 14:36	4.10	3.98	4.04	8.1	2.13	0.25	1.46
083	B	2 07:45	2.41	1.98	2.20	8.1	2.38	0.31	0.11
016	C	1 09:08	3.61	3.74	3.68	8.4	2.74	-0.02	-0.38
039	C	1 11:44	4.05	4.09	4.07	7.8	2.29	0.01	-0.11
062	C	1 14:42	2.78	3.20	2.99	8.0	2.74	-0.14	-0.16
085	C	2 07:45	2.54	2.59	2.56	8.0	2.26	-0.03	0.27
018	D	1 09:15	3.60	3.58	3.59	8.4	2.44	0.37	0.09
041	D	1 11:52	2.61	2.66	2.63	8.0	2.13	-0.33	-0.12
064	D	1 14:52	2.35	1.98	2.16	8.0	2.56	-0.42	0.01
087	D	2 07:45	2.54	2.21	2.38	8.3	2.32	-0.01	0.07
024	E	1 09:43	2.23	2.12	2.18	8.5	0.91	0.23	-0.09
047	E	1 12:20	3.12	3.31	3.21	8.1	1.52	-0.31	0.28
070	E	1 15:56	3.47	3.32	3.40	8.1	1.83	-0.42	0.26
023	E	2 08:25		1.98	1.98	8.1	1.52		
020	F	1 09:21	2.47	2.80	2.64	7.7	5.79	0.17	0.32
043	F	1 12:00	3.24	3.24	3.24	7.6	6.40	-0.25	-0.24
066	F	1 14:56	3.07	1.90	2.49	7.6	7.01	0.30	0.00
089	F	2 08:02	2.47	2.28	2.38	7.8	7.01	-0.05	0.20
022	G	1 09:30	2.02	1.88	2.00	7.5	4.27	-0.01	0.51
045	G	1 12:06	2.07	1.73	1.90	7.7	3.65	-0.32	0.06
068	G	1 15:03	1.79	2.21	2.00	8.0	4.11	-0.05	-0.41
091	G	2 08:11	2.95	2.73	2.84	8.1	3.35	0.02	0.62
029	H	1 11:00	1.73	1.73	1.73	8.2	3.96	-0.06	0.01
054	H	1 14:15	2.06	1.70	1.88	8.4	4.45	0.46	-0.20
077	H	2 07:20	1.80	1.68	1.74	8.0	2.13	-0.25	0.11
026	I	1 09:52	2.78	2.74	2.76	8.5	1.80	-0.21	0.04
049	I	1 12:28	2.18	2.41	2.29	9.2	1.74	0.29	0.09
072	I	1 15:27	3.57	3.49	3.53	8.4	2.29	-0.25	0.10
094	I	2 09:37	2.36	2.07	2.21	8.0	1.89		

Table 5.5
Results from the Tracy wastewater dilution study: November 1996

Sample information			Rb [ppb]			DO [mg/l]	River data		
ID	Sta-tion	Day & Time	Btm.	Surf.	Avg.	Surf.	Depth [m]	N Speed [m/s]	E Speed [m/s]
027	J	1 10:01	3.20		3.20	8.4	0.91		
050	J	1 12:34	2.63		2.63	9.0	0.91		
073	J	1 15:45	2.70		2.70	8.4	1.52		
095	J	2 09:40	2.35		2.35	7.7	1.28		
004	M	1 08:08	2.06	2.89	2.48	8.5	1.37	0.22	1.20
006	N	1 08:23	2.36	1.68	2.02	8.7	7.62	-0.08	0.22
008	O	1 08:34	1.87	1.91	1.89	9.1	3.66	0.08	0.28
031	O	1 11:11	3.98	1.86	2.92	8.4	3.51	-0.12	0.18
052	O	1 14:06	1.77	1.62	1.70	8.4	3.81	0.18	-0.23
075	O	2 07:13	1.89	1.71	1.80	8.1	3.96	-0.02	0.15
002	OF	1 07:28	9.07	4.21	6.64	8.6	4.11		
012	OF	1 08:50	2.02	4.54	3.28	8.4	3.35	0.14	0.38
035	OF	1 11:28	2.01	2.13	2.07	8.1	4.08	-0.10	0.32
058	OF	1 14:29	6.56	7.62	7.09	8.1	3.90	-0.21	-0.05
081	OF	2 07:40	2.55	2.25	2.40	8.1	4.11	-0.04	0.14
Samples collected from the treatment plant: "Upstream" is prior to tracer injection and "downstream" is after tracer injection:									
			Up	Down	stream				
01	STP	1 06:20	[a]	325.7					
02	STP	1 07:19	[a]	324.9					
03	STP	1 08:10	[a]	371.0					
04	STP	1 09:09	56.21	419.9					
05	STP	1 10:06	[a]	208.2					
06	STP	1 11:06		44.42					
07	STP	1 09:15		17.33					

[a] Concentrations are not reported for these samples, as significant cross-contamination occurred during collection.

Despite the less than ideal conditions, some general observations can be made. The highest observed Rb concentration at the outfall location was 6.64 ppb; assuming an average effluent concentration of about 350 ppm (as in the September study) and using the observed river background concentration of approximately 1.8 ppb (as measured at Station H), this corresponds to a dilution of about 71:1. This sample contained the

highest Rb concentration observed in samples collected during this study period. Concentrations are elevated above background levels in samples collected from Stations B, C, D, E, F, and, toward the end of the sampling period, G, indicating that most effluent from the outfall probably travels along this flow path. Concentrations are elevated at stations I and J but are not as high as concentrations at the stations mentioned above. This indicated that the northern flow path, traced out as OF - (B or E) - C - D - F - G, is probably more important than the southern flow path. Observations in the field, including flow velocity and water depth, also led to this conclusion.

5.4.3 Additional observations

Several flow parameters can be estimated from the data collected in the field. First, it is reasonable to assume that vertical mixing occurs very quickly, as the jet exit velocity is fairly high and the river relatively shallow (see Fischer *et al.*, 1979). The distance required for the river to become well-mixed laterally can be predicted by estimating the transverse diffusion coefficient, then solving the advection-diffusion equation for a distributed source. The transverse diffusion coefficient can be estimated as $\varepsilon_y \cong 0.6u_* d$ (Fischer *et al.*, 1979). Taking a Darcy-Weisbach friction factor f = 0.020 (typical for sand beds), the average velocity estimated from field observations, and a depth of 16 feet (4.88 m), this coefficient is computed to be roughly 0.013 m^2s^{-1}. The calculation was made by treating the diffuser as a distributed source with a length of 36 feet (10.97 m) centered in the river with a width of 180 feet (54.9 m), assuming complete vertical mixing, and using four images; the approximate distance downstream at which

the concentration at the side of the channel equals 0.95 times the centerline concentration is 910 m (3000 feet). This is roughly the distance from the outfall to the midpoint between Stations B and C.

As shown in Fischer *et al.* (1979), the longitudinal dispersion coefficient can be estimated from various parameters observed during the field study as

$$K = 0.011 \frac{U^2 W^2}{d u_*}.$$

The value calculated using the observed mean velocity of 0.09 m/s, the channel width of 55 m, the depth of 4.88 m, and u_* as calculated above, is K = 12.3 $m^2 s^{-1}$. During the September tracer release, a large spike of Rb was observed moving downstream from the outfall (see data in Table 5.3). This spike was likely caused by tidal influences at the outfall, and the analysis could be made because the tracer injection during the September study was continuous (unlike the November study, where tracer injection was interrupted for a period during the night). During the flood tide, the water surface elevation rises and the flow rate of the river is reduced, potentially to a condition of no net flow or even reverse flow. Comparison with stage records from a gauging station located in Old River near Tracy show that the slack tide between flood and ebb tides occurred at approximately 5 am on September 6, 1996, the first day of sampling. Peak concentrations were observed at stations downstream of the outfall at travel times corresponding approximately to travel times computed from the mean flow velocity and the distance between stations; these data are shown in Table 5.6. The travel time to all stations is underestimated, as the velocity must transition from near zero (at slack tide) to the mean

observed velocity, and this rough calculation does not account for this transition; also, the maximum observed concentration may represent a "shoulder" of the peak and not the absolute maximum concentration that occurred at a given location. Nonetheless, it is clear that a spike of tracer material did travel from the outfall to Station F (and presumably beyond, to Station G).

Table 5.6
Estimated travel times and observed peak concentrations for September, 1996

Path	Travel distance [m]	Travel time [hr]	Estimated time of peak arrival	Observed concentration [ppb]	Time of sample collection
OF-B	800	3.0	08:00	9.65	11:54
OF-C	1800	5.6	10:30	8.75	14:59
OF-D	2650	8.1	13:05	7.10	15:06
OF-F	3500	10.7	15:42	7.14	17:58
OF-G	5100	15.6	20:33	no spike observed	latest at 15:30

5.5 Conclusions

The three studies presented in this chapter involved shorter observation periods and simpler systems than the detailed studies presented in Chapters 3 and 4. All involved the mixing of only two sources. Because of the relative simplicity of these systems, fewer complications were encountered in applying the method for tracing flows. In the Napa River estuary and the Weymouth Filtration Plant, the natural chemistry of the waters was used; in both cases, several elements successfully predicted mixing, including many of the elements that were used to predict mixing in the Delta and Hawai'i study areas. It is particularly noteworthy that thirteen elements consistently predicted mixing in the

Weymouth Filtration Plant in spite of extensive treatment between the point where source samples were collected and the point where the plant effluent was collected. In the south Delta near Tracy, a rubidium chloride tracer was added to amplify the chemical differences between the wastewater and the receiving water. The addition of a tracer in this simple, two-source, freshwater system was also successful and allowed the determination of dilution to much higher levels than would have been possible using the natural chemistry of the two source waters alone.

These results demonstrate the effectiveness of the ICP-MS tracer method in simpler systems. Where concentration differences between two sources are large enough, the natural chemistry of the source waters can be used. When higher resolution is required than could be achieved using the natural chemistry of source waters, a tracer can be added to enhance that resolution. In two-source systems, mixing is likely to be conservative for many elements when both sources are freshwater sources; adding a tracer to one of two freshwater sources is also an effective way to determine dilution and source fractions. When one source is saline and the other fresh, the difference between the two can also be readily determined using a variety of elements naturally present in the more saline source water.

Figure 5.1: Napa River estuary study area

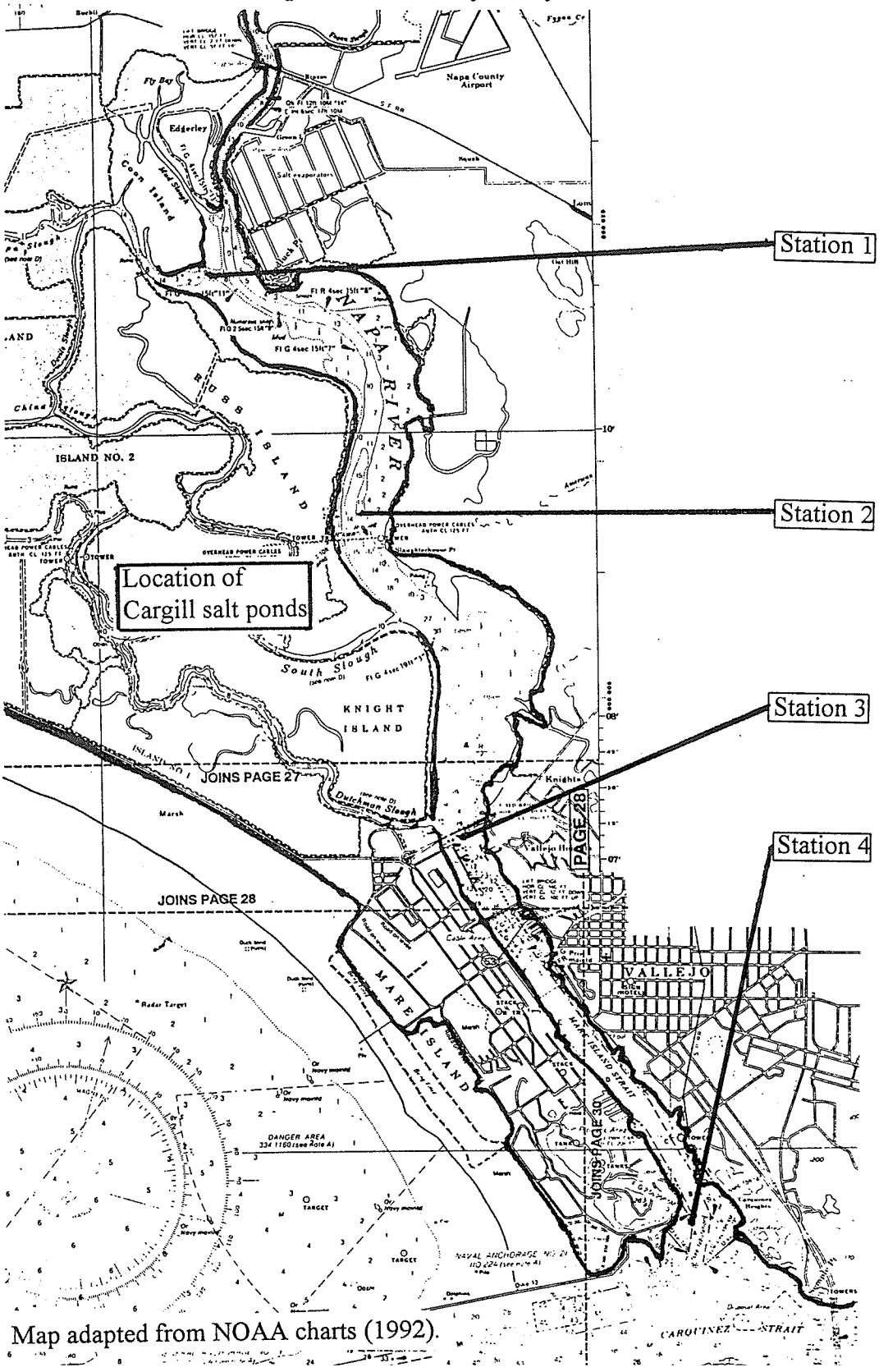

Map adapted from NOAA charts (1992).

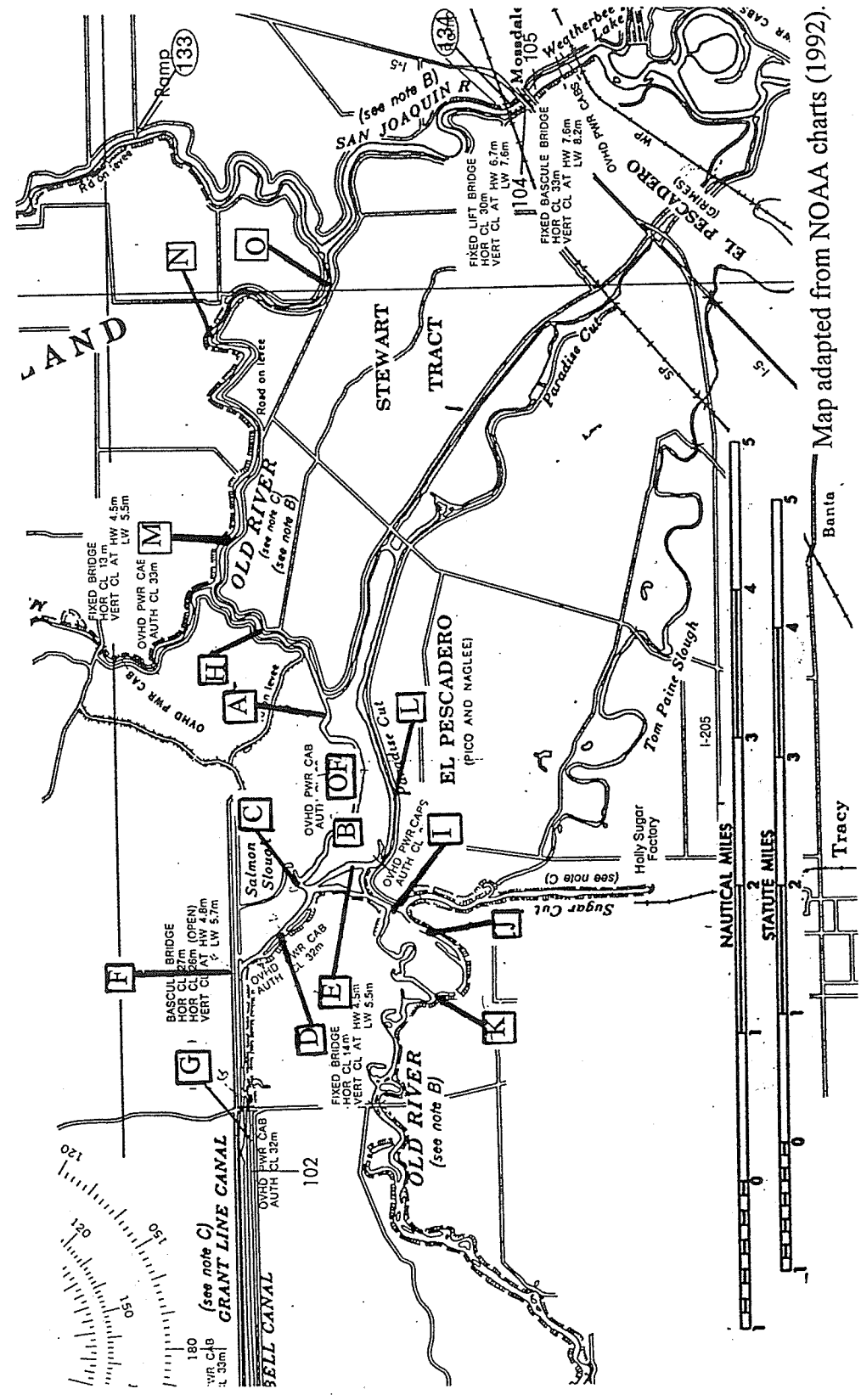

Figure 5.2: Sample collection locations for Tracy wastewater dilution study

Map adapted from NOAA charts (1992).

6 Summary and conclusions

6.1 General observations

The objective of this study was to develop a method to trace flows that would utilize the natural chemistry of the waters being traced. Thousands of samples were collected from several different study areas; in most cases, the source waters exhibited sufficiently different elemental compositions to enable tracing flows using the natural water chemistry. In a few cases, an elemental tracer was selected and added to a source flow to allow dilution of this flow to be measured to much higher levels than would otherwise have been possible. In all cases, elemental tracers existed (whether naturally present or added) that behaved conservatively, or nearly conservatively, on the timescales relevant to each study area. The characteristics of flow fields and mixing fractions were determined in freshwater, estuarine, and coastal environments for a wide variety of conditions.

This method of tracing flows potentially has several advantages over traditional methods, which involve the addition of tracer substances to source waters. Dye tracing, in which a dye is added to a source flow, involves the measurement of fluorescence in samples collected from a study area. Fluorescence can vary significantly with temperature and pH and can be affected by interactions between the dye and the source water or particulate matter (particularly particulate matter with high organic content) in the source water, leading to non-conservative behavior. Photolysis can also lead to non-conservative behavior. Although particle-water interactions also may occur for elemental

tracers, the wide range of choice of elemental tracers should allow the selection of conservative tracers. The range of elements available for use as tracers should also allow tracers to be selected that are not toxic and that do not experience solubility problems when added to source flows. By definition, tracing flows using added tracers limits the study period to the period of time over which a tracer is added plus the time in which it disperses; this time may be brief, particularly when residence times are short, due both to the expense of the tracers themselves and to the effort required to collect and analyze samples.

Computer models, often used to predict flows and the distribution of chemical constituents in natural systems, also have disadvantages. The formulation of flow models necessarily requires simplification of the equations describing the flow: flow models are generally one- or two-dimensional, and broad assumptions are made to linearize the governing equations of motion. These models often provide time-averaged statistical estimates of flow conditions and cannot be used to estimate instantaneous flow conditions. It is difficult to validate such models, and important parameters are often estimated or "fit" to the data. Often, the results of dye studies are used to calibrate computer models.

Because the method developed in this study utilizes naturally occurring elements, there is generally no need to add dyes or other tracers. Conditions within a study area can be monitored over longer periods of time, and because the method generally does not require addition of tracers, no special permits or permissions are required. In special situations, enhanced resolution can be obtained by adding elemental tracers that are

present in low concentrations in source waters (to minimize the mass of tracer added) and that behave conservatively. Because ICP-MS can measure the concentrations of many elements to very low detection limits, there is a wide range of choice in selecting an elemental tracer to be added. The main disadvantage of this type of flow tracing is that generally there are no visual clues to dilution levels, *i.e.*, differences in elemental composition are not observable in the field as are dye solutions.

The method developed in this study can be used to monitor existing conditions over either very short or long periods of time. If concentrations of tracer elements are measured at frequent intervals at receptor sites, nearly instantaneous estimates can be made of the fractions of water contributed by various sources. Alternatively, composite samples collected over longer periods of time can be used to yield time-averaged estimates of source fractions. Finally, results obtained from receptor or chemical mass balance models are objective; as stated by Olmez *et al.*, 1994:

> The data are mathematically manipulated only in the calculation of statistical measures. The only subjective part of the analysis is in the identification of source types influencing the sample... If the analyst chooses poorly the sources to consider or leaves out an important source influence altogether, the model statistics will indicate such a poor choice. Therefore, the receptor modeling calculations have an inherent consistency check built into the modeling framework.

For situations in which the use of computer models is necessary (*e.g.*, to predict changes in flow patterns resulting from different management scenarios or for the evaluation of the construction of new facilities), model calibration and validation using the results presented in this work should give greater confidence to these model estimates.

6.2 Summary and conclusions for each study area

6.2.1 Sacramento-San Joaquin Delta system

The Delta is a highly managed estuary that is central to the use of California's freshwater resources. Although hydrodynamic models exist to describe flows and the distribution of salinity within the Delta, they have difficulty in providing validated descriptions of the distribution of freshwaters. They also rely upon empirical estimates of important parameters (*e.g.*, channel flow distributions) and thus have not resolved many of the issues relating to the management of the system. Because the Delta system is very large and complex, large-scale tracer studies to describe the movement of water through the system have not been used. The method developed in this study addresses fundamental questions about the distribution of freshwater in the Delta and the effect of artificial channel barriers and diversions.

Four elements were found to behave conservatively within the estuary unequivocally: sodium, magnesium, calcium, and strontium. These elements are present in much higher concentrations in ocean water (and Bay water) than in fresh waters due to their inert chemical behavior. Water-particle interactions were found to be the main source of non-conservative behavior for most other elements; because the elements that were present in higher concentrations in river waters than in Bay water failed to behave conservatively, no estimate could be made of the net Delta outflow. Fingerprints assembled from concentrations of Na, Mg, Ca, and Sr for each of the major sources of water to the system were found to be unique. The concentrations of these elements were

steady on timescales shorter than mixing timescales during the dry season. During wet periods, concentrations varied more, and model predictions for these periods are less certain. During the major flood event of January 1997, saline Bay water was flushed from the system and other sources (*e.g.*, agricultural drainage) became important; use of the method during extreme flood events would require characterization of these additional sources but would be difficult due to enhanced water-particle effects. Model results using only three sources for this flood period do not make physical sense, confirming that the model fails when model assumptions are invalidated.

The most significant finding of this study involves water arriving at Clifton Court, the export point to the State Water Project in the south Delta. Many involved in the operation and study of the Delta have speculated that poor quality water arriving at the export pumps originated in the Bay and was carried to Clifton Court by tides. This study has established that this was not the case during the study period; the water arriving at Clifton Court originated almost entirely from the Sacramento and San Joaquin Rivers, and the San Joaquin River provided slightly more sodium (a surrogate for salinity) to Clifton Court than the Bay.

This method was also used to show how the distribution of source waters changed in the Delta in response to changes in artificial flow barriers and diversions. Opening the Delta Cross-Channel gates, for example, significantly increased the amount of Sacramento River water that reached the south Delta. The agricultural barriers in the south Delta and the barrier at the head of Old River altered the flow regime of the south

Delta considerably, restricting the flow of San Joaquin River water westward toward Clifton Court.

The successful use of this method in the Delta suggests that it could also be used in other estuarine environments. Because of their inert chemistry, elements that were used as tracers in the Delta were present in high concentrations in Bay waters and low concentrations in river waters; this would also be true for these elements in other estuaries. By diluting samples as appropriate, these elements could be measured accurately from river waters into fully saline ocean waters. Because the chemical behavior of elements varies from one estuary to another, it is also possible that additional elements could be used as tracers in other estuaries, and net outflow in other systems could be measured.

6.2.2 Oahu, Hawai'i

In Oahu, mixing between fresh and saline ocean waters occurs over much shorter distances than in the Delta estuary. The objective of the work conducted in Oahu was to extend the flow tracing method developed for use in the Delta to this environment and to address specific questions about pollution observed in the nearshore waters of Oahu.

Samples were collected from twelve streams and one wastewater discharge in this study area; unfortunately, for this study the geology within the study area was very uniform, and the fingerprints of the streams were not distinct enough to allow use of their natural chemistry to distinguish one from another. The main difficulty in extending this method into fully saline waters was the accurate measurement of elements present in low

concentrations in ocean waters. Accurate analysis by ICP-MS was difficult for all elements for which concentrations were higher in stream and wastewaters than in ocean waters. Elements that were present in higher concentrations in seawater samples were used as "inverse tracers," thus indicating the difference between fresh and saline waters. In this way, dilutions within Pearl Harbor and near the Ala Wai Canal were measured to levels of 25:1. If samples had been diluted even further, concentrations of major cations, including Na, Mg, and Ca, could have been measured in saline samples, and dilution could have been predicted to much higher levels. Direct measurements of chloride ion concentrations or conductivity (a surrogate for salinity) may well have been as accurate.

Because of the difficulty of analyzing trace elements at their naturally occurring concentration levels, a rare earth tracer containing lanthanum, praseodymium, and neodymium was added to the wastewater discharge from Waianae. In spite of the fact that these elements were present in concentrations many orders of magnitude higher than in background seawater, measurement of the rare earth elements was still difficult, and dilutions could be accurately determined only to levels of about 300:1. Beyond the level of 300:1, dilution levels predicted by Pr and Nd agreed with each other but not with dilution levels predicted by La. The cause of measurement difficulties remains unknown but is most likely matrix effects caused by major ions present in saline samples. For this reason, other tracer techniques may be more appropriate in seawater. Qualitatively, the main features of the flow field were determined to much higher dilution levels. The concentration field was observed to be "lumpy" or "blobby," with local peaks of high concentration, rather than a smooth distribution.

6.2.3 Other study areas

The method developed during this study was successfully used in a number of other study areas using both the natural chemistry of the source waters and added tracers. The difference between fresh and saline waters is easily determined by measuring the concentrations of just a few elements and can be used to determine estuarine mixing and tidal flushing characteristics. The mixing of freshwaters of varying elemental compositions is also easily determined, even when waters are subjected to extensive treatment processes; most of the elements that predict conservative mixing under these conditions are those that accurately predict mixing in laboratory mixing studies and at the confluences of rivers.

In the south Delta, Rb was added as a tracer to a wastewater flow. From concentrations measured in hundreds of samples, dilution levels within this area of the Delta were easily estimated. Tidal effects were shown to be significant, particularly for the late fall configuration of artificial flow barriers. Although the chemistry of the wastewater and the receiving water varied measurably, addition of a tracer allowed the measurement of much higher dilution levels than would have been possible using the natural chemistry of these waters. These applications demonstrate that this method is broadly applicable to a wide variety of flow systems; further, it was generally observed that the simpler the system, the fewer were the complications experienced in applying the method.

6.3 Procedures for use of the method in other systems

Extending this method to other study areas and other types of systems should be relatively straightforward, as the knowledge gained from this research should be directly applicable to other systems. The three conditions that must be met for selection of a tracer should be addressed for the specific system of interest. Finally, a suitable mathematical model should be used to predict source fractions in a sample from a receptor location.

6.3.1 Selection of elements for inclusion in a fingerprint

To screen water bodies for differences in elemental concentrations, samples should be analyzed to determine the concentrations of a wide range of elements. Those chosen for inclusion in a fingerprint should be easily and reproducibly quantifiable, *i.e.*, there should be no difficulties in applying ICP-MS analysis techniques to the measurement of the chosen elements. Additionally, the concentrations of elements chosen for inclusion in a fingerprint should vary significantly from one source to another. For elements that exhibit a high signal-to-noise ratio, concentrations need not vary by as much as for elements with a low signal-to-noise ratio. Acceptable differences in concentrations between sources should be based upon project requirements for estimated dilution levels.

If concentration differences for naturally-occurring elements are not large enough to meet project requirements, a tracer (or tracers) should be selected for addition to one (or more) source waters. Tracers should be selected that are non-toxic at required levels,

affordable, and that behave conservatively. Fortunately, the requirements of conservative behavior and a lack of toxicity are generally compatible, as elements that behave conservatively are generally relatively inert chemically in aqueous solution. Again, project requirements will determine the final concentration of added tracer in a source water.

6.3.2 Evaluation of relevant timescales

In designing the sample collection scheme for the chosen study area, relevant timescales should be identified. Simple methods can be used to estimate travel times and timescales of mixing. The advection-diffusion coefficient can be estimated from field observations of the various length and velocity scales of the study area, often available as charted bathymetry, measured flow velocities and flow rates, etc. This coefficient can then be used to gauge the distance required for lateral mixing in a study area. For example, this coefficient can be used to predict the distance and the travel time downstream of a river confluence where waters become well-mixed, in which case a natural tracer present in higher concentrations in one river would be evenly distributed over the cross-section. Similarly, a longitudinal dispersion coefficient can also be estimated from the length and velocity scales of the study area (see Section 5.4 for one example). This coefficient can then be used in simple calculations to estimate the dispersion (change in concentration) that is expected as a slug of an added tracer moves downstream. The time-of-travel from one location to another can be estimated based upon observed or estimated travel distances and flow velocities. Computer programs

designed to describe a given study area may also be useful in estimating the timescales relevant to a given problem.

Once relevant timescales have been estimated, they can be used to evaluate temporal fluctuations in the concentrations of natural elements; they can also be used to design a tracer addition study. When the existing chemistry of the sources is used, elements that are chosen for inclusion in a source fingerprint should exhibit variations in concentration that are small over the timescales relevant to the problem. If a tracer is added, it may be added over a time comparable to estimated timescales or as a single "spike." Observations of the spreading and mixing of a single spike of tracer can be used to estimate various flow parameters (*e.g.*, the longitudinal dispersion coefficient), while a longer tracer addition can be used to determine steady-state mixing conditions. Samples should be collected from the study area for longer periods of time than the relevant timescales; these samples could be collected as single grab samples over the entire study period or as composited samples (or both).

6.3.3 Evaluation of elemental behavior within the study area

For a given study area, relevant water quality parameters should be identified and measured. Measurements of pH and observations of redox conditions may be particularly significant, as these two parameters exert control over the solubility and ion exchange behavior of a wide variety of elements. Any unusual conditions within the study area, such as the occurrence of algal blooms or high pulses of turbidity, should also be noted and evaluated. Unusual conditions may indicate that an element may behave non-

conservatively; for example, both Mo and U are almost insoluble in aqueous solution under reducing conditions. Likewise, waters with low pH (*e.g.*, acid mine drainage) may affect the speciation of ionic compounds and lead to volatility (as with F) or enhanced ion exchange behavior (for elements, such as Mo and U, present as anionic species).

In the Delta study area, in Hawai'i, and in the smaller studies, several elements were shown to behave conservatively during mixing. These elements exhibit an uncomplicated chemistry in aqueous solutions and include Na, Mg, K, Ca, and Sr. All are present in higher concentrations in ocean waters than in freshwaters, due largely to their conservative behavior; barring unusual local conditions, all should predict mixing between freshwaters well also. Non-conservative behavior could result from the loss of salt from solution due to evaporation-induced precipitation, the loss from solution due to intense biological activity (of these elements, this is most likely for Ca and Sr), or the loss from solution as solid precipitates (again, most likely for Ca and Sr). In studies of river mixing and estuarine mixing, particle effects may be important, especially for study areas in which waters of significantly different salinities mix together. In these areas, the comparison of filtered and unfiltered samples is useful in identifying which elements are most likely subject to non-conservative behavior; the elements that are most likely to behave conservatively are those for which concentration is not altered to any large extent by filtration. If available, analysis of the variations in concentration with flow rate may also be useful; as noted in Chapter 3, elements that show a positive correlation between concentration and flow rate do not behave conservatively in the Delta estuary.

Laboratory mixing studies can also be useful in determining chemical behavior. Source waters collected in the field can be brought back to the laboratory and mixed in known proportions; when the concentrations of elements in these mixtures are plotted against the known fraction of source waters, elements that are likely to behave conservatively should plot as a straight line between two endpoints (this line is often termed the "theoretical dilution" line). Although not all elements exhibiting conservative behavior in the laboratory will exhibit conservative behavior in the field, elements that behave non-conservatively in laboratory studies should also behave non-conservatively in the field. Thus, laboratory studies can assist the selection of elements for inclusion in a fingerprint and use as a tracer, particularly in the absence of extended field observations.

6.3.4 Use of a model to predict source fractions

A mathematical model used to estimate source fractions may be quite simple (as in this study) or very sophisticated (as in complex air pollution studies). The choice of a model should depend upon the project requirements and the complexity of the study area. A more sophisticated model would be the proper choice for a system that has many sources or many elements in a fingerprint. A simpler model may be appropriate for a simple system (particularly a two-source system) or for a system that has source fingerprints that include relatively few elements (such as was successfully employed in this study for the Delta).

6.4 Recommendations for future work

The adaptation and application of existing receptor or chemical mass balance models would produce more robust model results. These models, which were developed for use in air pollution studies, use an effective variance least squares estimation algorithm or similar, more sophisticated mathematical algorithm to calculate source contributions and their standard errors; they also evaluate the model fit and validate model results, neither of which was done in the relatively simple model presented in this study. The Chemical Mass Balance Model Version 7.0 (CMB 7.0) is one model that would be relatively easy to adapt for use with the data presented in this study. The potential of such techniques has been shown using a relatively simple approach for the Delta study area, and the application of sophisticated modeling techniques would improve the accuracy and confidence of model predictions, particularly for multiple-source systems or for fingerprints that include a large number of elements. In the Delta study area, such an approach was not warranted, as source fingerprints were composed of only four elements, and independent results for all possible pairs of tracer elements were in close agreement (see Chapter 3).

The results obtained for the Delta study area could be used to improve existing computer models, which until now have been calibrated and validated using only the distribution of salinity from the Bay. After adjusting these models to reproduce the distribution of Sacramento and San Joaquin River waters within the system, they could be used to provide a better understanding of mixing patterns within the Delta and of how such mixing patterns evolve over time. Questions about the source of water exported

from the Delta could be addressed using models of possible gate and barrier configurations and possible management scenarios. Finally, computer models could be used with greater confidence to predict water quality and mixing within the Delta during extreme low flow (drought) periods.

It is possible also that the results of this study could be used to generate a " water chemistry module" that would be coupled to one of the existing flow models. This would allow water quality questions to be addressed with greater confidence; in addition to predicting the source of water within a system, a water chemistry module could be used to predict the quality of water at a given location within the study area. For example, if the concentration of a given pesticide is known at the source locations, then the computed travel time (and resultant decay of pesticide) and fraction of water from each source could be used by the model to predict the concentration of that pesticide at a given location within the study area.

One difficulty that was encountered during this study was the determination of elemental concentrations in fully saline waters. The most promising way to improve ICP-MS analysis techniques to extend the method into fully saline ocean waters would be to remove the major seawater ions prior to analysis using ion exchange techniques. Automation of an ion exchange procedure would provide the easiest solution, still enabling high sample throughput. Ion exchange would allow the determination of elements present in higher concentrations in stream and wastewaters than in ocean water, and dilutions could then be measured to much higher levels. This would allow the method to be used in a much wider variety of study areas than is currently possible; for

example, mixing in environments similar to that encountered in Hawai'i could be determined more accurately, and the method could be used for discharges into saline waters. One potential application would be to study mixing and tidal flushing in south San Francisco Bay.

Solving the problem of the measurement of elemental concentrations in saline waters would enable the method developed in this study to be used in almost any surface water environment to trace flows and better understand mixing behavior. The successful application in freshwater and estuarine environments demonstrates its suitability in those systems. Potentially, some of the many additional applications of the method would include: the determination of mixing behavior in groundwater systems (see Olmez *et al.* (1994) and Olmez and Hayes (1990) for similar approaches utilizing other analysis techniques); the determination of mixing behavior and residence times of reservoirs and other water storage and treatment systems; the understanding of mixing behavior and the location of cross-connections within water distribution systems; and the use of elemental tracer techniques in other systems to validate and calibrate computer models.

References

Anderson, L. C. D. and K. W. Bruland. "Biogeochemistry of arsenic in natural waters: The importance of methylated species." Environmental Science and Technology 25 (1991): 420-427.

Andersson, P. S., G. J. Wasserburg, and J. Ingri. "The sources and transport of Sr and Nd isotopes in the Baltic Sea." Earth and Planetary Science Letters 113 (1992): 459-472.

Andersson, P. S., G. J. Wasserburg, J. Ingri, et al. "Strontium, dissolved and particulate loads in fresh and brackish waters: the Baltic Sea and Mississippi Delta." Earth and Planetary Science Letters 124 (1994): 195-210.

Aston, S. R. "Estuarine chemistry." Chemical Oceanography, Volume 7. Ed. Riley, J. P. and R. Chester. 2nd ed. London: Academic Press, 1978. pp. 362-438.

Beauchemin, D. and S. Berman. "Determination of Trace Metals in Reference Water Standards by Inductively Coupled Plasma Mass Spectrometry with On-Line Preconcentration." Analytical Chemistry 61 (1989): 1857-1862.

Beauchemin, D., J. W. McLaren, and S. S. Berman. "Study of the effects of concomitant elements in inductively coupled plasma mass spectrometry." Spectrochimica Acta 42B (1987): 467-490.

Benoit, G. "Clean technique measurement of Pb, Ag, and Cd in freshwater: A redefinition of metal pollution." Environmental Science and Technology 28 (1994): 1987-1991.

Bergeron, M. and J. Lebel. "On the boron content in the sediments from the St. Lawrence Estuary off Rimouski, Quebec, Canada." Chemical Geology 42 (1984): 77-83.

Borole, D., S. Krishnaswami, and B. Somayajulu. "Investigations on dissolved uranium, silicon and on particulate trace elements in estuaries." Estuarine and Coastal Marine Science 5 (1977): 743-754.

Bradford, G., D. Bakhtar, and D. Westcot. "Uranium, Vanadium, and Molybdenum in Saline Waters of California." Journal of Environmental Quality 19 (1990): 105-108.

Brooks, N. H. Personal communication. "Determination of element pair producing the smallest error in predicted element concentrations." 1997.

Bruland, K. W. "Trace Elements in Sea-water." Chemical Oceanography, Volume 8. Ed. Riley, J. P. and R. Chester. London: Academic Press, 1983. pp. 157-220.

Bruland, K. W., J. R. Donat, and D. A. Hutchins. "Interactive influences of bioactive trace metals on biological production in oceanic waters." Limnology and Oceanography 36 (1991): 1555-1577.

Burton, J. D. and P. S. Liss. "Estuarine Chemistry." London, New York, San Francisco: Academic Press, 1976.

Byrne, R. H. and K.-H. Kim. "Rare earth element scavenging in seawater." Geochimica et Cosmochimica Acta 54 (1990): 2645-2656.

Byrne, R. H. and K.-H. Kim. "Rare earth precipitation and coprecipitation behavior: The limiting role of PO_4^{3-} on dissolved rare earth concentrations in seawater." Geochimica et Cosmochimica Acta 57 (1993): 519-526.

Byrne, R. H., L. R. Kump, and K. J. Cantrell. "The influence of temperature and pH on trace metal speciation in seawater." Marine Chemistry 25 (1988): 163-181.

California Data Exchange Center. "Current and historical information." (1997) http://cyclone.water.ca.gov/. Sacramento. State of California Department of Water Resources. (access: 15 April 1997).

California State Lands Commission. "Delta-Estuary: California's inland coast, a public trust report." 1991. Sacramento: California State Lands Commission.

California State Lands Commission. "California's rivers, a public trust report (2nd edition)." 1994. Sacramento: California State Lands Commission.

Callaway, R. and D. Specht. "Dissolved silicon in the Yaquina Estuary, Oregon." Estuarine, Coastal and Shelf Science 15 (1982): 561-567.

Carroll, J. and W. S. Moore. "Uranium removal during low discharge in the Ganges-Brahmaputra mixing zone." Geochimica et Cosmochimica Acta 58 (1994): 4987-4995.

Chemical Rubber Company, I. "CRC Handbook of Chemistry and Physics." 66th ed. Boca Raton: CRC Press, Inc. 1986. A-1-I-37.

Cochran, J. K. "The oceanic chemistry of the Uranium- and Thorium-series nuclides." Uranium-series Disequilibrium: Applications to Earth, Marine, and Environmental Sciences. Ed. Ivanovich, M. and R. S. Harmon. 2nd ed. Oxford: Clarendon Press, 1992. pp. 334-395.

Cooke, T. D. and K. W. Bruland. "Aquatic chemistry of selenium: evidence of biomethylation." Environmental Science and Technology 21 (1987): 1214-1219.

Cotton, F. A. and G. Wilkinson. "Advanced Inorganic Chemistry: A Comprehensive Text." 4th ed. New York: Wiley, 1980.

Cotton, F. A. and G. Wilkinson. "Advanced Inorganic Chemistry: A Comprehensive Text." 5th ed. New York: Wiley, 1988.

Creed, J. T., T. D. Martin, and M. Sivaganesan. "Preservation of trace metals in water samples." Journal of the American Water Works Association 87 (1995): 104-114.

Cutter, G. A. and K. W. Bruland. "The marine biogeochemistry of selenium: A re-evaluation." Limnology and Oceanography 29 (1984): 1179-1192.

Date, A. R. and A. L. Gray. "Applications of inductively coupled plasma mass spectrometry." Glasgow: Blackie, 1989. 1-254.

de Baar, H. J. W., M. P. Bacon, and P. G. Brewer. "Rare earth elements in the Pacific and Atlantic Oceans." Geochimica et Cosmochimica Acta 49 (1985): 1943-1959.

de Baar, H. J. W., P. G. Brewer, and M. P. Bacon. "Anomalies in rare earth distributions in seawater: Gd and Tb." Geochimica et Cosmochimica Acta 49 (1985): 1961-1969.

de Baar, H. J. W., J. Schijf, and R. H. Byrne. "Solution chemistry of rare earth elements in seawater." European Journal of Solid State and Inorganic Chemistry 28 (1991): 357-373.

Deverel, S. J. and S. P. Millard. "Distribution and mobility of selenium and other trace elements in shallow groundwater of the Western San Joaquin Valley, California." Environmental Science & Technology 22 (1988): 697-702.

Domagalski, J. Personal communication. "Alkalinity and pH data for the Sacramento River at Freeport, February 1996 - February 1997." 1997.

Dzubay, T. G., R. K. Stevens, G. E. Gordon, et al. "A composite receptor method applied to Philadelphia aerosol." Environmental Science & Technology 22 (1988): 46-52.

Emerson, S. R. and S. S. Huestad. "Ocean anoxia and the concentrations of molybdenum and vanadium in seawater." Marine Chemistry 34 (1991): 177-196.

Erel, Y., J. Morgan, and C. Patterson. "Natural levels of lead and cadmium in a remote mountain stream." Geochimica et Cosmochimica Acta 55 (1990a): 707-719.

Erel, Y., C. Patterson, M. Scott, et al. "Transport of industrial lead in snow through soil to stream water and groundwater." Chemical Geology 85 (1990b): 383-392.

Erel, Y. and E. M. Stolper. "Modeling of rare-earth element partitioning between particles and solution in aquatic environments." Geochimica et Cosmochimica Acta 57 (1993): 513-518.

Fischer, H. B., E. J. List, R. C. Y. Koh, et al. "Mixing in inland and coastal waters." Orlando: Academic Press, 1979. 1-483.

Flegal, A., G. Smith, G. Gill, et al. "Dissolved trace element cycles in the San Francisco Bay estuary." Marine Chemistry 36 (1991): 329-363.

Friedlander, S. K. "Chemical element balanced and identification of air pollution sources." Environmental Science & Technology 7 (1973): 235-240.

Gascoyne, M. "Geochemistry of the actinides and their daughters." Uranium-series Disequilibrium: Applications to Earth, Marine, and Environmental Sciences. Ed. Ivanovich, M. and R. S. Harmon. 2nd ed. Oxford: Clarendon Press, 1992. pp. 34-61.

Goldstein, S. J. and S. B. Jacobsen. "Rare earth elements in river waters." Earth and Planetary Science Letters 89 (1988a): 35-47.

Goldstein, S. J. and S. B. Jacobsen. "REE in the Great Whale River estuary, northwest Quebec." Earth and Planetary Science Letters 88 (1988b): 241-252.

Gordon, G. E. "Receptor models." Environmental Science & Technology 22 (1988): 1132-1142.

Greenberg, M. D. "Advanced engineering mathematics." Englewood Cliffs, New Jersey: Prentice-Hall, 1988. 1-946.

Hanor, J. S. and L.-H. Chan. "Non-conservative behavior of barium during mixing of Mississippi River and Gulf of Mexico waters." Earth and Planetary Science Letters 37 (1977): 242-250.

Hasany, S. M. and M. H. Chaudhary. "Sorption potential of Hare River sand for the removal of antimony from acidic aqueous-solution." Applied Radiation and Isotopes 47 (1996): 467-471.

Heaton, R. W., K. A. Rahn, and D. H. Lowenthal. "Regional apportionment of sulfate and tracer elements in Rhode Island precipitation." Atmospheric Environment 26A (1992): 1529-1543.

Henshaw, J. M., E. M. Heithmar, and T. A. Hinners. "Inductively coupled plasma mass spectrometric determination of trace elements in surface waters subject to acidic deposition." Analytical Chemistry 61 (1989): 335-342.

Hopke, P. K. "Receptor modeling in environmental chemistry." New York: John Wiley & Sons, 1985. 1-319.

Hopke, P. K., E. S. Gladney, G. E. Gordon, et al. "The use of multivariate anlaysis to identify sources of selected elements in the Boston urban aerosol." Atmospheric Environment 10 (1976): 1015-1025.

Houk, R. S. and J. J. Thompson. "Inductively coupled plasma mass spectrometry." Mass Spectrometry Reviews. Ed. Gross, H. L. New York: Wiley, 1988. 7. pp. 425-461.

Hoyle, J., H. Elderfield, A. Gledhill, et al. "The behaviour of the rare earth elements during mixing of river and sea waters." Geochimica et Cosmochimica Acta 48 (1984): 143-149.

Hunter, K. A. and S. R. Tyler. "The distribution of zinc and reactive silicate in the Otago Harbor, New Zealand." Marine Chemistry 20 (1987): 377-387.

Hunter, K. A. and M. W. Leonard. "Colloid stability and aggregation in estuaries: 1. Aggregation kinetics of riverine dissolved iron after mixing with seawater." Geochimica et Cosmochimica Acta 52 (1988): 1123-1130.

Ingri, J. and A. Widerlund. "Uptake of alkali and alkaline-earth elements on suspended iron and manganese in the Kalix River, northern Sweden." Geochimica et Cosmochimica Acta 58 (1994): 5433-5442.

Jarvis, K. E., A. L. Gray, and R. S. Houk. "Handbook of inductively coupled plasma mass spectrometry." Suffolk: St Edmundsbury Press Limited, 1992. 1-380.

Jeandel, C., M. Caisso, and J. F. Minster. "Vanadium behaviour in the global ocean and in the Mediterranean Sea." Marine Chemistry 21 (1987): 51-74.

Kadlec, R. H. "Detention and mixing in free water wetlands." Ecological Engineering 3 (1994): 345-380.

Koeppenkastrop, D. and E. H. De Carlo. "Sorption of rare-earth elements from seawater onto synthetic mineral particles: An experimental approach." Chemical Geology 95 (1992): 251-263.

Koeppenkastrop, D. and E. H. De Carlo. "Uptake of rare earth elements from solution by metal oxides." Environmental Science & Technology 27 (1993): 1796-1802.

Krishnaswami, S., J. R. Trivedi, M. M. Sarin, et al. "Strontium isotopes and rubidium in the Ganga-Brahmaputra river system: Weathering in the Himalaya, fluxes to the Bay of Bengal and contributions to the evolution of oceanic $^{87}Sr/^{86}Sr$." Earth and Planetary Science Letters 109 (1992): 243-253.

Liddicoat, M. I., D. R. Turner, and M. Whitfield. "Conservative behaviour of boron in the Tamar Estuary." Estuarine, Coastal and Shelf Science 17 (1983): 467-472.

Lienert, C., S. A. Short, and H. R. von Gunten. "Uranium infiltration from a river to shallow groundwater." Geochimica et Cosmochimica Acta 58 (1994): 5455-5463.

Liss, P. S. and M. Pointon. "Removal of dissolved boron and silicon during estuarine mixing of sea and river waters." Geochimica et Cosmochimica Acta 37 (1973): 1493-1498.

List, E. J. Personal communication. "Use of a rare earth tracer in a drinking water reservoir in San Diego." 1997.

Löfvendahl, R. "Dissolved uranium in the Baltic Sea." Marine Chemistry 21 (1987): 213-227.

Long, S. E. and T. D. Martin. "Determination of trace elements in waters and wastes by inductively coupled plasma-mass spectrometry. In: Methods for the Determination of Metals in Environmental Samples." EPA/600/4-91/010 1991. EPA. microfiche in Env library.

Luther, G., T. Ferdelman, C. Culberson, et al. "Iodine chemistry in the water column of the Chesapeake Bay: evidence for organic iodine forms." Estuarine, Coastal and Shelf Science 32 (1991): 267-279.

Martin, J. M. and M. Meybeck. "Elemental mass balance of material carried by major world rivers." Marine Chemistry 7 (1979): 173-206.

Miller, J. C. and J. N. Miller. "Statistics for analytical chemistry." 2nd ed. New York: Halsted Press, 1988. 1-227.

Millero, F. J. "Stability constants for the formation of rare earth inorganic complexes as a function of ionic strength." Geochimica et Cosmochimica Acta 56 (1992): 3123-3132.

Moller, P., P. Dulski, and J. Luck. "Determination of rare earth elements in sea water by inductively coupled plasma-mass spectrometry." Spectrochimica Acta 47B (1992): 1379-1387.

Morales-Juberias, T., P. Zafra, M. Olazar, et al. "Modeling solute transport in river channels using dispersion theory." Environmental Geology 24 (1994): 275-280.

Motekaitis, R. J. and A. E. Martell. "Speciation of metals in the oceans. I. Inorganic complexes in seawater, and influence of added chelating agents." Marine Chemistry 21 (1987): 101-116.

Mullen, J. R., S. W. Anderson, and P. D. Hayes. "Water resources data: California, water year 1993. Volume 3. Southern Central Valley Basins and the Great Basin from Walker River to Truckee River." Anonymous CA-93-3 1993. Menlo Park: U.S. Geological Survey.

Murray, J. W. "The Oceans." Global Biogeochemical Cycles. Ed. Butcher, S. S. R. J. Charlson G. H. Orians, et al. London: Academic Press, 1992. pp. 175-211.

Narvekar, P. V., M. D. Zingde, and V. N. Kamat Dalal. "Behaviour of boron, calcium and magnesium in a polluted estuary." Estuarine, Coastal and Shelf Science 16 (1983): 9-16.

Nicholls, G. D. "Weathering of the earth's crust." Chemical Oceanography, Volume 5. Ed. Riley, J. P. and R. Chester. 2nd ed. London: Academic Press, 1976. pp. 81-102.

Olivares, J. A. and R. S. Houk. "Suppression of analyte signal by various concomitant salts in inductively coupled plasma mass spectrometry." Analytical Chemistry 58 (1986): 20-25.

Olmez, I., J. W. Beal, and J. F. Villaume. "A new approach to understanding multiple-source groundwater contamination: factor analysis and chemical mass balances." Water Research 28 (1994): 1095-1101.

Olmez, I. and M. J. Hayes. "Identifying sources of groundwater pollution using trace element signatures." Biological Trace Element Research 26 (1990): 355-361.

Olmez, I., F. X. Pink, and R. A. Wheatcroft. "New particle-labeling technique for use in biological and physical sediment transport studies." Environmental Science & Technology 28 (1994): 1487-1490.

Orians, K. J., E. A. Boyle, and K. W. Bruland. "Dissolved titanium in the open ocean." Nature 348 (1990): 322-325.

Orians, K. J. and K. W. Bruland. "The marine geochemistry of dissolved gallium: A comparison with dissolved aluminum." Geochimica et Cosmochimica Acta 52 (1988a): 2955-2962.

Orians, K. J. and K. W. Bruland. "Dissolved gallium in the open ocean." Nature 332 (1988b): 717-719.

Palmer, M. R. and J. M. Edmond. "Controls over the strontium isotope composition of river water." Geochimica et Cosmochimica Acta 56 (1992): 2099-2111.

Pande, K., M. M. Sarin, J. R. Trivedi, et al. "The Indus river system (India-Pakistan): Major-ion chemistry, uranium and strontium isotopes." Chemical Geology 116 (1994): 245-259.

Peterson, D. H., R. E. Smith, S. W. Hager, et al. "Interannual variability in dissolved inorganic nutrients in Northern San Francisco Bay Estuary." Hydrobiologia 129 (1985): 37-58.

Plater, A. J., M. Ivanovich, and R. E. Dugdale. "Uranium series disequilibrium in river sediments and waters: the significance of anomalous activity ratios." Applied Geochemistry 7 (1992): 101-110.

Quevauviller, P., K. Kramer, E. Van der Vlies, et al. "Improvements in the determination of trace elements in seawater leading to the certification of Cd, Cu, Mo, Ni, Pb, and Zn." Marine Pollution Bulletin 24 (1992): 33-38.

Random House. "Random House Webster's College Dictionary." 3rd ed. New York: Random House, 1995. 1-1568.

Ray, S., M. Mohanti, and B. L. K. Somayajulu. "Suspended matter, major cations and dissolved silicon in the estuarine waters on the Mahanadi River, India." Journal of Hydrology 69 (1984): 183-196.

Ray, S. B., M. Mohanti, and B. L. K. Somayajulu. "Uranium isotopes in the Mahanadi River-Estuarine system, India." Estuarine, Coastal and Shelf Science 40 (1995): 635-645.

Rogge, W. "Molecular Tracers for Sources of Atmospheric Carbon Particles: Measurements and Model Predictions." (1993) California Institute of Technology. Ph.D. thesis.

Salomons, W. and R. Foerstner. "Metals in the Hydrocycle." Berlin: Springer-Verlag, 1984. 1 -349.

Santschi, P. H., E. Hoehn, A. Lueck, et al. "Tritium as a tracer for the movement of surface water and groundwater in the Glatt Valley, Switzerland." Environmental Science & Technology 21 (1987): 909-916.

Sarin, M. M. and T. M. Church. "Behaviour of uranium during mixing in the Delaware and Chesapeake estuaries." Estuarine, Coastal and Shelf Science 39 (1994): 619-631.

Sayles, F. L. and P. C. J. Mangelsdorf. "The equilibration of clay minerals with seawater: exchange reactions." Geochimica et Cosmochimica Acta 41 (1977): 951-960.

Schlesinger, W. H. "Biogeochemistry: an analysis of global change." San Diego: Academic Press, 1991. 3-443.

Sea Engineering, Inc. and California Institute of Technology. "Development of a technique to identify pollutant sources and impacts in coastal and oceanic waters." 1996. Waimanalo, Hawaii: Sea Engineering, Inc.

Sholkovitz, E. R. "The aquatic chemistry of rare earth elements in rivers and estuaries." Aquatic Geochemistry 1 (1995): 1-34.

Sholkovitz, E. R., W. M. Landing, and B. L. Lewis. "Ocean particle chemistry: The fractionation of rare earth elements between suspended particles and seawater." Geochimica et Cosmochimica Acta 58 (1994): 1567-1579.

Skrabal, S. A. "Distributions of dissolved titanium in Chesapeake Bay and the Amazon River Estuary." Geochimica et Cosmochimica Acta 59 (1995): 2449-2458.

Smith, P. E., R. N. Oltmann, and L. H. Smith. "Summary report on the interagency hydrodynamic study of the San Francisco Bay-Delta estuary." 1995. Sacramento: Interagency Ecological Program for the Sacramento-San Joaquin Estuary.

Somayajulu, B. L. K. "Uranium isotopes in the Hooghly estuary, India." Marine Chemistry 47 (1994): 291-296.

Stetzenbach, K. J., M. Amano, D. K. Kreamer, et al. "Testing the limits of ICP-MS: Determination of trace elements in ground water at the part-per-trillion level." Ground Water 32 (1994): 976-985.

Stewart, A. J. and L. A. Kszos. "Caution on using lithium (Li^+) as a conservative tracer in hydrological studies." Limnology and Oceanography 41 (1996): 190-191.

Stoffyn-Egli, P. "Conservative behavior of dissolved lithium in estuarine waters." Estuarine, Coastal and Shelf Science 14 (1982): 577-587.

Stumm, W. and J. J. Morgan. "Aquatic chemistry." 2nd ed. New York: John Wiley & Sons, 1981. 1-780.

Suijlen, J. M. and J. J. Buyse. "Potentials of photolytic rhodamine WT as a large-scale water tracer assessed in a long-term experiment in the Loosdrecht lakes." Limnology and Oceanography 39 (1994): 1411-1423.

Swarzenski, P. W., B. A. McKee, and J. G. Booth. "Uranium geochemistry on the Amazon shelf: Chemical phase partitioning and cycling across a salinity gradient." Geochimica et Cosmochimica Acta 59 (1995): 7-18.

Taylor, H. and J. Garbarino. "Assessment of the Analytical Capabilities of Inductively Coupled Plasma-Mass Spectrometry." Journal of Research of the National Bureau of Standards 93 (1988): 433-435.

The Mamala Bay Study Commission. "Mamala Bay Study." Honolulu: The Mamala Bay Study Commission. 1996.

The Royal Society of Chemistry. "The Dictionary of Substances and Their Effects." Cambridge: The Royal Society of Chemistry, 1994. 1-875.

Thompson, J. J. and R. S. Houk. "A study of internal standardization in inductively coupled plasma-mass spectrometry." Applied Spectroscopy 41 (1987): 801-806.

Toole, J., M. Baxter, and J. Thomson. "Behaviour of uranium isotopes with salinity change in three U.K. estuaries." Estuarine, Coastal and Shelf Science 25 (1987): 283-297.

U.S.Geological Survey. "San Francisco Bay Wind Pattern (Archival)." (1997) http://sfbay7.wr.usgs.gov/wind. Menlo Park. U.S. Geological Survey. (Access date: 15 April 1997).

van den Berg, C. M. G. "Complex formation and the chemistry of selected trace elements in estuaries." Estuaries 16 (1993): 512-520.

van den Berg, C. M. G., S. Khan, P. Daly, et al. "Electrochemical study of Ni, Sb, Se, Sn, U, and V in the estuary of the Tamar." Estuarine, Coastal and Shelf Science 33 (1991): 309-322.

Ward, N. "Multi-Element Analysis of Natural Water Using Inductively Coupled Plasma-Source Mass Spectrometry (ICP-MS)." Watershed 89: The Future for Water Quality in Europe, Volume II: Proceedings of the IAWPRC Conference, Guildford, UK, April 17-20, 1989. New York: Pergamon Press, 1989.

Watson, A. J., J. R. Ledwell, and S. C. Sutherland. "The Santa Monica Basin tracer experiment: Comparison of release methods and performance of perfluorodecalin and sulfur hexafluoride." Journal of Geophysical Research 96 (1991): 8719-8725.

Watson, J. G., J. A. Cooper, and J. J. Huntzicker. "The effective variance weighting for least squares calculations applied to the mass balance receptor model." Atmospheric Environment 18 (1984): 1347-1355.

Watson, J. G., N. F. Robinson, J. C. Chow, et al. "Model, CMB 7.0." Environmental Software 5 (1990): 38-49.

Wilson, J. F. J., E. D. Cobb, and F. A. Kilpatrick. "Fluorometric procedures for dye tracing." Anonymous TWI 3-A12 1 p. 1986. Denver: U.S. Geological Survey. Techniques of water-resources investigations of the United States Geological Survey.

Wilson, R. D. and D. M. Mackay. "SF_6 as a conservative tracers in saturated media with high intragranular porosity or high organic carbon content." Ground Water 34 (1996): 241-249.

Wong, G. T. F. "The stability of dissolved inorganic species of iodine in seawater." Marine Chemistry 9 (1980): 13-24.

Wong, G. T. F. "The stability of molecular iodine in seawater." Marine Chemistry 11 (1982): 91-95.

Wood, S. A. "The aqueous geochemistry of the rare-earth elements and yttrium. 1. Review of available low-temperature data for inorganic complexes and the inorganic REE speciation of natural waters." Chemical Geology 82(1990): 159-186.

Appendix A

Element listing and literature review

Appendix A
Element listing and literature review

Table of contents

Element symbols and element names

Ac	actinium	Ge	germanium	Pr	praseodymium
Ag	silver	H	hydrogen	Pt	platinum
Al	aluminum	He	helium	Pu	plutonium
Am	americium	Hf	hafnium	Ra	radium
Ar	argon	Hg	mercury	Rb	rubidium
As	arsenic	Ho	holmium	Re	rhenium
At	astatine	I	iodine	Rh	rhodium
Au	gold	In	indium	Rn	radon
B	boron	Ir	iridium	Ru	ruthenium
Ba	barium	K	potassium	S	sulfur
Be	beryllium	Kr	krypton	Sb	antimony
Bi	bismuth	La	lanthanum	Sc	scandium
Bk	berkelium	Li	lithium	Se	selenium
Br	bromine	Lr	lawrencium	Si	silicon
C	carbon	Lu	lutetium	Sm	samarium
Ca	calcium	Md	mendelevium	Sn	tin
Cd	cadmium	Mg	magnesium	Sr	strontium
Ce	cerium	Mn	manganese	Ta	tantalum
Cf	californium	Mo	molybdenum	Tb	terbium
Cl	chlorine	N	nitrogen	Tc	technecium
Cm	curium	Na	sodium	Te	tellurium
Co	cobalt	Nb	niobium	Th	thorium
Cr	chromium	Nd	neodymium	Ti	titanium
Cs	cesium	Ne	neon	Tl	thallium
Cu	copper	Ni	nickel	Tm	thulium
Dy	dysprosium	No	nobelium	U	uranium
Er	erbium	Np	neptunium	V	vanadium
Es	einsteinium	O	oxygen	W	tungsten
Eu	europium	Os	osmium	Xe	xenon
F	fluorine	P	phosphorus	Y	yttrium
Fe	iron	Pa	protactinium	Yb	ytterbium
Fm	fermium	Pb	lead	Zn	zinc
Fr	francium	Pd	palladium	Zr	zirconium
Ga	gallium	Pm	promethium		
Gd	gadolinium	Po	polonium		

Introduction. An extensive literature review has been conducted to understand the chemistry of many elements in freshwater, estuarine, and ocean environments. This information has been used to predict which elements are likely to behave conservatively as tracers and to narrow the range of elements analyzed. In general, elements that are likely to behave conservatively when fresh and saline waters mix are those that are present in higher concentrations in seawater; it is their inert behavior that leads to their higher concentrations in seawater. Although concentrations of these elements vary from one freshwater source to another, it is necessary in some systems (like the Hawai'i study area, see Chapter 4) to use as tracers elements that are present in higher concentrations in fresh waters and that can delineate between two or more freshwater sources. A review of some of the available literature was conducted to determine the chemical behavior of some of these elements. The information provided below is based upon observed behavior in other systems and known speciation information. This summary of information is provided for chemical "families" and for select individual elements. References from this appendix are included in the thesis reference list.

Alkali metals. This group of elements includes lithium, sodium, potassium, rubidium, and cesium (Li, Na, K, Rb, and Cs). In general, these elements are stable in aqueous solution, due primarily to their electronic structures, which consist of a single s electron outside a noble gas core. This electron is easily stripped and these elements tend to exist as singly-charged, largely non-reactive cations in solution. Reactivity increases from Li to Cs, as does the mobility of the ions in electrolytic conduction. The hydrated

radii and hydration energies decrease from Li to Cs, indicating that Li is less likely than the other alkali metals to coordinate with ligands other than water.

Lithium. Li is usually tetrahedrally surrounded by water molecules to form $Li(H_2O)_4^+$ in solution; its hydrated radius is exceptionally large at 3.40 Å (Cotton and Wilkinson, 1988). Analyses of Li in the St. Lawrence River estuary in Canada and the Scheldt River estuary in Belgium indicate that Li behaves conservatively, with a concentration increasing linearly in direct proportion to salinity; laboratory experiments have demonstrated that suspended matter in the Scheldt River estuary does not participate in adsorption or desorption reactions with Li (Stoffyn-Egli, 1982). Li is believed to behave conservatively in seawater, where its concentration is about 180 ppb; Li^+ is the main aqueous specie with a slight tendency to complexation with either chloride (Bruland, 1983) or perhaps with sulfate (Byrne et al., 1988). Li has been shown to behave conservatively in a variety of systems where it has been added as a tracer (see, for example, Kadlec, 1994, and Morales-Juberias et al., 1994). Li should be used as an added tracer only after careful consideration, as some researchers believe that it may be toxic to aquatic organisms (Stewart and Kszos, 1996).

Sodium. Na is an abundant element, comprising 2.6% of the earth's lithosphere; although not as large as the hydrated radius of Li, the hydrated radius of Na is large at 2.76 Å, and Na probably exists in aqueous solution as $Na(H_2O)_4^+$ (Cotton and Wilkinson, 1980). In river water, Na has been observed to have the following speciation: 99.83%

Na^+, 0.05% $NaSO_4$, 0.12% $NaHCO_3$, and 0% as either $NaCO_3$ or NaOH (Aston, 1978). Na is the major cation present in seawater, existing as about 99% Na^+ with about 1% present in solution in association with anions (Motekaitis and Martell, 1987). It is generally assumed that Na behaves conservatively in aqueous solution and in seawater, where it has a concentration of 11‰ (Bruland, 1983). Slight deviations from conservative behavior may occur due to the presence of Na in particulate matter in river water and due to the ability of Na to exchange with other cations in clay minerals in solution (Sayles and Mangelsdorf, 1977). This effect likely involves only a small fraction of the total amount of dissolved Na.

Potassium. The chemistry of K is similar to that of Li and Na; K has a hydration number of 4 and a fairly large hydrated radius of 2.32 Å (Cotton and Wilkinson, 1980). Its speciation in river water is similar to that of Na, with 99.92% present as K^+ and 0.08% associated with sulfate (Aston, 1978). In seawater, a small fraction of K (<1%) is associated with anions (Motekaitis and Martell, 1987). K has a conservative distribution in seawater and an average concentration of 400 ppm (Bruland, 1983).

Rubidium. Rb has a conservative distribution in the oceans, with an average concentration of about 120 ppb (Bruland, 1983). Approximately 1% of Rb in seawater is associated with sulfate and 99% is present as free hydrated Rb^+ (see Byrne et al., 1988, for stability constants). Rb is present primarily as a hydrated cation but with a hydration coordination number probably of 6 ($Rb(H_2O)_6^+$) (Cotton and Wilkinson, 1980). Although

little information is available on the speciation of Rb in freshwater, it is generally assumed that, like the other alkali metals, this is the dominant specie. In the Ganges-Brahmaputra and Indus river systems, concentrations of Rb and K are highly correlated; it is speculated that adsorption loss of Rb is responsible for observed increases in the ratio of K to Rb in these rivers (Krishnaswami et al., 1992; Pande et al., 1994).

Cesium. Cs has the smallest hydrated radius of the alkali metals at 2.28 Å; Cs probably has a hydration coordination number of 6 or perhaps greater (Cotton and Wilkinson, 1980). Cs has the strongest tendency of the alkali metals to complexation with chloride, but it still exists primarily as a simple hydrated cation with a conservative distribution in the oceans (Bruland, 1983). There may be a slight tendency to complexation with sulfate in seawater (see Byrne et al., 1988, for stability constants).

Alkaline earths. The alkaline earths, also known as the Group II elements, include beryllium, magnesium, calcium, strontium, barium, and radium (Be, Mg, Ca, Sr, Ba, and Ra). Be exhibits behavior that is distinct from that of the rest of the group and has the highest charge-to-radius ratio of all elements except H^+ and B^{3+} (Cotton and Wilkinson, 1980). The behavior of Mg is intermediate between Be and the rest of the group; Mg has a tendency to bond covalently and, like Be, can be precipitated from aqueous solution under special conditions (ibid.). Metal atomic radii are smaller for the alkaline earths than for the alkali metals, and all the alkaline earths are highly electropositive (ibid.).

Beryllium. Be differs from the rest of the elements in this group in its strong tendency to form hydrolysis products; it exists in seawater primarily as $Be(OH)^+$ and $Be(OH)_2^0$. Concentrations in seawater are low (< 1 ppt), its residence time is low (< 1000 years), and it exhibits a non-conservative nutrient-type profile in the oceans, indicative of scavenging (Bruland, 1983). Almost no Be is present in seawater as free cations, and Be, along with Sc, is one of the only strongly hydrolyzed metals with solution chemistry in seawater that includes reactions other than hydrolysis (see Byrne et al., 1988, for stability constants).

Magnesium. Mg is present in aqueous solution primarily as a hydrated cation with a coordination number of 6 ($Mg(H_2O)_6^{2+}$) (Cotton and Wilkinson, 1980). Its speciation in river water has been observed as 97.54% Mg^{2+}, 1.15% $MgSO_4$, 1.21% $MgHCO_3$, 0.08% $MgCO_3$, and 0.01% MgOH (Aston, 1978). In seawater, Mg complexes to a small extent with bicarbonate and carbonate (see Motekaitis and Martell, 1987, for stability constants). Mg exhibits a conservative profile in the oceans with an average concentration of 1.33‰ (Bruland, 1983). Slight non-conservative behavior may be observed with mixing between fresh and saline waters due to the exchange of Mg from clay particles (Sayles and Mangelsdorf, 1977); this effect is probably negligible due to the relatively high concentration of Mg in both river and seawater.

Calcium. The speciation of Ca in river water has been observed as 96.89% Ca^{2+}, 1.45% $CaSO_4$, 1.32% $CaHCO_3$, 0.33% $CaCO_3$, and 0.01% CaOH (Aston, 1978). In seawater, Ca forms complexes primarily with bicarbonate, carbonate, and sulfate (see Motekaitis and Martell, 1987, for stability constants). The average concentration of Ca in seawater is about 420 ppm (Bruland, 1983). The major sink for dissolved Ca in ocean waters is the incorporation of Ca into the calcareous tests of marine organisms, which sink and dissolve at depth; the result is a slight surface depletion of Ca (roughly 1.5% compared with deep waters) (ibid.). In a given region, this depletion tends to be uniform, such that the use of Ca as a tracer in seawater should not be eliminated due to this characteristic.

Strontium. Sr is present in relatively high concentrations in seawater (roughly 7.9 ppm) (Bruland, 1983). It is probably depleted by roughly the same amount as Ca in the surface waters of the oceans due to its incorporation into the tests of various species of plankton (Bruland, 1983). The speciation of Sr in river waters is probably similar to that of Ca and Mg. Scavenging of non-detrital Sr was observed to non-detrital Fe throughout all seasons for the Kalix River, a river in northern Sweden; Sr concentrations were significantly lower than observed in the Delta study area (Ingri and Widerlund, 1994). Sr isotope ratios have been studied in several river systems (for further information, see Andersson et al., 1994; Andersson et al., 1992; Krishnaswami et al., 1992; Pande et al., 1994; and Palmer and Edmond, 1992).

Barium. Interestingly, Ba is probably the most accurately determined trace element in oceanwater because it has been very widely studied; Ba exists in seawater primarily as a hydrated cation (Bruland, 1983). It has a non-conservative, nutrient-type distribution in the oceans similar to that of silicate; it follows a cycle of surface uptake and regeneration at depth similar to those of biogenic opal and calcium carbonate (ibid.). Ba in oceanwater has a small tendency to complexation with sulfate (see Byrne et al., 1988, for stability constants). Ba has been observed to behave strongly non-conservatively in mixing in the Mississippi River estuary, with strong addition at low salinities; this behavior is due to adsorption by clay minerals of Ba, which is preferentially sorbed over many other cations (Hanor and Chan, 1977). Observations on the Kalix River in northern Sweden show that sediment porewater concentrations of Ba are twenty-five times higher than river water concentrations, suggesting strong adsorption to and removal with particles (Ingri and Widerlund, 1994).

Group III elements. This group includes boron, aluminum, gallium, indium, and thallium (B, Al, Ga, In, and Tl). Although B is in the same column of the periodic table, it is smaller than the others and has no cationic chemistry. The main oxidation state for these elements is +III. In general, these elements are strongly hydrolyzed in solution and thus may behave more conservatively than other elements in adjacent positions in the periodic table.

Boron. B is the least metallic and least ionic of this family of elements. It is a conservative major element of seawater, existing primarily as boric acid (H_3BO_3) with about 1% present as ionized borate ($B(OH)_4^-$) (Bruland, 1983). Removal of B seems to occur upon mixing of fresh and saline waters in some estuaries but not in others. Removal has been observed in the River Alde estuary in England, while conservative behavior has been observed in the Chikugogawa and Beaulieu estuaries of Japan and England (Burton and Liss, 1976). Conservative behavior has been observed in the Tamar estuary, where dissolved B derives almost entirely from seawater (Liddicoat et al., 1983).

Studies of borate adsorption to soils show substantial adsorption above a pH of about 7; this adsorption is likely onto surface aluminol groups on particles (Sposito, 1988). Laboratory studies have shown that dissolved B may be removed in estuaries through reaction with clay minerals (Liss and Pointon, 1973). B removal to sediments has been observed in the Ambika estuary of India, where industrially added B raises freshwater concentrations substantially; this work supports the theory that B is incorporated into sediments in amounts proportional to salinity (Narvekar et al., 1983). Finally, estuarine sediments in the St. Lawrence estuary showed that B was associated with iron hydroxides near the sediment surface, with organic materials at intermediate depths, and was incorporated into the crystal lattices of clays after long burial times (Bergeron and Lebel, 1983); this work suggests that re-release after burial will be an insignificant source of B to overlying waters. For estuaries where non-conservative behavior is observed, adsorption to clay minerals with subsequent coagulation and loss of particles is the likely cause.

Aluminum. Al occurs widely in the earth's crust. Most Al from weathering rocks reaches the oceans as alumino-silicate minerals, and concentrations of dissolved Al are very low, ranging in river water from 5 - 800 ppb (Aston, 1978). Seawater contains typically less than 1 to 10 ppb of dissolved Al, and much of this is present as colloidal particles (ibid.; Bruland, 1983). The residence time of Al in the central North Pacific is about 1 to 4 years (Orians and Bruland, 1988a). Al can easily undergo hydrolysis, polymerization, and precipitation when fresh and saline waters mix. Significant removal has been observed in several estuaries, and humic substances may play a major role in removal processes (Aston, 1978). Dissolved Al in ocean waters is present primarily as $Al(OH)_4^-$ and $Al(OH)_3$ (Bruland, 1983). Thermodynamic stability constants for these species in seawater can be found in Byrne et al. (1988). It is significant to note that Al is a major component of alum, a flocculant used in wastewater treatment ($Al_2(SO_4)_3 \cdot 18H_2O$ or $Al_2(SO_4)_3 \cdot 14H_2O$); it reacts to form $Al(OH)_3$, a gelatinous floc that is insoluble and settles out, thus removing particulate matter. The chemistry of Al was not investigated further, as it was not expected to behave conservatively.

Gallium. Little is known about the aquatic chemistry of Ga. It is strongly hydrolyzed in ocean waters and is present primarily as $Ga(OH)_4^-$ (Bruland, 1983). Ga concentrations in oceanic waters exhibit a subsurface maximum, a mid-depth minimum, and a maximum in bottom waters; scavenging removal is evident (Orians and Bruland, 1988b). The residence time for dissolved Ga in the surface waters of the ocean is on the

order of hundreds of years, indicating that it is less reactive than Al (ibid.). Stability constants for the formation of Ga hydrolysis products in seawater can be found in Byrne et al. (1988). No details were found regarding the speciation and chemical behavior of Ga in fresh waters, but its behavior is probably analogous to that of Al.

Indium. Concentrations of In are low in both river and ocean waters. In ocean waters, In is present as the strongly hydrolyzed $In(OH)_3$ and related ions (Bruland, 1983; Byrne et al., 1988). Its concentration in ocean waters averages about 20 ppt (Bruland, 1983). Estimated stability constants for seawater can be found in Byrne et al. (1988). Because of its low concentration in natural waters, its moderate ionization potential, and its mass, In makes a good internal standard for ICP-MS analysis (Jarvis et al., 1992; Date and Gray, 1989).

Thallium. Both the trivalent and univalent states are important for Tl in ocean waters. Tl probably exists primarily as Tl(III) in ocean water, present as strongly hydrolyzed $Tl(OH)_3$ and related species (Byrne et al., 1988). Concentrations of Tl are very low (tens of parts per trillion) in both fresh and saline waters. Like In, its chemical properties and low abundance in natural waters suggest its use as an internal standard in ICP-MS analysis (Jarvis et al., 1992; Date and Gray, 1989).

Group IV elements. These elements include carbon, silicon, germanium, tin, and lead (C, Si, Ge, Sn, and Pb). C is strictly non-metallic, Si is essentially non-metallic, Ge

is a metalloid, and both Sn and Pb are metallic (Cotton and Wilkinson, 1980). C has a tendency to form long chains, while bond strengths generally decrease from Si to Pb (ibid.). Only Si and Ge are likely to behave conservatively in natural waters, as shown below.

Carbon. Carbon is present in natural waters in both organic and inorganic forms; inorganic carbon is present primarily as dissolved CO_2, HCO_3^-, and CO_3^{2-}. Organic carbon is present in almost every living thing, from plants to animals, and its geochemical cycling is complex, although the transport of organic carbon in rivers is a minor part of the global cycle (Schlesinger, 1991). C shows a nutrient-type distribution in the oceans (Bruland, 1983) and total C is not expected to behave conservatively during mixing.

Silicon. Si accounts for approximately 28% of the earth's crustal material and is generally unreactive (Cotton and Wilkinson, 1980). It forms many compounds with oxygen, including SiO_2 (quartz or cristobalite), which is perhaps the most common (ibid.). For waters of pH < 9, dissolved Si will be present almost exclusively as silicic acid, H_4SiO_4 (Aston, 1978; Stumm and Morgan, 1981). Laboratory testing has shown that removal of dissolved Si from river water requires both suspended sedimentary particles and seawater electrolytes (Aston, 1978). In ocean waters, Si is present in concentrations of about 2.9 ppm, and it exhibits a nutrient-type, non-conservative profile; here, it exhibits a large fractionation between surface waters and depths due to uptake of

silicic acid by organisms for test formation (Bruland, 1983). In fact, it is believed that Si is the biolimiting nutrient for planktonic organisms over much of the open oceans (ibid.).

Silicon has been observed to behave conservatively in some estuaries, including the Merrimack (Burton and Liss, 1976) and the Narbada (Borole et al., 1977). In other estuaries, removal is observed; these include the estuary of the River Alde in England (Liss and Pointon, 1973), the Godavari in India (Borole et al., 1977), and the Mahanadi (Ray et al., 1984). In still other estuaries, including the Yaquina in Washington state (Callaway and Specht, 1982), the San Francisco Bay estuary (Peterson et al., 1985; Flegal et al., 1991), and Otago Harbor of New Zealand (Hunter and Tyler, 1987), the behavior of Si is conservative only during certain times of the year.

Germanium. Ge is thought to exist in oceanwater primarily as H_4GeO_4 and $H_3GeO_4^-$ (Bruland, 1983). Ge has been reported in concentrations of about 0.5 to 8.3 ppt in ocean waters, where it has a nutrient-type concentration profile that resembles the profile of H_4SiO_4 (ibid.). Interestingly, concentrations of methylated Ge species in the deep sea have also been reported (ibid.). Little information is available on the speciation of Ge in freshwaters, but it is present in low concentrations and is not expected to behave conservatively.

Tin. Tin is believed to exist in ocean water primarily in the +IV oxidation state as $Sn(OH)_4$ and $SnO(OH)_3^-$; because most common water samplers are constructed in part of PVC, which can be a major source of Sn contamination, there has been little study of Sn

in the oceans (Bruland, 1983). Concentrations of 0.5 to 4.5 ppt have been reported in ocean surface waters (ibid.). Methylated Sn compounds have been observed to concentration levels roughly ten times below those reported for inorganic Sn (ibid.). Tributyl tin (TBT) is an extremely toxic organic Sn compound used on boat hulls as an antifouling component of paint; this use may introduce Sn to areas that support recreational and commercial boating (California State Lands Commission, 1991), but concentrations in freshwater are generally unknown. Sn was not extensively studied, as it is not expected to behave conservatively.

Lead. Because of contamination problems, sampling for lead is extremely difficult. In the open ocean, the concentration of Pb ranges from about 1 to 36 ppt, and its distribution is significantly influenced by man's activities (Bruland, 1983). Anthropogenic influences account for its observed oceanic distribution, which exhibits high concentrations in surface waters with depletion at depth; particle scavenging is the main means of removal and accounts for its short oceanic residence time (~ 100 years in the deep water column) (ibid.). Because of its highly non-conservative behavior and the difficulty of cleanly collecting samples for Pb analysis, the literature review conducted was not extensive. The reader is referred to several studies of Pb in freshwater, including: Benoit (1994); Quevauviller (1992); and Erel et al. (1990a and 1990b).

Group VN elements. This group includes nitrogen, phosphorus, arsenic, antimony, and bismuth (N, P, As, Sb, and Bi). All elements in this group are moderately electronegative; none forms any simple anion (Cotton and Wilkinson, 1980). P and N are

essentially covalent chemically, while As, Sb, and Bi show increasing tendencies to cationic behavior (ibid.). Both P and N are difficult to measure accurately with ICP-MS; additionally, they each exhibit a very complex chemistry involving multiple oxidation states and a wide variety of chemical and biological reactions. These elements are not discussed in greater detail.

Arsenic. In seawater, As(V) forms oxoanions, existing primarily as $HAsO_4^{2-}$; it has a nutrient-type distribution with concentrations in the range of a couple ppb (Bruland, 1983). In freshwater environments, removal by settling has been observed (Aston, 1978). Biological reactions involving methylation and interactions with particulate matter in freshwaters affect both the speciation and solution concentrations of As; probably all methylated forms are As(IV), but this is not certain (Anderson and Bruland, 1991). Inorganic As forms are predominant in river waters, while 13% of the As present in Suisun Bay was present as methylated As (ibid.). Strong parallels between arsenate (AsO_4^{3-}) and phosphate (PO_4^{3-}) exist in lake and reservoir waters, suggesting that As is taken up in biological reactions involving P (ibid.). As has only a single isotope, which experiences significant interferences during ICP-MS analysis with ArCl. Because of these difficulties, As was not studied further.

Antimony. Sb exists in seawater primarily in the +III and +V oxidation states and at concentrations of several hundred ppt (Bruland, 1983). Sb(V) occurs as $Sb(OH)_6^-$; Sb(III) is present primarily as $HSbO_2$ but also as methylated species in certain waters; the

distribution with salinity is largely unknown (ibid.). Sb is also present in low concentrations in fresh waters. Sb has been shown to sorb to sand (Hasany and Chaudhary, 1996), and estuarine chemistry is non-conservative, particularly at low salinities, in the Tamar estuary (van den Berg, 1993).

Bismuth. Little is known about the chemistry and speciation of Bi in ocean waters. It is present in low concentrations (part per trillion range) and exhibits enrichment at depth (Bruland, 1983). Its profile is consistent with the element's metallic characteristics and with its probably occurrence as a geochemically reactive hydroxy species (ibid.). Dissolved Bi probably exists in seawater primarily as $Bi(OH)_3$ (see Byrne et al., 1988, for stability constants). Little literature is available on the speciation and behavior of Bi in freshwaters.

Group VI elements. Group VI elements include oxygen, sulfur, selenium, and tellurium (O, S, Se, and Te). The metallic character of these elements increases from S to Te (Cotton and Wilkinson, 1980). As one of the major components of water, O is not measurable by ICP-MS in water samples. Sulfur, because of its high ionization potential, is difficult to quantify. The chemistry of sulfur is quite complex, as sulfur has several oxidation states and forms a wide variety of compounds with many elements; many ionic species form complexes with the inorganic sulfate ion in natural waters. These elements therefore were not considered as tracers and are not discussed in greater detail below. Even though its quantification is difficult by ICP-MS, the chemistry of Se is of particular

interest in the Delta study area, and some detail is presented below. Very little information is available about the existence of Te in natural waters, and it is not treated here.

Selenium. Profiles taken in the Pacific show three dissolved Se species: selenate (Se(VI)), selenite (Se(IV)), and organic selenide (Se(-II)). In surface waters, organic selenide comprises about 80% of total Se, and Se has a nutrient-type profile in the ocean (Cutter and Bruland, 1984). In surface waters, Se(VI) is probably the dominant specie present (ibid.). Se is highly enriched in atmospheric aerosols relative to its crustal abundance, with an enrichment factor of between 1000 and 6000; the largest fraction of this Se is an unidentified vapor phase (Cooke and Bruland, 1987). One pathway for enrichment could be Se biomethylation followed by the release of dimethyl selenide (DMSe) (ibid.). In surface waters, dissolved inorganic Se can exist as: Se(-II), primarily present as biselenide (HSe^-); Se(0) as colloidal elemental Se; Se(IV), primarily as a selenite oxyanion ($HSeO_3^-$ and SeO_3^{2-}); and Se(VI) as the selenate oxyanion (SeO_4^{2-}) (ibid.). In high Se freshwater environments, removal of Se(VI) has been observed to occur very quickly. In the San Joaquin River, selenate was the major specie present, accounting for 56 - 71% of the total Se observed. Selenite accounted for 5 - 10 %, and Se ((-II) + (0)) accounted for 14 - 38%. $DMSe^+$-R was detected in 2 of 5 samples at levels of 1% and 19%; although DMSe was not detected, it may be produced an transfer into the gas phase very quickly (ibid.). A study of Se in shallow groundwater collected from the western San Joaquin Valley showed that concentrations in shallow groundwater are likely

affected by the salinity of the groundwater and the geologic source of the alluvial material (Deverel and Millard, 1988).

Halogens. Also known as the Group VII elements, the halogens include fluorine, chlorine, bromine, iodine, and astatine (F, Cl, Br, I, and At). These elements are one electron short of having a noble gas electron configuration and readily gain an electron to form X- anion or single covalent bonds (Cotton and Wilkinson, 1980). Once in noble gas configuration, they are quite stable. The electronegativity of the elements in this group decreases from F (the most electronegative of all elements) to At (ibid.). At is radioactive with several short-lived isotopes; the longest half-life is 8.3 hours.

Fluorine. F is the most chemically reactive of all elements (Cotton and Wilkinson, 1980). F probably occurs largely as F^- in seawater, although the MgF^+ pair may account for up to 50% of the total F in solution (Burton and Liss, 1976). In river water, only about 1% of F is complexed as MgF^+, and complexation by Al is more important than in seawater (ibid.). Fluorine speciation in river water has been observed by others to be: 98.79% F, 0.01% NaF, 0.88% MgF, and 0.32% CaF (Aston, 1978). F has been assumed to behave conservatively during estuarine mixing, and this has been confirmed in coastal/estuarine areas in Georgia, in Chesapeake Bay, and in the Chikugogawa estuary of Japan (Burton and Liss, 1976). Note that because the pK of hydrofluoric acid is 3.45 at 25°C (CRC Handbook of Chemistry and Physics, 1986) and

because HF is volatile, acidification of samples below this pH level could result in significant loss of F.

Chlorine. Cl is assumed to behave conservatively during estuarine mixing, and chlorinity and/or chlorosity are often used to judge the conservative nature of mixing of various estuarine constituents (Burton and Liss, 1976). Cl is present at a level of 18.9‰ in seawater and is assumed to be almost completely uncomplexed (Bruland, 1983). Several of the REEs, Mn, Fe, Co, Ni, Zn, and Tl are present as weak Cl^- complexes in seawater (Byrne et al., 1988). In river water, Cl is present entirely as Cl^- (Aston, 1978). Cl should behave conservatively but was not studied in greater detail because it cannot be easily measured using ICP-MS.

Bromine. Br is present in much higher concentrations in ocean waters (about 69 ppm) than in freshwaters; it is present in seawater primarily as Br^-, where it is believed to behave conservatively (Bruland, 1983). Its speciation in freshwater is likely similar to that of Cl, and Br is likely to behave conservatively during estuarine mixing. Unfortunately, it could not be measured reproducibly by ICP-MS.

Iodine. I differs from the other halogens in that its primary oxidation state in natural waters is not -I. In oxygenated seawater, I occurs principally as iodate (I(V), present as IO_3^-); under anoxic conditions, I^- is the stable form (Bruland, 1983). In the oceans, I is observed to have a nutrient-type, non-conservative distribution (ibid.). At the

pH of ocean water, loss of molecular I by volatilization should not occur (Wong, 1980). Molecular I is unstable in seawater and undergoes rapid hydrolysis to form IO^-, which has a limited lifetime in seawater, possibly due to reactions with naturally occurring organic compounds (Wong, 1982). I is delivered to the oceans by rivers primarily as I^-; due to kinetic limitations, conversion to iodate likely occurs beyond the estuary (Bruland, 1983). Studies conducted in Chesapeake Bay found that total I did behave conservatively in spite of changes in speciation and oxidation state and the presence of large quantities of organic I (Luther et al., 1991); here, up to 90% of total I was present in organic forms in surface waters, which had a high primary productivity. As with F, acidification of samples may result in loss of I.

Noble gases. These elements include helium, neon, argon, krypton, xenon, and radon (He, Ne, Ar, Kr, Xe, and Rn). Many are present in the atmosphere in measurable concentrations (most notably Ar) but are not present in detectable quantities in aqueous solution. Because of their stable electron configuration, they are remarkably inert (Cotton and Wilkinson, 1980).

Elements of the first transition series. Scandium, titanium, vanadium, chromium, manganese, iron, cobalt, nickel, copper, and zinc (Sc, Ti, V, Cr, Mn, Fe, Co, Ni, Cu, and Zn) comprise the first transition series. Although the aqueous chemistry of the first transition elements is simpler than that of the second or third transition elements, the chemistry is still quite complicated compared to many of the elements discussed

above. All these elements except Sc and Zn form multiple oxidation states; the remaining elements occur in the +II and +III oxidation states, while the +IV oxidation state is the most important for Ti and is also important for V. The V, VI, and VII states occur only as Cr(V, VI), Mn(V, VI, VII), and Fe(V, VI) (Cotton and Wilkinson, 1980). Many of these elements are subject to significant fluctuations caused by man-made inputs of these elements (e.g., as sewage or industrial wastes). None of these elements (with the possible exception of Sc) has a conservative profile in the oceans (ibid.). Fe is particularly important to estuarine mixing behavior where fresh and saline waters mix, where it often forms particles that settle and that can sweep out other elements. Because of their complex chemistry and because they were not considered for use as tracers, only an extremely small fraction of the literature available regarding the chemical behavior of these elements was reviewed. Details are provided below.

Scandium. Sc is often grouped with the REEs because its chemistry resembles lanthanide chemistry more closely than the chemistry of the other elements in the first transition series. In seawater with pH values near that of the open ocean, Sc is strongly hydrolyzed, and it is believed that almost all Sc is present as $Sc(OH)_4^-$, $Sc(OH)_3$, and $Sc(OH)_2^+$ (see Byrne et al., 1988, for stability constants). Sc is present at very low concentrations in seawater (<1 ppt), and its behavior is unknown (Bruland, 1983). Laboratory experiments performed by mixing riverine suspended matter with filtered seawater showed no significant desorption (Burton and Liss, 1976). Removal by settling was not observed to a significant degree in the Rhine River estuary; however, estuarine

and near-shore sediments, when anaerobic, are capable of taking up and retaining Sc (Aston, 1978). Little is known about the freshwater speciation of Sc, but it is likely similar to that of Sc in the oceans, perhaps with some carbonate complexation as well as hydrolysis.

Titanium. Ti is unusual in that it is relatively abundant in the earth's crust but is present only in very low concentrations in seawater (100 ppt or less) (Orians et al., 1990; Bruland, 1983). It is depleted in ocean surface waters but strongly enriched in bottom waters, often by two orders of magnitude; this indicates that it is scavenged by particles (Orians et al., 1990). Thermodynamic speciation models suggest that $TiO(OH)_2$ should be the dominant species (ibid.). In both the Amazon River estuary and Chesapeake Bay, Ti is present in very low concentrations (about 50 ppt or less) and is removed at low salinities, most likely by the "coagulation of colloidal metal, perhaps with stabilization of the aggregates by organic material or by adsorption onto other particles" (Skrabal, 1995). Comparison of oxic surface waters to anoxic bottom waters demonstrated no consistent evidence for Ti release upon Fe or Mn dissolution (ibid.).

Vanadium. V is relatively unreactive in seawater and is concentrated in sediments overlain by anoxic or nearly anoxic waters (Emerson and Huestad, 1991). V in oxic seawater should be present as V(V) and hydrolyzed to $VO_2(OH)_3^{2-}$ at neutral pH (ibid.; Jeandel et al., 1987); this is analogous to U in seawater, which occurs primarily as $UO_2(CO_3)_3^{4-}$ and $UO_2(CO_3)_2^{3-}$. Concentrations of V in the surface waters of the ocean

correlate roughly with phosphate, but V behaves conservatively below the surface (Emerson and Huestad, 1991). Similarities between the chemistries of the vanadates and phosphates may be responsible for the biological activity of V, which may be involved in phosphatase enzyme regulation (Jeandel et al., 1987). Both V(V) and V(IV) are surface active, but V(IV) should be far more strongly adsorbed in natural waters (ibid.). The probable mechanism for removal onto sediments is adsorption of V(IV) onto surface oxide phases in sediments (ibid.). High concentrations of V have been observed in the inlet waters to evaporation ponds in the San Joaquin Valley, suggesting that soils derived from marine sediments are the likely source (Bradford et al., 1990); in shallow groundwaters of this valley, V is probably present as dissolved oxyanions (Deverel and Millard, 1988).

Chromium. Cr has many oxidation states, including Cr(VI) (which is highly toxic in aqueous solutions), Cr(V), Cr(IV), Cr(III), Cr(II), and Cr(0); of these, Cr(V) and Cr(IV) are relatively rare (Cotton and Wilkinson, 1980). Cr(III) complexes are relatively inert in aqueous solution (ibid.). Cr has a nutrient-type distribution in seawater with an average concentration of about 0.2 ppb (Bruland, 1983). Complexation data for Cr(III) can be found in Byrne et al. (1988).

Manganese. Manganese comprises 0.085% of the earth's crust; only iron is a more abundant heavy metal (Cotton and Wilkinson, 1980). In the oceans, Mn occurs in the +II oxidation state, existing mainly as free hydrated Mn^{2+}; the concentration ranges

from 5 to 16 ppt (Bruland et al., 1991). Estuarine and near-shore anaerobic sediments are capable of taking up and retaining Mn (Aston, 1978), and hydrous Mn-oxides can be very efficient scavengers for trace metals (Burton and Liss, 1976). Equilibrium constants for Mn in seawater can be found in Byrne et al. (1988) and in Motekaitis and Martell (1987), which also includes dissolution constants for $Mn(OH)_2(s)$ and $MnCO_3(s)$. In the dissolved phase, Mn is shown to complex with a variety of anions.

Iron. Iron is the second most abundant metal (after Al) and the fourth most abundant element in the earth's crust (Cotton and Wilkinson, 1980). Iron oxides, including goethite, hematite, maghemite, and lepidocrocite, are only sparingly soluble in oxidizing waters; solubility increases as pH decreases and as the redox potential decreases (Nicholls, 1976). Fe(II) and Fe(III) are the main oxidation states in natural waters (Cotton and Wilkinson, 1980). In seawater, dissolved Fe^{3+} is strongly hydrolyzed, and $Fe(OH)_3^0$ is probably the dominant Fe(III) specie (Bruland et al., 1991). Although important, the colloidal fraction is not well-characterized; where resuspension occurs in the deep sea, rescavenging and removal to sediments probably prevent mixing back to surface waters (ibid.). Fe uptake in the oceans is enhanced by organic complexation (ibid.).

In natural waters, Fe may form soluble complexes with naturally occurring organic compounds; hydrous Fe-oxides can be very efficient scavengers for many trace metals (Burton and Liss, 1976). In laboratory experiments, the surface charge on suspended sediment particles is neutralized as Fe(III) is removed from solution; the likely

explanation is the formation of an Fe oxide-hydroxide surface coating (Aston, 1978). Hunter and Leonard (1988) found that riverine iron exists primarily as colloidal Fe(III) oxides stabilized by association with humic substances; during estuarine mixing, colloids are destabilized by high concentrations of seawater ions and aggregation occurs when particles collide. Observed behavior was shown to be highly dependent upon the history of freshwater/seawater mixing: the distance and timescales over which mixing occurs may have a significant effect on the aggregation and settling behavior. As an example, the authors noted that the fraction of Fe aggregated upon the addition of salt to riverine samples decreased the longer those samples had been stored prior to laboratory use; this finding also has implications for laboratory mixing studies of other elements that may be associated with river-borne particulate matter. Stability constants for dissolved Fe in seawater can be found in Motekaitis and Martell (1987) and Byrne et al.(1988).

Cobalt. In nature, Co always occurs in association with Ni and usually also with As (Cotton and Wilkinson, 1980). Co(II) and Co(III) are the most common oxidation states, and Co(II) is the most common in aqueous solutions (ibid.). In the Pacific, concentrations of 0.2 to 5 ppt have been observed (Bruland et al., 1991). Co is a central atom in the vitamin B_{12} and is involved in biological reactions, with uptake enhanced by organic complexation (ibid.). Co^{2+} complexes in seawater with various anions, including chloride, sulfate, and carbonate; stability constants are estimated in Byrne et al.(1988).

Nickel. In general, only Ni(II) is stable under ordinary conditions (Cotton and Wilkinson, 1980). In the oceans, Ni exhibits a nutrient-type distribution with observed concentrations ranging from 100 to 700 ppt; as an essential cofactor in the enzyme urease, it is involved in biological reactions (Bruland et al., 1991). Dissolved Ni was found to behave conservatively in the Merrimack estuary (Burton and Liss, 1976). Stability constants are estimated by both Motekaitis and Martell (1987) and Byrne et al. (1988), and Ni^{2+} shows a strong tendency to complexation with a variety of anions.

Copper. In addition to elemental copper, Cu(I) and Cu(II) exist and form compounds that are stable in aqueous solution; however, Cu(I) is readily oxidized to Cu(II), and Cu(II) is by far the most important oxidation state for Cu in aqueous solutions (Cotton and Wilkinson, 1980). Cu(III) is important biologically and is present in peptides and other compounds (ibid.). In the oceans, Cu exhibits a linear increase in concentration with depth; this behavior is the result of two processes: in-situ scavenging in deep waters and nutrient-type assimilation and regeneration (Bruland et al., 1991). Removal from riverine environments has been observed, and estuarine and near-shore anaerobic sediments may take up and retain Cu (Aston, 1978). Conservative behavior for dissolved Cu was observed in the Merrimack estuary (Burton and Liss, 1976). Estimates of stability constants are given by Motekaitis and Martell (1987) and by Byrne et al. (1988).

Zinc. Zn comprises about 10^{-6}% of the earth's crust and exists only in the +II oxidation state, in sharp contrast to the other elements of the first transition series (Cotton

and Wilkinson, 1980). Zn is important biologically, and a variety of zinc-containing proteins have been identified, most of them enzymes (ibid.). In the water column, biogenic uptake of Zn followed by transport to bottom sediments is counteracted by organic decomposition processes at the sediment surface, which return Zn to the water column (Aston, 1978). Nonetheless, net settling has been observed in freshwater environments (ibid.). Although Zn exists commonly in the +II oxidation state, it does form complexes that resemble those of the neighboring transition metals (Bruland, 1983). In seawater, Zn exists primarily as the free ion and a hydroxy-, carbonato-, and chloro-complexes (ibid.). The concentration of free Zn^{2+} in seawater ranges from 0.1 to 160 ppt, and the shape of the Zn concentration profile closely resembles that of H_4SiO_4, silicic acid (Bruland et al., 1991). Zn was observed to behave nearly conservatively in the estuary of Otago Harbor, New Zealand, where relationships between Zn and Si suggest a coupling between the rates of supply and uptake for these elements (Hunter and Tyler, 1987). Speciation of Zn in seawater can be estimated using stability constants provided by Motekaitis and Martell (1987) and by Byrne et al. (1988); in seawater, only about 60 to 75% of dissolved Zn is present as Zn^{2+}.

Elements of the second and third transition series. The second transition series includes yttrium, zirconium, niobium, molybdenum, ruthenium, palladium, and silver (Y, Zr, Nb, Mo, Ru, Pd, and Ag). The third transition series includes hafnium, tantalum, tungsten, rhenium, osmium, iridium, platinum, and gold (Hf, Ta, W, Re, Os, Ir, Pt, and

Au). Like Sc in the first transition series, Y is generally considered to have lanthanide-like chemistry and thus is considered separately. The aqua ions of the low and medium valence states are not well-defined or important for any of the heavier of these elements. For most, anionic oxo- and halo- complexes play an important role in the aqueous chemistry; some, such as a few of the platinum metals, do also form cationic complexes. The platinum metals (which include Ru, Os, Rh, Ir, Pd, and Pt) form complex compounds in aqueous solution, and the oxides of these metals are generally inert to aqueous acids (Cotton and Wilkinson, 1980); these metals are largely insoluble in aqueous solution and are present in very low concentrations (sub-ppt) in natural waters. Both Zr and Hf probably exist in the oceans as hydrolysis products; Nb and Ta probably exist in the +V oxidation state (Bruland, 1983). There is very little data available on the concentrations or behavior of these elements in natural waters, but behavior is not likely to be conservative. Mo is an interesting exception in this group of elements in that it exhibits conservative behavior in the oceans; its chemistry is discussed in greater detail below. W is largely unstudied, although concentrations in freshwaters tend to reflect anthropogenic influences, and it has a strong affinity for particles. Tc does not occur naturally, although it may be injected into the oceans as a waste product of the nuclear industry (Bruland, 1983). Re probably exists in the +VII oxidation state as the oxyanion ReO_4^- (ibid.). Both Ag and Au exist primarily in the +I oxidation state as $AgCl_2^-$ and $AuCl_2^-$ complexes (ibid.). Thermodynamic stability constants for the complexation of Ag with chloride can be found in Byrne et al., 1988. The distributions of these elements are largely unknown but are likely to be non-conservative and possibly nutrient-type.

Yttrium. The chemistry of Y is analogous to that of U in that the predominant species in seawater (98% at pH 8.2) is a carbonate complex, $Y(CO_3)_2^-$ (Byrne et al., 1988). Very little is know about its distribution within the oceans, but concentrations are in the 10 ppt range (Bruland, 1983). Concentrations in freshwaters are generally higher. At pH values lower than that of seawater, more complexation with anions other than carbonate probably occurs, and some Y is probably present as free ion (Byrne et al., 1988).

Molybdenum. Mo can exist in a variety of oxidation states, although in oxygenated natural waters, Mo(+VI) is predominant (Emerson and Huestad, 1991). In seawater, Mo is strongly hydrolyzed and is present as the molybdate anion, MoO_4^{2-}, at neutral pH (ibid.). In seawater, its distribution is conservative, and its high concentration (at 11 ppb, more than 10 times that of "average" river water) indicates a general lack of reactivity (ibid.; Bruland, 1983). Mo is a highly biologically active element that is involved in the functioning of nitrogenase enzymes (Cotton and Wilkinson, 1980), and biological cycling may affect its concentrations in low concentration environments.

Mo has been found to behave approximately conservatively in estuarine mixing in the Conway estuary, although some desorption from particulate matter may occur (Burton and Liss, 1976). Mo is often enriched in anoxic sediments (Burton and Liss, 1976), where it probably exists in the +V oxidation state as MoO_2^+ (Bruland, 1983; Emerson and Huestad, 1991). Mo was found in high concentrations (averaging 26 ppm) in anaerobic

sediments of the Saanich Inlet, B.C., and was below detection limits in aerobic sediments (Aston, 1978), which suggests that reduction may be important in removing dissolved Mo from the water column. Mo(IV) is likely coprecipitated with iron sulfides in strongly reducing environments, with complexation by organic matter in sediments likely (Emerson and Huestad, 1991). In shallow groundwater in the San Joaquin Valley, concentrations of Mo are high, and Mo is geochemically mobile and present as oxyanions (Deverel and Millard, 1988). High concentrations of Mo have been observed in the inlet waters to evaporation ponds in the San Joaquin Valley; surrounding soils derived from the marine sediments of the coast range are the most likely source, and V, Mo, and U all tend to be mobile with other salts in soil solution (Bradford et al., 1990).

Rare earth elements (REEs). These elements are also known as the lanthanides (denoted Ln) and include lanthanum, cerium, praseodymium, neodymium, samarium, europium, gadolinium, terbium, dysprosium, holmium, erbium, thulium, ytterbium, and lutetium (La, Ce, Pr, Nd, Sm, Eu, Gd, Tb, Dy, Ho, Er, Tm, Yb, and Lu). These elements are generally studied as a group rather than individually; the information presented here will be in this format, with exceptions noted.

All the REEs are highly electropositive, and the +III oxidation state is the primary oxidation state. All the lanthanides form +III ions in solution as aqua ions $[Ln(H_2O)_n]^{3+}$ (Cotton and Wilkinson, 1980). The predominant species in seawater are probably the carbonato- complex $Ln(CO_3)^+$, although some variable amounts of sulfato-, chloro-, and hydroxy- complexes should also be present along with small amounts of hydrated ion

(Bruland, 1983). The tendency to complexation with carbonate increases from the light to the heavy REEs (Sholkovitz et al., 1994). Because it can be oxidized to the +IV oxidation state, the chemistry and oceanic distribution of Ce is often anomalous. All the REEs except Ce increase in concentration with depth, a trend that is especially prominent for the heavier REEs (de Baar et al., 1985; Bruland, 1983). Ce, which is readily oxidized to the +IV state in ocean waters, is strongly depleted compared to the other REEs (de Baar et al., 1991; de Baar et al., 1985). In ocean waters, the REEs are strongly depleted in surface waters, with the light REEs preferentially adsorbed to particles over the heavy REEs (Sholkovitz et al., 1994; Erel and Stolper, 1993; de Baar et al., 1985). This is likely because the heavier REEs are stabilized by stronger inorganic complexation (de Baar et al., 1985) relative to the lighter REEs, particularly by stronger complexation with carbonate (Erel and Stolper, 1993).

The speciation and complexation of the REEs have also been extensively studied in river waters. Studies of river waters from the Connecticut, Hudson, and Mississippi Rivers by Sholkovitz (1995) showed that the concentration and fractionation of the REEs in river waters are highly pH dependent, with higher pH resulting in lower concentrations and greater fractionation; adsorption to particles is greater for the light REEs than for the heavy REEs as a result of increasing pH. Further, this study used ultrafiltration to determine that Fe-organic colloids are the major REE carriers of "dissolved" REEs. Field results indicated that the mixing of river waters with seawater induces coagulation and particle removal, with the light REEs preferentially removed over the heavy REEs; laboratory experiments showed that release of REEs can occur when river-borne particles

are leached with seawater. Goldstein and Jacobsen (1988a) found that rivers with high pH and alkalinity are likely enriched in the heavy REEs relative to source rocks; they observed estuarine removal of about 60% for the light REEs and about 40% for the heavy REEs for estuaries of both high and low river pH. Rivers studied included the Amazon, Indus, Mississippi, Murray-Darling, and Ohio. Observations by Hoyle et al. (1984) showed that in the organic-rich waters of the Luce river, the REEs were primarily associated with Fe-organic matter colloids that flocculated during mixing, while little REE removal occurred in organic-poor Kex Beck (a tributary to the River Wharfe in England). In the Great Whale River, which flows into Hudson Bay, removal was observed to occur primarily at very low salinities, less than 2‰ (Goldstein and Jacobsen, 1988b).

In laboratory studies, the REEs were found to sorb to both synthetic Fe-oxyhydroxides (α-FeOOH) and Mn-oxides (δ-MnO_2); REE sorption patterns on hydroxylapatite also suggest that the light to intermediate REEs may substitute for Ca^{2+} in the mineral lattice structure of this mineral (Koeppenkastrop and DeCarlo, 1992). Koeppenkastrop and DeCarlo (1993) found that carbonate complexation influences the uptake of the REEs by δ-MnO_2 more strongly than uptake by FeOOH. The stability constant of EDTA with the REEs increases with atomic number but is lower for La and Gd than for the rest of the REEs (de Baar et al., 1991). The same observations are made for the formation constants for 15 monocarboxylic acids with these elements by Byrne and Kim (1990), who found that the affinity of REEs for surfaces is affected strongly by thin organic surface coatings. Sequential digestion of suspended particles collected from

the Sargasso Sea also indicated that surface coatings are responsible for the removal and fractionation of the REEs from seawater, as detrital phases had REE compositions typical of crustal materials (Sholkovitz et al., 1994). Particularly when phosphate concentrations are high, the solubility of the REEs in seawater may be limited by the formation of REE-phosphate coprecipitates, as the lanthanide-phosphate phases have very low solubility products (Byrne and Kim, 1993). Stability constants for the formation of REE-anion and REE-cation complexes can be found in Millero (1992).

Actinides. The actinides include the heaviest of elements. All are radioactive, with only two (thorium and uranium, Th and U) having longer half-lives and playing important role in aqueous solution.

Thorium. Th is widely distributed in nature but is present in very low concentrations in natural waters due to its low solubility. In aqueous solution, Th is hydrolyzed, forming Th(OH) complexes (Byrne et al., 1988). Th is largely transported in insoluble resistate minerals or adsorbed to the surfaces of clay minerals (Gascoyne, 1992). Because of its rapid removal (mainly via particle scavenging), Th is not expected to behave conservatively.

Uranium. U is remarkably common in natural waters. Estimates of speciation in saline waters show that U is strongly hydrolyzed and present primarily as carbonato-complexes; at the salinity of ocean water, approximately 7.1% of dissolved U is present

as $UO_2(CO_3)_2^{2-}$, while the remaining 92.9% is present as $UO_2(CO_3)_3^{4-}$ (van den Berg, 1991). At 0‰ salinity, 78.1% is present as $UO_2(CO_3)_2^{2-}$ and 21.8% as $UO_2(CO_3)_3^{4-}$ (ibid.). U occurs as stable anionic complexes of cations and is not readily complexed by organic matter (ibid.). U is generally removed from solution in reducing environments (where it converts from the soluble +VI oxidation state to the highly insoluble +IV oxidation state) and can also adsorb to iron hydroxides that are removed by flocculation in estuaries (ibid). U may also be removed on phosphate particles in waters containing high concentrations of phosphates (Somayajulu, 1994). Estimates of stability constants of U with inorganic ions in seawater can be found in van den Berg (1993), Byrne et al. (1988), and Motekaitis and Martell (1987).

U behaves conservatively in a number of estuaries, including: the Clyde and Tamar (Toole et al., 1987); the Narbada, Tapti, and Godavari (Borole et al., 1977); the Baltic Sea, where it remains oxic (Löfvendahl, 1987), and the Mahanadi (Ray et al., 1995). U behaves non-conservatively in a number of estuaries, generally where conditions become reducing (such as in mangrove swamps), where dissolved oxygen is seasonally depleted in the water column, or where phosphate concentrations are extremely high due to the discharge of untreated sewage. These estuaries include: the Tamar (van den Berg, 1991); the Forth (Toole et al., 1987); the Ogeechee and Savannah River and the Amazon estuary (Cochran, 1992); Delaware and Chesapeake Bay (Sarin and Church, 1994); the Hooghly (Somayajulu, 1994); the Fenland catchment (Plater et al., 1992); and the Ganges-Brahmaputra (Carroll and Moore, 1993). The distribution in the

oceans is likely to be conservative with an average concentration of about 3.2 to 3.3 ppb (higher than average river water).

Additional studies have shown that particles and colloids played only a minor role for the transport of U in an aquifer hydraulically connected to the River Glatt in Switzerland, and the formation of phosphate and organic complexes was negligible (Lienert et al., 1994). In the Amazon River, up to 92% of dissolved U is associated with colloids, with removal likely as Fe-oxyhydroxides precipitate (Swarzenski et al., 1995). U is often concentrated in petroleum and associated brines; in evaporation pond waters in the San Joaquin Valley, concentrations of U can be as high as 9.90 mgl^{-1} (Bradford et al., 1990). Surrounding soils derived from marine sediments are the likely source, as U tends to be mobile with other salts in solution in this valley (ibid.).

Appendix B

ICP-MS Interferences

ICP-MS Interferences

Mass	Element		Hydride		Oxide		Argide	Dimer and M^{2+}		Chloride
1	H	99.985						H^{2+}	0.015	
2	H	0.015	HH	99.970				HH	99.970	
								He^{2+}	100.00	
3	He	0.0001	HH	0.030				HH	0.030	
4	He	99.999								
5			HeH	99.985						
6	Li	7.42	HeH	0.015						
7	**Li**	92.58	LiH	7.499						
8			LiH	92.487				HeHe	100	
9	**Be**	100	LiH	0.014						
10	B	19.78	BeH	99.985				Ne^{2+}	90.480	
11	**B**	80.22	BeH	0.015				Ne^{2+}	9.250	
			BH	19.897						
12	C	98.89	BH	80.091				LiLi	0.563	
13	C	1.11	BH	0.012				LiLi	13.875	
			CH	98.885						
14	N	99.63	CH	1.115				LiLi	85.563	
15	N	0.37	NH	99.619						
16	O	99.759	NH	0.381						
17	O	0.037	OH	99.747	HO	99.747				
18	O	0.204	OH	0.053	HO	0.053		BeBe	100	
								Ar^{2+}	0.337	
19	F	100	OH	0.200	HO	0.200		Ar^{2+}	0.063	
20	Ne	90.92	FH	99.985	HeO	99.762		BB	3.960	
								Ar^{2+}	99.600	
								Ca^{2+}	96.941	
21	Ne	0.257	FH	0.015	HeO	0.038		BB	31.880	
			NeH	90.466				Ca^{2+}	0.647	
22	Ne	8.82	NeH	0.284	HeO	0.200		BB	64.160	
					LiO	7.482		Ca^{2+}	2.086	
23	**Na**	100	NeH	9.249	LiO	92.283		Ti^{2+}	8.000	
24	**Mg**	78.7	NaH	99.985	LiO	0.050		CC	97.812	
								Ca^{2+}	0.187	
								Ti^{2+}	73.800	
25	Mg	10.13	NaH	0.015	LiO	0.185		CC	2.176	
			MgH	78.978	BeO	99.762		Ti^{2+}	5.400	
								V^{2+}	0.250	
26	Mg	11.17	MgH	10.010	BeO	0.038		CC	0.012	
					BO	19.853				
27	**Al**	100	MgH	11.010	BeO	0.200		Fe^{2+}	5.800	
					BO	79.917				
28	Si	92.21	AlH	99.985	BO	0.070		NN	99.269	
					CO	98.665		Fe^{2+}	91.720	
29	**Si**	4.7	AlH	0.015	BO	0.160		NN	0.729	
			SiH	92.216	CO	1.135		Fe^{2+}	0.280	
								Ni^{2+}	68.077	
30	Si	3.09	SiH	4.683	CO	0.198		Ni^{2+}	26.223	

Masses used for analysis and species for which corrections were made are shown in boldface.

ICP-MS Interferences

Mass	Element		Hydride		Oxide		Argide		Dimer and M^{2+}		Chloride	
					NO	99.397						
31	P	100	SiH	3.100	NO	0.403			Ni^{2+}	3.634		
32	S	95	PH	99.985	NO	0.199			OO	99.525		
					OO	99.525			Ni^{2+}	0.926		
33	S	0.76	PH	0.015	OO	0.076			OO	0.076		
			SH	95.006								
34	S	4.22	SH	0.764	OO	0.399			OO	0.399		
35	Cl	75.53	SH	4.209	FO	99.762						
36	S	0.014	ClH	75.759	FO	0.038					HCl	75.759
	Ar	0.337			NeO	90.265						
37	Cl	24.47	SH	0.020	FO	0.200	HAr	0.337			HCl	0.011
			ClH	0.011	NeO	0.304						
			ArH	0.337								
38	Ar	0.063	ClH	24.226	NeO	9.409			FF	100	HCl	24.226
39	K	93.1	ArH	0.063	NaO	99.762	HAr	0.063			HeCl	75.77
40	K	0.00118	KH	93.244	NeO	0.019	HeAr	0.337	NeNe	81.866		
	Ca	96.97			NaO	0.038						
	Ar	99.6			MgO	78.802						
41	K	6.88	ArH	99.585	NaO	0.200	HAr	99.585	NeNe	0.489	HeCl	24.23
			KH	0.026	MgO	10.006					LiCl	5.683
			CaH	96.926								
42	Ca	0.64	ArH	0.015	MgO	11.146	HAr	0.015	NeNe	16.740	LiCl	70.087
			KH	6.729			HeAr	0.063	Sr^{2+}	0.560		
			CaH	0.015			LiAr	0.025				
43	Ca	0.145	CaH	0.647	MgO	0.024	LiAr	0.312	NeNe	0.050	LiCl	1.817
					AlO	99.762			Sr^{2+}	9.860		
44	Ca	2.06	CaH	0.135	MgO	0.022	HeAr	99.600	NeNe	0.856	LiCl	22.413
					AlO	0.038			Sr^{2+}	82.580	BeCl	75.77
					SiO	92.010						
45	Sc	100	CaH	2.086	AlO	0.200	LiAr	0.058	Zr^{2+}	51.450	BCl	15.078
					SiO	4.694	BeAr	0.337				
46	Ti	7.93	ScH	99.985	SiO	3.279	LiAr	7.470	NaNa	100	BeCl	24.23
	Ca	0.0033					BAr	0.067	Zr^{2+}	17.150	BCl	60.692
									Mo^{2+}	14.840		
47	Ti	7.28	ScH	0.015	SiO	0.011	LiAr	92.130	Zr^{2+}	17.380	BCl	4.822
			TiH	7.999	PO	99.762	BeAr	0.063	Mo^{2+}	9.250	CCl	74.937
							BAr	0.270				
48	Ti	73.94	TiH	7.300	PO	0.038	BAr	0.013	MgMg	62.394	BCl	19.408
	Ca	0.18			SO	94.794	CAr	0.333	Zr^{2+}	2.800	CCl	0.833
									Mo^{2+}	16.680		
									Ru^{2+}	5.520		
49	Ti	5.51	CaH	0.187	PO	0.200	BeAr	99.600	MgMg	15.798	CCl	23.963
			TiH	73.790	SO	0.784	BAr	0.050	Mo^{2+}	24.130	NCl	75.493
									Ru^{2+}	1.880		
50	Ti	5.34	TiH	5.510	SO	4.390	BAr	19.820	MgMg	18.394	CCl	0.267
	V	0.24					CAr	0.062	Mo^{2+}	9.630	NCl	0.277
	Cr	4.31					NAr	0.336	Ru^{2+}	12.600		

Masses used for analysis and species for which corrections were made are shown in boldface.

ICP-MS Interferences

Mass	Element		Hydride		Oxide		Argide		Dimer and M^{2+}		Chloride	
51	V	99.76	TiH	5.400	ClO	75.590	BAr	79.780	MgMg	2.202	NCl	24.141
			VH	0.250					Ru^{2+}	31.600	OCl	75.59
			CrH	4.344					Pd^{2+}	1.021		
52	Cr	83.76	VH	99.735	SO	0.028	CAr	98.504	MgMg	1.212	NCl	0.089
					ClO	0.029	NAr	0.063	Ru^{2+}	18.700	OCl	0.029
					ArO	0.336	OAr	0.336	Pd^{2+}	11.151		
53	Cr	9.55	VH	0.015	ClO	24.324	CAr	1.096	Pd^{2+}	27.357	OCl	24.324
			CrH	83.766					Cd^{2+}	1.250		
54	Fe	5.82	CrH	9.512	ArO	0.064	NAr	99.235	AlAl	100	FCl	75.77
	Cr	2.38					OAr	0.064	Pd^{2+}	26.486		
									Cd^{2+}	0.890		
55	Mn	100	CrH	2.366	ClO	0.048	NAr	0.365	Pd^{2+}	11.732	OCl	0.048
			FeH	5.799	KO	93.036	FAr	0.337	Cd^{2+}	12.490	NeCl	68.557
56	Fe	91.66	MnH	99.985	ArO	99.363	OAr	99.363	SiSi	85.064	FCl	24.23
					KO	0.047	NeAr	0.305	Cd^{2+}	24.130	NeCl	0.205
					CaO	96.710			Sn^{2+}	0.970		
57	Fe	2.19	MnH	0.015	ArO	0.038	FAr	0.063	SiSi	8.614	NeCl	28.932
			FeH	91.706	KO	6.901	OAr	0.038	Cd^{2+}	28.730		
					CaO	0.037			Sn^{2+}	0.650		
58	Fe	0.33	FeH	2.213	ArO	0.199	OAr	0.199	SiSi	5.936	NeCl	0.065
	Ni	67.84			CaO	0.839	NeAr	0.088	Cd^{2+}	7.490	NaCl	75.77
									Sn^{2+}	14.530		
59	Co	100	FeH	0.280	KO	0.013	FAr	99.600	SiSi	0.290	NeCl	2.241
			NiH	68.067	CaO	0.135	NaAr	0.337	Sn^{2+}	24.230	MgCl	59.851
60	Ni	26.23	CoH	99.985	CaO	2.082	NeAr	90.124	SiSi	0.096	NaCl	24.23
			NiH	0.010			MgAr	0.266	Sn^{2+}	32.590	MgCl	7.577
									Te^{2+}	0.096		
61	Ni	1.19	CoH	0.015	ScO	99.762	NeAr	0.269	Sn^{2+}	4.630	MgCl	27.482
			NiH	26.219			NaAr	0.063	Te^{2+}	2.603		
							MgAr	0.034				
62	Ni	3.66	NiH	1.144	ScO	0.038	NeAr	9.213	PP	100	MgCl	2.423
					TiO	7.981	MgAr	0.087	Sn^{2+}	5.790	AlCl	75.77
									Te^{2+}	4.816		
									Xe^{2+}	0.100		
63	Cu	69.09	NiH	3.634	ScO	0.200	NaAr	99.600	Te^{2+}	18.950	MgCl	2.668
					TiO	7.286	AlAr	0.337	Xe^{2+}	0.090	SiCl	69.883
64	Zn	48.89	CuH	69.160	CaO	0.187	MgAr	78.681	SS	90.288	AlCl	24.23
	Ni	1.08			TiO	73.643	SiAr	0.311	Te^{2+}	31.689	SiCl	3.538
									Xe^{2+}	1.910		
65	Cu	30.91	NiH	0.926	TiO	5.530	MgAr	9.960	SS	1.425	SiCl	24.696
			CuH	0.010			AlAr	0.063	Te^{2+}	33.799		
			ZnH	48.593			SiAr	0.016	Xe^{2+}	4.100		
									Ba^{2+}	0.106		
66	Zn	27.81	CuH	30.825	TiO	5.537	MgAr	10.966	SS	8.006	SiCl	1.132
					VO	0.249	SiAr	0.069	Xe^{2+}	26.900	PCl	75.77
					CrO	4.335			Ba^{2+}	0.101		
67	Zn	4.11	ZnH	27.896	TiO	0.013	AlAr	99.600	SS	0.063	SiCl	0.751
					VO	99.513	PAr	0.337	Xe^{2+}	10.400	SCl	71.997

Masses used for analysis and species for which corrections were made are shown in boldface.

ICP-MS Interferences

Mass	Element		Hydride		Oxide		Argide		Dimer and M^{2+}		Chloride	
									Ba^{2+}	2.417		
68	Zn	18.57	ZnH	4.104	TiO	0.011	SiAr	91.863	SS	0.215	PCl	24.23
					VO	0.038	SAr	0.320	Xe^{2+}	8.900	SCl	0.568
					CrO	83.598			Ba^{2+}	7.854		
									Ce^{2+}	0.190		
69	**Ga**	60.4	ZnH	18.798	VO	0.200	SiAr	4.651	Ba^{2+}	71.700	SCl	26.213
					CrO	9.510	PAr	0.063	La^{2+}	0.090		
									Ce^{2+}	0.250		
70	Ge	20.52	GaH	60.099	CrO	2.531	SiAr	3.088	ClCl	57.411	SCl	0.182
	Zn	0.62			FeO	5.786	SAr	0.074	Ce^{2+}	88.480	ClCl	57.411
71	Ga	39.6	ZnH	0.600	CrO	0.020	PAr	99.600	Ce^{2+}	11.080	SCl	1.035
			GeH	21.227	MnO	99.762	ClAr	0.255	Nd^{2+}	27.130	ArCl	0.255
72	Ge	27.43	GaH	39.886	MnO	0.038	SAr	94.643	ClCl	36.718	ClCl	36.718
					FeO	91.513			Nd^{2+}	23.800		
									Sm^{2+}	3.100		
73	Ge	7.76	GeH	27.656	MnO	0.200	SAr	0.747	Nd^{2+}	17.190	ArCl	0.129
					FeO	2.230	ClAr	0.129				
74	Ge	36.54	GeH	7.733	FeO	0.464	SAr	4.193	ClCl	5.871	ClCl	5.871
	Se	0.87			NiO	67.915			Nd^{2+}	5.760	KCl	70.662
									Sm^{2+}	11.300		
75	**As**	100	GeH	35.936	CoO	99.762	**ClAr**	75.482	Nd^{2+}	5.640	**ArCl**	75.482
			SeH	0.890	NiO	0.026	KAr	0.314	Sm^{2+}	7.400	**CaCl**	73.452
76	Ge	7.76	AsH	99.985	CoO	0.038	SAr	0.020	ArAr	0.671	KCl	27.696
	Se	9.02			NiO	26.297	ArAr	0.671	Sm^{2+}	26.700		
							CaAr	0.327	Gd^{2+}	0.200		
77	Se	7.58	GeH	7.439	CoO	0.200	ClAr	24.133	Sm^{2+}	22.700	ArCl	24.133
			AsH	0.015	NiO	1.147	KAr	0.081	Gd^{2+}	2.180	CaCl	23.979
			SeH	9.359								
78	Kr	0.35	SeH	7.630	NiO	3.678	ArAr	0.125	ArAr	0.125	KCl	1.631
	Se	23.52					CaAr	0.063	KK	86.971	CaCl	0.102
									Gd^{2+}	20.470		
									Dy^{2+}	0.060		
79	Br	50.54	SeH	23.778	CuO	69.005	KAr	92.889	KK	0.022	CaCl	1.737
			KrH	0.350					Gd^{2+}	24.840		
									Dy^{2+}	0.100		
80	Kr	2.27	BrH	50.682	NiO	0.931	ArAr	99.202	ArAr	99.202	CaCl	0.033
	Se	49.82			CuO	0.026	KAr	0.012	KK	12.553	ScCl	75.77
					ZnO	48.484	CaAr	96.561	CaCa	93.976		
									Gd^{2+}	21.860		
									Dy^{2+}	2.340		
81	**Br**	49.46	SeH	49.603	CuO	30.895	KAr	6.703	Dy^{2+}	25.500	CaCl	0.508
			KrH	2.250	ZnO	0.018	ScAr	0.337	Er^{2+}	0.140	TiCl	6.062
82	Kr	11.56	BrH	49.303	CuO	0.012	CaAr	0.646	KK	0.453	ScCl	24.23
	Se	9.19			ZnO	27.931	TiAr	0.027	CaCa	1.254	TiCl	5.531
									Dy^{2+}	28.200		
									Er^{2+}	1.610		
83	Kr	11.55	SeH	8.729	CuO	0.062	CaAr	0.134	CaCa	0.262	CaCl	0.143
			KrH	11.598	ZnO	4.101	ScAr	0.063	Er^{2+}	33.600	TiCl	57.857

Masses used for analysis and species for which corrections were made are shown in boldface.

ICP-MS Interferences

Mass	Element		Hydride		Oxide		Argide		Dimer and M^{2+}		Chloride	
							TiAr	0.025				
84	Kr	56.9	KrH	11.500	ZnO	18.813	CaAr	2.078	CaCa	4.049	TiCl	5.936
	Sr	0.56					TiAr	0.254	Er^{2+}	26.800		
									Yb^{2+}	0.130		
85	**Rb**	72.15	KrH	56.993	ZnO	0.015	ScAr	99.600	Er^{2+}	14.900	CaCl	0.045
			SrH	0.560	GaO	59.965	TiAr	0.023	Yb^{2+}	3.050	TiCl	21.973
											VCl	0.189
											CrCl	3.292
86	Kr	17.37	RbH	72.154	ZnO	0.636	TiAr	8.033	CaCa	0.035	TiCl	1.333
	Sr	9.86			GaO	0.023	CrAr	0.015	Yb^{2+}	21.900	VCl	75.581
					GeO	21.179						
87	**Sr**	7.02	KrH	17.297	GaO	39.917	TiAr	7.274	Yb^{2+}	31.800	TiCl	1.308
	Rb	27.85	RbH	0.011			VAr	0.336	Hf^{2+}	0.162	VCl	0.061
			SrH	9.859							CrCl	64.54
88	Sr	82.56	RbH	27.831	GaO	0.015	CaAr	0.186	CaCa	0.406	VCl	24.169
			SrH	7.000	GeO	27.637	TiAr	73.508	Yb^{2+}	12.700	CrCl	7.199
							CrAr	0.285	Lu^{2+}	2.590		
									Hf^{2+}	5.206		
89	**Y**	100	SrH	82.569	GaO	0.080	TiAr	5.478	Hf^{2+}	27.297	CrCl	22.094
					GeO	7.722	VAr	0.063			FeCl	4.395
							CrAr	0.032				
90	Zr	51.46	SrH	0.012	GeO	35.913	TiAr	5.378	ScSc	100	CrCl	2.302
			YH	99.985	SeO	0.888	VAr	0.249	Hf^{2+}	35.100	MnCl	75.77
							CrAr	4.388	Ta^{2+}	0.012		
							FeAr	0.020	W^{2+}	0.130		
91	Zr	11.23	YH	0.015	GeO	0.029	VAr	99.351	W^{2+}	26.300	CrCl	0.573
			ZrH	51.442	AsO	99.762	MnAr	0.337			FeCl	70.902
92	Zr	17.11	ZrH	11.226	GeO	7.494	CrAr	83.455	TiTi	0.640	MnCl	24.23
	Mo	15.84			AsO	0.038	FeAr	0.313	W^{2+}	30.670	FeCl	1.667
					SeO	9.340			Os^{2+}	0.020		
93	Nb	100	ZrH	17.149	AsO	0.200	CrAr	9.463	TiTi	1.168	FeCl	22.436
			MoH	14.838	SeO	7.615	MnAr	0.063	W^{2+}	28.600	NiCl	51.582
									Os^{2+}	1.580		
94	Zr	17.4	NbH	99.985	GeO	0.015	CrAr	2.356	TiTi	12.341	FeCl	0.533
	Mo	9.04			SeO	23.745	FeAr	5.836	Os^{2+}	13.300	CoCl	75.77
					KrO	0.349	NiAr	0.229				
95	Mo	15.72	ZrH	17.377	SeO	0.024	MnAr	99.600	TiTi	11.655	FeCl	0.068
			NbH	0.015	BrO	50.569	CoAr	0.337	Os^{2+}	26.400	NiCl	36.364
			MoH	9.249					Pt^{2+}	0.010		
96	Zr	2.8	MoH	15.919	SeO	49.539	FeAr	91.353	TiTi	56.131	CoCl	24.23
	Mo	16.53			BrO	0.019	CoAr	0.131	Os^{2+}	41.000	NiCl	0.864
	Ru	5.51			KrO	2.245			Pt^{2+}	0.790		
97	Mo	9.46	ZrH	2.800	SeO	0.019	FeAr	2.191	TiTi	8.906	NiCl	9.107
			MoH	16.680	BrO	49.294	CoAr	0.063	Pt^{2+}	32.900		
			RuH	5.519								
98	**Mo**	23.78	MoH	9.551	SeO	8.808	FeAr	0.279	TiTi	8.273	NiCl	0.276
	Ru	1.87			BrO	0.019	CoAr	67.833	Pt^{2+}	25.300	CuCl	52.41
					KrO	11.577			Hg^{2+}	0.150		

Masses used for analysis and species for which corrections were made are shown in boldface.

ICP-MS Interferences

Mass	Element		Hydride		Oxide		Argide		Dimer and M^{2+}		Chloride	
99	Ru	12.72	MoH	24.128	BrO	0.099	CoAr	99.600	TiTi	0.594	NiCl	1.582
			RuH	1.880	KrO	11.477	CuAr	0.233	Pt^{2+}	7.200	ZnCl	36.824
									Hg^{2+}	9.970		
100	Mo	9.63	TcH	99.985	SeO	0.017	CoAr	26.124	TiTi	0.292	CuCl	40.12
	Ru	12.62	RuH	12.698	KrO	56.892	ZnAr	0.164	CrCr	0.189		
					SrO	0.559			Hg^{2+}	23.100		
101	Ru	17.07	MoH	9.629	KrO	0.045	CoAr	1.135	VV	0.499	NiCl	0.224
			TcH	0.015	RbO	71.993	CuAr	0.147	Hg^{2+}	29.860	ZnCl	32.916
			RuH	12.600								
102	Pd	0.96	RuH	16.999	KrO	17.373	CoAr	3.620	VV	99.501	CuCl	7.47
	Ru	31.61			RbO	0.027	ZnAr	0.125	CrCr	7.281	ZnCl	3.107
					SrO	9.838			Hg^{2+}	6.870		
									Pb^{2+}	1.400		
103	Rh	100	RuH	31.598	RbO	27.913	CuAr	68.913	CrCr	0.826	ZnCl	21.005
			PdH	1.021	SrO	6.987	ZnAr	0.014	Pb^{2+}	24.100		
104	Pd	10.97	RhH	99.985	KrO	0.035	CoAr	0.922	CrCr	70.411	ZnCl	0.993
	Ru	18.58			RbO	0.011	ZnAr	48.487	Pb^{2+}	52.400	GaCl	45.544
					SrO	82.406						
105	Pd	22.23	RuH	18.697	RbO	0.056	CuAr	30.707	CrCr	15.922	ZnCl	5.01
			RhH	0.015	SrO	0.045	GaAr	0.203			GeCl	16.086
			PdH	11.149	YO	99.762						
106	Pd	27.33	PdH	22.251	SrO	0.165	ZnAr	27.802	CrCr	4.866	GaCl	44.79
	Cd	1.22			YO	0.038	GeAr	0.072				
					ZrO	51.328						
107	Ag	51.82	PdH	27.357	YO	0.200	ZnAr	4.084	CrCr	0.449	ZnCl	0.145
			CdH	1.250	ZrO	11.213	GaAr	0.172			GeCl	26.102
108	Pd	26.71	AgH	51.831	ZrO	17.216	ZnAr	18.725	CrCr	0.056	GaCl	9.666
	Cd	0.88			MoO	14.805	GeAr	0.107	FeFe	0.336	GeCl	5.857
109	Ag	48.18	PdH	26.483	ZrO	0.029	GaAr	59.893			GeCl	33.934
			CdH	0.890	NbO	99.762	GeAr	0.026			SeCl	0.674
110	Pd	11.81	AgH	48.154	ZrO	17.373	ZnAr	0.598	MnMn	100	GeCl	1.873
	Cd	12.39			NbO	0.038	GeAr	21.284	FeFe	10.640	AsCl	75.77
					MoO	9.258						
111	**Cd**	12.75	PdH	11.730	NbO	0.200	GaAr	39.372	FeFe	0.255	GeCl	14.346
			CdH	12.488	MoO	15.886	AsAr	0.337			SeCl	7.308
112	Sn	0.96	CdH	12.800	ZrO	2.828	GeAr	27.597	FeFe	84.158	AsCl	24.23
	Cd	24.07			MoO	16.665	SeAr	0.032			SeCl	5.781
					RuO	5.507						
113	Cd	12.26	CdH	24.128	MoO	9.565	GeAr	7.699	FeFe	4.036	GeCl	1.803
	In	4.28	SnH	0.970			AsAr	0.063			SeCl	20.286
							SeAr	0.026			KrCl	0.265
114	Sn	0.66	CdH	12.222	MoO	24.110	GeAr	35.801	FeFe	0.562	SeCl	1.849
	Cd	28.86	InH	4.299	RuO	1.887	AsAr	0.972			BrCl	38.408
115	Sn	0.35	CdH	28.728	MoO	0.028	AsAr	99.600	FeFe	0.012	SeCl	43.351
	In	95.72	SnH	0.650	TcO	99.762	BrAr	0.171			KrCl	1.79
					RuO	12.670						
116	Sn	14.3	InH	95.686	MoO	9.655	GeAr	7.410	NiNi	46.345	BrCl	49.664
	Cd	7.58	SnH	0.340	TcO	0.038	AsAr	9.505	Th^{2+}	100.00		

Masses used for analysis and species for which corrections were made are shown in boldface.

ICP-MS Interferences

Mass	Element		Hydride		Oxide		Argide		Dimer and M^{2+}		Chloride	
					RuO	12.579						
117	Sn	7.61	CdH	7.489	TcO	0.200	AsAr	7.599			SeCl	18.635
			InH	0.014	RuO	16.990	BrAr	0.198			KrCl	9.334
			SnH	14.528								
118	Sn	24.03	SnH	7.681	MoO	0.019	AsAr	23.746	CoCo	100	BrCl	11.948
					RuO	31.556	KrAr	0.389	NiNi	35.704	KrCl	8.714
					PdO	1.019						
119	Sn	8.58	SnH	24.228	RuO	0.046	BrAr	50.518	NiNi	1.552	SeCl	2.115
					RhO	99.762	KrAr	0.039	U^{2+}	99.274	KrCl	46
											SrCl	0.424
120	Sn	32.85	SnH	8.592	RuO	18.719	AsAr	49.417	NiNi	11.824	KrCl	2.786
	Te	0.089			RhO	0.038	KrAr	2.440			RbCl	54.679
					PdO	11.127						
121	**Sb**	57.25	SnH	32.586	RhO	0.200	BrAr	49.113	NiNi	0.598	KrCl	26.919
			TeH	0.096	PdO	22.204	RbAr	0.243			SrCl	7.607
122	Sn	4.72	SbH	57.351	RuO	0.037	AsAr	8.695	NiNi	3.180	RbCl	38.576
	Te	2.46			PdO	27.323	KrAr	11.648			SrCl	5.304
					CdO	1.247	SrAr	0.034				
123	Te	0.87	SnH	4.629	PdO	0.055	KrAr	11.454	NiNi	0.083	KrCl	4.192
	Sb	42.75	TeH	2.603	AgO	51.716	RbAr	0.139			SrCl	64.96
							SrAr	0.024				
124	Sn	5.94	SbH	42.634	PdO	26.478	KrAr	56.783	NiNi	0.618	RbCl	6.744
	Te	4.61	TeH	0.908	AgO	0.020	SrAr	0.842			SrCl	1.696
	Xe	0.096			CdO	0.890					YCl	75.77
125	Te	6.99	SnH	5.789	PdO	0.010	RbAr	71.894	NiNi	0.021	SrCl	20.009
			TeH	4.815	AgO	48.150	YAr	0.337			ZrCl	29.984
			XeH	0.100								
126	Te	18.71	TeH	7.139	PdO	11.757	KrAr	17.231	NiNi	0.067	YCl	24.23
	Xe	0.09			AgO	0.018	SrAr	9.873	CuCu	47.845	ZrCl	8.501
					CdO	12.462	ZrAr	0.173				
127	I	100	TeH	18.948	AgO	0.096	RbAr	27.724			ZrCl	25.461
			XeH	0.090	CdO	12.774	SrAr	6.972			MoCl	11.244
							YAr	0.063				
							ZrAr	0.038				
128	Te	31.79	IH	99.985	PdO	0.023	SrAr	82.250	CuCu	42.650	ZrCl	2.719
	Xe	1.92			CdO	24.102	ZrAr	0.090	ZnZn	23.620	NbCl	75.77
					SnO	0.968	MoAr	0.050				
129	Xe	26.44	TeH	31.685	CdO	12.226	YAr	99.600			ZrCl	17.324
			IH	0.015	InO	4.290	NbAr	0.337			MoCl	10.604
			XeH	1.910								
130	Ba	0.101	XeH	26.396	CdO	28.715	ZrAr	51.314	CuCu	9.505	NbCl	24.23
	Te	34.48			SnO	0.650			ZnZn	27.119	MoCl	12.063
	Xe	4.08										
131	Xe	21.18	TeH	33.794	CdO	0.035	ZrAr	11.175	ZnZn	3.985	ZrCl	6.333
			XeH	4.103	InO	95.481	NbAr	0.063			MoCl	14.88
			BaH	0.106	SnO	0.339	MoAr	0.054			RuCl	4.183
132	Ba	0.097	XeH	21.197	CdO	7.530	ZrAr	17.102	ZnZn	26.058	MoCl	11.093
	Xe	26.89			InO	0.036	MoAr	14.843				

Masses used for analysis and species for which corrections were made are shown in boldface.

ICP-MS Interferences

Mass	Element		Hydride		Oxide		Argide		Dimer and M^{2+}		Chloride	
					SnO	14.497	RuAr	0.019				
133	Cs	100	XeH	26.899	**InO**	0.191	NbAr	99.600	ZnZn	2.288	ZrCl	0.678
			BaH	0.101	SnO	7.668	MoAr	0.042			MoCl	22.325
											RuCl	2.762
134	Ba	2.42	CsH	99.985	CdO	0.015	ZrAr	17.312	ZnZn	11.242	MoCl	2.314
	Xe	10.44			SnO	24.204	MoAr	9.305			TcCl	75.77
											RuCl	9.623
135	Ba	6.59	XeH	10.398	SnO	8.594	MoAr	15.862	ZnZn	1.542	MoCl	13.143
			CsH	0.015			TcAr	0.337			RuCl	10.003
			BaH	2.417			RuAr	0.043				
136	Ba	7.81	BaH	6.591	SnO	32.564	ZrAr	2.789	ZnZn	3.869	TcCl	24.23
	Ce	0.193			TeO	0.096	MoAr	16.661			RuCl	15.958
	Xe	8.87					RuAr	5.542				
137	**Ba**	11.32	XeH	8.899	SbO	57.223	MoAr	9.512	ZnZn	0.049	MoCl	2.333
			BaH	7.854			TcAr	0.063			RuCl	26.996
			CeH	0.190			RuAr	0.065			PdCl	0.774
138	Ba	71.66	BaH	11.229	SnO	4.684	MoAr	24.040	ZnZn	0.226	RuCl	4.119
	Ce	0.25			SbO	0.022	RuAr	1.987	GaGa	36.130	RhCl	75.77
	La	0.089			TeO	2.597						
139	**La**	99.911	BaH	71.691	SbO	42.653	TcAr	99.600			RuCl	21.826
			LaH	0.090	TeO	0.907	RuAr	12.660			PdCl	8.697
			CeH	0.250			RhAr	0.337				
140	Ce	88.48	BaH	0.011	SnO	5.785	MoAr	9.591	GaGa	47.957	RhCl	24.23
			LaH	99.895	SbO	0.016	RuAr	12.633	GeGe	4.507	PdCl	16.861
					TeO	4.810	PdAr	0.038				
					XeO	0.100						
141	**Pr**	100	LaH	0.015	SbO	0.085	RuAr	16.932			RuCl	4.531
			CeH	88.467	TeO	7.126	RhAr	0.063			PdCl	23.431
							PdAr	0.075			CdCl	0.947
142	Nd	27.11	CeH	0.013	TeO	18.917	RuAr	31.485	GaGa	15.914	PdCl	5.392
	Ce	11.07	PrH	99.985	XeO	0.090	PdAr	1.116	GeGe	11.744	AgCl	39.278
143	Nd	12.17	CeH	11.078	TeO	0.021	RhAr	99.600	GeGe	3.282	PdCl	26.697
			PrH	0.015	IO	99.762	PdAr	0.014			CdCl	0.977
			NdH	27.156			AgAr	0.175				
144	Nd	23.85	NdH	12.182	TeO	31.652	RuAr	18.625	GeGe	22.911	AgCl	49.052
	Sm	3.09			IO	0.038	PdAr	11.213				
					XeO	1.906						
145	Nd	8.3	NdH	23.798	IO	0.200	PdAr	22.163	GeGe	4.276	PdCl	15.307
			SmH	3.100	XeO	26.338	AgAr	0.195			CdCl	9.679
146	**Nd**	17.62	NdH	8.302	TeO	33.782	PdAr	27.304	GeGe	23.639	AgCl	11.669
					XeO	4.104	CdAr	1.288			CdCl	9.699
					BaO	0.106						
147	**Sm**	14.97	NdH	17.189	XeO	21.204	AgAr	51.662	GeGe	5.556	PdCl	2.843
							CdAr	0.043			CdCl	21.31
											SnCl	0.735
148	Nd	5.73	SmH	14.998	TeO	0.068	PdAr	26.388	GeGe	17.033	CdCl	12.361
	Sm	11.24			XeO	26.852	CdAr	0.976			InCl	3.258
					BaO	0.101						

Masses used for analysis and species for which corrections were made are shown in boldface.

ICP-MS Interferences

Mass	Element		Hydride		Oxide		Argide		Dimer and M^{2+}		Chloride	
149	Sm	13.83	NdH	5.759	XeO	0.053	AgAr	47.968	GeGe	1.150	CdCl	27.615
			SmH	11.301	CsO	99.762	CdAr	0.049				
							InAr	0.014				
150	Nd	5.62	SmH	13.800	XeO	10.429	PdAr	11.685	GeGe	5.348	CdCl	2.961
	Sm	7.44			CsO	0.038	CdAr	12.552	AsAs	100	InCl	73.554
					BaO	2.411						
151	**Eu**	47.82	NdH	5.639	CsO	0.200	CdAr	12.756			CdCl	12.636
			SmH	7.401	BaO	6.577	InAr	0.325			SnCl	11.167
152	Gd	0.2	EuH	47.793	XeO	8.900	CdAr	24.077	SeSe	1.299	InCl	23.188
	Sm	26.72			BaO	7.843	SnAr	1.015			SnCl	5.902
					CeO	0.190						
153	Eu	52.18	SmH	26.696	BaO	11.219	CdAr	12.171	SeSe	1.428	CdCl	1.815
			GdH	0.200			InAr	4.343			SnCl	21.88
154	Gd	2.15	EuH	52.192	BaO	71.549	CdAr	28.620	SeSe	5.917	SnCl	8.37
	Sm	22.71			LaO	0.090	SnAr	0.738				
					CeO	0.250						
155	Gd	14.73	SmH	22.697	BaO	0.050	InAr	95.317	SeSe	3.629	SnCl	30.564
			GdH	2.180	LaO	99.672	SnAr	0.372			TeCl	0.073
156	Gd	20.47	GdH	14.798	BaO	0.143	CdAr	7.460	SeSe	15.097	SnCl	2.081
	Dy	0.052			LaO	0.038	SnAr	14.597			SbCl	43.462
					CeO	88.270						
157	**Gd**	15.68	GdH	20.469	LaO	0.200	SnAr	7.655	SeSe	7.570	SnCl	11.405
			DyH	0.060	CeO	0.034	SbAr	0.193			TeCl	1.996
					PrO	99.762						
158	Gd	24.87	GdH	15.651	CeO	11.231	SnAr	24.169	SeSe	25.229	SnCl	46.207
	Dy	0.09			PrO	0.038			BrBr	25.695	TeCl	0.688
					NdO	27.065						
159	**Tb**	100	GdH	24.839	PrO	0.200	SnAr	8.556	SeSe	1.332	SnCl	5.509
			DyH	0.100	NdO	12.161	SbAr	0.180			TeCl	4.28
160	Gd	21.9	TbH	99.985	CeO	0.022	SnAr	32.482	SeSe	28.764	SbCl	10.332
	Dy	2.29			NdO	23.802	TeAr	0.113	BrBr	49.990	TeCl	5.629
					SmO	3.093						
161	Dy	18.88	GdH	21.857	NdO	8.314	SbAr	57.157			SnCl	1.403
			TbH	0.015			TeAr	0.025			TeCl	15.525
			DyH	2.340							XeCl	0.092
162	Er	0.136	DyH	18.898	NdO	17.200	SnAr	4.615	SeSe	8.662	TeCl	1.73
	Dy	25.53					TeAr	2.659	BrBr	24.315	ICl	75.77
									KrKr	0.921		
163	**Dy**	24.97	DyH	25.499	NdO	0.023	SbAr	42.469	KrKr	0.518	TeCl	28.603
			ErH	0.140	SmO	14.964	TeAr	0.909			XeCl	1.469
							IAr	0.337				
164	Er	1.56	DyH	24.900	NdO	5.781	SnAr	5.767	KrKr	4.032	ICl	24.23
	Dy	28.18			SmO	11.279	TeAr	4.915			XeCl	20.003
							XeAr	0.106				
165	**Ho**	100	DyH	28.200	SmO	13.801	TeAr	7.110	KrKr	2.668	TeCl	33.288
			ErH	1.610			IAr	0.063			XeCl	3.569
							XeAr	0.089			BaCl	0.08
166	Er	33.41	HoH	99.985	NdO	5.638	TeAr	19.008	KrKr	15.325	XeCl	22.46

Masses used for analysis and species for which corrections were made are shown in boldface.

ICP-MS Interferences

Mass	Element		Hydride		Oxide		Argide		Dimer and M^{2+}		Chloride	
					SmO	7.410	XeAr	0.105				
167	Er	22.94	HoH	0.015	SmO	0.030	IAr	99.600	KrKr	13.110	TeCl	8.19
			ErH	33.595	EuO	47.686					XeCl	21.376
											BaCl	0.102
168	Er	27.07	ErH	22.952	NdO	0.011	TeAr	31.584	KrKr	36.504	XeCl	5.137
	Yb	0.135			SmO	26.651	XeAr	1.996			CsCl	75.77
					EuO	0.018						
					GdO	0.200						
169	Tm	100	ErH	26.799	SmO	0.010	XeAr	26.308	KrKr	3.979	XeCl	14.398
			YbH	0.130	EuO	52.171	CsAr	0.337			BaCl	1.856
170	Er	14.88	TmH	99.985	SmO	22.699	TeAr	33.664	KrKr	19.722	CsCl	24.23
	Yb	3.03			EuO	0.020	XeAr	4.136	RbRb	52.078	BaCl	4.995
					GdO	2.175	BaAr	0.114	SrSr	0.110		
171	Yb	14.31	ErH	14.898	EuO	0.104	XeAr	21.115	SrSr	0.078	XeCl	9.263
			TmH	0.015	GdO	14.766	CsAr	0.063			BaCl	6.537
			YbH	3.050			BaAr	0.022			CeCl	0.144
172	**Yb**	21.82	YbH	14.298	SmO	0.045	XeAr	26.829	KrKr	2.993	BaCl	10.06
					GdO	20.431	BaAr	0.129	RbRb	40.174		
					DyO	0.060			SrSr	1.897		
173	Yb	16.13	YbH	21.899	GdO	15.650	CsAr	99.600	SrSr	1.380	XeCl	2.156
							BaAr	0.042			BaCl	56.23
											LaCl	0.068
											CeCl	0.235
174	Yb	31.84	YbH	16.121	GdO	24.828	XeAr	10.364	RbRb	7.748	BaCl	2.721
	Hf	0.18			DyO	0.100	BaAr	2.654	SrSr	16.775	LaCl	75.702
175	**Lu**	97.41	YbH	31.798	GdO	0.041	BaAr	6.573	SrSr	11.561	BaCl	17.373
			HfH	0.162	TbO	99.762	LaAr	0.337			LaCl	0.022
											CeCl	67.102
176	Lu	2.59	LuH	97.395	GdO	21.858	XeAr	8.864	SrSr	68.195	LaCl	24.208
	Yb	12.73			TbO	0.038	BaAr	7.868			PrCl	75.77
	Hf	5.2			DyO	2.335	CeAr	0.488				
177	Hf	18.5	YbH	12.698	TbO	0.200	BaAr	11.185			CeCl	29.834
			LuH	2.604	DyO	18.856	LaAr	0.063			NdCl	20.556
			HfH	5.205			PrAr	0.337				
178	Hf	27.14	HfH	18.604	GdO	0.044	BaAr	71.413	YY	100	PrCl	24.23
					DyO	25.451	LaAr	0.090			NdCl	9.229
					ErO	0.140	CeAr	0.342				
							NdAr	0.091				
179	Hf	13.75	HfH	27.296	DyO	24.888	LaAr	99.510			CeCl	2.685
							PrAr	0.063			NdCl	24.607
							NdAr	0.041			SmCl	2.349
180	Ta	0.0123	HfH	13.631	DyO	28.193	CeAr	88.133	ZrZr	26.471	NdCl	9.24
	W	0.14			ErO	1.606	NdAr	0.097				
	Hf	35.24										
181	Ta	99.988	HfH	35.097	DyO	0.061	PrAr	99.600	ZrZr	11.545	NdCl	18.792
			TaH	0.012	HoO	99.762					SmCl	0.751
			WH	0.130								
182	W	26.41	TaH	99.973	DyO	0.056	CeAr	11.036	ZrZr	18.906	NdCl	2.011

Masses used for analysis and species for which corrections were made are shown in boldface.

ICP-MS Interferences

Mass	Element		Hydride		Oxide		Argide		Dimer and M^{2+}		Chloride	
					HoO	0.038	NdAr	27.094			SmCl	11.366
					ErO	33.523						
183	W	14.4	TaH	0.015	HoO	0.200	NdAr	12.137	ZrZr	3.848	NdCl	8.529
			WH	26.296	ErO	22.908	SmAr	0.051			SmCl	8.562
184	Os	0.018	WH	14.302	ErO	26.812	NdAr	23.735	ZrZr	20.825	SmCl	14.091
	W	30.64			YbO	0.130	SmAr	3.126				
185	Re	37.07	WH	30.668	ErO	0.056	NdAr	8.267	ZrZr	3.900	NdCl	5.669
			OsH	0.020	TmO	99.762	SmAr	0.056			SmCl	8.345
186	Os	1.59	ReH	37.394	ErO	14.918	NdAr	17.144	ZrZr	8.843	SmCl	3.344
	W	28.41			TmO	0.038	SmAr	0.032	NbNb	100	EuCl	36.218
					YbO	3.043						
187	Os	1.64	WH	28.596	TmO	0.200	SmAr	14.949	ZrZr	0.628	NdCl	1.367
	Re	62.93	OsH	1.580	YbO	14.267	EuAr	0.161	MoMo	4.725	SmCl	22.024
											GdCl	0.152
188	Os	13.3	ReH	62.591	ErO	0.030	NdAr	5.741	ZrZr	3.981	EuCl	51.134
			OsH	1.600	YbO	21.859	SmAr	11.349	MoMo	5.806		
189	Os	16.1	OsH	13.298	YbO	16.119	SmAr	13.745	MoMo	5.780	SmCl	23.669
							EuAr	0.206			GdCl	1.7
190	Os	26.4	OsH	16.100	YbO	31.774	NdAr	5.617	ZrZr	0.973	EuCl	12.648
	Pt	0.0127			HfO	0.162	SmAr	7.464	MoMo	12.782	GdCl	11.214
191	Ir	37.3	OsH	26.398	YbO	0.044	EuAr	47.642	MoMo	7.078	SmCl	5.5
			PtH	0.010	LuO	97.178	GdAr	0.050			GdCl	16.038
											DyCl	0.045
192	Os	41	IrH	37.294	YbO	12.733	SmAr	26.608	MoMo	13.145	GdCl	15.444
	Pt	0.78			LuO	2.621	GdAr	0.270				
					HfO	5.194						
193	Ir	62.7	OsH	40.994	LuO	0.196	EuAr	51.991	MoMo	10.869	GdCl	23.781
			PtH	0.790	HfO	18.564	GdAr	0.062			DyCl	0.09
194	Pt	32.9	IrH	62.691	YbO	0.025	SmAr	22.609	MoMo	10.743	GdCl	3.792
					HfO	27.250	GdAr	2.268			TbCl	75.77
195	Pt	33.8	PtH	32.895	HfO	13.644	GdAr	14.751	MoMo	7.675	GdCl	22.582
							TbAr	0.337			DyCl	1.797
196	Hg	0.146	PtH	33.800	HfO	35.076	GdAr	20.477	MoMo	9.035	TbCl	24.23
	Pt	25.3			TaO	0.012	DyAr	0.068			DyCl	14.321
					WO	0.130						
197	Au	100	PtH	25.301	HfO	0.041	GdAr	15.587			GdCl	5.297
			HgH	0.150	TaO	99.750	TbAr	0.063			DyCl	19.888
							DyAr	0.064			ErCl	0.106
198	Hg	10.02	AuH	99.985	HfO	0.070	GdAr	24.754	TcTc	100	DyCl	23.446
	Pt	7.21			TaO	0.038	DyAr	0.187	RuRu	5.575		
					WO	26.238						
199	Hg	16.84	PtH	7.199	TaO	0.200	TbAr	99.600	RuRu	3.840	DyCl	27.546
			AuH	0.015	WO	14.276	DyAr	0.096			ErCl	1.254
			HgH	9.969								
200	Hg	23.13	AuH	16.869	WO	30.655	GdAr	21.773	RuRu	9.158	DyCl	6.033
					OsO	0.020	DyAr	2.442			HoCl	75.77
201	Hg	13.22	AuH	23.099	WO	0.040	DyAr	18.840	RuRu	12.310	DyCl	6.833
					ReO	37.311	HoAr	0.337			ErCl	25.849

Masses used for analysis and species for which corrections were made are shown in boldface.

ICP-MS Interferences

Mass	Element		Hydride		Oxide		Argide		Dimer and M^{2+}		Chloride	
202	Hg	29.8	AuH	13.181	WO	28.593	DyAr	25.416	RuRu	11.556	HoCl	24.23
					ReO	0.014	ErAr	0.254			ErCl	17.389
					OsO	1.576						
203	Tl	29.5	AuH	29.857	WO	0.011	DyAr	24.800	RuRu	15.494	ErCl	28.448
					ReO	62.526	HoAr	0.063			YbCl	0.099
					OsO	1.597	ErAr	0.077				
204	Hg	6.85	TlH	29.516	WO	0.057	DyAr	28.087	RuRu	14.698	ErCl	5.561
	Pb	1.48			ReO	0.024	ErAr	1.715			TmCl	75.77
					OsO	13.272						
205	Tl	70.5	AuH	6.869	ReO	0.125	HoAr	99.600	RuRu	6.358	ErCl	17.783
			PbH	1.400	OsO	16.070	ErAr	0.014			YbCl	2.342
							TmAr	0.337				
206	Pb	23.6	TlH	70.469	OsO	26.370	ErAr	33.533	RuRu	11.818	TmCl	24.23
					PtO	0.010	YAr	0.010	RhRh	100	YbCl	10.835
207	Pb	22.6	TlH	0.011	OsO	0.042	ErAr	22.858			ErCl	3.61
			PbH	24.096	IrO	37.211	TmAr	0.063			YbCl	17.333
							YAr	0.048				
208	Pb	52.3	PbH	22.100	OsO	40.955	ErAr	26.702	RuRu	3.497	YbCl	15.679
					IrO	0.014	YAr	0.205	PdPd	1.802		
					PtO	0.788						
209	Bi	100	PbH	52.395	OsO	0.016	TmAr	99.600	PdPd	4.963	YbCl	29.401
					IrO	62.625	YAr	0.063			HfCl	0.123
232	**Th**	100					OsAr	40.836	SnSn	3.111	PtCl	8.19
							PtAr	0.893			AuCl	75.77
234	U	0.0057					PtAr	32.809	SnSn	8.203	AuCl	24.23
							HgAr	0.034			HgCl	12.782
235	U	0.7196					PtAr	33.665	SnSn	6.440	PtCl	1.745
							AuAr	0.063			HgCl	19.919
							HgAr	0.057				
238	U	99.276					PtAr	7.171	SnSn	17.952	HgCl	3.194
							HgAr	10.045			TlCl	22.367

Masses used for analysis and species for which corrections were made are shown in boldface.

Appendix C

Results of standard addition investigations

Appendix C
Results of standard addition investigations

Table of Contents

Standard addition investigations on Sacramento River water:

Standard addition investigations on Sacramento River water:

Standard addition investigations on San Joaquin River water:

Standard addition investigations on San Joaquin River water:

Standard addition investigations on water collected from Martinez:

Standard addition investigations on water collected from Martinez:

Standard addition investigations on water collected from Martinez:

Standard addition investigations on water collected from Pinole:

Standard addition investigations on water collected from Pinole:

Standard addition investigations on water collected from Pinole:

Standard addition investigations on ocean water collected in Hawai'i:

Standard addition investigations on ocean water collected in Hawai'i:

Standard Addition Test for Li in Sacramento River Water

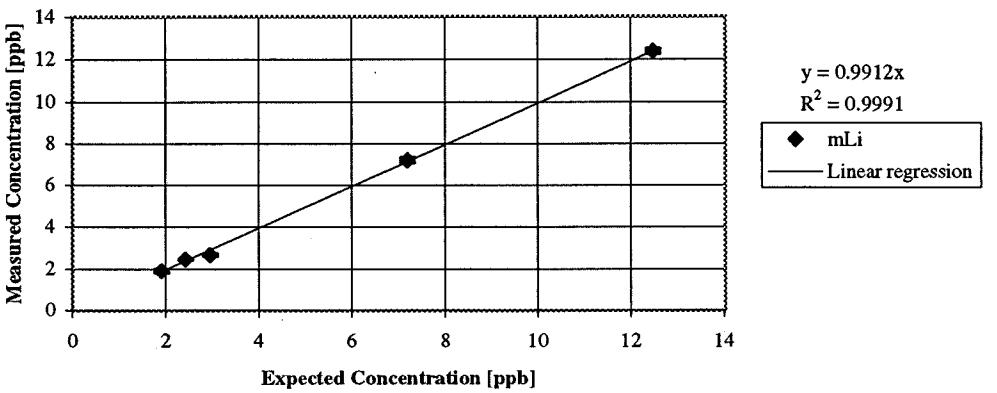

Standard Addition Test for B in Sacramento River Water

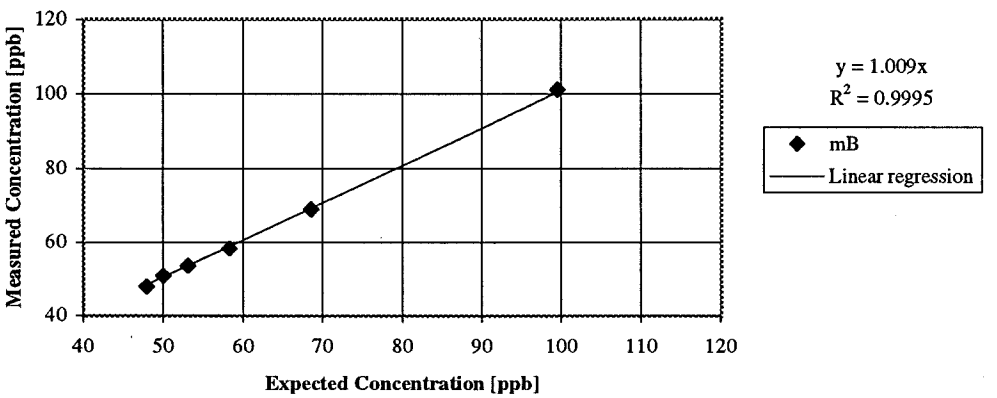

Standard Addition Test for Na in 10:1 Sacramento River Water

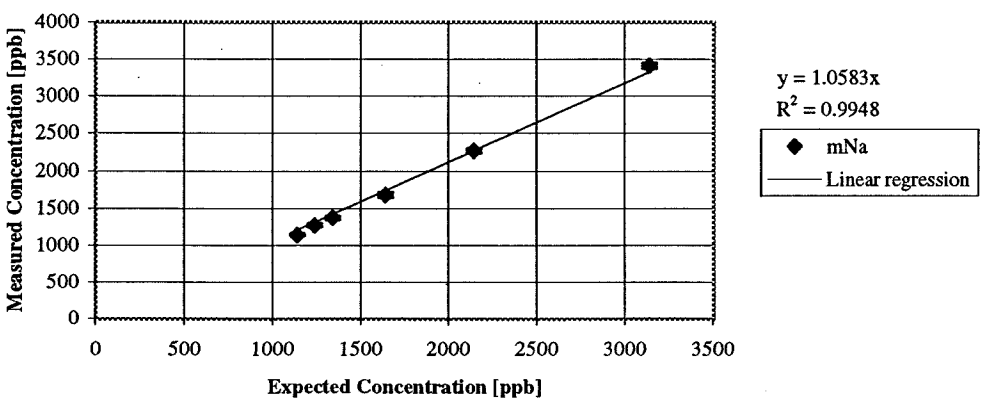

Standard Addition Test for Mg in 10:1 Sacramento River Water

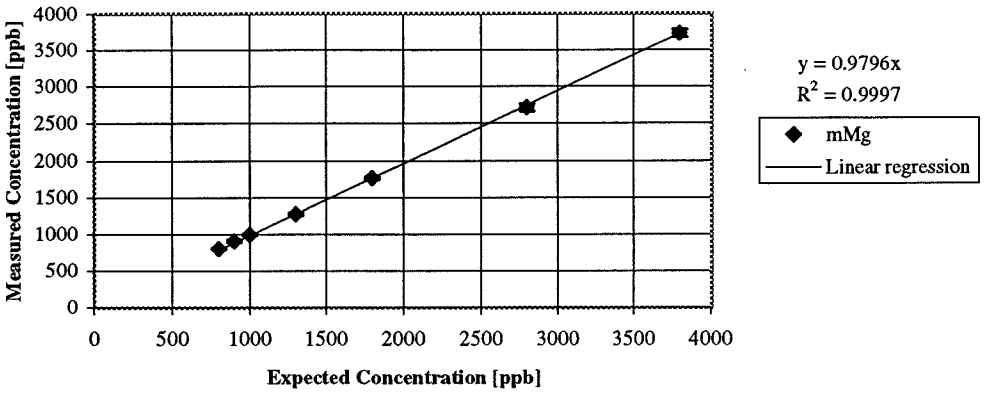

Standard Addition Test for Si in 10:1 Sacramento River Water

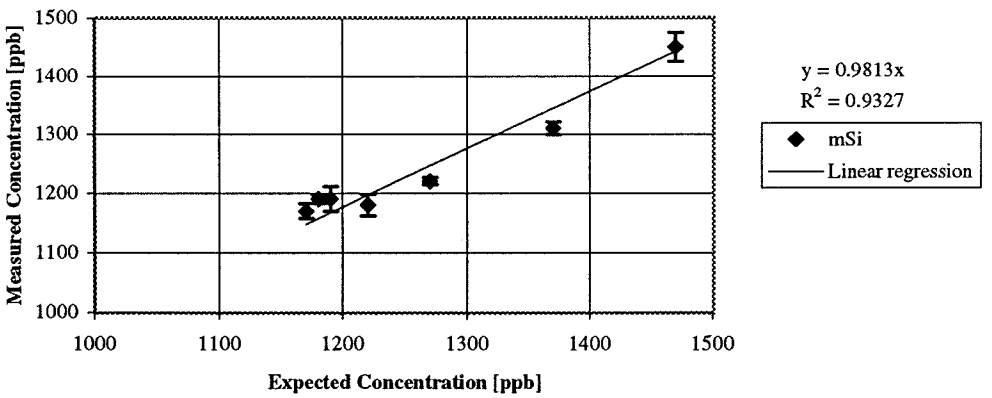

Standard Addition Test for K in 10:1 Sacramento River Water

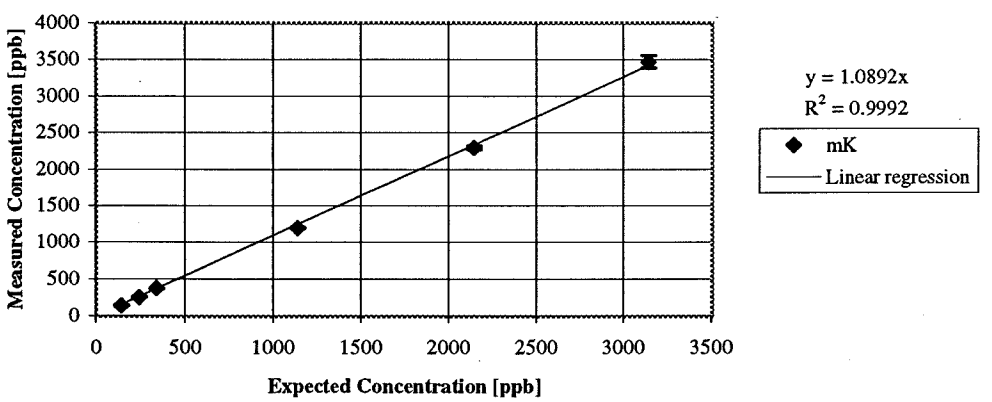

Standard Addition Test for Ca in 10:1 Sacramento River Water

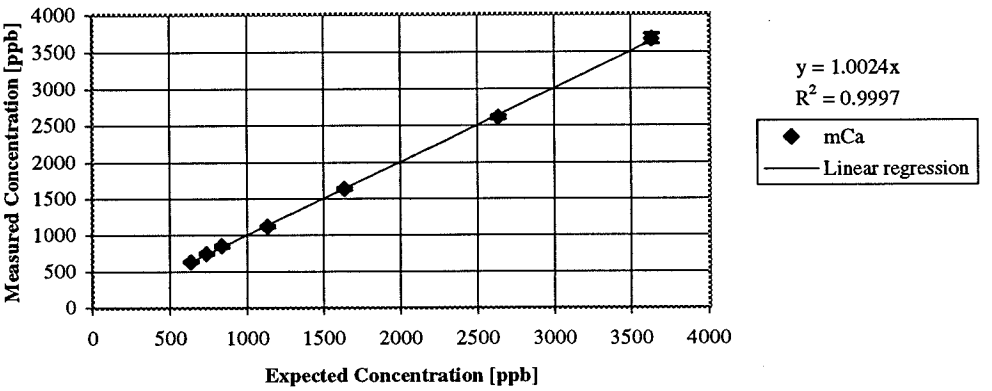

Standard Addition Test for V in Sacramento River Water

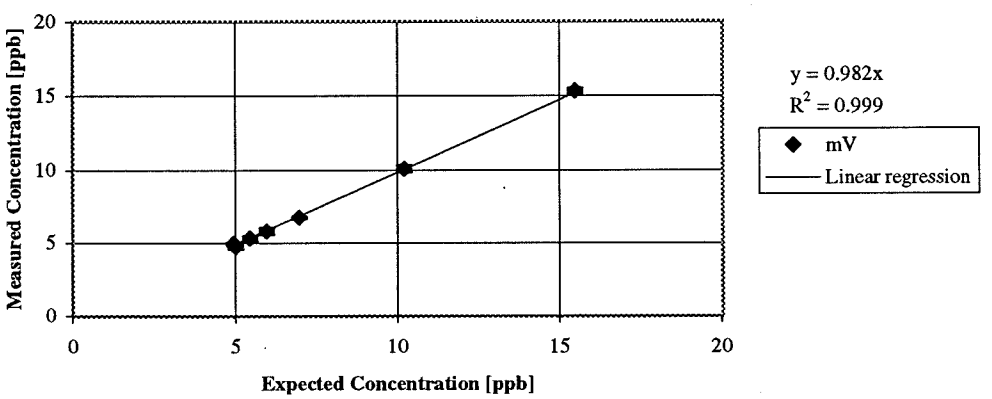

Standard Addition Test for Cr in Sacramento River Water

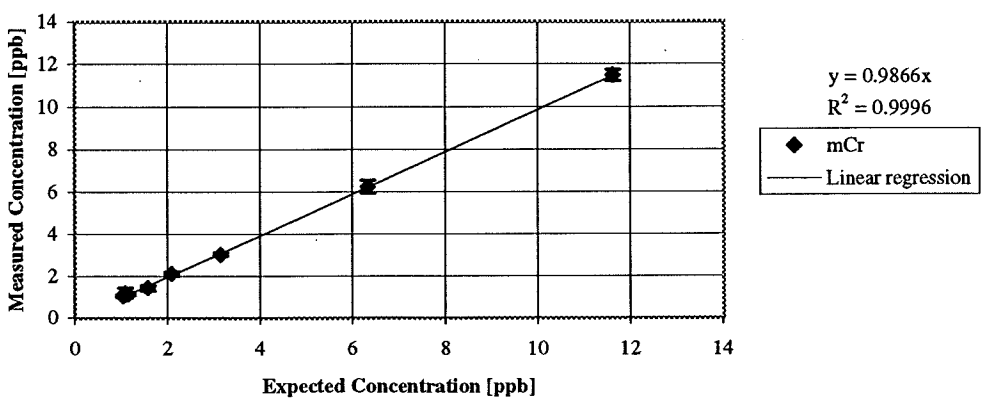

Standard Addition Test for Fe in Sacramento River Water

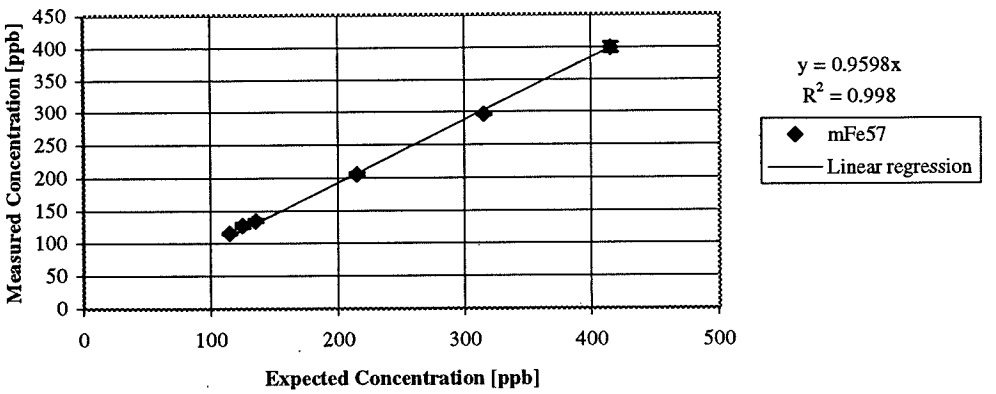

Standard Addition Test for Mn in Sacramento River Water

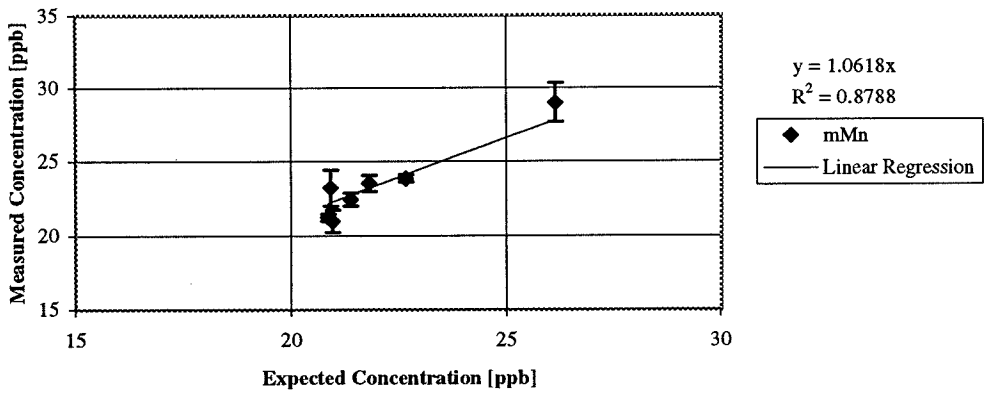

Standard Addition Test for Co in Sacramento River Water

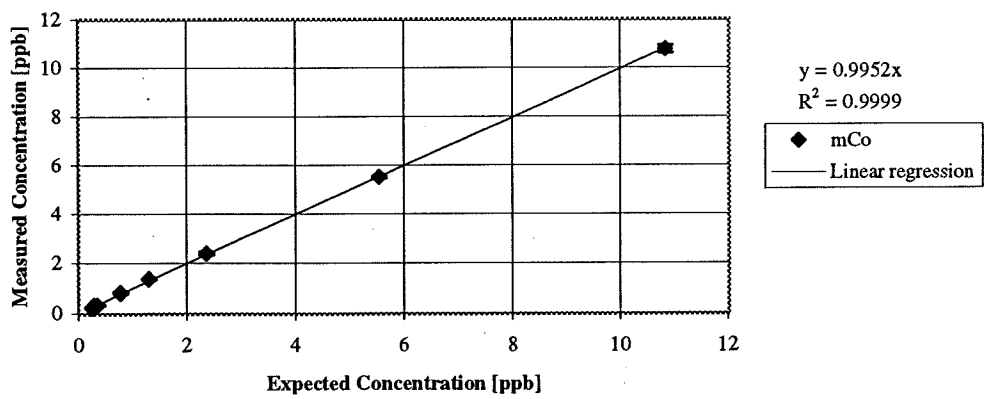

Standard Addition Test for Ni in Sacramento River Water

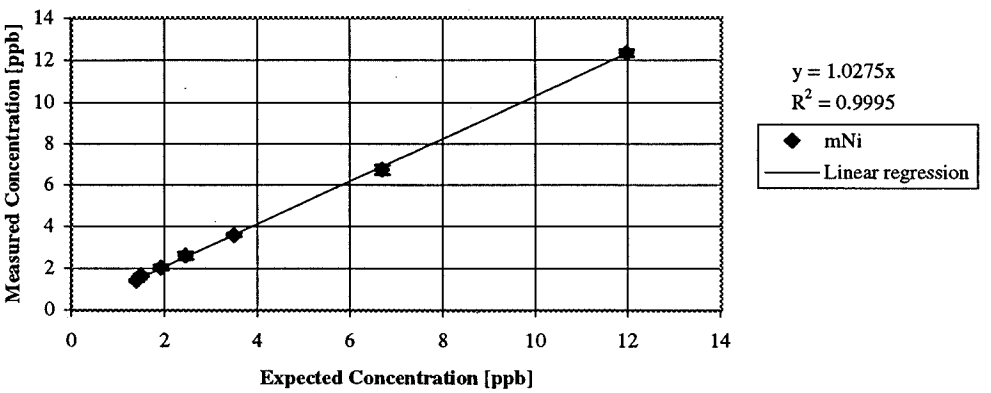

Standard Addition Test for Cu63 in Sacramento River Water

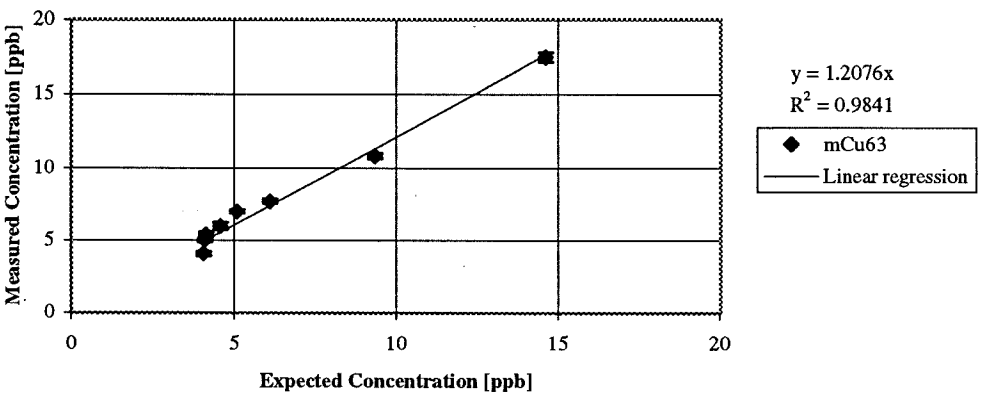

Standard Addition Test for Cu65 in Sacramento River Water

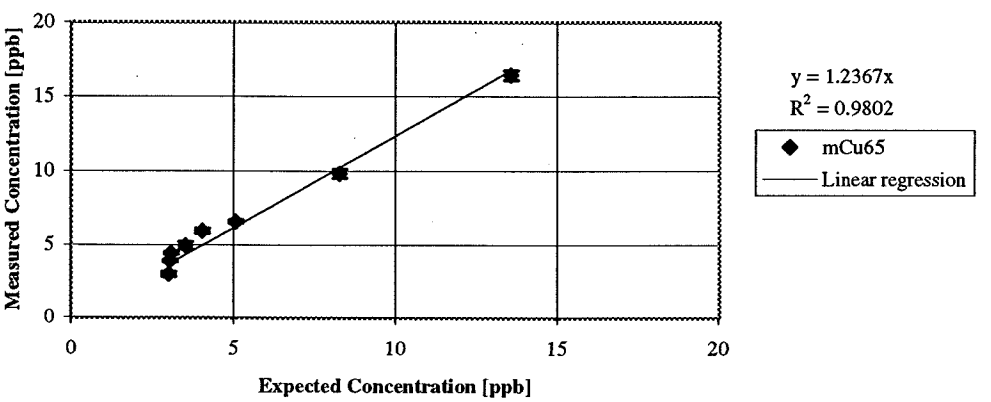

Standard Addition Test for Zn in Sacramento River Water

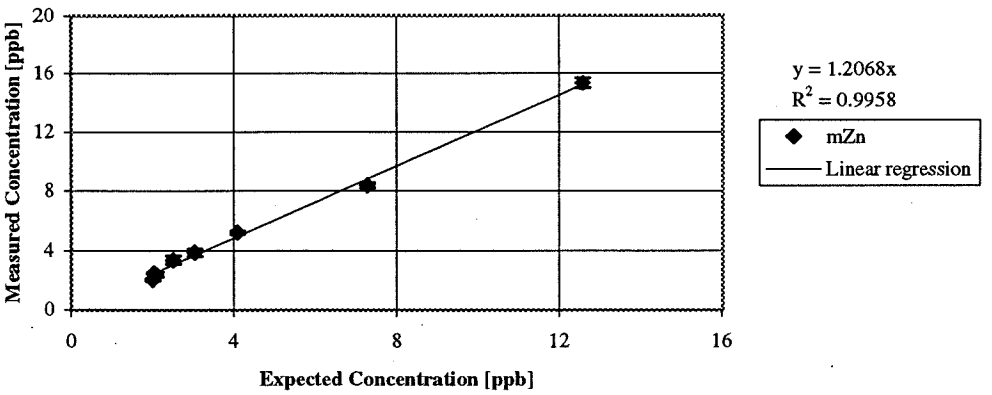

Standard Addition Test for Ga in Sacramento River Water

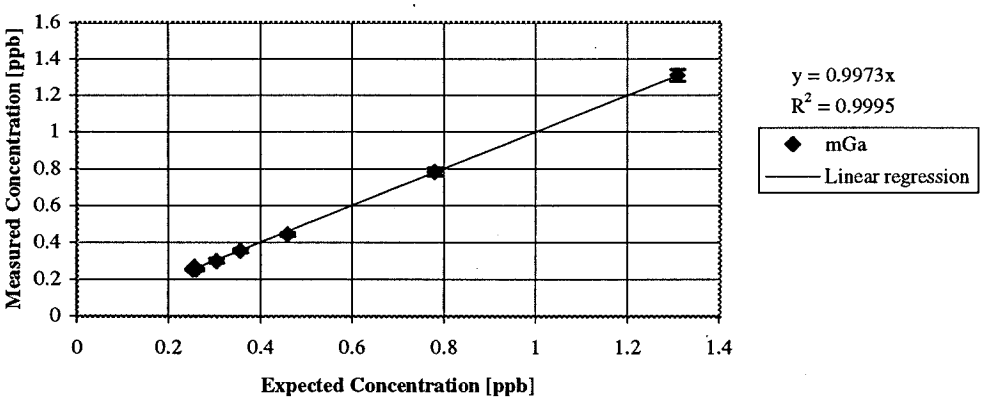

Standard Addition Test for Rb in Sacramento River Water

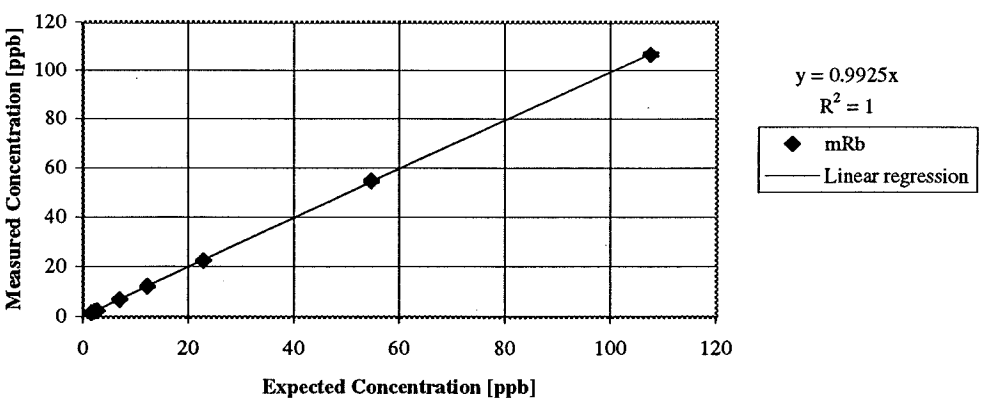

Standard Addition Test for Sr in Sacramento River Water

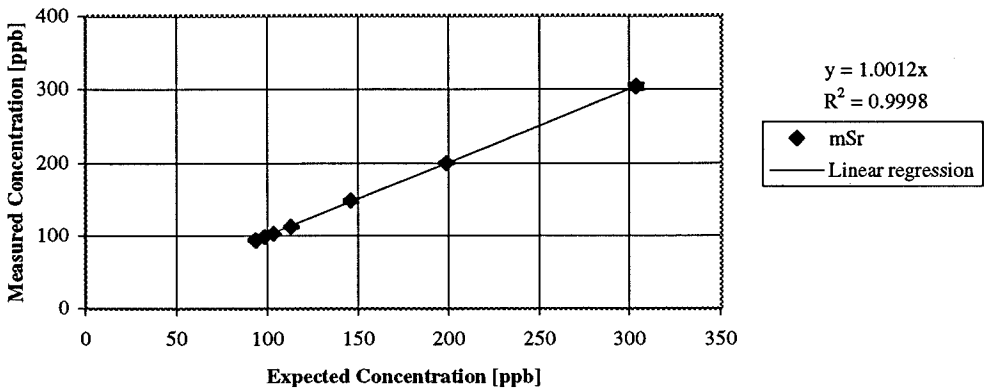

Standard Addition Test for Y in Sacramento River Water

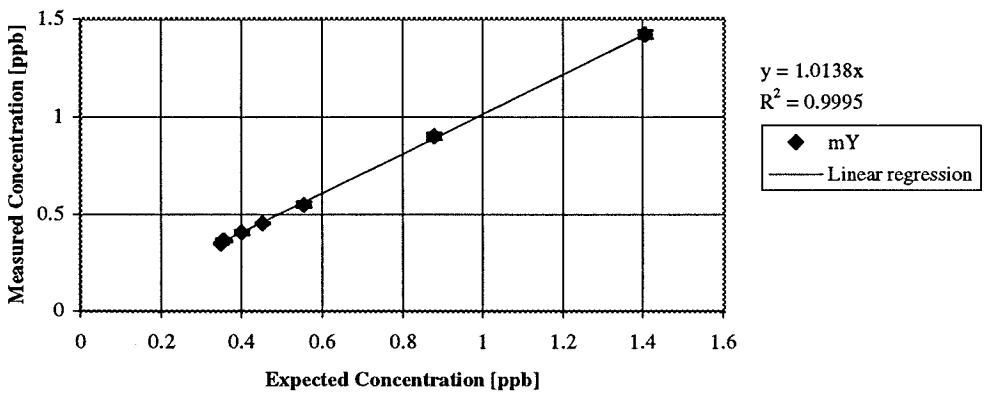

Standard Addition Test for Mo in Sacramento River Water

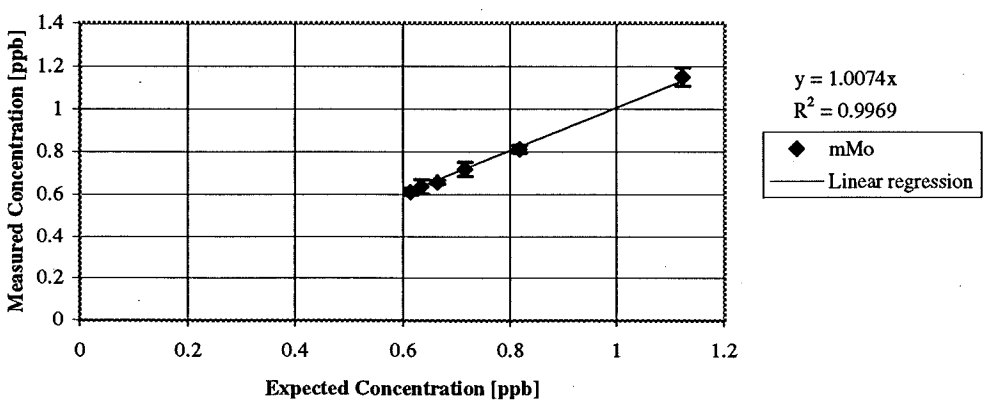

Standard Addition Test for Cd in Sacramento River Water

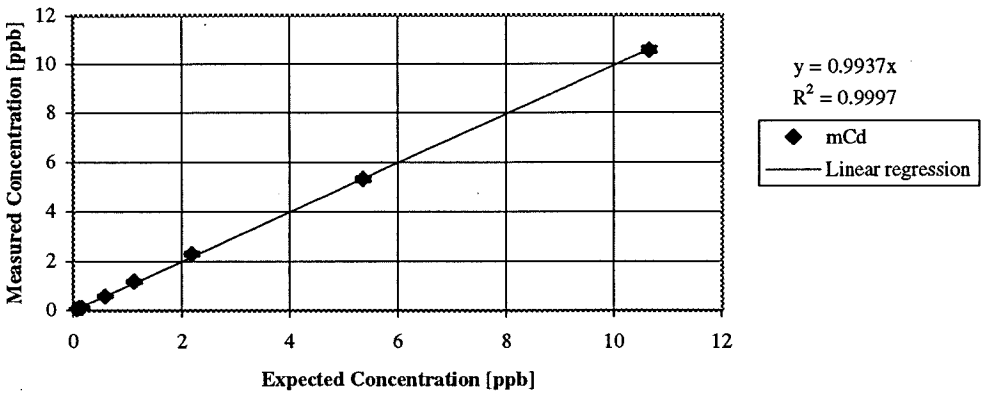

Standard Addition Test for Cs in Sacramento River Water

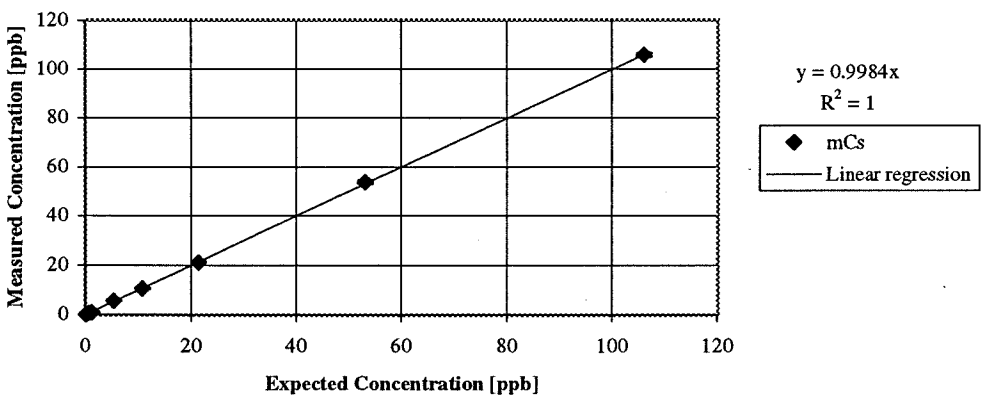

Standard Addition Test for Ba in Sacramento River Water

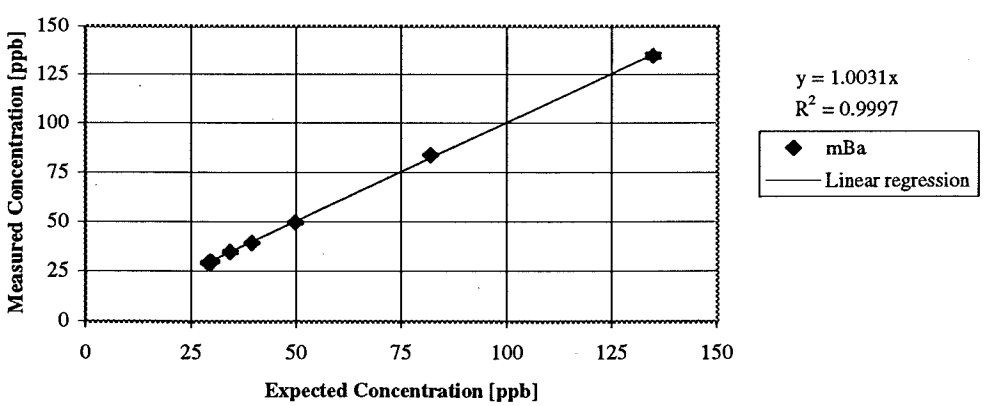

Standard Addition Test for La in Sacramento River Water

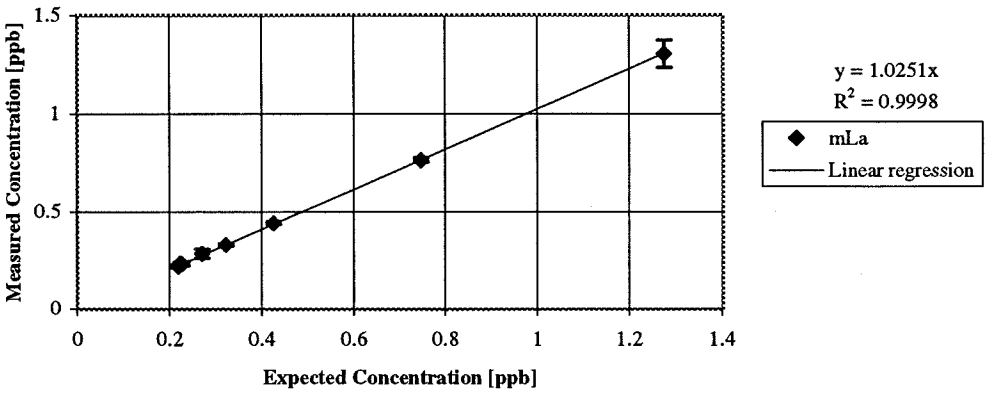

Standard Addition Test for Ce in Sacramento River Water

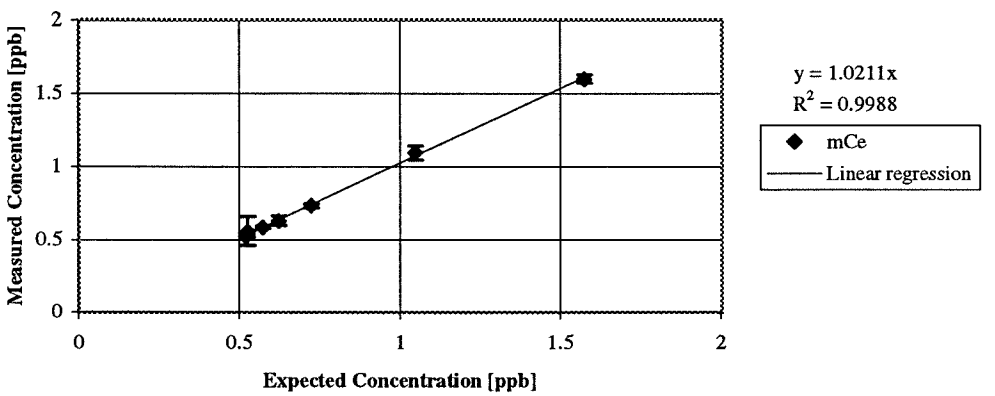

Standard Addition Test for Pr in Sacramento River Water

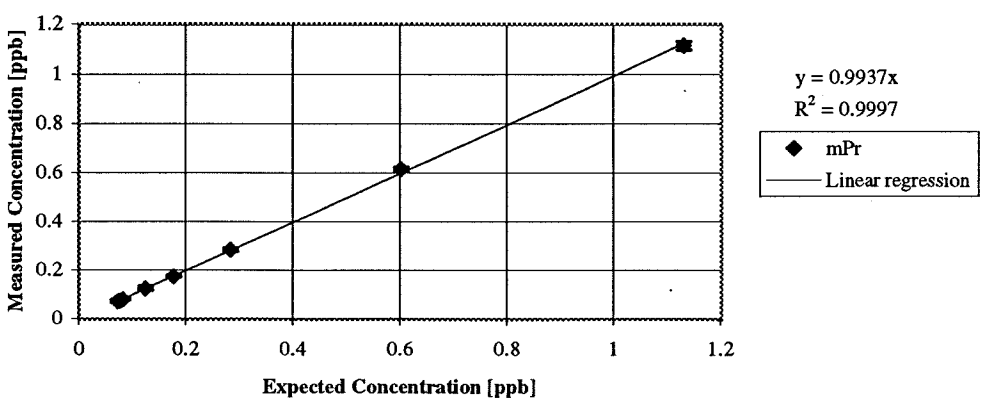

Standard Addition Test for Nd in Sacramento River Water

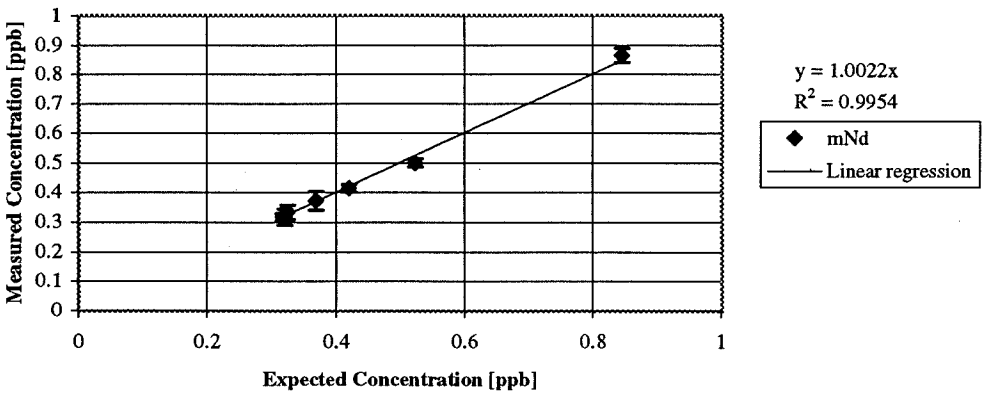

Standard Addition Test for Sm in Sacramento River Water

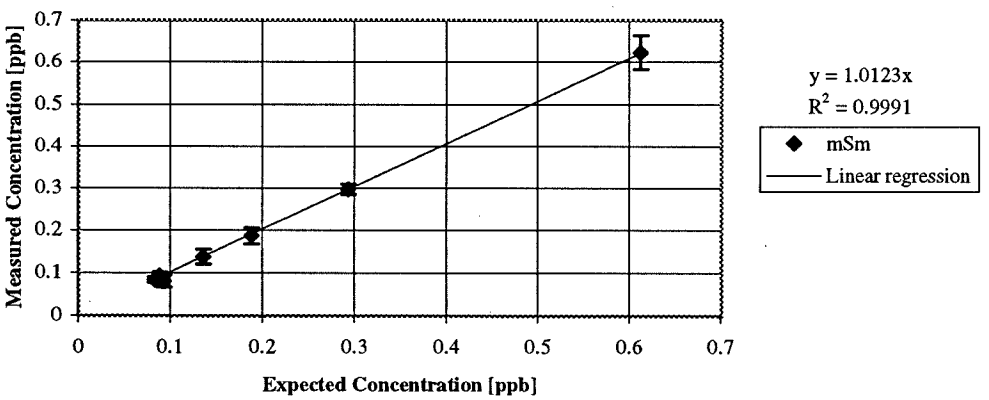

Standard Addition Test for Eu in Sacramento River Water

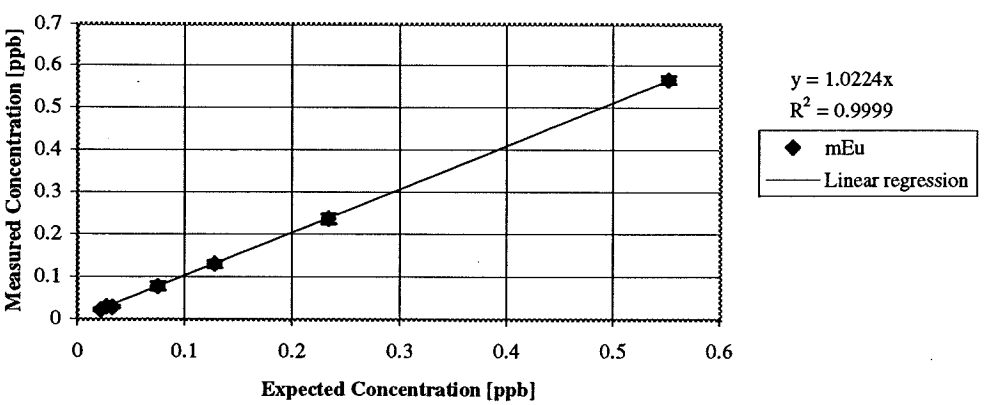

Standard Addition Test for Gd in Sacramento River Water

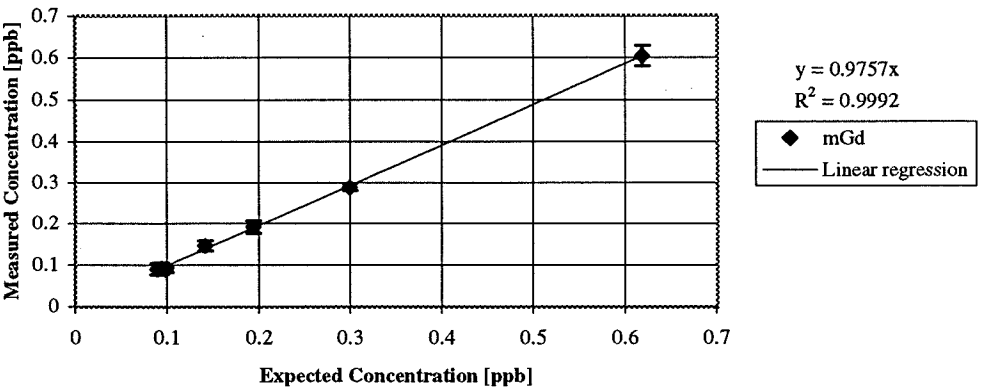

Standard Addition Test for Tb in Sacramento River Water

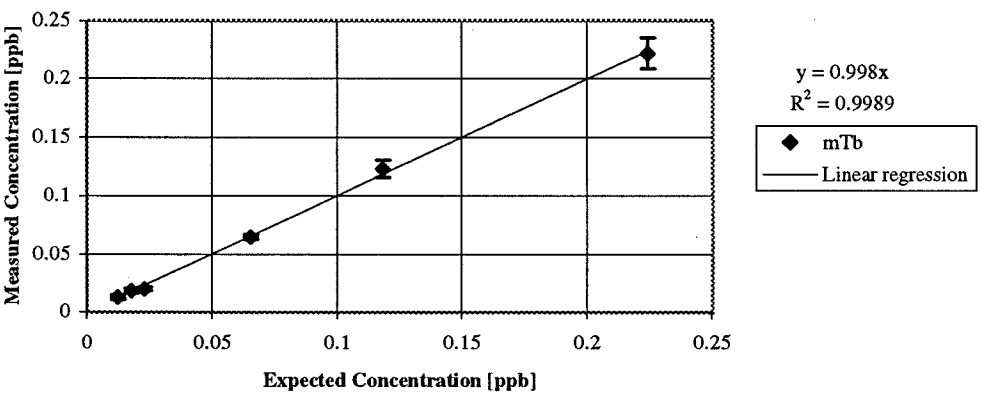

Standard Addition Test for Dy in Sacramento River Water

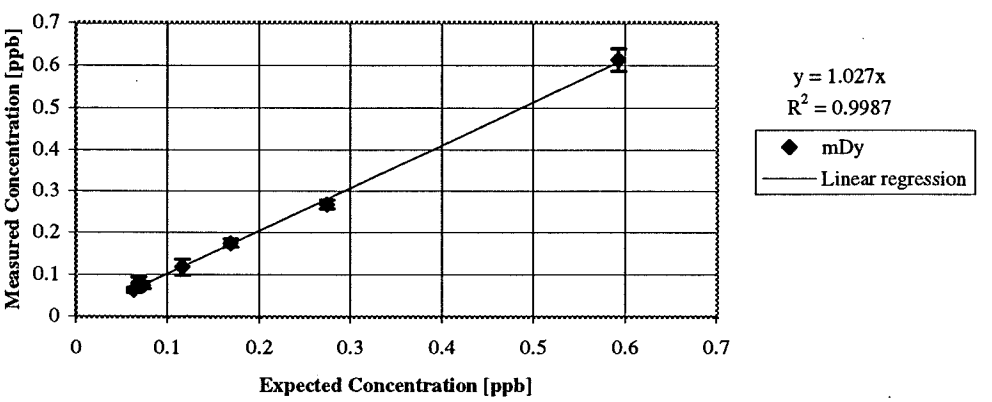

Standard Addition Test for Ho in Sacramento River Water

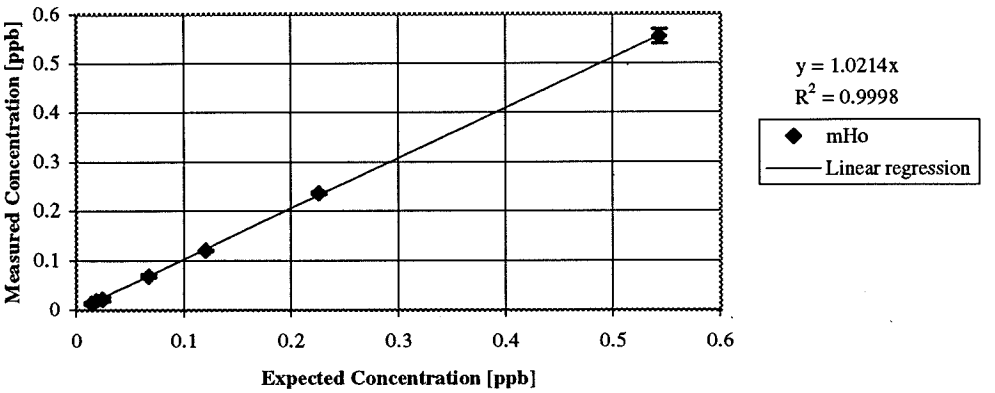

Standard Addition Test for Er in Sacramento River Water

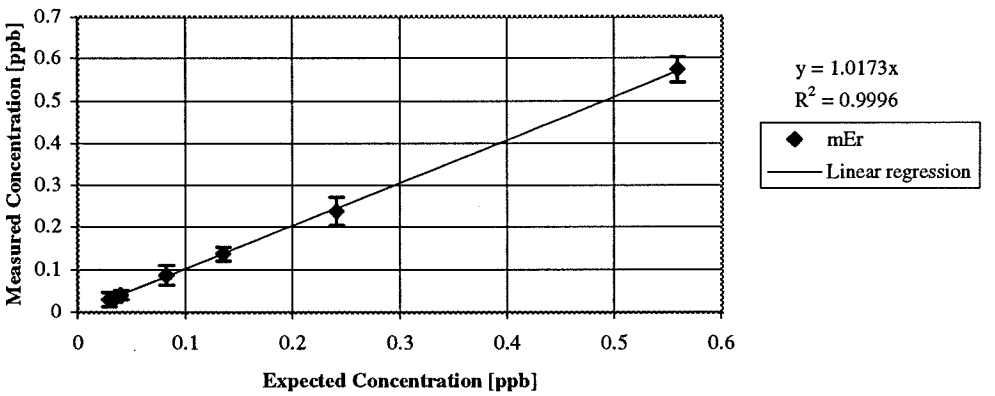

Standard Addition Test for Yb in Sacramento River Water

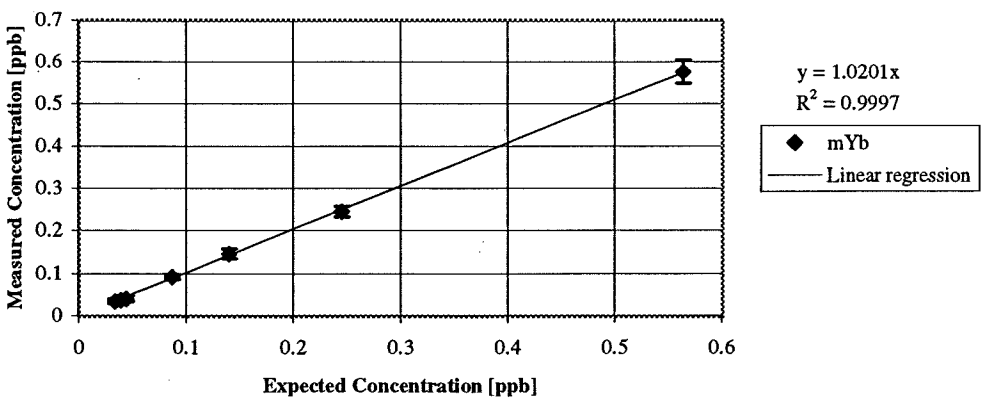

Standard Addition Test for Lu in Sacramento River Water

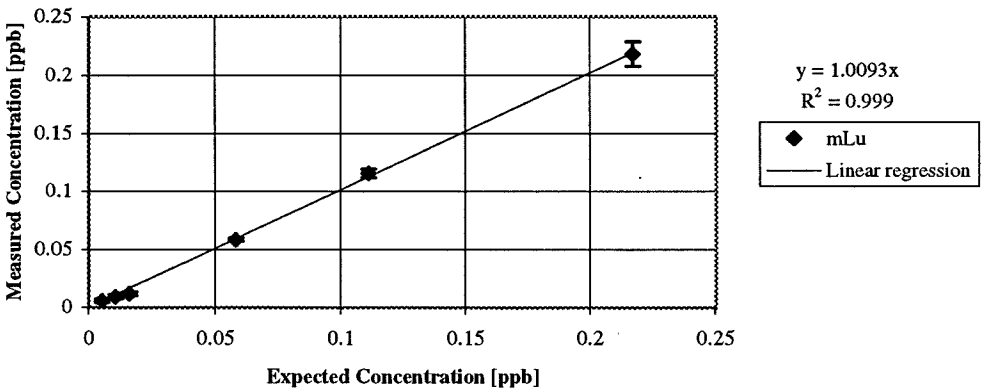

Standard Addition Test for Th in Sacramento River Water

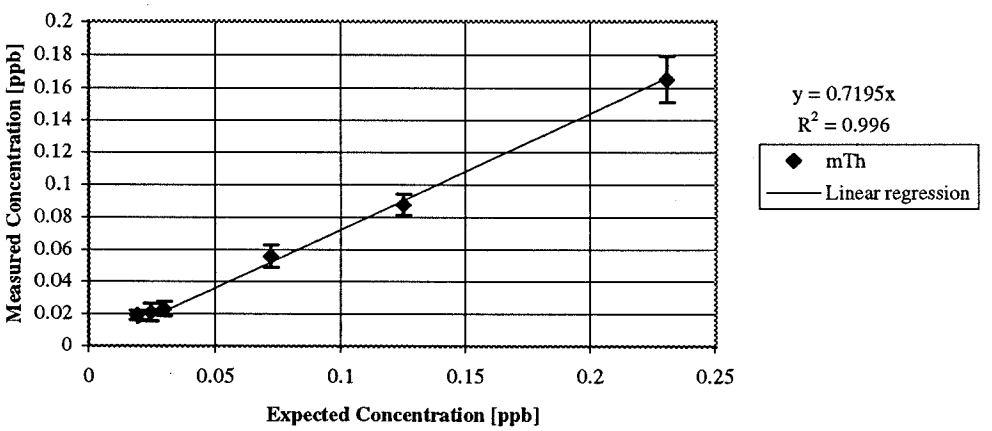

Standard Addition Test for U in Sacramento River Water

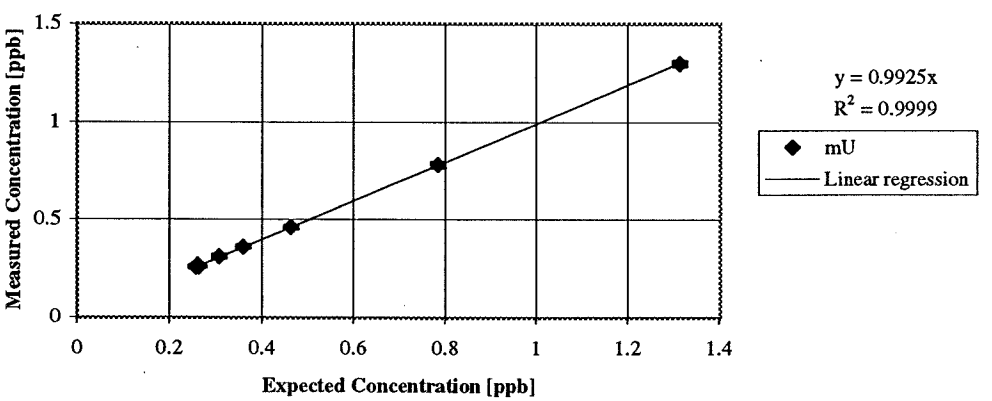

Standard Addition Test for Li in San Joaquin River Water

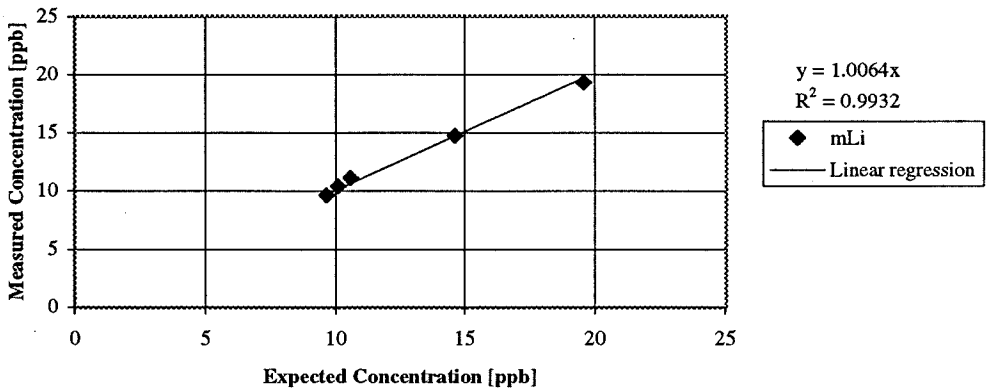

Standard Addition Test for B in San Joaquin River Water

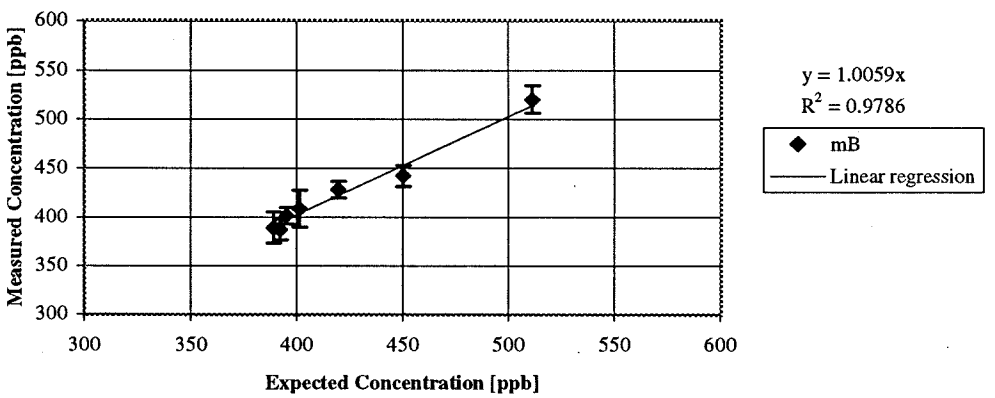

Standard Addition Test for Na in 10:1 San Joaquin River Water

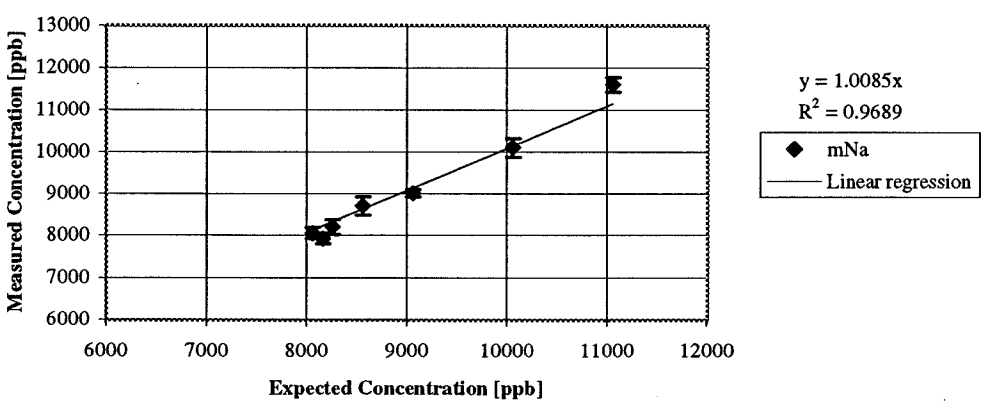

Standard Addition Test for Mg in 10:1 San Joaquin River Water

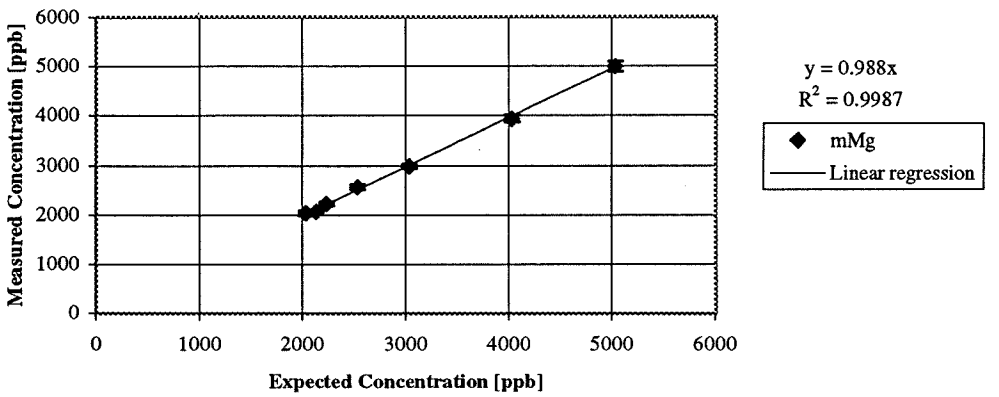

Standard Addition Test for Si in 10:1 San Joaquin River Water

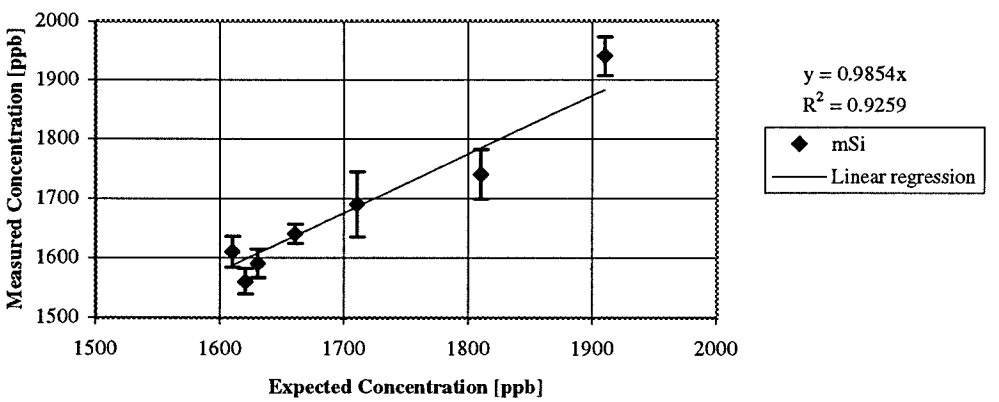

Standard Addition Test for K in 10:1 San Joaquin River Water

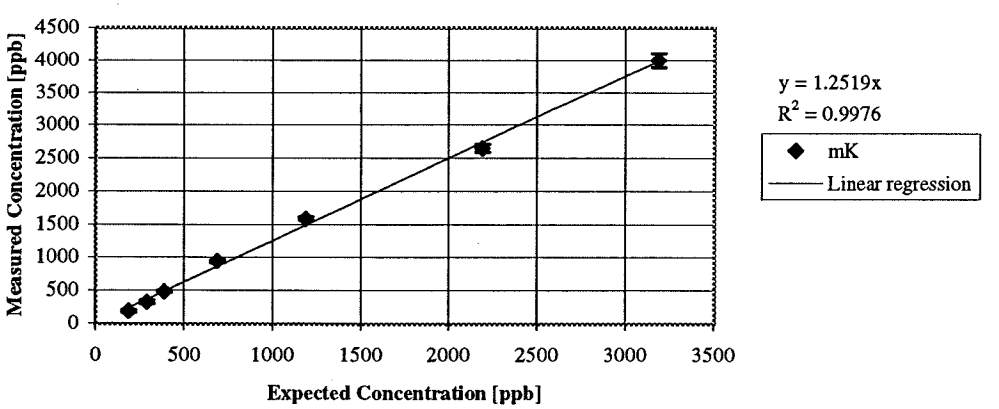

Standard Addition Test for Ca in 10:1 San Joaquin River Water

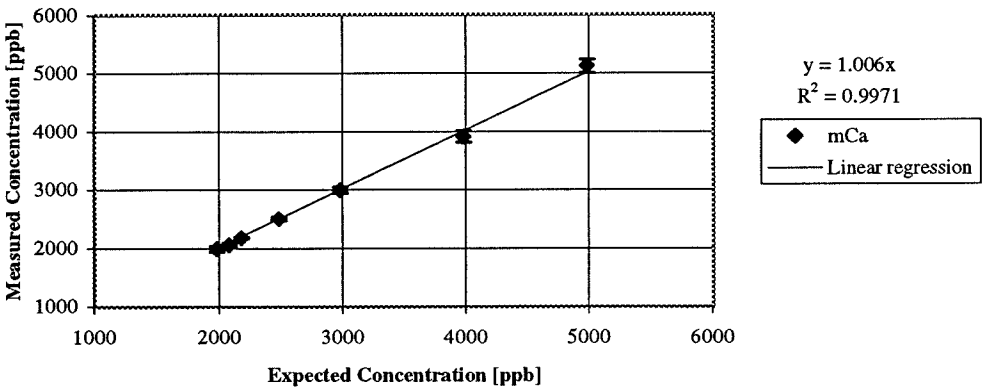

Standard Addition Test for V in San Joaquin River Water

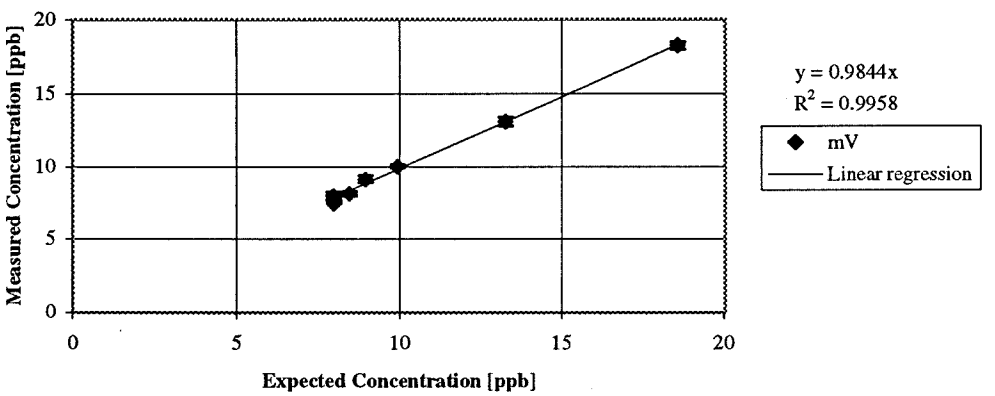

Standard Addition Test for Cr in San Joaquin River Water

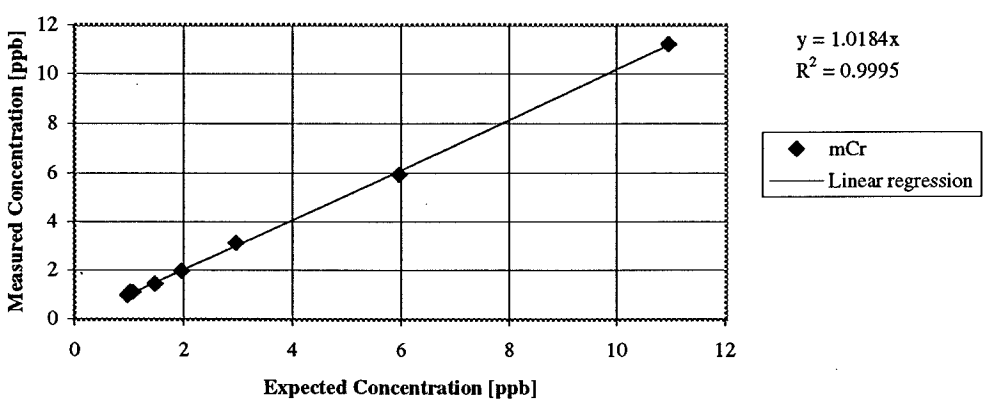

Standard Addition Test for Fe in San Joaquin River Water

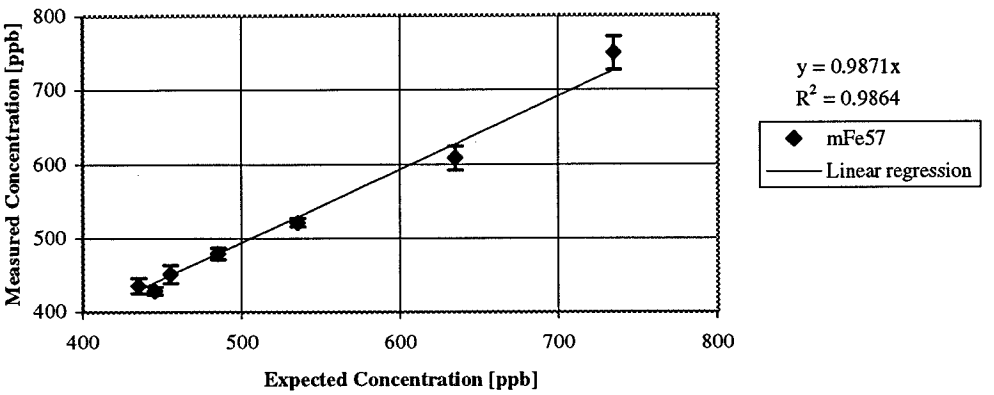

Standard Addition Test for Mn in San Joaquin River Water

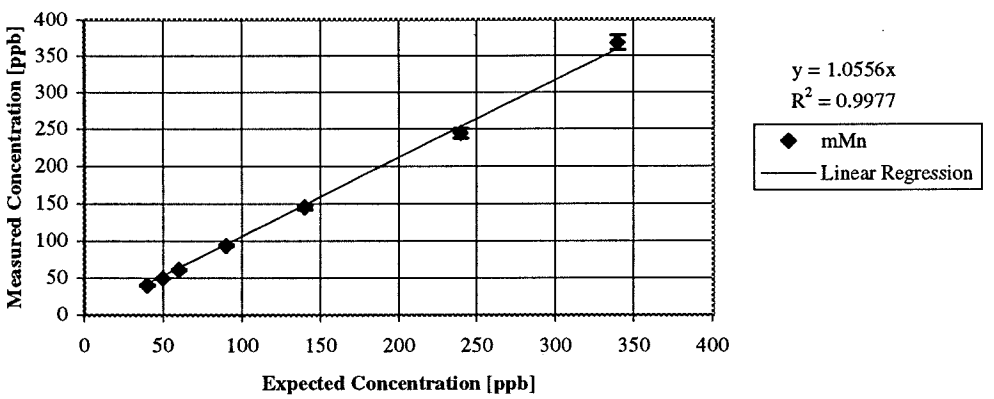

Standard Addition Test for Co in San Joaquin River Water

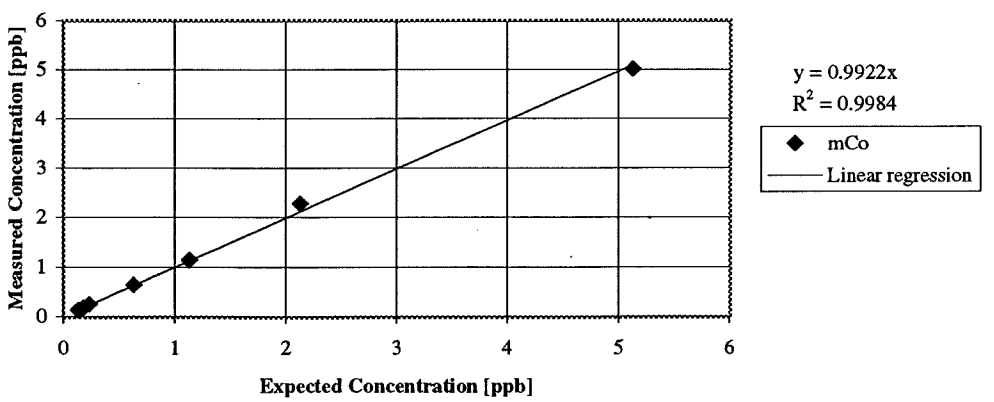

Standard Addition Test for Ni in San Joaquin River Water

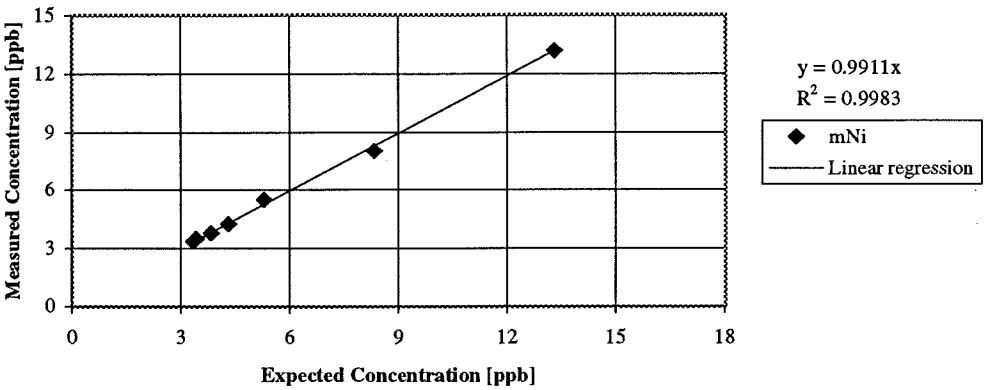

Standard Addition Test for Cu63 in San Joaquin River Water

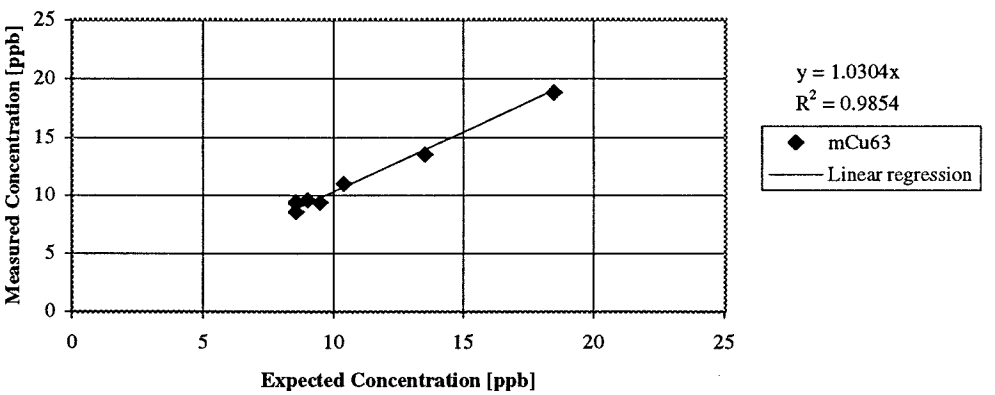

Standard Addition Test for Cu65 in San Joaquin River Water

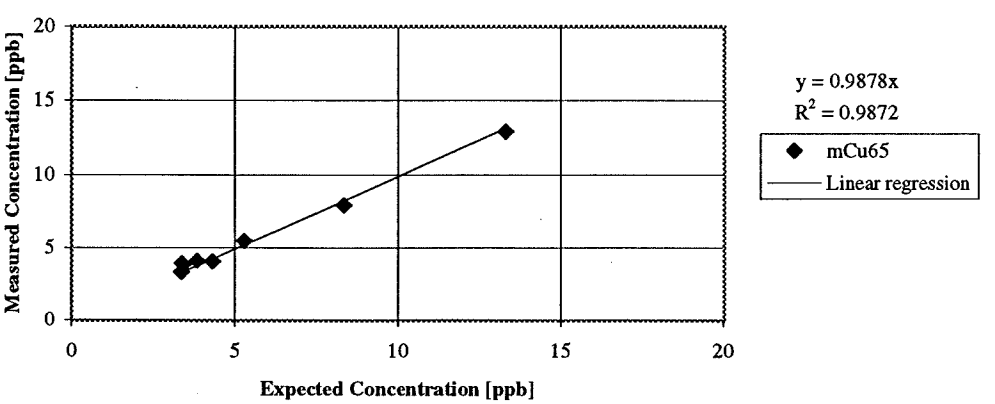

Standard Addition Test for Zn in San Joaquin River Water

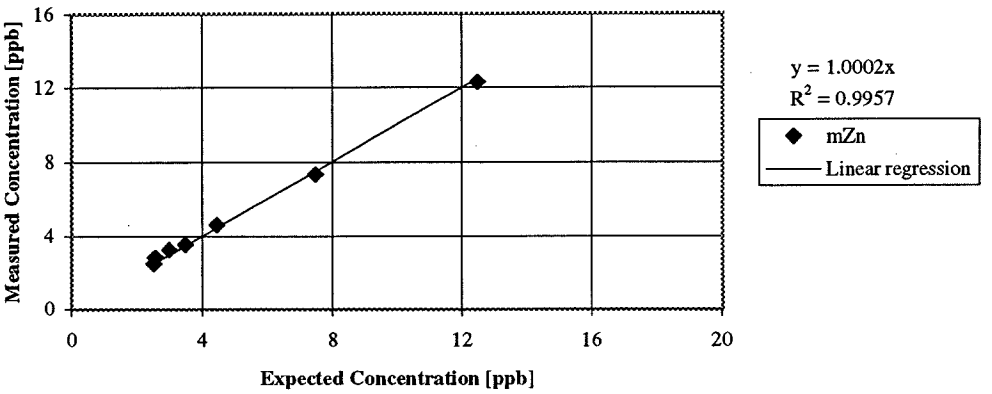

Standard Addition Test for Ga in San Joaquin River Water

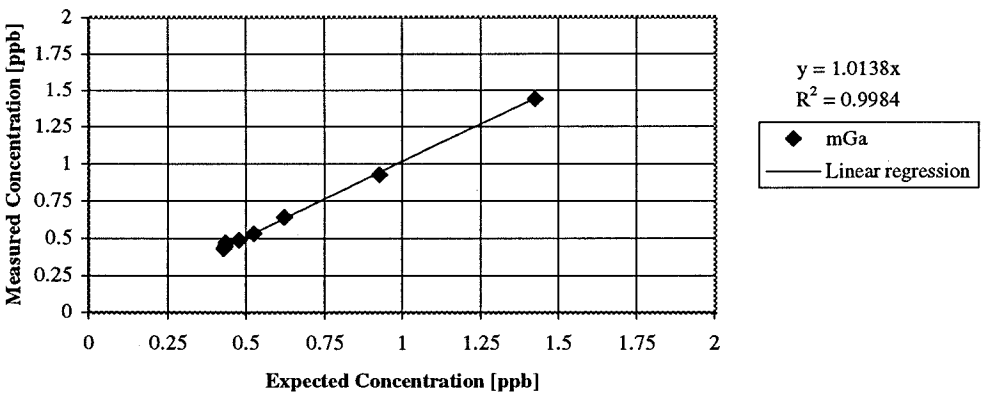

Standard Addition Test for Rb in San Joaquin River Water

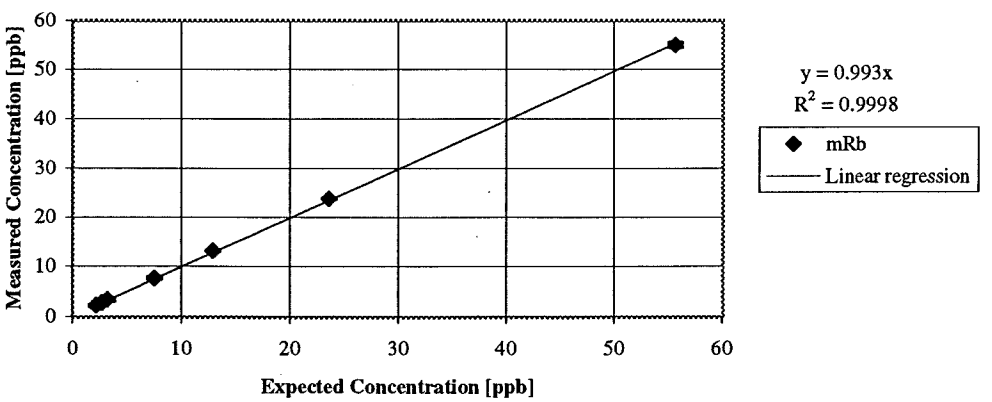

Standard Addition Test for Sr in San Joaquin River Water

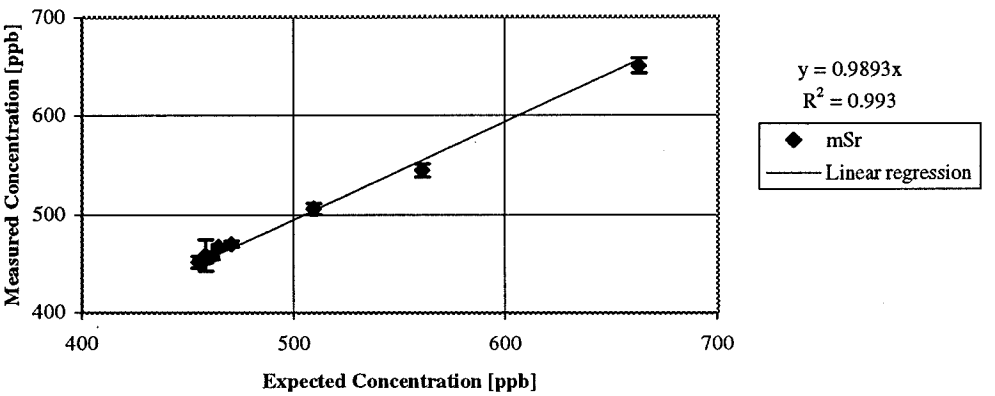

Standard Addition Test for Y in San Joaquin River Water

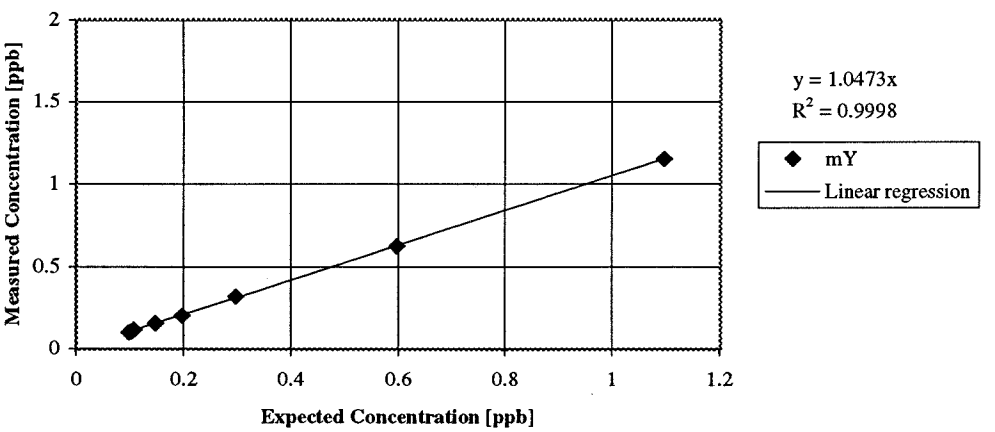

Standard Addition Test for Mo in San Joaquin River Water

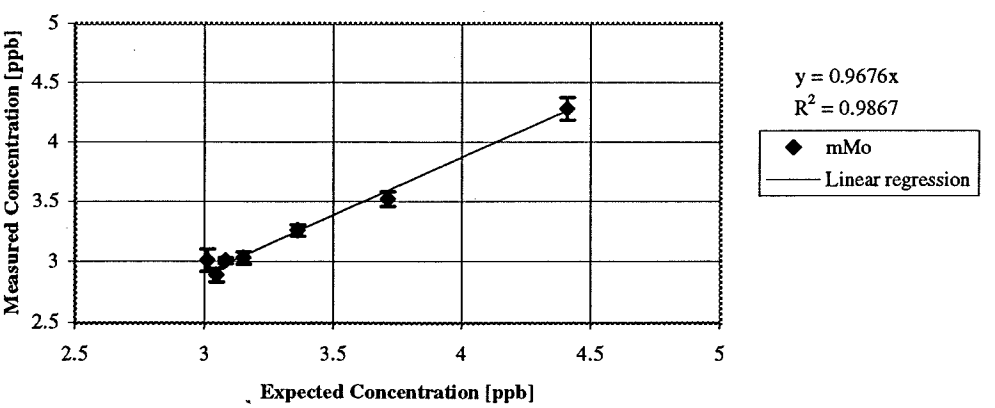

Standard Addition Test for Cd in San Joaquin River Water

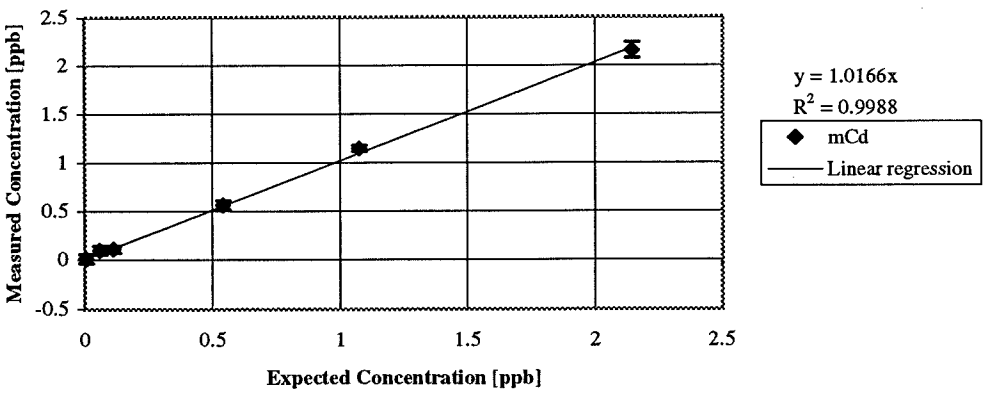

Standard Addition Test for Cs in San Joaquin River Water

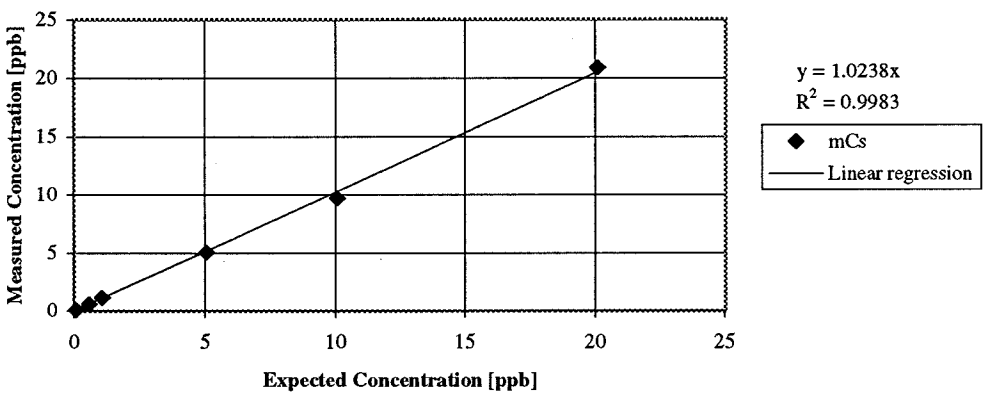

Standard Addition Test for Ba in San Joaquin River Water

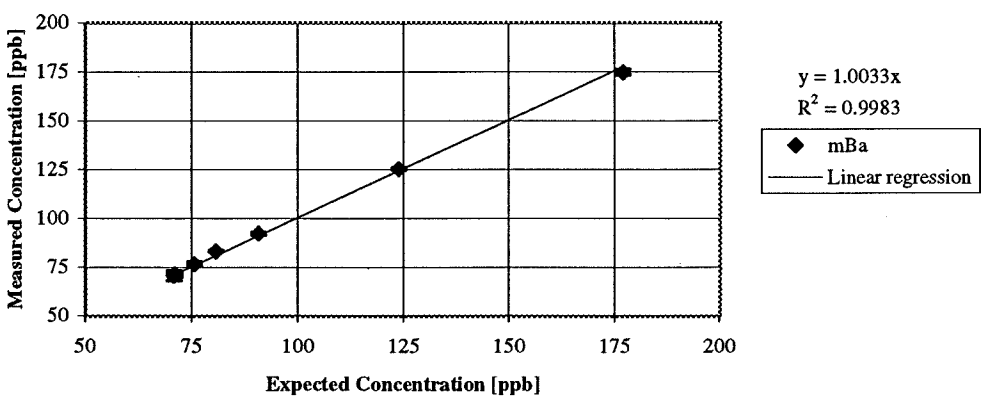

Standard Addition Test for La in San Joaquin River Water

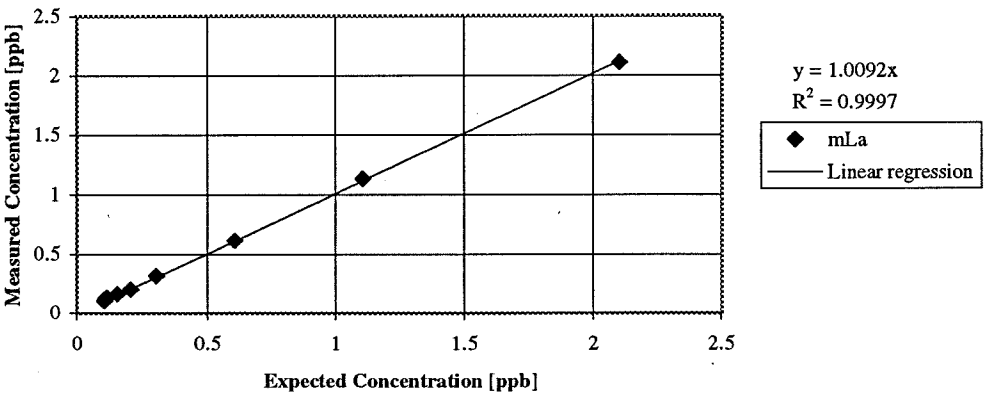

Standard Addition Test for Ce in San Joaquin River Water

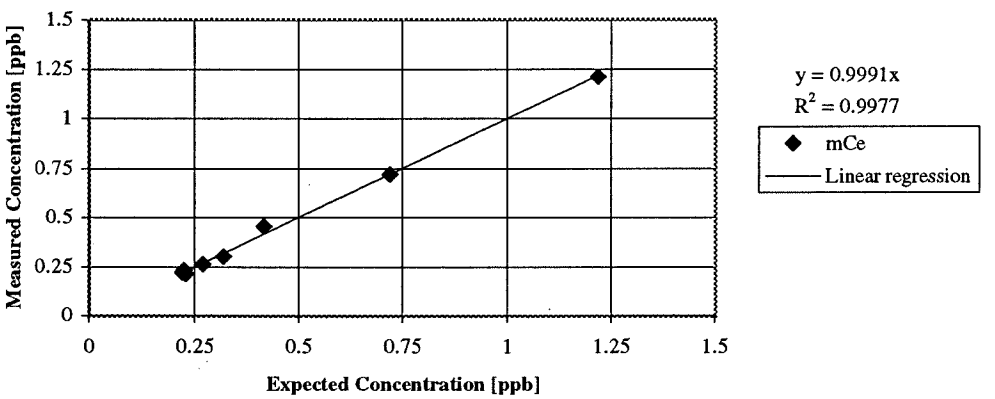

Standard Addition Test for Pr in San Joaquin River Water

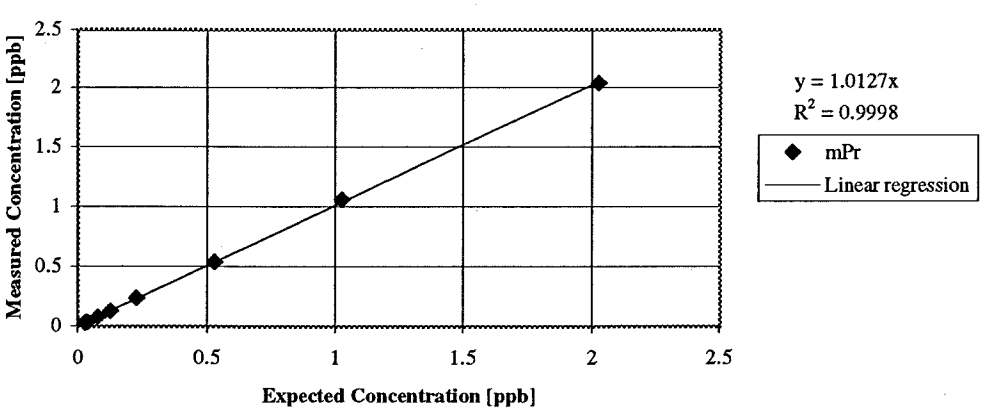

Standard Addition Test for Nd in San Joaquin River Water

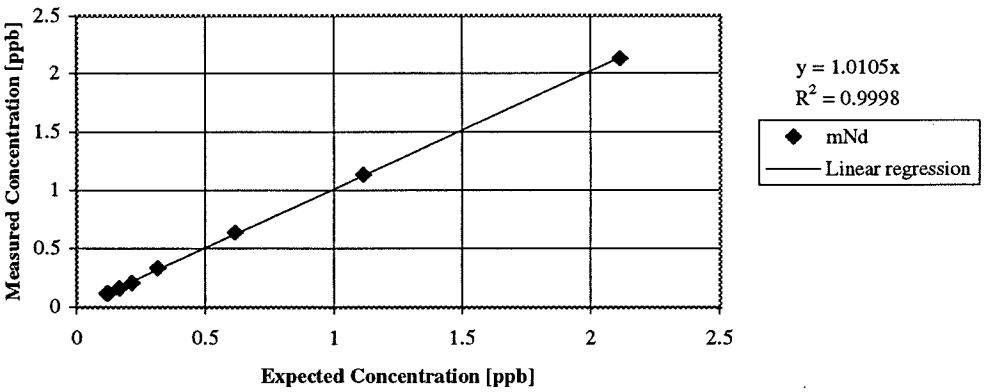

Standard Addition Test for Sm in San Joaquin River Water

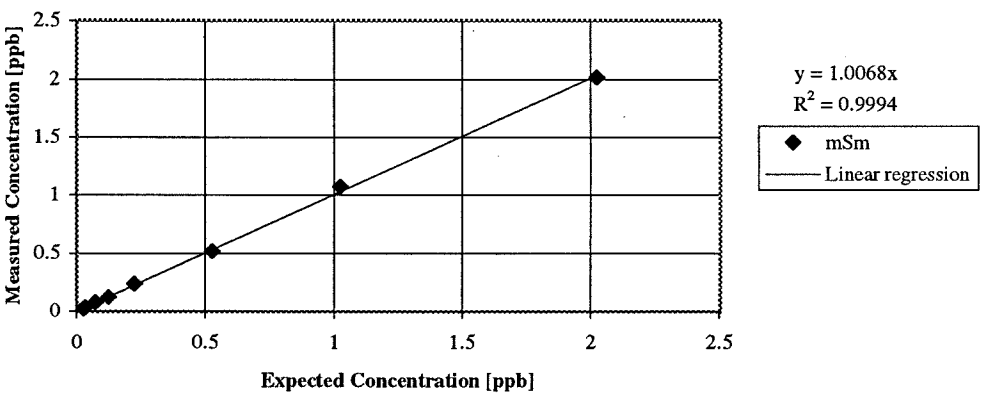

Standard Addition Test for Eu in San Joaquin River Water

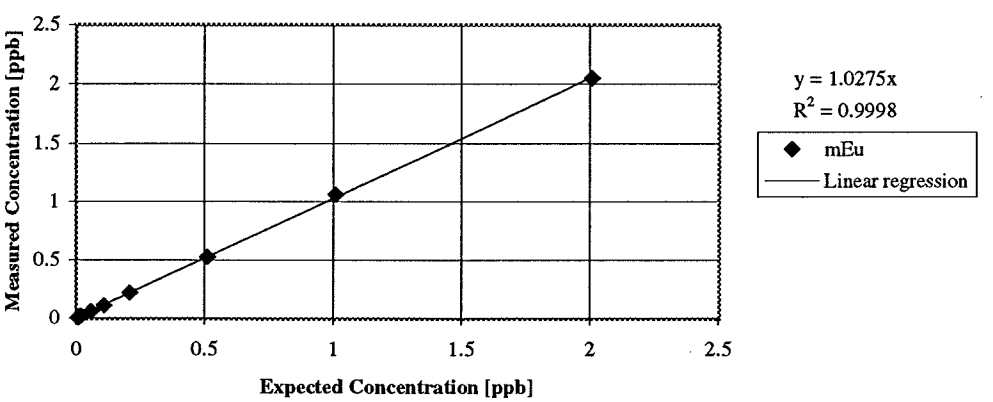

Standard Addition Test for Gd in San Joaquin River Water

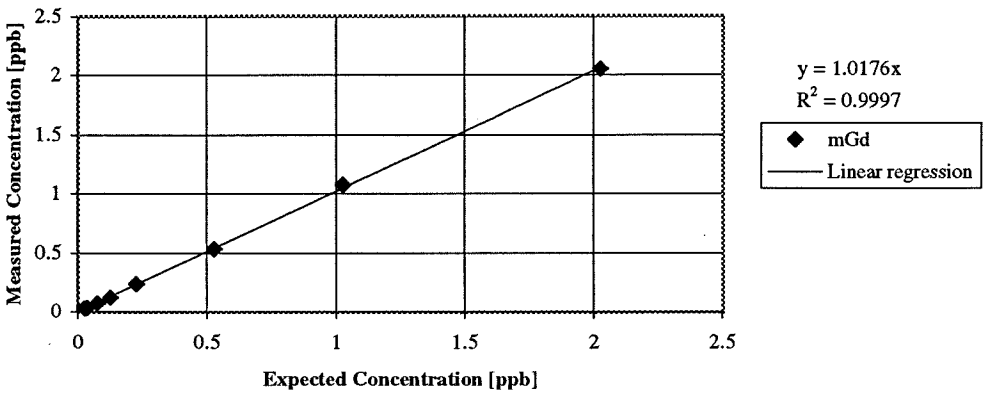

Standard Addition Test for Tb in San Joaquin River Water

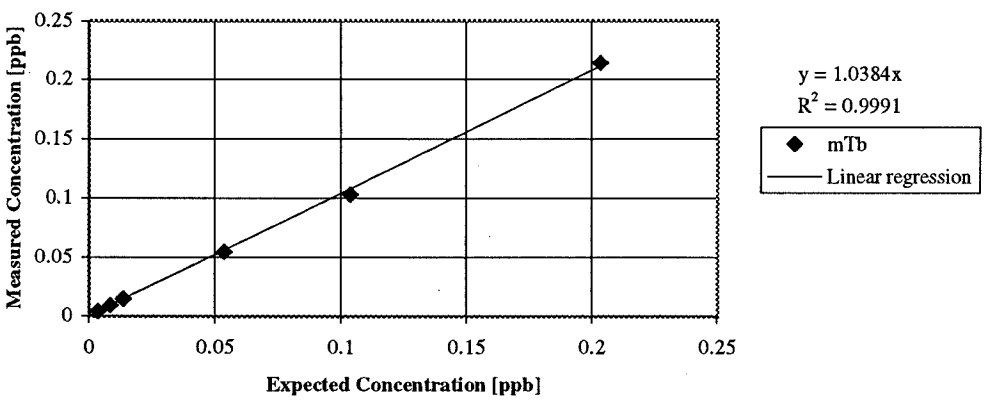

Standard Addition Test for Dy in San Joaquin River Water

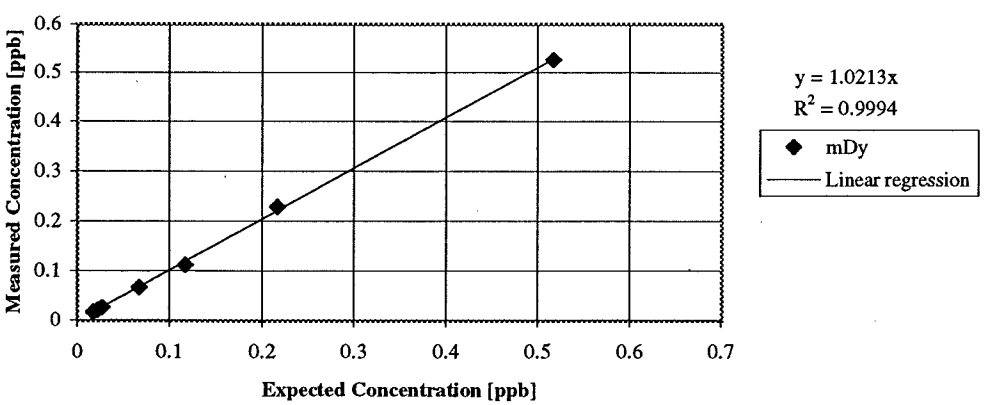

Standard Addition Test for Ho in San Joaquin River Water

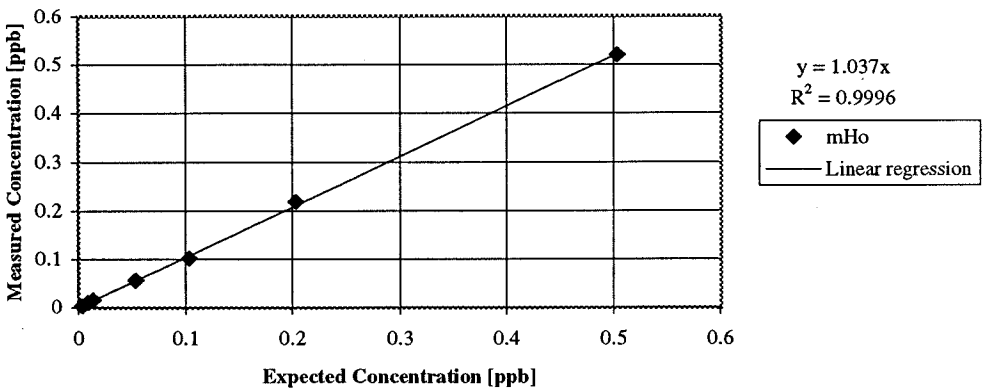

Standard Addition Test for Er in San Joaquin River Water

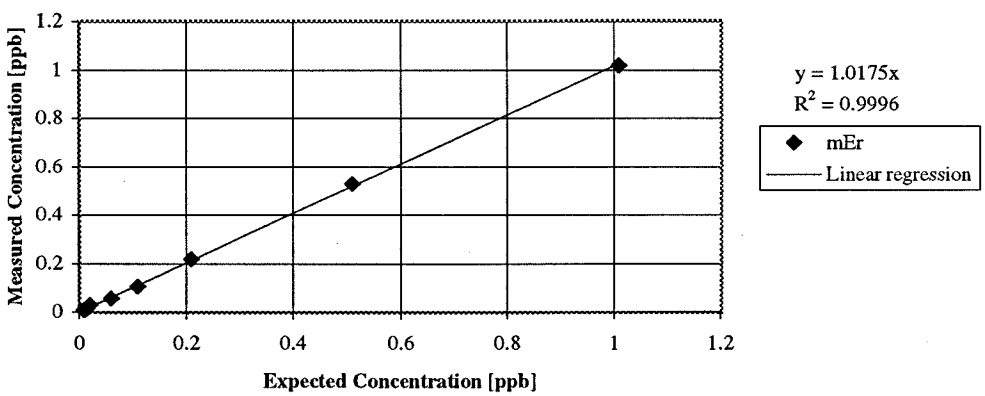

Standard Addition Test for Yb in San Joaquin River Water

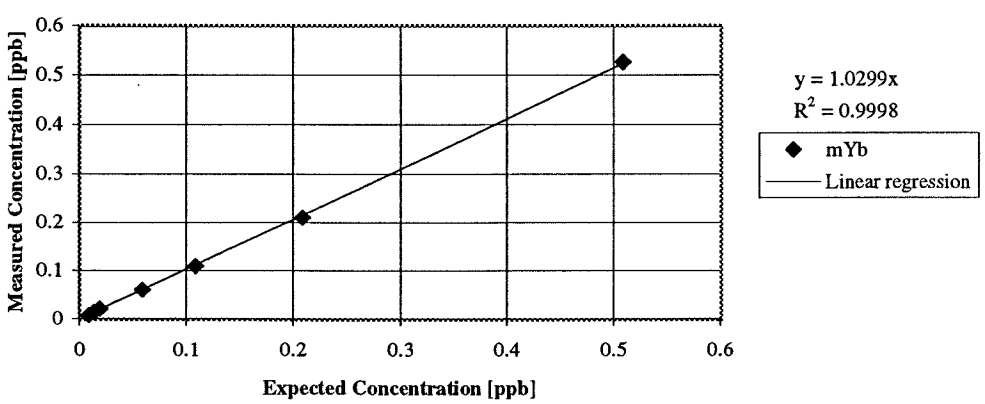

Standard Addition Test for Lu in San Joaquin River Water

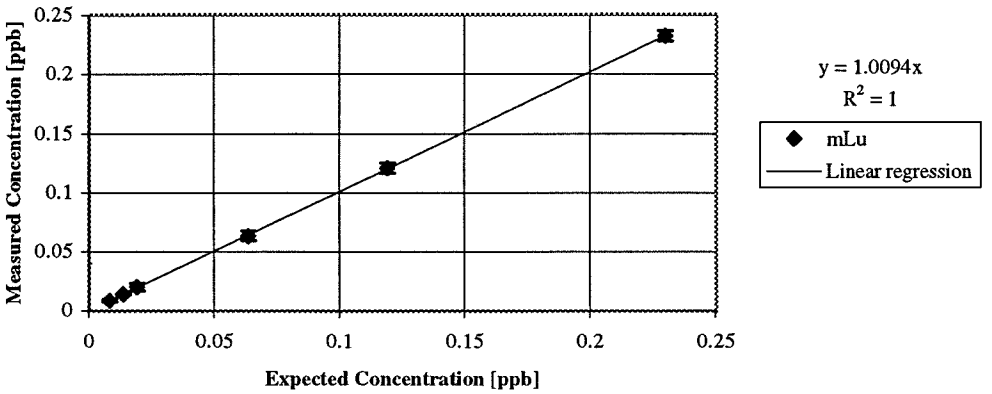

Standard Addition Test for Th in San Joaquin River Water

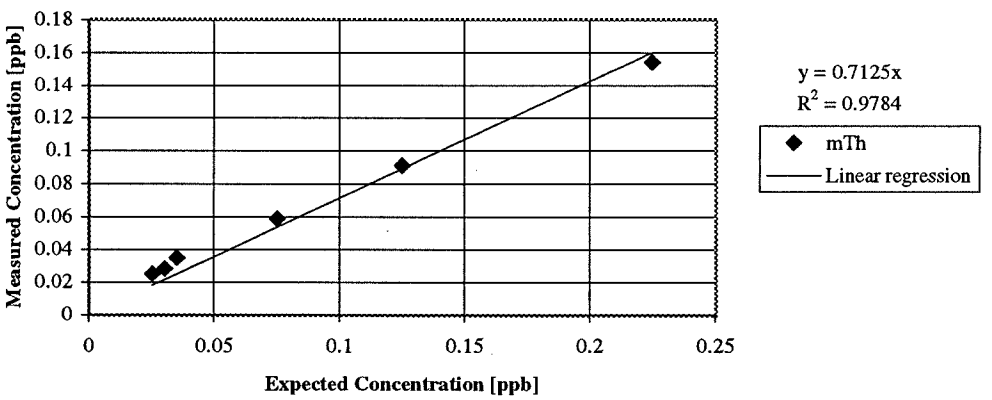

Standard Addition Test for U in San Joaquin River Water

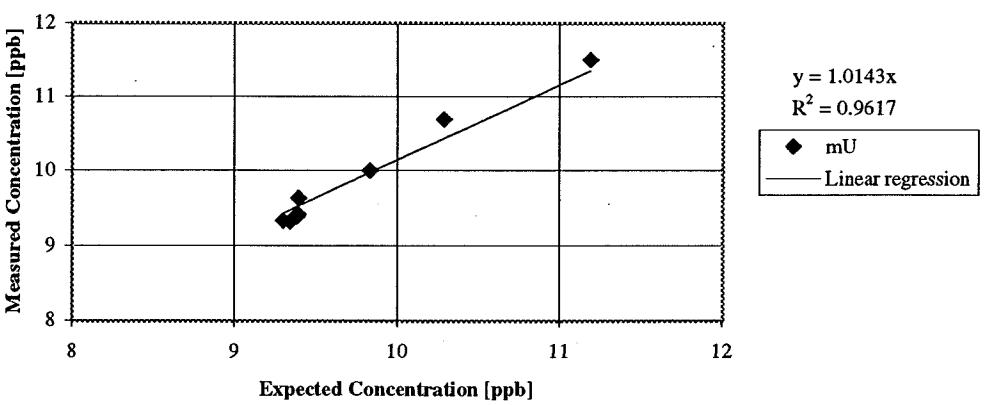

Standard Addition Test for Li in Water from Martinez

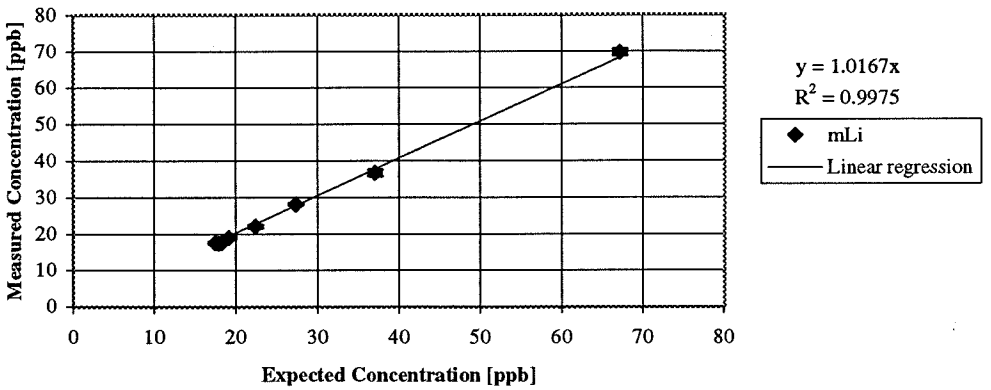

Standard Addition Test for B in Water from Martinez

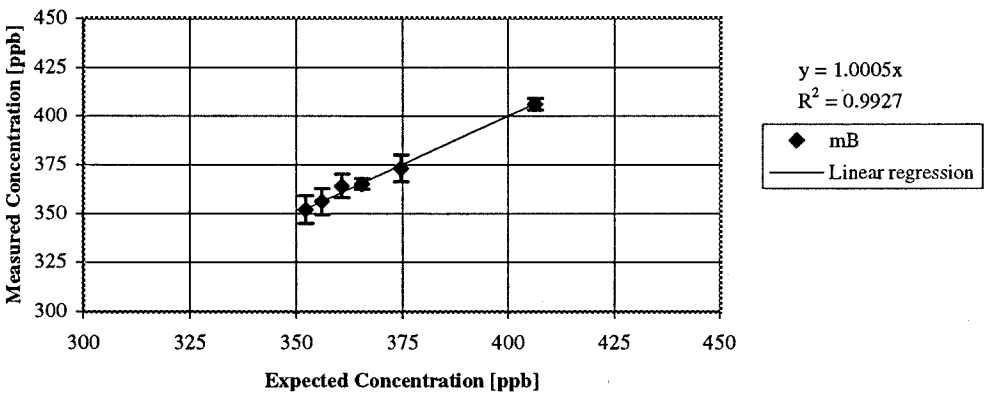

Standard Addition Test for Mg in 100:1 Water from Martinez

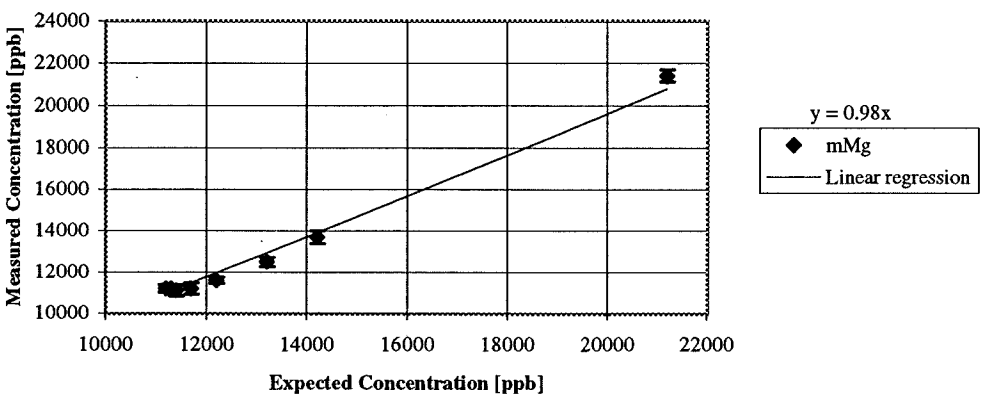

Standard Addition Test for Si in 10:1 Water from Martinez

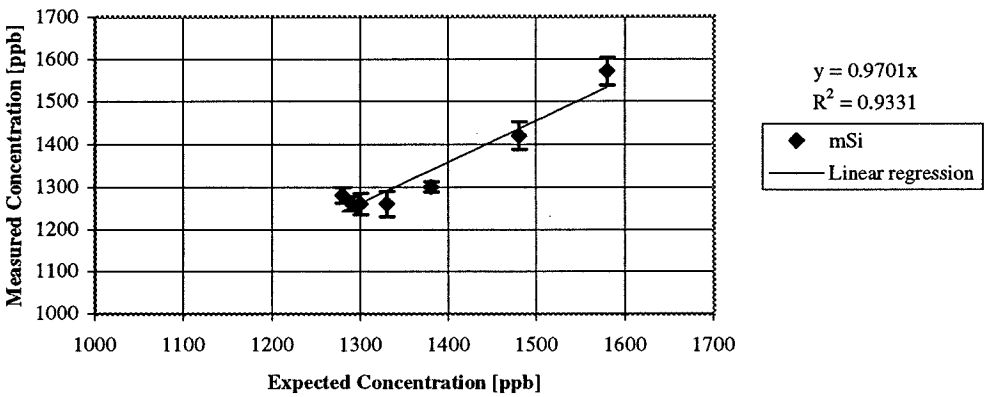

Standard Addition Test for K in 100:1 Water from Martinez

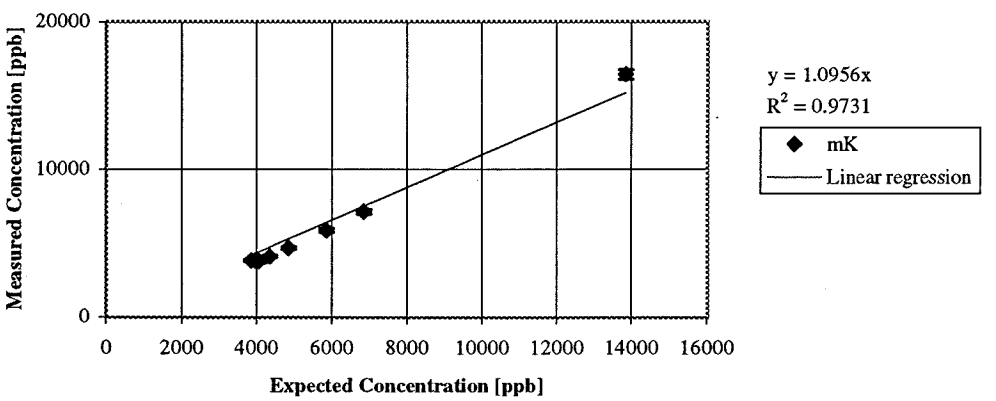

Standard Addition Test for Ca in 100:1 Water from Martinez

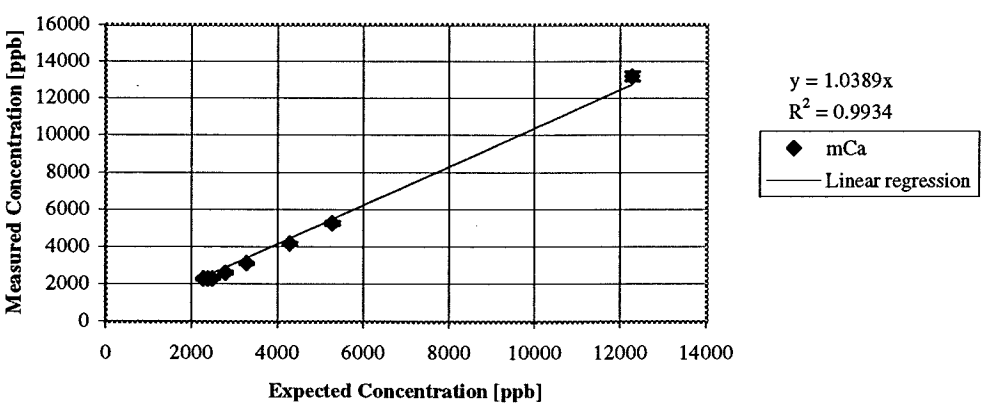

Standard Addition Test for V in Water from Martinez

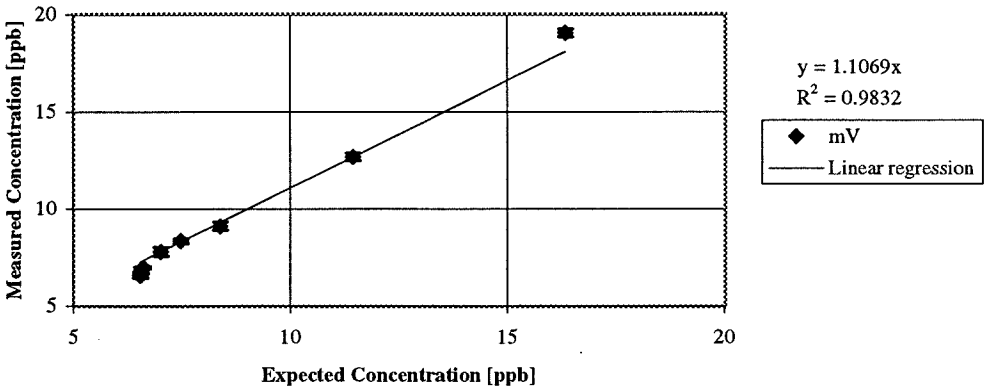

Standard Addition Test for Cr in Water from Martinez

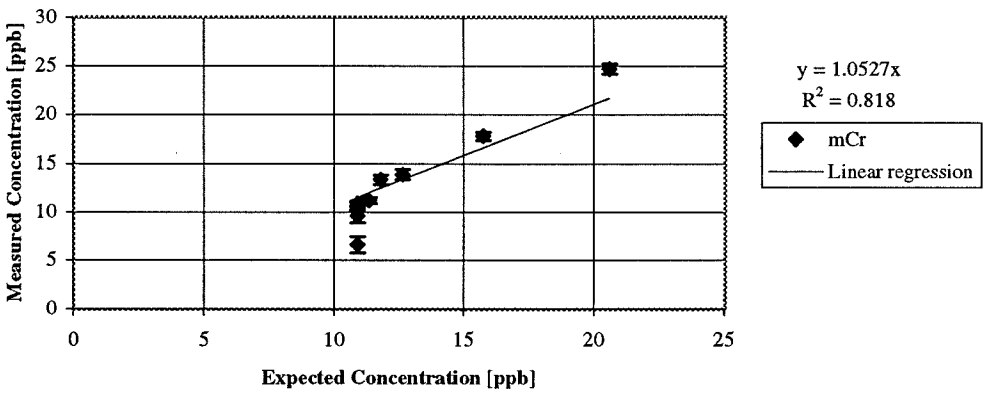

Standard Addition Test for Fe in 10:1 Water from Martinez

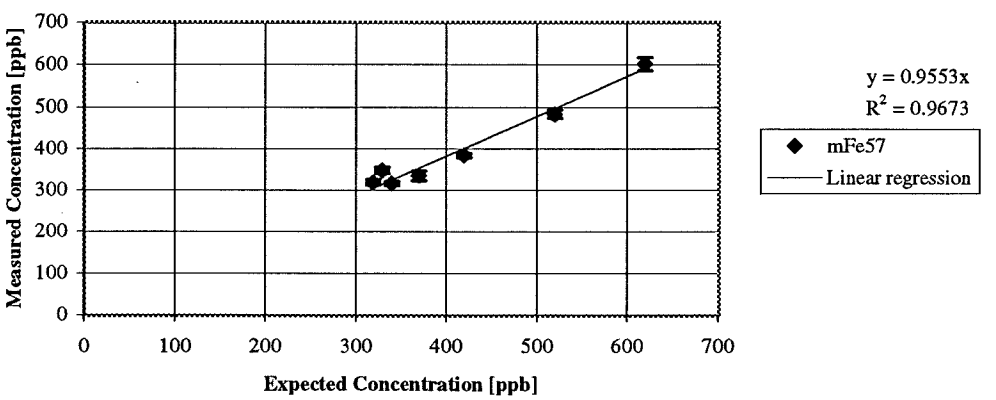

Standard Addition Test for Mn in 10:1 Water from Martinez

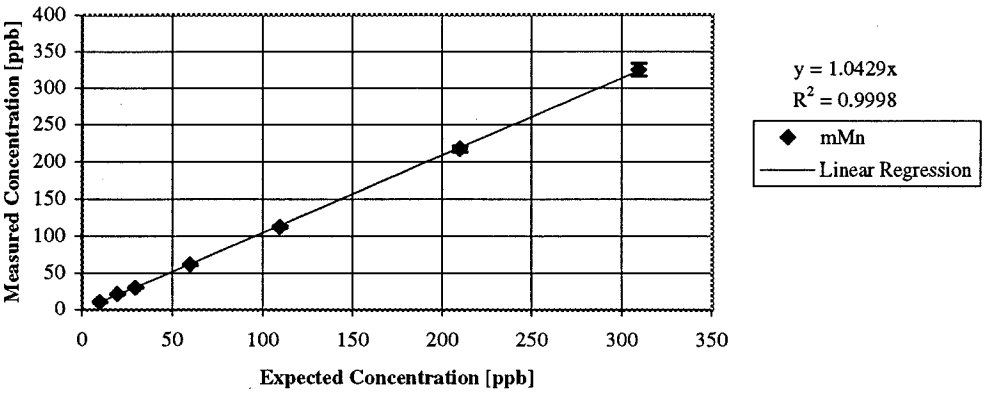

Standard Addition Test for Co in Water from Martinez

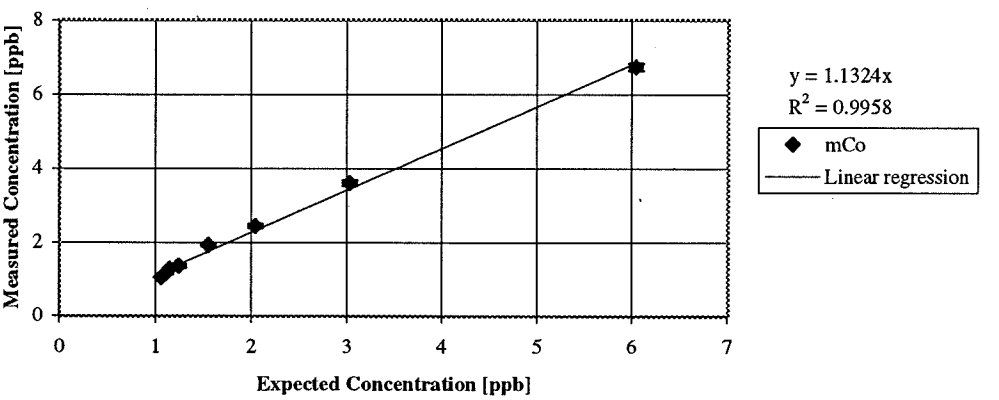

Standard Addition Test for Ni in Water from Martinez

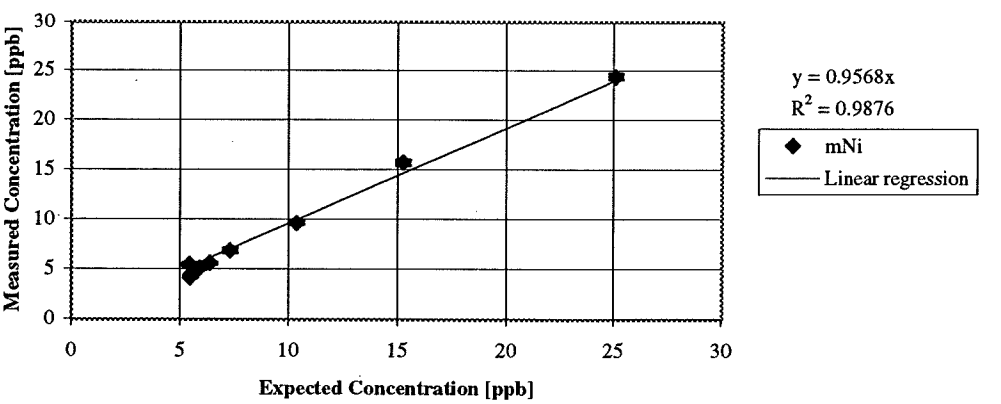

Standard Addition Test for Cu63 in Water from Martinez

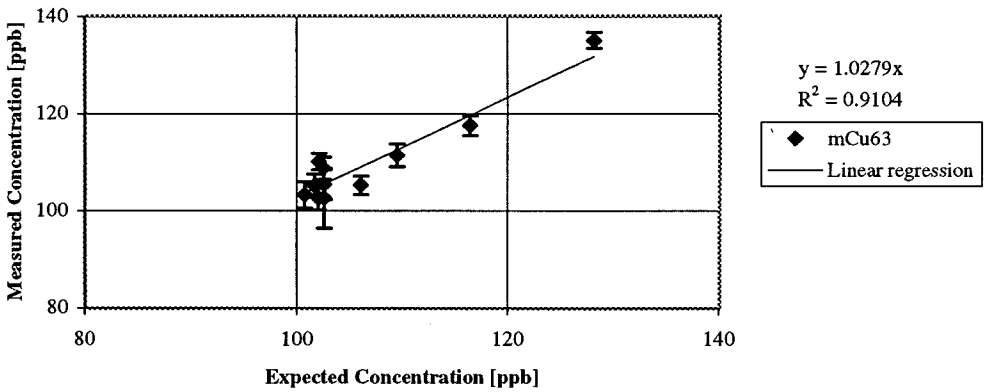

Standard Addition Test for Cu65 in Water from Martinez

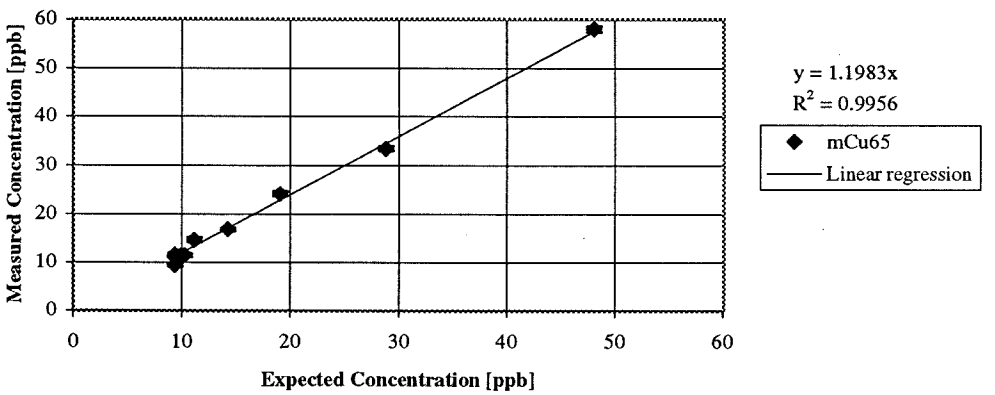

Standard Addition Test for Zn in Water from Martinez

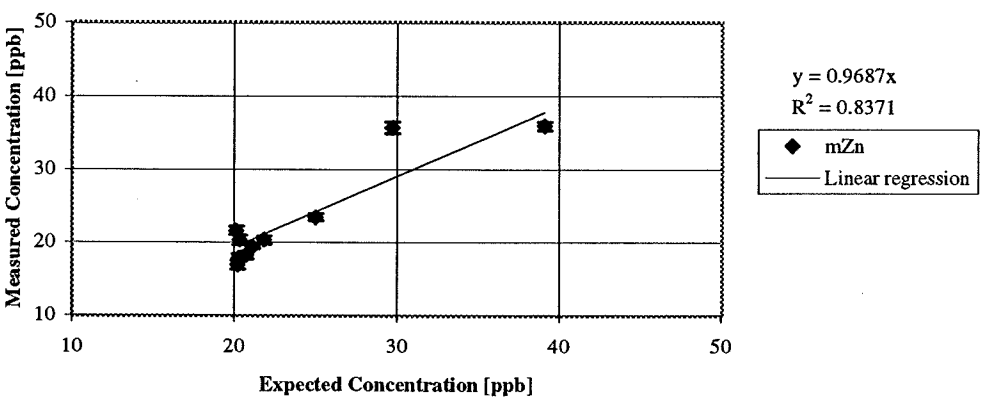

Standard Addition Test for Ga in Water from Martinez

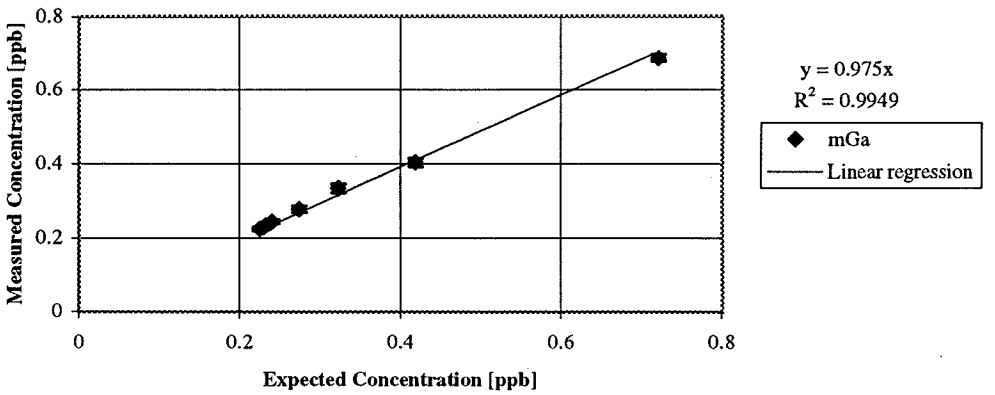

Standard Addition Test for Rb in Water from Martinez

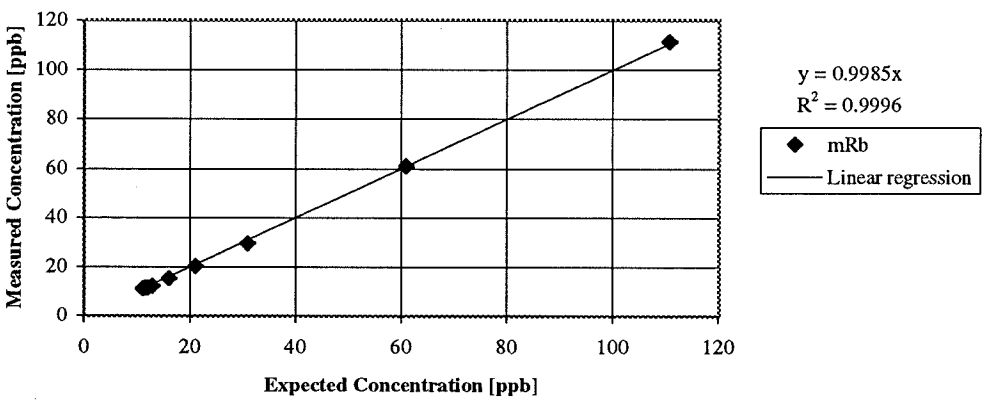

Standard Addition Test for Sr in Water from Martinez

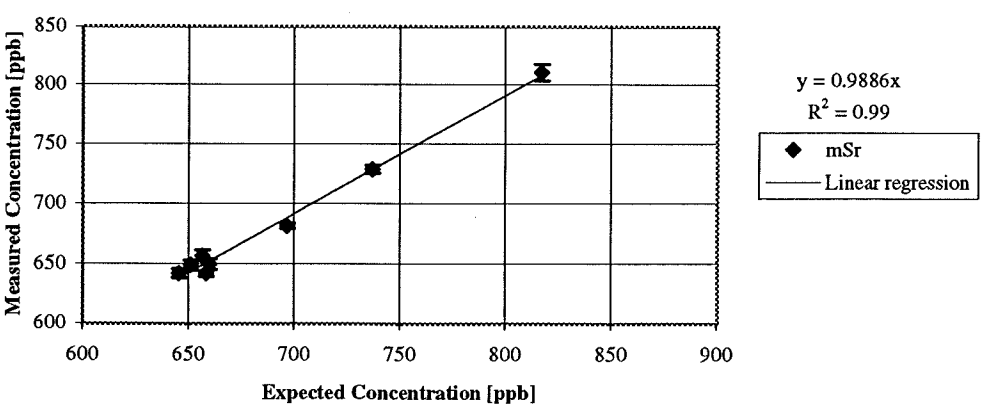

Standard Addition Test for Y in Water from Martinez

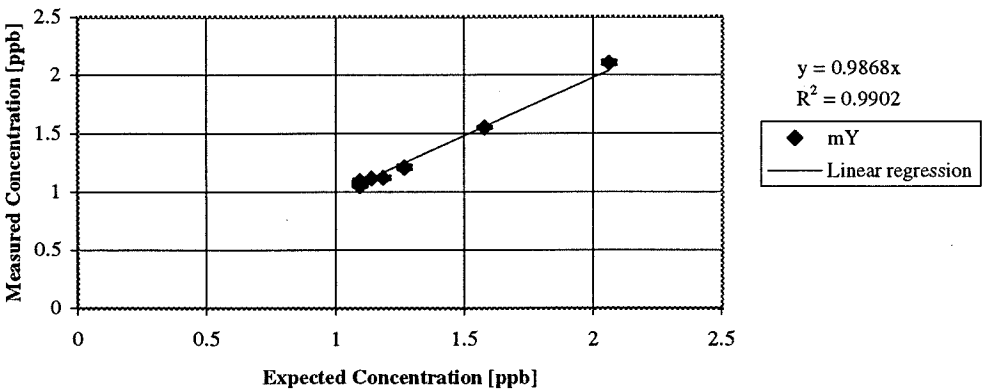

Standard Addition Test for Mo in Water from Martinez

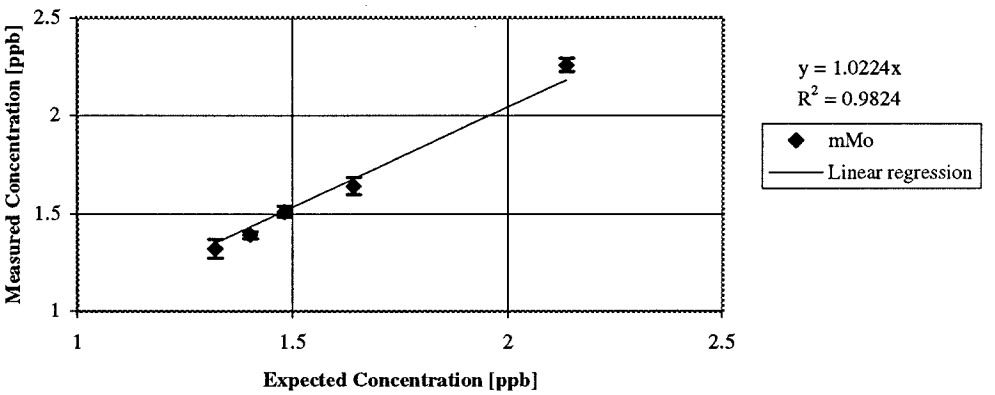

Standard Addition Test for Cd in Water from Martinez

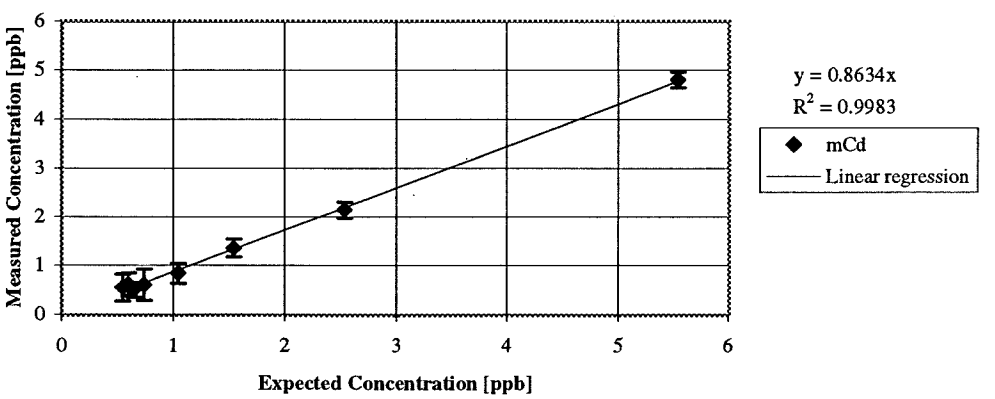

Standard Addition Test for Cs in Water from Martinez

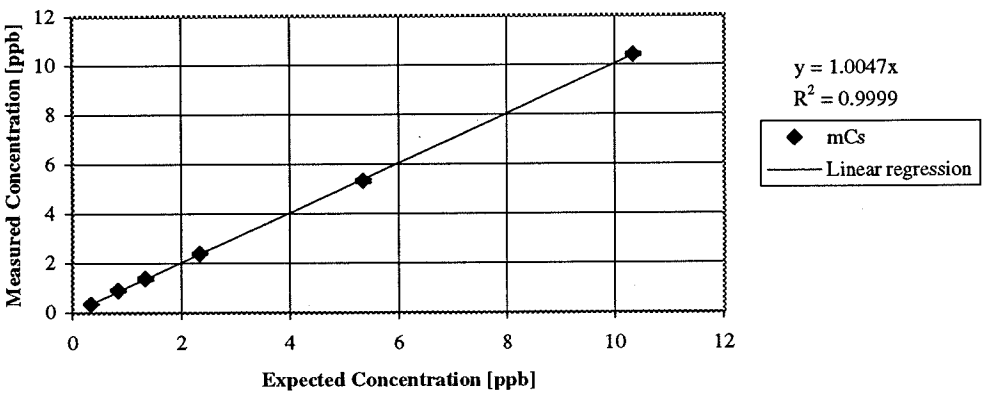

Standard Addition Test for Ba in Water from Martinez

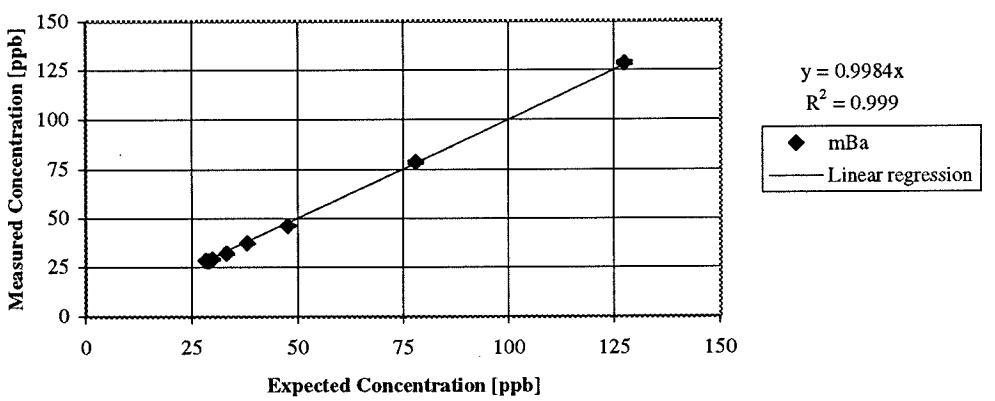

Standard Addition Test for La in Water from Martinez

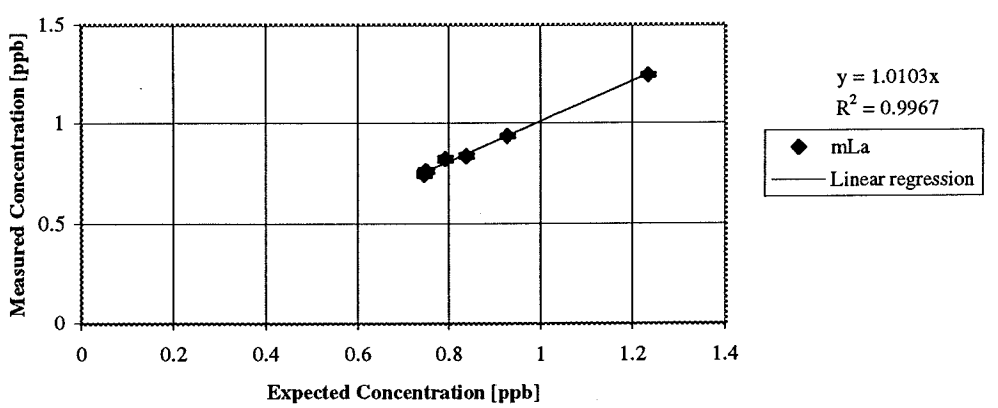

Standard Addition Test for Ce in Water from Martinez

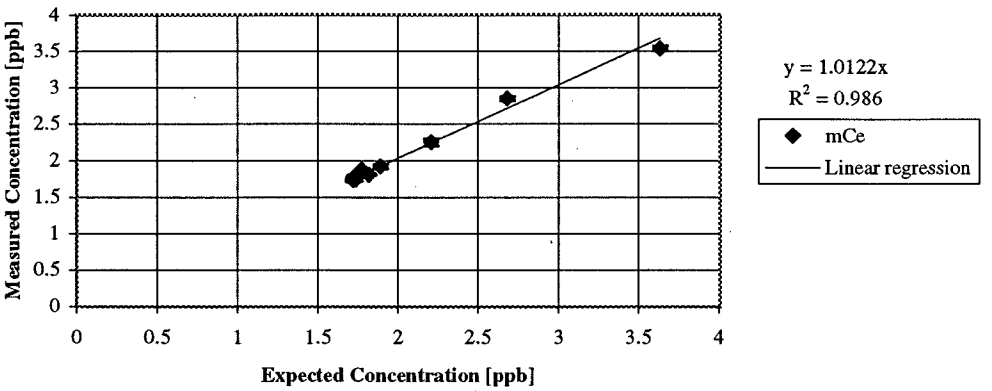

Standard Addition Test for Pr in Water from Martinez

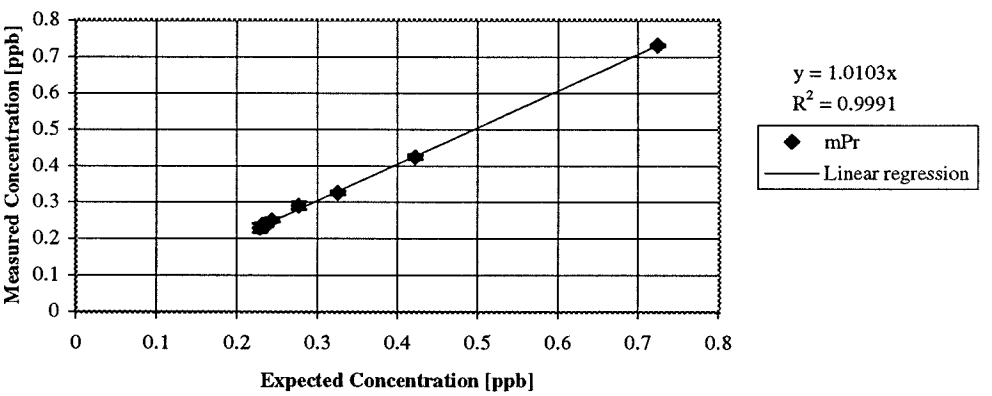

Standard Addition Test for Nd in Water from Martinez

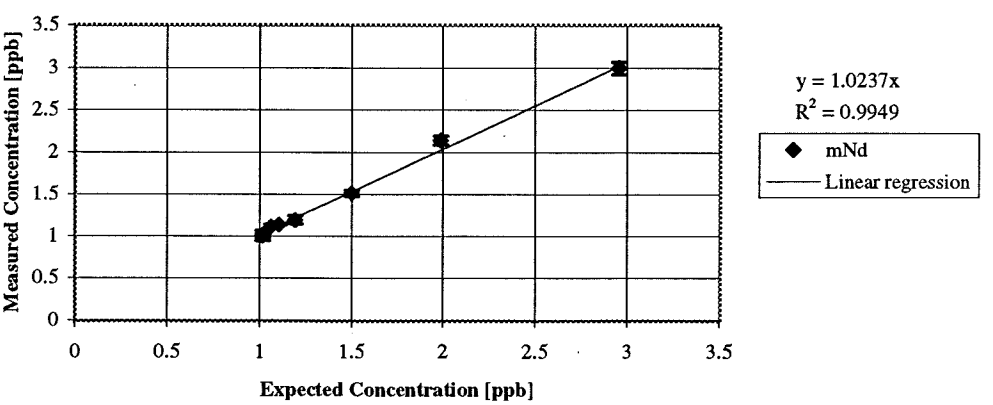

Standard Addition Test for Sm in Water from Martinez

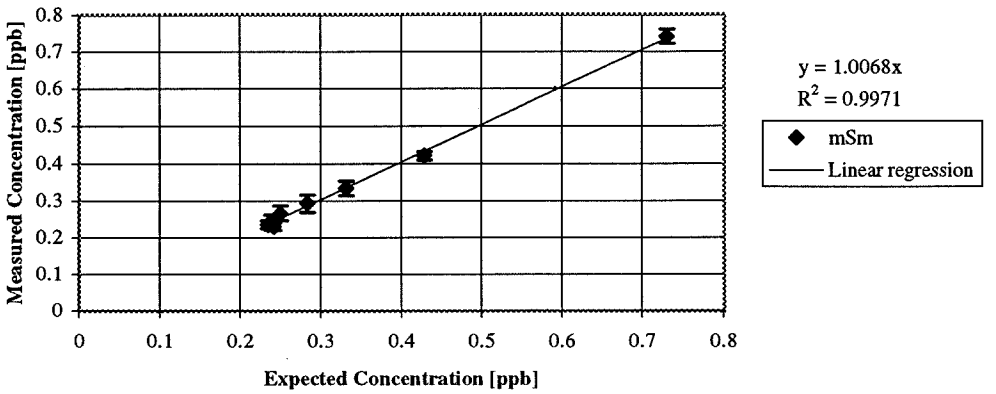

Standard Addition Test for Eu in Water from Martinez

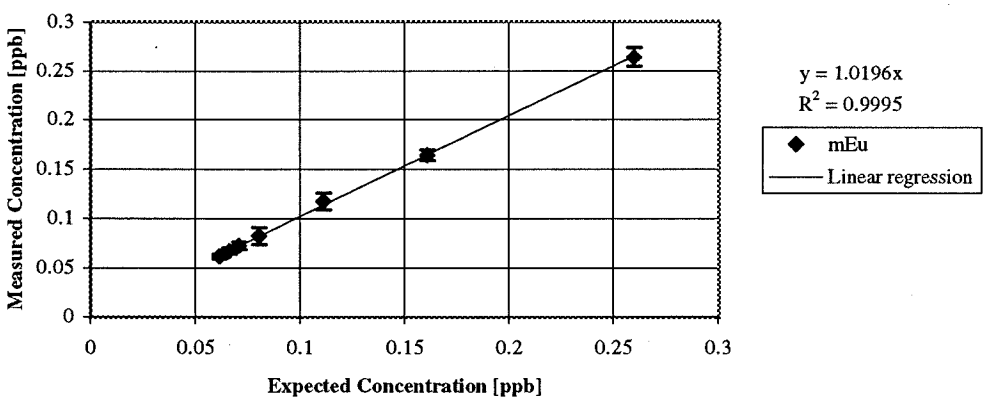

Standard Addition Test for Gd in Water from Martinez

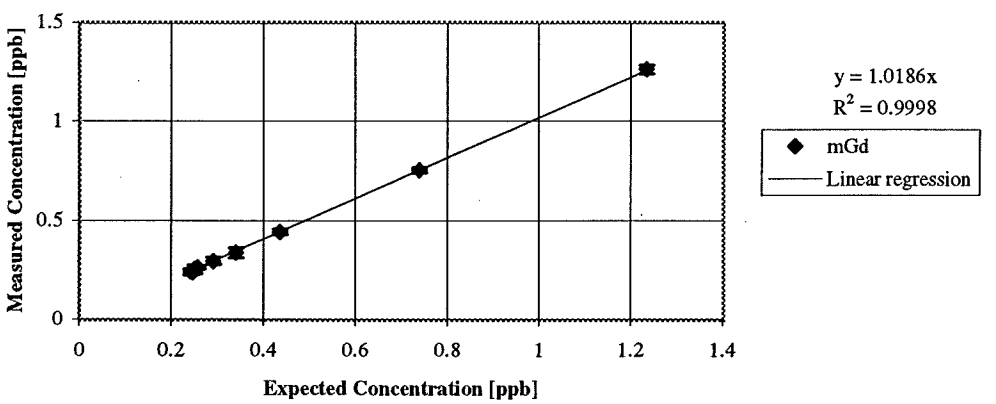

Standard Addition Test for Tb in Water from Martinez

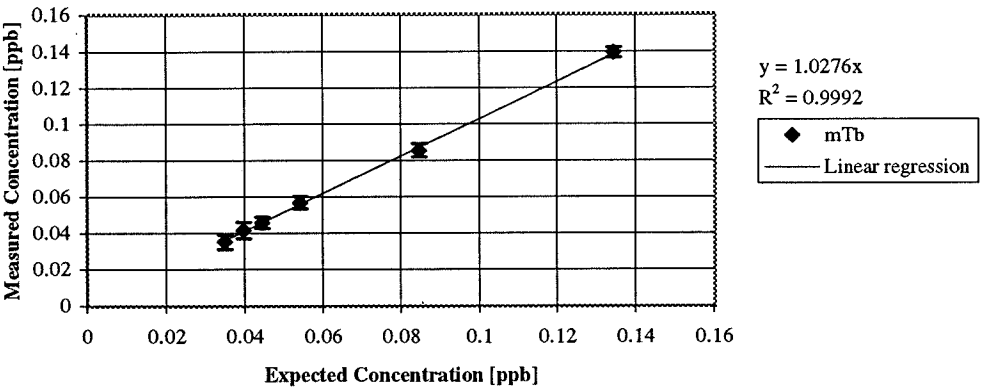

Standard Addition Test for Dy in Water from Martinez

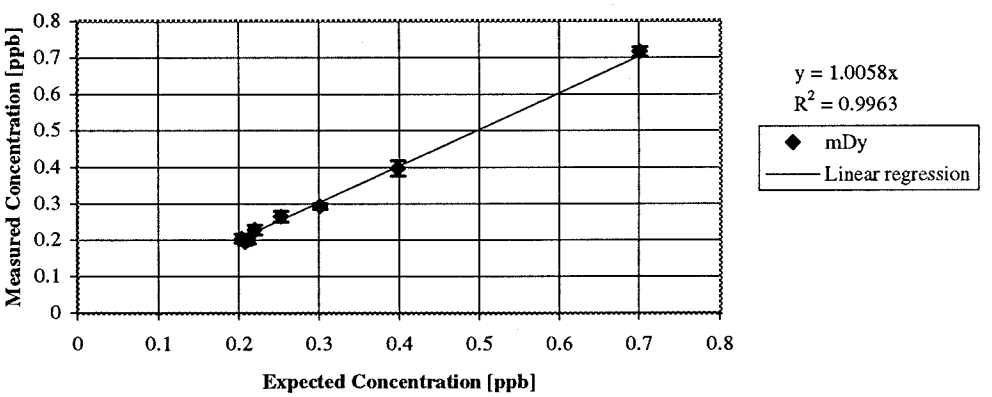

Standard Addition Test for Ho in Water from Martinez

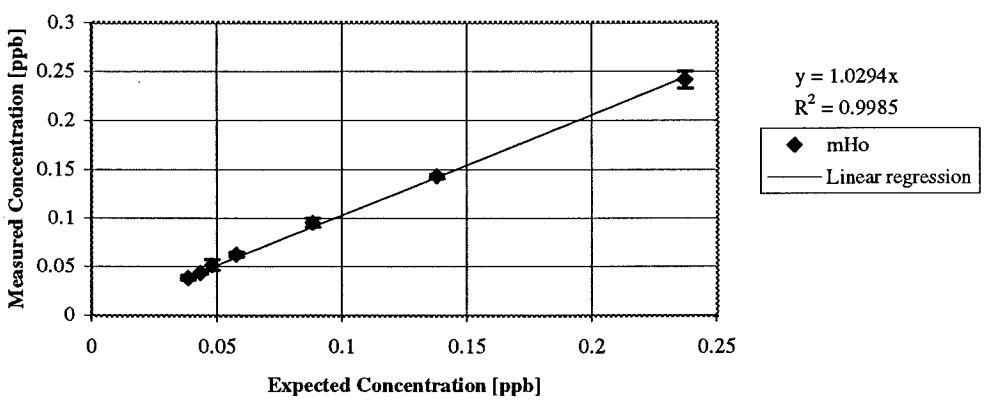

Standard Addition Test for Er in Water from Martinez

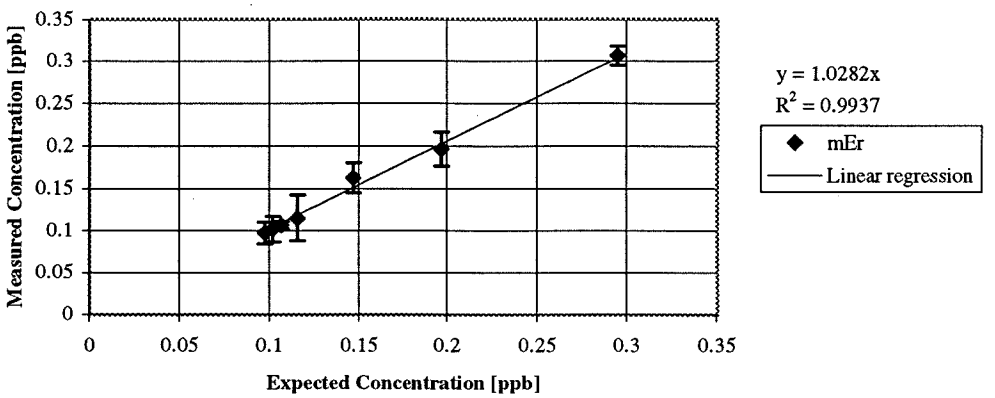

Standard Addition Test for Yb in Water from Martinez

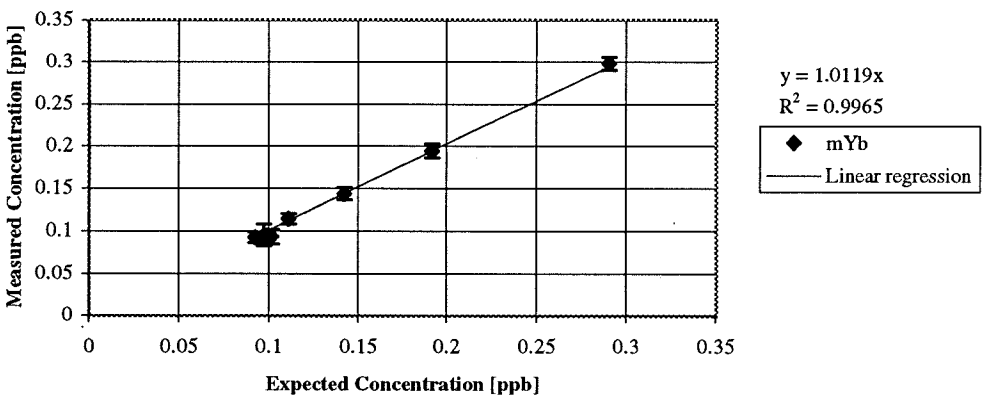

Standard Addition Test for Lu in Water from Martinez

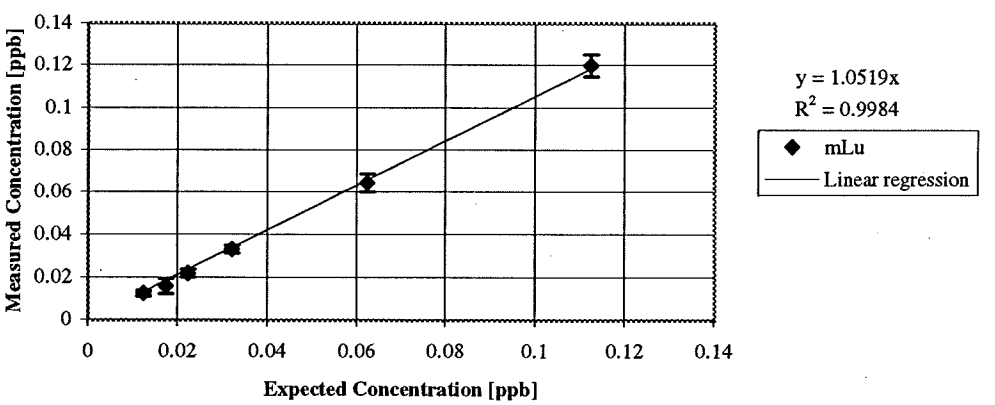

Standard Addition Test for Th in Water from Martinez

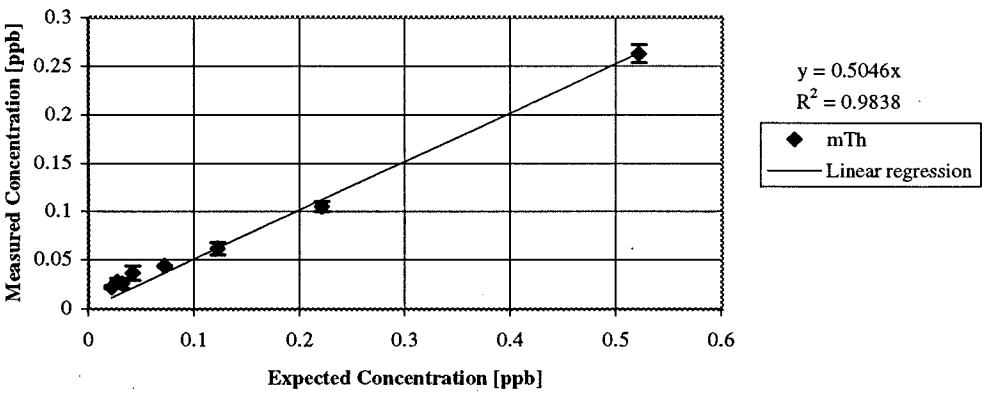

Standard Addition Test for U in Water from Martinez

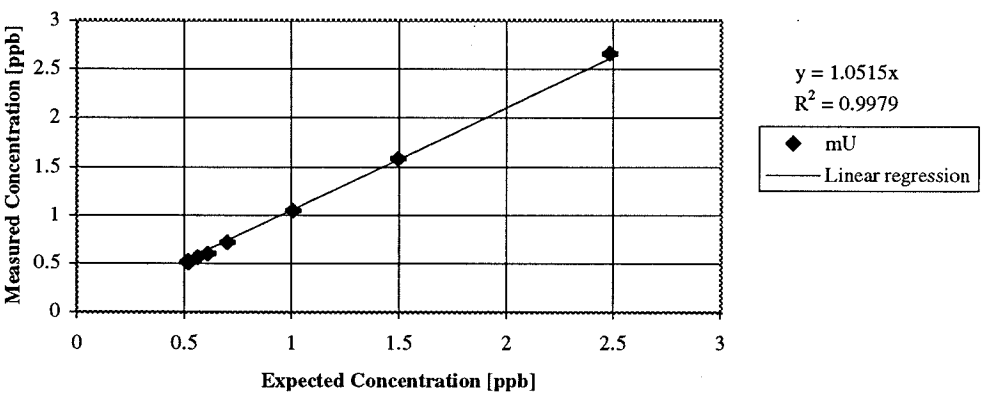

Standard Addition Test for Li in Water from Pinole

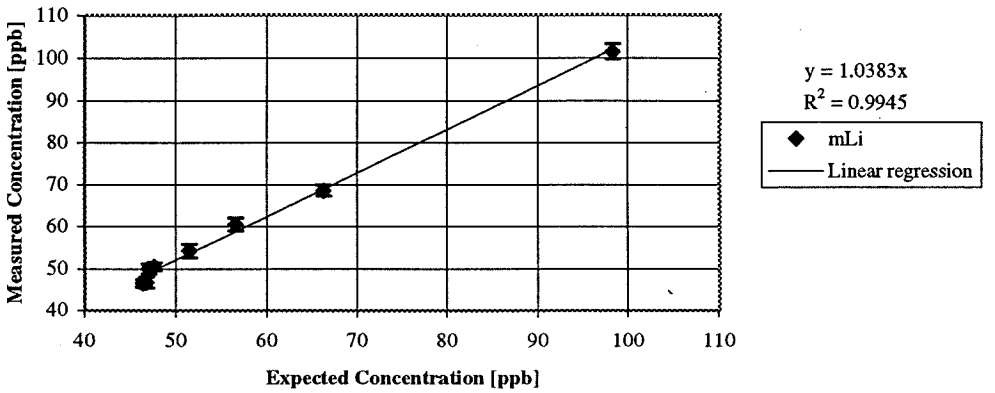

Standard Addition Test for B in Water from Pinole

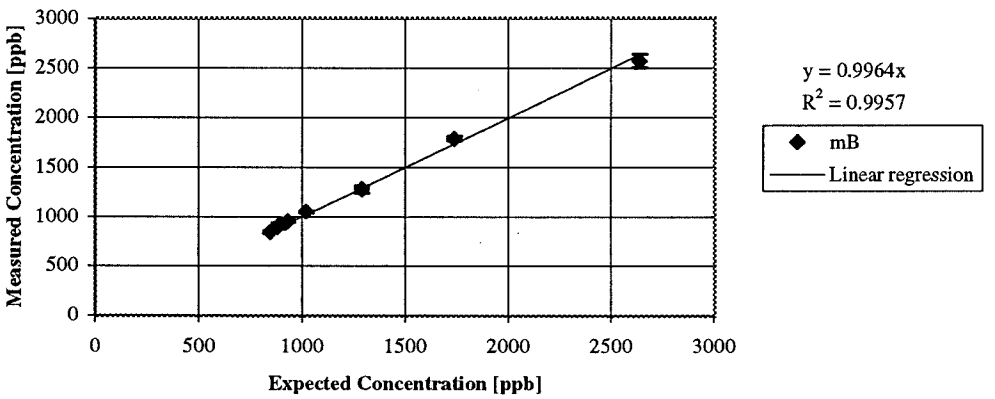

Standard Addition Test for Na in 200:1 Water from Pinole

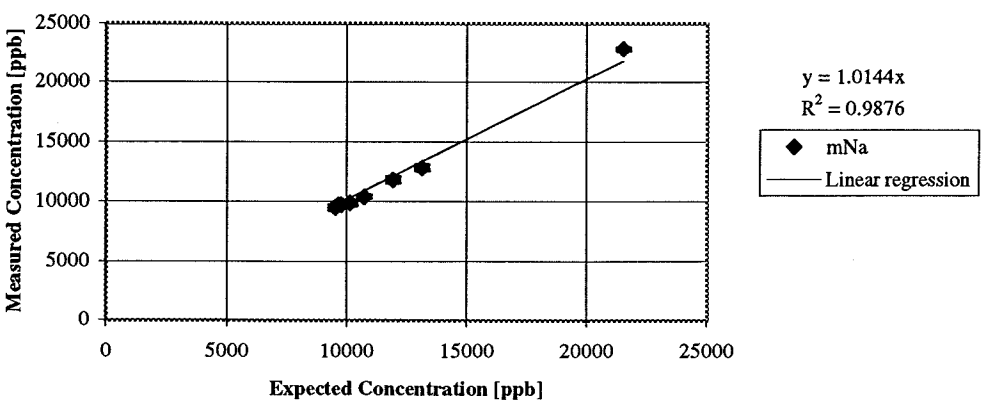

Standard Addition Test for Mg in 100:1 Water from Pinole

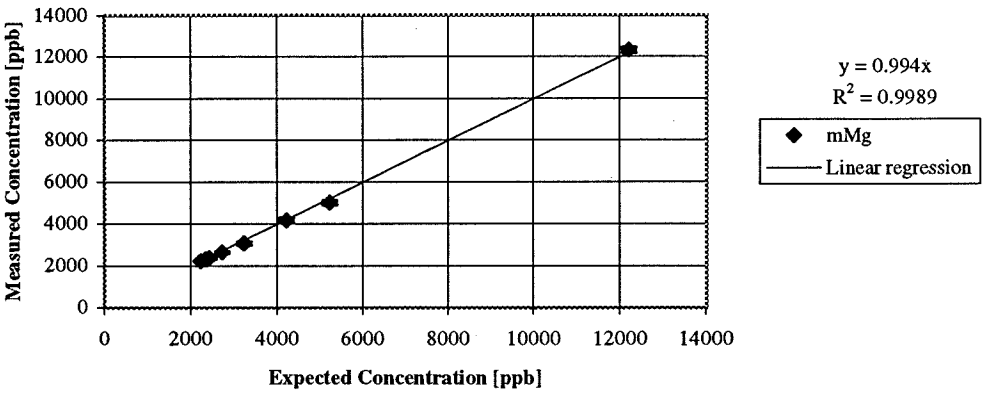

Standard Addition Test for K in 100:1 Water from Pinole

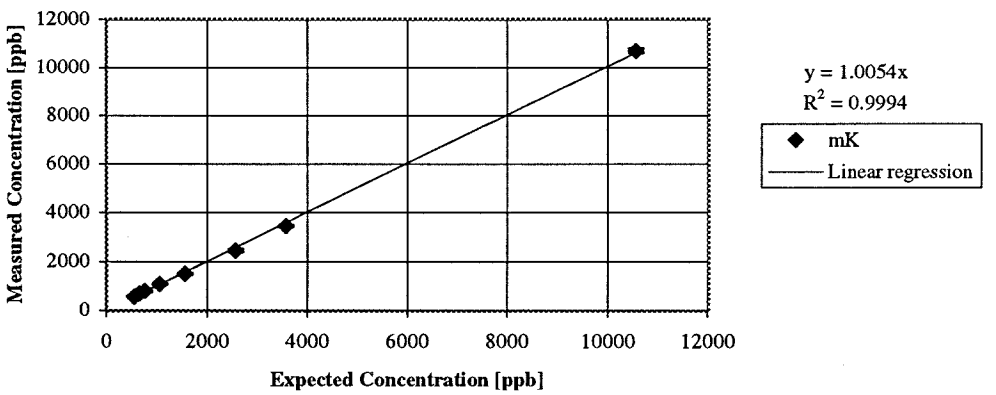

Standard Addition Test for Ca in 100:1 Water from Pinole

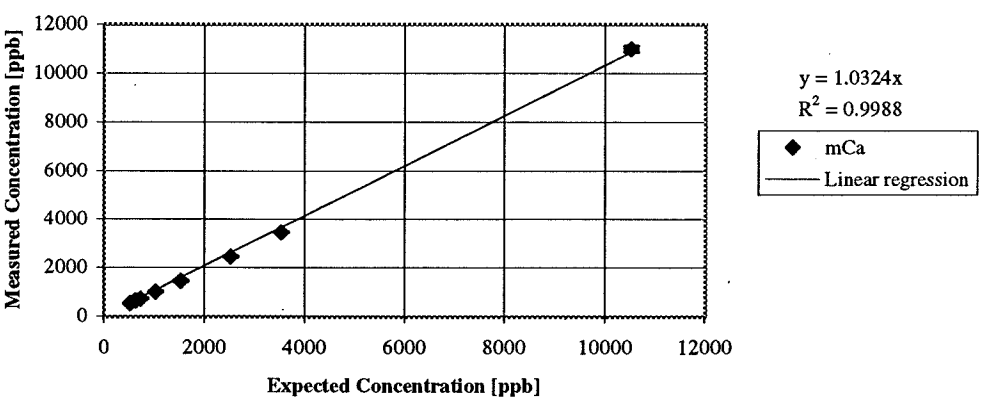

Standard Addition Test for V in Water from Pinole

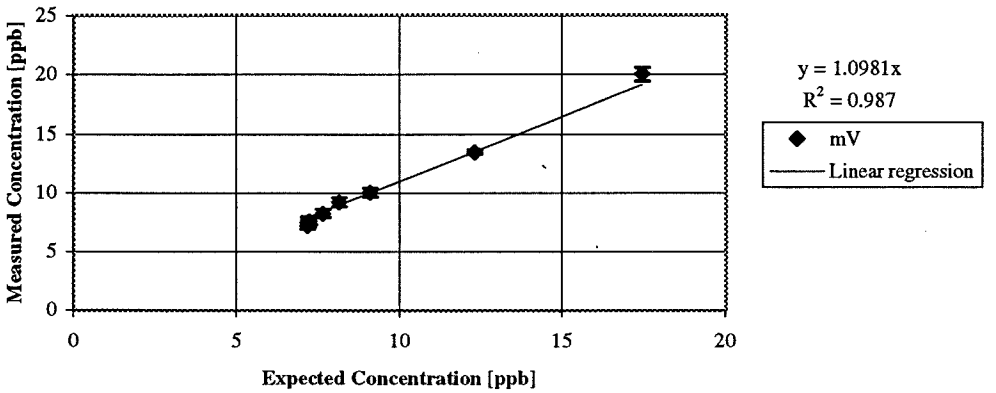

Standard Addition Test for Cr in Water from Pinole

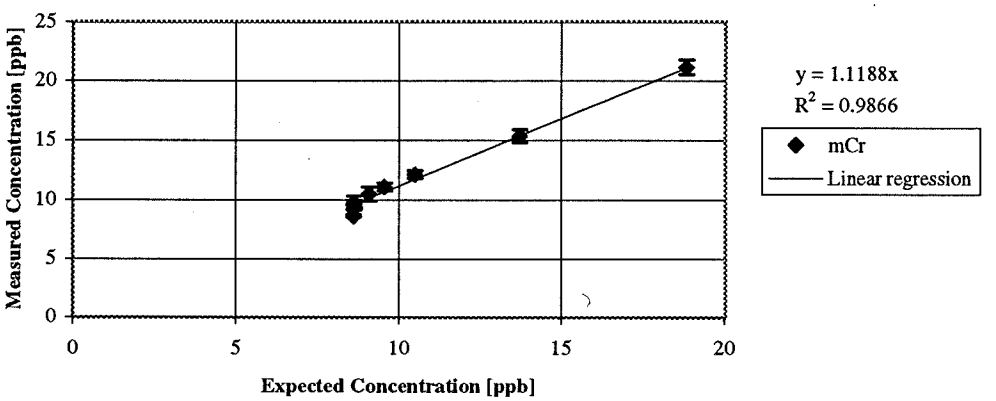

Standard Addition Test for Mn in Water from Pinole

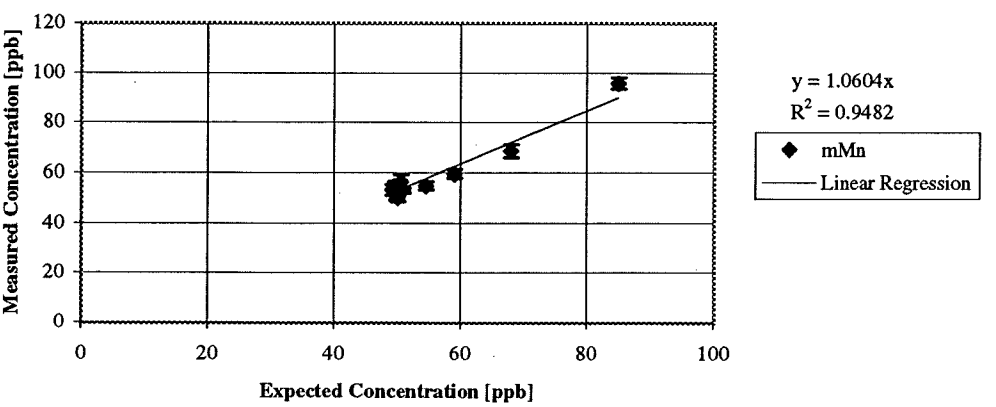

Standard Addition Test for Co in Water from Pinole

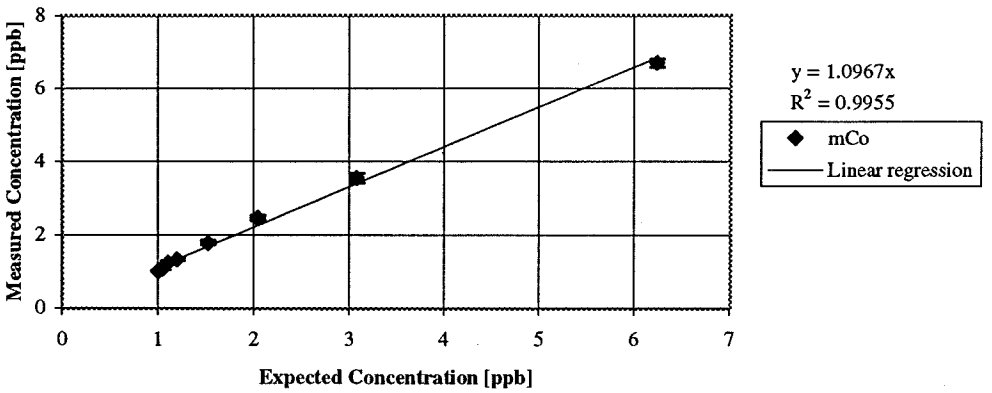

Standard Addition Test for Ni in Water from Pinole

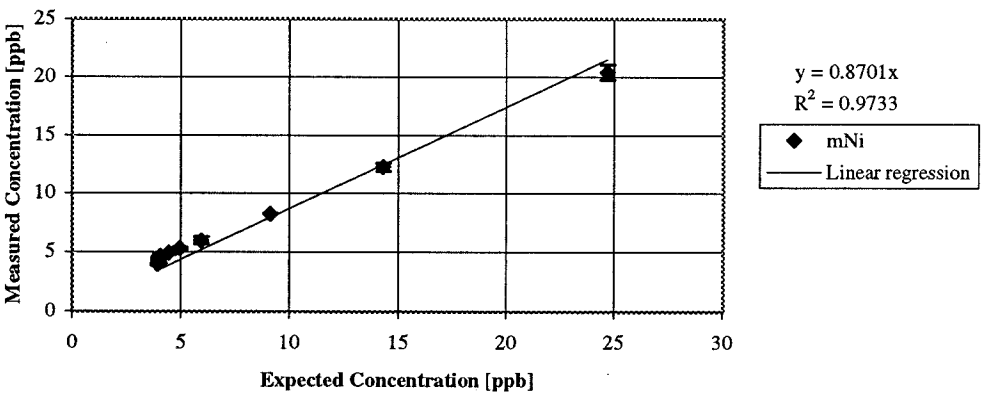

Standard Addition Test for Cu63 in Water from Pinole

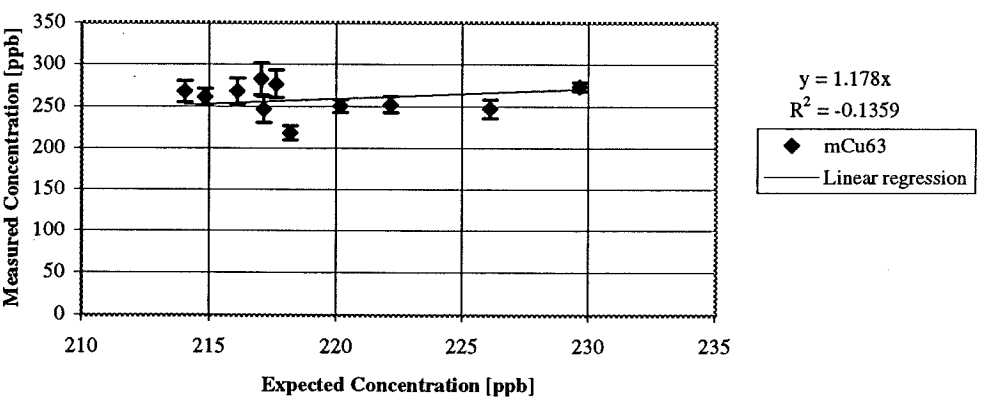

Standard Addition Test for Cu65 in Water from Pinole

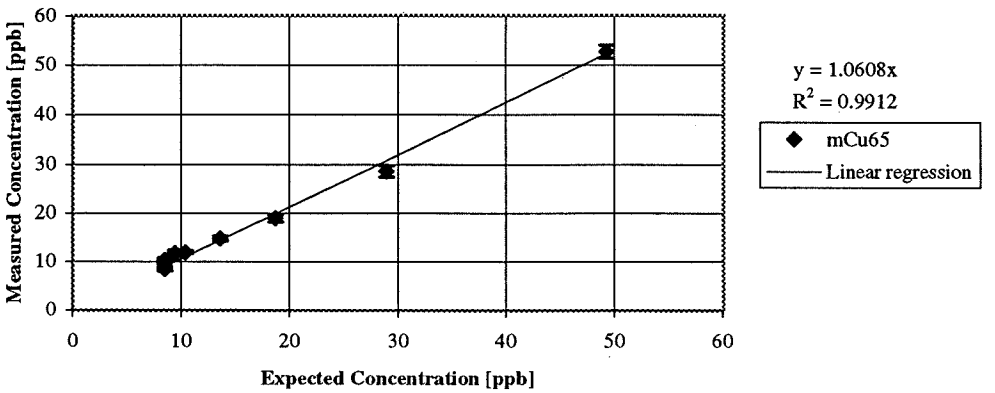

Standard Addition Test for Zn in Water from Pinole

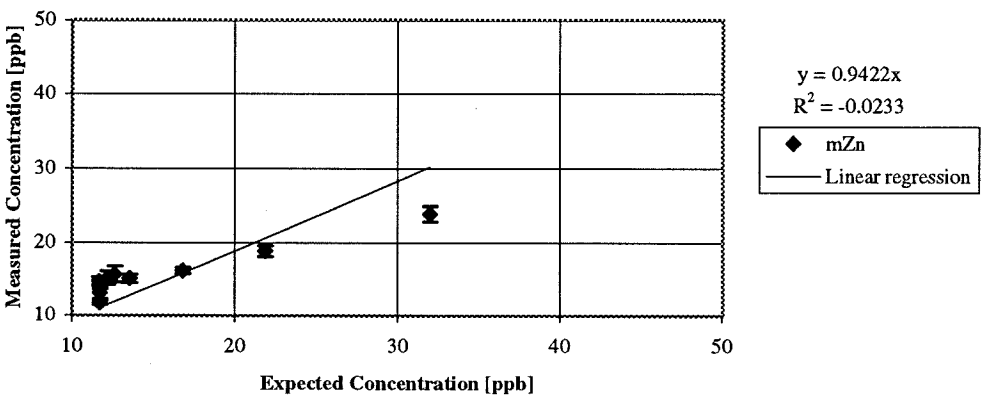

Standard Addition Test for Ga in Water from Pinole

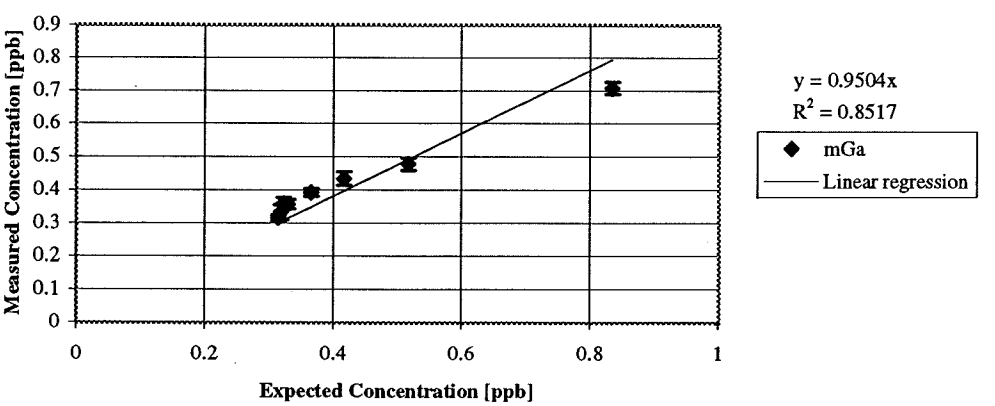

Standard Addition Test for Rb in Water from Pinole

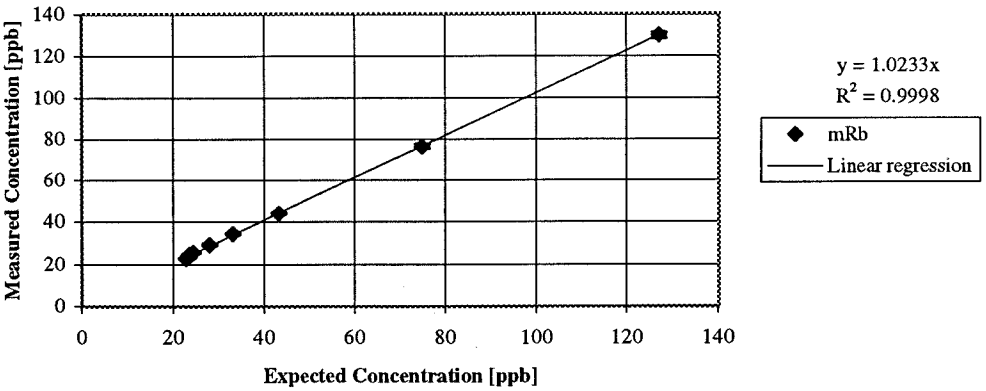

Standard Addition Test for Sr in 100:1 Water from Pinole

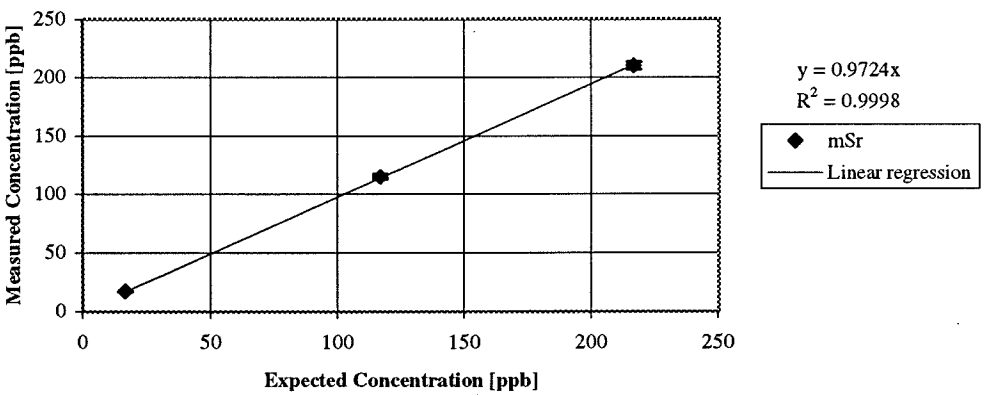

Standard Addition Test for Y in Water from Pinole

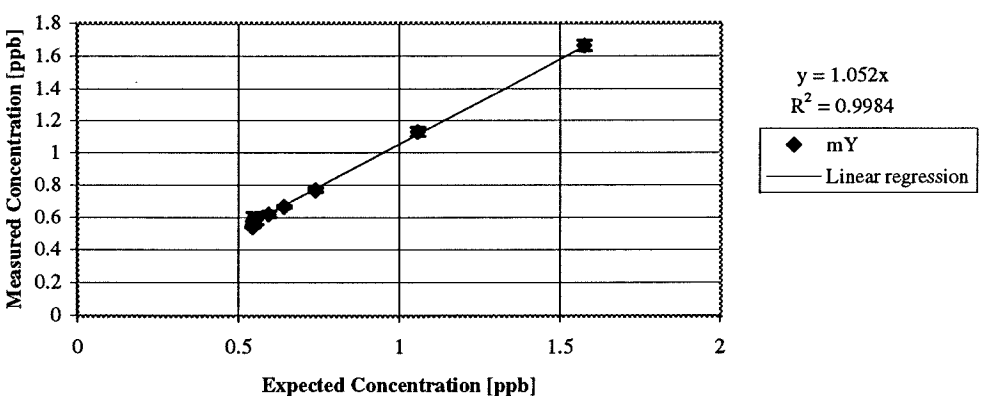

Standard Addition Test for Mo in Water from Pinole

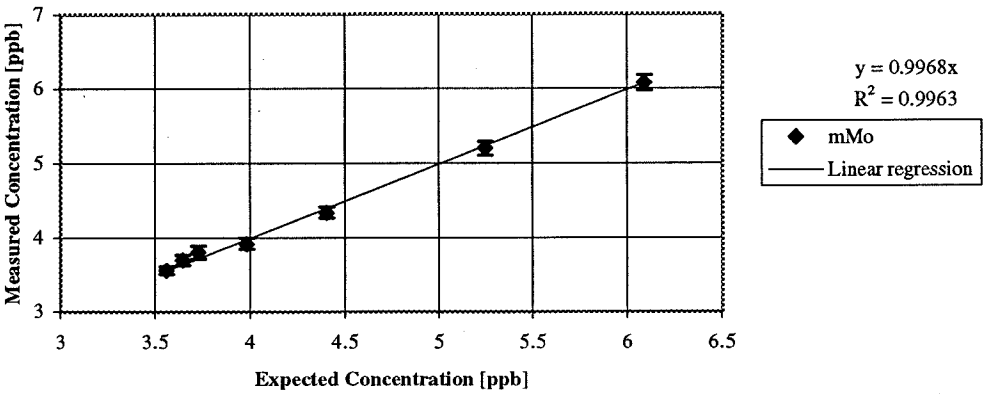

Standard Addition Test for Cd in Water from Pinole

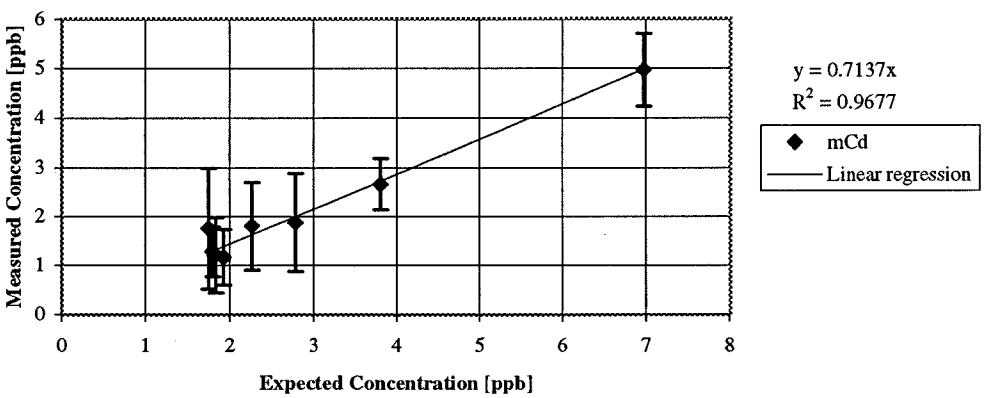

Standard Addition Test for Cs Water from Pinole

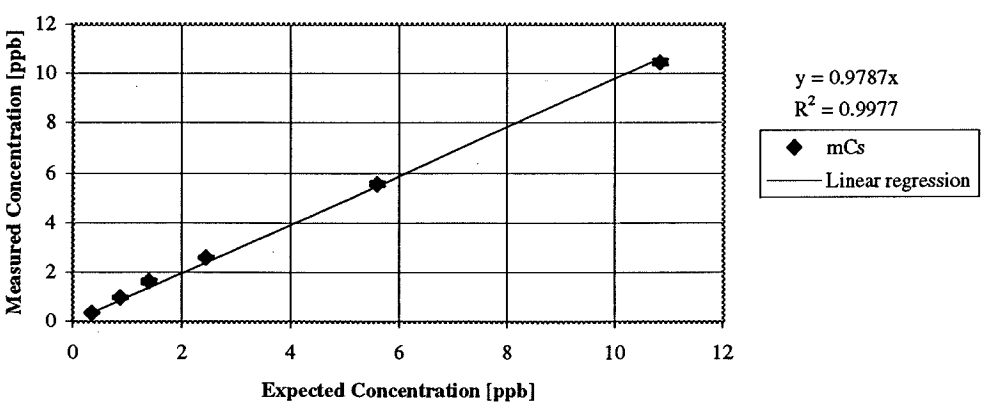

Standard Addition Test for Ba in Water from Pinole

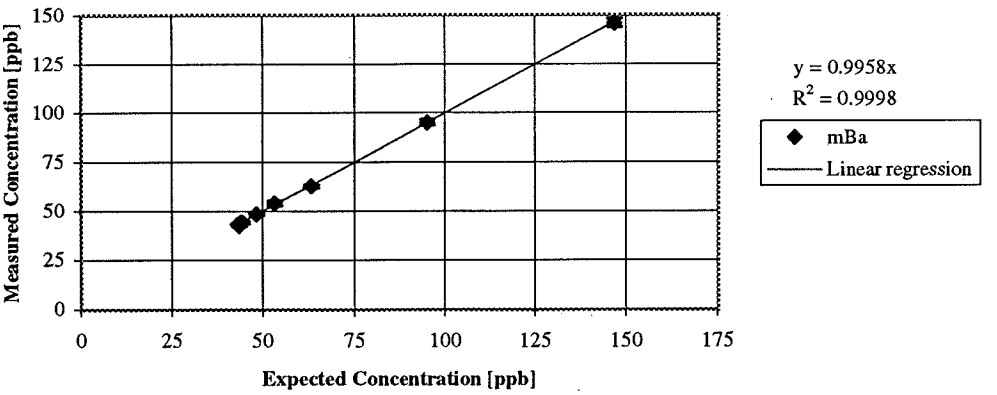

Standard Addition Test for La in Water from Pinole

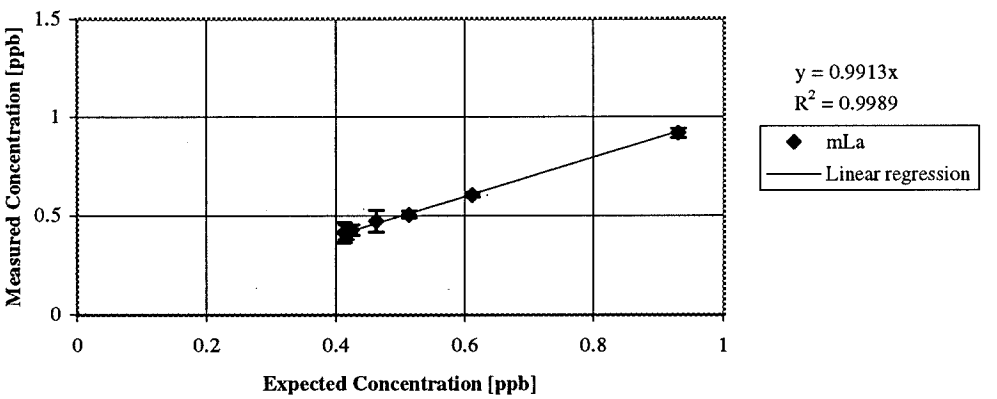

Standard Addition Test for Ce in Water from Pinole

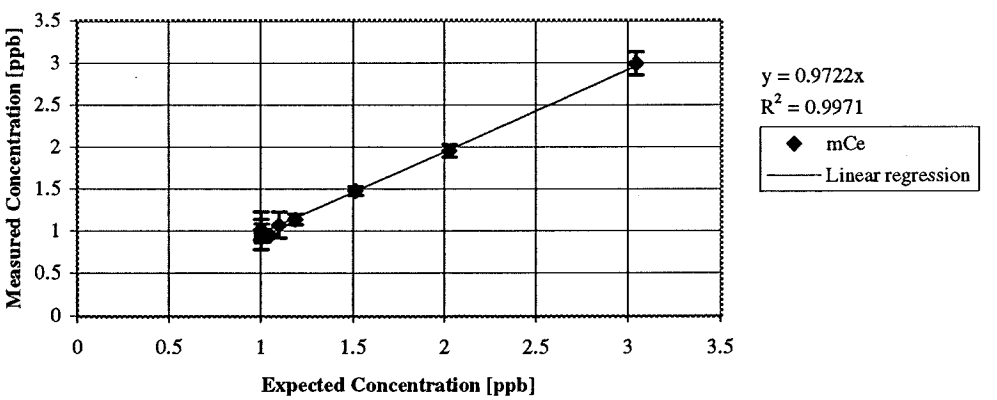

Standard Addition Test for Pr in Water from Pinole

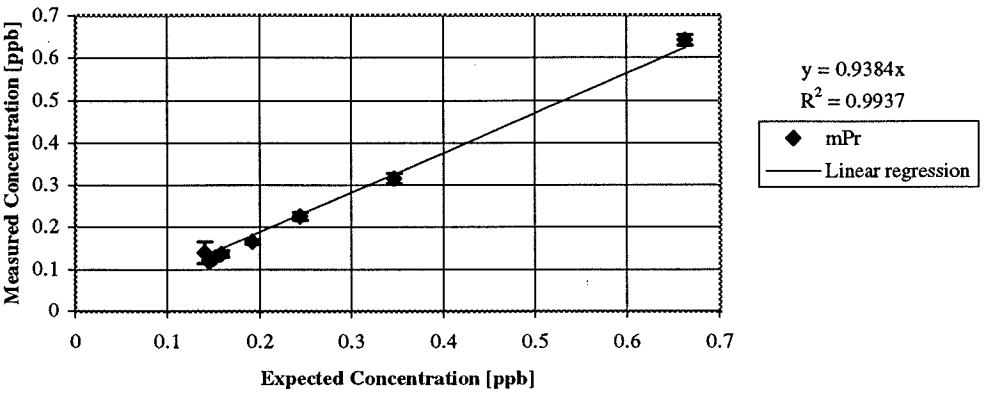

Standard Addition Test for Nd in Water from Pinole

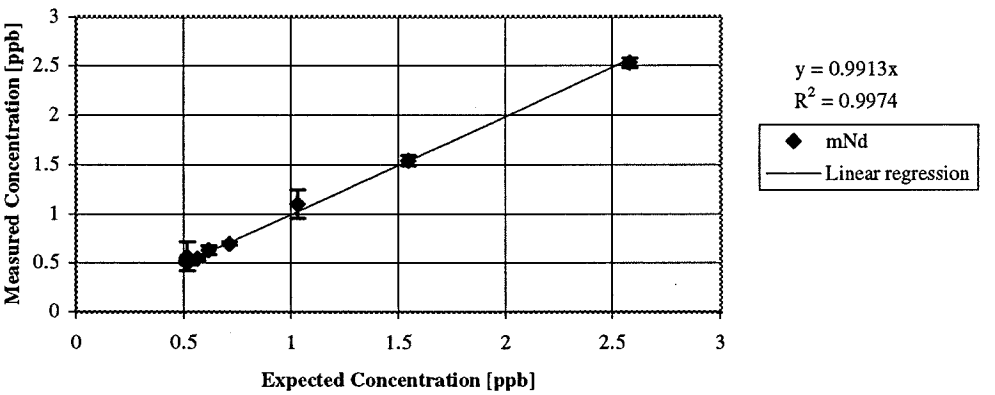

Standard Addition Test for Sm in Water from Pinole

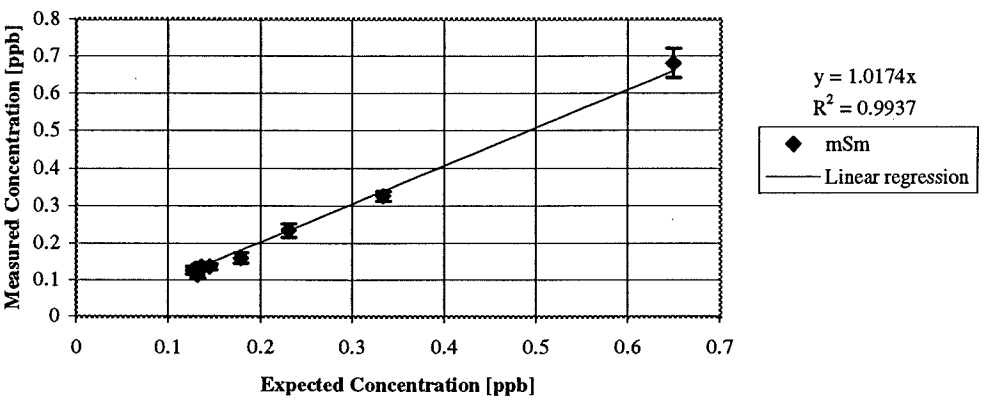

Standard Addition Test for Eu in Water from Pinole

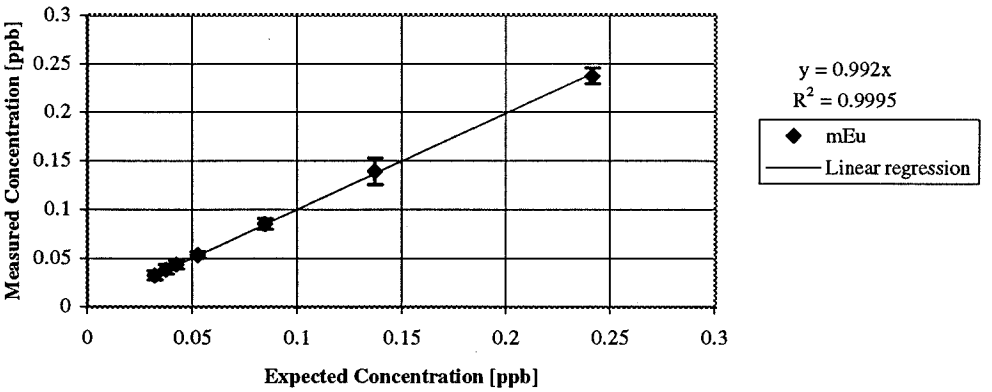

Standard Addition Test for Gd in Water from Pinole

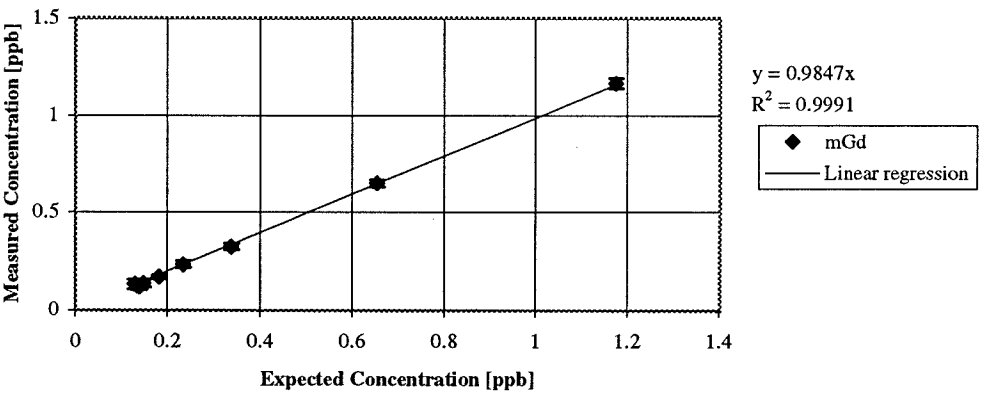

Standard Addition Test for Tb in Water from Pinole

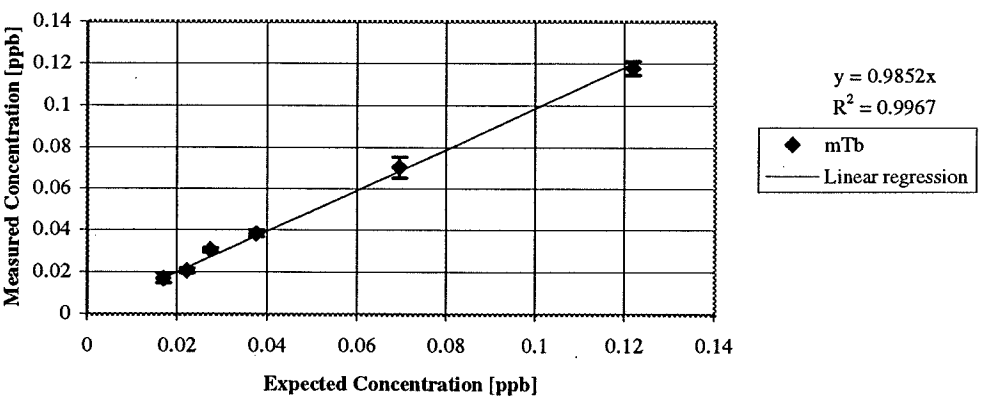

Standard Addition Test for Dy in Water from Pinole

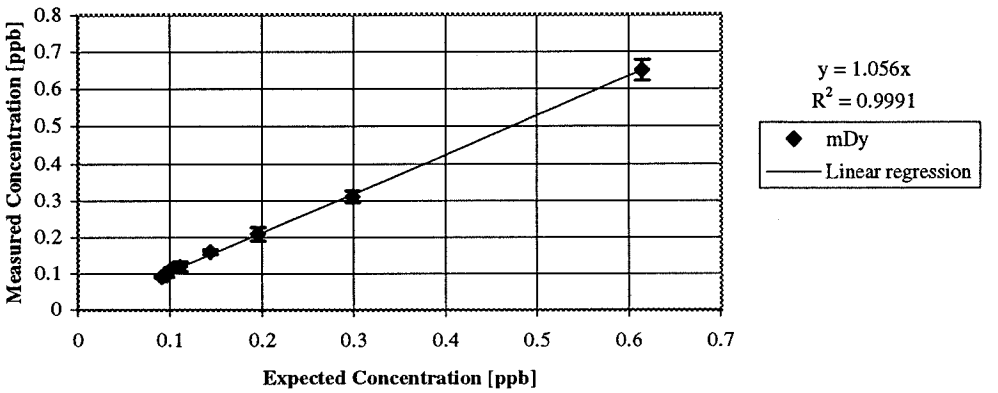

Standard Addition Test for Ho in Water from Pinole

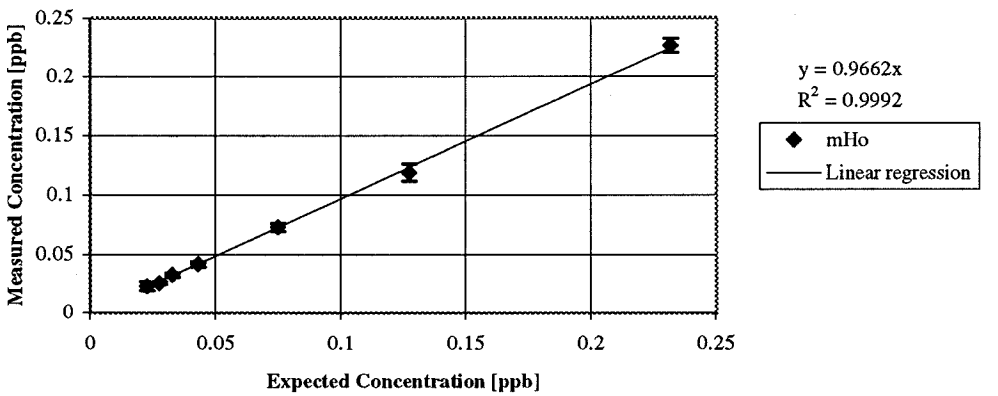

Standard Addition Test for Er in Water from Pinole

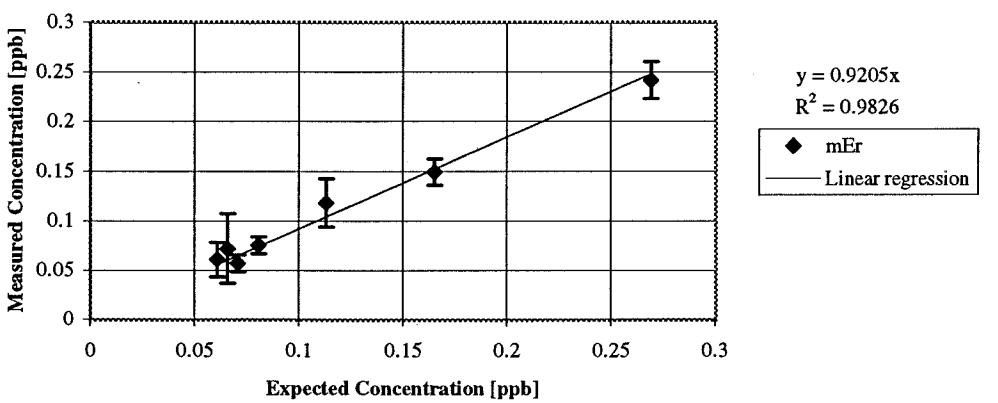

Standard Addition Test for Yb in Water from Pinole

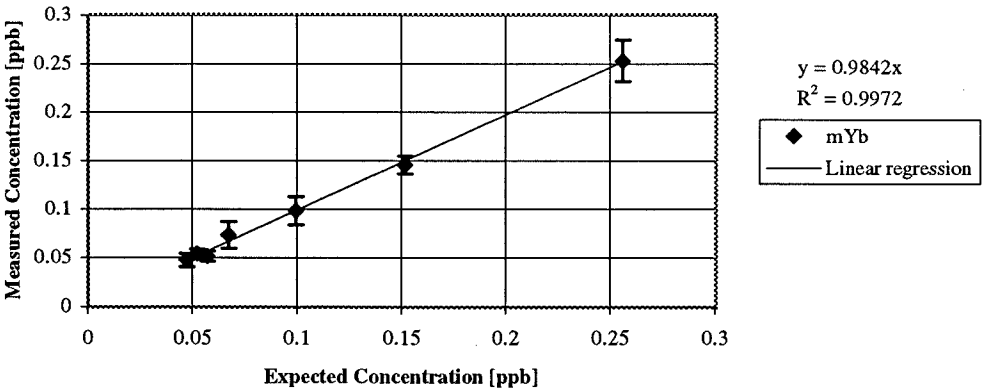

Standard Addition Test for Lu in Water from Pinole

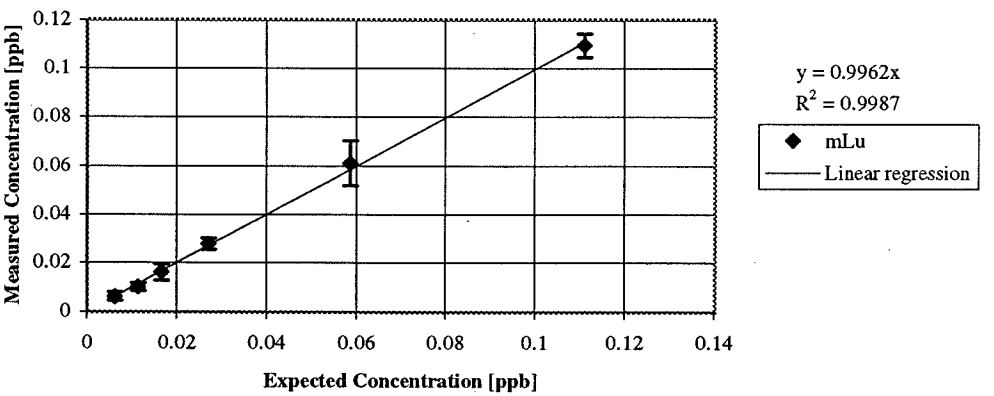

Standard Addition Test for Th in Water from Pinole

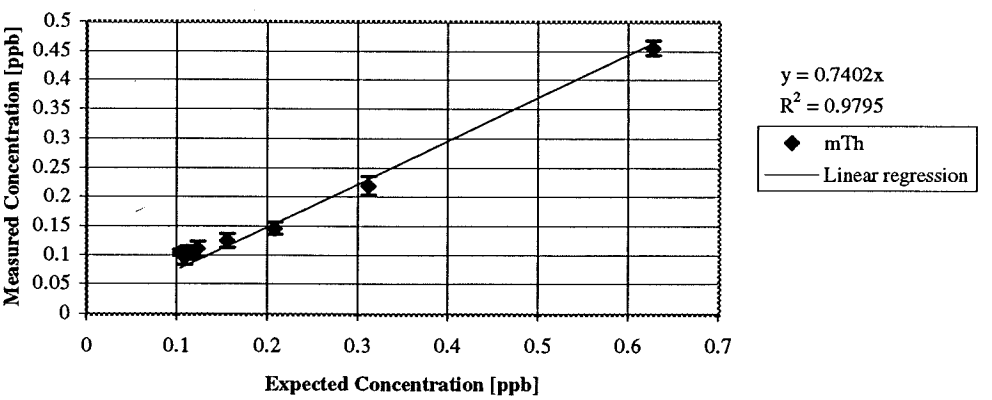

Standard Addition Test for U in Water from Pinole

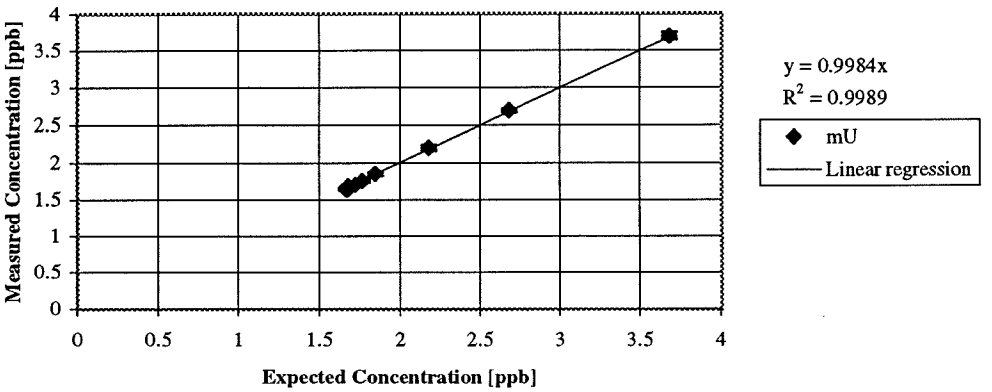

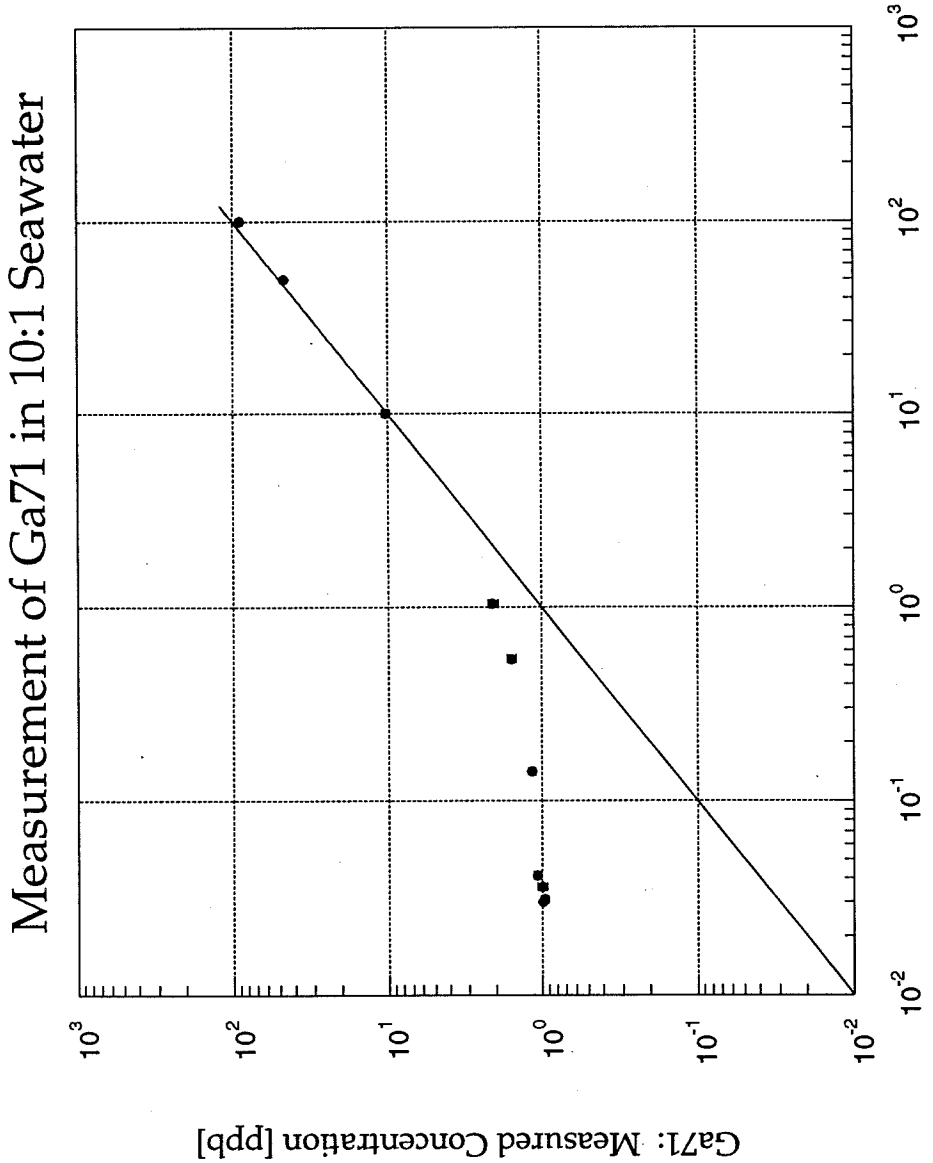
Measurement of Ga71 in 10:1 Seawater
Ga71: Measured Concentration [ppb]
Ga71: Actual Concentration [ppb]
10^3
10^2
10^1
10^0
10^-1
10^-2

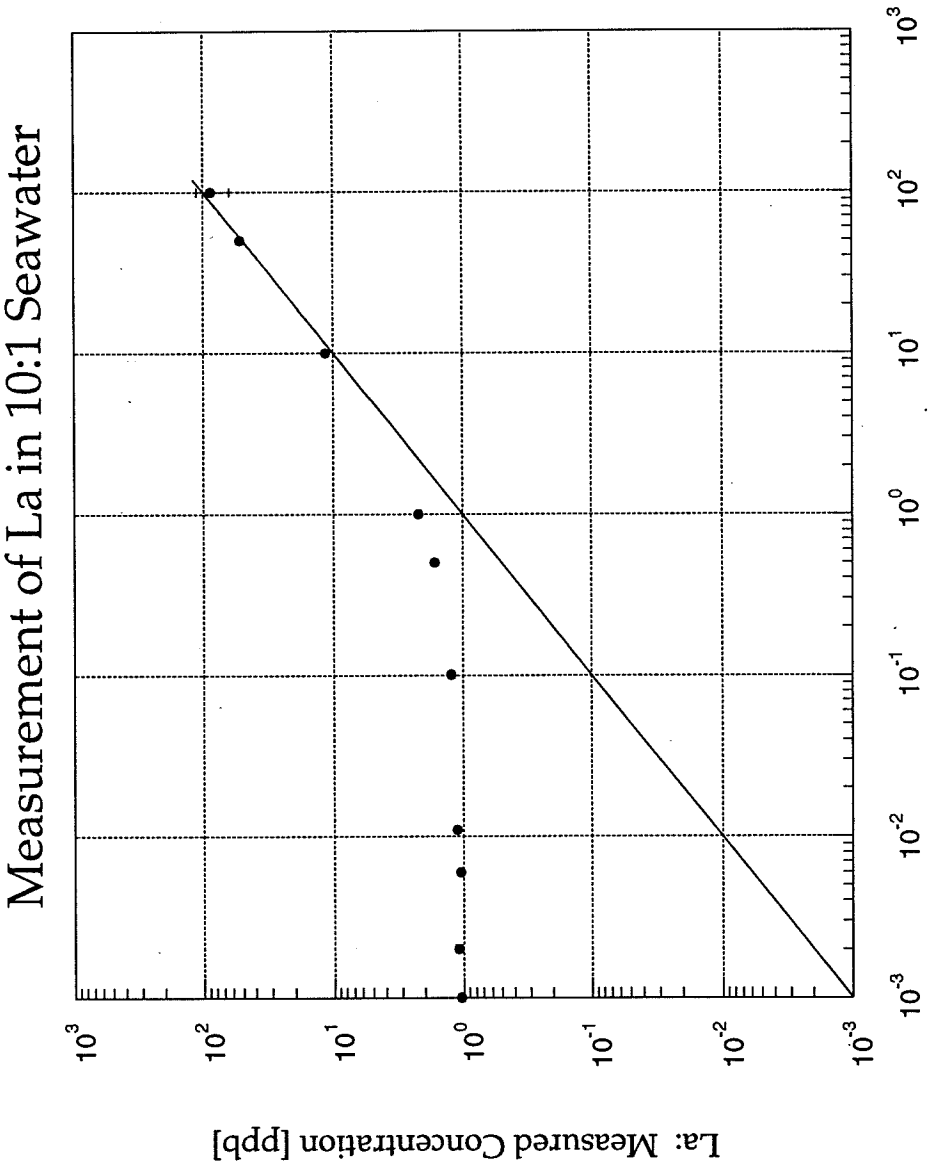
Measurement of La in 10:1 Seawater
La: Measured Concentration [ppb]
La: Actual Concentration [ppb]
10^3
10^2
10^1
10^0
10^-1
10^-2
10^-3

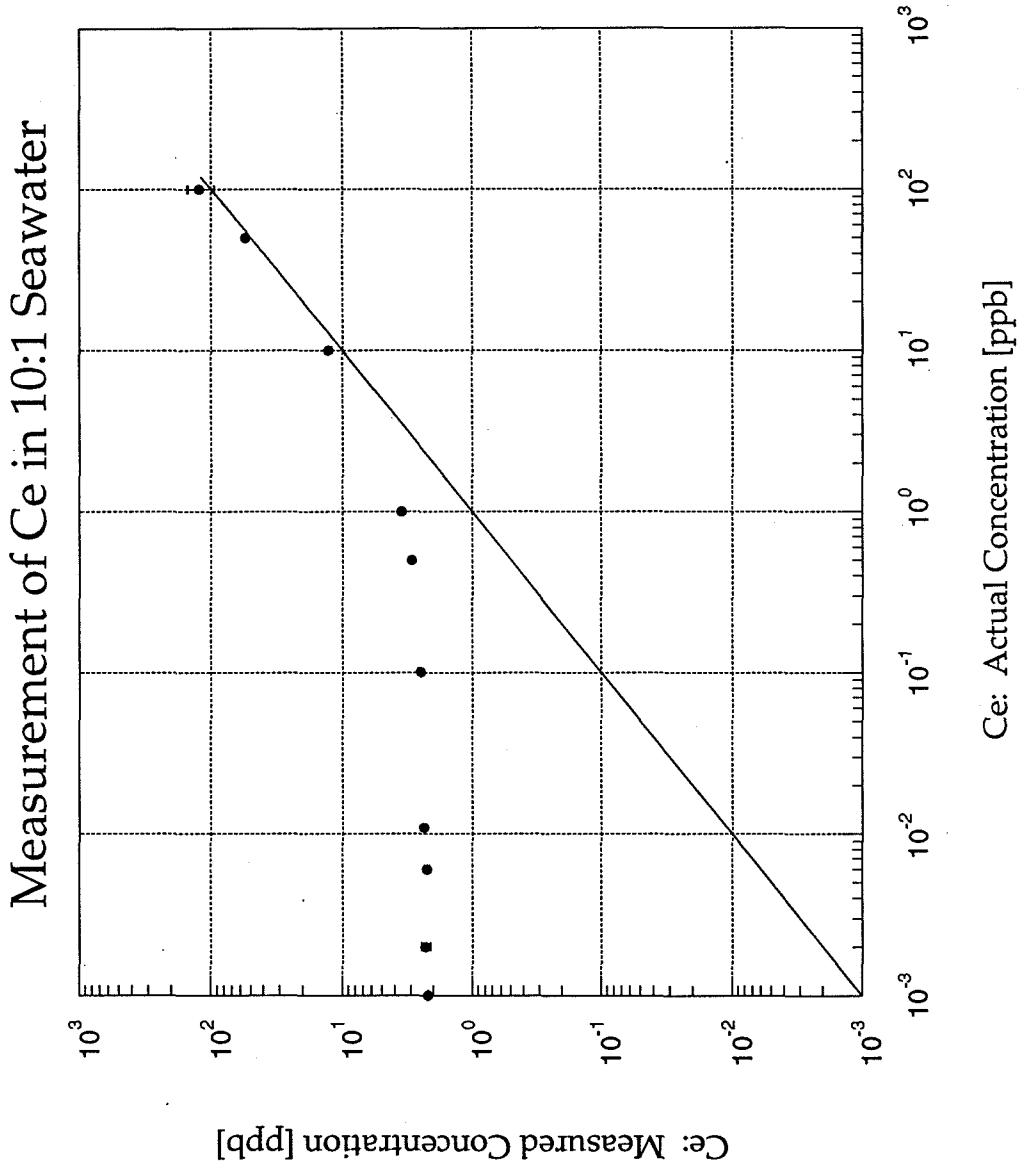
Measurement of Ce in 10:1 Seawater
Ce: Measured Concentration [ppb]
Ce: Actual Concentration [ppb]
10^-3
10^-2
10^-1
10^0
10^1
10^2
10^3

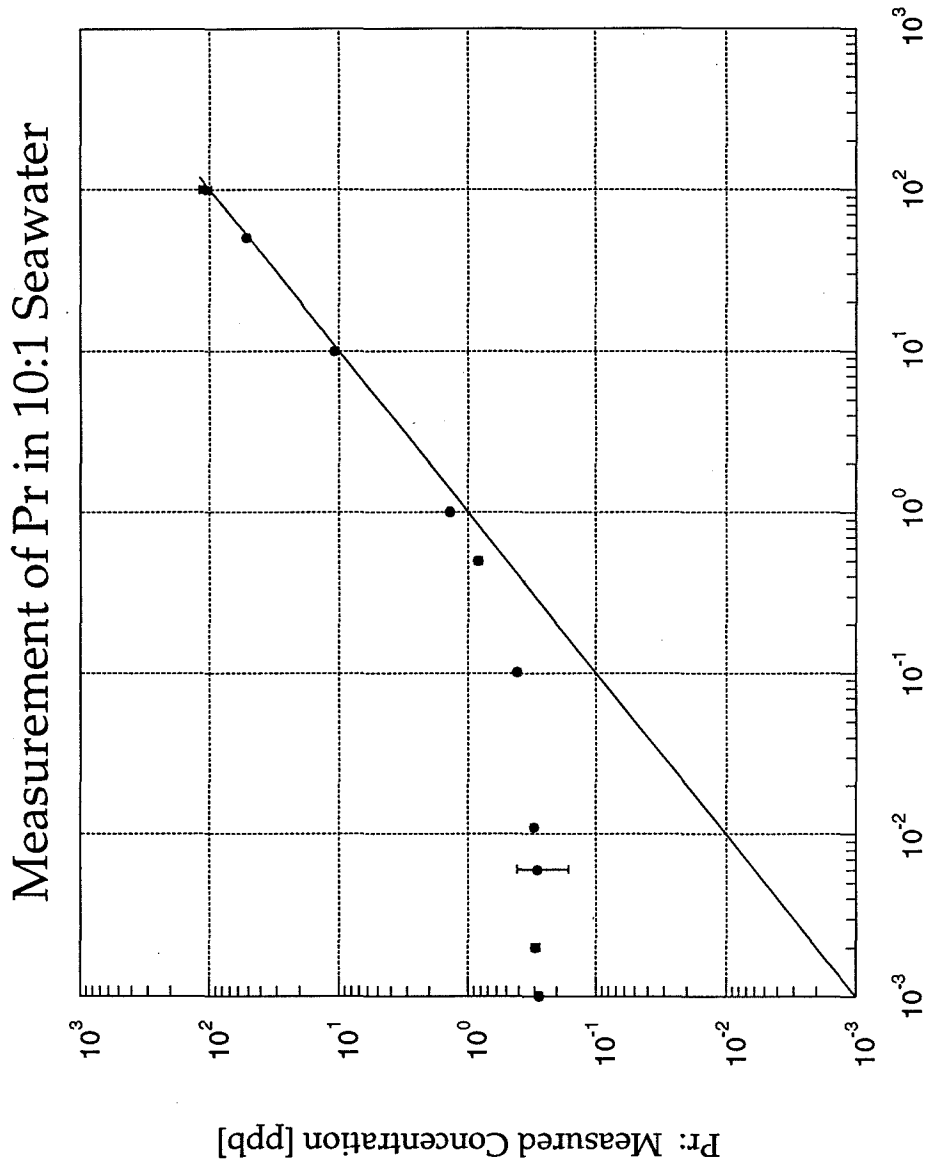
Measurement of Pr in 10:1 Seawater
Pr: Measured Concentration [ppb]
Pr: Actual Concentration [ppb]
10^-3
10^-2
10^-1
10^0
10^1
10^2
10^3

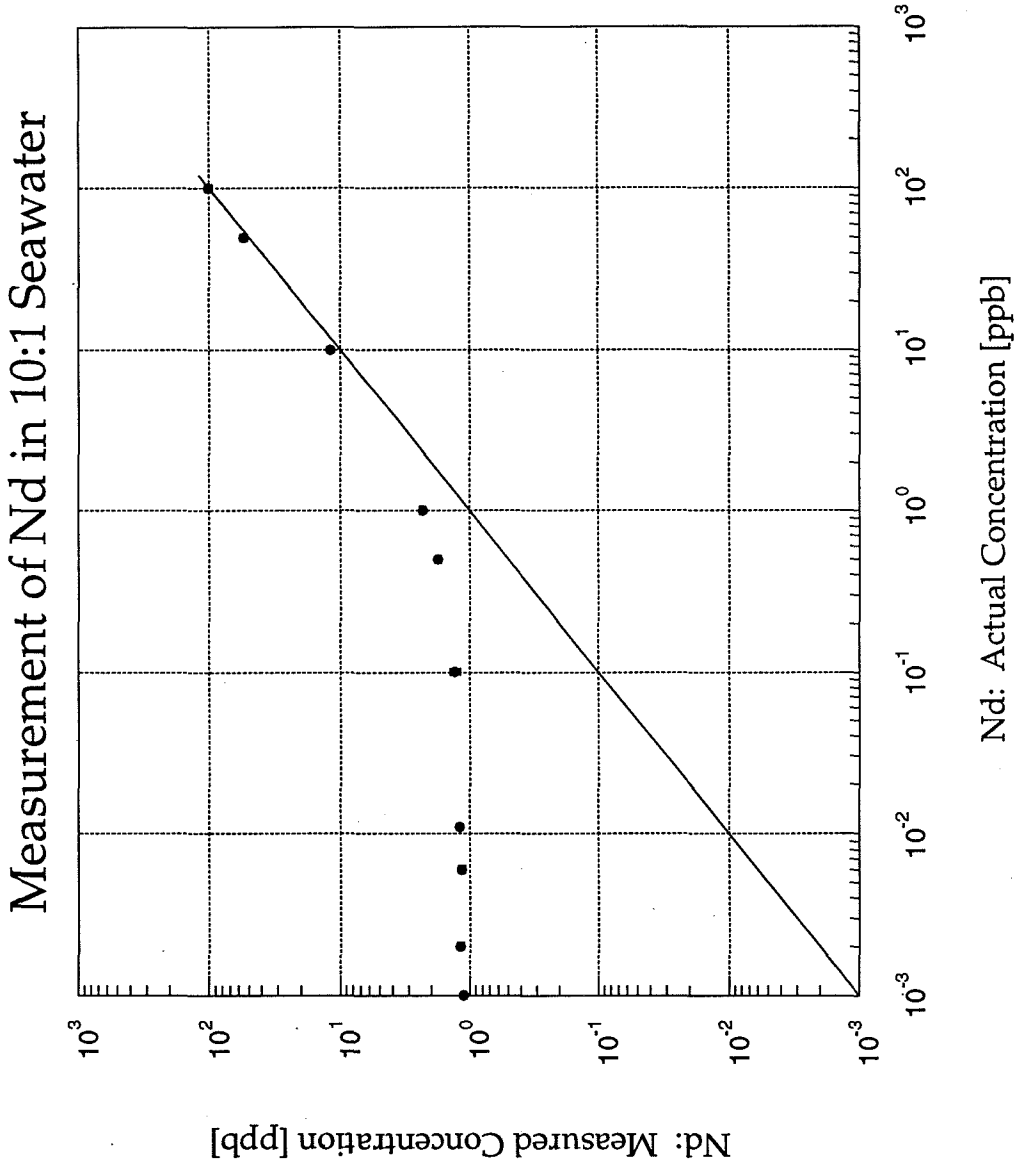
Measurement of Nd in 10:1 Seawater
Nd: Measured Concentration [ppb]
Nd: Actual Concentration [ppb]
10^3
10^2
10^1
10^0
10^-1
10^-2
10^-3

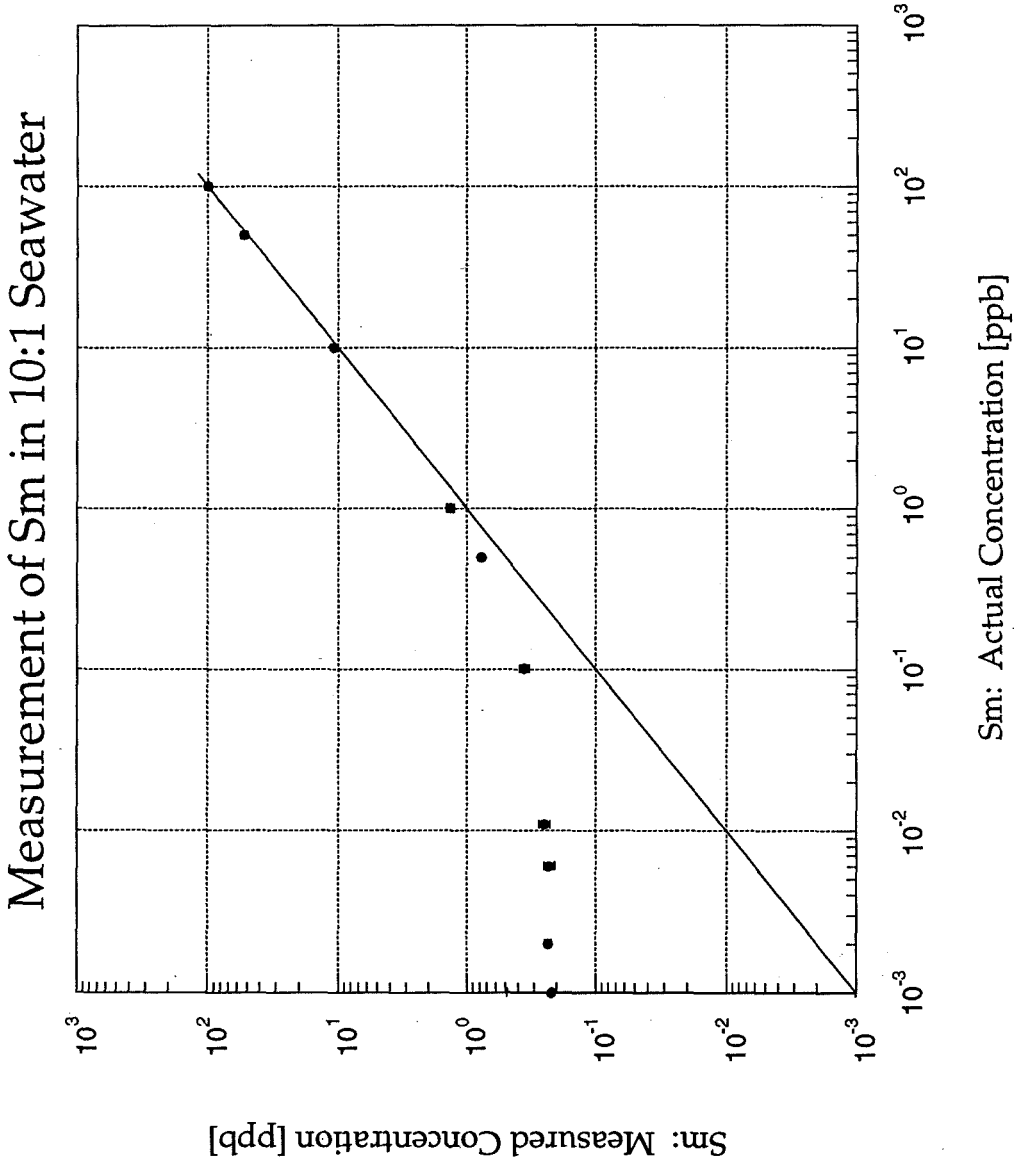
Measurement of Sm in 10:1 Seawater
Sm: Measured Concentration [ppb]
Sm: Actual Concentration [ppb]
10^3
10^2
10^1
10^0
10^-1
10^-2
10^-3

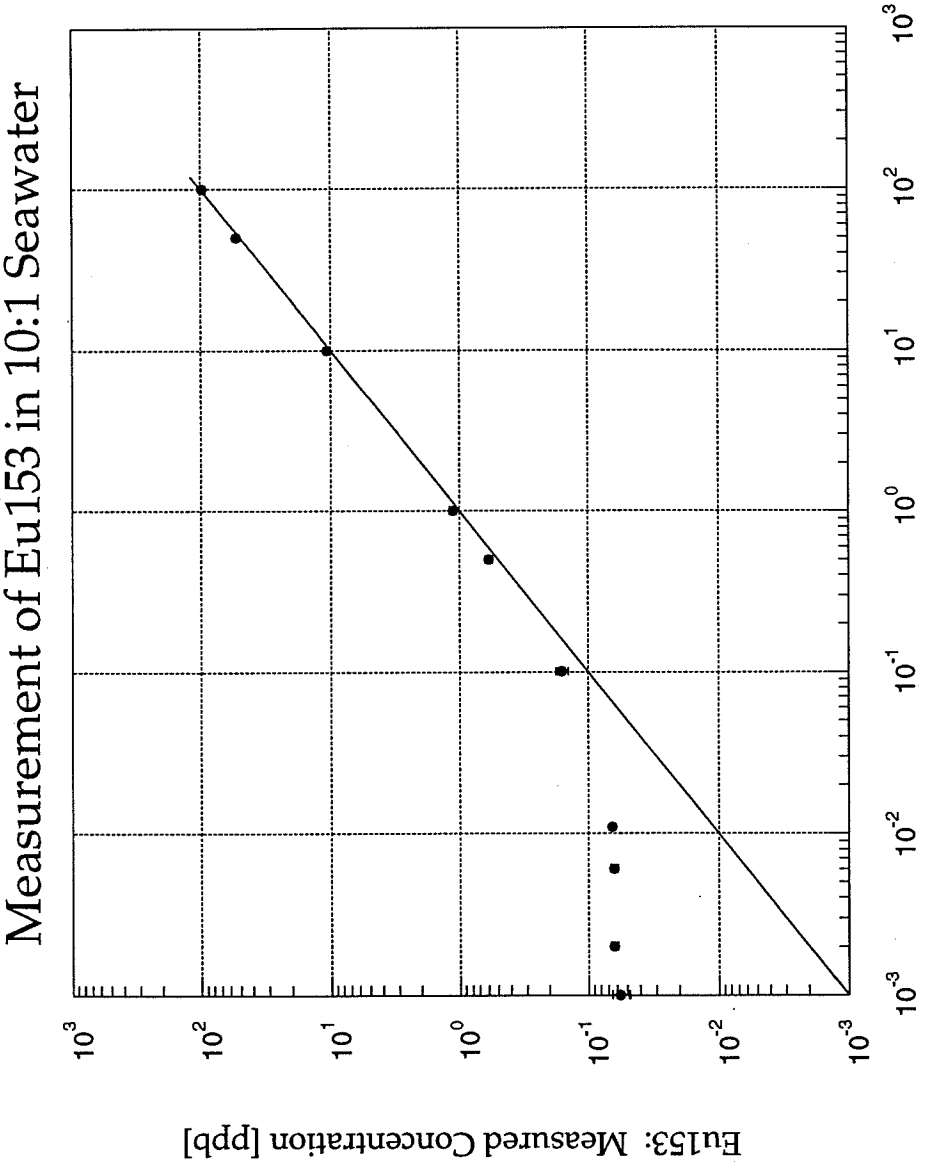

Eu153: Actual Concentration [ppb]

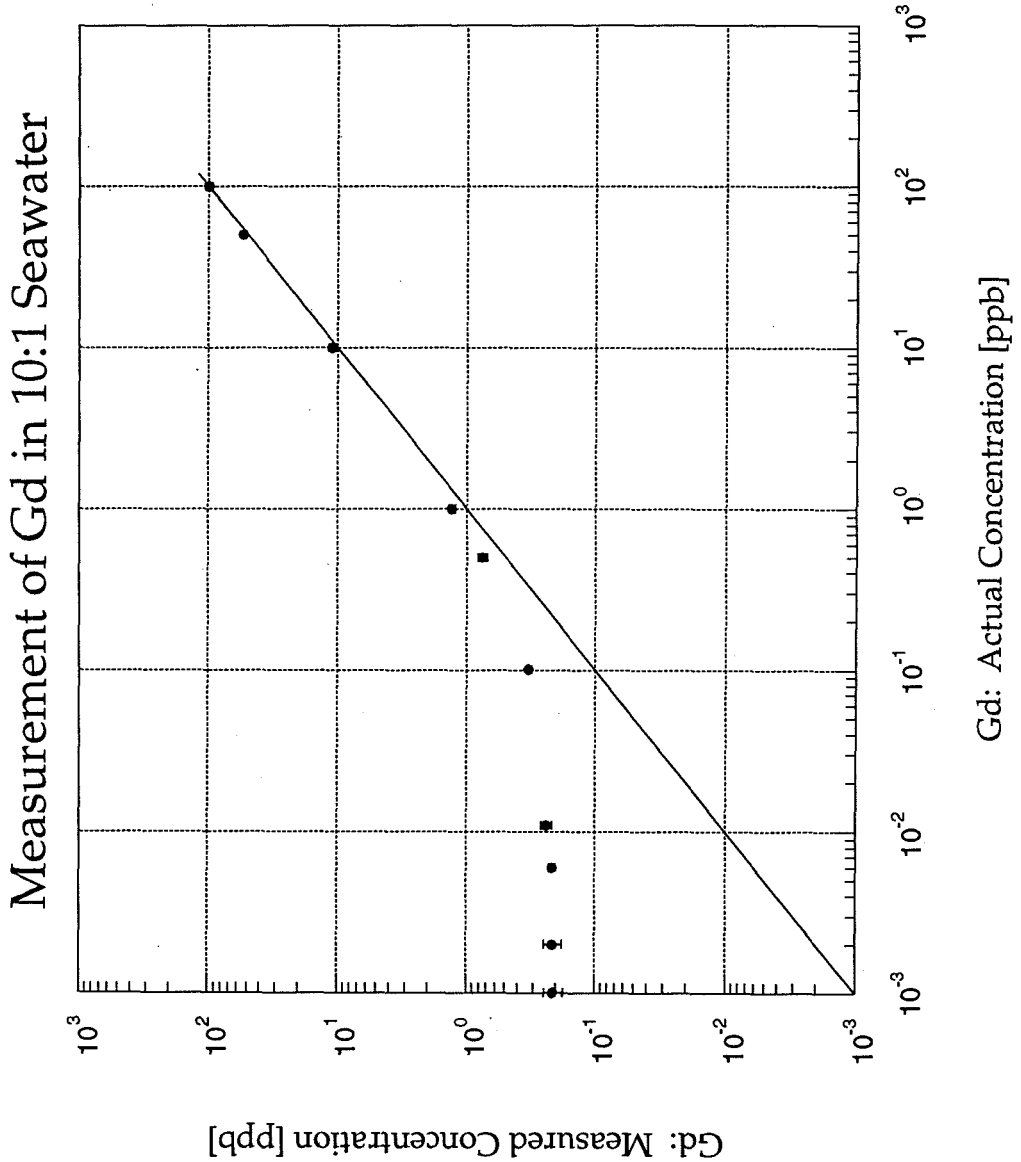
Measurement of Gd in 10:1 Seawater
Gd: Measured Concentration [ppb]
Gd: Actual Concentration [ppb]
10^3
10^2
10^1
10^0
10^-1
10^-2
10^-3

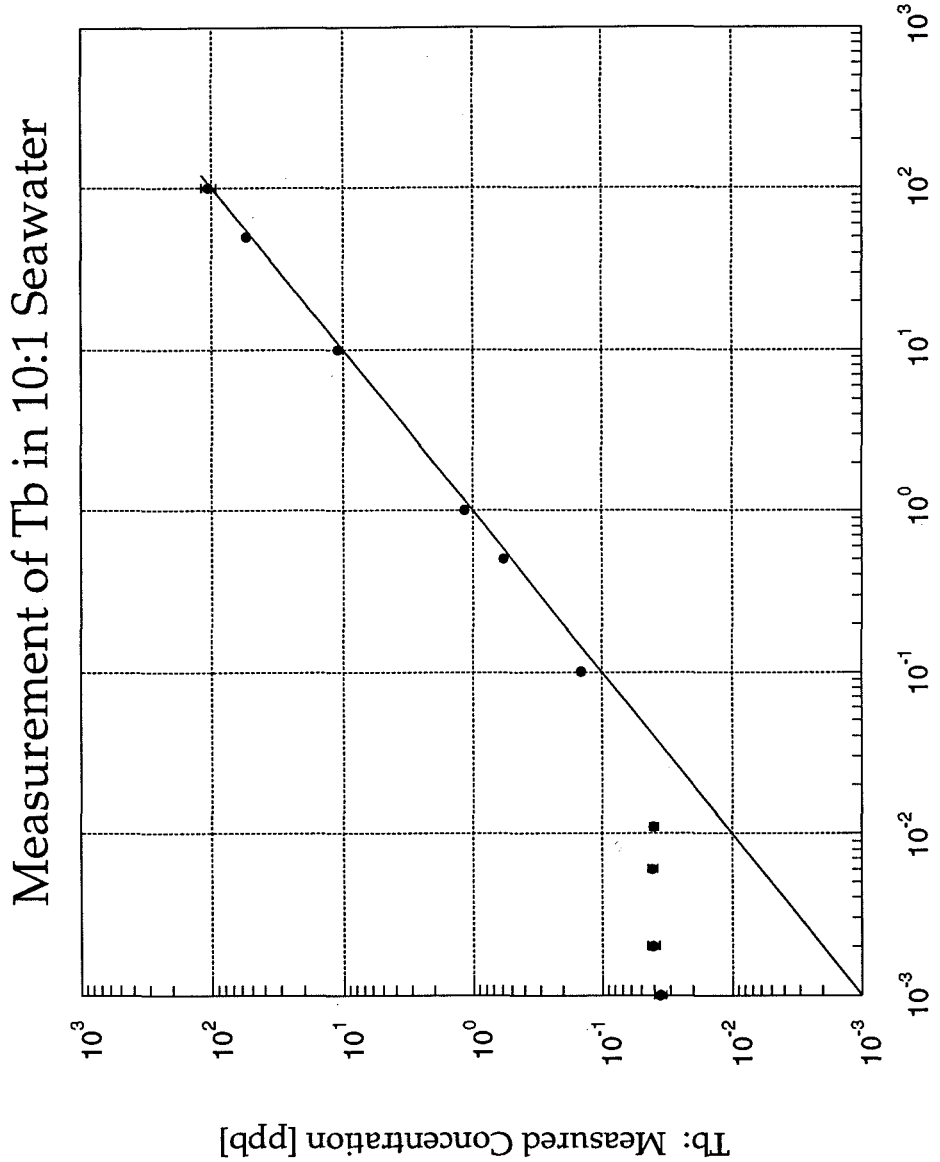
Measurement of Tb in 10:1 Seawater
Tb: Measured Concentration [ppb]
Tb: Actual Concentration [ppb]
10^-3
10^-2
10^-1
10^0
10^1
10^2
10^3

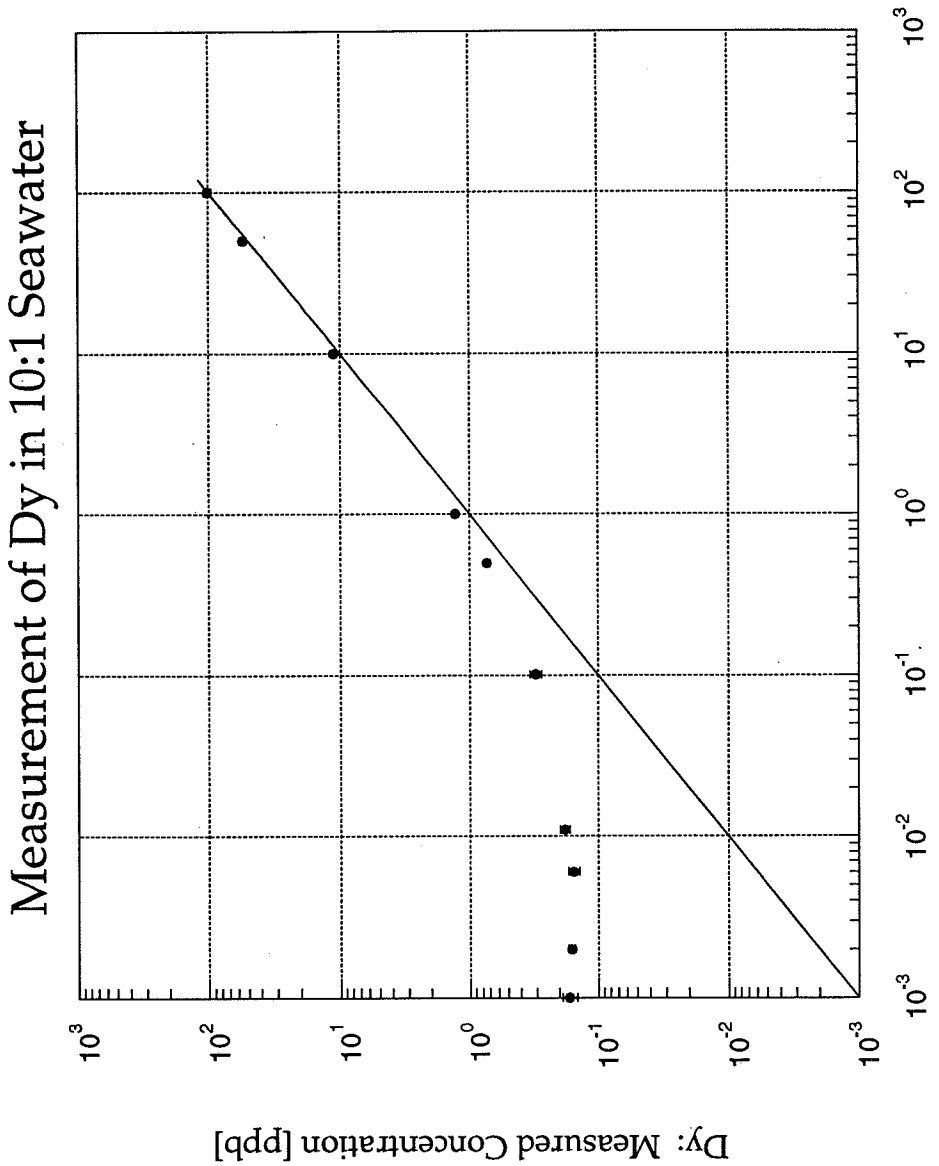
Measurement of Dy in 10:1 Seawater
Dy: Measured Concentration [ppb]
Dy: Actual Concentration [ppb]
10^3
10^2
10^1
10^0
10^-1
10^-2
10^-3

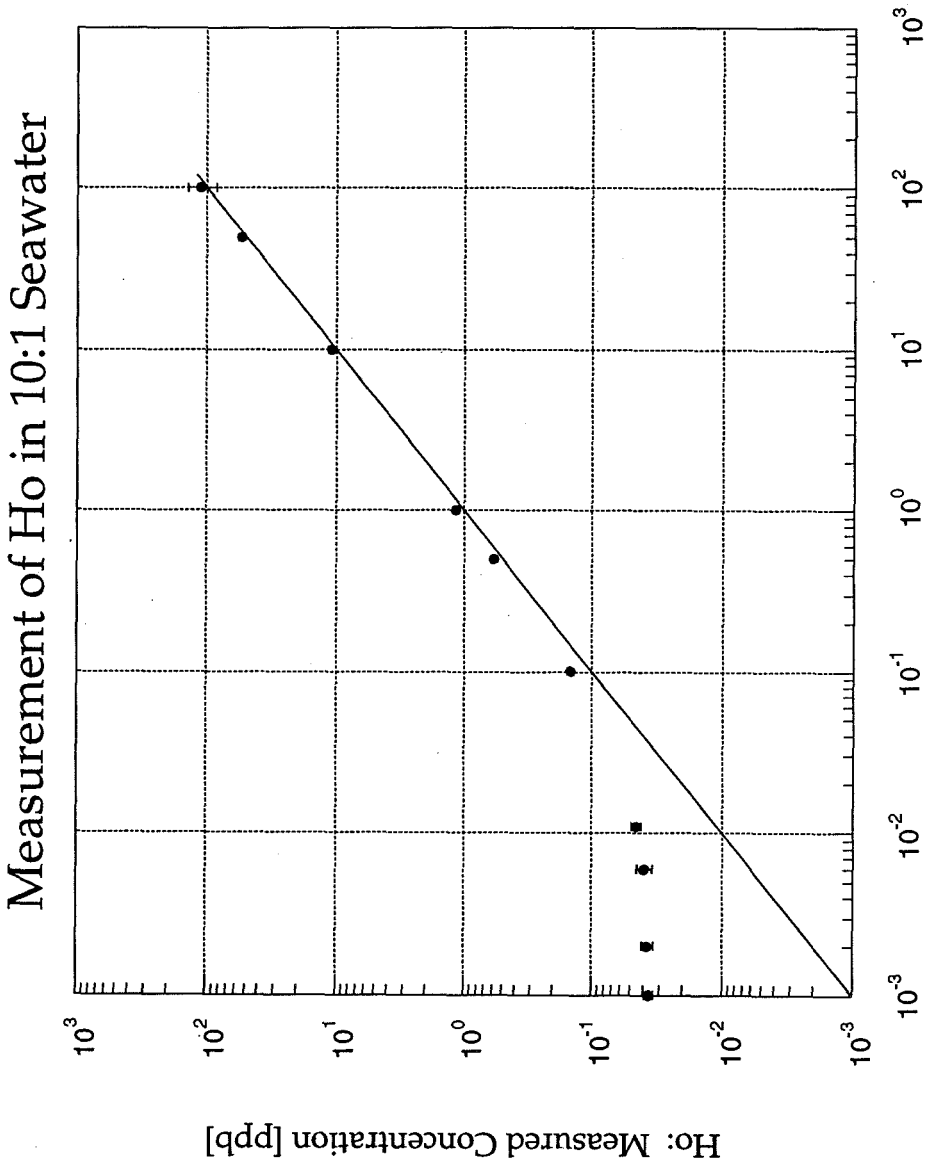
Measurement of Ho in 10:1 Seawater
Ho: Measured Concentration [ppb]
Ho: Actual Concentration [ppb]
10^3
10^2
10^1
10^0
10^-1
10^-2
10^-3

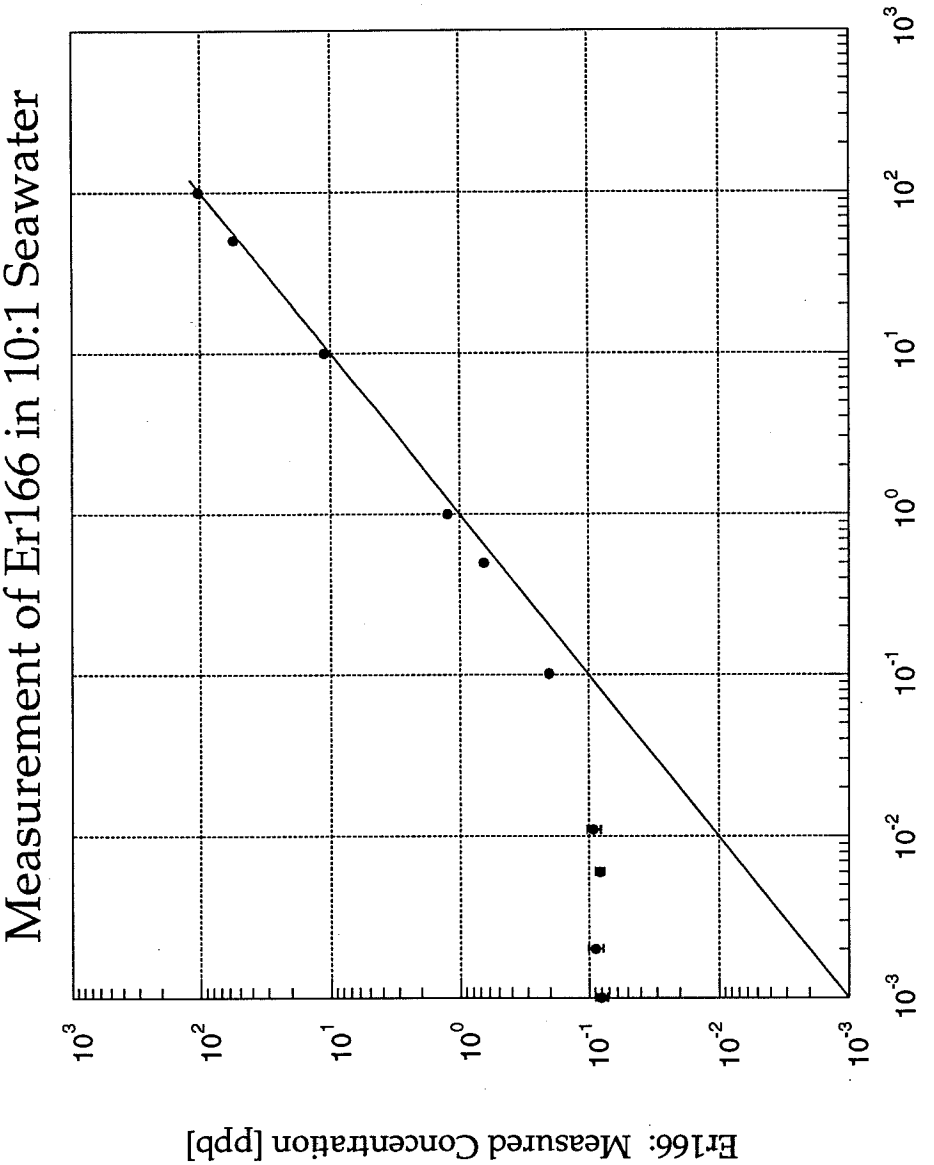

Er166: Actual Concentration [ppb]

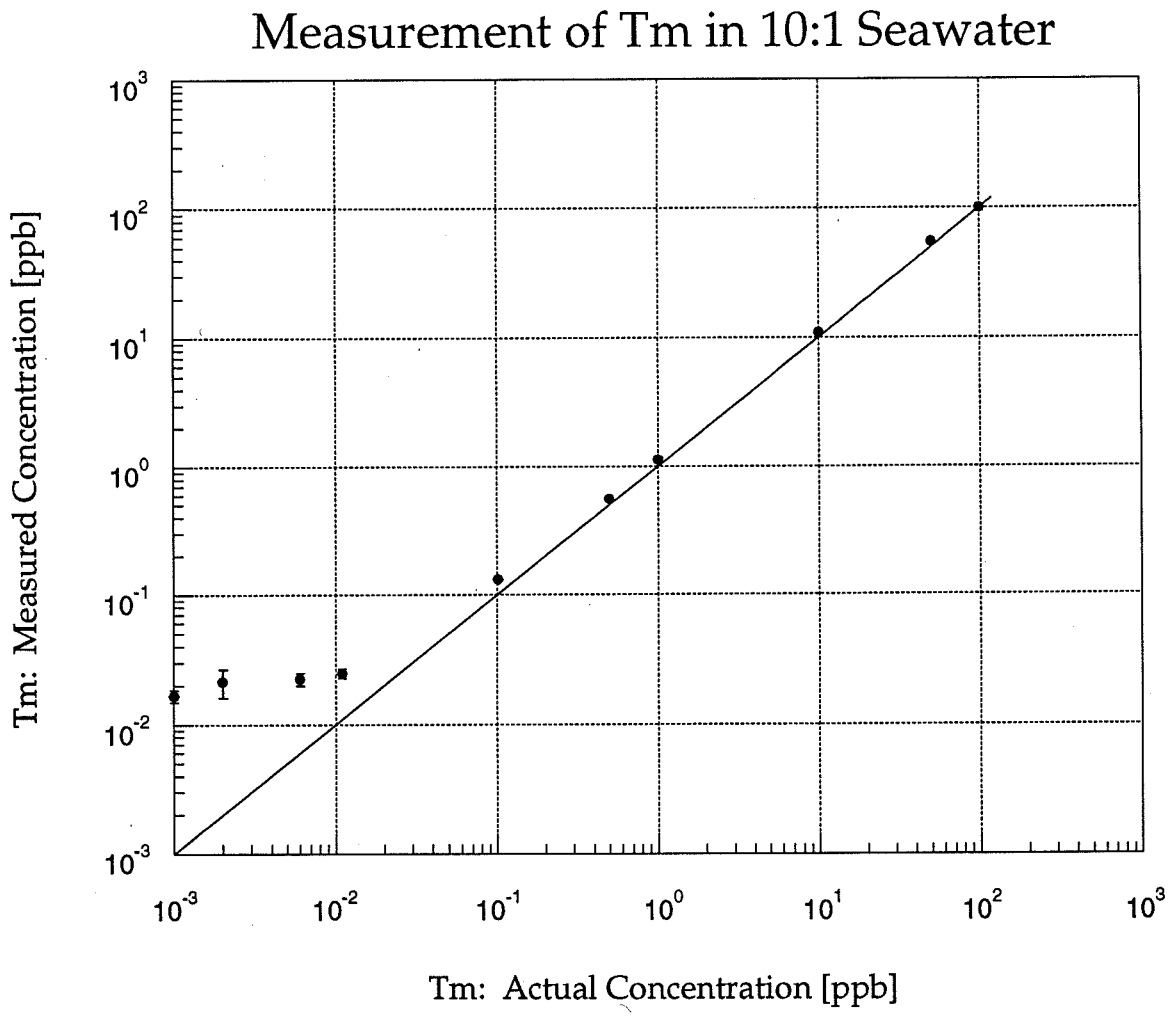
Measurement of Tm in 10:1 Seawater
Tm: Measured Concentration [ppb]
Tm: Actual Concentration [ppb]
10^3
10^2
10^1
10^0
10^-1
10^-2
10^-3

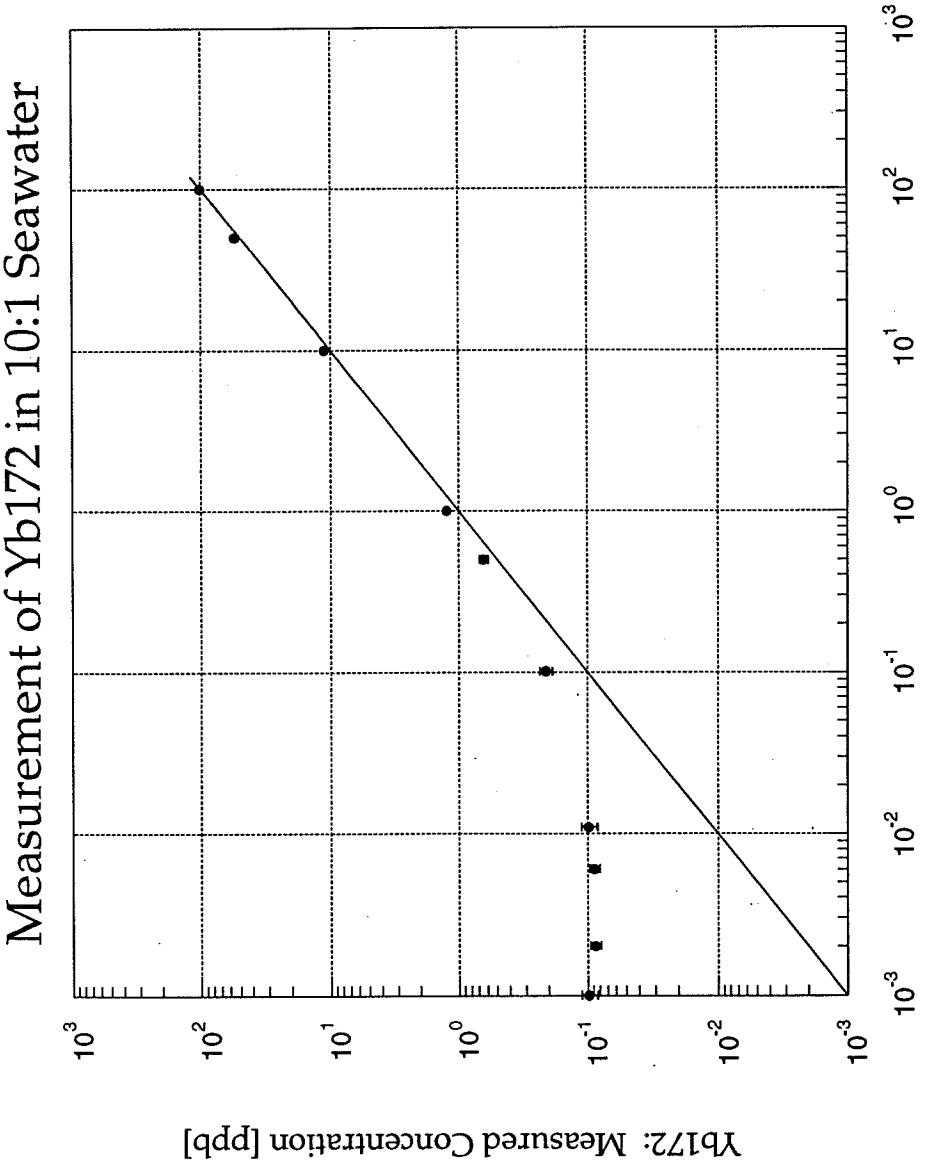
Measurement of Yb172 in 10:1 Seawater
Yb172: Measured Concentration [ppb]
Yb172: Actual Concentration [ppb]
10^3
10^2
10^1
10^0
10^-1
10^-2
10^-3

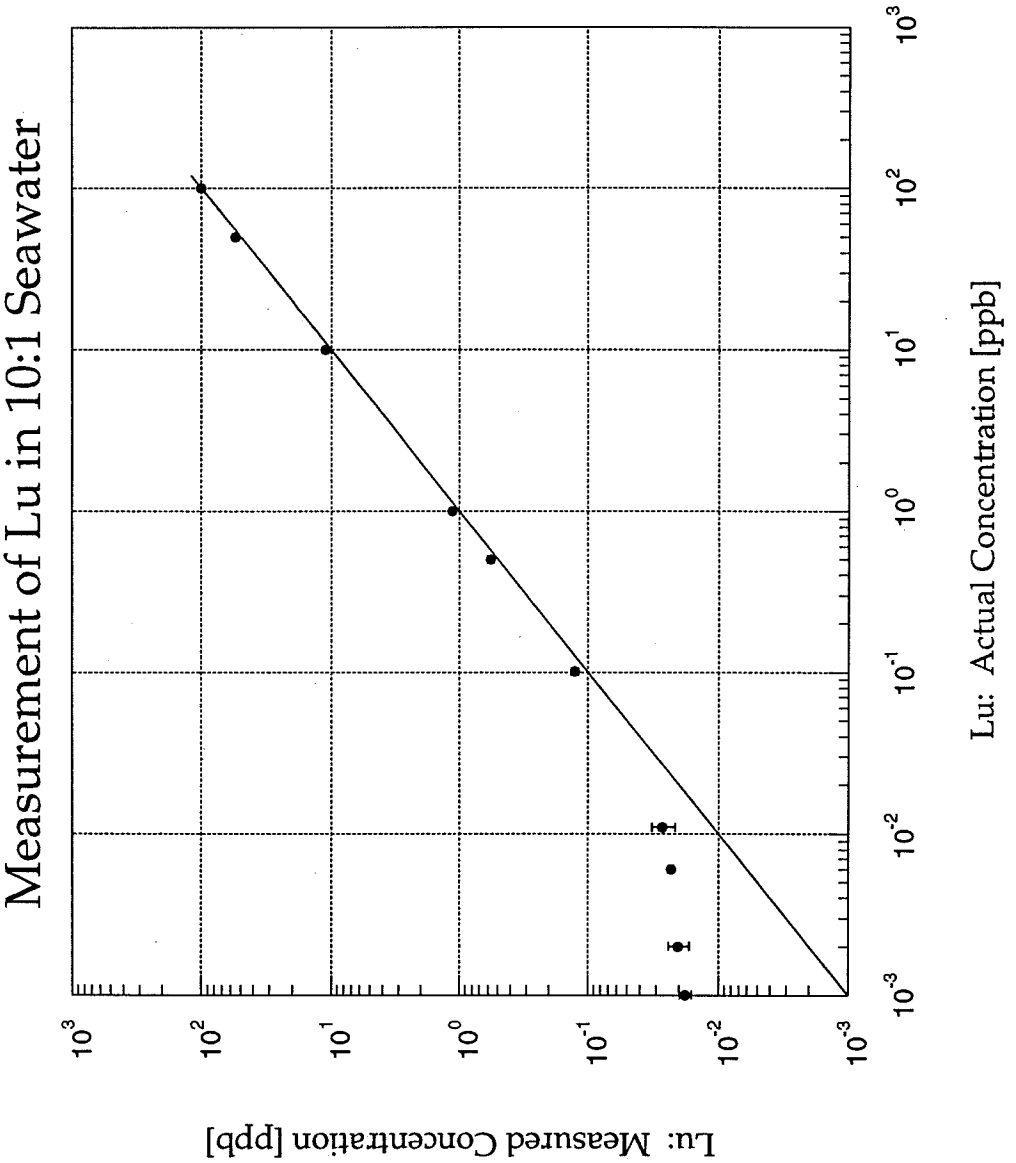
Measurement of Lu in 10:1 Seawater
Lu: Measured Concentration [ppb]
Lu: Actual Concentration [ppb]
10^3
10^2
10^1
10^0
10^-1
10^-2
10^-3

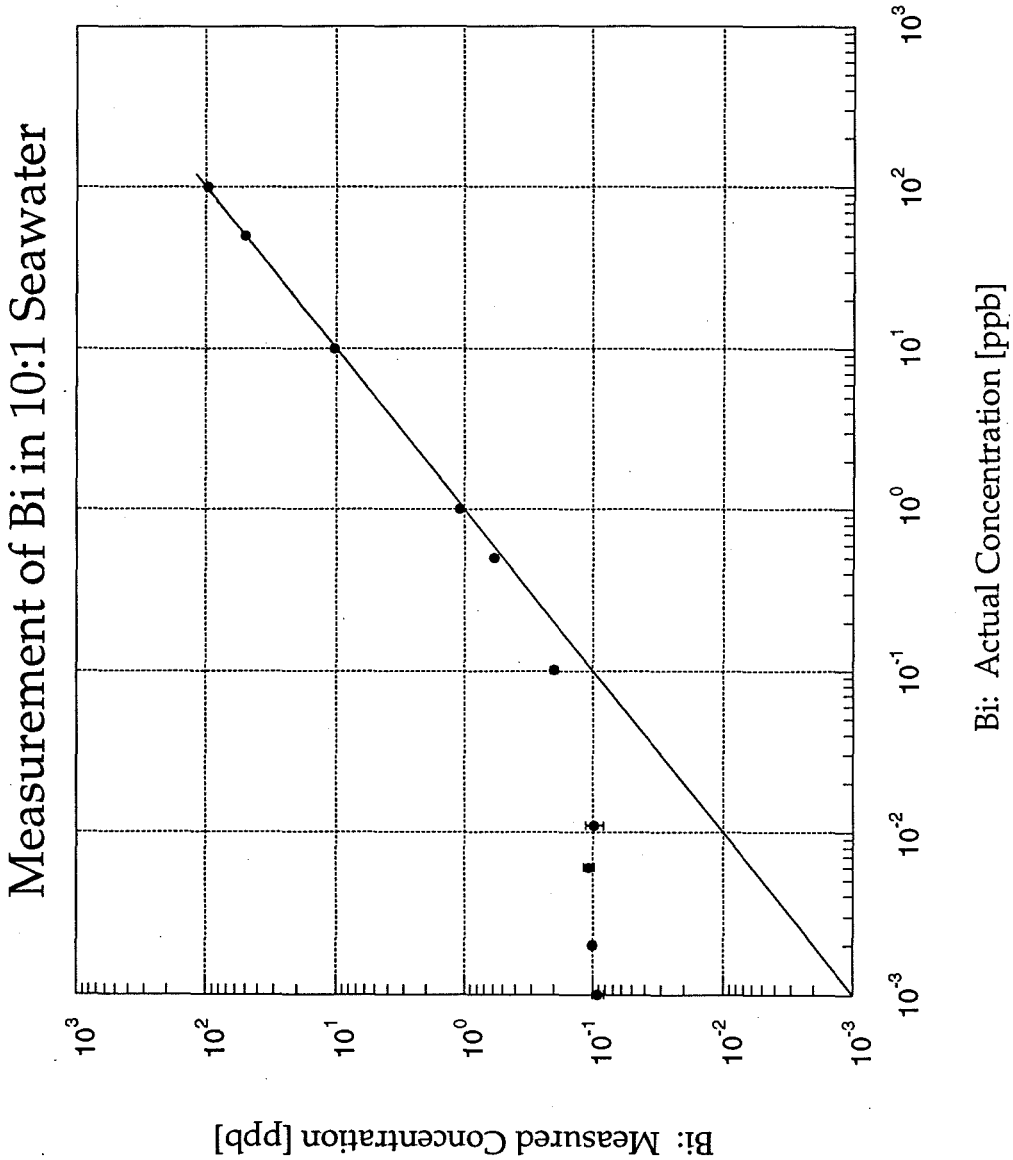
Measurement of Bi in 10:1 Seawater
Bi: Measured Concentration [ppb]
Bi: Actual Concentration [ppb]
10^3
10^2
10^1
10^0
10^-1
10^-2
10^-3

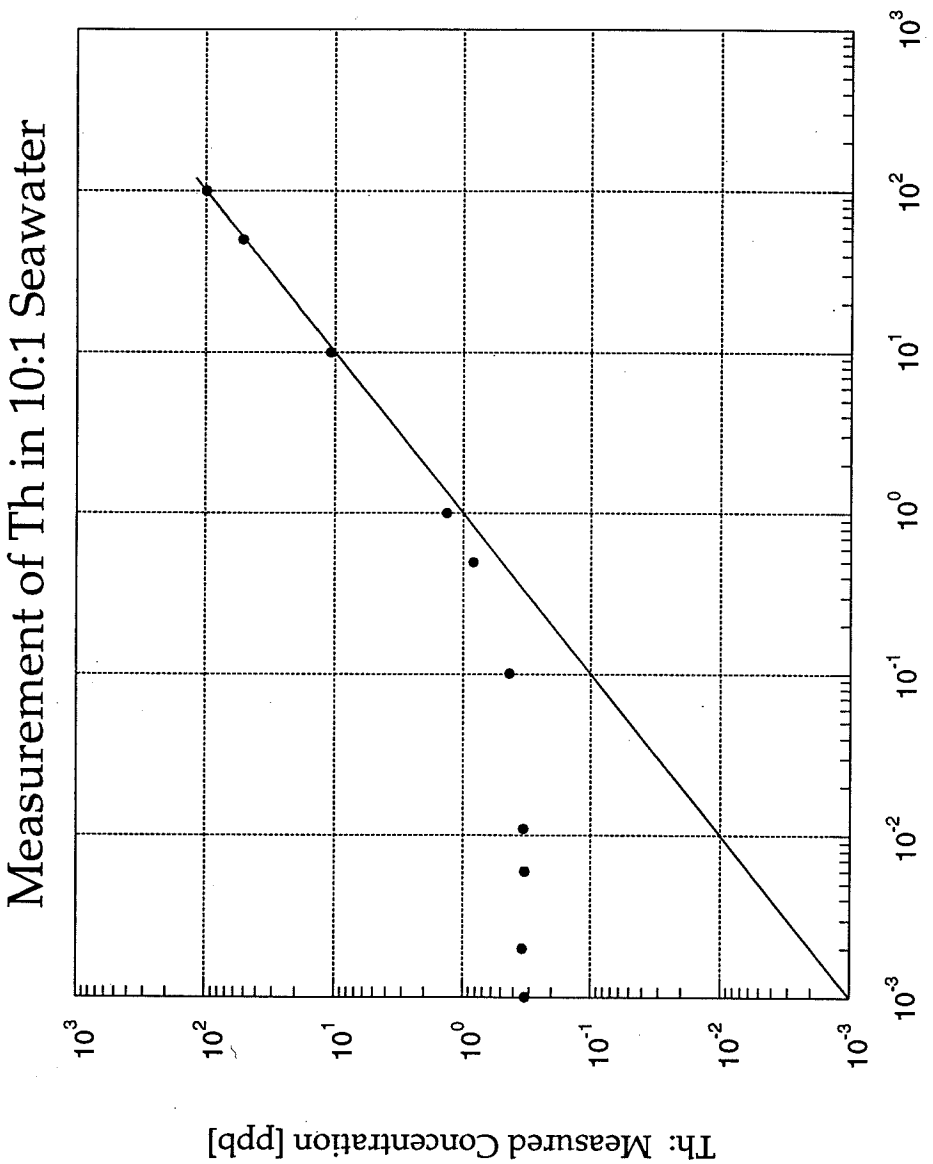
Measurement of Th in 10:1 Seawater
Th: Measured Concentration [ppb]
Th: Actual Concentration [ppb]
10^3
10^2
10^1
10^0
10^-1
10^-2
10^-3

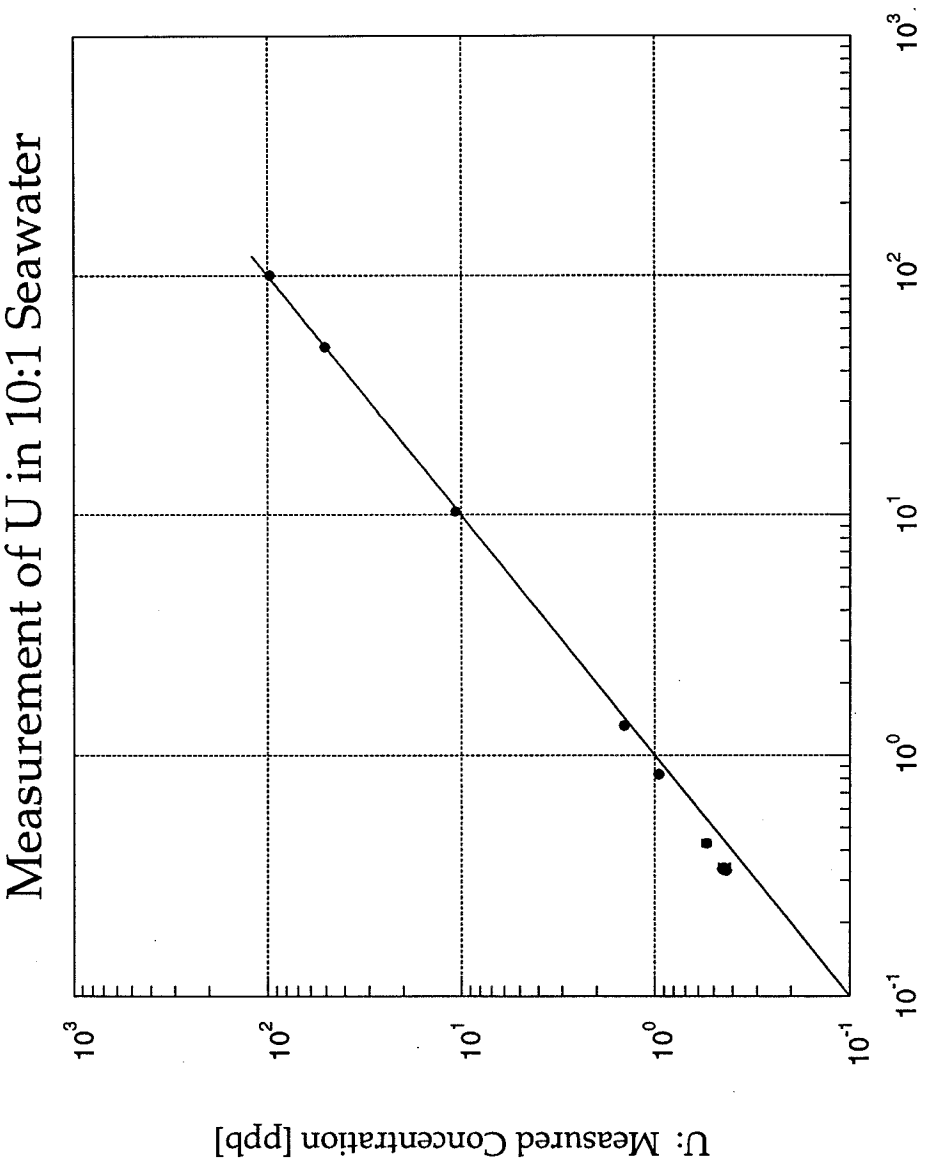
Measurement of U in 10:1 Seawater
U: Measured Concentration [ppb]
U: Actual Concentration [ppb]
10^{3}
10^{2}
10^{1}
10^{0}
10^{-1}
10^{-1}
10^{0}
10^{1}
10^{2}
10^{3}

Appendix D

Variations in elemental concentrations for daily composite samples at five locations in the Delta

Appendix D
Variations in elemental concentrations for daily composite samples at five locations in the Delta

Table of Contents

Measured quantities in the Sacramento River at Locke:

Measured quantities in the Sacramento River at Locke:

Measured quantities in the San Joaquin River at Mossdale Landing:

Measured quantities in the San Joaquin River at Mossdale Landing:

Measured quantities in the San Joaquin River at Mossdale Landing:

Measured quantities in San Pablo Bay at Martinez:

Measured quantities in San Pablo Bay at Martinez:

Measured quantities in water collected from Bethel Island:

Measured quantities in water collected from Bethel Island:

Measured quantities in water collected from Clifton Court:

Measured quantities in water collected from Clifton Court:

Measured quantities in water collected from Clifton Court:

location:
Locke
element:
river flow (cfs)
Flow rate [cfs]
120000
100000
80000
60000
40000
20000
0
3/2/96
3/16/96
3/30/96
4/13/96
4/27/96
5/11/96
5/25/96
6/8/96
6/22/96
7/6/96
7/20/96
8/3/96
8/17/96
8/31/96
9/14/96
9/28/96
10/12/96
10/26/96
11/9/96
11/23/96
12/7/96
12/21/96
1/4/97
1/18/97
2/1/97
2/15/97
3/1/97
3/15/97
sample date

location:
Locke
element:
Li7
concentration [ppb]
0
1
2
3
4
5
6
sample date
3/2/96
3/16/96
3/30/96
4/13/96
4/27/96
5/11/96
5/25/96
6/8/96
6/22/96
7/6/96
7/20/96
8/3/96
8/17/96
8/31/96
9/14/96
9/28/96
10/12/96
10/26/96
11/9/96
11/23/96
12/7/96
12/21/96
1/4/97
1/18/97
2/1/97
2/15/97
3/1/97
3/15/97

location:
Locke
element:
B11
concentration [ppb]
0
10
20
30
40
50
60
70
sample date
3/2/96
3/16/96
3/30/96
4/13/96
4/27/96
5/11/96
5/25/96
6/8/96
6/22/96
7/6/96
7/20/96
8/3/96
8/17/96
8/31/96
9/14/96
9/28/96
10/12/96
10/26/96
11/9/96
11/23/96
12/7/96
12/21/96
1/4/97
1/18/97
2/1/97
2/15/97
3/1/97
3/15/97

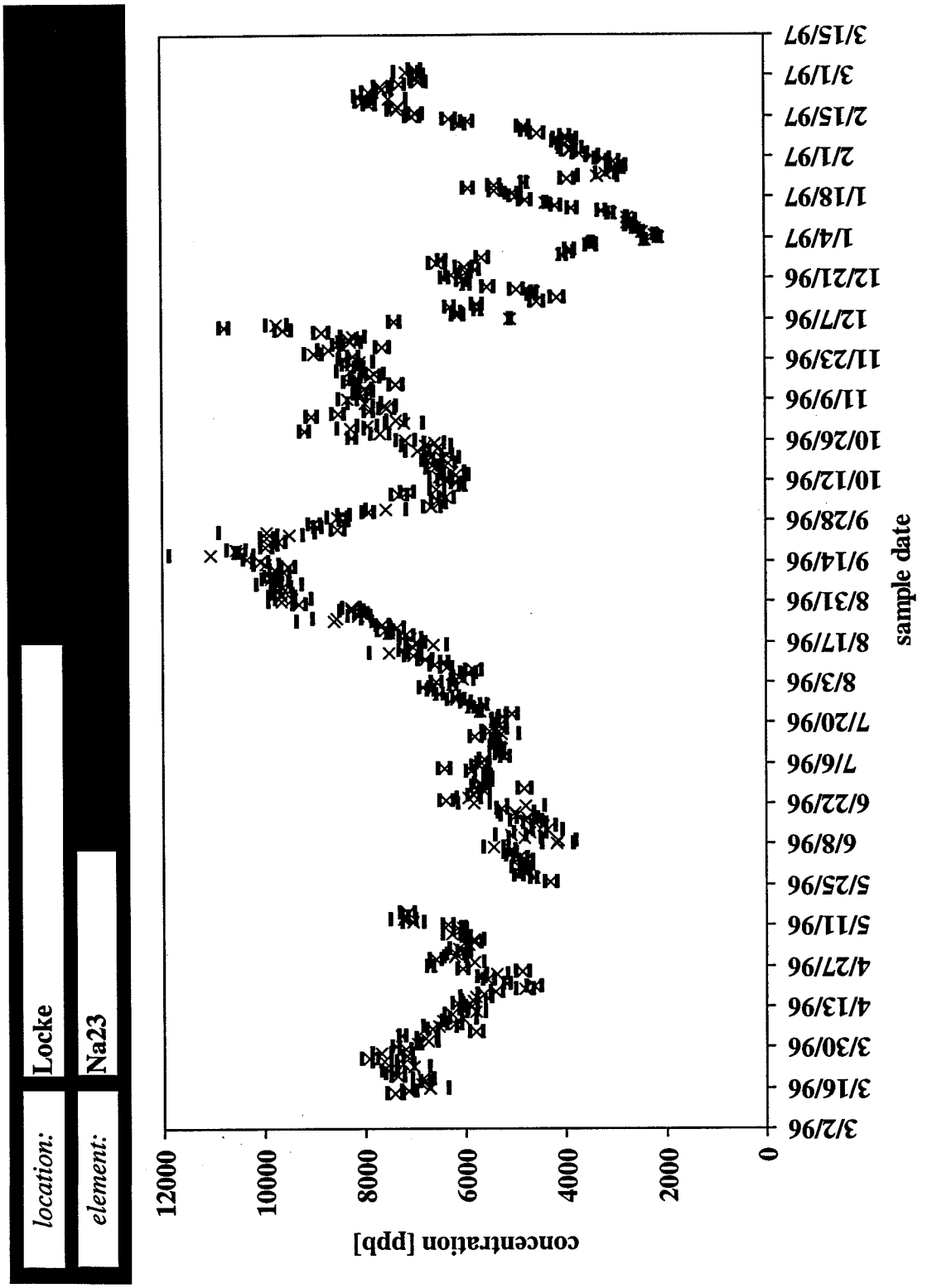
location:
Locke
element:
Na23
concentration [ppb]
12000
10000
8000
6000
4000
2000
0
sample date
3/2/96
3/16/96
3/30/96
4/13/96
4/27/96
5/11/96
5/25/96
6/8/96
6/22/96
7/6/96
7/20/96
8/3/96
8/17/96
8/31/96
9/14/96
9/28/96
10/12/96
10/26/96
11/9/96
11/23/96
12/7/96
12/21/96
1/4/97
1/18/97
2/1/97
2/15/97
3/1/97
3/15/97

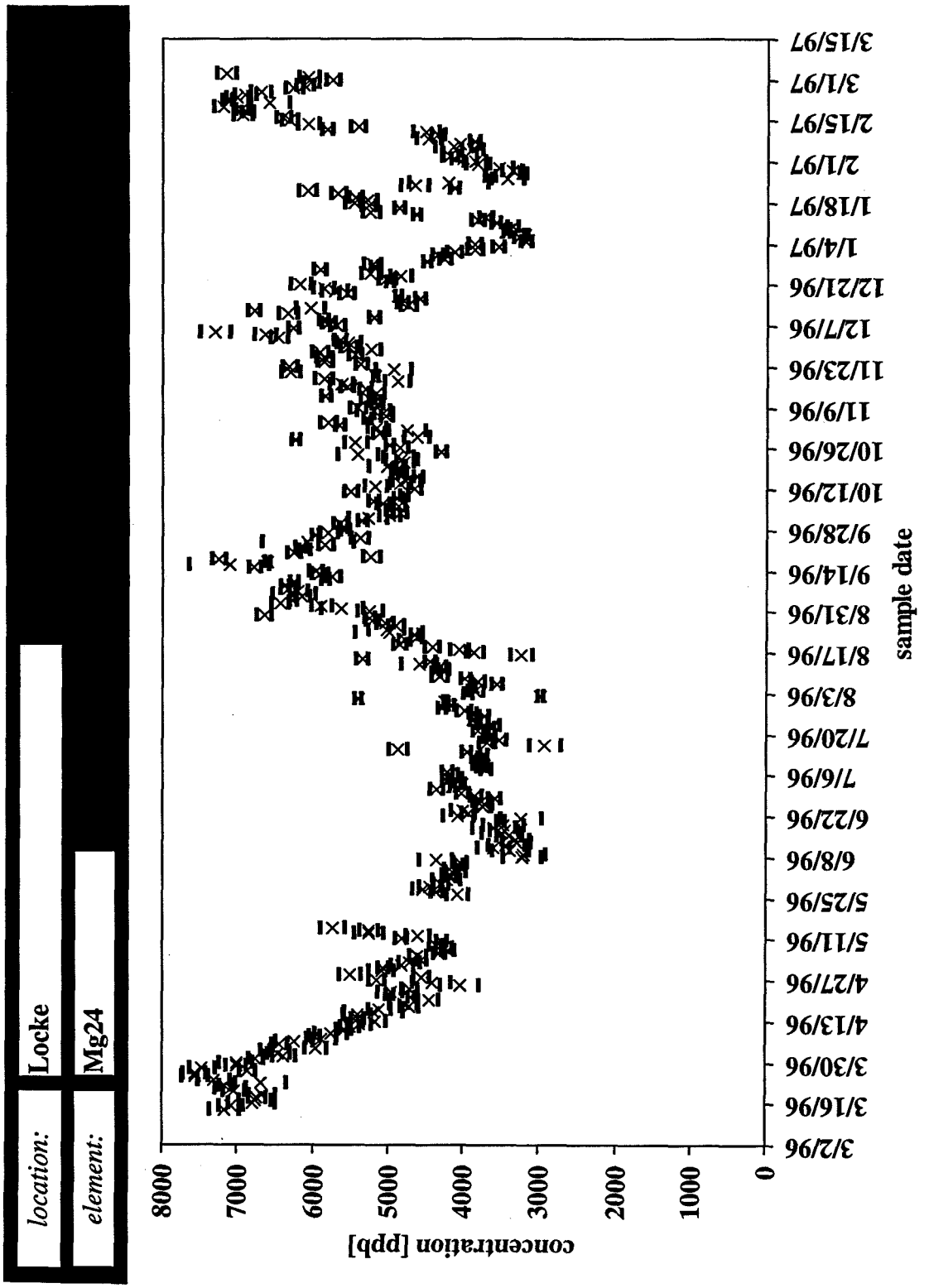
location:
Locke
element:
Mg24
concentration [ppb]
8000
7000
6000
5000
4000
3000
2000
1000
0
sample date
3/2/96
3/16/96
3/30/96
4/13/96
4/27/96
5/11/96
5/25/96
6/8/96
6/22/96
7/6/96
7/20/96
8/3/96
8/17/96
8/31/96
9/14/96
9/28/96
10/12/96
10/26/96
11/9/96
11/23/96
12/7/96
12/21/96
1/4/97
1/18/97
2/1/97
2/15/97
3/1/97
3/15/97

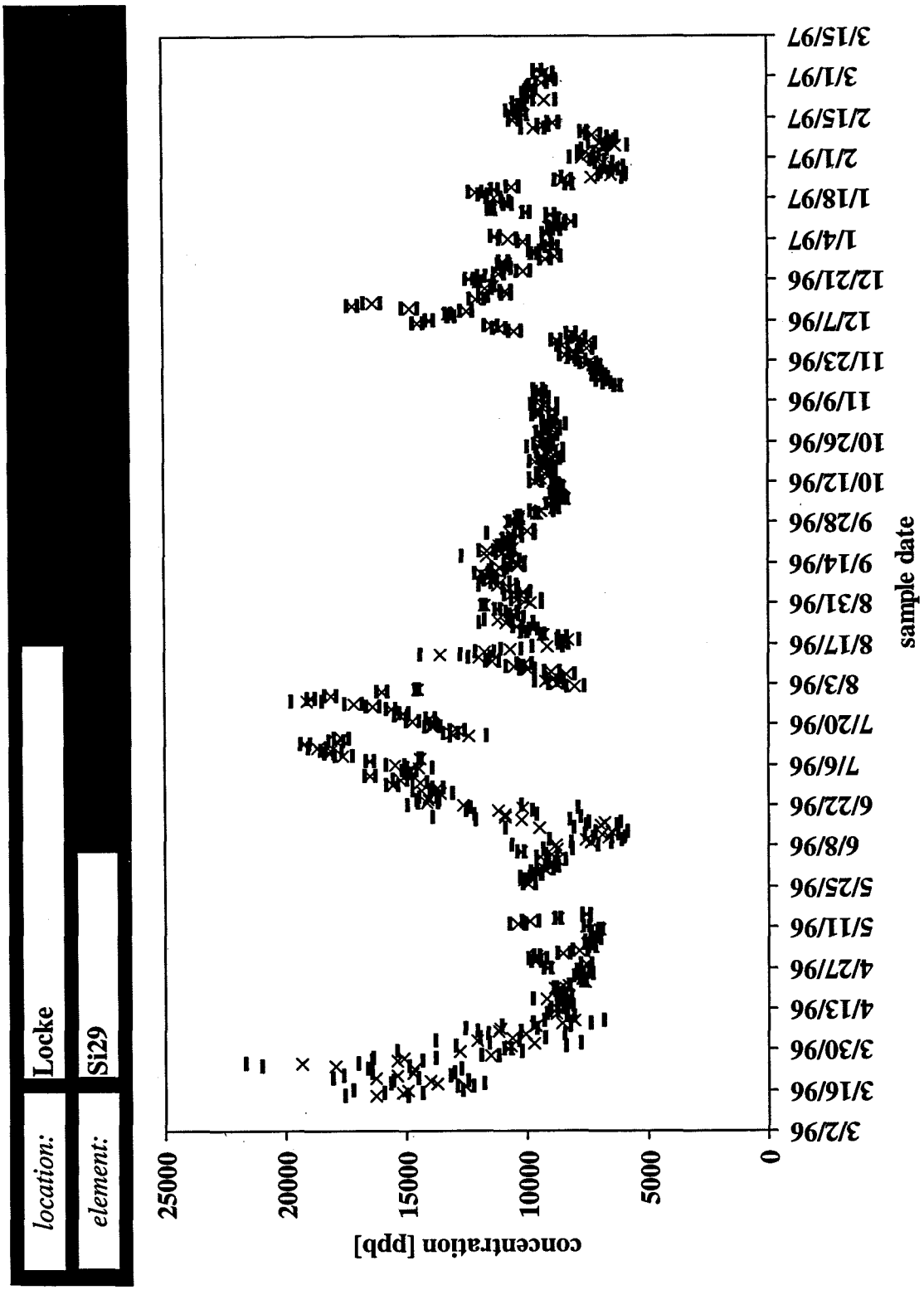
location:
Locke
element:
Si29
concentration [ppb]
25000
20000
15000
10000
5000
0
sample date
3/2/96
3/16/96
3/30/96
4/13/96
4/27/96
5/11/96
5/25/96
6/8/96
6/22/96
7/6/96
7/20/96
8/3/96
8/17/96
8/31/96
9/14/96
9/28/96
10/12/96
10/26/96
11/9/96
11/23/96
12/7/96
12/21/96
1/4/97
1/18/97
2/1/97
2/15/97
3/1/97
3/15/97

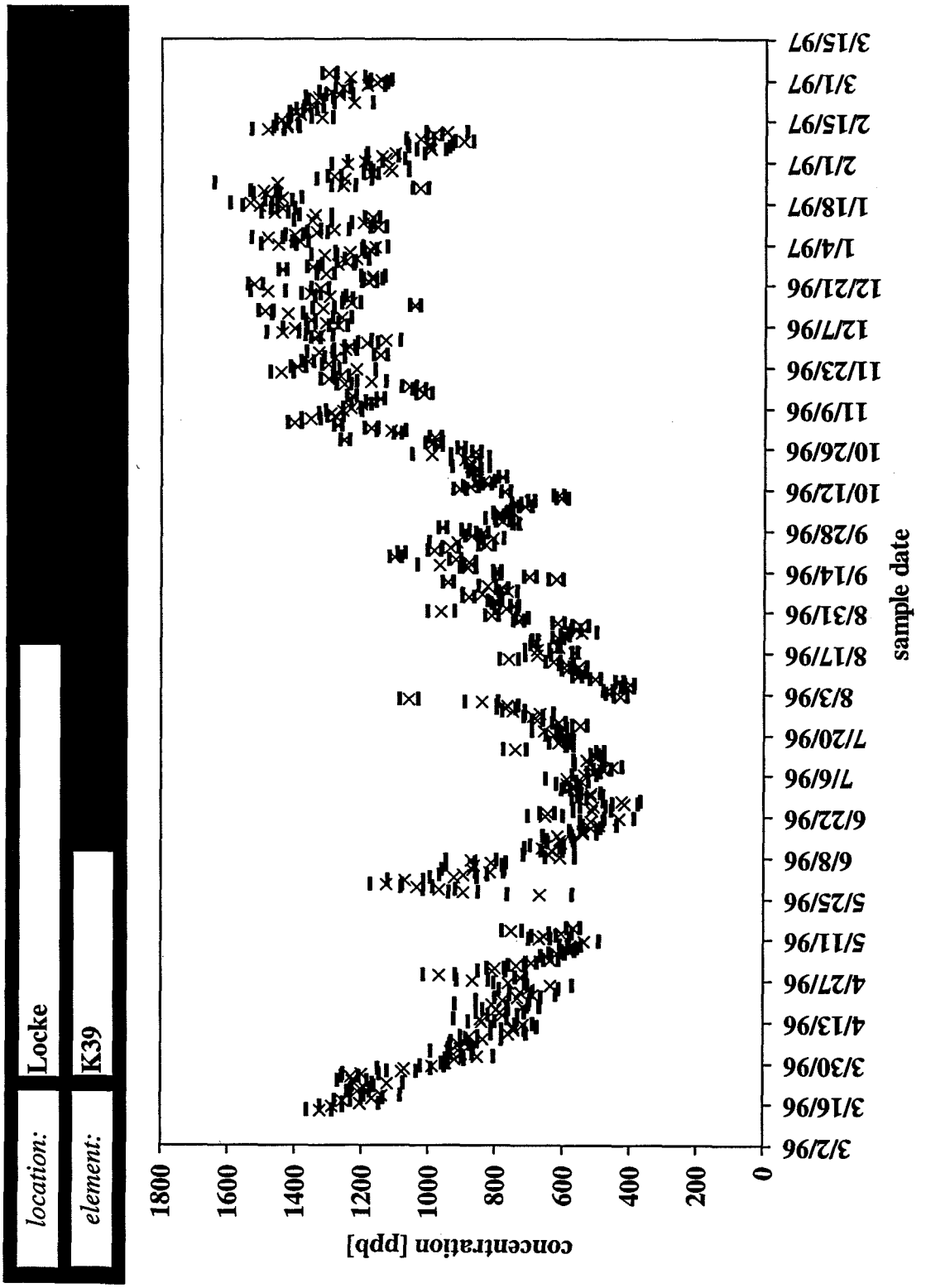
location:
Locke
element:
K39
concentration [ppb]
0
200
400
600
800
1000
1200
1400
1600
1800
sample date
3/2/96
3/16/96
3/30/96
4/13/96
4/27/96
5/11/96
5/25/96
6/8/96
6/22/96
7/6/96
7/20/96
8/3/96
8/17/96
8/31/96
9/14/96
9/28/96
10/12/96
10/26/96
11/9/96
11/23/96
12/7/96
12/21/96
1/4/97
1/18/97
2/1/97
2/15/97
3/1/97
3/15/97

location:
Locke
element:
Ca43
concentration [ppb]
8000
7000
6000
5000
4000
3000
2000
1000
0
sample date
3/2/96
3/16/96
3/30/96
4/13/96
4/27/96
5/11/96
5/25/96
6/8/96
6/22/96
7/6/96
7/20/96
8/3/96
8/17/96
8/31/96
9/14/96
9/28/96
10/12/96
10/26/96
11/9/96
11/23/96
12/7/96
12/21/96
1/4/97
1/18/97
2/1/97
2/15/97
3/1/97
3/15/97

location:
Locke
element:
V51
concentration [ppb]
0
2
4
6
8
10
12
14
16
sample date
3/2/96
3/16/96
3/30/96
4/13/96
4/27/96
5/11/96
5/25/96
6/8/96
6/22/96
7/6/96
7/20/96
8/3/96
8/17/96
8/31/96
9/14/96
9/28/96
10/12/96
10/26/96
11/9/96
11/23/96
12/7/96
12/21/96
1/4/97
1/18/97
2/1/97
2/15/97
3/1/97
3/15/97

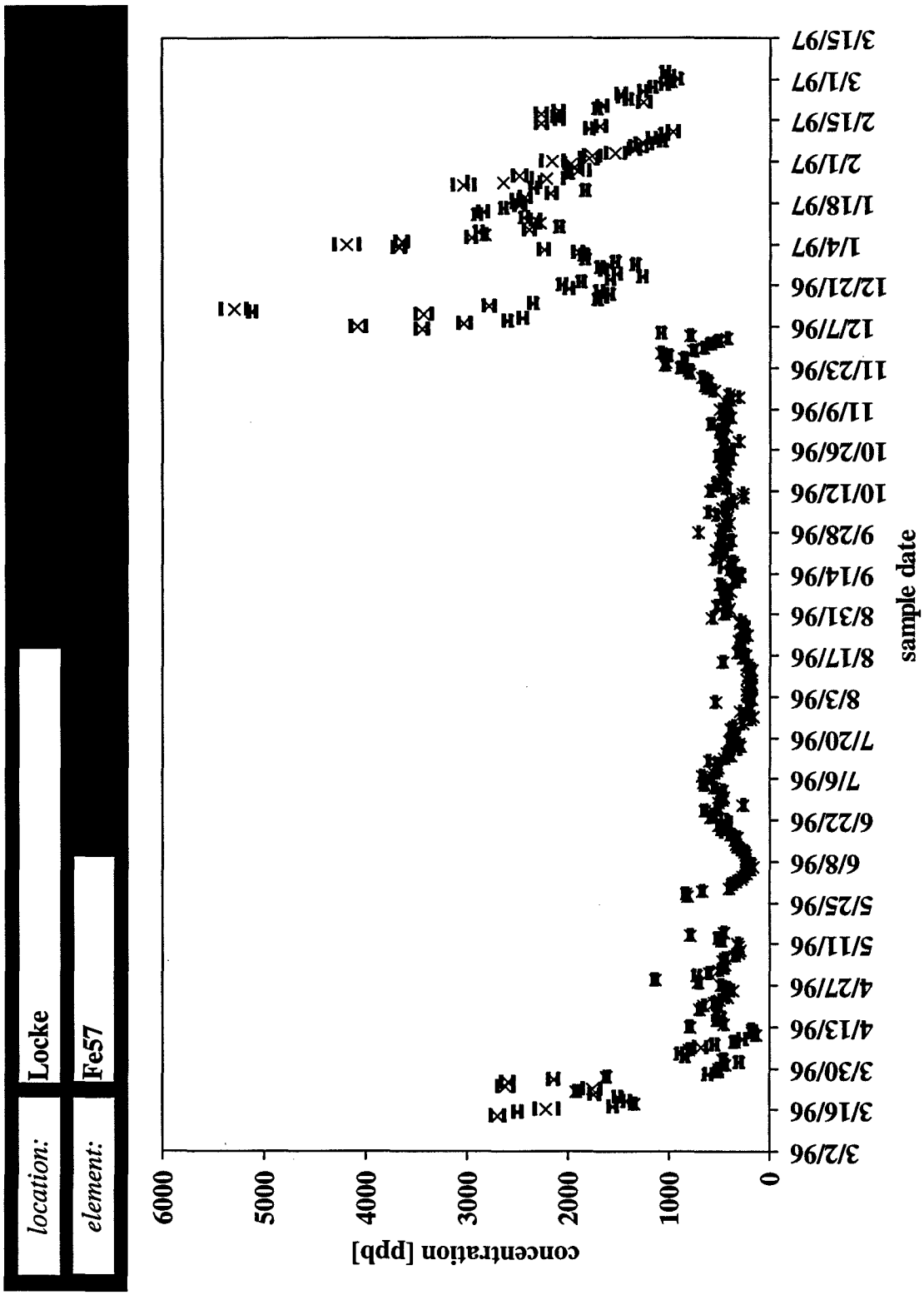
location:
Locke
element:
Fe57
concentration [ppb]
0
1000
2000
3000
4000
5000
6000
sample date
3/2/96
3/16/96
3/30/96
4/13/96
4/27/96
5/11/96
5/25/96
6/8/96
6/22/96
7/6/96
7/20/96
8/3/96
8/17/96
8/31/96
9/14/96
9/28/96
10/12/96
10/26/96
11/9/96
11/23/96
12/7/96
12/21/96
1/4/97
1/18/97
2/1/97
2/15/97
3/1/97
3/15/97

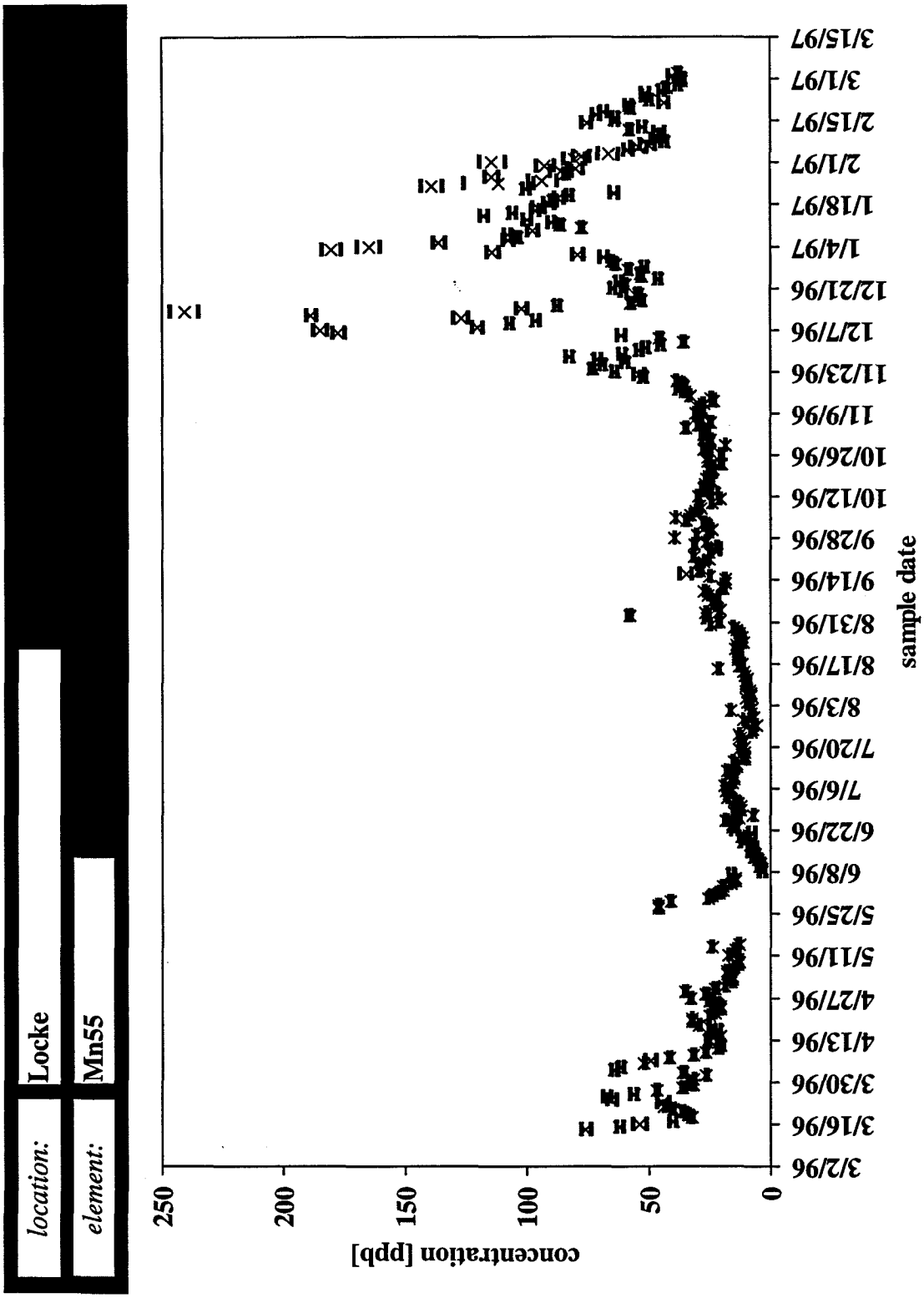
location:
Locke
element:
Mn55
concentration [ppb]
250
200
150
100
50
0
sample date
3/2/96
3/16/96
3/30/96
4/13/96
4/27/96
5/11/96
5/25/96
6/8/96
6/22/96
7/6/96
7/20/96
8/3/96
8/17/96
8/31/96
9/14/96
9/28/96
10/12/96
10/26/96
11/9/96
11/23/96
12/7/96
12/21/96
1/4/97
1/18/97
2/1/97
2/15/97
3/1/97
3/15/97

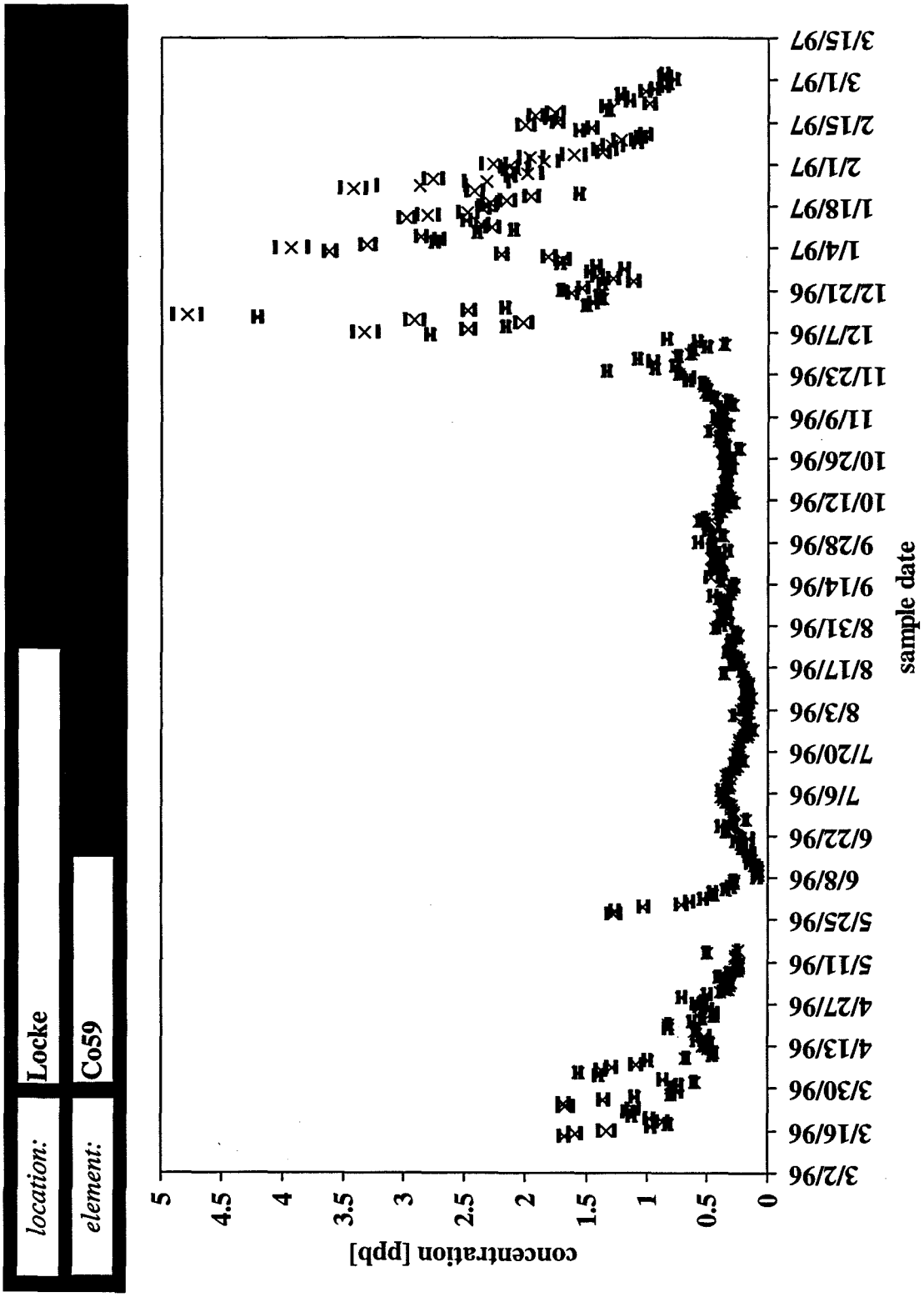
location:
Locke
element:
Co59
concentration [ppb]
0
0.5
1
1.5
2
2.5
3
3.5
4
4.5
5
sample date
3/2/96
3/16/96
3/30/96
4/13/96
4/27/96
5/11/96
5/25/96
6/8/96
6/22/96
7/6/96
7/20/96
8/3/96
8/17/96
8/31/96
9/14/96
9/28/96
10/12/96
10/26/96
11/9/96
11/23/96
12/7/96
12/21/96
1/4/97
1/18/97
2/1/97
2/15/97
3/1/97
3/15/97

location:
Locke
element:
Zn66
concentration [ppb]
60
50
40
30
20
10
0
-10
sample date
3/2/96
3/16/96
3/30/96
4/13/96
4/27/96
5/11/96
5/25/96
6/8/96
6/22/96
7/6/96
7/20/96
8/3/96
8/17/96
8/31/96
9/14/96
9/28/96
10/12/96
10/26/96
11/9/96
11/23/96
12/7/96
12/21/96
1/4/97
1/18/97
2/1/97
2/15/97
3/1/97
3/15/97

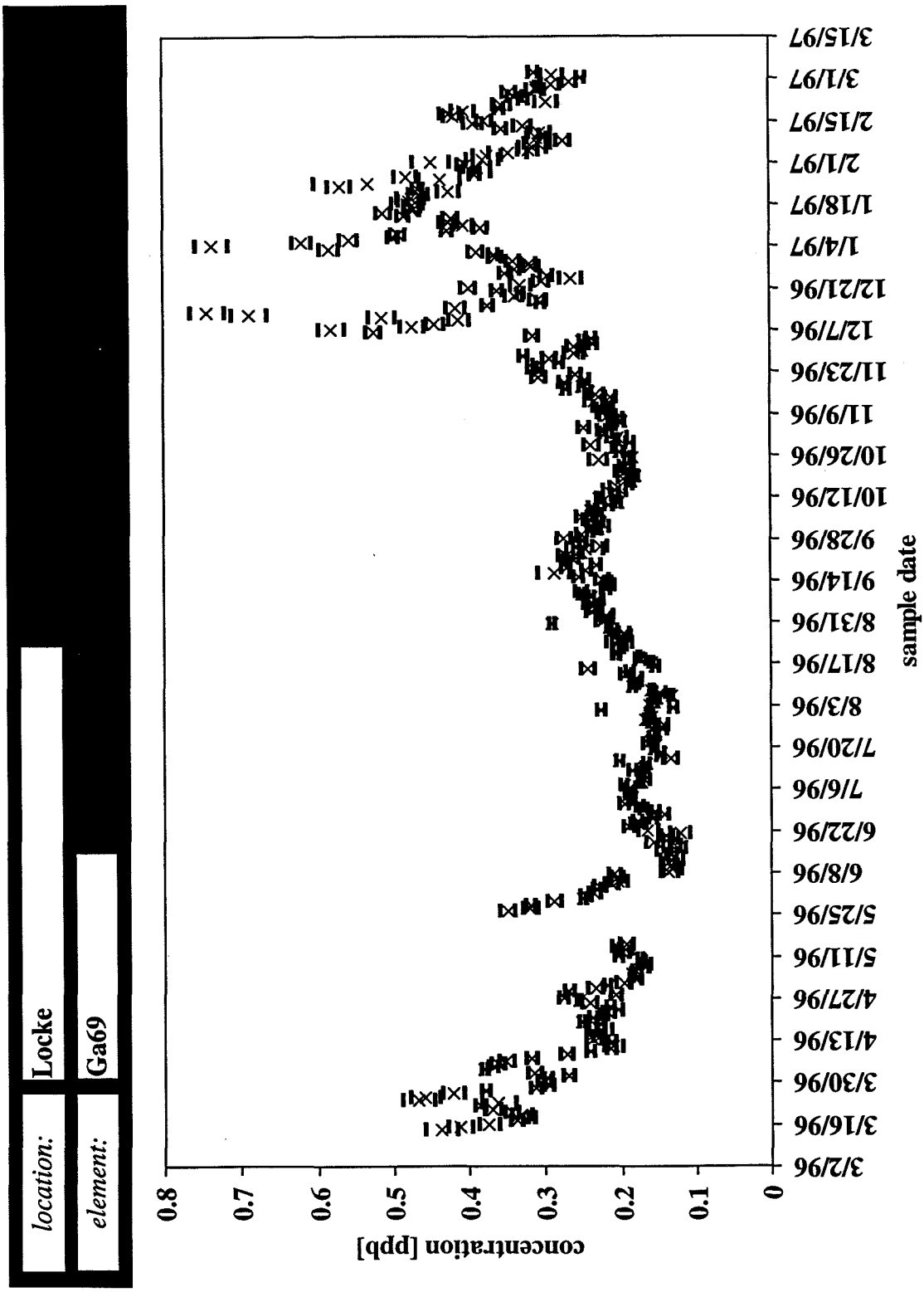
location:
Locke
element:
Ga69
concentration [ppb]
0.8
0.7
0.6
0.5
0.4
0.3
0.2
0.1
0
sample date
3/2/96
3/16/96
3/30/96
4/13/96
4/27/96
5/11/96
5/25/96
6/8/96
6/22/96
7/6/96
7/20/96
8/3/96
8/17/96
8/31/96
9/14/96
9/28/96
10/12/96
10/26/96
11/9/96
11/23/96
12/7/96
12/21/96
1/4/97
1/18/97
2/1/97
2/15/97
3/1/97
3/15/97

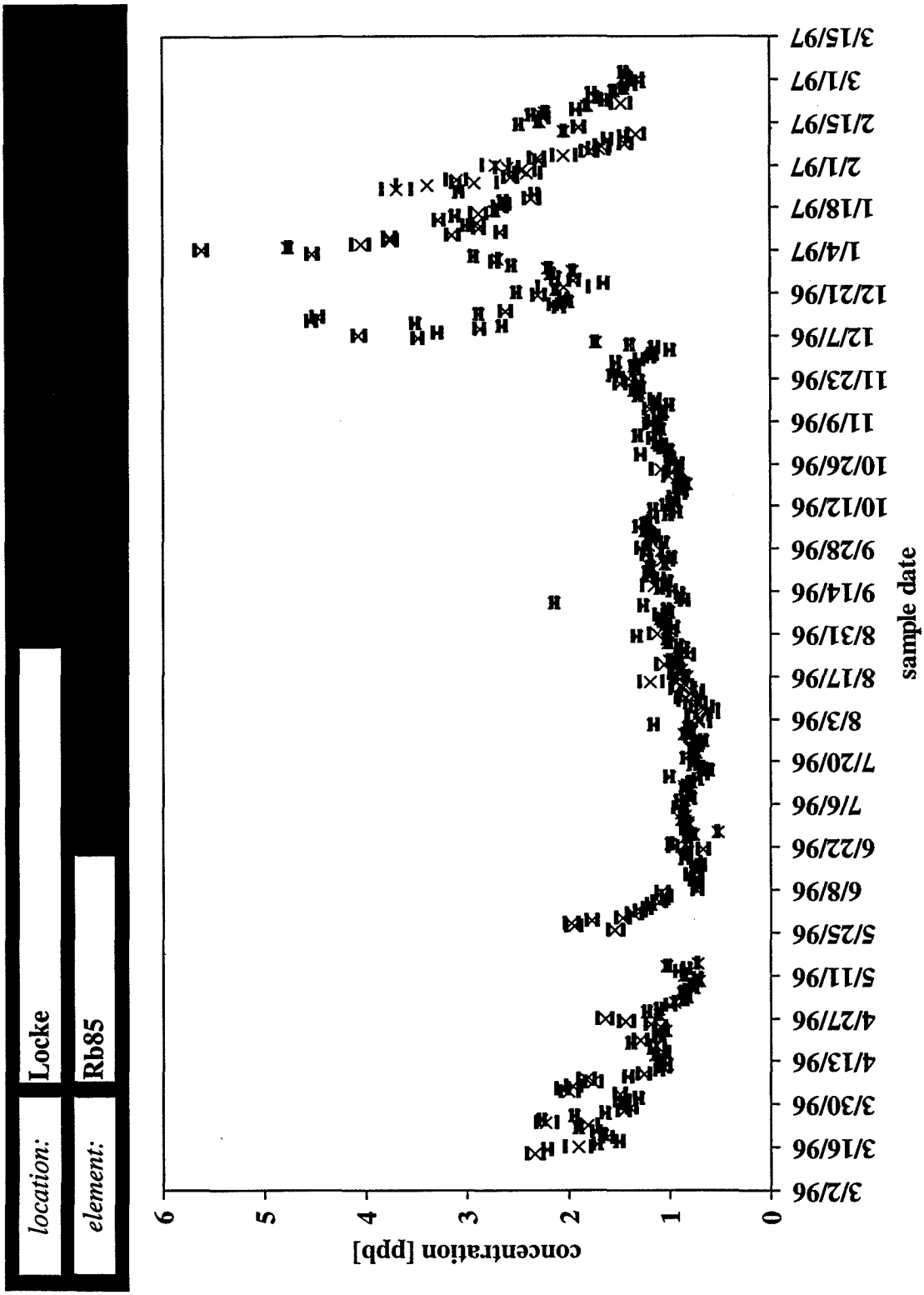
location:
Locke
element:
Rb85
concentration [ppb]
0
1
2
3
4
5
6
sample date
3/2/96
3/16/96
3/30/96
4/13/96
4/27/96
5/11/96
5/25/96
6/8/96
6/22/96
7/6/96
7/20/96
8/3/96
8/17/96
8/31/96
9/14/96
9/28/96
10/12/96
10/26/96
11/9/96
11/23/96
12/7/96
12/21/96
1/4/97
1/18/97
2/1/97
2/15/97
3/1/97
3/15/97

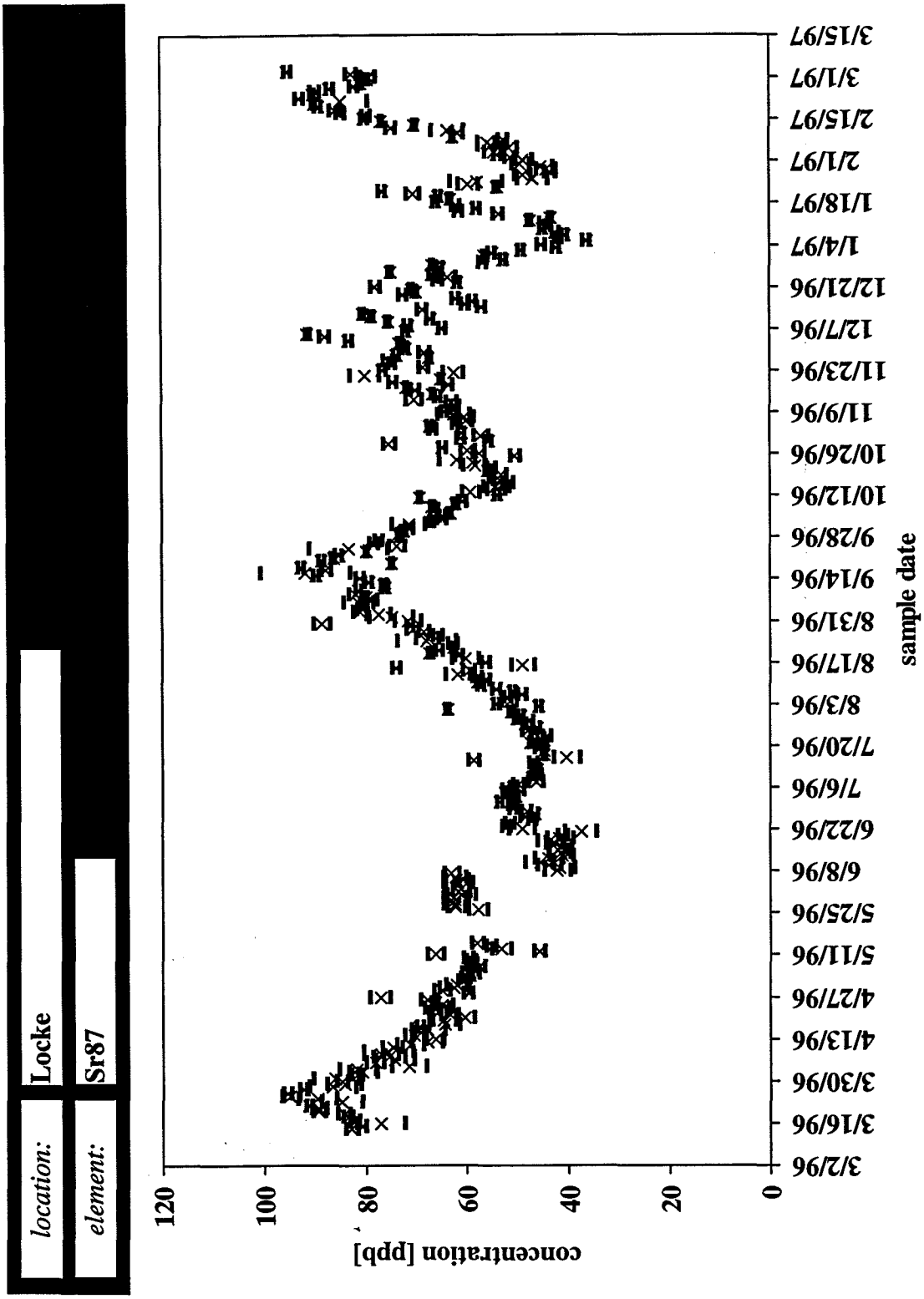
location:
Locke
element:
Sr87
concentration [ppb]
0
20
40
60
80
100
120
sample date
3/2/96
3/16/96
3/30/96
4/13/96
4/27/96
5/11/96
5/25/96
6/8/96
6/22/96
7/6/96
7/20/96
8/3/96
8/17/96
8/31/96
9/14/96
9/28/96
10/12/96
10/26/96
11/9/96
11/23/96
12/7/96
12/21/96
1/4/97
1/18/97
2/1/97
2/15/97
3/1/97
3/15/97

location:
Locke
element:
Y89
concentration [ppb]
0
0.5
1
1.5
2
2.5
3
3.5
4
sample date
3/2/96
3/16/96
3/30/96
4/13/96
4/27/96
5/11/96
5/25/96
6/8/96
6/22/96
7/6/96
7/20/96
8/3/96
8/17/96
8/31/96
9/14/96
9/28/96
10/12/96
10/26/96
11/9/96
11/23/96
12/7/96
12/21/96
1/4/97
1/18/97
2/1/97
2/15/97
3/1/97
3/15/97

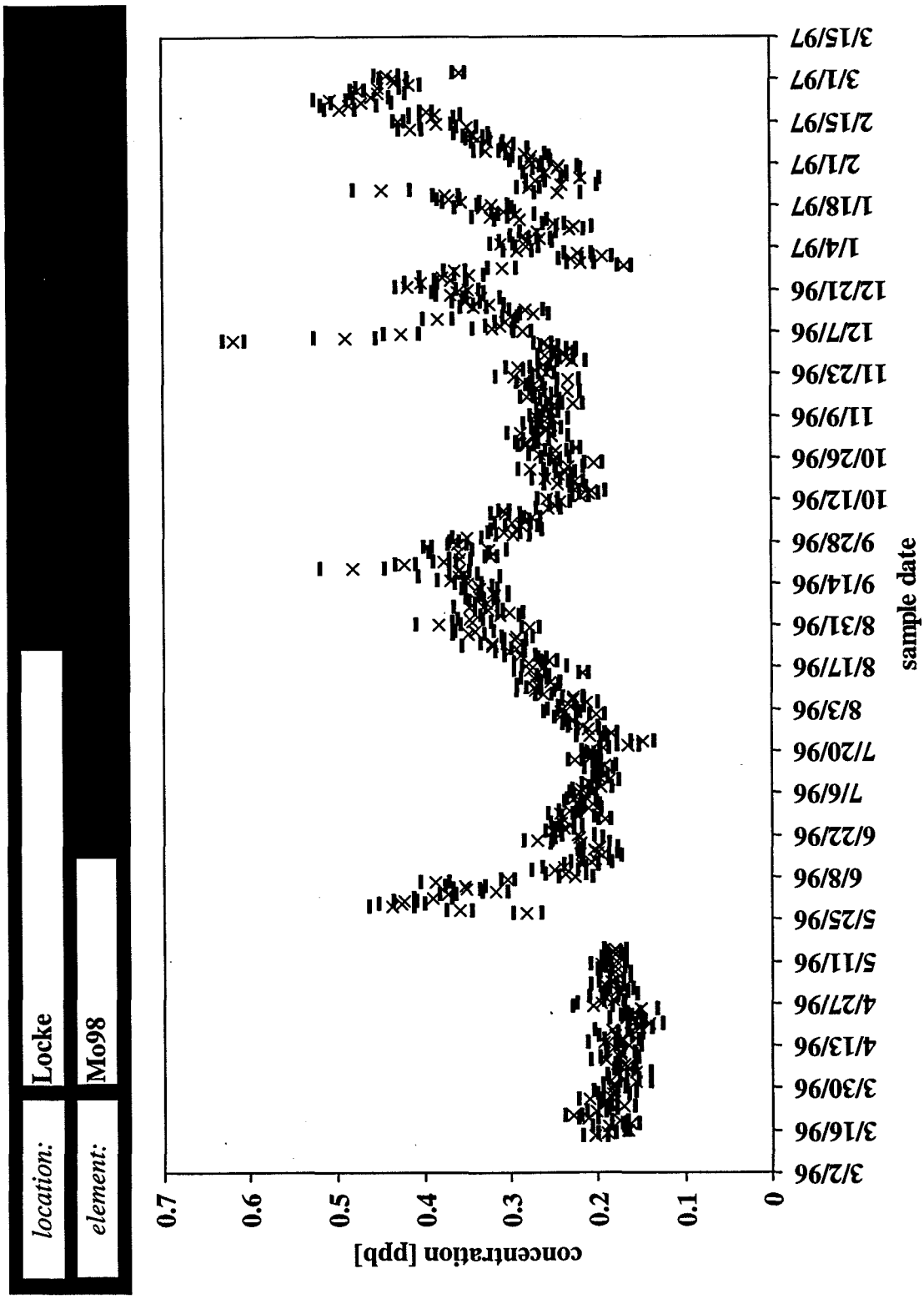
location:
Locke
element:
Mo98
concentration [ppb]
0.7
0.6
0.5
0.4
0.3
0.2
0.1
0
sample date
3/2/96
3/16/96
3/30/96
4/13/96
4/27/96
5/11/96
5/25/96
6/8/96
6/22/96
7/6/96
7/20/96
8/3/96
8/17/96
8/31/96
9/14/96
9/28/96
10/12/96
10/26/96
11/9/96
11/23/96
12/7/96
12/21/96
1/4/97
1/18/97
2/1/97
2/15/97
3/1/97
3/15/97

location:
Locke
element:
Ba137
concentration [ppb]
0
10
20
30
40
50
60
70
80
sample date
3/2/96
3/16/96
3/30/96
4/13/96
4/27/96
5/11/96
5/25/96
6/8/96
6/22/96
7/6/96
7/20/96
8/3/96
8/17/96
8/31/96
9/14/96
9/28/96
10/12/96
10/26/96
11/9/96
11/23/96
12/7/96
12/21/96
1/4/97
1/18/97
2/1/97
2/15/97
3/1/97
3/15/97

location:
Locke
element:
La139
concentration [ppb]
0
0.5
1
1.5
2
2.5
3
3.5
sample date
3/2/96
3/16/96
3/30/96
4/13/96
4/27/96
5/11/96
5/25/96
6/8/96
6/22/96
7/6/96
7/20/96
8/3/96
8/17/96
8/31/96
9/14/96
9/28/96
10/12/96
10/26/96
11/9/96
11/23/96
12/7/96
12/21/96
1/4/97
1/18/97
2/1/97
2/15/97
3/1/97
3/15/97

location:
Locke
element:
Ce140
concentration [ppb]
0
1
2
3
4
5
6
7
8
9
sample date
3/2/96
3/16/96
3/30/96
4/13/96
4/27/96
5/11/96
5/25/96
6/8/96
6/22/96
7/6/96
7/20/96
8/3/96
8/17/96
8/31/96
9/14/96
9/28/96
10/12/96
10/26/96
11/9/96
11/23/96
12/7/96
12/21/96
1/4/97
1/18/97
2/1/97
2/15/97
3/1/97
3/15/97

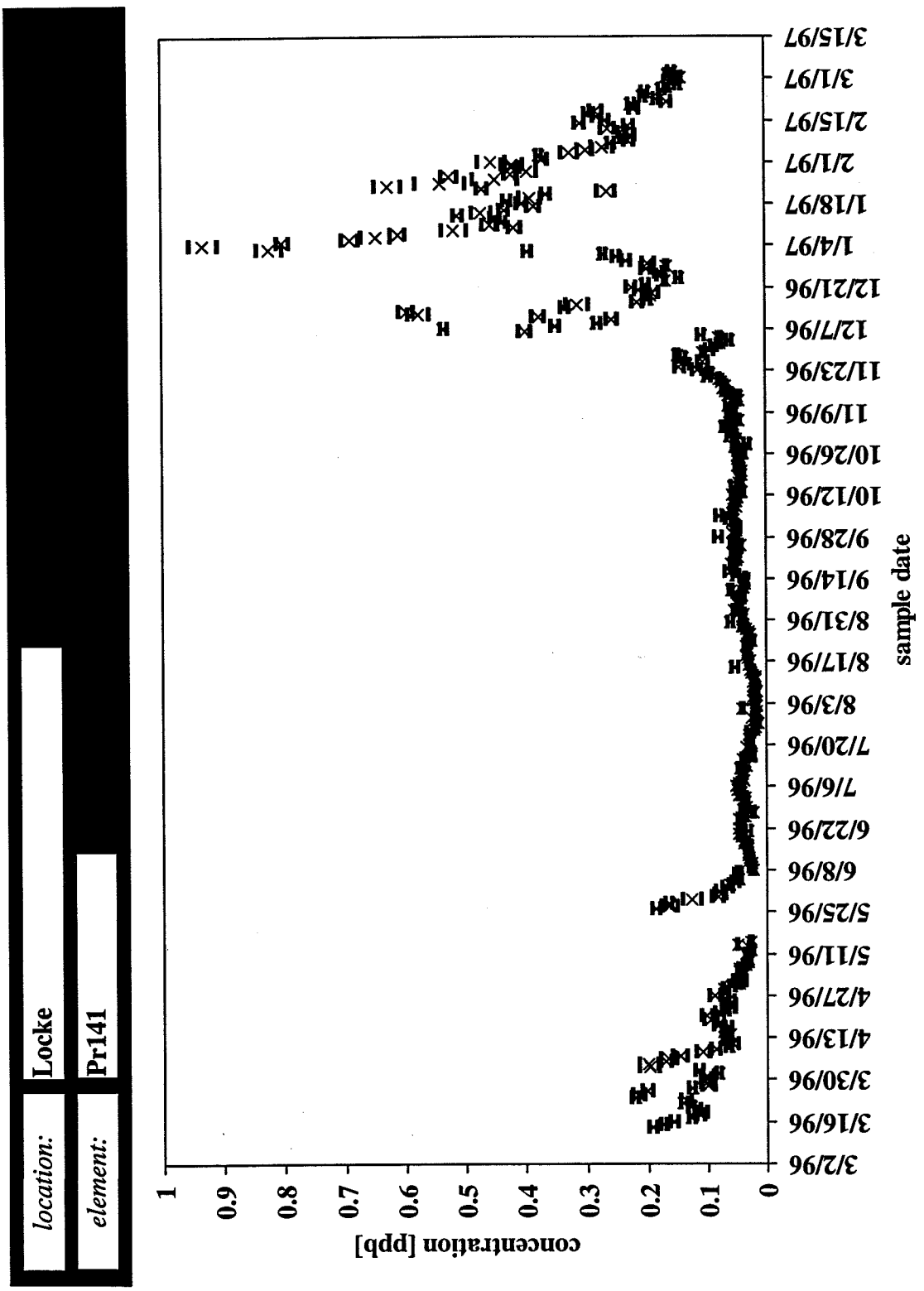
location:
Locke
element:
Pr141
concentration [ppb]
0
0.1
0.2
0.3
0.4
0.5
0.6
0.7
0.8
0.9
1
sample date
3/2/96
3/16/96
3/30/96
4/13/96
4/27/96
5/11/96
5/25/96
6/8/96
6/22/96
7/6/96
7/20/96
8/3/96
8/17/96
8/31/96
9/14/96
9/28/96
10/12/96
10/26/96
11/9/96
11/23/96
12/7/96
12/21/96
1/4/97
1/18/97
2/1/97
2/15/97
3/1/97
3/15/97

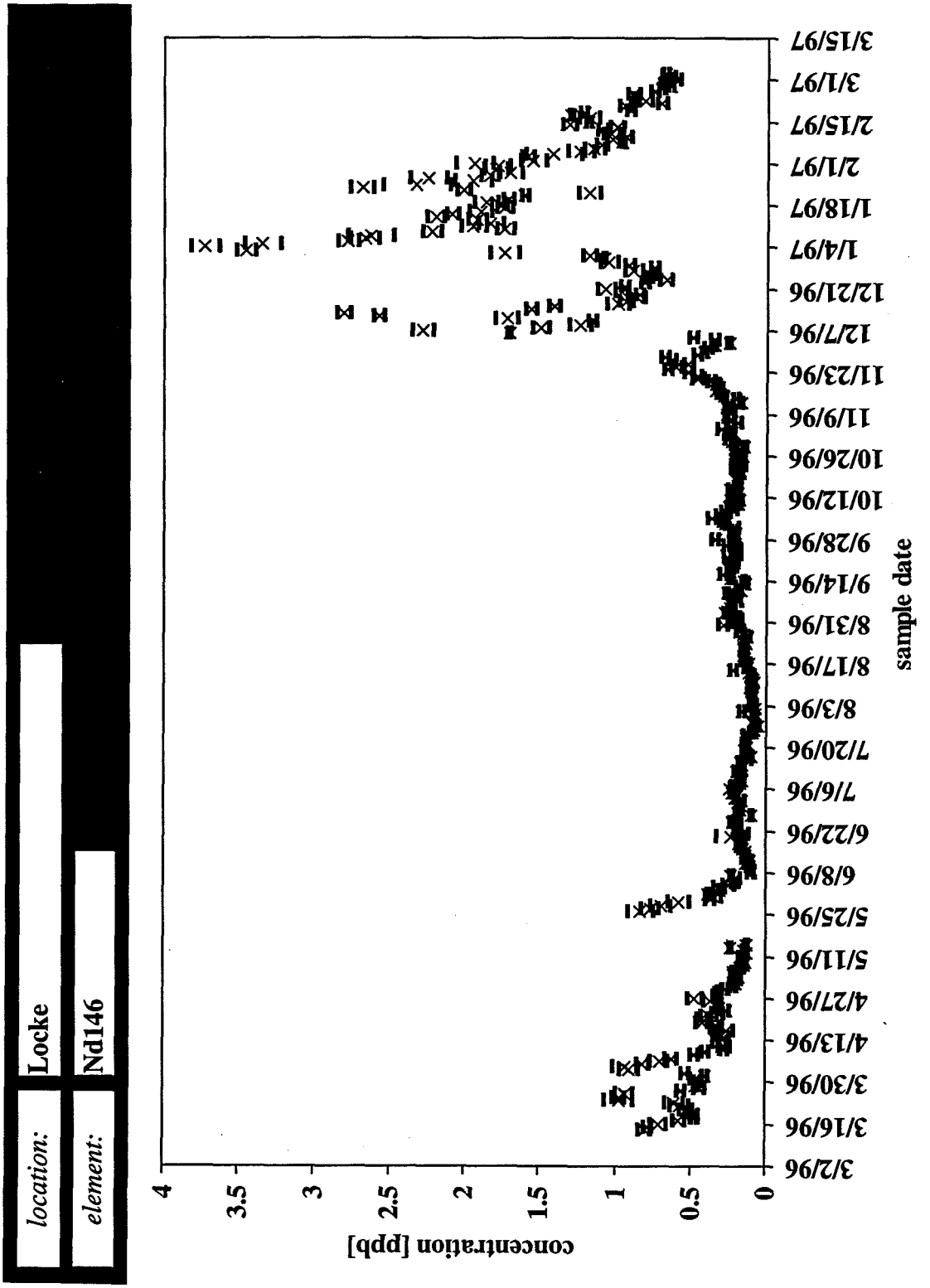
location:
Locke
element:
Nd146
concentration [ppb]
0
0.5
1
1.5
2
2.5
3
3.5
4
sample date
3/2/96
3/16/96
3/30/96
4/13/96
4/27/96
5/11/96
5/25/96
6/8/96
6/22/96
7/6/96
7/20/96
8/3/96
8/17/96
8/31/96
9/14/96
9/28/96
10/12/96
10/26/96
11/9/96
11/23/96
12/7/96
12/21/96
1/4/97
1/18/97
2/1/97
2/15/97
3/1/97
3/15/97

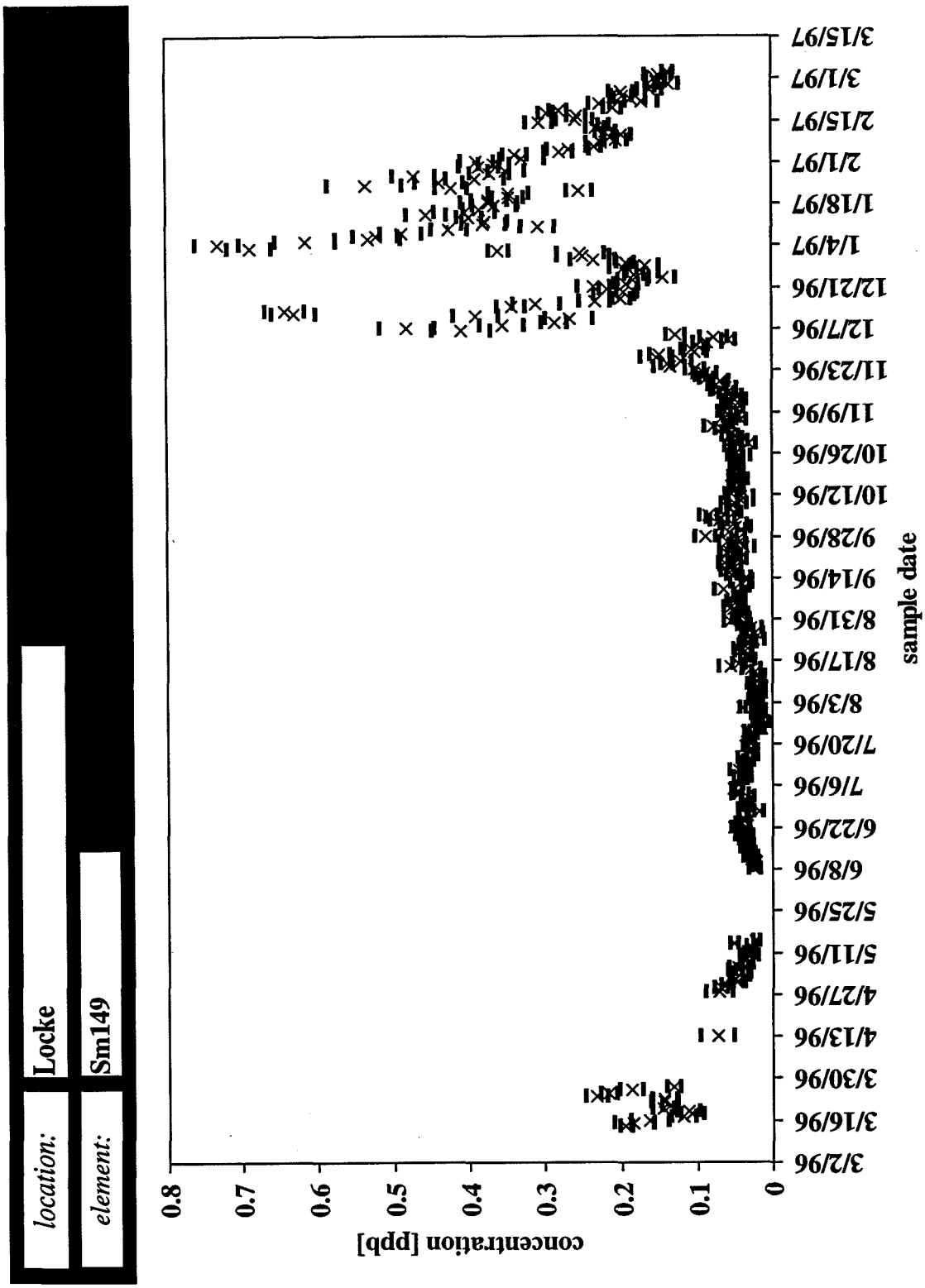
location:
Locke
element:
Sm149
concentration [ppb]
0
0.1
0.2
0.3
0.4
0.5
0.6
0.7
0.8
sample date
3/2/96
3/16/96
3/30/96
4/13/96
4/27/96
5/11/96
5/25/96
6/8/96
6/22/96
7/6/96
7/20/96
8/3/96
8/17/96
8/31/96
9/14/96
9/28/96
10/12/96
10/26/96
11/9/96
11/23/96
12/7/96
12/21/96
1/4/97
1/18/97
2/1/97
2/15/97
3/1/97
3/15/97

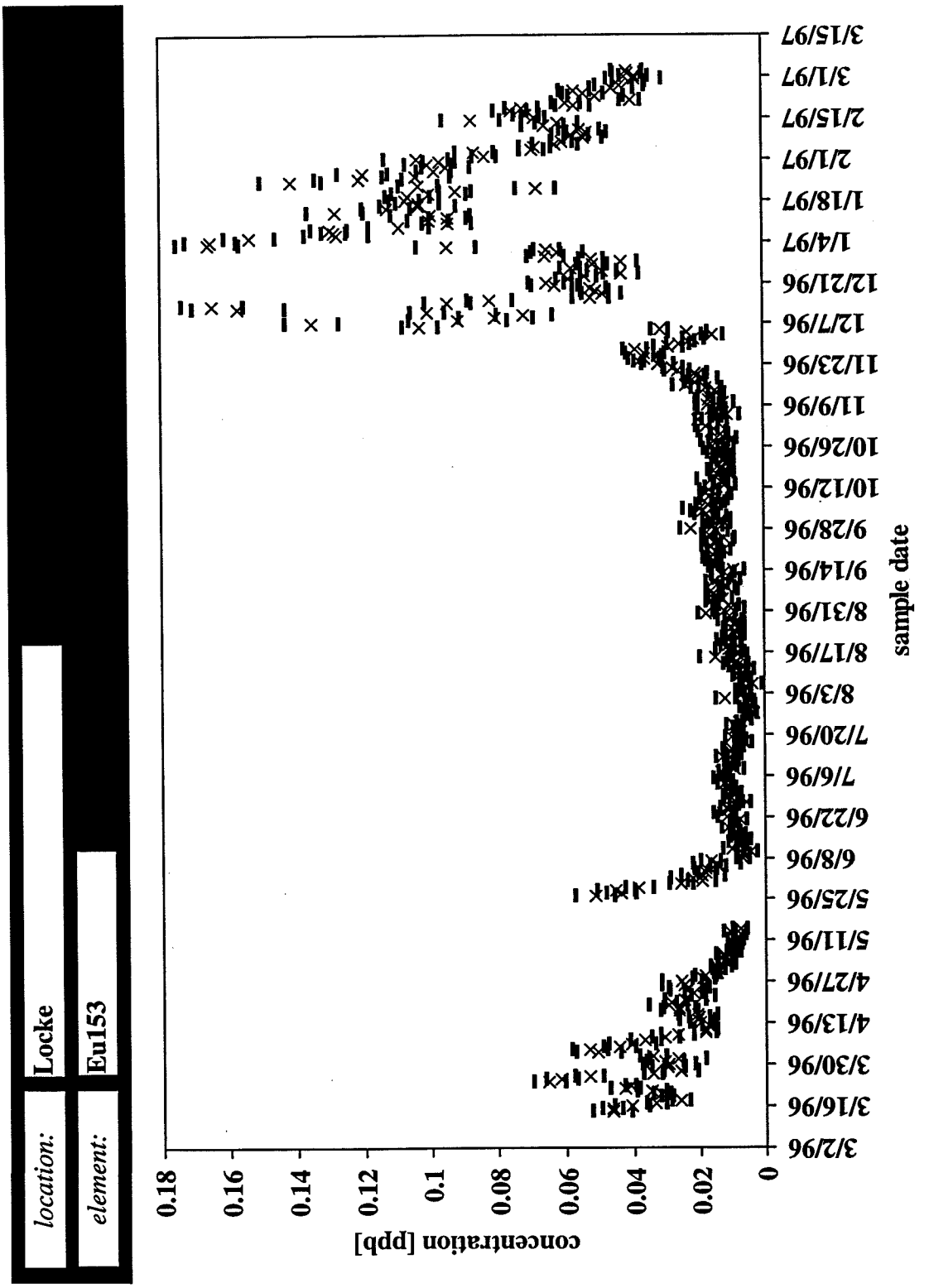
location:
Locke
element:
Eu153
concentration [ppb]
0.18
0.16
0.14
0.12
0.1
0.08
0.06
0.04
0.02
0
sample date
3/2/96
3/16/96
3/30/96
4/13/96
4/27/96
5/11/96
5/25/96
6/8/96
6/22/96
7/6/96
7/20/96
8/3/96
8/17/96
8/31/96
9/14/96
9/28/96
10/12/96
10/26/96
11/9/96
11/23/96
12/7/96
12/21/96
1/4/97
1/18/97
2/1/97
2/15/97
3/1/97
3/15/97

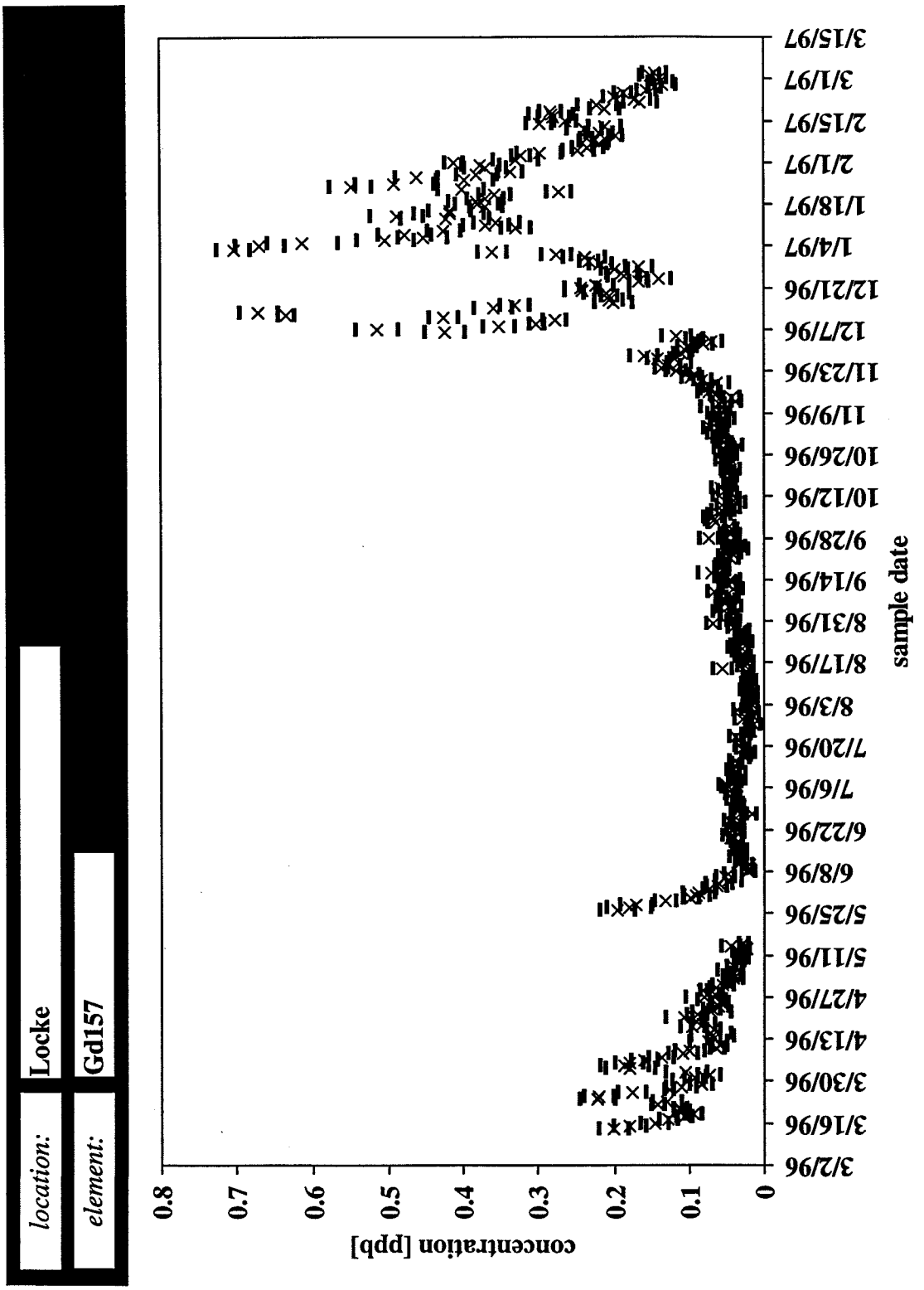
location:
Locke
element:
Gd157
concentration [ppb]
0.8
0.7
0.6
0.5
0.4
0.3
0.2
0.1
0
sample date
3/2/96
3/16/96
3/30/96
4/13/96
4/27/96
5/11/96
5/25/96
6/8/96
6/22/96
7/6/96
7/20/96
8/3/96
8/17/96
8/31/96
9/14/96
9/28/96
10/12/96
10/26/96
11/9/96
11/23/96
12/7/96
12/21/96
1/4/97
1/18/97
2/1/97
2/15/97
3/1/97
3/15/97

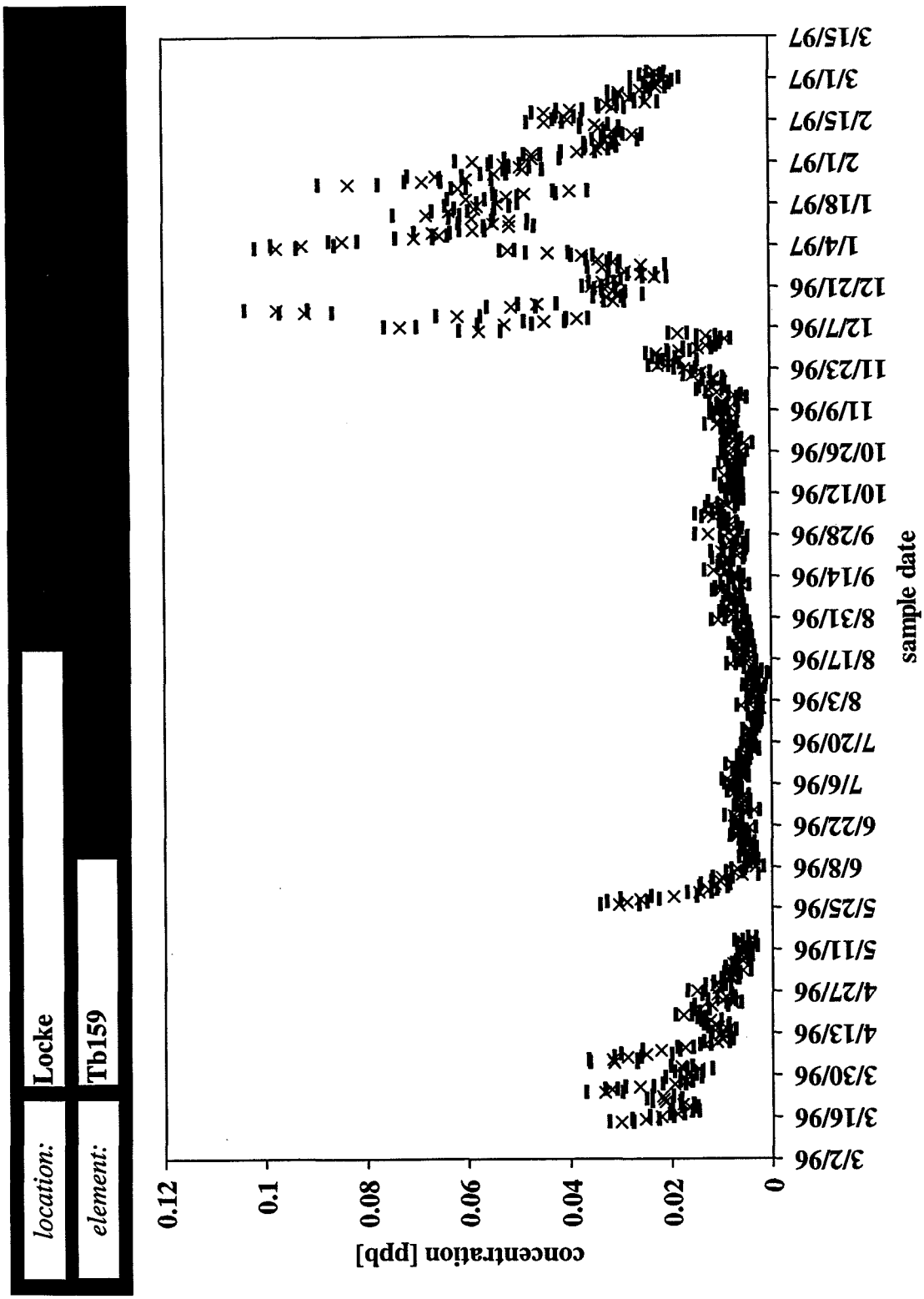
location:
Locke
element:
Tb159
concentration [ppb]
0.12
0.1
0.08
0.06
0.04
0.02
0
sample date
3/2/96
3/16/96
3/30/96
4/13/96
4/27/96
5/11/96
5/25/96
6/8/96
6/22/96
7/6/96
7/20/96
8/3/96
8/17/96
8/31/96
9/14/96
9/28/96
10/12/96
10/26/96
11/9/96
11/23/96
12/7/96
12/21/96
1/4/97
1/18/97
2/1/97
2/15/97
3/1/97
3/15/97

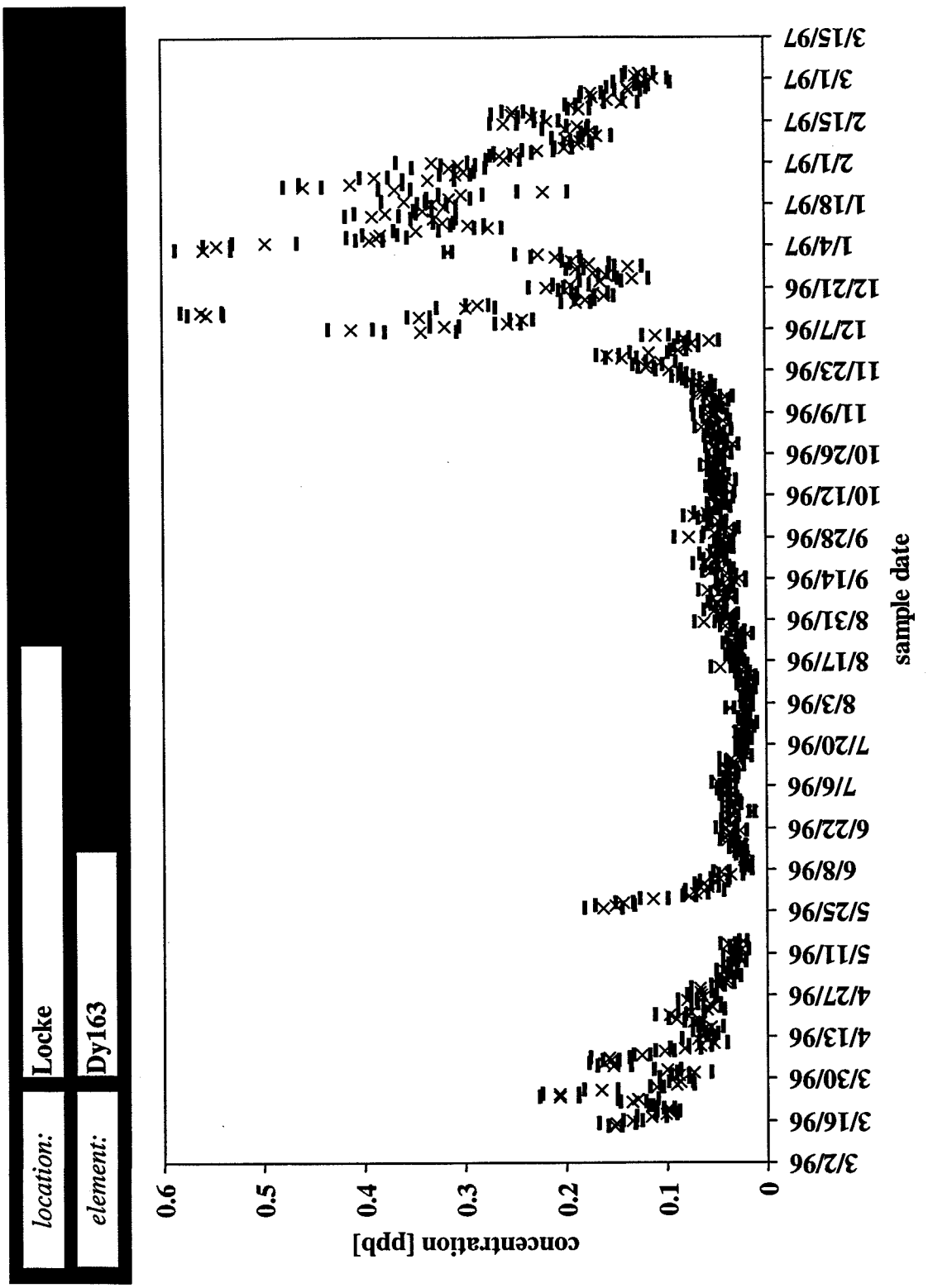
location:
Locke
element:
Dy163
concentration [ppb]
0.6
0.5
0.4
0.3
0.2
0.1
0
sample date
3/2/96
3/16/96
3/30/96
4/13/96
4/27/96
5/11/96
5/25/96
6/8/96
6/22/96
7/6/96
7/20/96
8/3/96
8/17/96
8/31/96
9/14/96
9/28/96
10/12/96
10/26/96
11/9/96
11/23/96
12/7/96
12/21/96
1/4/97
1/18/97
2/1/97
2/15/97
3/1/97
3/15/97

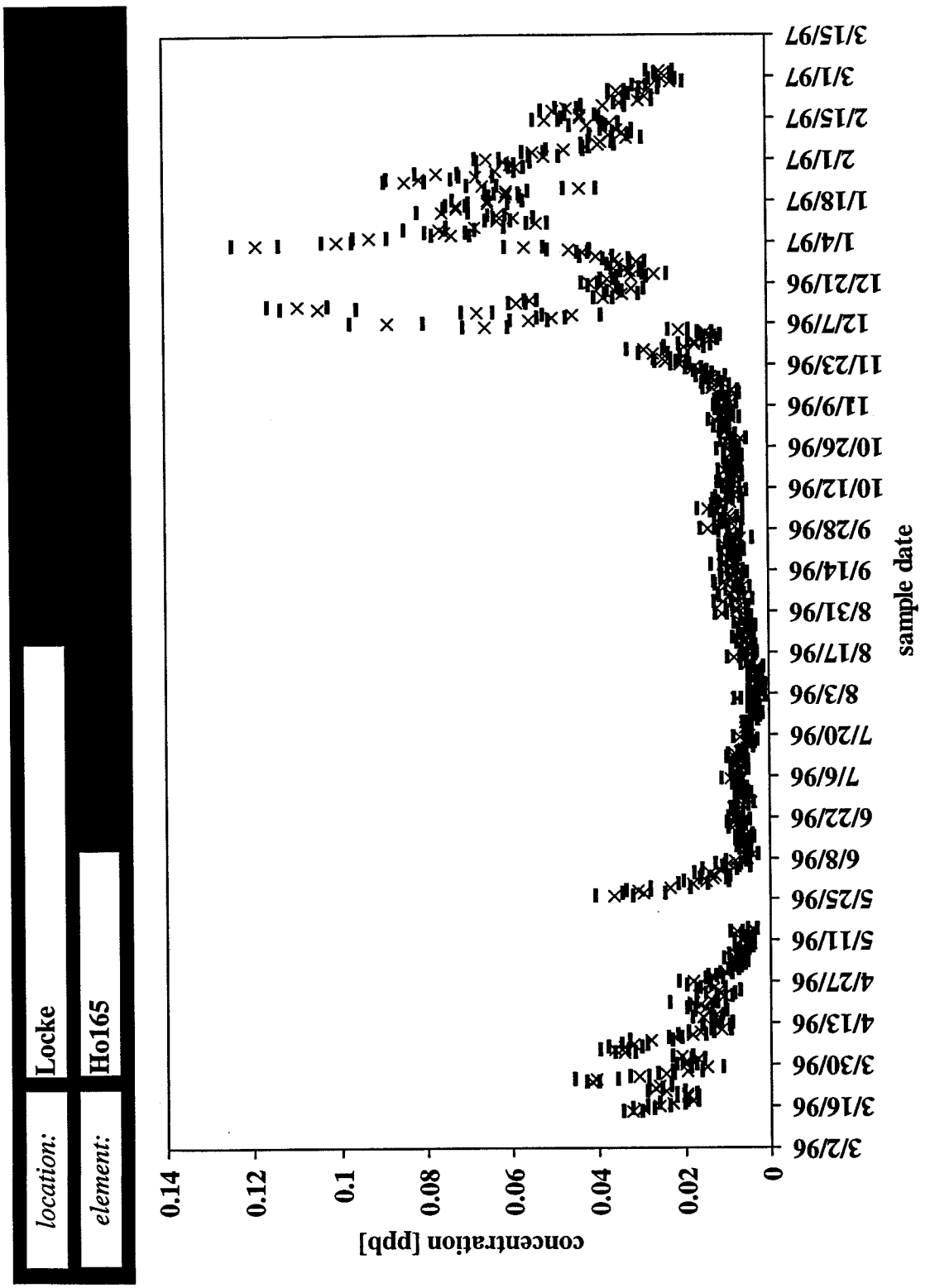
location:
Locke
element:
Ho165
concentration [ppb]
0.14
0.12
0.1
0.08
0.06
0.04
0.02
0
sample date
3/2/96
3/16/96
3/30/96
4/13/96
4/27/96
5/11/96
5/25/96
6/8/96
6/22/96
7/6/96
7/20/96
8/3/96
8/17/96
8/31/96
9/14/96
9/28/96
10/12/96
10/26/96
11/9/96
11/23/96
12/7/96
12/21/96
1/4/97
1/18/97
2/1/97
2/15/97
3/1/97
3/15/97

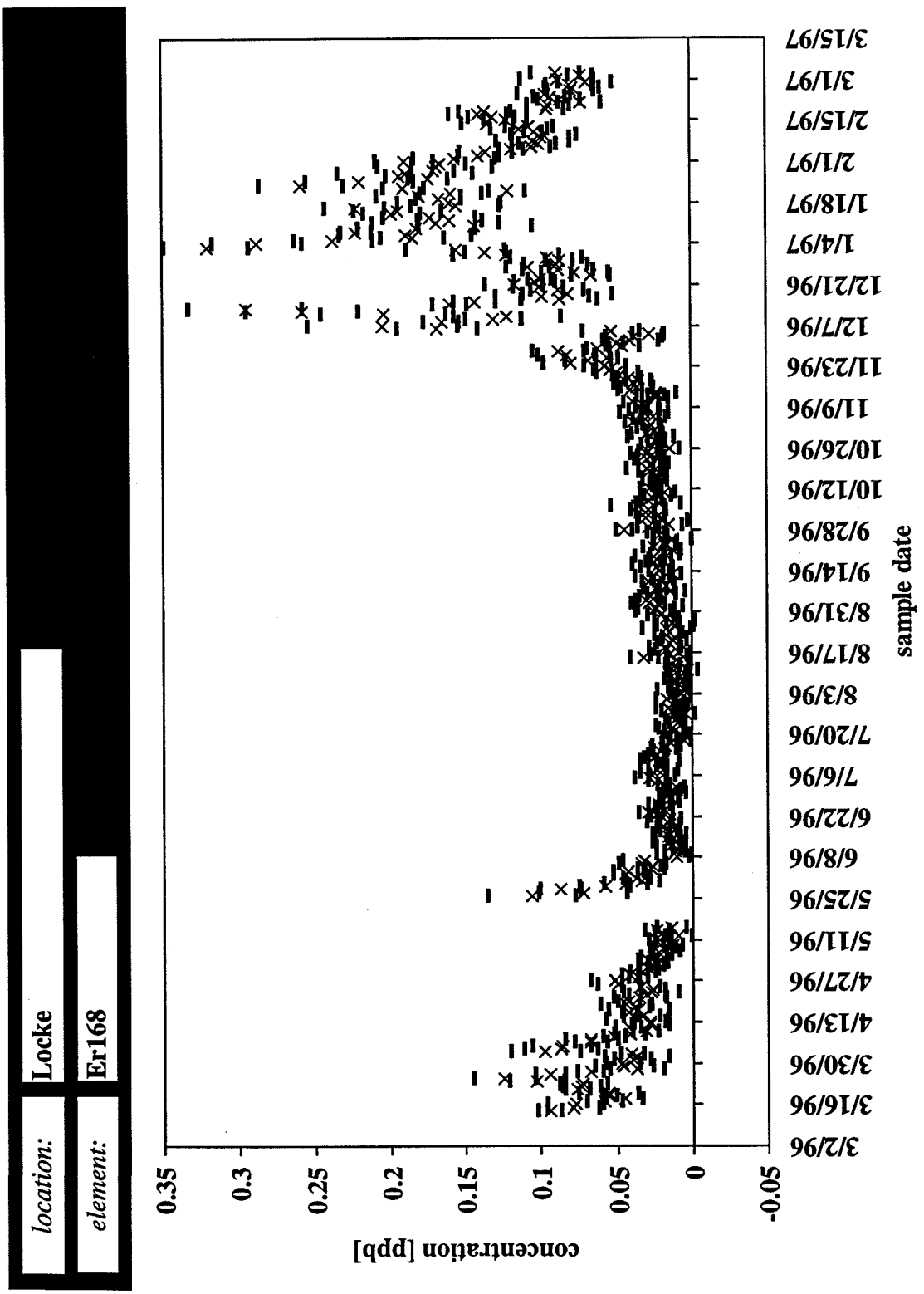
location:
Locke
element:
Er168
concentration [ppb]
0.35
0.3
0.25
0.2
0.15
0.1
0.05
0
-0.05
sample date
3/2/96
3/16/96
3/30/96
4/13/96
4/27/96
5/11/96
5/25/96
6/8/96
6/22/96
7/6/96
7/20/96
8/3/96
8/17/96
8/31/96
9/14/96
9/28/96
10/12/96
10/26/96
11/9/96
11/23/96
12/7/96
12/21/96
1/4/97
1/18/97
2/1/97
2/15/97
3/1/97
3/15/97

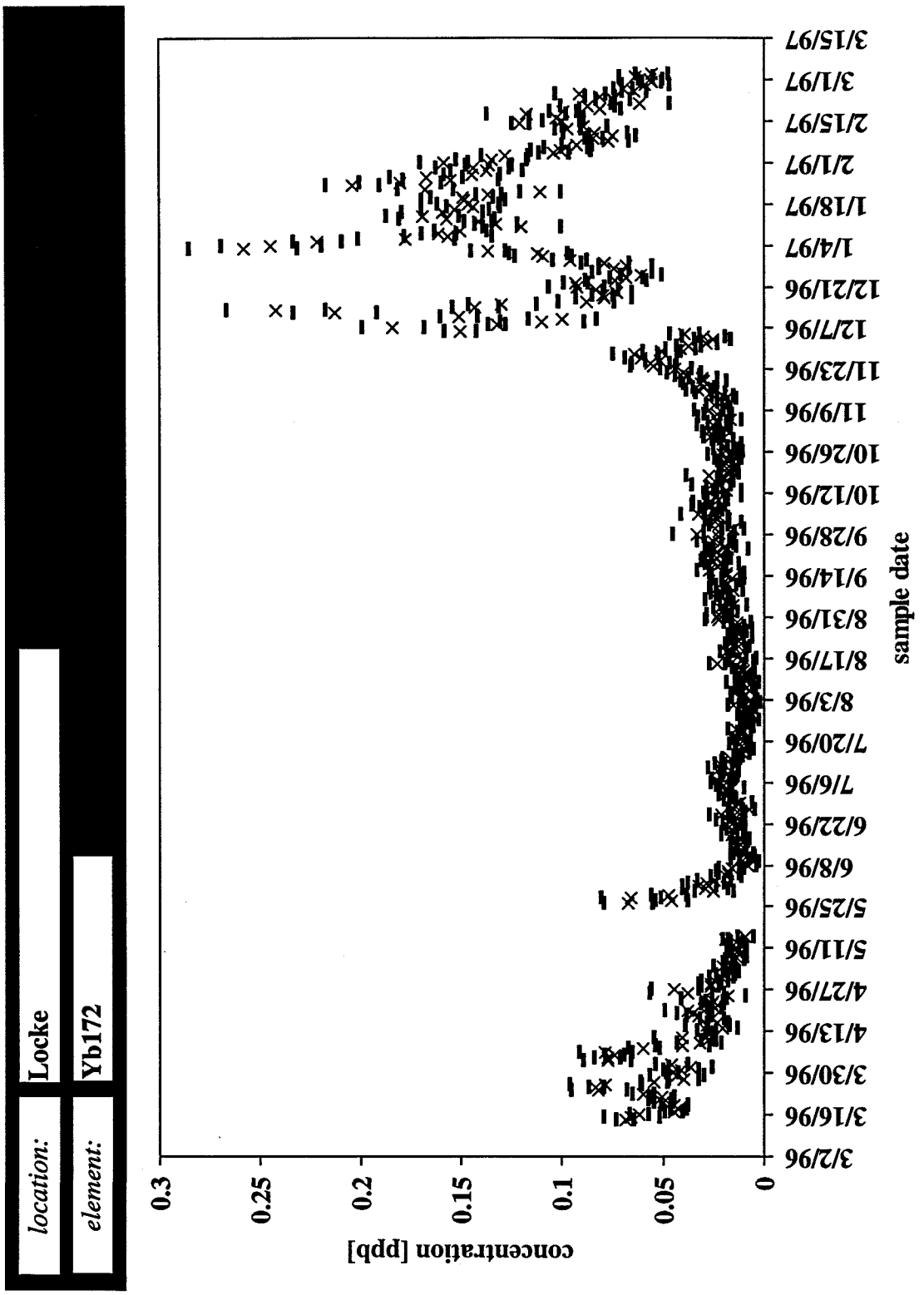
location:
Locke
element:
Yb172
concentration [ppb]
0.3
0.25
0.2
0.15
0.1
0.05
0
sample date
3/2/96
3/16/96
3/30/96
4/13/96
4/27/96
5/11/96
5/25/96
6/8/96
6/22/96
7/6/96
7/20/96
8/3/96
8/17/96
8/31/96
9/14/96
9/28/96
10/12/96
10/26/96
11/9/96
11/23/96
12/7/96
12/21/96
1/4/97
1/18/97
2/1/97
2/15/97
3/1/97
3/15/97

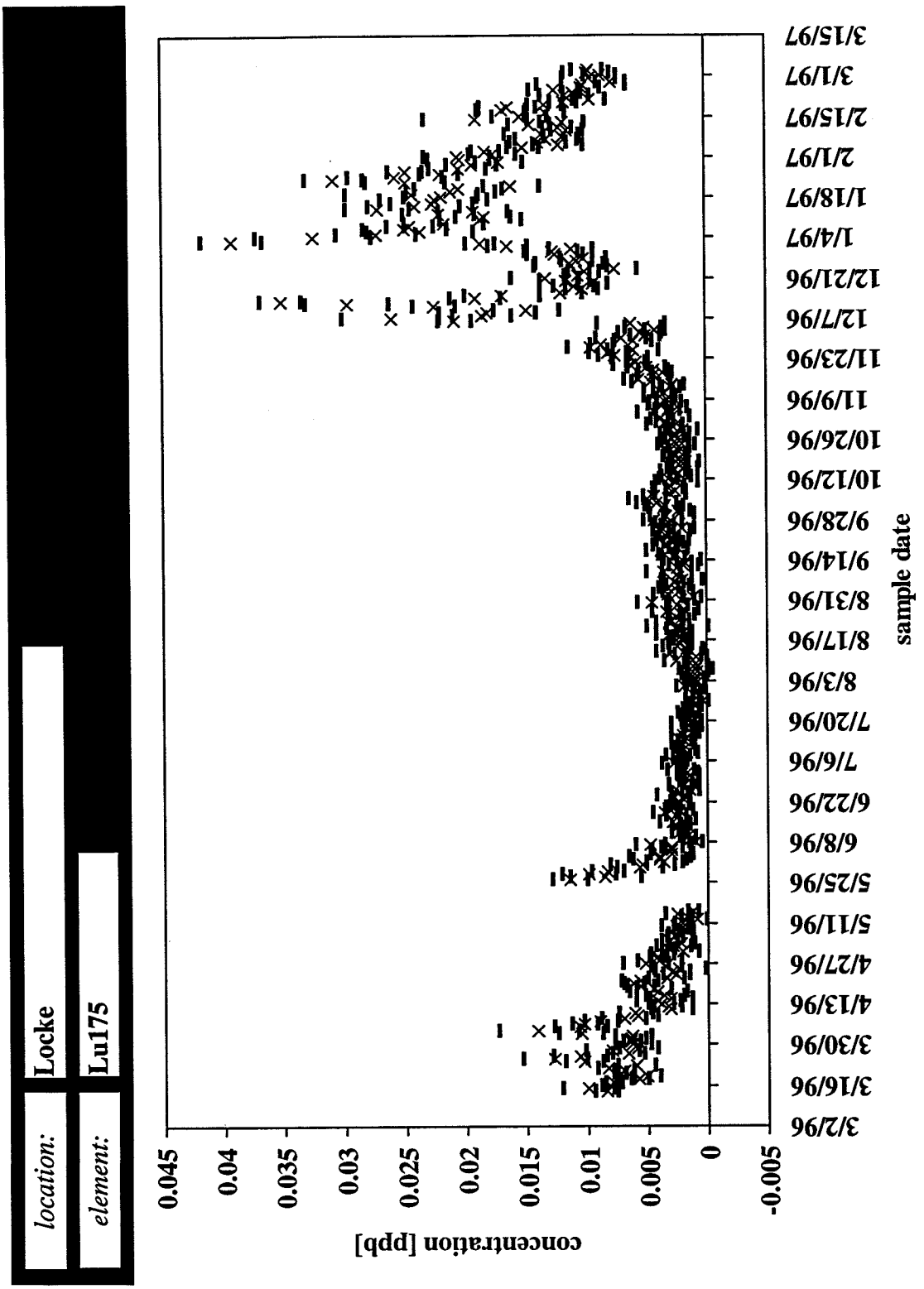
location:
Locke
element:
Lu175
concentration [ppb]
0.045
0.04
0.035
0.03
0.025
0.02
0.015
0.01
0.005
0
-0.005
sample date
3/2/96
3/16/96
3/30/96
4/13/96
4/27/96
5/11/96
5/25/96
6/8/96
6/22/96
7/6/96
7/20/96
8/3/96
8/17/96
8/31/96
9/14/96
9/28/96
10/12/96
10/26/96
11/9/96
11/23/96
12/7/96
12/21/96
1/4/97
1/18/97
2/1/97
2/15/97
3/1/97
3/15/97

location:
Locke
element:
Th232
concentration [ppb]
0.5
0.45
0.4
0.35
0.3
0.25
0.2
0.15
0.1
0.05
0
-0.05
sample date
3/2/96
3/16/96
3/30/96
4/13/96
4/27/96
5/11/96
5/25/96
6/8/96
6/22/96
7/6/96
7/20/96
8/3/96
8/17/96
8/31/96
9/14/96
9/28/96
10/12/96
10/26/96
11/9/96
11/23/96
12/7/96
12/21/96
1/4/97
1/18/97
2/1/97
2/15/97
3/1/97
3/15/97

location:
Locke
element:
U238
concentration [ppb]
0.5
0.45
0.4
0.35
0.3
0.25
0.2
0.15
0.1
0.05
0
sample date
3/2/96
3/16/96
3/30/96
4/13/96
4/27/96
5/11/96
5/25/96
6/8/96
6/22/96
7/6/96
7/20/96
8/3/96
8/17/96
8/31/96
9/14/96
9/28/96
10/12/96
10/26/96
11/9/96
11/23/96
12/7/96
12/21/96
1/4/97
1/18/97
2/1/97
2/15/97
3/1/97
3/15/97

location:
Mossdale Landing
element:
river flow (cfs)
flow rate [cfs]
50000
45000
40000
35000
30000
25000
20000
15000
10000
5000
0
sample date
3/2/96
3/16/96
3/30/96
4/13/96
4/27/96
5/11/96
5/25/96
6/8/96
6/22/96
7/6/96
7/20/96
8/3/96
8/17/96
8/31/96
9/14/96
9/28/96
10/12/96
10/26/96
11/9/96
11/23/96
12/7/96
12/21/96
1/4/97
1/18/97
2/1/97
2/15/97
3/1/97
3/15/97

location:
Mossdale Landing
element:
Li7
concentration [ppb]
0
10
20
30
40
50
60
70
sample date
3/2/96
3/16/96
3/30/96
4/13/96
4/27/96
5/11/96
5/25/96
6/8/96
6/22/96
7/6/96
7/20/96
8/3/96
8/17/96
8/31/96
9/14/96
9/28/96
10/12/96
10/26/96
11/9/96
11/23/96
12/7/96
12/21/96
1/4/97
1/18/97
2/1/97
2/15/97
3/1/97
3/15/97

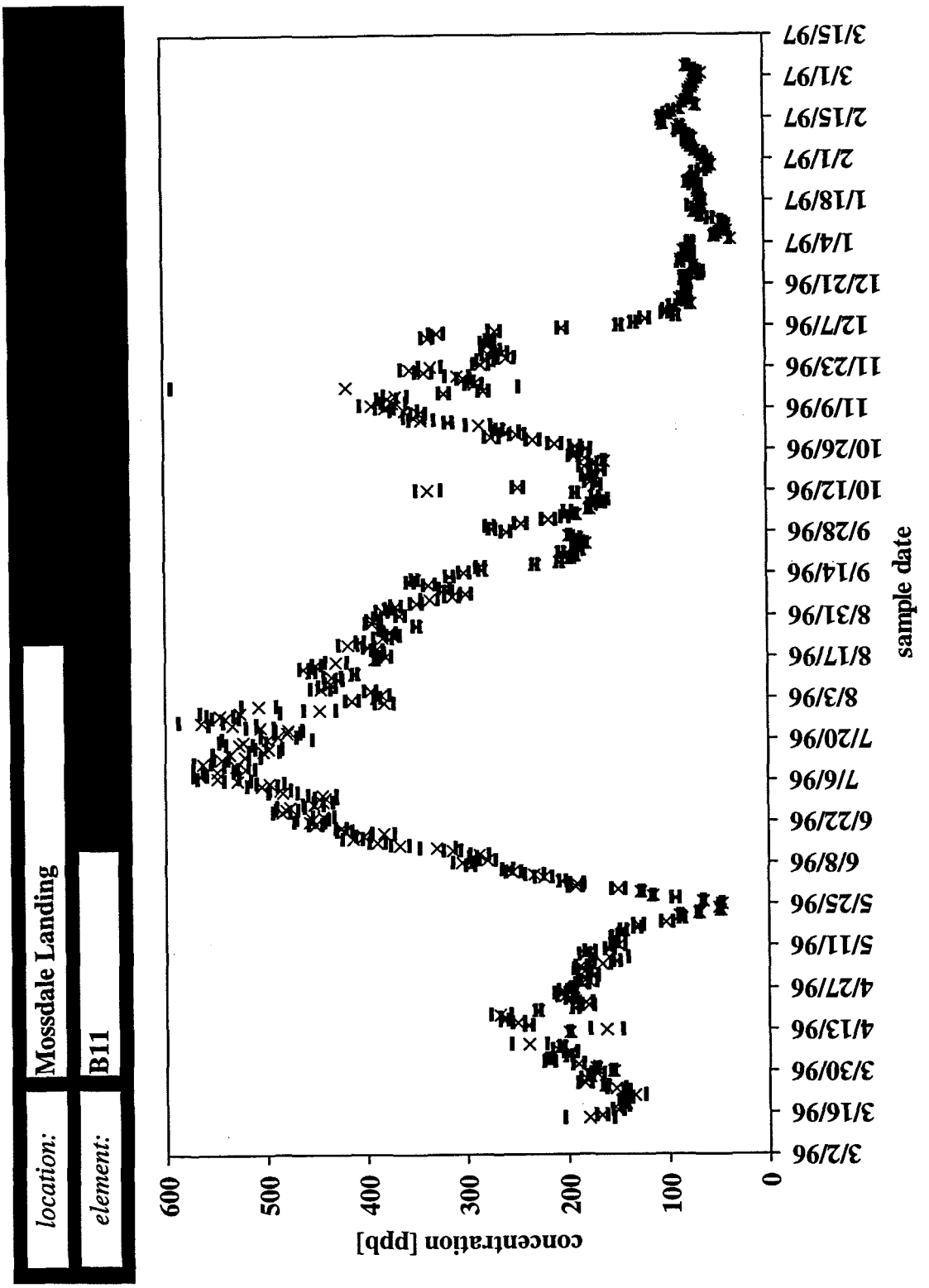
location:
Mossdale Landing
element:
B11
concentration [ppb]
0
100
200
300
400
500
600
sample date
3/2/96
3/16/96
3/30/96
4/13/96
4/27/96
5/11/96
5/25/96
6/8/96
6/22/96
7/6/96
7/20/96
8/3/96
8/17/96
8/31/96
9/14/96
9/28/96
10/12/96
10/26/96
11/9/96
11/23/96
12/7/96
12/21/96
1/4/97
1/18/97
2/1/97
2/15/97
3/1/97
3/15/97

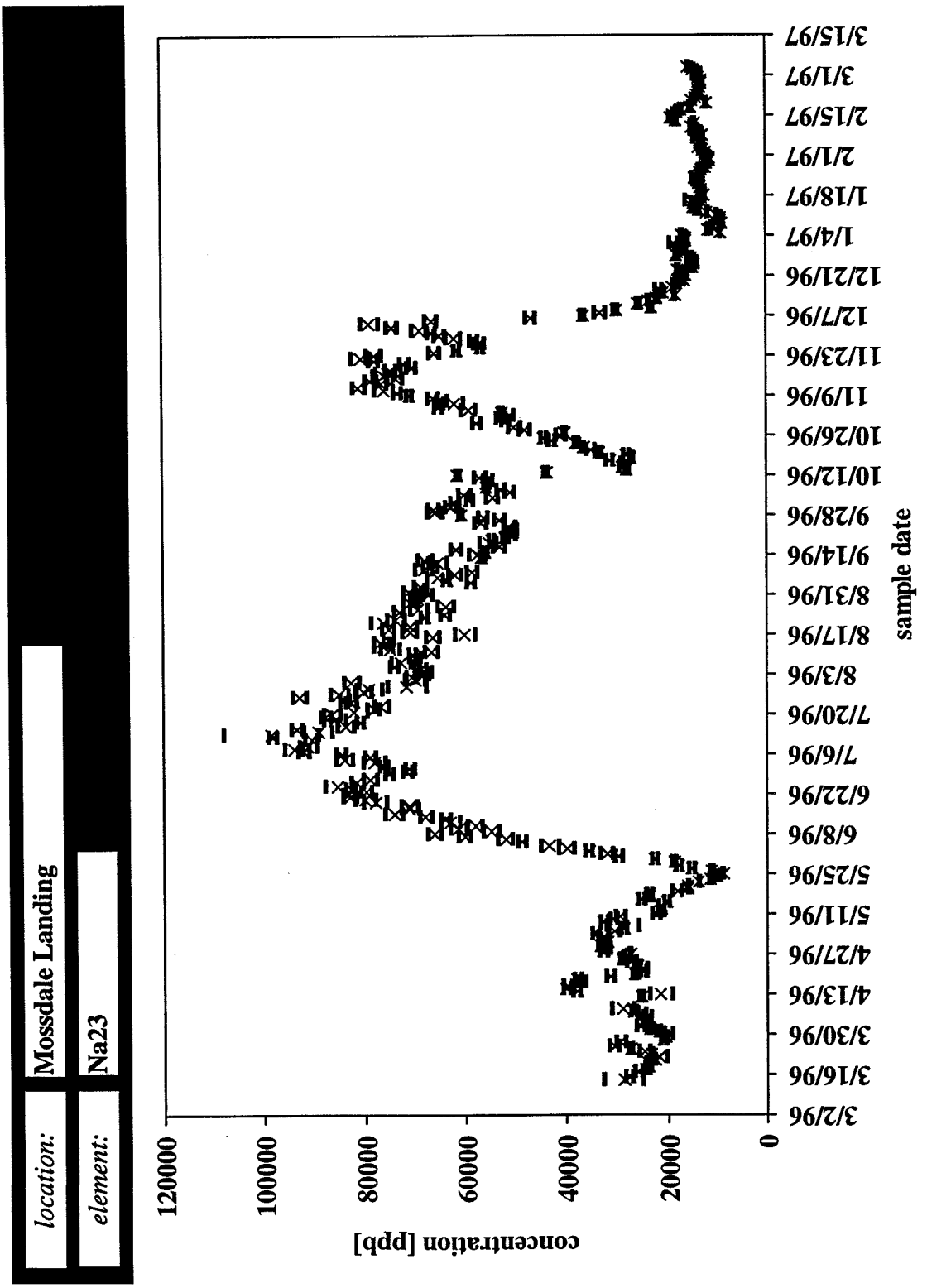
location:
Mossdale Landing
element:
Na23
concentration [ppb]
120000
100000
80000
60000
40000
20000
0
sample date
3/2/96
3/16/96
3/30/96
4/13/96
4/27/96
5/11/96
5/25/96
6/8/96
6/22/96
7/6/96
7/20/96
8/3/96
8/17/96
8/31/96
9/14/96
9/28/96
10/12/96
10/26/96
11/9/96
11/23/96
12/7/96
12/21/96
1/4/97
1/18/97
2/1/97
2/15/97
3/1/97
3/15/97

location:
Mossdale Landing
element:
Mg24
concentration [ppb]
35000
30000
25000
20000
15000
10000
5000
0
sample date
3/2/96
3/16/96
3/30/96
4/13/96
4/27/96
5/11/96
5/25/96
6/8/96
6/22/96
7/6/96
7/20/96
8/3/96
8/17/96
8/31/96
9/14/96
9/28/96
10/12/96
10/26/96
11/9/96
11/23/96
12/7/96
12/21/96
1/4/97
1/18/97
2/1/97
2/15/97
3/1/97
3/15/97

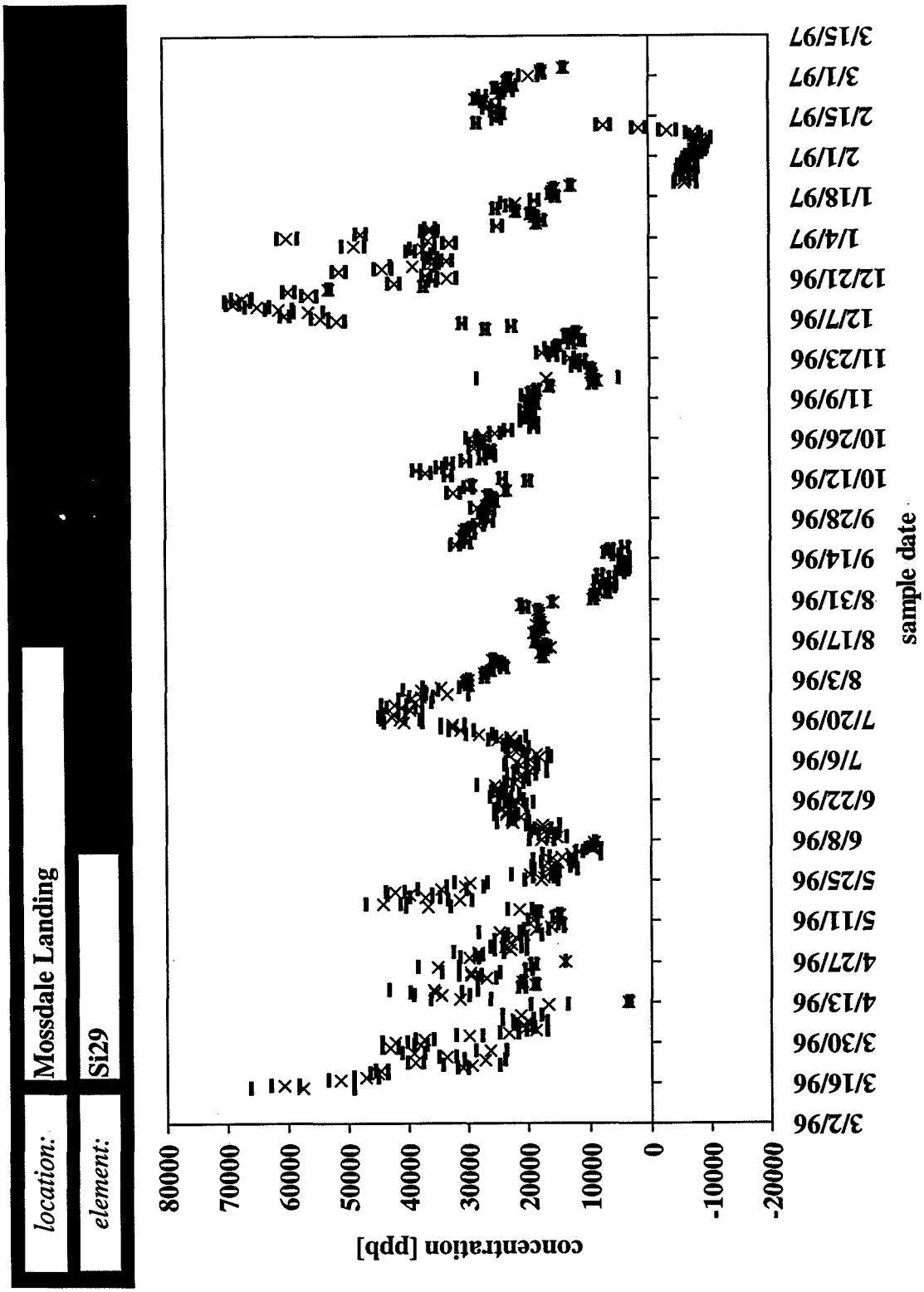
location:
Mossdale Landing
element:
Si29
concentration [ppb]
80000
70000
60000
50000
40000
30000
20000
10000
0
-10000
-20000
sample date
3/2/96
3/16/96
3/30/96
4/13/96
4/27/96
5/11/96
5/25/96
6/8/96
6/22/96
7/6/96
7/20/96
8/3/96
8/17/96
8/31/96
9/14/96
9/28/96
10/12/96
10/26/96
11/9/96
11/23/96
12/7/96
12/21/96
1/4/97
1/18/97
2/1/97
2/15/97
3/1/97
3/15/97

location:	**Mossdale Landing**
element:	**K39**

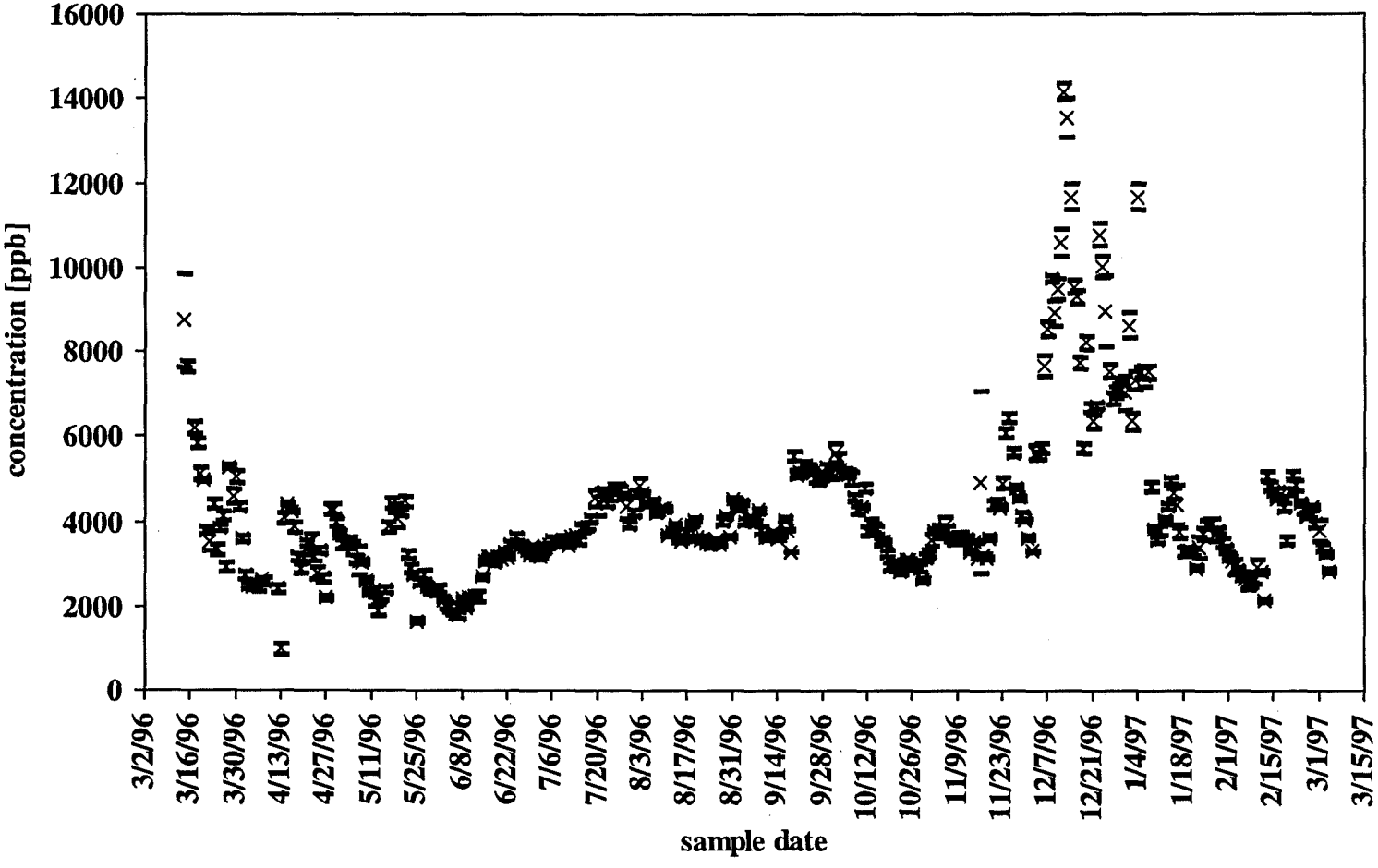

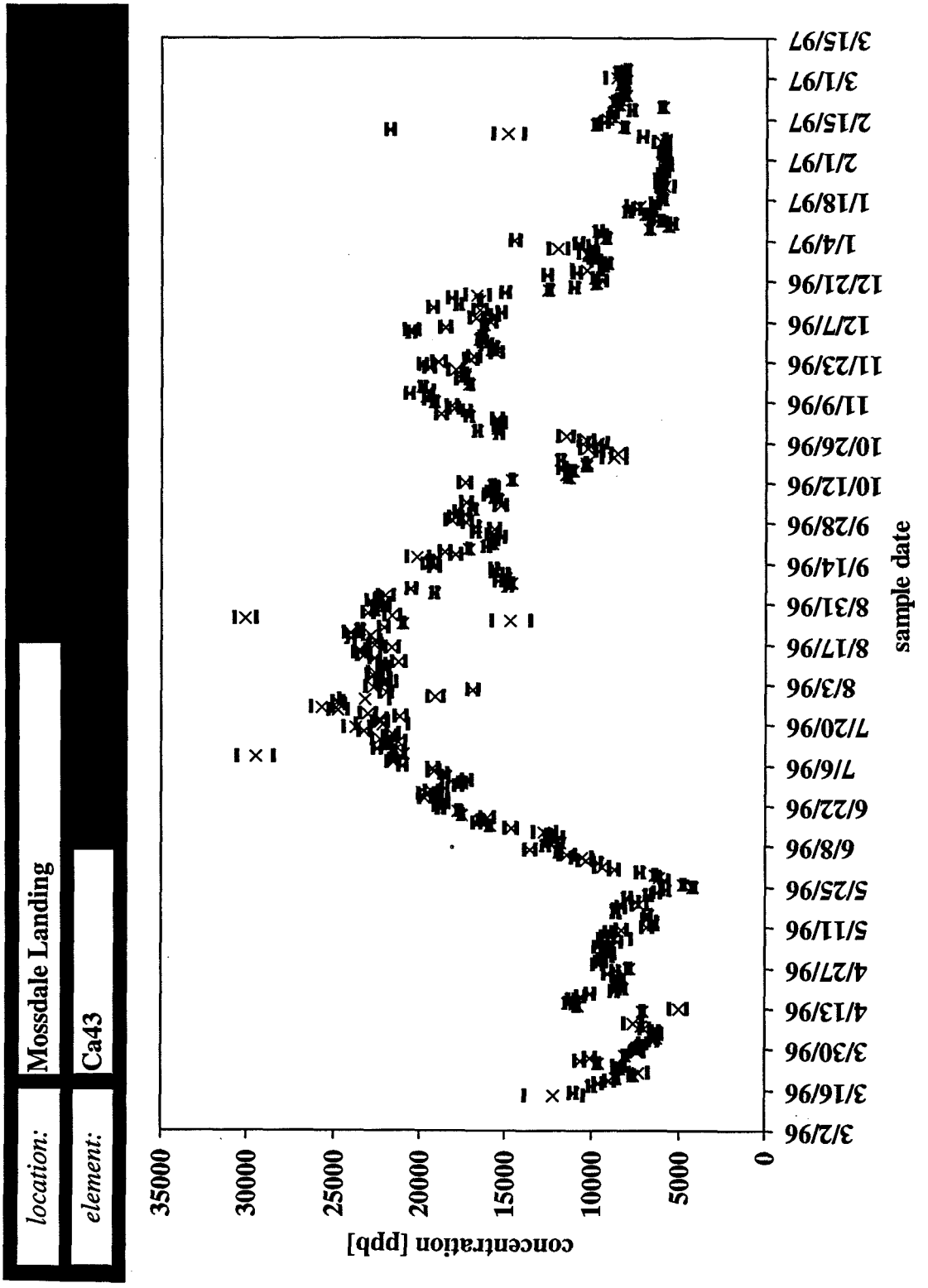
location:
Mossdale Landing
element:
Ca43
concentration [ppb]
35000
30000
25000
20000
15000
10000
5000
0
sample date
3/2/96
3/16/96
3/30/96
4/13/96
4/27/96
5/11/96
5/25/96
6/8/96
6/22/96
7/6/96
7/20/96
8/3/96
8/17/96
8/31/96
9/14/96
9/28/96
10/12/96
10/26/96
11/9/96
11/23/96
12/7/96
12/21/96
1/4/97
1/18/97
2/1/97
2/15/97
3/1/97
3/15/97

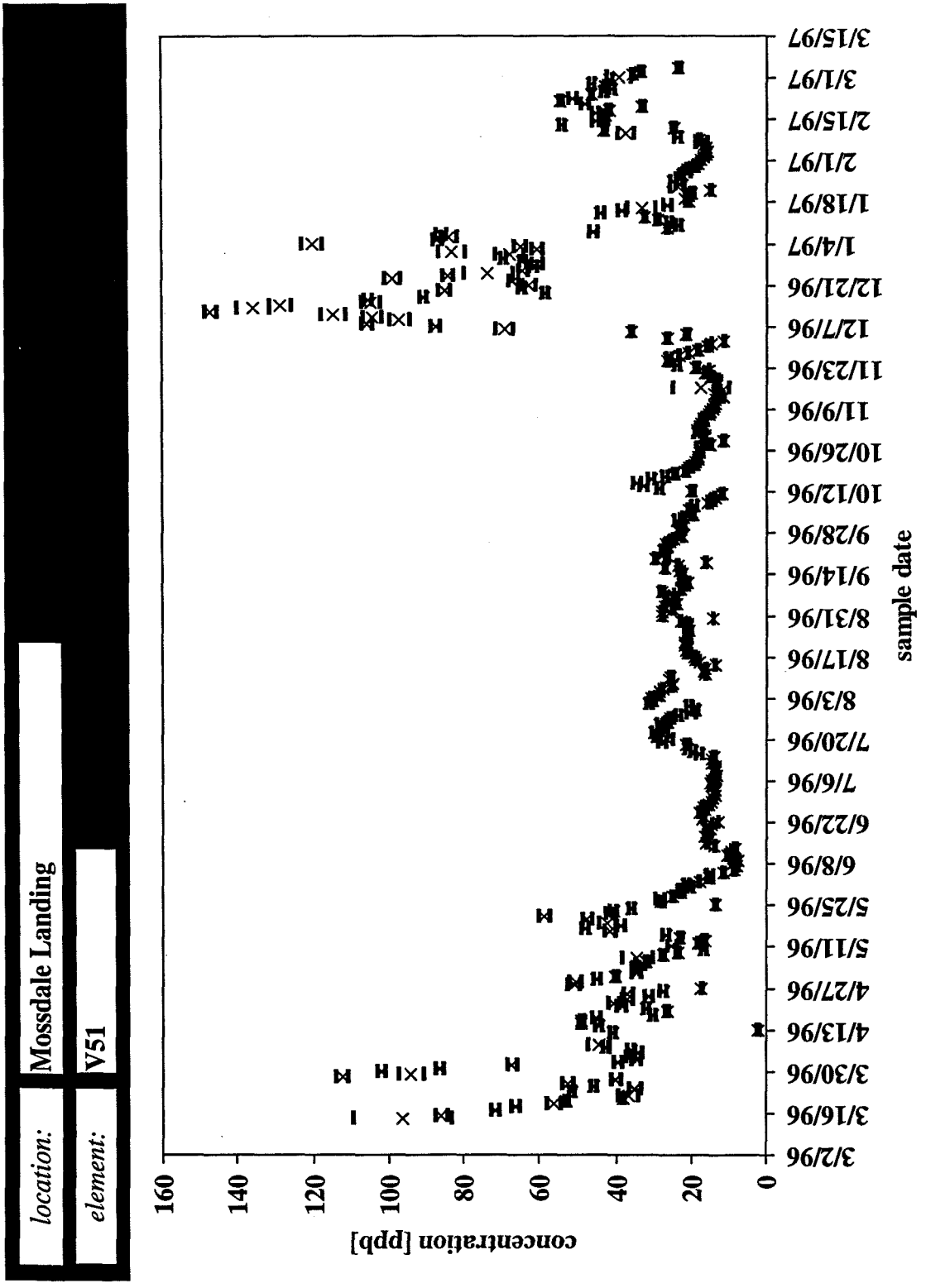
location:
Mossdale Landing
element:
V51
concentration [ppb]
0
20
40
60
80
100
120
140
160
sample date
3/2/96
3/16/96
3/30/96
4/13/96
4/27/96
5/11/96
5/25/96
6/8/96
6/22/96
7/6/96
7/20/96
8/3/96
8/17/96
8/31/96
9/14/96
9/28/96
10/12/96
10/26/96
11/9/96
11/23/96
12/7/96
12/21/96
1/4/97
1/18/97
2/1/97
2/15/97
3/1/97
3/15/97

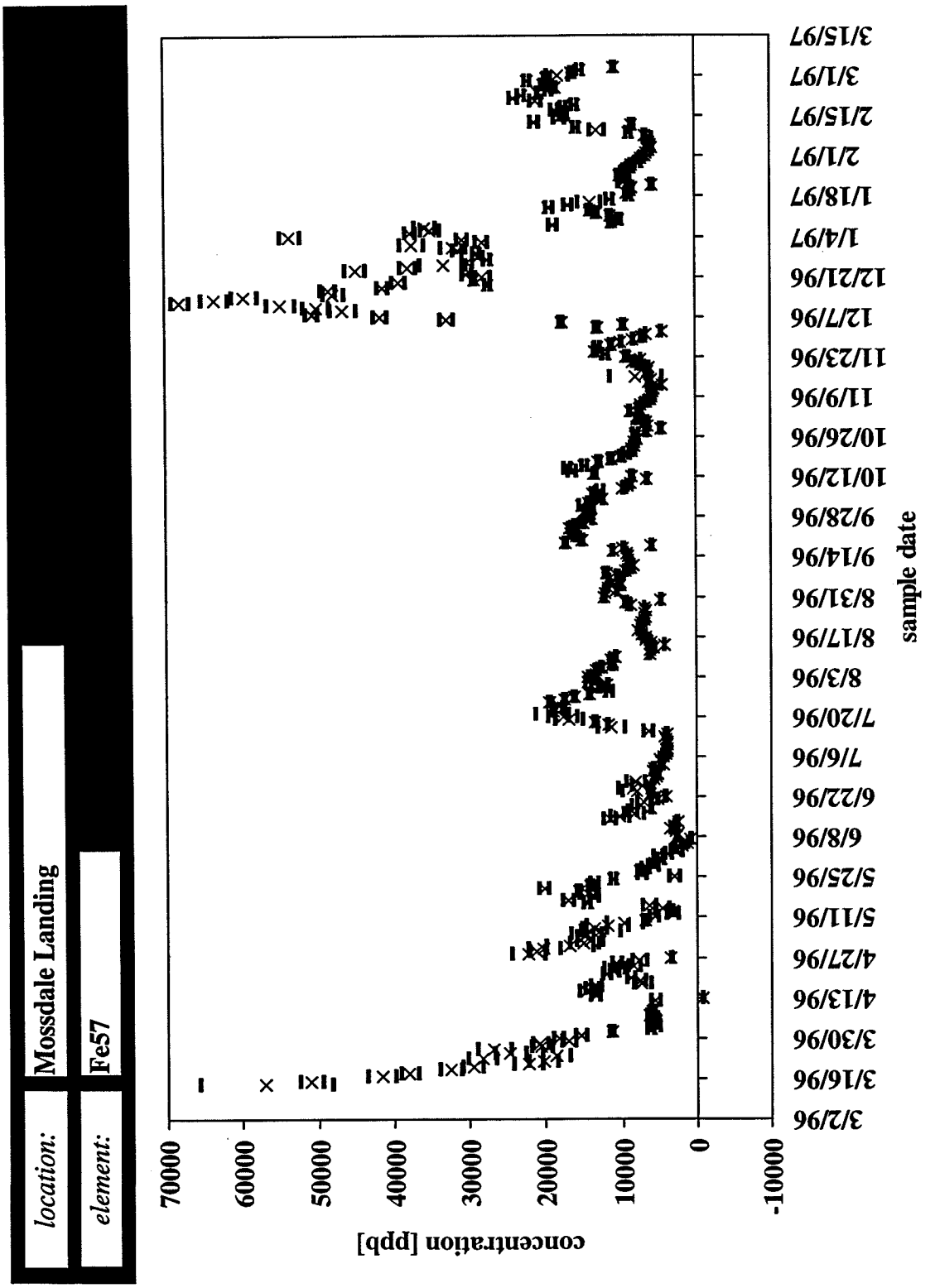
location:
Mossdale Landing
element:
Fe57
concentration [ppb]
70000
60000
50000
40000
30000
20000
10000
0
-10000
sample date
3/2/96
3/16/96
3/30/96
4/13/96
4/27/96
5/11/96
5/25/96
6/8/96
6/22/96
7/6/96
7/20/96
8/3/96
8/17/96
8/31/96
9/14/96
9/28/96
10/12/96
10/26/96
11/9/96
11/23/96
12/7/96
12/21/96
1/4/97
1/18/97
2/1/97
2/15/97
3/1/97
3/15/97

location:
Mossdale Landing
element:
Mn55
concentration [ppb]
3000
2500
2000
1500
1000
500
0
-500
sample date
3/2/96
3/16/96
3/30/96
4/13/96
4/27/96
5/11/96
5/25/96
6/8/96
6/22/96
7/6/96
7/20/96
8/3/96
8/17/96
8/31/96
9/14/96
9/28/96
10/12/96
10/26/96
11/9/96
11/23/96
12/7/96
12/21/96
1/4/97
1/18/97
2/1/97
2/15/97
3/1/97
3/15/97

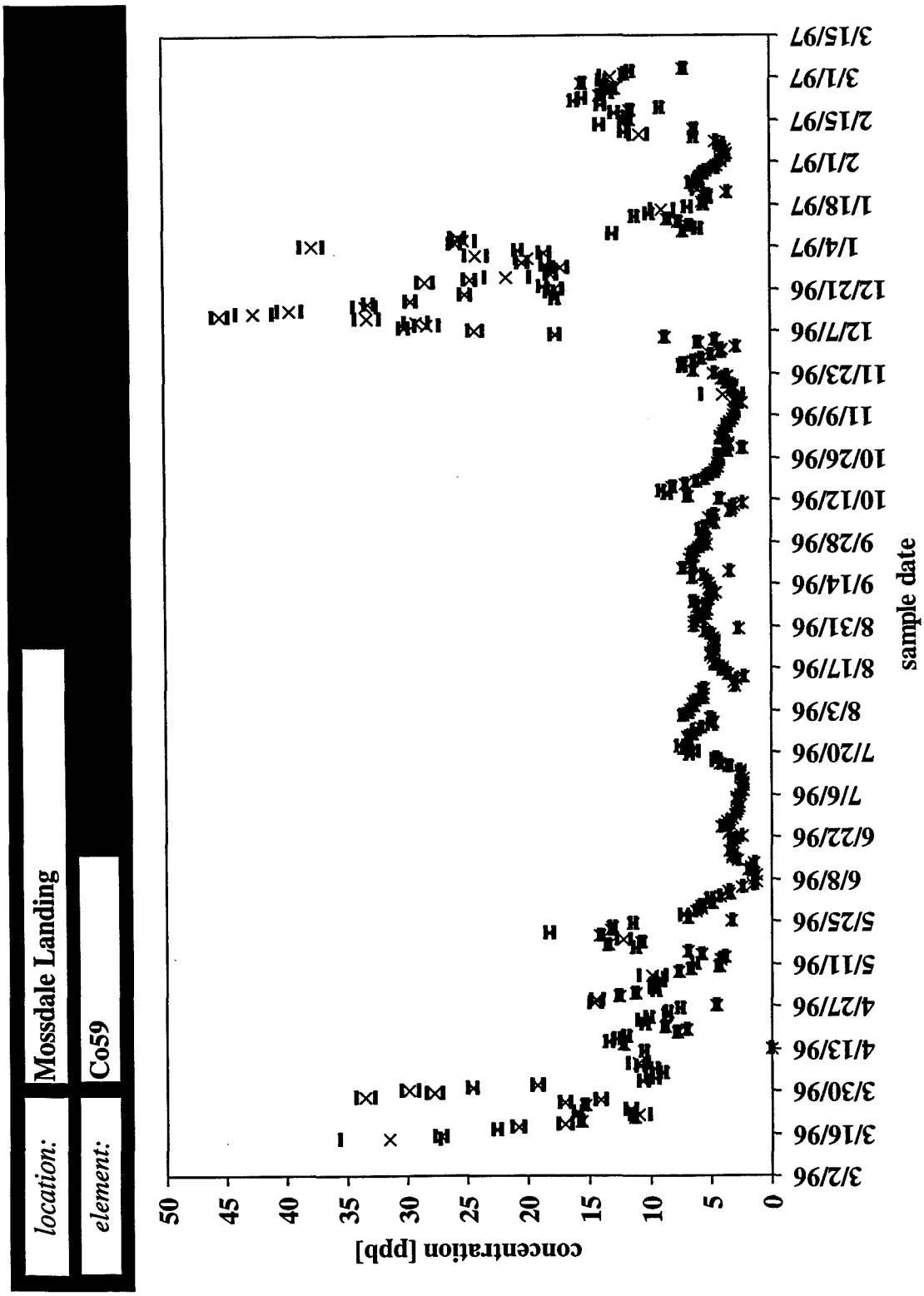
location:
Mossdale Landing
element:
Co59
concentration [ppb]
0
5
10
15
20
25
30
35
40
45
50
sample date
3/2/96
3/16/96
3/30/96
4/13/96
4/27/96
5/11/96
5/25/96
6/8/96
6/22/96
7/6/96
7/20/96
8/3/96
8/17/96
8/31/96
9/14/96
9/28/96
10/12/96
10/26/96
11/9/96
11/23/96
12/7/96
12/21/96
1/4/97
1/18/97
2/1/97
2/15/97
3/1/97
3/15/97

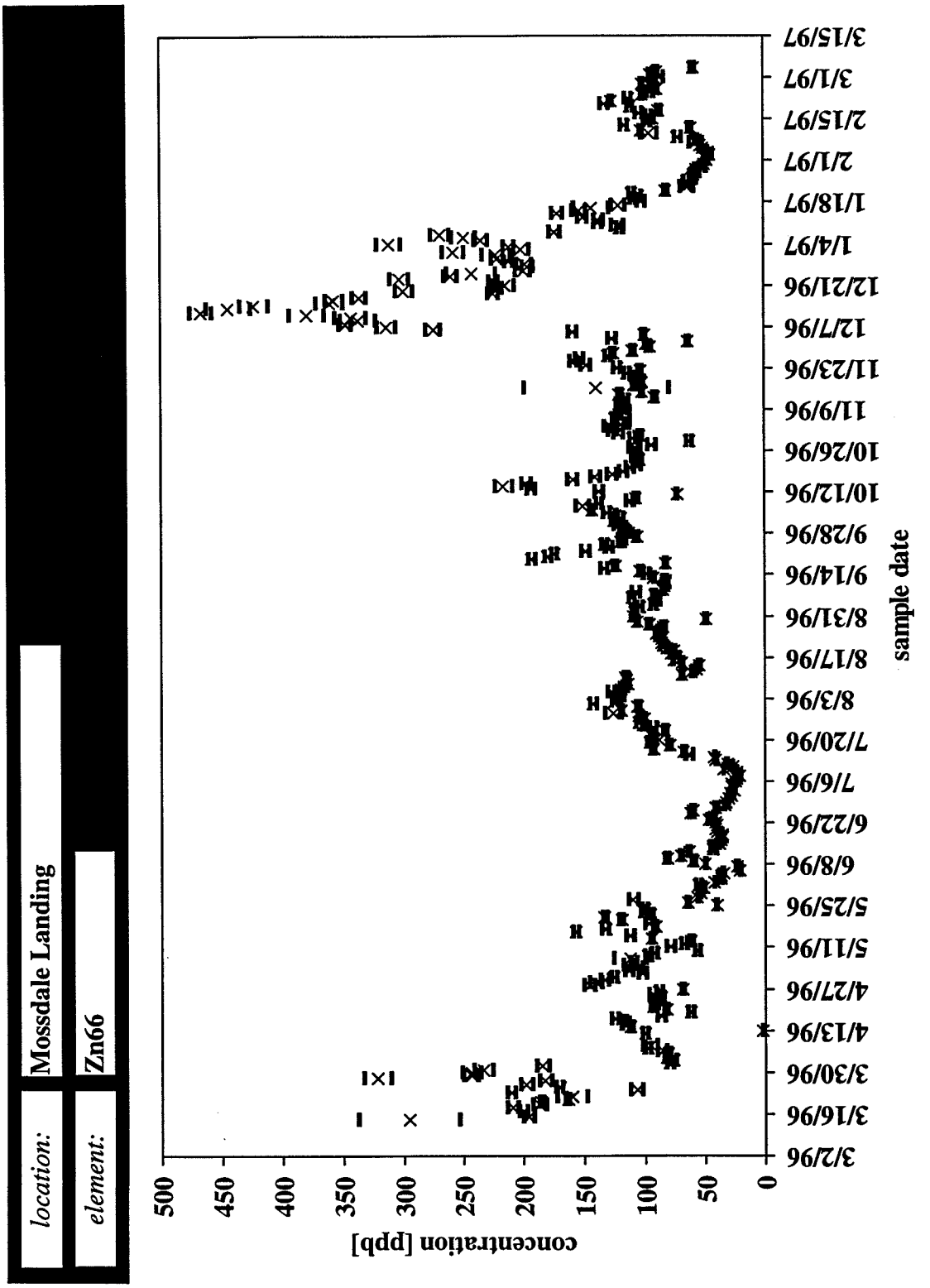
location:
Mossdale Landing
element:
Zn66
concentration [ppb]
0
50
100
150
200
250
300
350
400
450
500
sample date
3/2/96
3/16/96
3/30/96
4/13/96
4/27/96
5/11/96
5/25/96
6/8/96
6/22/96
7/6/96
7/20/96
8/3/96
8/17/96
8/31/96
9/14/96
9/28/96
10/12/96
10/26/96
11/9/96
11/23/96
12/7/96
12/21/96
1/4/97
1/18/97
2/1/97
2/15/97
3/1/97
3/15/97

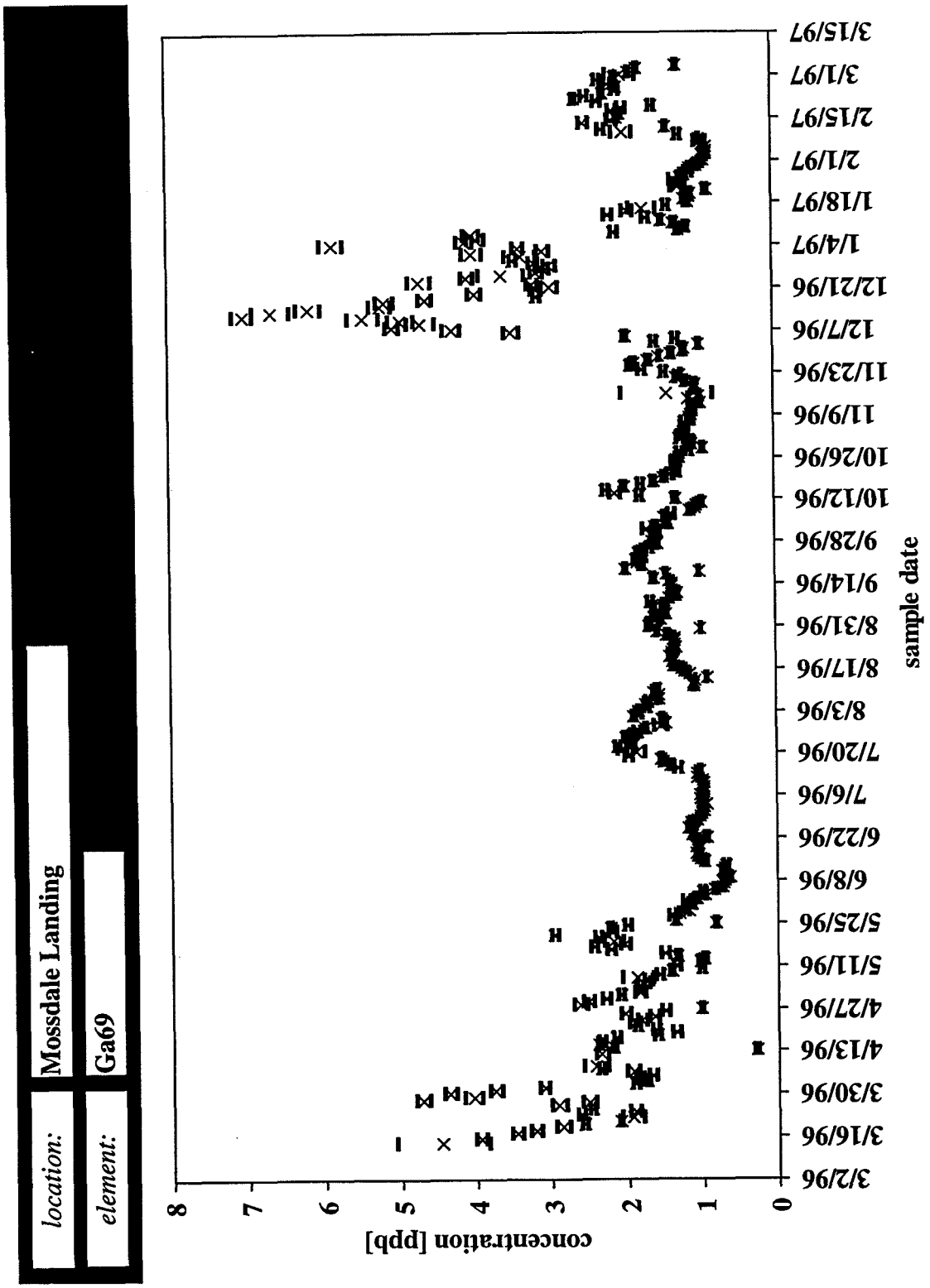
location:
Mossdale Landing
element:
Ga69
concentration [ppb]
0
1
2
3
4
5
6
7
8
sample date
3/2/96
3/16/96
3/30/96
4/13/96
4/27/96
5/11/96
5/25/96
6/8/96
6/22/96
7/6/96
7/20/96
8/3/96
8/17/96
8/31/96
9/14/96
9/28/96
10/12/96
10/26/96
11/9/96
11/23/96
12/7/96
12/21/96
1/4/97
1/18/97
2/1/97
2/15/97
3/1/97
3/15/97

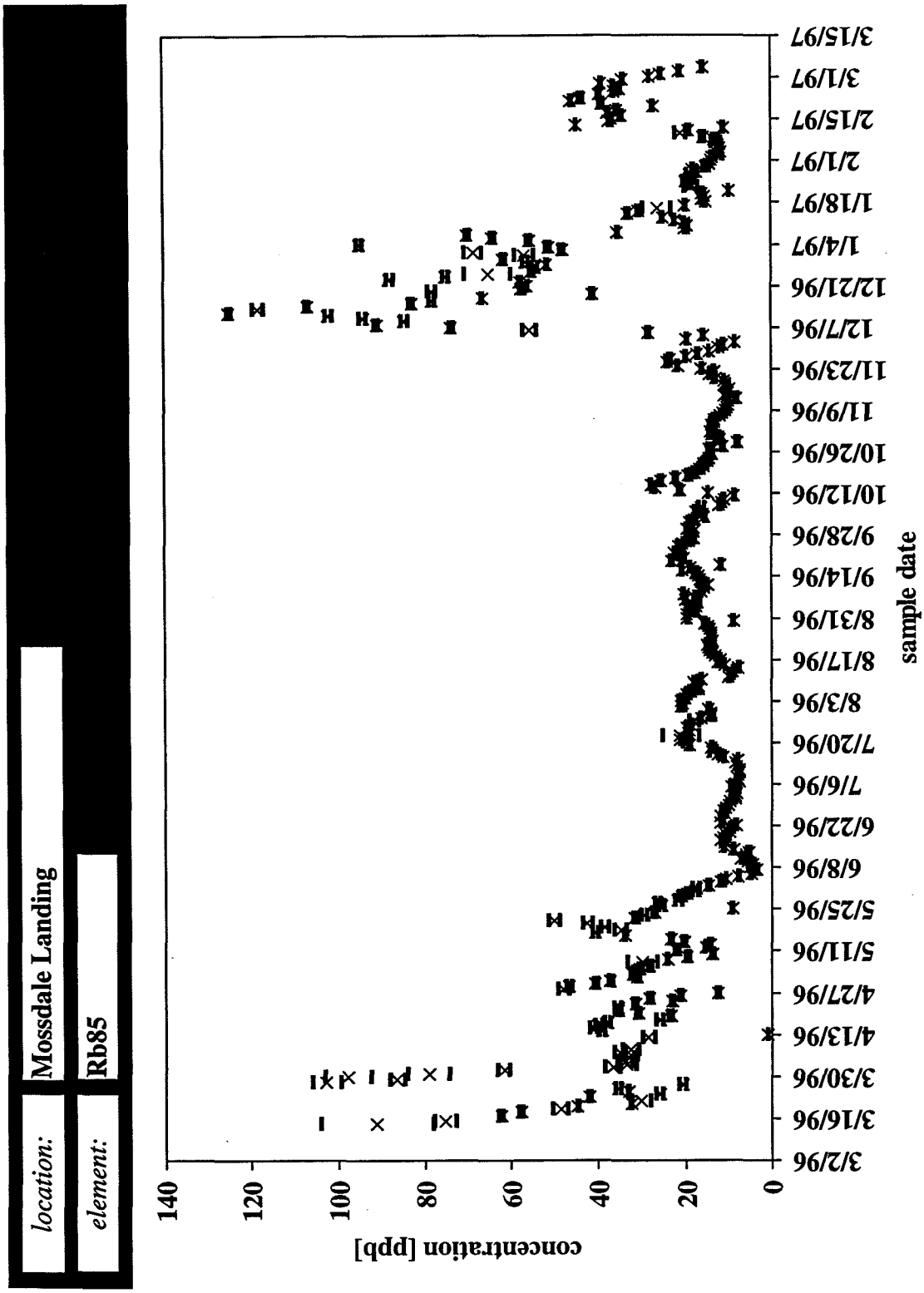
location:
Mossdale Landing
element:
Rb85
concentration [ppb]
0
20
40
60
80
100
120
140
sample date
3/2/96
3/16/96
3/30/96
4/13/96
4/27/96
5/11/96
5/25/96
6/8/96
6/22/96
7/6/96
7/20/96
8/3/96
8/17/96
8/31/96
9/14/96
9/28/96
10/12/96
10/26/96
11/9/96
11/23/96
12/7/96
12/21/96
1/4/97
1/18/97
2/1/97
2/15/97
3/1/97
3/15/97

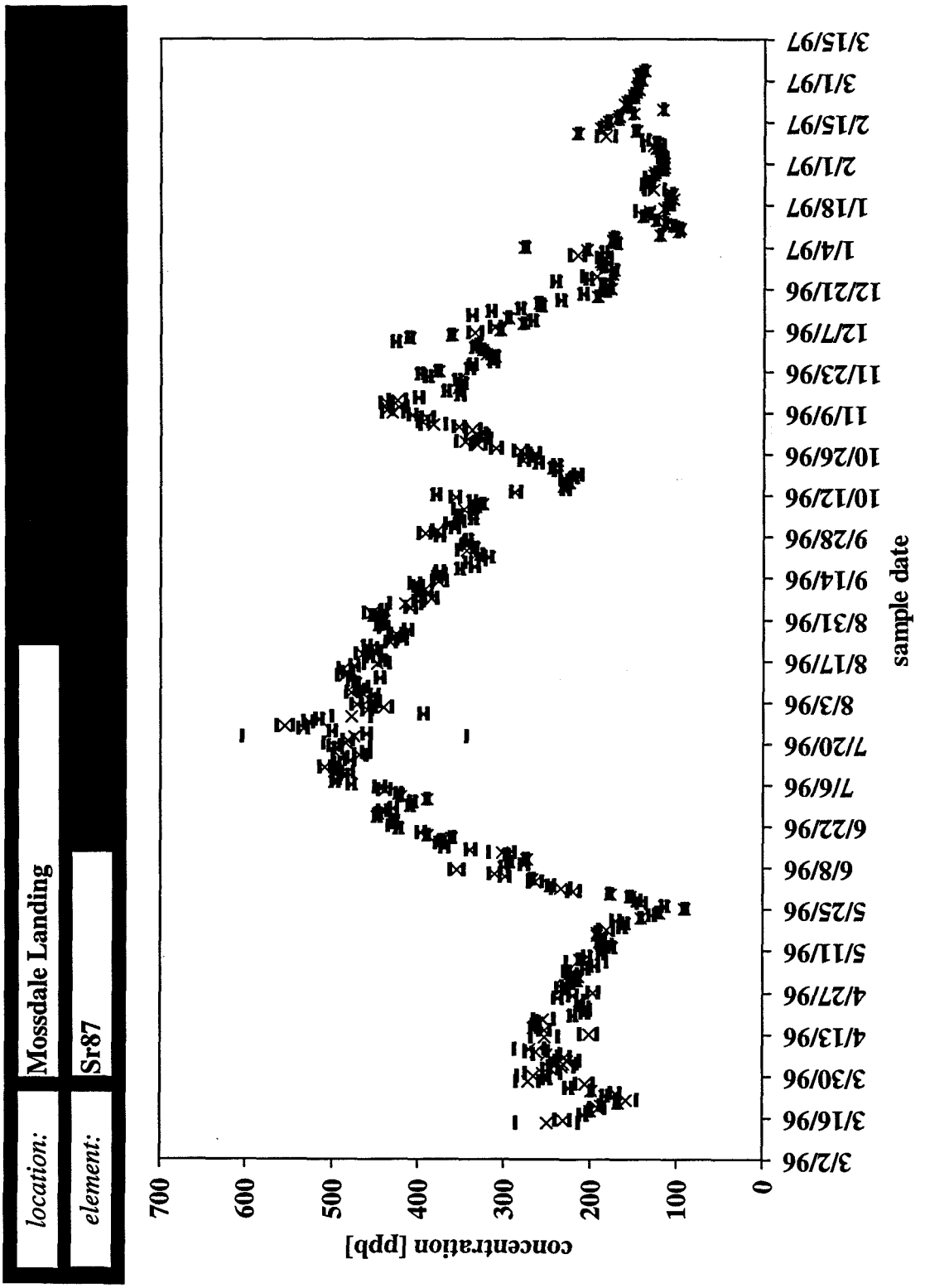
location:
Mossdale Landing
element:
Sr87
concentration [ppb]
0
100
200
300
400
500
600
700
sample date
3/2/96
3/16/96
3/30/96
4/13/96
4/27/96
5/11/96
5/25/96
6/8/96
6/22/96
7/6/96
7/20/96
8/3/96
8/17/96
8/31/96
9/14/96
9/28/96
10/12/96
10/26/96
11/9/96
11/23/96
12/7/96
12/21/96
1/4/97
1/18/97
2/1/97
2/15/97
3/1/97
3/15/97

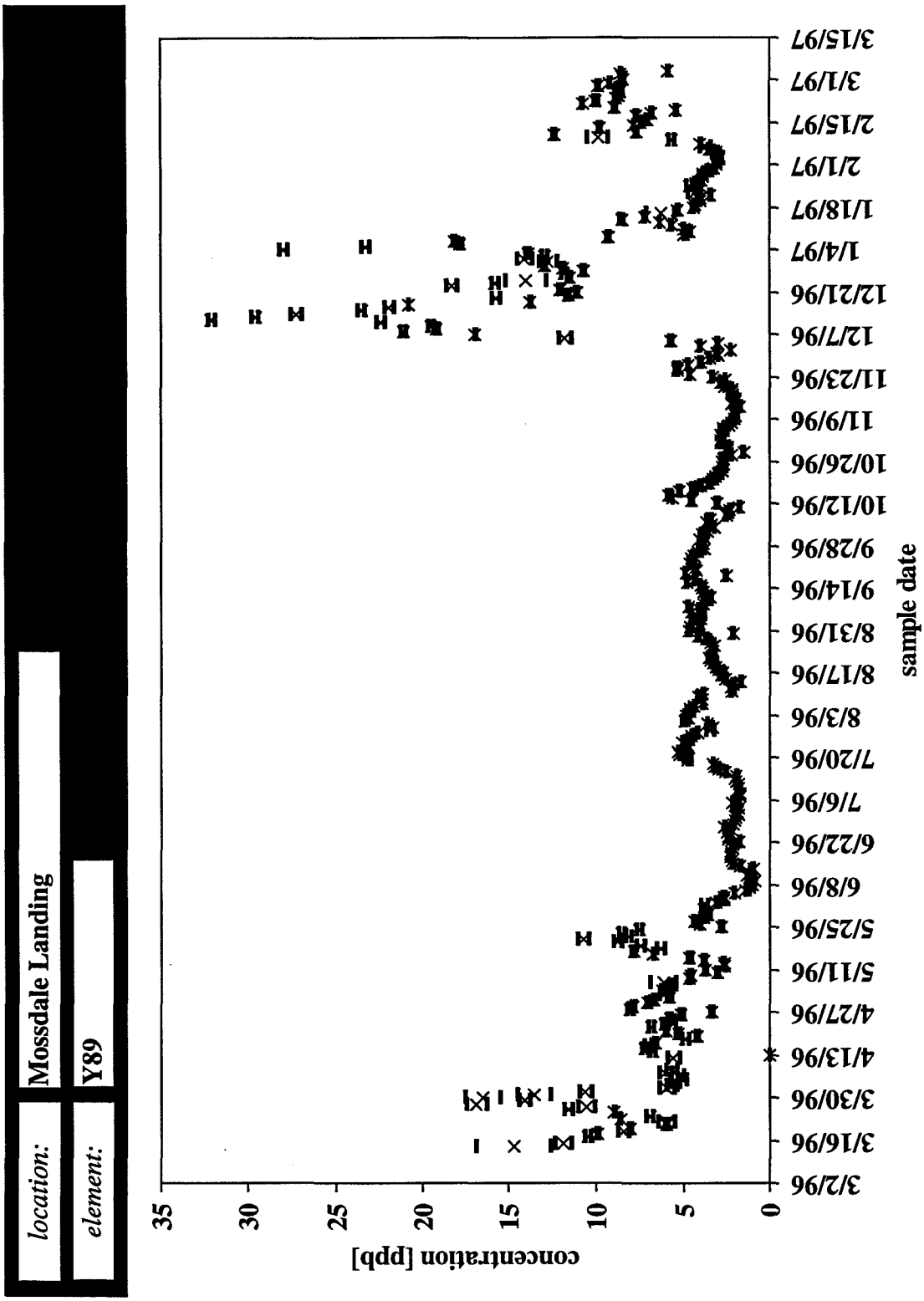
location:
Mossdale Landing
element:
Y89
concentration [ppb]
0
5
10
15
20
25
30
35
sample date
3/2/96
3/16/96
3/30/96
4/13/96
4/27/96
5/11/96
5/25/96
6/8/96
6/22/96
7/6/96
7/20/96
8/3/96
8/17/96
8/31/96
9/14/96
9/28/96
10/12/96
10/26/96
11/9/96
11/23/96
12/7/96
12/21/96
1/4/97
1/18/97
2/1/97
2/15/97
3/1/97
3/15/97

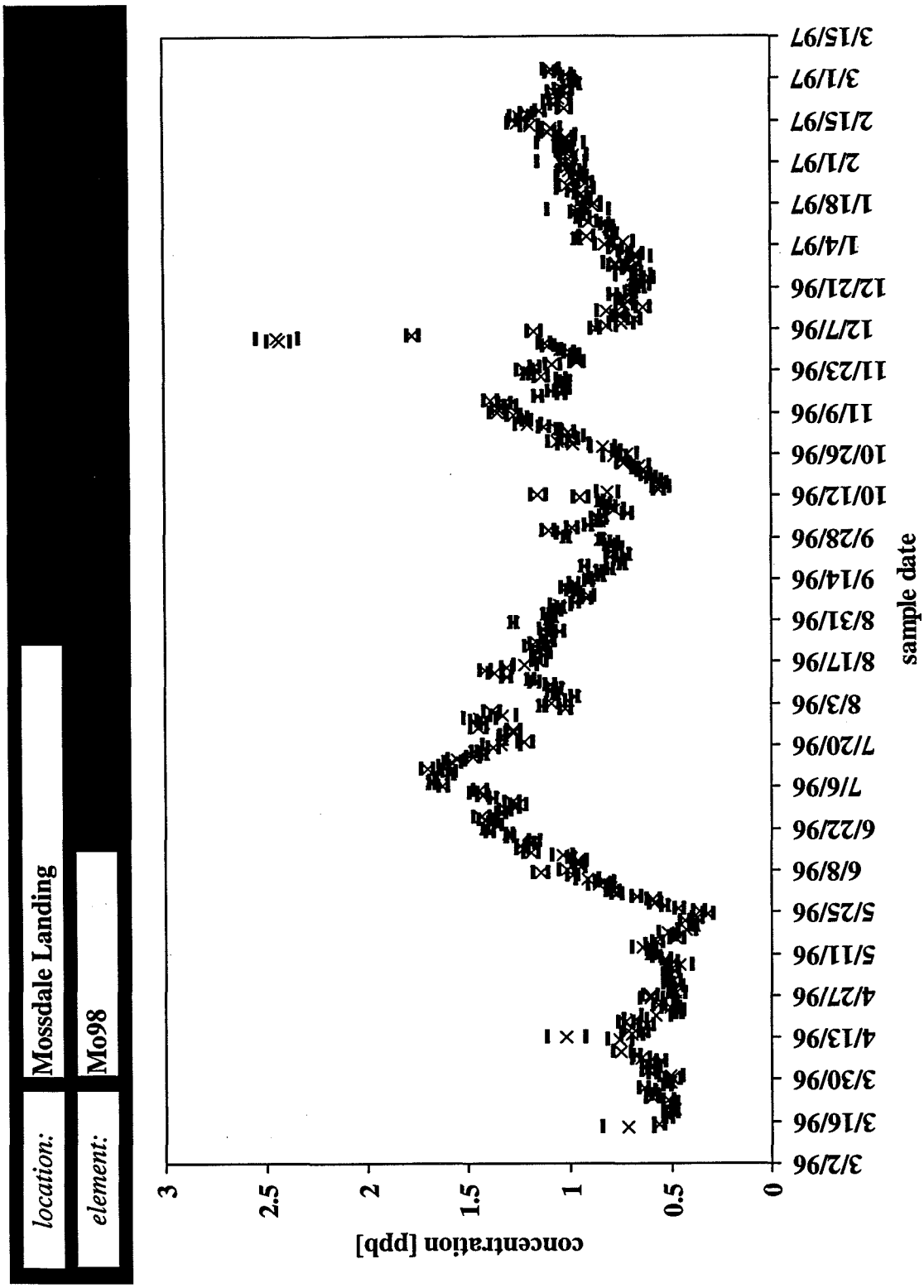
location:
Mossdale Landing
element:
Mo98
concentration [ppb]
0
0.5
1
1.5
2
2.5
3
sample date
3/2/96
3/16/96
3/30/96
4/13/96
4/27/96
5/11/96
5/25/96
6/8/96
6/22/96
7/6/96
7/20/96
8/3/96
8/17/96
8/31/96
9/14/96
9/28/96
10/12/96
10/26/96
11/9/96
11/23/96
12/7/96
12/21/96
1/4/97
1/18/97
2/1/97
2/15/97
3/1/97
3/15/97

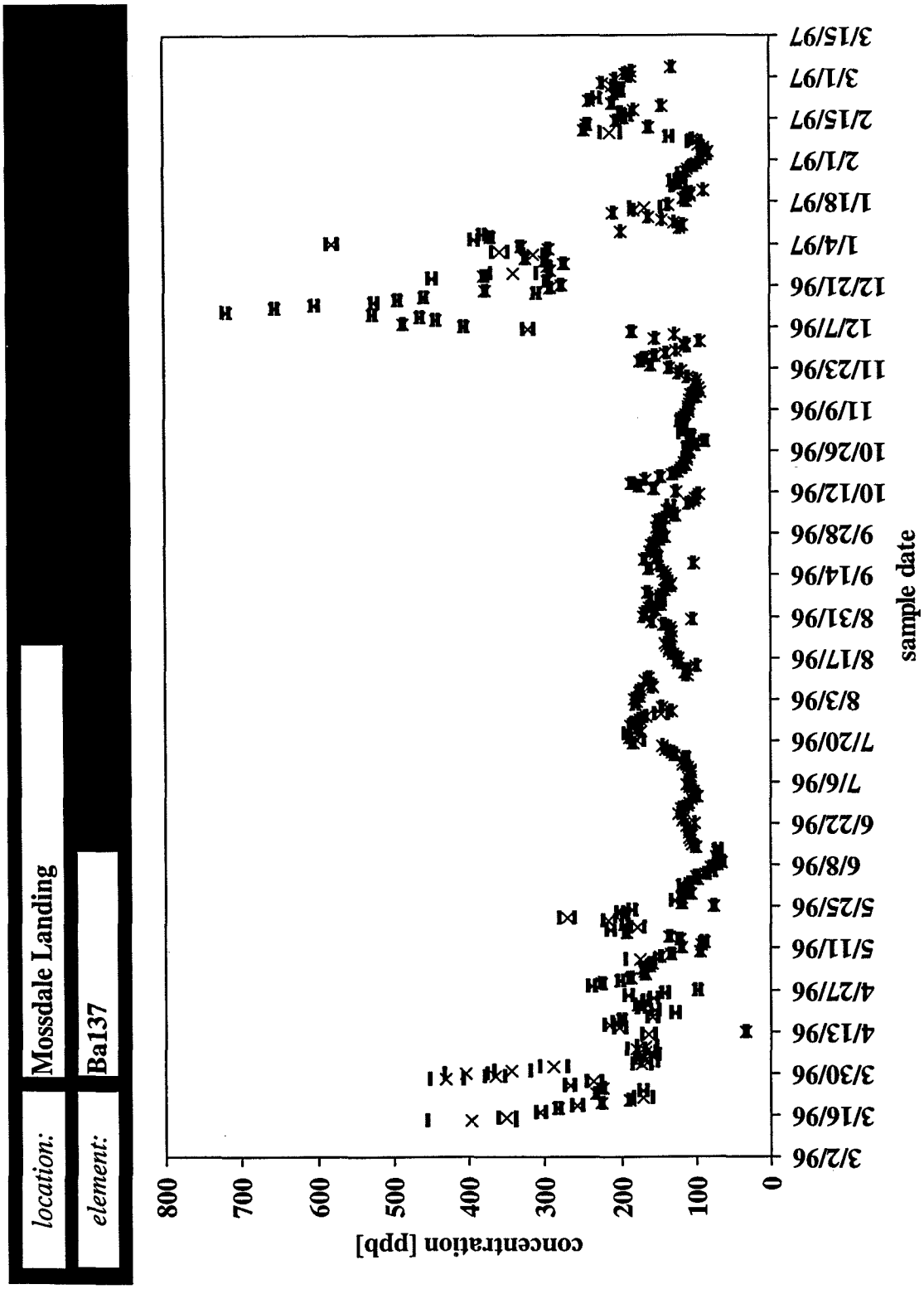
location:
Mossdale Landing
element:
Ba137
concentration [ppb]
0
100
200
300
400
500
600
700
800
sample date
3/2/96
3/16/96
3/30/96
4/13/96
4/27/96
5/11/96
5/25/96
6/8/96
6/22/96
7/6/96
7/20/96
8/3/96
8/17/96
8/31/96
9/14/96
9/28/96
10/12/96
10/26/96
11/9/96
11/23/96
12/7/96
12/21/96
1/4/97
1/18/97
2/1/97
2/15/97
3/1/97
3/15/97

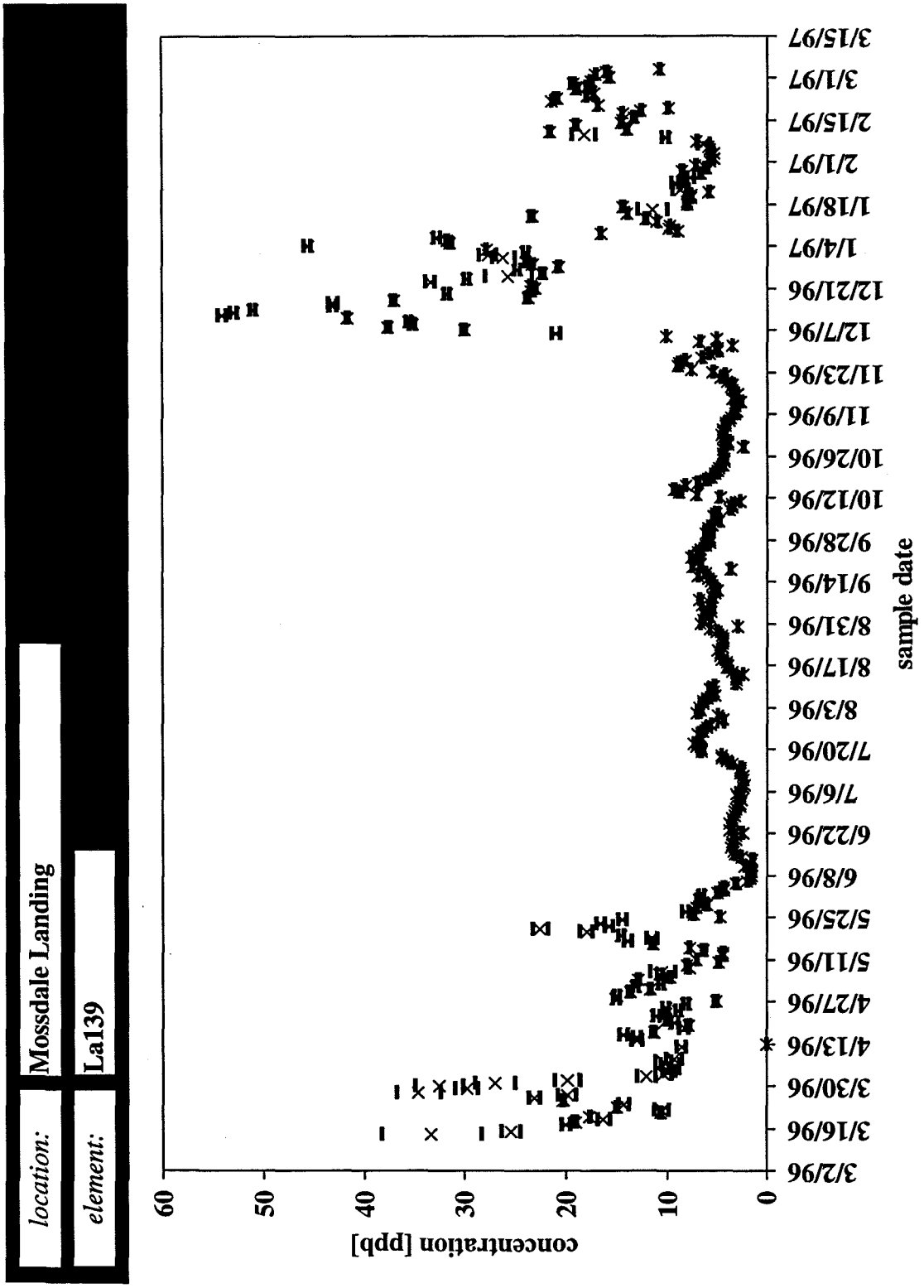
location:
Mossdale Landing
element:
La139
concentration [ppb]
0
10
20
30
40
50
60
sample date
3/2/96
3/16/96
3/30/96
4/13/96
4/27/96
5/11/96
5/25/96
6/8/96
6/22/96
7/6/96
7/20/96
8/3/96
8/17/96
8/31/96
9/14/96
9/28/96
10/12/96
10/26/96
11/9/96
11/23/96
12/7/96
12/21/96
1/4/97
1/18/97
2/1/97
2/15/97
3/1/97
3/15/97

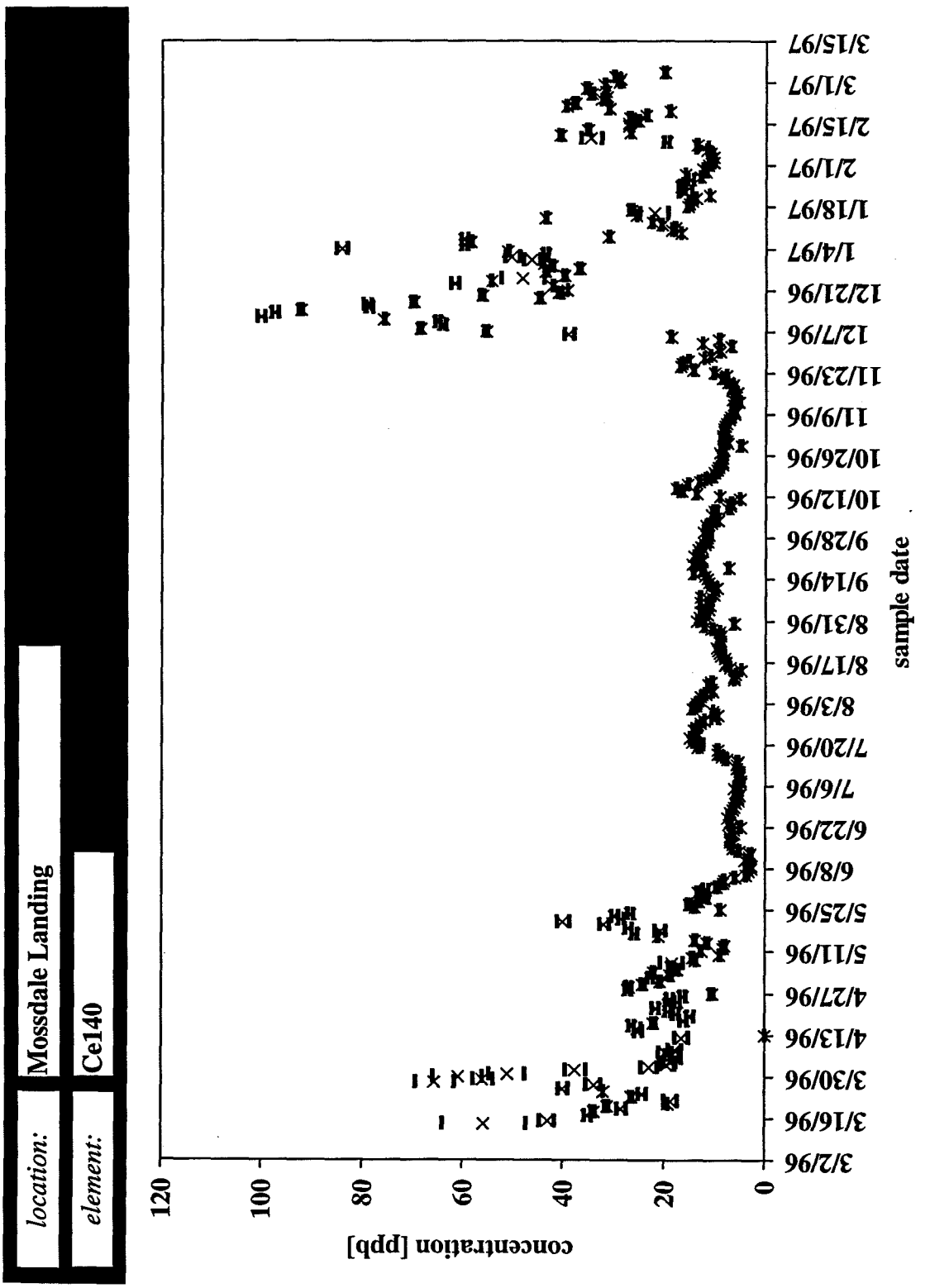
location:
Mossdale Landing
element:
Ce140
concentration [ppb]
0
20
40
60
80
100
120
sample date
3/2/96
3/16/96
3/30/96
4/13/96
4/27/96
5/11/96
5/25/96
6/8/96
6/22/96
7/6/96
7/20/96
8/3/96
8/17/96
8/31/96
9/14/96
9/28/96
10/12/96
10/26/96
11/9/96
11/23/96
12/7/96
12/21/96
1/4/97
1/18/97
2/1/97
2/15/97
3/1/97
3/15/97

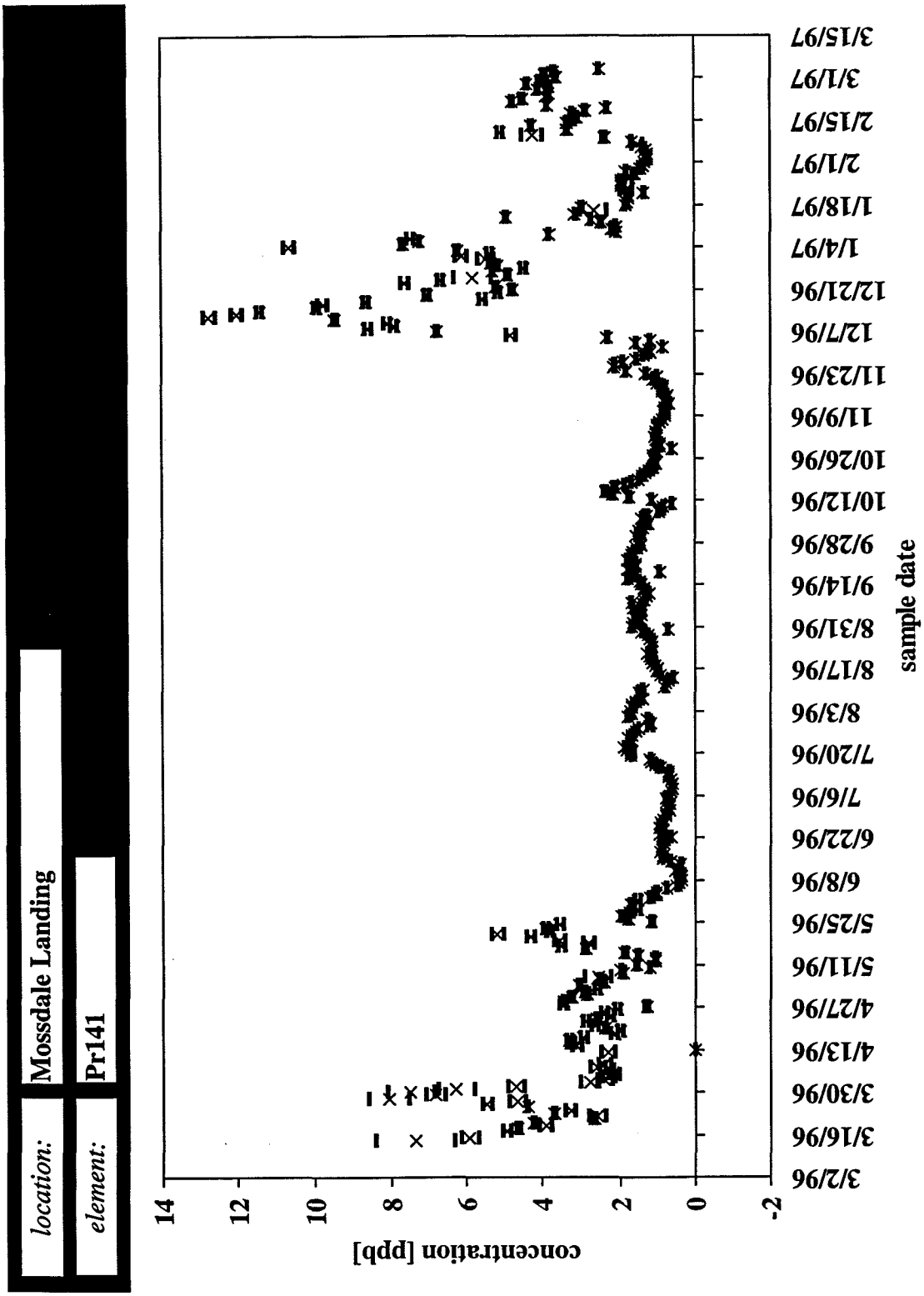
location:
Mossdale Landing
element:
Pr141
concentration [ppb]
14
12
10
8
6
4
2
0
-2
sample date
3/2/96
3/16/96
3/30/96
4/13/96
4/27/96
5/11/96
5/25/96
6/8/96
6/22/96
7/6/96
7/20/96
8/3/96
8/17/96
8/31/96
9/14/96
9/28/96
10/12/96
10/26/96
11/9/96
11/23/96
12/7/96
12/21/96
1/4/97
1/18/97
2/1/97
2/15/97
3/1/97
3/15/97

location:
Mossdale Landing
element:
Nd146
concentration [ppb]
0
10
20
30
40
50
60
sample date
3/2/96
3/16/96
3/30/96
4/13/96
4/27/96
5/11/96
5/25/96
6/8/96
6/22/96
7/6/96
7/20/96
8/3/96
8/17/96
8/31/96
9/14/96
9/28/96
10/12/96
10/26/96
11/9/96
11/23/96
12/7/96
12/21/96
1/4/97
1/18/97
2/1/97
2/15/97
3/1/97
3/15/97

location:
Mossdale Landing
element:
Sm149
concentration [ppb]
0
1
2
3
4
5
6
7
8
9
10
sample date
3/2/96
3/16/96
3/30/96
4/13/96
4/27/96
5/11/96
5/25/96
6/8/96
6/22/96
7/6/96
7/20/96
8/3/96
8/17/96
8/31/96
9/14/96
9/28/96
10/12/96
10/26/96
11/9/96
11/23/96
12/7/96
12/21/96
1/4/97
1/18/97
2/1/97
2/15/97
3/1/97
3/15/97

location:
Mossdale Landing
element:
Eu153
concentration [ppb]
0
0.2
0.4
0.6
0.8
1
1.2
1.4
1.6
1.8
2
sample date
3/2/96
3/16/96
3/30/96
4/13/96
4/27/96
5/11/96
5/25/96
6/8/96
6/22/96
7/6/96
7/20/96
8/3/96
8/17/96
8/31/96
9/14/96
9/28/96
10/12/96
10/26/96
11/9/96
11/23/96
12/7/96
12/21/96
1/4/97
1/18/97
2/1/97
2/15/97
3/1/97
3/15/97

location:
Mossdale Landing
element:
Gd157
concentration [ppb]
9
8
7
6
5
4
3
2
1
0
-1
sample date
3/2/96
3/16/96
3/30/96
4/13/96
4/27/96
5/11/96
5/25/96
6/8/96
6/22/96
7/6/96
7/20/96
8/3/96
8/17/96
8/31/96
9/14/96
9/28/96
10/12/96
10/26/96
11/9/96
11/23/96
12/7/96
12/21/96
1/4/97
1/18/97
2/1/97
2/15/97
3/1/97
3/15/97

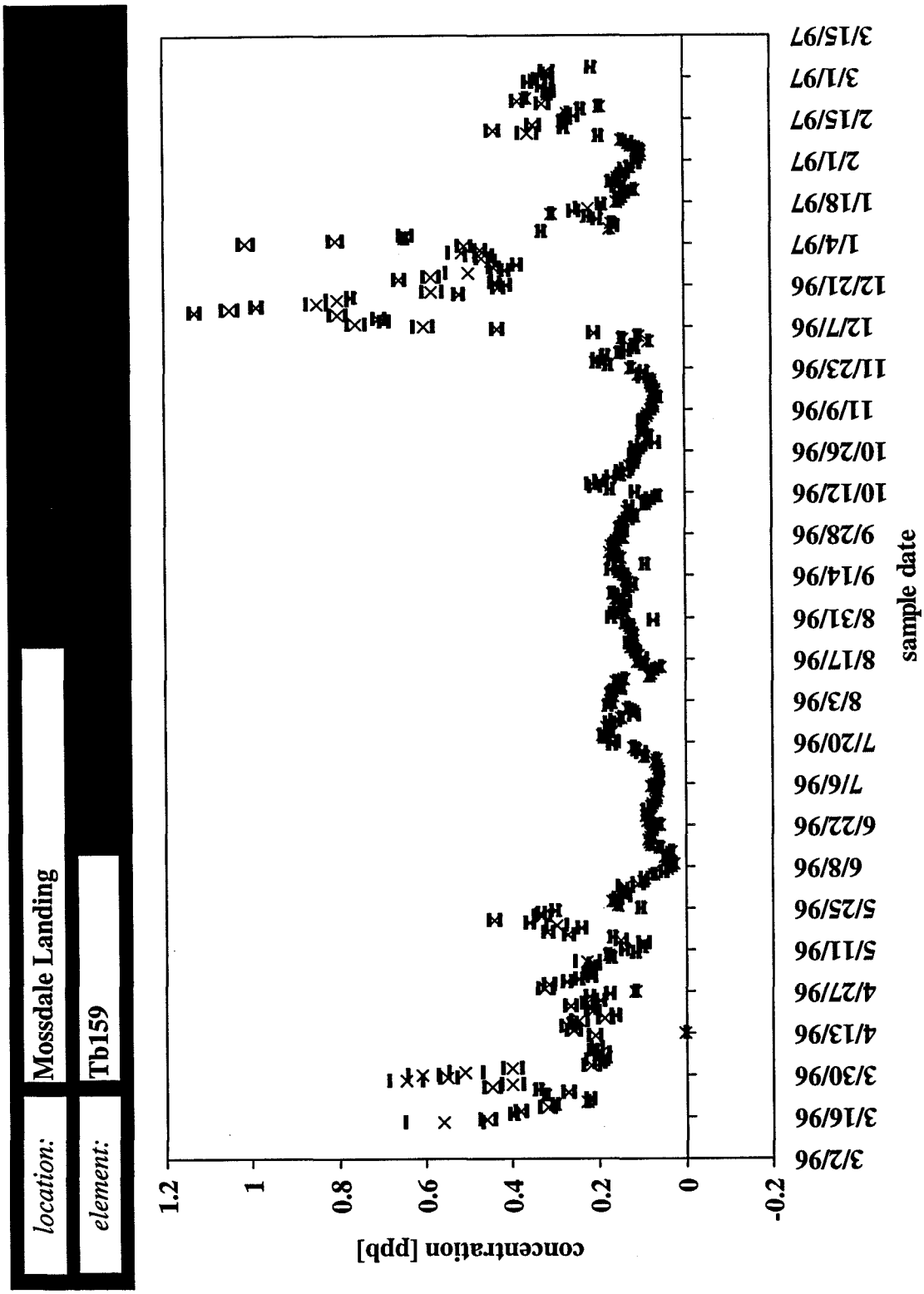
location:
Mossdale Landing
element:
Tb159
concentration [ppb]
1.2
1
0.8
0.6
0.4
0.2
0
-0.2
sample date
3/2/96
3/16/96
3/30/96
4/13/96
4/27/96
5/11/96
5/25/96
6/8/96
6/22/96
7/6/96
7/20/96
8/3/96
8/17/96
8/31/96
9/14/96
9/28/96
10/12/96
10/26/96
11/9/96
11/23/96
12/7/96
12/21/96
1/4/97
1/18/97
2/1/97
2/15/97
3/1/97
3/15/97

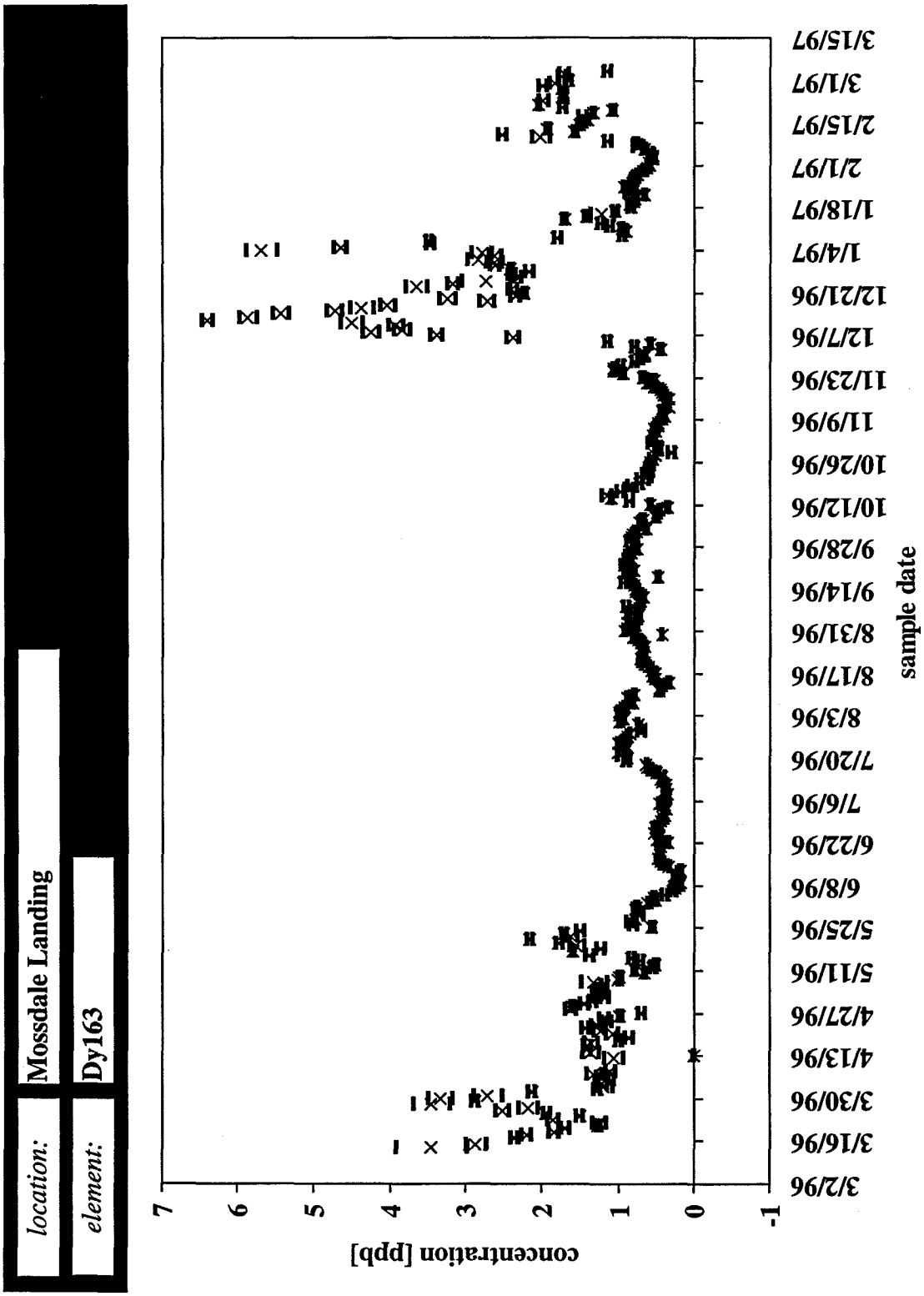
location:
Mossdale Landing
element:
Dy163
concentration [ppb]
7
6
5
4
3
2
1
0
-1
sample date
3/2/96
3/16/96
3/30/96
4/13/96
4/27/96
5/11/96
5/25/96
6/8/96
6/22/96
7/6/96
7/20/96
8/3/96
8/17/96
8/31/96
9/14/96
9/28/96
10/12/96
10/26/96
11/9/96
11/23/96
12/7/96
12/21/96
1/4/97
1/18/97
2/1/97
2/15/97
3/1/97
3/15/97

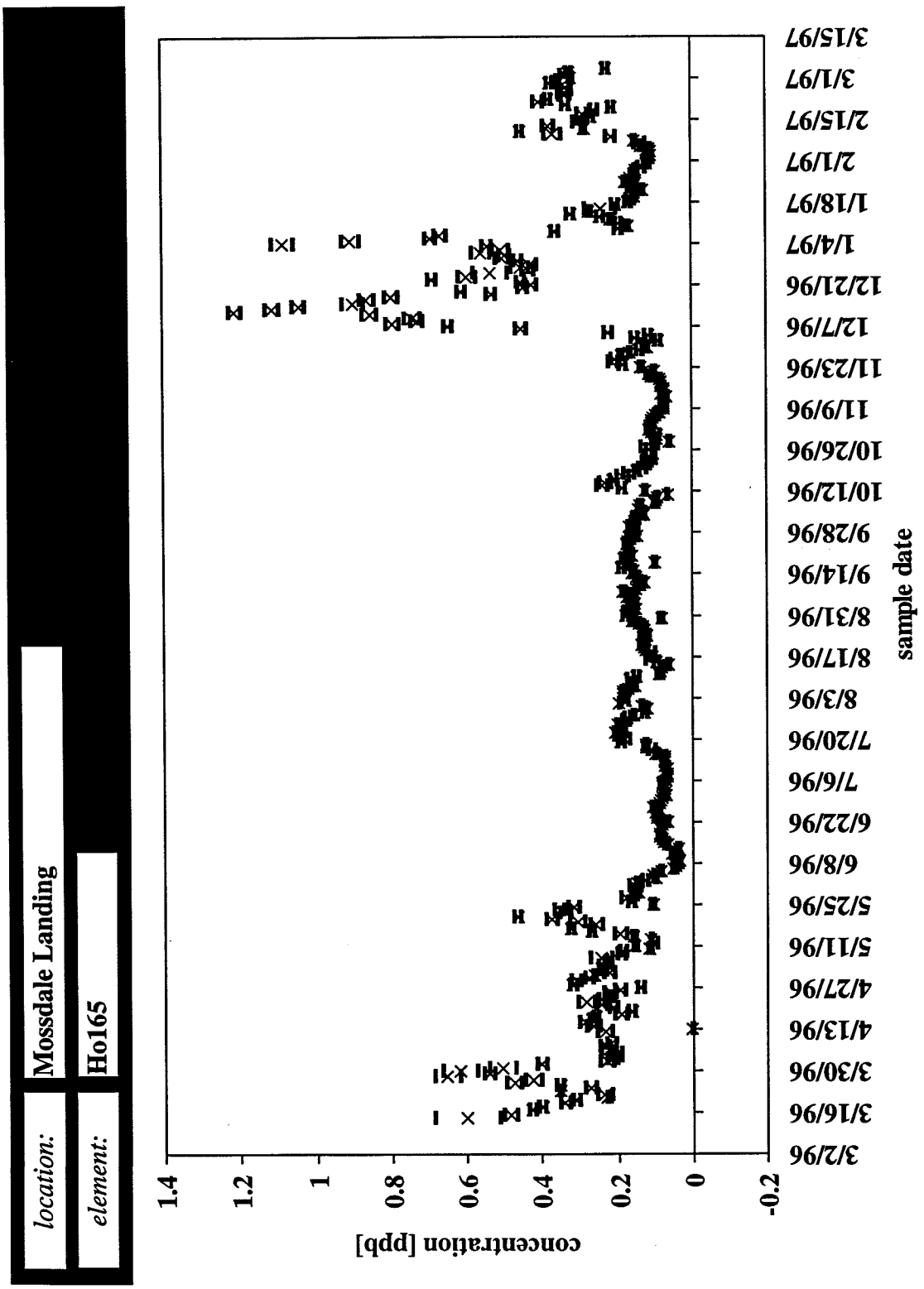
location:
Mossdale Landing
element:
Ho165
concentration [ppb]
1.4
1.2
1
0.8
0.6
0.4
0.2
0
-0.2
sample date
3/2/96
3/16/96
3/30/96
4/13/96
4/27/96
5/11/96
5/25/96
6/8/96
6/22/96
7/6/96
7/20/96
8/3/96
8/17/96
8/31/96
9/14/96
9/28/96
10/12/96
10/26/96
11/9/96
11/23/96
12/7/96
12/21/96
1/4/97
1/18/97
2/1/97
2/15/97
3/1/97
3/15/97

location:
Mossdale Landing
element:
Er168
concentration [ppb]
3.5
3
2.5
2
1.5
1
0.5
0
-0.5
sample date
3/2/96
3/16/96
3/30/96
4/13/96
4/27/96
5/11/96
5/25/96
6/8/96
6/22/96
7/6/96
7/20/96
8/3/96
8/17/96
8/31/96
9/14/96
9/28/96
10/12/96
10/26/96
11/9/96
11/23/96
12/7/96
12/21/96
1/4/97
1/18/97
2/1/97
2/15/97
3/1/97
3/15/97

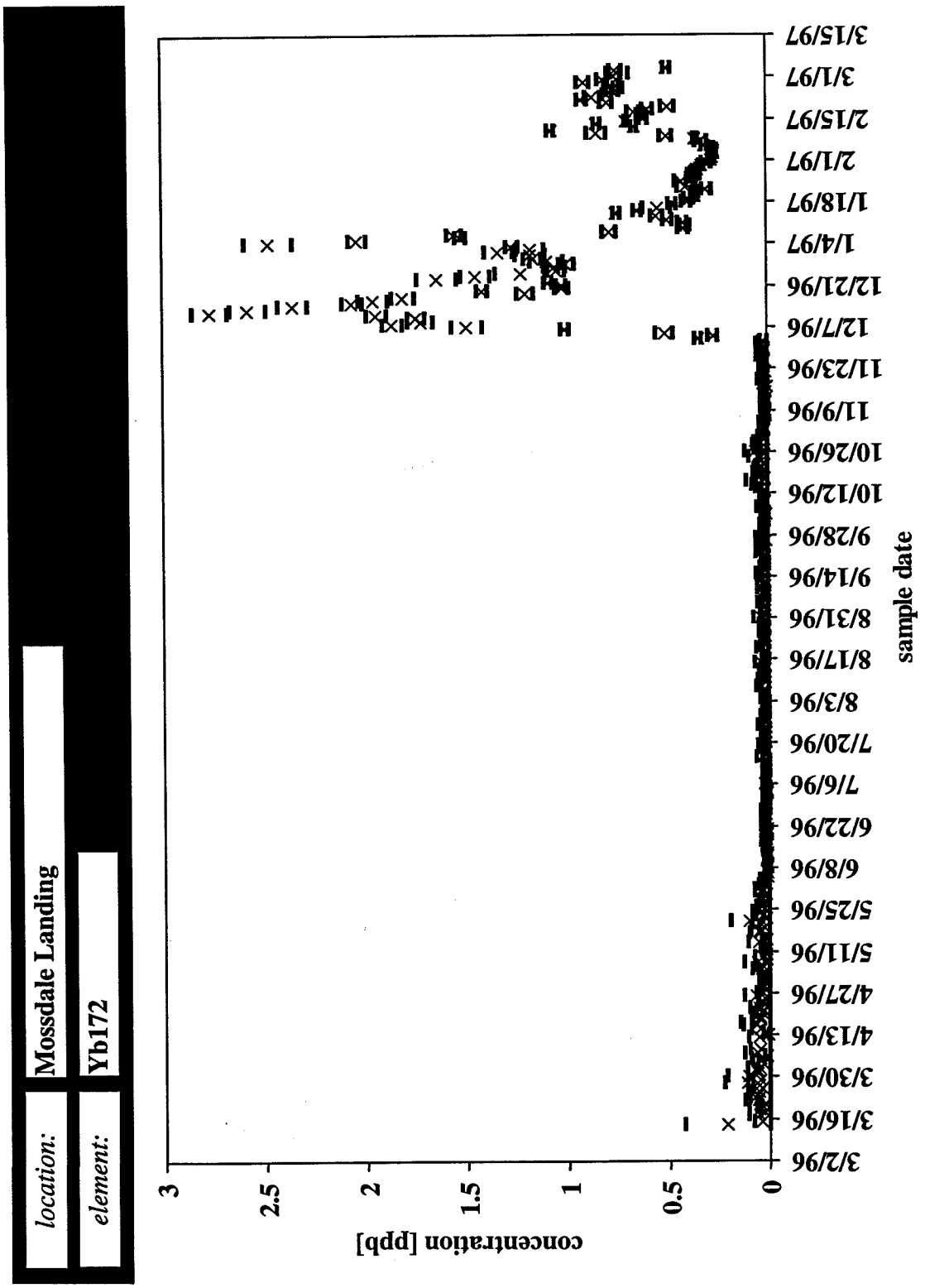
location:
Mossdale Landing
element:
Yb172
concentration [ppb]
0
0.5
1
1.5
2
2.5
3
sample date
3/2/96
3/16/96
3/30/96
4/13/96
4/27/96
5/11/96
5/25/96
6/8/96
6/22/96
7/6/96
7/20/96
8/3/96
8/17/96
8/31/96
9/14/96
9/28/96
10/12/96
10/26/96
11/9/96
11/23/96
12/7/96
12/21/96
1/4/97
1/18/97
2/1/97
2/15/97
3/1/97
3/15/97

location:
Mossdale Landing
element:
Lu175
concentration [ppb]
0.45
0.4
0.35
0.3
0.25
0.2
0.15
0.1
0.05
0
-0.05
sample date
3/2/96
3/16/96
3/30/96
4/13/96
4/27/96
5/11/96
5/25/96
6/8/96
6/22/96
7/6/96
7/20/96
8/3/96
8/17/96
8/31/96
9/14/96
9/28/96
10/12/96
10/26/96
11/9/96
11/23/96
12/7/96
12/21/96
1/4/97
1/18/97
2/1/97
2/15/97
3/1/97
3/15/97

location:
Mossdale Landing
element:
Th232
concentration [ppb]
0
10
20
30
40
50
60
70
sample date
3/2/96
3/16/96
3/30/96
4/13/96
4/27/96
5/11/96
5/25/96
6/8/96
6/22/96
7/6/96
7/20/96
8/3/96
8/17/96
8/31/96
9/14/96
9/28/96
10/12/96
10/26/96
11/9/96
11/23/96
12/7/96
12/21/96
1/4/97
1/18/97
2/1/97
2/15/97
3/1/97
3/15/97

location:
Mossdale Landing
element:
U238
concentration [ppb]
0
2
4
6
8
10
12
14
16
18
20
sample date
3/2/96
3/16/96
3/30/96
4/13/96
4/27/96
5/11/96
5/25/96
6/8/96
6/22/96
7/6/96
7/20/96
8/3/96
8/17/96
8/31/96
9/14/96
9/28/96
10/12/96
10/26/96
11/9/96
11/23/96
12/7/96
12/21/96
1/4/97
1/18/97
2/1/97
2/15/97
3/1/97
3/15/97

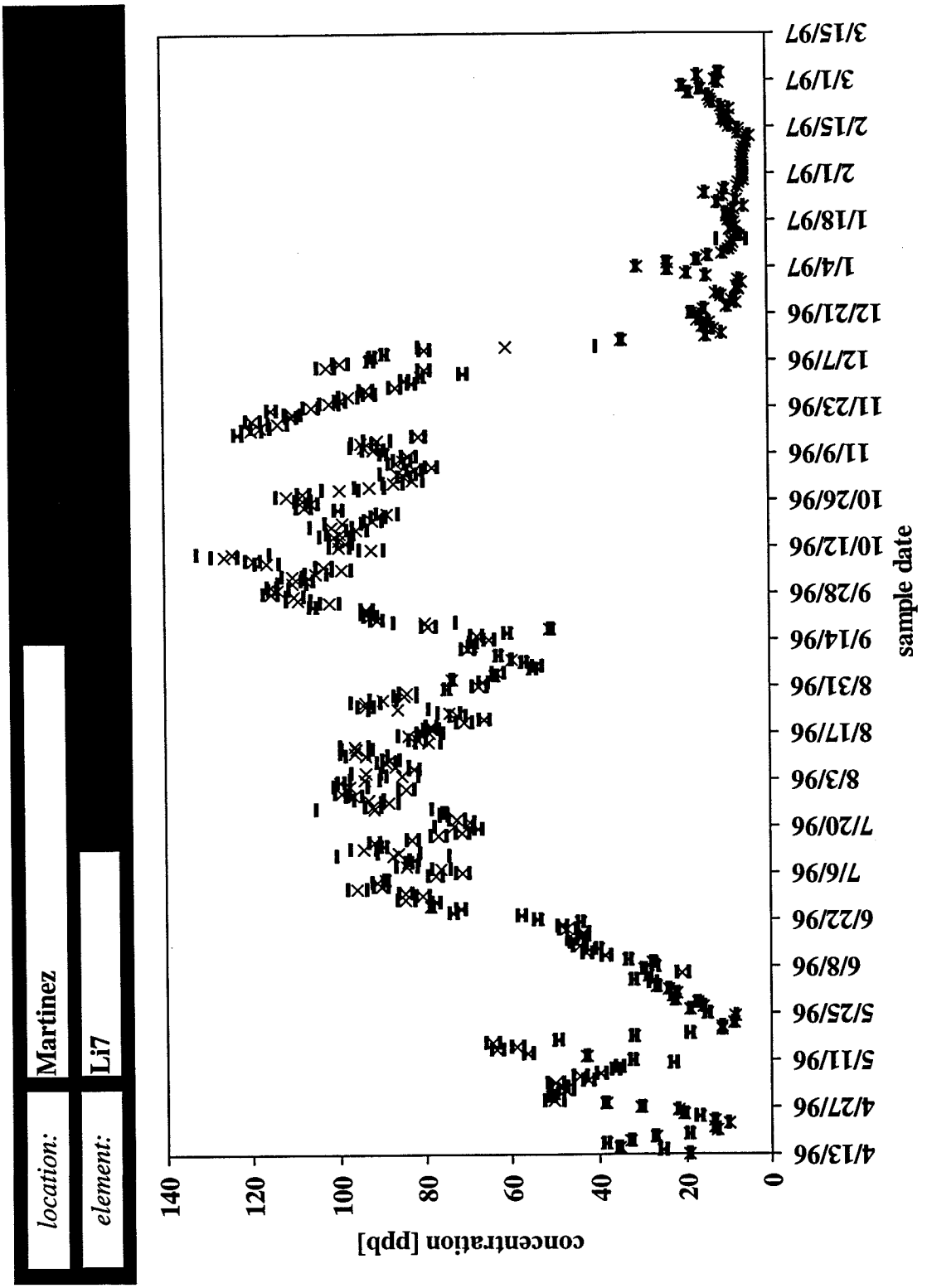
location:
Martinez
element:
Li7
concentration [ppb]
0
20
40
60
80
100
120
140
sample date
4/13/96
4/27/96
5/11/96
5/25/96
6/8/96
6/22/96
7/6/96
7/20/96
8/3/96
8/17/96
8/31/96
9/14/96
9/28/96
10/12/96
10/26/96
11/9/96
11/23/96
12/7/96
12/21/96
1/4/97
1/18/97
2/1/97
2/15/97
3/1/97
3/15/97

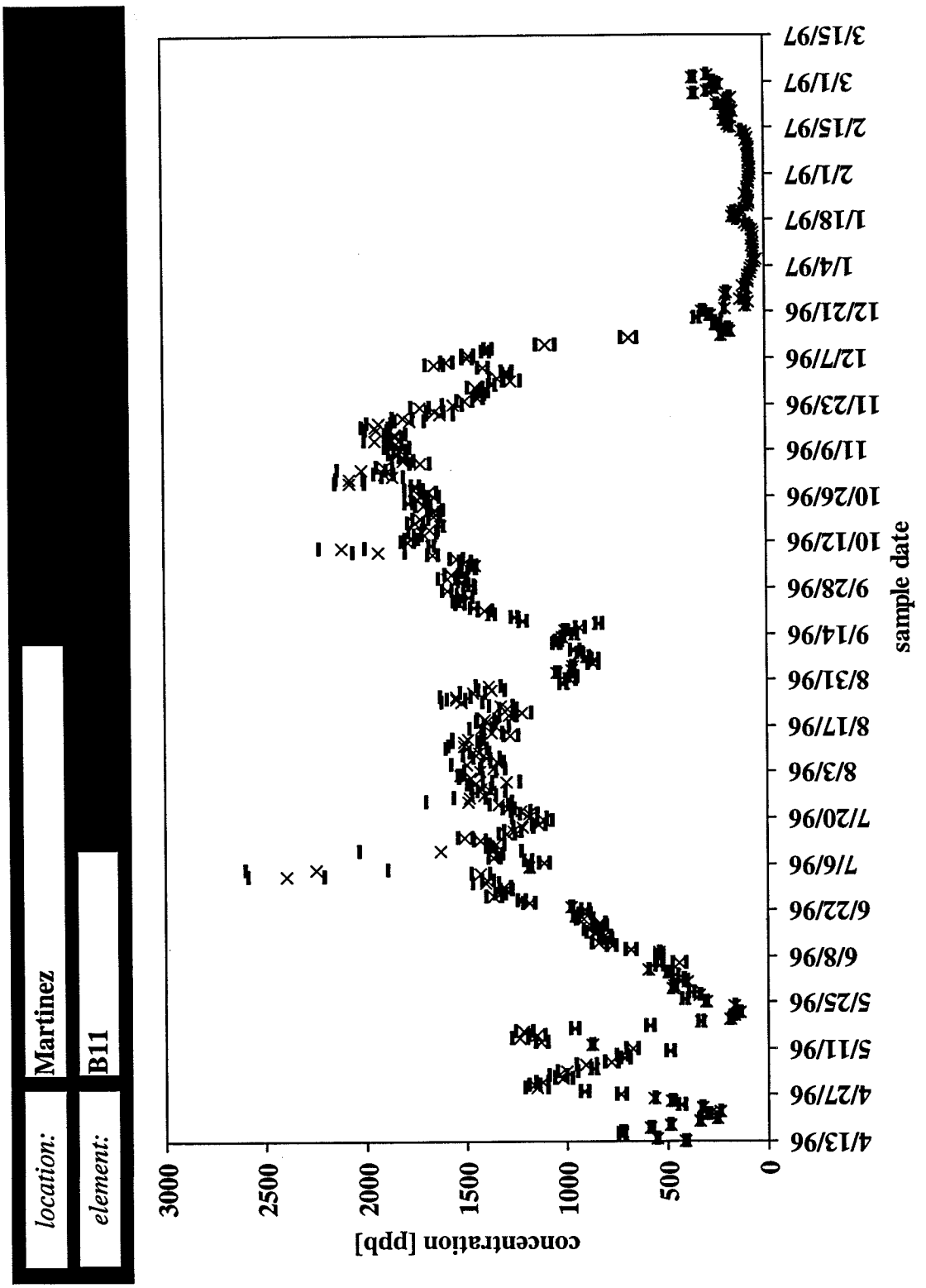
location:
Martinez
element:
B11
concentration [ppb]
3000
2500
2000
1500
1000
500
0
sample date
4/13/96
4/27/96
5/11/96
5/25/96
6/8/96
6/22/96
7/6/96
7/20/96
8/3/96
8/17/96
8/31/96
9/14/96
9/28/96
10/12/96
10/26/96
11/9/96
11/23/96
12/7/96
12/21/96
1/4/97
1/18/97
2/1/97
2/15/97
3/1/97
3/15/97

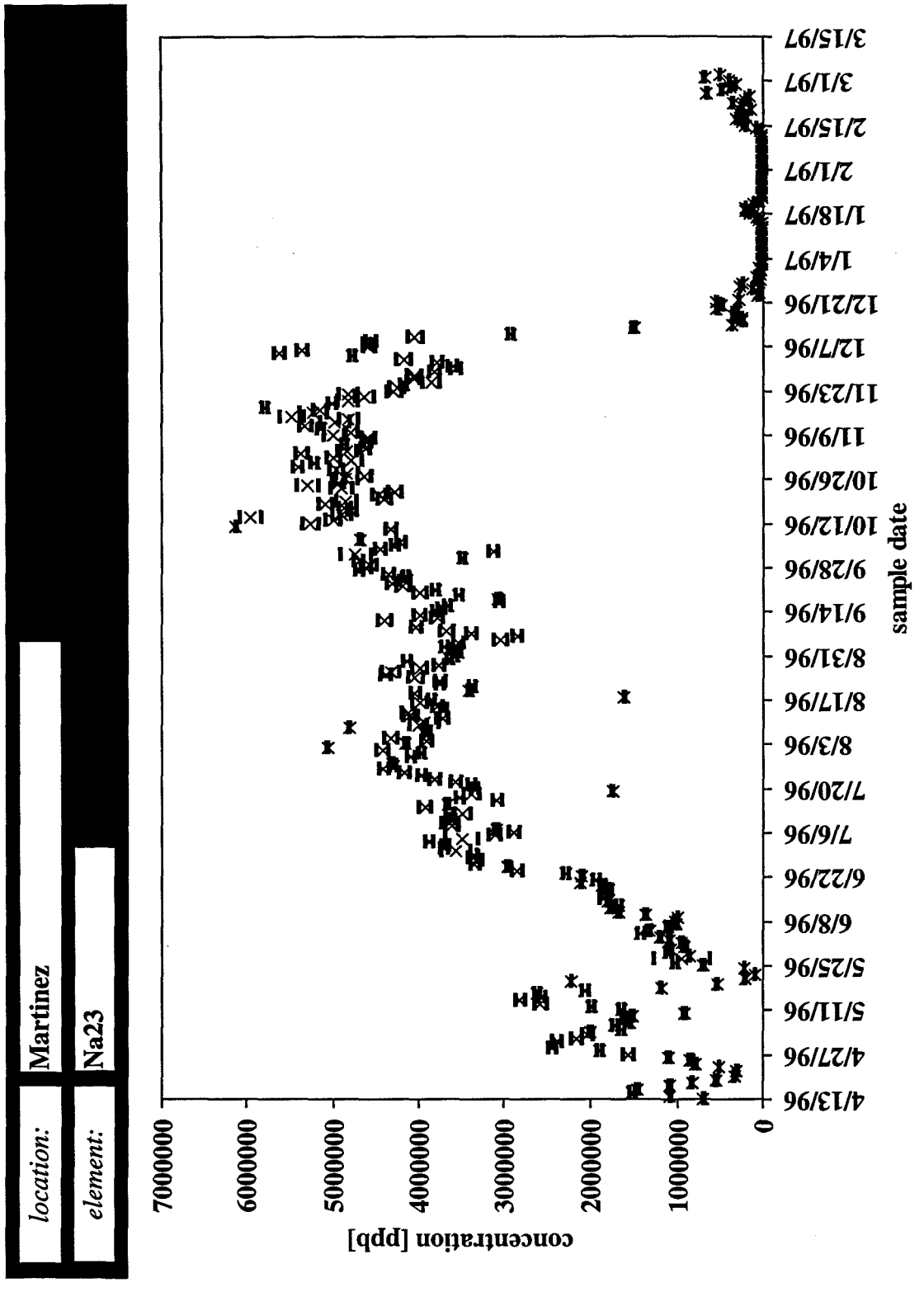
location:
Martinez
element:
Na23
concentration [ppb]
7000000
6000000
5000000
4000000
3000000
2000000
1000000
0
sample date
4/13/96
4/27/96
5/11/96
5/25/96
6/8/96
6/22/96
7/6/96
7/20/96
8/3/96
8/17/96
8/31/96
9/14/96
9/28/96
10/12/96
10/26/96
11/9/96
11/23/96
12/7/96
12/21/96
1/4/97
1/18/97
2/1/97
2/15/97
3/1/97
3/15/97

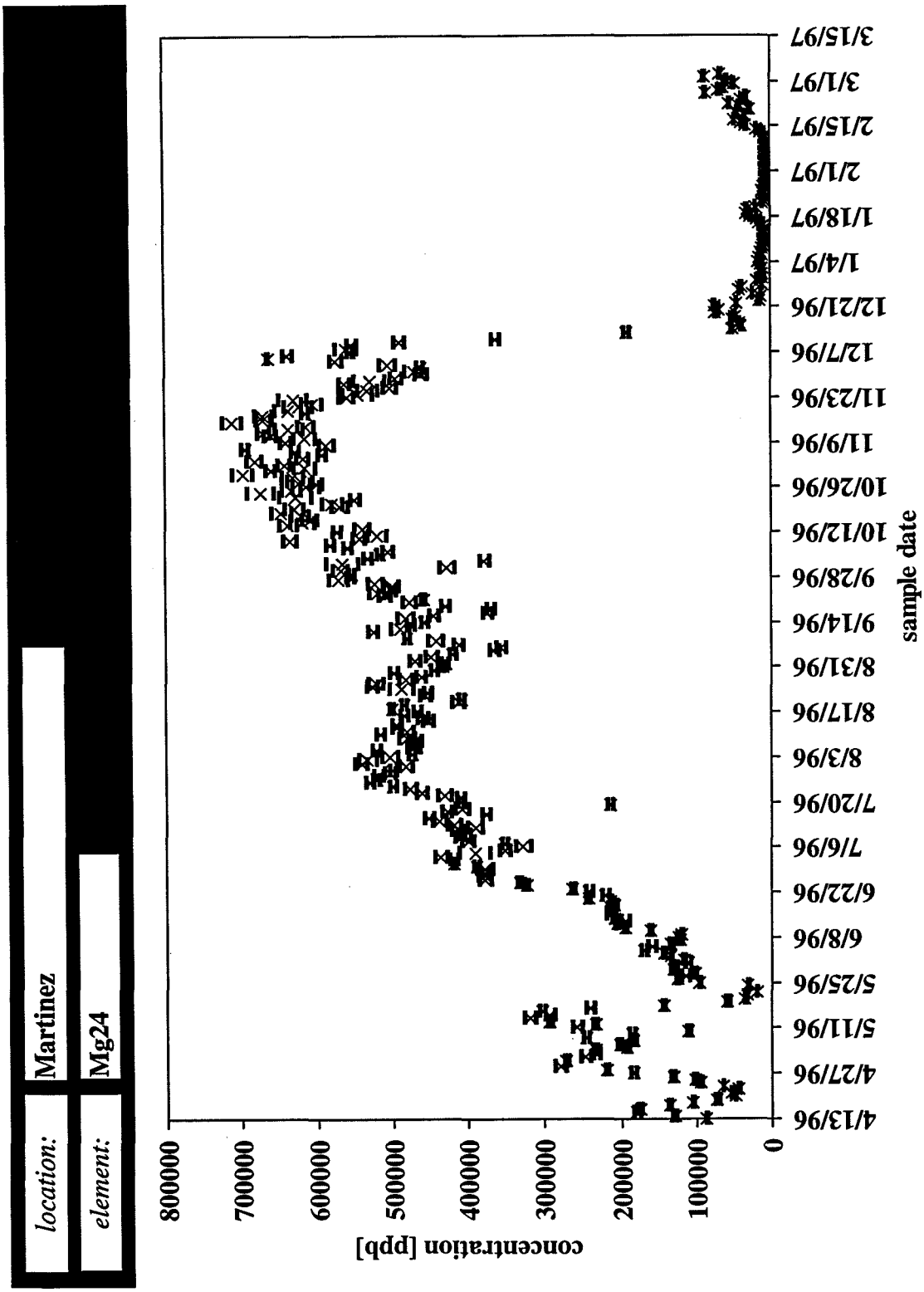
location:
Martinez
element:
Mg24
concentration [ppb]
800000
700000
600000
500000
400000
300000
200000
100000
0
sample date
4/13/96
4/27/96
5/11/96
5/25/96
6/8/96
6/22/96
7/6/96
7/20/96
8/3/96
8/17/96
8/31/96
9/14/96
9/28/96
10/12/96
10/26/96
11/9/96
11/23/96
12/7/96
12/21/96
1/4/97
1/18/97
2/1/97
2/15/97
3/1/97
3/15/97

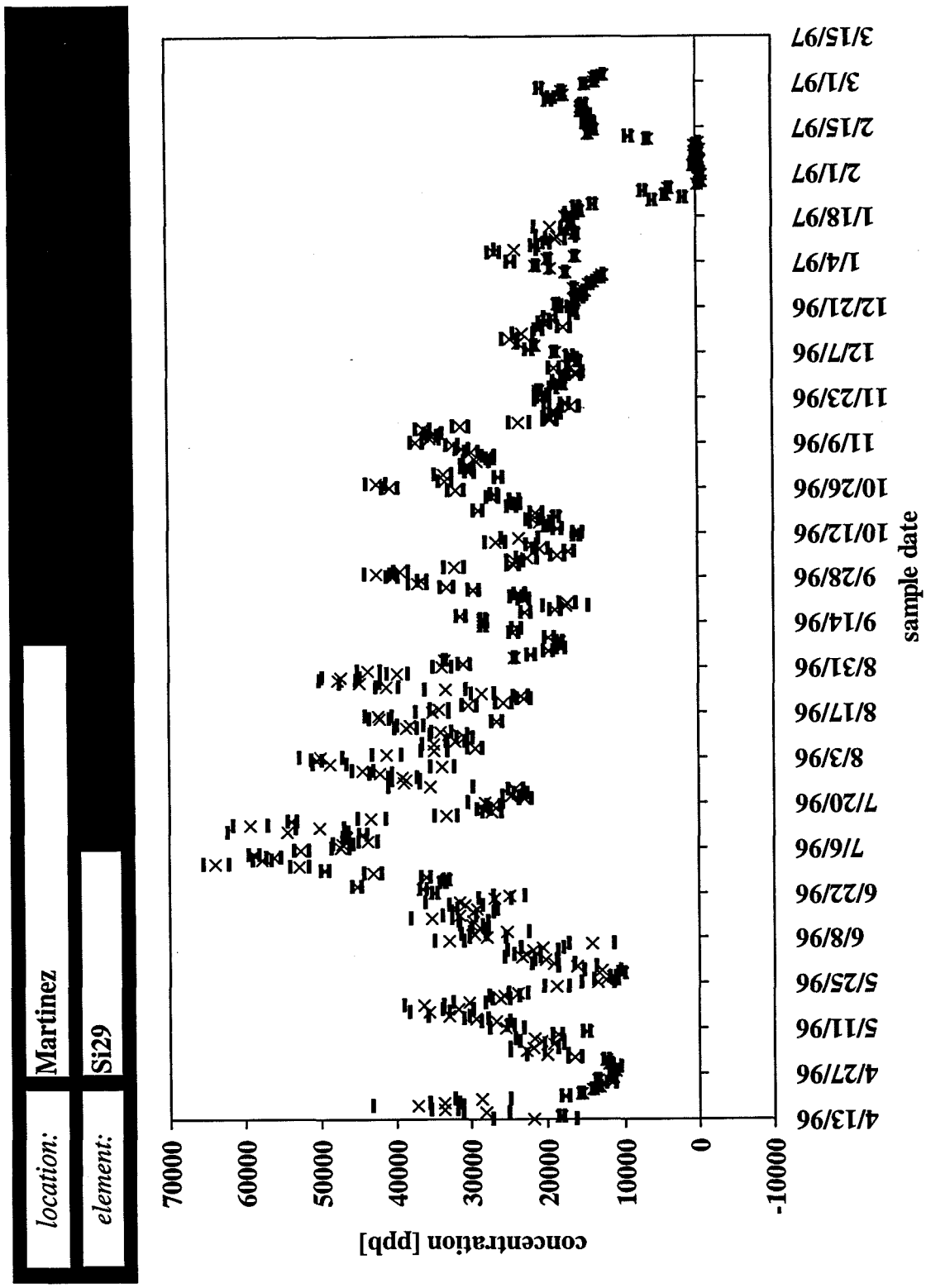
location:
Martinez
element:
Si29
concentration [ppb]
70000
60000
50000
40000
30000
20000
10000
0
-10000
sample date
4/13/96
4/27/96
5/11/96
5/25/96
6/8/96
6/22/96
7/6/96
7/20/96
8/3/96
8/17/96
8/31/96
9/14/96
9/28/96
10/12/96
10/26/96
11/9/96
11/23/96
12/7/96
12/21/96
1/4/97
1/18/97
2/1/97
2/15/97
3/1/97
3/15/97

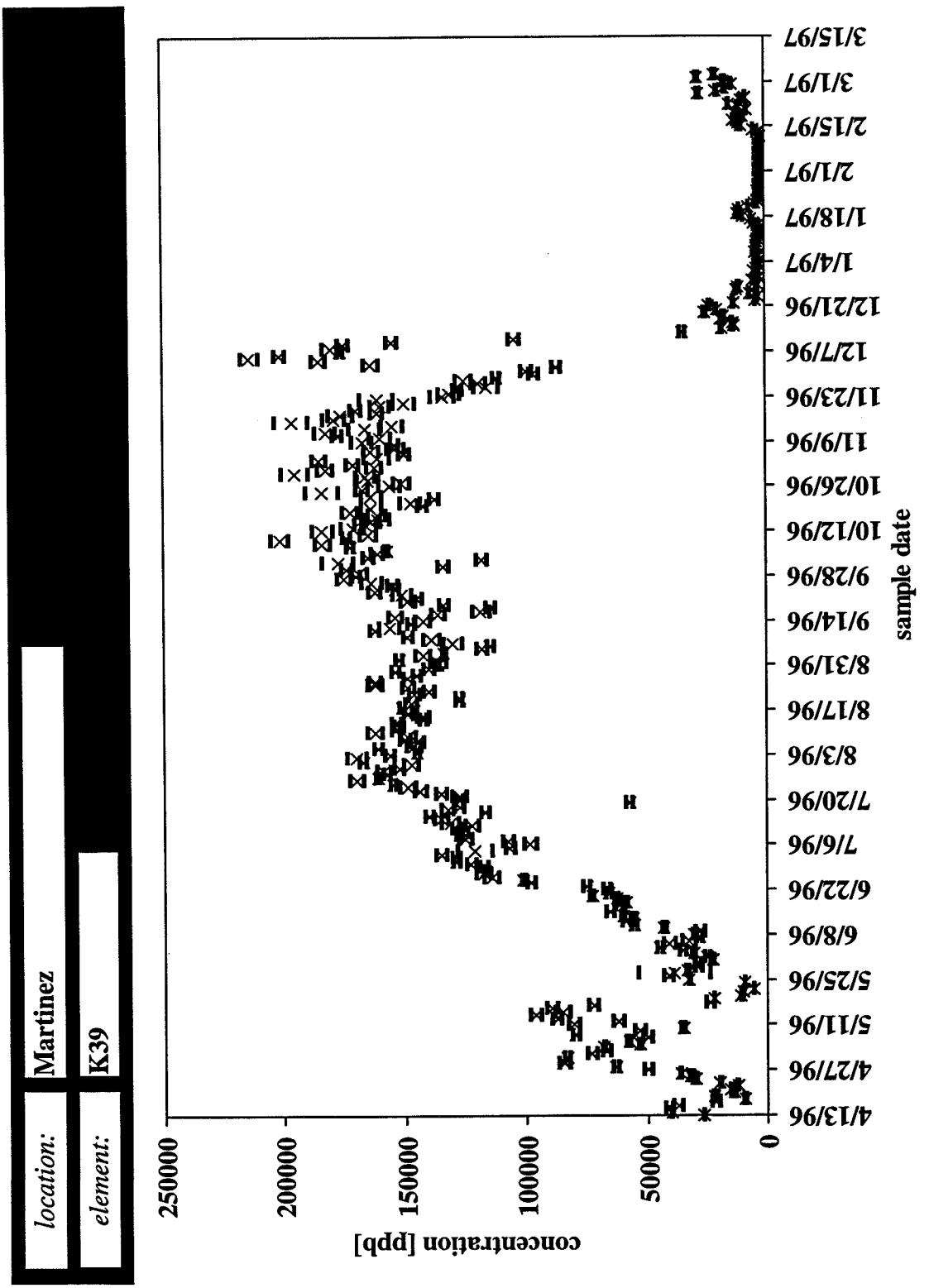
location:
Martinez
element:
K39
concentration [ppb]
250000
200000
150000
100000
50000
0
sample date
4/13/96
4/27/96
5/11/96
5/25/96
6/8/96
6/22/96
7/6/96
7/20/96
8/3/96
8/17/96
8/31/96
9/14/96
9/28/96
10/12/96
10/26/96
11/9/96
11/23/96
12/7/96
12/21/96
1/4/97
1/18/97
2/1/97
2/15/97
3/1/97
3/15/97

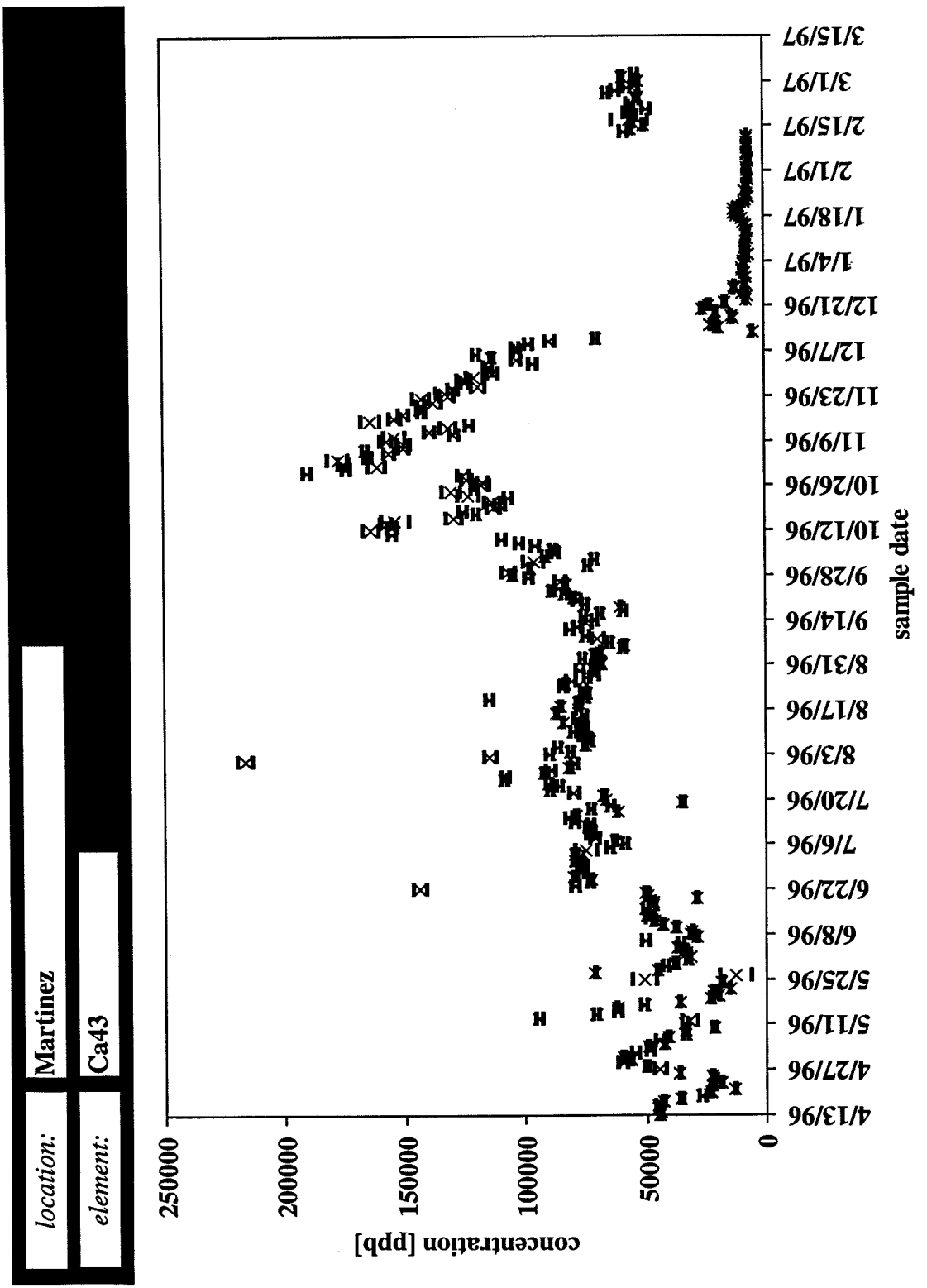
location:
Martinez
element:
Ca43
concentration [ppb]
250000
200000
150000
100000
50000
0
sample date
4/13/96
4/27/96
5/11/96
5/25/96
6/8/96
6/22/96
7/6/96
7/20/96
8/3/96
8/17/96
8/31/96
9/14/96
9/28/96
10/12/96
10/26/96
11/9/96
11/23/96
12/7/96
12/21/96
1/4/97
1/18/97
2/1/97
2/15/97
3/1/97
3/15/97

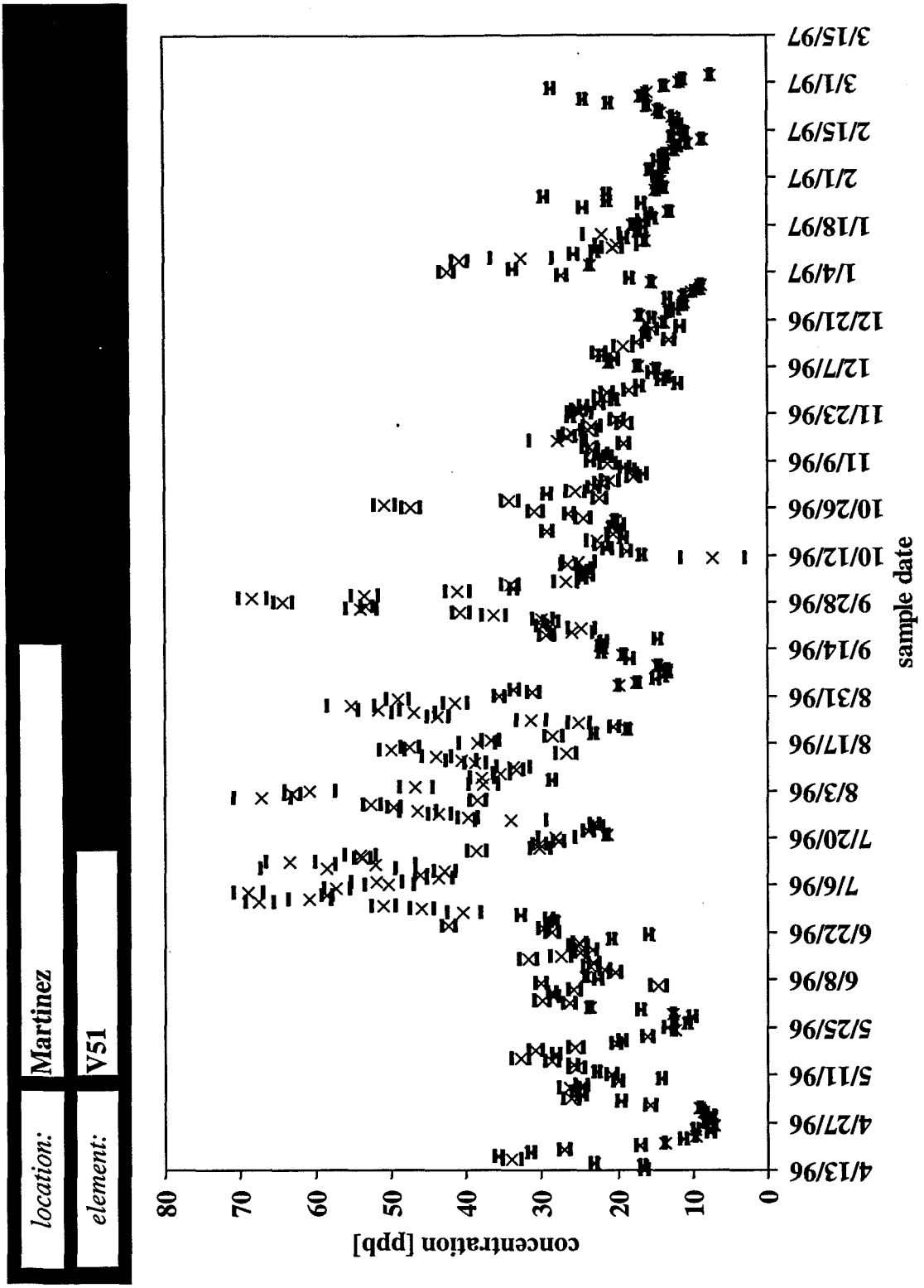
location:
Martinez
element:
V51
concentration [ppb]
0
10
20
30
40
50
60
70
80
sample date
4/13/96
4/27/96
5/11/96
5/25/96
6/8/96
6/22/96
7/6/96
7/20/96
8/3/96
8/17/96
8/31/96
9/14/96
9/28/96
10/12/96
10/26/96
11/9/96
11/23/96
12/7/96
12/21/96
1/4/97
1/18/97
2/1/97
2/15/97
3/1/97
3/15/97

location:
Martinez
element:
Fe57
concentration [ppb]
35000
30000
25000
20000
15000
10000
5000
0
sample date
4/13/96
4/27/96
5/11/96
5/25/96
6/8/96
6/22/96
7/6/96
7/20/96
8/3/96
8/17/96
8/31/96
9/14/96
9/28/96
10/12/96
10/26/96
11/9/96
11/23/96
12/7/96
12/21/96
1/4/97
1/18/97
2/1/97
2/15/97
3/1/97
3/15/97

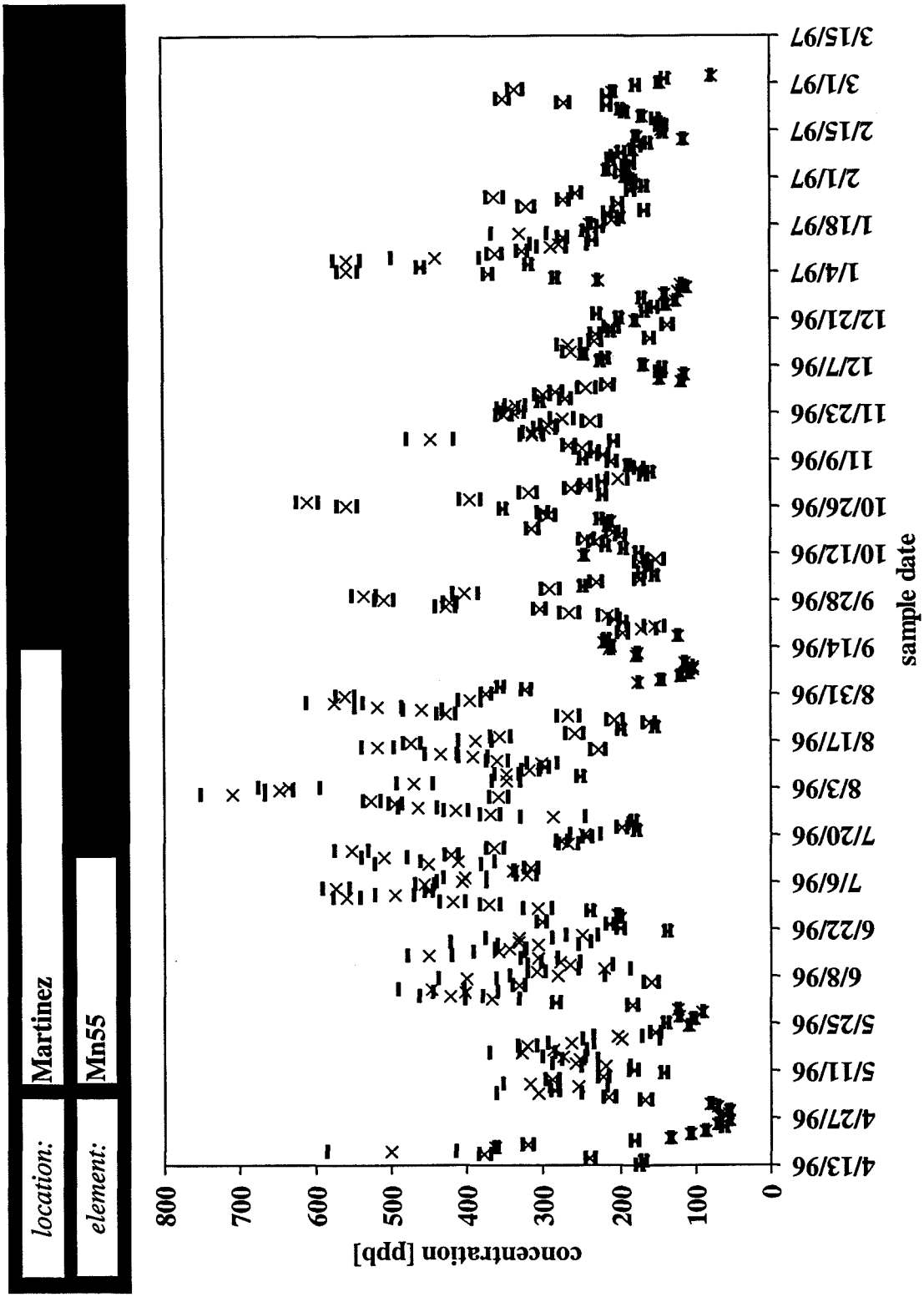
location:
Martinez
element:
Mn55
concentration [ppb]
0
100
200
300
400
500
600
700
800
sample date
4/13/96
4/27/96
5/11/96
5/25/96
6/8/96
6/22/96
7/6/96
7/20/96
8/3/96
8/17/96
8/31/96
9/14/96
9/28/96
10/12/96
10/26/96
11/9/96
11/23/96
12/7/96
12/21/96
1/4/97
1/18/97
2/1/97
2/15/97
3/1/97
3/15/97

location:
Martinez
element:
Co59
concentration [ppb]
0
2
4
6
8
10
12
14
16
sample date
4/13/96
4/27/96
5/11/96
5/25/96
6/8/96
6/22/96
7/6/96
7/20/96
8/3/96
8/17/96
8/31/96
9/14/96
9/28/96
10/12/96
10/26/96
11/9/96
11/23/96
12/7/96
12/21/96
1/4/97
1/18/97
2/1/97
2/15/97
3/1/97
3/15/97

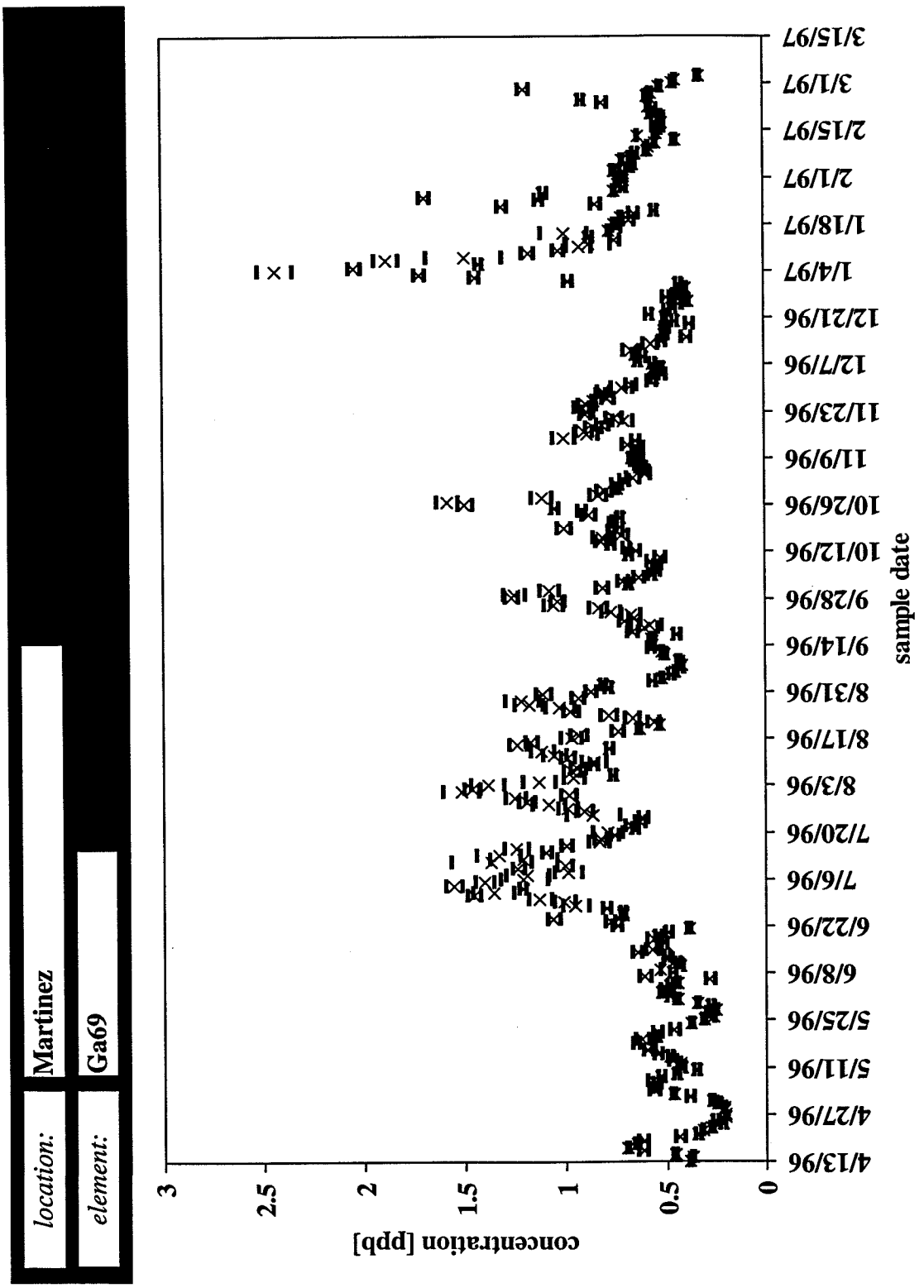
location:
Martinez
element:
Ga69
concentration [ppb]
0
0.5
1
1.5
2
2.5
3
sample date
4/13/96
4/27/96
5/11/96
5/25/96
6/8/96
6/22/96
7/6/96
7/20/96
8/3/96
8/17/96
8/31/96
9/14/96
9/28/96
10/12/96
10/26/96
11/9/96
11/23/96
12/7/96
12/21/96
1/4/97
1/18/97
2/1/97
2/15/97
3/1/97
3/15/97

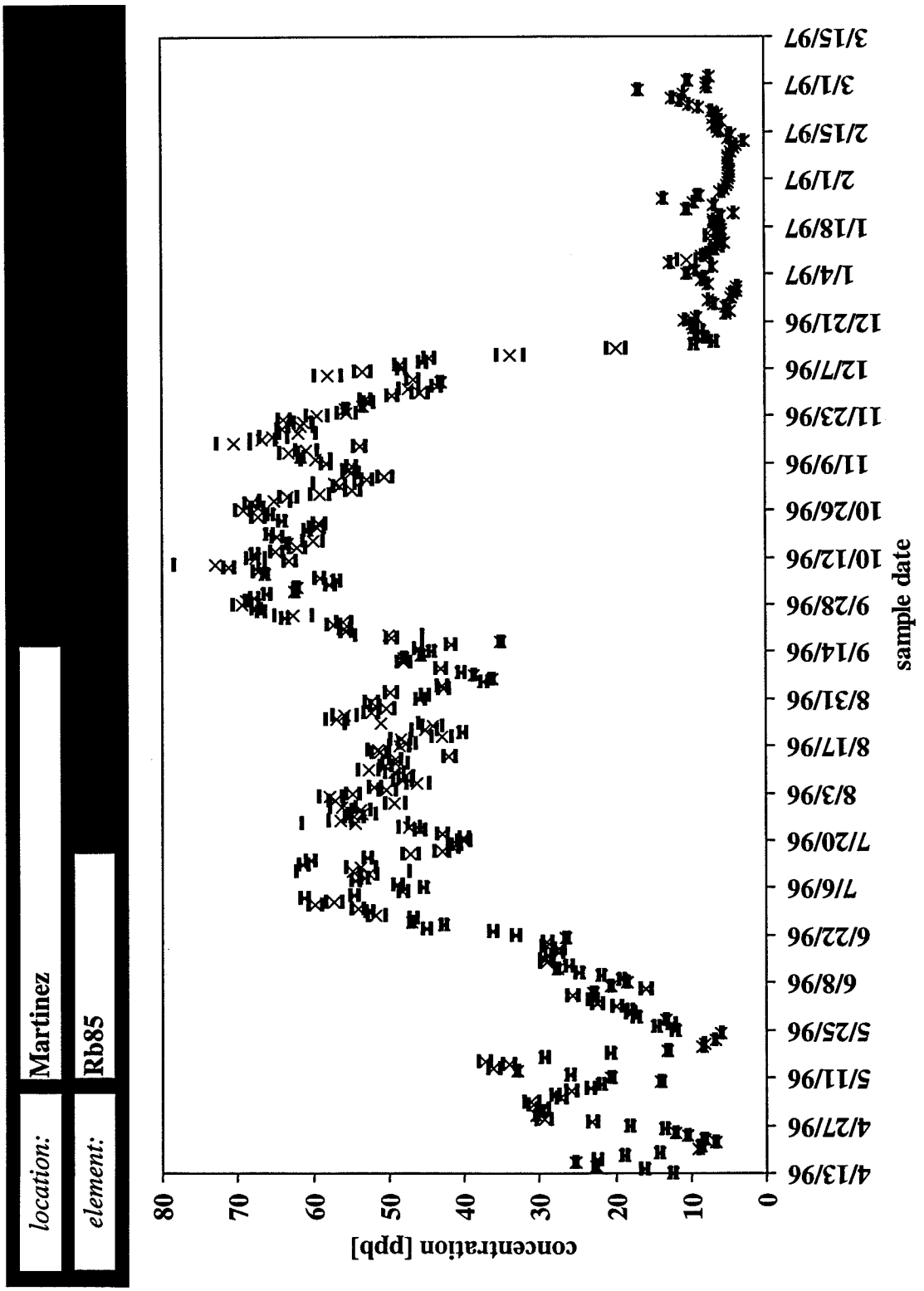
location:
Martinez
element:
Rb85
concentration [ppb]
0
10
20
30
40
50
60
70
80
sample date
4/13/96
4/27/96
5/11/96
5/25/96
6/8/96
6/22/96
7/6/96
7/20/96
8/3/96
8/17/96
8/31/96
9/14/96
9/28/96
10/12/96
10/26/96
11/9/96
11/23/96
12/7/96
12/21/96
1/4/97
1/18/97
2/1/97
2/15/97
3/1/97
3/15/97

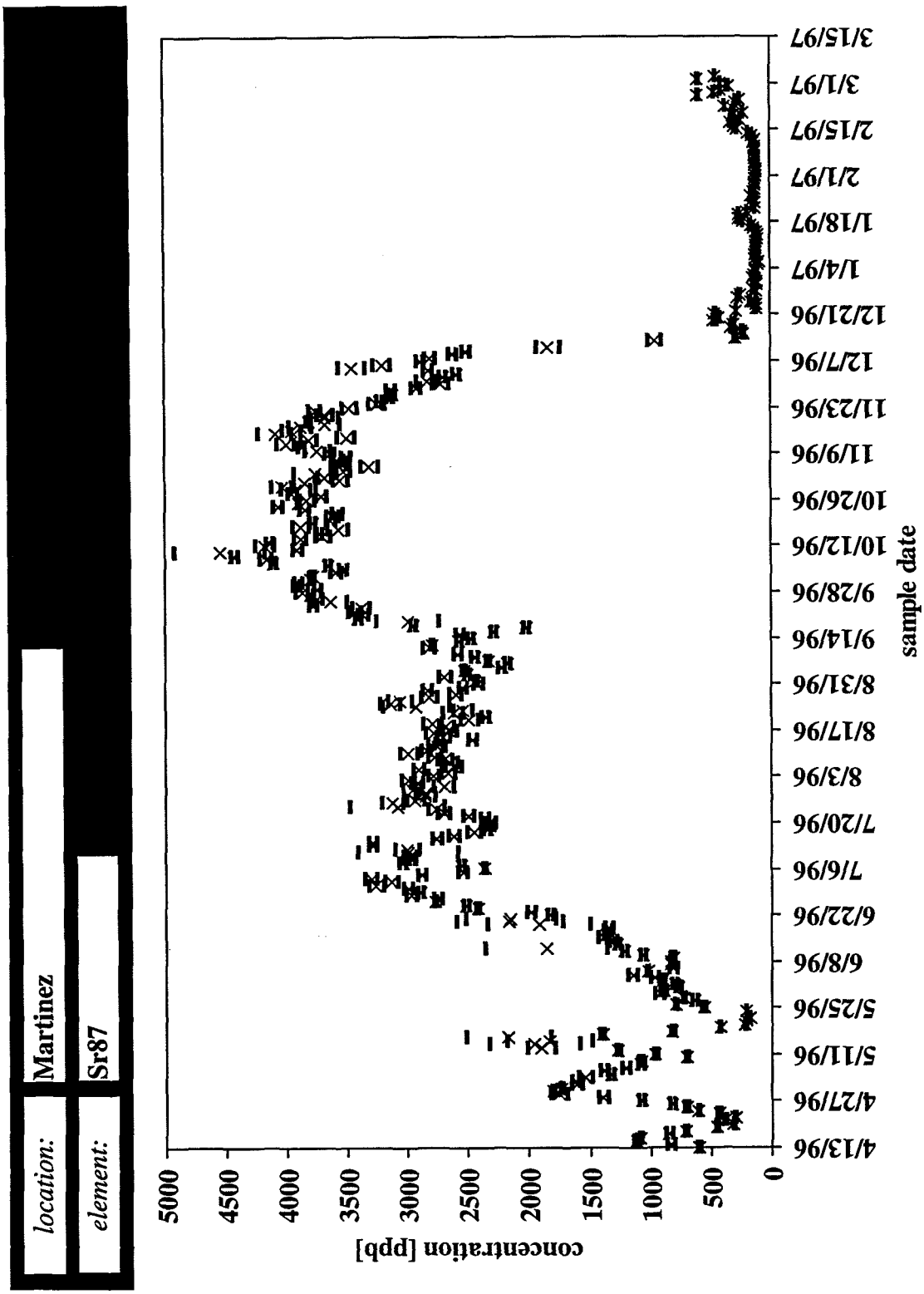
location:
Martinez
element:
Sr87
concentration [ppb]
0
500
1000
1500
2000
2500
3000
3500
4000
4500
5000
sample date
4/13/96
4/27/96
5/11/96
5/25/96
6/8/96
6/22/96
7/6/96
7/20/96
8/3/96
8/17/96
8/31/96
9/14/96
9/28/96
10/12/96
10/26/96
11/9/96
11/23/96
12/7/96
12/21/96
1/4/97
1/18/97
2/1/97
2/15/97
3/1/97
3/15/97

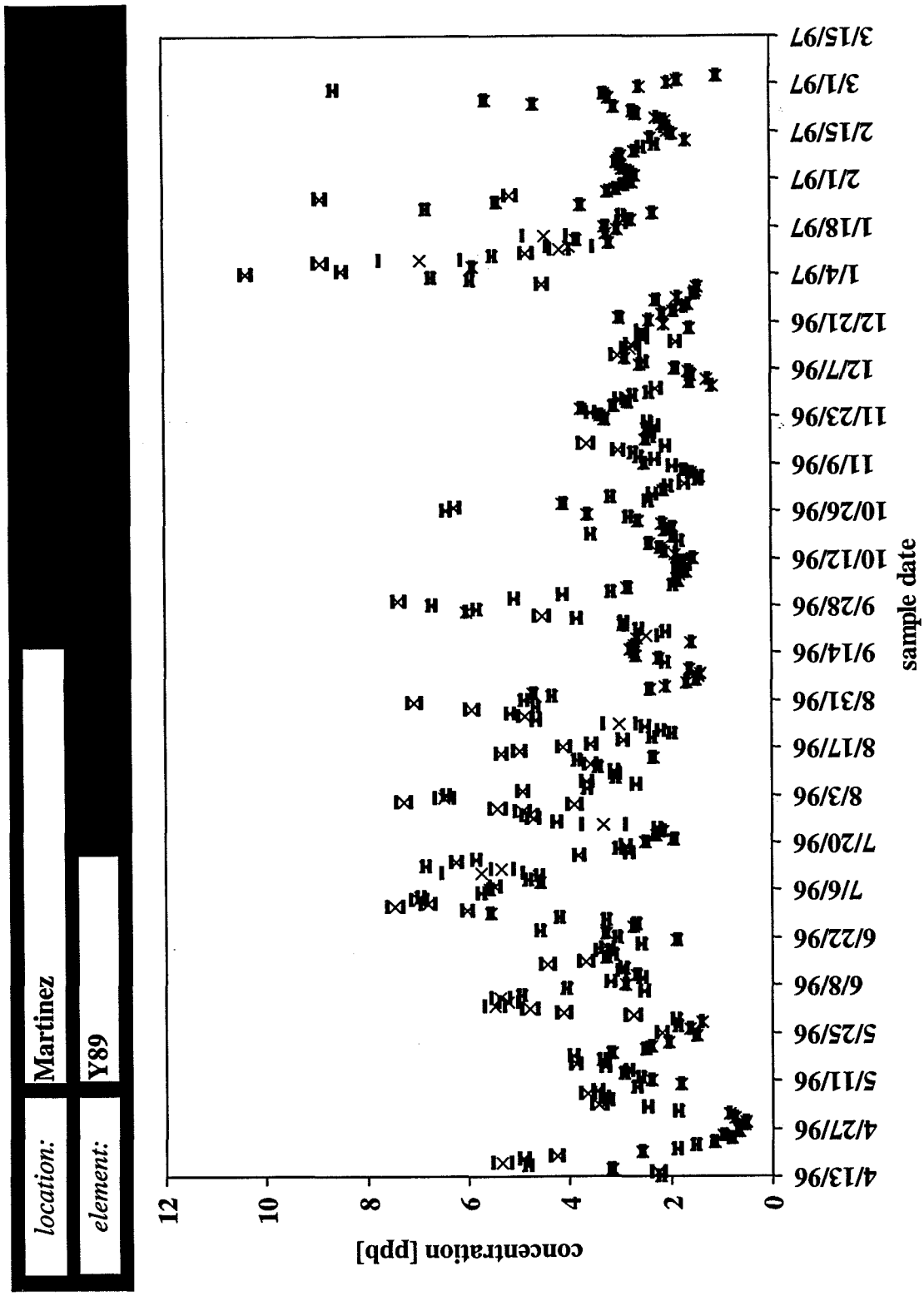
location:
Martinez
element:
Y89
concentration [ppb]
0
2
4
6
8
10
12
sample date
4/13/96
4/27/96
5/11/96
5/25/96
6/8/96
6/22/96
7/6/96
7/20/96
8/3/96
8/17/96
8/31/96
9/14/96
9/28/96
10/12/96
10/26/96
11/9/96
11/23/96
12/7/96
12/21/96
1/4/97
1/18/97
2/1/97
2/15/97
3/1/97
3/15/97

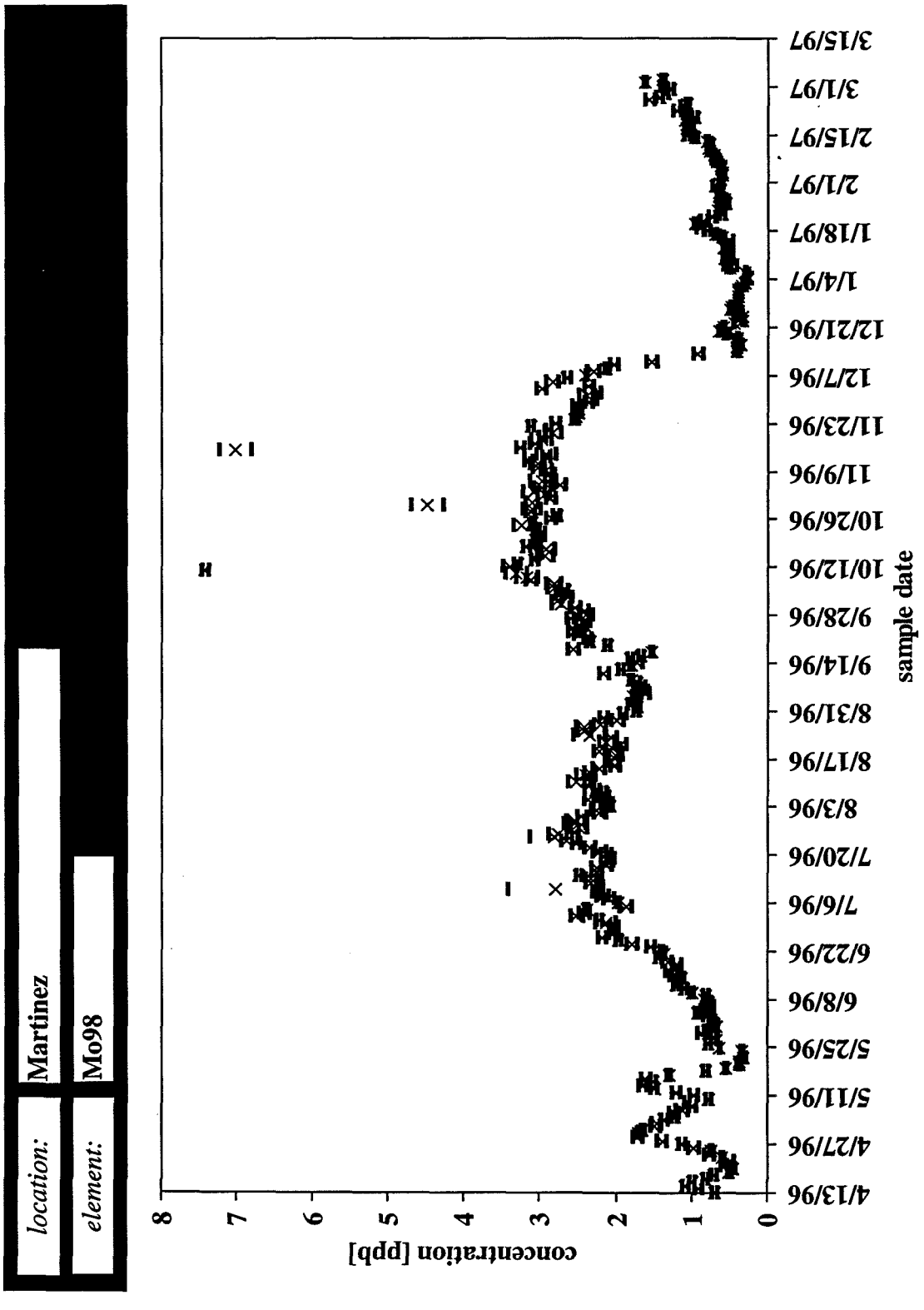
location:
Martinez
element:
Mo98
concentration [ppb]
0
1
2
3
4
5
6
7
8
sample date
4/13/96
4/27/96
5/11/96
5/25/96
6/8/96
6/22/96
7/6/96
7/20/96
8/3/96
8/17/96
8/31/96
9/14/96
9/28/96
10/12/96
10/26/96
11/9/96
11/23/96
12/7/96
12/21/96
1/4/97
1/18/97
2/1/97
2/15/97
3/1/97
3/15/97

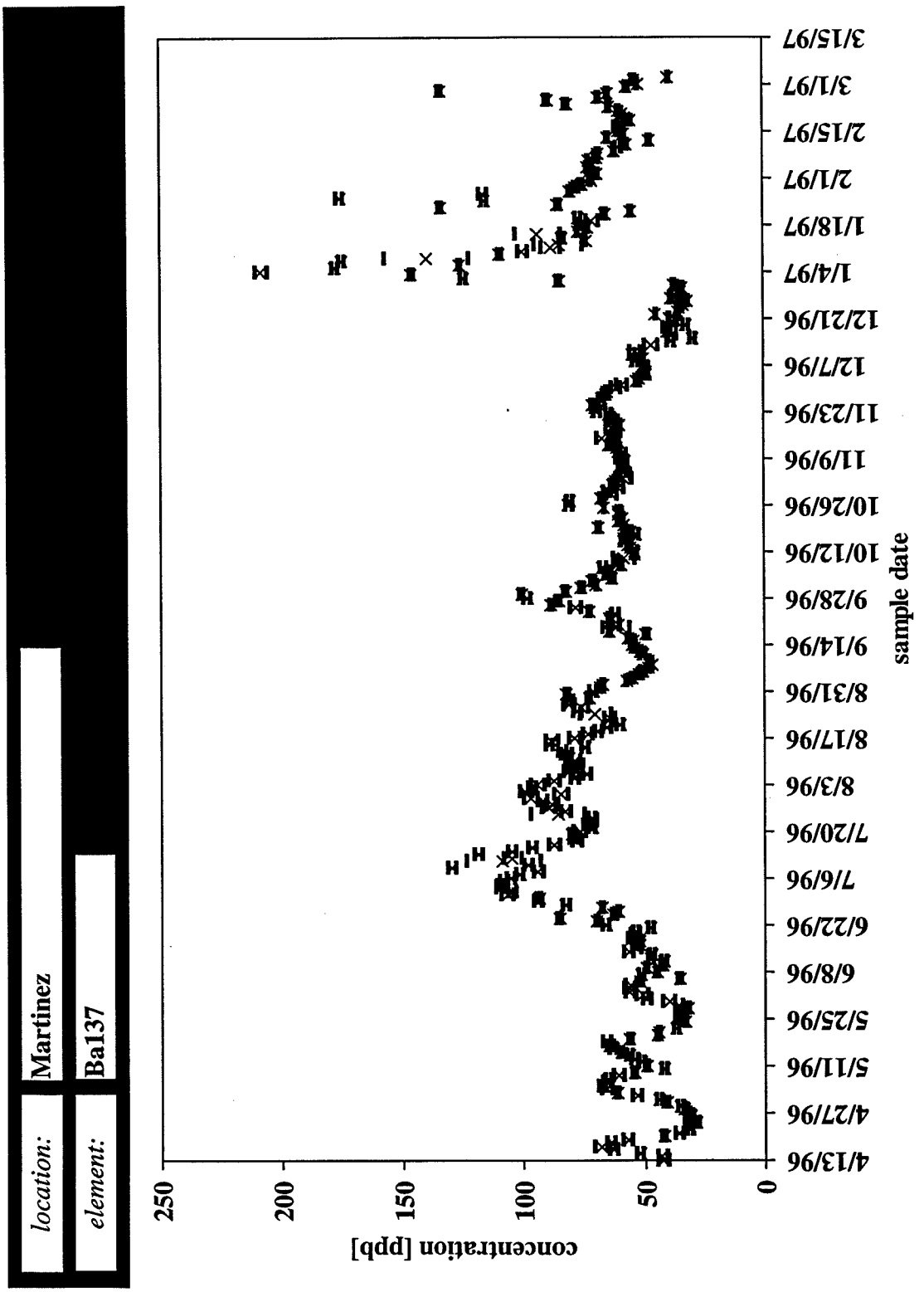
location:
Martinez
element:
Ba137
concentration [ppb]
250
200
150
100
50
0
sample date
4/13/96
4/27/96
5/11/96
5/25/96
6/8/96
6/22/96
7/6/96
7/20/96
8/3/96
8/17/96
8/31/96
9/14/96
9/28/96
10/12/96
10/26/96
11/9/96
11/23/96
12/7/96
12/21/96
1/4/97
1/18/97
2/1/97
2/15/97
3/1/97
3/15/97

location:
Martinez
element:
La139
concentration [ppb]
0
1
2
3
4
5
6
7
8
9
10
sample date
4/13/96
4/27/96
5/11/96
5/25/96
6/8/96
6/22/96
7/6/96
7/20/96
8/3/96
8/17/96
8/31/96
9/14/96
9/28/96
10/12/96
10/26/96
11/9/96
11/23/96
12/7/96
12/21/96
1/4/97
1/18/97
2/1/97
2/15/97
3/1/97
3/15/97

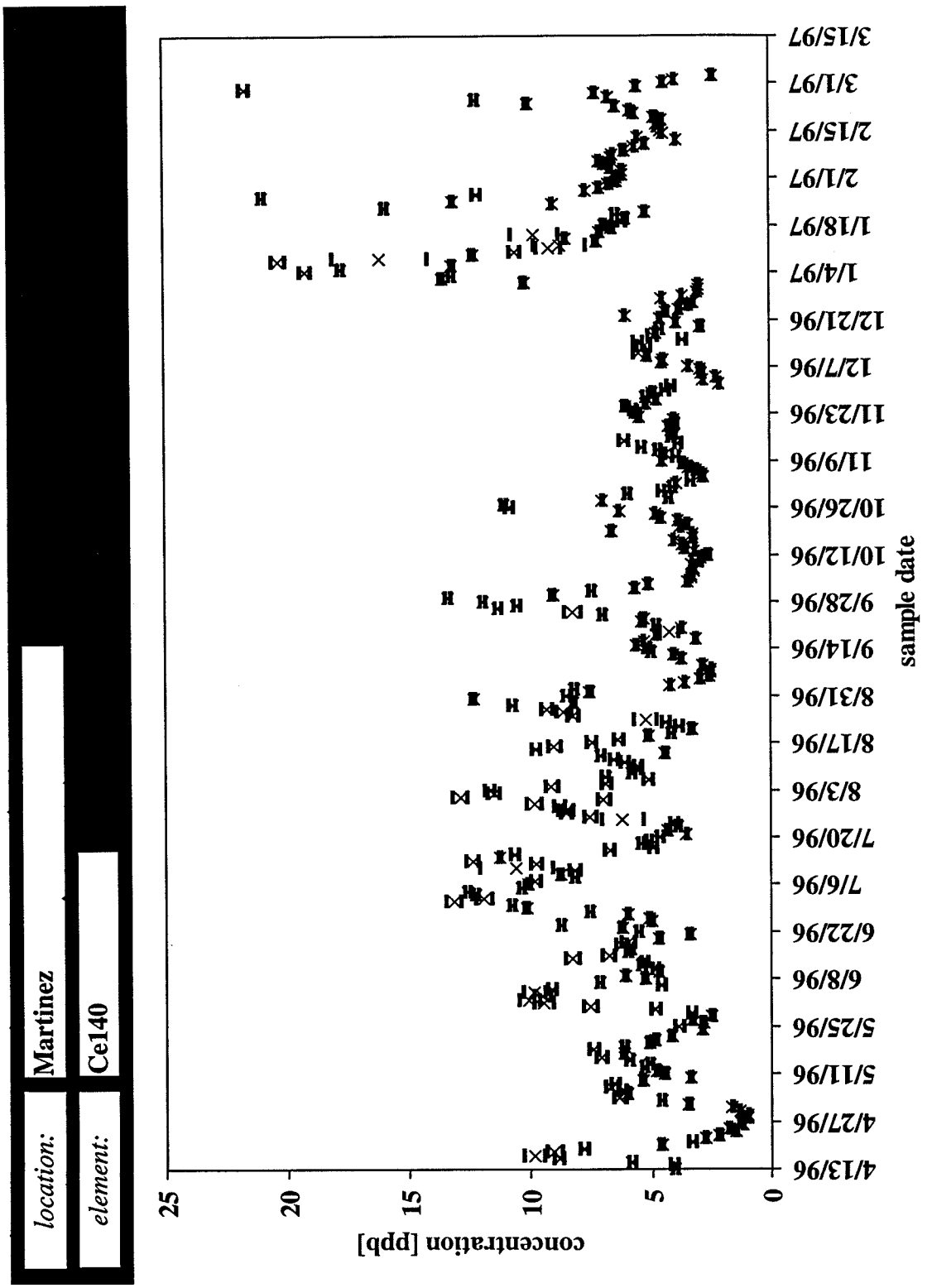
location:
Martinez
element:
Ce140
concentration [ppb]
0
5
10
15
20
25
sample date
4/13/96
4/27/96
5/11/96
5/25/96
6/8/96
6/22/96
7/6/96
7/20/96
8/3/96
8/17/96
8/31/96
9/14/96
9/28/96
10/12/96
10/26/96
11/9/96
11/23/96
12/7/96
12/21/96
1/4/97
1/18/97
2/1/97
2/15/97
3/1/97
3/15/97

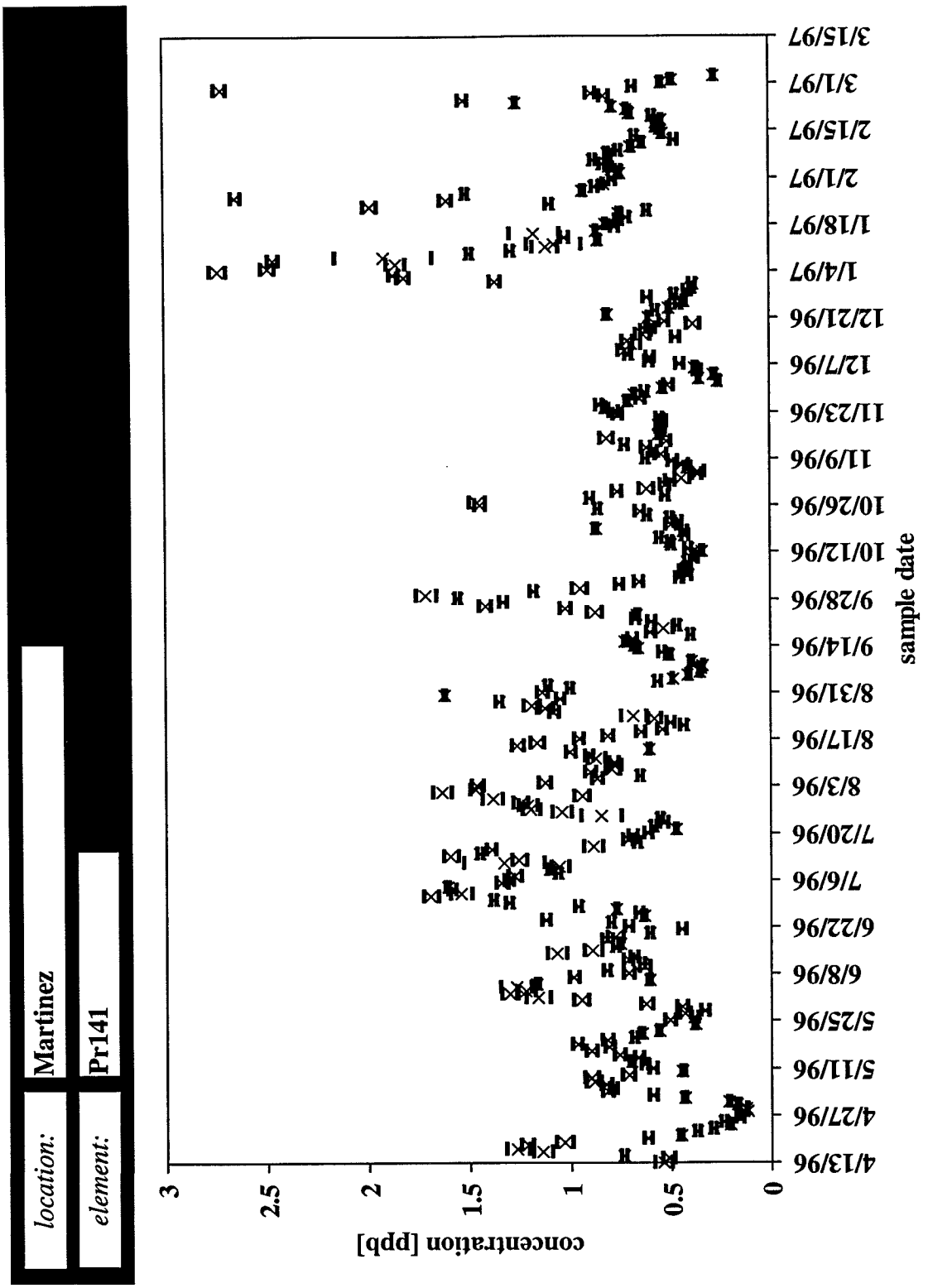
location:
Martinez
element:
Pr141
concentration [ppb]
0
0.5
1
1.5
2
2.5
3
sample date
4/13/96
4/27/96
5/11/96
5/25/96
6/8/96
6/22/96
7/6/96
7/20/96
8/3/96
8/17/96
8/31/96
9/14/96
9/28/96
10/12/96
10/26/96
11/9/96
11/23/96
12/7/96
12/21/96
1/4/97
1/18/97
2/1/97
2/15/97
3/1/97
3/15/97

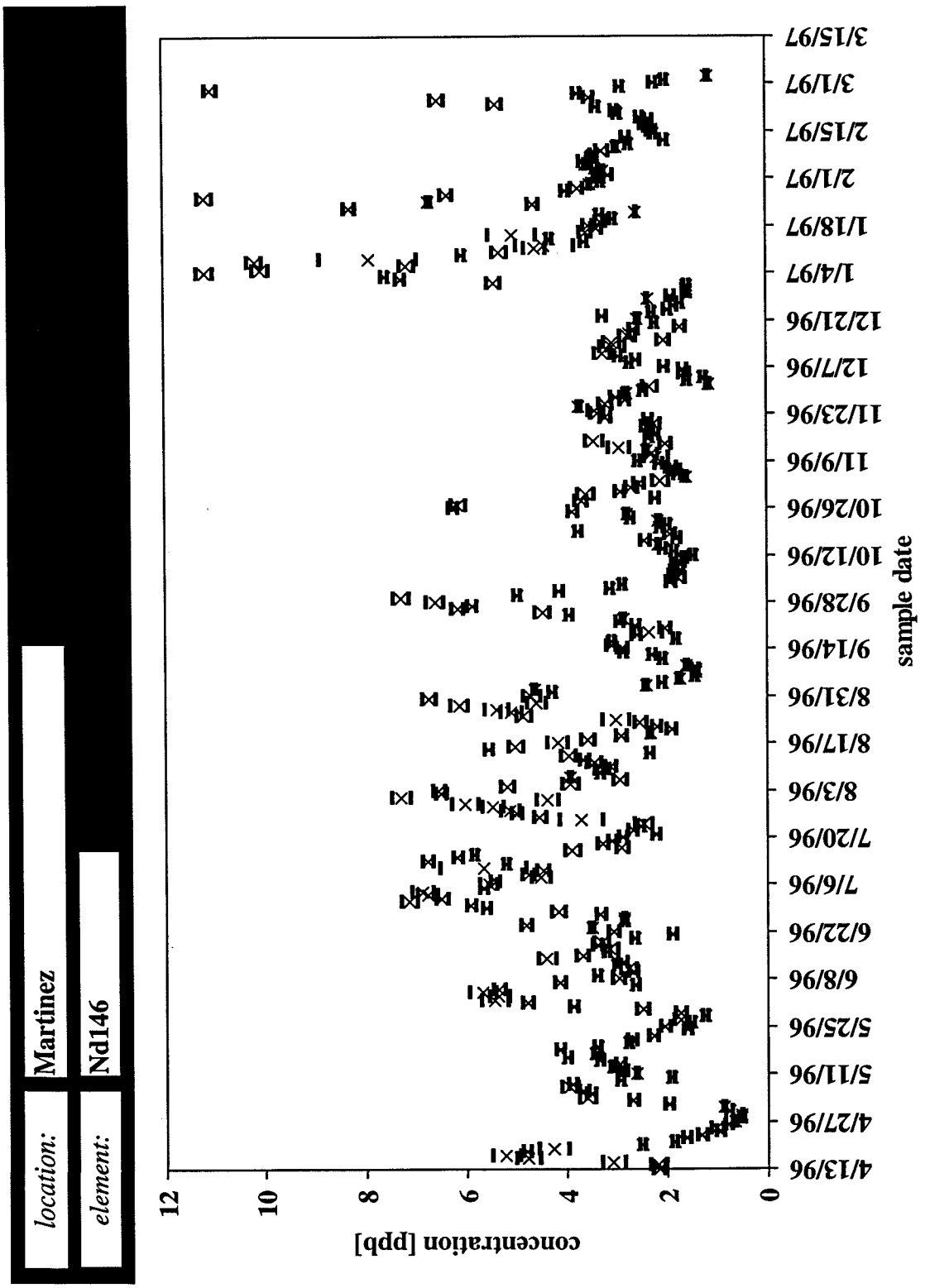
location:
Martinez
element:
Nd146
concentration [ppb]
0
2
4
6
8
10
12
sample date
4/13/96
4/27/96
5/11/96
5/25/96
6/8/96
6/22/96
7/6/96
7/20/96
8/3/96
8/17/96
8/31/96
9/14/96
9/28/96
10/12/96
10/26/96
11/9/96
11/23/96
12/7/96
12/21/96
1/4/97
1/18/97
2/1/97
2/15/97
3/1/97
3/15/97

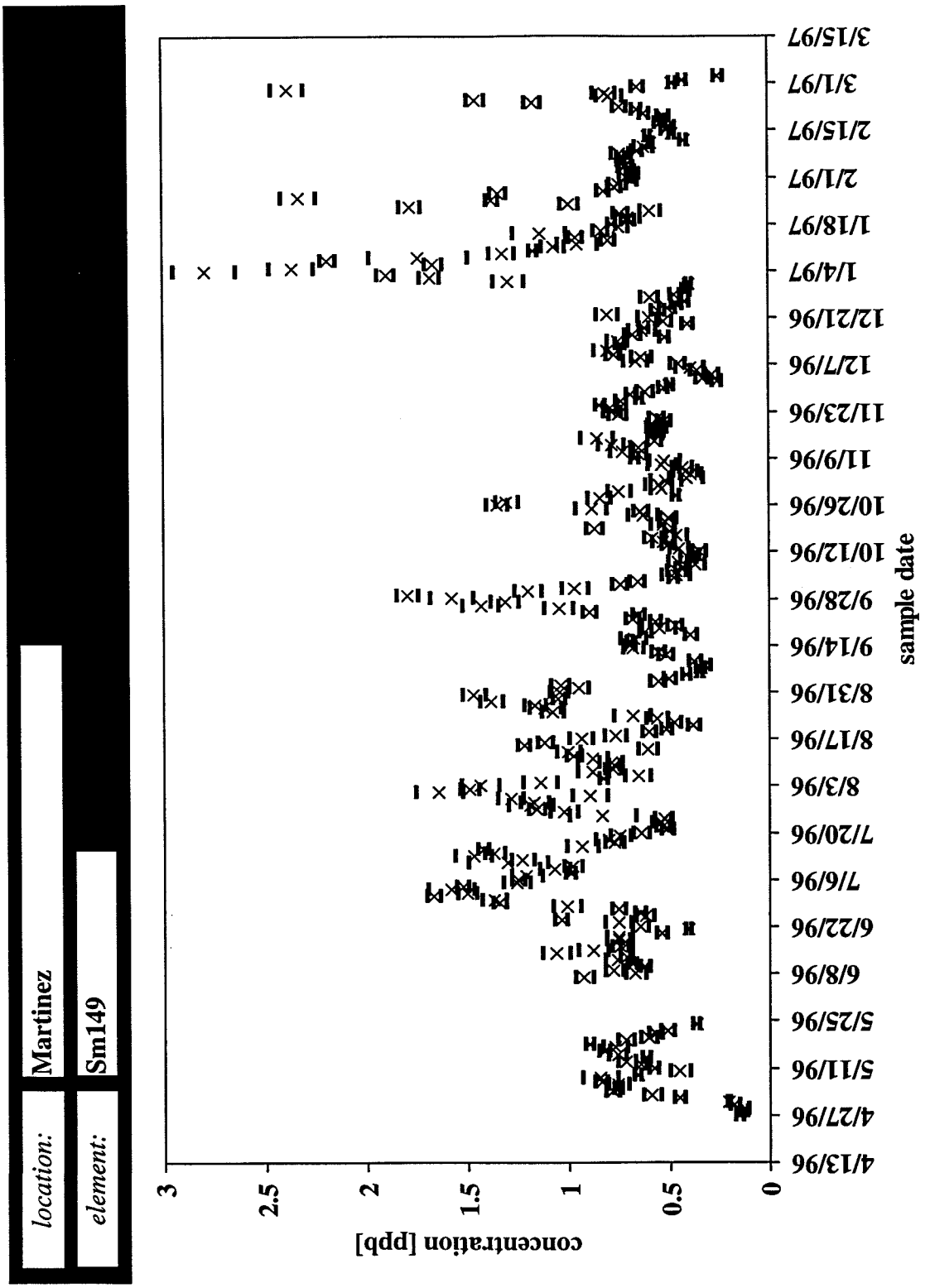
location:
Martinez
element:
Sm149
concentration [ppb]
0
0.5
1
1.5
2
2.5
3
sample date
4/13/96
4/27/96
5/11/96
5/25/96
6/8/96
6/22/96
7/6/96
7/20/96
8/3/96
8/17/96
8/31/96
9/14/96
9/28/96
10/12/96
10/26/96
11/9/96
11/23/96
12/7/96
12/21/96
1/4/97
1/18/97
2/1/97
2/15/97
3/1/97
3/15/97

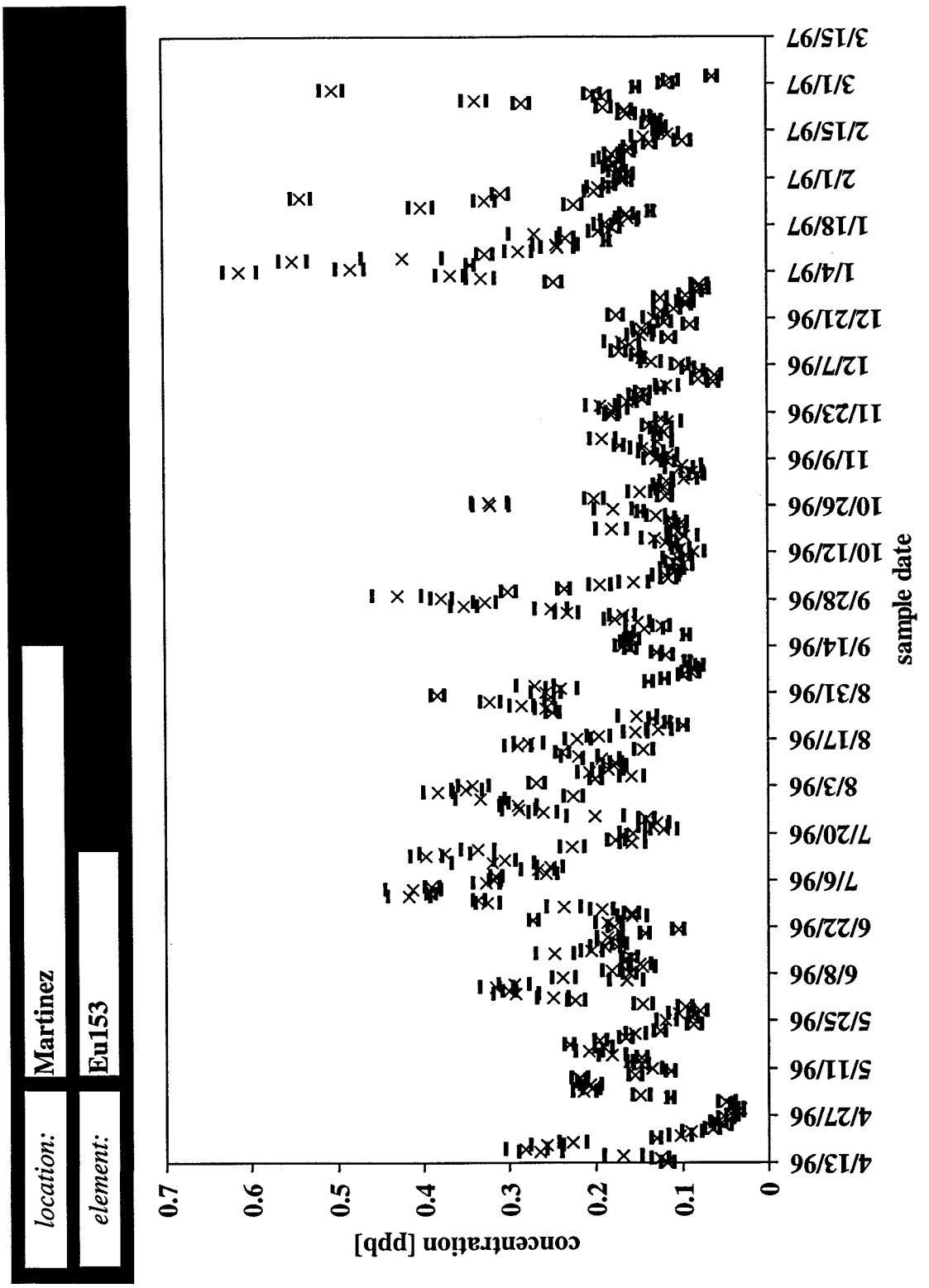
location:
Martinez
element:
Eu153
concentration [ppb]
0.7
0.6
0.5
0.4
0.3
0.2
0.1
0
sample date
4/13/96
4/27/96
5/11/96
5/25/96
6/8/96
6/22/96
7/6/96
7/20/96
8/3/96
8/17/96
8/31/96
9/14/96
9/28/96
10/12/96
10/26/96
11/9/96
11/23/96
12/7/96
12/21/96
1/4/97
1/18/97
2/1/97
2/15/97
3/1/97
3/15/97

location:
Martinez
element:
Gd157
concentration [ppb]
3
2.5
2
1.5
1
0.5
0
sample date
4/13/96
4/27/96
5/11/96
5/25/96
6/8/96
6/22/96
7/6/96
7/20/96
8/3/96
8/17/96
8/31/96
9/14/96
9/28/96
10/12/96
10/26/96
11/9/96
11/23/96
12/7/96
12/21/96
1/4/97
1/18/97
2/1/97
2/15/97
3/1/97
3/15/97

location:
Martinez
element:
Tb159
concentration [ppb]
0.4
0.35
0.3
0.25
0.2
0.15
0.1
0.05
0
sample date
4/13/96
4/27/96
5/11/96
5/25/96
6/8/96
6/22/96
7/6/96
7/20/96
8/3/96
8/17/96
8/31/96
9/14/96
9/28/96
10/12/96
10/26/96
11/9/96
11/23/96
12/7/96
12/21/96
1/4/97
1/18/97
2/1/97
2/15/97
3/1/97
3/15/97

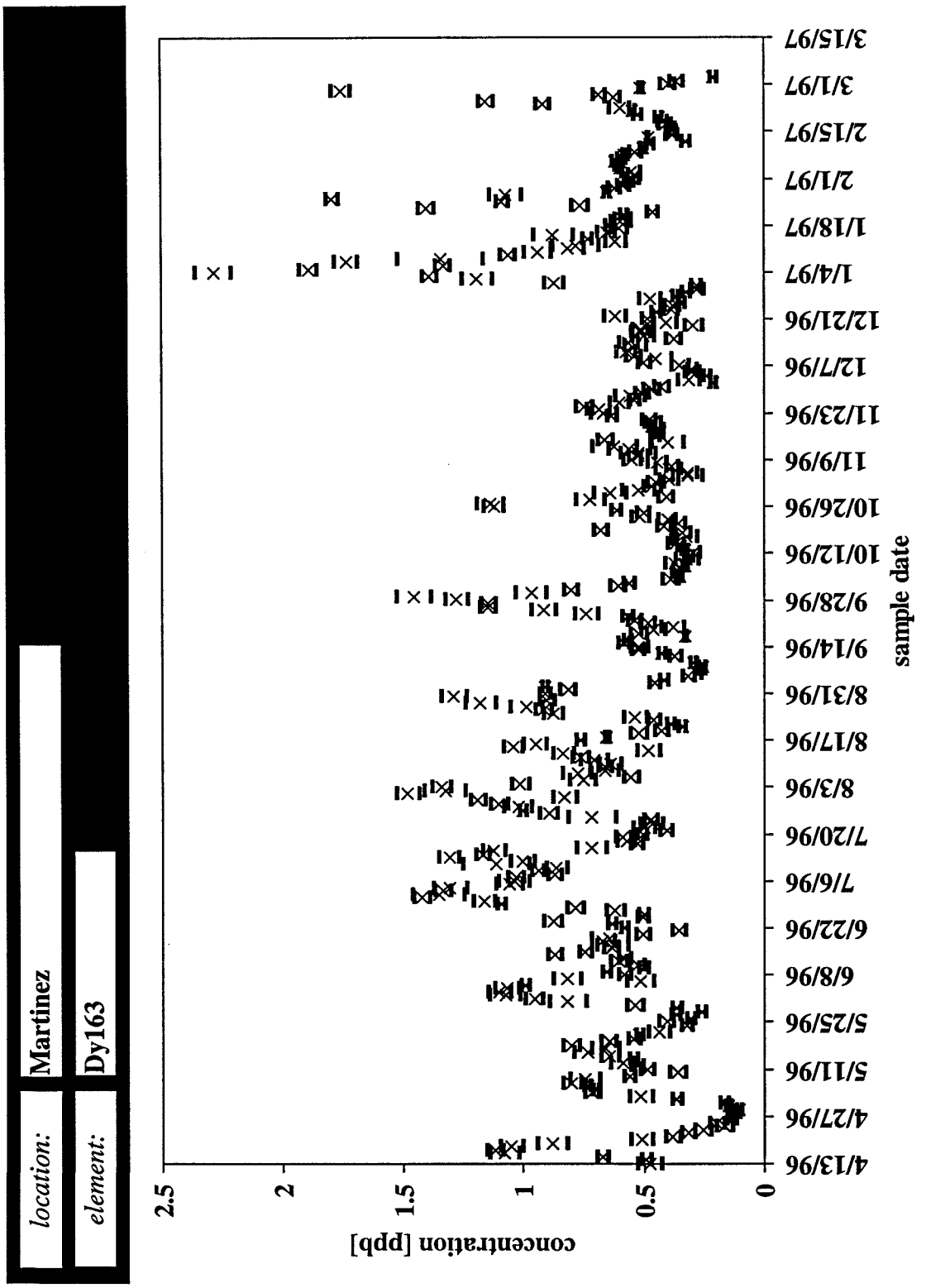
location:
Martinez
element:
Dy163
concentration [ppb]
2.5
2
1.5
1
0.5
0
sample date
4/13/96
4/27/96
5/11/96
5/25/96
6/8/96
6/22/96
7/6/96
7/20/96
8/3/96
8/17/96
8/31/96
9/14/96
9/28/96
10/12/96
10/26/96
11/9/96
11/23/96
12/7/96
12/21/96
1/4/97
1/18/97
2/1/97
2/15/97
3/1/97
3/15/97

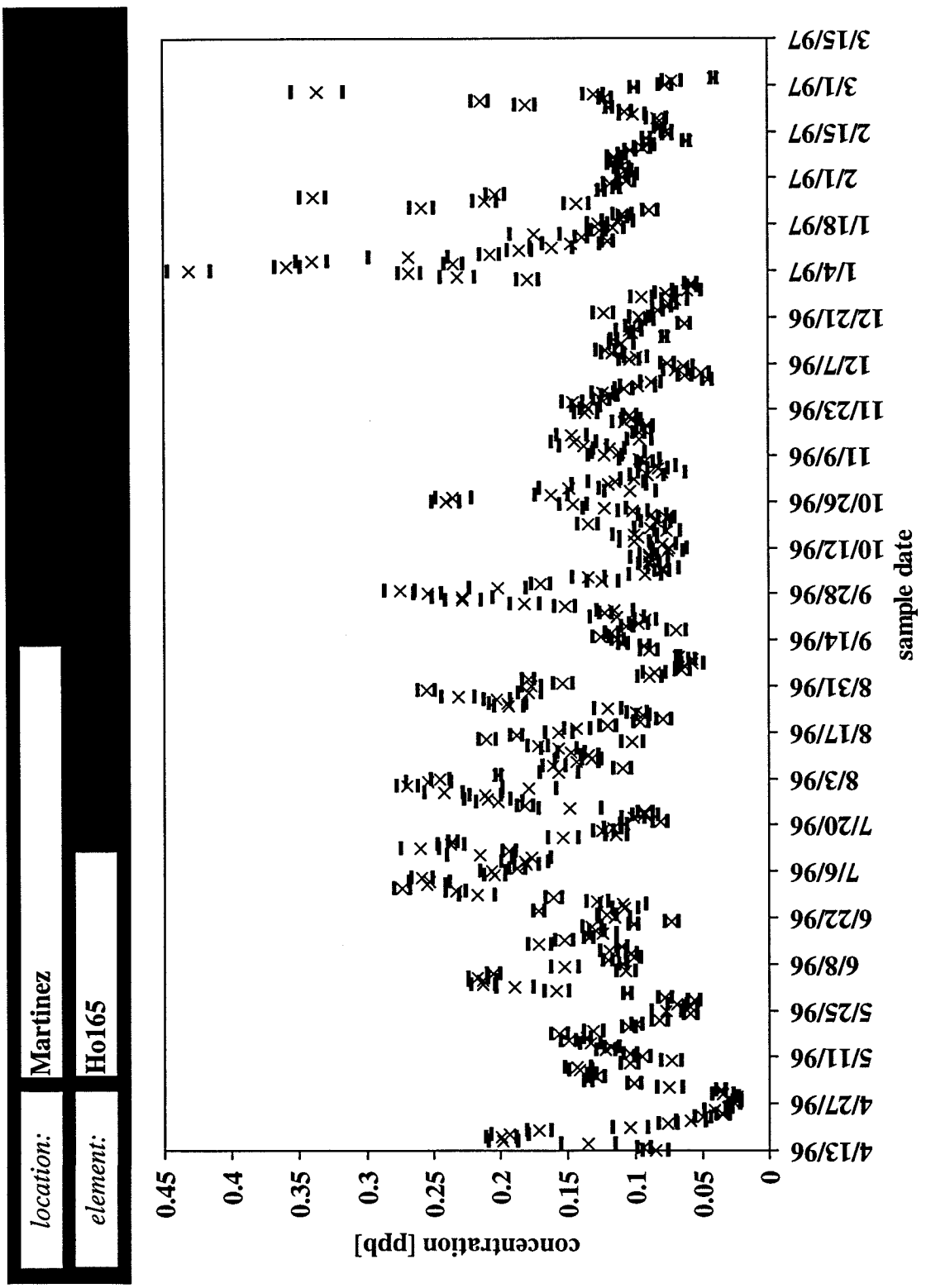
location:
Martinez
element:
Ho165
concentration [ppb]
0.45
0.4
0.35
0.3
0.25
0.2
0.15
0.1
0.05
0
sample date
4/13/96
4/27/96
5/11/96
5/25/96
6/8/96
6/22/96
7/6/96
7/20/96
8/3/96
8/17/96
8/31/96
9/14/96
9/28/96
10/12/96
10/26/96
11/9/96
11/23/96
12/7/96
12/21/96
1/4/97
1/18/97
2/1/97
2/15/97
3/1/97
3/15/97

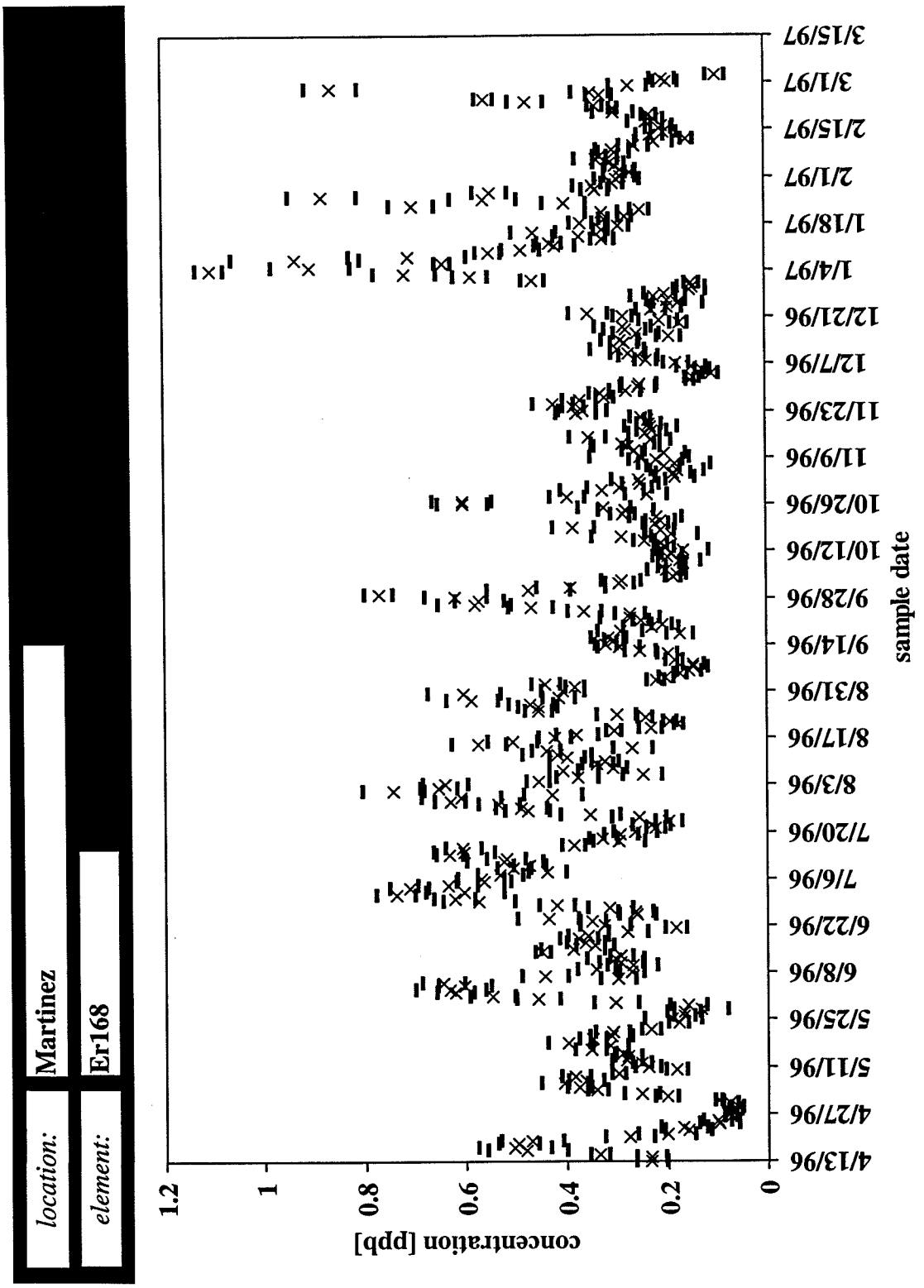
location:
Martinez
element:
Er168
concentration [ppb]
1.2
1
0.8
0.6
0.4
0.2
0
sample date
4/13/96
4/27/96
5/11/96
5/25/96
6/8/96
6/22/96
7/6/96
7/20/96
8/3/96
8/17/96
8/31/96
9/14/96
9/28/96
10/12/96
10/26/96
11/9/96
11/23/96
12/7/96
12/21/96
1/4/97
1/18/97
2/1/97
2/15/97
3/1/97
3/15/97

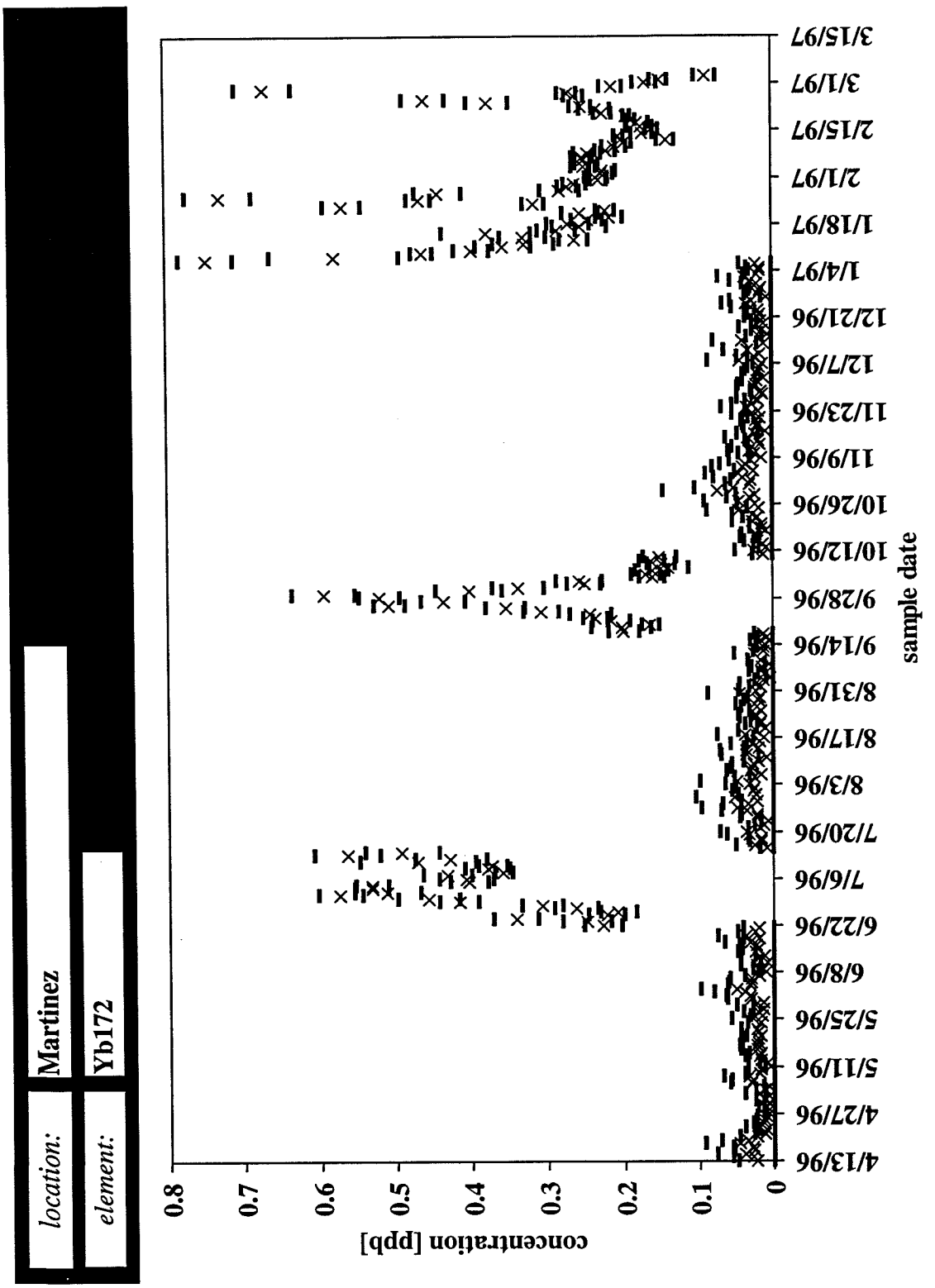
location:
Martinez
element:
Yb172
concentration [ppb]
0.8
0.7
0.6
0.5
0.4
0.3
0.2
0.1
0
sample date
4/13/96
4/27/96
5/11/96
5/25/96
6/8/96
6/22/96
7/6/96
7/20/96
8/3/96
8/17/96
8/31/96
9/14/96
9/28/96
10/12/96
10/26/96
11/9/96
11/23/96
12/7/96
12/21/96
1/4/97
1/18/97
2/1/97
2/15/97
3/1/97
3/15/97

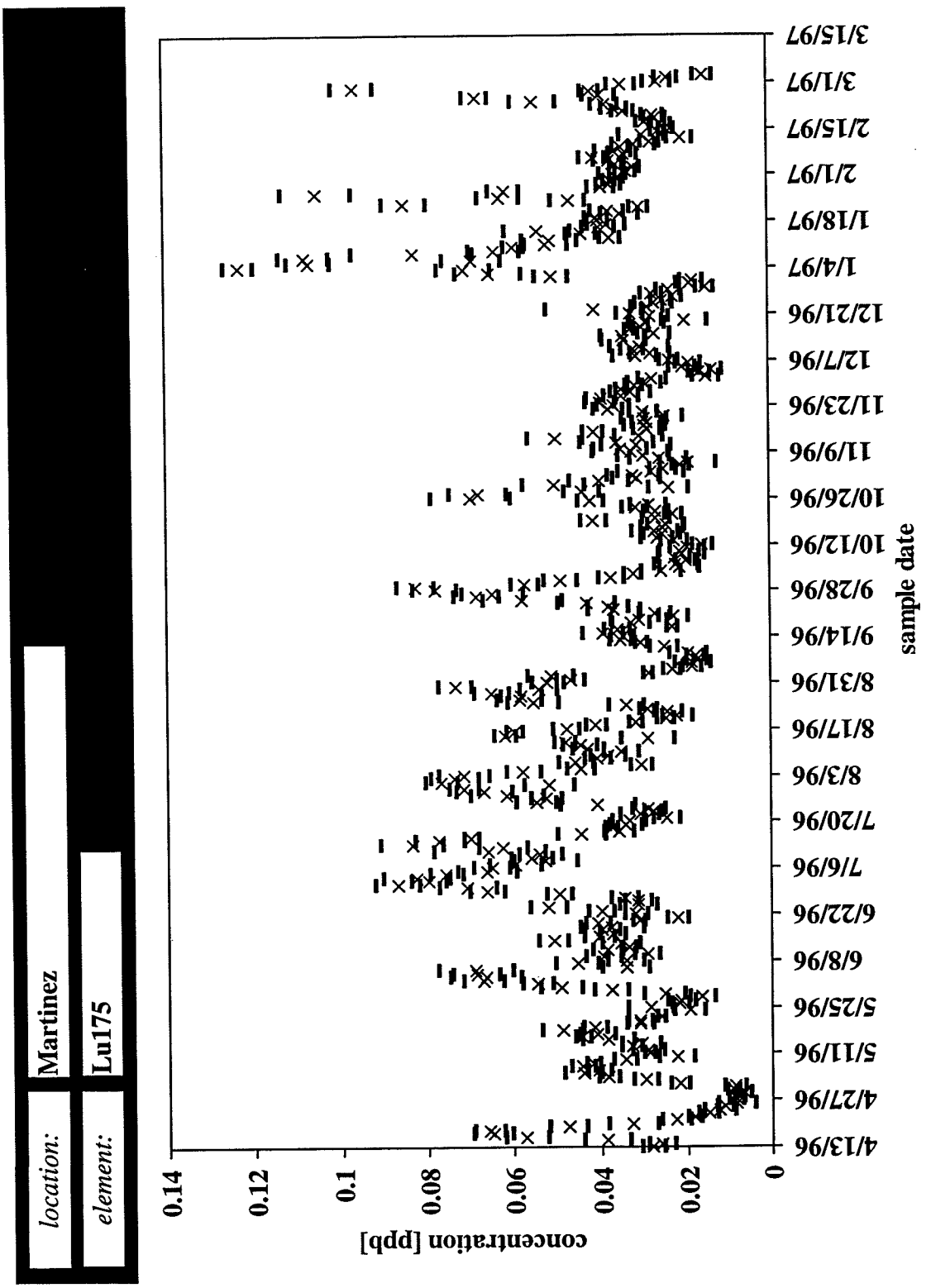
location:
Martinez
element:
Lu175
concentration [ppb]
0.14
0.12
0.1
0.08
0.06
0.04
0.02
0
sample date
4/13/96
4/27/96
5/11/96
5/25/96
6/8/96
6/22/96
7/6/96
7/20/96
8/3/96
8/17/96
8/31/96
9/14/96
9/28/96
10/12/96
10/26/96
11/9/96
11/23/96
12/7/96
12/21/96
1/4/97
1/18/97
2/1/97
2/15/97
3/1/97
3/15/97

location:
Martinez
element:
Th232
concentration [ppb]
2.5
2
1.5
1
0.5
0
sample date
4/13/96
4/27/96
5/11/96
5/25/96
6/8/96
6/22/96
7/6/96
7/20/96
8/3/96
8/17/96
8/31/96
9/14/96
9/28/96
10/12/96
10/26/96
11/9/96
11/23/96
12/7/96
12/21/96
1/4/97
1/18/97
2/1/97
2/15/97
3/1/97
3/15/97

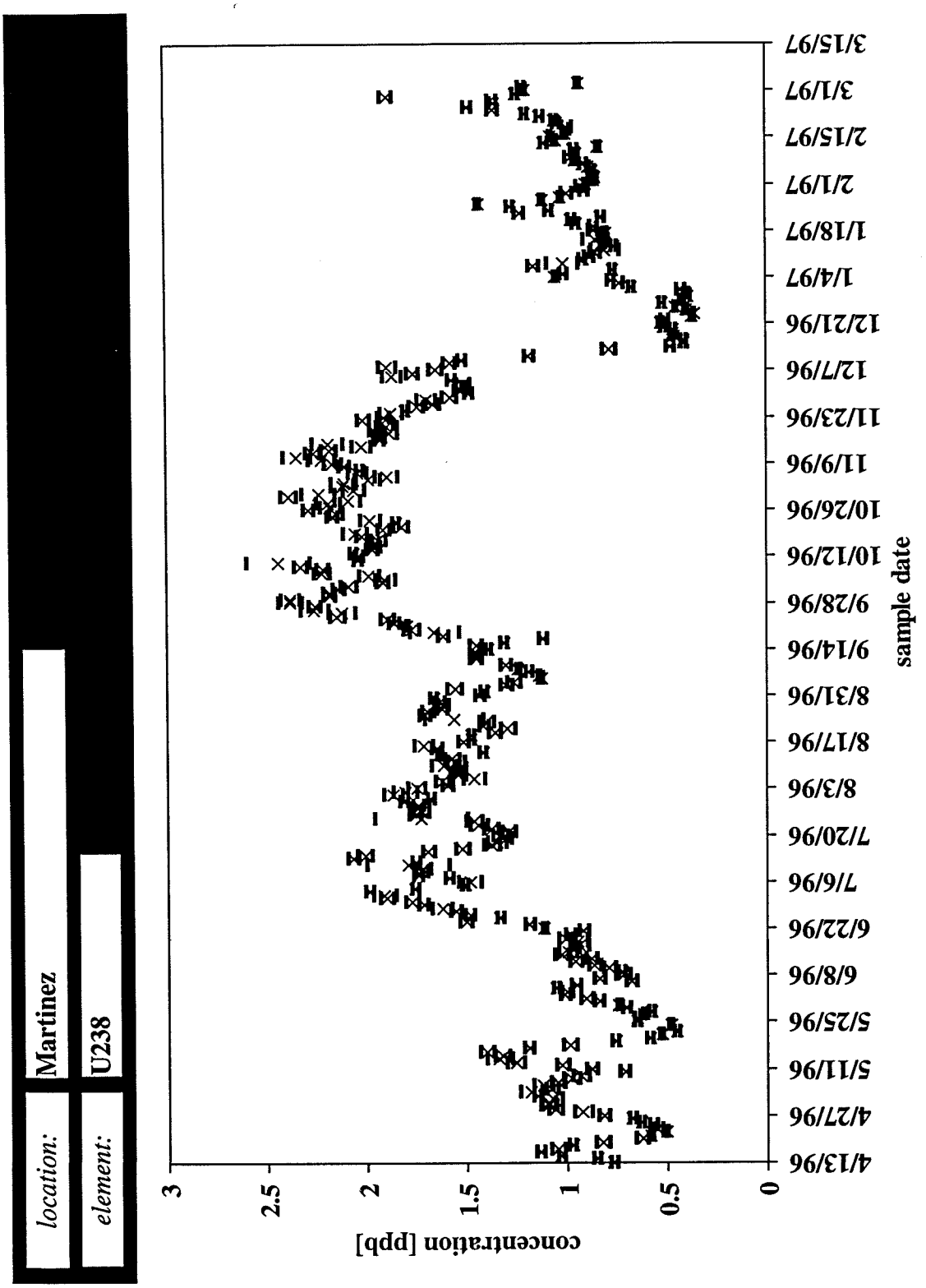
location:
Martinez
element:
U238
concentration [ppb]
0
0.5
1
1.5
2
2.5
3
sample date
4/13/96
4/27/96
5/11/96
5/25/96
6/8/96
6/22/96
7/6/96
7/20/96
8/3/96
8/17/96
8/31/96
9/14/96
9/28/96
10/12/96
10/26/96
11/9/96
11/23/96
12/7/96
12/21/96
1/4/97
1/18/97
2/1/97
2/15/97
3/1/97
3/15/97

location:
Bethel Island
element:
Li7
concentration [ppb]
0
2
4
6
8
10
12
14
sample date
3/2/96
3/16/96
3/30/96
4/13/96
4/27/96
5/11/96
5/25/96
6/8/96
6/22/96
7/6/96
7/20/96
8/3/96
8/17/96
8/31/96
9/14/96
9/28/96
10/12/96
10/26/96
11/9/96
11/23/96
12/7/96
12/21/96
1/4/97
1/18/97
2/1/97
2/15/97
3/1/97
3/15/97

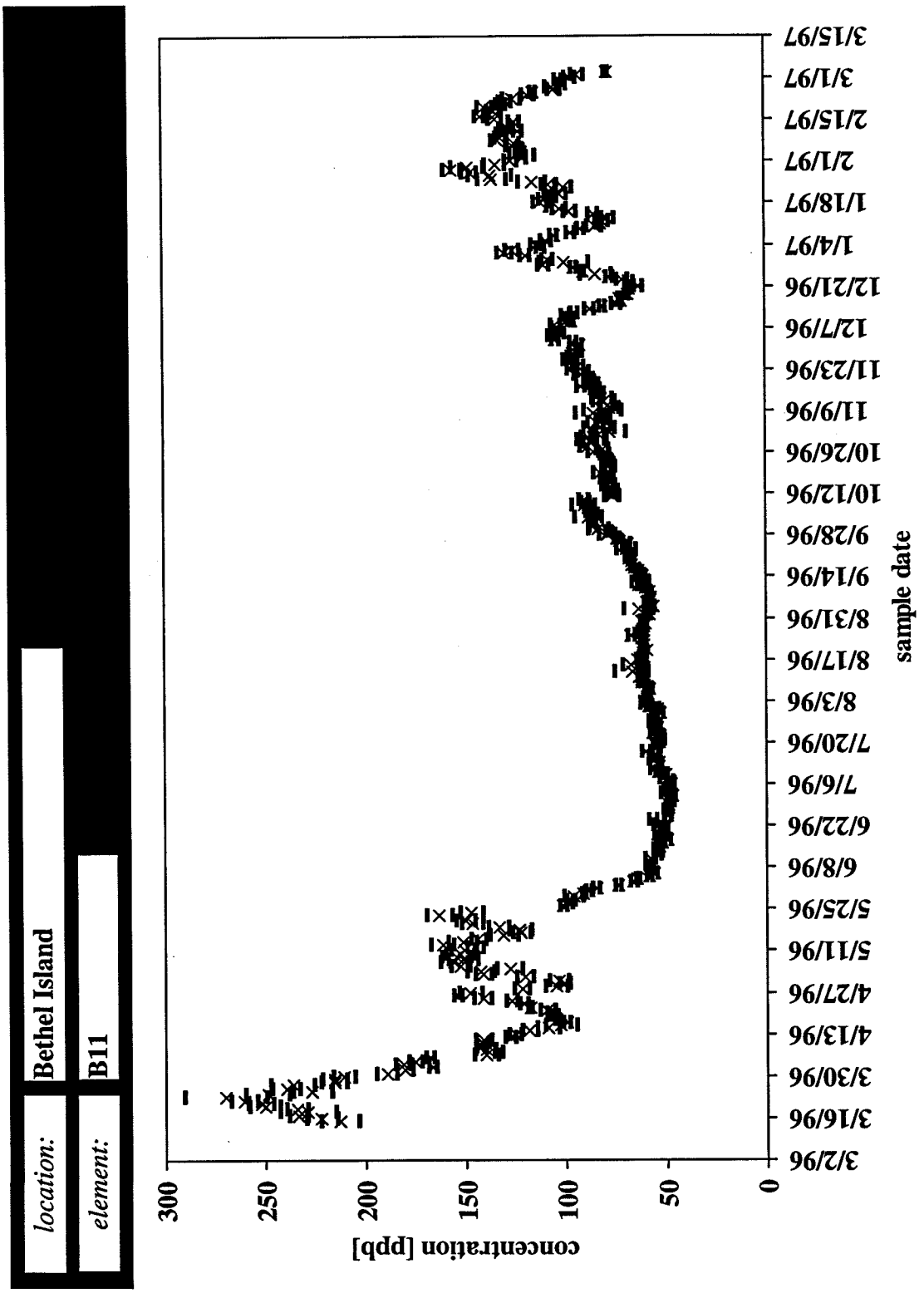
location:
Bethel Island
element:
B11
concentration [ppb]
300
250
200
150
100
50
0
sample date
3/2/96
3/16/96
3/30/96
4/13/96
4/27/96
5/11/96
5/25/96
6/8/96
6/22/96
7/6/96
7/20/96
8/3/96
8/17/96
8/31/96
9/14/96
9/28/96
10/12/96
10/26/96
11/9/96
11/23/96
12/7/96
12/21/96
1/4/97
1/18/97
2/1/97
2/15/97
3/1/97
3/15/97

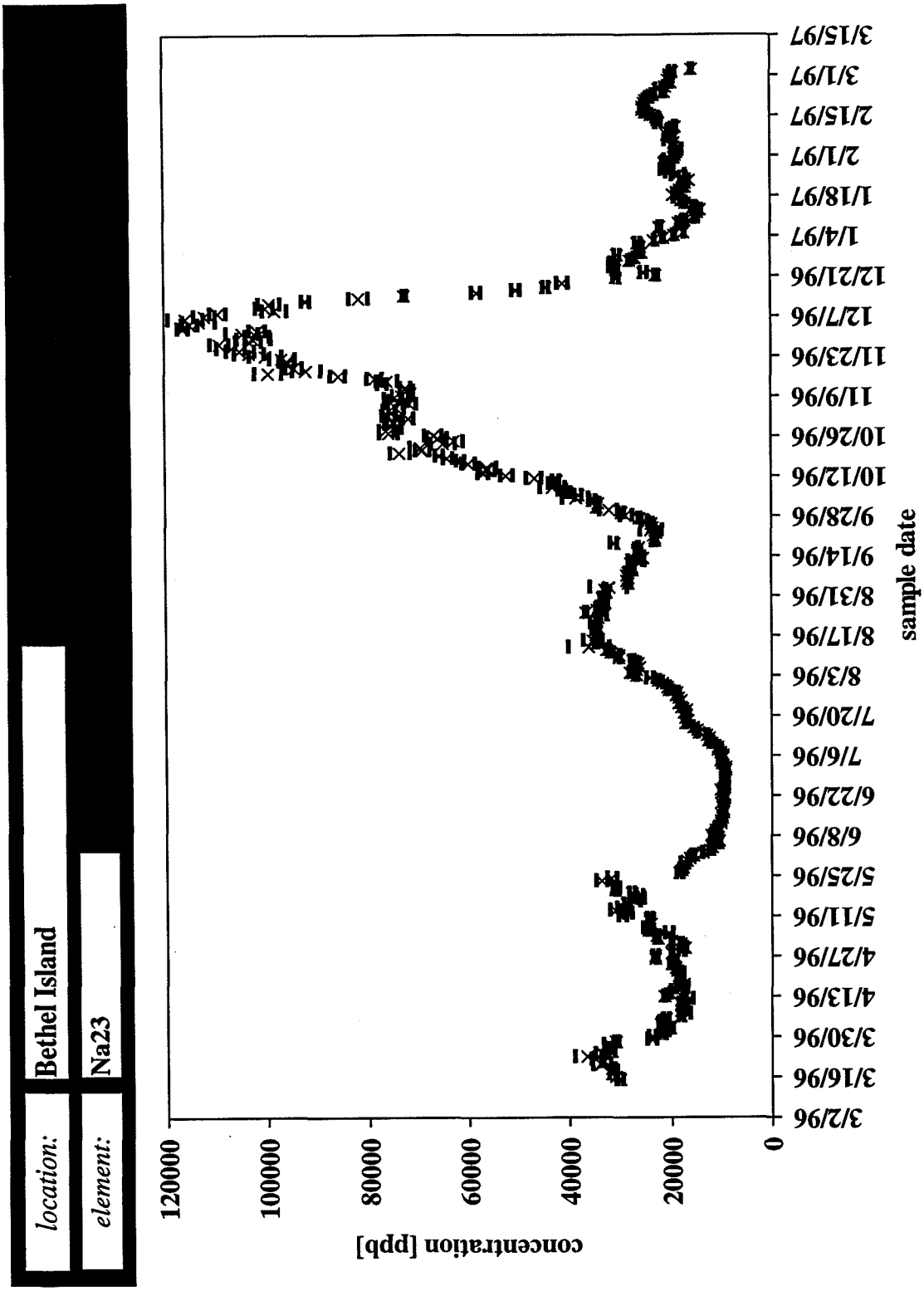
location:
Bethel Island
element:
Na23
concentration [ppb]
120000
100000
80000
60000
40000
20000
0
sample date
3/2/96
3/16/96
3/30/96
4/13/96
4/27/96
5/11/96
5/25/96
6/8/96
6/22/96
7/6/96
7/20/96
8/3/96
8/17/96
8/31/96
9/14/96
9/28/96
10/12/96
10/26/96
11/9/96
11/23/96
12/7/96
12/21/96
1/4/97
1/18/97
2/1/97
2/15/97
3/1/97
3/15/97

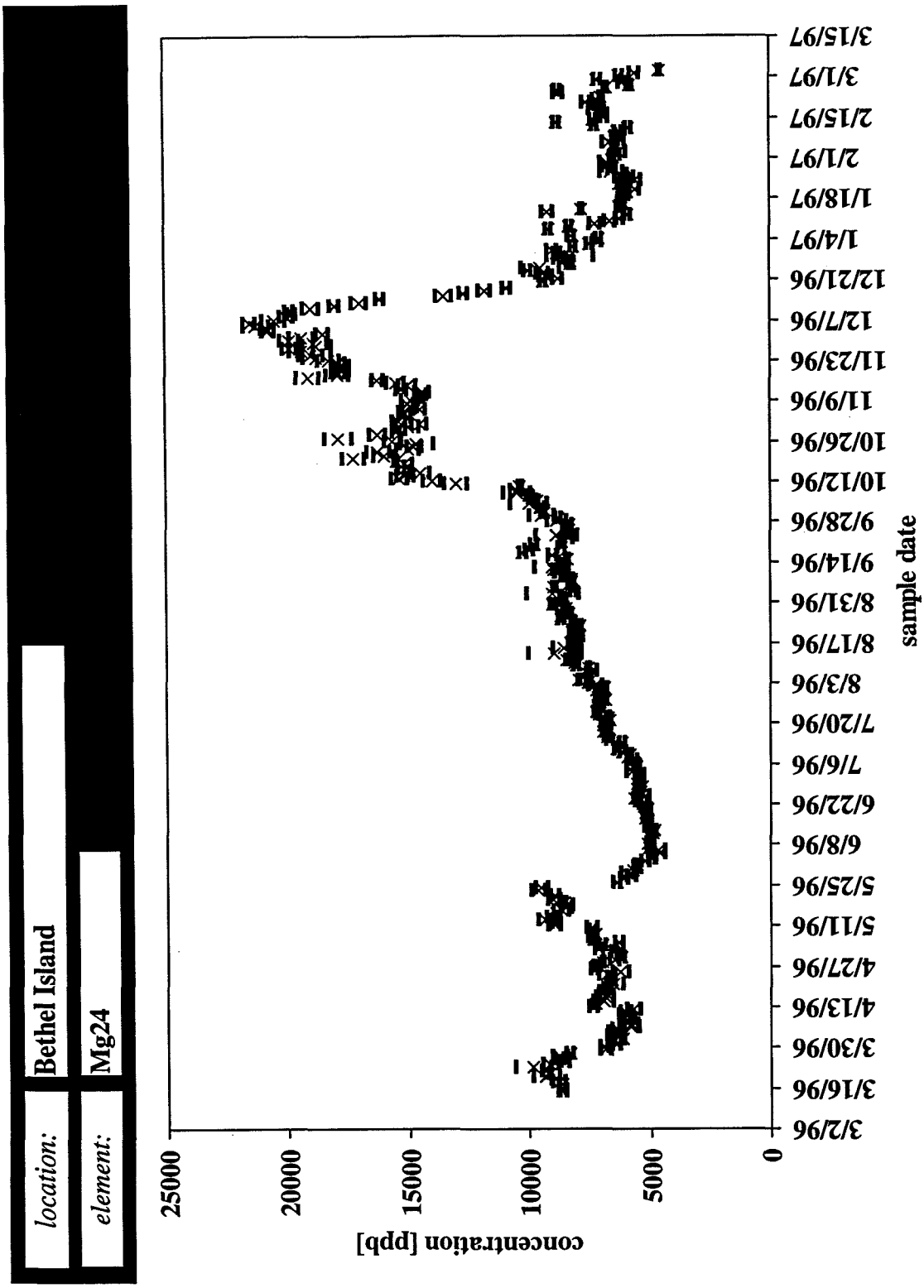
location:
Bethel Island
element:
Mg24
concentration [ppb]
25000
20000
15000
10000
5000
0
sample date
3/2/96
3/16/96
3/30/96
4/13/96
4/27/96
5/11/96
5/25/96
6/8/96
6/22/96
7/6/96
7/20/96
8/3/96
8/17/96
8/31/96
9/14/96
9/28/96
10/12/96
10/26/96
11/9/96
11/23/96
12/7/96
12/21/96
1/4/97
1/18/97
2/1/97
2/15/97
3/1/97
3/15/97

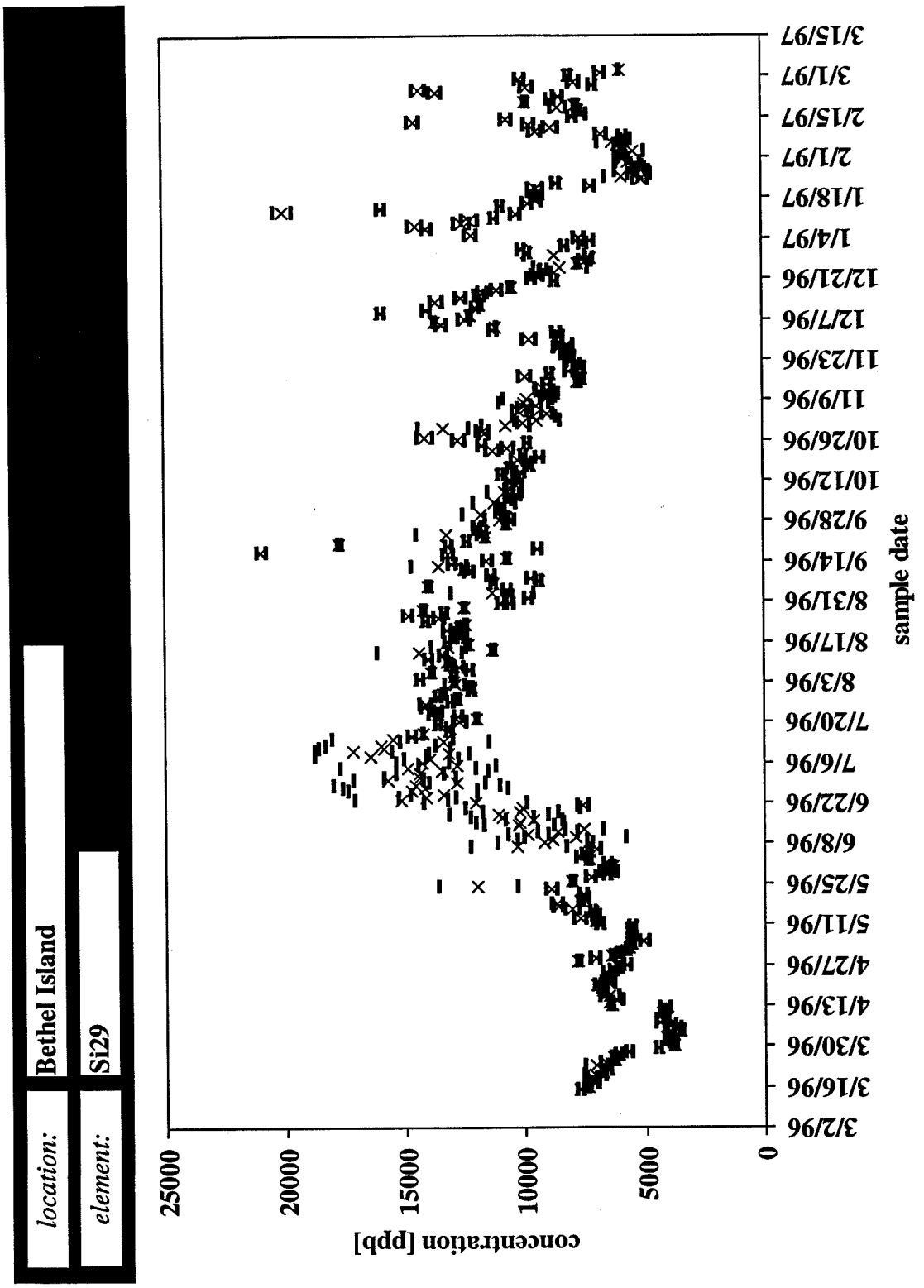
location:
Bethel Island
element:
Si29
concentration [ppb]
25000
20000
15000
10000
5000
0
sample date
3/2/96
3/16/96
3/30/96
4/13/96
4/27/96
5/11/96
5/25/96
6/8/96
6/22/96
7/6/96
7/20/96
8/3/96
8/17/96
8/31/96
9/14/96
9/28/96
10/12/96
10/26/96
11/9/96
11/23/96
12/7/96
12/21/96
1/4/97
1/18/97
2/1/97
2/15/97
3/1/97
3/15/97

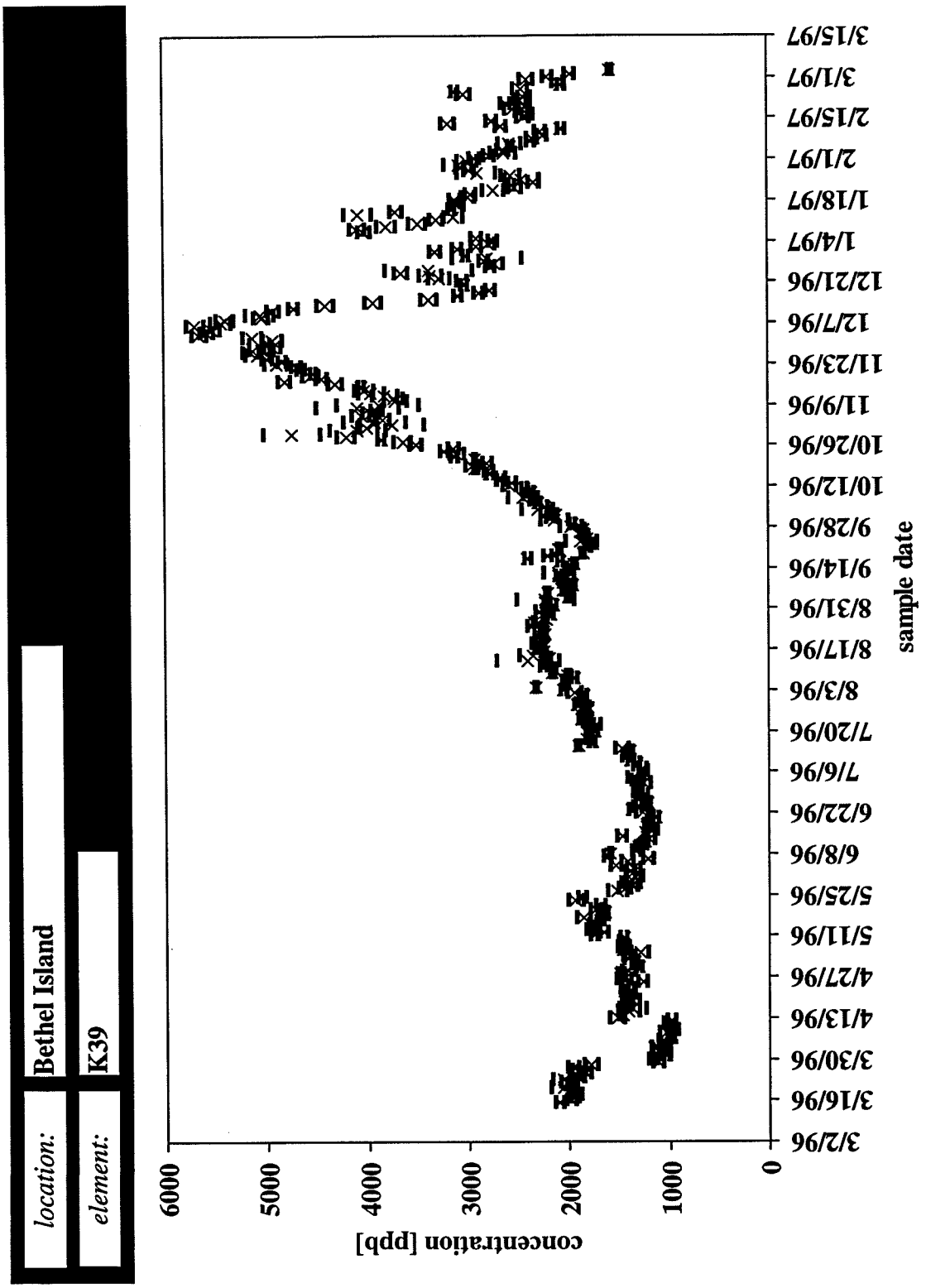
location:
Bethel Island
element:
K39
concentration [ppb]
6000
5000
4000
3000
2000
1000
0
sample date
3/2/96
3/16/96
3/30/96
4/13/96
4/27/96
5/11/96
5/25/96
6/8/96
6/22/96
7/6/96
7/20/96
8/3/96
8/17/96
8/31/96
9/14/96
9/28/96
10/12/96
10/26/96
11/9/96
11/23/96
12/7/96
12/21/96
1/4/97
1/18/97
2/1/97
2/15/97
3/1/97
3/15/97

location:
Bethel Island
element:
Ca43
concentration [ppb]
12000
10000
8000
6000
4000
2000
0
sample date
3/2/96
3/16/96
3/30/96
4/13/96
4/27/96
5/11/96
5/25/96
6/8/96
6/22/96
7/6/96
7/20/96
8/3/96
8/17/96
8/31/96
9/14/96
9/28/96
10/12/96
10/26/96
11/9/96
11/23/96
12/7/96
12/21/96
1/4/97
1/18/97
2/1/97
2/15/97
3/1/97
3/15/97

location:
Bethel Island
element:
V51
concentration [ppb]
0
5
10
15
20
25
30
35
sample date
3/2/96
3/16/96
3/30/96
4/13/96
4/27/96
5/11/96
5/25/96
6/8/96
6/22/96
7/6/96
7/20/96
8/3/96
8/17/96
8/31/96
9/14/96
9/28/96
10/12/96
10/26/96
11/9/96
11/23/96
12/7/96
12/21/96
1/4/97
1/18/97
2/1/97
2/15/97
3/1/97
3/15/97

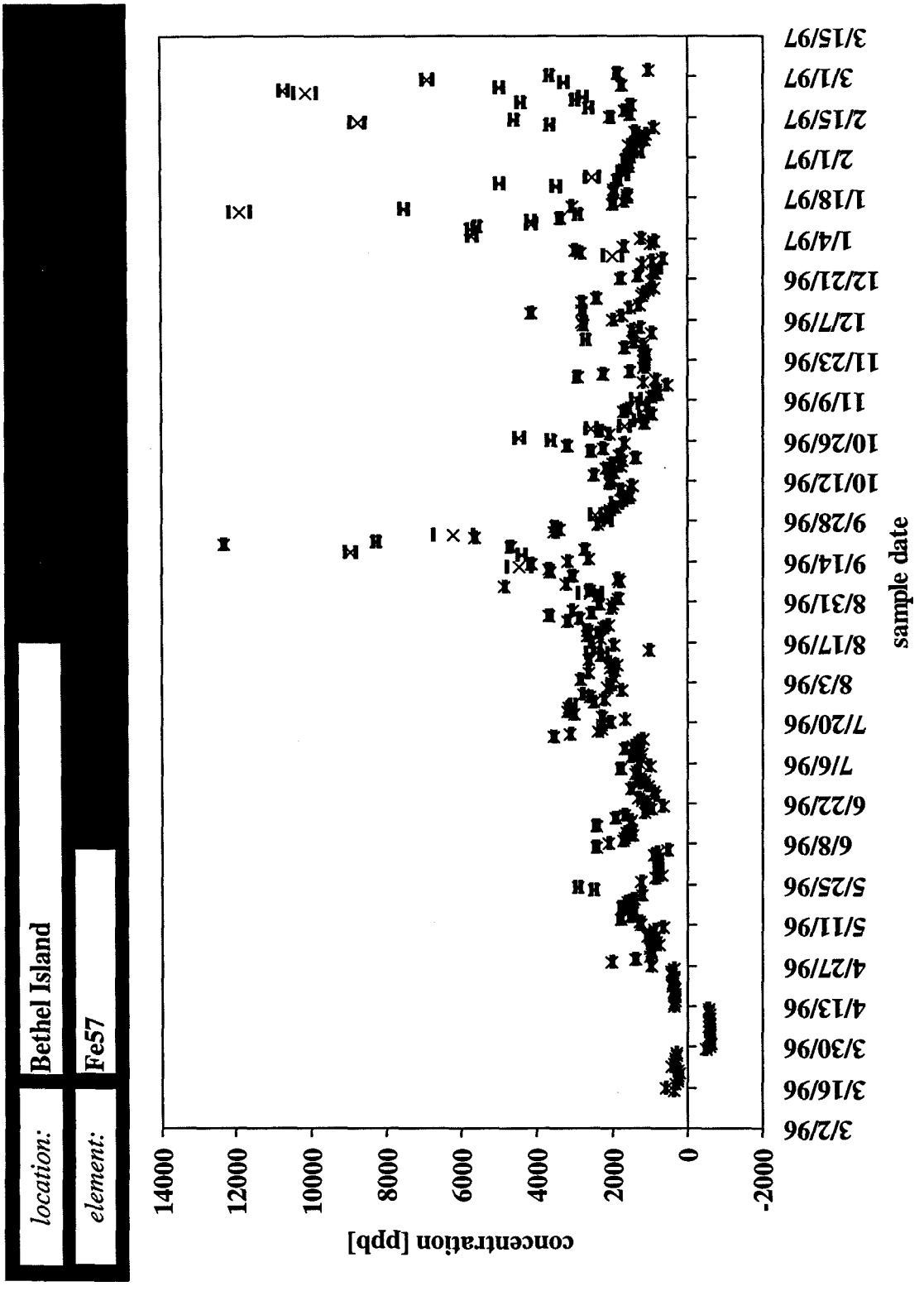
location:
Bethel Island
element:
Fe57
concentration [ppb]
14000
12000
10000
8000
6000
4000
2000
0
-2000
sample date
3/2/96
3/16/96
3/30/96
4/13/96
4/27/96
5/11/96
5/25/96
6/8/96
6/22/96
7/6/96
7/20/96
8/3/96
8/17/96
8/31/96
9/14/96
9/28/96
10/12/96
10/26/96
11/9/96
11/23/96
12/7/96
12/21/96
1/4/97
1/18/97
2/1/97
2/15/97
3/1/97
3/15/97

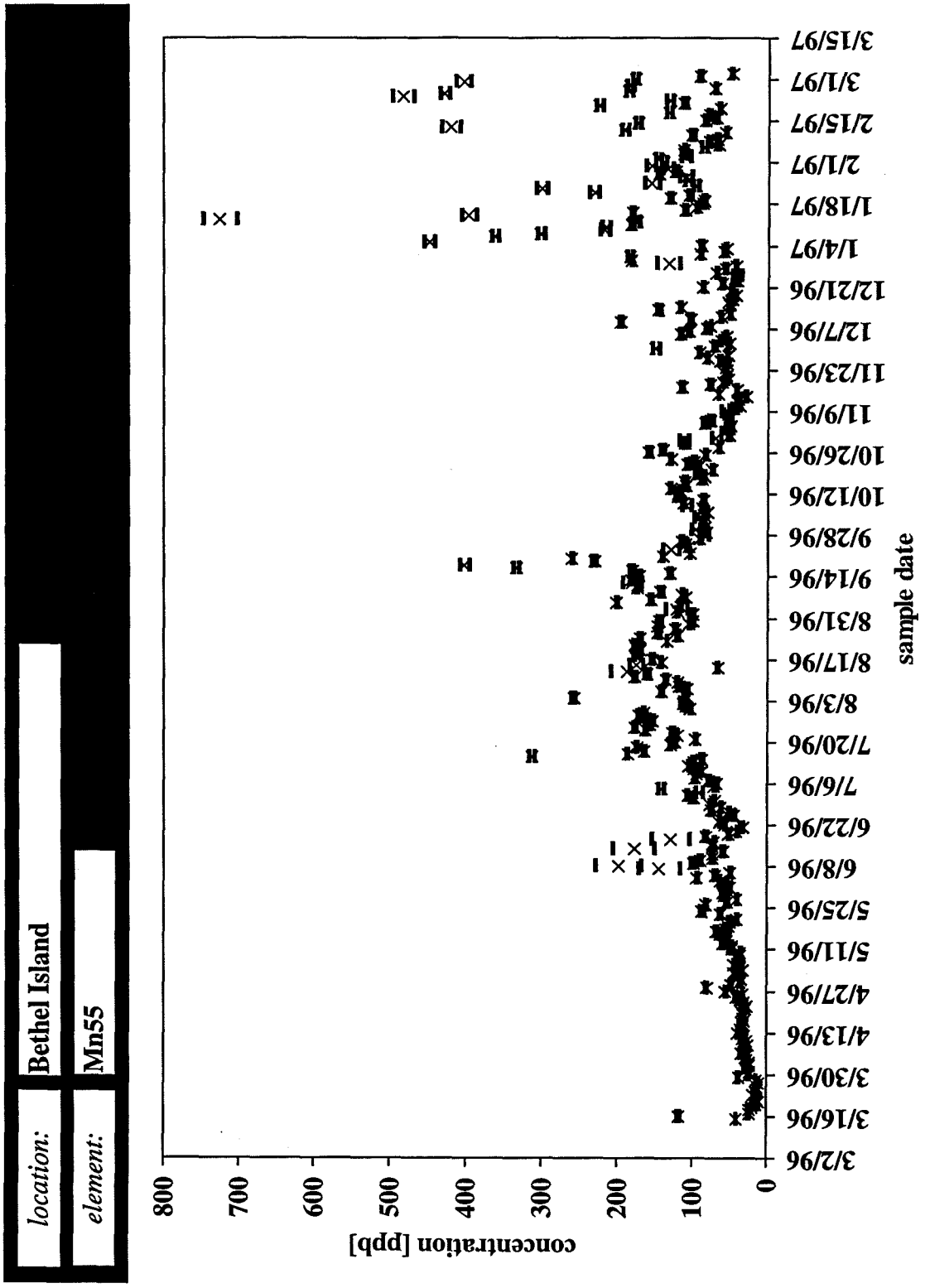
location:
Bethel Island
element:
Mn55
concentration [ppb]
0
100
200
300
400
500
600
700
800
sample date
3/2/96
3/16/96
3/30/96
4/13/96
4/27/96
5/11/96
5/25/96
6/8/96
6/22/96
7/6/96
7/20/96
8/3/96
8/17/96
8/31/96
9/14/96
9/28/96
10/12/96
10/26/96
11/9/96
11/23/96
12/7/96
12/21/96
1/4/97
1/18/97
2/1/97
2/15/97
3/1/97
3/15/97

location:
Bethel Island
element:
Co59
concentration [ppb]
0
1
2
3
4
5
6
7
8
sample date
3/2/96
3/16/96
3/30/96
4/13/96
4/27/96
5/11/96
5/25/96
6/8/96
6/22/96
7/6/96
7/20/96
8/3/96
8/17/96
8/31/96
9/14/96
9/28/96
10/12/96
10/26/96
11/9/96
11/23/96
12/7/96
12/21/96
1/4/97
1/18/97
2/1/97
2/15/97
3/1/97
3/15/97

location:
Bethel Island
element:
Ga69
concentration [ppb]
1.6
1.4
1.2
1
0.8
0.6
0.4
0.2
0
sample date
3/2/96
3/16/96
3/30/96
4/13/96
4/27/96
5/11/96
5/25/96
6/8/96
6/22/96
7/6/96
7/20/96
8/3/96
8/17/96
8/31/96
9/14/96
9/28/96
10/12/96
10/26/96
11/9/96
11/23/96
12/7/96
12/21/96
1/4/97
1/18/97
2/1/97
2/15/97
3/1/97
3/15/97

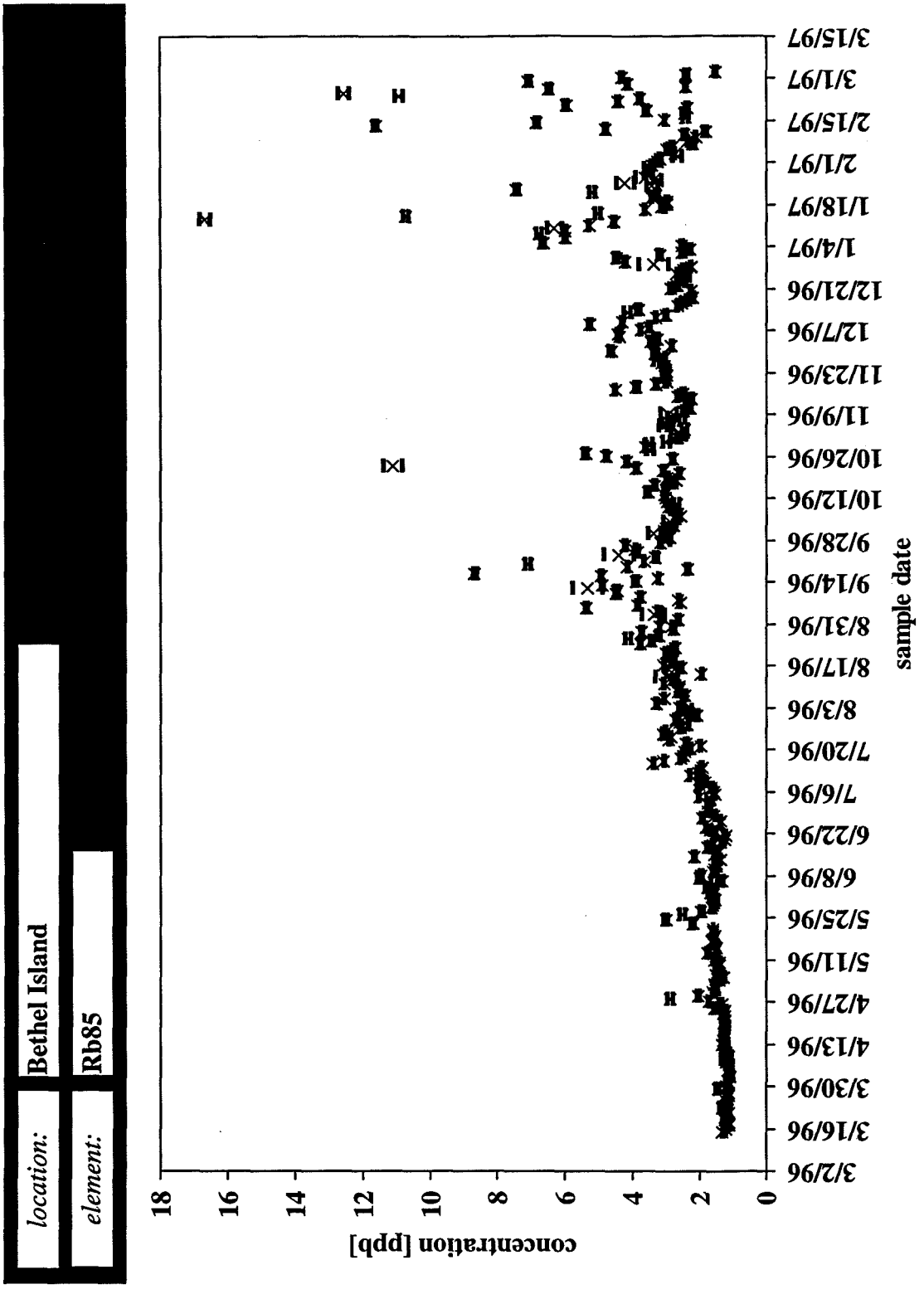
location:
Bethel Island
element:
Rb85
concentration [ppb]
0
2
4
6
8
10
12
14
16
18
sample date
3/2/96
3/16/96
3/30/96
4/13/96
4/27/96
5/11/96
5/25/96
6/8/96
6/22/96
7/6/96
7/20/96
8/3/96
8/17/96
8/31/96
9/14/96
9/28/96
10/12/96
10/26/96
11/9/96
11/23/96
12/7/96
12/21/96
1/4/97
1/18/97
2/1/97
2/15/97
3/1/97
3/15/97

location:
Bethel Island
element:
Sr87
concentration [ppb]
200
180
160
140
120
100
80
60
40
20
0
sample date
3/2/96
3/16/96
3/30/96
4/13/96
4/27/96
5/11/96
5/25/96
6/8/96
6/22/96
7/6/96
7/20/96
8/3/96
8/17/96
8/31/96
9/14/96
9/28/96
10/12/96
10/26/96
11/9/96
11/23/96
12/7/96
12/21/96
1/4/97
1/18/97
2/1/97
2/15/97
3/1/97
3/15/97

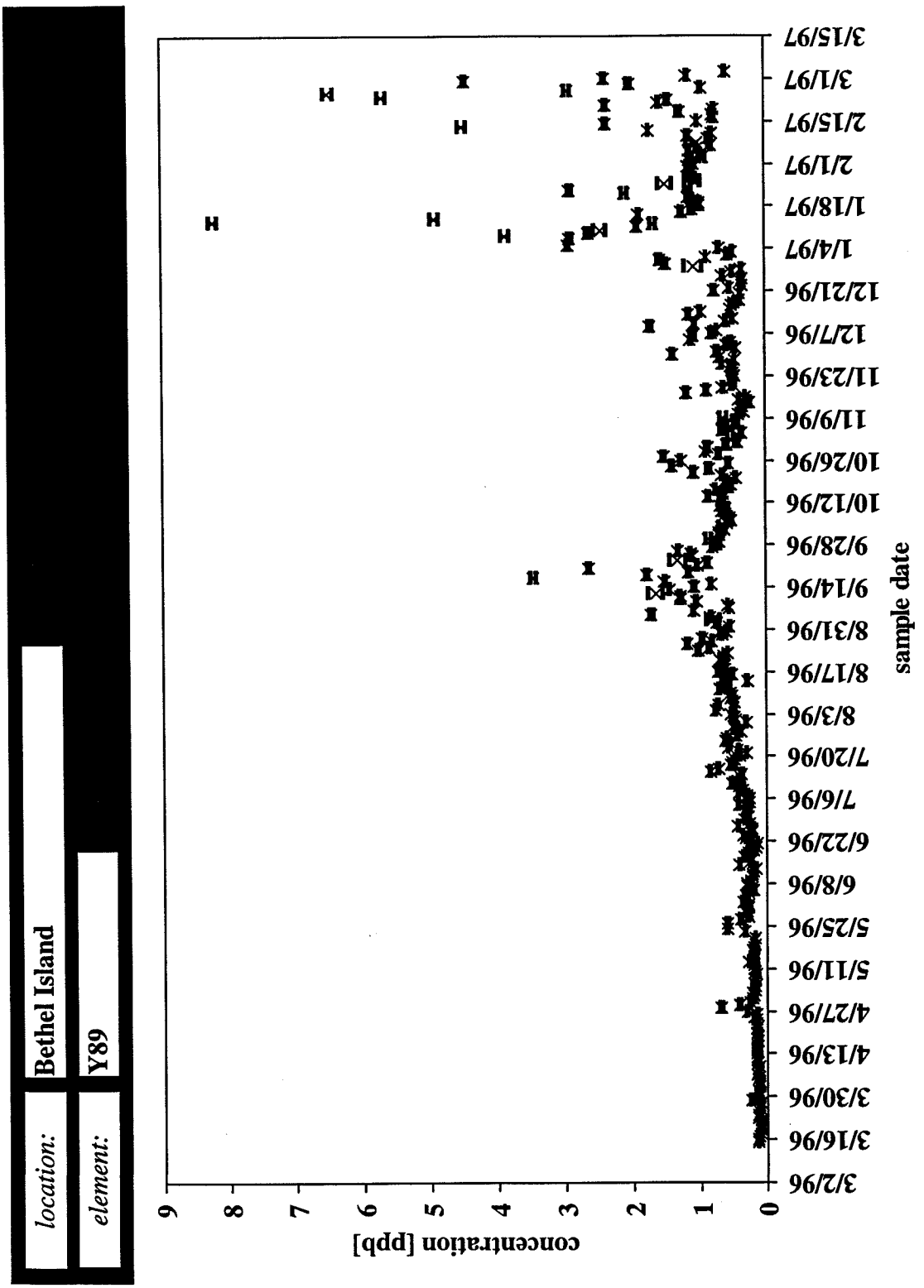
location:
Bethel Island
element:
Y89
concentration [ppb]
0
1
2
3
4
5
6
7
8
9
sample date
3/2/96
3/16/96
3/30/96
4/13/96
4/27/96
5/11/96
5/25/96
6/8/96
6/22/96
7/6/96
7/20/96
8/3/96
8/17/96
8/31/96
9/14/96
9/28/96
10/12/96
10/26/96
11/9/96
11/23/96
12/7/96
12/21/96
1/4/97
1/18/97
2/1/97
2/15/97
3/1/97
3/15/97

location:
Bethel Island
element:
Mo98
concentration [ppb]
1.6
1.4
1.2
1
0.8
0.6
0.4
0.2
0
sample date
3/2/96
3/16/96
3/30/96
4/13/96
4/27/96
5/11/96
5/25/96
6/8/96
6/22/96
7/6/96
7/20/96
8/3/96
8/17/96
8/31/96
9/14/96
9/28/96
10/12/96
10/26/96
11/9/96
11/23/96
12/7/96
12/21/96
1/4/97
1/18/97
2/1/97
2/15/97
3/1/97
3/15/97

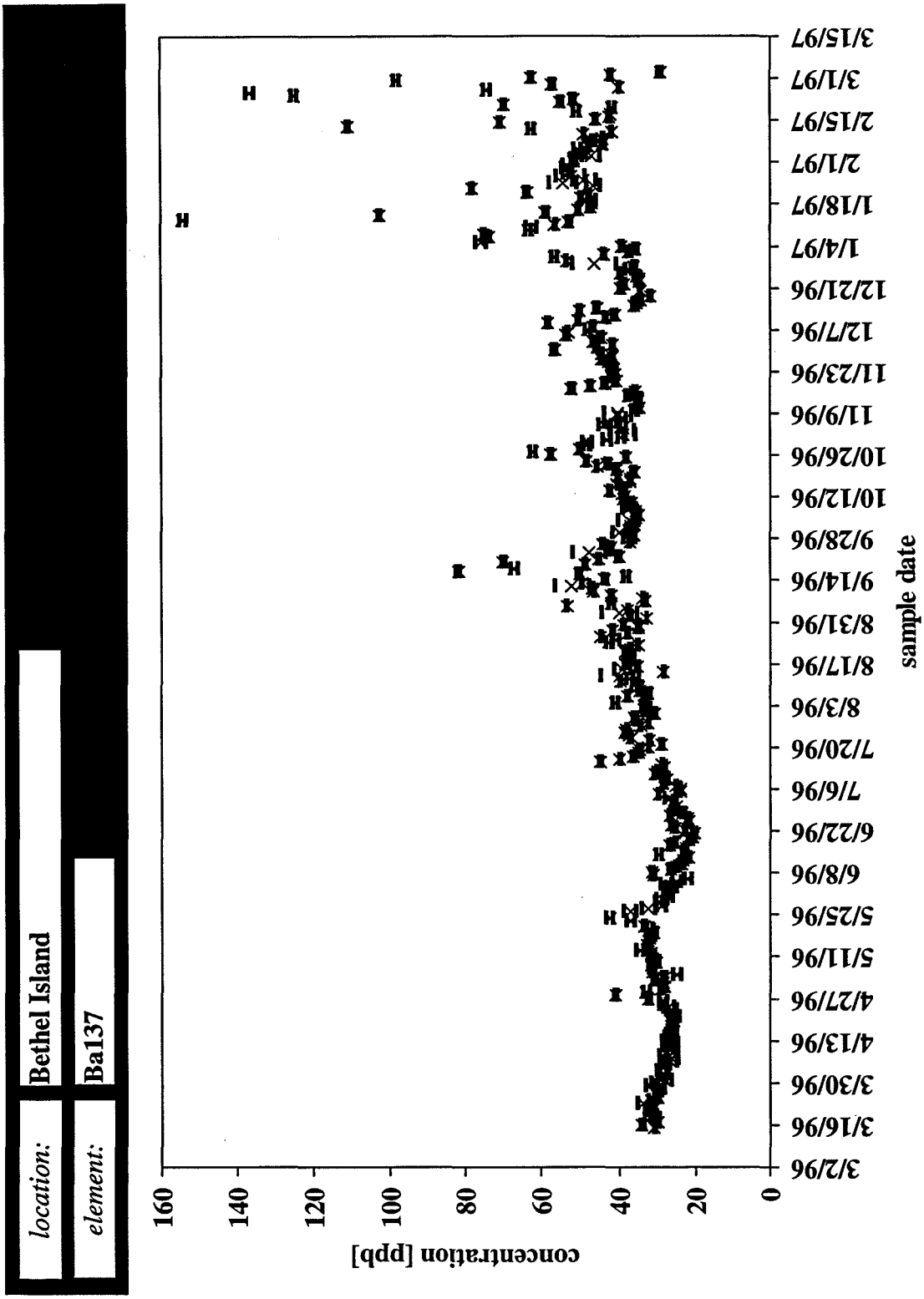
location:
Bethel Island
element:
Ba137
concentration [ppb]
0
20
40
60
80
100
120
140
160
sample date
3/2/96
3/16/96
3/30/96
4/13/96
4/27/96
5/11/96
5/25/96
6/8/96
6/22/96
7/6/96
7/20/96
8/3/96
8/17/96
8/31/96
9/14/96
9/28/96
10/12/96
10/26/96
11/9/96
11/23/96
12/7/96
12/21/96
1/4/97
1/18/97
2/1/97
2/15/97
3/1/97
3/15/97

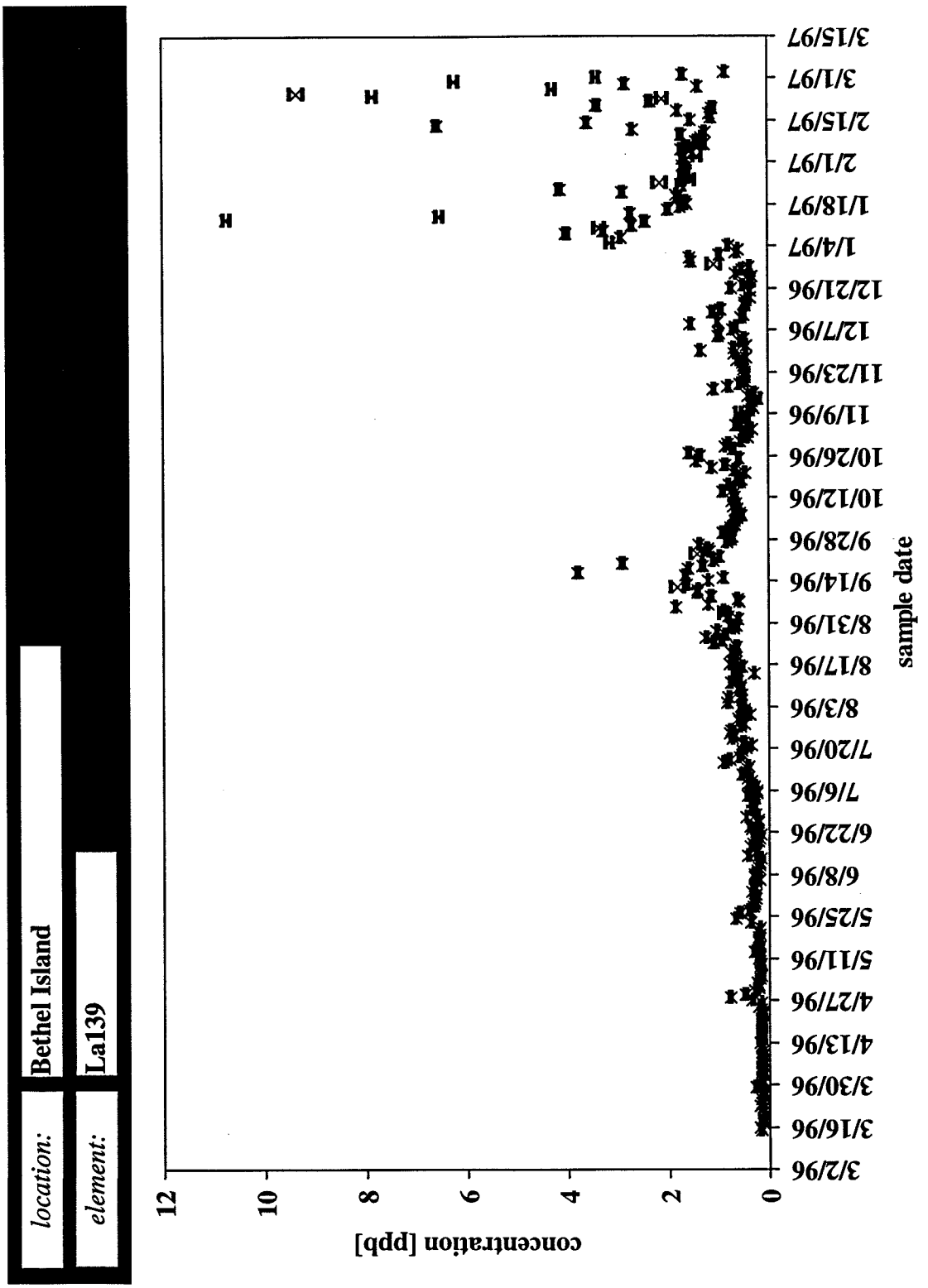
location:
Bethel Island
element:
La139
concentration [ppb]
0
2
4
6
8
10
12
sample date
3/2/96
3/16/96
3/30/96
4/13/96
4/27/96
5/11/96
5/25/96
6/8/96
6/22/96
7/6/96
7/20/96
8/3/96
8/17/96
8/31/96
9/14/96
9/28/96
10/12/96
10/26/96
11/9/96
11/23/96
12/7/96
12/21/96
1/4/97
1/18/97
2/1/97
2/15/97
3/1/97
3/15/97

location:
Bethel Island
element:
Ce140
concentration [ppb]
0
5
10
15
20
25
sample date
3/2/96
3/16/96
3/30/96
4/13/96
4/27/96
5/11/96
5/25/96
6/8/96
6/22/96
7/6/96
7/20/96
8/3/96
8/17/96
8/31/96
9/14/96
9/28/96
10/12/96
10/26/96
11/9/96
11/23/96
12/7/96
12/21/96
1/4/97
1/18/97
2/1/97
2/15/97
3/1/97
3/15/97

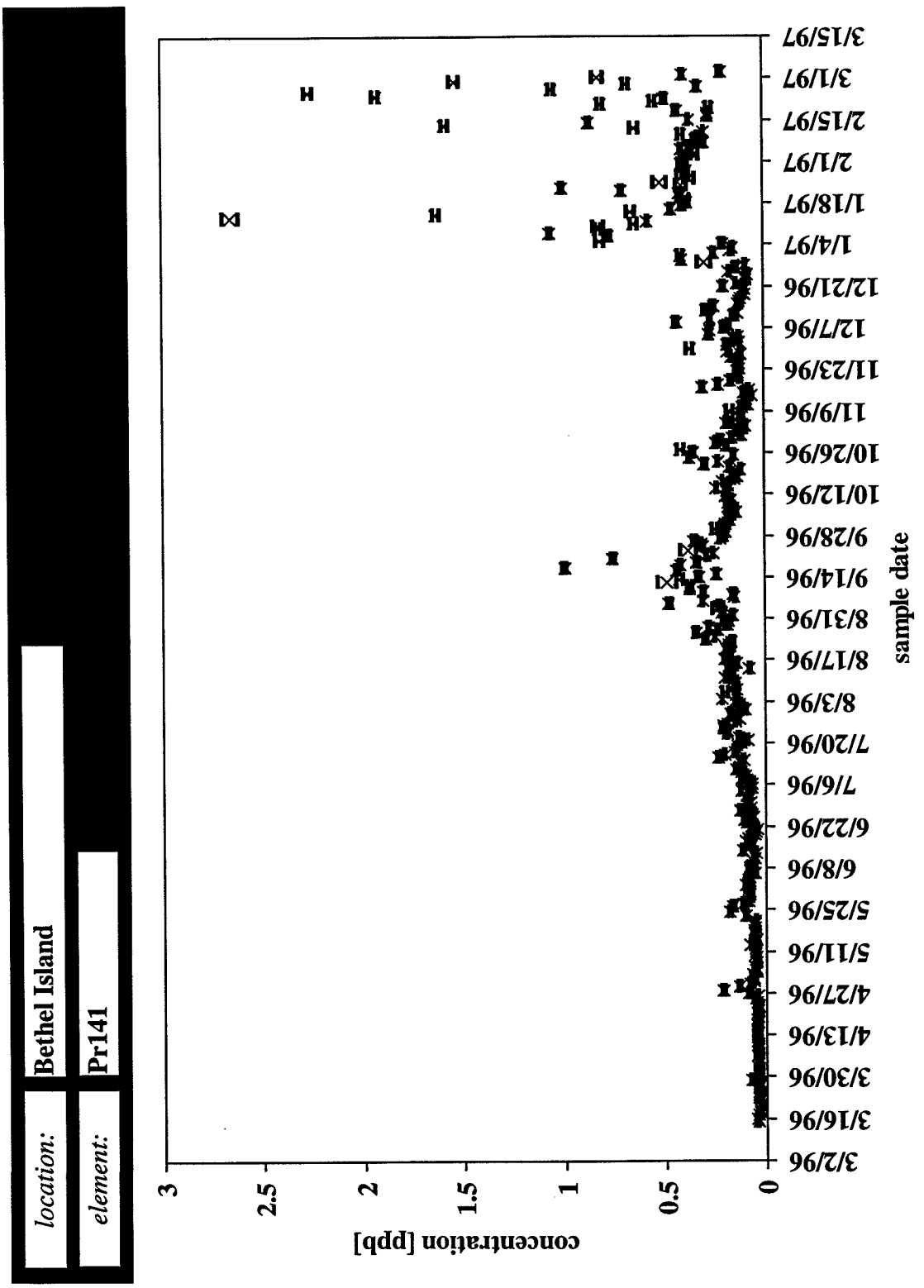
location:
Bethel Island
element:
Pr141
concentration [ppb]
0
0.5
1
1.5
2
2.5
3
sample date
3/2/96
3/16/96
3/30/96
4/13/96
4/27/96
5/11/96
5/25/96
6/8/96
6/22/96
7/6/96
7/20/96
8/3/96
8/17/96
8/31/96
9/14/96
9/28/96
10/12/96
10/26/96
11/9/96
11/23/96
12/7/96
12/21/96
1/4/97
1/18/97
2/1/97
2/15/97
3/1/97
3/15/97

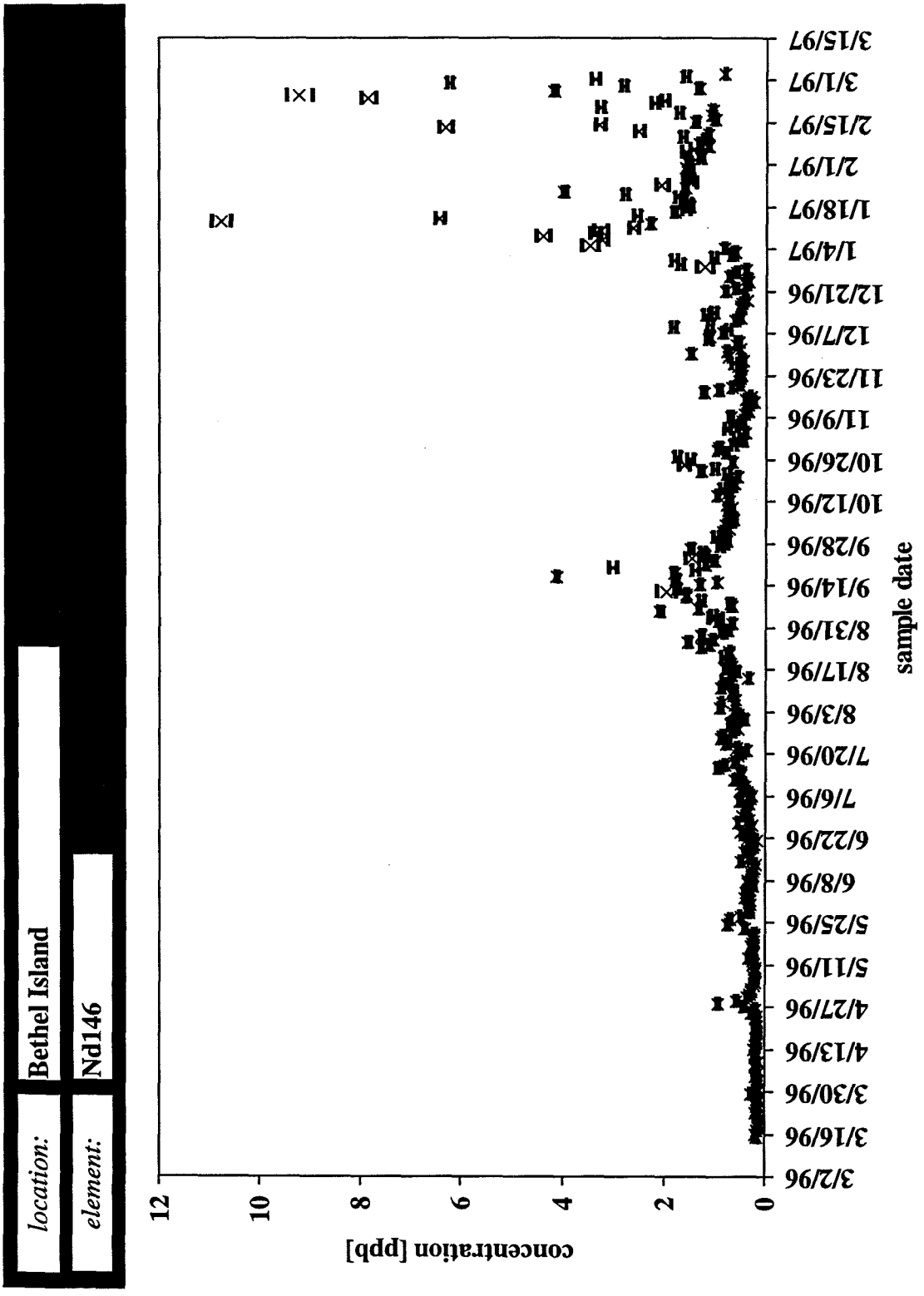
location:
Bethel Island
element:
Nd146
concentration [ppb]
0
2
4
6
8
10
12
sample date
3/2/96
3/16/96
3/30/96
4/13/96
4/27/96
5/11/96
5/25/96
6/8/96
6/22/96
7/6/96
7/20/96
8/3/96
8/17/96
8/31/96
9/14/96
9/28/96
10/12/96
10/26/96
11/9/96
11/23/96
12/7/96
12/21/96
1/4/97
1/18/97
2/1/97
2/15/97
3/1/97
3/15/97

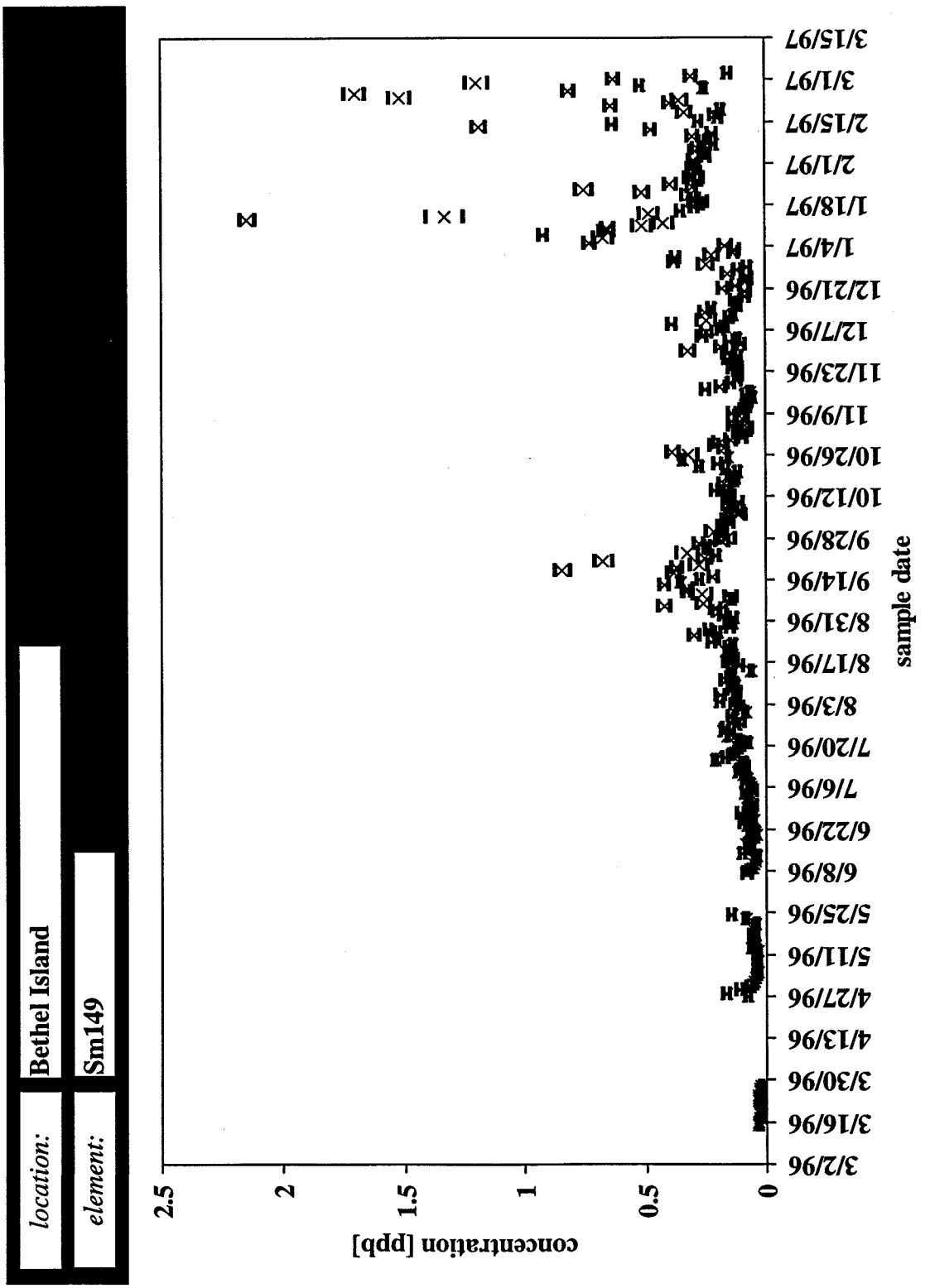
location:
Bethel Island
element:
Sm149
concentration [ppb]
2.5
2
1.5
1
0.5
0
sample date
3/2/96
3/16/96
3/30/96
4/13/96
4/27/96
5/11/96
5/25/96
6/8/96
6/22/96
7/6/96
7/20/96
8/3/96
8/17/96
8/31/96
9/14/96
9/28/96
10/12/96
10/26/96
11/9/96
11/23/96
12/7/96
12/21/96
1/4/97
1/18/97
2/1/97
2/15/97
3/1/97
3/15/97

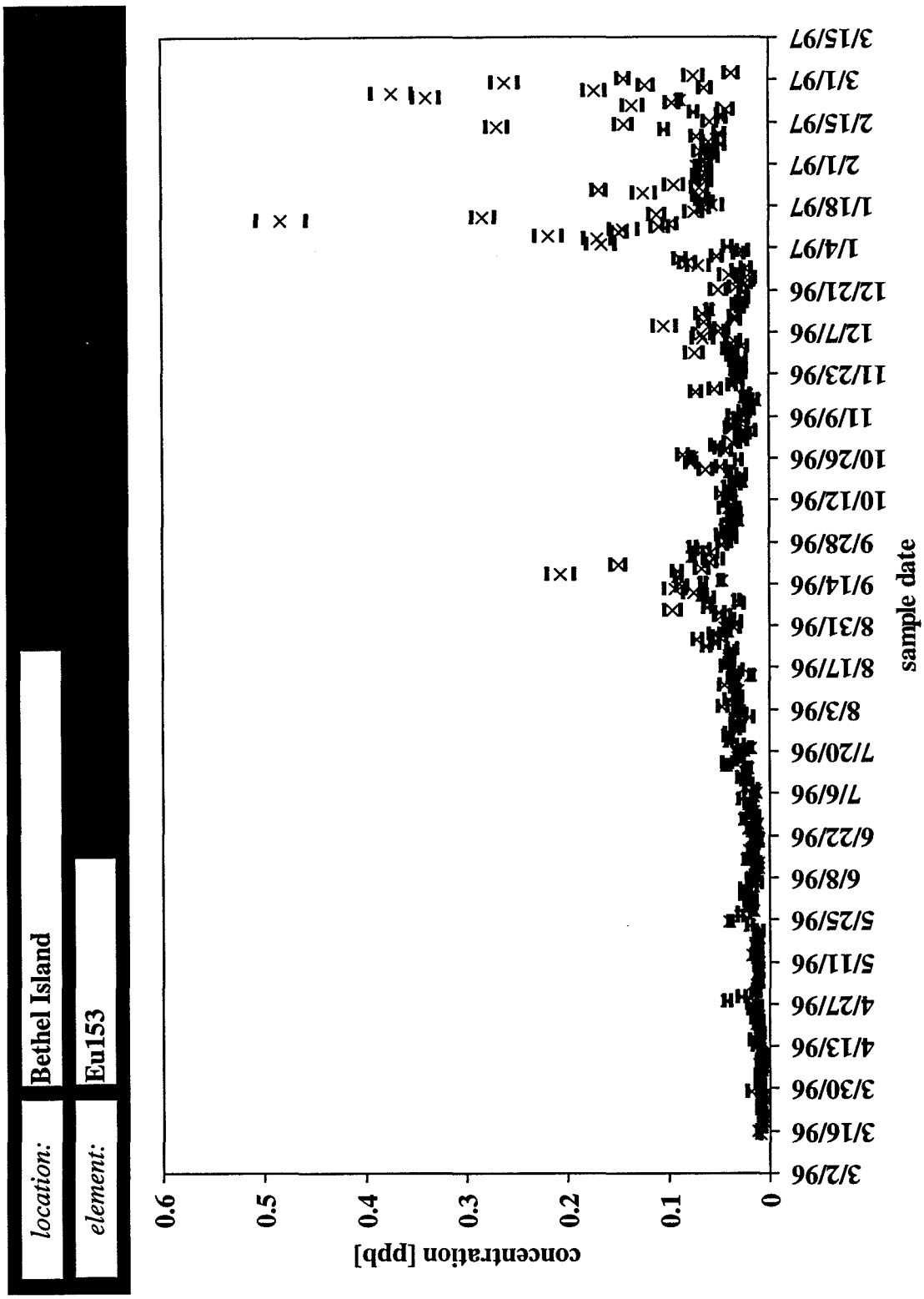
location:
Bethel Island
element:
Eu153
concentration [ppb]
0.6
0.5
0.4
0.3
0.2
0.1
0
sample date
3/2/96
3/16/96
3/30/96
4/13/96
4/27/96
5/11/96
5/25/96
6/8/96
6/22/96
7/6/96
7/20/96
8/3/96
8/17/96
8/31/96
9/14/96
9/28/96
10/12/96
10/26/96
11/9/96
11/23/96
12/7/96
12/21/96
1/4/97
1/18/97
2/1/97
2/15/97
3/1/97
3/15/97

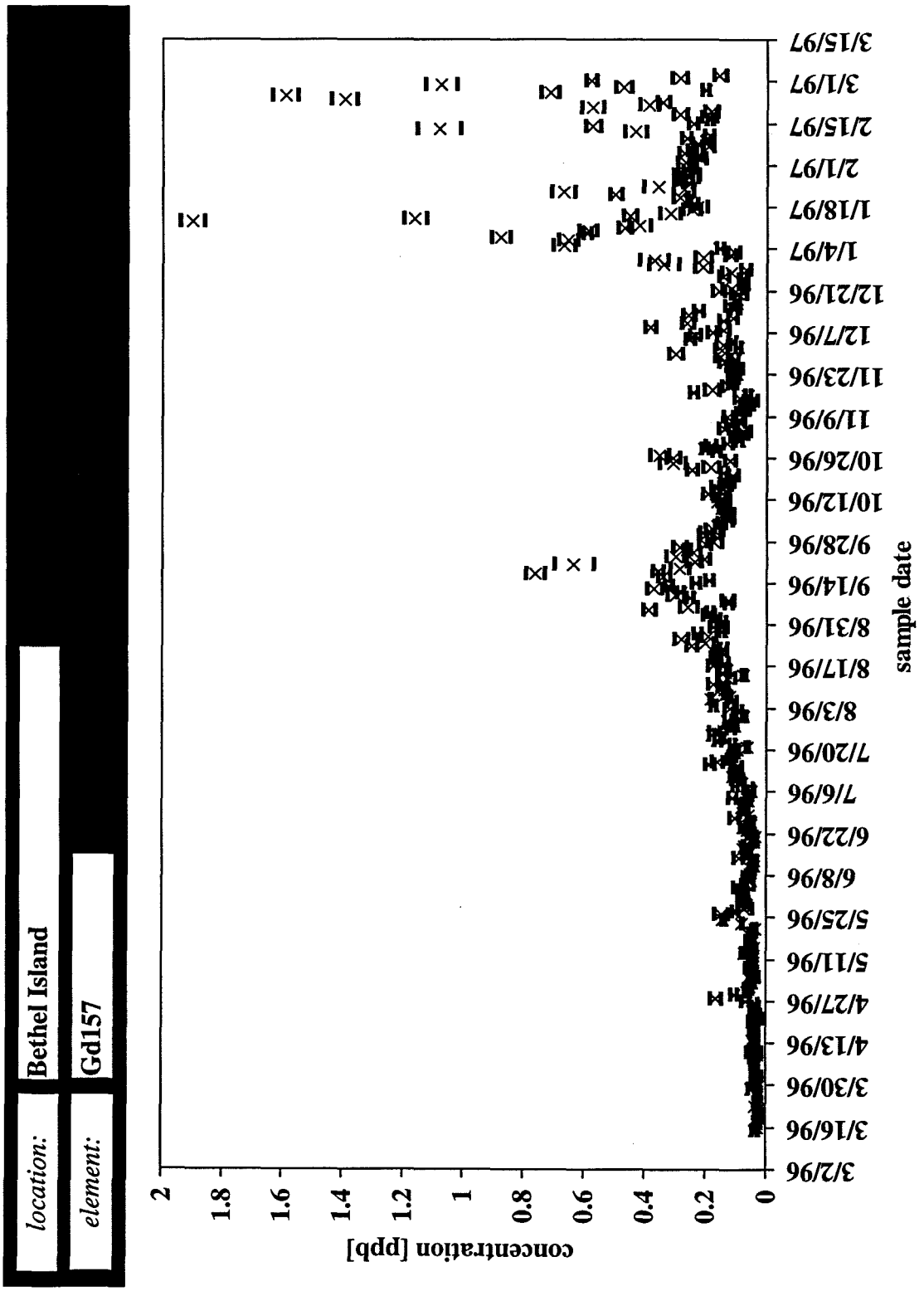
location:
Bethel Island
element:
Gd157
concentration [ppb]
0
0.2
0.4
0.6
0.8
1
1.2
1.4
1.6
1.8
2
sample date
3/2/96
3/16/96
3/30/96
4/13/96
4/27/96
5/11/96
5/25/96
6/8/96
6/22/96
7/6/96
7/20/96
8/3/96
8/17/96
8/31/96
9/14/96
9/28/96
10/12/96
10/26/96
11/9/96
11/23/96
12/7/96
12/21/96
1/4/97
1/18/97
2/1/97
2/15/97
3/1/97
3/15/97

location:
Bethel Island
element:
Tb159
concentration [ppb]
0.3
0.25
0.2
0.15
0.1
0.05
0
sample date
3/2/96
3/16/96
3/30/96
4/13/96
4/27/96
5/11/96
5/25/96
6/8/96
6/22/96
7/6/96
7/20/96
8/3/96
8/17/96
8/31/96
9/14/96
9/28/96
10/12/96
10/26/96
11/9/96
11/23/96
12/7/96
12/21/96
1/4/97
1/18/97
2/1/97
2/15/97
3/1/97
3/15/97

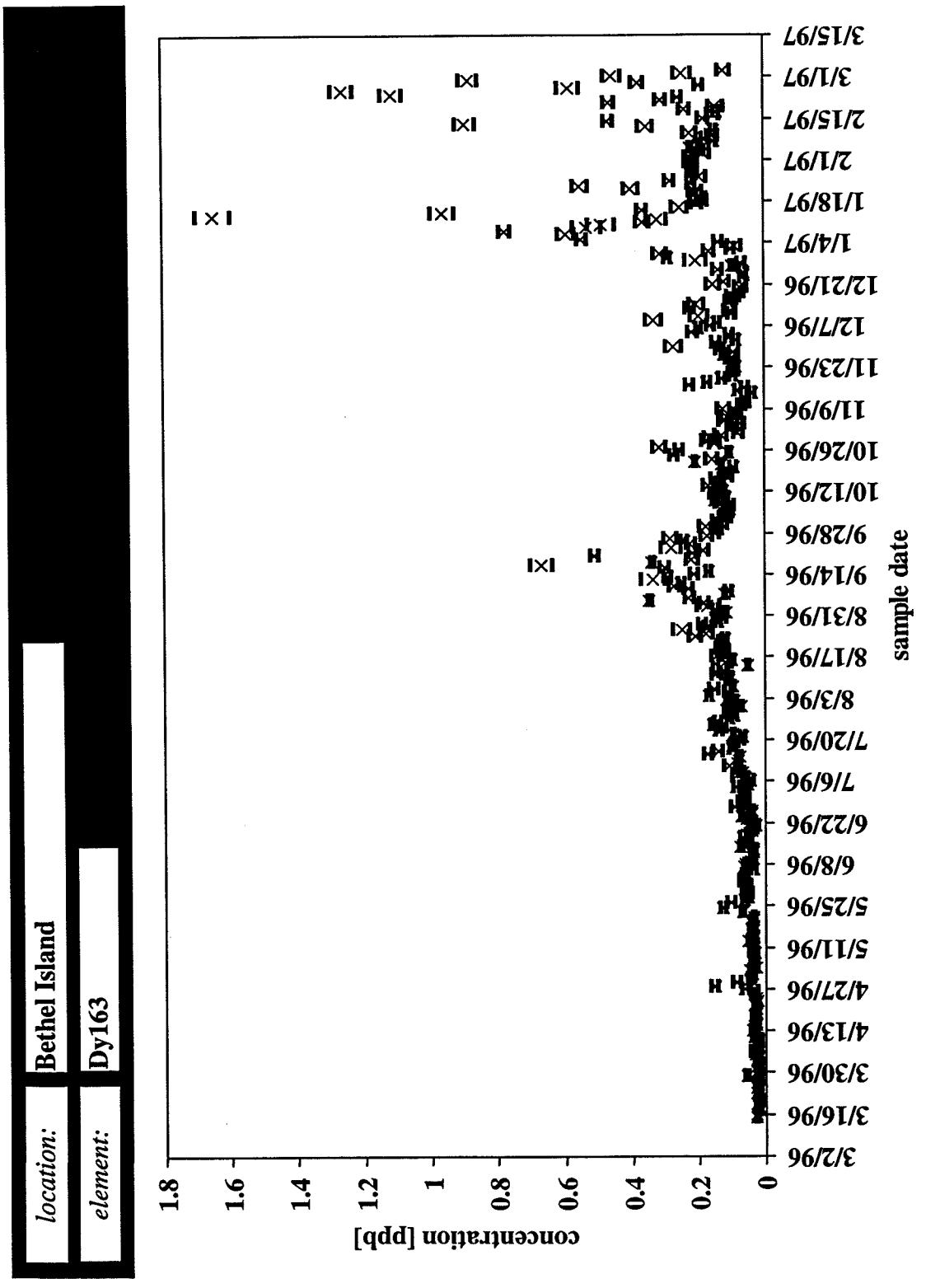
location:
Bethel Island
element:
Dy163
concentration [ppb]
0
0.2
0.4
0.6
0.8
1
1.2
1.4
1.6
1.8
sample date
3/2/96
3/16/96
3/30/96
4/13/96
4/27/96
5/11/96
5/25/96
6/8/96
6/22/96
7/6/96
7/20/96
8/3/96
8/17/96
8/31/96
9/14/96
9/28/96
10/12/96
10/26/96
11/9/96
11/23/96
12/7/96
12/21/96
1/4/97
1/18/97
2/1/97
2/15/97
3/1/97
3/15/97

location:
Bethel Island
element:
Ho165
concentration [ppb]
0.35
0.3
0.25
0.2
0.15
0.1
0.05
0
sample date
3/2/96
3/16/96
3/30/96
4/13/96
4/27/96
5/11/96
5/25/96
6/8/96
6/22/96
7/6/96
7/20/96
8/3/96
8/17/96
8/31/96
9/14/96
9/28/96
10/12/96
10/26/96
11/9/96
11/23/96
12/7/96
12/21/96
1/4/97
1/18/97
2/1/97
2/15/97
3/1/97
3/15/97

location:
Bethel Island
element:
Er168
concentration [ppb]
0.9
0.8
0.7
0.6
0.5
0.4
0.3
0.2
0.1
0
-0.1
sample date
3/2/96
3/16/96
3/30/96
4/13/96
4/27/96
5/11/96
5/25/96
6/8/96
6/22/96
7/6/96
7/20/96
8/3/96
8/17/96
8/31/96
9/14/96
9/28/96
10/12/96
10/26/96
11/9/96
11/23/96
12/7/96
12/21/96
1/4/97
1/18/97
2/1/97
2/15/97
3/1/97
3/15/97

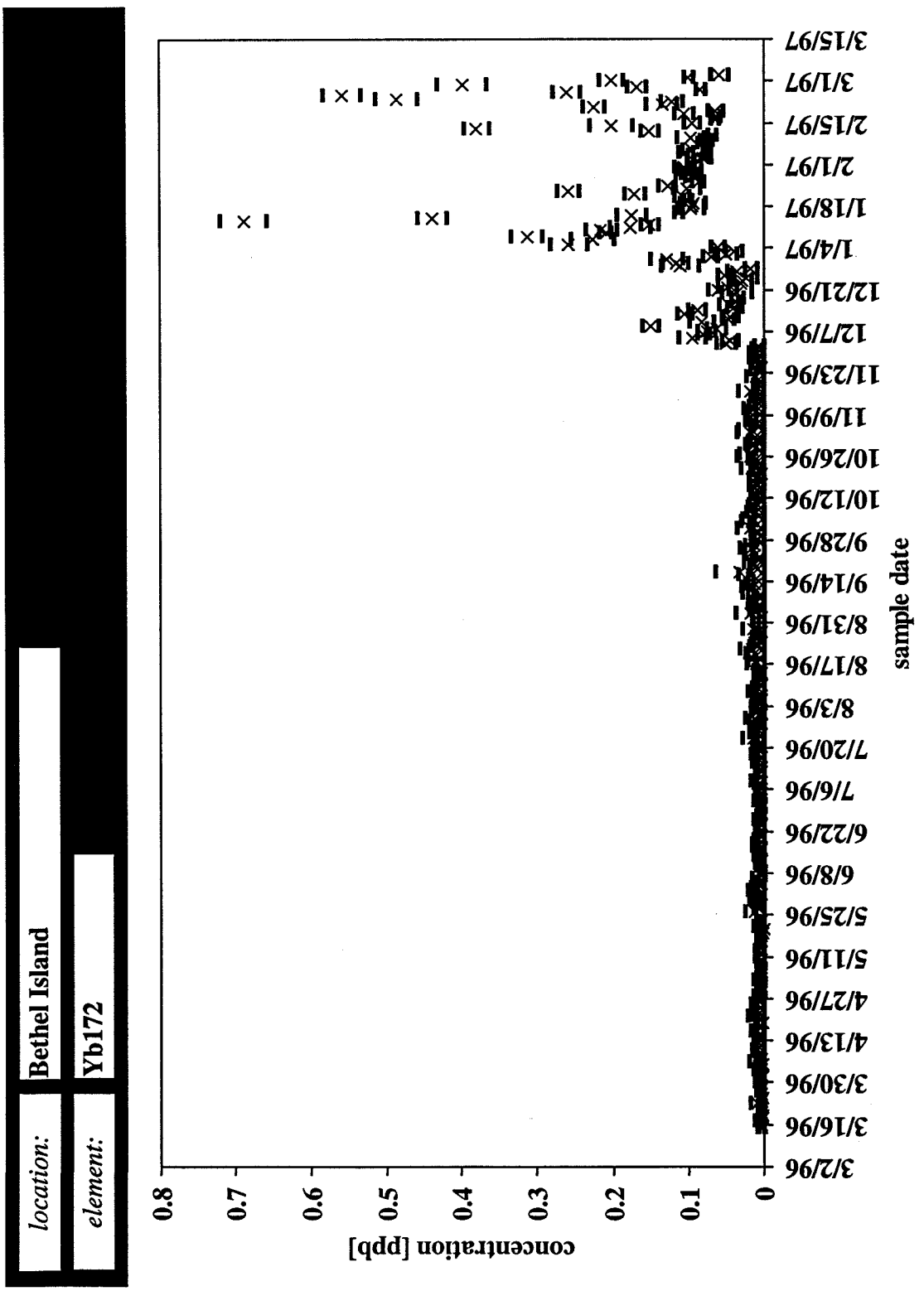
location:
Bethel Island
element:
Yb172
concentration [ppb]
0.8
0.7
0.6
0.5
0.4
0.3
0.2
0.1
0
sample date
3/2/96
3/16/96
3/30/96
4/13/96
4/27/96
5/11/96
5/25/96
6/8/96
6/22/96
7/6/96
7/20/96
8/3/96
8/17/96
8/31/96
9/14/96
9/28/96
10/12/96
10/26/96
11/9/96
11/23/96
12/7/96
12/21/96
1/4/97
1/18/97
2/1/97
2/15/97
3/1/97
3/15/97

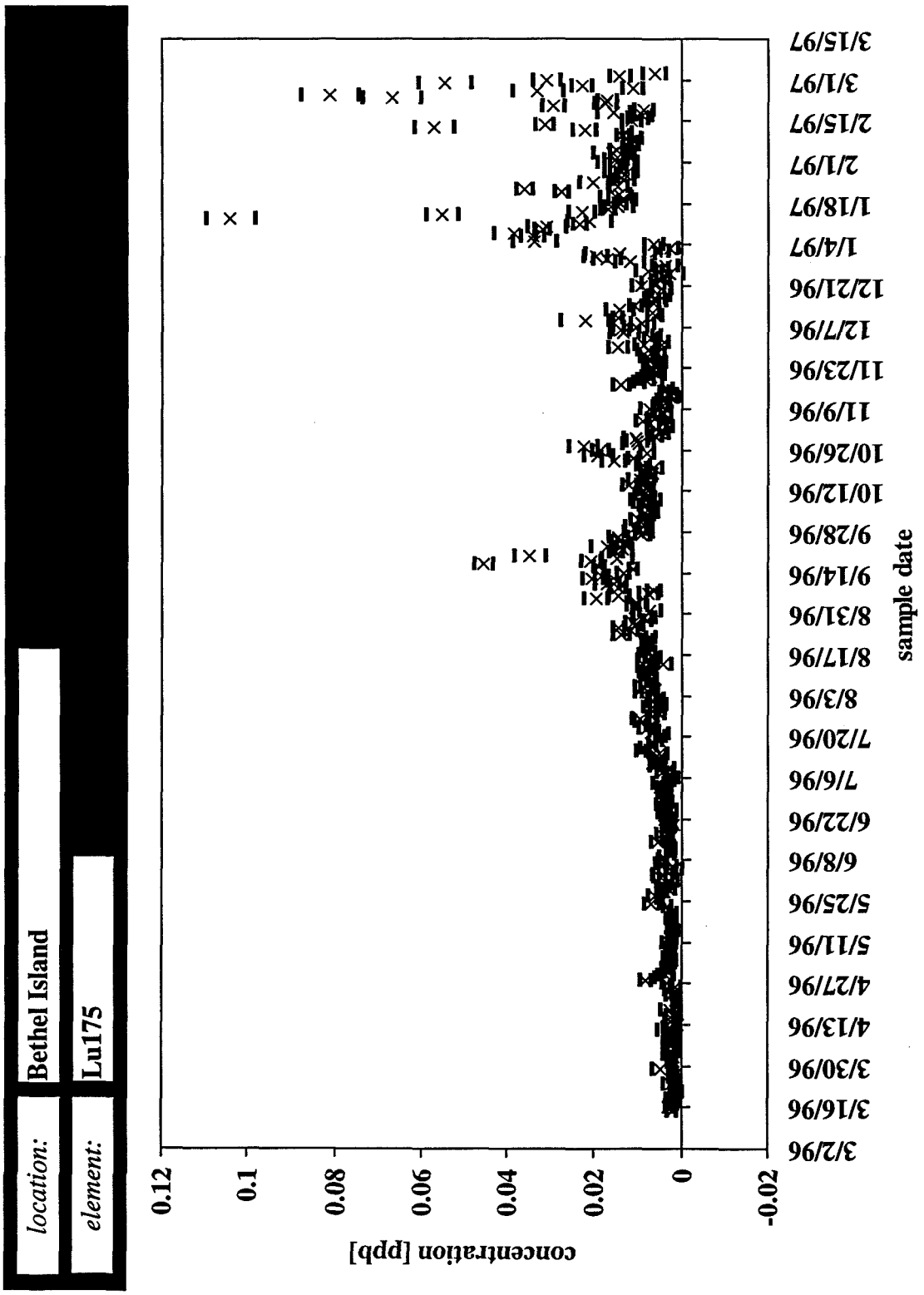
location:
Bethel Island
element:
Lu175
concentration [ppb]
0.12
0.1
0.08
0.06
0.04
0.02
0
-0.02
sample date
3/2/96
3/16/96
3/30/96
4/13/96
4/27/96
5/11/96
5/25/96
6/8/96
6/22/96
7/6/96
7/20/96
8/3/96
8/17/96
8/31/96
9/14/96
9/28/96
10/12/96
10/26/96
11/9/96
11/23/96
12/7/96
12/21/96
1/4/97
1/18/97
2/1/97
2/15/97
3/1/97
3/15/97

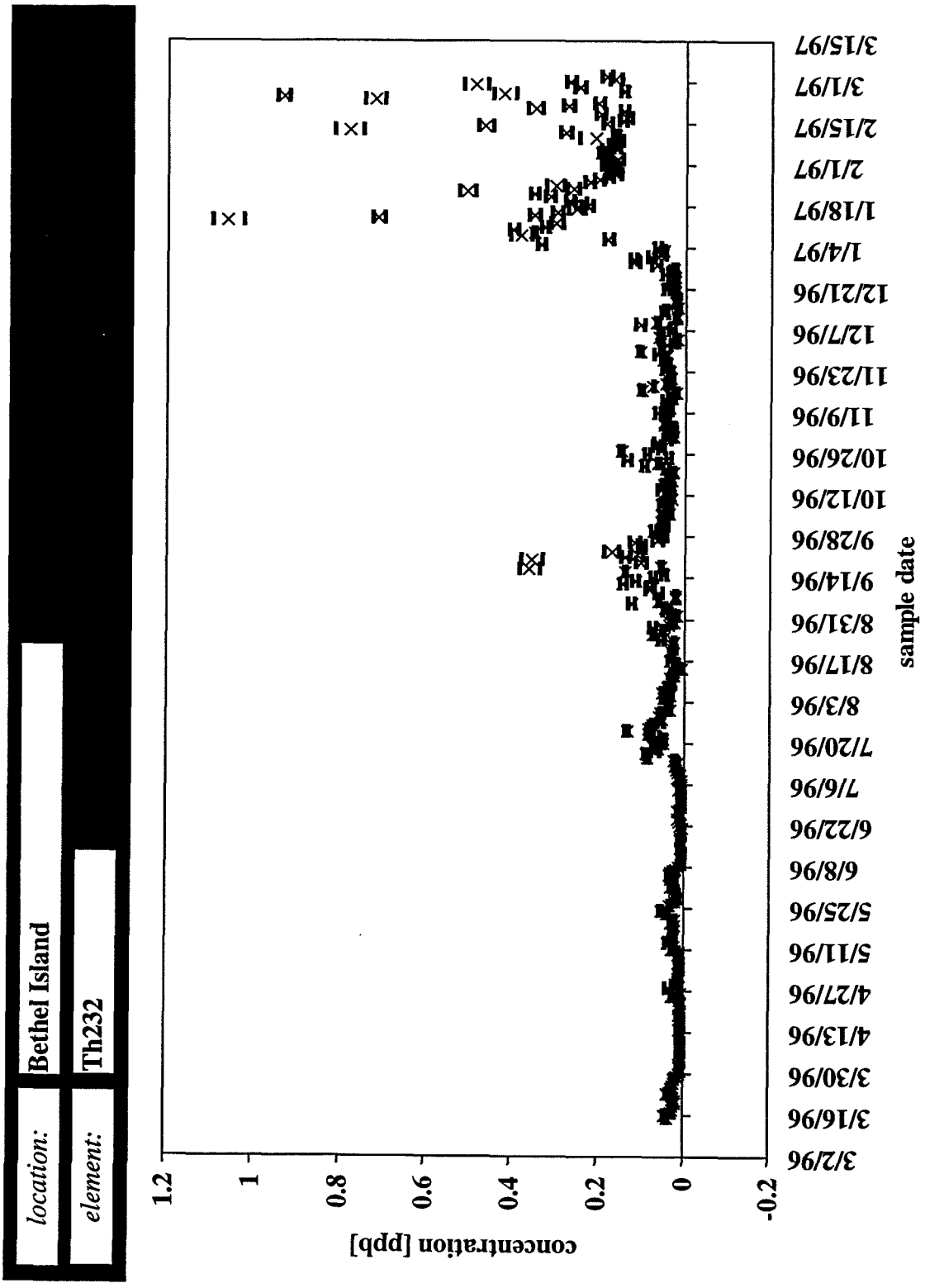
location:
Bethel Island
element:
Th232
concentration [ppb]
1.2
1
0.8
0.6
0.4
0.2
0
-0.2
sample date
3/2/96
3/16/96
3/30/96
4/13/96
4/27/96
5/11/96
5/25/96
6/8/96
6/22/96
7/6/96
7/20/96
8/3/96
8/17/96
8/31/96
9/14/96
9/28/96
10/12/96
10/26/96
11/9/96
11/23/96
12/7/96
12/21/96
1/4/97
1/18/97
2/1/97
2/15/97
3/1/97
3/15/97

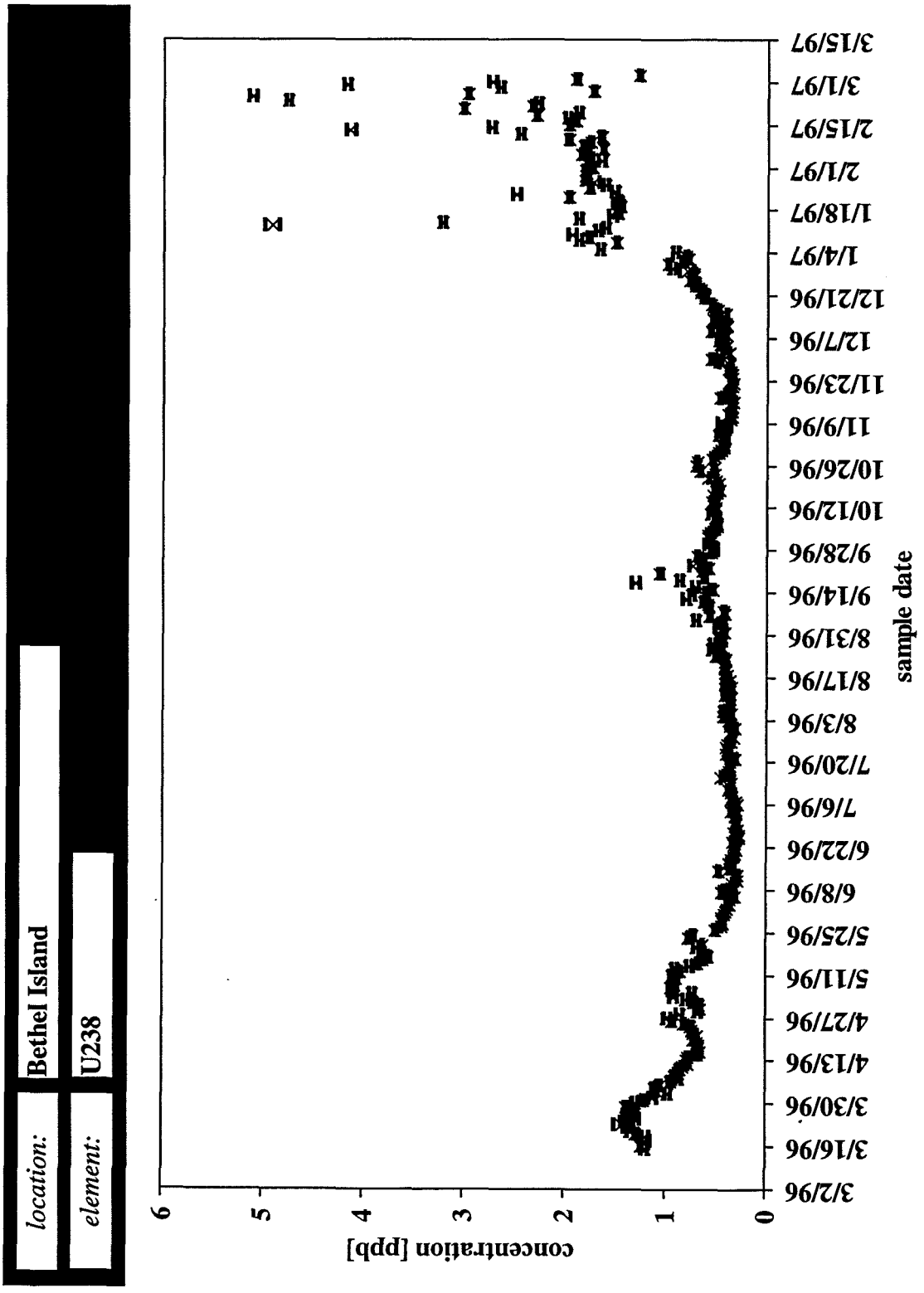
location:
Bethel Island
element:
U238
concentration [ppb]
0
1
2
3
4
5
6
sample date
3/2/96
3/16/96
3/30/96
4/13/96
4/27/96
5/11/96
5/25/96
6/8/96
6/22/96
7/6/96
7/20/96
8/3/96
8/17/96
8/31/96
9/14/96
9/28/96
10/12/96
10/26/96
11/9/96
11/23/96
12/7/96
12/21/96
1/4/97
1/18/97
2/1/97
2/15/97
3/1/97
3/15/97

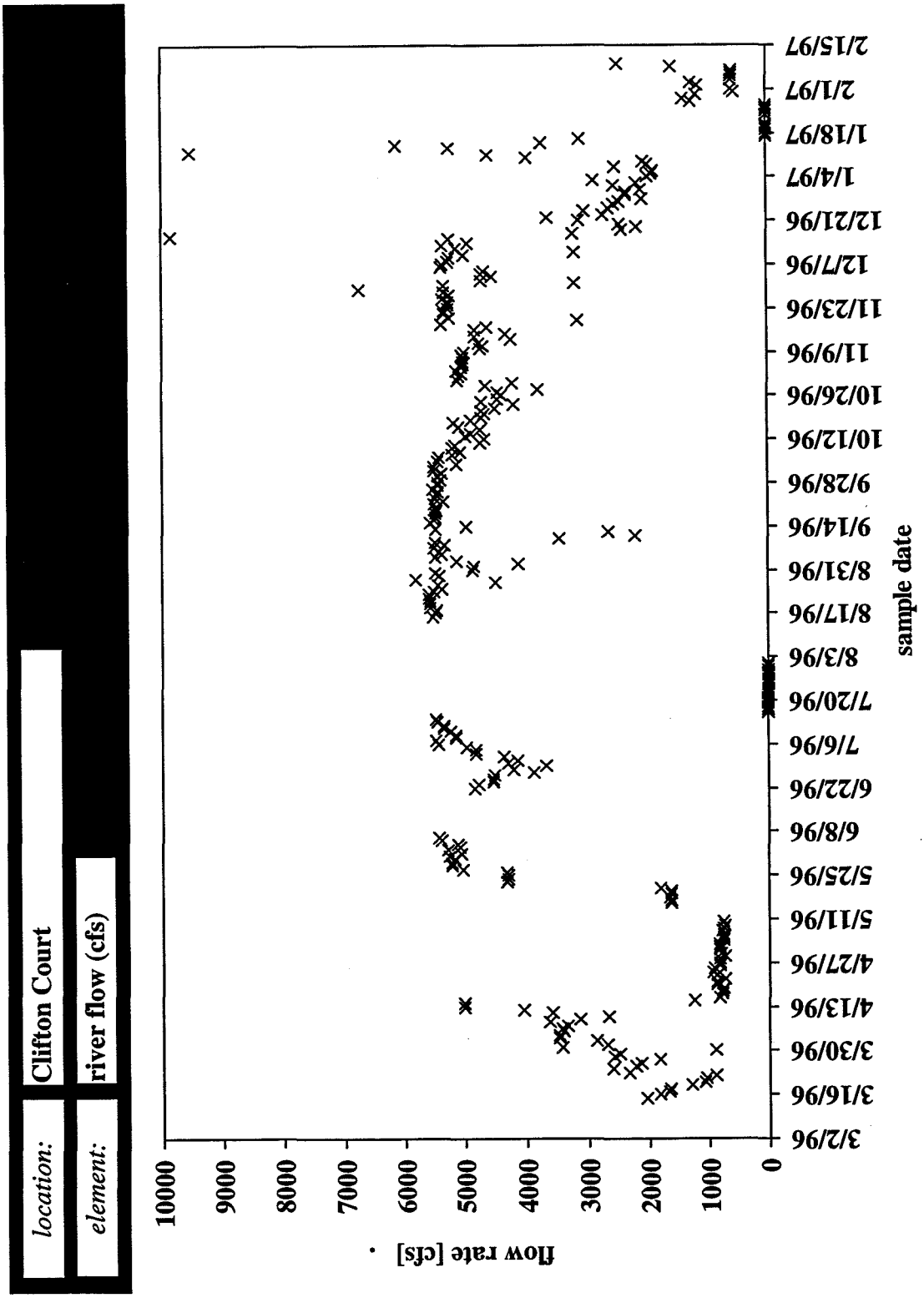
location:
Clifton Court
element:
river flow (cfs)
flow rate [cfs]
10000
9000
8000
7000
6000
5000
4000
3000
2000
1000
0
3/2/96
3/16/96
3/30/96
4/13/96
4/27/96
5/11/96
5/25/96
6/8/96
6/22/96
7/6/96
7/20/96
8/3/96
8/17/96
8/31/96
9/14/96
9/28/96
10/12/96
10/26/96
11/9/96
11/23/96
12/7/96
12/21/96
1/4/97
1/18/97
2/1/97
2/15/97
sample date

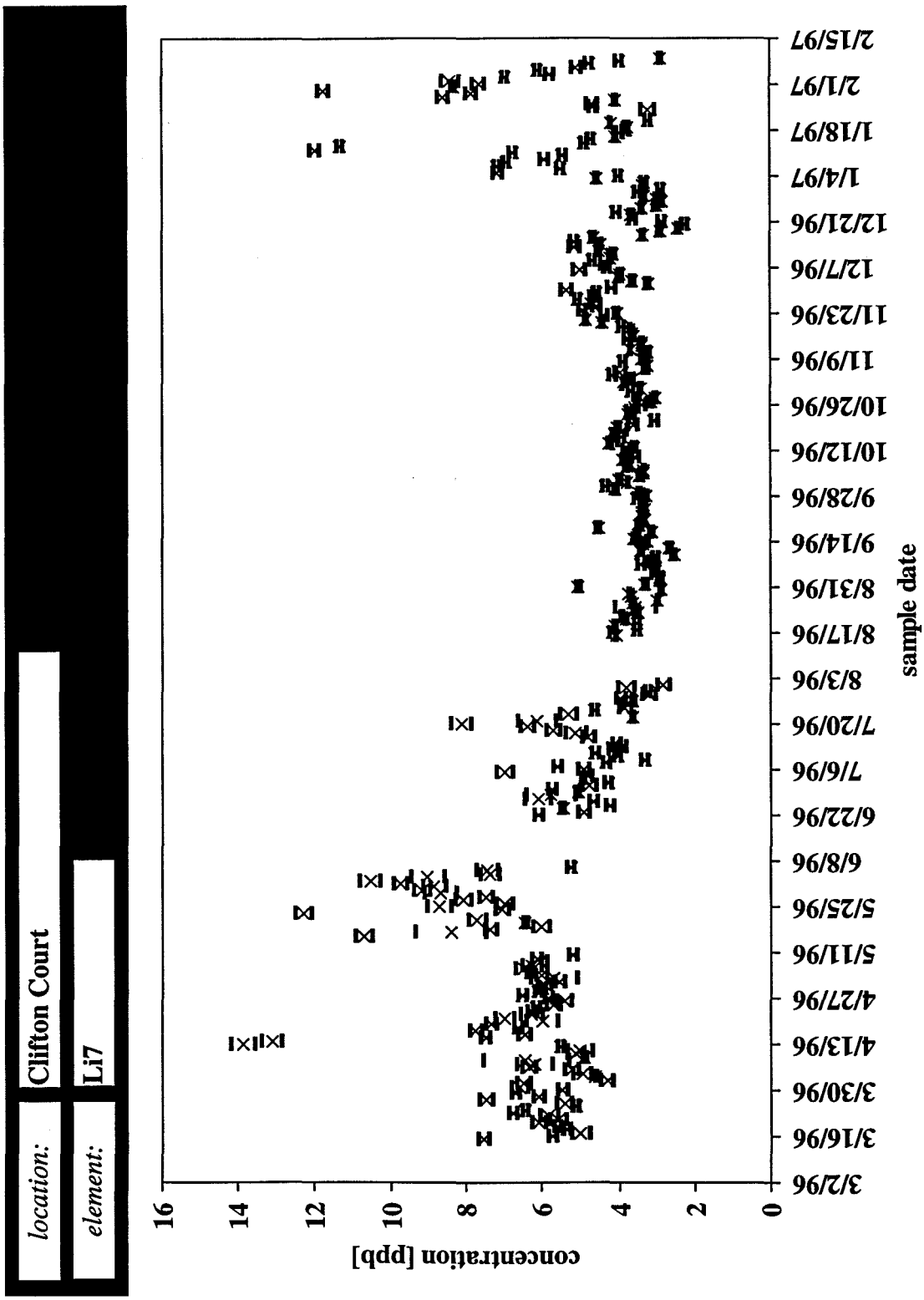
location:
Clifton Court
element:
Li7
concentration [ppb]
0
2
4
6
8
10
12
14
16
sample date
3/2/96
3/16/96
3/30/96
4/13/96
4/27/96
5/11/96
5/25/96
6/8/96
6/22/96
7/6/96
7/20/96
8/3/96
8/17/96
8/31/96
9/14/96
9/28/96
10/12/96
10/26/96
11/9/96
11/23/96
12/7/96
12/21/96
1/4/97
1/18/97
2/1/97
2/15/97

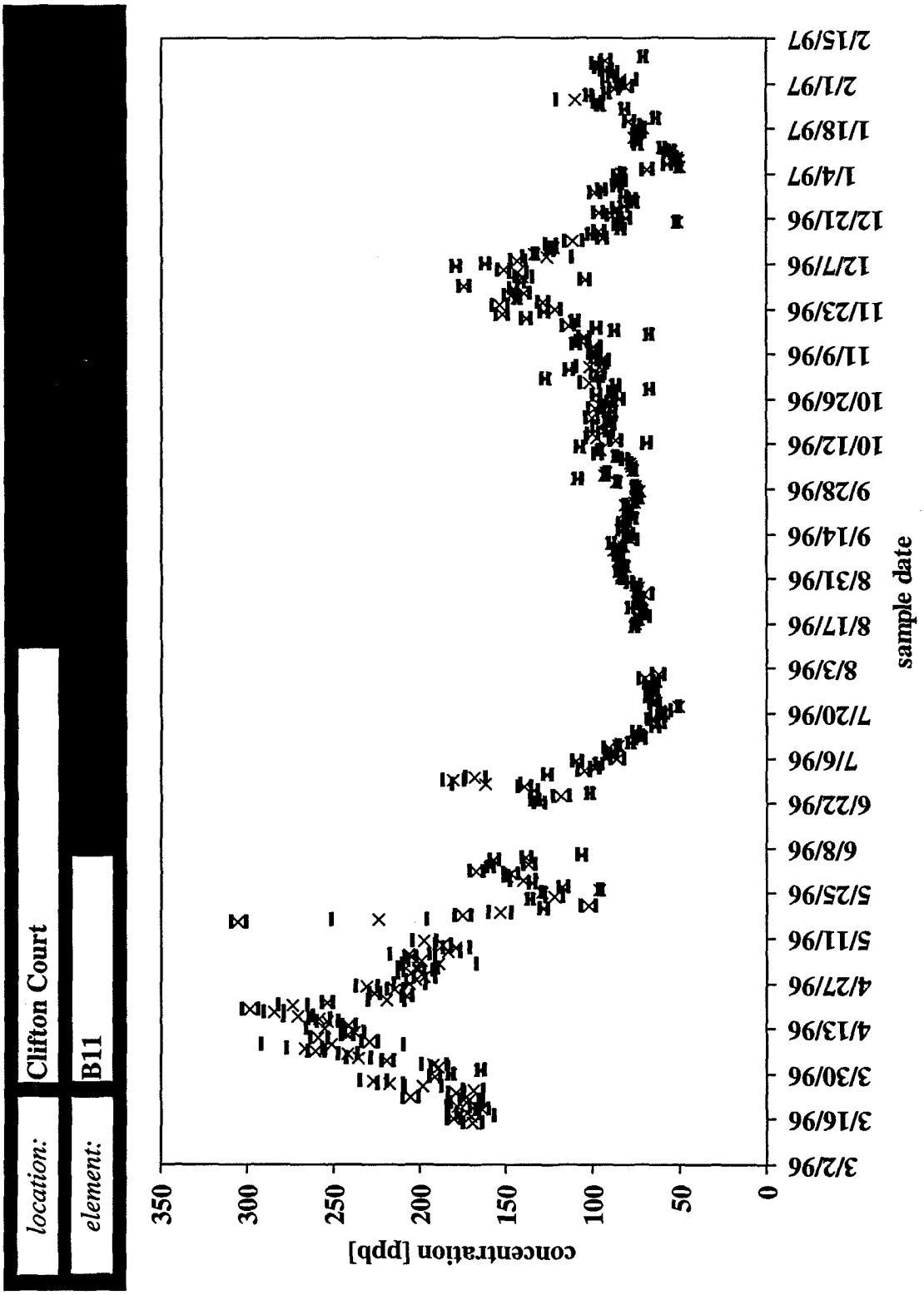
location:
Clifton Court
element:
B11
concentration [ppb]
0
50
100
150
200
250
300
350
sample date
3/2/96
3/16/96
3/30/96
4/13/96
4/27/96
5/11/96
5/25/96
6/8/96
6/22/96
7/6/96
7/20/96
8/3/96
8/17/96
8/31/96
9/14/96
9/28/96
10/12/96
10/26/96
11/9/96
11/23/96
12/7/96
12/21/96
1/4/97
1/18/97
2/1/97
2/15/97

location:
Clifton Court
element:
Na23
concentration [ppb]
80000
70000
60000
50000
40000
30000
20000
10000
0
sample date
3/2/96
3/16/96
3/30/96
4/13/96
4/27/96
5/11/96
5/25/96
6/8/96
6/22/96
7/6/96
7/20/96
8/3/96
8/17/96
8/31/96
9/14/96
9/28/96
10/12/96
10/26/96
11/9/96
11/23/96
12/7/96
12/21/96
1/4/97
1/18/97
2/1/97
2/15/97

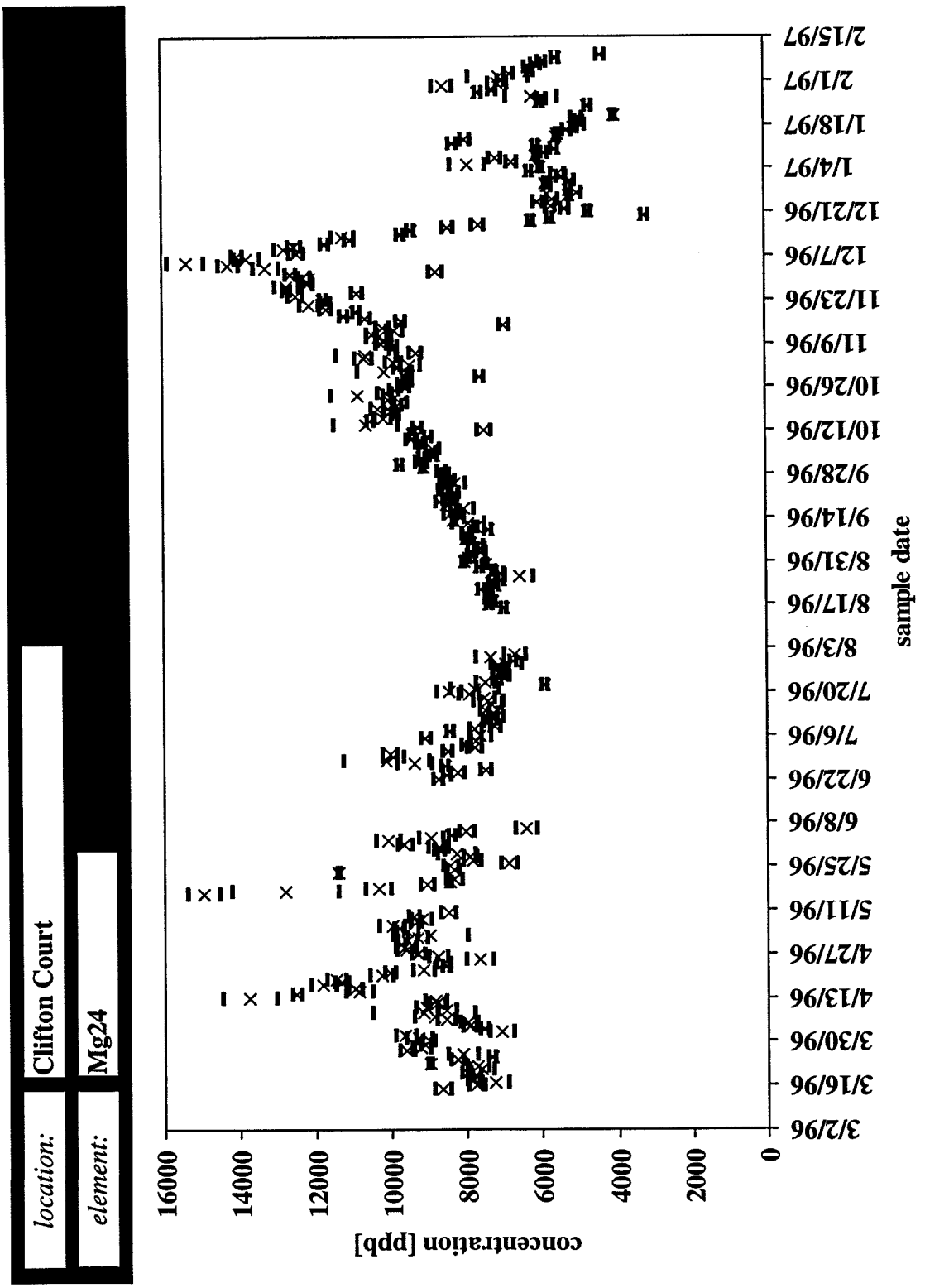
location:
Clifton Court
element:
Mg24
concentration [ppb]
16000
14000
12000
10000
8000
6000
4000
2000
0
sample date
3/2/96
3/16/96
3/30/96
4/13/96
4/27/96
5/11/96
5/25/96
6/8/96
6/22/96
7/6/96
7/20/96
8/3/96
8/17/96
8/31/96
9/14/96
9/28/96
10/12/96
10/26/96
11/9/96
11/23/96
12/7/96
12/21/96
1/4/97
1/18/97
2/1/97
2/15/97

location:
Clifton Court
element:
Si29
concentration [ppb]
35000
30000
25000
20000
15000
10000
5000
0
-5000
-10000
sample date
3/2/96
3/16/96
3/30/96
4/13/96
4/27/96
5/11/96
5/25/96
6/8/96
6/22/96
7/6/96
7/20/96
8/3/96
8/17/96
8/31/96
9/14/96
9/28/96
10/12/96
10/26/96
11/9/96
11/23/96
12/7/96
12/21/96
1/4/97
1/18/97
2/1/97
2/15/97

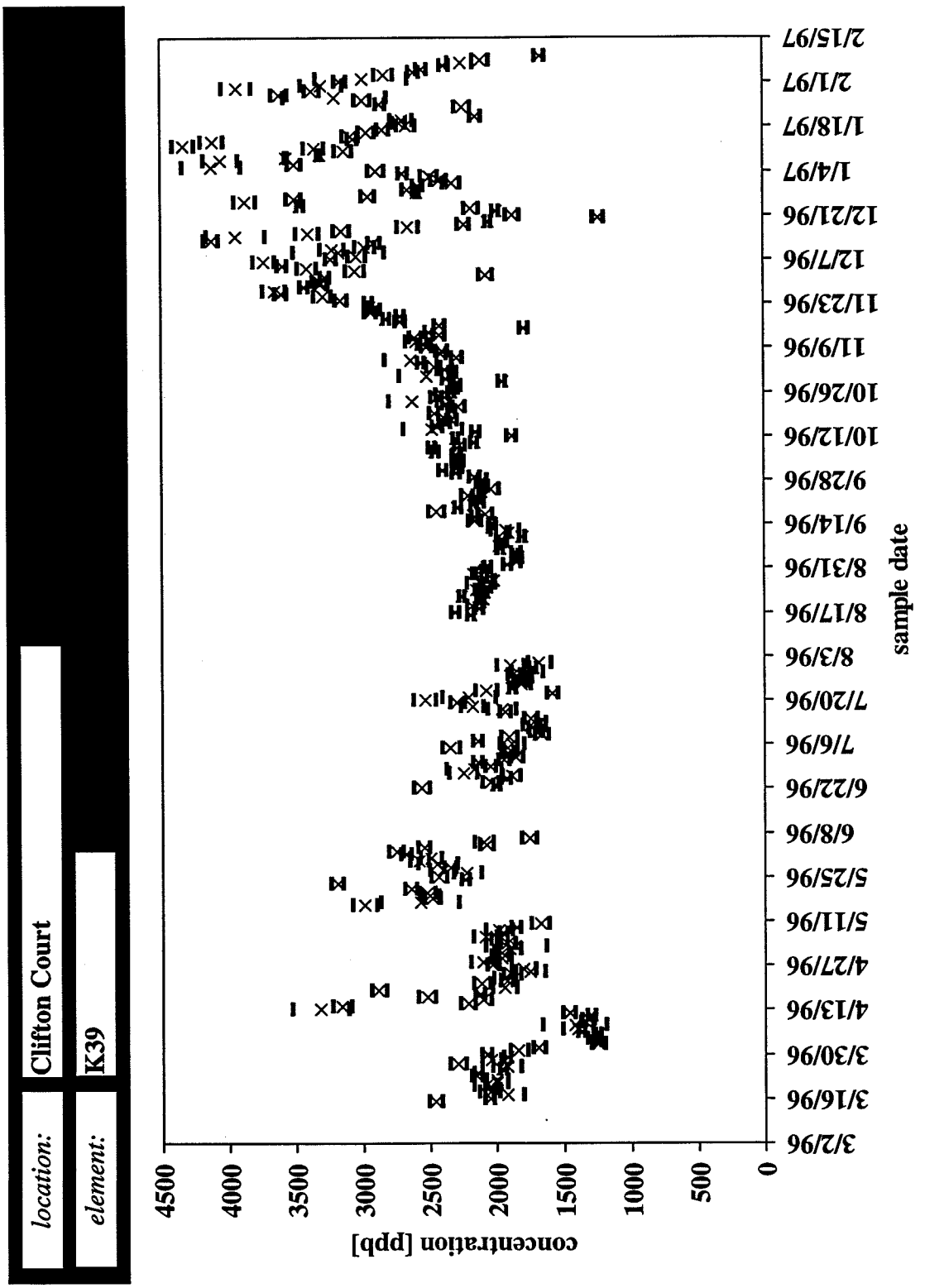
location:
Clifton Court
element:
K39
concentration [ppb]
4500
4000
3500
3000
2500
2000
1500
1000
500
0
sample date
3/2/96
3/16/96
3/30/96
4/13/96
4/27/96
5/11/96
5/25/96
6/8/96
6/22/96
7/6/96
7/20/96
8/3/96
8/17/96
8/31/96
9/14/96
9/28/96
10/12/96
10/26/96
11/9/96
11/23/96
12/7/96
12/21/96
1/4/97
1/18/97
2/1/97
2/15/97

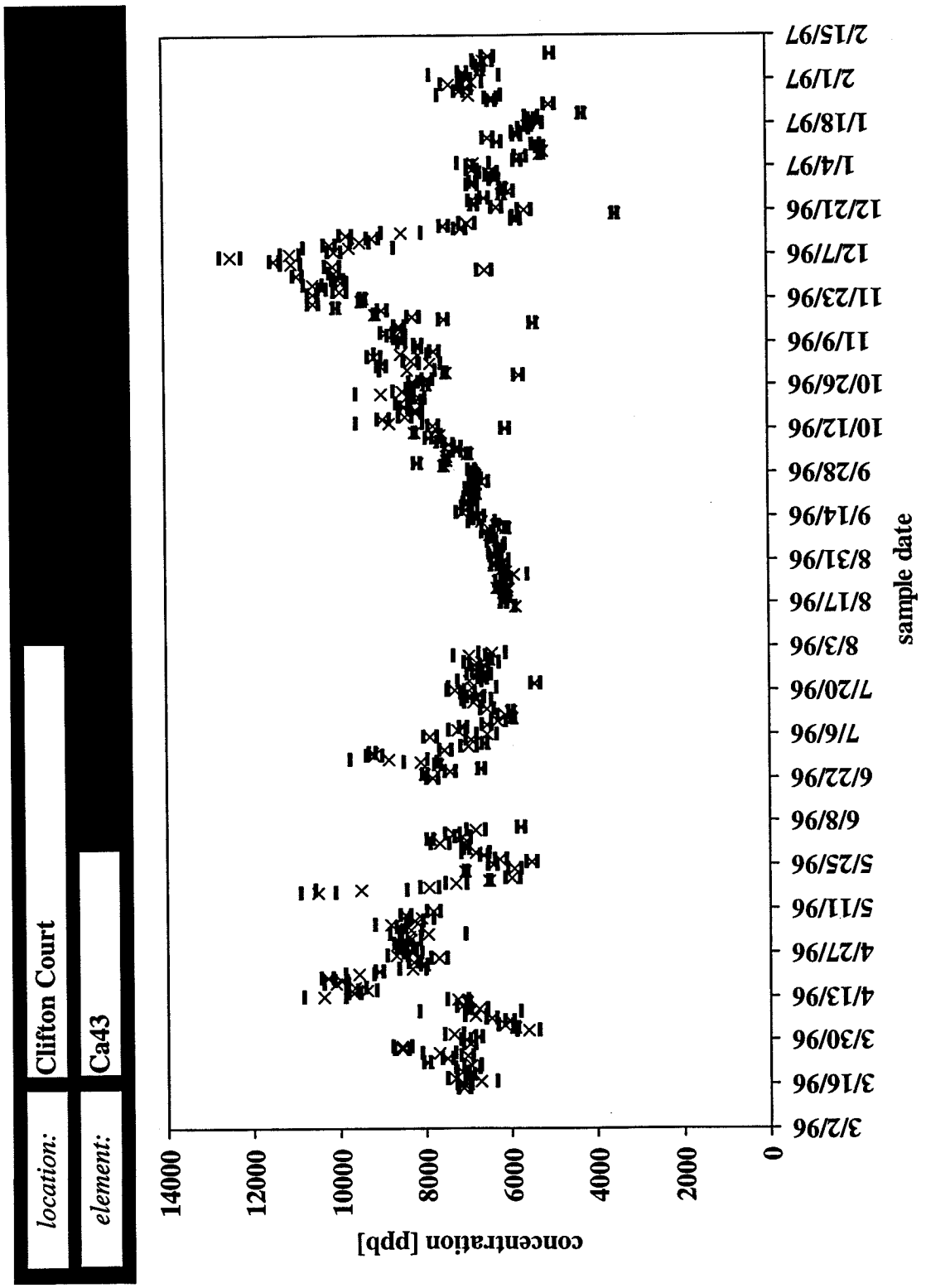
location:
Clifton Court
element:
Ca43
concentration [ppb]
0
2000
4000
6000
8000
10000
12000
14000
sample date
3/2/96
3/16/96
3/30/96
4/13/96
4/27/96
5/11/96
5/25/96
6/8/96
6/22/96
7/6/96
7/20/96
8/3/96
8/17/96
8/31/96
9/14/96
9/28/96
10/12/96
10/26/96
11/9/96
11/23/96
12/7/96
12/21/96
1/4/97
1/18/97
2/1/97
2/15/97

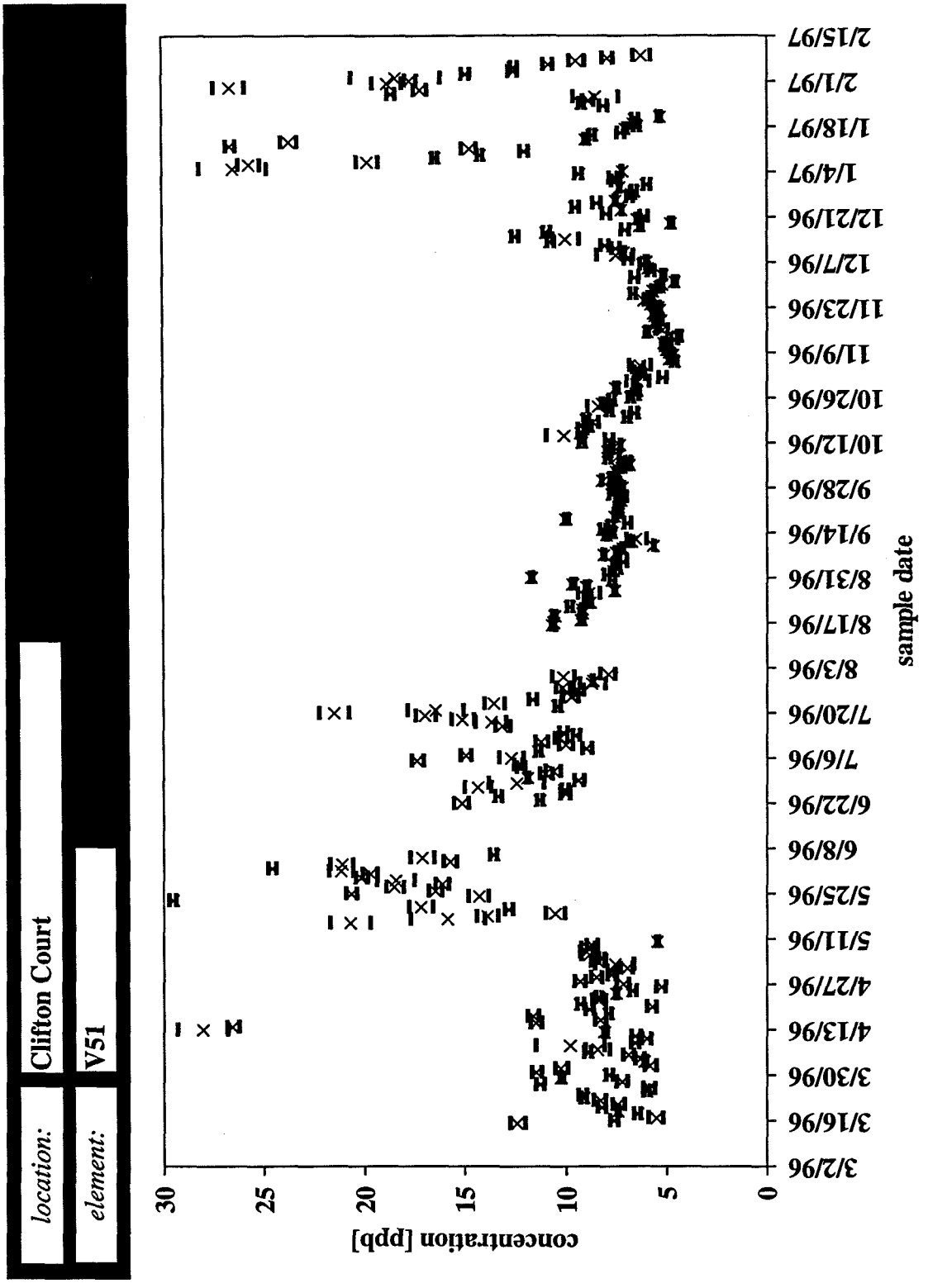
location:
Clifton Court
element:
V51
concentration [ppb]
0
5
10
15
20
25
30
sample date
3/2/96
3/16/96
3/30/96
4/13/96
4/27/96
5/11/96
5/25/96
6/8/96
6/22/96
7/6/96
7/20/96
8/3/96
8/17/96
8/31/96
9/14/96
9/28/96
10/12/96
10/26/96
11/9/96
11/23/96
12/7/96
12/21/96
1/4/97
1/18/97
2/1/97
2/15/97

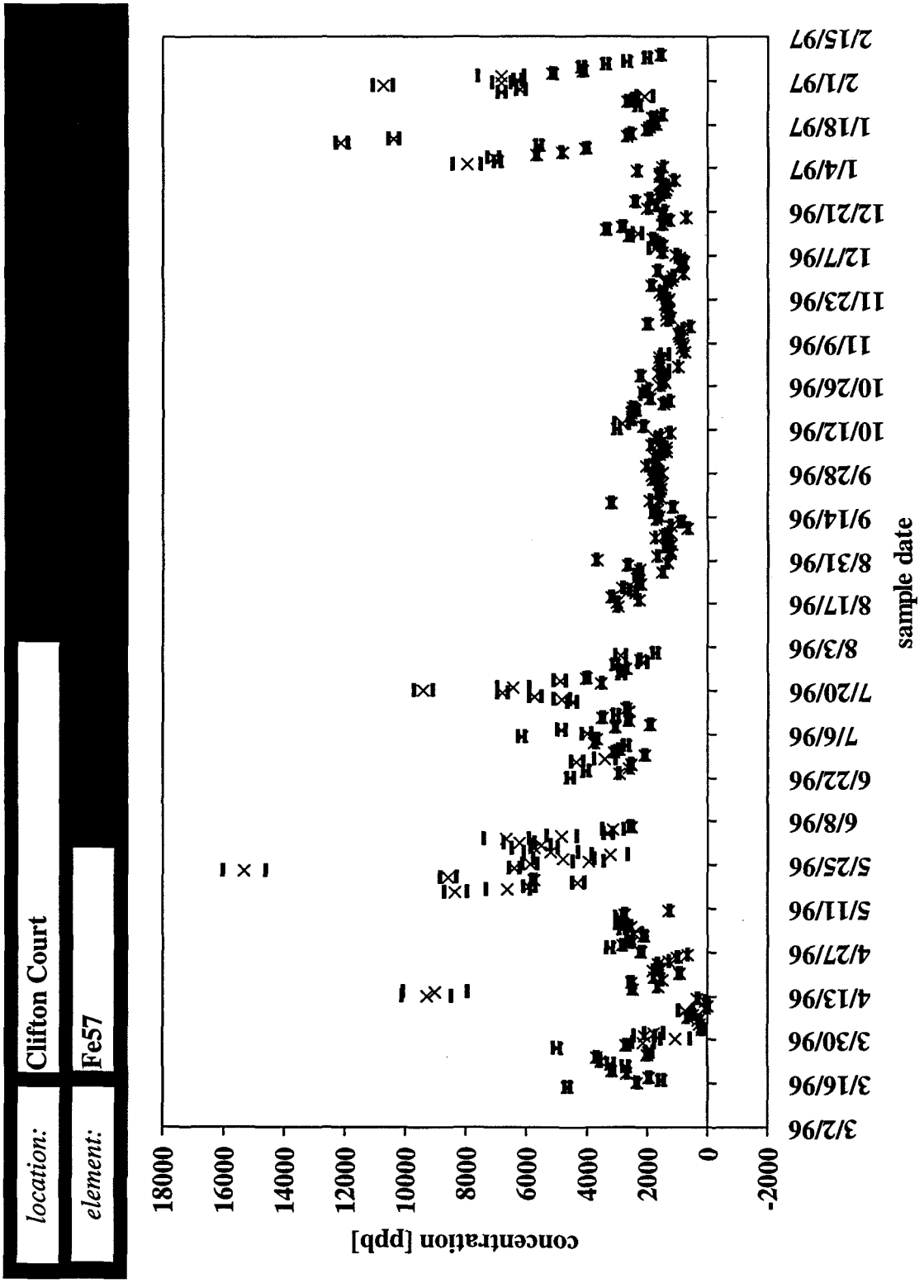
location:
Clifton Court
element:
Fe57
concentration [ppb]
18000
16000
14000
12000
10000
8000
6000
4000
2000
0
-2000
sample date
3/2/96
3/16/96
3/30/96
4/13/96
4/27/96
5/11/96
5/25/96
6/8/96
6/22/96
7/6/96
7/20/96
8/3/96
8/17/96
8/31/96
9/14/96
9/28/96
10/12/96
10/26/96
11/9/96
11/23/96
12/7/96
12/21/96
1/4/97
1/18/97
2/1/97
2/15/97

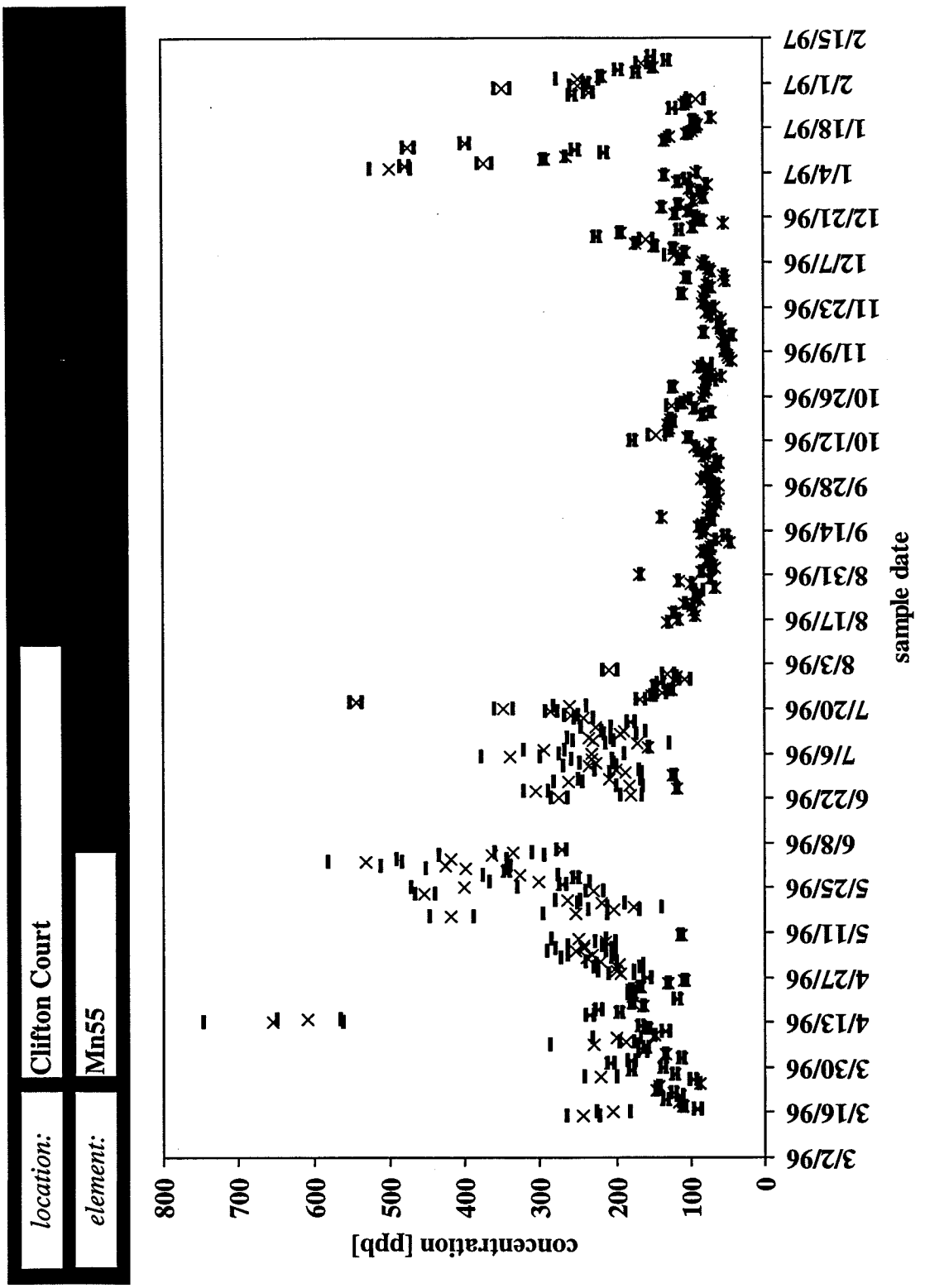
location:
Clifton Court
element:
Mn55
concentration [ppb]
0
100
200
300
400
500
600
700
800
sample date
3/2/96
3/16/96
3/30/96
4/13/96
4/27/96
5/11/96
5/25/96
6/8/96
6/22/96
7/6/96
7/20/96
8/3/96
8/17/96
8/31/96
9/14/96
9/28/96
10/12/96
10/26/96
11/9/96
11/23/96
12/7/96
12/21/96
1/4/97
1/18/97
2/1/97
2/15/97

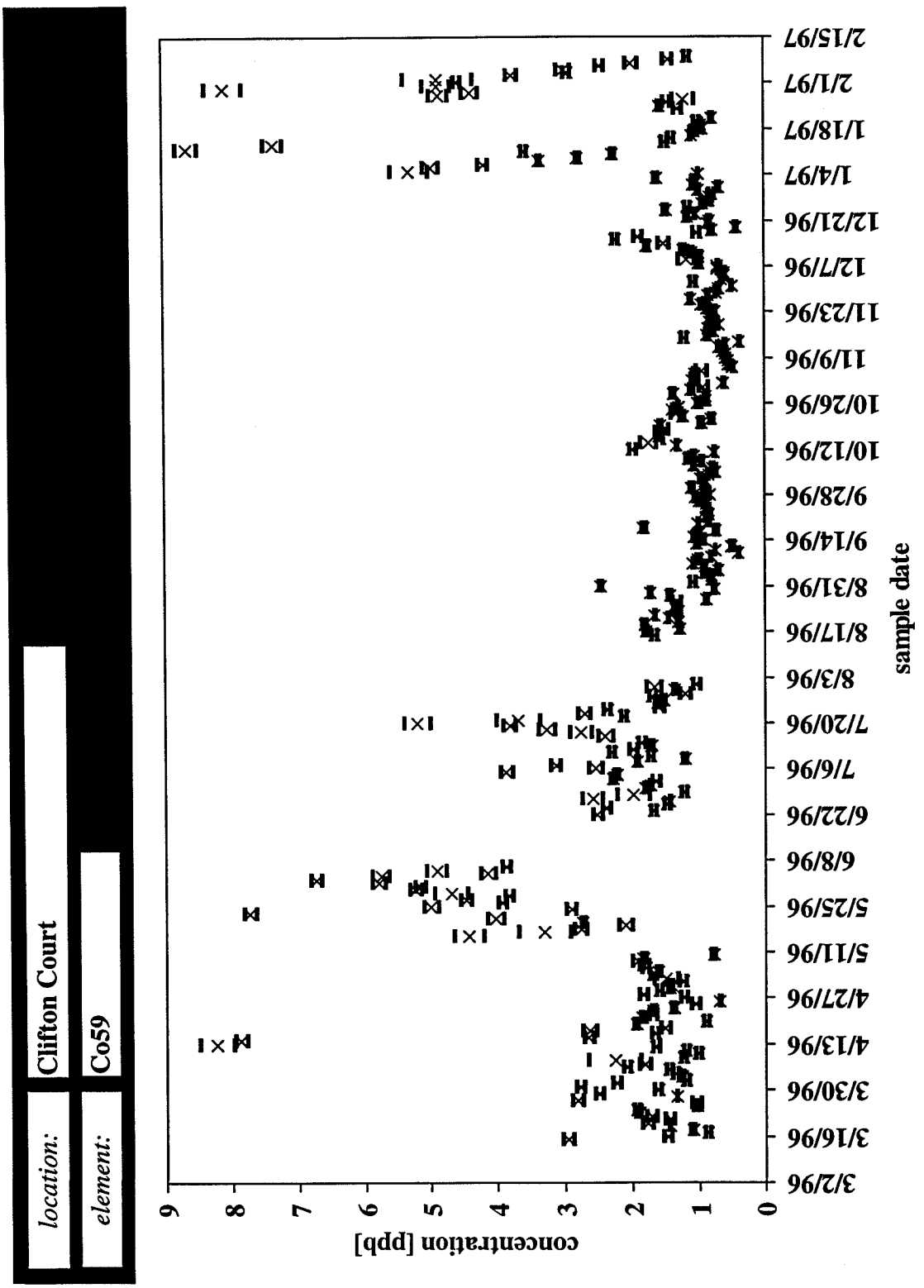
location:
Clifton Court
element:
Co59
concentration [ppb]
0
1
2
3
4
5
6
7
8
9
sample date
3/2/96
3/16/96
3/30/96
4/13/96
4/27/96
5/11/96
5/25/96
6/8/96
6/22/96
7/6/96
7/20/96
8/3/96
8/17/96
8/31/96
9/14/96
9/28/96
10/12/96
10/26/96
11/9/96
11/23/96
12/7/96
12/21/96
1/4/97
1/18/97
2/1/97
2/15/97

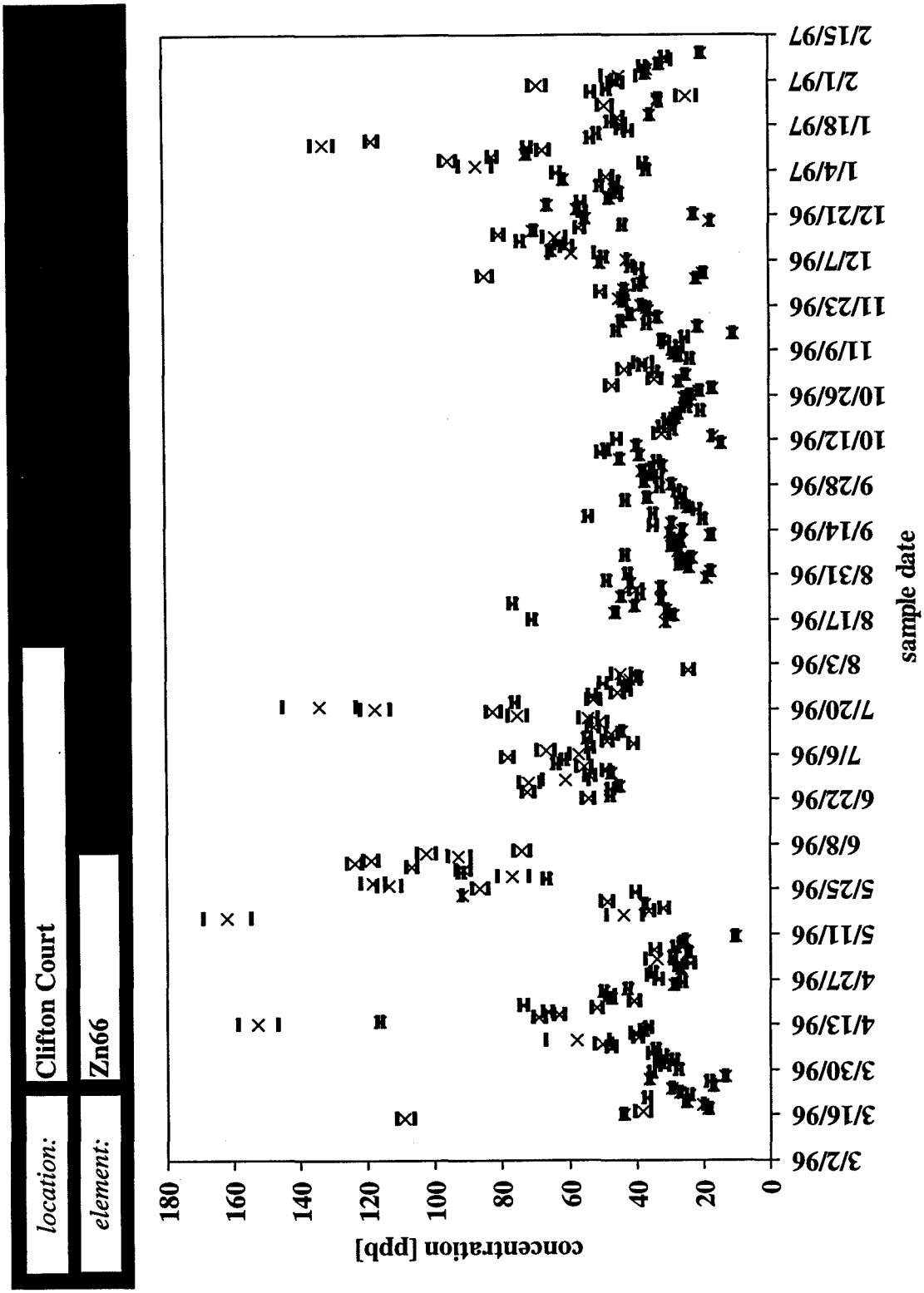
location:
Clifton Court
element:
Zn66
concentration [ppb]
0
20
40
60
80
100
120
140
160
180
sample date
3/2/96
3/16/96
3/30/96
4/13/96
4/27/96
5/11/96
5/25/96
6/8/96
6/22/96
7/6/96
7/20/96
8/3/96
8/17/96
8/31/96
9/14/96
9/28/96
10/12/96
10/26/96
11/9/96
11/23/96
12/7/96
12/21/96
1/4/97
1/18/97
2/1/97
2/15/97

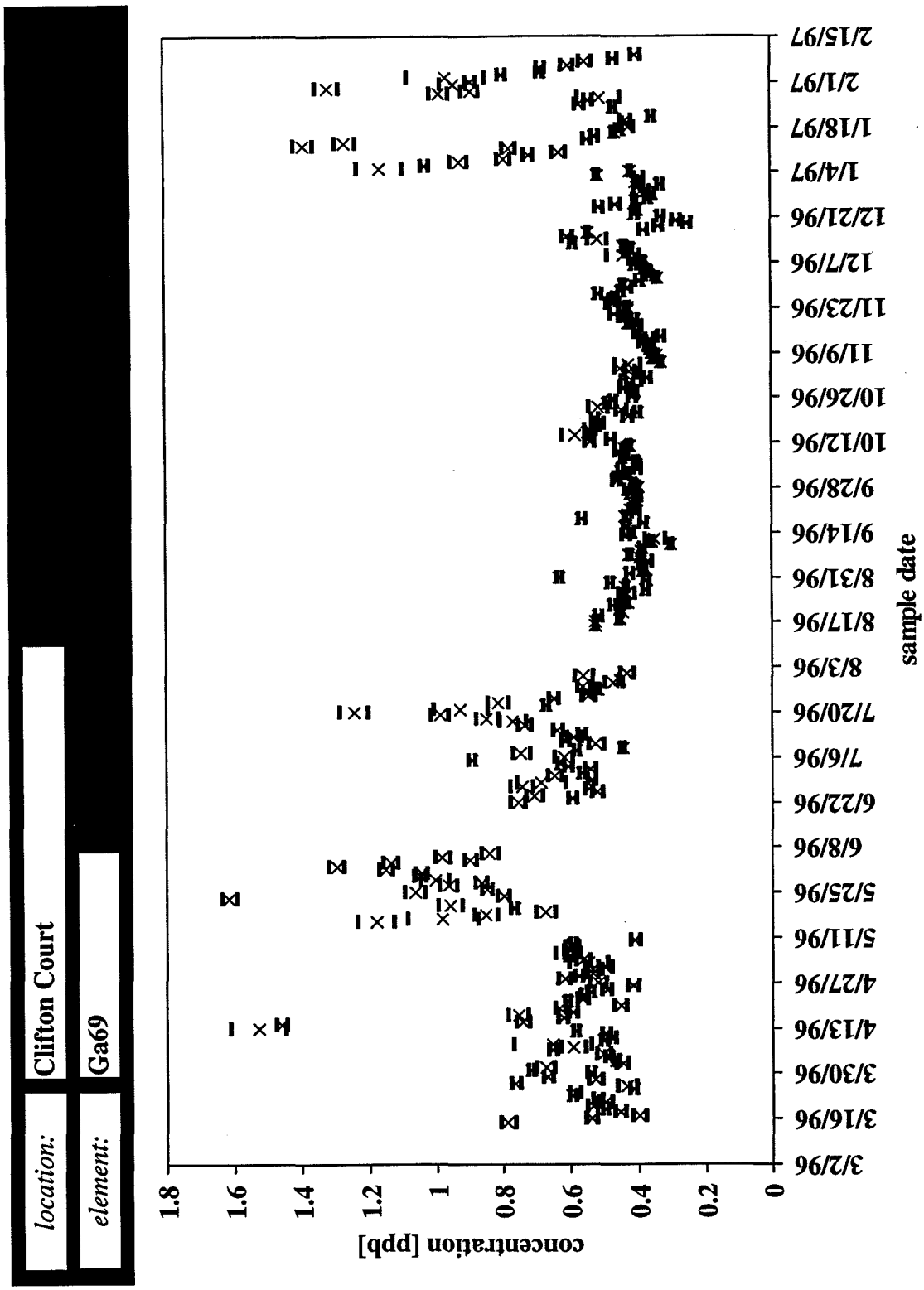
location:
Clifton Court
element:
Ga69
concentration [ppb]
1.8
1.6
1.4
1.2
1
0.8
0.6
0.4
0.2
0
sample date
3/2/96
3/16/96
3/30/96
4/13/96
4/27/96
5/11/96
5/25/96
6/8/96
6/22/96
7/6/96
7/20/96
8/3/96
8/17/96
8/31/96
9/14/96
9/28/96
10/12/96
10/26/96
11/9/96
11/23/96
12/7/96
12/21/96
1/4/97
1/18/97
2/1/97
2/15/97

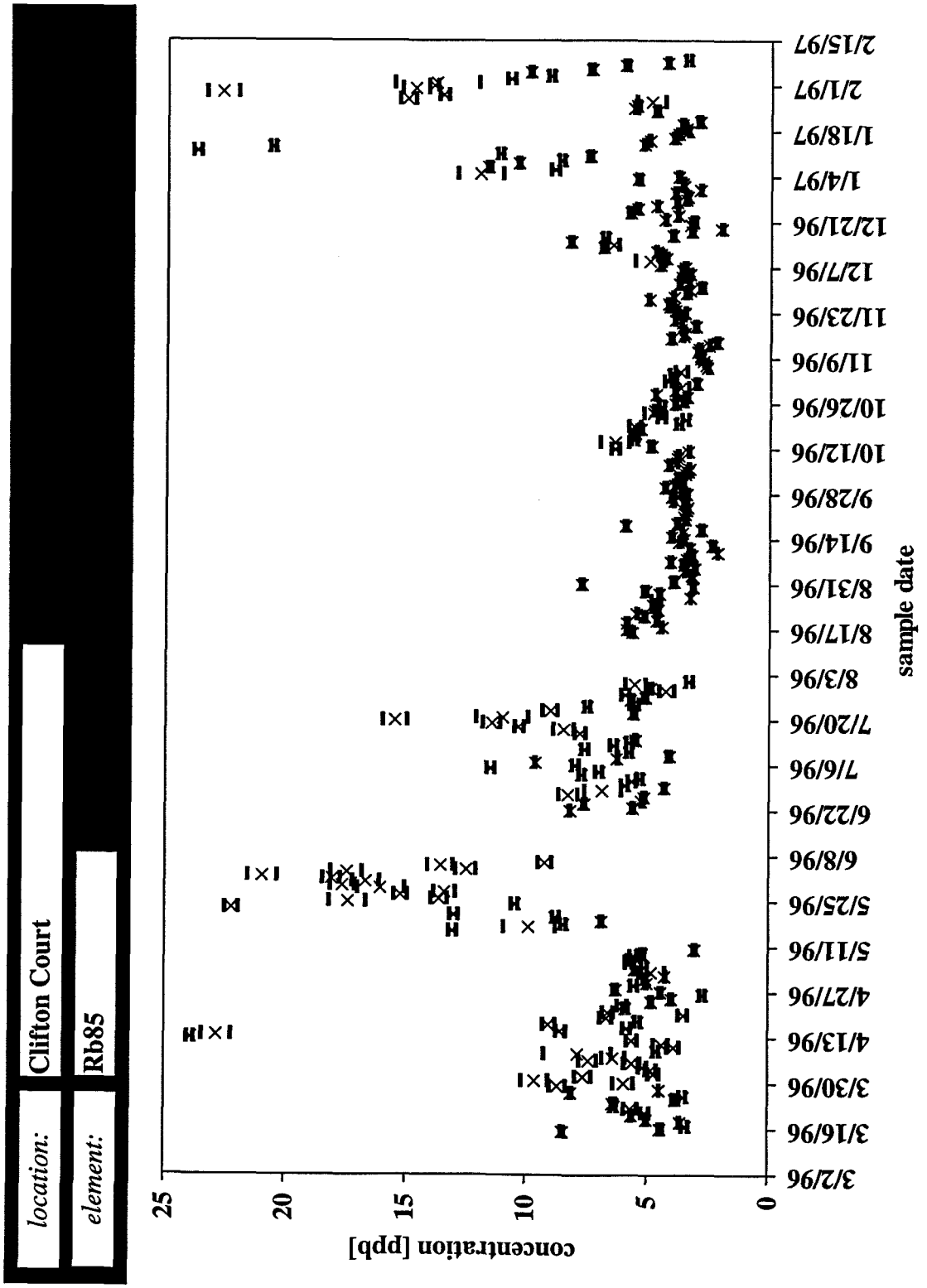
location:
Clifton Court
element:
Rb85
concentration [ppb]
0
5
10
15
20
25
sample date
3/2/96
3/16/96
3/30/96
4/13/96
4/27/96
5/11/96
5/25/96
6/8/96
6/22/96
7/6/96
7/20/96
8/3/96
8/17/96
8/31/96
9/14/96
9/28/96
10/12/96
10/26/96
11/9/96
11/23/96
12/7/96
12/21/96
1/4/97
1/18/97
2/1/97
2/15/97

location:
Clifton Court
element:
Sr87
concentration [ppb]
300
250
200
150
100
50
0
sample date
3/2/96
3/16/96
3/30/96
4/13/96
4/27/96
5/11/96
5/25/96
6/8/96
6/22/96
7/6/96
7/20/96
8/3/96
8/17/96
8/31/96
9/14/96
9/28/96
10/12/96
10/26/96
11/9/96
11/23/96
12/7/96
12/21/96
1/4/97
1/18/97
2/1/97
2/15/97

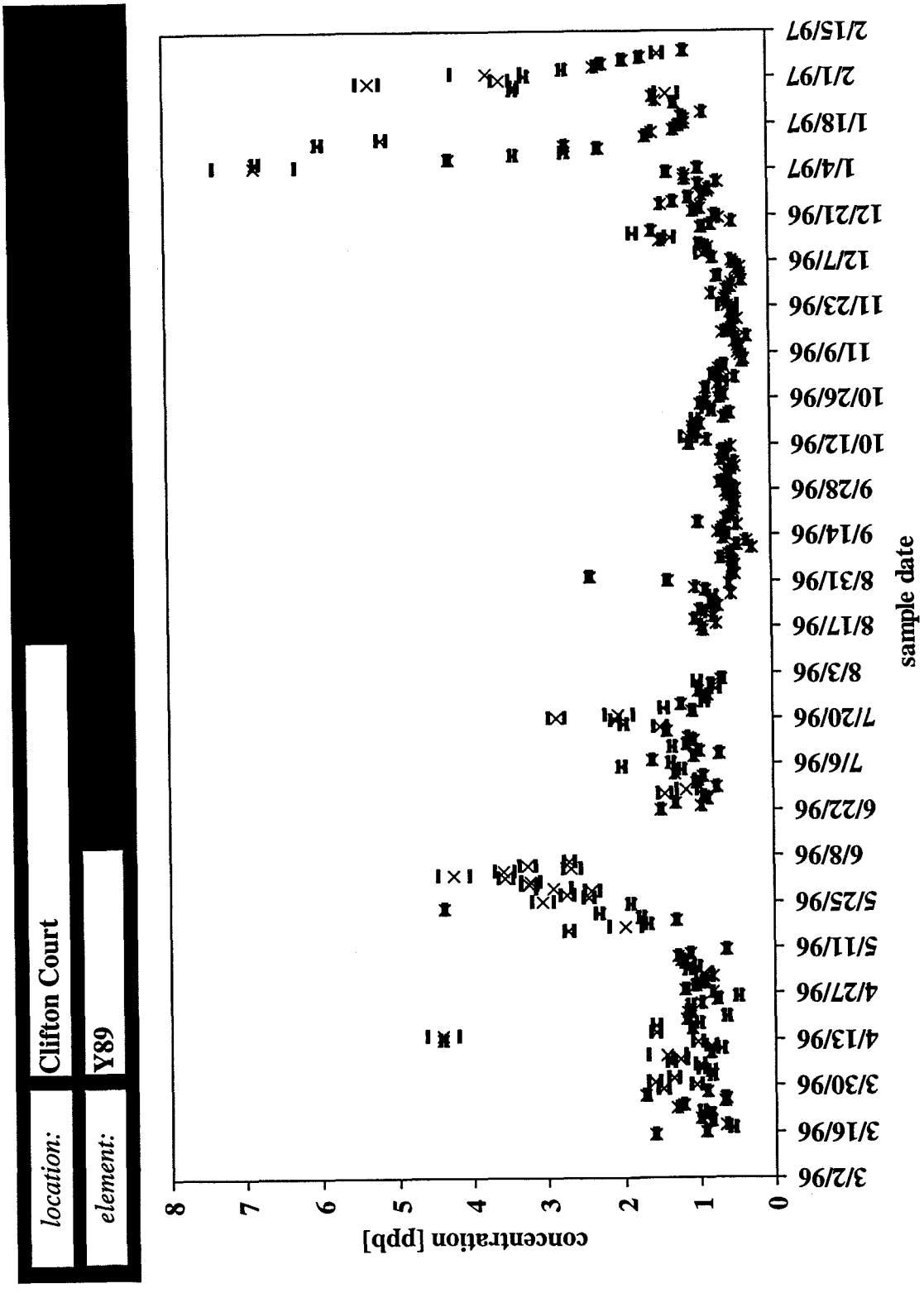
location:
Clifton Court
element:
Y89
concentration [ppb]
0
1
2
3
4
5
6
7
8
sample date
3/2/96
3/16/96
3/30/96
4/13/96
4/27/96
5/11/96
5/25/96
6/8/96
6/22/96
7/6/96
7/20/96
8/3/96
8/17/96
8/31/96
9/14/96
9/28/96
10/12/96
10/26/96
11/9/96
11/23/96
12/7/96
12/21/96
1/4/97
1/18/97
2/1/97
2/15/97

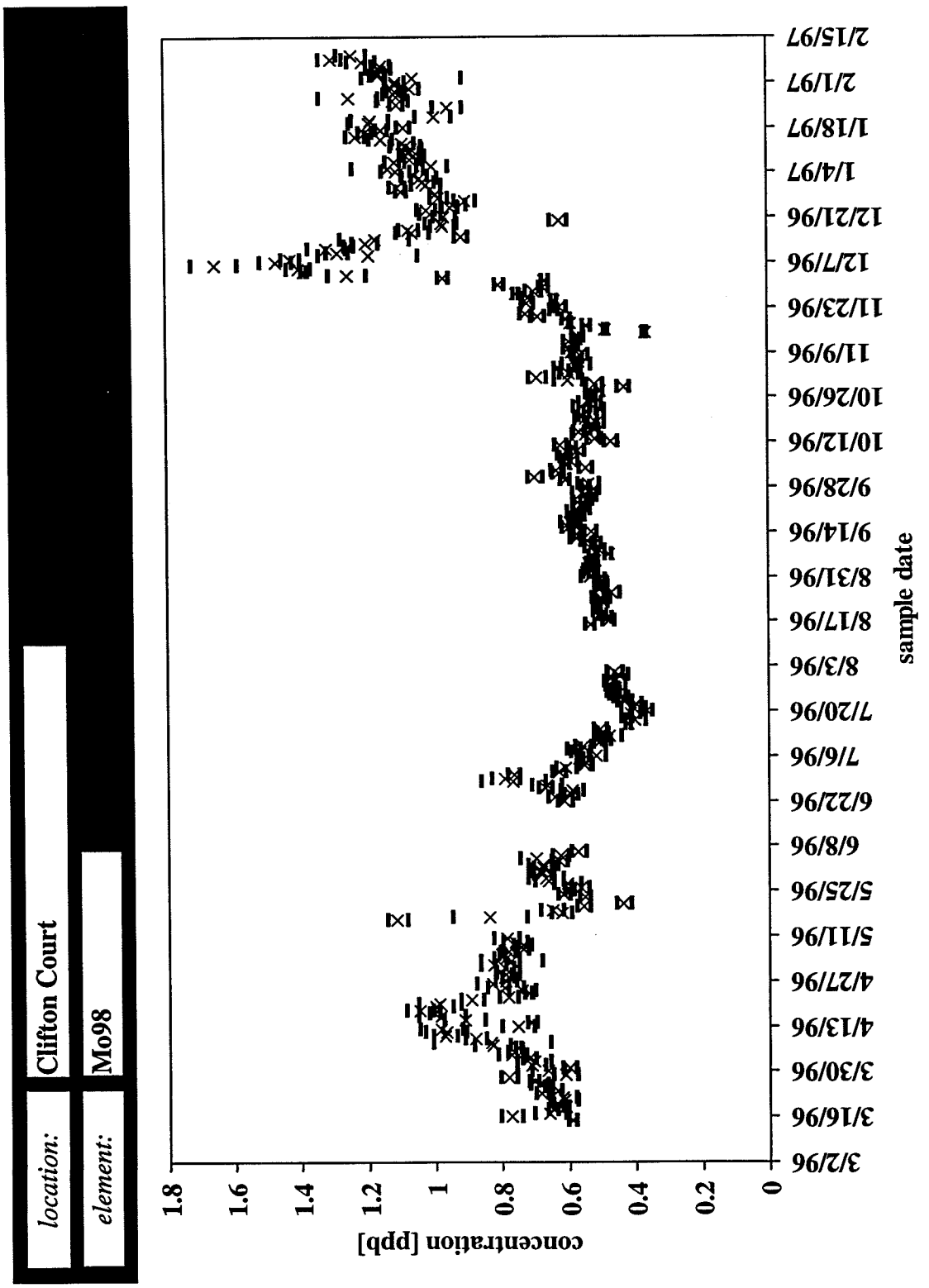
location:
Clifton Court
element:
Mo98
concentration [ppb]
1.8
1.6
1.4
1.2
1
0.8
0.6
0.4
0.2
0
sample date
3/2/96
3/16/96
3/30/96
4/13/96
4/27/96
5/11/96
5/25/96
6/8/96
6/22/96
7/6/96
7/20/96
8/3/96
8/17/96
8/31/96
9/14/96
9/28/96
10/12/96
10/26/96
11/9/96
11/23/96
12/7/96
12/21/96
1/4/97
1/18/97
2/1/97
2/15/97

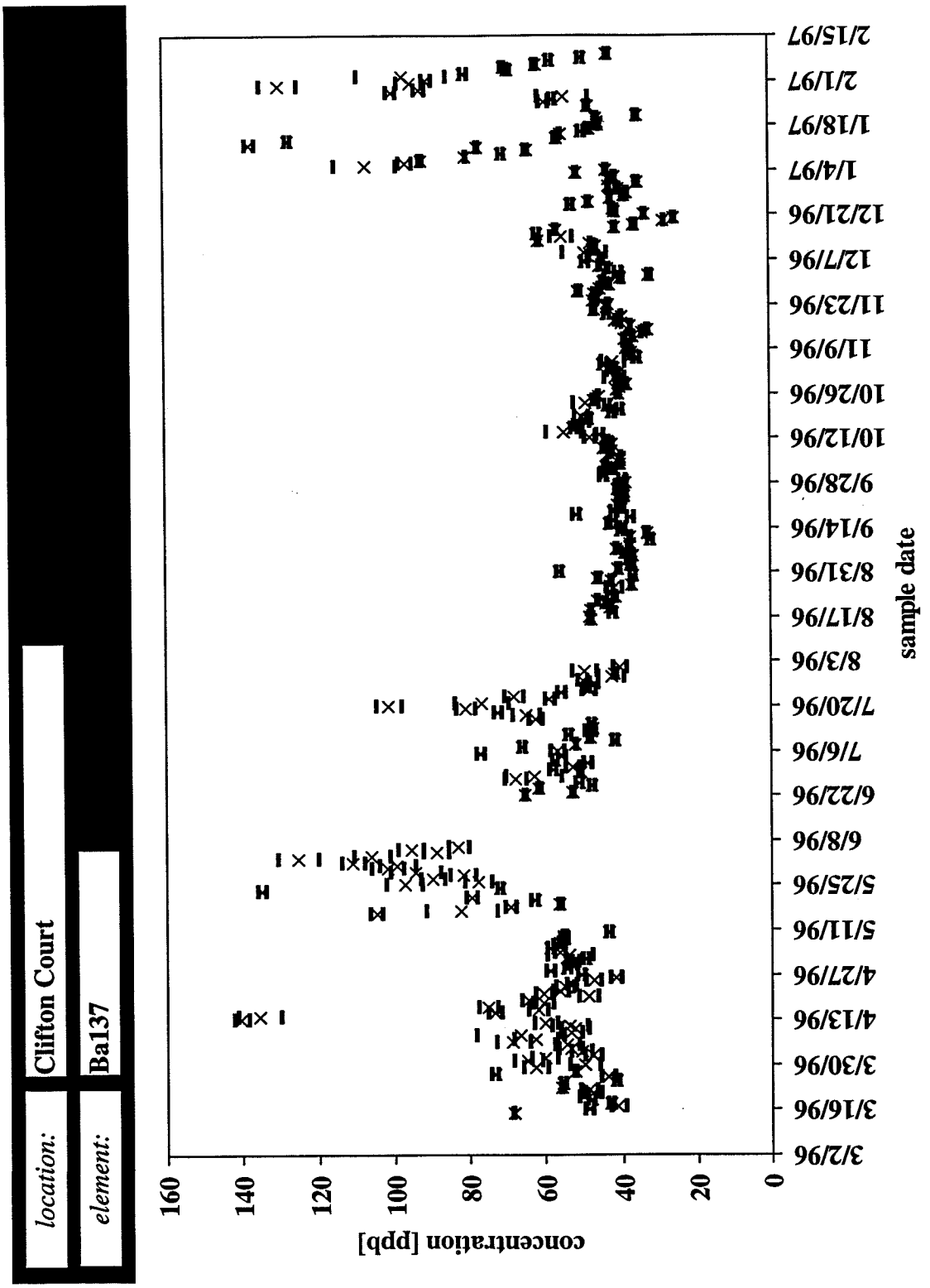
location:
Clifton Court
element:
Ba137
concentration [ppb]
0
20
40
60
80
100
120
140
160
sample date
3/2/96
3/16/96
3/30/96
4/13/96
4/27/96
5/11/96
5/25/96
6/8/96
6/22/96
7/6/96
7/20/96
8/3/96
8/17/96
8/31/96
9/14/96
9/28/96
10/12/96
10/26/96
11/9/96
11/23/96
12/7/96
12/21/96
1/4/97
1/18/97
2/1/97
2/15/97

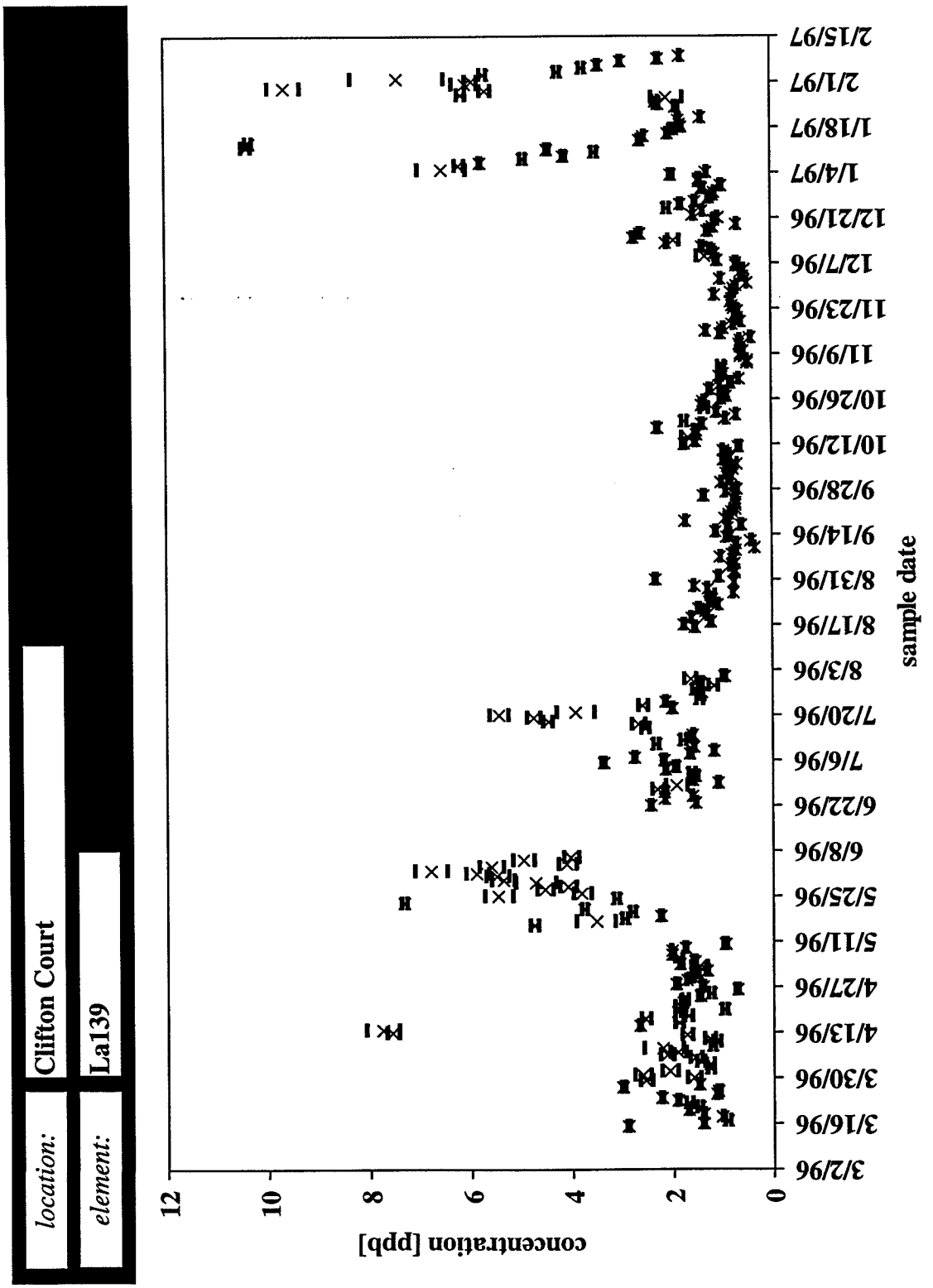
location:
Clifton Court
element:
La139
concentration [ppb]
0
2
4
6
8
10
12
sample date
3/2/96
3/16/96
3/30/96
4/13/96
4/27/96
5/11/96
5/25/96
6/8/96
6/22/96
7/6/96
7/20/96
8/3/96
8/17/96
8/31/96
9/14/96
9/28/96
10/12/96
10/26/96
11/9/96
11/23/96
12/7/96
12/21/96
1/4/97
1/18/97
2/1/97
2/15/97

location:
Clifton Court
element:
Ce140
concentration [ppb]
0
5
10
15
20
25
sample date
3/2/96
3/16/96
3/30/96
4/13/96
4/27/96
5/11/96
5/25/96
6/8/96
6/22/96
7/6/96
7/20/96
8/3/96
8/17/96
8/31/96
9/14/96
9/28/96
10/12/96
10/26/96
11/9/96
11/23/96
12/7/96
12/21/96
1/4/97
1/18/97
2/1/97
2/15/97

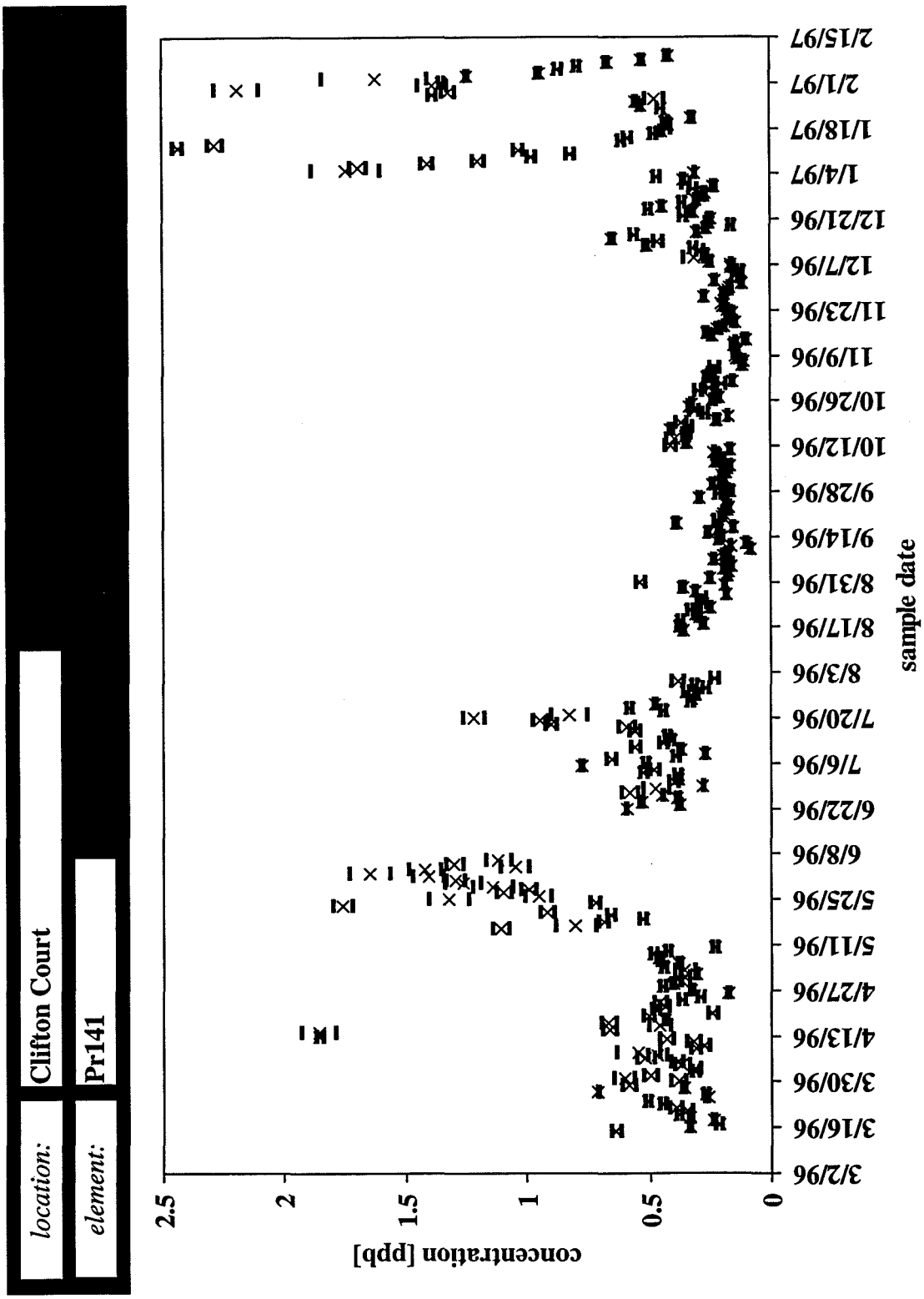
location:
Clifton Court
element:
Pr141
concentration [ppb]
2.5
2
1.5
1
0.5
0
sample date
3/2/96
3/16/96
3/30/96
4/13/96
4/27/96
5/11/96
5/25/96
6/8/96
6/22/96
7/6/96
7/20/96
8/3/96
8/17/96
8/31/96
9/14/96
9/28/96
10/12/96
10/26/96
11/9/96
11/23/96
12/7/96
12/21/96
1/4/97
1/18/97
2/1/97
2/15/97

location:
Clifton Court
element:
Nd146
concentration [ppb]
0
1
2
3
4
5
6
7
8
9
10
sample date
3/2/96
3/16/96
3/30/96
4/13/96
4/27/96
5/11/96
5/25/96
6/8/96
6/22/96
7/6/96
7/20/96
8/3/96
8/17/96
8/31/96
9/14/96
9/28/96
10/12/96
10/26/96
11/9/96
11/23/96
12/7/96
12/21/96
1/4/97
1/18/97
2/1/97
2/15/97

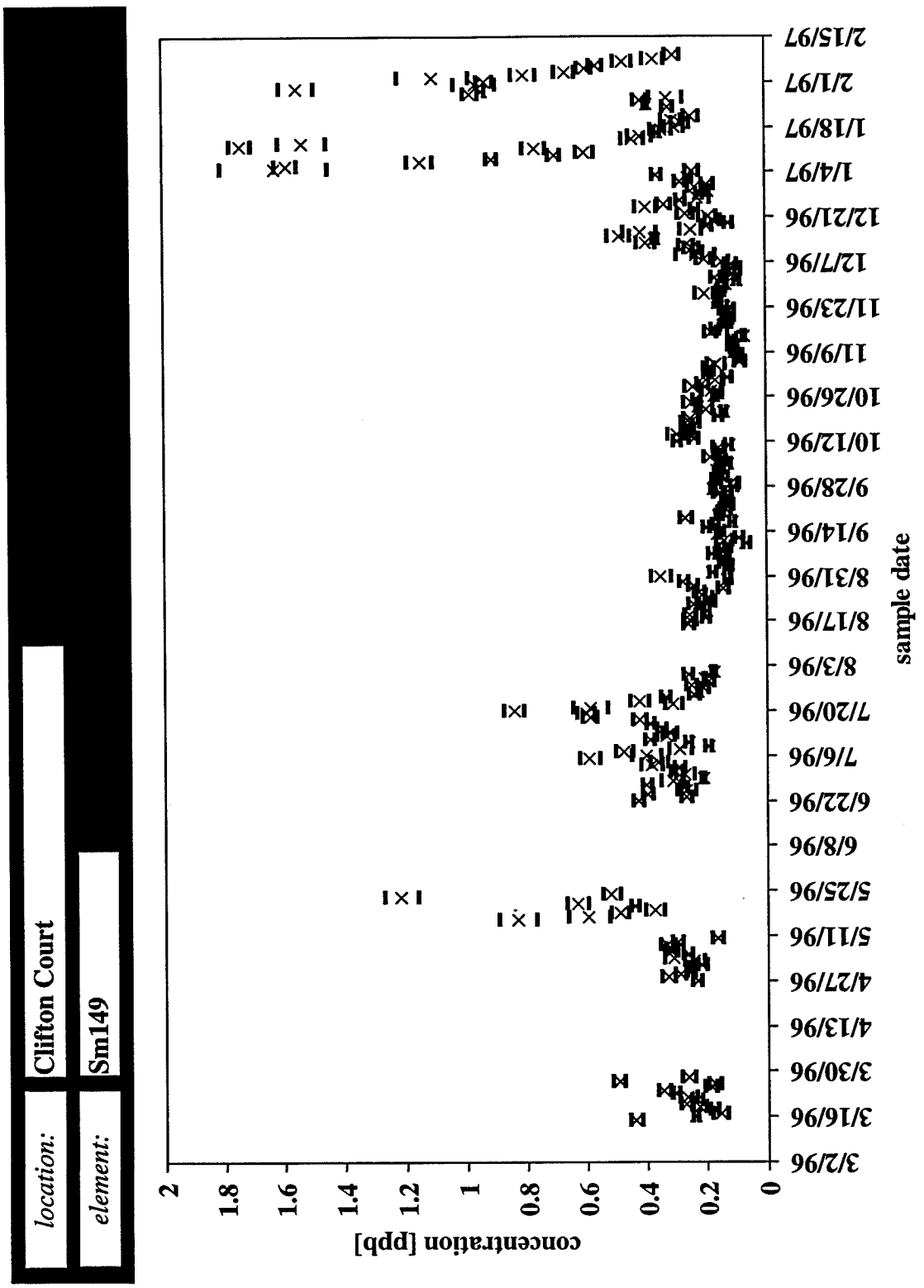
location:
Clifton Court
element:
Sm149
concentration [ppb]
0
0.2
0.4
0.6
0.8
1
1.2
1.4
1.6
1.8
2
sample date
3/2/96
3/16/96
3/30/96
4/13/96
4/27/96
5/11/96
5/25/96
6/8/96
6/22/96
7/6/96
7/20/96
8/3/96
8/17/96
8/31/96
9/14/96
9/28/96
10/12/96
10/26/96
11/9/96
11/23/96
12/7/96
12/21/96
1/4/97
1/18/97
2/1/97
2/15/97

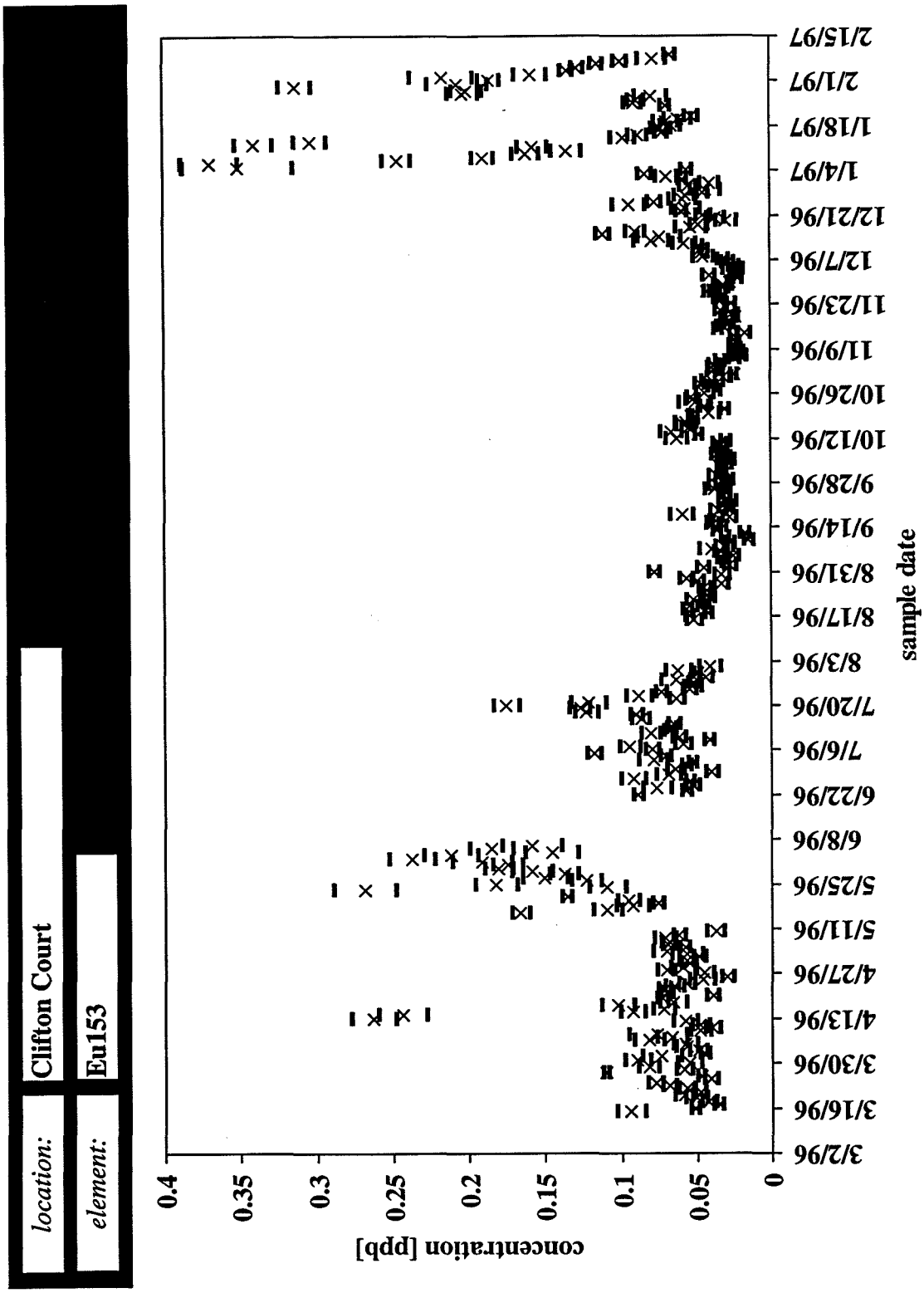
location:
Clifton Court
element:
Eu153
concentration [ppb]
0.4
0.35
0.3
0.25
0.2
0.15
0.1
0.05
0
sample date
3/2/96
3/16/96
3/30/96
4/13/96
4/27/96
5/11/96
5/25/96
6/8/96
6/22/96
7/6/96
7/20/96
8/3/96
8/17/96
8/31/96
9/14/96
9/28/96
10/12/96
10/26/96
11/9/96
11/23/96
12/7/96
12/21/96
1/4/97
1/18/97
2/1/97
2/15/97

location:
Clifton Court
element:
Gd157
concentration [ppb]
0
0.2
0.4
0.6
0.8
1
1.2
1.4
1.6
1.8
sample date
3/2/96
3/16/96
3/30/96
4/13/96
4/27/96
5/11/96
5/25/96
6/8/96
6/22/96
7/6/96
7/20/96
8/3/96
8/17/96
8/31/96
9/14/96
9/28/96
10/12/96
10/26/96
11/9/96
11/23/96
12/7/96
12/21/96
1/4/97
1/18/97
2/1/97
2/15/97

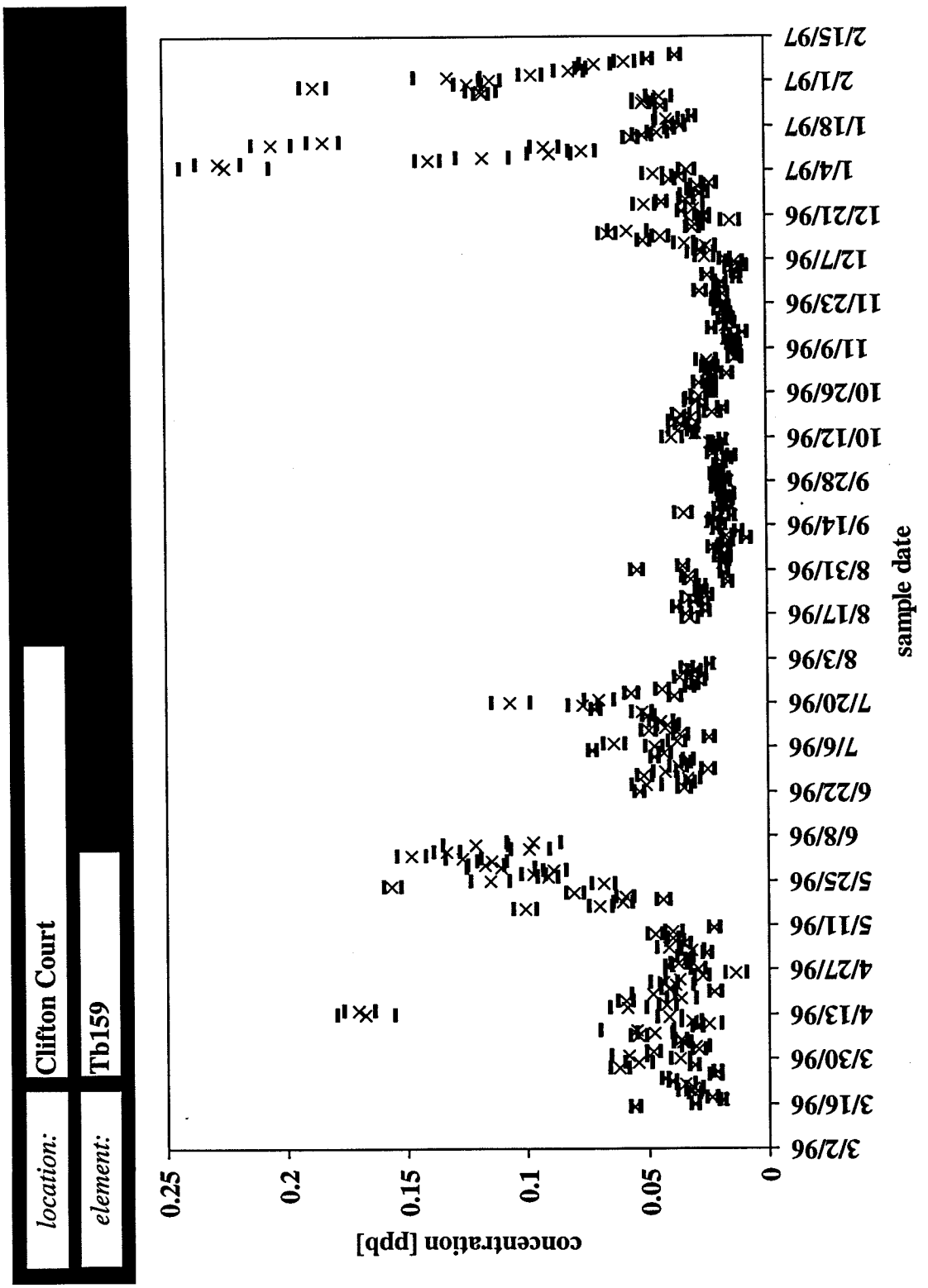
location:
Clifton Court
element:
Tb159
concentration [ppb]
0.25
0.2
0.15
0.1
0.05
0
sample date
3/2/96
3/16/96
3/30/96
4/13/96
4/27/96
5/11/96
5/25/96
6/8/96
6/22/96
7/6/96
7/20/96
8/3/96
8/17/96
8/31/96
9/14/96
9/28/96
10/12/96
10/26/96
11/9/96
11/23/96
12/7/96
12/21/96
1/4/97
1/18/97
2/1/97
2/15/97

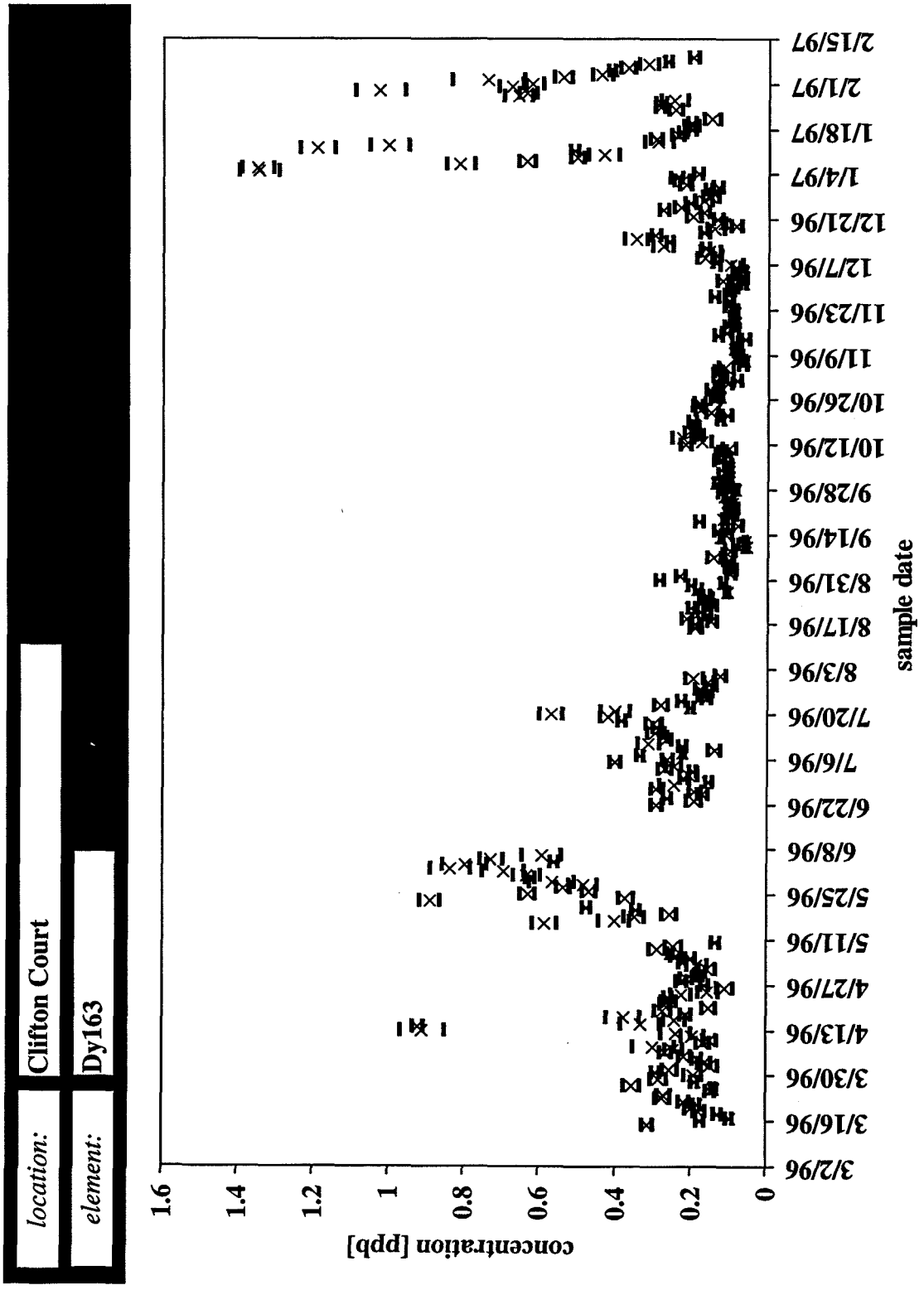
location:
Clifton Court
element:
Dy163
concentration [ppb]
0
0.2
0.4
0.6
0.8
1
1.2
1.4
1.6
sample date
3/2/96
3/16/96
3/30/96
4/13/96
4/27/96
5/11/96
5/25/96
6/8/96
6/22/96
7/6/96
7/20/96
8/3/96
8/17/96
8/31/96
9/14/96
9/28/96
10/12/96
10/26/96
11/9/96
11/23/96
12/7/96
12/21/96
1/4/97
1/18/97
2/1/97
2/15/97

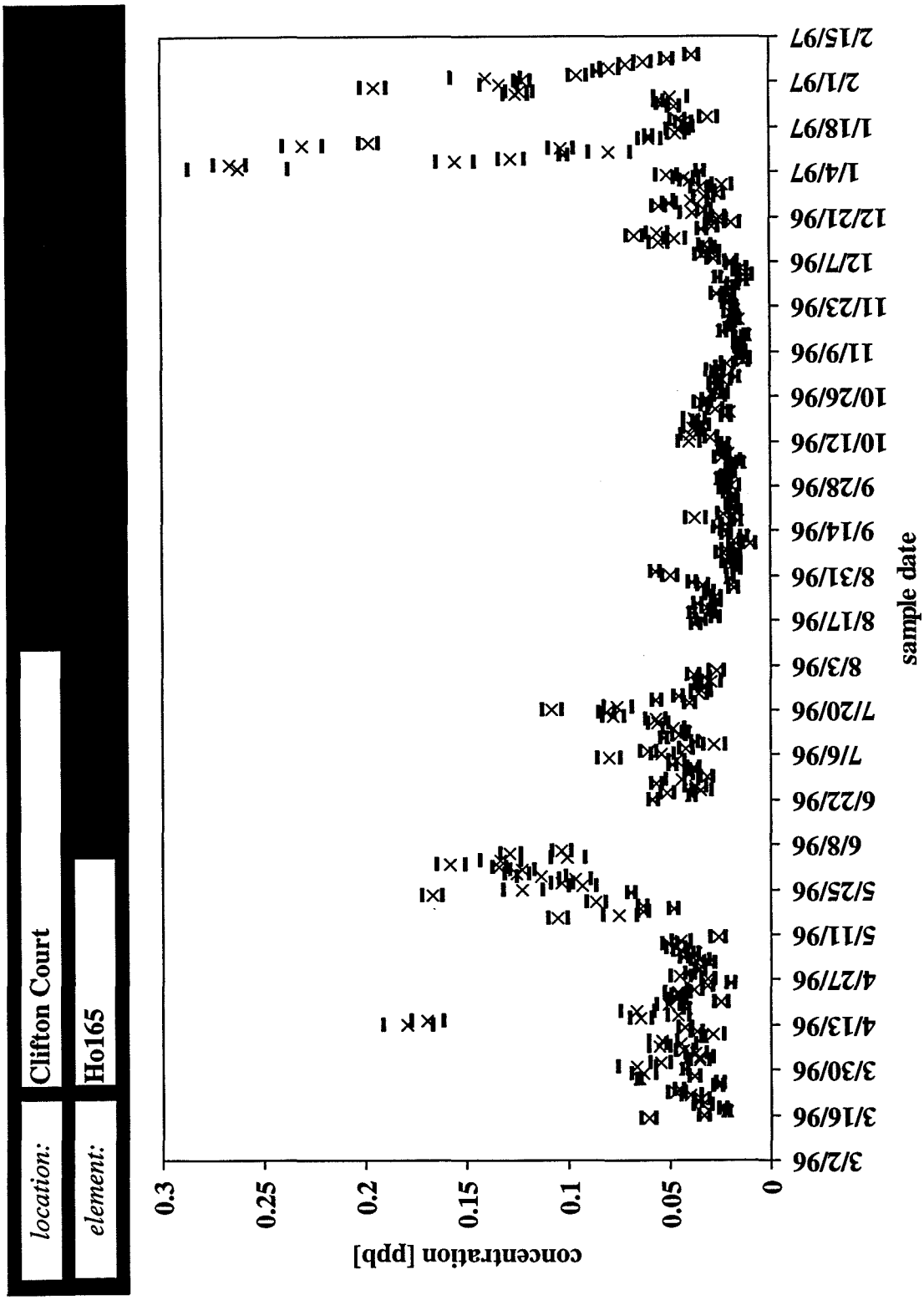
location:
Clifton Court
element:
Ho165
concentration [ppb]
0.3
0.25
0.2
0.15
0.1
0.05
0
sample date
3/2/96
3/16/96
3/30/96
4/13/96
4/27/96
5/11/96
5/25/96
6/8/96
6/22/96
7/6/96
7/20/96
8/3/96
8/17/96
8/31/96
9/14/96
9/28/96
10/12/96
10/26/96
11/9/96
11/23/96
12/7/96
12/21/96
1/4/97
1/18/97
2/1/97
2/15/97

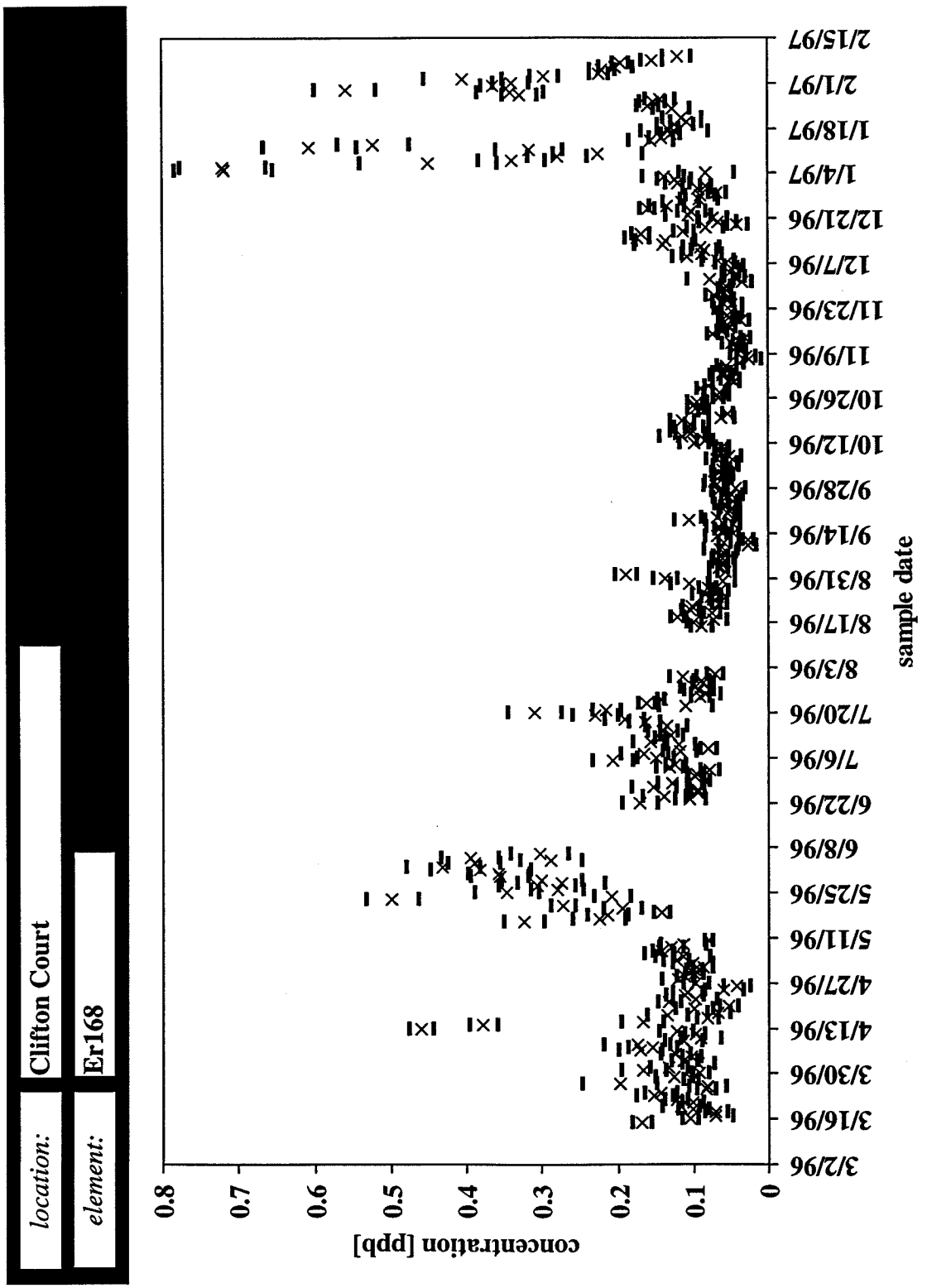
location:
Clifton Court
element:
Er168
concentration [ppb]
0.8
0.7
0.6
0.5
0.4
0.3
0.2
0.1
0
sample date
3/2/96
3/16/96
3/30/96
4/13/96
4/27/96
5/11/96
5/25/96
6/8/96
6/22/96
7/6/96
7/20/96
8/3/96
8/17/96
8/31/96
9/14/96
9/28/96
10/12/96
10/26/96
11/9/96
11/23/96
12/7/96
12/21/96
1/4/97
1/18/97
2/1/97
2/15/97

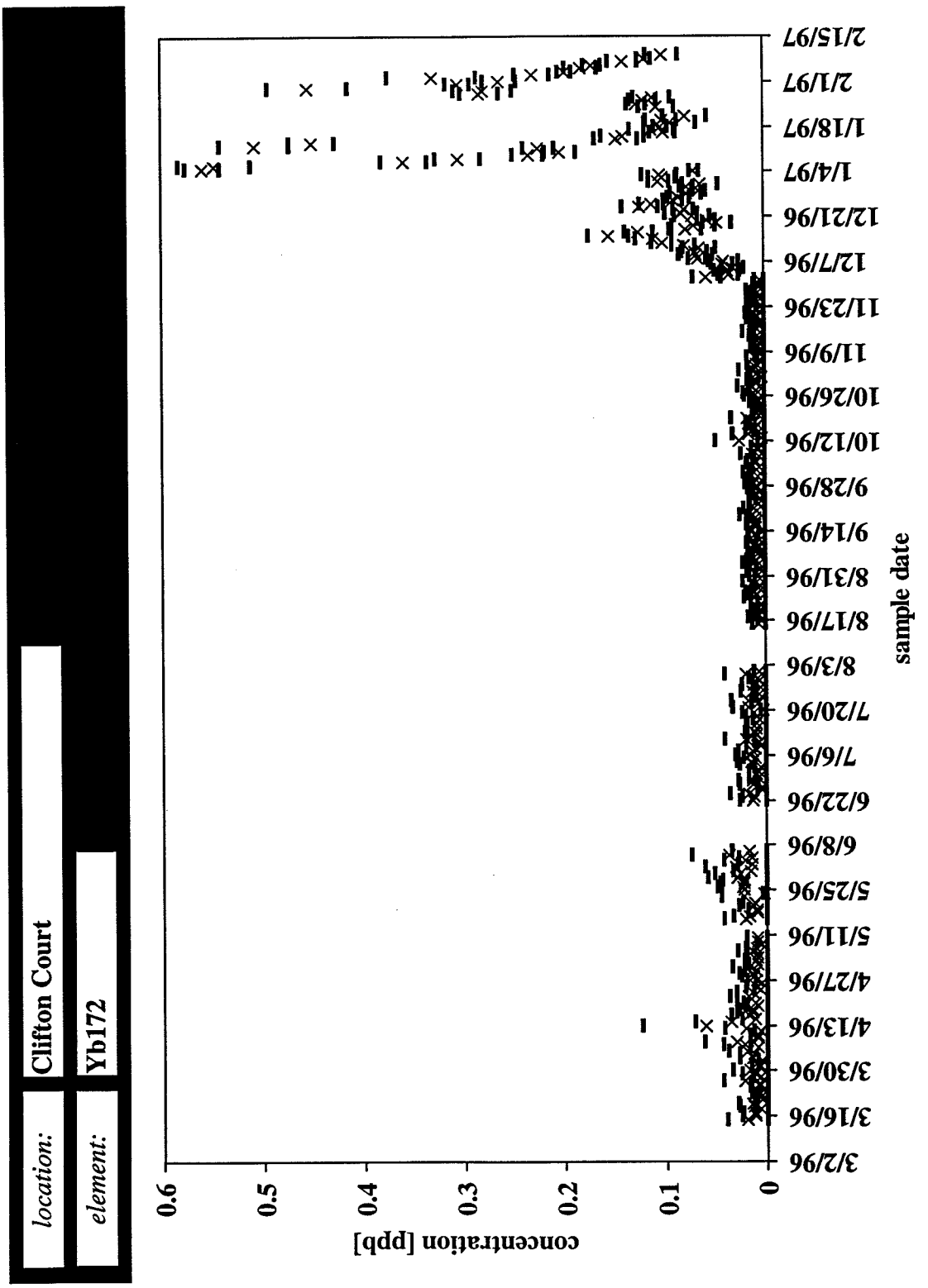
location:
Clifton Court
element:
Yb172
concentration [ppb]
0.6
0.5
0.4
0.3
0.2
0.1
0
sample date
3/2/96
3/16/96
3/30/96
4/13/96
4/27/96
5/11/96
5/25/96
6/8/96
6/22/96
7/6/96
7/20/96
8/3/96
8/17/96
8/31/96
9/14/96
9/28/96
10/12/96
10/26/96
11/9/96
11/23/96
12/7/96
12/21/96
1/4/97
1/18/97
2/1/97
2/15/97

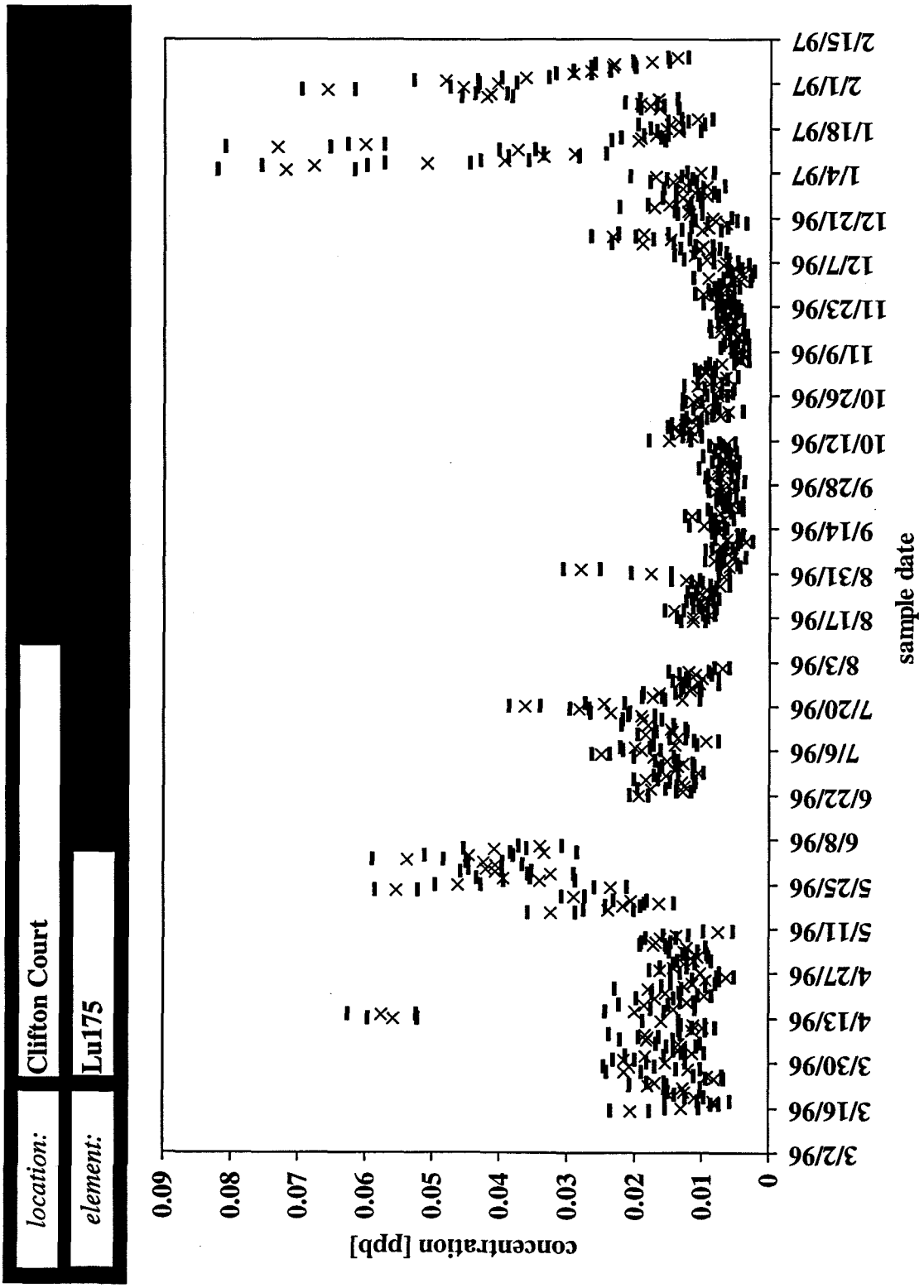
location:
Clifton Court
element:
Lu175
concentration [ppb]
0.09
0.08
0.07
0.06
0.05
0.04
0.03
0.02
0.01
0
sample date
3/2/96
3/16/96
3/30/96
4/13/96
4/27/96
5/11/96
5/25/96
6/8/96
6/22/96
7/6/96
7/20/96
8/3/96
8/17/96
8/31/96
9/14/96
9/28/96
10/12/96
10/26/96
11/9/96
11/23/96
12/7/96
12/21/96
1/4/97
1/18/97
2/1/97
2/15/97

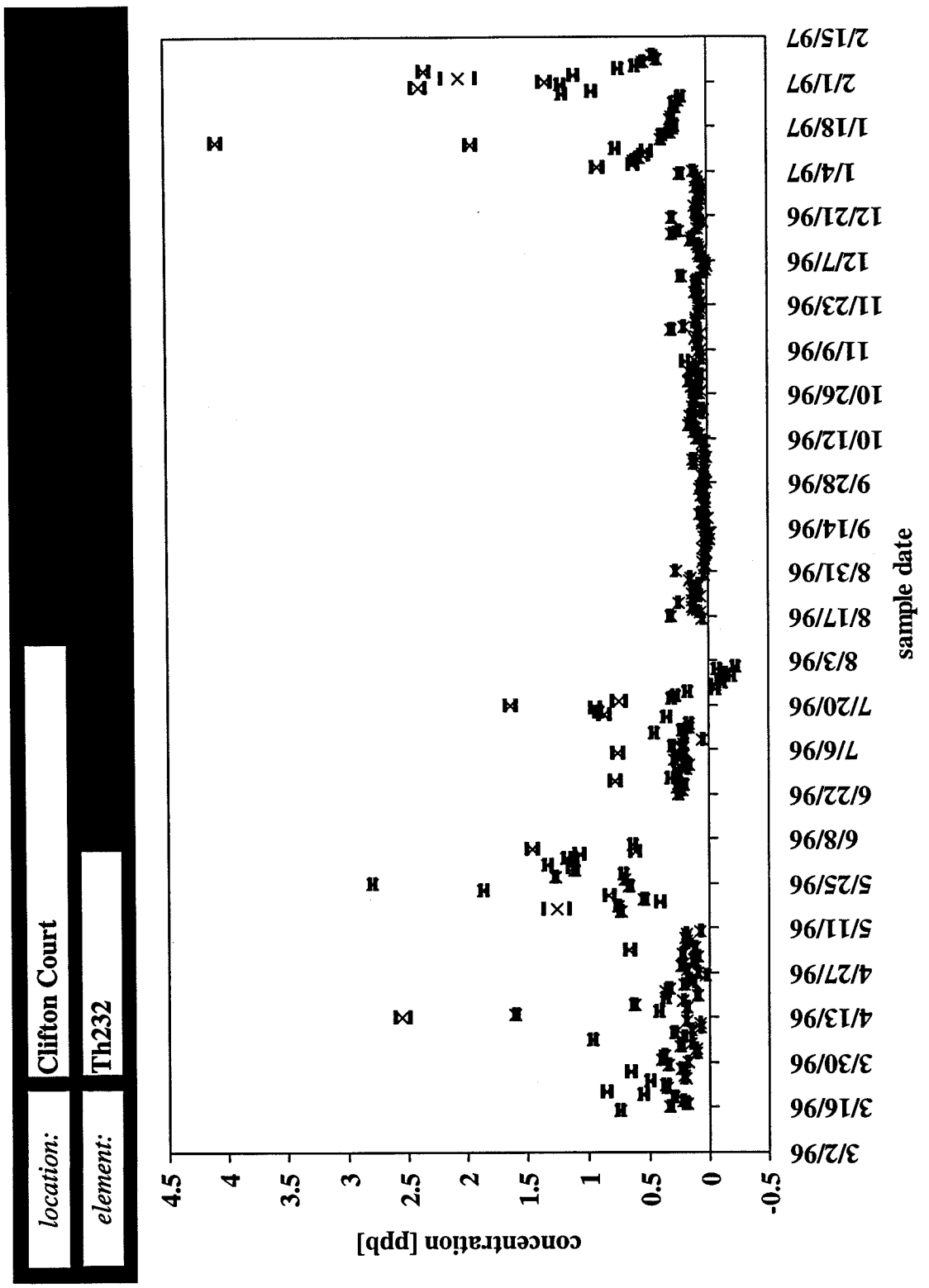
location:
Clifton Court
element:
Th232
concentration [ppb]
4.5
4
3.5
3
2.5
2
1.5
1
0.5
0
-0.5
sample date
3/2/96
3/16/96
3/30/96
4/13/96
4/27/96
5/11/96
5/25/96
6/8/96
6/22/96
7/6/96
7/20/96
8/3/96
8/17/96
8/31/96
9/14/96
9/28/96
10/12/96
10/26/96
11/9/96
11/23/96
12/7/96
12/21/96
1/4/97
1/18/97
2/1/97
2/15/97

location:
Clifton Court
element:
U238
concentration [ppb]
0
0.5
1
1.5
2
2.5
3
3.5
4
4.5
5
sample date
3/2/96
3/16/96
3/30/96
4/13/96
4/27/96
5/11/96
5/25/96
6/8/96
6/22/96
7/6/96
7/20/96
8/3/96
8/17/96
8/31/96
9/14/96
9/28/96
10/12/96
10/26/96
11/9/96
11/23/96
12/7/96
12/21/96
1/4/97
1/18/97
2/1/97
2/15/97

Appendix E

Variations in elemental concentrations along the Sacramento River

Appendix E
Variations in elemental concentrations along the Sacramento River

Table of Contents

Concentrations measured along the Sacramento River:

Concentrations measured along the Sacramento River:

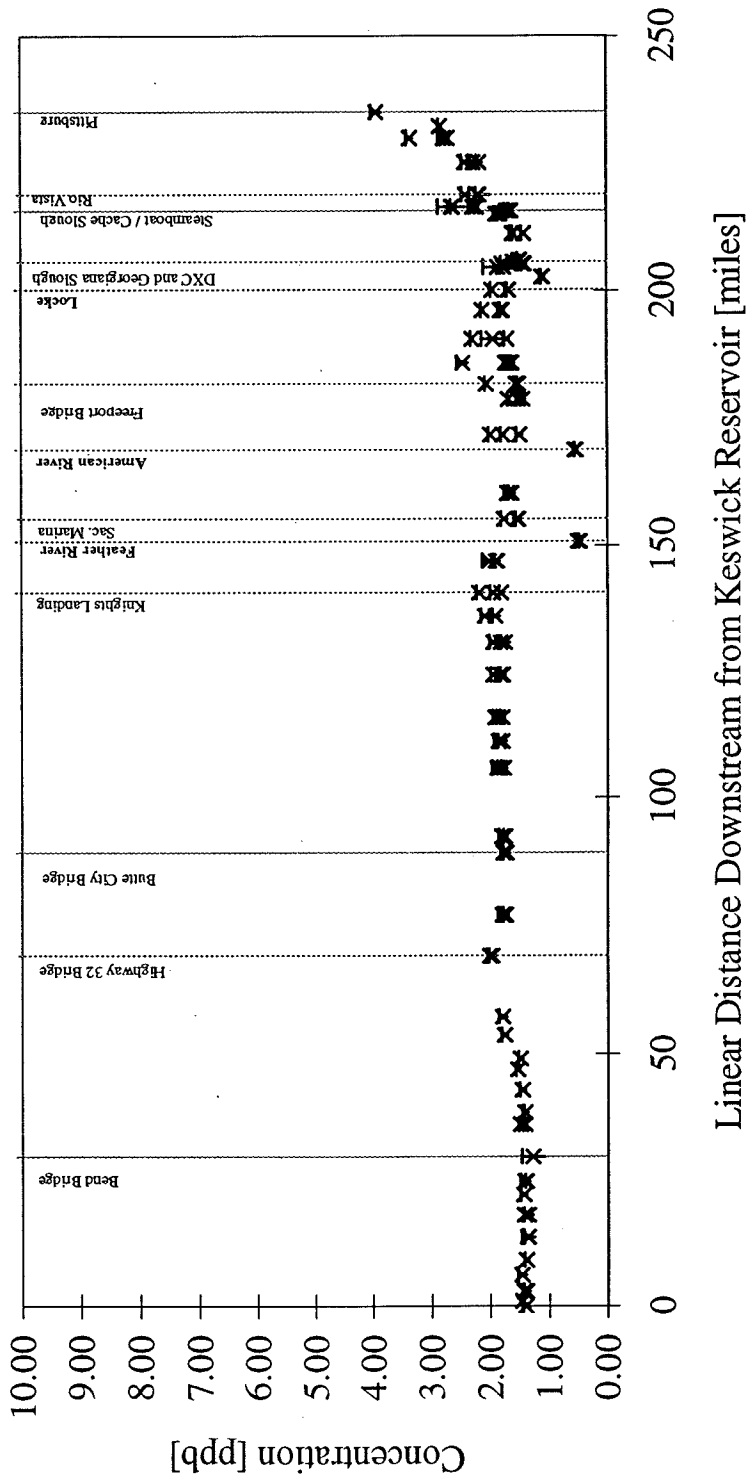
Concentration along the Sacramento River:
× Li
Concentration [ppb]
10.00
9.00
8.00
7.00
6.00
5.00
4.00
3.00
2.00
1.00
0.00
0
50
100
150
200
250
Linear Distance Downstream from Keswick Reservoir [miles]
Bend Bridge
Highway 32 Bridge
Butte City Bridge
Knights Landing
Feather River
Sac. Martina
American River
Freeport Bridge
Locke
DXC and Georgiana Slough
Steamboat / Cache Slough
Rio Vista
Pittsburg

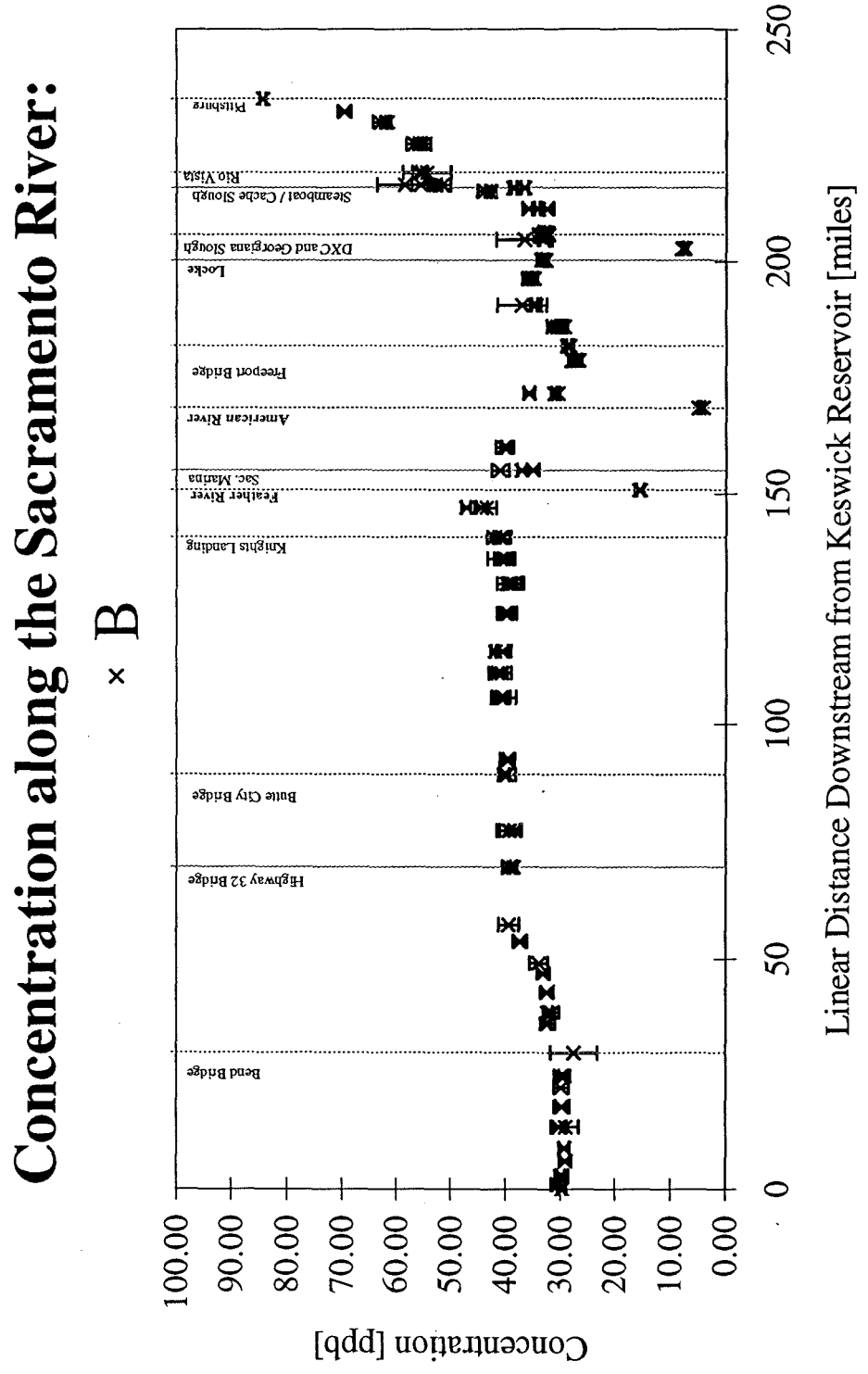
Concentration along the Sacramento River:
× B
Concentration [ppb]
100.00
90.00
80.00
70.00
60.00
50.00
40.00
30.00
20.00
10.00
0.00
0
50
100
150
200
250
Linear Distance Downstream from Keswick Reservoir [miles]
Bend Bridge
Highway 32 Bridge
Butte City Bridge
Knights Landing
Feather River
Sac. Mainna
American River
Freeport Bridge
Locke
DXC and Georgiana Slough
Steamboat / Cache Slough
Rio Vista
Pittsburg

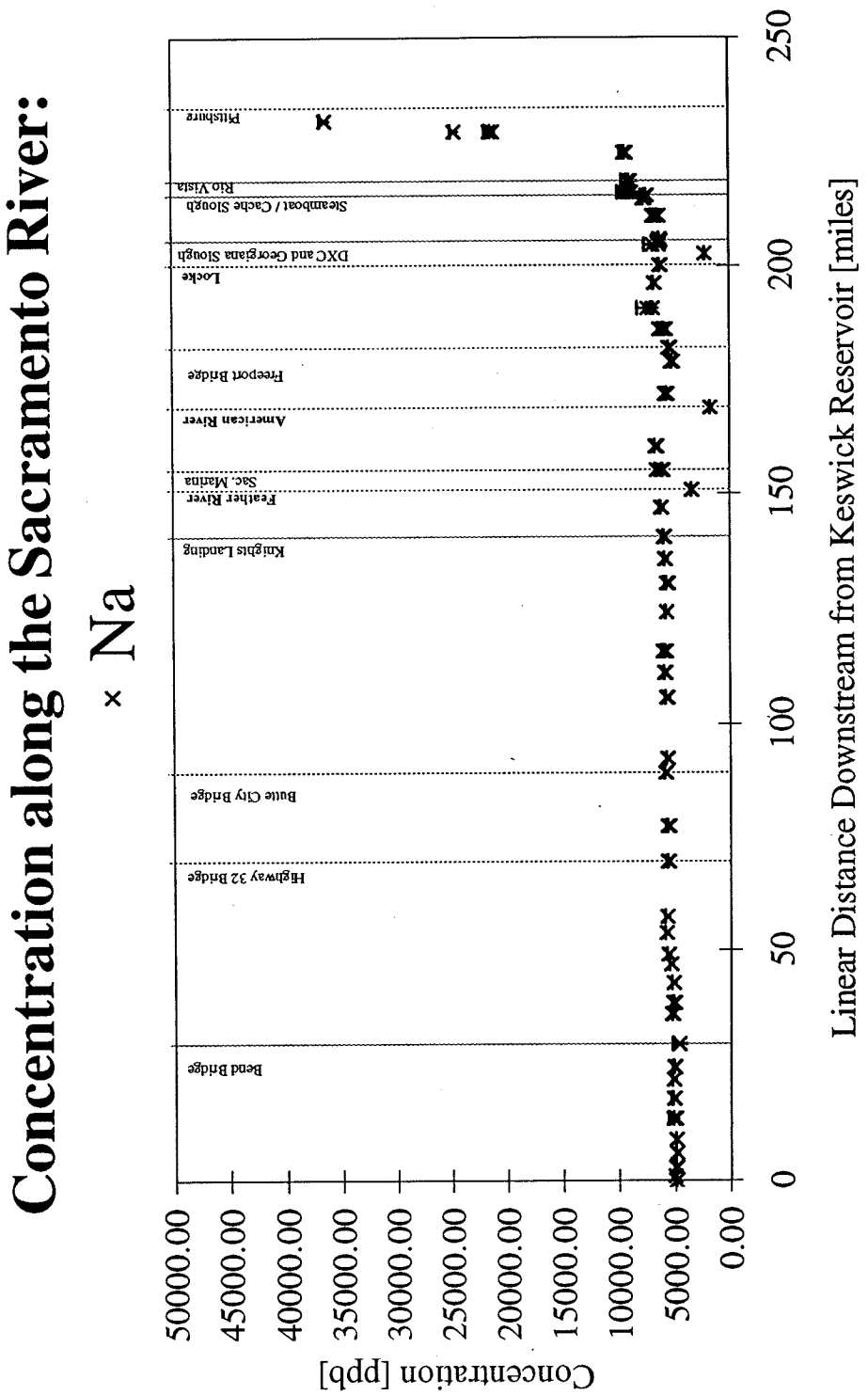
Concentration along the Sacramento River:
× Na
Concentration [ppb]
50000.00
45000.00
40000.00
35000.00
30000.00
25000.00
20000.00
15000.00
10000.00
5000.00
0.00
0
50
100
150
200
250
Linear Distance Downstream from Keswick Reservoir [miles]
Bend Bridge
Highway 32 Bridge
Butte City Bridge
Knights Landing
Feather River
Sac. Marina
American River
Freeport Bridge
Locke
DXC and Georgiana Slough
Steamboat / Cache Slough
Rio Vista
Pittsburg

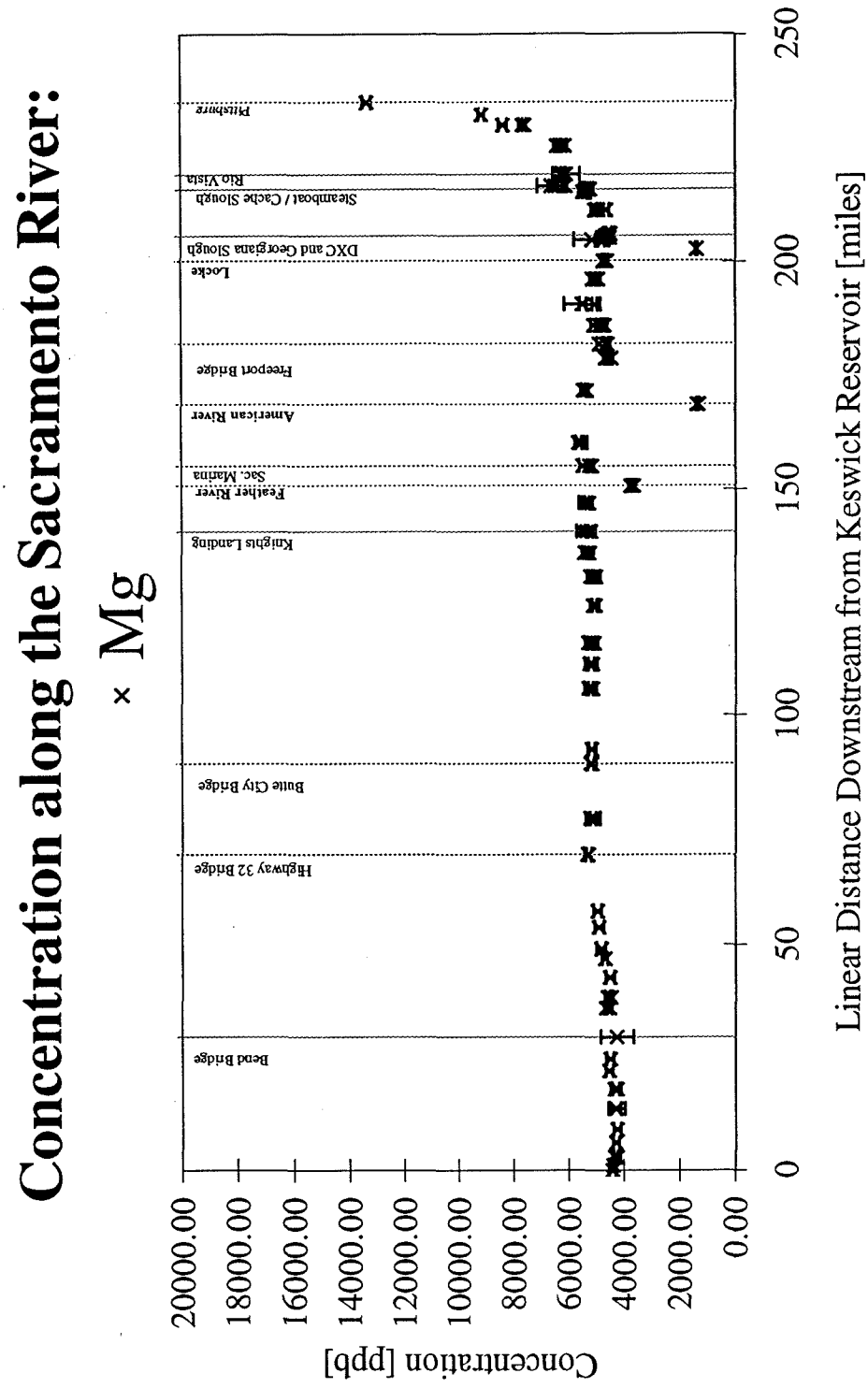
Concentration along the Sacramento River:
× Mg
Concentration [ppb]
20000.00
18000.00
16000.00
14000.00
12000.00
10000.00
8000.00
6000.00
4000.00
2000.00
0.00
0
50
100
150
200
250
Linear Distance Downstream from Keswick Reservoir [miles]
Bend Bridge
Highway 32 Bridge
Butte City Bridge
Knights Landing
Feather River
Sac. Marina
American River
Freeport Bridge
Locke
DXC and Georgiana Slough
Steamboat / Cache Slough
Rio Vista
Pittsburg

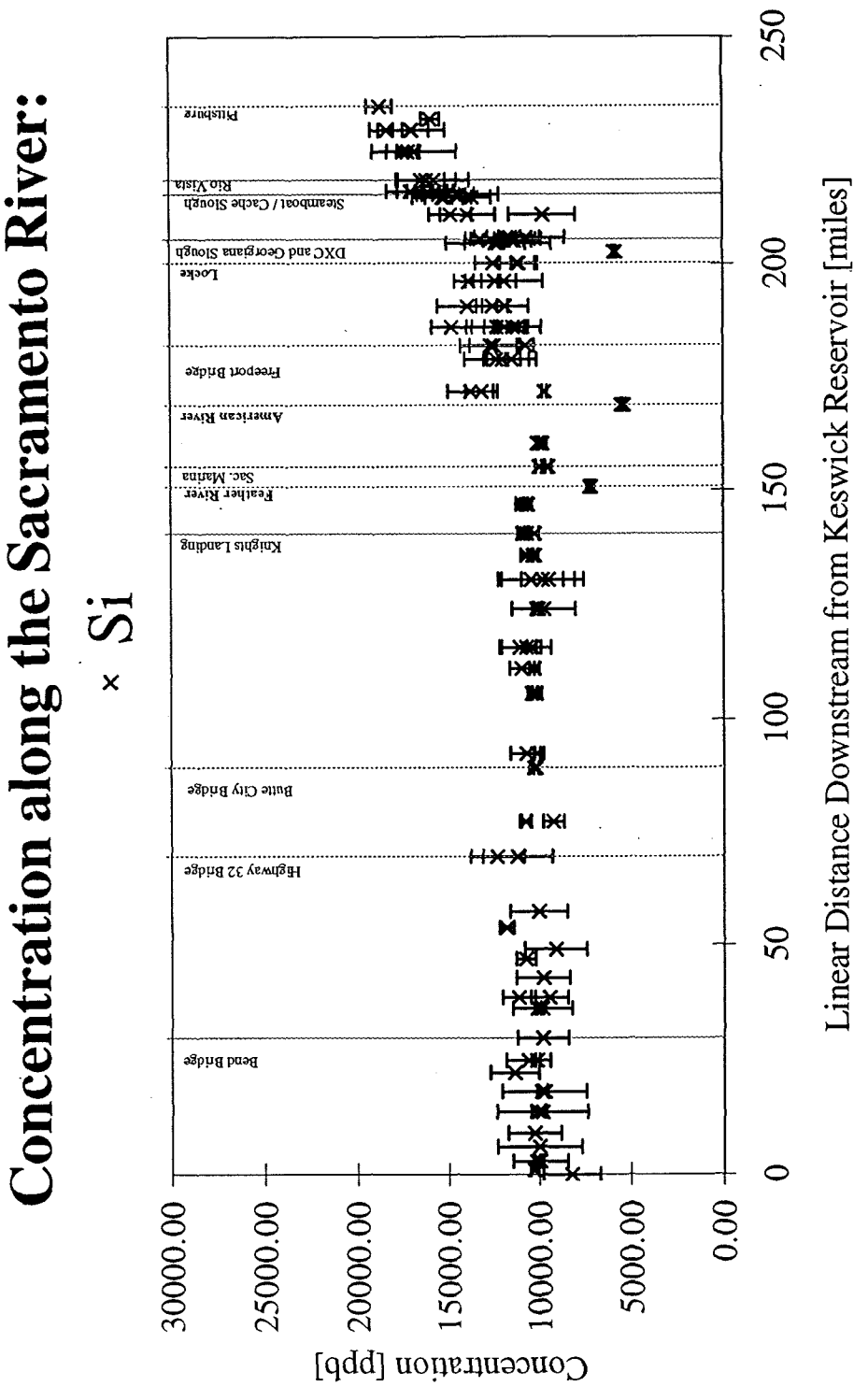
Concentration along the Sacramento River:
× Si
Concentration [ppb]
30000.00
25000.00
20000.00
15000.00
10000.00
5000.00
0.00
0
50
100
150
200
250
Linear Distance Downstream from Keswick Reservoir [miles]
Bend Bridge
Highway 32 Bridge
Butte City Bridge
Knights Landing
Feather River
Sac. Marina
American River
Freeport Bridge
Locke
DXC and Georgiana Slough
Steamboat / Cache Slough
Rio Vista
Pittsburg

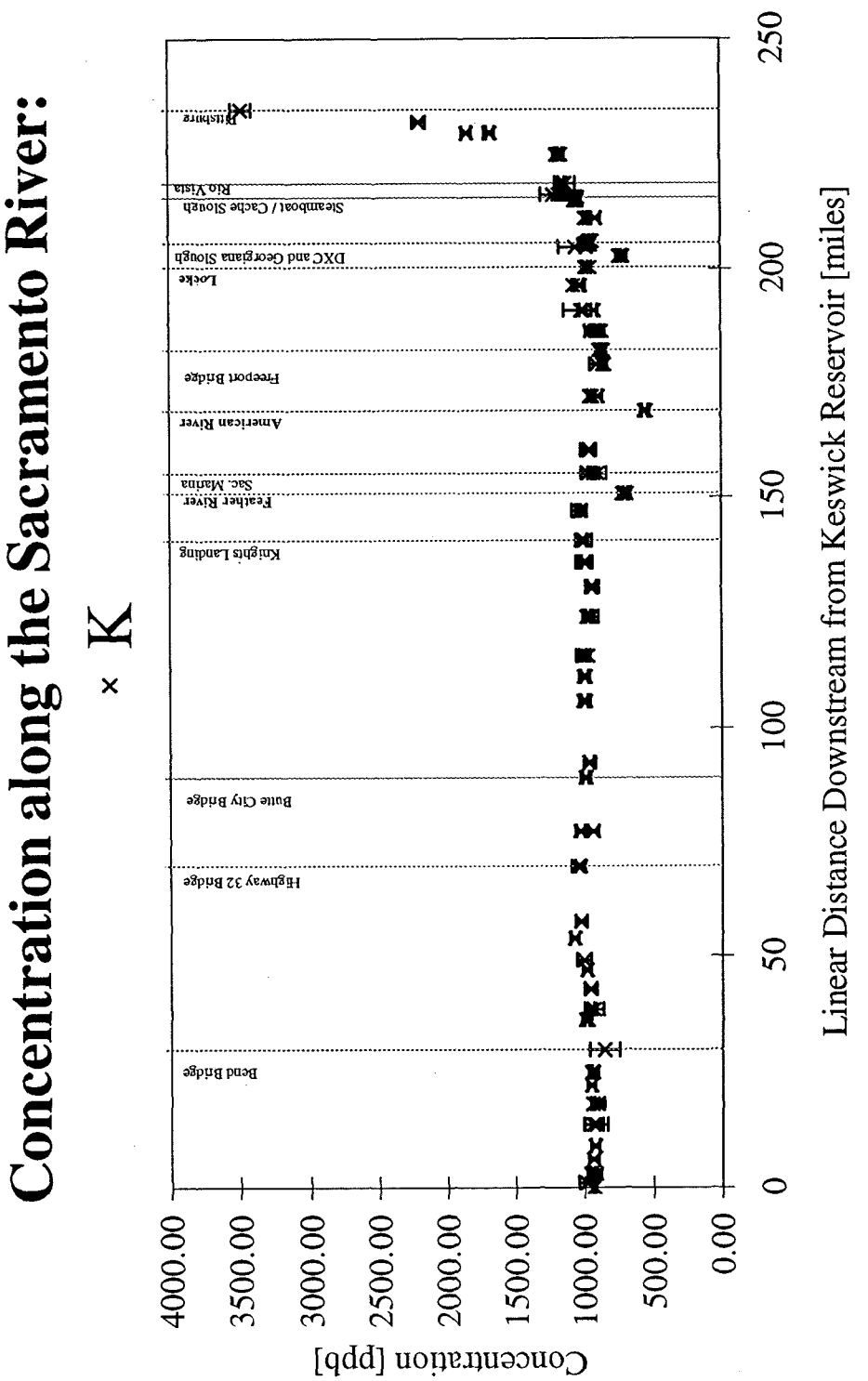
Concentration along the Sacramento River:
× K
Concentration [ppb]
4000.00
3500.00
3000.00
2500.00
2000.00
1500.00
1000.00
500.00
0.00
0
50
100
150
200
250
Linear Distance Downstream from Keswick Reservoir [miles]
Bend Bridge
Highway 32 Bridge
Butte City Bridge
Knights Landing
Feather River
Sac. Marina
American River
Freeport Bridge
Locke
DXC and Georgiana Slough
Steamboat / Cache Slough
Rio Vista
Bluffsnire

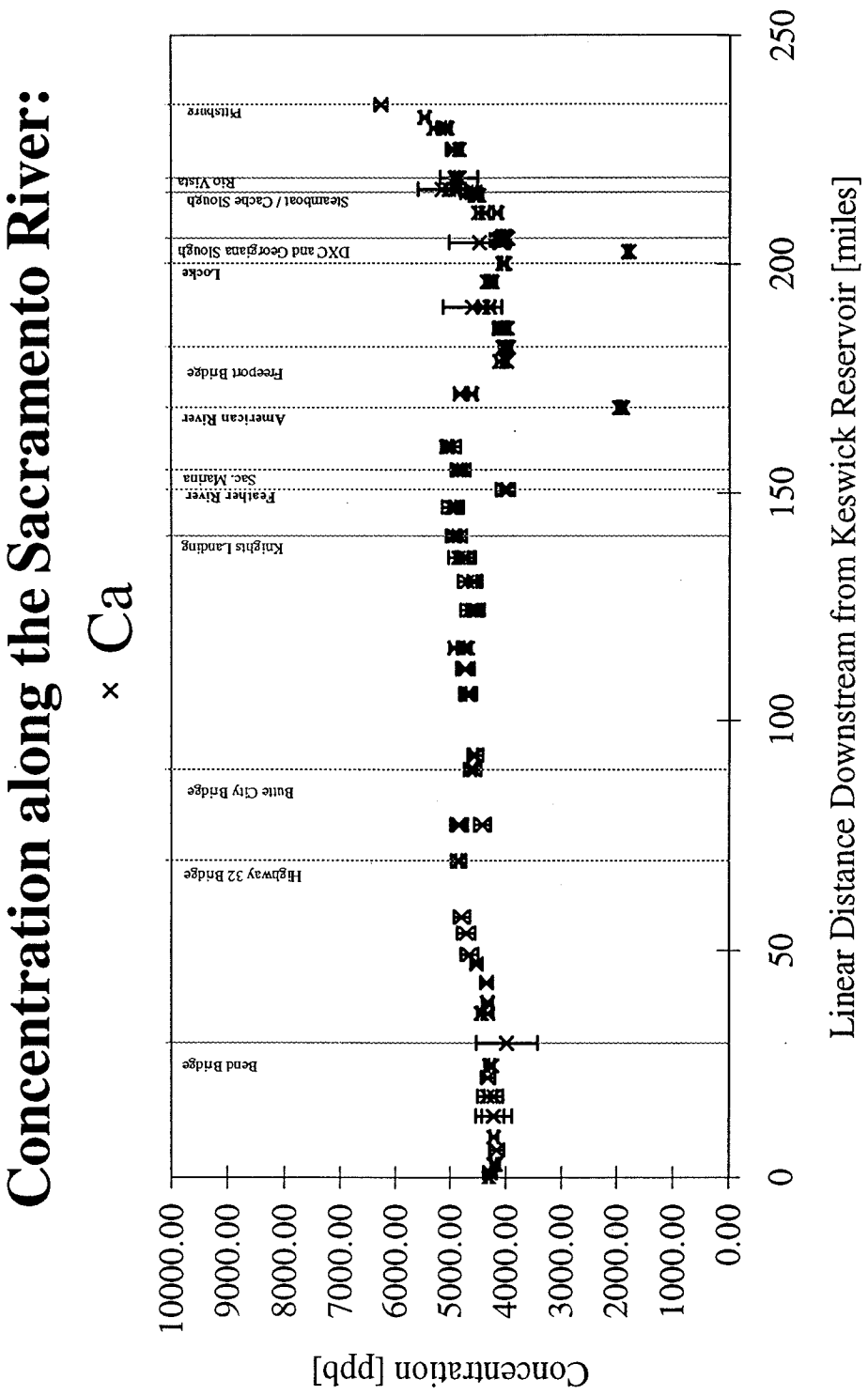
Concentration along the Sacramento River:
× Ca
Concentration [ppb]
10000.00
9000.00
8000.00
7000.00
6000.00
5000.00
4000.00
3000.00
2000.00
1000.00
0.00
0
50
100
150
200
250
Linear Distance Downstream from Keswick Reservoir [miles]
Bend Bridge
Highway 32 Bridge
Butte City Bridge
Knights Landing
Feather River
Sac. Marina
American River
Freeport Bridge
Locke
DXC and Georgiana Slough
Steamboat / Cache Slough
Rio Vista
Pittsburg

Concentration along the Sacramento River:

× V

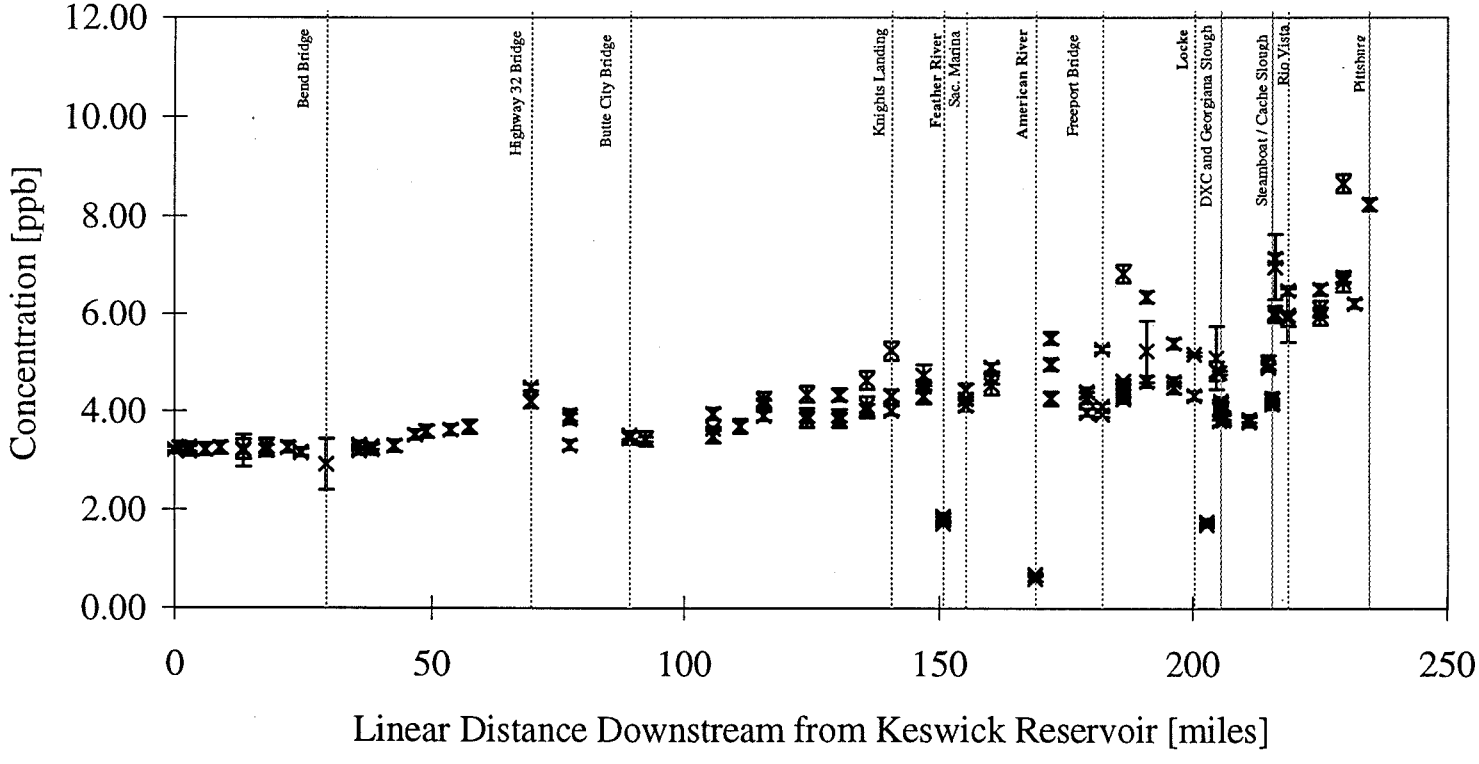

Concentration along the Sacramento River:

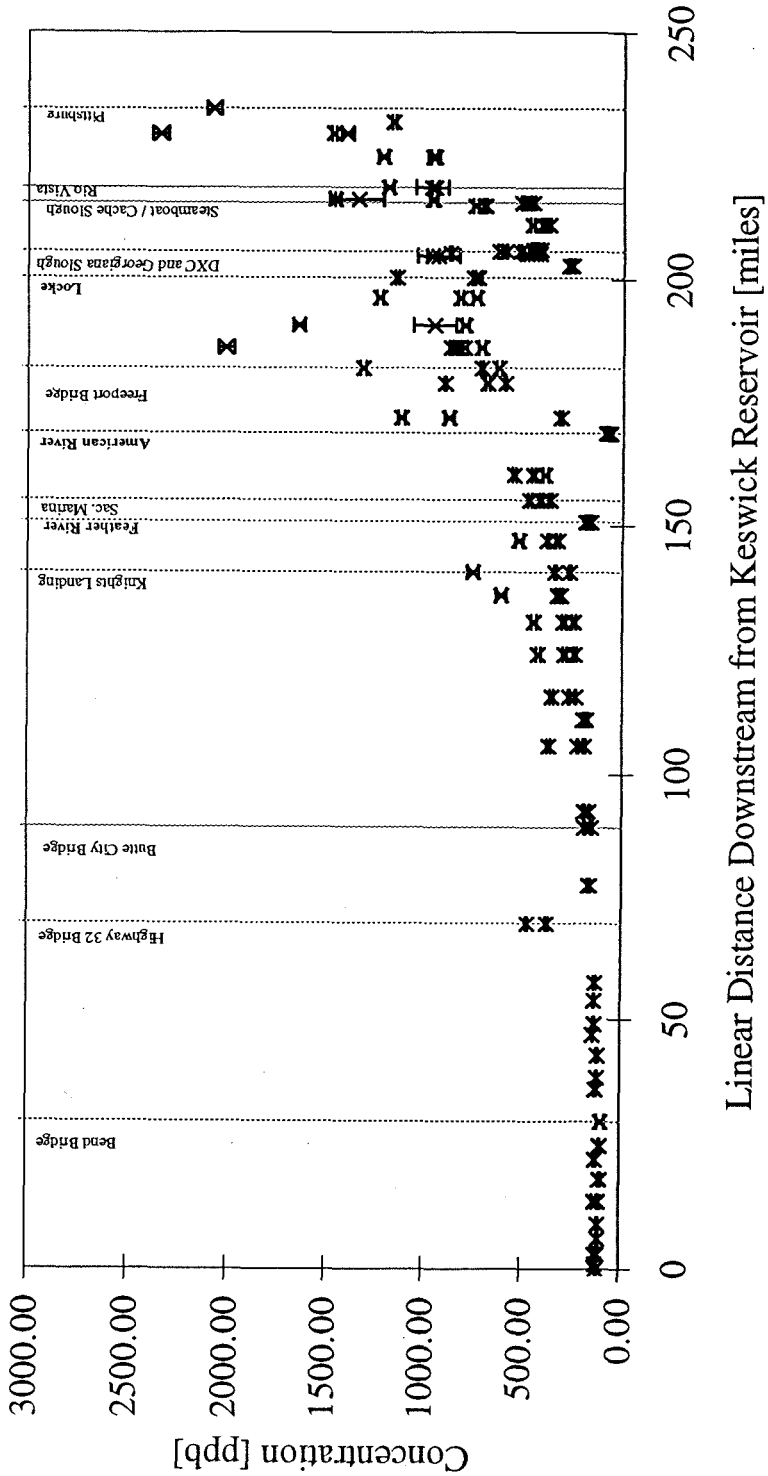

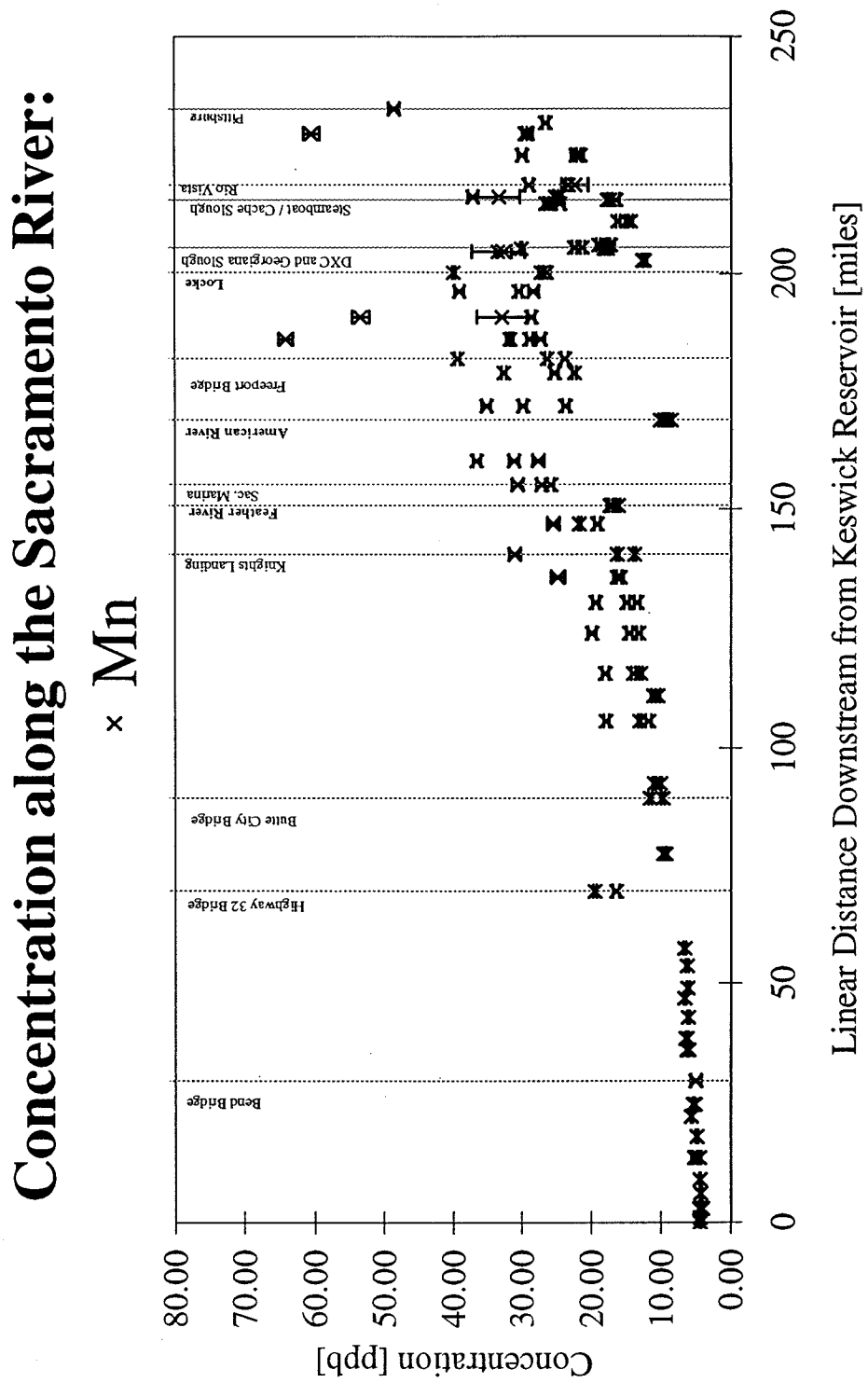
Concentration along the Sacramento River:
× Mn
Concentration [ppb]
80.00
70.00
60.00
50.00
40.00
30.00
20.00
10.00
0.00
0
50
100
150
200
250
Linear Distance Downstream from Keswick Reservoir [miles]
Bend Bridge
Highway 32 Bridge
Butte City Bridge
Knights Landing
Feather River
Sac. Marina
American River
Freeport Bridge
Locke
DXC and Georgiana Slough
Steamboat / Cache Slough
Rio Vista
Pittsburg

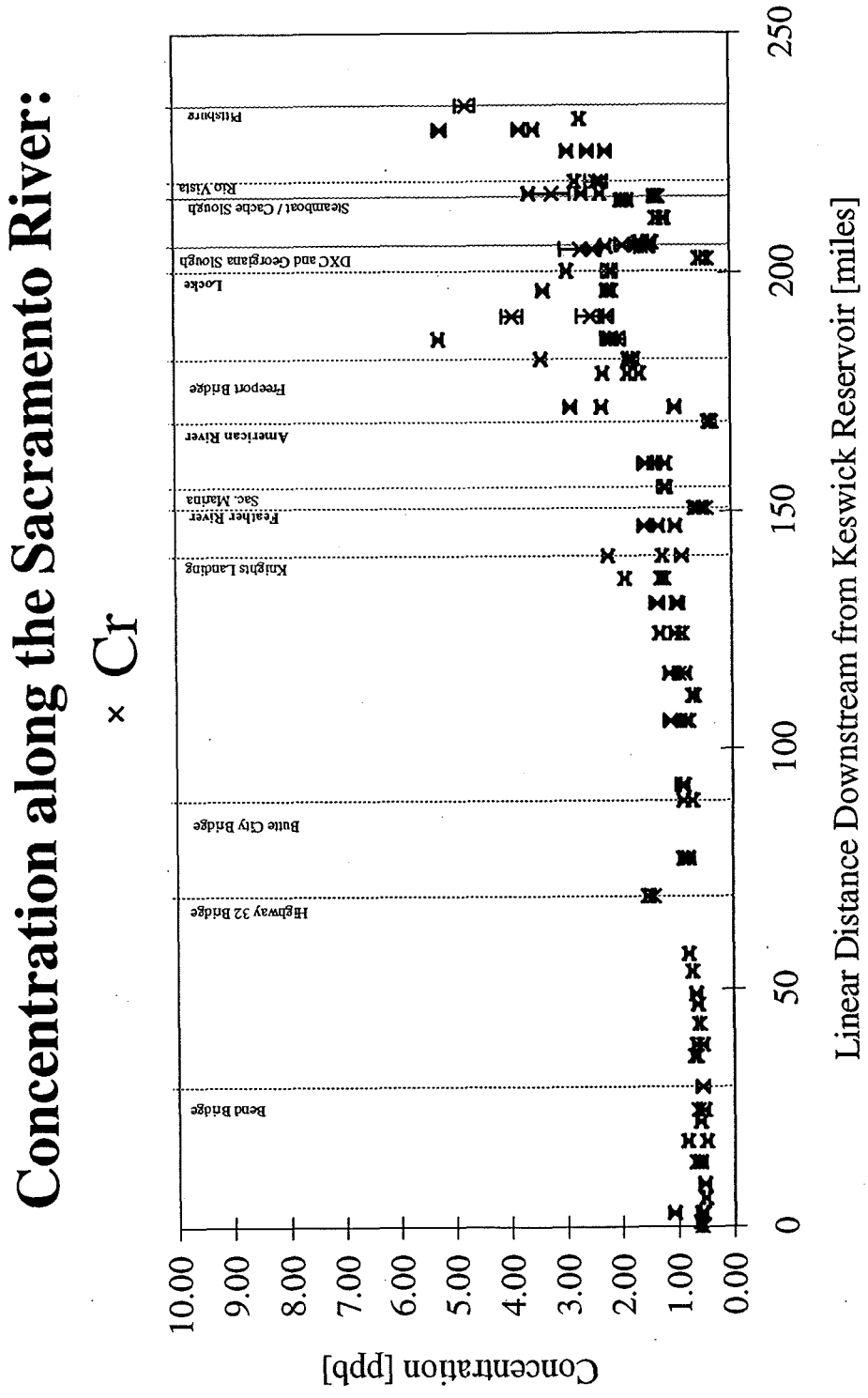
Concentration along the Sacramento River:
× Cr
Concentration [ppb]
10.00
9.00
8.00
7.00
6.00
5.00
4.00
3.00
2.00
1.00
0.00
0
50
100
150
200
250
Linear Distance Downstream from Keswick Reservoir [miles]
Bend Bridge
Highway 32 Bridge
Butte City Bridge
Knights Landing
Feather River
Sac. Marina
American River
Freeport Bridge
Locke
DXC and Georgiana Slough
Steamboat / Cache Slough
Rio Vista
Pittsburg

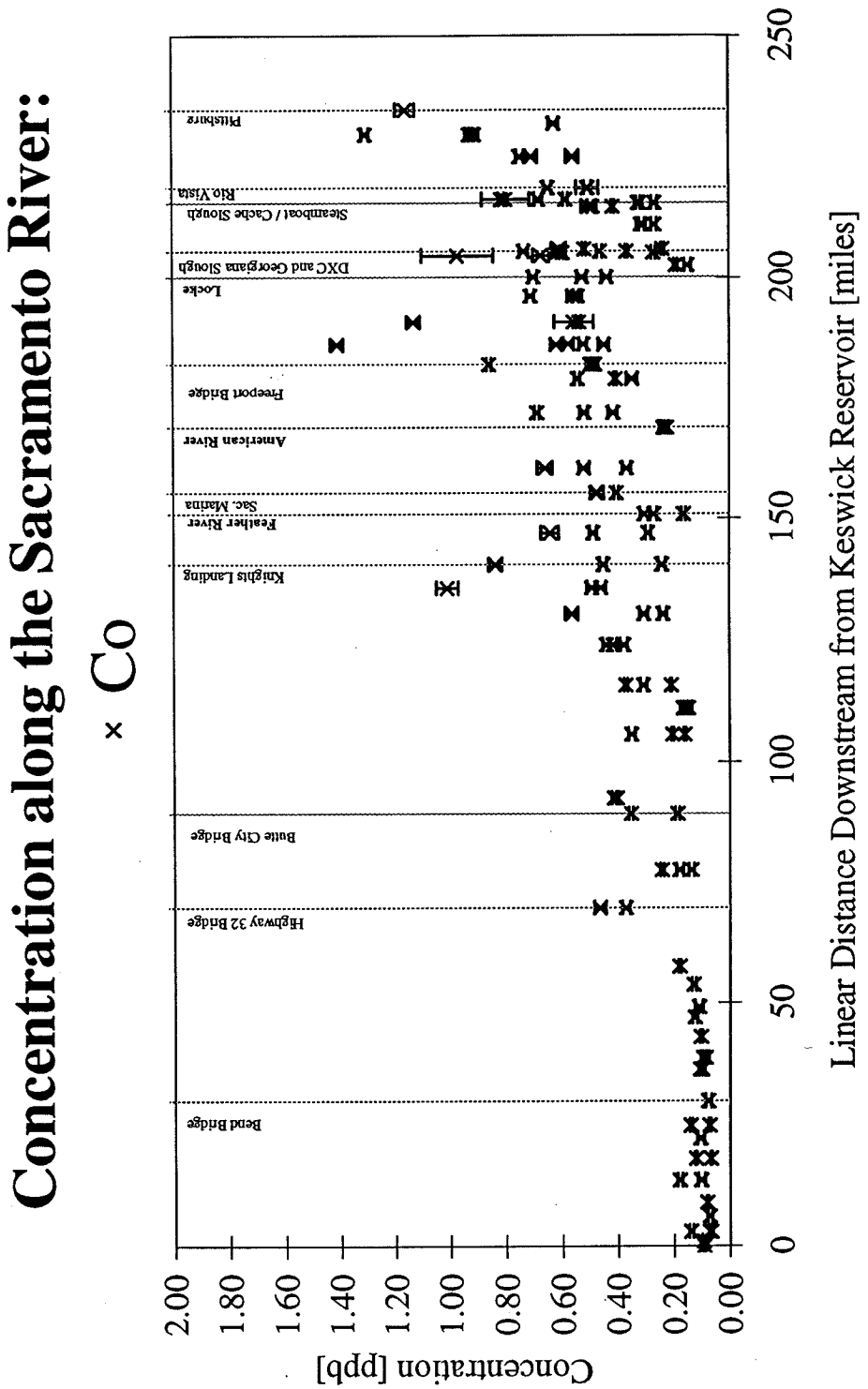
Concentration along the Sacramento River:
× Co
Concentration [ppb]
2.00
1.80
1.60
1.40
1.20
1.00
0.80
0.60
0.40
0.20
0.00
0
50
100
150
200
250
Linear Distance Downstream from Keswick Reservoir [miles]
Bend Bridge
Highway 32 Bridge
Butte City Bridge
Knights Landing
Feather River
Sac. Marina
American River
Freeport Bridge
Locke
DXC and Georgiana Slough
Steamboat / Cache Slough
Rio Vista
Pittsburg

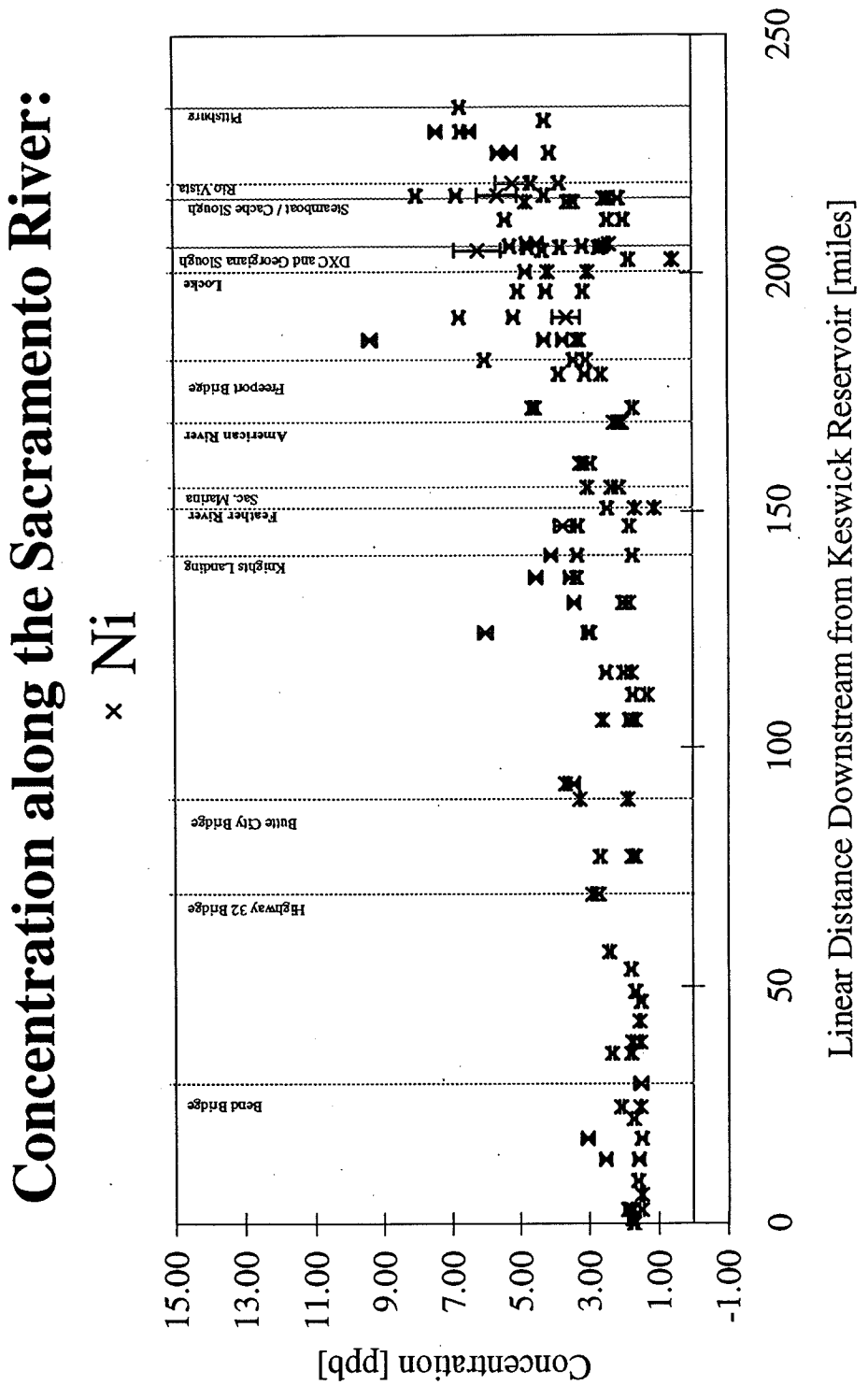
Concentration along the Sacramento River:
× Ni
Concentration [ppb]
15.00
13.00
11.00
9.00
7.00
5.00
3.00
1.00
-1.00
0
50
100
150
200
250
Linear Distance Downstream from Keswick Reservoir [miles]
Bend Bridge
Highway 32 Bridge
Butte City Bridge
Knights Landing
Feather River
Sac. Marina
American River
Freeport Bridge
Locke
DXC and Georgiana Slough
Steamboat / Cache Slough
Rio Vista
Pittsburg

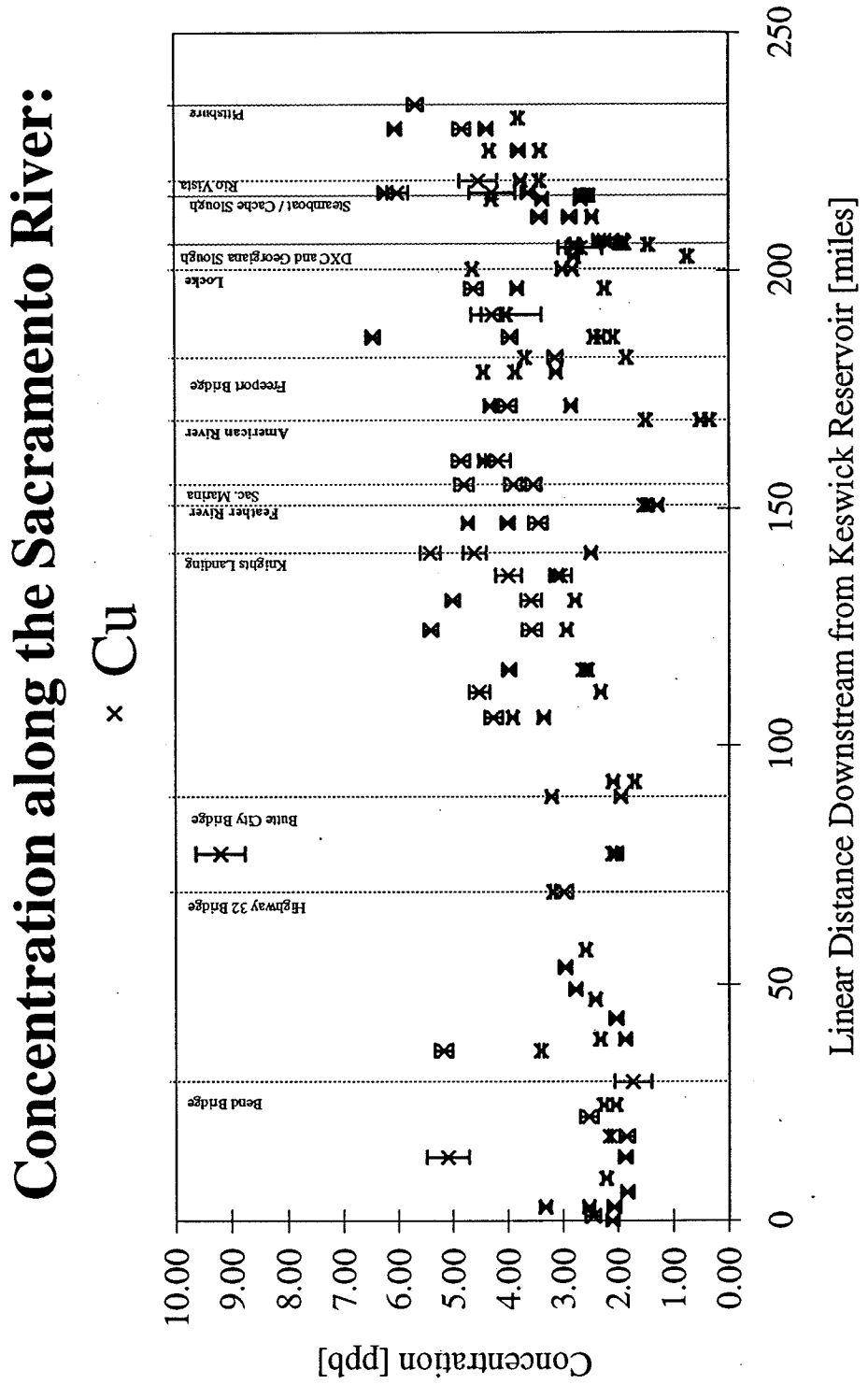
Concentration along the Sacramento River:
× Cu
Concentration [ppb]
10.00
9.00
8.00
7.00
6.00
5.00
4.00
3.00
2.00
1.00
0.00
0
50
100
150
200
250
Linear Distance Downstream from Keswick Reservoir [miles]
Bend Bridge
Highway 32 Bridge
Butte City Bridge
Knights Landing
Feather River
Sac. Marina
American River
Freeport Bridge
Locke
DXC and Georgiana Slough
Steamboat / Cache Slough
Rio Vista
Pittsburg

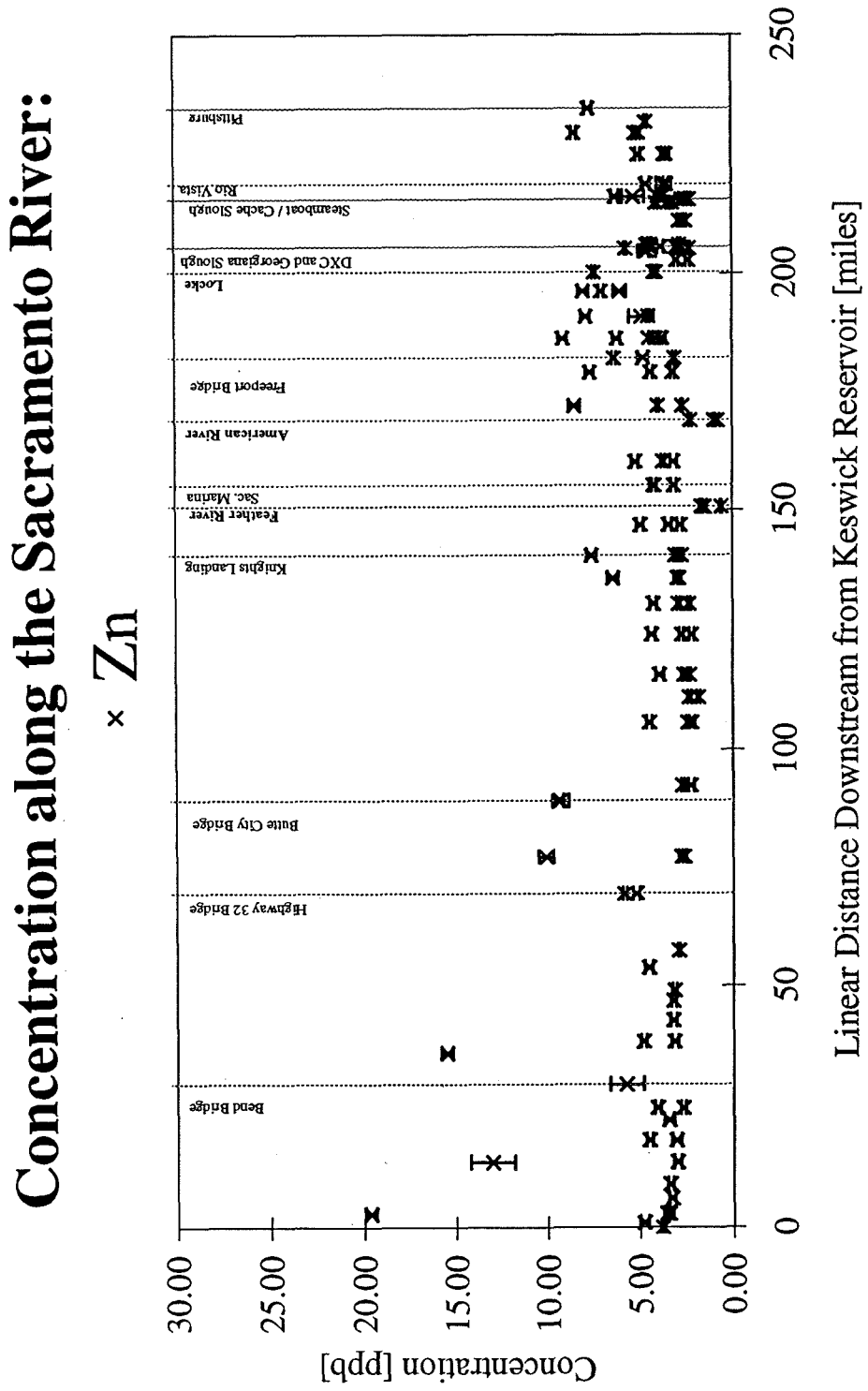
Concentration along the Sacramento River:
× Zn
Concentration [ppb]
30.00
25.00
20.00
15.00
10.00
5.00
0.00
0
50
100
150
200
250
Linear Distance Downstream from Keswick Reservoir [miles]
Bend Bridge
Highway 32 Bridge
Butte City Bridge
Knights Landing
Feather River
Sac. Marina
American River
Freeport Bridge
Locke
DXC and Georgiana Slough
Steamboat / Cache Slough
Rio Vista
Pittshurg

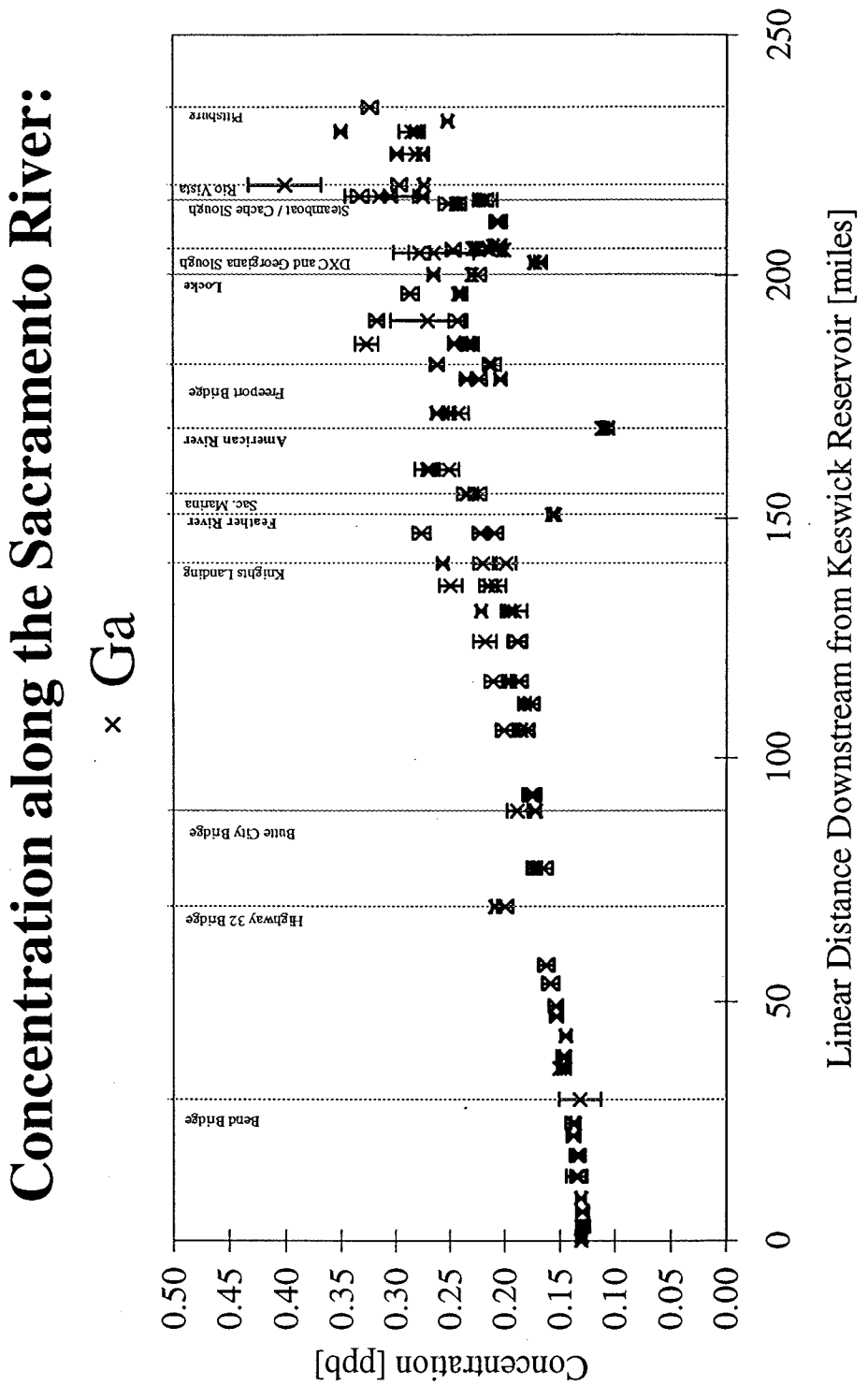
Concentration along the Sacramento River:
× Ga
Concentration [ppb]
0.50
0.45
0.40
0.35
0.30
0.25
0.20
0.15
0.10
0.05
0.00
0
50
100
150
200
250
Linear Distance Downstream from Keswick Reservoir [miles]
Bend Bridge
Highway 32 Bridge
Butte City Bridge
Knights Landing
Feather River
Sac. Marina
American River
Freeport Bridge
Locke
DXC and Georgiana Slough
Steamboat / Cache Slough
Rio Vista
Pittsburg

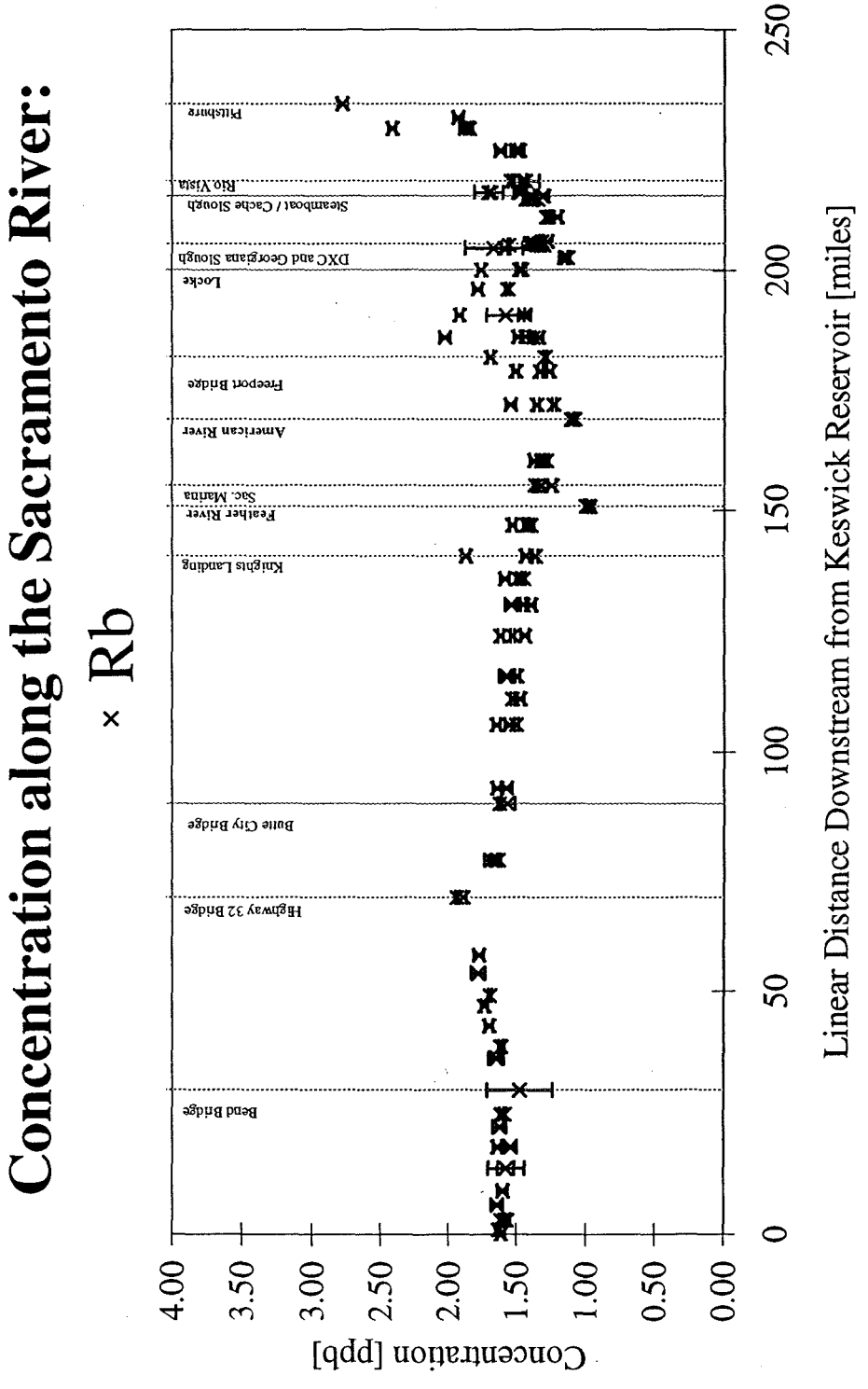
Concentration along the Sacramento River:
× Rb
Concentration [ppb]
4.00
3.50
3.00
2.50
2.00
1.50
1.00
0.50
0.00
0
50
100
150
200
250
Linear Distance Downstream from Keswick Reservoir [miles]
Bend Bridge
Highway 32 Bridge
Butte City Bridge
Knights Landing
Feather River
Sac. Marina
American River
Freeport Bridge
Locke
DXC and Georgiana Slough
Steamboat / Cache Slough
Rio Vista
Pittsburg

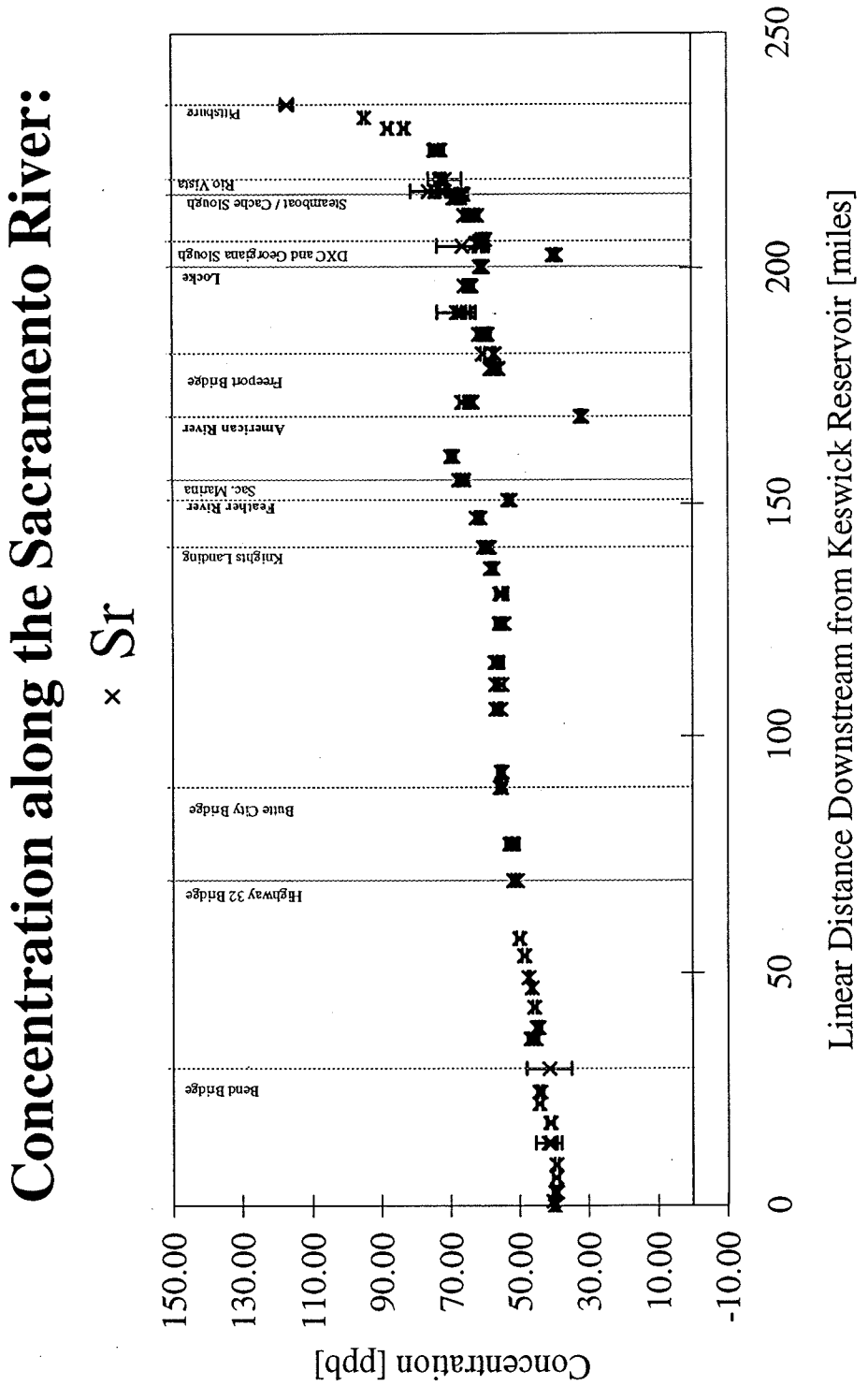
Concentration along the Sacramento River:
× Sr
Concentration [ppb]
150.00
130.00
110.00
90.00
70.00
50.00
30.00
10.00
-10.00
0
50
100
150
200
250
Linear Distance Downstream from Keswick Reservoir [miles]
Bend Bridge
Highway 32 Bridge
Butte City Bridge
Knights Landing
Feather River
Sac. Manna
American River
Freeport Bridge
Locke
DXC and Georgiana Slough
Steamboat / Cache Slough
Rio Vista
Pittshire

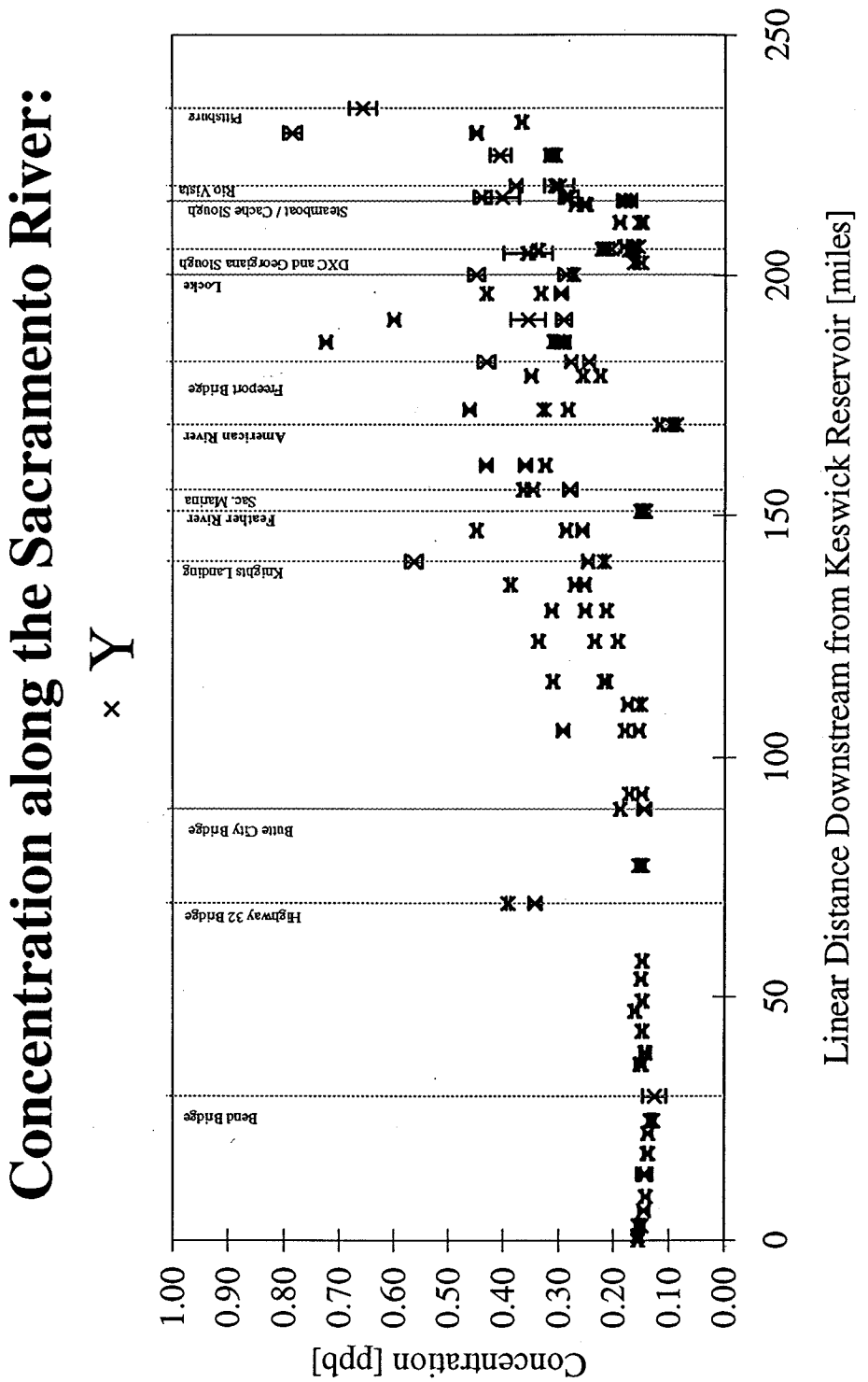
Concentration along the Sacramento River:
Y
Concentration [ppb]
1.00
0.90
0.80
0.70
0.60
0.50
0.40
0.30
0.20
0.10
0.00
0
50
100
150
200
250
Linear Distance Downstream from Keswick Reservoir [miles]
Bend Bridge
Highway 32 Bridge
Butte City Bridge
Knights Landing
Feather River
Sac. Marina
American River
Freeport Bridge
Locke
DXC and Georgiana Slough
Steamboat / Cache Slough
Rio Vista
Pittsburg

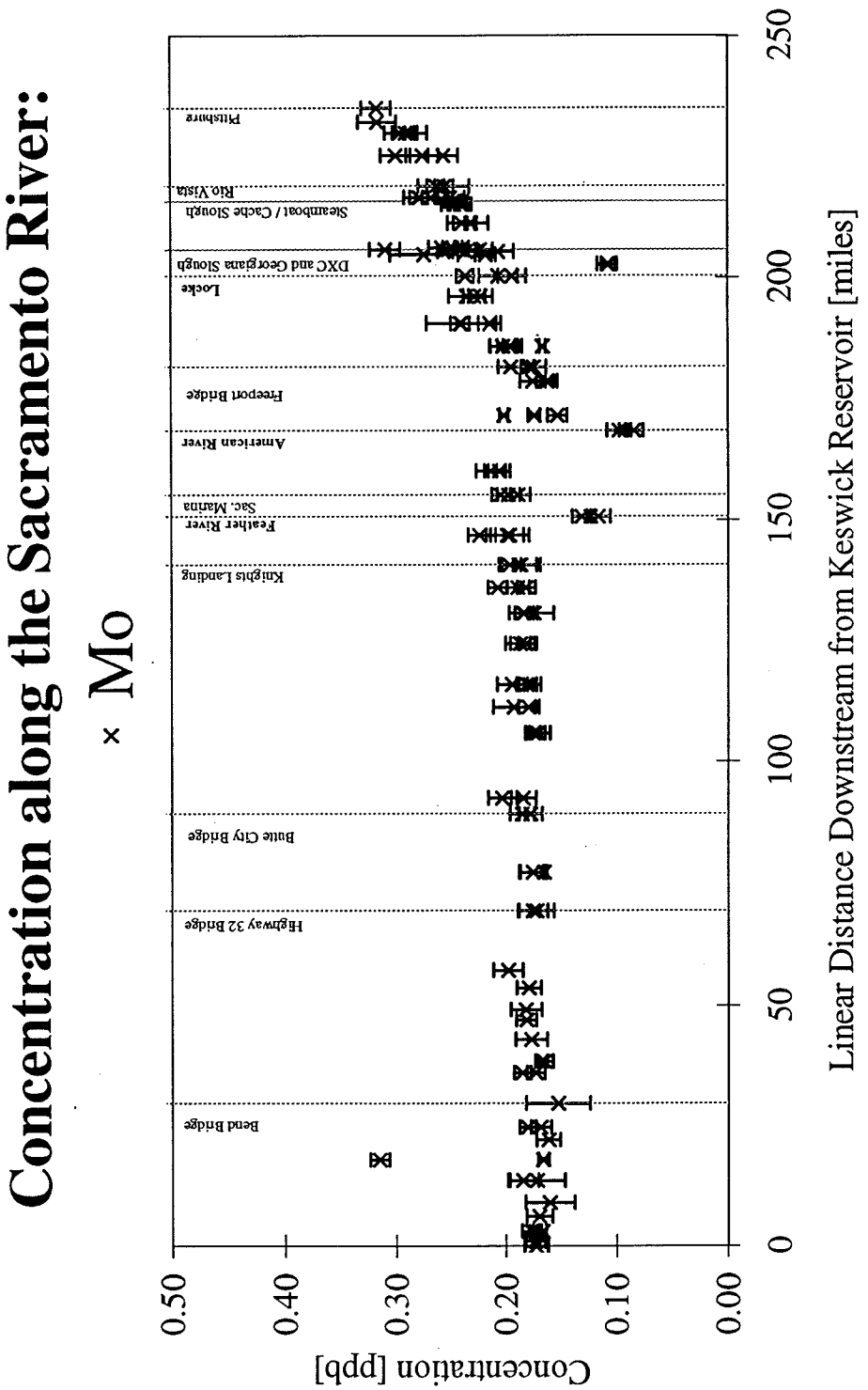
Concentration along the Sacramento River:
× Mo
Concentration [ppb]
0.50
0.40
0.30
0.20
0.10
0.00
0
50
100
150
200
250
Linear Distance Downstream from Keswick Reservoir [miles]
Bend Bridge
Highway 32 Bridge
Blue Ctry Bridge
Knights Landing
Feather River
Sac. Manna
American River
Freeport Bridge
Locke
DXC and Georgiana Slough
Steamboat / Cache Slough
Rio Vista
Pittsburg

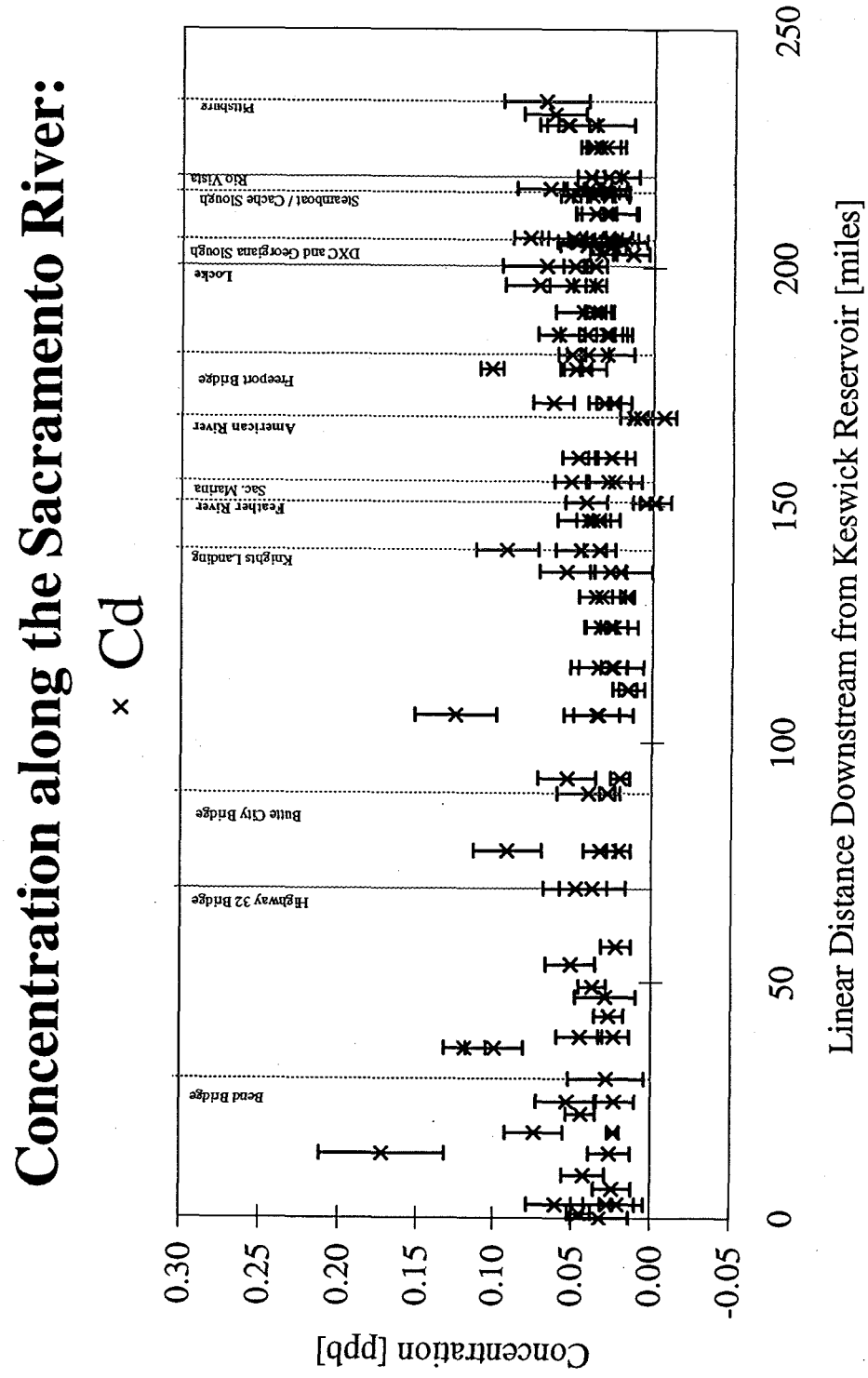
Concentration along the Sacramento River:
× Cd
Concentration [ppb]
0.30
0.25
0.20
0.15
0.10
0.05
0.00
-0.05
0
50
100
150
200
250
Linear Distance Downstream from Keswick Reservoir [miles]
Bend Bridge
Highway 32 Bridge
Butte City Bridge
Knights Landing
Feather River
Sac. Mantua
American River
Freeport Bridge
Locke
DXC and Georgiana Slough
Steamboat / Cache Slough
Rio Vista
Pittsburg

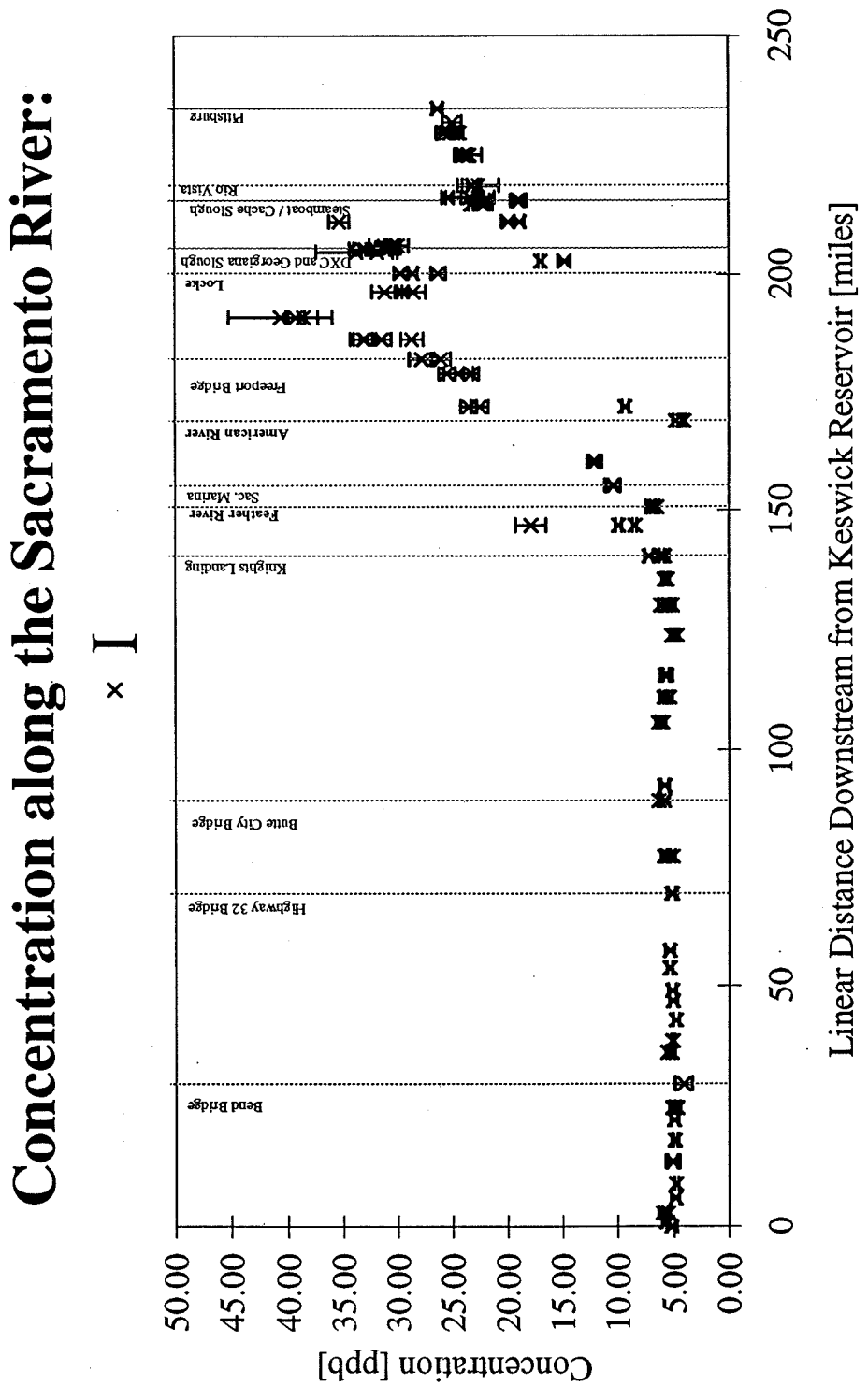
Concentration along the Sacramento River:
Concentration [ppb]
50.00
45.00
40.00
35.00
30.00
25.00
20.00
15.00
10.00
5.00
0.00
0
50
100
150
200
250
Linear Distance Downstream from Keswick Reservoir [miles]
Bend Bridge
Highway 32 Bridge
Butte City Bridge
Knights Landing
Feather River
Sac. Mainta
American River
Freeport Bridge
Locke
DXC and Georgiana Slough
Steamboat / Cache Slough
Rio Vista
Pittsburg

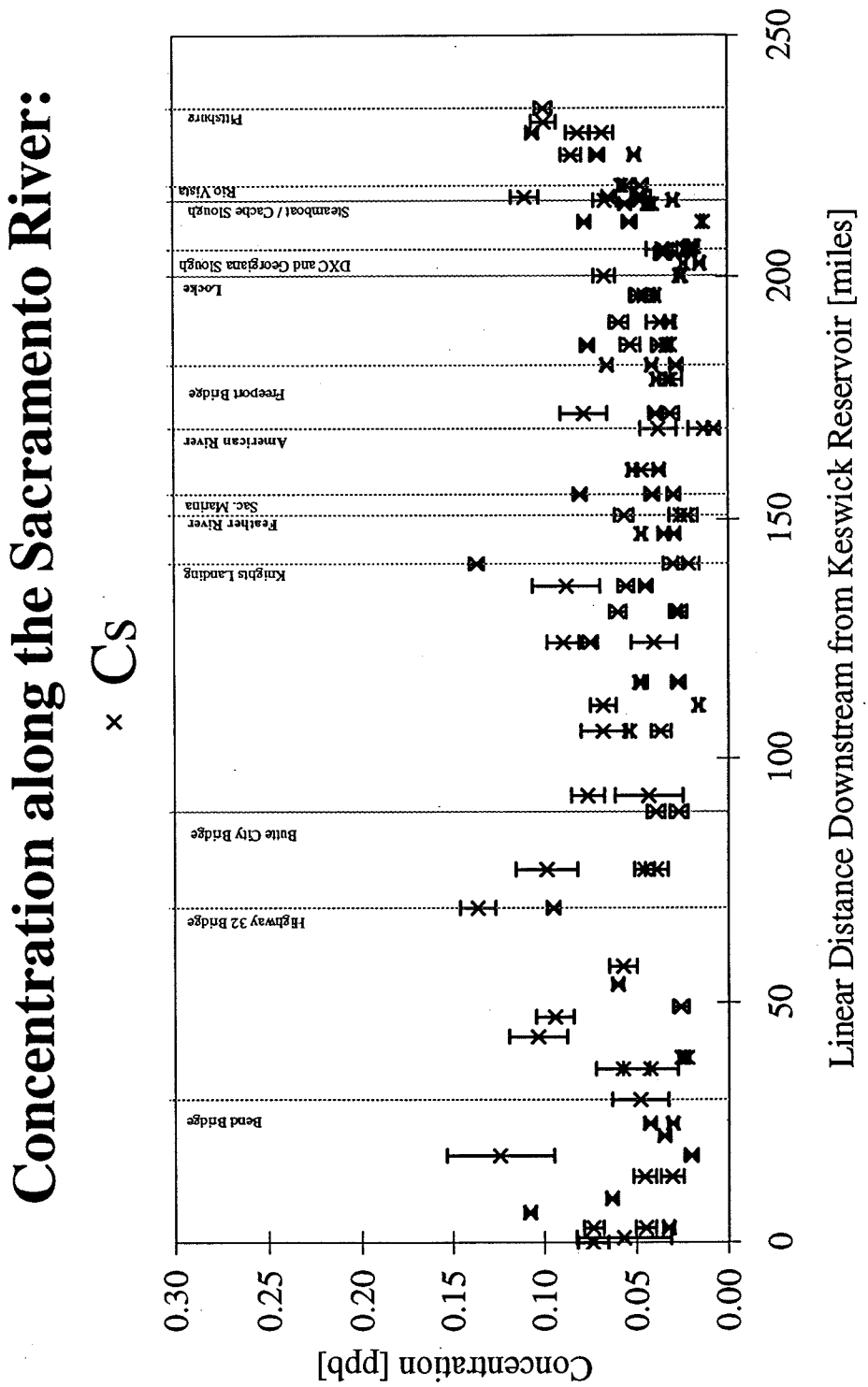
Concentration along the Sacramento River:
× Cs
Concentration [ppb]
0.30
0.25
0.20
0.15
0.10
0.05
0.00
0
50
100
150
200
250
Linear Distance Downstream from Keswick Reservoir [miles]
Bend Bridge
Highway 32 Bridge
Butte City Bridge
Knights Landing
Feather River
Sac. Matnia
American River
Freeport Bridge
Locke
DXC and Georgiana Slough
Steamboat / Cache Slough
Rio Vista
Mtlshnre

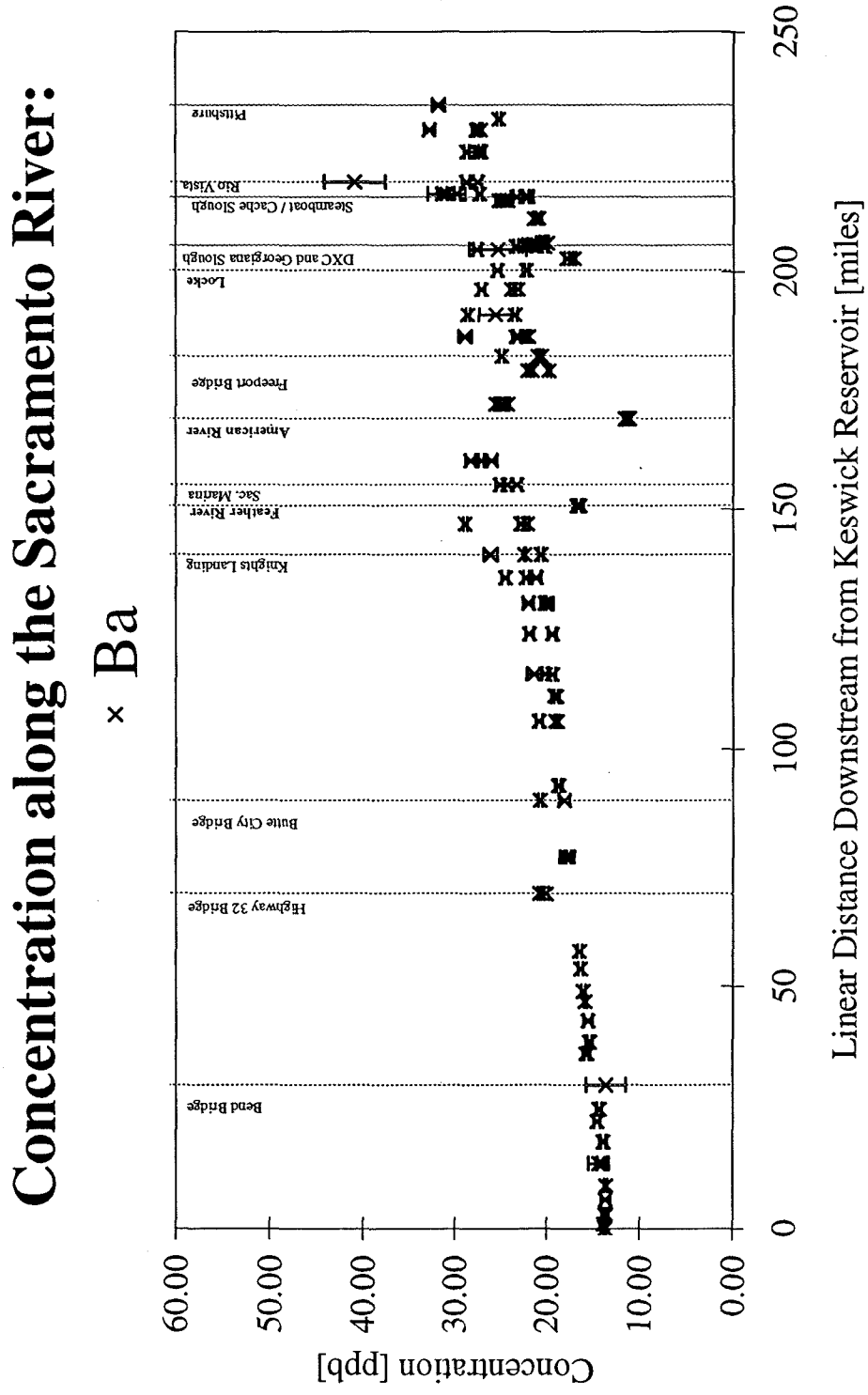
Concentration along the Sacramento River:
× Ba
Concentration [ppb]
60.00
50.00
40.00
30.00
20.00
10.00
0.00
0
50
100
150
200
250
Linear Distance Downstream from Keswick Reservoir [miles]
Bend Bridge
Highway 32 Bridge
Butte City Bridge
Knights Landing
Feather River
Sac. Matina
American River
Freeport Bridge
Locke
DXC and Georgiana Slough
Steamboat / Cache Slough
Rio Vista
Pittshire

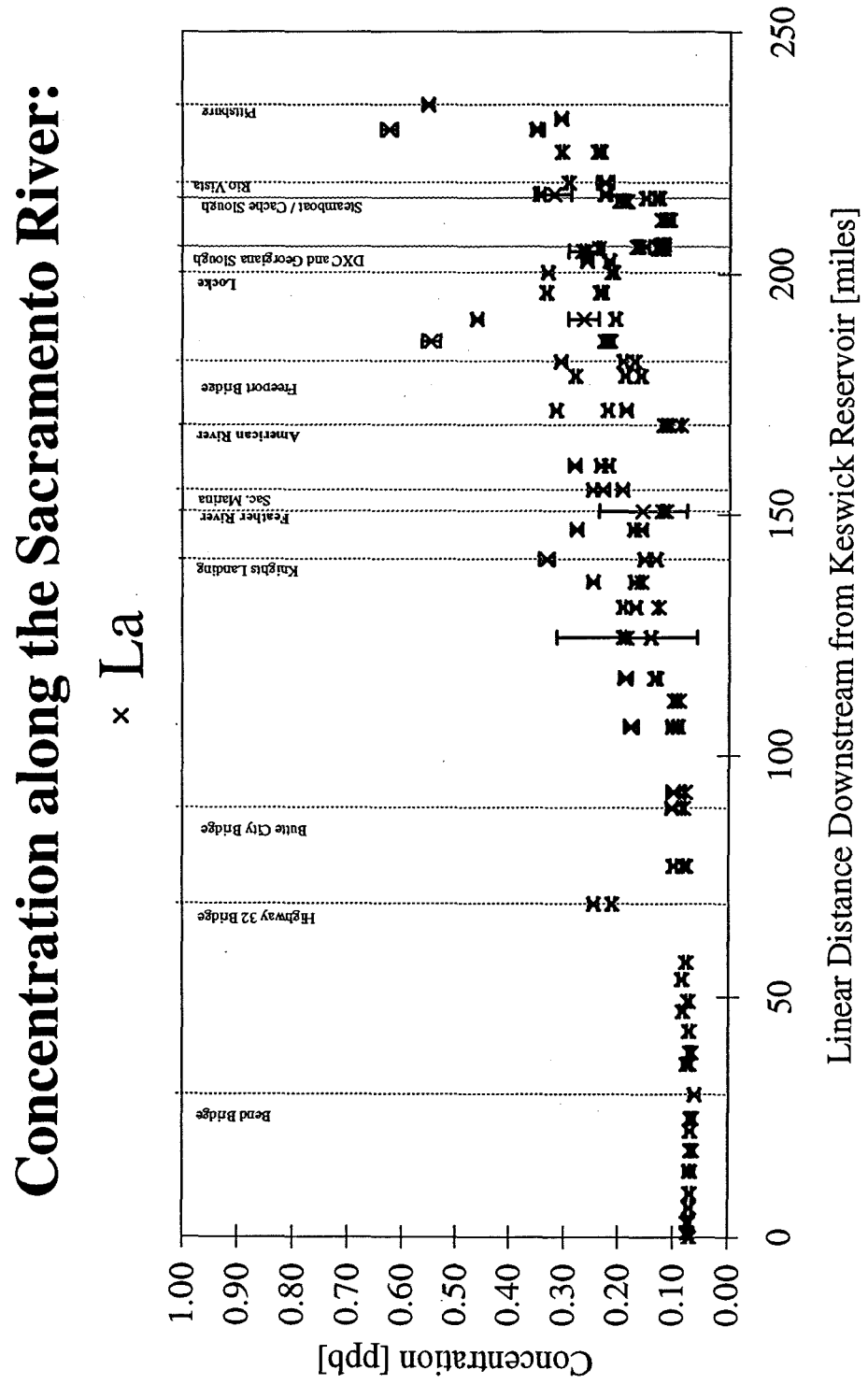
Concentration along the Sacramento River:
× La
Concentration [ppb]
1.00
0.90
0.80
0.70
0.60
0.50
0.40
0.30
0.20
0.10
0.00
0
50
100
150
200
250
Linear Distance Downstream from Keswick Reservoir [miles]
Bend Bridge
Highway 32 Bridge
Butte City Bridge
Knights Landing
Feather River
Sac. Marina
American River
Freeport Bridge
Locke
DXC and Georgiana Slough
Steamboat / Cache Slough
Rio Vista
Pittsburg

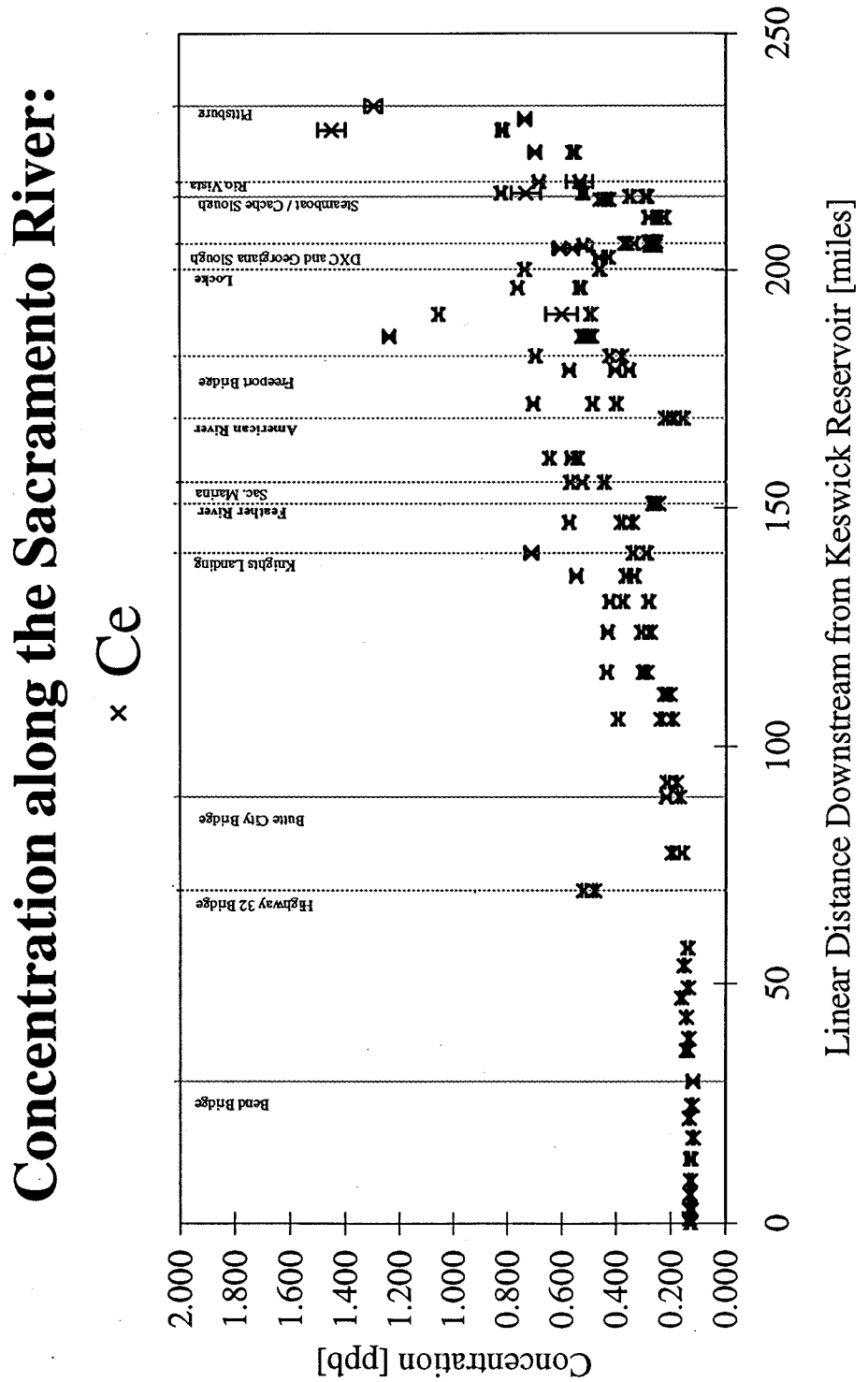
Concentration along the Sacramento River:
× Ce
Concentration [ppb]
2.000
1.800
1.600
1.400
1.200
1.000
0.800
0.600
0.400
0.200
0.000
0
50
100
150
200
250
Linear Distance Downstream from Keswick Reservoir [miles]
Bend Bridge
Highway 32 Bridge
Butte City Bridge
Knights Landing
Feather River
Sac. Marina
American River
Freeport Bridge
Locke
DXC and Georgiana Slough
Steamboat / Cache Slough
Rio Vista
Pittsburg

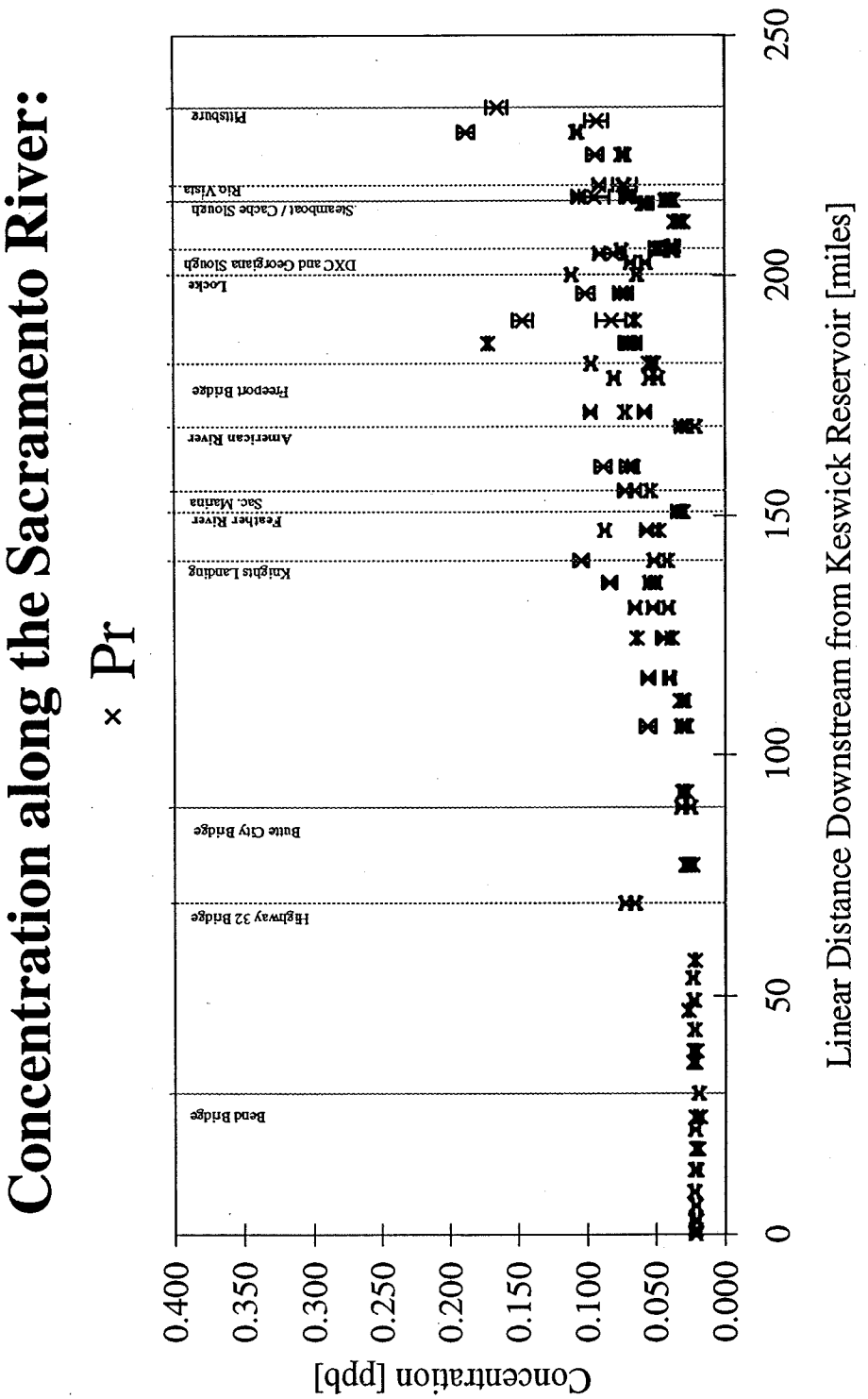
Concentration along the Sacramento River:
× Pr
Concentration [ppb]
0.400
0.350
0.300
0.250
0.200
0.150
0.100
0.050
0.000
0
50
100
150
200
250
Linear Distance Downstream from Keswick Reservoir [miles]
Bend Bridge
Highway 32 Bridge
Butte City Bridge
Knights Landing
Feather River
Sac. Marina
American River
Freeport Bridge
Locke
DXC and Georgiana Slough
Steamboat / Cache Slough
Rio Vista
Pittsburg

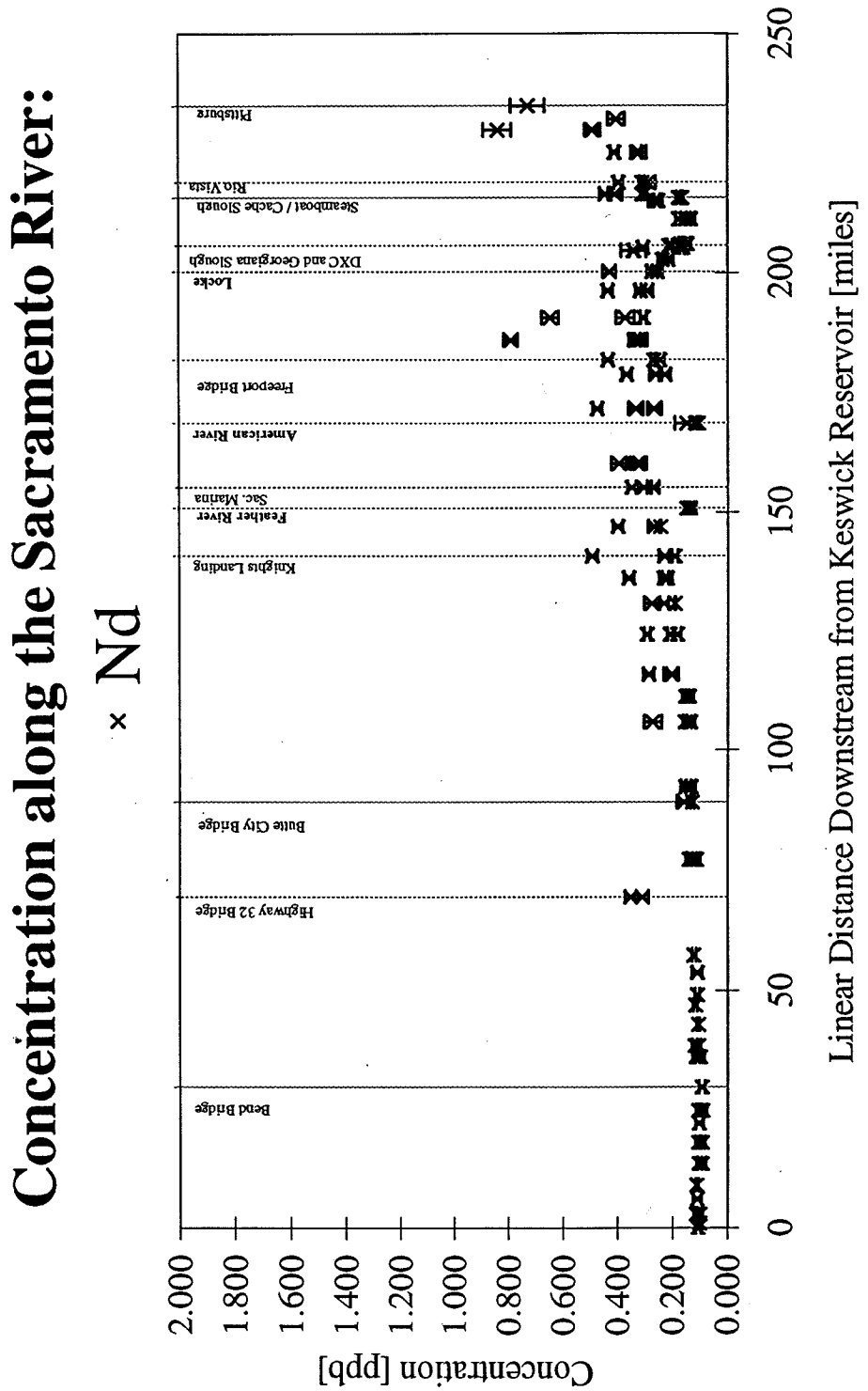
Concentration along the Sacramento River:
× Nd
Concentration [ppb]
2.000
1.800
1.600
1.400
1.200
1.000
0.800
0.600
0.400
0.200
0.000
0
50
100
150
200
250
Linear Distance Downstream from Keswick Reservoir [miles]
Bend Bridge
Highway 32 Bridge
Butte City Bridge
Knights Landing
Feather River
Sac. Marina
American River
Freeport Bridge
Locke
DXC and Georgiana Slough
Steamboat / Cache Slough
Rio Vista
Pittsburg

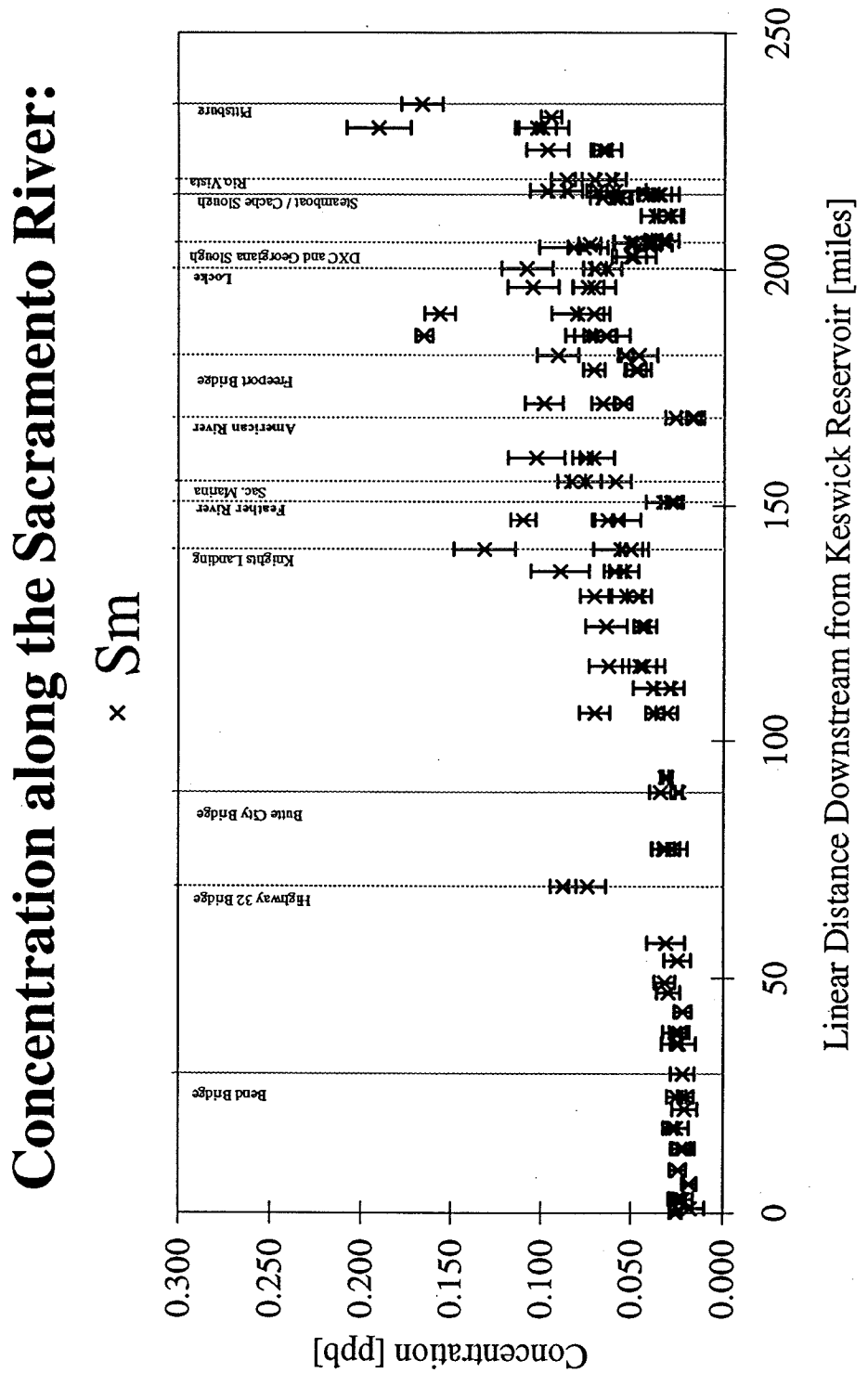
Concentration along the Sacramento River:
× Sm
Concentration [ppb]
0.300
0.250
0.200
0.150
0.100
0.050
0.000
0
50
100
150
200
250
Linear Distance Downstream from Keswick Reservoir [miles]
Bend Bridge
Highway 32 Bridge
Butte City Bridge
Knights Landing
Feather River
Sac. Marina
American River
Freeport Bridge
Locke
DXC and Georgiana Slough
Steamboat / Cache Slough
Rio Vista
Pittsburg

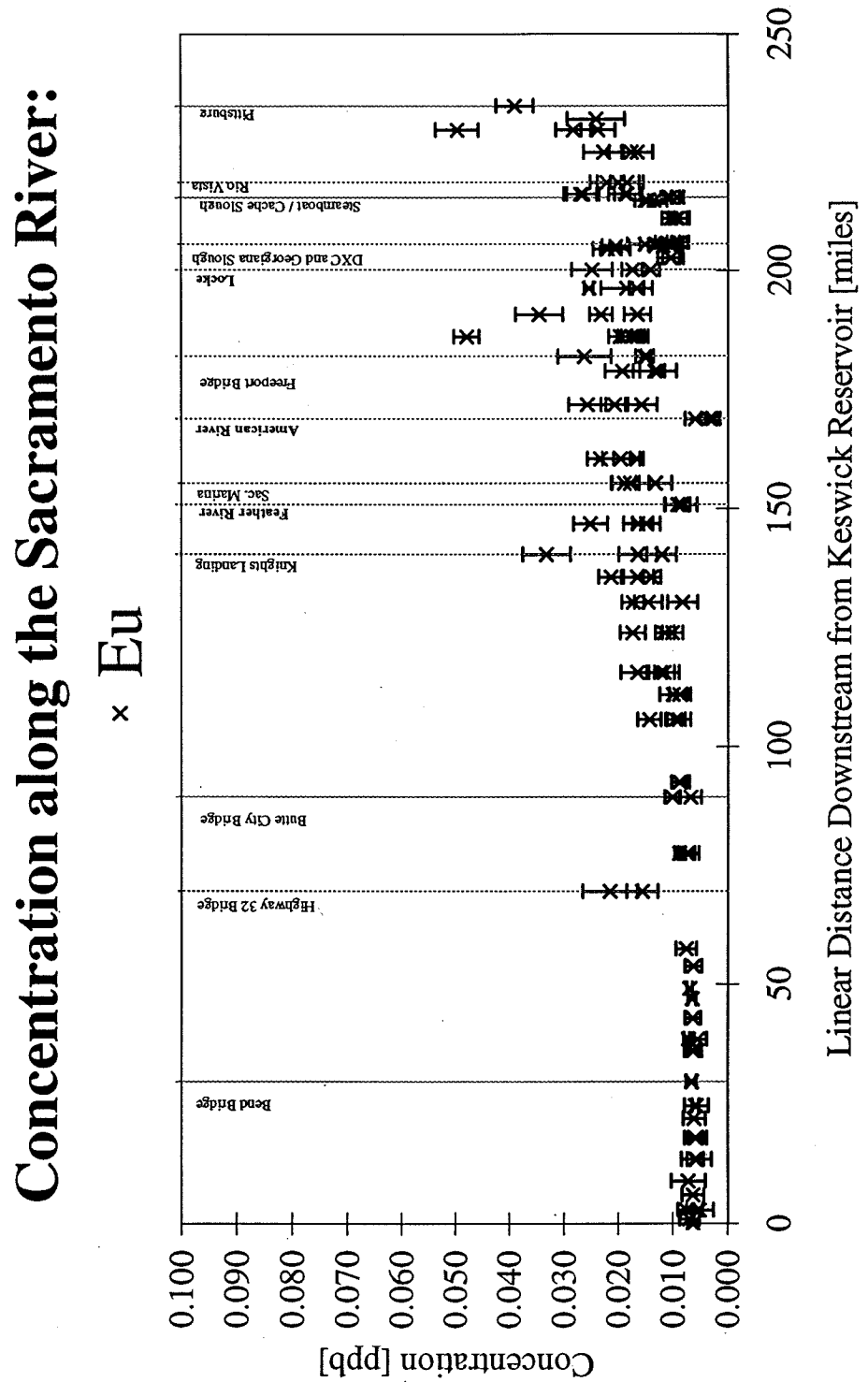
Concentration along the Sacramento River:
× Eu
Concentration [ppb]
0.100
0.090
0.080
0.070
0.060
0.050
0.040
0.030
0.020
0.010
0.000
0
50
100
150
200
250
Linear Distance Downstream from Keswick Reservoir [miles]
Bend Bridge
Highway 32 Bridge
Butte City Bridge
Knights Landing
Feather River
Sac. Martina
American River
Freeport Bridge
Locke
DXC and Georgiana Slough
Steamboat / Cache Slough
Rio Vista
Pittsburg

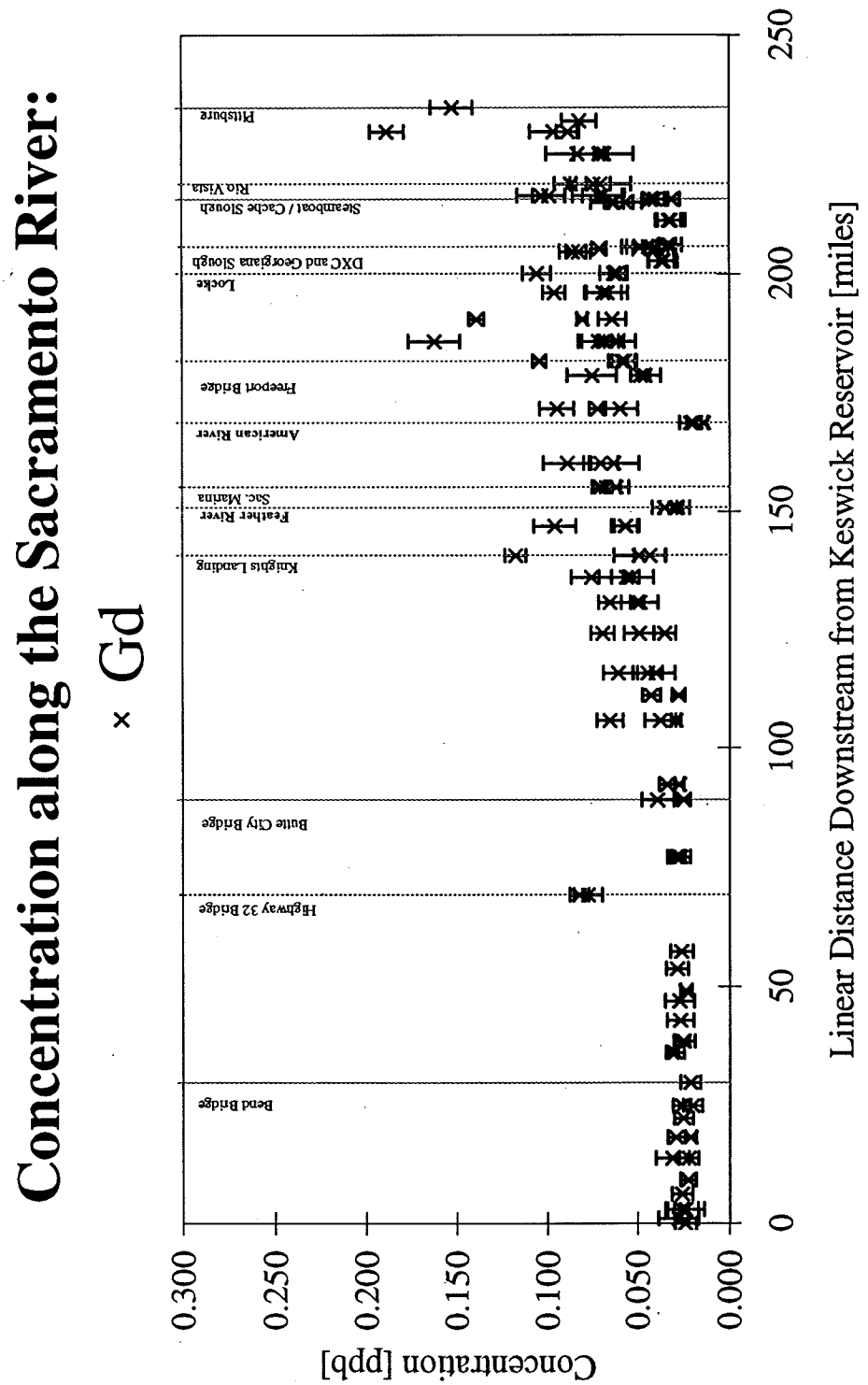
Concentration along the Sacramento River:
× Gd
Concentration [ppb]
0.300
0.250
0.200
0.150
0.100
0.050
0.000
0
50
100
150
200
250
Linear Distance Downstream from Keswick Reservoir [miles]
Bend Bridge
Highway 32 Bridge
Butte City Bridge
Knights Landing
Feather River
Sac. Mainta
American River
Freeport Bridge
Locke
DXC and Georgiana Slough
Steamboat / Cache Slough
Rio Vista
Pittsburg

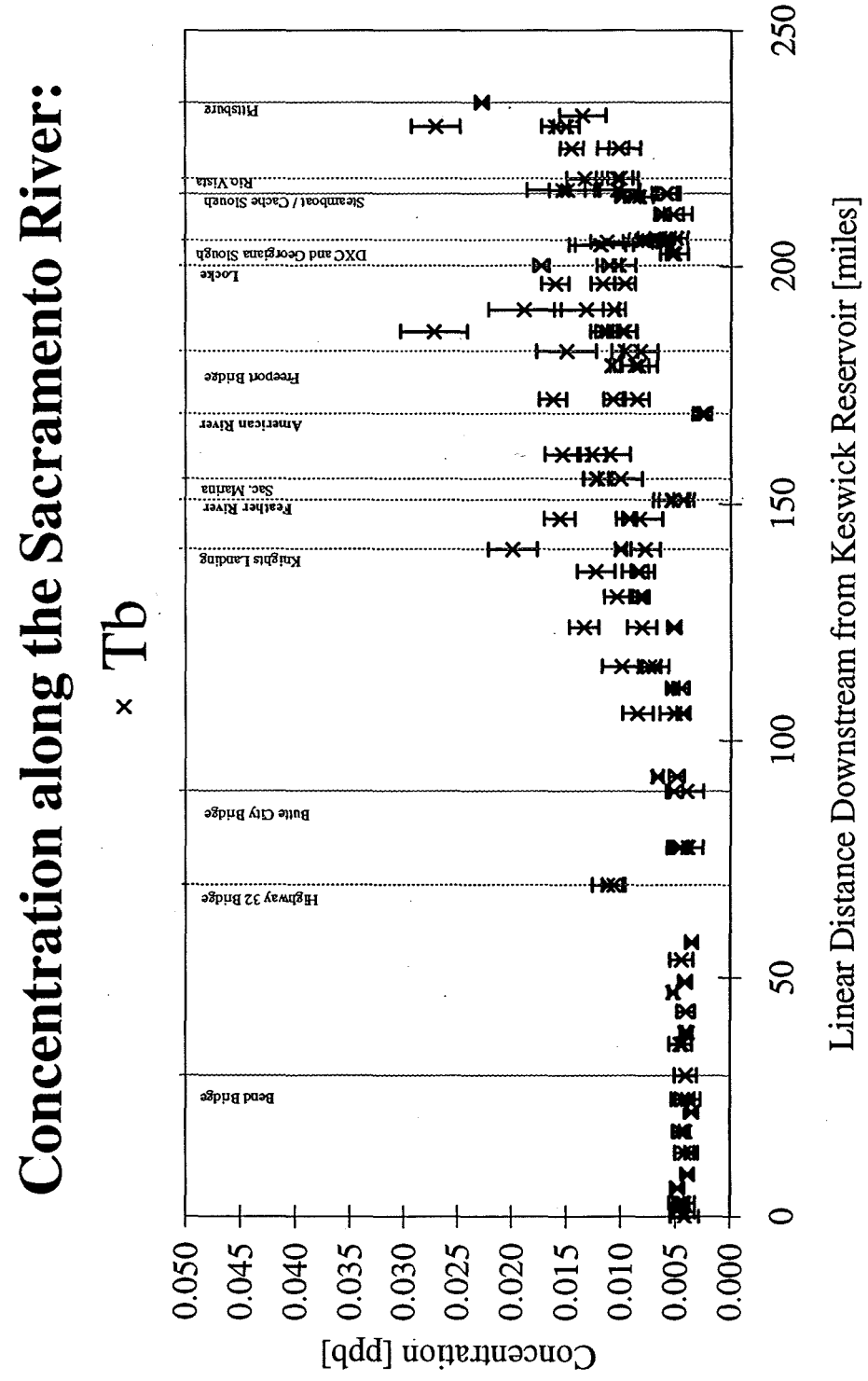
Concentration along the Sacramento River:
× Tb
Concentration [ppb]
0.050
0.045
0.040
0.035
0.030
0.025
0.020
0.015
0.010
0.005
0.000
0
50
100
150
200
250
Linear Distance Downstream from Keswick Reservoir [miles]
Bend Bridge
Highway 32 Bridge
Butte City Bridge
Knights Landing
Feather River
Sac. Marina
American River
Freeport Bridge
Locke
DXC and Georgiana Slough
Steamboat / Cache Slough
Rio Vista
Pittsburg

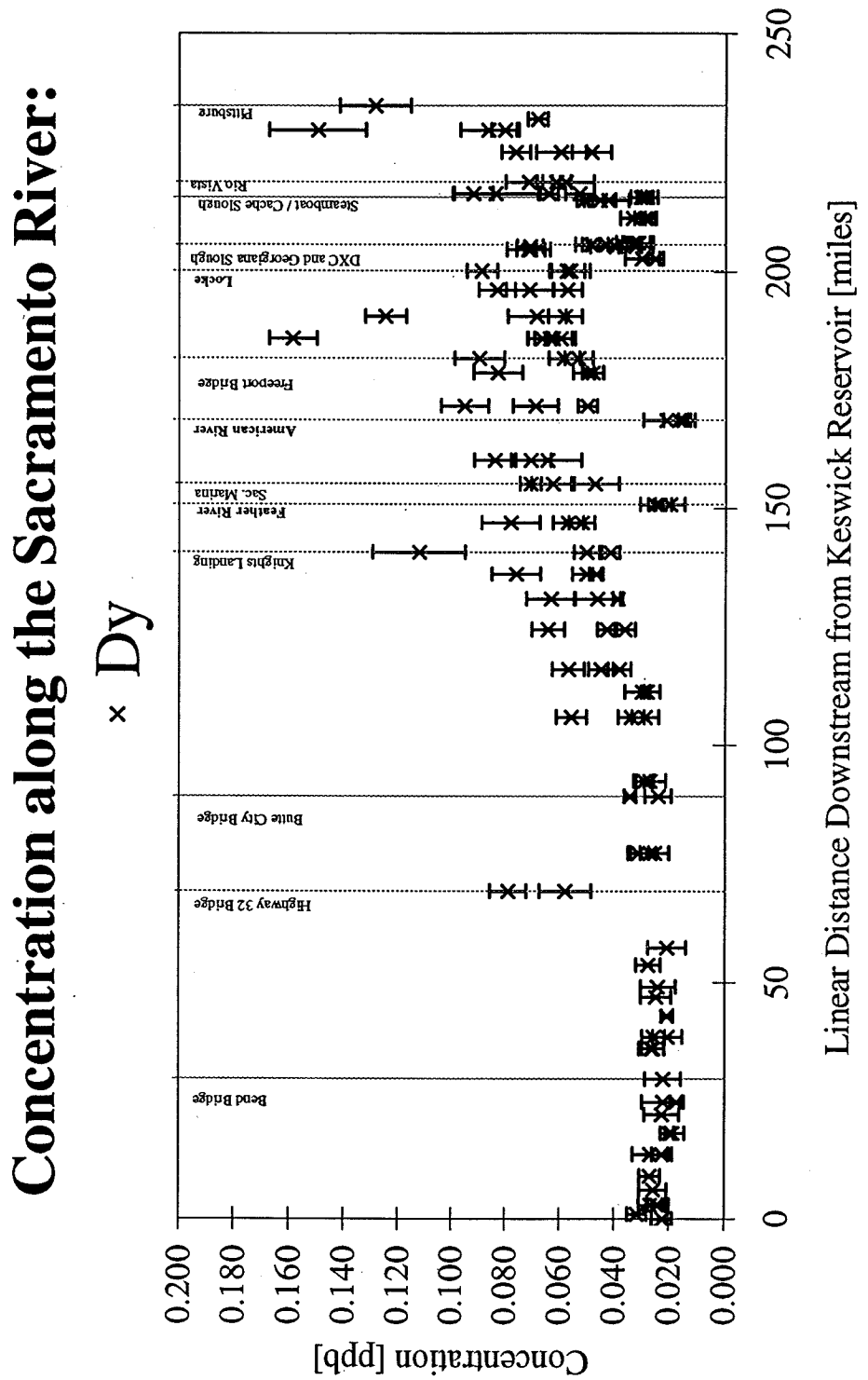
Concentration along the Sacramento River:
× Dy
Concentration [ppb]
0.200
0.180
0.160
0.140
0.120
0.100
0.080
0.060
0.040
0.020
0.000
0
50
100
150
200
250
Linear Distance Downstream from Keswick Reservoir [miles]
Bend Bridge
Highway 32 Bridge
Butte City Bridge
Knights Landing
Feather River
Sac. Marina
American River
Freeport Bridge
Locke
DXC and Georgiana Slough
Steamboat / Cache Slough
Rio Vista
Pittsburg

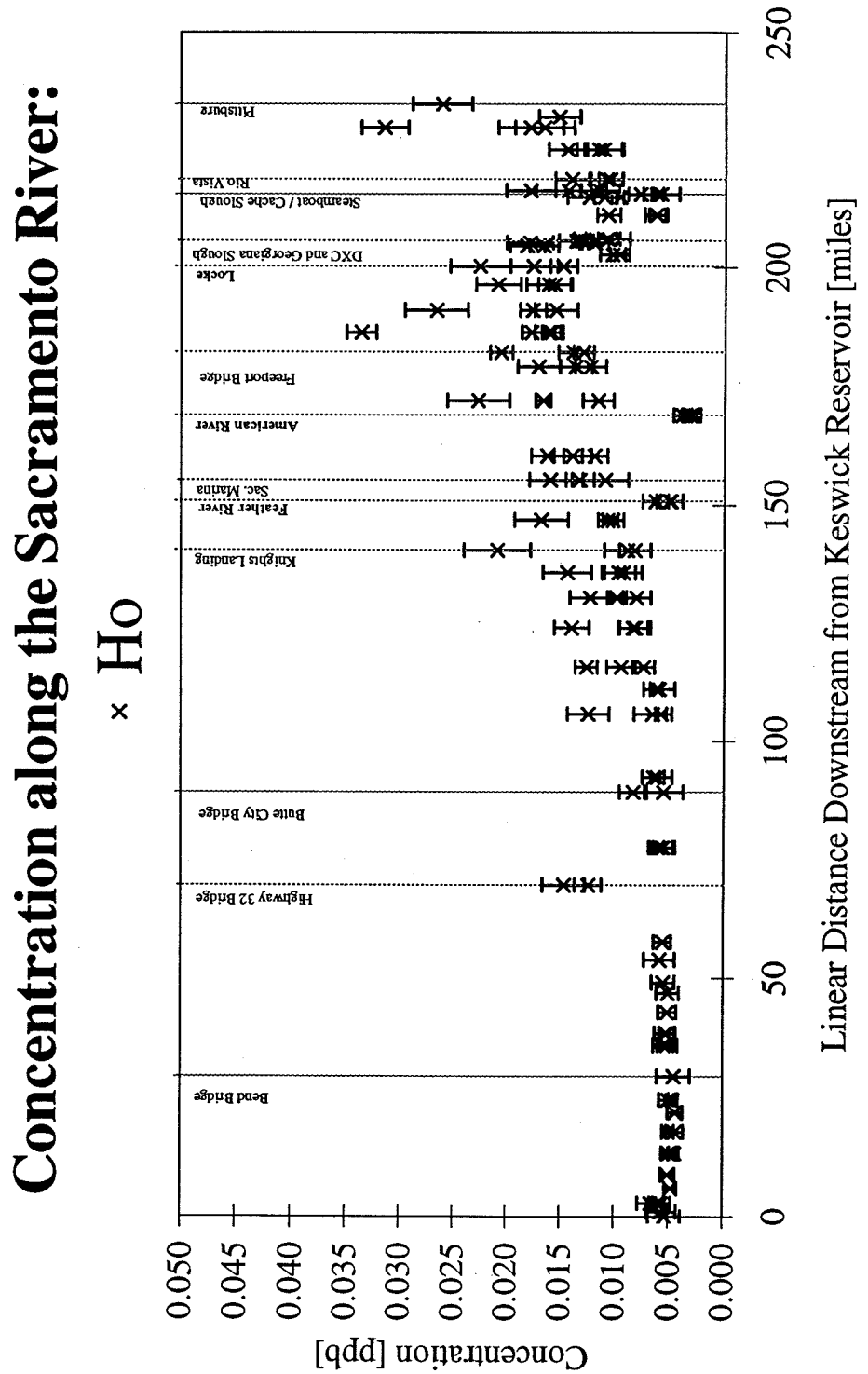
Concentration along the Sacramento River:
× Ho
Concentration [ppb]
0.050
0.045
0.040
0.035
0.030
0.025
0.020
0.015
0.010
0.005
0.000
0
50
100
150
200
250
Linear Distance Downstream from Keswick Reservoir [miles]
Bend Bridge
Highway 32 Bridge
Butte City Bridge
Knights Landing
Feather River
Sac. Mainta
American River
Freeport Bridge
Locke
DXC and Georgiana Slough
Steamboat / Cache Slough
Rio Vista
Pittsburg

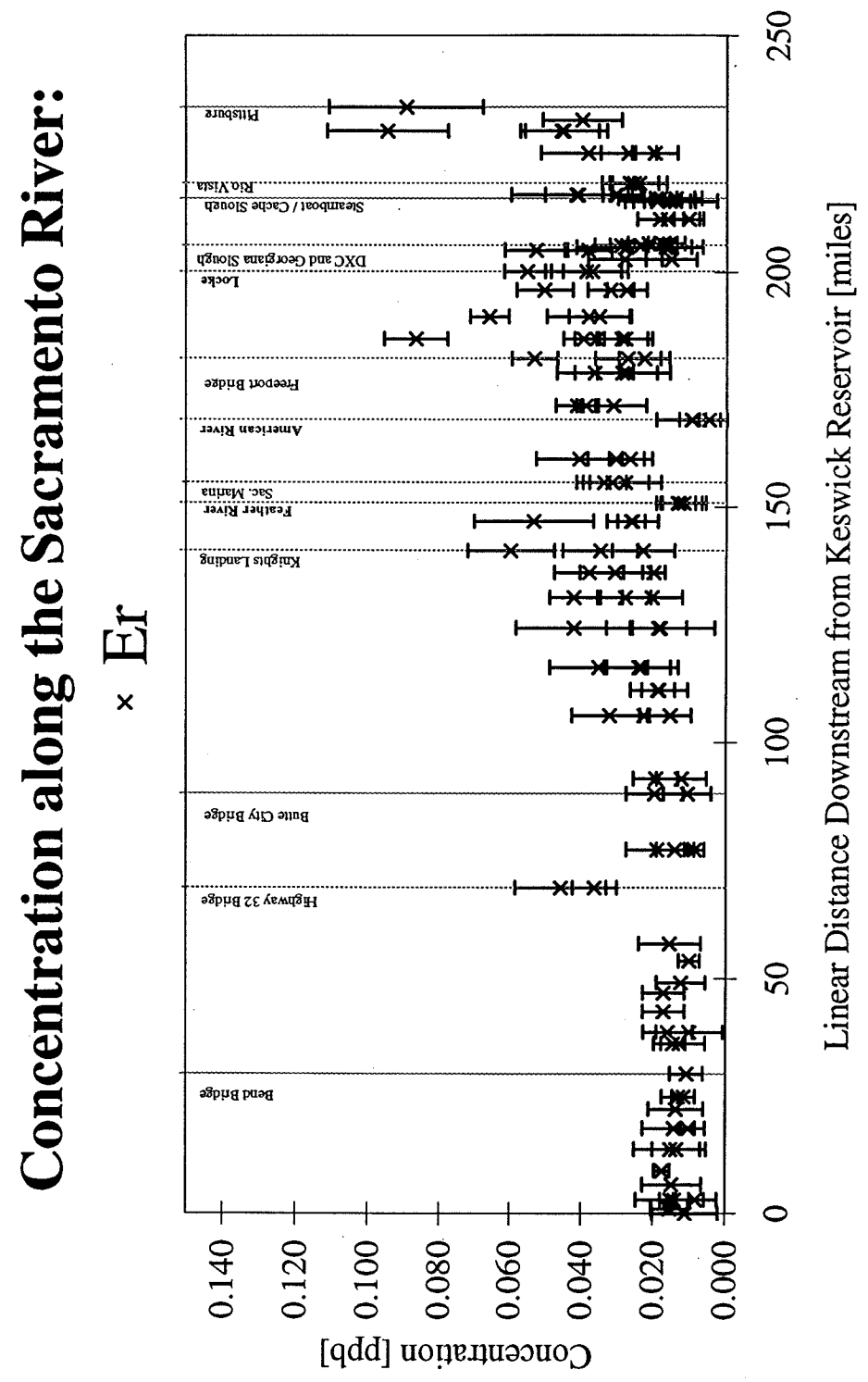
Concentration along the Sacramento River:
× Er
Concentration [ppb]
0.140
0.120
0.100
0.080
0.060
0.040
0.020
0.000
0
50
100
150
200
250
Linear Distance Downstream from Keswick Reservoir [miles]
Bend Bridge
Highway 32 Bridge
Butte City Bridge
Knights Landing
Feather River
Sac. Mainta
American River
Freeport Bridge
Locke
DXC and Georgiana Slough
Steamboat / Cache Slough
Rio Vista
Pittsburg

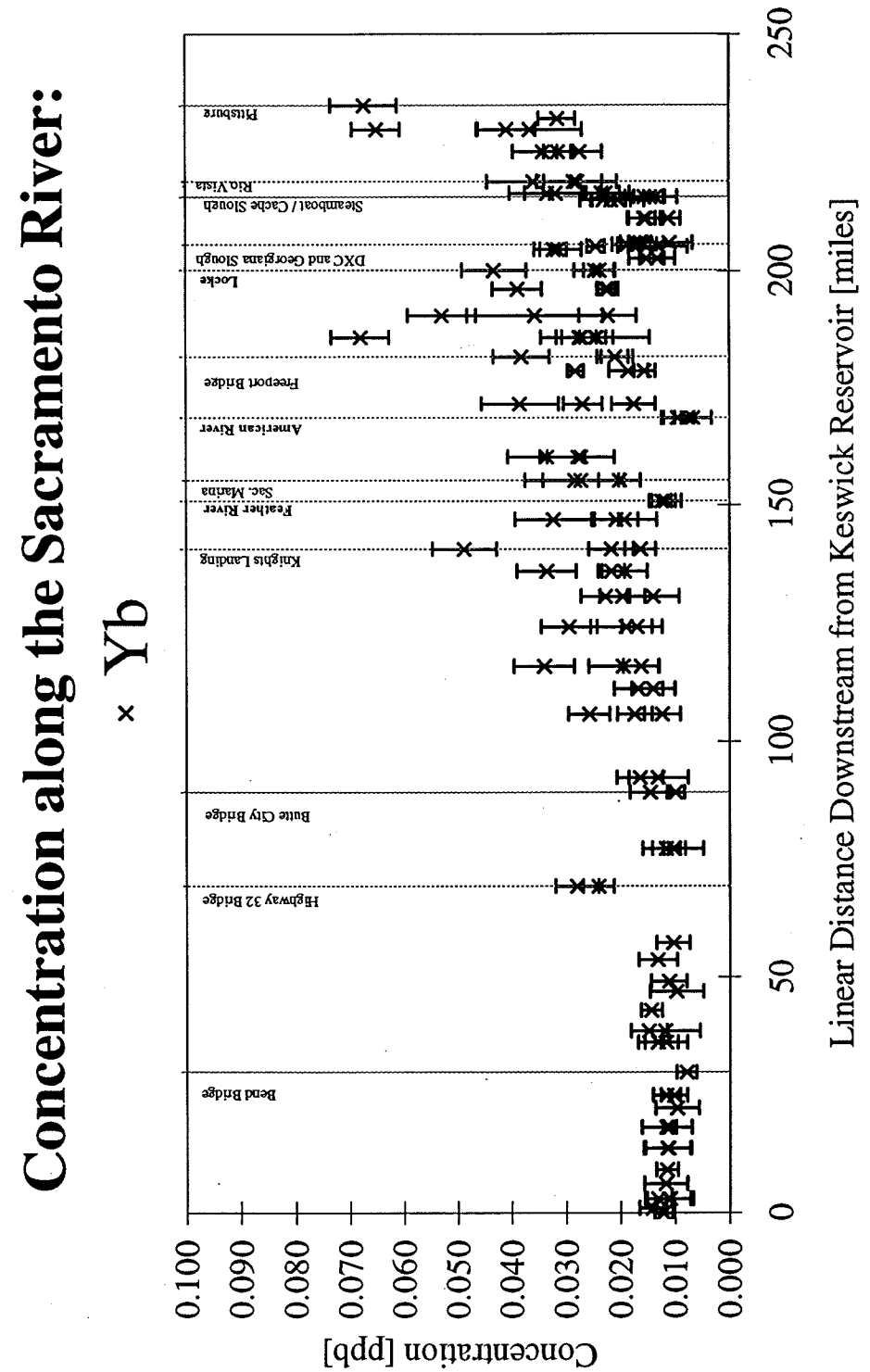
Concentration along the Sacramento River:
× Yb
Concentration [ppb]
0.100
0.090
0.080
0.070
0.060
0.050
0.040
0.030
0.020
0.010
0.000
0
50
100
150
200
250
Linear Distance Downstream from Keswick Reservoir [miles]
Bend Bridge
Highway 32 Bridge
Butte City Bridge
Knights Landing
Feather River
Sac. Marina
American River
Freeport Bridge
Locke
DXC and Georgiana Slough
Steamboat / Cache Slough
Rio Vista
Pittsburg

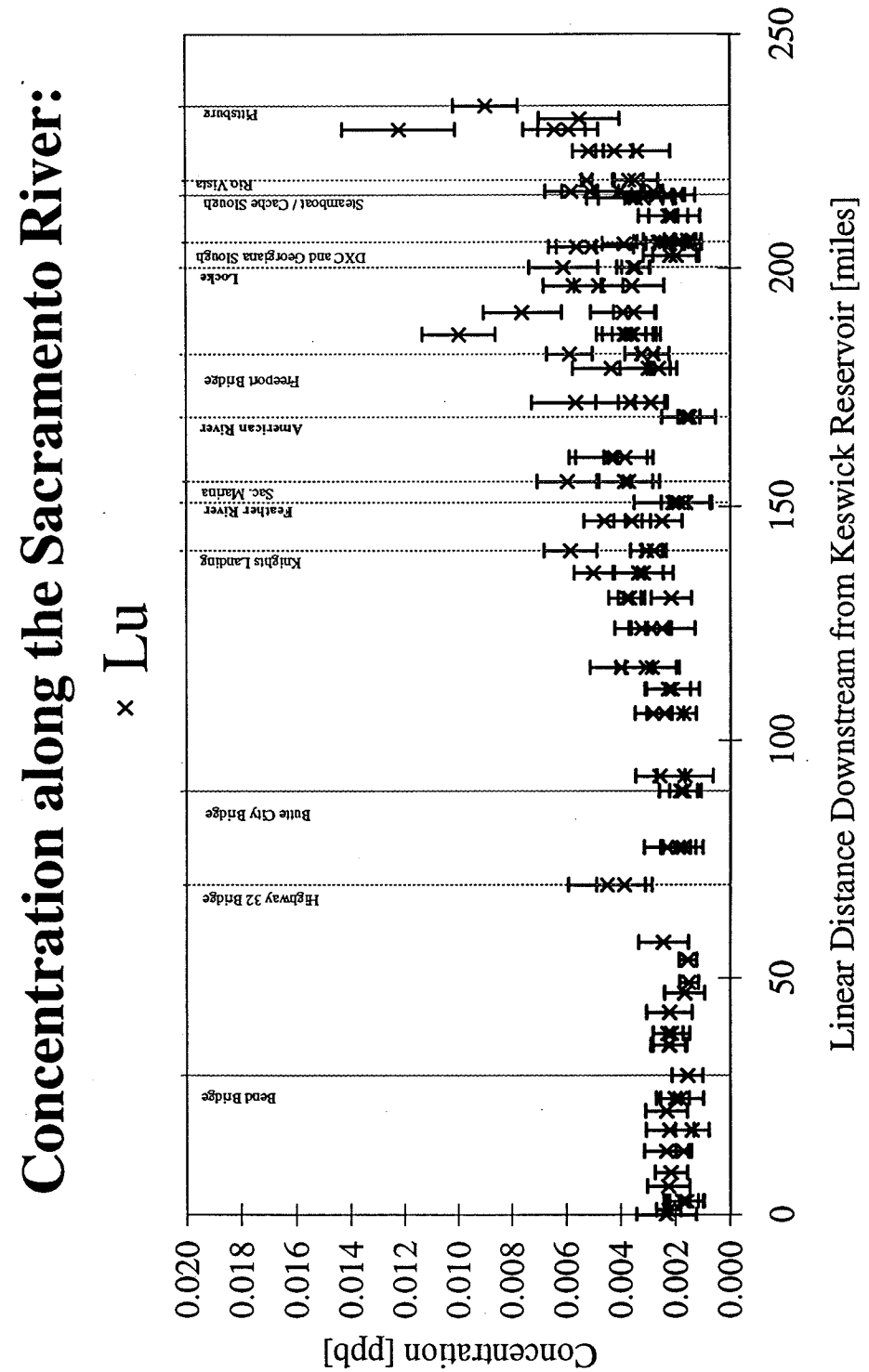
Concentration along the Sacramento River:
× Lu
Concentration [ppb]
0.020
0.018
0.016
0.014
0.012
0.010
0.008
0.006
0.004
0.002
0.000
0
50
100
150
200
250
Linear Distance Downstream from Keswick Reservoir [miles]
Bend Bridge
Highway 32 Bridge
Butte City Bridge
Knights Landing
Feather River
Sac. Marina
American River
Freeport Bridge
Locke
DXC and Georgiana Slough
Steamboat / Cache Slough
Rio Vista
Pittsburg

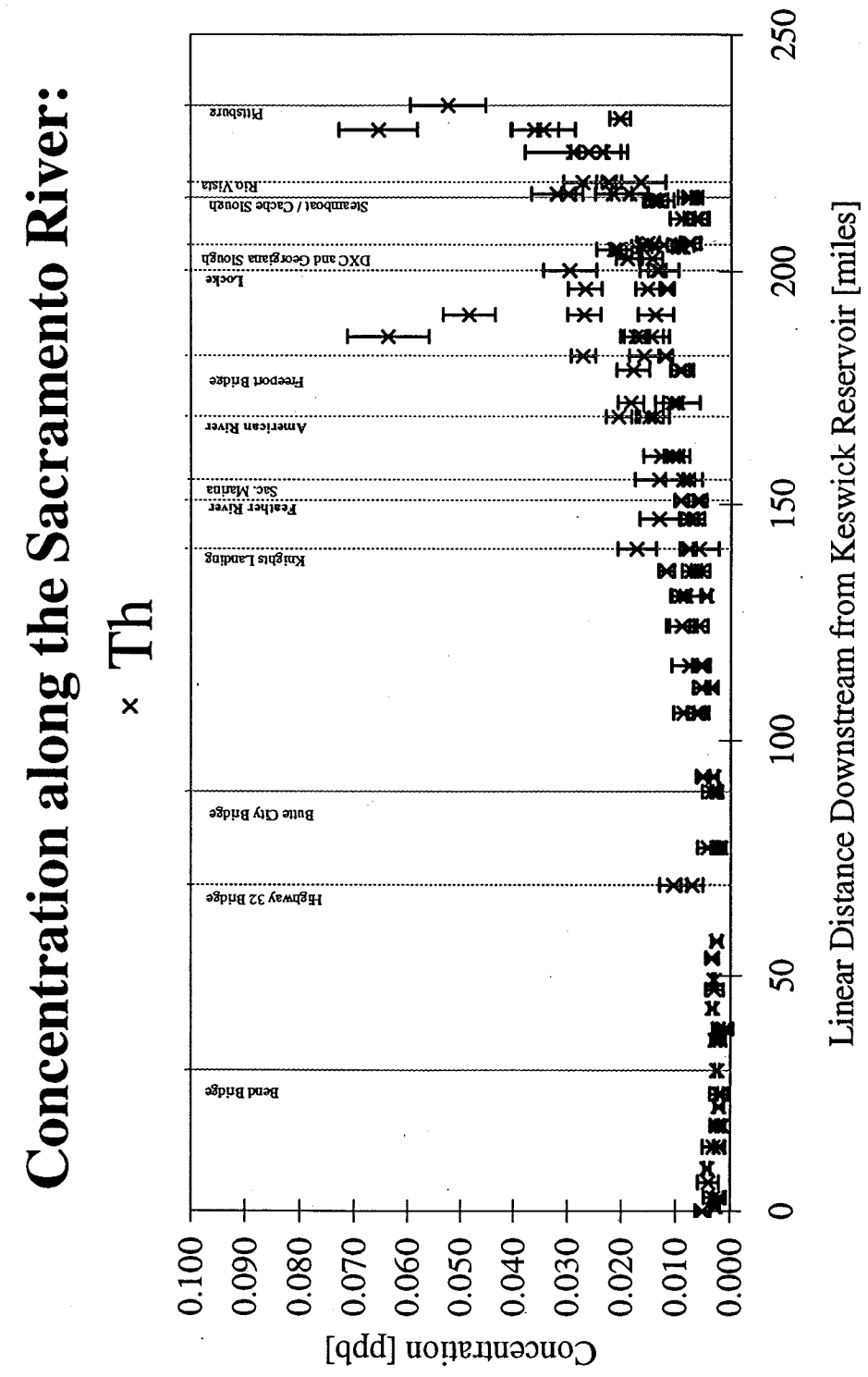
Concentration along the Sacramento River:
× Th
Concentration [ppb]
0.100
0.090
0.080
0.070
0.060
0.050
0.040
0.030
0.020
0.010
0.000
0
50
100
150
200
250
Linear Distance Downstream from Keswick Reservoir [miles]
Bend Bridge
Highway 32 Bridge
Butte City Bridge
Knights Landing
Feather River
Sac. Marina
American River
Freeport Bridge
Locke
DXC and Georgiana Slough
Steamboat / Cache Slough
Rio Vista
Pittsburg

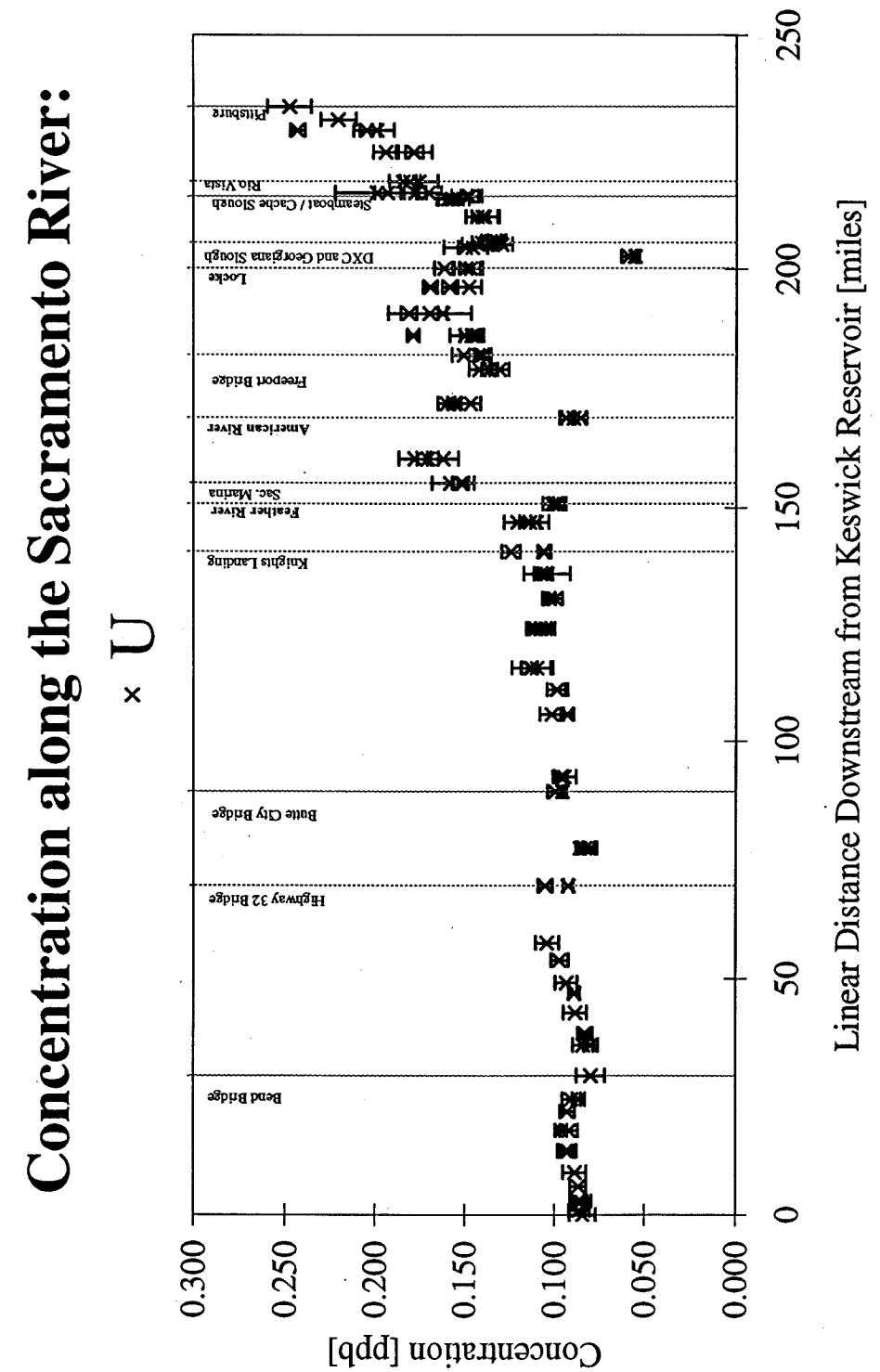
Concentration along the Sacramento River:
× U
Concentration [ppb]
0.300
0.250
0.200
0.150
0.100
0.050
0.000
0
50
100
150
200
250
Linear Distance Downstream from Keswick Reservoir [miles]
Bend Bridge
Highway 32 Bridge
Butte City Bridge
Knights Landing
Feather River
Sac. Marina
American River
Freeport Bridge
Locke
DXC and Georgiana Slough
Steamboat / Cache Slough
Rio Vista
Pittsburg

Appendix F

Results of filtration experiments to determine maximum cation exchange capacity in the Delta

Appendix F
Results of filtration experiments to determine maximum cation exchange capacity in the Delta

Table of Contents

Flow on Sacramento and San Joaquin Rivers during filtration experiments

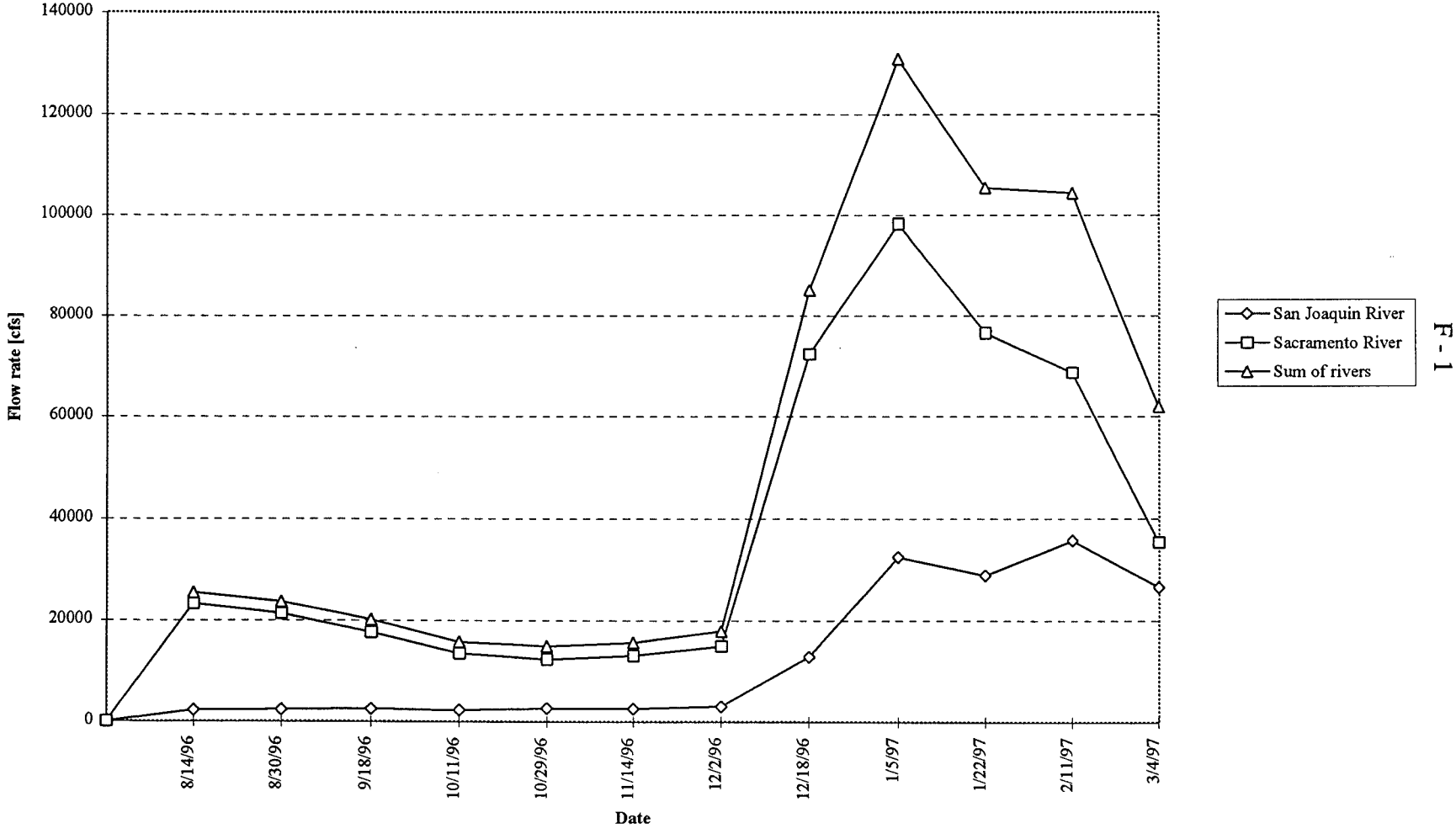

F - 1

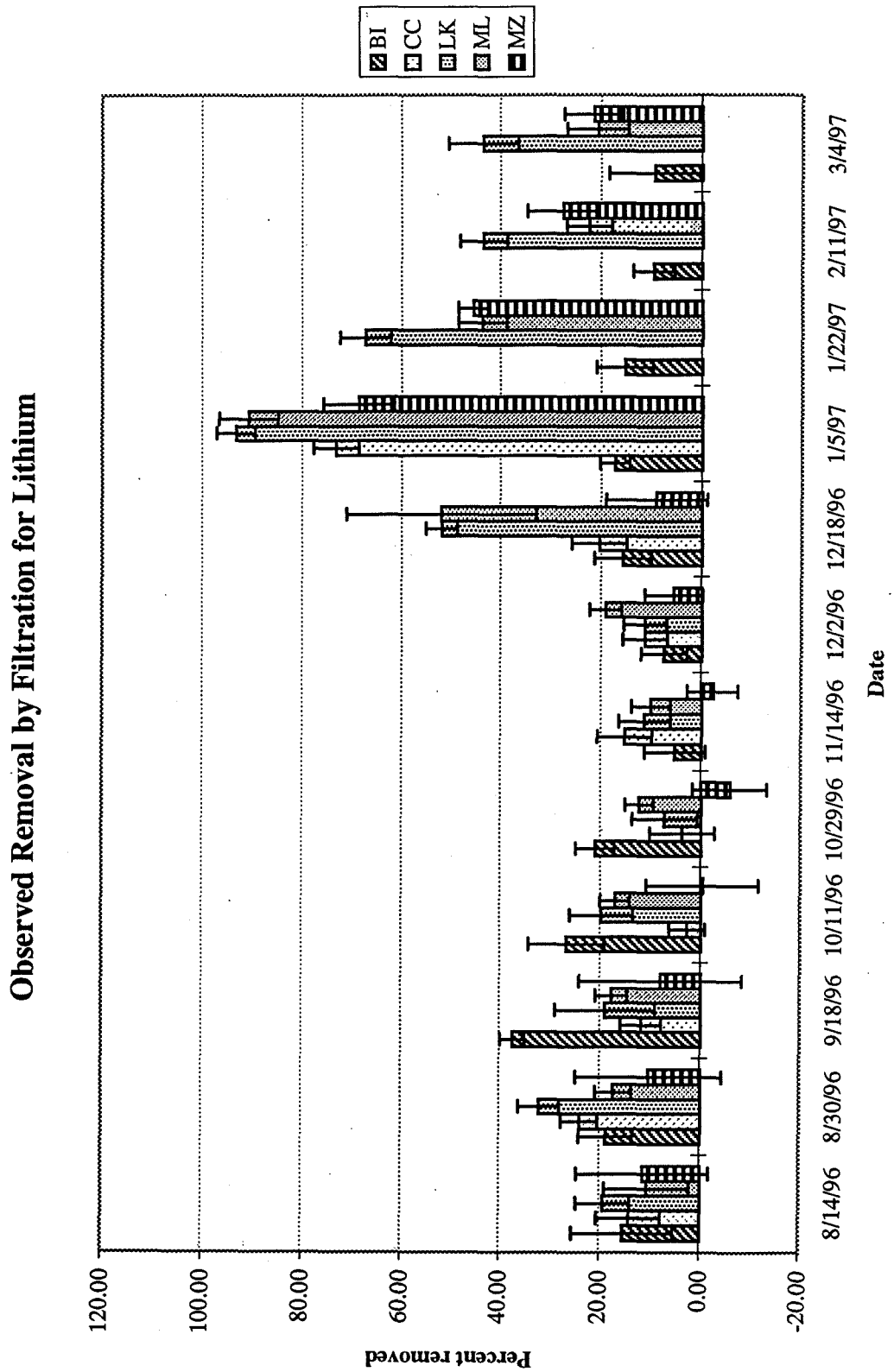
Observed Removal by Filtration for Lithium
BI
CC
LK
ML
MZ
120.00
100.00
80.00
60.00
40.00
20.00
0.00
-20.00
Percent removed
8/14/96
8/30/96
9/18/96
10/11/96
10/29/96
11/14/96
12/2/96
12/18/96
1/5/97
1/22/97
2/11/97
3/4/97
Date

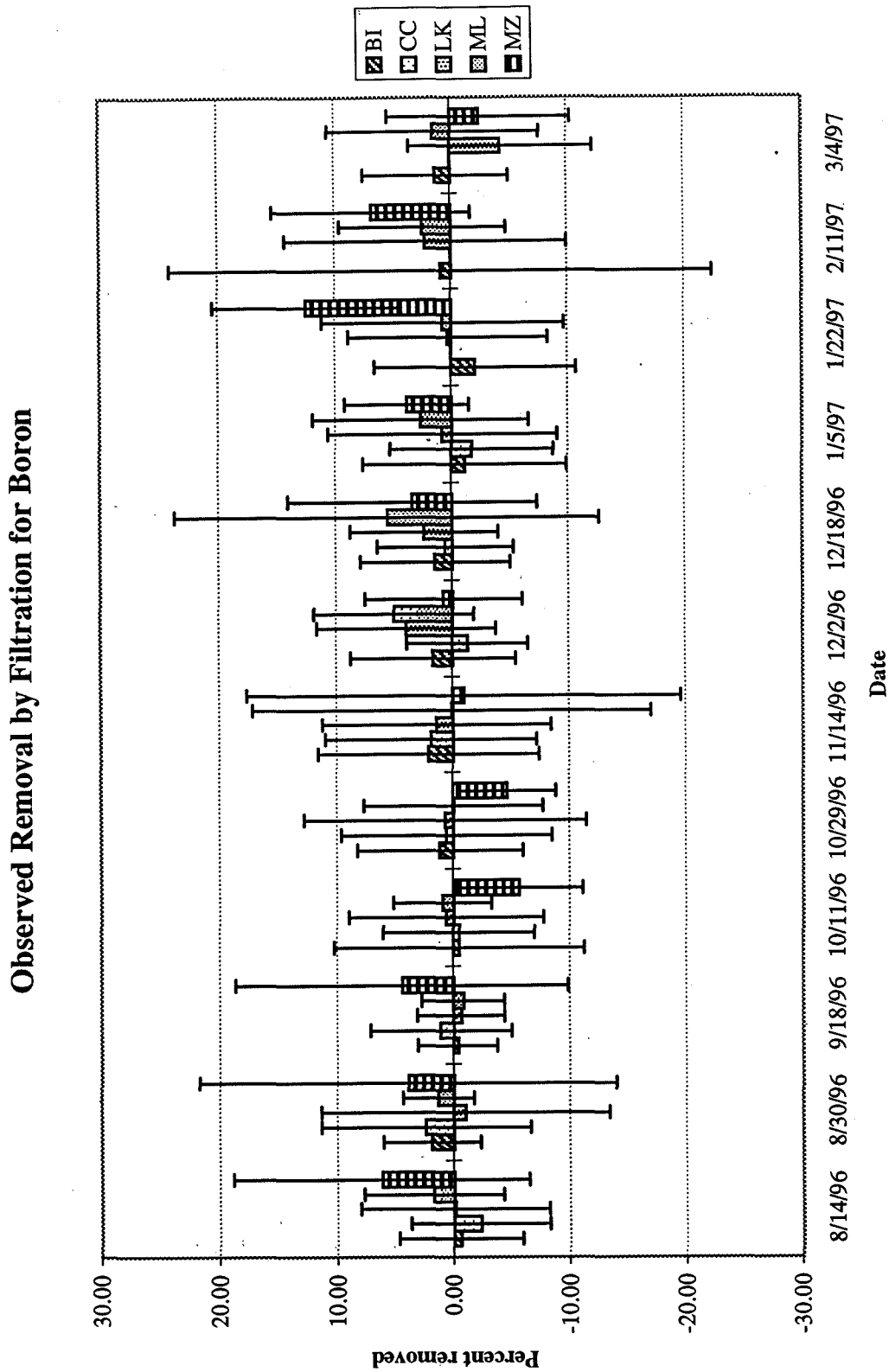
Observed Removal by Filtration for Boron
BI
CC
LK
ML
MZ
30.00
20.00
10.00
0.00
-10.00
-20.00
-30.00
Percent removed
8/14/96
8/30/96
9/18/96
10/11/96
10/29/96
11/14/96
12/2/96
12/18/96
1/5/97
1/22/97
2/11/97
3/4/97
Date

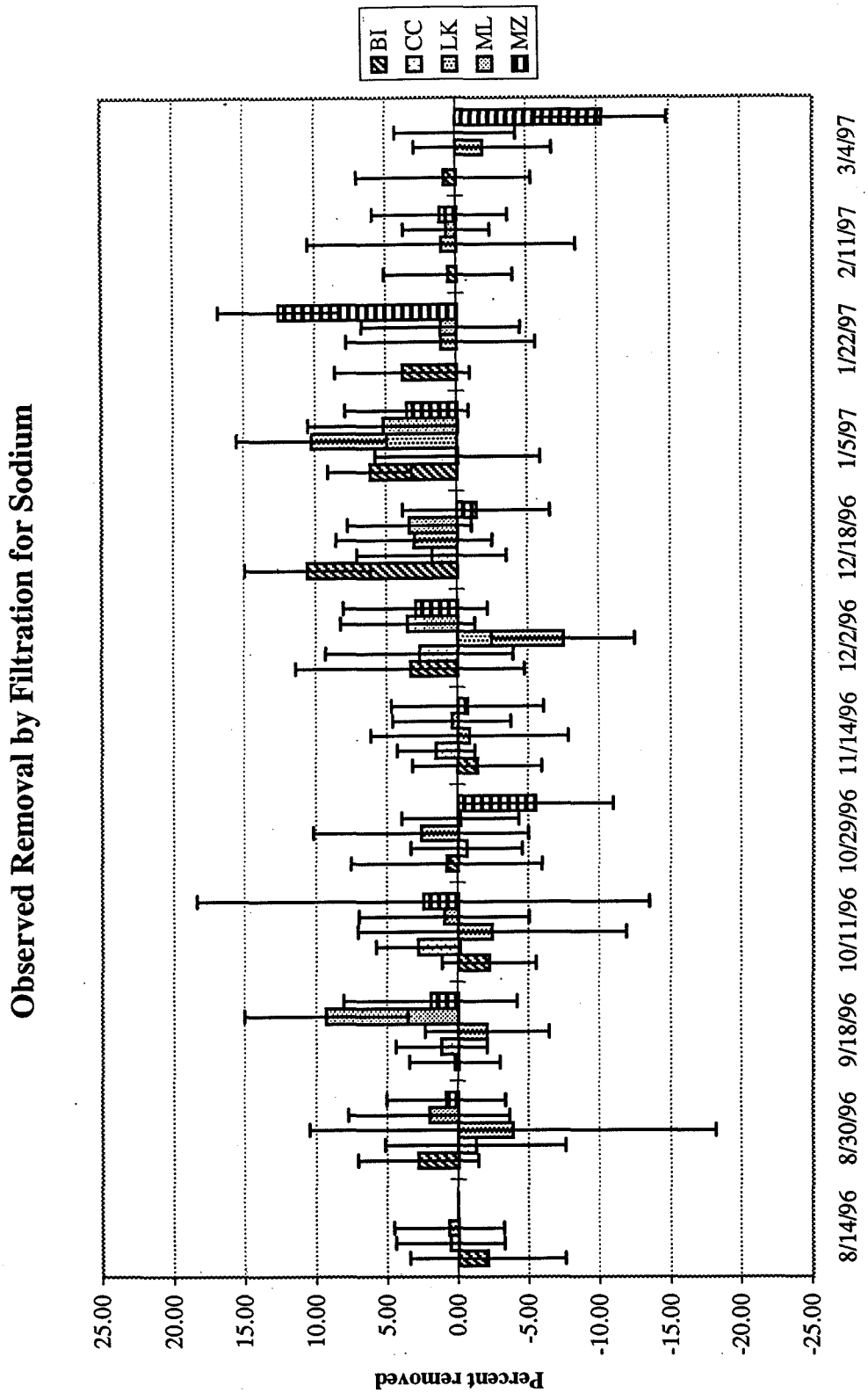
Observed Removal by Filtration for Sodium
BI
CC
LK
ML
MZ
25.00
20.00
15.00
10.00
5.00
0.00
-5.00
-10.00
-15.00
-20.00
-25.00
Percent removed
8/14/96
8/30/96
9/18/96
10/11/96
10/29/96
11/14/96
12/2/96
12/18/96
1/5/97
1/22/97
2/11/97
3/4/97
Date

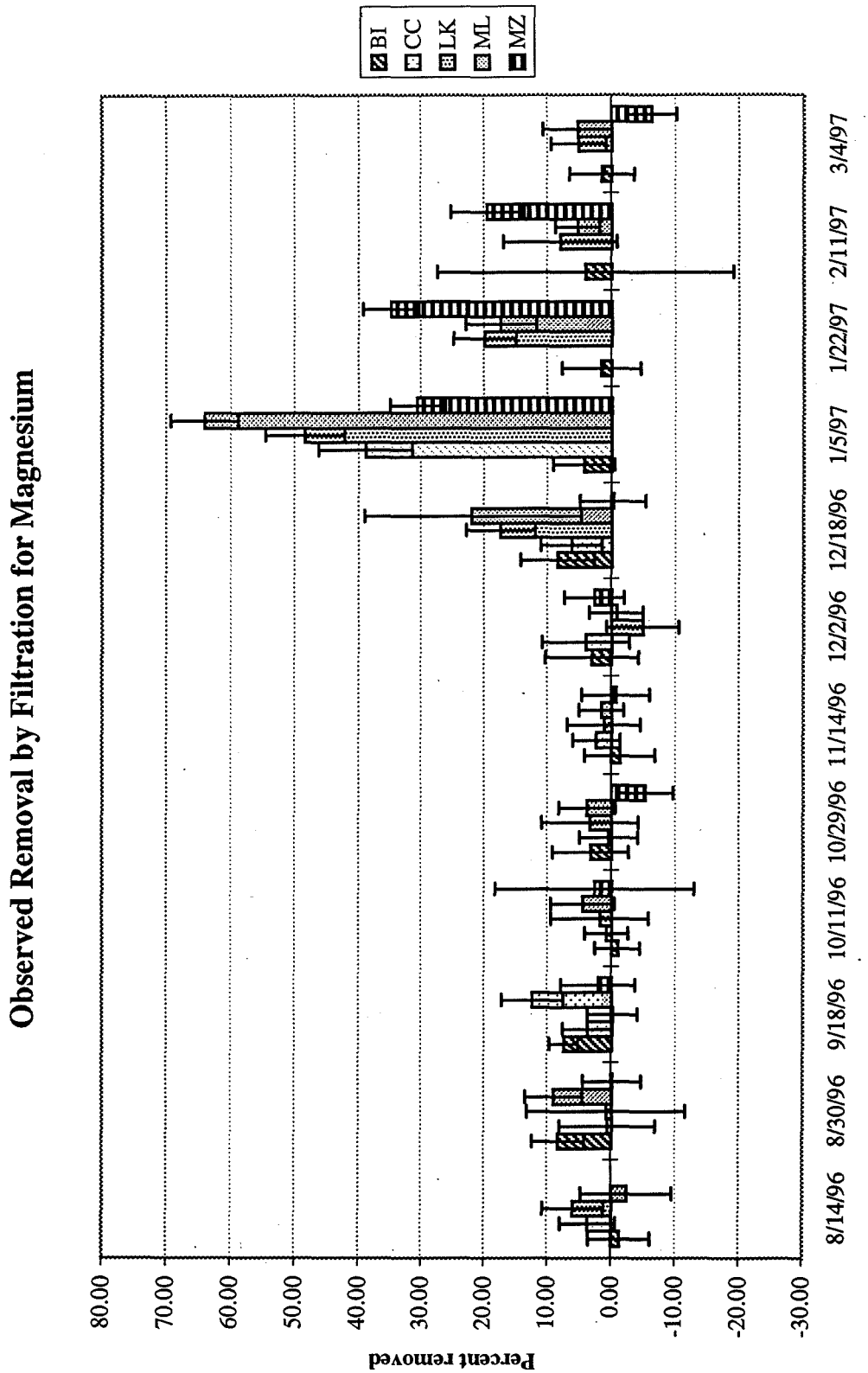
Observed Removal by Filtration for Magnesium
BI
CC
LK
ML
MZ
80.00
70.00
60.00
50.00
40.00
30.00
20.00
10.00
0.00
-10.00
-20.00
-30.00
Percent removed
8/14/96
8/30/96
9/18/96
10/11/96
10/29/96
11/14/96
12/2/96
12/18/96
1/5/97
1/22/97
2/11/97
3/4/97
Date

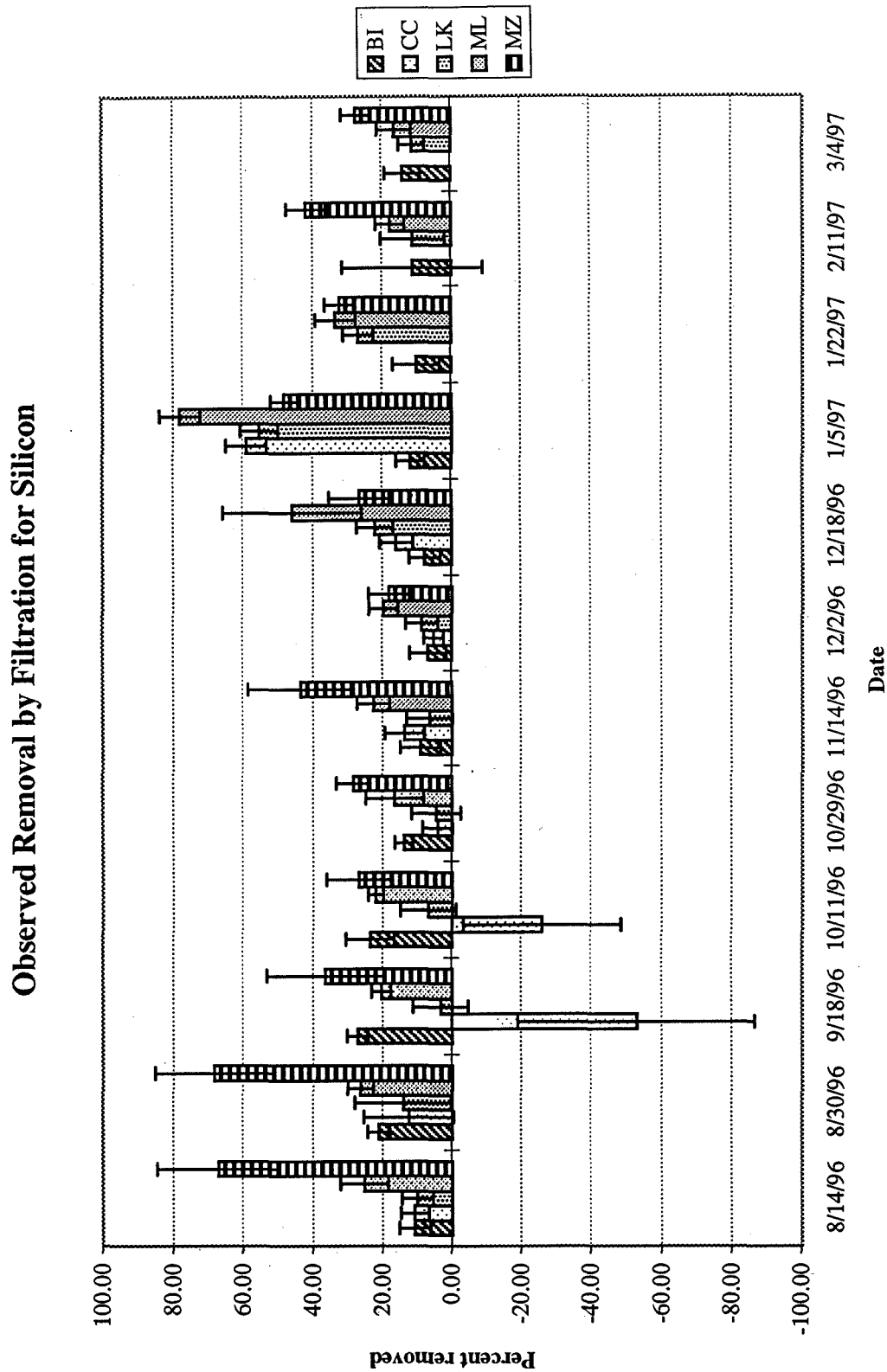
Observed Removal by Filtration for Silicon
BI
CC
LK
ML
MZ
100.00
80.00
60.00
40.00
20.00
0.00
-20.00
-40.00
-60.00
-80.00
-100.00
Percent removed
8/14/96
8/30/96
9/18/96
10/11/96
10/29/96
11/14/96
12/2/96
12/18/96
1/5/97
1/22/97
2/11/97
3/4/97
Date

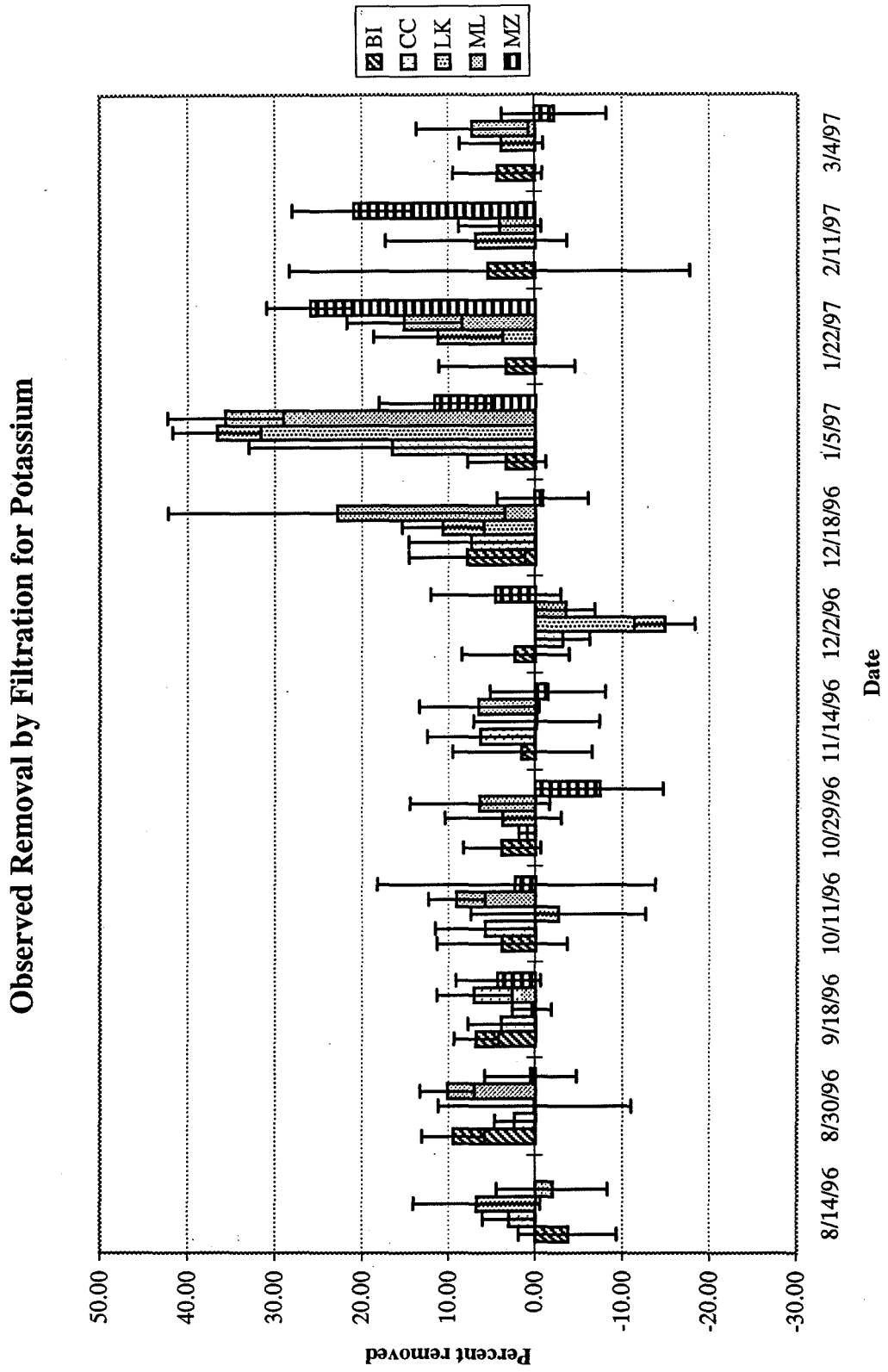
Observed Removal by Filtration for Potassium
BI
CC
LK
ML
MZ
50.00
40.00
30.00
20.00
10.00
0.00
-10.00
-20.00
-30.00
Percent removed
8/14/96
8/30/96
9/18/96
10/11/96
10/29/96
11/14/96
12/2/96
12/18/96
1/5/97
1/22/97
2/11/97
3/4/97
Date

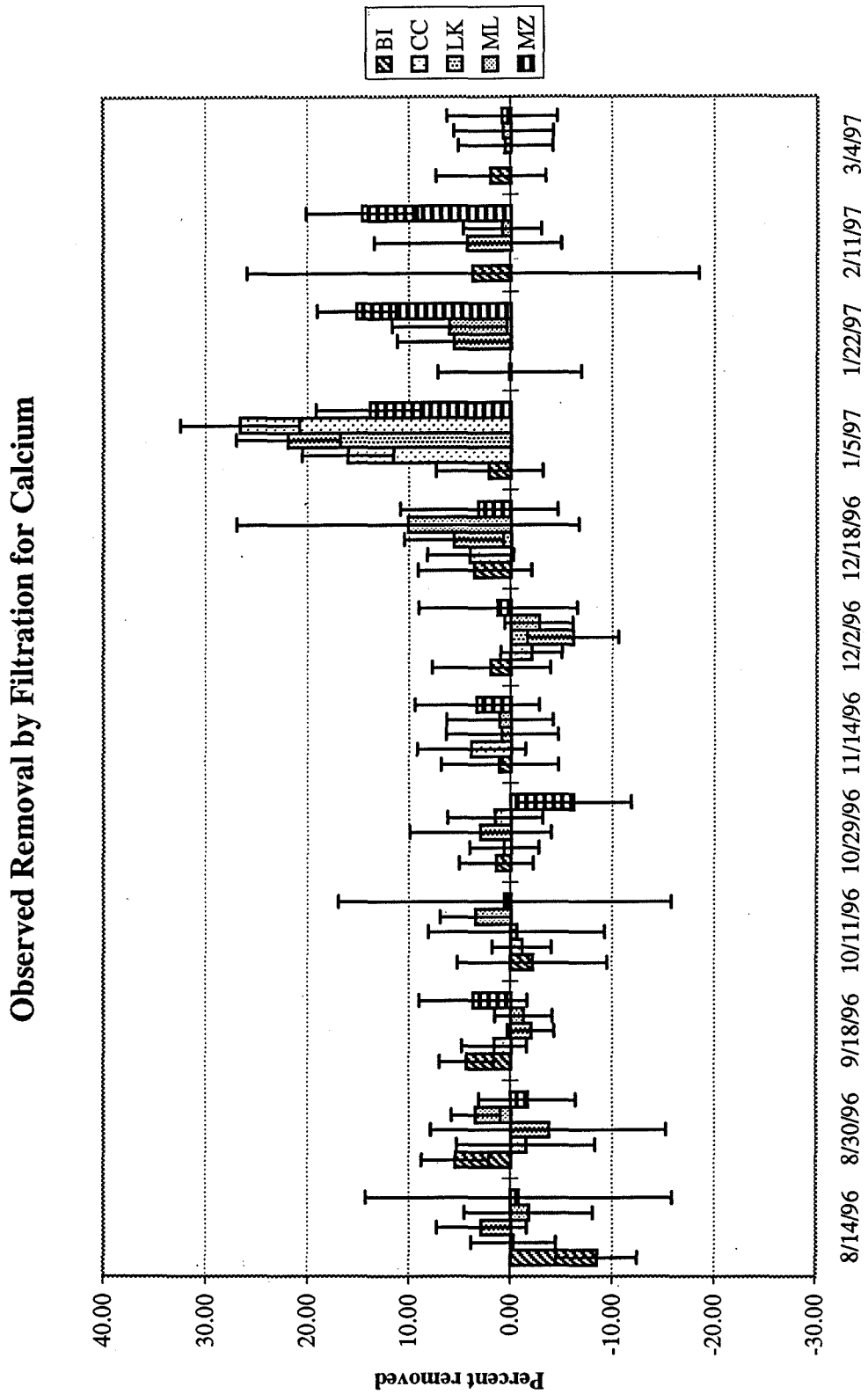
Observed Removal by Filtration for Calcium
BI
CC
LK
ML
MZ
40.00
30.00
20.00
10.00
0.00
-10.00
-20.00
-30.00
Percent removed
8/14/96
8/30/96
9/18/96
10/11/96
10/29/96
11/14/96
12/2/96
12/18/96
1/5/97
1/22/97
2/11/97
3/4/97
Date

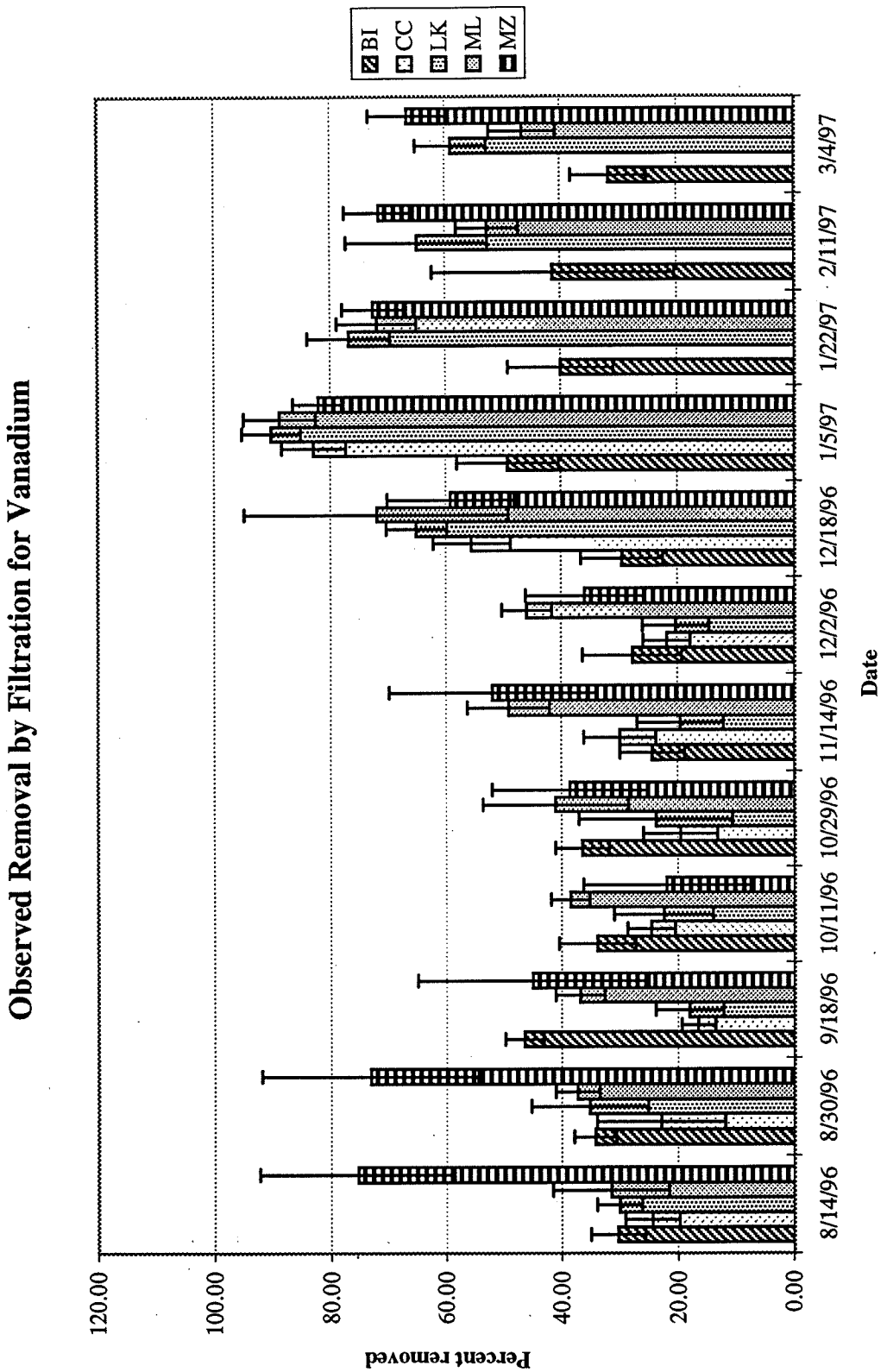
Observed Removal by Filtration for Vanadium
BI
CC
LK
ML
MZ
Percent removed
120.00
100.00
80.00
60.00
40.00
20.00
0.00
8/14/96
8/30/96
9/18/96
10/11/96
10/29/96
11/14/96
12/2/96
12/18/96
1/5/97
1/22/97
2/11/97
3/4/97
Date

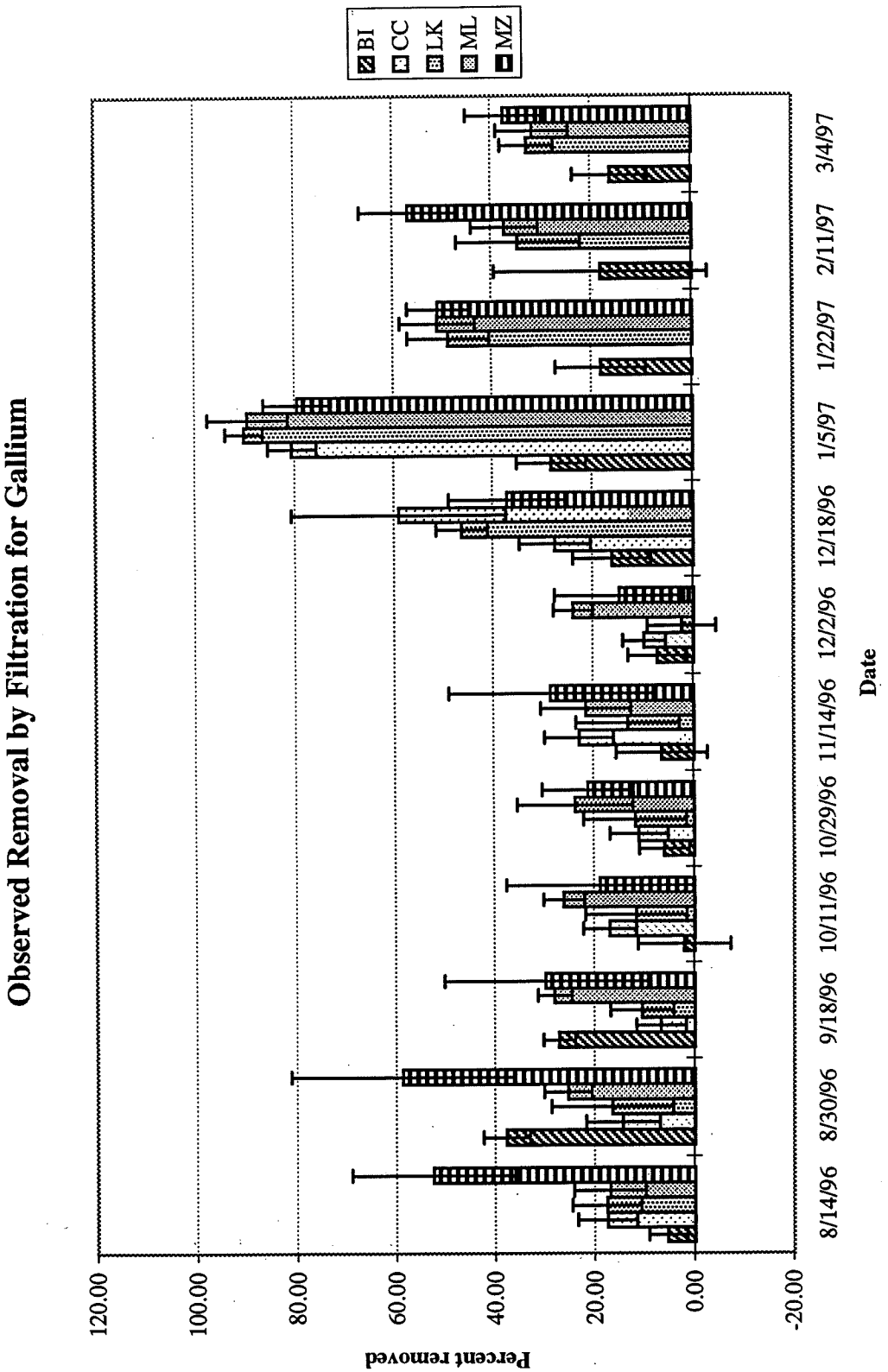
Observed Removal by Filtration for Gallium
BI
CC
LK
ML
MZ
120.00
100.00
80.00
60.00
40.00
20.00
0.00
-20.00
Percent removed
8/14/96
8/30/96
9/18/96
10/11/96
10/29/96
11/14/96
12/2/96
12/18/96
1/5/97
1/22/97
2/11/97
3/4/97
Date

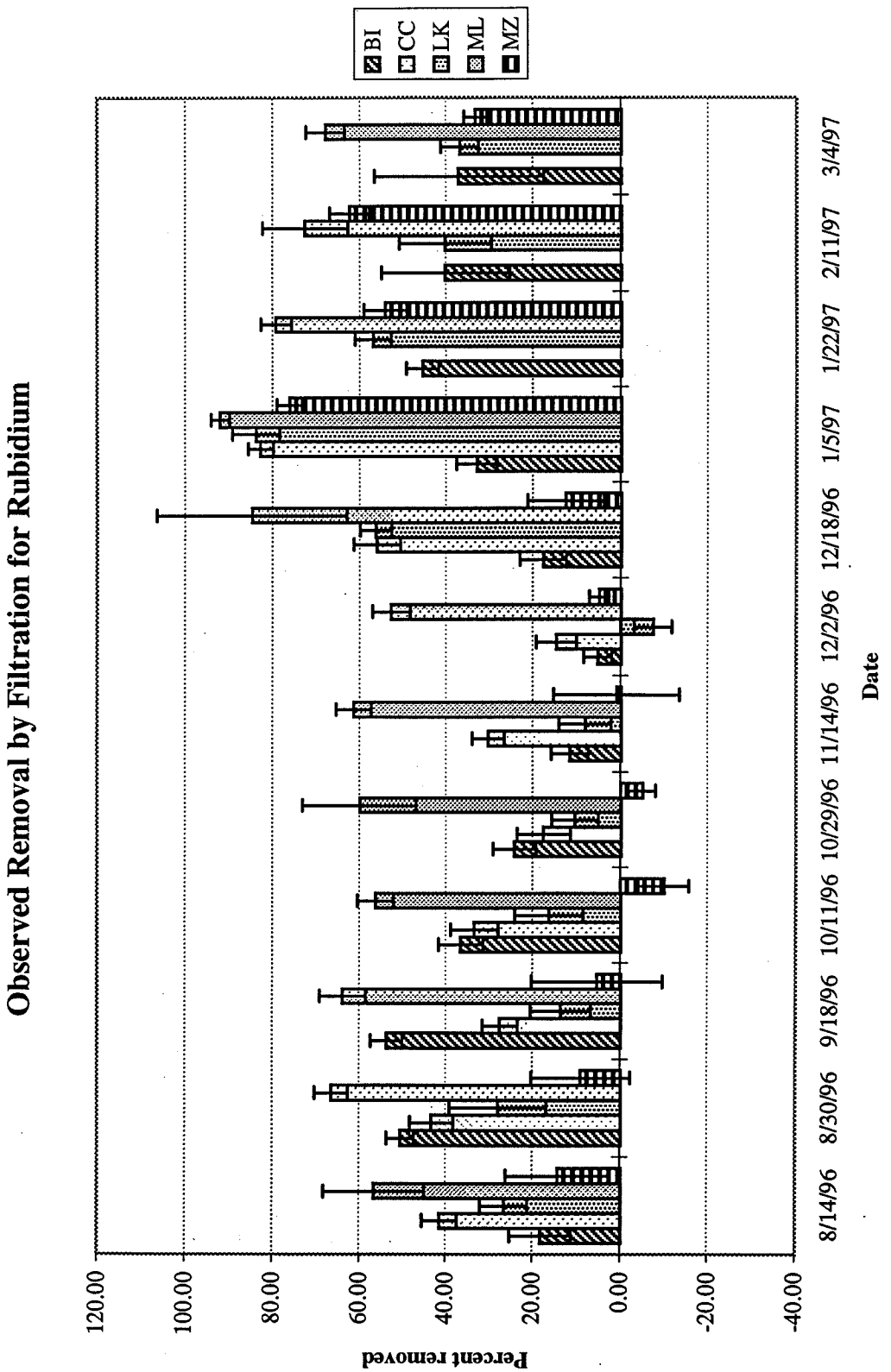
Observed Removal by Filtration for Rubidium
BI
CC
LK
ML
MZ
120.00
100.00
80.00
60.00
40.00
20.00
0.00
-20.00
-40.00
Percent removed
8/14/96
8/30/96
9/18/96
10/11/96
10/29/96
11/14/96
12/2/96
12/18/96
1/5/97
1/22/97
2/11/97
3/4/97
Date

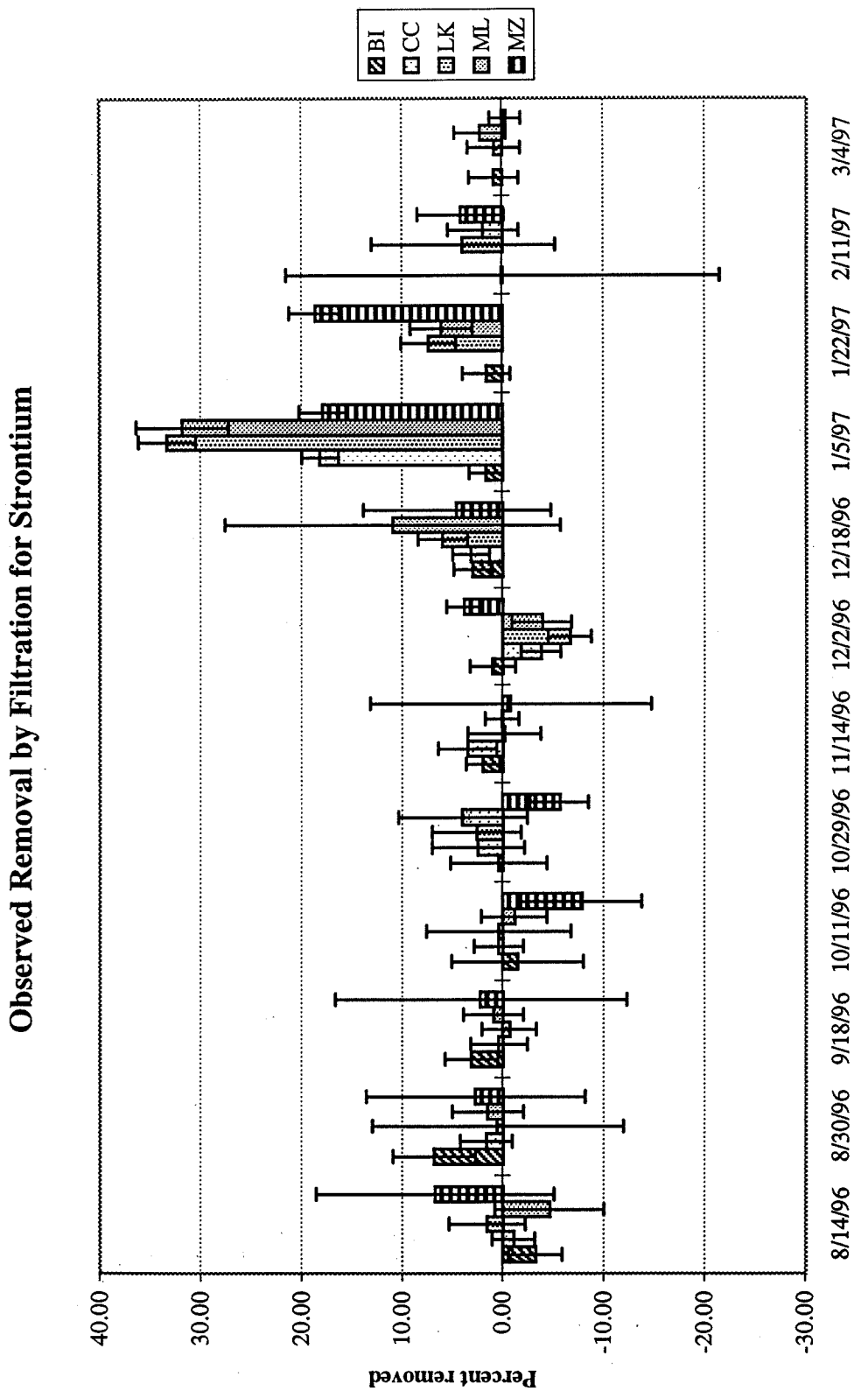
Observed Removal by Filtration for Strontium
BI
CC
LK
ML
MZ
40.00
30.00
20.00
10.00
0.00
-10.00
-20.00
-30.00
Percent removed
8/14/96
8/30/96
9/18/96
10/11/96
10/29/96
11/14/96
12/2/96
12/18/96
1/5/97
1/22/97
2/11/97
3/4/97
Date

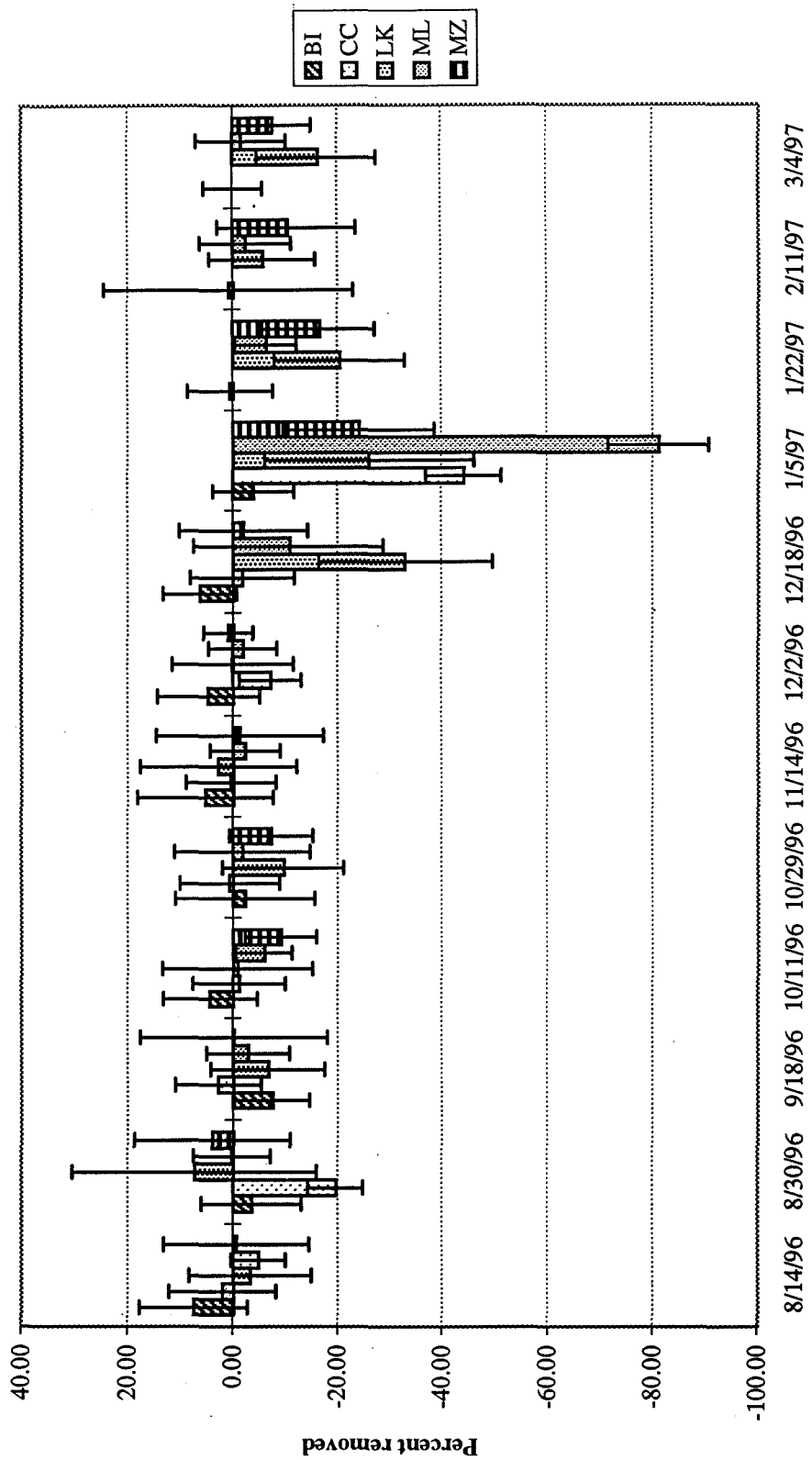

Note: Sample contamination is evident and results are inconclusive.

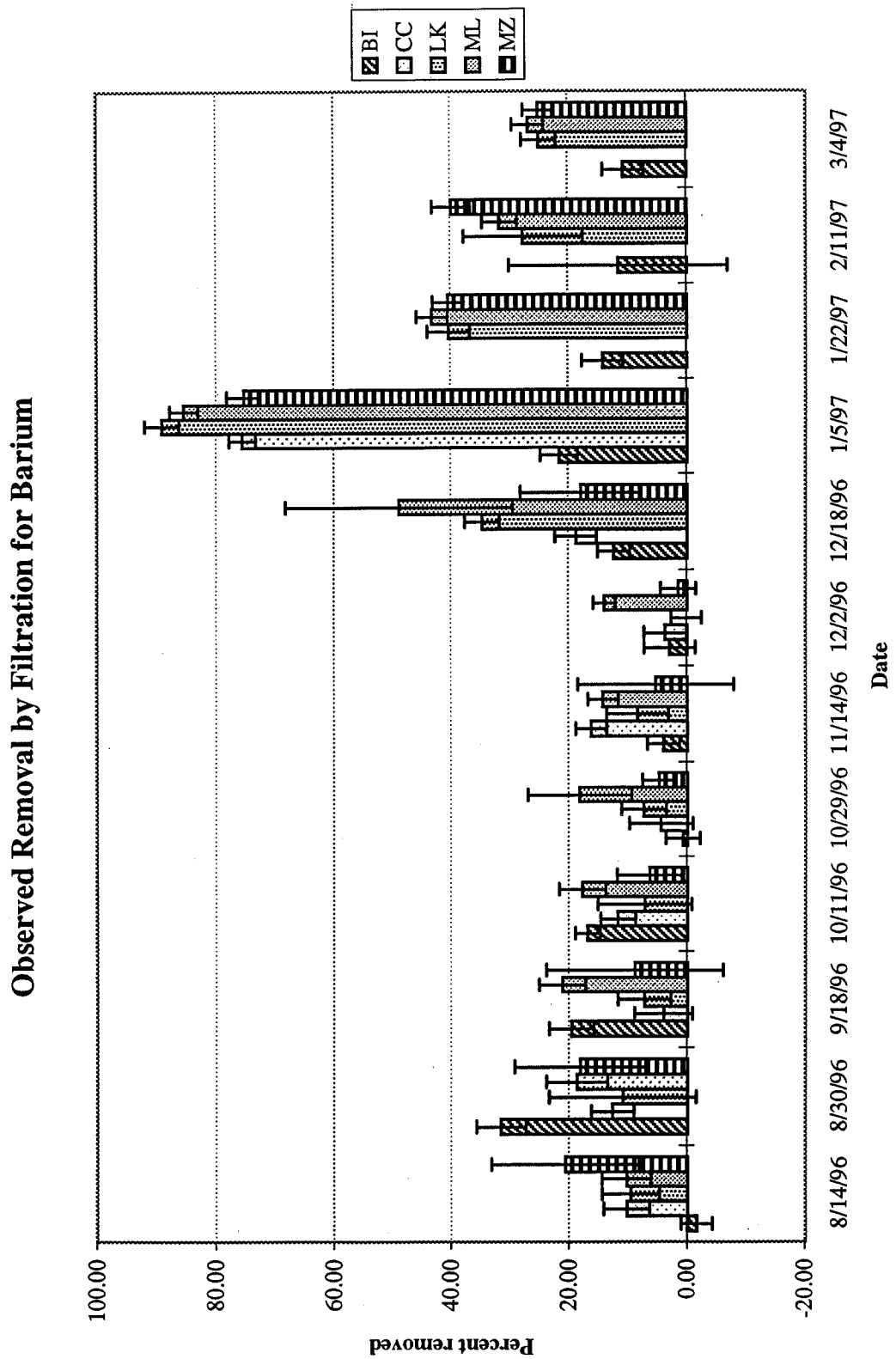
Observed Removal by Filtration for Barium
BI
CC
LK
ML
MZ
100.00
80.00
60.00
40.00
20.00
0.00
-20.00
Percent removed
8/14/96
8/30/96
9/18/96
10/11/96
10/29/96
11/14/96
12/2/96
12/18/96
1/5/97
1/22/97
2/11/97
3/4/97
Date

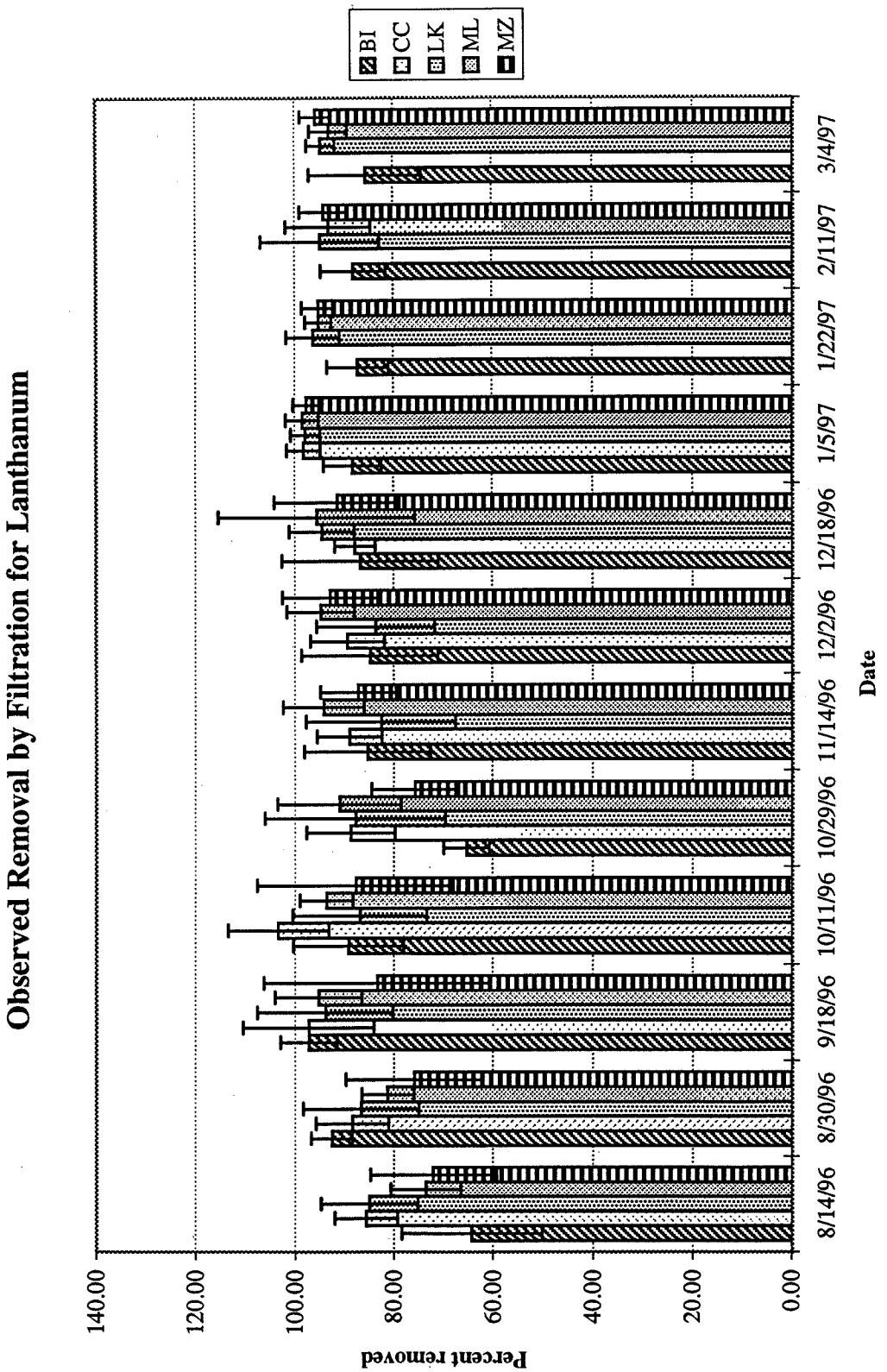
Observed Removal by Filtration for Lanthanum
BI
CC
LK
ML
MZ
140.00
120.00
100.00
80.00
60.00
40.00
20.00
0.00
Percent removed
8/14/96
8/30/96
9/18/96
10/11/96
10/29/96
11/14/96
12/2/96
12/18/96
1/5/97
1/22/97
2/11/97
3/4/97
Date

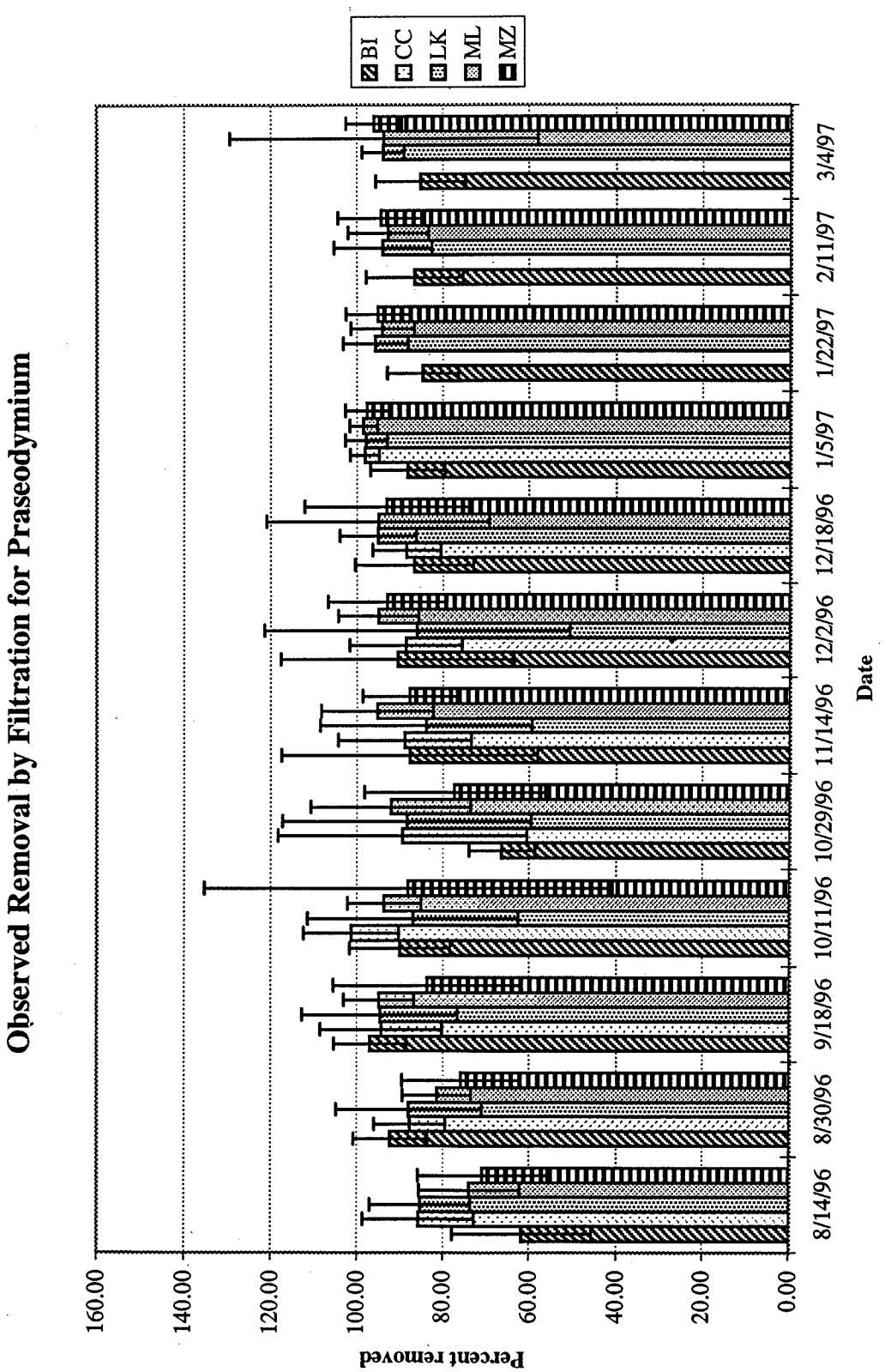
Observed Removal by Filtration for Praseodymium
BI
CC
LK
ML
MZ
160.00
140.00
120.00
100.00
80.00
60.00
40.00
20.00
0.00
Percent removed
8/14/96
8/30/96
9/18/96
10/11/96
10/29/96
11/14/96
12/2/96
12/18/96
1/5/97
1/22/97
2/11/97
3/4/97
Date

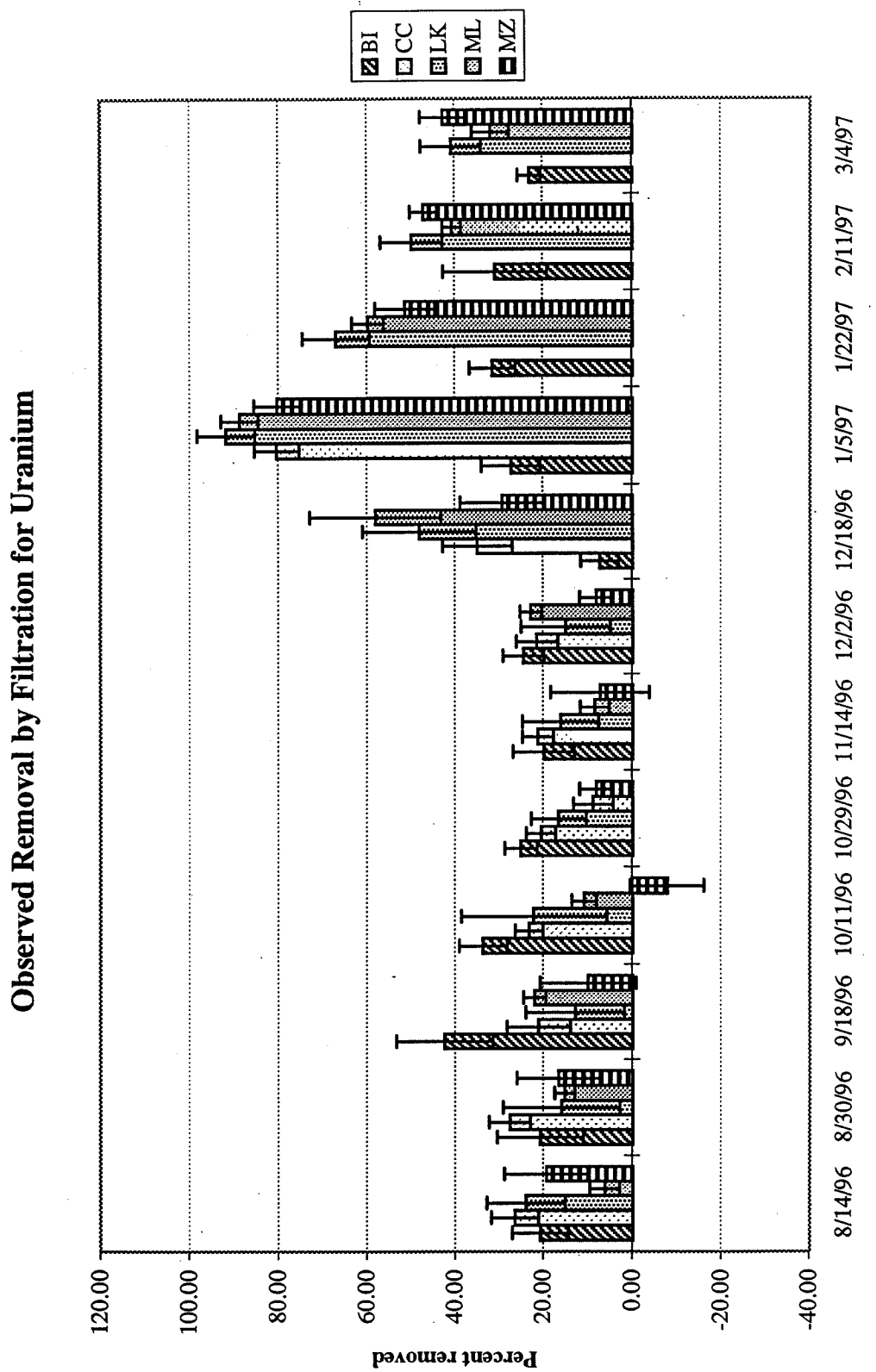
Observed Removal by Filtration for Uranium
BI
CC
LK
ML
MZ
120.00
100.00
80.00
60.00
40.00
20.00
0.00
-20.00
-40.00
Percent removed
8/14/96
8/30/96
9/18/96
10/11/96
10/29/96
11/14/96
12/2/96
12/18/96
1/5/97
1/22/97
2/11/97
3/4/97
Date

Appendix G

Models results for entire study period

for the Delta

Appendix G
Model results for entire study period for the Delta

Table of Contents

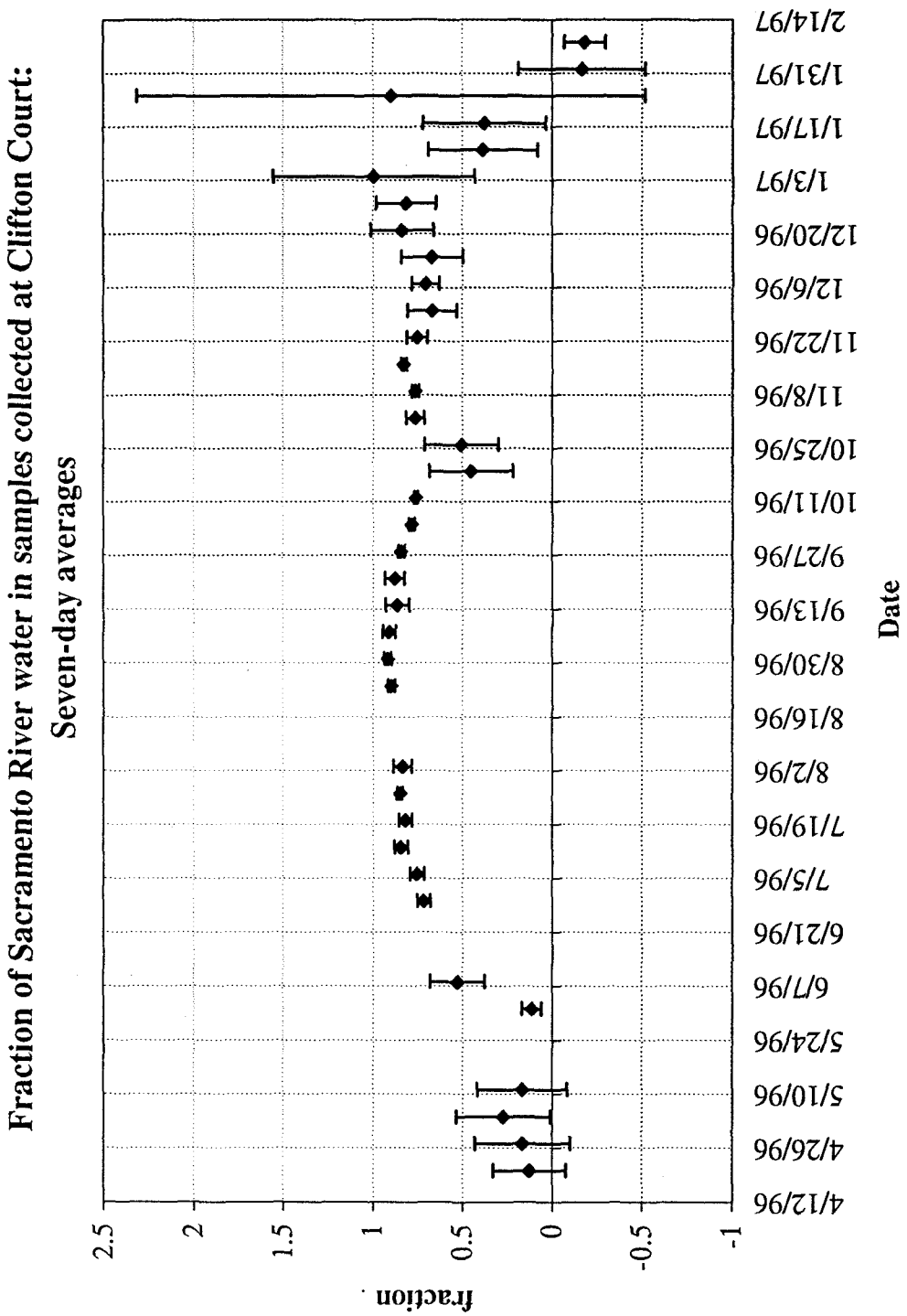
Fraction of Sacramento River water in samples collected at Clifton Court:
Seven-day averages
fraction
2.5
2
1.5
1
0.5
0
-0.5
-1
4/12/96
4/26/96
5/10/96
5/24/96
6/7/96
6/21/96
7/5/96
7/19/96
8/2/96
8/16/96
8/30/96
9/13/96
9/27/96
10/11/96
10/25/96
11/8/96
11/22/96
12/6/96
12/20/96
1/3/97
1/17/97
1/31/97
2/14/97
Date

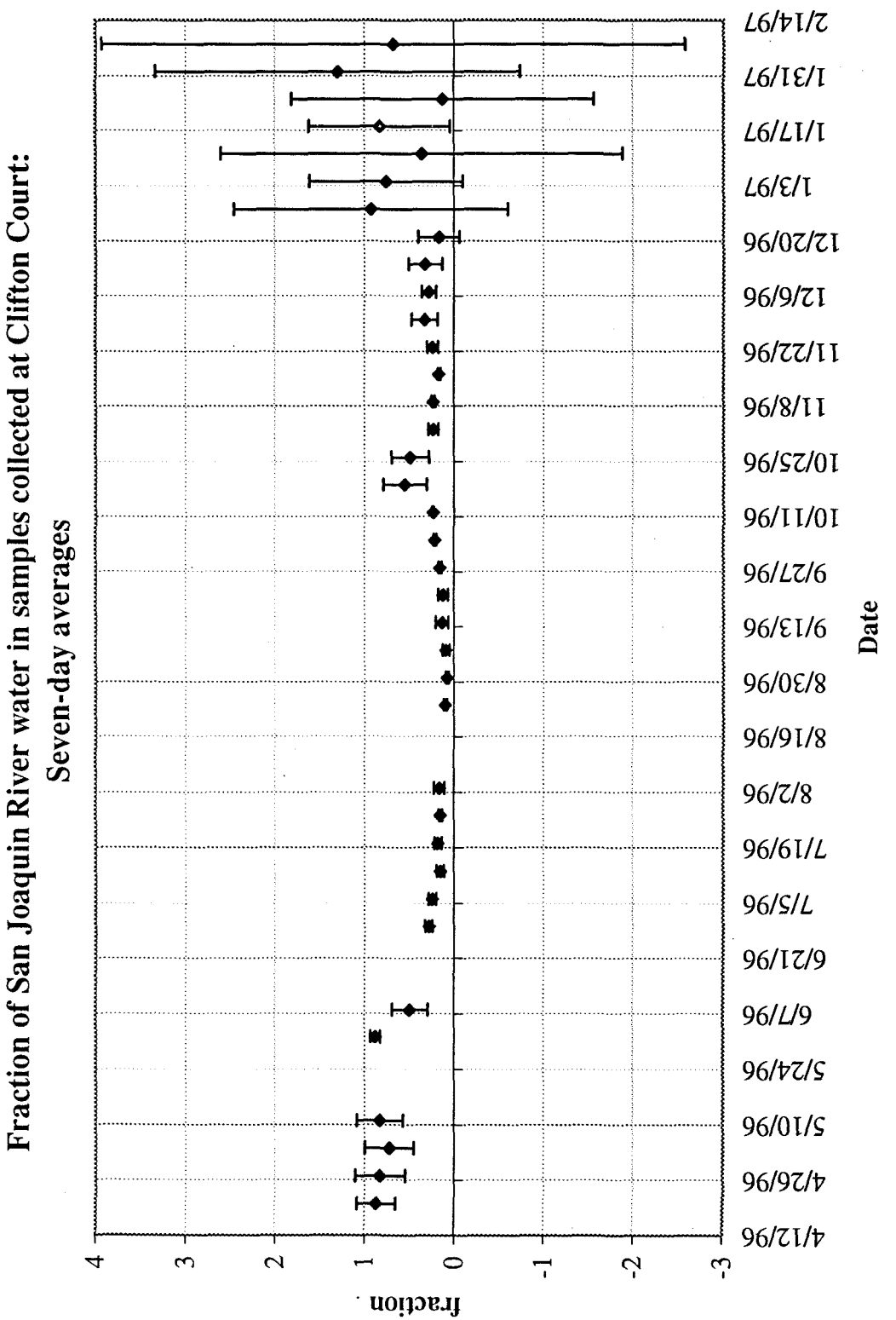
Fraction of San Joaquin River water in samples collected at Clifton Court:
Seven-day averages
Fraction
4
3
2
1
0
-1
-2
-3
Date
4/12/96
4/26/96
5/10/96
5/24/96
6/7/96
6/21/96
7/5/96
7/19/96
8/2/96
8/16/96
8/30/96
9/13/96
9/27/96
10/11/96
10/25/96
11/8/96
11/22/96
12/6/96
12/20/96
1/3/97
1/17/97
1/31/97
2/14/97

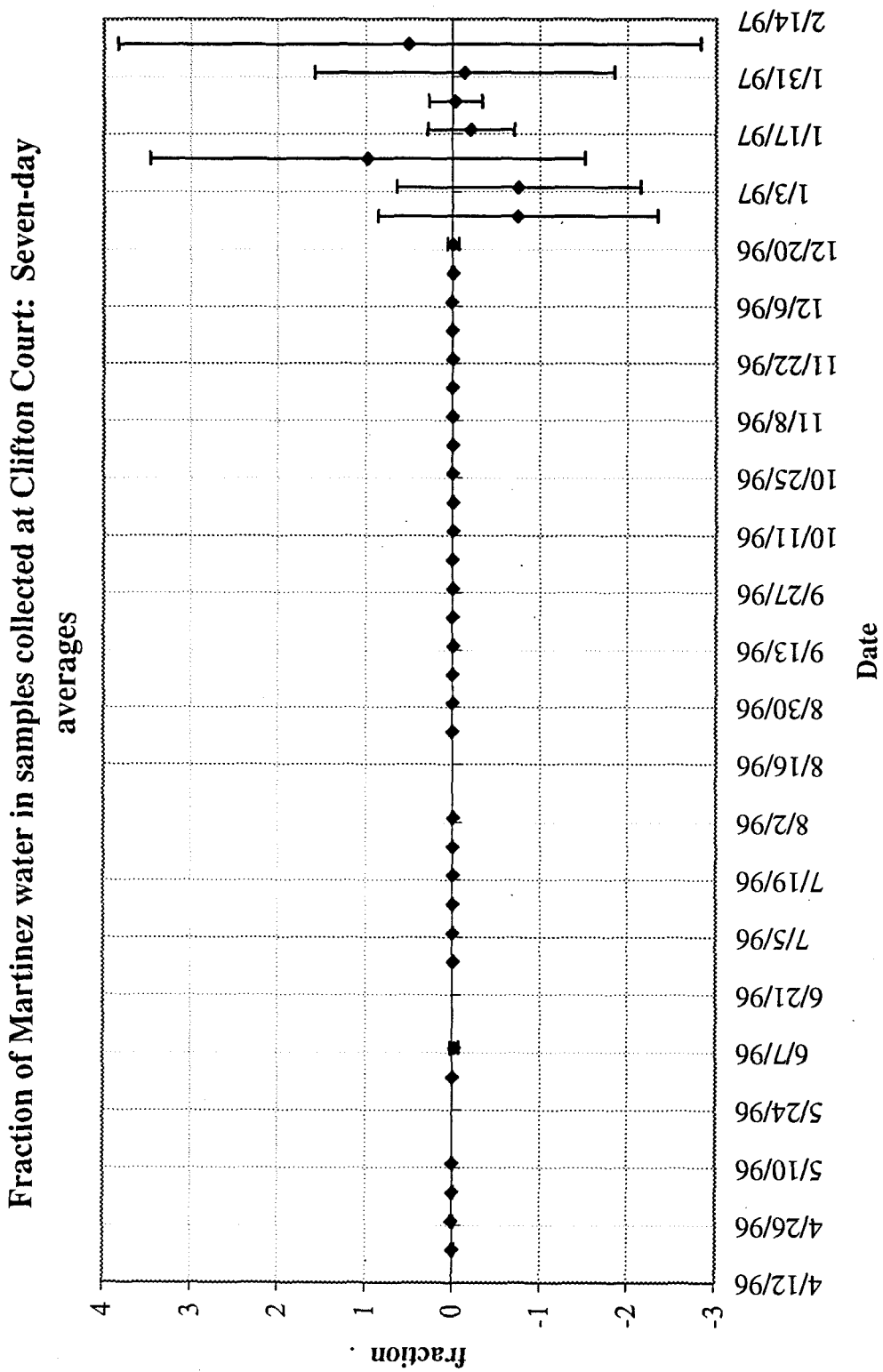
Fraction of Martinez water in samples collected at Clifton Court: Seven-day averages
Fraction
4
3
2
1
0
-1
-2
-3
Date
4/12/96
4/26/96
5/10/96
5/24/96
6/7/96
6/21/96
7/5/96
7/19/96
8/2/96
8/16/96
8/30/96
9/13/96
9/27/96
10/11/96
10/25/96
11/8/96
11/22/96
12/6/96
12/20/96
1/3/97
1/17/97
1/31/97
2/14/97

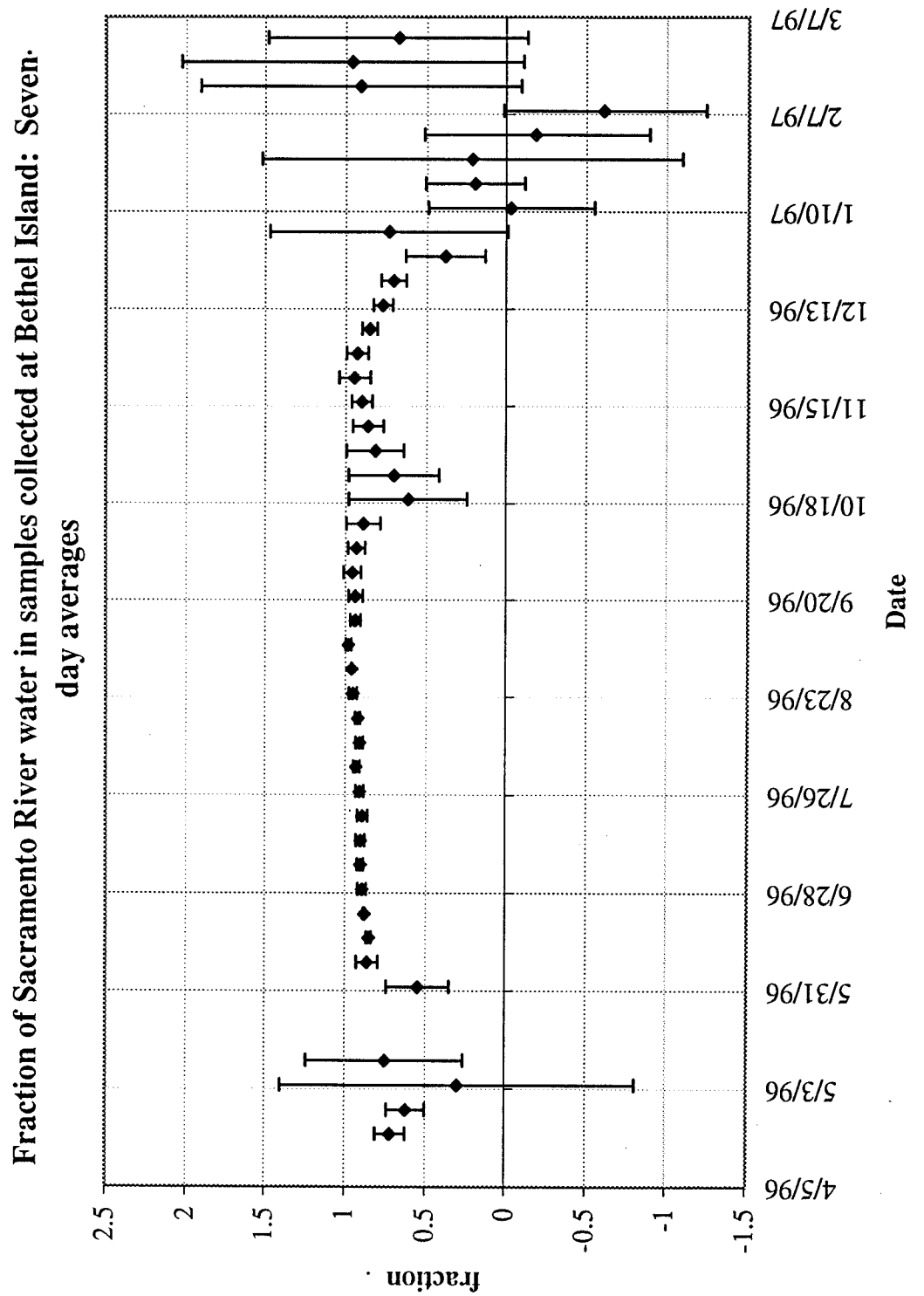
Fraction of Sacramento River water in samples collected at Bethel Island: Seven-day averages
Fraction
2.5
2
1.5
1
0.5
0
-0.5
-1
-1.5
4/5/96
5/3/96
5/31/96
6/28/96
7/26/96
8/23/96
9/20/96
10/18/96
11/15/96
12/13/96
1/10/97
2/7/97
3/7/97
Date

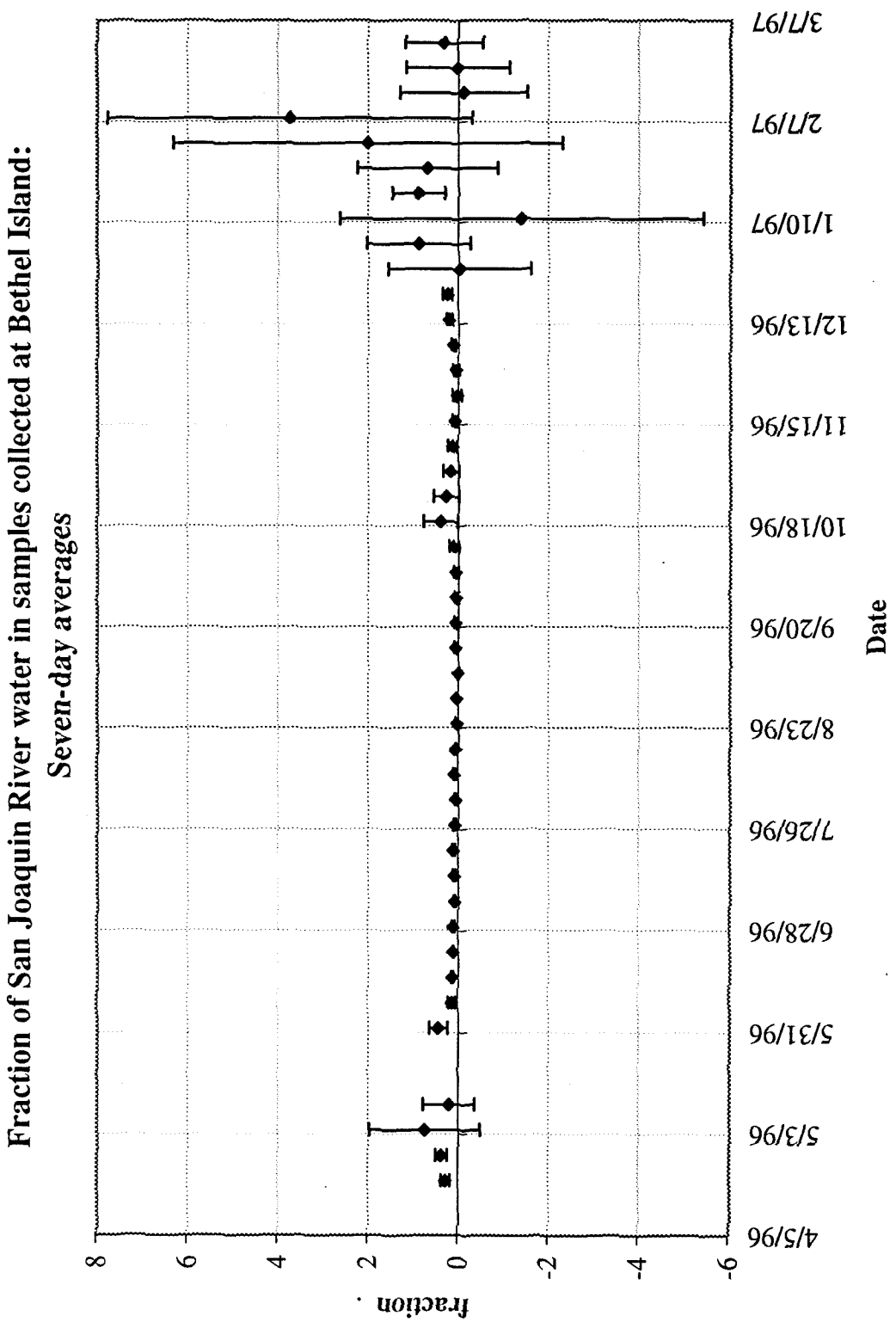
Fraction of San Joaquin River water in samples collected at Bethel Island:
Seven-day averages
fraction
8
6
4
2
0
-2
-4
-6
4/5/96
5/3/96
5/31/96
6/28/96
7/26/96
8/23/96
9/20/96
10/18/96
11/15/96
12/13/96
1/10/97
2/7/97
3/7/97
Date

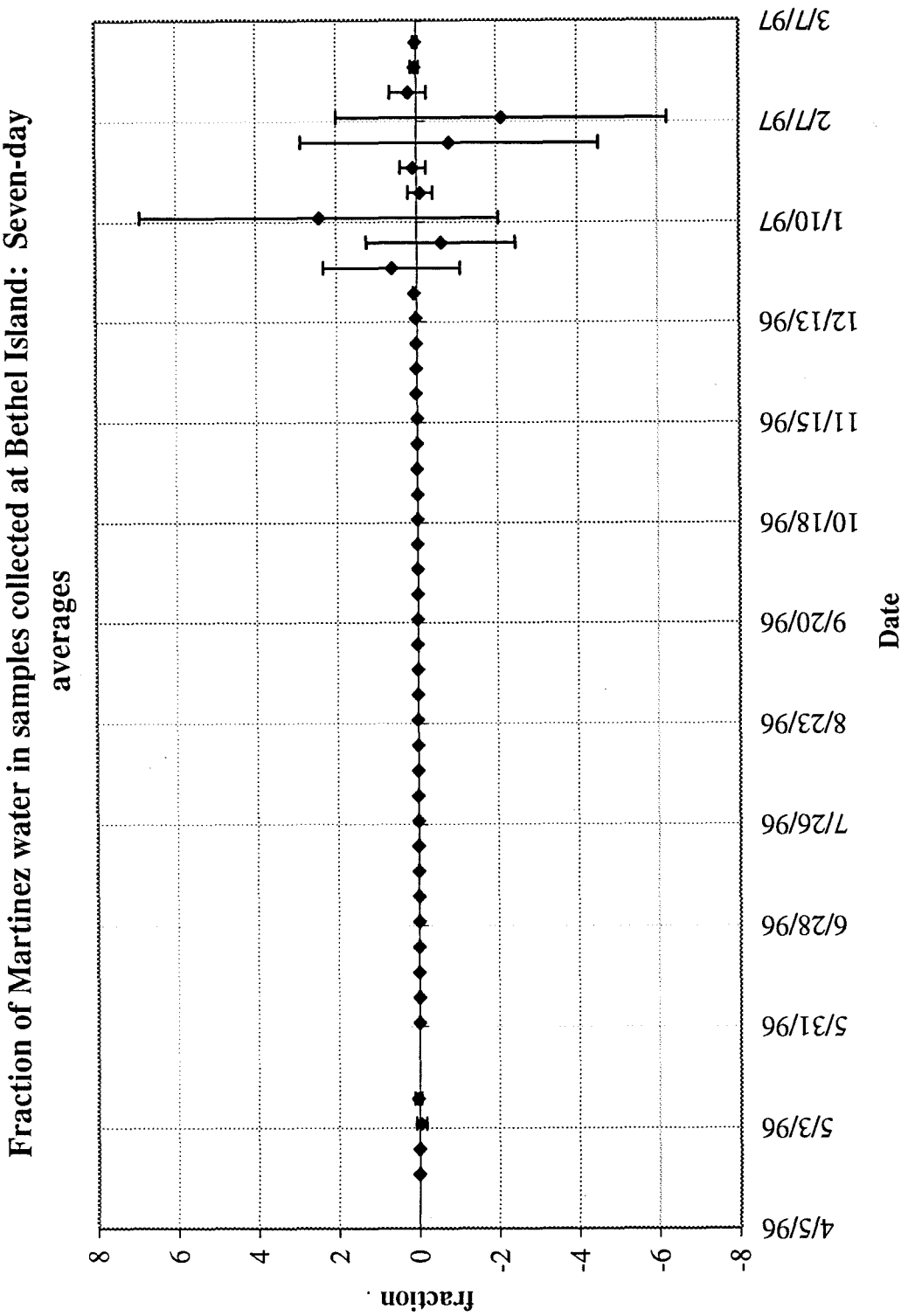
Fraction of Martinez water in samples collected at Bethel Island: Seven-day averages
fraction
8
6
4
2
0
-2
-4
-6
-8
4/5/96
5/3/96
5/31/96
6/28/96
7/26/96
8/23/96
9/20/96
10/18/96
11/15/96
12/13/96
1/10/97
2/7/97
3/7/97
Date

Appendix H

Variations in elemental concentrations in stream samples collected from streams in Oahu, Hawai'i

Appendix H
Variations in elemental concentrations in stream samples collected from streams in Oahu, Hawai'i

Table of Contents

location: Waikele

element: Rb85

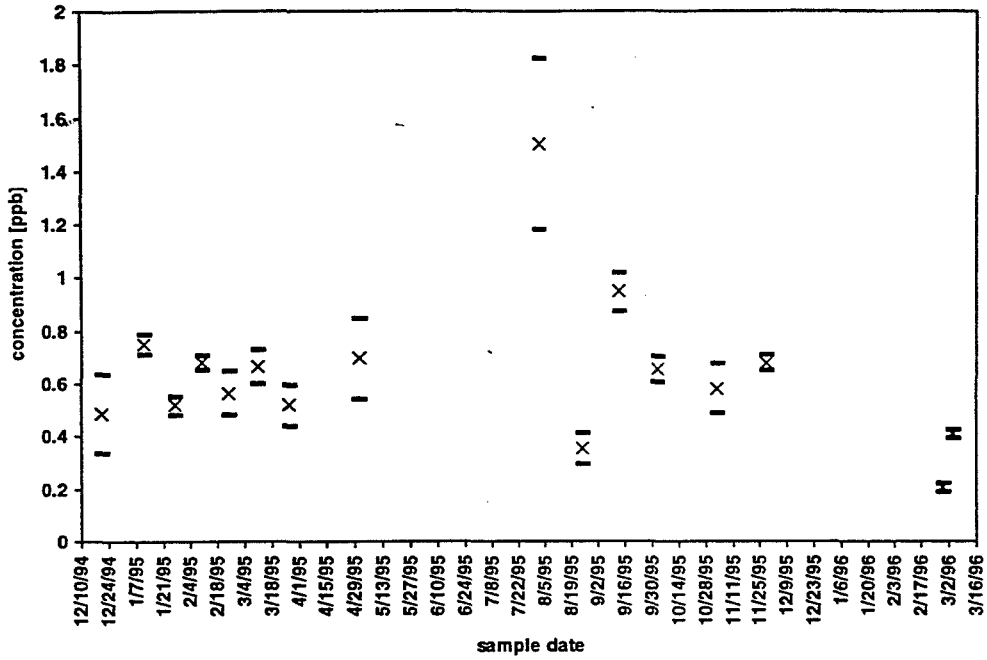

location: Waianae STP

element: Rb85

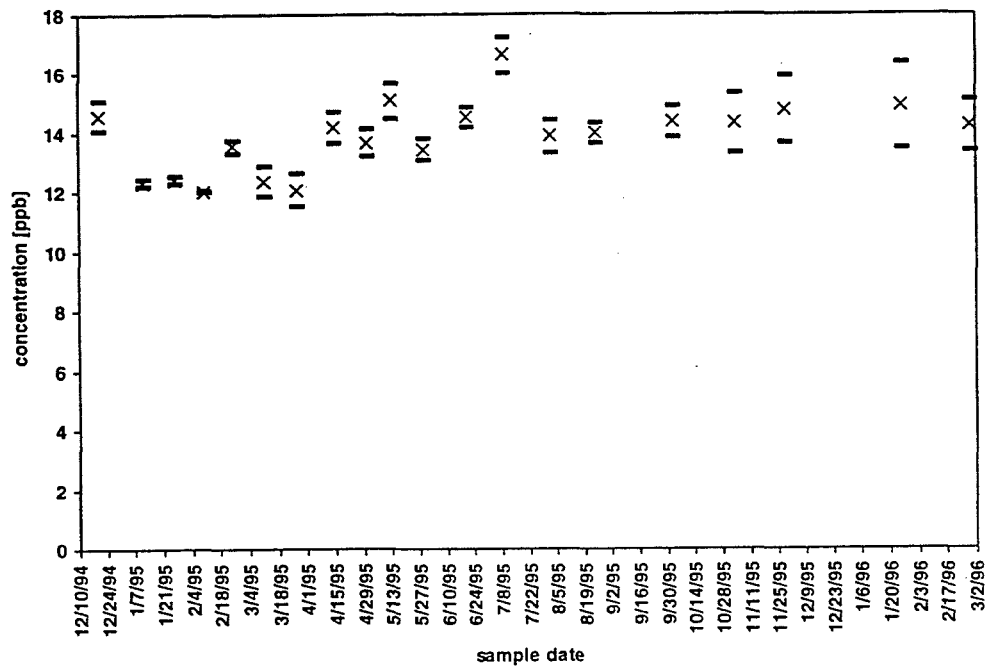

location: Manoa

element: Rb85

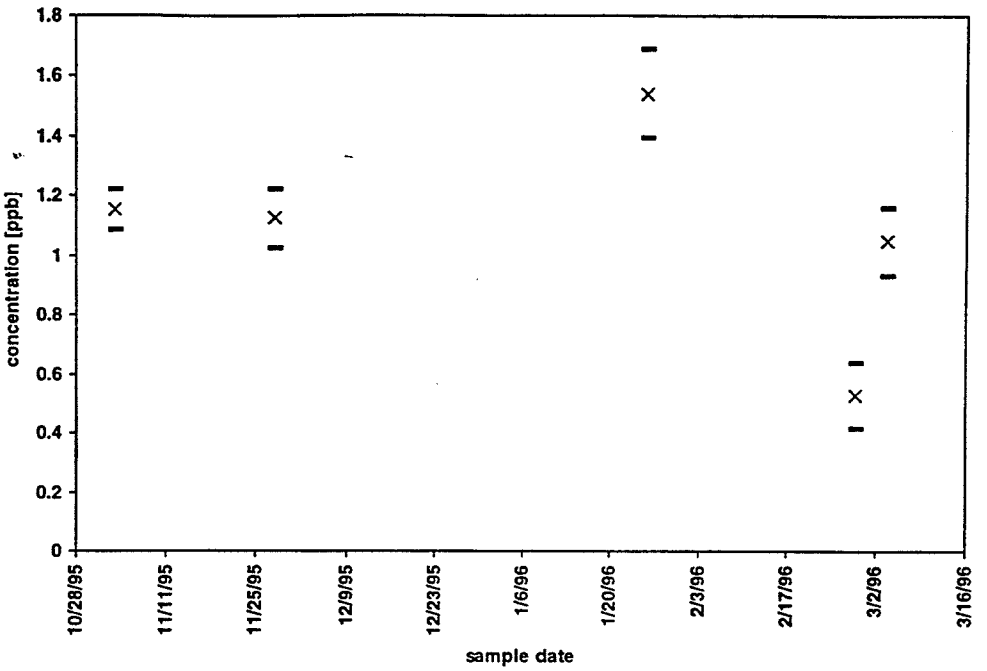

location: Palolo

element: Rb85

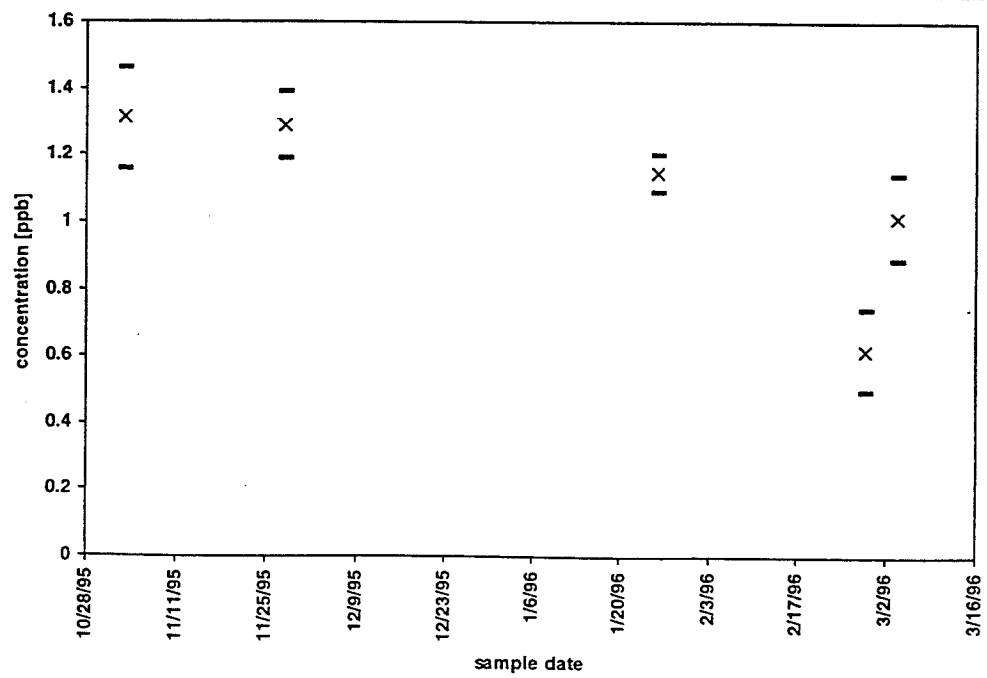

location: Waikele

element: U238

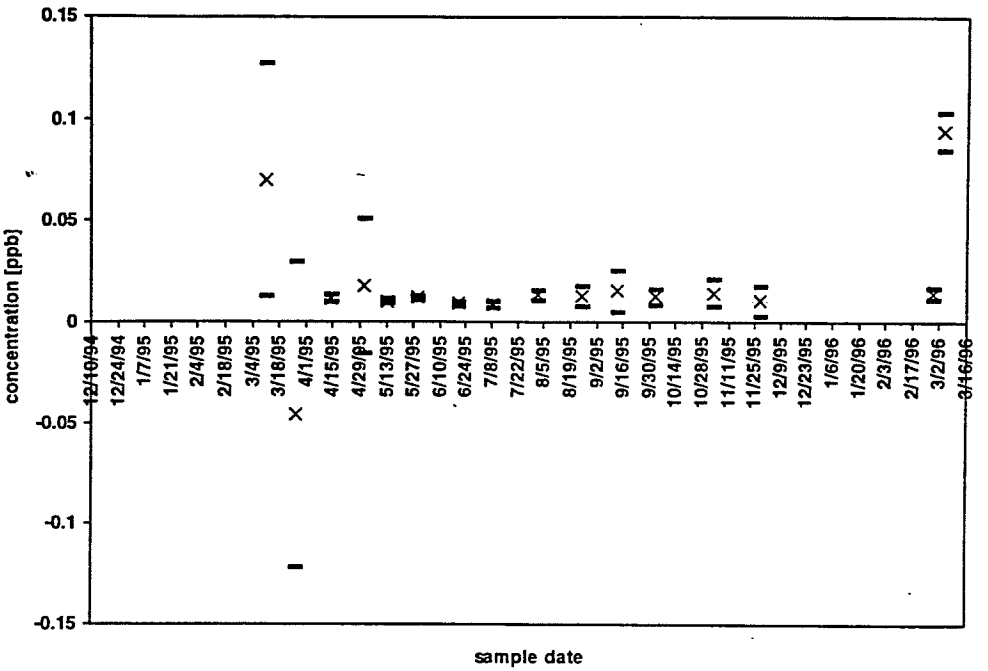

location: Waianae STP

element: U238

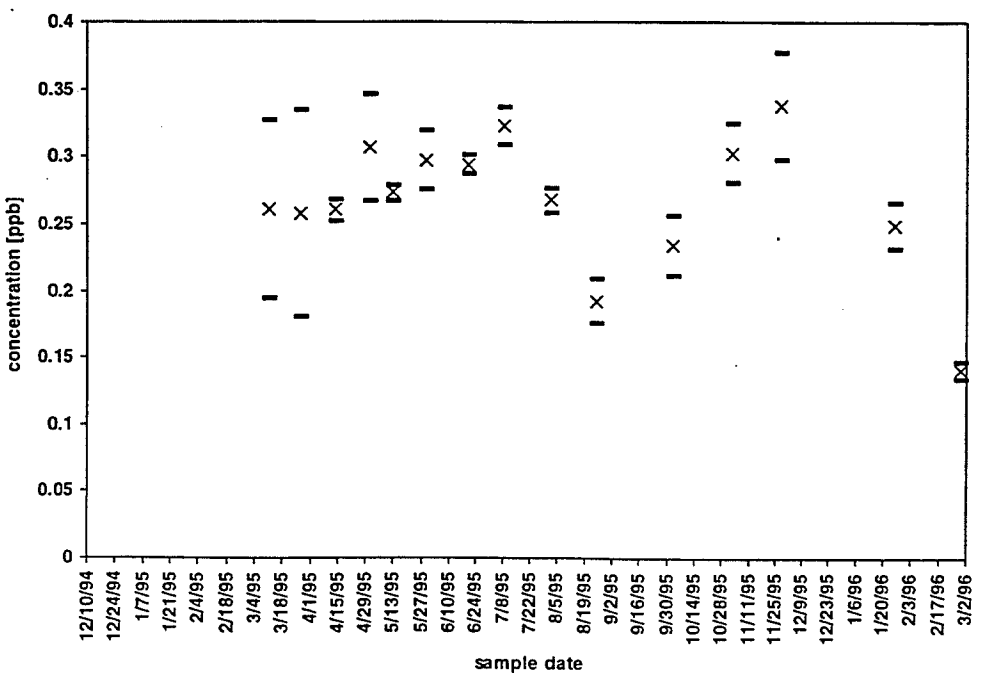

location: Manoa

element: U238

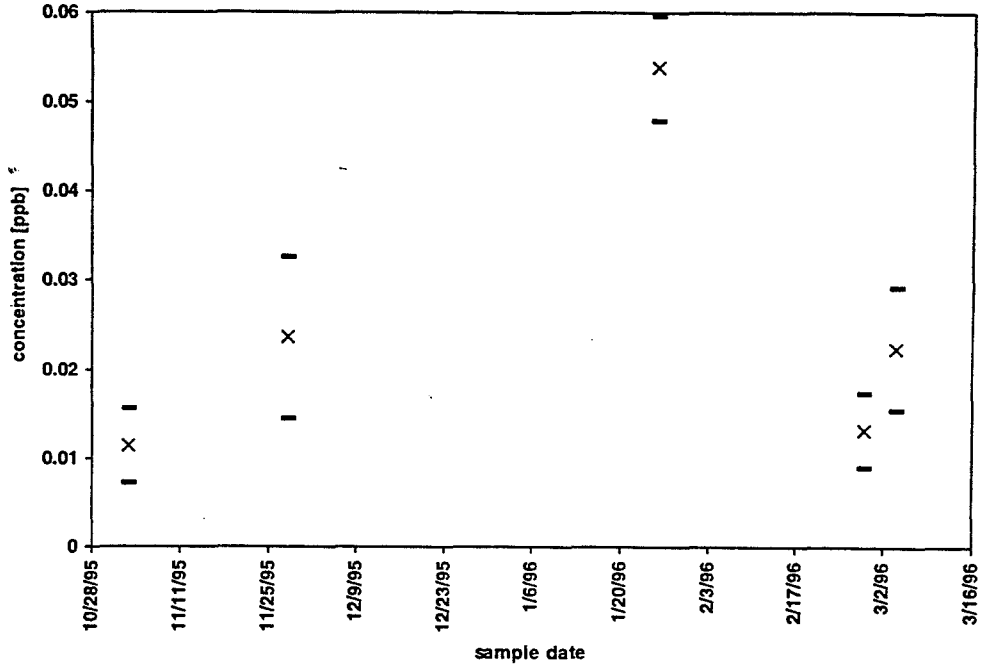

location: Palolo

element: U238

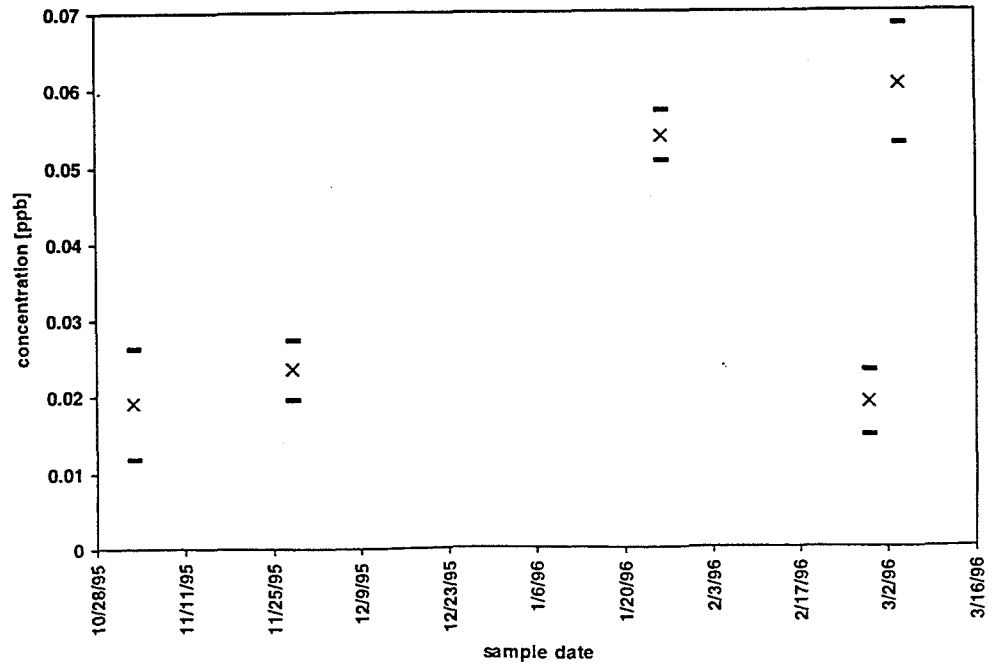

location: Waikele

element: La139

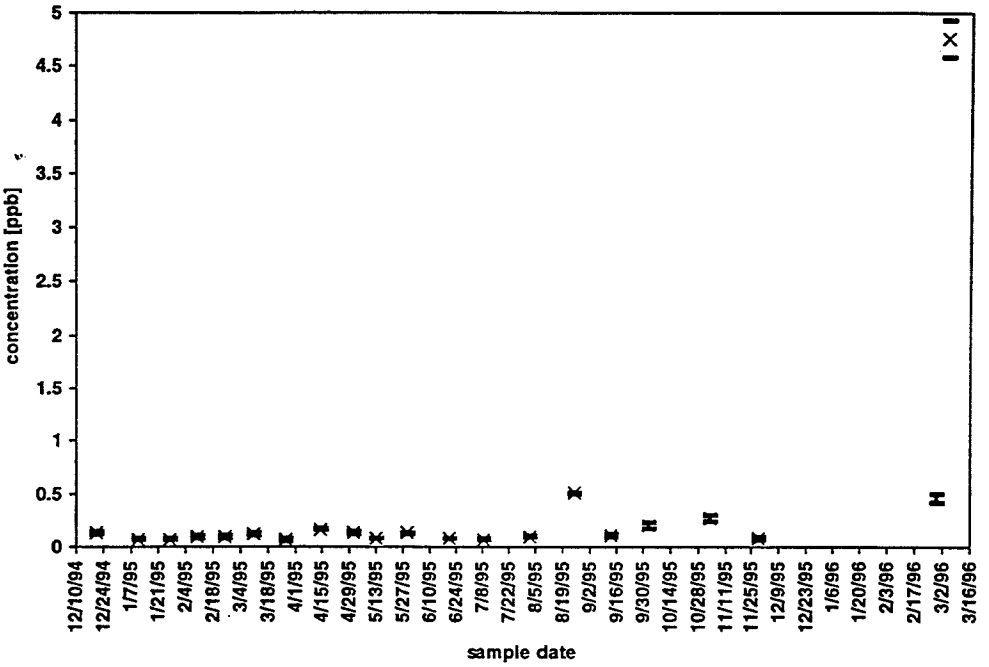

location: Waianae STP

element: La139

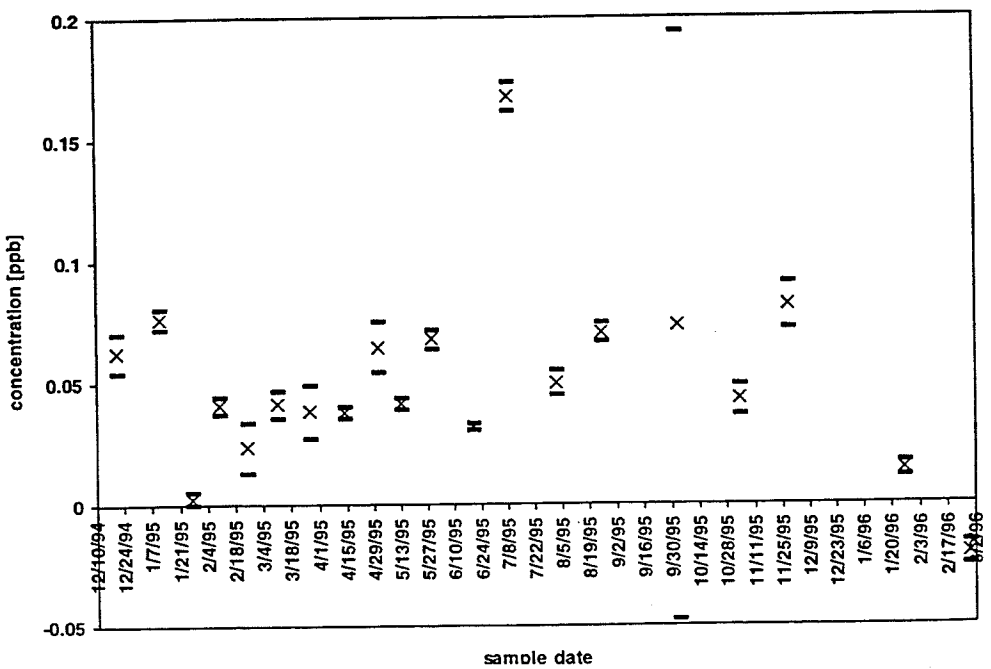

location: Manoa

element: La139

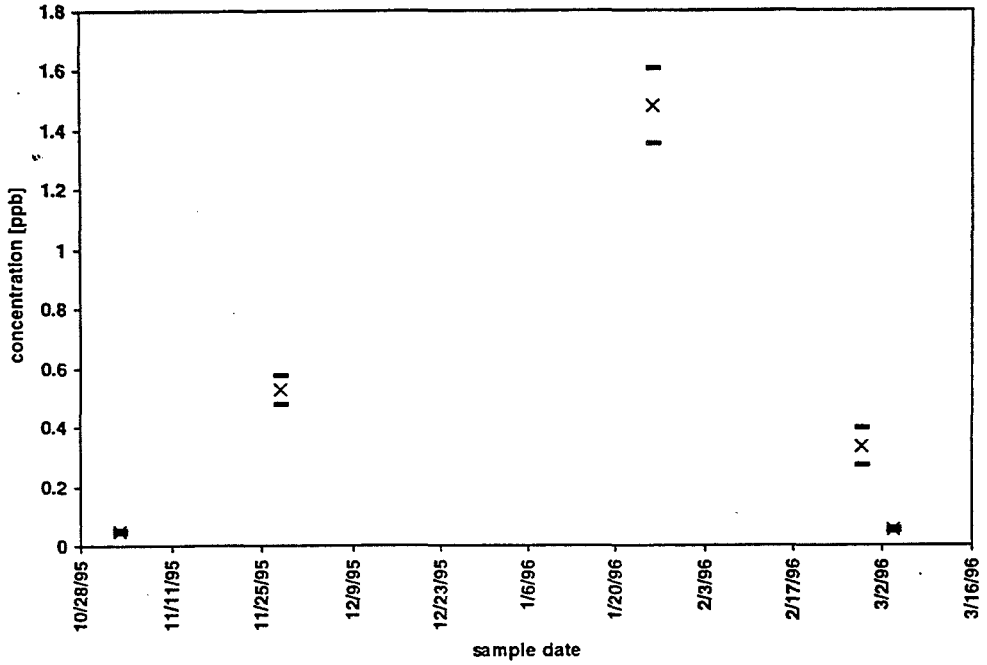

location: Palolo

element: La139

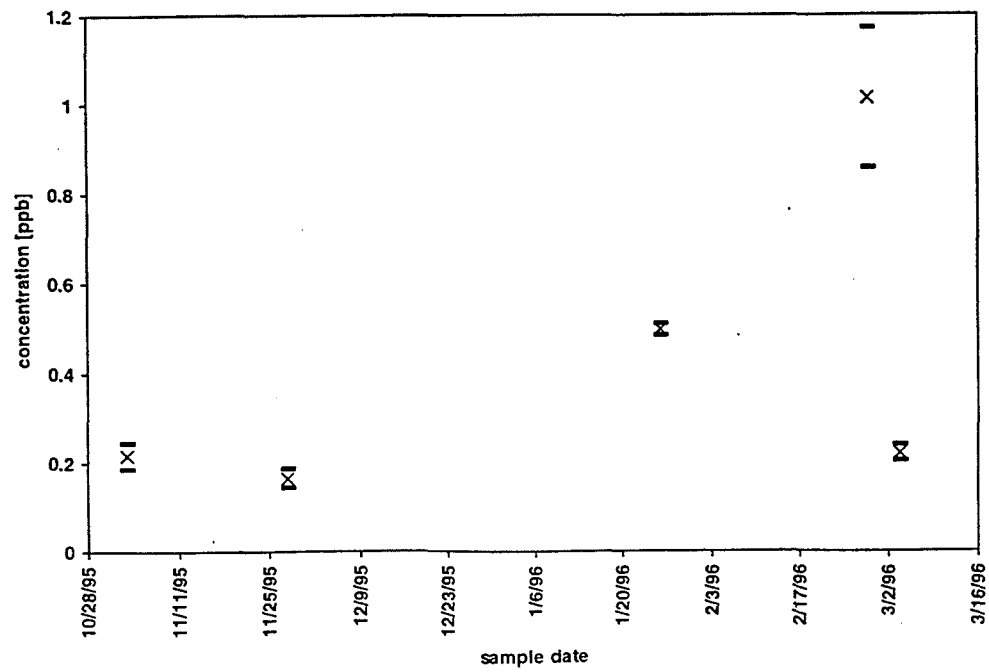

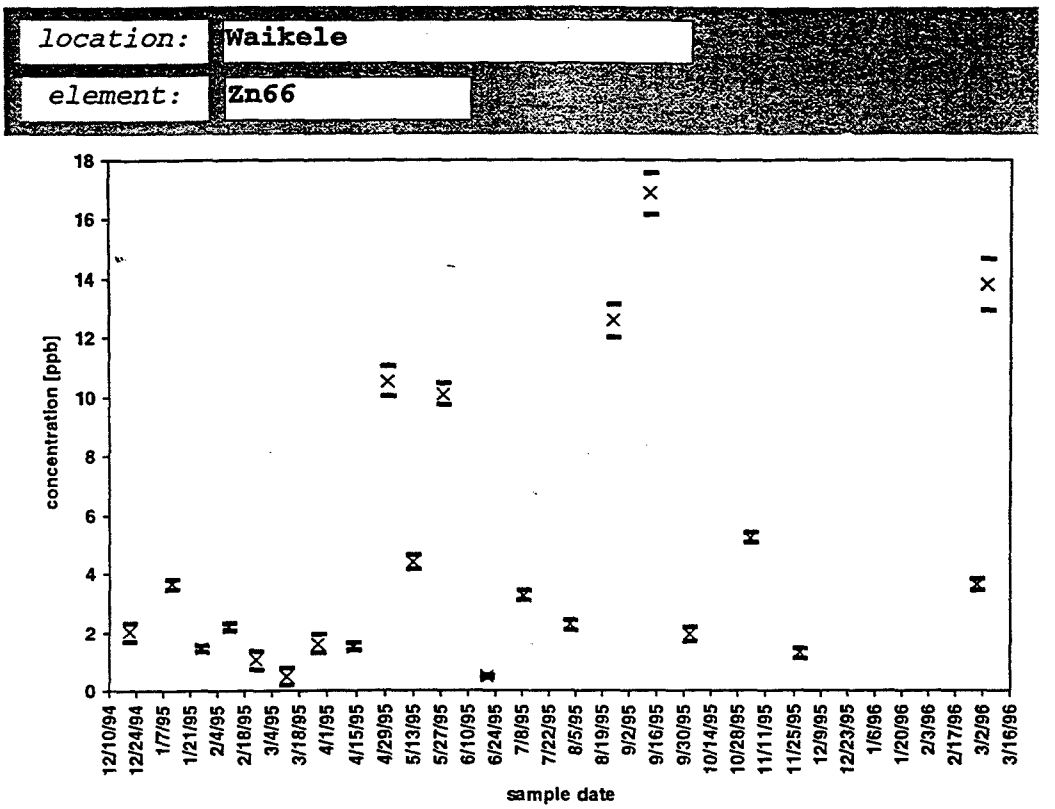
location:
Waikele
element:
Zn66
concentration [ppb]
sample date

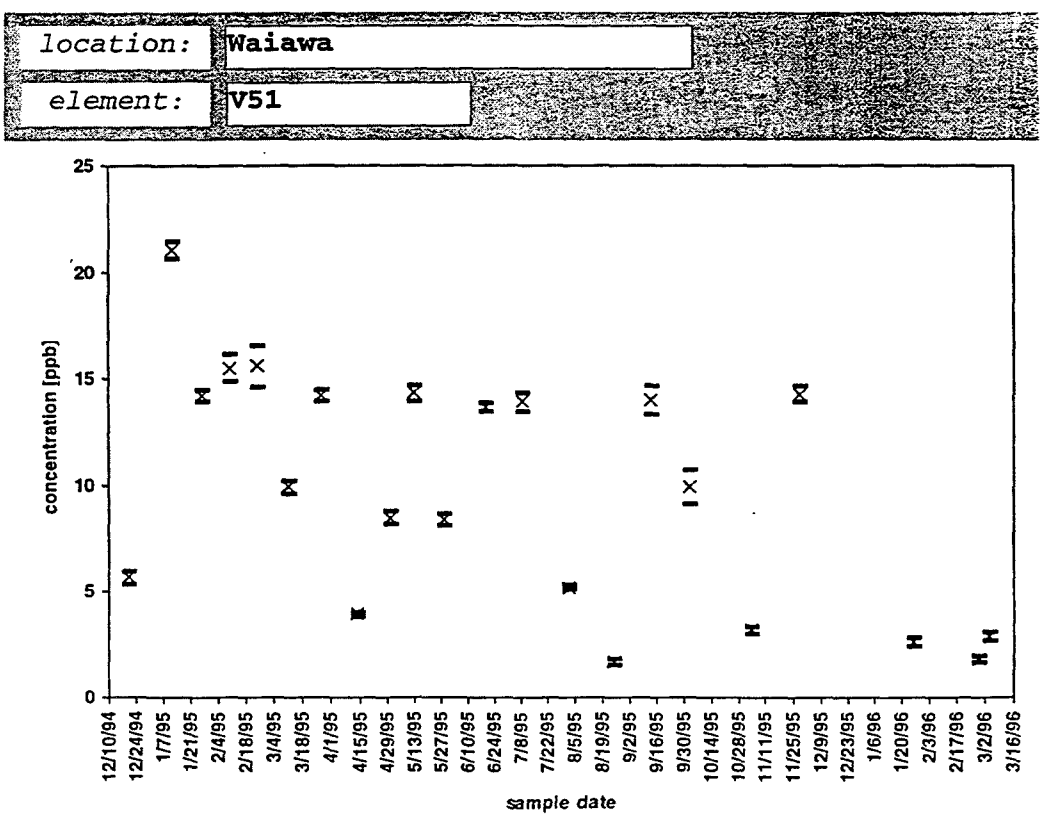
location:
Waiawa
element:
V51
concentration [ppb]
sample date

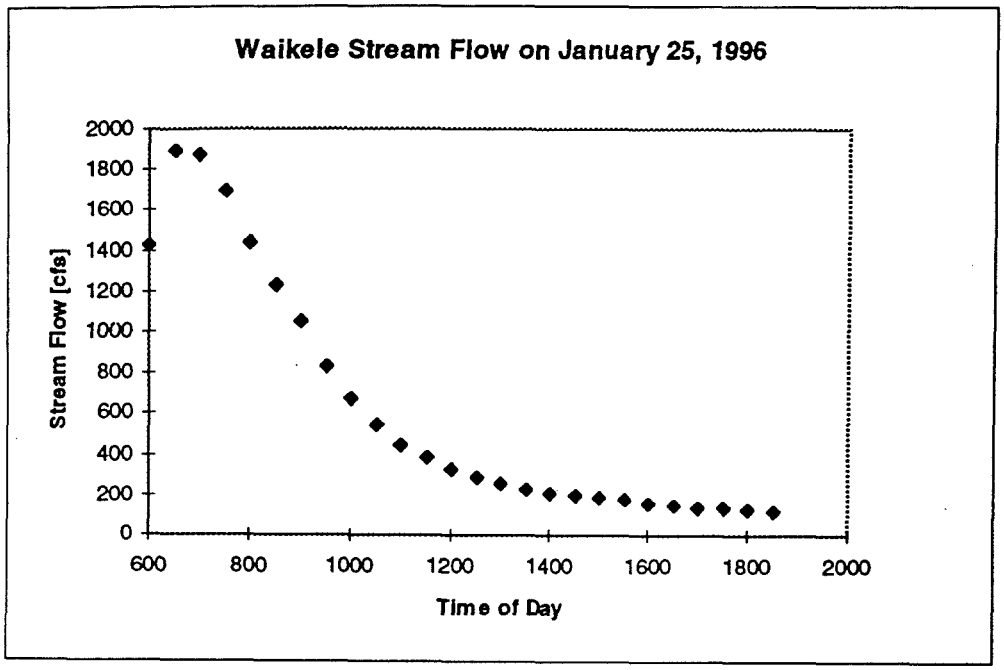
Waikele Stream Flow on January 25, 1996
Stream Flow [cfs]
2000
1800
1600
1400
1200
1000
800
600
400
200
0
600
800
1000
1200
1400
1600
1800
2000
Time of Day

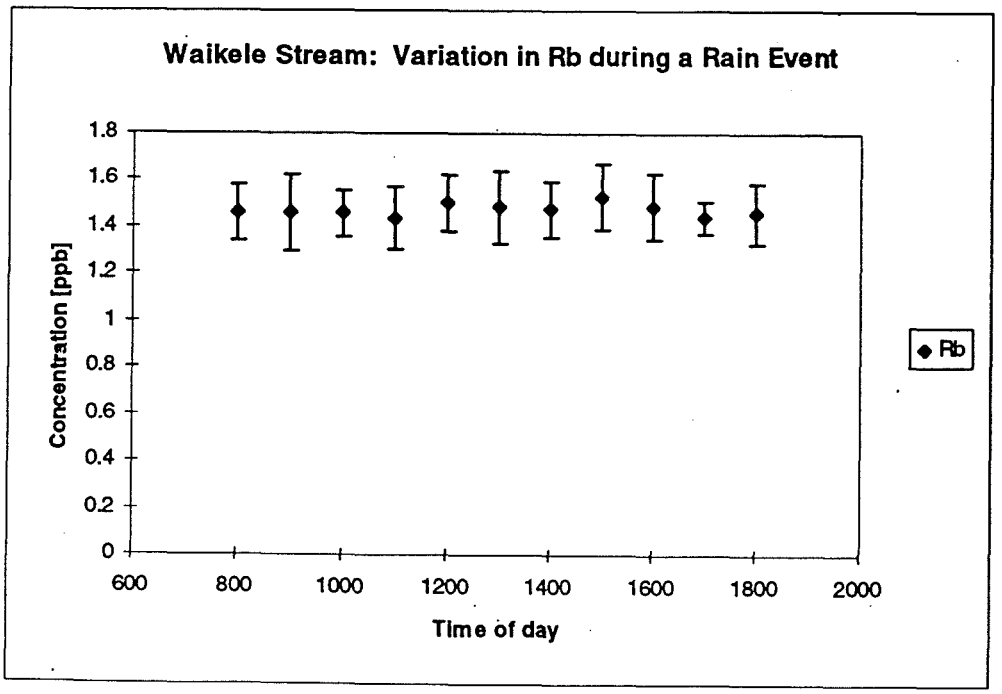
Waikele Stream: Variation in Rb during a Rain Event
Concentration [ppb]
1.8
1.6
1.4
1.2
1
0.8
0.6
0.4
0.2
0
600
800
1000
1200
1400
1600
1800
2000
Time of day
Rb

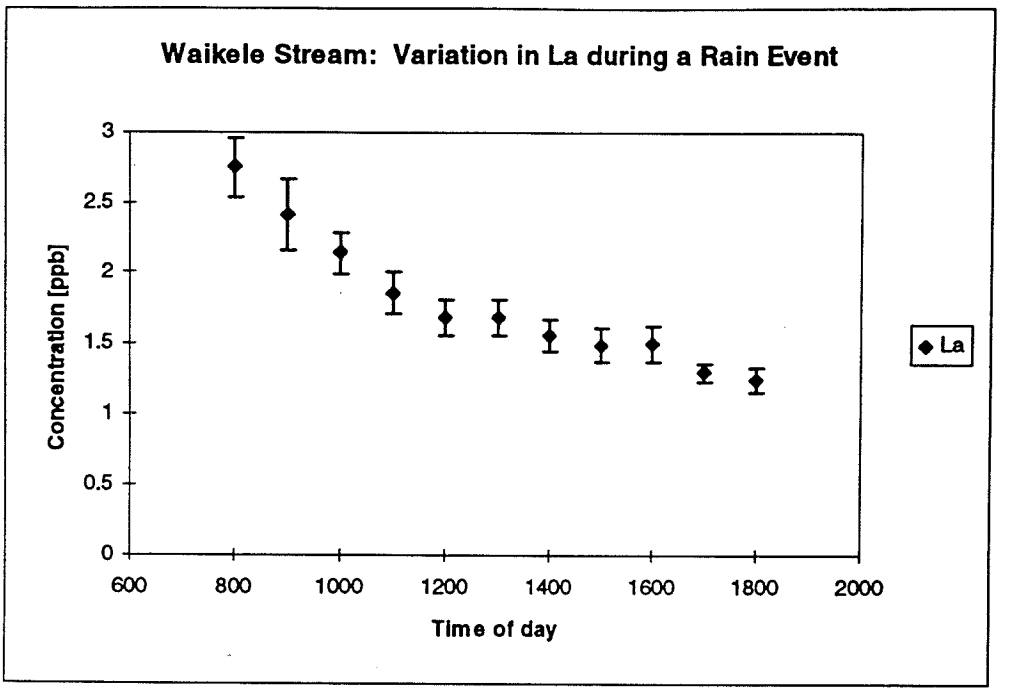
Waikele Stream: Variation in La during a Rain Event
Concentration [ppb]
3
2.5
2
1.5
1
0.5
0
600
800
1000
1200
1400
1600
1800
2000
Time of day
La

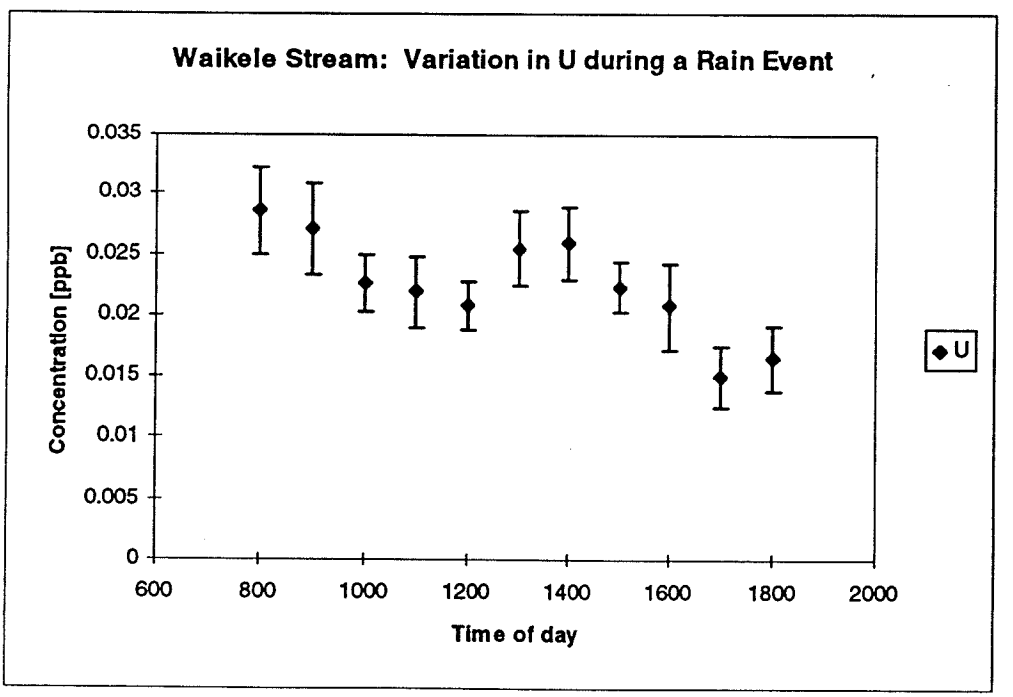
Waikele Stream: Variation in U during a Rain Event
Concentration [ppb]
0.035
0.03
0.025
0.02
0.015
0.01
0.005
0
600
800
1000
1200
1400
1600
1800
2000
Time of day
U

Appendix I

Contour and point value plots of La, Pr, and Nd data for Waianae Outfall tracer injection event

Appendix I
Contour and point value plots of La, Pr, and Nd data for Waianae Outfall tracer injection event

Table of Contents

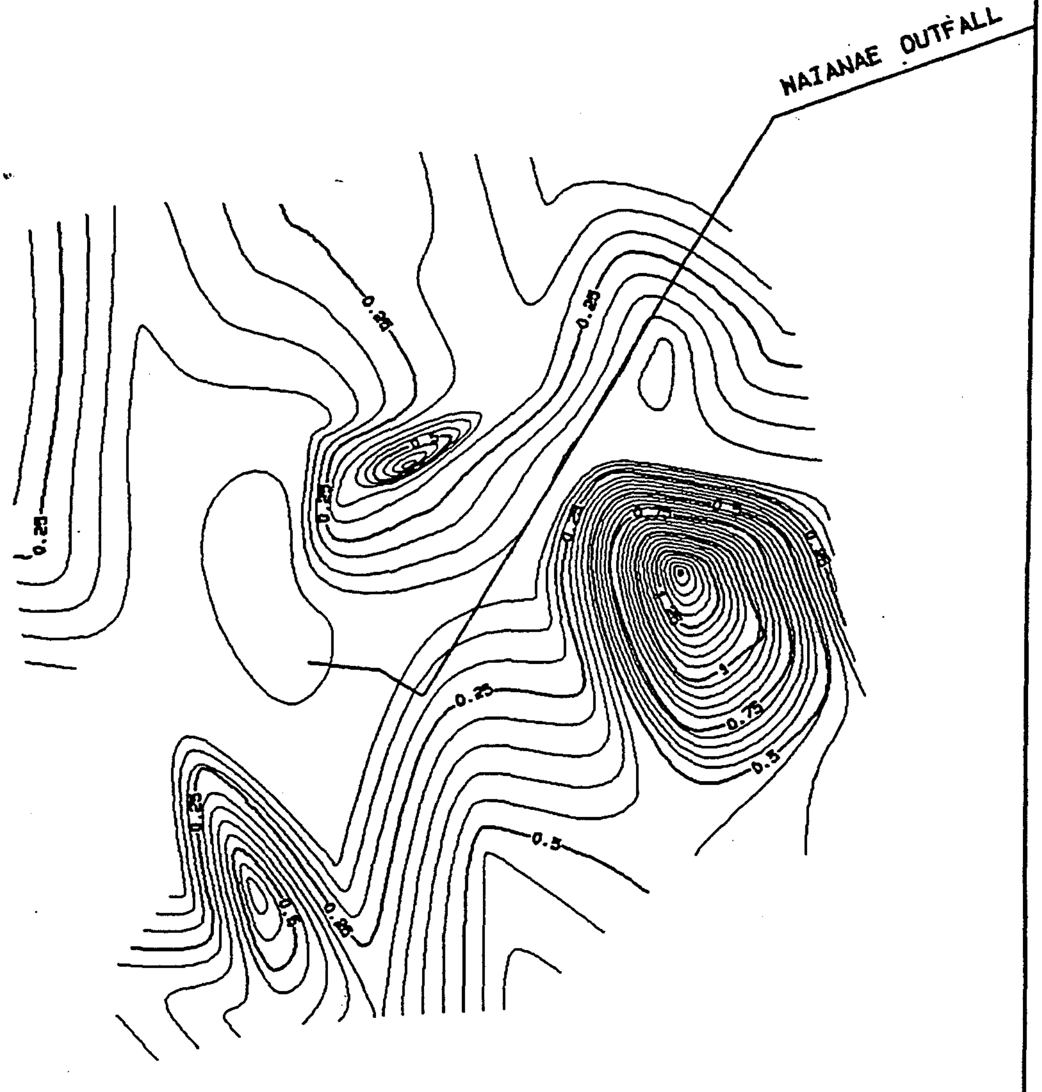

La. Surface

NORMALIZED CONCENTRATION X 1000

SCALE: 1" = 700'

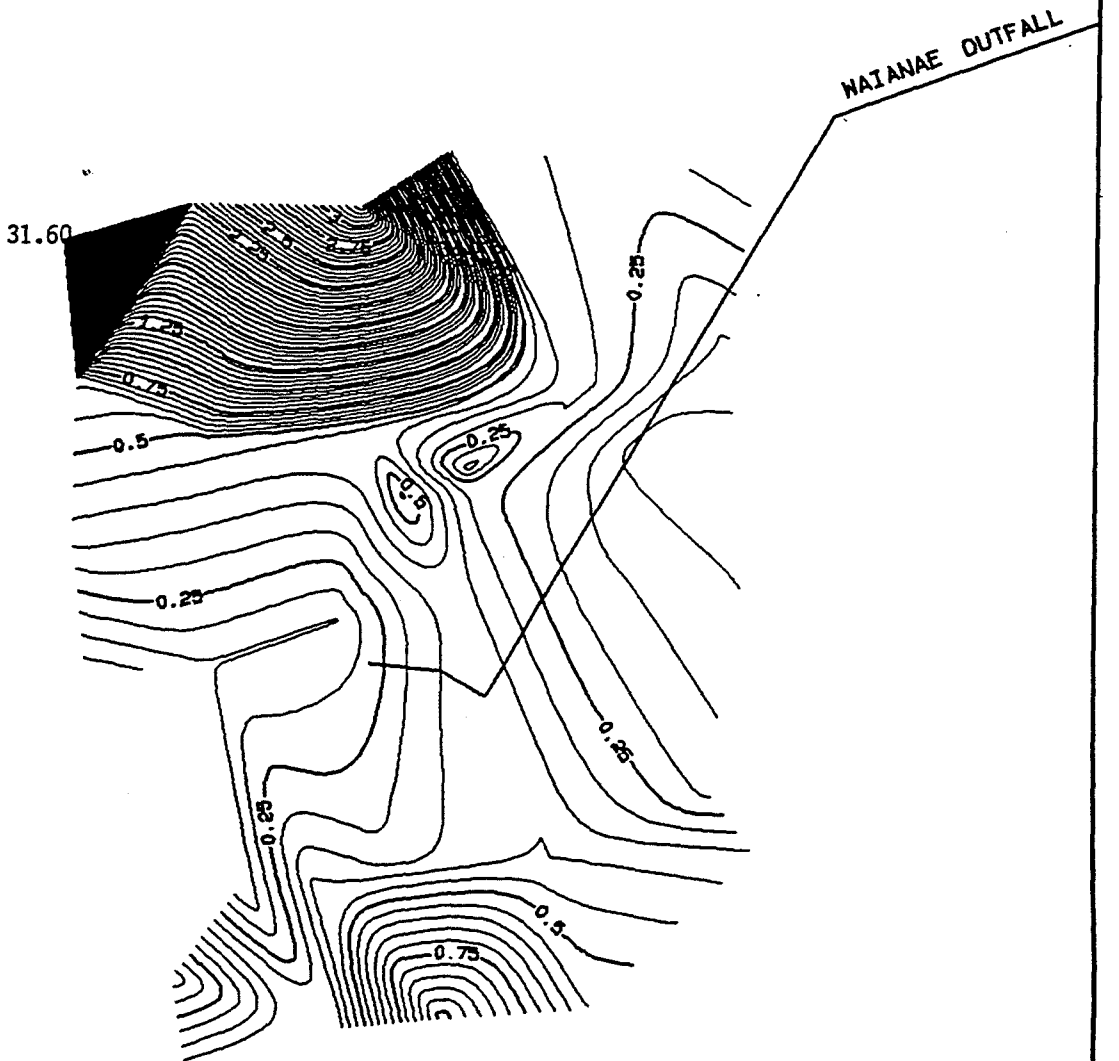

La. -35 ft

NORMALIZED CONCENTRATION X 1000

SCALE: 1" = 700'

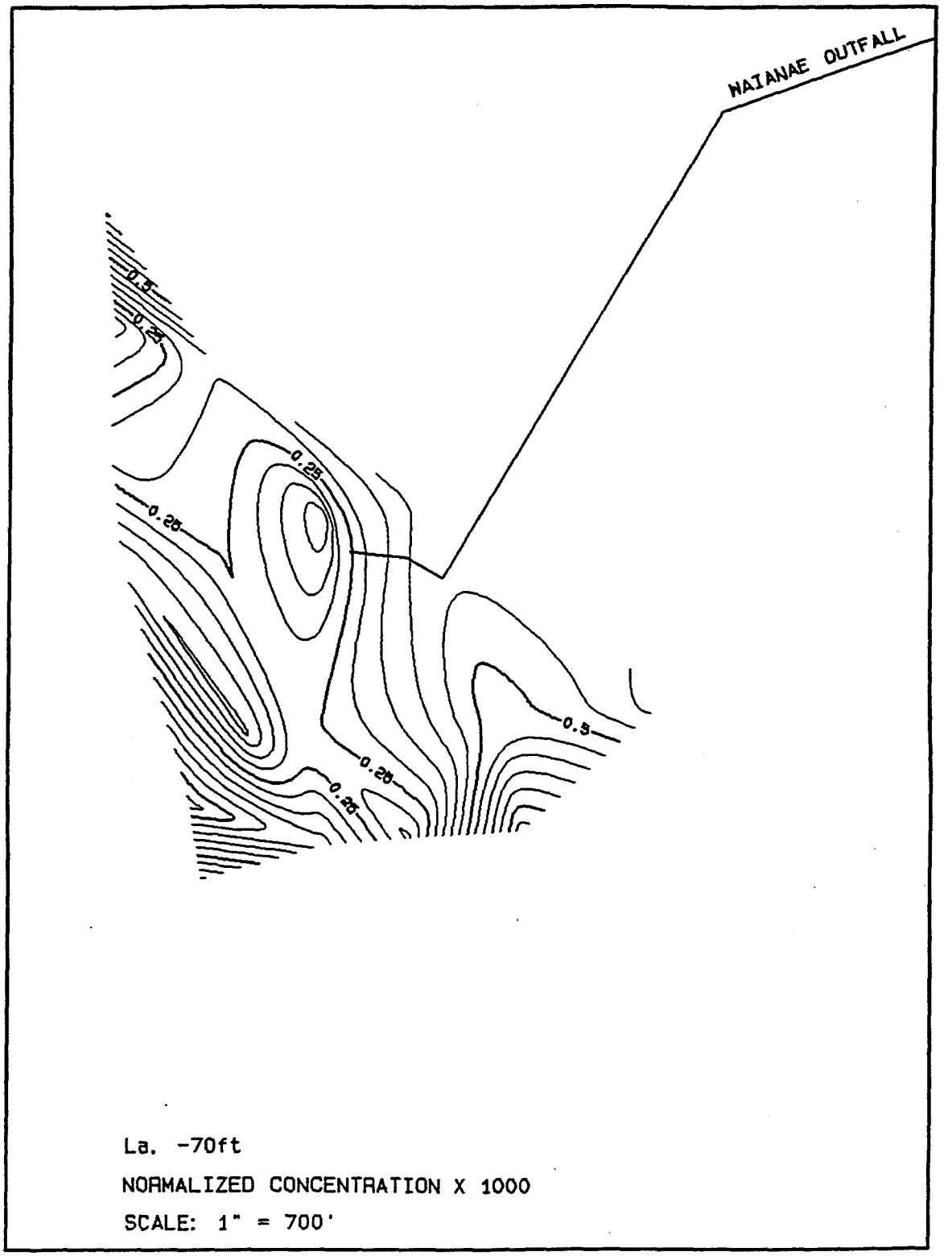
NAIANAE OUTFALL
0.5
0.25
0.25
0.25
0.5
0.25
0.25
La. -70ft
NORMALIZED CONCENTRATION X 1000
SCALE: 1" = 700'

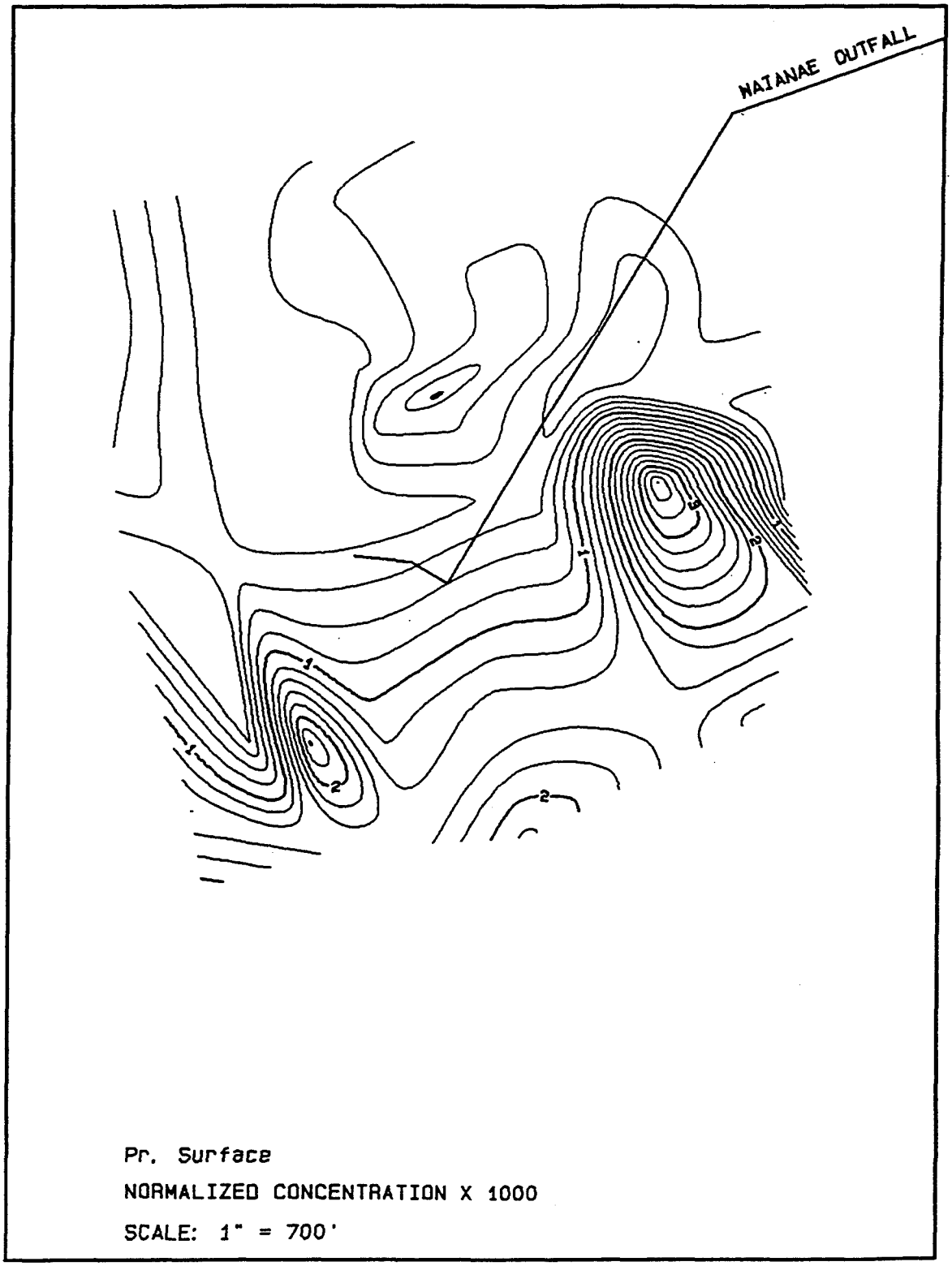
MAIANAE OUTFALL
1
1
2
2
1
1
1
1
Pr. Surface
NORMALIZED CONCENTRATION X 1000
SCALE: 1" = 700'

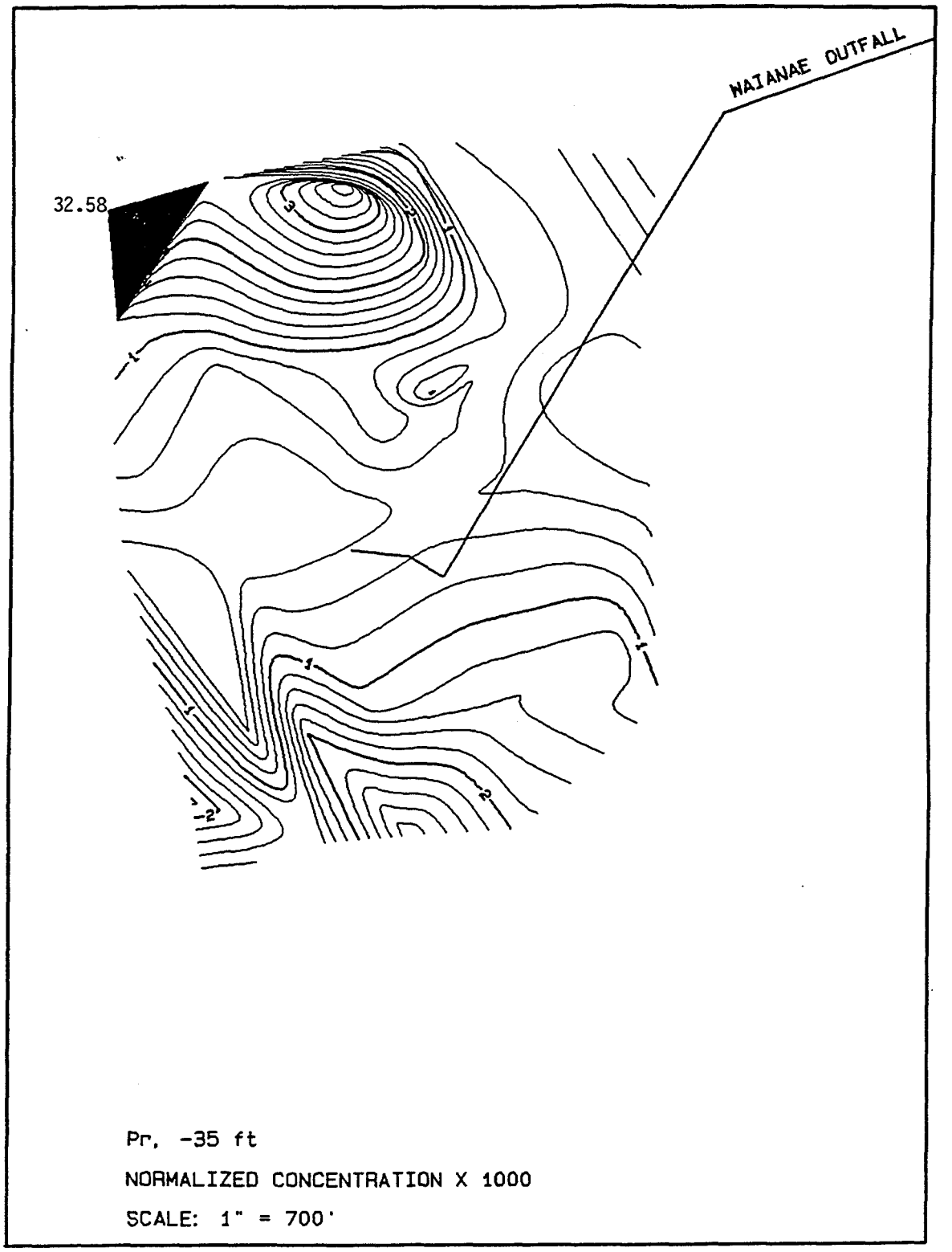

Pr, -35 ft

NORMALIZED CONCENTRATION X 1000

SCALE: 1" = 700'

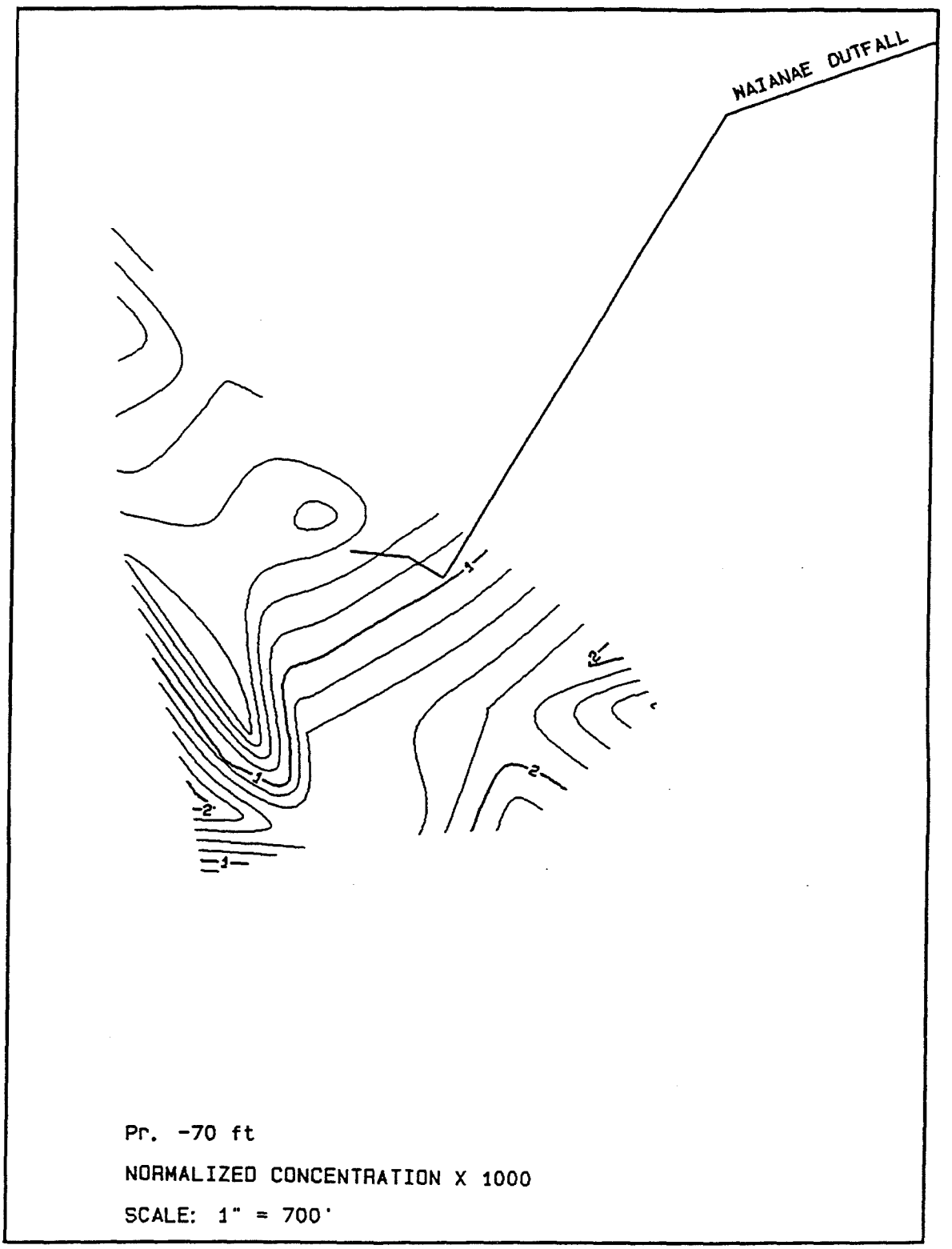

Pr. -70 ft

NORMALIZED CONCENTRATION X 1000

SCALE: 1" = 700'

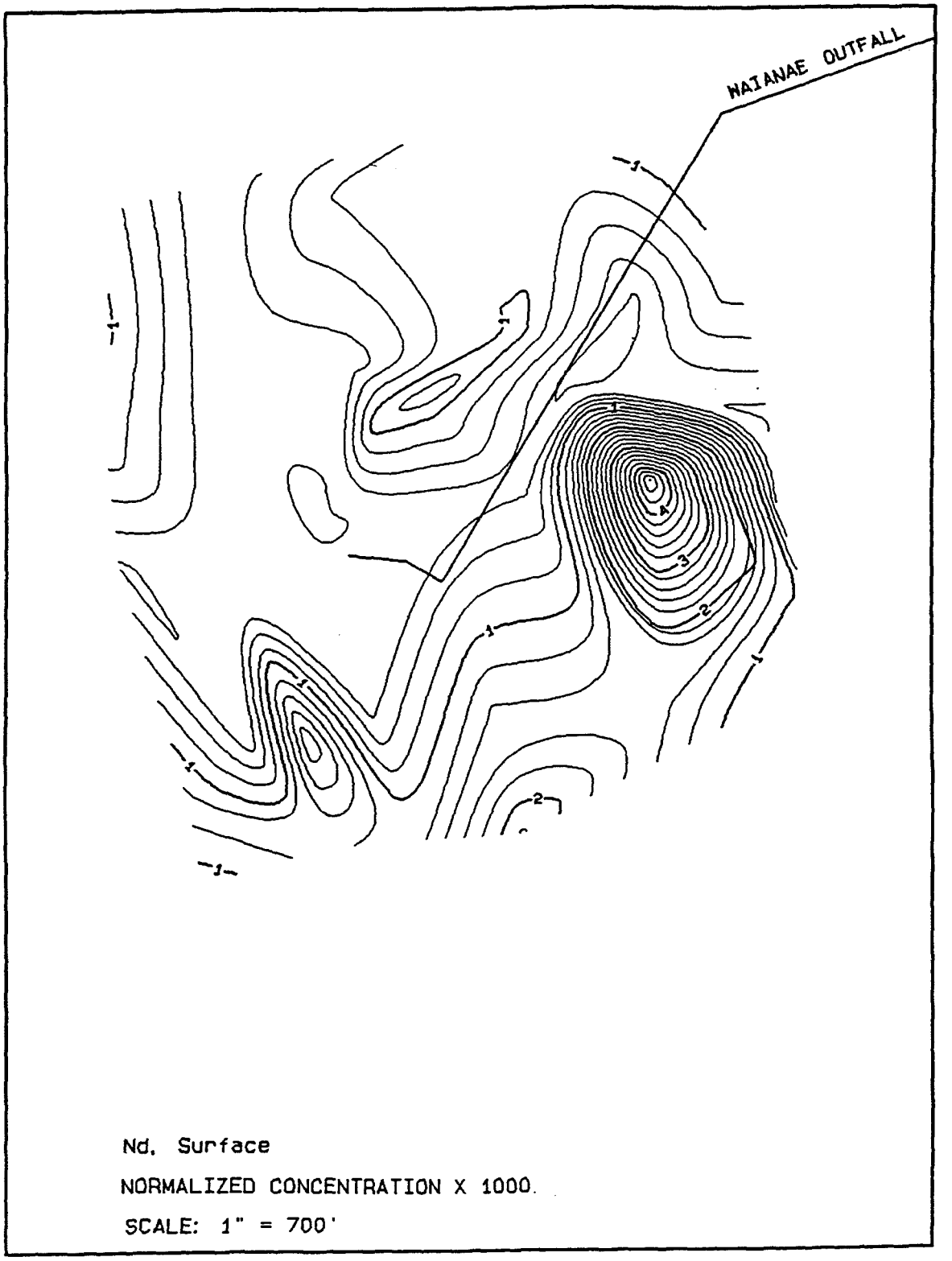

Nd, Surface

NORMALIZED CONCENTRATION X 1000.

SCALE: 1" = 700'

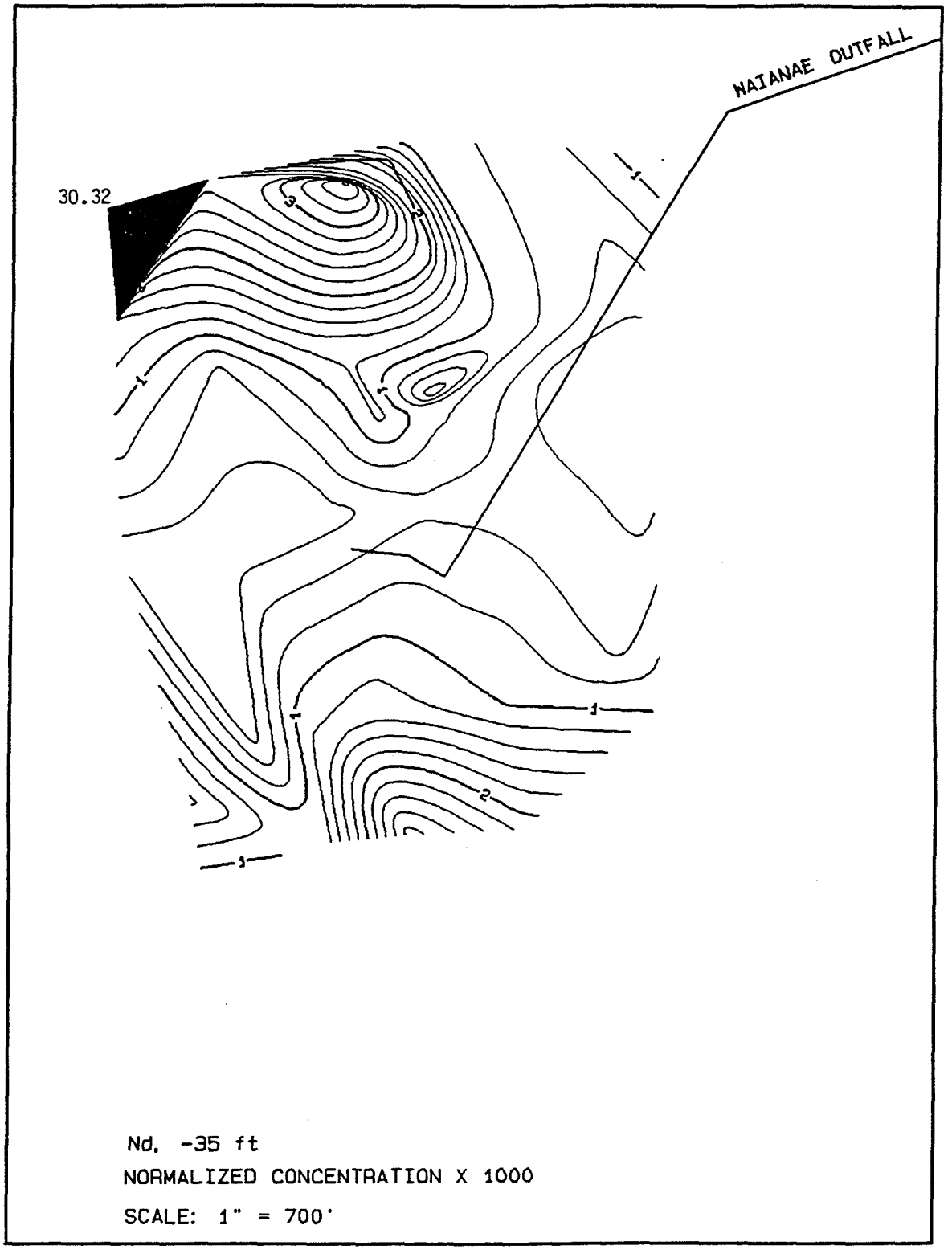

Nd, -35 ft

NORMALIZED CONCENTRATION X 1000

SCALE: 1" = 700'

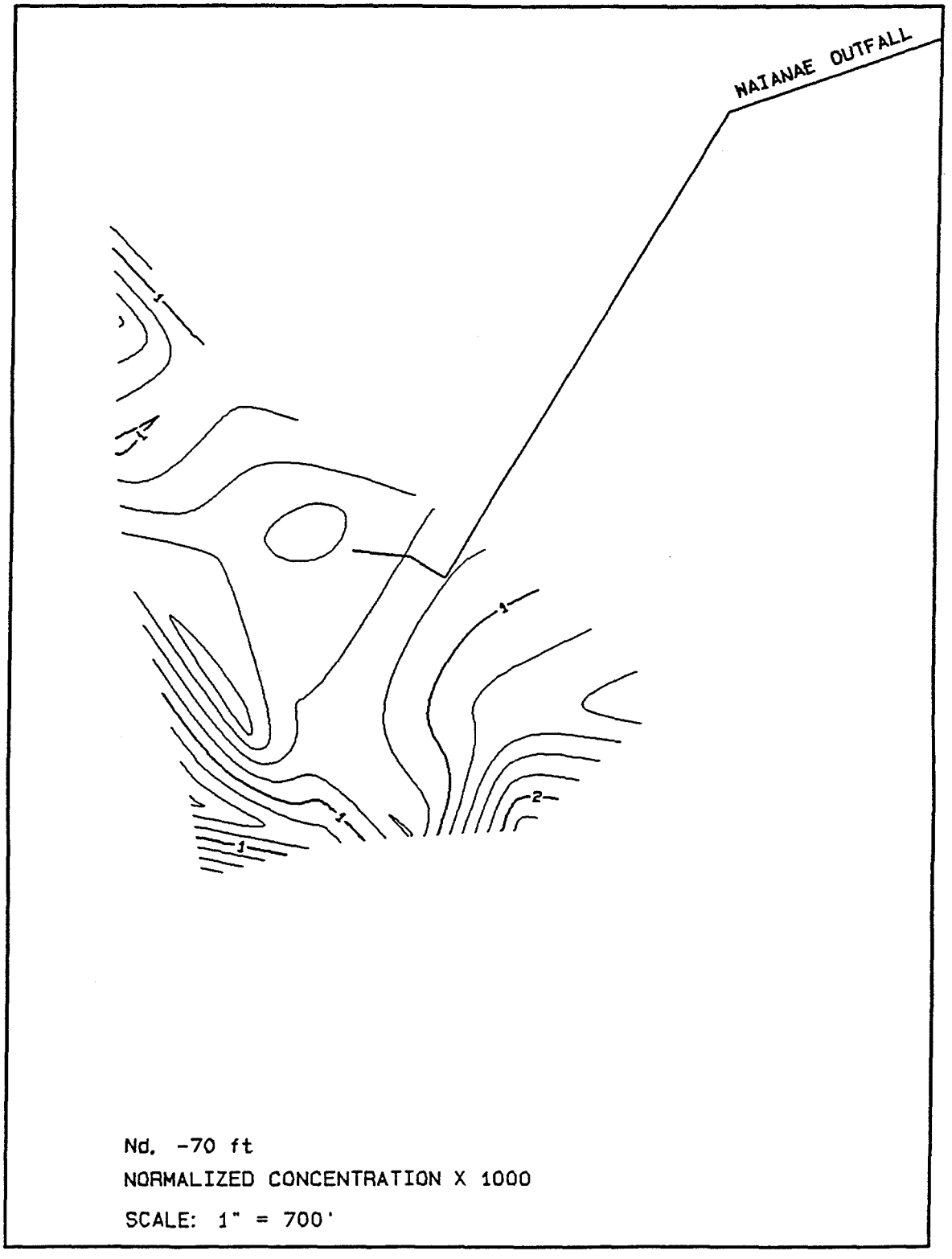

Nd, -70 ft

NORMALIZED CONCENTRATION X 1000

SCALE: 1" = 700'

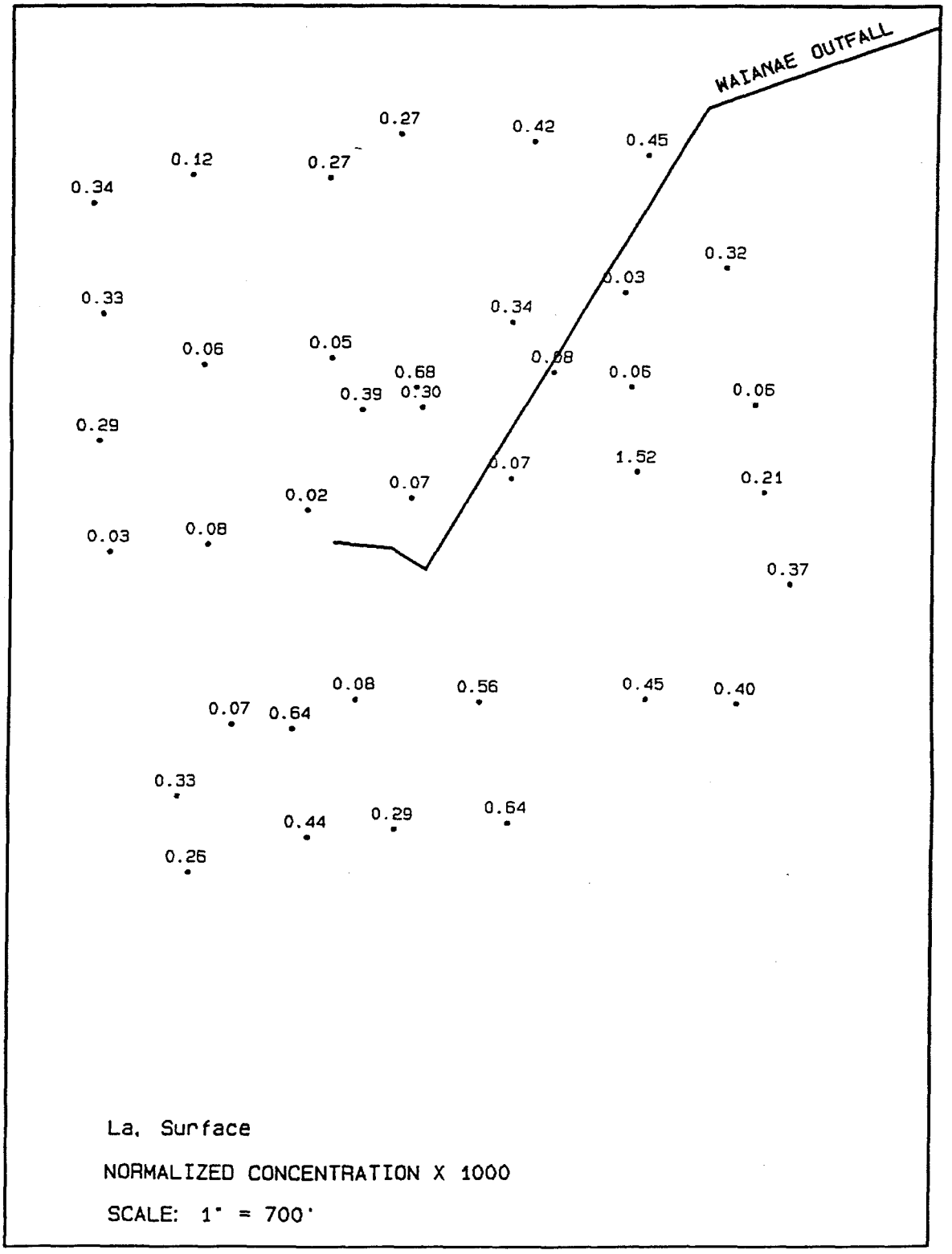
WAIANAE OUTFALL
0.27
0.42
0.45
0.12
0.27
0.34
0.32
0.03
0.33
0.34
0.06
0.05
0.68
0.08
0.06
0.39
0.30
0.06
0.29
0.07
1.52
0.02
0.07
0.21
0.03
0.08
0.37
0.08
0.56
0.45
0.40
0.07
0.64
0.33
0.44
0.29
0.64
0.26
La, Surface
NORMALIZED CONCENTRATION X 1000
SCALE: 1" = 700'

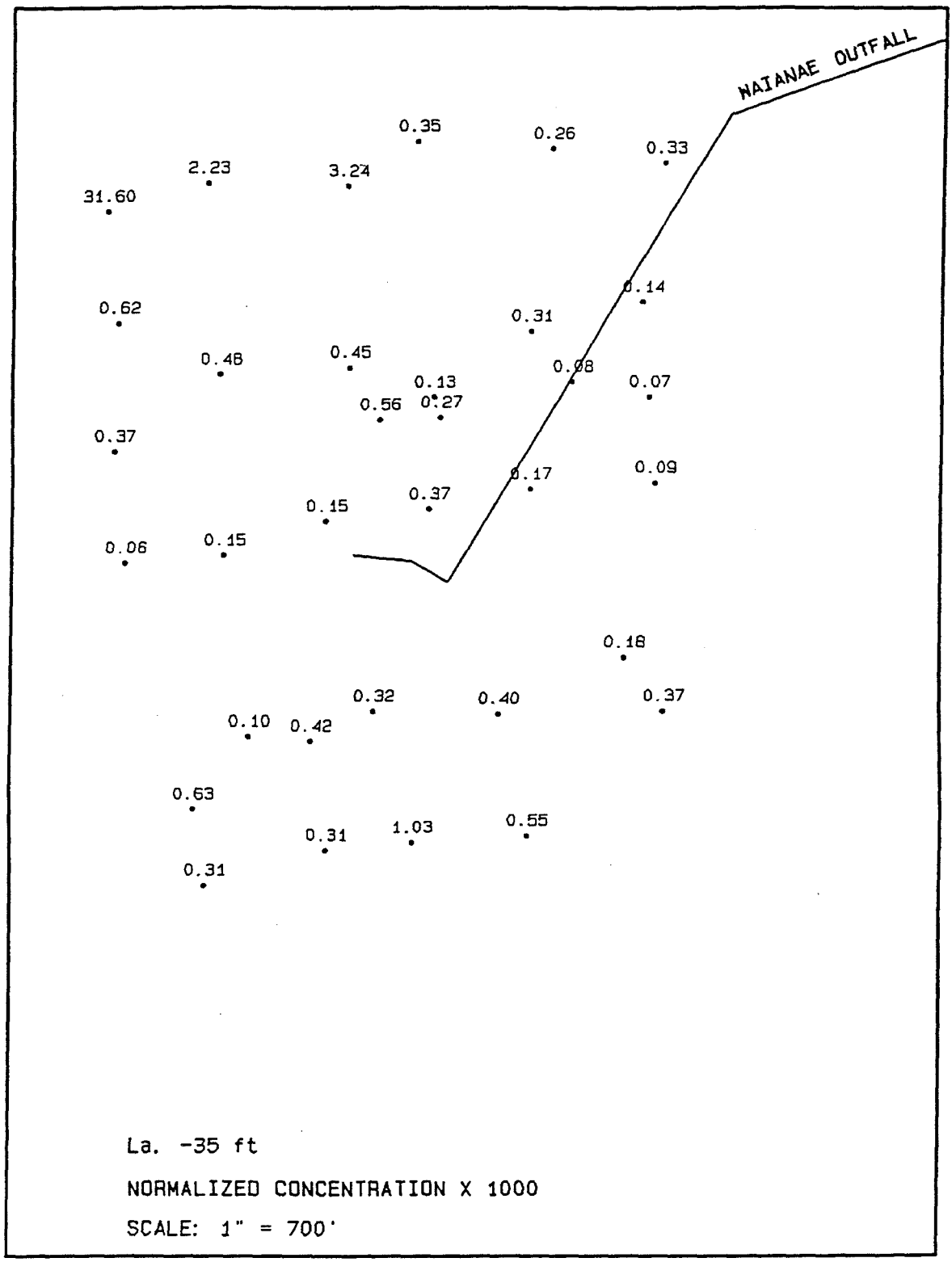
NAIANAE OUTFALL
0.35
0.26
0.33
2.23
3.24
31.60
0.14
0.62
0.31
0.48
0.45
0.08
0.13
0.07
0.56
0.27
0.37
0.17
0.09
0.37
0.15
0.06
0.15
0.18
0.32
0.40
0.37
0.10
0.42
0.63
0.55
0.31
1.03
0.31
La. -35 ft
NORMALIZED CONCENTRATION X 1000
SCALE: 1" = 700'

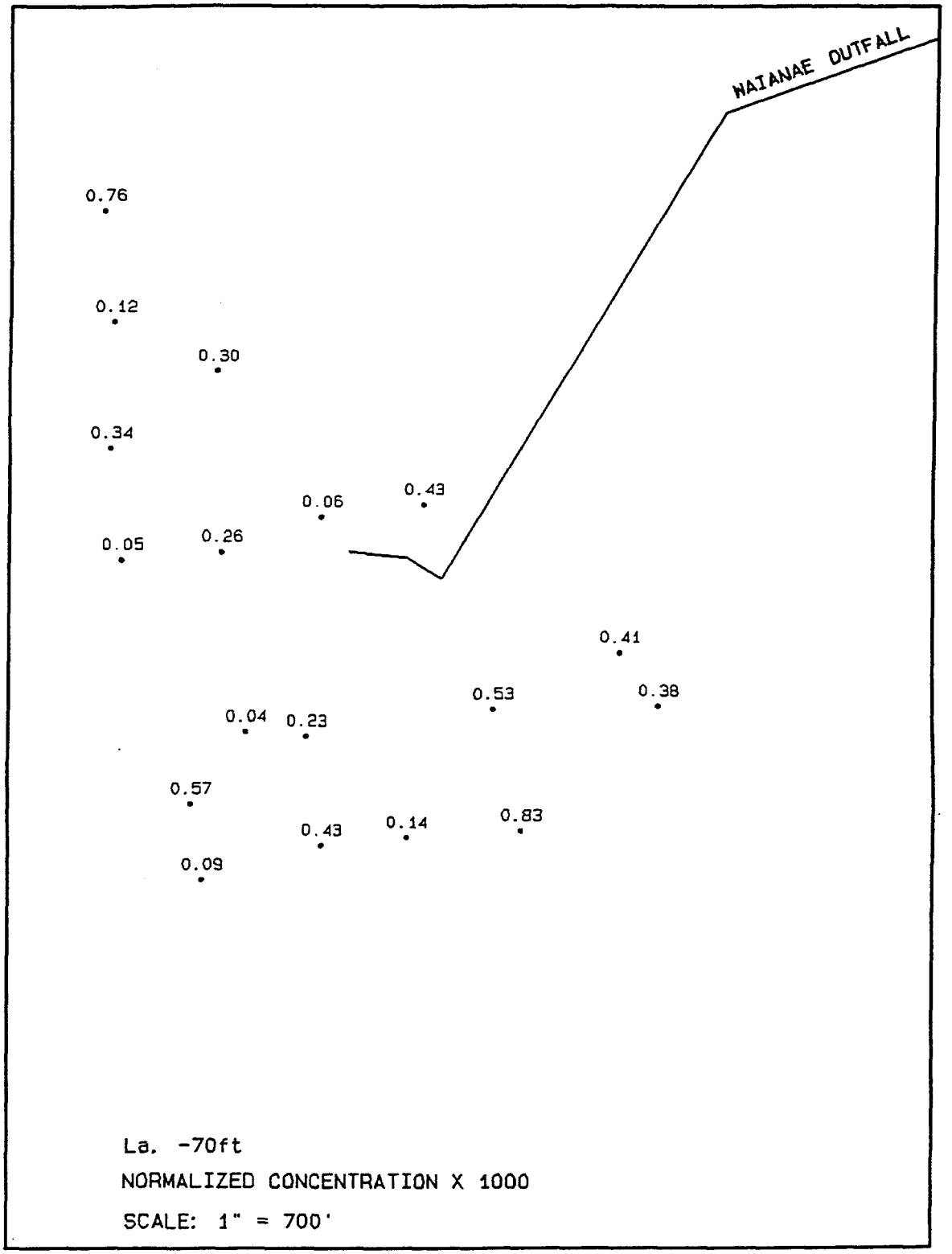
WAIANAE OUTFALL
0.76
0.12
0.30
0.34
0.06
0.43
0.05
0.26
0.41
0.53
0.38
0.04
0.23
0.57
0.43
0.14
0.83
0.09
La. -70ft
NORMALIZED CONCENTRATION X 1000
SCALE: 1" = 700'

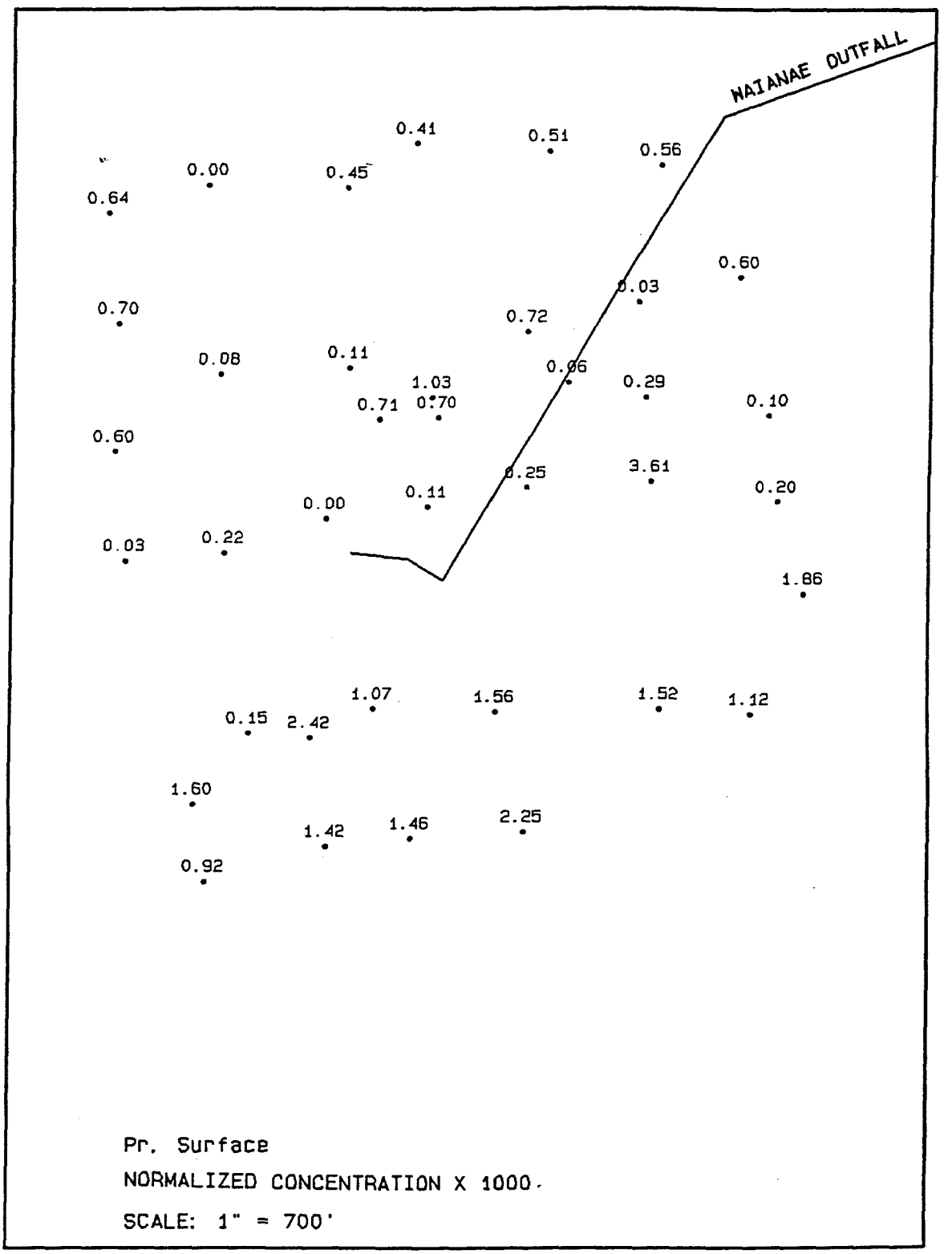
WAIANAE OUTFALL
0.41
0.51
0.56
0.00
0.45
0.64
0.60
0.03
0.70
0.72
0.11
0.08
0.06
0.29
1.03
0.71
0.70
0.10
0.60
3.61
0.25
0.11
0.20
0.00
0.03
0.22
1.86
1.07
1.56
1.52
1.12
0.15
2.42
1.60
1.42
1.46
2.25
0.92
Pr. Surface
NORMALIZED CONCENTRATION X 1000.
SCALE: 1" = 700'

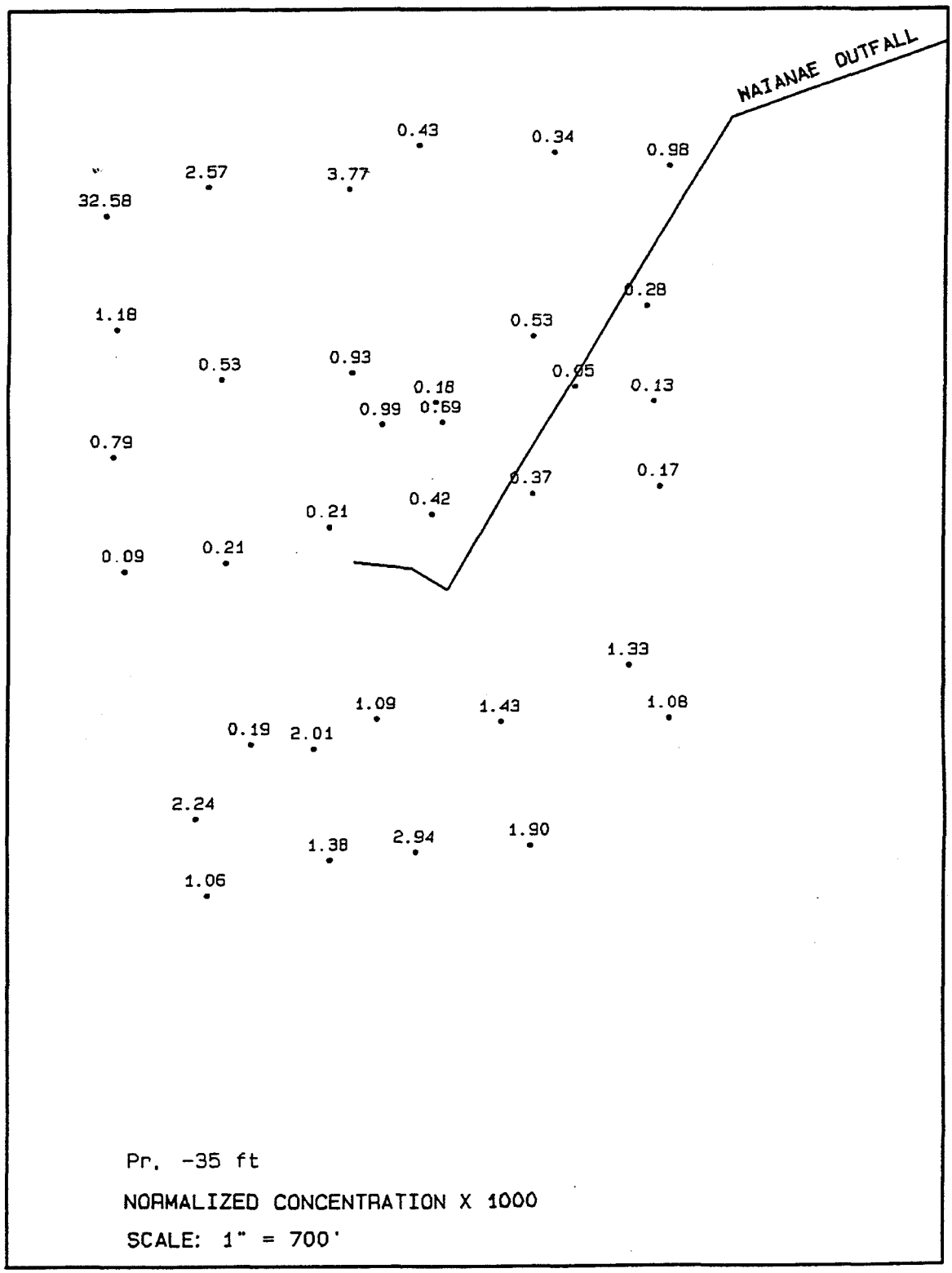
HAIANAE OUTFALL
0.43
0.34
0.98
2.57
3.77
32.58
0.28
1.18
0.53
0.53
0.93
0.05
0.18
0.13
0.99
0.69
0.79
0.37
0.17
0.42
0.21
0.21
0.09
1.33
1.09
1.43
1.08
0.19
2.01
2.24
1.38
2.94
1.90
1.06
Pr. -35 ft
NORMALIZED CONCENTRATION X 1000
SCALE: 1" = 700'

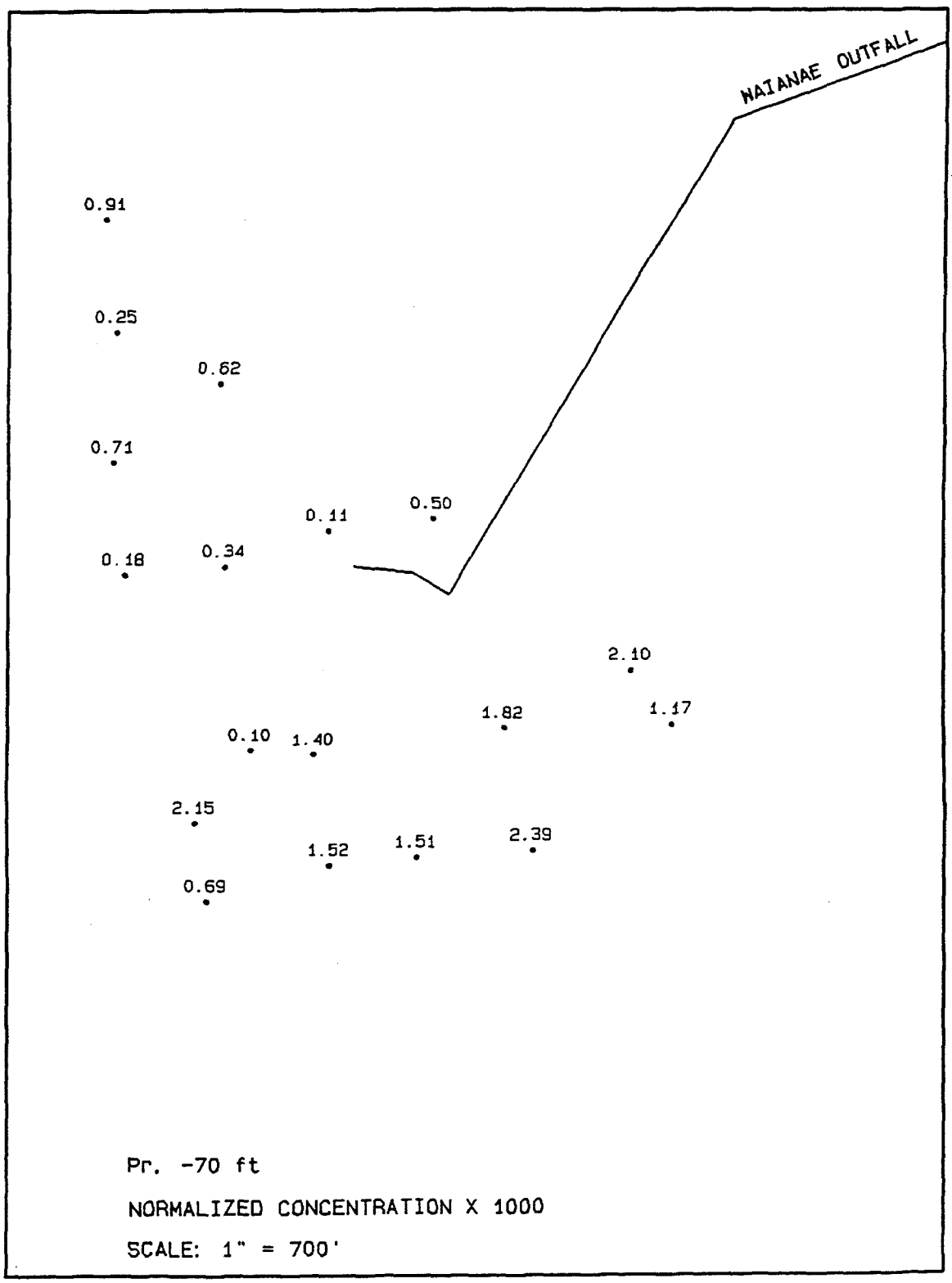
WAIANAE OUTFALL
0.91
0.25
0.62
0.71
0.11
0.50
0.18
0.34
2.10
1.82
1.17
0.10
1.40
2.15
1.52
1.51
2.39
0.69
Pr. -70 ft
NORMALIZED CONCENTRATION X 1000
SCALE: 1" = 700'

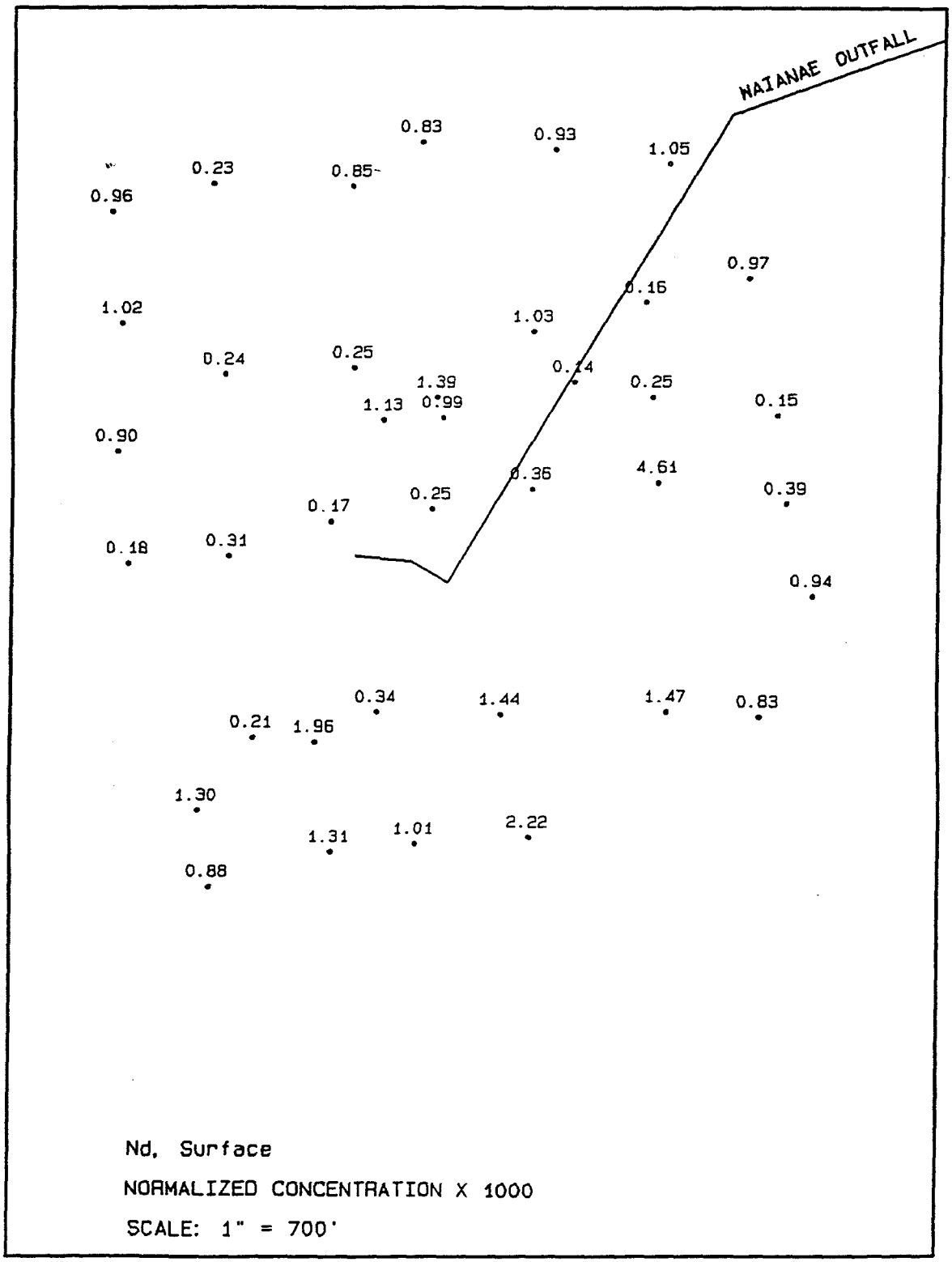
NAIANAE OUTFALL
0.83
0.93
1.05
0.23
0.85
0.96
0.97
0.16
1.02
1.03
0.24
0.25
0.14
1.39
0.25
1.13
0.99
0.15
0.90
0.36
4.61
0.25
0.39
0.17
0.18
0.31
0.94
0.34
1.44
1.47
0.83
0.21
1.96
1.30
1.31
1.01
2.22
0.88
Nd, Surface
NORMALIZED CONCENTRATION X 1000
SCALE: 1" = 700'

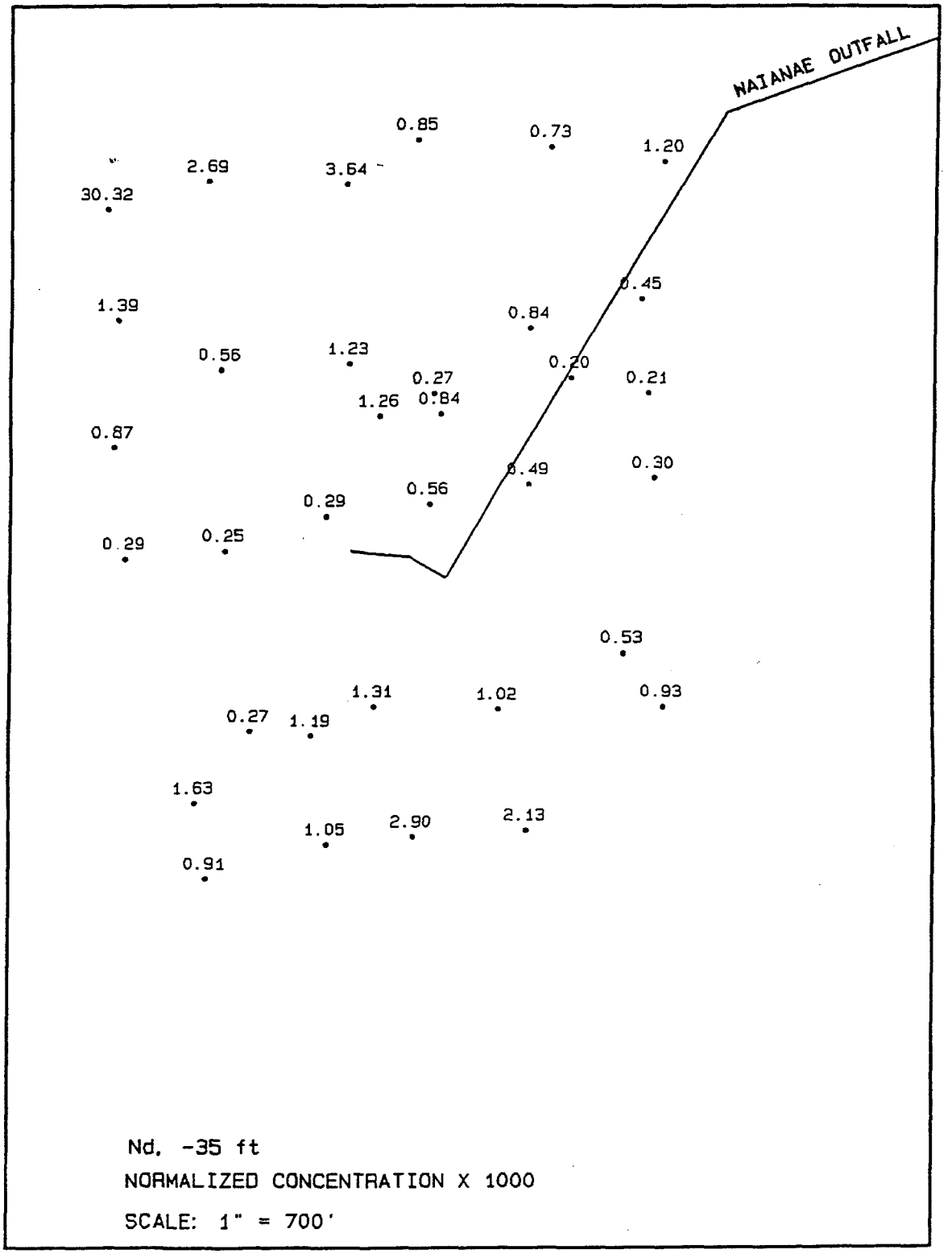
NAIANAE OUTFALL
0.85
0.73
1.20
2.69
3.64
30.32
0.45
1.39
0.84
0.56
1.23
0.20
0.27
0.21
1.26
0.84
0.87
0.49
0.30
0.56
0.29
0.29
0.25
0.53
1.31
1.02
0.93
0.27
1.19
1.63
1.05
2.90
2.13
0.91
Nd, -35 ft
NORMALIZED CONCENTRATION X 1000
SCALE: 1" = 700'

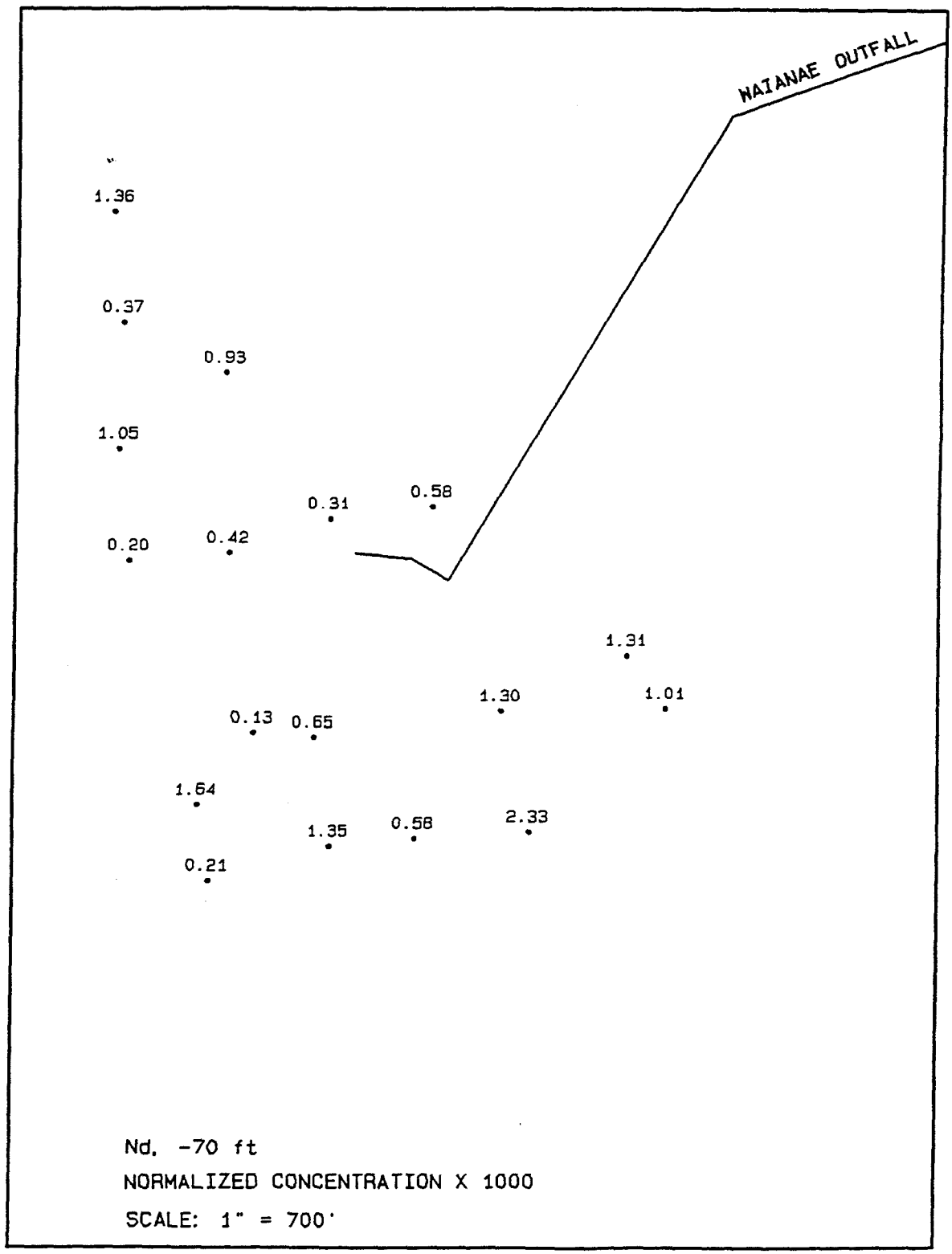
NAIANAE OUTFALL
1.36
0.37
0.93
1.05
0.31
0.58
0.20
0.42
1.31
1.30
1.01
0.13
0.65
1.64
1.35
0.58
2.33
0.21
Nd, -70 ft
NORMALIZED CONCENTRATION X 1000
SCALE: 1" = 700'